Scientific and Technical Aerospace Reports

STAR

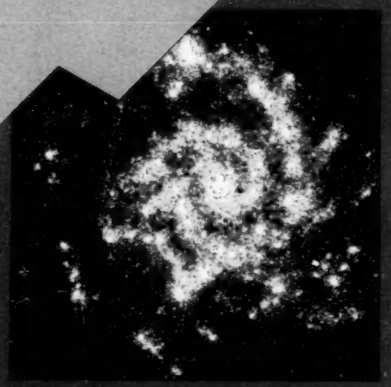

An Abstract Journal

STI PROGRAM
SCIENTIFIC & TECHNICAL INFORMATION

Volume 30, Number 14
July 23, 1992
N92-23121 to N92-24070

Scientific and Technical Aerospace Reports

Scientific and Technical Aerospace Reports (STAR) is an abstract journal that provides comprehensive coverage of worldwide aerospace-related reports. It is a major product of the International Aerospace Database managed by the NASA Scientific and Technical Information (STI) Program. The coverage includes reports on aeronautics, space, and supporting disciplines. *STAR* lists current, publicly available reports entered into the NASA STI Database during the 2-week period preceding publication. A typical citation and abstract appear on page viii. They explain how to read the items that are announced in this journal.

NASA sponsors a companion journal, *International Aerospace Abstracts (IAA)* (*NOVA* for internal NASA use) that lists abstracts of the open literature on aerospace subjects available worldwide. *IAA* is available for sale through the AIAA.

Entries found in *STAR* and *IAA* are available through NASA's online service, RECON, as the International Aerospace Database and through DIALOG as the Aerospace Database.

Information on aerospace and related subjects is gathered by the NASA STI Program through national and international agreements and exchanges and is made available to the NASA community as well as to the public in many forms through various outlets. The section on NASA STI Program Products and Services contains additional information.

For further information please contact:
NASA Center for AeroSpace Information (CASI)
P.O. Box 8757
Baltimore, Maryland 21240-0757
(301) 621-0390

US ISSN 0036-8741

Volume 30 Number 14 / July 23, 1992

TABLE OF CONTENTS

AERONAUTICS For related information see also *Astronautics.*

01 AERONAUTICS (GENERAL) **2301**

02 AERODYNAMICS **2304**
Includes aerodynamics of bodies, combinations, wings, rotors, and control surfaces; and internal flow in ducts and turbomachinery. For related information see also *34 Fluid Mechanics and Heat Transfer.*

03 AIR TRANSPORTATION AND SAFETY **2305**
Includes passenger and cargo air transport operations; and aircraft accidents. For related information see also *16 Space Transportation* and *85 Urban Technology and Transportation.*

04 AIRCRAFT COMMUNICATIONS AND NAVIGATION **2306**
Includes digital and voice communication with aircraft; air navigation systems (satellite and ground based); and air traffic control. For related information see also *17 Space Communications, Spacecraft Communications, Command and Tracking* and *32 Communications and Radar.*

05 AIRCRAFT DESIGN, TESTING AND PERFORMANCE **2306**
Includes aircraft simulation technology. For related information see also *18 Spacecraft Design, Testing and Performance* and *39 Structural Mechanics.* For land transportation vehicles see *85 Urban Technology and Transportation.*

06 AIRCRAFT INSTRUMENTATION ..... **N.A.**
Includes cockpit and cabin display devices; and flight instruments. For related information see also *19 Spacecraft Instrumentation* and *35 Instrumentation and Photography.*

07 AIRCRAFT PROPULSION AND POWER **2310**
Includes prime propulsion systems and systems components, e.g., gas turbine engines and compressors; and onboard auxiliary power plants for aircraft. For related information see also *20 Spacecraft Propulsion and Power, 28 Propellants and Fuels,* and *44 Energy Production and Conversion.*

08 AIRCRAFT STABILITY AND CONTROL ..... **N.A.**
Includes aircraft handling qualities; piloting; flight controls; and autopilots. For related information see also *05 Aircraft Design, Testing and Performance.*

09 RESEARCH AND SUPPORT FACILITIES (AIR) **2312**
Includes airports, hangars and runways; aircraft repair and overhaul facilities; wind tunnels; shock tubes; and aircraft engine test stands. For related information see also *14 Ground Support Systems and Facilities (Space).*

ASTRONAUTICS For related information see also *Aeronautics.*

12 ASTRONAUTICS (GENERAL) **2312**
For extraterrestrial exploration see *91 Lunar and Planetary Exploration.*

13 ASTRODYNAMICS **2317**
Includes powered and free-flight trajectories; and orbital and launching dynamics.

14 GROUND SUPPORT SYSTEMS AND FACILITIES (SPACE) ..... **N.A.**
Includes launch complexes, research and production facilities; ground support equipment, e.g., mobile transporters; and simulators. For related information see also *09 Research and Support Facilities (Air).*

15 LAUNCH VEHICLES AND SPACE VEHICLES **2318**
Includes boosters; operating problems of launch/space vehicle systems; and reusable vehicles. For related information see also *20 Spacecraft Propulsion and Power.*

16 SPACE TRANSPORTATION **2321**
Includes passenger and cargo space transportation, e.g., shuttle operations; and space rescue techniques. For related information see also *03 Air Transportation and Safety* and *18 Spacecraft Design, Testing and Performance.* For space suits see *54 Man/System Technology and Life Support.*

17 SPACE COMMUNICATIONS, SPACECRAFT COMMUNICATIONS, COMMAND AND TRACKING . **2322**
Includes telemetry; space communications networks; astronavigation and guidance; and radio blackout. For related information see also *04 Aircraft Communications and Navigation* and *32 Communications and Radar.*

N.A.—no abstracts were assigned to this category for this issue.

18 SPACECRAFT DESIGN, TESTING AND PERFORMANCE **2322**
Includes satellites; space platforms; space stations; spacecraft systems and components such as thermal and environmental controls; and attitude controls. For life support systems see *54 Man/System Technology and Life Support.* For related information see also *05 Aircraft Design, Testing and Performance, 39 Structural Mechanics,* and *16 Space Transportation.*

19 SPACECRAFT INSTRUMENTATION ..... **N.A.**
For related information see also *06 Aircraft Instrumentation* and *35 Instrumentation and Photography.*

20 SPACECRAFT PROPULSION AND POWER **2337**
Includes main propulsion systems and components, e.g., rocket engines; and spacecraft auxiliary power sources. For related information see also *07 Aircraft Propulsion and Power, 28 Propellants and Fuels, 44 Energy Production and Conversion,* and *15 Launch Vehicles and Space Vehicles.*

CHEMISTRY AND MATERIALS

23 CHEMISTRY AND MATERIALS (GENERAL) **2339**

24 COMPOSITE MATERIALS **2339**
Includes physical, chemical, and mechanical properties of laminates and other composite materials. For ceramic materials see *27 Nonmetallic Materials.*

25 INORGANIC AND PHYSICAL CHEMISTRY **2346**
Includes chemical analysis, e.g., chromatography; combustion theory; electrochemistry; and photochemistry. For related information see also *77 Thermodynamics and Statistical Physics.*

26 METALLIC MATERIALS **2350**
Includes physical, chemical, and mechanical properties of metals, e.g., corrosion; and metallurgy.

27 NONMETALLIC MATERIALS **2353**
Includes physical, chemical, and mechanical properties of plastics, elastomers, lubricants, polymers, textiles, adhesives, and ceramic materials. For composite materials see *24 Composite Materials.*

28 PROPELLANTS AND FUELS **2356**
Includes rocket propellants, igniters and oxidizers; their storage and handling procedures; and aircraft fuels. For related information see also *07 Aircraft Propulsion and Power, 20 Spacecraft Propulsion and Power,* and *44 Energy Production and Conversion.*

29 MATERIALS PROCESSING **2356**
Includes space-based development of products and processes for commercial application. For biological materials see *55 Space Biology.*

ENGINEERING For related information see also *Physics.*

31 ENGINEERING (GENERAL) **2363**
Includes vacuum technology; control engineering; display engineering; cryogenics; and fire prevention.

32 COMMUNICATIONS AND RADAR **2364**
Includes radar; land and global communications; communications theory; and optical communications. For related information see also *04 Aircraft Communications and Navigation* and *17 Space Communications, Spacecraft Communications, Command and Tracking.* For search and rescue see *03 Air Transportation and Safety,* and *16 Space Transportation.*

33 ELECTRONICS AND ELECTRICAL ENGINEERING **2368**
Includes test equipment and maintainability; components, e.g., tunnel diodes and transistors; microminiaturization; and integrated circuitry. For related information see also *60 Computer Operations and Hardware* and *76 Solid-State Physics.*

34 FLUID MECHANICS AND HEAT TRANSFER **2372**
Includes boundary layers; hydrodynamics; fluidics; mass transfer and ablation cooling. For related information see also *02 Aerodynamics* and *77 Thermodynamics and Statistical Physics.*

35 INSTRUMENTATION AND PHOTOGRAPHY **2377**
Includes remote sensors; measuring instruments and gauges; detectors; cameras and photographic supplies; and holography. For aerial photography see *43 Earth Resources and Remote Sensing.* For related information see also *06 Aircraft Instrumentation* and *19 Spacecraft Instrumentation.*

36 LASERS AND MASERS **2379**
Includes parametric amplifiers. For related information see also *76 Solid-State Physics.*

37 MECHANICAL ENGINEERING **2380**
Includes auxiliary systems (nonpower); machine elements and processes; and mechanical equipment.

38 QUALITY ASSURANCE AND RELIABILITY **2386**
Includes product sampling procedures and techniques; and quality control.

39 STRUCTURAL MECHANICS **2387**
Includes structural element design and weight analysis; fatigue; and thermal stress. For applications see *05 Aircraft Design, Testing and Performance* and *18 Spacecraft Design, Testing and Performance.*

GEOSCIENCES For related information see also *Space Sciences.*

42 GEOSCIENCES (GENERAL) **2392**

43 EARTH RESOURCES AND REMOTE SENSING **2392**
Includes remote sensing of earth resources by aircraft and spacecraft; photogrammetry; and aerial photography. For instrumentation see *35 Instrumentation and Photography.*

44 ENERGY PRODUCTION AND CONVERSION **2402**
Includes specific energy conversion systems, e.g., fuel cells; global sources of energy; geophysical conversion; and windpower. For related information see also *07 Aircraft Propulsion and Power, 20 Spacecraft Propulsion and Power,* and *28 Propellants and Fuels.*

45 ENVIRONMENT POLLUTION **2404**
Includes atmospheric, noise, thermal, and water pollution.

46 GEOPHYSICS **2407**
Includes aeronomy; upper and lower atmosphere studies; ionospheric and magnetospheric physics; and geomagnetism. For space radiation see *93 Space Radiation.*

47 METEOROLOGY AND CLIMATOLOGY **2409**
Includes weather forecasting and modification.

48 OCEANOGRAPHY **2412**
Includes biological, dynamic, and physical oceanography; and marine resources. For related information see also *43 Earth Resources and Remote Sensing.*

LIFE SCIENCES

51 LIFE SCIENCES (GENERAL) **2412**

52 AEROSPACE MEDICINE **2414**
Includes physiological factors; biological effects of radiation; and effects of weightlessness on man and animals.

53 BEHAVIORAL SCIENCES ..... **N.A.**
Includes psychological factors; individual and group behavior; crew training and evaluation; and psychiatric research.

54 MAN/SYSTEM TECHNOLOGY AND LIFE SUPPORT **2415**
Includes human engineering; biotechnology; and space suits and protective clothing. For related information see also *16 Space Transportation.*

55 SPACE BIOLOGY **2416**
Includes exobiology; planetary biology; and extraterrestrial life.

MATHEMATICAL AND COMPUTER SCIENCES

59 MATHEMATICAL AND COMPUTER SCIENCES (GENERAL) **2416**

60 COMPUT4R OPERATIONS AND HARDWARE **2416**
Includes hardware for computer graphics, firmware, and data processing. For components see *33 Electronics and Electrical Engineering.*

61 COMPUTER PROGRAMMING AND SOFTWARE **2417**
Includes computer programs, routines, algorithms, and specific applications, e.g., CAD/CAM.

62 COMPUTER SYSTEMS **2425**
Includes computer networks and special application computer systems.

63 CYBERNETICS **2426**
Includes feedback and control theory, artificial intelligence, robotics and expert systems. For related information see also *54 Man/System Technology and Life Support.*

64 NUMERICAL ANALYSIS **2431**
Includes iteration, difference equations, and numerical approximation.

65 STATISTICS AND PROBABILITY **2434**
Includes data sampling and smoothing; Monte Carlo method; and stochastic processes.

66 SYSTEMS ANALYSIS **2434**
Includes mathematical modeling; network analysis; and operations research.

67 THEORETICAL MATHEMATICS **2435**
Includes topology and number theory.

PHYSICS For related information see also *Engineering.*

70 PHYSICS (GENERAL) **2435**
For precision time and time interval (PTTI) see *35 Instrumentation and Photography;* for geophysics, astrophysics or solar physics see *46 Geophysics, 90 Astrophysics,* or *92 Solar Physics.*

71 ACOUSTICS **2435**
Includes sound generation, transmission, and attenuation. For noise pollution see *45 Environment Pollution.*

72 ATOMIC AND MOLECULAR PHYSICS **2436**
Includes atomic structure, electron properties, and molecular spectra.

73 NUCLEAR AND HIGH-ENERGY PHYSICS **2440**
Includes elementary and nuclear particles; and reactor theory. For space radiation see *93 Space Radiation.*

74 OPTICS **2441**
Includes light phenomena and optical devices. For lasers see *36 Lasers and Masers.*

75 PLASMA PHYSICS **2443**
Includes magnetohydrodynamics and plasma fusion. For ionospheric plasmas see *46 Geophysics.* For space plasmas see *90 Astrophysics.*

76 SOLID-STATE PHYSICS **2446**
Includes superconductivity. For related information see also *33 Electronics and Electrical Engineering* and *36 Lasers and Masers.*

77 THERMODYNAMICS AND STATISTICAL PHYSICS **2451**
Includes quantum mechanics; theoretical physics; and Bose and Fermi statistics. For related information see also *25 Inorganic and Physical Chemistry* and *34 Fluid Mechanics and Heat Transfer.*

SOCIAL SCIENCES

80 SOCIAL SCIENCES (GENERAL) ..... **N.A.**
Includes educational matters.

81 ADMINISTRATION AND MANAGEMENT **2451**
Includes management planning and research.

82 DOCUMENTATION AND INFORMATION SCIENCE **2452**
Includes information management; information storage and retrieval technology; technical writing; graphic arts; and micrography. For computer documentation see *61 Computer Programming and Software.*

83 ECONOMICS AND COST ANALYSIS ..... **N.A.**
Includes cost effectiveness studies.

84 LAW, POLITICAL SCIENCE AND SPACE POLICY ..... **N.A.**
Includes NASA appropriation hearings; aviation law; space law and policy; international law; international cooperation; and patent policy.

85 URBAN TECHNOLOGY AND TRANSPORTATION ..... **N.A.**
Includes applications of space technology to urban problems; technology transfer; technology assessment; and surface and mass transportation. For related information see *03 Air Transportation and Safety, 16 Space Transportation,* and *44 Energy Production and Conversion.*

SPACE SCIENCES For related information see also *Geosciences.*

88 SPACE SCIENCES (GENERAL) ..... **N.A.**

89 ASTRONOMY **2454**
Includes radio, gamma-ray, and infrared astronomy; and astrometry.

90 ASTROPHYSICS **2456**
Includes cosmology; celestial mechanics; space plasmas; and interstellar and interplanetary gases and dust. For related information see also *75 Plasma Physics.*

91 LUNAR AND PLANETARY EXPLORATION **2459**
Includes planetology; and manned and unmanned flights. For spacecraft design or space stations see *18 Spacecraft Design, Testing and Performance.*

92 SOLAR PHYSICS **2459**
Includes solar activity, solar flares, solar radiation and sunspots. For related information see *93 Space Radiation.*

93 SPACE RADIATION **2460**
Includes cosmic radiation; and inner and outer earth's radiation belts. For biological effects of radiation see *52 Aerospace Medicine.* For theory see *73 Nuclear and High-Energy Physics.*

GENERAL

Includes aeronautical, astronautical, and space science related histories, biographies, and pertinent reports too broad for categorization; histories or broad overviews of NASA programs.

99 GENERAL **2461**

SUBJECT INDEX **I-1**

PERSONAL AUTHOR INDEX **I-65**

CORPORATE SOURCE INDEX **I-73**

CONTRACT NUMBER INDEX **I-85**

REPORT NUMBER INDEX **I-87**

ACCESSION NUMBER INDEX **I-93**

APPENDIX **A-1**

TYPICAL CITATION AND ABSTRACT

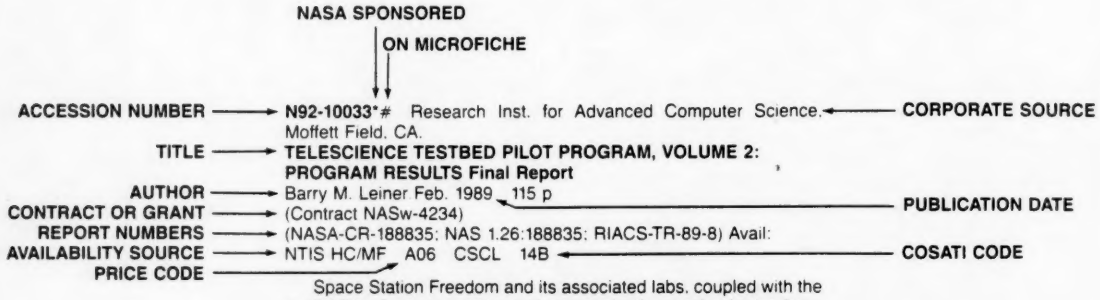

Space Station Freedom and its associated labs, coupled with the availability of new computing and communications technologies, have the potential for significantly enhancing scientific research. A Telescience Testbed Pilot Program (TTPP), aimed at developing the experience base to deal with issues in the design of the future information system of the Space Station era. The testbeds represented four scientific disciplines (astronomy and astrophysics, earth sciences, life sciences, and microgravity sciences) and studied issues in payload design, operation, and data analysis. This volume, of a 3 volume set, which all contain the results of the TTPP, contains the integrated results. Background is provided of the program and highlights of the program results. The various testbed experiments and the programmatic approach is summarized. The results are summarized on a discipline by discipline basis, highlighting the lessons learned for each discipline. Then the results are integrated across each discipline, summarizing the lessons learned overall.

Author

VOLUME 30 NUMBER 14 / JULY 23, 1992

Scientific and Technical Aerospace Reports

A Semimonthly Publication of the National Aeronautics and Space Administration

01 AERONAUTICS (GENERAL)

N92-23336*# National Aeronautics and Space Administration. Lewis Research Center, Cleveland, OH.
CENTER FOR MODELING OF TURBULENCE AND TRANSITION (CMOTT). RESEARCH BRIEFS: 1990
Louis A. Povinelli, comp., Meng-Sing Liou, comp., and Tsan-Hsing Shih, comp. Oct. 1991 166 p
(NASA Order C-99066-6)
(NASA-TM-105243; ICOMP-91-17; CMOTT-91-07; E-6570; NAS 1.15:105243) Avail: NTIS HC/MF A08 CSCL 01B

Brief progress reports of the Center for Modeling of Turbulence and Transition (CMOTT) research staff from May 1990 to May 1991 are given. The objectives of the CMOTT are to develop, validate, and implement the models for turbulence and boundary layer transition in the practical engineering flows. The flows of interest are three dimensional, incompressible, and compressible flows with chemistry. The schemes being studied include the two-equation and algebraic Reynolds stress models, the full Reynolds stress (or second moment closure) models, the probability density function models, the Renormalization Group Theory (RNG) and Interaction Approximation (DIA), the Large Eddy Simulation (LES) and Direct Numerical Simulation (DNS). For individual titles, see N92-23337 through N92-23355.

N92-23337*# Sverdrup Technology, Inc., Cleveland, OH.
THE STUDY OF PDF TURBULENCE MODELS IN COMBUSTION **c25**
Andrew T. Hsu *In* NASA. Lewis Research Center, Center for Modeling of Turbulence and Transition (CMOTT). Research Briefs: 1990 Oct. 1991 p 1-3 (For primary document see N92-23336 14-01)
Avail: NTIS HC/MF A08 CSCL 21B

The accurate prediction of turbulent combustion is still beyond reach for today's computation techniques. It is the consensus of the combustion profession that the predictions of chemically reacting flow were poor if conventional turbulence models were used. The main difficulty lies in the fact that the reaction rate is highly nonlinear, and the use of averaged temperature, pressure, and density produces excessively large errors. The probability density function (PDF) method is the only alternative at the present time that uses local instant values of the temperature, density, etc. in predicting chemical reaction rate, and thus it is the only viable approach for turbulent combustion calculations. Author

N92-23338*# National Aeronautics and Space Administration. Lewis Research Center, Cleveland, OH.
TURBULENCE MODELING **c34**
Tsan-Hsing Shih *In its* Center for Modeling of Turbulence and Transition (CMOTT). Research Briefs: 1990 Oct. 1991 p 4-8 Prepared in cooperation with Stanford Univ., CA (For primary document see N92-23336 14-01)
Avail: NTIS HC/MF A08 CSCL 20D

The performance of existing two-equation eddy viscosity models was examined. An effort was made to develop better models for near-wall turbulence using direct numerical simulations of plane channel and boundary layer flows. The asymptotic near-wall behavior of turbulence was used to examine the problems of current second order closure models and develop new models with the correct near-wall behavior. Rapid Distortion Theory was used to analytically study the effects of mean deformation on turbulence, obtain analytical solutions for the spectrum tensor, Reynolds stress tensor, anisotropy tensor and its invariants, which can be used in the turbulence model development. The potential of the renormalization group theory in turbulence modeling was studied, as well as compressible turbulent flows, and modeling of bypass transition. Author

N92-23339*# State Univ. of New York, Buffalo.
EXPERIMENTS AND MODELING **c34**
Aamir Shabbir *In* NASA. Lewis Research Center, Center for Modeling of Turbulence and Transition (CMOTT). Research Briefs: 1990 Oct. 1991 p 9-12 (For primary document see N92-23336 14-01)
Avail: NTIS HC/MF A08 CSCL 20D

The usual approach in establishing the correctness and accuracy of turbulence models is to numerically solve the modeled differential equations and then compare the results with the experiment. However, in the case of a discrepancy, this procedure does not pinpoint where in the model the drawback lies. It is also possible that the model overcompensates one physical phenomenon and undercompensates the other so that the net result is a good agreement between the two. Therefore, a more desirable approach is to directly compare the individual terms in the equations with their models. To achieve this objective, primary physical experiments were used to carry out the second moment budgets. These can then be used to analyze and assess various models and closure assumptions and seek improvements/modifications where models prove deficient. Author

N92-23340*# National Aeronautics and Space Administration. Lewis Research Center, Cleveland, OH.
MODELING OF COMPRESSIBLE TURBULENT SHEAR FLOWS **c34**
William W. Liou *In its* Center for Modeling of Turbulence and Transition (CMOTT). Research Briefs: 1990 Oct. 1991 p 13-15 (For primary document see N92-23336 14-01)
Avail: NTIS HC/MF A08 CSCL 20D

Despite all the recent developments in computer technologies and numerical algorithms, full numerical simulations of turbulent flows are feasible only at moderate Reynolds numbers and for flows with relatively simple geometries. The main goal of this research is to develop new second order moment closures for compressible turbulence. It has been shown that the models based on the extension of those developed originally for incompressible flows fail to adequately predict turbulent flows at high Mach numbers. In this attempt, the compressibility effects are explicitly considered. A successful development of these models that directly takes into account the compressibility effects may have a range of technological implications in the design of supersonic and hypersonic vehicles. Author

N92-23341*# Cornell Univ., Ithaca, NY.
RNG IN TURBULENCE AND MODELING OF BYPASS TRANSITION **c34**
Zhigang Yang *In* NASA. Lewis Research Center, Center for Modeling of Turbulence and Transition (CMOTT). Research Briefs:

1990 Oct. 1991 p 16-18 (For primary document see N92-23336 14-01)
Avail: NTIS HC/MF A08 CSCL 20D

Two projects are considered: the Renormalization Group (RNG) analysis of turbulence modeling, and the calculation of bypass transition through turbulence modeling. RNG is a process which eliminates small scales on the uneliminated large scales as the change in the transport properties. It is because of this property of RNG that it was previously suggested that RNG could be used as a model builder in turbulence modeling. The possibility is studied of constructing RNG based turbulence models, and to try to proceed to do the modeling through RNG in parallel with the classical approach. The numerical predictions made by RNG models and by classical models is compared against data from Direct Numerical Simulation. While in an environment with freestream turbulence, the transition initiated by the instability of the laminar boundary layer to Tollmien-Schlichting waves is found to be a bypass one in which turbulent spots are formed without T-S wave amplification. The formation is a random process, and flow within a turbulent spot is almost fully turbulent. This suggests the possibility of using turbulence modeling to describe and predict the bypass transition. Author

N92-23342*# Vigyan Research Associates, Inc., Hampton, VA.
TURBULENCE MODELING IN SUPERSONIC COMBUSTING FLOWS **c25**
Tawit Chitsomboon *In* NASA. Lewis Research Center, Center for Modeling of Turbulence and Transition (CMOTT). Research Briefs: 1990 Oct. 1991 p 19-21 (For primary document see N92-23336 14-01)
Avail: NTIS HC/MF A08 CSCL 21B

To support the National Aerospace Plane project, the RPLUS3D CFD code has been developed at NASA Lewis. The code has the ability to solve three-dimensional flowfields with finite rate combustion of hydrogen and air. The combustion processes of the hydrogen-air system are simulated by an 18-reaction path, 8-species chemical kinetic mechanism. The code uses a Lower-Upper (LU) decomposition numerical algorithm as its basis, making it a very efficient and robust code. Except for the Jacobian matrix for the implicit chemistry source terms, there is no inversion of a matrix even though it uses a fully implicit numerical algorithm. A k-epsilon (two equation) turbulence model is incorporated into the RPLUS3D code. Author

N92-23343*# National Aeronautics and Space Administration. Lewis Research Center, Cleveland, OH.
DEVELOPMENT OF NEW FLUX SPLITTING SCHEMES **c34**
Meng-S. Liou and Christopher J. Steffen, Jr. *In its* Center for Modeling of Turbulence and Transition (CMOTT). Research Briefs: 1990 Oct. 1991 p 22-23 (For primary document see N92-23336 14-01)
Avail: NTIS HC/MF A08 CSCL 20D

Maximizing both accuracy and efficiency has been the primary objective in designing a numerical algorithm for CFD. This is especially important for solution of complex three-dimensional systems of Navier-Stokes equations which often include turbulence modeling and chemistry effects. Recently, upwind schemes have been well received for both their capability of resolving discontinuities and their sound theoretical basis in characteristic theory for hyperbolic systems. With this in mind, two new flux splitting techniques are presented for upwind differencing. Author

N92-23344*# Sverdrup Technology, Inc., Cleveland, OH.
PROGRESS OF SIMULATIONS FOR REACTING SHEAR LAYERS **c34**
Sheng-Tao Yu *In* NASA. Lewis Research Center, Center for Modeling of Turbulence and Transition (CMOTT). Research Briefs: 1990 Oct. 1991 p 24-25 (For primary document see N92-23336 14-01)
Avail: NTIS HC/MF A08 CSCL 20D

An attempt was made to develop a high speed, chemically reactive shear layer test rig. The purpose of the experiment was to study the mixing of oxidizer and fuel streams in reacting shear layers for various density, velocity, and Mach number. The primary goal was to understand the effects of the compressibility upon mixing and combustion in a fundamental way. Therefore, a two-dimensional shear layer is highly desirable for its simplicity to quantify the compressibility effects. The RPLUS 2D code is used to calculate the flow fields of different sections of the test rig. The emphasis was on the supersonic nozzle design, the vitiation process for the hot air stream and the overall thermodynamic conditions of the test matrix. The k-epsilon turbulence model with wall function was successfully implemented in the RPLUS code. The k and epsilon equations are solved simultaneously and the LU scheme is used to make it compatible with the flow solver. Author

N92-23345*# Sverdrup Technology, Inc., Cleveland, OH.
THE STUDY OF PDF TURBULENCE MODELS IN COMBUSTION **c25**
Andrew T. Hsu *In* NASA. Lewis Research Center, Center for Modeling of Turbulence and Transition (CMOTT). Research Briefs: 1990 Oct. 1991 p 53-65 Presented at the 9th National Aero-Space Plane Technology Symposium, 1-2 Nov. 1990 (For primary document see N92-23336 14-01)
(Paper-107) Avail: NTIS HC/MF A08 CSCL 21B

In combustion computations, it is known that the predictions of chemical reaction rates are poor if conventional turbulence models are used. The probability density function (pdf) method seems to be the only alternative that uses local instantaneous values of the temperature, density, etc., in predicting chemical reaction rates, and thus is the only viable approach for more accurate turbulent combustion calculations. The fact that the pdf equation has a very large dimensionality renders finite difference schemes extremely demanding on computer memories and thus impractical. A logical alternative is the Monte Carlo scheme. Since CFD has a certain maturity as well as acceptance, it seems that the use of a combined CFD and Monte Carlo scheme is more beneficial. Therefore, a scheme is chosen that uses a conventional CFD flow solver in calculating the flow field properties such as velocity, pressure, etc., while the chemical reaction part is solved using a Monte Carlo scheme. The discharge of a heated turbulent plane jet into quiescent air was studied. Experimental data for this problem shows that when the temperature difference between the jet and the surrounding air is small, buoyancy effect can be neglected and the temperature can be treated as a passive scalar. The fact that jet flows have a self-similar solution lends convenience in the modeling study. Futhermore, the existence of experimental data for turbulent shear stress and temperature variance make the case ideal for the testing of pdf models wherein these values can be directly evaluated. Author

N92-23346*# Sverdrup Technology, Inc., Cleveland, OH.
ON RECONTAMINATION AND DIRECTIONAL-BIAS PROBLEMS IN MONTE CARLO SIMULATION OF PDF TURBULENCE MODELS **c34**
Andrew T. Hsu *In* NASA. Lewis Research Center, Center for Modeling of Turbulence and Transition (CMOTT). Research Briefs: 1990 Oct. 1991 p 66-67 (For primary document see N92-23336 14-01)
Avail: NTIS HC/MF A08 CSCL 20D

Turbulent combustion can not be simulated adequately by conventional moment closure turbulence models. The difficulty lies in the fact that the reaction rate is in general an exponential function of the temperature, and the higher order correlations in the conventional moment closure models of the chemical source term can not be neglected, making the applications of such models impractical. The probability density function (pdf) method offers an attractive alternative: in a pdf model, the chemical source terms are closed and do not require additional models. A grid dependent Monte Carlo scheme was studied, since it is a logical alternative, wherein the number of computer operations increases only linearly with the increase of number of independent variables, as compared to the exponential increase in a conventional finite difference scheme. A new algorithm was devised that satisfies a restriction

in the case of pure diffusion or uniform flow problems. Although for nonuniform flows absolute conservation seems impossible, the present scheme has reduced the error considerably. Author

N92-23347*# Sverdrup Technology, Inc., Cleveland, OH.
PROGRESS IN THE DEVELOPMENT OF PDF TURBULENCE MODELS FOR COMBUSTION **c25**
Andrew T. Hsu *In* NASA. Lewis Research Center, Center for Modeling of Turbulence and Transition (CMOTT). Research Briefs: 1990 Oct. 1991 p 68-76 Presented at the 10th National Aero-Space Plane Technology Symposium, 23-26 Apr. 1991 (For primary document see N92-23336 14-01)
(Contract NAS3-25266)
(Paper-213) Avail: NTIS HC/MF A08 CSCL 21B

A combined Monte Carlo-computational fluid dynamic (CFD) algorithm was developed recently at Lewis Research Center (LeRC) for turbulent reacting flows. In this algorithm, conventional CFD schemes are employed to obtain the velocity field and other velocity related turbulent quantities, and a Monte Carlo scheme is used to solve the evolution equation for the probability density function (pdf) of species mass fraction and temperature. In combustion computations, the predictions of chemical reaction rates (the source terms in the species conservation equation) are poor if conventional turbulence modles are used. The main difficulty lies in the fact that the reaction rate is highly nonlinear, and the use of averaged temperature produces excessively large errors. Moment closure models for the source terms have attained only limited success. The probability density function (pdf) method seems to be the only alternative at the present time that uses local instantaneous values of the temperature, density, etc., in predicting chemical reaction rates, and thus may be the only viable approach for more accurate turbulent combustion calculations. Assumed pdf's are useful in simple problems; however, for more general combustion problems, the solution of an evolution equation for the pdf is necessary. Author

N92-23348*# Sverdrup Technology, Inc., Cleveland, OH.
A STUDY OF HYDROGEN DIFFUSION FLAMES USING PDF TURBULENCE MODEL **c25**
Andrew T. Hsu *In* NASA. Lewis Research Center, Center for Modeling of Turbulence and Transition (CMOTT). Research Briefs: 1990 Oct. 1991 p 77-86 Previously announced in IAA as A91-45549 (For primary document see N92-23336 14-01)
(Contract NAS2-5266)
Avail: NTIS HC/MF A08 CSCL 21B

The application of probability density function (pdf) turbulence models is addressed. For the purpose of accurate prediction of turbulent combustion, an algorithm that combines a conventional computational fluid dynamic (CFD) flow solver with the Monte Carlo simulation of the pdf evolution equation was developed. The algorithm was validated using experimental data for a heated turbulent plane jet. The study of H2-F2 diffusion flames was carried out using this algorithm. Numerical results compared favorably with experimental data. The computations show that the flame center shifts as the equivalence ratio changes, and that for the same equivalence ratio, similarity solutions for flames exist.
Author

N92-23349*# Sverdrup Technology, Inc., Cleveland, OH.
AN IMPROVED K-EPSILON MODEL FOR NEAR WALL TURBULENCE **c34**
T. H. Shih (National Aeronautics and Space Administration. Lewis Research Center, Cleveland, OH.) and Andrew T. Hsu *In* NASA. Lewis Research Center, Center for Modeling of Turbulence and Transition (CMOTT). Research Briefs: 1990 Oct. 1991 p 87-104 (For primary document see N92-23336 14-01)
Avail: NTIS HC/MF A08 CSCL 21B

An improved k-epsilon model for low Reynolds number turbulence near a wall is presented. In the first part of this work, the near-wall asymptotic behavior of the eddy viscosity and the pressure transport term in the turbulent kinetic energy equation are analyzed. Based on these analyses, a modified eddy viscosity model with the correct near-wall behavior is suggested, and a model for the pressure transport term in the k-equation is proposed. In addition, a modeled dissipation rate equation is reformulated, and a boundary condition for the dissipation rate is suggested. In the second part of the work, one of the deficiencies of the existing k-epsilon models, namely, the wall distance dependency of the equations and the damping functions, is examined. An improved model that does not depend on any wall distance is introduced. Fully developed turbulent channel flows and turbulent boundary layers over a flat plate are studied as validations for the proposed new models. Numerical results obtained from the present and other previous k-epsilon models are compared with data from direct numerical simulation. The results show that the present k-epsilon model, with added robustness, performs as well as or better than other existing models in predicting the behavior of near-wall turbulence. Author

N92-23350*# National Aeronautics and Space Administration. Lewis Research Center, Cleveland, OH.
ADVANCEMENTS IN ENGINEERING TURBULENCE MODELING **c34**
T.-H. Shih *In its* Center for Modeling of Turbulence and Transition (CMOTT). Research Briefs: 1990 Oct. 1991 p 108-125 Presented at the 9th National Aero-Space Plane Technology Symposium, 1-2 Nov. 1990 (For primary document see N92-23336 14-01)
(Paper-105) Avail: NTIS HC/MF A08 CSCL 20D

Some new developments in two-equation models and second order closure models are presented. Two-equation models (k-epsilon models) have been widely used in computational fluid dynamics (CFD) for engineering problems. Most of low-Reynolds number two-equation models contain some wall-distance damping functions to account for the effect of wall on turbulence. However, this often causes the confusion and difficulties in computing flows with complex geometry and also needs an ad hoc treatment near the separation and reattachment points. A set of modified two-equation models is proposed to remove the aforementioned shortcomings. The calculations using various two-equation models are compared with direct numerical simulations of channel flow and flat boundary layers. Development of a second order closure model is also discussed with emphasis on the modeling of pressure related correlation terms and dissipation rates in the second moment equations. All the existing models poorly predict the normal stresses near the wall and fail to predict the 3-D effect of mean flow on the turbulence (e.g. decrease in the shear stress caused by the cross flow in the boundary layer). The newly developed second order near-wall turbulence model is described and is capable of capturing the near-wall behavior of turbulence as well as the effect of 3-D mean flow on the turbulence. Author

N92-23351*# National Aeronautics and Space Administration. Lewis Research Center, Cleveland, OH.
ON THE BASIC EQUATIONS FOR THE SECOND-ORDER MODELING OF COMPRESSIBLE TURBULENCE **c34**
William W. Liou and T.-H. Shih *In its* Center for Modeling of Turbulence and Transition (CMOTT). Research Briefs: 1990 Oct. 1991 p 134 (For primary document see N92-23336 14-01)
Avail: NTIS HC/MF A08 CSCL 20D

Equations for the mean and the turbulence quantities of compressible turbulent flows are derived in this report. Both the conventional Reynolds average and the mass-weighted Favre average were employed to decompose the flow variable into mean and turbulent quantities. These equations are to be used later in developing second-order Reynolds stress models for high-speed compressible flows. A few recent advances in modeling some of the terms in the equation due to compressibility effects are also summarized. Author

N92-23352*# National Aeronautics and Space Administration. Lewis Research Center, Cleveland, OH.
DEVELOPMENT OF A NEW FLUX SPLITTING SCHEME **c34**
Meng-Sing Liou and Christopher J. Steffen, Jr. *In its* Center for Modeling of Turbulence and Transition (CMOTT). Research Briefs:

1990 Oct. 1991 p 144-145 Previously announced in IAA as A91-40793 (For primary document see N92-23336 14-01)
Avail: NTIS HC/MF A08 CSCL 20D

The use of a new splitting scheme, the advection upstream splitting method, for model aerodynamic problems where Van Leer and Roe schemes had failed previously is discussed. The present scheme is based on splitting in which the convective and pressure terms are separated and treated differently depending on the underlying physical conditions. The present method is found to be both simple and accurate. Author

N92-23353*# National Aeronautics and Space Administration. Lewis Research Center, Cleveland, OH.
HIGH-ORDER POLYNOMIAL EXPANSIONS (HOPE) FOR FLUX-VECTOR SPLITTING **c34**
Meng-Sing Liou and Chris J. Steffen, Jr. *In its* Center for Modeling of Turbulence and Transition (CMOTT). Research Briefs: 1990 Oct. 1991 p 146-150 Previously announced as N91-25739 (For primary document see N92-23336 14-01)
Avail: NTIS HC/MF A08 CSCL 20D

The Van Leer flux splitting is known to produce excessive numerical dissipation for Navier-Stokes calculations. Researchers attempt to remedy this deficiency by introducing a higher order polynomial expansion (HOPE) for the mass flux. In addition to Van Leer's splitting, a term is introduced so that the mass diffusion error vanishes at M = 0. Several splittings for pressure are proposed and examined. The effectiveness of the HOPE scheme is illustrated for 1-D hypersonic conical viscous flow and 2-D supersonic shock-wave boundary layer interactions. Author

N92-23354*# Sverdrup Technology, Inc., Cleveland, OH.
THREE-DIMENSIONAL CALCULATIONS OF SUPERSONIC REACTING FLOWS USING AN LU SCHEME **c02**
Sheng-Tao Yu, Y.-L. Peter Tsai, and Jian-Shun Shuen *In* NASA. Lewis Research Center, Center for Modeling of Turbulence and Transition (CMOTT). Research Briefs: 1990 Oct. 1991 p 151 (For primary document see N92-23336 14-01)
Avail: NTIS HC/MF A08 CSCL 01A

A 3-D numerical program that incorporates comprehensive real gas property models was developed to simulate supersonic reacting flows. The code employs an implicit, finite volume, Lower-Upper (LU), time-marching method to solve the complete Navier-Stokes and species equations in a fully-coupled and efficient manner. A chemistry model with 9 species and 18 reaction steps is adopted in the program to represent the chemical reactions of H2 and air. To demonstrate the capability of the program, flow fields of underexpanded hydrogen jets transversely injected into the supersonic airstream inside the combustors of scramjets are calculated. Results clearly depict the flow characteristics, including the shock structure, the separated flow regions around the injector, and the distribution of the combustion products. Author

N92-23355*# National Aeronautics and Space Administration. Lewis Research Center, Cleveland, OH.
SIMULATIONS OF FREE SHEAR LAYERS USING A COMPRESSIBLE KAPPA-EPSILON MODEL **c34**
S. T. Yu (Sverdrup Technology, Inc., Cleveland, OH.), C. T. Chang, and C. J. Marek *In its* Center for Modeling of Turbulence and Transition (CMOTT). Research Briefs: 1990 Oct. 1991 p 152-160 Previously announced in IAA as A91-45778 (For primary document see N92-23336 14-01)
Avail: NTIS HC/MF A08 CSCL 20D

A two-dimensional, compressible Navier-Stokes equation with a k-epsilon turbulence model is solved numerically to simulate the flow of a compressible free shear layer. The appropriate form of k and epsilon equations for compressible flow is discussed. Sarkar's modeling is adopted to simulate the compressibility effects in the k and epsilon equations. The numerical results show that the spreading rate of the shear layers decreases with increasing convective Mach number. In addition, favorable comparison was found between the calculated results and experimental data. Author

02 AERODYNAMICS

Includes aerodynamics of bodies, combinations, wings, rotors, and control surfaces; and internal flow in ducts and turbomachinery.

For related information see also *34 Fluid Mechanics and Heat Transfer.*

N92-23168# Aeronautical Research Inst. of Sweden, Stockholm. Aerodynamics Dept.
HYPERSONIC LAMINAR FLOW COMPUTATIONS OVER A BLUNT LEADING EDGED DELTA WING AT THREE DIFFERENT CHORD REYNOLDS NUMBERS
Shivakumar Srinivasan, Peter Eliasson, and Arthur Rizzi Oct. 1991 17 p
(Contract VUB-8356/89/NL/FG(SG))
(FFA-TN-1991-40; ETN-92-91194) Avail: NTIS HC/MF A03

The hypersonic flow past a blunt leading edged and a blunt nosed delta wing was simulated numerically by solving the three dimensional Navier-Stokes equation. The laminar flow simulations were performed for three different chord Reynolds numbers. The Navier-Stokes equations were solved using the explicit finite volume four stage Runge-Kutta scheme. The intent is to reach a reasonable understanding of the separation characteristics of the flow in the leeside. It was observed that in the case of blunt edged delta wings at high angles of attack, the hypersonic flow is dominated by a shear layer that separates just past the blunt leading edge forming a more distributed vortical region over the wing, rather than a concentrated vortex structure as observed at lower speeds. As the Reynolds number increases, the separation characteristic on the lee side of the wing changes from a primary separation near the wing mid semi span to a primary separation close to the leading edge and a secondary separation near the wing mid semi span. The shape of the wing apex determines the location of the chords plane where the separation begins. The solutions were not compared with experimental data due to the nonavailability of the data at the time of writing. Sensitivity of the flow field to mesh refinement was investigated for the low Reynolds number case and it was found that the characteristics of the flow field remains the same even after mesh refinement. ESA

N92-23269*# National Aeronautics and Space Administration. Lewis Research Center, Cleveland, OH.
THE FLIP-FLOP NOZZLE EXTENDED TO SUPERSONIC FLOWS
Ganesh Raman, Michael Hailye (Michigan Univ., Ann Arbor.), and Edward J. Rice 1992 26 p Proposed for presentation at the Tenth Applied Aerodynamic Conference, Palo Alto, CA, 22-24 Jun. 1992; sponsored by AIAA
(Contract NAS3-25266)
(NASA-TM-105570; E-6895; NAS 1.15:105570) Avail: NTIS HC/MF A03 CSCL 01A

An experiment studying a fluidically oscillated rectangular jet flow was conducted. The Mach number was varied over a range from low subsonic to supersonic. Unsteady velocity and pressure measurements were made using hot wires and piezoresistive pressure transducers. In addition smoke flow visualization using high speed photography was used to document the oscillation of the jet. For the subsonic flip-flop jet it was found that the apparent time-mean widening of the jet was not accompanied by an increase in mass flux. It was found that it is possible to extend the operation of these devices to supersonic flows. Most of the measurements were made for a fixed nozzle geometry for which the oscillations ceased at a fully expanded Mach number of 1.58. By varying the nozzle geometry this limitation was overcome and operation was extended to Mach 1.8. The streamwise velocity perturbation levels produced by this device were much higher than the perturbation levels that could be produced using conventional excitation sources such as acoustic drivers. In view of this ability to produce high amplitudes, the potential for using small scale fluidically oscillated jet as an unsteady excitation source for the control of shear flows in full scale practical applications seems promising. Author

N92-23533*# National Aeronautics and Space Administration. Langley Research Center, Hampton, VA.
GRID GENERATION AND FLOW SOLUTION METHOD FOR EULER EQUATIONS ON UNSTRUCTURED GRIDS
W. Kyle Anderson Apr. 1992 20 p
(NASA-TM-4295; L16986; NAS 1.15:4295) Avail: NTIS HC/MF A03 CSCL 01A

A grid generation and flow solution algorithm for the Euler equations on unstructured grids is presented. The grid generation scheme, which uses Delaunay triangulation, generates the field points for the mesh based on cell aspect ratios and allows clustering of grid points near solid surfaces. The flow solution method is an implicit algorithm in which the linear set of equations arising at each time step is solved using a Gauss-Seidel procedure that is completely vectorizable. Also, a study is conducted to examine the number of subiterations required for good convergence of the overall algorithm. Grid generation results are shown in two dimensions for an NACA 0012 airfoil as well as a two element configuration. Flow solution results are shown for a two dimensional flow over the NACA 0012 airfoil and for a two element configuration in which the solution was obtained through an adaptation procedure and compared with an exact solution. Preliminary three dimensional results also are shown in which the subsonic flow over a business jet is computed. Author

N92-23563*# National Aeronautics and Space Administration. Lewis Research Center, Cleveland, OH.
INTERACTIVE SOLUTION-ADAPTIVE GRID GENERATION PROCEDURE
Todd L. Henderson, Yung K. Choo, and Ki D. Lee (Illinois Univ., Urbana.) Apr. 1992 28 p Original contains color illustrations
(NASA-TM-105432; E-6853; NAS 1.15:105432) Avail: NTIS HC/MF A03; 10 functional color pages CSCL 01A

TURBO-AD is an interactive solution adaptive grid generation program under development. The program combines an interactive algebraic grid generation technique and a solution adaptive grid generation technique into a single interactive package. The control point form uses a sparse collection of control points to algebraically generate a field grid. This technique provides local grid control capability and is well suited to interactive work due to its speed and efficiency. A mapping from the physical domain to a parametric domain was used to improve difficulties encountered near outwardly concave boundaries in the control point technique. Therefore, all grid modifications are performed on the unit square in the parametric domain, and the new adapted grid is then mapped back to the physical domain. The grid adaption is achieved by adapting the control points to a numerical solution in the parametric domain using control sources obtained from the flow properties. Then a new modified grid is generated from the adapted control net. This process is efficient because the number of control points is much less than the number of grid points and the generation of the grid is an efficient algebraic process. TURBO-AD provides the user with both local and global controls. Author

N92-23717 Virginia Polytechnic Inst. and State Univ., Blacksburg.
EFFICIENT AND ROBUST DESIGN OPTIMIZATION OF TRANSONIC AIRFOILS Ph.D. Thesis
Changyeol Joh 1991 153 p
Avail: Univ. Microfilms Order No. DA9136288

Numerical optimization procedures were employed for the design of airfoils in transonic flow based on the transonic small-disturbance (TSD) and Euler equations. A sequential approximation optimization technique was implemented for solving the design problem of lift maximization with wave drag and area constraints. A simple linear approximation was used for the approximation of the lift. Accurate approximations for sensitivity derivatives of the wave drag were obtained through the use of Nixon's coordinate straining approach. A modification of the Euler surface boundary conditions was implemented in order to efficiently compute design sensitivities without recreating the grid. Our design procedures experienced convergence problems for some TSD solutions, where the wave drag was found not to vary smoothly with the design parameters and consequently create local optimum problems. A procedure interchanging the role of the objective function and constraint, initially minimizing drag with a constraint on the lift, was found to be effective in producing converged designs, usually in approximately 10 global iterations. This procedure was also shown to be robust and efficient for cases where the drag varied smoothly, such as with the Euler solutions. Dissert. Abstr.

N92-23354*# Sverdrup Technology, Inc., Cleveland, OH.
THREE-DIMENSIONAL CALCULATIONS OF SUPERSONIC REACTING FLOWS USING AN LU SCHEME
Sheng-Tao Yu, Y.-L. Peter Tsai, and Jian-Shun Shuen *In* NASA. Lewis Research Center, Center for Modeling of Turbulence and Transition (CMOTT). Research Briefs: 1990 Oct. 1991 p 151 (For primary document see N92-23336 14-01)
Avail: NTIS HC/MF A08 CSCL 01A

N92-23956*# National Aeronautics and Space Administration. Langley Research Center, Hampton, VA.
HIGH ANGLE OF ATTACK: AERODYNAMICS
John E. Lamar *In* AGARD, Special Course on Engineering Methods in Aerodynamic Analysis and Design of Aircraft Jan. 1992 39 p (For primary document see N92-23950 14-05)
Copyright Avail: NTIS HC/MF A11; Non-NATO Nationals requests available only from AGARD/Scientific Publications Executive CSCL 01A

03 AIR TRANSPORTATION AND SAFETY

Includes passenger and cargo air transport operations; and aircraft accidents.

For related information see also *16 Space Transportation* and *85 Urban Technology and Transportation.*

N92-23596# National Transportation Safety Board, Washington, DC.
AIRCRAFT ACCIDENT REPORT: RUNWAY COLLISION OF USAIR FLIGHT 1493, BOEING 737 AND SKYWEST FLIGHT 5569 FAIRCHILD METROLINER, LOS ANGELES INTERNATIONAL AIRPORT, LOS ANGELES, CA, FEBRUARY 1, 1991
22 Oct. 1991 168 p
(PB91-910409; NTSB/AAR-91/08) Avail: NTIS HC/MF A08; paper copy available on Standing Order, deposit account required (minimum deposit $100 US, Canada, and Mexico; all others $200) CSCL 01C

On 1 Feb. 1991, at 1807 Pacific standard time, USAir flight 1493, a Boeing 737-300, collided with Skywest flight 5569, a Fairchild Metroliner, while USA1493 was landing at L.A. International Airport (LAX), Calif. Flight 5569 was positioned on the same runway, at intersection 45, awaiting clearance for takeoff. The NTSB determines that the probable cause of the accident was the failure of the LA Air Traffic Facility Management to implement procedures that provided redundancy comparable to the requirements contained in the National Operational Position Standards and the failure of the FAA Air Traffic Service to provide adequate policy direction and oversight to its air traffic control facility managers. These failures created an environment in the LA ATC tower that ultimately led to the failure of the local controller 2 to maintain an awareness of the traffic situation, culminating in the inappropriate clearances and subsequent collision of the aircrafts. Author

N92-23597# National Transportation Safety Board, Washington, DC.
AIRCRAFT ACCIDENT REPORT: RYAN INTERNATIONAL AIRLINES DC-9-15, N565PC, LOSS OF CONTROL ON TAKEOFF, CLEVELAND-HOPKINS INTERNATIONAL AIRPORT, CLEVELAND, OHIO, FEBRUARY 17, 1991
16 Nov. 1991 106 p

(PB91-910410; NTSB/AAR-91/09) Avail: NTIS HC/MF A06; available on Standing Order, deposit account required (minimum deposit $100 US, Canada, and Mexico; all others $200) CSCL 01C

The crash on takeoff of Ryan International Airlines flight 590 at Cleveland, Ohio, on 17 Feb. 1991 is examined. Ryan International Airlines flight 590, a DC-9 series 10 airplane, crashed while taking off from Cleveland-Hopkins International Airport. The flight crew consisted of two pilots. There were no other crewmembers or passengers on the flight, which was contracted to carry mail for the U.S. Postal Service. Both pilots were fatally injured, and the airplane was destroyed as a result of the accident. The National Transportation Safety Board determines that the probable cause of the accident was the failure of the flightcrew to detect and remove ice contamination on the airplane's wings. The ice formation led to wing stall and loss of control during the attempted takeoff. Author

04 AIRCRAFT COMMUNICATIONS AND NAVIGATION

Includes digital and voice communication with aircraft; air navigation systems (satellite and ground based); and air traffic control.

For related information see also *17 Space Communications, Spacecraft Communications, Command and Tracking* and *Communications and Radar.*

N92-23541*# Texas Univ., Austin. Center for Space Research.
PRECISION GPS EPHEMERIDES AND BASELINES Final Report, 1 Jan. - 31 Dec. 1991
Dec. 1991 59 p
(Grant NAGw-2717)
(NASA-CR-190247; NAS 1.26:190247) Avail: NTIS HC/MF A04 CSCL 17G

Based on the research, the area of precise ephemerides for GPS satellites, the following observations can be made pertaining to the status and future work needed regarding orbit accuracy. There are several aspects which need to be addressed in discussing determination of precise orbits, such as force models, kinematic models, measurement models, data reduction/estimation methods, etc. Although each one of these aspects was studied at CSR in research efforts, only points pertaining to the force modeling aspect are addressed. Author

N92-23729 Nottingham Univ. (England).
DYNAMIC POSITIONING BY GPS Ph.D. Thesis
Jane M. Westrop 1990 260 p
Avail: Univ. Microfilms Order No. BRD-93584

Techniques for improving the accuracy of the differential Global Positioning System (GPS) are examined. Also investigated is how the methods and measurements employed in static GPS surveying may be enhanced to allow their use in true dynamic environments, such that the one meter accuracy criterion may be reached. The theory required for these improvements is explained and the software written to process GPS data in this manner is described. The results of tests undertaken using static and semi-dynamic GPS data show that the one meter accuracy criterion may be reached in certain circumstances, by suitably combining the pseudorange and carrier phase measurements. Author

05 AIRCRAFT DESIGN, TESTING AND PERFORMANCE

Includes aircraft simulation technology.

For related information see also *18 Spacecraft Design, Testing and Performance* and *39 Structural Mechanics.*For land transportation vehicles see *85 Urban Technology and Transportation.*

N92-23227# Advisory Group for Aerospace Research and Development, Neuilly-Sur-Seine (France). Structures and Materials Panel.
INTEGRATED DESIGN ANALYSIS AND OPTIMISATION OF AIRCRAFT STRUCTURES
Feb. 1992 212 p The 72nd meeting was held in Bath, England, 29 Apr. - 3 May 1991
(AGARD-R-784; ISBN-92-835-0653-7) Copyright Avail: NTIS HC/MF A10; Non-NATO Nationals requests available only from AGARD/Scientific Publications Executive

At its 72nd meeting, the Structures and Materials Panel held a workshop to address the role of integrated design analysis and optimization of aircraft structures in order to review and evaluate modern computer codes, and the methodologies for their use. The workshop provided a very useful forum for the exchange of information which is reflected in the papers presented in this report. Among the topics covered are: aerodynamics, aeroelasticity, active control, composite materials, multidisciplinary design and optimization, fin design and optimization, and sensitivity analysis. For individual titles, see N92-23228 through N92-23239.

N92-23228*# National Aeronautics and Space Administration. Langley Research Center, Hampton, VA.
A SYSTEM APPROACH TO AIRCRAFT OPTIMIZATION
Jaroslaw Sobieszczanski-Sobieski *In* AGARD, Integrated Design Analysis and Optimisation of Aircraft Structures Feb. 1992 15 p (For primary document see N92-23227 14-05)
Copyright Avail: NTIS HC/MF A10; Non-NATO Nationals requests available only from AGARD/Scientific Publications Executive CSCL 01C

Mutual couplings among the mathematical models of physical phenomenon and parts of a system such as an aircraft complicate the design process because each contemplated design change may have far reaching consequences throughout the system. This paper outlines techniques for computing these influences as system design derivatives useful in both judgmental and formal optimization purposes. The techniques facilitate decomposition of the design process into smaller, more manageable tasks and they form a methodology that can easily fit into existing engineering optimizations and incorporate their design tools. Author

N92-23229*# Virginia Polytechnic Inst. and State Univ., Blacksburg.
SENSITIVITY ANALYSIS OF DYNAMIC AEROELASTIC RESPONSES **c08**
Rakesh K. Kapania *In* AGARD, Integrated Design Analysis and Optimisation of Aircraft Structures Feb. 1992 12 p (For primary document see N92-23227 14-05)
(Contract NAS1-18471)
Copyright Avail: NTIS HC/MF A10; Non-NATO Nationals requests available only from AGARD/Scientific Publications Executive CSCL 01C

This paper summarizes ongoing research on the sensitivity analysis of dynamic aeroelastic response of wings. Two approaches are being used to express the unsteady aerodynamic loads: (1) the frequency-domain approach, and (2) the state-space approach. The frequency-domain approach is demonstrated on a three-dimensional box wing and the state-space domain approach is demonstrated on a simple two-dimensional sectional model. Three different methods are used to find the sensitivities: (1) a purely finite difference approach, (2) a semi-analytical approach in which an analytical expression is used for calculating the sensitivity of an eigenvalue of the complex valued aeroelastic matrix, however, the derivatives of the components of the matrix are obtained using

finite difference, and (3) a semi-analytic approach that differs from (2) in the sense that the sensitivity of the aerodynamic matrix is now obtained analytically. A good agreement is seen between the three sets of results. For the two-dimensional sectional model the results for the sensitivities of the flutter speed with respect to the various parameters are obtained. Author

N92-23230*# National Aeronautics and Space Administration. Langley Research Center, Hampton, VA.
APPLICATION OF MULTIDISCIPLINARY OPTIMIZATION METHODS TO THE DESIGN OF A SUPERSONIC TRANSPORT
J.-F. M. Barthelemy, P. G. Coen, G. A. Wrenn, M. F. Riley, A. R. Dovi, and L. E. Hall (Unisys Corp., Hampton, VA.) *In* AGARD, Integrated Design Analysis and Optimisation of Aircraft Structures Feb. 1992 5 p Previously announced as N91-23135 (For primary document see N92-23227 14-05)
Copyright Avail: NTIS HC/MF A10; Non-NATO Nationals requests available only from AGARD/Scientific Publications Executive CSCL 01C

A new optimization based design method is discussed. This method is based on integrating existing disciplinary analysis and sensitivity analysis techniques by means of generalized sensitivity equations. A generic design system implementing this method is described. The system is being used to design the configuration and internal structure of a supersonic transport wing for optimum performance. This problem combines the disciplines of linear aerodynamics, structures, and performance. Initial results which include the disciplines of aerodynamics and structures in a conventional minimum weight design under static aeroelastic constraints are presented. Author

N92-23231# General Dynamics Corp., Fort Worth, TX.
APPLICATION OF ANALYTICAL AND DESIGN TOOLS FOR FIGHTER WING AEROELASTIC TAILORING
Jonathan D. Bohlmann, Michael H. Love, Daniel K. Barker, William A. Rogers, and Beth E. Paul *In* AGARD, Integrated Design Analysis and Optimisation of Aircraft Structures Feb. 1992 14 p (For primary document see N92-23227 14-05)
Copyright Avail: NTIS HC/MF A10; Non-NATO Nationals requests available only from AGARD/Scientific Publications Executive

Wing analysis and design studies have been performed for the Validation of Aeroelastic Tailoring (VAT) configuration. The VAT represents a series of static and dynamic wind tunnel tests, performed in the 1970's, to verify the beneficial use of aeroelastic tailoring for fighter aircraft wing design. The VAT provides a useful database for evaluation of various aeroelastic methodologies. Static analysis predictions for ELAPS, a Ritz structural analysis code, are compared to the VAT results, with excellent agreement. ASTROS, a new multidisciplinary finite element optimization code, is also used for static and dynamic analyses of the VAT. The results demonstrate several analysis capabilities of ASTROS. The composite wing skin of the VAT is also optimized by ASTROS for strength and displacement constraints simulating aeroelastic loads. ASTROS was able to design the composite skin to achieve a desired twist and camber deformation behavior. ASTROS is thus a viable tool for aeroelastic tailoring design. Author

N92-23232# Saab-Scania, Linkoping (Sweden). Aircraft Div.
THE STRUCTURAL OPTIMIZATION SYSTEM OPTSYS: CURRENT STATUS AND APPLICATIONS
Torsten Brama *In* AGARD, Integrated Design Analysis and Optimisation of Aircraft Structures Feb. 1992 9 p (For primary document see N92-23227 14-05)
Copyright Avail: NTIS HC/MF A10; Non-NATO Nationals requests available only from AGARD/Scientific Publications Executive

OPTSYS is a modular structural optimization system with well-defined interfaces to finite element (FE) programs and codes for aeroelasticity. A mathematical programming approach is adopted where a sequence of convex approximations of the initial problem is solved, using the method of moving asymptotes (MMA). This approach makes it possible to take all design criteria into account simultaneously. Gradients are calculated semi-analytically. OPTSYS can treat design variables associated to the shape of the structure, the element cross section properties, or the material direction in the case of composite materials. Constraints can be defined on displacement, stress, eigenfrequency, local buckling, flutter, and aileron efficiency. Recent developments have concerned the constraints on dynamic response and acoustics. Other important gradients are: the integration of a preprocessor to define shape variables, the treatment of discrete variables, and the possibility to deal with substructured FE models. The current status of the system capabilities and methods will be discussed and illustrated with applications on aircraft and automotive structures. Author

N92-23233# British Aerospace Public Ltd. Co., Lancashire (England).
APPLICATION OF AN AUTOMATED MULTIDISCIPLINARY ANALYSIS AND OPTIMISATION SYSTEM TO THE DESIGN OF AIRCRAFT STRUCTURES
D. Thompson and J. C. Ayres *In* AGARD, Integrated Design Analysis and Optimisation of Aircraft Structures Feb. 1992 61 p (For primary document see N92-23227 14-05)
Copyright Avail: NTIS HC/MF A10; Non-NATO Nationals requests available only from AGARD/Scientific Publications Executive

Prior to the development of the ECLIPSE system, structural optimization was performed by a combination of software and manual methods. These methods proved their worth by the reduction in costs and improvements in quality resulting from their use. The program used for optimization of structures subject to stiffness criteria became the focus for development of the aeroelastic constraints. This was later extended to incorporate strength constraints, fabrication constraints, and was coupled directly to the NASTRAN analysis system. This process of development continued with the result of the present general resizing, optimization, and post-processing system. This paper describes the application of the system to the optimization of three structures: tail plane, fin/rudder, and foreplane. The emphasis is on the use of the system to optimize for a flutter speed constraint in all three cases. However, in the case of the foreplane, the adaption of the system to include a detail stressing constraint is illustrated. A brief description of some of the developments proposed for the future is also given. Author

N92-23234# Oklahoma Univ., Norman.
MULTIDISCIPLINARY OPTIMIZATION STUDIES USING ASTROS **c08**
Alfred G. Striz and Vipperla B. Venkayya (Wright Research Development Center, Wright-Patterson AFB, OH.) *In* AGARD, Integrated Design Analysis and Optimisation of Aircraft Structures Feb. 1992 29 p (For primary document see N92-23227 14-05)
Copyright Avail: NTIS HC/MF A10; Non-NATO Nationals requests available only from AGARD/Scientific Publications Executive

The influences of the structural and aerodynamic modeling on flutter analysis and multidisciplinary optimization of fully built-up finite element wing models in an aeroelastic environment are not yet well understood. Therefore, the dynamic aeroelastic and optimization capabilities in the Automated Structural Optimization System (ASTROS) were used to evaluate the flutter behavior and the behavior of structural optimization with flutter constraints of various representative fully built-up finite element wing models in subsonic and supersonic flow. ASTROS was here used as a tool to calculate flutter speeds and frequencies and to minimize the weight of these wing models in subsonic and supersonic flow under given flutter and frequency constraints to determine the effect that these modeling factors have. Author

N92-23235# McDonnell Aircraft Co., Saint Louis, MO.
DESIGN OF A FIGHTER AIRCRAFT VERTICAL TAIL ENHANCED BUFFET ENVIRONMENT SURVIVABILITY
Dale M. Pitt and Robert W. Scanlon *In* AGARD, Integrated Design Analysis and Optimisation of Aircraft Structures Feb. 1992 6 p (For primary document see N92-23227 14-05)
Copyright Avail: NTIS HC/MF A10; Non-NATO Nationals requests available only from AGARD/Scientific Publications Executive

A method developed for multidisciplinary design of aircraft primary surfaces to include buffet fatigue life improvements is presented. The method is a multistep approach. First, measured buffet pressures are used as the source of excitation. These pressures excite the primary structural modes of the tail and result in high dynamic strains. Second, the Automated Structural Optimization System (ASTROS) multidisciplinary code is used to either raise or lower the primary modal frequencies. Third, a NASTRAN random analysis is used to determine the buffet dynamic strains. Fourth, a subsequent fatigue analysis is used to compute the change in fatigue life. The process was demonstrated on a generic vertical tail. Author

N92-23236# Messerschmitt-Boelkow-Blohm G.m.b.H., Munich (Germany, F.R.). Airplane Div.
FIRST APPROACH TO AN INTEGRATED FIN DESIGN
G. Schneider, J. Krammer, and H. R. E. M. Hoernlein *In* AGARD, Integrated Design Analysis and Optimisation of Aircraft Structures Feb. 1992 10 p (For primary document see N92-23227 14-05)
Copyright Avail: NTIS HC/MF A10; Non-NATO Nationals requests available only from AGARD/Scientific Publications Executive

The present paper is focused on findings and results of an integrated design optimization study for an aircraft fin. The basic flight mechanics design requirement for a vertical fin is to provide a specified control power inside the whole flight envelope with a minimum weight structure. A method of implicit function theorem has been applied on our MBB fin sample problem. The definition of state variables and independent variables will be discussed in detail. Three basic aerodynamic parameters have been chosen for the sensitivity analysis: taper ratio, aspect ratio, and surface area. This aerodynamic sensitivity analysis has been performed by the finite difference method. The necessary finite element models of the structure have been generated in the same way as the aerodynamic model for the finite difference method. The applied method based on implicit function theorem has proven its capability to provide a transparent method with clear defined discipline interfaces which are essential to monitor a complex system.
Author

N92-23237# Alenia, Torino (Italy). Defence Aircraft Group.
A FIN OPTIMISATION STUDY
G. Pollano *In* AGARD, Integrated Design Analysis and Optimisation of Aircraft Structures Feb. 1992 10 p (For primary document see N92-23227 14-05)
Copyright Avail: NTIS HC/MF A10; Non-NATO Nationals requests available only from AGARD/Scientific Publications Executive

This paper details the ALENIA activities performed in order to optimize the design of a fin proposed by MBB in an AGARD sub-committee, using the in house optimization program SOS (Structural Optimization System). A series of different optimization studies using stress, efficiency, and flutter constraints was carried out. In addition comparisons between these results and optimizations having frequency separation and displacements as constraints were done. Author

N92-23238# British Aerospace Public Ltd. Co., Bristol (England). Airbus Div.
SIMULTANEOUS STRESS AND FLUTTER OPTIMIZATION FOR THE WING OF A TRANSPORT AIRCRAFT EQUIPPED WITH FOUR ENGINES **c08**
J. M. D. Snee, H. Zimmermann, D. Schierenbeck, and P. Heinze (Deutsche Airbus G.m.b H., Bremen, Germany, F.R.) *In* AGARD, Integrated Design Analysis and Optimisation of Aircraft Structures Feb. 1992 12 p (For primary document see N92-23227 14-05)
Copyright Avail: NTIS HC/MF A10; Non-NATO Nationals requests available only from AGARD/Scientific Publications Executive

The main objective of this work is to demonstrate the benefits of interdisciplinary optimization techniques to a modern aircraft design. The optimization is related to a four engine transport aircraft series equipped with a common wing. The series comprises of two aircraft differing in fuselage length by approximately 4 m but with the same maximum takeoff weight. Wing commonality in terms of optimization means that all the significant aeroelastic and static constraints are taken into account in order to achieve a weight optimized but also valid design proposal. In effect, this means that critical flutter situations of both aircraft types dependent on the fuel and load conditions as well as the dimensioning static load cases in combination with the stresses allowable must be introduced into a mathematical optimization model and the weight optimized solution must be sought with the aid of various optimization techniques. Author

N92-23239# Dassault Espace, Saint-Cloud (France).
STRUCTURAL OPTIMIZATION OF AIRCRAFT PRACTICE AND TRENDS
C. Cornuault, C. Petiau, B. Coiffier, and A. Paret *In* AGARD, Integrated Design Analysis and Optimisation of Aircraft Structures Feb. 1992 12 p (For primary document see N92-23227 14-05)
Copyright Avail: NTIS HC/MF A10; Non-NATO Nationals requests available only from AGARD/Scientific Publications Executive

After a general presentation of the CATIA-ELFINI tool, developed by DASSAULT, where computer aided design (CAD), structural analysis, and optimization are fully embedded, we focus on a detailed description of the optimization algorithm. We show the special features of optimization with composite materials. We present: (1) the new organization of design resulting from use of optimization techniques; (2) the application of our optimization techniques on the case of the MBB fin; and (3) techniques neighboring optimization as model adjustment and computation with uncertain data. We conclude by presenting further developments. Author

N92-23950# Advisory Group for Aerospace Research and Development, Neuilly-Sur-Seine (France). Fluid Dynamics Panel.
SPECIAL COURSE ON ENGINEERING METHODS IN AERODYNAMIC ANALYSIS AND DESIGN OF AIRCRAFT
Jan. 1992 248 p Special course held in Ankara, Turkey, 6-10 May 1991, in Rhode-Saint-Genese, Belgium, 13-17 May 1991, and in Madrid, Spain, 20-24 May 1991; sponsored in cooperation with the von Karman Inst. for Fluid Dynamics
(AGARD-R-783; ISBN-92-835-0652-9) Copyright Avail: NTIS HC/MF A11; Non-NATO Nationals requests available only from AGARD/Scientific Publications Executive

Lecture notes for the AGARD Fluid Dynamics Panel Special Course on 'Engineering Methods in Aerodynamic Analysis and Design of Aircraft' have been assembled in this report. Proven engineering methods used during conceptual and preliminary design and development of new aircraft concepts are presented. These methods focus on simple computational procedures for conceptual and preliminary design, low level analysis computer codes, and experimental techniques for aircraft performance predictions. The course was aimed at helping train young engineers to appreciate and work with simple engineering tools to enhance the art of cost effective preliminary design of new aircraft. For individual titles, see N92-23951 through N92-23957.

N92-23951# Messerschmitt-Boelkow-Blohm G.m.b.H., Munich (Germany, F.R.). Military Aircraft Div.
[INTRODUCTION TO SPECIAL COURSE ON ENGINEERING METHODS IN AERODYNAMIC ANALYSIS AND DESIGN OF AIRCRAFT]
P. W. Sacher *In* AGARD, Special Course on Engineering Methods in Aerodynamic Analysis and Design of Aircraft Jan. 1992 10 p (For primary document see N92-23950 14-05)
Copyright Avail: NTIS HC/MF A11; Non-NATO Nationals requests available only from AGARD/Scientific Publications Executive

There are three major statements that characterize the findings of this special course. First, engineering work in aeronautical analysis and design is traditionally performed both through experiments and through numerical analysis. Second, an interdisciplinary approach is mandatory in conceptual and preliminary design work because although experiments will not be replaced by computational fluid dynamics (CFD), CFD may

complement experiments by allowing quicker and more reliable selection of promising configurations. Third, engineering methods are indispensable because: high level CFD analysis is excluded in preliminary design; experimental work may be unavailable for configuration conception; and empirical low level flow code analysis and extrapolation from previous experience is the only logical consequence. H.A.

N92-23952# Dassault Espace, Saint-Cloud (France). Departement d'Aerodynamique Theorique.
COMPUTATIONAL PROCEDURES FOR PRELIMINARY DESIGN
P. Perrier *In* AGARD, Special Course on Engineering Methods in Aerodynamic Analysis and Design of Aircraft Jan. 1992 10 p (For primary document see N92-23950 14-05)
Copyright Avail: NTIS HC/MF A11; Non-NATO Nationals requests available only from AGARD/Scientific Publications Executive

Preliminary design of aircraft has evolved largely over the past ten years. The main origin of the evolution came from the rationalization and broadening of the preliminary emphasis on new project development. The project has to be evaluated more quickly and the capability of a project to meet its requirements must be satisfied. This paper deals specifically with low level computations for preliminary design, and covers such areas as: center of pressure evaluation; lift evaluation; drag evaluation; air-intake integration; afterbody integration; and interactions with non aerodynamic requirements. H.A.

N92-23953# Conceptual Research Corp., Sylmar, CA.
CONFIGURATION DEVELOPMENT
Daniel P. Raymer *In* AGARD, Special Course on Engineering Methods in Aerodynamic Analysis and Design of Aircraft Jan. 1992 20 p (For primary document see N92-23950 14-05)
Copyright Avail: NTIS HC/MF A11; Non-NATO Nationals requests available only from AGARD/Scientific Publications Executive

Aircraft conceptual design is a complex, multidisciplinary process involving many aspects of engineering. Although this paper focuses on aerodynamic aspects of aircraft design, the overall configuration of the aircraft must both provide good aerodynamics and reflect a wide variety of other considerations. This paper will discuss the configuration development and its key role in aerodynamic design. Author

N92-23954# Aircraft Research Association Ltd., Bedford (England).
SURVEY OF EXPERIMENTAL TECHNIQUES FOR PERFORMANCE PREDICTION
A. B. Haines *In* AGARD, Special Course on Engineering Methods in Aerodynamic Analysis and Design of Aircraft Jan. 1992 60 p (For primary document see N92-23950 14-05)
Copyright Avail: NTIS HC/MF A11; Non-NATO Nationals requests available only from AGARD/Scientific Publications Executive

This paper reviews the present state of the art in experimental testing in large wind tunnels as a means of predicting aircraft performance. Desirable and attainable standards of accuracy are defined and the paper lists and discusses the factors that contribute to this accuracy. Topics covered include: balances and pressure scanners; quality of tunnel flow; correction of data for wall interference; extrapolation of scale model data to full scale aircraft Reynolds numbers; and propulsion interference effects. Author

N92-23955# National Aerospace Lab., Amsterdam (Netherlands).
PANEL METHODS FOR AERODYNAMIC ANALYSIS AND DESIGN
H. W. M. Hoeijmakers *In* AGARD, Special Course on Engineering Methods in Aerodynamic Analysis and Design of Aircraft Jan. 1992 47 p (For primary document see N92-23950 14-05)
Copyright Avail: NTIS HC/MF A11; Non-NATO Nationals requests available only from AGARD/Scientific Publications Executive

An overview is presented of several aspects of panel methods used in the aerodynamic analysis and design of aircraft or aircraft components. Panel methods can provide the flow about complex configurations and are routinely used in the analysis of the aerodynamics of realistic aircraft shapes. However, panel methods are based on a mathematical model in which much of the fluid physics is ignored. The report discusses the capabilities and limitations of panel methods, the basic concepts of the panel method, choices that can be made in the basic implementation of the concepts, as well as possible types of boundary conditions that can be utilized to creatively model subsonic and supersonic flow. The discussion also includes aspects of the accuracy of the approximation, consistent formulations, aspects of low and high order panel methods, etc. Also discussed are the computational aspects of panel methods and possible extensions to nonlinear compressible flows, coupling with viscous flow methods, and applications to other flow problems. Author

N92-23956*# National Aeronautics and Space Administration. Langley Research Center, Hampton, VA.
HIGH ANGLE OF ATTACK: AERODYNAMICS **c02**
John E. Lamar *In* AGARD, Special Course on Engineering Methods in Aerodynamic Analysis and Design of Aircraft Jan. 1992 39 p (For primary document see N92-23950 14-05)
Copyright Avail: NTIS HC/MF A11; Non-NATO Nationals requests available only from AGARD/Scientific Publications Executive CSCL 01A

The ability to predict high angle of attack, nonlinear, aerodynamic characteristics of flight vehicles, including aircraft, has made significant progress in the last 25 years using computational tools and analyses. The key technological element which has made these analyses possible is the ability to account for the influence of the shed vortical flow, prevalent in this angle of attack range, on geometries of interest. Using selected analysis techniques, applications have also been made to wing design in order to improve their high speed maneuver performance. Various techniques, associated with different levels of accuracy, exist to model this vortical flow influence. The ones included in this paper cover: suction analogy with extensions; free vortex filaments; free vortex sheet modeling; and Euler and Navier-Stokes solutions. Associated relevant features of vortices are also addressed, including: the wing and flow conditions which cause vortex formation; and how the vortex strength varies with angle of attack and wing sweep. Author

N92-23957# Grumman Aerospace Corp., Bethpage, NY. Aircraft Systems Div.
AIRCRAFT DRAG ANALYSIS METHODS
Charles W. Boppe *In* AGARD, Special Course on Engineering Methods in Aerodynamic Analysis and Design of Aircraft Jan. 1992 50 p (For primary document see N92-23950 14-05)
Copyright Avail: NTIS HC/MF A11; Non-NATO Nationals requests available only from AGARD/Scientific Publications Executive

A collection of aircraft drag analysis methods and drag reduction techniques has been prepared. Pressure, skin friction (viscous), wave (compressibility), lift induced (vortex), interference, throttle dependent, and trim drag source predictions are included. The need to establish a computational drag prediction experience base is emphasized and illustrated. Project type applications are described in which these drag prediction tools have been implemented for drag reduction processes. The paper concludes by summarizing the role played by computerized drag prediction methods in aircraft design programs. Author

N92-24009 ESDU International Ltd., London (England).
NORMAL FORCE OF LOW ASPECT RATIO WING-BODY COMBINATIONS UP TO HIGH ANGLES OF ATTACK AT SUPERSONIC SPEEDS
Nov. 1991 15 p Supersedes ESDU-68022 (ESDU-91042; ESDU-68022; ISBN-0-85679-804-5; ISSN-0141-397X) Avail: ESDU

ESDU 91042 presents a method that applies to delta, cropped delta, or rectangular wings mounted on an axisymmetric body at mid-height. It applies to Mach numbers between 1.2 and 5 to configurations with thin, sharp-edged wings with aspect ratio between 0.2 and 4 at angles of attack up to 60 degrees. The method takes the isolated wing normal force (from ESDU 90013),

factored to account for body interference on the wing and wing interferences on the body (using ESDU 91007) and to account for interference from the body vortices, and adds the body contribution (from ESDU 89014 or 90034). The vortex interference factor is provided graphically and depends on the point of separation of the vortices for which another graph provides data. The method applies for zero or near zero roll angle to both cruciform and monoplane wings. When predicted values were compared with experimental values extracted from the literature an accuracy of 10 percent was indicated. This is illustrated for results in the angles of attack range of 20 to 25 degrees, and the ranges of experimental parameters used are tabulated. A worked example illustrates the use of the method. ESDU

N92-24010 California Univ., Los Angeles.
ADAPTIVE ACTIVE FLUTTER SUPPRESSION OF WINGS IN SUBSONIC AND TRANSONIC FLIGHT REGIMES Ph.D. Thesis
Chan-Gi Pak 1991 227 p
Avail: Univ. Microfilms Order No. DA9207716

A digital adaptive controller is applied to the active flutter suppression problem of a wind under time varying flight conditions in subsonic and transonic flow. Linear quadratic controller gain at each time step is obtained using an iterative Riccati solver. The digital adaptive optimal controller is robust with respect to the unknown external loads. Flutter and divergence instabilities are simultaneously suppressed using a trailing edge control surface and displacement sensing. A new transonic unsteady aerodynamic approximation methodology is developed which enables one to carry out the rapid calculation required for transonic aeroservoelastic applications. This approximation is based on unsteady subsonic aerodynamics combined with a transonic correction procedure. Aeroservoelastic transient time response is obtained using Roger's approximation, state transition matrices and an iterative time marching algorithm. The aeroservoelastic system in the time domain is modeled using a deterministic ARMA model together with a parameter estimator. Transonic flutter boundaries of a wing structure are computed, in time domain, using an estimated aeroelastic system matrix and are in agreement with experimental data for the low transonic Mach number range. Dissert. Abstr.

N92-23822# Air Force Systems Command, Wright-Patterson AFB, OH. National Aero-Space Plane Joint Program Office.
DESIGN CHALLENGES FOR THE NATIONAL AERO-SPACE PLANE
Frank D. Boensch *In* ESA, Spacecraft Structures and Mechanical Testing, Volume 1 Oct. 1991 p 293-297 (For primary document see N92-23780 14-18)
Copyright Avail: NTIS HC/MF A21

06 AIRCRAFT INSTRUMENTATION

Includes cockpit and cabin display devices; and flight instruments.

For related information see also *19 Spacecraft Instrumentation* and *35 Instrumentation and Photography.*

No abstracts in this category.

07 AIRCRAFT PROPULSION AND POWER

Includes prime propulsion systems and systems components, e.g., gas turbine engines and compressors; and onboard auxilliary power plants for aircraft.

For related information see also *20 Spacecraft Propulsion and Power, 28 Propellants and Fuels,* and *44 Energy Production and Conversion.*

N92-23122 Stanford Univ., CA.
CONTROL OF A HELICOPTER ENGINE IN LOW ALTITUDE FLIGHT Ph.D. Thesis
Link Ching Jaw 1991 151 p
Avail: Univ. Microfilms Order No. DA9206794

Helicopters flying at low altitude must maneuver constantly to avoid terrain contours and obstacles above the ground, hence rapid responses to control commands are critical to the safety of the vehicle and its crew. To obtain these features, the engine control system must react quickly to change engine power. For most helicopters, the engine control bandwidth is lowered to avoid exciting rotor/engine system vibrational modes. This degrades engine control effectiveness to maintain a desired rotor speed during maneuvers. To increase the engine control bandwidth, accurate modeling of coupled rotor/engine torsional modes is essential. This research shows that the two way coupling between rotor and engine increases the frequency and damping of rotor collective lead lag modes, and it slows down the turbine speed lag mode. A simplified, fourth order model expressed in multiblade coordinates is derived to represent the coupled rotor/engine system. Even with increased fuel control bandwidth, the engine power can not be changed fast enough, because the allowable maximum fuel flow is limited to protect the engine. This shows that controlling free turbine inlet bleed flow is a feasible supplement to controlling fuel flow in affecting a rapid and large power change. The bleed flow control reduces speed variations and increases vehicle agility significantly. Dissert. Abstr.

N92-23169# Loughborough Univ. of Technology (England). Dept. of Transport Technology.
ADVANCED RAMJET SYSTEMS FOR THE PROPULSION OF GUIDED WEAPONS M.S. Thesis
K. MacKenzie 1990 129 p Sponsored by Ministry of Defence Prepared in cooperation with Royal Air Force Coll., Cranwell, England
(ETN-92-91195) Copyright Avail: NTIS HC/MF A07

The characteristics and shortcomings of gas turbine, rocket, and ramjet engines are outlined and the combustion and regression mechanism of solid fuel ramjets is described. The advantages in propulsion system mass and volume reduction of hybrid engines over separated powerplants to cover wide flight envelopes are discussed, and a variety of air breathing hybrid engines are examined to consider the suitability as means of propulsion for future guided weapons. The powered range of the ramjet-propelled missiles evaluated is estimated to be some 5 1/2 times greater than that obtained by rocket propulsion. A metallized solid ramjet fuel enabled the required thrust to be developed for the most economical fuel mass consumption rate, although variations in propulsion system efficiencies could easily erode the apparent advantage. Nonetheless, the greater density of the metallized fuel offered a clear advantage for volume-limited applications. Solid fuels and propellants offer significant benefits in reducing servicing and preparation activities; and the integral rocket solid fuel ramjet provides the best prospect for the propulsion of future air-lanched tactical missiles. The gas generator ramrocket's potential to provide a more compact, but heavier, engine makes it more attractive for land and ship launched applications. The ejector ramjet and air turbo ramjet/ramjet-rocket concepts are unsuitable for guided weapons use, and their greater flexibility and complexity make them more appropriate for multi-mission atmospheric and trans-atmospheric vehicle propulsion. ESA

N92-23225*# National Aeronautics and Space Administration. Lewis Research Center, Cleveland, OH.
DEPOSITION OF ADHERENT Ag-Ti DUPLEX FILMS ON CERAMICS IN A MULTIPLE-CATHODE SPUTTER DEPOSITION SYSTEM
Frank S. Honecy Apr. 1992 10 p
(NASA-TM-105586; E-6914; NAS 1.15:105586) Avail: NTIS HC/MF A02 CSCL 21E

The adhesion of Ag films deposited on oxide ceramics can be increased by first depositing intermediate films of active metals such as Ti. Such duplex coatings can be fabricated in a widely used three target sputter deposition system. It is shown here that the beneficial effect of the intermediate Ti film can be defeated by commonly used in situ target and substrate sputter cleaning procedures which result in Ag under the Ti. Auger electron spectroscopy and wear testing of the coatings are used to develop a cleaning strategy resulting in an adherent film system. Author

N92-23254*# National Aeronautics and Space Administration. Lewis Research Center, Cleveland, OH.
EFFECTS OF CHEMICAL EQUILIBRIUM ON TURBINE ENGINE PERFORMANCE FOR VARIOUS FUELS AND COMBUSTOR TEMPERATURES
Donald H. Tran and Christopher A. Snyder Apr. 1992 22 p
(NASA-TM-105399; E-6795; NAS 1.15:105399) Avail: NTIS HC/MF A03 CSCL 21E

A study was performed to quantify the differences in turbine engine performance with and without the chemical dissociation effects for various fuel types over a range of combustor temperatures. Both turbojet and turbofan engines were studied with hydrocarbon fuels and cryogenic, nonhydrocarbon fuels. Results of the study indicate that accuracy of engine performance decreases when nonhydrocarbon fuels are used, especially at high temperatures where chemical dissociation becomes more significant. For instance, the deviation in net thrust for liquid hydrogen fuel can become as high as 20 percent at 4160 R. This study reveals that computer central processing unit (CPU) time increases significantly when dissociation effects are included in the cycle analysis. Author

N92-23537*# National Aeronautics and Space Administration. Lewis Research Center, Cleveland, OH.
EFFECTS OF TURBINE COOLING ASSUMPTIONS ON PERFORMANCE AND SIZING OF HIGH-SPEED CIVIL TRANSPORT
Paul F. Senick May 1992 11 p
(NASA-TM-105610; E-6948; NAS 1.15:105610) Avail: NTIS HC/MF A03 CSCL 21E

The analytical study presented examines the effects of varying turbine cooling assumptions on the performance of a high speed civil transport propulsion system as well as the sizing sensitivity of this aircraft to these performance variations. The propulsion concept employed in this study was a two spool, variable cycle engine with a sea level thrust of 55,000 lbf. The aircraft used for this study was a 250 passenger vehicle with a cruise Mach number of 2.4 and 5000 nautical mile range. The differences in turbine cooling assumptions were represented by varying the amount of high pressure compressor bleed air used to cool the turbines. It was found that as this cooling amount increased, engine size and weight increased, but specific fuel consumption (SFC) decreased at takeoff and climb only. Because most time is spent at cruise, the SFC advantage of the higher bleed engines seen during subsonic flight was minimized and the lower bleed, lighter engines led to the lowest takeoff gross weight vehicles. Finally, the change in aircraft takeoff gross weight versus turbine cooling level is presented. Author

N92-23671 Stanford Univ., CA.
COMPUTATIONS OF UNSTEADY MULTISTAGE TURBOMACHINERY FLOWS Ph.D. Thesis
Karen Leann Gundy-Burlet 1991 142 p
Avail: Univ. Microfilms Order No. DA9206774

The fluid dynamic environment within multistage turbomachines is extremely complex because of aerodynamic interactions between rotors and stators. Designers need to minimize the weight and size of turbomachines to improve overall efficiency of an airplane. However, this can cause large inviscid and viscous interactions between rotors and stators within an engine. A computational tool that can analyze these interactions can be useful in understanding these effects and will aid in the design of turbomachines that are light and compact as well as reliable and efficient. Two and three dimensional, unsteady, thin layer Euler/Navier-Stokes zonal codes were developed to analyze flows within multistage turbomachines (STAGE 2 and STAGE 3). The nonlinear equations are advanced in time using a third order accurate, implicit, upwind biased Roe algorithm. Body conforming 'O' grids are used to accurately resolve the viscous effects associated with each airfoil. These grids are overlayed on sheared cartesian grids which resolve the inviscid flow field between blades. The cartesian grids are allowed to slip past each other, simulating the relative motion between rotors and stators. The implementation of two and three dimensional zonal algorithms for multistage turbomachinery flows is discussed. Dissert. Abstr.

08 AIRCRAFT STABILITY AND CONTROL

Includes aircraft handling qualities; piloting; flight controls; and autopilots.

For related information see also *05 Aircraft Design, Testing and Performance.*

N92-23229*# Virginia Polytechnic Inst. and State Univ., Blacksburg.
SENSITIVITY ANALYSIS OF DYNAMIC AEROELASTIC RESPONSES
Rakesh K. Kapania *In* AGARD, Integrated Design Analysis and Optimisation of Aircraft Structures Feb. 1992 12 p (For primary document see N92-23227 14-05)
(Contract NAS1-18471)
Copyright Avail: NTIS HC/MF A10; Non-NATO Nationals requests available only from AGARD/Scientific Publications Executive CSCL 01C

N92-23234# Oklahoma Univ., Norman.
MULTIDISCIPLINARY OPTIMIZATION STUDIES USING ASTROS
Alfred G. Striz and Vipperla B. Venkayya (Wright Research Development Center, Wright-Patterson AFB, OH.) *In* AGARD, Integrated Design Analysis and Optimisation of Aircraft Structures Feb. 1992 29 p (For primary document see N92-23227 14-05)
Copyright Avail: NTIS HC/MF A10; Non-NATO Nationals requests available only from AGARD/Scientific Publications Executive

N92-23238# British Aerospace Public Ltd. Co., Bristol (England). Airbus Div.
SIMULTANEOUS STRESS AND FLUTTER OPTIMIZATION FOR THE WING OF A TRANSPORT AIRCRAFT EQUIPPED WITH FOUR ENGINES
J. M. D. Snee, H. Zimmermann, D. Schierenbeck, and P. Heinze (Deutsche Airbus G.m.b.H., Bremen, Germany, F.R.) *In* AGARD, Integrated Design Analysis and Optimisation of Aircraft Structures Feb. 1992 12 p (For primary document see N92-23227 14-05)
Copyright Avail: NTIS HC/MF A10; Non-NATO Nationals requests available only from AGARD/Scientific Publications Executive

09 RESEARCH AND SUPPORT FACILITIES (AIR)

Includes airports, hangars and runways; aircraft repair and overhaul facilities; wind tunnels; shock tubes; and aircraft engine test stands.

For related information see also *14 Ground Support Systems and Facilities (Space).*

N92-23778# National Aerospace Lab., Tokyo (Japan). Aerodynamics Div.

DEVELOPMENT OF WALL PRESSURE MEASURING APPARATUS FOR AN EXISTING TRANSONIC WIND TUNNEL TEST SECTION

Seizo Sakakibara, Hideo Sawada, Koichi Suzuki, Seigo Nakamura, and Nobuyuki Hosoe Mar. 1987 29 p In JAPANESE; ENGLISH summary

(NAL-TM-565; ISSN-0452-2982; JTN-92-80309) Avail: NTIS HC/MF A03

An apparatus for measuring ventilated wall pressure distributions in the NAL 2 m x 2 m transonic wind tunnel was developed. Described in this paper is the necessity for transonic wind tunnel test section pressure distribution data. Secondly, the construction and function of each component of the apparatus, which were designed for the transonic wind tunnel without altering the existing wall configurations, are described. Finally, typical examples of pressure distribution data obtained with this apparatus are shown. The results of detailed analysis of this pressure distribution data will be separately reported. Author (NASDA)

N92-23979# National Aerospace Lab., Tokyo (Japan). Aircraft Aerodynamics Div.

DISTRIBUTED COMPUTER SYSTEM IN THE LARGE SCALE LOW SPEED WIND TUNNEL [OGATA TEISOKU FUDO NI OKERU BUNSAN SHORI SHISUTEMU NI TSUITE]

Hideo Hoshino, Katsuichi Murota, and Hirofumi Kondo Nov. 1990 34 p In JAPANESE

(NAL-TM-629; ISSN-0452-2982; JTN-92-80327) Avail: NTIS HC/MF A03

In 1987 the static quantity instrumentation equipment of the large wind tunnel in the NAL was replaced. In the new equipment the number of measurement channels was increased and test results monitoring functions and data gathering functions were distributed. The measurements and monitoring of air flow parameters such as flow rate, dynamics pressure, static pressure and angle of attack in model settings and data gathering are automated with the use of FA (Factory Automation) computer system. Simple calculations of test results, such as averaging, were made possible in the new equipment. The host computer in the old system was improved to transmit and record data in disk file according to the predetermined formats and to calculate the air flow coefficients and graphic data. Main configurations and functions of the new distributed system were described. As for the host computer system, data transmission function which transmits observed data to the distributed system and data display functions of the transmitted data were described.

Author (NASDA)

12 ASTRONAUTICS (GENERAL)

For extraterrestrial exploration see *91 Lunar and Planetary Exploration.*

N92-23240*# National Aeronautics and Space Administration, Washington, DC.

MISSION SAFETY EVALUATION REPORT FOR STS-43, POSTFLIGHT EDITION

William C. Hill and Seymour I. Finkel (Vitro Corp., Washington, DC.) 31 Oct. 1991 127 p

(NASA-TM-107801; NAS 1.15:107801) Avail: NTIS HC/MF A07 CSCL 22A

Some of the topics covered include: (1) an STS-43 mission summary; (2) safety risks factors/issues; (3) resolved STS-43 safety risk factors; (4) STS-40 inflight anomalies; (5) STS-37 inflight anomalies; and (6) STS-43 inflight anomalies. Background information and a list of acronyms are also presented. Author

N92-23241*# National Aeronautics and Space Administration, Washington, DC.

MISSION SAFETY EVALUATION REPORT FOR STS-29, POSTFLIGHT EDITION

8 May 1989 89 p

(NASA-TM-107773; NAS 1.15:107773) Avail: NTIS HC/MF A05 CSCL 22A

The topics covered include: (1) an STS-29 mission summary; (2) safety risk factors/issues; (3) resolved STS-29 safety risk factors; (4) STS-27 flight anomalies; (5) STS-26 flight anomalies; and (6) the STS-29 official inflight anomaly report. Background information and a list of acronyms are also presented. Author

N92-23242*# National Aeronautics and Space Administration, Washington, DC.

MISSION SAFETY EVALUATION REPORT FOR STS-30, POSTFLIGHT EDITION

Seymour I. Finkel (Vitro Corp., Washington, DC.) 25 Aug. 1989 64 p

(NASA-TM-107774; NAS 1.15:107774) Avail: NTIS HC/MF A04 CSCL 22A

The topics covered include: (1) an STS-30 mission summary; (2) safety risk factors/issues; (3) resolved STS-30 safety risk factors; (4) STS-29 inflight anomalies; (5) STS-27 inflight anomalies; and (6) the STS-30 official inflight anomaly report. Background information and a list of acronyms are also presented. Author

N92-23243*# National Aeronautics and Space Administration, Washington, DC.

MISSION SAFETY EVALUATION REPORT FOR STS-32, POSTFLIGHT EDITION

William C. Hill and Seymour I. Finkel (Vitro Corp., Washington, DC.) 20 Jul. 1990 134 p

(NASA-TM-107775; NAS 1.15:107775) Avail: NTIS HC/MF A07 CSCL 22A

The topics covered include: (1) an STS-32 mission summary; (2) safety risk factors/issues; (3) resolved STS-32 safety risk factors; (4) STS-32 inflight anomalies; (5) STS-28 inflight anomalies; and (6) STS-32 inflight anomalies. Background information and a list of acronyms are also presented. Author

N92-23244*# National Aeronautics and Space Administration, Washington, DC.

MISSION SAFETY EVALUATION REPORT FOR STS-36, POSTFLIGHT EDITION

William C. Hill and Seymour I. Finkel (Vitro Corp., Washington, DC.) 15 Jun. 1990 151 p

(NASA-TM-107780; NAS 1.15:107780) Avail: NTIS HC/MF A08 CSCL 22A

The topics covered include: (1) an STS-36 mission summary; (2) safety risk factors/issues; (3) resolved STS-36 safety risk factors; (4) STS-32 inflight anomalies; (5) STS-34 inflight anomalies; and (6) STS-36 inflight anomalies. Background information and a list of acronyms are also presented. Author

N92-23643*# National Aeronautics and Space Administration, Washington, DC.

PROCEEDINGS OF THE SECOND ANNUAL SYMPOSIUM ON INDUSTRIAL INVOLVEMENT AND SUCCESSES IN COMMERCIAL SPACE

1991 250 p Symposium held in Washington, DC, 14 May 1991

(NASA-TM-107812; NAS 1.15:107812) Avail: NTIS HC/MF A11 CSCL 22A

The proceedings of the conference are presented. It is proposed that commercial development in space is an important element in the future competitive posture of the industrial nations of the world. The resources and characteristics of space will play a major role

in opening a new economic frontier for all the spacefaring nations of the world. Some topics of discussion are as follow: NASA's mission and the role of CCD's; A balanced commercial access to space; Systems for COMET; SPACEHAB; Space Station Freedom; The center for macromolecular crystallography; Center for space power and advanced electronics; and The center for mapping. For individual titles, see N92-23644 through N92-23655.

N92-23644*# Orbital Sciences Corp., Fairfax, VA.
SUBORBITAL MISSIONS: THE JOUST
Bruce W. Ferguson *In* NASA, Washington, Proceedings of the Second Annual Symposium on Industrial Involvement and Successes in Commercial Space 1991 20 p (For primary document see N92-23643 14-12)
Avail: NTIS HC/MF A11 CSCL 22A

Joust 1 will carry a payload of 10 experiments. The experiments in the payload module will be mated with a service module containing accelerometers, avionics, a low gravity rate control system, and battery packs. This suborbital mission will last approximately 21 minutes, providing at least 13 minutes of microgravity time. The experiments are as follow: study into polymer membrane processes; polymer curing; plasma particle generation; automated generic bioprocessing apparatus; biomodule; thin films; materials dispersion apparatus; foam formation; electrodeposition process; and powdered materials processing. E.R.

N92-23645*# Engineering and Economics Research, Inc., Houston, TX. Space Services Div.
LAUNCH VEHICLE FOR ORBITAL MISSIONS: COMET c15
Deke Slayton *In* NASA, Washington, Proceedings of the Second Annual Symposium on Industrial Involvement and Successes in Commercial Space 1991 42 p (For primary document see N92-23643 14-12)
Avail: NTIS HC/MF A11 CSCL 22B

A group of viewgraphs are presented which seem to be designed to persuade that EER Systems Space Services Div. is capable of designing, testing, and launching spacecraft. Some representative viewgraphs are entitled as follow: corporate profile; corporate revenues; corporate organization; commercial space products; space systems pursuits; space services heritage; capabilities demonstrated; and commercial approach. E.R.

N92-23646*# Westinghouse Defense and Electronic Systems Center, Baltimore, MD. Commercial and Civil Space Dept.
SYSTEMS FOR COMET
Harry Andrews *In* NASA, Washington, Proceedings of the Second Annual Symposium on Industrial Involvement and Successes in Commercial Space 1991 16 p (For primary document see N92-23643 14-12)
Avail: NTIS HC/MF A11 CSCL 22A

The Centers for Commercial Development of Space (CCDS) have become the nation's primary focus for stimulating private sector investment in space. In establishing the COMmercial Experiment Transporter (COMET) program, the CCDS's have taken a major step toward the full scale commercial development of space. The COMET program will enable the CCDS community to turn the goal of commercial space into reality, and in the process, establish U.S. leadership in the global market for space systems and services. Some details are presented on the systems that make up the COMET missions, specifically as they describe the accommodation for potential users and mission parameters. Author

N92-23647*# Spacehab, Inc., Washington, DC.
SPACEHAB c18
David Rossi *In* NASA, Washington, Proceedings of the Second Annual Symposium on Industrial Involvement and Successes in Commercial Space 1991 19 p (For primary document see N92-23643 14-12)
Avail: NTIS HC/MF A11 CSCL 22B

Information is given in viewgraph form on the Spacehab company and its work on a pressurized module to be carried on the Space Shuttle. The module augments the Shuttle's capability to support man-tended microgravity experiments. The augmentation modules are designed to duplicate the resources, such as power, environmental control, and data management that are available in the Shuttle's middeck. Topics covered include a company overview, company financing, system overview, module description, payload resources, locker accommodations, program status, and a listing of candidate payloads. Author

N92-23648*# Space Industries, Inc., Webster, TX.
THE WAKE SHIELD FACILITY: A SPACE EXPERIMENT PLATFORM c18
Joseph P. Allen *In* NASA, Washington, Proceedings of the Second Annual Symposium on Industrial Involvement and Successes in Commercial Space 1991 7 p (For primary document see N92-23643 14-12)
Avail: NTIS HC/MF A11 CSCL 22B

Information is given in viewgraph form on Wakeshield, a space experiment platform. The Wake Shield Facility (WSF) flight program objectives, product applications, commercial development approach, and cooperative experiments are listed. The program objectives are to produce new industry-driven electronic, magnetic, and superconducting thin-film materials and devices both in terrestrial laboratories and in space; utilize the ultra-vacuum of space for thin film epitaxial growth and materials processing; and develop commercial space hardware for research and development and enhanced access to space. Author

N92-23649*# Boeing Commercial Airplane Co., Seattle, WA.
SPACE STATION FREEDOM c18
Gilbert Keyes *In* NASA, Washington, Proceedings of the Second Annual Symposium on Industrial Involvement and Successes in Commercial Space 1991 27 p (For primary document see N92-23643 14-12)
Avail: NTIS HC/MF A11 CSCL 22B

Information is given in viewgraph form on Space Station Freedom. Topics covered include future evolution, man-tended capability, permanently manned capability, standard payload rack dimensions, the Crystals by Vapor Transport Experiment (CVTE), commercial space projects interfaces, and pricing policy. Author

N92-23650*# Vertex Pharmaceuticals, Cambridge, MA.
CENTER FOR MACROMOLECULAR CRYSTALLOGRAPHY, UNIVERSITY OF ALABAMA IN BIRMINGHAM c16
Manuel A. Navia *In* NASA, Washington, Proceedings of the Second Annual Symposium on Industrial Involvement and Successes in Commercial Space 1991 3 p (For primary document see N92-23643 14-12)
Avail: NTIS HC/MF A11 CSCL 10B

Porcine pancreatic elastase (PPE) crystals grown under microgravity conditions on mission STS-26 of the Space Shuttle Discovery were shown to diffract to considerably higher resolution than the best PPE crystals grown by us on the ground. We have now independently refined both the microgravity and ground-based data. Preliminary results of these refinements are summarized. These results show nearly a doubling of experimental diffraction data for this structure, exceeding 1.3 A resolution. Improved phase information derived from the refined structure of PPE based on this microgravity data has allowed us to interpret previously-uninterpretable electron density obtained from ground-based crystals of a complex of PPE with a chemically-reactive inhibitor. Intermediate stages in the enzyme-inhibitor reaction mechanism in the crystal can now be directly observed. Further refinement of PPE structures is in progress. Author

N92-23651*# Johnson Controls, Inc., Butler, WI. Nickel Hydrogen Batteries Div.
CENTER FOR SPACE POWER, TEXAS A AND M UNIVERSITY c33
Ken Jones *In* NASA, Washington, Proceedings of the Second Annual Symposium on Industrial Involvement and Successes in Commercial Space 1991 5 p (For primary document see

N92-23643 14-12)
Avail: NTIS HC/MF A11 CSCL 11D

Johnson Controls is a 106 year old company employing 42,000 people worldwide with $4.7 billion annual sales. Though we are new to the aerospace industry we are a world leader in automobile battery manufacturing, automotive seating, plastic bottling, and facilities environment controls. The battery division produces over 24,000,000 batteries annually under private label for the new car manufacturers and the replacement market. We are entering the aerospace market with the nickel hydrogen battery with the help of NASA's Center for Space Power at Texas A&M. Unlike traditional nickel hydrogen battery manufacturers, we are reaching beyond the space applications to the higher volume markets of aircraft starting and utility load leveling. Though space applications alone will not provide sufficient volume to support the economies of scale and opportunities for statistical process control, these additional terrestrial applications will. For example, nickel hydrogen batteries do not have the environmental problems of nickel cadmium or lead acid and may someday start your car or power your electric vehicle. However you envision the future, keep in mind that no manufacturer moves into a large volume market without fine tuning their process. The Center for Space Power at Texas A&M is providing indepth technical analysis of all of the materials and fabricated parts of our battery as well as thermal and mechanical design computer modeling. Several examples of what we are doing with nickel hydrogen chemistry to lead to these production efficiencies are presented. Author

N92-23652*# Du Pont de Nemours (E. I.) and Co., Deepwater, NJ. Chemicals and Pigments Dept.
ADVANCED MATERIALS CENTER, BATTELLE c24
Harold Bellis *In* NASA, Washington, Proceedings of the Second Annual Symposium on Industrial Involvement and Successes in Commercial Space 1991 7 p (For primary document see N92-23643 14-12)
Avail: NTIS HC/MF A11 CSCL 06A

The goal of the Mixed Oxide Program is to determine the results obtained by using microgravity processing on a commercially significant catalyst - V-P-O System. The topics are presented in viewgraph form and include the following: (1) reasons for using microgravity; (2) the synthesis process; (3) novel results of the earth based program; and (4) Dupont interests. Author

N92-23653*# Genetech, Inc., San Francisco, CA. Endocrine Research Div.
CENTER FOR CELL RESEARCH, PENNSYLVANIA STATE UNIVERSITY c51
Mike Cronin *In* NASA, Washington, Proceedings of the Second Annual Symposium on Industrial Involvement and Successes in Commercial Space 1991 11 p (For primary document see N92-23643 14-12)
Avail: NTIS HC/MF A11 CSCL 10B

A brief review of Genentech, Inc., is presented. Additionally, the Physiological Systems Experiment (PSE-01) is discussed in terms of its development history. The PSE-01 was developed to investigate the bone wasting, muscle wasting, and immune cell dysfunction that occur in microgravity conditions. Specifically, a number of human disorders are associated with maladaptive changes in bone, muscle, and immune function. The physiological adjustments that the body makes in response to space flight can be monitored and may aid in the discovery of new protein forms and patterns. This research may also provide strategies for protecting the health of flight crews enduring prolonged space flight. Results are discussed. D.R.D.

N92-23654*# Westinghouse Electric Corp., Pittsburgh, PA. Science and Technology Center.
CENTER FOR SPACE POWER AND ADVANCED ELECTRONICS, AUBURN UNIVERSITY c33
Dan W. Deis and Richard H. Hopkins *In* NASA, Washington, Proceedings of the Second Annual Symposium on Industrial Involvement and Successes in Commercial Space 1991 21 p (For primary document see N92-23643 14-12)
Avail: NTIS HC/MF A11 CSCL 08B

The union of Auburn University's Center for Space Power and Advanced Electronics and the Westinghouse Science and Technology Center to form a Center for the Commercial Development of Space (CCDS) is discussed. An area of focus for the CCDS will be the development of silicon carbide electronics technology, in terms of semiconductors and crystal growth. The discussion is presented in viewgraph form. D.R.D.

N92-23655*# Intergraph Corp., Reston, VA. International Marketing Div.
CENTER FOR MAPPING, OHIO STATE UNIVERSITY c43
Lowell Starr *In* NASA, Washington, Proceedings of the Second Annual Symposium on Industrial Involvement and Successes in Commercial Space 1991 17 p (For primary document see N92-23643 14-12)
Avail: NTIS HC/MF A11 CSCL 08B

There are many future opportunities for Centers for the Commercial Development of Space (CCDS) activities that are directly linked to industry strategic objectives. In the fields of mapping, remote sensing, and geographic information systems (GIS), the near term opportunities may exceed all that have occurred in the past 10 years. It is strongly believed that a national spatial data infrastructure must be established in this country, if we are to remain a leader in the information age. Author

N92-23705# Joint Publications Research Service, Arlington, VA.
JPRS REPORT: SCIENCE AND TECHNOLOGY. CENTRAL EURASIA: SPACE
1 Apr. 1992 59 p Transl. into ENGLISH from various Russian articles
(JPRS-USP-92-002) Avail: NTIS HC/MF A04

A bibliography is given of Central Eurasian research in space sciences. Topics covered include solar sails, satellite motion prediction, magnetic storms, the Earth radiation belt, magnetic field vector measurement from a rotating spacecraft, the formation of planetary systems in the course of the evolution of close binary stars, and estimating the mass of Halley's Comet dust particles. Author

N92-23910# European Space Agency, Paris (France).
THE SOLID-EARTH MISSION ARISTOTELES
C. Mattok, ed. Dec. 1991 123 p International workshop held in Anacapri, Italy, 23-24 Sep. 1991; sponsored by NASA, ESA, Italian Space Agency, and Alenia Spazio S.p.A.
(ESA-SP-329; ISBN-92-9092-158-7; ISSN-0379-6566; ETN-92-91383) Avail: NTIS HC/MF A06; ESA, EPD, ESTEC, Noordwijk, Netherlands, HC 50 Dutch guilders

Various aspects of the Aristoteles mission are discussed. The gradiometer payload, and the design and development status of the GRADIO accelemometer are described. NASA's Global Positioning System (GPS) tracking system for Aristoteles is described. The magnetometer system and the Delta 2 launcher to be used in the mission are described. The mission ground segment and the potential use of fiducial ground networks are discussed. Gravity field data products from the mission and approaches to data distribution are considered. For individual titles, see N92-23911 through N92-23927.

N92-23911# Technische Univ., Delft (Netherlands). Faculty of Geodetic Engineering.
ON THE PRINCIPLE OF ARISTOTELES
Reiner Rummel *In* ESA, The Solid-Earth Mission Aristoteles Dec. 1991 p 11-15 (For primary document see N92-23910 14-12)
Avail: NTIS HC/MF A06; ESA, EPD, ESTEC, Noordwijk, Netherlands, HC 50 Dutch guilders

Aristoteles is to be the first spacecraft with a gravity gradiometer on board. The gradiometer consists of a symmetrical set of four test masses arranged in the normal plane of the trajectory and electrically kept in levitated position inside four housings. Due to the frequency band limitation of the gradiometer, the long

wavelength part of the gravitational field is to be determined from the carrier phase measurements of a Global Positioning System (GPS) receiver on board the spacecraft. The expected outcomes are less than 5 cm for the geoid and less than 0.00001 m/sq s for gravity anomalies, both with a spatial resolution of 100 km half wavelength. The mission will contribute in important ways to geodesy, solid Earth physics and oceanography. In particular, it is to allow the determination of ocean surface circulation in conjunction with satellite altimetry. ESA

N92-23912*# National Aeronautics and Space Administration. Goddard Space Flight Center, Greenbelt, MD.
MISSION OBJECTIVES AND SCIENTIFIC RATIONALE FOR THE MAGNETOMETER MISSION
Robert A. Langel *In* ESA, The Solid-Earth Mission Aristoteles Dec. 1991 p 17-26 (For primary document see N92-23910 14-12)
Avail: NTIS HC/MF A06; ESA, EPD, ESTEC, Noordwijk, Netherlands, HC 50 Dutch guilders

Based on a review of the characteristics of the geomagnetic field, objectives for the magnetic portion of the Aristoteles mission are described. They are to derive a description of the main magnetic field and its secular variation, to investigate the correlation between the geomagnetic field and variations in the length of day, to study properties of the fluid core, to study the conductivity of the mantle, to model the state and evolution of the crust and upper lithosphere, to measure and characterize field aligned currents and ionospheric currents and to understand their generation mechanisms and their role in energy coupling in the interplanetary-magnetospheric-ionospheric systems. Procedures for these investigations are outlined. Required measurement accuracies are 2.0 nT for the field magnitude and 4.5 nT for each component. Error sources and a possible error budget are discussed. Planned data rates are 2 samples/second for the scalar field and 16 samples/second/axis for the vector components. ESA

N92-23913# Ohio State Univ., Columbus. Dept. of Geodetic Science and Surveying.
THE EARTH'S GRAVITY FIELD FROM SATELLITE GEODESY: A 30 YEAR ADVENTURE **c46**
Richard H. Rapp *In* ESA, The Solid-Earth Mission Aristoteles Dec. 1991 p 29-32 (For primary document see N92-23910 14-12)
Avail: NTIS HC/MF A06; ESA, EPD, ESTEC, Noordwijk, Netherlands, HC 50 Dutch guilders

The history of research in the Earth's gravity field from satellite geodesy is described and limitations of existing geopotential models are indicated. Although current solutions have made outstanding achievements, their limited accuracy restricts their use for some oceanographic applications. An example is discussed where there appears to be an incompatibility of the long wavelength geoid undulation obtained through satellite analysis with independent estimates that have become available. The future Aristoteles mission is seen as providing a significant leap in Earth gravity field knowledge improvement. ESA

N92-23914# Politecnico di Milano (Italy). Dipartimento di Ingegneria Idraulica, Ambientale e del Rilevamento.
PROGRESS IN THE SPACEWISE APPROACH TO ARISTOTELES DATA REDUCTION **c43**
M. Bassanino, Frederica Migliaccio, and Fernando Sanso *In* ESA, The Solid-Earth Mission Aristoteles Dec. 1991 p 33-43 (For primary document see N92-23910 14-12)
Avail: NTIS HC/MF A06; ESA, EPD, ESTEC, Noordwijk, Netherlands, HC 50 Dutch guilders

Aristoteles, a satellite mission conceived to determine a global model of the Earth's gravity field, in a homogeneous way, with high resolution and high accuracy is described. It is shown, after some simplifications and idealizations, how this task can be accomplished by using in a Boundary Value Problem (BVP) mode the data available from the satellite. Gradiometry, accelerometry and Global Positioning System (GPS) data are to be used to this end. Comparison of the BVP method and a least squares approach is carried out. It is concluded that each approach has its own specific pros and cons. ESA

N92-23915*# National Aeronautics and Space Administration. Goddard Space Flight Center, Greenbelt, MD.
THE GEOPHYSICAL IMPACT OF THE ARISTOTELES MISSION **c46**
Allen Joel Anderson, E. Klingele, R. Sabadini, S. Tinti, and Suzanna Zerbini (Bologna Univ., Italy) *In* ESA, The Solid-Earth Mission Aristoteles Dec. 1991 p 45-50 (For primary document see N92-23910 14-12)
Avail: NTIS HC/MF A06; ESA, EPD, ESTEC, Noordwijk, Netherlands, HC 50 Dutch guilders CSCL 08G

The importance of a precise, high resolution gradiometric and magnetometric mission in some topics of geophysical interest is stressed. Ways in which the planned Aristoteles mission can allow the geophysical community to improve the knowledge and the physical understanding of several important geodynamical processes involving the coupled system consisting of the lithosphere, asthenosphere and upper mantle are discussed. Particular attention is devoted to the inversion of anomalous density structures in collision and subduction zones by means of the joint use of gradiometric and seismic tomographic data. Some modeling efforts accomplished to study the capability of the mission to invert the rheological parameters of the lithosphere and upper mantle through the gravimetric signals of internal and surface density anomalies are described. ESA

N92-23916# European Space Agency. European Space Research and Technology Center, ESTEC, Noordwijk (Netherlands).
INTRODUCTORY REMARKS TO THE MISSION AND SYSTEM ASPECTS SESSION **c46**
Rene Bonnefoy and M. Schuyer *In its* The Solid-Earth Mission Aristoteles Dec. 1991 p 53-5 (For primary document see N92-23910 14-12)
Avail: NTIS HC/MF A06; ESA, EPD, ESTEC, Noordwijk, Netherlands, HC 50 Dutch guilders

A brief history of the measurement of Earth potential fields is presented. The scientific objectives of the Aristoteles mission are summarized. Cooperation between NASA and ESA in developing the Aristoteles mission constraints are presented in tabular form. Correspondence between major mission and technical constraints is discussed. Program status of the Aristoteles mission and the mission baseline are described. The planned configuration of the Aristoteles satellite is shown in diagrammatic form. ESA

N92-23917# MATRA Marconi Space, Toulouse (France).
THE GRADIOMETER PAYLOAD **c19**
P. Meyer and Patrick Peyrot *In* ESA, The Solid-Earth Mission Aristoteles Dec. 1991 p 57-60 (For primary document see N92-23910 14-12)
Avail: NTIS HC/MF A06; ESA, EPD, ESTEC, Noordwijk, Netherlands, HC 50 Dutch guilders

The Aristoteles gravity mission is achieved in part by performing gradiometry measurements using an instrument called GRADIO. Its principle is based on the simultaneous measurement of acceleration on several locations of a very stable plate (the GRADIO plate) equipped with high accuracy three axes accelerometers. To correct misalignment errors and accelerometer parameters (scale factors, nonlinearities), a calibration system, fixed in the center of the GRADIO plate is used. The requirements placed on GRADIO components resulting in the design described are presented. A gradiometry performance analysis is presented taking into account mission and spacecraft considerations. This analysis gives good confidence in meeting the gradiometry requirement which is to measure components Tyy and Tzz of the gravity gradient tensor in the 0.005, 0.125 Hz frequency bandwidth with an accuracy of 0.01 EU. ESA

N92-23918# Office National d'Etudes et de Recherches Aerospatiales, Paris (France).
THE GRADIO ACCELEROMETER: DESIGN AND DEVELOPMENT STATUS **c19**
Alain Bernard and M. P. Touboul *In* ESA, The Solid-Earth Mission Aristoteles Dec. 1991 p 61-67 (For primary document see N92-23910 14-12)
Avail: NTIS HC/MF A06; ESA, EPD, ESTEC, Noordwijk, Netherlands, HC 50 Dutch guilders

The concept of Satellite Gravity Gradiometry (SGG) based on differential microaccelerometry as proposed in the early eighties is summarized. Work devoted to the development of the GRADIO accelerometers is described. The configuration was optimized for the Aristoteles mission with the objective of increasing resolution for an integrating time of 4 s. Thanks to the selected three axis configuration, very sensitive differential tests were carried out between two very representative laboratory models, in directions perpendicular to gravity. The resolution of these tests, limited by the actual stability of alignments of the testing equipment is described. ESA

N92-23919*# Jet Propulsion Lab., California Inst. of Tech., Pasadena.
NASA'S GPS TRACKING SYSTEM FOR ARISTOTELES **c13**
E. S. Davis, G. Hajj, E. R. Kursinski, C. Kyriacou, T. K. Meehan, William G. Melbourne, R. E. Neilan, L. E. Young, and Thomas P. Yunck *In* ESA, The Solid-Earth Mission Aristoteles Dec. 1991 p 69-82 Sponsored by NASA, Washington (For primary document see N92-23910 14-12)
Avail: NTIS HC/MF A06; ESA, EPD, ESTEC, Noordwijk, Netherlands, HC 50 Dutch guilders

NASA 's Global Positioning System (GPS) tracking system for Artistoteles receivers and a GPS flight receiver aboard Aristoteles is described. It will include a global network of GPS ground receivers and a GPS flight receiver aboard Aristoteles. The flight receiver will operate autonomously; it will provide real time navigation solutions for Aristoteles and tracking data needed by ESOC for operational control of the satellite. The GPS flight and ground receivers will currently and continuously track all visible GPS satellites. These observations will yield high accuracy differential positions and velocities of Aristoteles in a terrestrial frame defined by the locations of the globally distributed ground work. The precise orbits and tracking data will be made available to science investigators as part of the geophysical data record. The characteristics of the GPS receivers, both flight and ground based, that NASA will be using to support Aristoteles are described. The operational aspects of the overall tracking system, including the data functions and the resulting data products are summarized. The expected performance of the tracking system is compared to Aristoteles requirements and the need to control key error sources such as multipath is identified. ESA

N92-23920*# National Aeronautics and Space Administration. Goddard Space Flight Center, Greenbelt, MD.
ARISTOTELES MAGNETOMETER SYSTEM **c19**
Edward J. Smith, Roy J. Marquedant (Jet Propulsion Lab., California Inst. of Tech., Pasadena.), Robert Langel, and Mario Acuna *In* ESA, The Solid-Earth Mission Aristoteles Dec. 1991 p 83-89 (For primary document see N92-23910 14-12)
Avail: NTIS HC/MF A06; ESA, EPD, ESTEC, Noordwijk, Netherlands, HC 50 Dutch guilders CSCL 14B

A magnetometer system capable of meeting the stringent requirements of the Aristoteles mission is described. The system will comprise a three axis or Vector Flux gas Magnetometer (VFM) and a highly accurate resonance magnetometer, the Scalar Helium Magnetometer (SHM). Basic operational features of these instruments are described and their performance is related to the scientific objectives of the mission appropriate to the geomagnetic field measurements. The major requirements imposed on the spacecraft are summarized. Photographs and diagrams of both instruments are presented along with graphs of the sensitivity of the SHM to magnetic field orientation. ESA

N92-23921*# National Aeronautics and Space Administration. Goddard Space Flight Center, Greenbelt, MD.
THE DELTA 2 LAUNCHER **c15**
Gilbert W. Ousley, Sr. *In* ESA, The Solid-Earth Mission Aristoteles Dec. 1991 p 91-94 (For primary document see N92-23910 14-12)
Avail: NTIS HC/MF A06; ESA, EPD, ESTEC, Noordwijk, Netherlands, HC 50 Dutch guilders CSCL 22B

The utilization of the Delta 2 as the vehicle for launching Aristoteles into its near Sun synchronous orbit is addressed. Delta is NASA's most reliable launch vehicle and is well suited for placing the present Aristoteles spacecraft into a 400 m circular orbit. A summary of some of the Delta 2 flight parameters is presented. Diagrams of a typical Delta 2 two stage separation are included along with statistics on delta reliability and launch plans. ESA

N92-23922# Alenia Spazio S.p.A., Turin (Italy).
THE ARISTOTELES MISSION PROFILE
Alberto Anselmi and Mario Izzo *In* ESA, The Solid-Earth Mission Aristoteles Dec. 1991 p 95-99 (For primary document see N92-23910 14-12)
Avail: NTIS HC/MF A06; ESA, EPD, ESTEC, Noordwijk, Netherlands, HC 50 Dutch guilders

The Aristoteles mission requires a near polar, circular orbit at low altitude. In years of preparatory studies, a complex mission profile has evolved, including altitude and inclination change maneuvers, as well as month long orbit maintenance at selected attitudes. The baseline mission profile adopted in the current system definition study is described. The main features of the mission are discussed and a rationale for the selected orbit parameters is given. Given the very low altitude at which the satellite is to fly in the gravity part of its mission, minimization of drag is identified as being of paramount importance. The mission is tailored to take place around minimum of the eleven year cycle of solar activity. This requires a launch in 1997 to 1998. A later launch date would demand substantial modification of mission design. ESA

N92-23923# European Space Agency. European Space Operations Center, Darmstadt (Germany, F.R.).
ARISTOTELES GROUND SEGMENT: OPERATIONAL CONCEPT **c14**
H. Houet *In its* The Solid-Earth Mission Aristoteles Dec. 1991 p 101-105 (For primary document see N92-23910 14-12)
Avail: NTIS HC/MF A06; ESA, EPD, ESTEC, Noordwijk, Netherlands, HC 50 Dutch guilders

The involvement of ESA/ESOC in support of the Aristoteles mission is described. The objective of the various components of the foreseen ground segment are presented. Based on the mission requirements, emphasis is put on the criticality of the operations which require highly redundant ground segment hardware. A diagram of the ground support configuration is shown. A map of typical ground track and station coverage is presented. The ground segment for operational phases is shown in diagram form. The uplink and downlink technical specifications are tabulated. Diagrams of the station front and the station backend are presented. ESA

N92-23924# Italian Space Agency, Rome. Centro di Geodesia Spaziale.
THE POTENTIAL USE OF FIDUCIAL GROUND NETWORKS **c14**
Giuseppe Bianco *In* ESA, The Solid-Earth Mission Aristoteles Dec. 1991 p 107-109 (For primary document see N92-23910 14-12)
Avail: NTIS HC/MF A06; ESA, EPD, ESTEC, Noordwijk, Netherlands, HC 50 Dutch guilders

Collocation of space geodetic techniques will play an important role for precision orbit determination of Aristoteles. The 'Fiducial Laboratories' for an International Natural science Network' (FLINN) concept is ideal for defining and maintaining a highly precise conventional terrestrial reference frame by means of collocated Satellite Laser Ranging (SLR), Very Long Baseline Interferometry (VLBI), and GPS stations. The proposed, online Aristoteles Global Positioning System (GPS) tracking network should be supported

by an extended, offline tracking network with several selected FLINN sites, in order to include the Aristoteles mission within a standard, high accuracy conventional terrestrial reference system. ESA

N92-23925# Centre National d'Etudes Spatiales, Toulouse (France). Groupe de Recherche de Geodesie Spatiale.
GRAVITY FIELD DATA PRODUCTS FROM THE ARISTOTELES MISSION **c43**
Georges Balmino *In* ESA, The Solid-Earth Mission Aristoteles Dec. 1991 p 111-113 (For primary document see N92-23910 14-12)
Avail: NTIS HC/MF A06; ESA, EPD, ESTEC, Noordwijk, Netherlands, HC 50 Dutch guilders

The Aristoteles mission will bring a wealth of homogeneous information about the Earth gravity field enabling new direct and inverse modeling of geophysical structures at various scales. A reference geoid surface quality will help in oceanographic studies, leading to global models (in spherical harmonics) of high resolution for versatile applications and precise orbit determination of artificial satellites (especially those of altimetric missions). The basic data coming from the microaccelerometers which compose the gradiometer will, in addition to gravity gradients, provide information on the surface forces acting on the spacecraft including the atmospheric drag, from which density models will be improved. The different types of measurements involved in these investigations, the various levels of processing and how they can be phased with the scientific activities, and the expected products are discussed. General schemes are proposed along which the different tasks can be undertaken. ESA

N92-23926# European Space Agency. ESRIN, Frascati (Italy).
DATA DISTRIBUTION AND REDUCTION APPROACHES TO DATA DISTRIBUTION: THE EARTHNET EXPERIENCE **c43**
Livio Marelli *In its* The Solid-Earth Mission Aristoteles Dec. 1991 p 115-116 (For primary document see N92-23910 14-12)
Avail: NTIS HC/MF A06; ESA, EPD, ESTEC, Noordwijk, Netherlands, HC 50 Dutch guilders

The scheme adopted within ESA for handling the ERS-1 and 2 payload is described. Integration of Aristoteles payload data within the same scheme is discussed. Use of such integration as a valuable reference for defining the ground component of the Aristoteles program is considered. Maximum synergy between Aristoteles measurements and those from other Earth observation missions is called for. The need to take advantage of the infrastructure, personnel and expertise gained in other missions, secure long term access to data on a standard operational basis, and ensure close interaction between the team in charge of the Aristoteles payload and the international scientific community in defining product specifications and standards, are all identified as crucial. The advantages to be gained through integration of the Aristoteles payload data into the ERS payload data handling system are outlined. ESA

N92-23927# Observatoire de la Cote d'Azur, Nice (France).
POSSIBLE ATMOSPHERIC RESEARCH WITH ARISTOTELES **c46**
Francois Barlier *In* ESA, The Solid-Earth Mission Aristoteles Dec. 1991 p 135-137 (For primary document see N92-23910 14-12)
Avail: NTIS HC/MF A06; ESA, EPD, ESTEC, Noordwijk, Netherlands, HC 50 Dutch guilders

Use of the Aristoteles mission in measuring atmospheric parameters is discussed. The total density of the thermosphere, the temperature of the stratosphere and the total electron count of the ionosphere are identified as three areas in which the Aristoteles mission could be of great use in carrying out research. Combining the accelerometer measurements yields the gravity tensor as well as the nongravitational acceleration acting upon the satellite. Ways in which the temperature of the stratosphere around the Earth, and the annual, seasonal and secular variations it goes through could be measured are discussed. ESA

N92-24048*# Boeing Aerospace Co., Huntsville, AL. Advanced Civil Space Systems.
SPACE TRANSFER CONCEPTS AND ANALYSES FOR EXPLORATION MISSIONS: TECHNICAL DIRECTIVE 10 Final Report, Oct. 1991 - Jan. 1992
Gordon R. Woodcock Feb. 1992 111 p
(Contract NAS8-37857)
(NASA-CR-184309; NAS 1.26:184309; D615-10051) Avail: NTIS HC/MF A06 CSCL 22A

The current technical effort is part of the third phase of a broad-scoped and systematic study of space transfer concepts for human lunar and Mars missions. The study addressed issues that were raised during the previous phases but specifically on launch vehicle size trades and MEV options. Author

13 ASTRODYNAMICS

Includes powered and free-flight trajectories; and orbital and launching dynamics.

N92-23529*# Georgia Inst. of Tech., Atlanta. School of Aerospace Engineering.
NONLINEAR FEEDBACK GUIDANCE LAW FOR AERO-ASSISTED ORBIT TRANSFER MANEUVERS Final Technical Report
P. K. A. Menon Mar. 1992 31 p
(Grant NAG1-1243)
(NASA-CR-190129; NAS 1.26:190129) Avail: NTIS HC/MF A03 CSCL 22A

Aero-assisted orbit transfer vehicles have the potential for significantly reducing the fuel requirements in certain classes of orbit transfer operations. Development of a nonlinear feedback guidance law for performing aero-assisted maneuvers that accomplish simultaneous change of all the orbital elements with least vehicle acceleration magnitude is discussed. The analysis is based on a sixth order nonlinear point-mass vehicle model with lift, bank angle, thrust and drag modulation as the control variables. The guidance law uses detailed vehicle aerodynamic and the atmosphere models in the feedback loop. Higher-order gravitational harmonics, planetary atmosphere rotation and ambient winds are included in the formulation. Due to modest computational requirements, the guidance law is implementable on-board an orbit transfer vehicle. The guidance performance is illustrated for three sets of boundary conditions. Author

N92-23531*# Massachusetts Inst. of Tech., Cambridge. Dept. of Physics.
DISCOVERY OF ORBITAL DECAY IN SMC X-1
A. Levine, S. Rappaport, P. Boynton, J. Deeter, and F. Nagase (Tokyo Univ., Japan) 7 Apr. 1992 33 p Submitted for publication
(Grants NAG8-762; NAGw-1545)
(NASA-CR-190214; NAS 1.26:190214; CSR-HEA-92-08) Avail: NTIS HC/MF A03 CSCL 22A

The results are reported of three observations of the binary X ray pulsar SMC X-1 with the Ginga satellite. Timing analyses of the 0.71 s X ray pulsations yield Doppler delay curves which, in turn, provide the most accurate determination of the SMC X-1 orbital parameters available to date. The orbital phase of the 3.9 day orbit is determined in May 1987, Aug. 1988, and Aug. 1988 with accuracies of 11, 1, and 3.5 s, respectively. These phases are combined with two previous determinations of the orbital phase to yield the rate of change in the orbital period: P sub orb/P sub orb = (-3.34 + or - 0.023) x 10(exp -6)/yr. An interpretation of this measurement and the known decay rate for the orbit of Cen X-3 is made in the context of tidal evolution. Finally, a discussion is presented of the relation among the stellar evolution, orbital decay, and neutron star spinup time scales for the SMC X-1 system. Author

N92-23919*# Jet Propulsion Lab., California Inst. of Tech., Pasadena.
NASA'S GPS TRACKING SYSTEM FOR ARISTOTELES
E. S. Davis, G. Hajj, E. R. Kursinski, C. Kyriacou, T. K. Meehan, William G. Melbourne, R. E. Neilan, L. E. Young, and Thomas P. Yunck *In* ESA, The Solid-Earth Mission Aristoteles Dec. 1991 p 69-82 Sponsored by NASA, Washington (For primary document see N92-23910 14-12)
Avail: NTIS HC/MF A06; ESA, EPD, ESTEC, Noordwijk, Netherlands, HC 50 Dutch guilders

N92-23969# Forschungsinstitut fuer Hochfrequenzphysik, Werthhoven (Germany, F.R.).
ORBIT ANALYSIS AND LIFETIME PREDICTION USING RADAR DATA BY REENTRY OF SALYUT-7/KOSMOS-1686
W. Liewehr, H. G. Peters, and D. Mehrholz *In* ESA, The Reentry of Salyut-7/Kosmos-1686 Aug. 1991 p 9-1 (For primary document see N92-23967 14-18)
Copyright Avail: NTIS HC/MF A05

N92-23973# Royal Aerospace Establishment, Farnborough (England). Space Dept.
DEBRIS REENTRY PREDICTION: SALYUT-7/KOSMOS-1686
R. Crowther *In* ESA, The Reentry of Salyut-7/Kosmos-1686 Aug. 1991 p 51-56 (For primary document see N92-23967 14-18)
Copyright Avail: NTIS HC/MF A05

N92-23976# European Space Agency. European Space Operations Center, Darmstadt (Germany, F.R.). Mission Analysis Section.
SALYUT-7/KOSMOS-1686 ORBIT DETERMINATION FROM RADAR DATA
R. Jehn *In its* The Reentry of Salyut-7/Kosmos-1686 Aug. 1991 p 73-7 (For primary document see N92-23967 14-18)
Copyright Avail: NTIS HC/MF A05

N92-23977# European Space Agency. European Space Operations Center, Darmstadt (Germany, F.R.). Mission Analysis Section.
LIFETIME OF OBJECTS IN GEOSTATIONARY TRANSFER ORBIT
G. Janin *In its* The Reentry of Salyut-7/Kosmos-1686 Aug. 1991 p 79-8 (For primary document see N92-23967 14-18)
Copyright Avail: NTIS HC/MF A05

14 GROUND SUPPORT SYSTEMS AND FACILITIES (SPACE)

Includes launch complexes, research and production facilities; ground support equipment, e.g., mobile transporters; and simulators.

For related information see also *09 Research and Support Facilities (Air).*

N92-23923# European Space Agency. European Space Operations Center, Darmstadt (Germany, F.R.).
ARISTOTELES GROUND SEGMENT: OPERATIONAL CONCEPT
H. Houet *In its* The Solid-Earth Mission Aristoteles Dec. 1991 p 101-105 (For primary document see N92-23910 14-12)
Avail: NTIS HC/MF A06; ESA, EPD, ESTEC, Noordwijk, Netherlands, HC 50 Dutch guilders

N92-23924# Italian Space Agency, Rome. Centro di Geodesia Spaziale.
THE POTENTIAL USE OF FIDUCIAL GROUND NETWORKS
Giuseppe Bianco *In* ESA, The Solid-Earth Mission Aristoteles Dec. 1991 p 107-109 (For primary document see N92-23910 14-12)
Avail: NTIS HC/MF A06; ESA, EPD, ESTEC, Noordwijk, Netherlands, HC 50 Dutch guilders

15 LAUNCH VEHICLES AND SPACE VEHICLES

Includes boosters; operating problems of launch/space vehicle systems; and reusable vehicles.

For related information see also *20 Spacecraft Propulsion and Power.*

N92-23750# European Space Agency, Paris (France).
LAUNCHER PROPULSION TOWARDS THE YEAR 2010
Valerie David, ed. Dec. 1991 185 p In ENGLISH and FRENCH Conference held in Bordeaux, France, 11-12 Jun. 1991
(ESA-SP-327; ISBN-92-9092-150-1; ETN-92-91381) Copyright
Avail: NTIS HC/MF A09; ESA, EPD, ESTEC, Noordwijk, Netherlands, HC 50 Dutch guilders

Conference papers covering the following sessions are presented: review of propulsion techniques used by the major space programs; technical status; and prospective developments. Several papers cover the Ariane 5 and Vulcain engine development. The Space Shuttle (U.S.) and other NASA and USSR launchers are covered. Other topics include health monitoring, reusable launch vehicles, materials for liquid propellant engines, nonpollutant solid propellants, and the future of hybrid rocket propulsion. For individual titles, see N92-23751 through N92-23768.

N92-23751# European Space Agency, Paris (France).
ARIANE TECHNOLOGY: FROM TODAY INTO THE NEXT CENTURY
J. Feustel-Bueechl *In its* Launcher Propulsion Towards the Year 2010 Dec. 1991 p 23-25 (For primary document see N92-23750 14-15)
Copyright Avail: NTIS HC/MF A09; ESA, EPD, ESTEC, Noordwijk, Netherlands, HC 50 Dutch guilders

The Ariane programs have enabled improvement of the technological level of the European space launcher industry. The successful implementation of past technologies and the progressive disappearance of technology drivers leaves little base for further advances. It is therefore necessary to implement a policy to meet the technological needs, whether immediate or still only outlined in the future. To cover the first need, ESA is implementing a low cost coordination effort, called ELITE (European Launcher Investigation and Technology Effort); to cover the second need, ESA proposes a program called FESTIP (Future European Space Transportation Investigation Program). These technological activities are to be carried out in close cooperation with industry, research organizations and national agencies. ESA

N92-23752*# National Aeronautics and Space Administration, Washington, DC.
LAUNCH SYSTEMS FOR FUTURE NASA MISSIONS
Ronald J. Harris *In* ESA, Launcher Propulsion Towards the Year 2010 Dec. 1991 p 27-31 (For primary document see N92-23750 14-15)
Copyright Avail: NTIS HC/MF A09; ESA, EPD, ESTEC, Noordwijk, Netherlands, HC 50 Dutch guilders CSCL 22B

The existing launch systems NASA plans to use in the 1990's to accomplish planned missions are reviewed. Current planning for potential new launch systems, both manned and unmanned, are discussed and the associated propulsion technology and development requirements are identified. The review of current launch systems covers small to large expandable launch vehicles. The current status of the Space Shuttle and planned improvements on its main engine and solid rocket boosters are summarized. Primary emphasis is devoted to the discussion of potential new launch system concepts, with particular emphasis given to current plans and concepts for a new heavy lift launch vehicle and a new Space Transportation Main Engine (STME) to be employed by this vehicle. Concepts for a new Personnel Launch System to complement the Space Shuttle, and an Advanced Manned Launch System which might eventually replace the Space Shuttle, are discussed. ESA

N92-23753# Moscow Inst. of Aviation Technology (USSR).
THE USSR LAUNCHERS PROGRAMME
Vasily B. Mishin *In* ESA, Launcher Propulsion Towards the Year 2010 Dec. 1991 p 33-38 (For primary document see N92-23750 14-15)
Copyright Avail: NTIS HC/MF A09; ESA, EPD, ESTEC, Noordwijk, Netherlands, HC 50 Dutch guilders

A review of the USSR launchers is presented. The first generation of Soviet launch vehicles were based on the intercontinental ballistic missile R7, first successfully launched on 22 Aug. 1957. Development of the R5 and R6 is outlined. The following launch vehicles are discussed: Vostok, Soyuz and Molniya, Proton, NI, Energiya, and Zenit. Further directions in the development of launch vehicles are described. ESA

N92-23754*# National Aeronautics and Space Administration. Marshall Space Flight Center, Huntsville, AL.
ROCKET PROPULSION FOR NASA'S EARTH TO ORBIT LAUNCHERS
John P. McCarty *In* ESA, Launcher Propulsion Towards the Year 2010 Dec. 1991 p 43-48 (For primary document see N92-23750 14-15)
Copyright Avail: NTIS HC/MF A09; ESA, EPD, ESTEC, Noordwijk, Netherlands, HC 50 Dutch guilders CSCL 22B

The U.S. and NASA currently use a diverse, flexible family of ETO (Earth To Orbit) launch systems. One element of this family is the expendable launch vehicles. For this element, NASA procures the requisite launch services directly from the commercial sector. The major current U.S. vehicles in this segment are Delta, Atlas, and Titan. The characteristics of these vehicles and rocket propulsion are described. The other element of the current launcher family is the Space Shuttle fleet. The Shuttle propulsion elements, including the Space Shuttle Main Engine (SSME), the Main Propulsion System (MPS), the External Tank (ET), and the Solid Rocket Booster (SRB), are described. Looking ahead, new launch vehicles featuring increased mission safety and reliability, reduced operations requirements and costs and enhanced performance are projected. The elements of these systems would support a modular approach capable of transporting a range of payload. The rocket propulsion elements under consideration for these vehicles, including the Space Transportation Main Engine (STME), propulsion modules, a modified STS external tank and solid rocket motors, are described. ESA

N92-23755# Europropulsion, Suresnes (France).
DEVELOPMENT STATUS OF THE ARIANE 5 SOLID PROPELLANT ENGINE [ETAT D'AVANCEMENT DU DEVELOPPEMENT DU MOTEUR A PROPERGOL SOLIDE D'ARIANE 5] **c20**
Alain Coutrot *In* ESA, Launcher Propulsion Towards the Year 2010 Dec. 1991 p 49-55 In FRENCH (For primary document see N92-23750 14-15)
Copyright Avail: NTIS HC/MF A09; ESA, EPD, ESTEC, Noordwijk, Netherlands, HC 50 Dutch guilders

The definition of the solid propellant engine of the Ariane 5 launch vehicle and its performance are reviewed, and the main results obtained to date in its subassemblies are presented. The objectives and configuration of 10 bench firings and reliability tests are presented. Planning development up to flight qualification is outlined. ESA

N92-23756# Bombrini Parodi-Delfino S.p.A., Colleferro (Italy). Coordination Industrielle Activities Spatiales.
MANUFACTURING PROCESS OF THE ARIANE 5 SEGMENTED PROPELLANT CHARGERS [PROCEDE DE FABRICATION DU CHARGEMENT SEGMENTE DES PROPULSEURS D'ARIANE 5] **c28**
Roberto Isopi and Michel Vidal (Societe Nationale des Poudres et Explosifs, Saint-Medard-en-Jalles, France) *In* ESA, Launcher Propulsion Towards the Year 2010 Dec. 1991 p 57-66 In FRENCH (For primary document see N92-23750 14-15)
Copyright Avail: NTIS HC/MF A09; ESA, EPD, ESTEC, Noordwijk, Netherlands, HC 50 Dutch guilders

Current procedures for the manufacturing of the Ariane 5 propellant chargers are described in the frame of three specially built factories (thermal protection and propellant factories in Italy and the propellant factory in French Guiana). Focus is on design problems to be resolved related principally to the size of the segments, and on original solutions adopted rather than those common to past experience. Nondestructive tests are described. ESA

N92-23757# Chemical Automatics Design Bureau, Voronezh (USSR).
EXPERIENCE OF THE CHEMICAL AUTOMATICS DESIGN BUREAU IN CREATION OF RD-0120 LOX/LH2 LIQUID ROCKET ENGINE WITH THRUST OF 2 mn FOR ENERGIA LAUNCHER **c20**
Stanislav P. Aksjonov, Vladimir S. Rachuk, and A. F. Efimochkin *In* ESA, Launcher Propulsion Towards the Year 2010 Dec. 1991 p 67-72 (For primary document see N92-23750 14-15)
Copyright Avail: NTIS HC/MF A09; ESA, EPD, ESTEC, Noordwijk, Netherlands, HC 50 Dutch guilders

A list of developed space Liquid Rocket Engines (LRE) is presented. More detailed data for the RD-0120 cryogenic engine for the core unit of the Energia launcher are presented. Science, technical and organization problems connected with this engine creation are given. The main specifications of the advanced hydrogen LRE are forecasted. ESA

N92-23758# Aerospatiale, Les Mureaux (France).
DEVELOPMENT STATUS OF THE CRYOTECHNICAL PRINCIPAL STAGE [ETAT DE DEVELOPPEMENT DE L'ETAGE PRINCIPAL CRYOTECHNIQUE]
Jean-Yves Heloret, Serge Eury, and G. Rivol (Cryospace, France) *In* ESA, Launcher Propulsion Towards the Year 2010 Dec. 1991 p 73-76 In FRENCH (For primary document see N92-23750 14-15)
Copyright Avail: NTIS HC/MF A09; ESA, EPD, ESTEC, Noordwijk, Netherlands, HC 50 Dutch guilders

The development status of the Ariane 5 launch vehicle cryotechnical principal stage is reported. The stage principally comprises a commonly based cryotechnic tank arranged front skirt, an arranged engine mount, and the Vulcain engine. The first firing tests of the front part of the stage with engine are planned for the beginning of 1993, and those for the complete stage mid 1993. The qualification should be announced at the beginning of 1995 for an inaugural Ariane 5 flight fixed for 1 Apr. 1995. ESA

N92-23759# Societe Europeenne de Propulsion, Vernon (France).
DEVELOPMENT STATUS OF THE VULCAIN ENGINE **c20**
Serge Eury and E. Kirner (Messerschmitt-Boelkow-Blohm G.m.b.H., Ottobrunn, Germany, F.R.) *In* ESA, Launcher Propulsion Towards the Year 2010 Dec. 1991 p 77-85 (For primary document see N92-23750 14-15)
Copyright Avail: NTIS HC/MF A09; ESA, EPD, ESTEC, Noordwijk, Netherlands, HC 50 Dutch guilders

The development status of the Ariane 5 main cryogenic engine, Vulcain, is presented. Basic project objectives are: low launch cost; very high level of reliability and safety; high payload capability and versatility. Today, the whole Ariane 5 program is in progress in order to insure the availability of a ready to fly launcher, first in an unmanned automatic configuration in the mid 90's, then in a man-rated configuration with the Hermes hypersonic glider. ESA

N92-23760# Aerospatiale, Les Mureaux (France). Div. Systemes Strategiques et Spatiaux.
REUSABLE LAUNCHERS: NEW CONCEPTS AND TECHNOLOGICAL ADVANCES FOR THE MANUFACTURING OF CRYOGENIC TANKS [LANCEURS REUTILISABLES: NOUVEAUX CONCEPTS ET AVANCEES TECHNOLOGIQUES POUR LA FABRICATION DE RESERVOIRS CRYOGENIQUES]
Jean-Pierre Clariou, Jacques Chanteranne, and Gerard Lassourd *In* ESA, Launcher Propulsion Towards the Year 2010 Dec. 1991 p 89-92 In FRENCH (For primary document see

N92-23750 14-15)
Copyright Avail: NTIS HC/MF A09; ESA, EPD, ESTEC, Noordwijk, Netherlands, HC 50 Dutch guilders

Studies on reusable launchers beyond the Ariane 5 program are reported. In the short term, progress on reliability and costs concerning fabrication processes and metallic structure control are being addressed. In the medium term, development characterization and implementation of new materials (metal and composite alloys) allow significant gains in specific performances to be envisaged. The emergence of 'adaptive systems' or 'intelligent materials' may contribute to the response to the specific structural lifetime problem, crucial to the design of reusable launchers. ESA

N92-23761# NPO Energomash, Khimki (USSR).
OXYGEN-KEROSENE LIQUID ROCKET ENGINES WITH POSTBURNING GENERATOR GAS AND HIGH PRESSURE IN COMBUSTION CHAMBER **c20**
Vladimir K. Tchvanov *In* ESA, Launcher Propulsion Towards the Year 2010 Dec. 1991 p 93-96 (For primary document see N92-23750 14-15)
Copyright Avail: NTIS HC/MF A09; ESA, EPD, ESTEC, Noordwijk, Netherlands, HC 50 Dutch guilders

Data on the last generation of RD-170 and RD-120 engines developed with postburning the generator gas in high pressure combustion chamber are given. The development distinction of liquid rocket engines with postburning generator gas in high pressure combustion chamber, reliability control problem and the maintenance quality control system are illustrated on the RD-120 example which was developed simultaneously with the RD-170 engine. The concepts of building the malfunction protection systems for increasing the payload and evaluation of engine technical state by means of functional and test diagnostics methods are considered. Information about the perfection of main aggregates of the engine chamber, gas generator, turbopump, automatic units, and defining engine reliability as a whole, is given. Characteristics of modifications, development of which are possible on the RTD-120 base, are given. ESA

N92-23762# Rockwell International Corp., Canoga Park, CA. Rocketdyne Div.
HEALTH MONITORING OF REUSABLE ROCKET ENGINES **c20**
W. Ezell, S. Barkhoudarian, and G. Cross *In* ESA, Launcher Propulsion Towards the Year 2010 Dec. 1991 p 97-102 (For primary document see N92-23750 14-15)
Copyright Avail: NTIS HC/MF A09; ESA, EPD, ESTEC, Noordwijk, Netherlands, HC 50 Dutch guilders

An extensive study of liquid propellant rocket engine test and flight history data has produced methods for advanced health monitoring currenty under development for application to the Advanced Shuttle, National AeroSpace Plane, and other future propulsion systems. Advanced health monitoring is a systematic approach to instrumentation design and development, signal processing, and knowledge based strategies to infer the operating status of any engine component or system. Properly implemented, advanced health monitoring increases safety and the probability of mission success, significantly reduces turnaround time and maintenance cost, prolongs component life, and reduces life cycle cost. ESA

N92-23763# Societe Europeenne de Propulsion, Vernon (France).
MATERIALS FOR HIGH LIQUID PROPULSION IN 2010 [LES MATERIAUX DESTINES A LA GROSSE PROPULSION LIQUIDE EN 2010] **c24**
Jean-Claude Sylvestre *In* ESA, Launcher Propulsion Towards the Year 2010 Dec. 1991 p 103-116 In FRENCH (For primary document see N92-23750 14-15)
Copyright Avail: NTIS HC/MF A09; ESA, EPD, ESTEC, Noordwijk, Netherlands, HC 50 Dutch guilders

Several examples of materials and processes developed for combustion chamber in the HM7 (cryogenic engine of the third stage of the Ariane 4 launcher) and Vulcain (Ariane 5 engine) programs are presented. The materials must work in extreme temperature conditions (20 to 3500K) and constraints, as well as in particularly aggressive (hydrogen and oxygen) environments. Of particular interest are the ceramic matrix composite materials developed. ESA

N92-23764# Messerschmitt-Boelkow-Blohm G.m.b.H., Munich (Germany, F.R.).
MATERIALS FOR LIQUID PROPELLANT ENGINES **c24**
Wolfgang Keinath and Dietmar Wolf *In* ESA, Launcher Propulsion Towards the Year 2010 Dec. 1991 p 117-131 (For primary document see N92-23750 14-15)
Copyright Avail: NTIS HC/MF A09; ESA, EPD, ESTEC, Noordwijk, Netherlands, HC 50 Dutch guilders

The development of the thrust chamber for the Vulcain engine, planned to power the cryogenic main stage of the future European launcher Ariane 5, is addressed. The development of the material for the combustion chamber liner of the Vulcain engine is described. Since the material selected had not yet been used in European engine technology, suppliers and manufacturers were not familiar with it. The process for manufacturing the liner is presented and some of its basic material properties are discussed. A survey of possible future combustion chamber designs is given in conclusion. ESA

N92-23765# Societe Nationale des Poudres et Explosifs, Vert-Le-Petit (France).
SMALL OR NON POLLUTANT SOLID PROPELLANTS FOR SPACE LAUNCHERS [PROPERGOLS SOLIDES PEU OU NON POLLUANTS POUR LANCEURS SPATIAUX] **c28**
Bernard Finck and Christian Perut *In* ESA, Launcher Propulsion Towards the Year 2010 Dec. 1991 p 137-141 In FRENCH (For primary document see N92-23750 14-15)
Copyright Avail: NTIS HC/MF A09; ESA, EPD, ESTEC, Noordwijk, Netherlands, HC 50 Dutch guilders

The risk of pollution at the propulsion phase product emission level by current or envisaged solid propellants for space launcher accelerator chargers is studied. These propellants contain about 20 percent gaseous hydrochloric acid, an important quantity of aluminum, and other particles or gas prejudicial to the environment. The type considered as most damaging is hydrochloric acid, which it is theoretically possible to suppress. This leads to new solid propellant species containing either hydrochloric gas absorbers, or nonhalogen solid oxidant charges. ESA

N92-23766# Aerospatiale, Les Mureaux (France). Departement Systemes Propulsifs.
FUTURE LAUNCHERS: LARGE SIZE SOLID PROPELLANT MONOLITHIC BOOSTER [LANCEURS FUTURS: PROPULSEUR MONOLITHIQUE DE GRANDES DIMENSIONS A PROPERGOL SOLIDE] **c20**
Max Calabro and Roland Lucas (Societe Nationale des Poudres et Explosifs, Saint-Medard-en-Jalles, France) *In* ESA, Launcher Propulsion Towards the Year 2010 Dec. 1991 p 143-152 In FRENCH (For primary document see N92-23750 14-15)
Copyright Avail: NTIS HC/MF A09; ESA, EPD, ESTEC, Noordwijk, Netherlands, HC 50 Dutch guilders

Problems related to the design and manufacturing of propellant chargers and of structure, for the development of Titan and Ariane 5, are discussed. In particular, the following are addressed: initial choice of profile, fluid flow, and nondestructive test methods; and cost gain on choice of booster structure. The advantage of an integrated factory in achieving cost reduction is shown. ESA

N92-23767# Centre National d'Etudes Spatiales, Paris (France).
DEVELOPMENT OF SOLID PROPELLANT BOOSTER [EVOLUTION DE LA CONCEPTION DES PROPULSEURS A PROPERGOL SOLIDE] **c20**
Michel Eymard and Yves Pelipenko *In* ESA, Launcher Propulsion Towards the Year 2010 Dec. 1991 p 153-158 (For primary document see N92-23750 14-15)
Copyright Avail: NTIS HC/MF A09; ESA, EPD, ESTEC, Noordwijk, Netherlands, HC 50 Dutch guilders

A study aimed at showing the possible development of solid propellant boosters is presented. Two examples are used: low stage boosters (the Ariane 5 P230) and upper stage boosters (MAGE engine). The three main parameters driving the development and improvement of launch vehicles such as Ariane 5 are functional safety (automatic and manned flight); competitiveness with other launch means; and performance.
ESA

N92-23768# Office National d'Etudes et de Recherches Aerospatiales, Paris (France). Energetics Dept.
WHAT FUTURE FOR HYBRID ROCKET PROPULSION? c20
Paul Kuentzmann and H. J. Sternfeld (Deutsche Forschungsanstalt fuer Luft- und Raumfahrt, Lampoldshausen, Germany, F.R.) *In* ESA, Launcher Propulsion Towards the Year 2010 Dec. 1991 p 159-169 (For primary document see N92-23750 14-15)
Copyright Avail: NTIS HC/MF A09; ESA, EPD, ESTEC, Noordwijk, Netherlands, HC 50 Dutch guilders

A few general concepts concerning hybrid propulsion are reviewed and a synopsis of European work and recent activities published in open literature is given. A critical examination of the potential advantages of hybrid propulsion compared with propulsion by liquid or solid propellants is given. The performance, operational flexibility, safety, security, reliability, cost and environmental impact characteristics are examined. A few specific problems of hybrid propulsion are mentioned. The possible applications of hybrid propulsion for space launchers are examined. Different versions of hybrid rockets are identified and the version best suited to each application is proposed. A strategy which would allow the future of hybrid propulsion in space activity to be clarified and development to be rationally started is outlined in conclusion.
ESA

N92-23645*# Engineering and Economics Research, Inc., Houston, TX. Space Services Div.
LAUNCH VEHICLE FOR ORBITAL MISSIONS: COMET
Deke Slayton *In* NASA, Washington, Proceedings of the Second Annual Symposium on Industrial Involvement and Successes in Commercial Space 1991 42 p (For primary document see N92-23643 14-12)
Avail: NTIS HC/MF A11 CSCL 22B

N92-23797# Centre National d'Etudes Spatiales, Toulouse (France).
DYNAMIC LOAD CASES ON ARIANE 5
B. Chemoul and E. Louaas *In* ESA, Spacecraft Structures and Mechanical Testing, Volume 1 Oct. 1991 p 117-122 (For primary document see N92-23780 14-18)
Copyright Avail: NTIS HC/MF A21

N92-23798# Aerospatiale, Les Mureaux (France). Secteur Etudes Mecaniques et de Synthese.
MULTI PARAMETER OPTIMIZATION ON ARIANE 5
G. Boullenger *In* ESA, Spacecraft Structures and Mechanical Testing, Volume 1 Oct. 1991 p 123-127 In FRENCH (For primary document see N92-23780 14-18)
Copyright Avail: NTIS HC/MF A21

N92-23808# European Space Agency, Paris (France).
ARIANE 5 STRUCTURAL DEFINITION OF THE UPPER COMPOSITE
A. L. GonzalezBlasquez *In its* Spacecraft Structures and Mechanical Testing, Volume 1 Oct. 1991 p 189-195 (For primary document see N92-23780 14-18)
Copyright Avail: NTIS HC/MF A21

N92-23810# Construcciones Aeronauticas S.A., Madrid (Spain). Div. Espacio.
BRIEF HISTORY OF THE DEVELOPMENT OF THE EPS-STRUCTURE
J. Martin *In* ESA, Spacecraft Structures and Mechanical Testing, Volume 1 Oct. 1991 p 203-208 (For primary document see N92-23780 14-18)
Copyright Avail: NTIS HC/MF A21

N92-23811# Centre National d'Etudes Spatiales, Paris (France). Direction des Lanceurs.
ARIANE 4 INTERNAL ACOUSTIC ENVIRONMENT: INTERPRETATION OF FLIGHT DATA WITH A VIBROACOUSTIC MODEL OF THE UPPER PART OF THE LAUNCHER
B. Ritchie and M. Beldi (STRACO S.A., Compiegne, France) *In* ESA, Spacecraft Structures and Mechanical Testing, Volume 1 Oct. 1991 p 211-217 (For primary document see N92-23780 14-18)
Copyright Avail: NTIS HC/MF A21

N92-23921*# National Aeronautics and Space Administration. Goddard Space Flight Center, Greenbelt, MD.
THE DELTA 2 LAUNCHER
Gilbert W. Ousley, Sr. *In* ESA, The Solid-Earth Mission Aristoteles Dec. 1991 p 91-94 (For primary document see N92-23910 14-12)
Avail: NTIS HC/MF A06; ESA, EPD, ESTEC, Noordwijk, Netherlands, HC 50 Dutch guilders CSCL 22B

16 SPACE TRANSPORTATION

Includes passenger and cargo space transportation, e.g., shuttle operations; and space rescue techniques.

For related information see also *03 Air Transportation and Safety* and *18 Spacecraft Design, Testing and Performance.* For space suits see *54 Man/System Technology and Life Support.*

N92-23524*# National Aeronautics and Space Administration. Marshall Space Flight Center, Huntsville, AL.
STS INVESTIGATORS' GUIDE
Oct. 1989 84 p Original contains color illustrations
(NASA-TM-105523; NAS 1.15:105523) Avail: NTIS HC/MF A05; 1 functional color page CSCL 22B

The capability of the Space Transportation System (STS), the Space Shuttle, to support crew tended and free flyer research in low Earth orbit has opened new possibilities for science in space. For the first time, research equipment can be put into orbit routinely, operated in either a shirtsleeve environment or exposed to space, and then returned to the investigator. NASA, operator of the Shuttle, has implemented a variety of programs to ensure that anyone with a worthy research idea can take advantage of this opportunity. Investigators ranging from high school students to renowned space scientists have already used the Shuttle as a platform for making Earth, atmospheric, and astronomical observations; for performing space plasma physics measurements; and for exploring the effects of microgravity on living organisms and physical processes. For investigators considering a flight experiment for the first time, this guide explains what the Shuttle has to offer, how to arrange to fly an experiment, and what to expect once preparations for the flight are under way.
Author

N92-23980*# National Academy of Sciences - National Research Council, Washington, DC.
FROM EARTH TO ORBIT
Joseph G. Gavin, Jr., Edmund Blond, Yvonne C. Brill, Bernard Budiansky, Robert S. Cooper, Wolfgang H. Demisch, Clark W. Hawk, Jack L. Kerrebrock, Byron K. Lichtenberg, and Arthur Mager (Mager, Artur, Los Angeles, CA) 1992 101 p
(Contract NASw-4003)
(NASA-CR-190216; NAS 1.26:190216) Avail: NTIS HC/MF A06 CSCL 22B

Within this document, the National Research Council (NRC) assesses the requirements, benefits, technological feasibility, and roles of Earth-to-orbit transportation options that could be developed in support of the national space program. Among the topics covered are launch vehicles and infrastructure, propulsion, and technology.
H.A.

N92-23650*# Vertex Pharmaceuticals, Cambridge, MA.
CENTER FOR MACROMOLECULAR CRYSTALLOGRAPHY, UNIVERSITY OF ALABAMA IN BIRMINGHAM
Manuel A. Navia *In* NASA, Washington, Proceedings of the Second Annual Symposium on Industrial Involvement and Successes in Commercial Space 1991 3 p (For primary document see N92-23643 14-12)
Avail: NTIS HC/MF A11 CSCL 10B

N92-23796*# National Aeronautics and Space Administration. Lyndon B. Johnson Space Center, Houston, TX.
A REVIEW OF SPACE SHUTTLE PAYLOAD-BAY LIFT-OFF FLIGHT DATA AND ANALYSIS COMPARISONS
David A. Hamilton, Nancy E. Tengler, B. N. Nguyen, and Carl A. Lauritzen (Lockheed Electronics Co., Houston, TX.) *In* ESA, Spacecraft Structures and Mechanical Testing, Volume 1 Oct. 1991 p 111-116 (For primary document see N92-23780 14-18)
Copyright Avail: NTIS HC/MF A21 CSCL 22B

N92-23823# Dassault Espace, Saint-Cloud (France). Centre Spatial.
THE CHALLENGE OF THE HERMES TPS SHINGLES
Christian Petiau *In* ESA, Spacecraft Structures and Mechanical Testing, Volume 1 Oct. 1991 p 299-306 (For primary document see N92-23780 14-18)
Copyright Avail: NTIS HC/MF A21

17 SPACE COMM., SPACECRAFT COMM., COMMAND & TRACKING

Includes telemetry; space communications networks; astronavigation and guidance; and radio blackout.

For related information see also *04 Aircraft Communications and Navigation* and *32 Communications and Radar.*

N92-23187*# National Aeronautics and Space Administration. Lewis Research Center, Cleveland, OH.
ACHIEVING SPECTRUM CONSERVATION FOR THE MINIMUM-SPAN AND MINIMUM-ORDER FREQUENCY ASSIGNMENT PROBLEMS
Ann O. Heyward 1992 28 p Presented at the 14th International Communications Satellite Systems Conference, Washington, DC, 22-26 Mar. 1992; sponsored by AIAA Previously announced in IAA as A92-29883
(NASA-TM-105649; E-7010; NAS 1.15:105649; AIAA-92-1960)
Avail: NTIS HC/MF A03 CSCL 17B

Effective and efficient solutions of frequency assignment problems assumes increasing importance as the radiofrequency spectrum experiences ever increasing utilization by diverse communications services, requiring that the most efficient use of this resource be achieved. The research presented explores a general approach to the frequency assignment problem, in which such problems are categorized by the appropriate spectrum conserving objective function, and are each treated as an N-job, M-machine scheduling problem appropriate for the objective. Results obtained and presented illustrate that such an approach presents an effective means of achieving spectrum conserving frequency assignments for communications systems in a variety of environments. Author

18 SPACECRAFT DESIGN, TESTING AND PERFORMANCE

Includes satellites; space platforms; space stations; spacecraft systems and components such as thermal and environmental controls; and attitude controls.

For life support systems see *54 Man/System Technology and Life Support.* For related information see also *05 Aircraft Design, Testing and Performance, 39 Structural Mechanics,* and *16 Space Transportation.*

N92-23526*# Virginia Polytechnic Inst. and State Univ., Blacksburg. Dept. of Aerospace and Ocean Engineering.
SOLAR-ELECTRIC-PROPULSION CARGO VEHICLES FOR SPLIT/SPRINT MARS MISSION
Christopher E. Callaghan, Michael D. Crowe, Matthew J. Swis, Marcus R. Mickney, C. Keith Montgomery, Robert Walters, and Scott Thoden Jun. 1991 84 p
(Contract NASw-4435)
(NASA-CR-189983; NAS 1.26:189983) Avail: NTIS HC/MF A05 CSCL 22B

In support of the proposed exploration of Mars, an unmanned cargo ferry SEMM1 (Solar Electric Mars Mission) was designed. The vehicle is based on solar electric propulsion, and required to transport a cargo of 61,000 kg. The trajectory is a combination of spirals; first, out from LEO, then around the sun, then spiral down to low Mars orbit. The spacecraft produces 3.03 MWe power using photovoltaic flexible blanket arrays. Ion thrusters using argon as a propellant were selected to drive the ship, providing about 60 Newtons of thrust in low Earth orbit. The configuration is based on two long truss beams to which the 24 individual, self-deployable, solar arrays are attached. The main body module supports the two beams and houses the computers, electrical, and control equipment. The thruster module is attached to the rear of the main body, and the cargo to the front. Author

N92-23530*# SECA, Inc., Huntsville, AL.
ORBITAL MANEUVERING VEHICLE (OMV) PLUME AND PLUME EFFECTS STUDY Final Report
Sheldon D. Smith 15 Dec. 1991 104 p
(Contract NAS8-38243)
(NASA-CR-184292; NAS 1.26:184292; SECA-TR-92-02) Avail: NTIS HC/MF A06 CSCL 22B

The objective was to characterize the Orbital Maneuvering Vehicle (OMV) propulsion and attitude control system engine exhaust plumes and predict the resultant plume impingement pressure, heat loads, forces, and moments. Detailed description is provided of the OMV gaseous nitrogen (GN2) thruster exhaust plume flow field characteristics calculated with the RAMP2 snd SFPGEN computer codes. Brief descriptions are included of the two models, GN2 thruster characteristics and RAMP2 input data files. The RAMP2 flow field could be recalculated by other organizations using the information presented. The GN2 flow field can be readily used by other organizations who are interested in GN2 plume induced environments which require local flow field properties which can be supplied using the SFPGEN GN2 model. Author

N92-23780# European Space Agency, Paris (France).
SPACECRAFT STRUCTURES AND MECHANICAL TESTING, VOLUME 1
W. R. Burke, comp. (European Space Agency. European Space Research and Technology Center, ESTEC, Noordwijk, Netherlands) Oct. 1991 487 p In ENGLISH and FRENCH Conference held in Noordwijk, Netherlands, 24-26 Apr. 1991; sponsored by ESA, CNES, and DLR
(ESA-SP-321-Vol-1; ISBN-92-9092-126-9; ISSN-0379-6566; ETN-92-91208) Copyright Avail: NTIS HC/MF A21

Papers presented at the conference were directly associated with space project applications of scientific, Earth observation and telecommunication satellites, reporting hardware design, development and testing and other related experiences. Volume 1 presents sessions on the following: space plane and reentry;

vibroacoustics; testing (systems); multibody dynamics (microgravity); launcher (development and loads/optimization); space stations; dynamic identification; analysis (methods, dynamics, fluid/structure interaction); and materials (composites, characterization, fracture/fatigue). The most important points identified are the need for a better understanding of launcher loads, qualification requirements imposed by launcher authorities to cover launch events, and particular qualification requirements imposed by space projects and programs to ensure mission success. For individual titles, see N92-23781 through N92-23850.

N92-23781# National Space Development Agency, Tokyo (Japan).

DEVELOPMENT OF JAPANESE EXPERIMENT MODULE

Fumio Otsuki, Kazuhiko Kamesaki, Kuniaki Shiraki, and Kazuyuki Tasaki *In* ESA, Spacecraft Structures and Mechanical Testing, Volume 1 Oct. 1991 p 3-8 (For primary document see N92-23780 14-18)

Copyright Avail: NTIS HC/MF A21

The National Space Development Agency of Japan (NASDA) started preliminary design of the JEM (Japanese Experiment Module) in Jan. 1990 along with the component development test activities, and has a plan to conduct the preliminary design review in early 1992. NASDA's JEM program faces many challenges as it strives to overcome the large number of technical obstacles associated with designing, developing and integrating the JEM. An overall picture of the JEM program structural development activities including design, testing and analysis activities, is presented with focus on some technical challenges which have been or must be surmounted in order to assure JEM structural safety. Some approaches taken to implement these solutions are introduced. ESA

N92-23782# Erno Raumfahrttechnik G.m.b.H. Bremen (Germany, F.R.).

THE COLUMBUS FREE FLYING LABORATORY: MECHANICAL DESIGN ASPECTS

Joachim Guelpen *In* ESA, Spacecraft Structures and Mechanical Testing, Volume 1 Oct. 1991 p 9-17 (For primary document see N92-23780 14-18)

Copyright Avail: NTIS HC/MF A21

The Columbus Free Flyer has a three year mission in low Earth orbit with the primary objective to provide microgravity laboratory capabilities. The particular mechanical requirements resulting from this mission are explained, relevant design features are presented, and the verification approach envisaged in the development program leading to a launch of the laboratory in 2001 is outlined. ESA

N92-23783# Boeing Aerospace and Electronics Co., Huntsville, AL. Defense and Space Group.

STRUCTURAL ASSESSMENT OF THE SPACE STATION FREEDOM'S PRESSURIZED ELEMENTS

R. L. Grant *In* ESA, Spacecraft Structures and Mechanical Testing, Volume 1 Oct. 1991 p 19-25 (For primary document see N92-23780 14-18)

Copyright Avail: NTIS HC/MF A21

The design of the Space Station Freedom (SSF) pressurized element structure and the requirements that affect the structure and its associated mechanisms are unique and particularized to the unique set of load and functional environments. The procedures to develop the most significant structural requirements are described and typical results as they are known at the end of the preliminary design phase are presented. Loads, acoustic, thermal environments, and the meteorite/orbital debris environments are discussed. The materials chosen for SSF, as well as the rationale, are discussed. The verification job is described. Detailed stress analyses, backed up with development tests, are used to ensure that the SSF pressurized element structure meets all imposed requirements. When the final design is complete, special flight quality hardware is built and tested to prove that the hardware is qualified for flight. The structural qualification program planned for SSF is briefly described. ESA

N92-23784# European Space Agency. European Space Research and Technology Center, ESTEC, Noordwijk (Netherlands).

THE VALIDATION OF HYDROCODES FOR ORBITAL DEBRIS IMPACT SIMULATION

M. Lambert, J. D. Frey, J. F. Rios, X. Garaud, J. Dubois, and E. Schneider (Fraunhofer Inst. fuer Kurzzeitdynamik, Freiburg im Breisgau, Germany, F.R.) *In its* Spacecraft Structures and Mechanical Testing, Volume 1 Oct. 1991 p 29-35 (For primary document see N92-23780 14-18)

Copyright Avail: NTIS HC/MF A21

Orbital debris poses a danger for spacecraft in orbit. Protection against this threat is obtained by shielding. One or more sheets placed at some distance from the structure to be protected can minimize the damage inflicted by projectiles at high velocity. The range of velocity between 0 and 8 km/s is well covered by tests. Unfortunately, the average velocity of debris in low Earth orbit is above 10 km/s with a maximum velocity around 15 km/s. A methodology aimed at validating the numerical approach and to predict and extrapolate the behavior of multishock shields in the velocity range between 8 and 15 km/s is presented. The formation of the debris cloud, after perforation of the shields on the one hand and the generation and propagation of damage in the backwall on the other hand, is a key factor. It is examined, discussed and illustrated with correlation between numerical simulation, analytical formulae and test results. ESA

N92-23785# McDonnell-Douglas Space Systems Co., Huntington Beach, CA.

MATERIAL CONSIDERATIONS FOR HABITABLE AREAS OF MANNED SPACECRAFT

Cherie Jones, Kaia Simpson, Brian Vickers, Paul Ledoux, and Hank Babel *In* ESA, Spacecraft Structures and Mechanical Testing, Volume 1 Oct. 1991 p 37-42 (For primary document see N92-23780 14-18)

Copyright Avail: NTIS HC/MF A21

Important material considerations relative to the design of habitable areas of manned spacecraft are examined. The issues considered include flammability, toxic offgassing, particulate generation, fungus growth, odor, and general corrosion. Specific material applications such as hook and loop (Velcro (trademark) type) fasteners and protective coatings for the interior of pressurized structures are also discussed relative to these issues. Greatest emphasis is shown to have been appropriately placed on characterizing material for flammability and toxic offgassing, areas where life threatening situations could occur if improper material selections are made. Less emphasis was placed on the areas of particulate generation and fungus growth. Unresolved issues were identified in all areas of the spacecraft. ESA

N92-23786# Messerschmitt-Boelkow-Blohm G.m.b.H., Bremen (Germany, F.R.).

PROTECTION OF SPACECRAFT AGAINST METEROID/ORBITAL DEBRIS IMPACTS

Hans-G. Reimerdes *In* ESA, Spacecraft Structures and Mechanical Testing, Volume 1 Oct. 1991 p 43-49 Prepared in cooperation with Erno Raumfahrttechnik G.m.b.H. Bremen, Germany, F.R. (For primary document see N92-23780 14-18)

Copyright Avail: NTIS HC/MF A21

As a result of the space activities during the last three decades there are lots of artificial particles orbiting the Earth, the so called orbital debris. These particles increase the probability that spacecraft will be hidden during mission considerably. Especially large spacecraft planned for long missions will be endangered and have to be protected against this new threat. Techniques for protection of spacecraft are presented and compared. Semi-empirical formulae for calculation of dimensions of protection systems are given. Based on these formulae and on the direction distribution of the particles, three different approaches for reduction of the required mass of the protection system are presented. ESA

N92-23787# Centre National d'Etudes Spatiales, Toulouse (France).
COUPLED LOAD ANALYSIS: SCATTER RELATED TO MODEL UNCERTAINTIES **c39**
P. W. Bousquet, F. Mercier, and M. Klein (European Space Agency. European Space Research and Technology Center, ESTEC, Noordwijk, Netherlands) *In* ESA, Spacecraft Structures and Mechanical Testing, Volume 1 Oct. 1991 p 53-58 (For primary document see N92-23780 14-18)
Copyright Avail: NTIS HC/MF A21

Work carried out within the frame of a transient test feasibility study dedicated to the influence of spacecraft structural misrepresentation on Coupled Load Analysis (CLA) results is presented. The CLA's are performed using the equivalent force method and model synthesis results. The study has a statistical approach in which regular Monte Carlo procedures are applied to estimate CLA scatter distribution. Two main applications are presented; both are limited to the launcher longitudinal axis, at one flight event (second stage burnout), for an Ariane 3 version. An envelope for the shock spectra of any satellite compatible with the Ariane user's manual is calculated in terms of model characteristics. Results can be compared with Ariane's first 15 flight measurements. The influence of the uncertainties about the modal parameters (frequency and effective masses) of a given specimen is simulated. In this case, at certain frequencies, the greatest shock spectra can reach values twice as high as the nominal level. ESA

N92-23788# Frazer-Nash Consultancy Ltd., Leatherhead (England).
THE USE OF MODAL SYNTHESIS IN CONJUNCTION WITH NONLINEAR TRANSIENT DYNAMIC ANALYSIS **c39**
S. A. Challener and A. J. Vibert *In* ESA, Spacecraft Structures and Mechanical Testing, Volume 1 Oct. 1991 p 59-62 Sponsored in part by Ministry of Defence (For primary document see N92-23780 14-18)
Copyright Avail: NTIS HC/MF A21

Two methods by which modal synthesis can be used as part of nonlinear dynamic analysis are presented. The first method is based on the DYNA3D finite element code and describes the approach taken to incorporate a model synthesis capability in the code. The second method is demonstrated for a missile rail launcher for which a particular computer code was developed based on the model synthesis approach. Examples of both methods are presented. ESA

N92-23789# MATRA Espace, Toulouse (France). Dept. of Mechanical Engineering.
IMPROVEMENTS FOR INTERPRETATION OF STRUCTURAL DYNAMICS CALCULATION USING EFFECTIVE PARAMETERS FOR SUBSTRUCTURES **c39**
T. Berthelon and A. Capitaine *In* ESA, Spacecraft Structures and Mechanical Testing, Volume 1 Oct. 1991 p 63-68 (For primary document see N92-23780 14-18)
Copyright Avail: NTIS HC/MF A21

In the past few years, with the extensive use of the finite element method, the concept of effective masses was introduced to analyze the satellites structure. Up to now, the results used were applied to the whole system. The transfer of the use of effective parameters from the whole structure to all the subsystems, in order to define precisely which part of the spacecraft will tend to vibrate, is proposed. The theoretical study, the introduction of the new effective parameters and some examples are presented. ESA

N92-23790# Intespace, Toulouse (France).
ACOUSTIC ABSORPTION DUE TO SPECIMEN IN TEST IN A REVERBERANT CHAMBER **c71**
A. Girard and C. Blanchard *In* ESA, Spacecraft Structures and Mechanical Testing, Volume 1 Oct. 1991 p 71-75 (For primary document see N92-23780 14-18)
(Contract ESA-7821/88)
Copyright Avail: NTIS HC/MF A21

With the objective of determining an empirical law for the acoustic absorption of a specimen in test in a reverberant chamber, a methodology using commonly available test data is presented. The approach is based on the determination of the reverberation times at test cut off, leading to the acoustic absorption losses, then to the specimen acoustic absorption coefficients. This methodology is then applied to the acoustic test results of five satellite specimens already tested in chamber. The empirical law is derived from these results by averaging, providing a quick estimation of acoustic absorption losses in any chamber with known characteristics and a check of the capability of acoustic generators to achieve specifications. ESA

N92-23791# MATRA Espace, Toulouse (France). Dept. of Mechanical Engineering.
MAXIMAL MODAL ENERGY METHOD: AN OVERVALUING TOOL FOR LOW FREQUENCY PREDICTION OF STRUCTURE ACOUSTIC RESPONSE **c71**
B. Laviron, P. Herman, and S. DeZotti *In* ESA, Spacecraft Structures and Mechanical Testing, Volume 1 Oct. 1991 p 77-82 (For primary document see N92-23780 14-18)
Copyright Avail: NTIS HC/MF A21

The development of a numerical tool for elastoacoustics, the Maximal Modal Energy (MME) method, is demonstrated. Stress is laid upon the advantages and limitations of the MME method. Comparisons are drawn between this method, results of tests performed on space structures, and a classical modal superposition tool. ESA

N92-23792# Industrieanlagen-Betriebsgesellschaft m.b.H., Ottobrunn (Germany, F.R.).
NUMERICAL AND EXPERIMENTAL STUDY OF NOISE GENERATED BY A VIBRATING PLATE **c71**
O. vonEstorff, A. Homm, and F. Bartels (Fraunhofer-Forschungsgruppe fuer Hydroakustik, Ottobrunn, Germany, F.R.) *In* ESA, Spacecraft Structures and Mechanical Testing, Volume 1 Oct. 1991 p 83-87 (For primary document see N92-23780 14-18)
Copyright Avail: NTIS HC/MF A21

Applying an indirect boundary element method the sound radiation of a vibrating cantilever plate is investigated. The numerically obtained results are compared with measured data in order to show the accuracy and applicability of the numerical approach. The study clearly enhances the confidence in the computational solution of noise problems which are of particular importance in connection with the qualification of large spacecraft structures like the Hermes. ESA

N92-23793# Cambridge Univ. (England). Dept. of Engineering.
DEVELOPMENT OF FATIGUE DAMAGE MECHANICS FOR APPLICATION TO THE DESIGN OF DAMAGE-TOLERANT COMPOSITE COMPONENTS **c39**
P. W. R. Beaumont, S. M. Spearing, and M. T. Kortschot *In* ESA, Spacecraft Structures and Mechanical Testing, Volume 1 Oct. 1991 p 91-96 Sponsored in part by Science Research Council (For primary document see N92-23780 14-18)
Copyright Avail: NTIS HC/MF A21

The extension of basic damage models of composite failure to design is a powerful tool in the development of design procedures for composite hardware. The basic principle that dominates is the recognition that the strength of a composite changes with accumulated damage and that the composite can retain adequate strength by creating a microstructure that permits regions of subcritical damage growth. This involves the development of computational models that describe changes in microstructure brought about by stress which simulate those in service. Application of practical damage mechanics analysis can be made to the prediction of residual strength and stiffness and fatigue life of fiber composites. ESA

N92-23794# Deutsche Forschungsanstalt fuer Luft- und Raumfahrt, Brunswick (Germany, F.R.). Inst. fuer Strukturmechanik.

CHARACTERIZATION OF INTERLAMINAR MODE 1 AND MODE 2 FRACTURE IN CFRP LAMINATES **c24**

Rudolf Prinz and Michael Gaedke *In* ESA, Spacecraft Structures and Mechanical Testing, Volume 1 Oct. 1991 p 97-102 (For primary document see N92-23780 14-18)

Copyright Avail: NTIS HC/MF A21

The interlaminar fracture toughness, in general, is determined by using double cantilever beam and end notched flexure tests for mode 1 and mode 2 fracture, respectively. The transverse crack tension test and the transverse crack tension compression test for mode 2 fracture, which utilized continuous graphite fiber epoxy laminates, whose central plies were separated at the specimen center prior to curing, are presented. In the course of cycling loading a lateral crack developed in the area of the separations from which two mode 2 delaminations initiated at each of the separated and the continuous ply interfaces. For the compliance and the energy release rate simple equations were derived. The maximum cyclic energy release rate as a function of the delamination (crack front) propagation rate in correlation with the critical buckling state of separated plies in transverse crack tension compression test can be used for fatigue life estimations or for residual compressive strength calculations. ESA

N92-23795# Framasoft + CSI, Paris (France).

FATIGUE ANALYSIS UNDER RANDOM STRESSES **c39**

A. Ricard *In* ESA, Spacecraft Structures and Mechanical Testing, Volume 1 Oct. 1991 p 103-107 Prepared in cooperation with Commission of the European Communities, Brussels, Belgium (For primary document see N92-23780 14-18)

(BRITE Proj. P2381-5)

Copyright Avail: NTIS HC/MF A21

Fatigue is a primary risk of failure of metallic structural and mechanical components which respond dynamically to random loading, oscillatory stresses producing fatigue at 'hot spots'. However an engineering description of fatigue behavior is complicated because the fatigue process consists of two phases (crack initiation and propagation), there is substantial variability in failure data even in well controlled experiments, and stress processes are often very complicated. A classification of the high cycle fatigue design procedures for a structural component subjected to a stationary random stress process which in general can be wide band is proposed. Different methods to estimate the fatigue life time of structures, including threshold and mean stress effects are described. Such procedures could be useful in design of components for motor cars, aerospace vehicles, and offshore platforms. ESA

N92-23796*# National Aeronautics and Space Administration. Lyndon B. Johnson Space Center, Houston, TX.

A REVIEW OF SPACE SHUTTLE PAYLOAD-BAY LIFT-OFF FLIGHT DATA AND ANALYSIS COMPARISONS **c16**

David A. Hamilton, Nancy E. Tengler, B. N. Nguyen, and Carl A. Lauritzen (Lockheed Electronics Co., Houston, TX.) *In* ESA, Spacecraft Structures and Mechanical Testing, Volume 1 Oct. 1991 p 111-116 (For primary document see N92-23780 14-18)

Copyright Avail: NTIS HC/MF A21 CSCL 22B

The design evolution of Space Shuttle payloads to be launched requires structural analyses and testing, based on Shuttle load environments, to ensure flight safety and mission success. The adequacy of predicted load environments is continually assessed against flight and ground measured data. The Space Shuttle program has utilized extensive flight measurements to assess payload bay environments. As part of the orbital flight test program on STS-1 through STS-5, the orbiter Columbia was equipped with a broad range of instrumentation, including accelerometers and microphone in the payload bay. The orbiter Challenger was equipped with payload bay measurement systems on six of its flights, and the orbiter Discovery was similarly instrumented beginning with STS-26. The payload bay data, along with other measurements recorded on these flights, are compared to design load requirements for payloads, and updates are made as necessary. ESA

N92-23797# Centre National d'Etudes Spatiales, Toulouse (France).

DYNAMIC LOAD CASES ON ARIANE 5 **c15**

B. Chemoul and E. Louaas *In* ESA, Spacecraft Structures and Mechanical Testing, Volume 1 Oct. 1991 p 117-122 (For primary document see N92-23780 14-18)

Copyright Avail: NTIS HC/MF A21

Ariane 5 will be able to launch payloads weighing up to 20 tons. The environmental requirements for these various payloads must be given early in the launcher's development's program. The first launcher's intrumented tests have not yet begun and for this reason some load cases still remain unknown (e.g. engines thrust decay). To find those load cases, assumptions must be made using the experience of previous programs. If this experience does not exist and if the expected load cases are supposed to be critical, particular studies must be carried out (e.g. blast wave). The low frequency load cases considered on Ariane 5 to establish the environmental requirements depend on the flight phases: lift off (blastwave, symmetrical and unsymmetrical ignition); aerodynamic flight (transonic or max dynamic pressure) gust; and end of stage's thrust (strap on boosters, Vulcain, upperstage). Several causes are presented and analyzed. Applications with Astral are shown considering the dynamical coupling between Ariane 5 and standard payloads. ESA

N92-23798# Aerospatiale, Les Mureaux (France). Secteur Etudes Mecaniques et de Synthese.

MULTI PARAMETER OPTIMIZATION ON ARIANE 5 **c15**

G. Boullenger *In* ESA, Spacecraft Structures and Mechanical Testing, Volume 1 Oct. 1991 p 123-127 In FRENCH (For primary document see N92-23780 14-18)

Copyright Avail: NTIS HC/MF A21

The OPTI software of the SAMCEF program was used to automatically optimize the forward skirt of the Ariane 5 launcher. The results obtained were used to confirm the dimensioning and evaluate the influence of certain specifications on the mass balance of the subassembly, so as to propose modifications to the architect. ESA

N92-23799# LMS International, Leuven (Belgium).

AN ADVANCED SYSTEM FOR ENVIRONMENTAL SINE TESTING: BASIC PRINCIPLES REVISITED **c39**

J. Leuridan, R. Mangelschots, F. Declerq, and G. Bossaert *In* ESA, Spacecraft Structures and Mechanical Testing, Volume 1 Oct. 1991 p 131-134 (For primary document see N92-23780 14-18)

Copyright Avail: NTIS HC/MF A21

The testing of ever more complex mechanical systems for more stringent environmental conditions has put increased requirements on the systems that are used for closed loop vibration control and data reduction from laboratory or fielded systems. For testing based on sine excitation, this implies increased capability for speed (sweep rates), while maintaining measurement accuracy and resolution even for structures that exhibit resonances with high Q factors, and from noisy data. An implementation of a sine data reduction system using state of the art hardware (computer workstation, modular multichannel front end) and based on accepted principles for sine data processing is described. ESA

N92-23800# Ometron Ltd., London (England).

NON CONTACTING MEASUREMENT OF VIBRATION **c39**

A. J. Barker *In* ESA, Spacecraft Structures and Mechanical Testing, Volume 1 Oct. 1991 p 135-138 (For primary document see N92-23780 14-18)

Copyright Avail: NTIS HC/MF A21

Non-contacting methods of measurement have intrinsic advantages in many engineering applications. A non-contacting laser Doppler sensor was developed which enables conventional vibration measurements to be obtained at up to 200 m range with

a 1 mW laser beam. The sensor is able to accommodate the examination of complex shapes without refocus by virtue of an exceptional working depth of field of several meters. Near real time mapping of full field vibration patterns was achieved by combining the new sensor with special purpose electronic hardware controlled through an industry standard personal computer. The principle of operation of this new system and its broad capabilities in non-destructive testing is described and vibrational mode shape visualization is illustrated by application examples. ESA

N92-23801# Indian Space Research Organization, Bangalore. Mechanical Systems Group.
ON DEVELOPMENT OF AUTOMATED STATIC LOADING SYSTEM FOR SPACECRAFT STRUCTURES **c39**
A. V. Patki and R. Samuel *In* ESA, Spacecraft Structures and Mechanical Testing, Volume 1 Oct. 1991 p 139-144 (For primary document see N92-23780 14-18)
Copyright Avail: NTIS HC/MF A21

The quasi static loads on large spacecraft structures experienced during launch are generally simulated by static loading. With optimized structure and the structural model being used as flight model spares, it is necessary that the static load tests are conducted in such a manner that overloading or catastrophic failure do not occur during such tests. With this objective an Automated Static Test System (ASTS) was successfully developed, evaluated and used on a large communication satellite to demonstrate its utility in smooth conduct of the qualification tests. ESA

N92-23802# Veritas Research A.S., Hovik (Norway).
NONLINEAR FINITE-ELEMENT ANALYSIS OF SANDWICH SHELLS **c39**
O. Amlid and P. G. Bergan *In* ESA, Spacecraft Structures and Mechanical Testing, Volume 1 Oct. 1991 p 147-152 (For primary document see N92-23780 14-18)
Copyright Avail: NTIS HC/MF A21

Analysis of sandwich plates and shells poses a series of theoretical and practical problems to the design engineer. Local and global deformation modes and phenomena which are negligible when analyzing homogeneous members can turn out to be of significance when the member is layered and of sandwich type. In addition to this, a sandwich panel can exhibit failure modes which are unknown to homogeneous panels. Highly comprehensive, nonlinear finite element analysis capabilties are required to solve such problems accurately. A nonlinear sandwich element based on the free formulation theory is described. It was implemented in a general purpose finite element program with capabilities for solving nonlinear static and dynamic problems (FENRIS). ESA

N92-23803# Rome Univ. (Italy). Dipartimento Aerospaziale.
INFLUENCE OF THE SUBSTRATE ON THE SOLAR CELLS INTERCONNECTOR: STRESS DISTRIBUTION AND FATIGUE LIFE PREDICTION **c39**
S. Tizzi, M. Marchetti, and S. LaTerza *In* ESA, Spacecraft Structures and Mechanical Testing, Volume 1 Oct. 1991 p 153-159 Sponsored by Fabrica Italiana Apparecchiature Radioelettriche S.p.A. (For primary document see N92-23780 14-18)
Copyright Avail: NTIS HC/MF A21

The analysis of the influence of the composite material substrates in the stress distribution in the solar array components, solar cell, adhesive, substrate and interconnector, is addressed. A fatigue study for the life prediction of the interconnector, in low and geostationary orbits, and a further study of the substrate composite material strength were performed. ESA

N92-23804# Politecnico di Torino (Italy). Dept. of Aerospace Engineering.
BUCKLING OF SIMPLY SUPPORTED AND CLAMPED ANISOTROPIC PLATES UNDER COMBINED LOADS **c39**
G. Romeo and G. Frulla *In* ESA, Spacecraft Structures and Mechanical Testing, Volume 1 Oct. 1991 p 161-166 Sponsored by Ministry of University (For primary document see N92-23780 14-18)
Copyright Avail: NTIS HC/MF A21

An analytical solution was developed for the buckling of laminated cylindrical plates under biaxial compression and shear loads. Linear equations for laminated cylindrical shells (Donnell-type equations) were used in conjunction with Galerkin's method to determine critical buckling loads. Several composite panels were tested under uniaxial compression or inplane shear load in order to verify the correlation between the above analysis and experimental results. Panels had several types of layup, balanced and symmetric as well as unbalanced and unsymmetric, and different boundary conditions. A good correlation between theoretical analysis and experimental results was obtained. A new test facility was built in order to apply both biaxial compression and shear load. ESA

N92-23805# Deutsche Forschungsanstalt fuer Luft- und Raumfahrt, Brunswick (Germany, F.R.). Inst. for Structural Mechanics.
DAMPING BEHAVIOUR OF UNIDIRECTIONAL FIBRE REINFORCED POLYMERS **c27**
Holger Hanselka *In* ESA, Spacecraft Structures and Mechanical Testing, Volume 1 Oct. 1991 p 169-174 (For primary document see N92-23780 14-18)
Copyright Avail: NTIS HC/MF A21

A method for the analytical description of damping for unidirectional fiber reinforced composites is shown. Generally the parameter damping can be described through the simple theory of a damped system with one degree of freedom or by the definition of complex modulus of elasticity. To describe damping behavior of composite materials, the complex modulus of elasticity is substituted into the orthotropic stress strain relationship of unidirectional fiber reinforced laminates. With this modulus, damping and stiffness can be described as a function of direction of fiber reinforcement. The analytical solution is compared with experimental data. As an investigation method, the thermal resonance vibration bending test is used. An optimization of dynamic behavior of a simple structure, a single cantilever beam, is carried out through variation of angle of fiber direction. ESA

N92-23806# DNV Ingemansson A.B. (Sweden).
COMPUTER SIMULATION OF MOISTURE PENETRATION IN STRUCTURES **c24**
Otto Wilmar *In* ESA, Spacecraft Structures and Mechanical Testing, Volume 1 Oct. 1991 p 175-179 Sponsored by Defence Material Administration (For primary document see N92-23780 14-18)
Copyright Avail: NTIS HC/MF A21

A method for computer simulation of the transient flow of moisture, heat and pressure in composite materials is described. The theoretical formulation is the Luikov coupled partial differential equations having the three mentioned potentials as variables. The solution is accomplished by finite elements in space and finite differences in time. Material property values are allowed to vary with the prevailing conditions at each step in time. Time dependent values of moisture, temperature and pressure may be applied to the boundaries of the computational model. At each step in time the distribution, content and flow of moisture in and through the structure are computed. The program was applied for simulation of moisture distribution in polymers and air cavities. ESA

N92-23807# Politecnico di Torino (Italy). Dept. of Aerospace Engineering.
A NEW TEST FACILITY FOR MEASURING THE COEFFICIENT OF MOISTURE EXPANSION OF ADVANCED COMPOSITE MATERIALS **c24**
G. Romeo, E. Miraldi, G. Ruscica, F. Bertoglio, and G. Ruvinetti *In* ESA, Spacecraft Structures and Mechanical Testing, Volume 1 Oct. 1991 p 181-185 (For primary document see N92-23780 14-18)
Copyright Avail: NTIS HC/MF A21

A new test facility designed in order to carefully measure the Coefficient of Moisture Expansion (CME) in specimens made of

advanced composite materials is described. The facility is composed essentially of a thermostat contained in a vacuum chamber (10(exp -3) Pa) in which five carbon fiber reinforced plastic samples are enclosed with the displacement transducers, where they can be measured and compared in the same environmental conditions between them and with an Invar reference specimen. With a long term stability in the temperature of plus or minus 0.1 K and a careful choice of displacement sensors, a maximum error of plus or minus 5 x 10(exp -6) in the CME was confirmed. A coefficient of moisture expansion of 3.85 x 10(exp -5) and 3.098 x 10(exp -3) was obtained along the fiber direction and normal to fiber direction, respectively. ESA

N92-23808# European Space Agency, Paris (France).
ARIANE 5 STRUCTURAL DEFINITION OF THE UPPER COMPOSITE **c15**
A. L. GonzalezBlasquez *In its* Spacecraft Structures and Mechanical Testing, Volume 1 Oct. 1991 p 189-195 (For primary document see N92-23780 14-18)
Copyright Avail: NTIS HC/MF A21

The definition of the upper structural assembly of the Ariane 5 launcher is addressed. The philosophy of multiple payload launching is analyzed and the different upper configurations presented. The general dimensioning requirements are reviewed: payload factors and flight environment, particular requirements coming from the kinematics and dynamics of the payloads, and general launcher architecture. Special attention is given to the non-uniform load flow transmission and the pyrotechnic shocks induced in structure separation. The main structural tests of the upper structures are outlined. ESA

N92-23809# Maschinenfabrik Augsburg-Nuernberg A.G., Munich (Germany, F.R.).
ADVANCED NUMERICAL ANALYSES FOR THE OPTIMISATION OF THE STRUCTURAL BEHAVIOUR OF THE INTERSEGMENT CONNECTION FOR THE ARIANE 5 BOOSTER CASE **c20**
P. Agatonovic and D. Sygulla *In* ESA, Spacecraft Structures and Mechanical Testing, Volume 1 Oct. 1991 p 197-202 (For primary document see N92-23780 14-18)
Copyright Avail: NTIS HC/MF A21

The results of the structural analysis of the clevis-tang connection for the Ariane 5 booster case, carried out to establish a connection design which is optimally adopted to the general requirements of weight and cost saving, structural integrity and functional performance, are summarized. The results were used to develop the baseline solution for the connection geometry and to improve the necessary technological basis of the engineering approach in this area. By comparison of the results with experimental measurements, full verification of the basic procedure and the analysis model was achieved. ESA

N92-23810# Construcciones Aeronauticas S.A., Madrid (Spain). Div. Espacio.
BRIEF HISTORY OF THE DEVELOPMENT OF THE EPS-STRUCTURE **c15**
J. Martin *In* ESA, Spacecraft Structures and Mechanical Testing, Volume 1 Oct. 1991 p 203-208 (For primary document see N92-23780 14-18)
Copyright Avail: NTIS HC/MF A21

The EPS structure is a part of the upper stage of the Ariane 5 launcher. The analysis of the functions and constraints required for the structure led to its present design. The functions and summaries of the constraints and the mechanical requirements are presented. A brief description of the structure and several comments regarding the selection of the configuration of the different parts of the structure are given. Interesting conclusions of the different analyses performed during the development phase are presented. Comments regarding the present status of the structure are included. ESA

N92-23811# Centre National d'Etudes Spatiales, Paris (France). Direction des Lanceurs.
ARIANE 4 INTERNAL ACOUSTIC ENVIRONMENT: INTERPRETATION OF FLIGHT DATA WITH A VIBROACOUSTIC MODEL OF THE UPPER PART OF THE LAUNCHER **c15**
B. Ritchie and M. Beldi (STRACO S.A., Compiegne, France) *In* ESA, Spacecraft Structures and Mechanical Testing, Volume 1 Oct. 1991 p 211-217 (For primary document see N92-23780 14-18)
Copyright Avail: NTIS HC/MF A21

The theoretical and experimental approach used for the study of the vibroacoustic environment of Ariane 4 payloads at liftoff is presented. Focus is on a comparison between computer predicted and measured flight acoustic levels under the fairing in the payload area, at low and medium frequencies. The good agreement between the predicted and measured levels allow the model to be used as a reliable interpretative tool of the flight data. ESA

N92-23812# METRAVIB, Lyon (France). Fluid Structure Group.
ACOUSTIC PREDICTION ON SATELLITE STRUCTURE
Christian Clerc and Jean-Noel Giraudbit *In* ESA, Spacecraft Structures and Mechanical Testing, Volume 1 Oct. 1991 p 219-222 Prepared in cooperation with Alcatel Espace, Toulouse, France (For primary document see N92-23780 14-18)
Copyright Avail: NTIS HC/MF A21

A numerical method for comparison between 'test configuration' and 'launch configuration' was developed. The acoustic computations are performed with ASTRYD, which is a general software for solving scattering and radiation problems. ASTRYD is based on space time scheme discretization; at first, acoustic pressures are obtained in time domain, and then, they are obtained in frequency domain by classical fast Fourier transform algorithms. The satellite structure considered is the Telecom 2 satellite; computations are performed on one antenna reflector in free space (test configuration) or mounted on the satellite (launch configuration). For both configurations, main results are the acoustic field by octave and the acoustic pressure differential at the reflectors surface. Several over or underpressures are highlighted by computations specifically in the low frequency octave. Computations enable screening of the total frequency spectrum in which acoustic pressures are sensitive to the geometrical environment (frequency spectrum lies from 0 to 2000 Hz for a 2 m size specimen). Consequently, ASTRYD appears to be a powerful tool for the acoustic and structural engineer to predict acoustic loads on sensitive structures. ESA

N92-23813# Alenia Spazio S.p.A., Rome (Italy).
ACOUSTIC CAVITY AND FLUID/STRUCTURE INTERACTION MODELS: A METHODOLOGICAL DETERMINISTIC APPROACH AND PROBLEMS ENCOUNTERED **c39**
Pietro Carlo Marucchi-Chierro *In* ESA, Spacecraft Structures and Mechanical Testing, Volume 1 Oct. 1991 p 223-232 (For primary document see N92-23780 14-18)
Copyright Avail: NTIS HC/MF A21

The aim is to demonstrate the feasibility and reliability of the mathematical model based on the acoustic structural analogy and its numerical simulation, only in the presence of low modal density, using the finite element method technique. To develop the methodology, the study was carried out on simple cases where it is also possible to control the numerical results by analytical approach. In this manner, it was possible to highlight numerical imprecisions when studying two dimensional and three dimensional acoustic cavities. A method which is able to transmit both the complex mode shapes and the complex modal model of the coupled/structure system to the SDRC/SUPERTAB and SDRC/SYSTAN postprocessors is shown. ESA

N92-23814# IKO Software Service G.m.b.H., Stuttgart (Germany, F.R.).
EMPLOYMENT OF C.B. (CRAIG-BAMPTON) MODELS FOR NONLINEAR DYNAMIC ANALYSIS **c39**
P. Deloo and M. R. M. Klein (European Space Agency. European

Space Research and Technology Center, ESTEC, Noordwijk, Netherlands) *In* ESA, Spacecraft Structures and Mechanical Testing, Volume 1 Oct. 1991 p 235-240 (For primary document see N92-23780 14-18)
Copyright Avail: NTIS HC/MF A21

The nonlinear dynamic analysis of large structures is always very time, effort and central processing consuming. Whenever possible, the reduction of the size of the mathematical model involved is of main importance to speed up the computational procedures. Such reduction can be performed for the part of the structure which performs linearly. Most of the time, the classical Guyan reduction process is used. For nonlinear dynamic process where the nonlinearity is present at interfaces between different structures, Craig-Bampton models can provide a very rich information and allow easy selection of the relevant modes with respect to the phenomenon driving the nonlinearity. The employment of Craig-Bampton models, combined with Newmark direct integration for solving nonlinear friction problems appearing at the interface between the Hubble Space Telescope and its solar arrays during the orbit maneuvers, is presented. Theory, implementation in the finite element code ASKA and practical results are shown. ESA

N92-23815# Centre National d'Etudes Spatiales, Toulouse (France).
FEASIBILITY OF PAYLOAD SENSITIVITY ANALYSES FOR AR4 DYNAMIC EVENTS **c39**
F. Mercier *In* ESA, Spacecraft Structures and Mechanical Testing, Volume 1 Oct. 1991 p 241-246 (For primary document see N92-23780 14-18)
Copyright Avail: NTIS HC/MF A21

The coupled load analysis is a very important stage for the mechanical design and testing of spacecraft. The effects of the spacecraft model precision are usually not considered. These effects are now very important to study because the spacecraft need deeper notches for the sine tests. A method to perform these analyses with the data coming from a standard coupled load analysis for uniaxial events, taking into account the corrections for the truncation effects, is proposed. Examples are presented for different spacecrafts including AR4 (Ariane 4). ESA

N92-23816# Innsbruck Univ. (Austria). Inst. of Engineering Mechanics.
THE RESPONSE SURFACE METHOD: AN EFFICIENT TOOL TO DETERMINE THE FAILURE PROBABILITY OF LARGE STRUCTURAL SYSTEMS **c39**
G. I. Schueeller, C. G. Bucher, and H. J. Pradlwarter *In* ESA, Spacecraft Structures and Mechanical Testing, Volume 1 Oct. 1991 p 247-251 (For primary document see N92-23780 14-18)
(Contract FFF-6/546)
Copyright Avail: NTIS HC/MF A21

An efficient computational procedure for the analysis and design of structures under random loading by considering the statistical variation of the structural resistance is introduced. The interrelation between flexible mechanical modeling (e.g. finite element procedures) and efficient stochastic analysis (e.g. by accurate variance reduction simulation techniques) allows the treatment of complex systems without excessive computational effort. Hence, the practicing engineer is provided with a tool which enables him to design structures according to particular target reliabilities, and which meets the requirements of the state of the art for both the structural mechanical and the probabilistic procedures respectively. This procedure is applied to sample structures. ESA

N92-23817# Deutsche Forschungsanstalt fuer Luft- und Raumfahrt, Brunswick (Germany, F.R.). Inst. for Structural Mechanics.
AGING OF POLYMER MATRIX COMPOSITES AT ELEVATED TEMPERATURES **c27**
H. Twardy *In* ESA, Spacecraft Structures and Mechanical Testing, Volume 1 Oct. 1991 p 255-261 (For primary document see N92-23780 14-18)
Copyright Avail: NTIS HC/MF A21

Experimental studies were performed to examine the influence of thermal aging on strength and stiffness of carbon fiber reinforced plastic. Exposure times up to 3300 hours were conducted, but interest was focused on elevated temperatures with the consequence of low exposure durations. Materials selected for tests were four bismaleimide composites (among these 5250-2/T800) and the polyimide composites PMR 15/T300 and LARC 160/T800. Isothermal aging was conducted at temperatures in the range of 200 to 340 C. Comparative studies were performed in nitrogen and oxidizing air environment. Results of mass loss measurement were compared with mechanical properties changes. ESA

N92-23818# Vrije Univ., Brussels (Belgium). Composite Systems and Research Group.
THE TORSIONAL FATIGUE BEHAVIOUR OF THE IN-PLANE AND OUT-OF-PLANE SHEAR MODULI OF COMPOSITE MATERIALS **c24**
D. vanHemelrijck, L. Schillemans, F. DeRoey, I. Daerden, F. Boulpaep, J. DeVisscher, and A. Cardon *In* ESA, Spacecraft Structures and Mechanical Testing, Volume 1 Oct. 1991 p 263-267 (For primary document see N92-23780 14-18)
Copyright Avail: NTIS HC/MF A21

An automated torsion test is proposed for the determination of the in-plane and out-of-plane shear modulus. The obtained results show that for some composite systems the out-of-plane shear modulus is much different from the in-plane shear modulus which allows it to be considered in some design applications. The results of the inplane shear modulus are in good agreement with the results obtained with the RESONALYSER, which is a method based on the vibration behavior of a testplate. Fatigue data for the studied composite systems are given. ESA

N92-23819# Deutsche Forschungsanstalt fuer Luft- und Raumfahrt, Brunswick (Germany, F.R.). Inst. for Structural Mechanics.
EXPERIMENTAL STUDY OF DELAMINATION GROWTH IN MULTIDIRECTIONAL CFRP-LAMINATES UNDER FATIGUE LOADING **c24**
H. C. Goetting *In* ESA, Spacecraft Structures and Mechanical Testing, Volume 1 Oct. 1991 p 269-274 (For primary document see N92-23780 14-18)
Copyright Avail: NTIS HC/MF A21

An experimental study in damage mechanisms and failure mechanism of multidirectional CFRP (Carbon Fiber Reinforced Plastic) laminates was conducted with special reference to delamination onset and growth under compression-compression and tension-compression fatigue loading. Different laminate stacking sequences of unnotched test specimens and of laminates containing holes, notches, and artificial delaminations were investigated. Besides the well known nondestructive test techniques for the evaluation of damage states new optical online measurement methods are applied. The basic damage mechanisms like cracks in off axis plies and their influence on delamination development were studied with respect to the final fatigue damage state, e.g. the transition from stable to unstable delamination growth caused by buckling of sublaminates. Characteristic delamination states were found for different notch sizes and notch shapes which affect the redistribution of strains or stresses, respectively, during cycling. ESA

N92-23820# National Space Development Agency, Ibaraki (Japan).
CONCEPTIONAL DESIGN TO HEAT-RESISTANT AIRFRAME OF HOPE
Masataka Yamamoto *In* ESA, Spacecraft Structures and Mechanical Testing, Volume 1 Oct. 1991 p 277-282 (For primary document see N92-23780 14-18)
Copyright Avail: NTIS HC/MF A21

The HOPE (Japanese Spaceplane) airframe is recognized to meet with severe thermal and mechanical environment through

the operation phases such as launch, reentry, and landing. The conceptional design model is studied using the results of research and development of heat resistance materials and of heat resistance structural design. The structural configuration of heat resistance is to fit the thermal protection panels out of the frame structure, in addition to mounting the onboard thermal insulation material. Primary structural materials are carbon fiber reinforced polyimide (up to 300 C) and carbon-carbon (up to 1700 C); thermal protection materials are ceramic tile, titanium alloy panel, and carbon-carbon panel. ESA

N92-23821# Societe Europeenne de Propulsion, Saint-Medard-en-Jalles (France).
LARGE THIN COMPOSITE THERMOSTRUCTURAL PARTS
D. Desnoyer, A. Lacombe, and J. M. Rouges *In* ESA, Spacecraft Structures and Mechanical Testing, Volume 1 Oct. 1991 p 283-291 (For primary document see N92-23780 14-18)
Copyright Avail: NTIS HC/MF A21

The new space transportation projects (Sanger, Hotol, STAR-H, STS 2000, NASP, and Hermes) have a challenge with their system mass performance. Due to the overall size of these systems, large surface high temperature parts are mandatory in order to increase the system reliability in decreasing the junction number (seals and fasteners) and to decrease the overall mass. To be mass efficient, these large parts should be thin. The rigidity is provided by integrated stiffeners. Depending on the reentry atmosphere, two main types of environment constraints should be considered: an oxidizing and nonoxidizing environment. For the oxidizing environment, an SiC matrix was selected and large parts were manufactured demonstrating the availability and validity of the technologies. Material tests performed under plasma arc jet showed the oxidizing resistance of the material. For the nonoxidizing environment (i.e. planetary reentry) carbon-carbon can be selected. A conic shaped panel with integrated stiffeners was studied and manufactured. The skin thickness is 0.5 mm with no delaminable preform. ESA

N92-23822# Air Force Systems Command, Wright-Patterson AFB, OH. National Aero-Space Plane Joint Program Office.
DESIGN CHALLENGES FOR THE NATIONAL AERO-SPACE PLANE **c05**
Frank D. Boensch *In* ESA, Spacecraft Structures and Mechanical Testing, Volume 1 Oct. 1991 p 293-297 (For primary document see N92-23780 14-18)
Copyright Avail: NTIS HC/MF A21

The National Aerospace Plane is a program conceived in 1986 by the U.S. Defense Advanced Research Projects Agency, to develop and demonstrate in flight, the technologies necessary for hypersonic flight including Single Stage To Orbit (SSTO) and cruise at sustained Mach numbers. In order to do this, a number of technologies, propulsion, structure aerodynamics, computational fluid dynamics, and materials must be matured to the point that hypersonic flight is practical. The progress made in the critical areas of materials and structures, highlighting advances in propulsion and computational fluid dynamics, made possible by high materials such as titanium aluminides and carbon-carbon, is shown. An examination of the utility of hypersonic flight both in terms of an SSTO mission and the commercial potential for hypersonic flight is given. ESA

N92-23823# Dassault Espace, Saint-Cloud (France). Centre Spatial.
THE CHALLENGE OF THE HERMES TPS SHINGLES **c16**
Christian Petiau *In* ESA, Spacecraft Structures and Mechanical Testing, Volume 1 Oct. 1991 p 299-306 (For primary document see N92-23780 14-18)
Copyright Avail: NTIS HC/MF A21

The general principles of the thermal protection and hot structure design for the space shuttle Hermes are outlined. The shingle type thermal protection, made of thin C-SiC ceramic composite panels protecting a very light multiscreen insulation, is detailed. A description is provided of the technical requirements, as well as of the particularly complex numerical simulations and tests that have to be conducted for analysis of all phenomena (thermoelastic, acoustic, aeroelastic, internal venting, oxidation, etc.) that have to be sustained by the shingles. A generalized computer aided design/manufacturing tool that is needed for automated designing and analysis, and for the production of the hundreds of shingles which, although all being quite similar, show some distinctive features, is presented. ESA

N92-23824*# National Aeronautics and Space Administration. Lewis Research Center, Cleveland, OH.
SIMULATION OF SPACE STATION LOADS WITH ACTIVE CONTROL SYSTEMS
P. A. Bielloch, N. R. Beagley (SDRC Engineering Services Ltd., Herts, England), D. R. Ludwiczak, and I. Yunis *In* ESA, Spacecraft Structures and Mechanical Testing, Volume 1 Oct. 1991 p 309-315 (For primary document see N92-23780 14-18)
Copyright Avail: NTIS HC/MF A21 CSCL 22B

A methodology for calculating dynamic loads for the Space Station Freedom is presented. The methodology minimizes the repeated calculation of duplicate structural elements, while analyzing a large number of different Space Station configurations with different alpha and beta joint angles. Particular attention is paid to the issue of model reduction using a combination of component mode synthesis (superelements) and component mode selection to generate accurate system level models with a minimum of modal degrees of freedom. The modeling of the control systems during simulation of the structural response is discussed. ESA

N92-23825# MATRA Espace, Toulouse (France).
INFLUENCE OF MICROVIBRATIONS ON SPACECRAFT PERFORMANCES
N. Jourdon and V. Guillaud *In* ESA, Spacecraft Structures and Mechanical Testing, Volume 1 Oct. 1991 p 317-322 (For primary document see N92-23780 14-18)
Copyright Avail: NTIS HC/MF A21

Along with technology advances in the field of optical and laser payload, spacecraft pointing accuracy requirements become more and more severe, especially for scientific and Earth observation satellites. Attitude and orbit control equipments and payload moving parts generate in-orbit microvibrations which are critical to instruments line of sight pointing performance. A number of activities aimed at characterizing the in-orbit microvibrations endured by spacecraft payloads such as SPOT 4, SILEX, and SOHO were undertaken. A ground test campaign performed on SPOT flight model 3 is focused on. Primary objectives were to measure the structural damping coefficient. The test led to the conclusion that damping coefficients of 0.5 can be anticipated in orbit. It also demonstrated a relatively good representativeness of finite element models used for performance predictions. ESA

N92-23826# Messerschmitt-Boelkow-Blohm G.m.b.H., Bremen (Germany, F.R.).
ON THE MODELLING OF A DEPLOYABLE TELESCOPE ELASTIC BEAM-TYPE ELEMENT FOR ON-ORBIT MULTIBODY SIMULATIONS **c39**
Bernhard Kotzias *In* ESA, Spacecraft Structures and Mechanical Testing, Volume 1 Oct. 1991 p 323-328 Prepared in cooperation with Erno Raumfahrttechnik G.m.b.H. Bremen, Germany, F.R. (For primary document see N92-23780 14-18)
Copyright Avail: NTIS HC/MF A21

The theory of a continuous deployable beam type element for telescope applications is presented. The inertia tensor of this element is described by third order theory for large deformations. Stress stiffening from gyroscopic and external forces is included. In order to save numerical operations, continuous base functions, dedicated to the actual length of deployment, are used. These satisfy Dirichlet boundary conditions on the moving telescope joint. They are selected as polynomials, representing transversal, torsional, and longitudinal motion in a cartesian deformation base. Precalculation of stiffening and nonlinear intertia terms is done in advance. The numerical extensive part is thereby separated from time integration. ESA

N92-23827# Alenia Spazio S.p.A., Turin (Italy).
DEVELOPMENT AND APPLICATION OF SUBSTRUCTURING TECHNIQUES FOR UNDERSTANDING AND CONTROLLING RESIDUAL VIBRATIONS (MICROGRAVITY ASPECTS) **c39**
Daniele Francesconi, Pietro Carlo Marucchi-Chierro, and Roberto Ullio *In* ESA, Spacecraft Structures and Mechanical Testing, Volume 1 Oct. 1991 p 329-338 (For primary document see N92-23780 14-18)
Copyright Avail: NTIS HC/MF A21

New computation and experimental methods are required to meet the targets of microgravity requirements in modern space system projects. For example, in the Columbus project accurate analysis needs detailed monitoring of the system dynamics behavior in terms of acceleration levels up to 1000 Hz for microgravity aspects. While Statistical Energy Analysis (SEA) will have to be introduced in order to analyze high model density ranges, a classical computation method such as finite element method has to be updated in order to increase its capabilities for the monitoring of the low modal density structural dynamics: Component Mode Synthesis (CMS), linking substructuring approach to efficient dynamics oriented reduction algorithms, permits a strong subsystem zooming which implies an accurate monitoring of the dynamics of the system. The main features of a particular CMS technique and the capabilities of the method are shown in simple but meaningful examples. ESA

N92-23828# Intespace, Toulouse (France).
MINIMIZATION OF VIBRATIONS BY BROADBAND SENSITIVITY APPROACH **c39**
A. Girard, J. Chatelain, and N. Roy *In* ESA, Spacecraft Structures and Mechanical Testing, Volume 1 Oct. 1991 p 341-346 Sponsored by Centre d'Etudes et de Recherche sur la Discretion Acoustique des Navires (For primary document see N92-23780 14-18)
Copyright Avail: NTIS HC/MF A21

The transmissibility of vibrations due to mechanical sources through complex structures may be reduced by adequate modification of structural parameters. In order to globally account for uncertainties in the frequency content of the real environment, a sensitivity analysis on frequency responses due to broadband excitation is performed. Simplifying assumptions on the relationship between the physical parameters and the element matrices lead to an efficient computation of model parameter derivatives expressed in the model basis. Localization of sensitive zones, followed by estimations of the modified structure's responses give the way to obtain a minimal vibration level. A theoretical description and an application to a beam truss are presented in order to illustrate the minimization of dynamic transmissibilities between excitation and reaction forces. ESA

N92-23829# TeWiSoft G.m.b.H., Soechtenau (Germany, F.R.).
THE CONTINUOUS ELEMENTS METHOD **c39**
Peter H. Kulla *In* ESA, Spacecraft Structures and Mechanical Testing, Volume 1 Oct. 1991 p 347-352 (For primary document see N92-23780 14-18)
Copyright Avail: NTIS HC/MF A21

The term Continuous Elements (CE) stands for a technique that avoids the discretization error inherent in finite elements. This is achieved by describing the dynamic stiffness matrix of an element of the structure in terms of the complete analytical solution of the underlying differential equations. The matrix elements are transcendental functions of the frequency and the matrix can not be split up into a mass and a stiffness matrix. Recently the method was generalized to include two dimensional CE, which broadens the scope of its applicability. In fact, it is the generalization which makes it a general purpose tool for structural dynamics. An outline of the CE method is given, the generalization to two dimensional CEs is highlighted, and the method is used to find the first eigensolutions of an L sharp cantilever plate. ESA

N92-23830# Politecnico di Milano (Italy). Dipartimento di Ingegneria Aerospaziale.
HARMONIC WAVE PROPAGATION IN TWO-DIMENSIONAL PERIODIC LARGE SPACE STRUCTURES **c39**
F. Bernelli-Zazzera and F. Ercoli-Finzi *In* ESA, Spacecraft Structures and Mechanical Testing, Volume 1 Oct. 1991 p 353-358 Sponsored by Fondazione Ing. Paolo Foresio (For primary document see N92-23780 14-18)
Copyright Avail: NTIS HC/MF A21

The development of a suitable method for the analysis of harmonic wave propagation in large two dimensional periodic space structures is addressed. The dynamic behavior of modular structures is synthesized by the propagation coefficients of the repetitive element. The finite element method is used to compute the dynamic stiffness matrix of the periodic element; the appliciation of the repetitive boundary equilibrium and compatibility conditions and the use of Floquet's theory on periodic differential equations leads to a nonlinear system of equations. The solution of this nonlinear system of equations gives the propagation coefficients for rectilinear wave fronts propagating along a generic direction. It is demonstrated that in some very special cases the solution of the nonlinear system is equivalent to an eigenvalue problem. ESA

N92-23831# Avions Marcel Dassault-Breguet Aviation, Saint-Cloud (France).
NON LINEAR STRUCTURAL ANALYSIS OF A THIN SKIN CARBON-CARBON RIGID DECELERATOR **c24**
C. Bonnet, J. P. Planas, and M. Rigault *In* ESA, Spacecraft Structures and Mechanical Testing, Volume 1 Oct. 1991 p 359-362 (For primary document see N92-23780 14-18)
Copyright Avail: NTIS HC/MF A21

Structural linear analysis on the Phase A carbon-carbon decelerator concept for the Huygens probe was carried out. The study showed that the validation of such thin skin structure design requires precise instability phenomena analysis. The buckling, locally or general is likely to be size determining. Nonlinear buckling and post buckling analysis of the carbon-carbon Huygens decelerator on internal funding was done using software taking into account the combined thermomechanical and mechanical loading. The results of this nonlinear structural analysis are presented. Experience in such an ultrathin and ultralight carbon-carbon structure is not available. The only way to give the necessary credibility to the concept definition is to rely on sophisticated structural analysis including nonlinearity in the equations under both mechanical and thermal loading. ESA

N92-23832# Vrije Univ., Brussels (Belgium). Composite Systems and Adhesion Group.
DYNAMIC CHARACTERIZATION OF COMPOSITE MATERIALS **c24**
I. Daerden, D. vanHemelrijck, L. Schillemans, F. DeRoey, F. Boulpaep, J. DeVisscher, and A. Cardon *In* ESA, Spacecraft Structures and Mechanical Testing, Volume 1 Oct. 1991 p 365-368 (For primary document see N92-23780 14-18)
Copyright Avail: NTIS HC/MF A21

The determination of axial and torsional damping ratio's by use of a dynamic testbench is addressed. The results are compared with those obtained by a mixed numerical/experimental technique, called RESONALYSER. During pure axial and torsional fatigue testing of carbon and glass fiber reinforced polymers, the evolution of phase shift between load and displacement, which is a measure for the damping, is observed. ESA

N92-23833# Aerospatiale, Les Mureaux (France).
MECHANICAL BEHAVIOR OF COMPOSITE MATERIALS AND ADHESIVE BONDS AT LOW TEMPERATURES [COMPORTEMENT MECANIQUE DES MATERIAUX COMPOSITES ET ASSEMBLAGES COLLES AUX BASSES TEMPERATURES] **c24**
C. Laurent *In* ESA, Spacecraft Structures and Mechanical Testing, Volume 1 Oct. 1991 p 369-373 In FRENCH (For primary

document see N92-23780 14-18)
Copyright Avail: NTIS HC/MF A21

The mechanical performance of carbon resin fibers and adhesive bonds were evaluated at cold temperatures (up to 90 K) with respect to the polymerization temperature of the carbon resin fibers or adhesives, and the character of the fibers. The results show that the resins (or the adhesives in the case of adhesive bonds) which polymerize at higher temperature and which present better firmness at hot temperature, often have better behavior at cold temperature despite the high level of thermal constraints.
ESA

N92-23834# Padua Univ. (Italy). Dipartimento di Ingegneria Meccanica.
MECHANICAL TESTING ON A COMPOSITE FLEXIBLE STRUCTURE **c39**
G. Fanti, F. Angrilli, P. Baglioni, and G. Bianchini *In* ESA, Spacecraft Structures and Mechanical Testing, Volume 1 Oct. 1991 p 375-381 Sponsored by Italian Space Agency (For primary document see N92-23780 14-18)
Copyright Avail: NTIS HC/MF A21

A measuring method for the evaluation of the mechanical parameters of very flexible structures like long, multilayered ropes, such as that used in the Tethered Subsatellite System (TSS-1), is presented. Stiffness, longitudinal propagation velocity, loss factor, and hysteresis are determined in tether samples with different lengths and submitted to different environmental conditions such as temperature, pressure, and humidity. Two stick/slip mechanisms among adjacent layers of the rope were detected; the first one, called macroslidings, shows up in tethers about 25 m long at room temperature, and in tethers about 7 m long at low temperature (about -100 C); the second mechanism, microslidings, is always present with a loading cycle. As a consequence of these slidings, a tension transfer among the layers occurs. To explain this behavior, a 'beads model' of the tether was considered. A finite element model of a three layer rope was also developed in order to clarify the behavior of the composite tether. ESA

N92-23835# Dornier System G.m.b.H., Friedrichshafen (Germany, F.R.). Technology and Mechanics Development Div.
BUCKLING AND FAILURE OF THIN ELLIPTICAL DELAMINATIONS IN COMPOSITES **c24**
J. Heitzer *In* ESA, Spacecraft Structures and Mechanical Testing, Volume 1 Oct. 1991 p 383-389 (For primary document see N92-23780 14-18)
Copyright Avail: NTIS HC/MF A21

The Raleigh-Ritz method is used to analyze the buckling of elliptical delaminations in linear and nonlinear regimes. The delaminated region is separating a thick isotropic base laminate from a thin, anisotropic sublaminate. The delamination is oriented arbitrarily with respect to the loading axis. The base laminate enters the calculation only by its Poisson ratio so that the problem can be reduced to the calculation of the buckling behavior of an elliptical plate under suitable boundary conditions and loading. In contrast to previous approaches all couplings (full A-B-D matrix) are considered. Buckling strains are calculated by formulating the stability condition in terms of the derivative of the total energy and solving the corresponding eigenvalue problem. Solutions are checked with finite element results for various aspect ratios and layups. ESA

N92-23836# Avions Marcel Dassault-Breguet Aviation, Saint-Cloud (France).
STRETCHED SKIN CONCEPT FOR THE ENTRY AERODYNAMIC DECELERATOR SYSTEM OF PLANETARY PROBES
C. Bonnet, J. F. Puech, and M. Rigault *In* ESA, Spacecraft Structures and Mechanical Testing, Volume 1 Oct. 1991 p 393-397 (For primary document see N92-23780 14-18)
Copyright Avail: NTIS HC/MF A21

The joint NASA/ESA Cassini/Huygens mission is one of the forthcoming planetary exploration missions making use of a high drag decelerator. The requirements of this mission were used to support studies on new concepts for entry devices. Preliminary linear analysis performed on a very lightweight concept decelerator, based on ultra thin carbon-carbon skin showed that buckling is a driver during the entry phase. To avoid the consequence in stability of these stresses in the skin, the idea of using only a carbon fiber fabric without carbon impregnation was suggested. This was the first step towards the stretched skin concept. The second step was to design a proper structure to stretch the fabric. This concept, composed of a high temperature annular fabric, stretched into a rigid medium temperature armature and connected to the cold descent module structure, is described. A performance analysis is globally performed, and the predicted mass of the stretched skin concept is competitive. The technical feasibility is outlined. ESA

N92-23837# Interatom G.m.b.H., Bergisch Gladbach (Germany, F.R.).
BERYLLIUM-THERMAL PROTECTION TECHNOLOGY
H. Leder, U. Lohse, W. Ohly, P. Rathjen, L. Schiwkosky, H. Weber, and G. Wierheim *In* ESA, Spacecraft Structures and Mechanical Testing, Volume 1 Oct. 1991 p 399-404 (For primary document see N92-23780 14-18)
Copyright Avail: NTIS HC/MF A21

Beryllium, known as the lightest metallic heat sink structural material, was considered for the construction of a Thermal Protection System (TPS) to be used by entry bodies in future space missions. In the context of a feasibility study for fabrication of a probe with a TPS manufactured out of beryllium, design considerations were carried out by considering the Huygens Titan Probe as an example. Special technological aspects related to material characteristics, manufacturing design, and analysis are addressed. ESA

N92-23838# Societe Europeenne de Propulsion, Saint-Medard-en-Jalles (France).
CNSR ROSETTA: EARTH RETURN CAPSULE
D. Desnoyer, J. M. Larrieu, and C. Buck *In* ESA, Spacecraft Structures and Mechanical Testing, Volume 1 Oct. 1991 p 405-411 (For primary document see N92-23780 14-18)
Copyright Avail: NTIS HC/MF A21

The CNSR (Comet Nucleus Sample Return) Rosetta mission will bring back to Earth comet nucleus samples. During the system definition study, a preliminary design of the Earth return capsule Thermal Protection Subsystem (TPS) was performed. Due to high heat flux level, a high density ablative material was chosen for the heatshield. This design lead to a mass that did not match the requirements. The Sepcore concept was proposed in order to reduce the heatshield thickness. This concept requires the introduction of a thermal resistance structure. The material with high specific characteristics proposed of the aeroshell is a ceramic matrix composite, and the insulation function is ensured by a lightweight internal multilayer material. The application of the Sepcore concept on the CNSR Rosetta Earth return capsule allows a mass saving of 50 percent at TPS level and of 20 percent at capsule system level. The mass budgets established with this design met the requirements. ESA

N92-23839# Deutsche Forschungsanstalt fuer Luft- und Raumfahrt, Brunswick (Germany, F.R.). Inst. for Structural Mechanics.
NOTCHED STRENGTH OF COMPOSITE MATERIALS **c24**
A. S. Herrmann *In* ESA, Spacecraft Structures and Mechanical Testing, Volume 1 Oct. 1991 p 415-420 (For primary document see N92-23780 14-18)
Copyright Avail: NTIS HC/MF A21

The plane stress and displacement fields around an elliptical opening in an anisotropic plate with linear elastic material properties under arbitrary tensional forces and fiber direction are analytically determined by the method of complex stress functions. For this purpose a plate with infinite extension under uniaxial load is used as the mathematical model. Using a glass fiber reinforced composite with orthotropic material properties as an example it is shown that the data gathered from isotropic materials on the

behavior of stress and displacement around elliptical and circular openings is not applicable to anisotropic materials. This is especially true if load and orthotropic principal directions (off axis load) do not coincide. For several particular cases the stress concentration factors which are decisive for constructual design are depicted in polar diagrams. The location of the maximum stress is given for these examples as well, which are generally not on the tip of the opening, in contrast to isotropic materials. ESA

N92-23840# Messerschmitt-Boelkow-Blohm G.m.b.H., Munich (Germany, F.R.).
STRENGTH AND DEFORMATION BEHAVIOUR OF KEVLAR AND CARBON COMPOSITE SANDWICH STRUCTURES FOR SPACE APPLICATIONS **c24**
H. Bansemir and O. Haider *In* ESA, Spacecraft Structures and Mechanical Testing, Volume 1 Oct. 1991 p 421-426 (For primary document see N92-23780 14-18)
Copyright Avail: NTIS HC/MF A21

Composite structures are of great importance because of their low weight, their high stiffness and strength, and their thermal deformation stability. A sandwich structure with Kevlar fabrics or filament wound high modulus carbon composite face sheets with 0/90 degree fiber orientation was chosen for the solar panels. A lightweight perforated aluminum honeycomb is used in the core. The panels are loaded by bending moments. Sandwich wrinkling is the critical failure mode. The face sheet thickness is small. The honeycomb core is of low density. The wrinkling strength was studied with the help of four point bending specimens. In several test series, with a high number of test samples, the influence of the Young's modulus, the thicknesses of the face sheets, and the core, on the wrinkling stress was examined. The results showed that the prefactor of the wrinkling formula has to be reduced in comparison to the theoretical value of 0.816. ESA

N92-23841# Alenia Spazio S.p.A., Rome (Italy).
MODELING OF HONEYCOMB CORE FOR SANDWICH CTE PREDICTION **c24**
L. Scolamiero *In* ESA, Spacecraft Structures and Mechanical Testing, Volume 1 Oct. 1991 p 427-430 (For primary document see N92-23780 14-18)
Copyright Avail: NTIS HC/MF A21

The overall mechanical behavior of sandwich panels depends on and can be predicted from the mechanical properties of their constituents: fibers, resins, core, and adhesives. As far as the honeycomb core is concerned, its inplane mechanical properties are difficult to define (it is expandible in nature), and they are often neglected. When performing thermoelastic analyses, in terms of high dimensional stability, this is not yet applicable. Different sandwich CTE (Coefficient of Thermal Expansion) prediction methodologies are reviewed and discussed. A new conceptually practical method, also based on core measured properties from material supplier data sheets is presented. ESA

N92-23842# Fraunhofer-Inst. fuer Treib- und Explosivstoffe, Pfinztal-Berghausen (Germany, F.R.).
INVESTIGATIONS OF THE DYNAMIC BEHAVIOUR OF COMPOUNDS UNDER PRELOADING **c27**
A. Giessler, W. Schmitt, and H. Weber (Karlsruhe Univ., Germany, F.R.) *In* ESA, Spacecraft Structures and Mechanical Testing, Volume 1 Oct. 1991 p 431-433 (For primary document see N92-23780 14-18)
Copyright Avail: NTIS HC/MF A21

Polymers with characteristic dissipation properties are obtained by compounding them with additives. The mechanical behavior of these compounds under vibration conditions are characterized by dynamic moduli, which depend on a static preload. The test results of a PU compound is presented. The obtained results enable the complex moduli of a special dynamic constitutive equation and the stress and strain of dynamic deformations of structures under static preload to be calculated. ESA

N92-23843# Kreis Consultancies, Pragg-Jenaz (Switzerland).
ON THE ANALYSIS OF LIQUID FILLED FREE-FREE TANKS **c34**
Andreas Kreis and Michel Klein (European Space Agency. European Space Research and Technology Center, ESTEC, Noordwijk, Netherlands) *In* ESA, Spacecraft Structures and Mechanical Testing, Volume 1 Oct. 1991 p 437-442 (For primary document see N92-23780 14-18)
Copyright Avail: NTIS HC/MF A21

The problem of analysis of free-free flexible tanks filled with an incompressible fluid is discussed. Gravity effects due to thrust forces are considered both for the fluid and the structure. A numerical analysis methodology is presented which uses the boundary element method for the fluid model and the finite element method for the structural model. For the analysis of free-free tank fluid systems under gravity conditions it is essential to include the rigid dregrees of freedom explicitly in the model in order to get a correct rigid mode behavior. Besides numerical solutions, two benchmark problems are presented which were solved analytically by means of Fourier series expansions. Only two dimensional problems are discussed although the generalization to three dimensions is straightforward. ESA

N92-23844# Industrieanlagen-Betriebsgesellschaft m.b.H., Ottobrunn (Germany, F.R.).
NUMERICAL INVESTIGATION OF FLUID-STRUCTURE-INTERACTION PROBLEMS WITH THE FINITE ELEMENT METHOD **c34**
H.-P. Flicke and W. Mohr *In* ESA, Spacecraft Structures and Mechanical Testing, Volume 1 Oct. 1991 p 443-449 (For primary document see N92-23780 14-18)
Copyright Avail: NTIS HC/MF A21

A procedure for the description and solution of Fluid Structure Interaction (FSI) problems is presented. In contrast to many other approaches a complete coupling of the fluid with the structure is obtained. The derived eigenvalue problem of the coupled system is solved with a modified subspace iteration method. The time integration is performed with the method of modal superposition. In two examples the influence of the FSI on the eigenfrequencies of mechanical systems is shown. ESA

N92-23845# European Space Agency. European Space Research and Technology Center, ESTEC, Noordwijk (Netherlands).
FLUID-STRUCTURE INTERACTION PROBLEMS: DEVELOPMENT OF SPECIAL PROCESSORS **c34**
M. Klein and Y. M. Lefevre (MATRA Espace, Toulouse, France) *In its* Spacecraft Structures and Mechanical Testing, Volume 1 Oct. 1991 p 451-455 (For primary document see N92-23780 14-18)
(Contract ESA-6468/86/NL/PH)
Copyright Avail: NTIS HC/MF A21

The dynamic analysis of liquid filled tanks has become an increasingly important topic as their mass may represent over half the total mass of some spacecrafts. However, the analysis of such coupled systems is difficult because of the particular behavior of fluids, especially when gravity effects are included. A general method applicable to three dimensional cases is presented, using fluid finite elements. A general variational principle including gravity effects is established, from which a classical set of coupled equations is derived. Emphasis is put on the implementation of the formulation and its interface with a general finite element code (NASTRAN) which is used to compute the structural matrices and to solve the system of equations. Test examples are shown which demonstrate the general usefulness of the procedure. ESA

N92-23846# Universite de Technologie de Compiegne (France). DAVI Centre de Recherche de Royallieu.
A SYMMETRIC COUPLING BETWEEN BEM AND FEM FOR DYNAMICAL ANALYSIS OF SPACECRAFT **c34**
A. Omrani and M. A. Hamdi (STRACO S.A., Compiegne, France) *In* ESA, Spacecraft Structures and Mechanical Testing, Volume 1

Oct. 1991 p 457-460 (For primary document see N92-23780 14-18)
Copyright Avail: NTIS HC/MF A21

In modern spacecraft, a large percentage of the total mass consists of fluids. For satellites, this percentage can go up to 50 percent, and can be even higher for launcher elements (90 percent for an Ariane 5 central body). To control the spacecraft behavior the phenomena of liquid sloshing for partially filled tanks and hydroelastic modes must be taken into account. To predict these phenomena a convenient mathematical fluid modeling is required. A fluid modeling formulation based on coupled BEM/FEM (Boundary Element Method/Finite Element Method) technique in order to calculate sloshing modes is proposed. ESA

N92-23847# Deutsche Forschungsanstalt fuer Luft- und Raumfahrt, Goettingen (Germany, F.R.). Dept. of Structural Dynamics.

OPTIMAL EXCITER PLACEMENT AND FORCE VECTOR TUNING REQUIRED FOR EXPERIMENTAL MODAL ANALYSIS **c39**

Norbert Niedbal and Erhard Klusowski *In* ESA, Spacecraft Structures and Mechanical Testing, Volume 1 Oct. 1991 p 463-473 (For primary document see N92-23780 14-18)
Copyright Avail: NTIS HC/MF A21

Experience gained with present modal survey test techniques range from excellent results to unrealistic normal mode parameters. Present experimental modal analysis procedures suffer under the absence of a criterion for optimal exciter placement. In order to increase the reliability and robustness of modern identification methods, a technique for optimal exciter point selection was developed based on combinatorial optimization. Applying three force tuning procedures published in the past and a new method, reliable normal mode parameters of an analytical eleven degree of freedom system and of a real structure can be determined, which verifies the performance of the proposed technique. ESA

N92-23848# Besancon Univ. (France). Lab. de Mecanique Appliquee.

MATCHING FINITE ELEMENT MODELS TO MODAL DATA **c39**

S. Cogan and G. Lallement *In* ESA, Spacecraft Structures and Mechanical Testing, Volume 1 Oct. 1991 p 475-482 (For primary document see N92-23780 14-18)
(Contract ESTEC-8219/89)
Copyright Avail: NTIS HC/MF A21

Recent developments in the area of parametric updating of finite element models are presented. The emphasis is placed on the preliminary step of localizing the dominant error zones prior to their correction. Two techniques for matching finite element models to modal data are presented, both of which exploit the identified real eigensolutions. The first procedure is based on the minimization of the distances between the eigensolutions introduced as output quantities and the second is based on the minimization of a mixed residual formed from the inputs and outputs. The advantages and disadvantages of these formulations are discussed. ESA

N92-23849# Construcciones Aeronauticas S.A., Madrid (Spain). Space Div.

COMPARISON OF MULTI-POINT MODAL TEST METHODS **c39**

Kimon Alexiou and Jan R. Wright (Manchester Univ., England) *In* ESA, Spacecraft Structures and Mechanical Testing, Volume 1 Oct. 1991 p 483-490 (For primary document see N92-23780 14-18)
Copyright Avail: NTIS HC/MF A21

In multipoint modal testing, the appropriate force distributions for identifying and isolating pure modes of vibration may be determined by iterative or direct methods. A number of these methods which are based on the classical phase resonance criterion and operate on measured receptance matrix data were investigated and compared using a simulated model. Of the methods which operate on square matrix data, a suggested variation on Asher's method was found useful for estimating the effective number of modes (and hence exciters needed) in the frequency range of interest. The Traill-Nash method provided the clearest estimate of appropriated forces but was more sensitive to noise. Of the methods which operate on rectangular matrices the Extended Asher method was not considered suitable. The multivariate mode indicator function method was the most promising but suffered from conditioning problems if too many exciters were used. An iterative method operating on updates of measured modal matrix data performed well and if improved could automate the modal tuning process. ESA

N92-23850# Dornier System G.m.b.H., Friedrichshafen (Germany, F.R.).

DESIGN PARAMETER UPDATE OF DYNAMIC MATHEMATICAL MODELS IN PRESENCE OF TEST NOISE AND MODE PAIRING PROBLEMS **c39**

B. Caesar, L. Eckert, and A. Hoppe (Stuttgart Univ., Germany, F.R.) *In* ESA, Spacecraft Structures and Mechanical Testing, Volume 1 Oct. 1991 p 491-499 (For primary document see N92-23780 14-18)
Copyright Avail: NTIS HC/MF A21

An update procedure is described, which improves design parameters towards the correct ones so that the eigenfrequencies and mode shapes of a mathematical model converge to the measured ones. A design parameter can be any input parameter of a Finite Element (FE) model. The objective is to minimize the weighted differences of measured and analyzed eigenfequencies and mode shapes with minimum changes of the design parameters. Any type of FE may be used in the FE model. The nonlinear functions of the eigenfrequencies and mode with reference to the design parameters are linearized based on FE sensitivity analyses. The new mode shapes are calculated as a linear combination of the initial one. Numerical examples using noisy and incomplete test data demonstrate the successful application of the update procedure. ESA

N92-23967# European Space Agency, Paris (France). Publications Div.

THE REENTRY OF SALYUT-7/KOSMOS-1686

B. Battrick, ed. Aug. 1991 99 p International workshop held in Darmstadt, Fed. Republic of Germany, 9 Apr. 1991
(ESA-SP-345; ISBN-92-9092-222-2; ISSN-0379-6566;
ETN-92-91187) Copyright Avail: NTIS HC/MF A05

The proceedings of an international workshop on the reentry of Salyut 7/Kosmos 1686, held two months after the event, are presented. An account of what happened is given, and the technical problems and difficulties are described. A general discussion of the accidental reentry of risk objects is included. The question of how the various facets of reentry predictions can be improved was of great importance. For individual titles, see N92-23968 through N92-23978.

N92-23968# Forschungsinstitut fuer Hochfrequenzphysik, Werthhoven (Germany, F.R.).

RADAR TRACKING AND OBSERVATION OF NONCOOPERATIVE SPACE OBJECTS BY REENTRY OF SALYUT-7/KOSMOS-1686

D. Mehrholz and K. Magura *In* ESA, The Reentry of Salyut-7/Kosmos-1686 Aug. 1991 p 1-8 (For primary document see N92-23967 14-18)
Copyright Avail: NTIS HC/MF A05

Radar observations of the decayed USSR space station Salyut-7/Kosmos-1686 were frequently performed beginning in 1990. The main objective was to support and advise the German government in all matters concerning the reentry. Narrowband, as well as high resolution radar data, were analyzed to assist reentry predictions. Background information on experimental radar research related to low Earth orbit is provided. The concept of the high resolution radar is discussed. Methods to determine physical characteristics like size, shape, and intrinsic motion of noncooperative space objects are highlighted. Results achieved

from Salyut-7/Kosmos-1686 reentry observations are shown. ESA

N92-23969# Forschungsinstitut fuer Hochfrequenzphysik, Werthhoven (Germany, F.R.).
ORBIT ANALYSIS AND LIFETIME PREDICTION USING RADAR DATA BY REENTRY OF SALYUT-7/KOSMOS-1686 **c13**
W. Liewehr, H. G. Peters, and D. Mehrholz *In* ESA, The Reentry of Salyut-7/Kosmos-1686 Aug. 1991 p 9-1 (For primary document see N92-23967 14-18)
Copyright Avail: NTIS HC/MF A05

Radar observations of the decayed USSR space station Salyut-7/Kosmos-1686 were frequently performed beginning in 1990. The main objective was to support and advise the German government in all matters concerned with the reentry. Methods for orbit analysis, long and short term lifetime prediction, and spacecraft mass assessment are discussed. Typical results like orbital history to identify maneuvers and changes in attitude are presented. The influence of solar activity on low Earth orbits is shown. The robustness and reliability of the analysis methods is demonstrated using radar data from Salyut-7/Kosmos-1686 reentry observations. ESA

N92-23970# European Space Agency. European Space Operations Center, Darmstadt (Germany, F.R.). Mission Analysis Section.
SALYUT-7/KOSMOS-1686 REENTRY PREDICTION ACTIVITIES AT ESOC
H. Klinkrad *In its* The Reentry of Salyut-7/Kosmos-1686 Aug. 1991 p 17-3 (For primary document see N92-23967 14-18)
Copyright Avail: NTIS HC/MF A05

Salyut-7, a precursor to the present Mir Space Station, was launched by the USSR in 1982. Following a series of crew visits and dockings with supply spacecraft, Salyut-7/Soyuz T-14 were joined by an unmanned Kosmos-1686 spacecraft. After the separation and return to Earth of Soyuz T-14 the Salyut-7/Kosmos-1686 configuration remained unchanged. The Salyut-7/Kosmos-1686 complex was left mothballed at an altitude of 475 km. From here, it descended into the atmosphere which led to its reentry above South America. An overview of activities at the European Space Agency/European Space Operations Center during the follow up of the Salyut-7/Kosmos-1686 decay is provided together with activities of related cooperations with space agencies, research institutes, and national bodies within the ESA member states, within the U.S., and within the USSR. ESA

N92-23971# Ministry of Defense, Moscow (USSR). Computer Center.
DETERMINATION AND PREDICTION OF SATELLITE MOTION AT THE END OF THE LIFETIME
A. I. Nazarenko *In* ESA, The Reentry of Salyut-7/Kosmos-1686 Aug. 1991 p 35-43 (For primary document see N92-23967 14-18)
Copyright Avail: NTIS HC/MF A05

New methods and technical aspects for improving accuracy and reliability in predicting the reentry region and the satellite falling time are discussed. Examples of their recent application to trajectory information from the orbital complex 'Salyut-7/Kosmos-1686' are given. ESA

N92-23972# Centro Nazionale Univ. per il Calcolo Elettronico, Pisa (Italy).
SALYUT-7/KOSMOS-1686 REENTRY PREDICTIONS FOR THE ITALIAN CIVIL DEFENCE AUTHORITY
L. Anselmo, C. Pardini, A. Santoro, S. Trumpy, and P. E. Battaglia (Italian Space Agency, Rome.) *In* ESA, The Reentry of Salyut-7/Kosmos-1686 Aug. 1991 p 45-50 (For primary document see N92-23967 14-18)
Copyright Avail: NTIS HC/MF A05

Work carried out during the Salyut-7/Kosmos-1686 reentry campaign is presented. The technical procedures adopted are described, as well as the data sources and the problems encountered in obtaining updated orbital elements for the space station. Forty five reentry predictions were computed during a 250 day time span and a percentage error less than 5 percent was obtained in 60 percent of the cases. The ballistic parameter of the space complex was estimated 54 times, using both the semi major axis evolution and the nodal crossing epochs. Another important aspect of the activity was the cooperation with the Italian Civil Defence Ministry. The kind of information that might be useful, its presentation, and its timely availability were crucial issues for the ministries, agencies, local authorities, and territorial units involved in the alert. ESA

N92-23973# Royal Aerospace Establishment, Farnborough (England). Space Dept.
DEBRIS REENTRY PREDICTION: SALYUT-7/KOSMOS-1686 **c13**
R. Crowther *In* ESA, The Reentry of Salyut-7/Kosmos-1686 Aug. 1991 p 51-56 (For primary document see N92-23967 14-18)
Copyright Avail: NTIS HC/MF A05

The problems encountered when attempting to predict the reentry of space debris are considered. The King-Hele rate of change of mean motion lifetime prediction method is applied to the reentry estimation of the Salyut-7/Kosmos-1686 complex. Deficiencies in the current status of the method are identified and new data computed to account for these deficiencies. A method is then proposed which can provide aerodynamic data on reentering objects from observation of their orbital evolution. Such data will enable the active deorbiting of objects using aerodynamic techniques as opposed to propulsive strategies which make great demands on the propellant budget. ESA

N92-23974# Hyperschall-Technologie-Goettingen, Lindau Harz (Germany, F.R.).
MODELLING OF AERODYNAMIC FORCES AND HEAT TRANSFER FOR ORBITAL DECAY AND REENTRY CALCULATIONS
G. Koppenwallner and D. Johannsmeier *In* ESA, The Reentry of Salyut-7/Kosmos-1686 Aug. 1991 p 57-62 (For primary document see N92-23967 14-18)
Copyright Avail: NTIS HC/MF A05

In order to improve orbital decay and reentry calculations of satellites, an appropriate aerodynamic model is necessary. The aerodynamic data along the trajectory can be provided either in numerical tables generated by large computer codes or by analytical formulas. The latter method requires a simplified description of the vehicle shape and aerodynamic flow models for free molecular flow, rarefied flow, and hypersonic continuum flow. ESA

N92-23975# European Space Agency. European Space Operations Center, Darmstadt (Germany, F.R.). Spacecraft Trajectory Branch.
PREDICTION OF SOLAR AND GEOMAGNETIC ACTIVITY FOR ESA LOW-FLYING SPACECRAFT **c93**
R. Mugellesi and D. J. Kerridge (Natural Environmental Research Council, Edinburgh, Scotland) *In its* The Reentry of Salyut-7/Kosmos-1686 Aug. 1991 p 63-7 (For primary document see N92-23967 14-18)
Copyright Avail: NTIS HC/MF A05

During the planning and operation of low altitude Earth orbit satellite missions, an important activity is orbit prediction over periods ranging from days to more than one year. It is also necessary to assess the impact of solar activity on the onboard electronics over the long term. In the orbital propagation model, the dominant, and most difficult component to predict, is the drag force, as it is sensitive to the continuous variations of solar and geomagnetic activity. In the air density models presently available, solar activity is parameterized in terms of the solar radio flux F10.7, whereas geomagnetic activity is represented by the Kp (or the equivalent Ap) index. The availability of long, medium and short term prediction of the solar and geomagnetic activity is fundamental for satisfying the current operational needs. A method for medium and long term forecasting of the activities has been developed and implemented in a computer system. The method

predicts monthly mean values of the F10.7 radio flux and Ap index. The SOLMAG software is currently used for mission analysis and in planning work for the ERS and EURECA missions. The performance of the prediction software is discussed. ESA

N92-23976# European Space Agency. European Space Operations Center, Darmstadt (Germany, F.R.). Mission Analysis Section.
SALYUT-7/KOSMOS-1686 ORBIT DETERMINATION FROM RADAR DATA c13
R. Jehn *In its* The Reentry of Salyut-7/Kosmos-1686 Aug. 1991 p 73-7 (For primary document see N92-23967 14-18)
Copyright Avail: NTIS HC/MF A05

During the final reentry phase of the Salyut-7 orbital complex, transmissions of radar data were received weekly (in January) and daily (last seven days). The radar data comprised measurements of slant range, range rate, azimuth, and elevation. The data were processed by an iterative least squares algorithm to derive the state vector and the ballistic coefficient of the space station. The algorithm is explained, and critical areas where straightforward convergence is hampered are highlighted. Methods to solve the problem of convergence are presented together with the solutions of the orbit determination. ESA

N92-23977# European Space Agency. European Space Operations Center, Darmstadt (Germany, F.R.). Mission Analysis Section.
LIFETIME OF OBJECTS IN GEOSTATIONARY TRANSFER ORBIT c13
G. Janin *In its* The Reentry of Salyut-7/Kosmos-1686 Aug. 1991 p 79-8 (For primary document see N92-23967 14-18)
Copyright Avail: NTIS HC/MF A05

Objects in Geostationary Transfer Orbit (GTO) result from the launch of satellites in geostationary orbit. There are close to 200 GTO, most of them third stage rockets used for transferring satellites from low Earth orbit to geostationary orbit. By crossing the low Earth orbit region at high speed more than twice a day, they represent a hazard for low Earth orbiting satellites. The situation in GTO is described and the danger presented by these objects for the low Earth satellite population is stressed. The source and accuracy of tracking data is indicated and the effect of orbital perturbations on the orbit evolution is recalled. First attempts to determine ballistic coefficients are outlined and the accuracy of reentry prediction is discussed. The range of expected lifetimes are given. ESA

N92-23978*# National Aeronautics and Space Administration. Lyndon B. Johnson Space Center, Houston, TX.
ORBITAL DECAY AND REENTRY OF THE SALYUT-7 ORBITAL COMPLEX
P. D. Anz-Meador (Lockheed Engineering and Sciences Co., Houston, TX.) and A. E. Potter *In* ESA, The Reentry of Salyut-7/Kosmos-1686 Aug. 1991 p 91-95 (For primary document see N92-23967 14-18)
Copyright Avail: NTIS HC/MF A05

Work associated with reentry predictions made for the Salyut-7/Kosmos-1686 orbital complex is discussed. The fidelity of the reentry prediction increased as the date of reentry approached, as expected. Results agreed well with European Space Operations Center predictions, which used more detailed and exact methods. However, it is clear that significant improvements are needed. The main problem is the lack of orbital element data in the last few hours prior to reentry. A byproduct of the analysis was an improved estimate of the exospheric temperature during the period of high solar activity which occurred during the last months before reentry. ESA

N92-24046*# GTE Government Systems Corp., Chantilly, VA. Contel Federal Systems.
INTERIM SERVICE ISDN SATELLITE (ISIS) HARDWARE EXPERIMENT DEVELOPMENT FOR ADVANCED ISDN SATELLITE DESIGNS AND EXPERIMENTS Report, 1 Oct. 1991 - 30 Apr. 1992
Gerard R. Pepin 30 Apr. 1992 129 p
(Contract NASw-4520)
(NASA-CR-190257; NAS 1.26:190257) Avail: NTIS HC/MF A07 CSCL 22B

The Interim Service Integrated Service Digital Network (ISDN) Satellite (ISIS) Hardware Experiment Development for Advanced Satellite Designs describes the development of the ISDN Satellite Terminal Adapter (ISTA) capable of translating ISDN protocol traffic into Time Division Multiple Access (TDMA) signals for use by a communications satellite. The ISTA connects the Type 1 Network Termination (NT1) via the U-interface on the line termination side of the CPE to the RS-499 interface for satellite uplink. The same ISTA converts in the opposite direction the RS-499 to U-interface data with a simple switch setting. Author

N92-23281*# National Aeronautics and Space Administration. Langley Research Center, Hampton, VA.
LONG DURATION EXPOSURE FACILITY: A GENERAL OVERVIEW
Robert L. ONeal and E. Burton Lightner *In its* LDEF: 69 Months in Space. First Post-Retrieval Symposium, Part 1 Jan. 1992 p 3-48 (For primary document see N92-23280 14-99)
Avail: NTIS HC/MF A99; 8 functional color pages CSCL 22B

N92-23282*# National Aeronautics and Space Administration. Langley Research Center, Hampton, VA.
LONG DURATION EXPOSURE FACILITY (LDEF) SPACE ENVIRONMENTS OVERVIEW
William H. Kinard and Glenna D. Martin *In its* LDEF: 69 Months in Space. First Post-Retrieval Symposium, Part 1 Jan. 1992 p 49-60 (For primary document see N92-23280 14-99)
Avail: NTIS HC/MF A99; 8 functional color pages CSCL 22B

N92-23285*# Science Applications International Corp., Glendora, CA.
MEASURED SPACE ENVIRONMENTAL EFFECTS TO LDEF DURING RETRIEVAL
Carl R. Maag and W. Kelly Linder (Air Force Systems Command, Houston, TX.) *In its* LDEF: 69 Months in Space. First Post-Retrieval Symposium, Part 1 Jan. 1992 p 85-99 (For primary document see N92-23280 14-99)
Avail: NTIS HC/MF A99; 8 functional color pages CSCL 22B

N92-23287*# Boeing Co., Seattle, WA. Defense and Space Group.
MIGRATION AND GENERATION OF CONTAMINANTS FROM LAUNCH THROUGH RECOVERY: LDEF CASE HISTORY
E. R. Crutcher, L. S. Nishimura, K. J. Warner, and W. W. Wascher *In* NASA. Langley Research Center, LDEF: 69 Months in Space. First Post-Retrieval Symposium, Part 1 Jan. 1992 p 121-140 (For primary document see N92-23280 14-99)
(Contract NAS1-18224)
Avail: NTIS HC/MF A99; 8 functional color pages CSCL 22B

N92-23309*# National Aeronautics and Space Administration. Langley Research Center, Hampton, VA.
LARGE CRATERS ON THE METEOROID AND SPACE DEBRIS IMPACT EXPERIMENT
Donald H. Humes *In its* LDEF: 69 Months in Space. First Post-Retrieval Symposium, Part 1 Jan. 1992 p 399-418 (For primary document see N92-23280 14-99)
Avail: NTIS HC/MF A99; 8 functional color pages CSCL 22B

N92-23311*# National Aeronautics and Space Administration. Marshall Space Flight Center, Huntsville, AL.
METEOROID/SPACE DEBRIS IMPACTS ON MSFC LDEF EXPERIMENTS
Miria Finckenor *In* NASA. Langley Research Center, LDEF: 69 Months in Space. First Post-Retrieval Symposium, Part 1 Jan. 1992 p 435-442 (For primary document see N92-23280 14-99)
Avail: NTIS HC/MF A99; 8 functional color pages CSCL 22B

N92-23312*# Kent Univ., Canterbury (England). Physics Lab.
HYPERVELOCITY IMPACT MICROFOIL PERFORATIONS IN THE LEO SPACE ENVIRONMENT (LDEF, MAP AO-023 EXPERIMENT)
J. A. M. McDonnell and T. J. Stevenson *In* NASA. Langley Research Center, LDEF: 69 Months in Space. First Post-Retrieval Symposium, Part 1 Jan. 1992 p 443-458 (For primary document see N92-23280 14-99)
Avail: NTIS HC/MF A99; 8 functional color pages CSCL 22B

N92-23314*# National Aeronautics and Space Administration. Lyndon B. Johnson Space Center, Houston, TX.
METEOROID, AND DEBRIS SPECIAL INVESTIGATION GROUP PRELIMINARY RESULTS: SIZE-FREQUENCY DISTRIBUTION AND SPATIAL DENSITY OF LARGE IMPACT FEATURES ON LDEF
Thomas H. See, Friedrich Hoerz, Michael E. Zolensky, Martha K. Allbrooks, Dale R. Atkinson, and Charles G. Simon (Institute for Space Science and Technology, Inc., Gainesville, FL.) *In* NASA. Langley Research Center, LDEF: 69 Months in Space. First Post-Retrieval Symposium, Part 1 Jan. 1992 p 477-486 (For primary document see N92-23280 14-99)
Avail: NTIS HC/MF A99; 8 functional color pages CSCL 22B

N92-23319*# National Aeronautics and Space Administration. Ames Research Center, Moffett Field, CA.
LDEF IMPACT CRATERS FORMED BY CARBON-RICH IMPACTORS: A PRELIMINARY REPORT
T. E. Bunch, F. Radicati diBrozolo, Ronald H. Fleming, David W. Harris, Don Brownlee, and Terrence W. Reilly (Hitachi Scientific Instruments, Mountain View, CA.) *In* NASA. Langley Research Center, LDEF: 69 Months in Space. First Post-Retrieval Symposium, Part 1 Jan. 1992 p 549-564 (For primary document see N92-23280 14-99)
Avail: NTIS HC/MF A99; 8 functional color pages CSCL 22B

N92-23321*# POD Associates, Inc., Albuquerque, NM.
LDEF DATA CORRELATION TO EXISTING NASA DEBRIS ENVIRONMENT MODELS Abstract Only
Dale R. Atkinson, Martha K. Allbrooks, and Alan J. Watts *In* NASA. Langley Research Center, LDEF: 69 Months in Space. First Post-Retrieval Symposium, Part 1 Jan. 1992 p 567 (For primary document see N92-23280 14-99)
Avail: NTIS HC/MF A99; 8 functional color pages CSCL 22B

N92-23323*# National Aeronautics and Space Administration. Lyndon B. Johnson Space Center, Houston, TX.
M AND D SIG PROGRESS REPORT: LABORATORY SIMULATIONS OF LDEF IMPACT FEATURES Abstract Only
Friedrich Horz, R. P. Bernhard, T. H. See, D. Atkinson, and M. Allbrooks (POD Associates, Inc., Albuquerque, NM.) *In* NASA. Langley Research Center, LDEF: 69 Months in Space. First Post-Retrieval Symposium, Part 1 Jan. 1992 p 581 (For primary document see N92-23280 14-99)
Avail: NTIS HC/MF A99; 8 functional color pages CSCL 22B

N92-23324*# National Aeronautics and Space Administration. Lyndon B. Johnson Space Center, Houston, TX.
PRELIMINARY MICROMETEOROID AND DEBRIS EFFECTS ON LDEF THERMAL CONTROL SURFACES Abstract Only
Martha K. Allbrooks, Dale R. Atkinson, Thomas See (Lockheed Engineering and Sciences Co., Houston, TX.), and Fred Horz *In* NASA. Langley Research Center, LDEF: 69 Months in Space. First Post-Retrieval Symposium, Part 1 Jan. 1992 p 583 (For primary document see N92-23280 14-99)
Avail: NTIS HC/MF A99; 8 functional color pages CSCL 22B

N92-23647*# Spacehab, Inc., Washington, DC.
SPACEHAB
David Rossi *In* NASA, Washington, Proceedings of the Second Annual Symposium on Industrial Involvement and Successes in Commercial Space 1991 19 p (For primary document see N92-23643 14-12)
Avail: NTIS HC/MF A11 CSCL 22B

N92-23648*# Space Industries, Inc., Webster, TX.
THE WAKE SHIELD FACILITY: A SPACE EXPERIMENT PLATFORM
Joseph P. Allen *In* NASA, Washington, Proceedings of the Second Annual Symposium on Industrial Involvement and Successes in Commercial Space 1991 7 p (For primary document see N92-23643 14-12)
Avail: NTIS HC/MF A11 CSCL 22B

N92-23649*# Boeing Commercial Airplane Co., Seattle, WA.
SPACE STATION FREEDOM
Gilbert Keyes *In* NASA, Washington, Proceedings of the Second Annual Symposium on Industrial Involvement and Successes in Commercial Space 1991 27 p (For primary document see N92-23643 14-12)
Avail: NTIS HC/MF A11 CSCL 22B

19 SPACECRAFT INSTRUMENTATION

For related information see also *06 Aircraft Instrumentation* and *35 Instrumentation and Photography.*

N92-23284*# National Aeronautics and Space Administration. Langley Research Center, Hampton, VA.
USE OF THE LONG DURATION EXPOSURE FACILITY'S THERMAL MEASUREMENT SYSTEM FOR THE VERIFICATION OF THERMAL MODELS
William M. Berrios *In its* LDEF: 69 Months in Space. First Post-Retrieval Symposium, Part 1 Jan. 1992 p 69-83 (For primary document see N92-23280 14-99)
Avail: NTIS HC/MF A99; 8 functional color pages CSCL 14B

N92-23917# MATRA Marconi Space, Toulouse (France).
THE GRADIOMETER PAYLOAD
P. Meyer and Patrick Peyrot *In* ESA, The Solid-Earth Mission Aristoteles Dec. 1991 p 57-60 (For primary document see N92-23910 14-12)
Avail: NTIS HC/MF A06; ESA, EPD, ESTEC, Noordwijk, Netherlands, HC 50 Dutch guilders

N92-23918# Office National d'Etudes et de Recherches Aerospatiales, Paris (France).
THE GRADIO ACCELEROMETER: DESIGN AND DEVELOPMENT STATUS
Alain Bernard and M. P. Touboul *In* ESA, The Solid-Earth Mission Aristoteles Dec. 1991 p 61-67 (For primary document see N92-23910 14-12)
Avail: NTIS HC/MF A06; ESA, EPD, ESTEC, Noordwijk, Netherlands, HC 50 Dutch guilders

N92-23920*# National Aeronautics and Space Administration. Goddard Space Flight Center, Greenbelt, MD.
ARISTOTELES MAGNETOMETER SYSTEM
Edward J. Smith, Roy J. Marquedant (Jet Propulsion Lab., California Inst. of Tech., Pasadena.), Robert Langel, and Mario Acuna *In* ESA, The Solid-Earth Mission Aristoteles Dec. 1991 p 83-89 (For primary document see N92-23910 14-12)
Avail: NTIS HC/MF A06; ESA, EPD, ESTEC, Noordwijk, Netherlands, HC 50 Dutch guilders CSCL 14B

20 SPACECRAFT PROPULSION AND POWER

Includes main propulsion systems and components, e.g., rocket engines; and spacecraft auxilliary power sources.

For related information see also *07 Aircraft Propulsion and Power, 28 Propellants and Fuels, 44 Energy Production and Conversion,* and *15 Launch Vehicles and Space Vehicles.*

N92-23151*# Research Inst. for Computing and Information Systems, Houston, TX.
LOW THRUST PROPULSION LITERATURE SURVEY
Darrel Monroe (Texas Univ., Austin.) Sep. 1989 54 p
(Contract NCC9-16; RICIS Proj. SE-21)
(NASA-CR-190179; NAS 1.26:190179) Avail: NTIS HC/MF A04 CSCL 21H

A literature search was performed to investigate the area of low thrust propulsion. In an effort to evaluate this technology, a number of articles, obtained through the use of the NASA-RECON database, were collected and categorized. The study indicates that although much was done, particularly in the 1960's and 1970's, more can be done in the area of practical navigation and guidance. It is suggested that the older studies be reinvestigated to see what potential there exists for future low thrust applications.
D.R.D.

N92-23252*# National Aeronautics and Space Administration. Lewis Research Center, Cleveland, OH.
BLAZING THE TRAILWAY: NUCLEAR ELECTRIC PROPULSION AND ITS TECHNOLOGY PROGRAM PLANS
Michael P. Doherty 1992 18 p Presented at the Conference on Advanced Space Exploration Initiative Technologies, Cleveland, OH, 4-6 Sep. 1991; sponsored by AIAA, and OAI Previously announced in IAA as A91-52353
(NASA-TM-105605; E-6941; NAS 1.15:105605; AIAA-91-3441) Avail: NTIS HC/MF A03 CSCL 18L

An overview is given of the plans for a program in nuclear electric propulsion (NEP) technology for space applications being considered by NASA, DOE, and DOD. Possible missions using NEP are examined, and NEP technology plans are addressed regarding concept development, systems engineering, nuclear fuels, power conversion, thermal management, power management and distribution, electric thrusters, facilities, and issues related to safety and environment. The programmatic characteristics are considered.
Author

N92-23534*# National Aeronautics and Space Administration. Lewis Research Center, Cleveland, OH.
DERATED ION THRUSTER DESIGN ISSUES
Michael J. Patterson and Vincent K. Rawlin Oct. 1991 16 p Presented at the 22nd International Electric Propulsion Conference, Viareggio, Italy, 14-17 Oct. 1991; sponsored by AIDAA, AIAA, DGLR, and JSASS
(NASA-TM-105576; E-6902; NAS 1.15:105576) Avail: NTIS HC/MF A03 CSCL 21C

Preliminary activities to develop and refine a lightweight 30 cm engineering model ion thruster are discussed. The approach is to develop a 'derated' ion thruster capable of performing both auxiliary and primary propulsion roles over an input power range of at least 0.5 to 5.0 kilo-W. Design modifications to a baseline thruster to reduce mass and volume are discussed. Performance data over an order of magnitude input power range are presented, with emphasis on the performance impact of engine throttling. Thruster design modifications to optimize performance over specific power envelopes are discussed. Additionally, lifetime estimates based on wear test measurements are made for the operation envelope of the engine.
Author

N92-23539*# Mississippi State Univ., Mississippi State.
PROCEEDINGS: NOZZLE INITIATIVE INDUSTRY ADVISORY COMMITTEE ON STANDARDIZATION OF CARBON-PHENOLIC TEST METHODS AND SPECIFICATIONS
31 Mar. 1992 246 p Meeting held in Sacramento, CA, 14-15 Nov. 1991
(Grant NAG8-545)
(NASA-CR-190203; NAS 1.26:190203) Avail: NTIS HC/MF A11 CSCL 21H

The proceedings of the meeting is presented in conversational form. Some areas of discussion are as follow: resin advancement at NASA Marshall new technologies studies; NMR studies; SPIP/PAN development summary; computer modeling support; composite testing; carbon assay testing; activity and aerospace computer database; alternate rayon yarn sizing; fiber morphology; and carbon microballoons specifications.
Author

N92-23694 Pennsylvania State Univ., University Park.
ANALYSIS OF SOLAR AND MICROWAVE THERMAL PROPULSION SYSTEMS Ph.D. Thesis
Sankaran Venkateswaran 1991 254 p
Avail: Univ. Microfilms Order No. DA9127441

Theoretical models are developed to assess the conceptual feasibility of employing solar and microwave energy to heat a propellant gas and generate thrust. Both these advanced electrothermal propulsion concepts promise high specific impulses and are, therefore, being considered as alternatives to chemical propulsion for space-based applications. The present research addresses two major feasibility issues: (1) the efficient coupling of electromagnetic energy to the propellant, and (2) the performance capabilities of these systems. Physical modeling of the direct absorption of solar radiation in gases involves the solution of the thermal radiation problem within the thruster. The absorption of the incident beam is modeled by a ray-tracing technique while the reradiation of the heated gas is treated by a thick-thin model. The analysis of the microwave problem involves the coupled solution of the Navier-Stokes equations for the gasdynamics and the Maxwell equations for the microwaves. Time-marching techniques are employed for the solution of both equation sets. Computational results are in good agreement with experimental data for resonant cavity plasmas - peak plasma temperatures are between 9000 and 10,000 K and high coupling efficiencies (up to 100 percent) are predicted.
Dissert. Abstr.

N92-23722# Oak Ridge National Lab., TN.
CHARACTERIZATION OF ROCKET PROPELLANT COMBUSTION PRODUCTS
R. A. Jenkins, C. W. Nestor, C. V. Thompson, T. M. Gayle, C. Y. Ma, B. A. Tomkins, and R. L. Moody Dec. 1991 128 p
(Contract DE-AC05-84OR-21400)
(DE92-007799; ORNL/TM-11759) Avail: NTIS HC/MF A07

The overall objective of the described research is four-fold: to (1) develop a standardized and experimentally validated approach to the sampling and chemical and physical characterization of the exhaust products of scaled-down rocket launch motors fired under experimentally controlled conditions at the Army's Signature Characterization Facility (ASCF) at Redstone Arsenal in Huntsville, Alabama; (2) determine the composition of the exhaust products; (3) assess the accuracy of a selected existing computer model for predicting the composition of major and minor chemical species; and (4) recommend alternations to both the sampling and analysis strategy and the computer model in order to achieve greater congruence between chemical measurements and computer prediction.
DOE

N92-23982*# Pratt and Whitney Aircraft, West Palm Beach, FL. Government Engines and Space Propulsion.
TUBULAR COPPER THRUST CHAMBER DESIGN STUDY Final Report, Oct. 1989 - Jun. 1990
A. I. Masters and D. E. Galler May 1992 106 p
(Contract NAS3-23858)
(NASA-CR-187206; NAS 1.26:187206; FR-21385) Avail: NTIS HC/MF A06 CSCL 21H

The use of copper tubular thrust chambers is particularly important in high performance expander cycle space engines. Tubular chambers have more surface area than flat wall chambers, and this extra surface area provides enhanced heat transfer for

additional energy to power the cycle. This paper was divided into two sections: (1) a thermal analysis and sensitivity study; and (2) a preliminary design of a selected thrust chamber configuration. The thermal analysis consisted of a statistical optimization to determine the optimum tube geometry, tube booking, thrust chamber geometry, and cooling routing to achieve the maximum upper limit chamber pressure for a 25,000 pound thrust engine. The preliminary design effort produced a layout drawing of a tubular thrust chamber that is three inches shorter than the Advanced Expander Test Bed (AETB) milled channel chamber but is predicted to provide a five percent increase in heat transfer. Testing this chamber in the AETB would confirm the inherent advantages of tubular chamber construction and heat transfer. Author

N92-24004*# Sverdrup Technology, Inc., Brook Park, OH.
SYNERGISTIC USE OF HIGH AND LOW THRUST PROPULSION SYSTEMS FOR PILOTED MISSIONS TO MARS
Final Report
James H. Gilland Mar. 1992 13 p Presented at the 27th Joint Propulsion Conference, Sacramento, CA, 24-26 Jun. 1991; sponsored by AIAA, SAE, ASME, and ASEE Previously announced in IAA as A91-45807
(Contract NAS3-25266)
(NASA-CR-189138; E-6940; NAS 1.26:189138; AIAA-91-2346)
Avail: NTIS HC/MF A03 CSCL 21H

The use of high thrust, relatively low specific impulse systems, such as chemical or nuclear thermal propulsion, in conjunction with low thrust, high specific impulse nuclear electric propulsion (NEP) was considered for a representative piloted Mars mission. It was concluded that the single burn option in an all-propulsive mission scenario does not yield a significant advantage in reduced trip time for reasonable masses. The multiple burn option allows significant reductions in trip time relative to the NEP system, and may provide a performance advantage over nuclear thermal propulsion, depending upon the system assumptions. The combined systems serve to reduce high thrust systems' sensitivity to mission opportunity. It is considered that 5 kg/kWe systems can provide significant improvements in mass and trip time over the single systems at power levels of 5 to 10 MWe. Author

N92-23755# Europropulsion, Suresnes (France).
DEVELOPMENT STATUS OF THE ARIANE 5 SOLID PROPELLANT ENGINE [ETAT D'AVANCEMENT DU DEVELOPPEMENT DU MOTEUR A PROPERGOL SOLIDE D'ARIANE 5]
Alain Coutrot *In* ESA, Launcher Propulsion Towards the Year 2010 Dec. 1991 p 49-55 In FRENCH (For primary document see N92-23750 14-15)
Copyright Avail: NTIS HC/MF A09; ESA, EPD, ESTEC, Noordwijk, Netherlands, HC 50 Dutch guilders

N92-23757# Chemical Automatics Design Bureau, Voronezh (USSR).
EXPERIENCE OF THE CHEMICAL AUTOMATICS DESIGN BUREAU IN CREATION OF RD-0120 LOX/LH2 LIQUID ROCKET ENGINE WITH THRUST OF 2 mn FOR ENERGIA LAUNCHER
Stanislav P. Aksjonov, Vladimir S. Rachuk, and A. F. Efimochkin *In* ESA, Launcher Propulsion Towards the Year 2010 Dec. 1991 p 67-72 (For primary document see N92-23750 14-15)
Copyright Avail: NTIS HC/MF A09; ESA, EPD, ESTEC, Noordwijk, Netherlands, HC 50 Dutch guilders

N92-23759# Societe Europeenne de Propulsion, Vernon (France).
DEVELOPMENT STATUS OF THE VULCAIN ENGINE
Serge Eury and E. Kirner (Messerschmitt-Boelkow-Blohm G.m.b.H., Ottobrunn, Germany, F.R.) *In* ESA, Launcher Propulsion Towards the Year 2010 Dec. 1991 p 77-85 (For primary document see N92-23750 14-15)
Copyright Avail: NTIS HC/MF A09; ESA, EPD, ESTEC, Noordwijk, Netherlands, HC 50 Dutch guilders

N92-23761# NPO Energomash, Khimki (USSR).
OXYGEN-KEROSENE LIQUID ROCKET ENGINES WITH POSTBURNING GENERATOR GAS AND HIGH PRESSURE IN COMBUSTION CHAMBER
Vladimir K. Tchvanov *In* ESA, Launcher Propulsion Towards the Year 2010 Dec. 1991 p 93-96 (For primary document see N92-23750 14-15)
Copyright Avail: NTIS HC/MF A09; ESA, EPD, ESTEC, Noordwijk, Netherlands, HC 50 Dutch guilders

N92-23762# Rockwell International Corp., Canoga Park, CA. Rocketdyne Div.
HEALTH MONITORING OF REUSABLE ROCKET ENGINES
W. Ezell, S. Barkhoudarian, and G. Cross *In* ESA, Launcher Propulsion Towards the Year 2010 Dec. 1991 p 97-102 (For primary document see N92-23750 14-15)
Copyright Avail: NTIS HC/MF A09; ESA, EPD, ESTEC, Noordwijk, Netherlands, HC 50 Dutch guilders

N92-23766# Aerospatiale, Les Mureaux (France). Departement Systemes Propulsifs.
FUTURE LAUNCHERS: LARGE SIZE SOLID PROPELLANT MONOLITHIC BOOSTER [LANCEURS FUTURS: PROPULSEUR MONOLITHIQUE DE GRANDES DIMENSIONS A PROPERGOL SOLIDE]
Max Calabro and Roland Lucas (Societe Nationale des Poudres et Explosifs, Saint-Medard-en-Jalles, France) *In* ESA, Launcher Propulsion Towards the Year 2010 Dec. 1991 p 143-152 In FRENCH (For primary document see N92-23750 14-15)
Copyright Avail: NTIS HC/MF A09; ESA, EPD, ESTEC, Noordwijk, Netherlands, HC 50 Dutch guilders

N92-23767# Centre National d'Etudes Spatiales, Paris (France).
DEVELOPMENT OF SOLID PROPELLANT BOOSTER [EVOLUTION DE LA CONCEPTION DES PROPULSEURS A PROPERGOL SOLIDE]
Michel Eymard and Yves Pelipenko *In* ESA, Launcher Propulsion Towards the Year 2010 Dec. 1991 p 153-158 (For primary document see N92-23750 14-15)
Copyright Avail: NTIS HC/MF A09; ESA, EPD, ESTEC, Noordwijk, Netherlands, HC 50 Dutch guilders

N92-23768# Office National d'Etudes et de Recherches Aerospatiales, Paris (France). Energetics Dept.
WHAT FUTURE FOR HYBRID ROCKET PROPULSION?
Paul Kuentzmann and H. J. Sternfeld (Deutsche Forschungsanstalt fuer Luft- und Raumfahrt, Lampoldshausen, Germany, F.R.) *In* ESA, Launcher Propulsion Towards the Year 2010 Dec. 1991 p 159-169 (For primary document see N92-23750 14-15)
Copyright Avail: NTIS HC/MF A09; ESA, EPD, ESTEC, Noordwijk, Netherlands, HC 50 Dutch guilders

N92-23809# Maschinenfabrik Augsburg-Nuernberg A.G., Munich (Germany, F.R.).
ADVANCED NUMERICAL ANALYSES FOR THE OPTIMISATION OF THE STRUCTURAL BEHAVIOUR OF THE INTERSEGMENT CONNECTION FOR THE ARIANE 5 BOOSTER CASE
P. Agatonovic and D. Sygulla *In* ESA, Spacecraft Structures and Mechanical Testing, Volume 1 Oct. 1991 p 197-202 (For primary document see N92-23780 14-18)
Copyright Avail: NTIS HC/MF A21

23 CHEMISTRY AND MATERIALS (GENERAL)

N92-23174# Technische Univ., Delft (Netherlands).
CHARACTERIZATION OF ORGANIC COATINGS WITH IMPEDANCE MEASUREMENTS: A STUDY OF COATING STRUCTURE, ADHESION AND UNDERFILM CORROSION Ph.D. Thesis
F. Geenen 23 Sep. 1991 184 p
(PB92-133479) Avail: NTIS HC/MF A09 CSCL 07A

Organic coatings of many different types and formulations are frequently employed to protect metal structures against corrosion and to simultaneously provide them with almost any color and gloss required. Obviously the matter of selecting the optimum coating for a specific substrate to be exposed to a specific environment from the multitude of different commercially available coatings, requires a thorough characterization of the most important coating properties. Furthermore a detailed characterization is a vital step in the development of new types of coatings, and new formulations. This is especially important as the use of a large number of proven types of coatings and components is soon to be prohibited under the new and very strict environmental legislations world-wide. In this thesis the possibilities for a successful application of impedance measurements to the broad characterization of coated metals are investigated in depth. Important in the study is the consideration that a successful data interpretation is possible only if the experimental conditions are highly optimized. This has resulted in the development of a novel cell design, optimization of noise reducing facilities, the optimization of a new technique to produce extremely well defined defects in coatings by laser ablation, and a large number of measurements on extremely controllable model coatings. GRA

N92-23190*# National Aeronautics and Space Administration. Lewis Research Center, Cleveland, OH.
TRIBOLOGICAL EVALUATION OF AN Al2O3-SiO2 CERAMIC FIBER CANDIDATE FOR HIGH TEMPERATURE SLIDING SEALS
Christopher DellaCorte and Bruce Steinetz Apr. 1992 19 p
(NASA-TM-105611; E-6949; NAS 1.15:105611) Avail: NTIS HC/MF A03 CSCL 07A

A test program to determine the relative sliding durability of an alumina-silica candidate ceramic fiber for high temperature sliding seal applications as described. This work represents the first reporting of the sliding durability of this material system. Pin-on-disk tests were used to evaluate the potential seal material by sliding a tow or bundle of the candidate ceramic fiber against a superalloy test disk. Friction was measured during the tests and fiber wear, indicated by the extent of fibers broken in the tow or bundle, was measured at the end of each test. Test variables studied included ambient temperatures from 25 C to 900 C, loads from 1.3 to 21.2 Newtons, and sliding velocities from 0.025 to 0.25 m/sec. In addition, the effects of fiber diameter, elastic modulus, and a pretest fiber heat treatment on friction and wear were measured. In most cases, wear increased with temperature. Friction ranged from about 0.36 at 500 C and low velocity (0.025 m/s) to over 1.1 at 900 C and high velocity (0.25 m/s). The pretest fiber heat treatment, which caused significant durability reductions for alumina-boria-silica ceramic fibers tested previously, had little effect on the alumina-silica fibers tested here. These results indicate that the alumina-silica (Al2O3-SiO2) fiber is a good candidate material system for high temperature sliding seal applications. Author

N92-23290*# National Aeronautics and Space Administration. Langley Research Center, Hampton, VA.
ORGANIC CONTAMINATION OF LDEF
Gale A. Harvey *In its* LDEF: 69 Months in Space. First Post-Retrieval Symposium, Part 1 Jan. 1992 p 179-197 (For primary document see N92-23280 14-99)
Avail: NTIS HC/MF A99; 8 functional color pages CSCL 07A

24 COMPOSITE MATERIALS

Includes physical, chemical, and mechanical properties of laminates and other composite materials.
For ceramic materials see *27 Nonmetallic Materials.*

N92-23157 Bath Univ. (England).
THE EFFECT OF FATIGUE-INDUCED DAMAGE ON THE MECHANICAL PROPERTIES OF CFRP COMPOSITES Ph.D. Thesis
Ansong Chen 1991 258 p
Avail: Univ. Microfilms Order No. BRDX94301

A study was made into fatigue induced damage mechanisms and their effects on the mechanical properties of carbon fiber reinforced plastics, emphasizing better understanding of the relationship of microstructure and macroscopic properties. A series of experimental works were conducted on XAS/914 and T800/5245 carbon fiber epoxy resin composites with ((+ or - 45, O sub 2)2)s and unidirectional (O)sub 8 layups. Damage conditions of the laminates subjected to repeated tension cycling (R = 0.1) were detected by means of destructive and nondestructive evaluation methods. And prior damage information is presented in the form of schematic 'damage maps'. The close property and damage state relationship which is confirmed by mechanical property measurements shows that it is possible to predict long term fatigue life by assuming that the final fatigue failure is an occurrence of the last damage mechanism. Dissert. Abstr.

N92-23167# Aeronautical Research Inst. of Sweden, Stockholm. Structures Dept.
EXPERIMENTAL VERIFICATION OF A THEORY FOR THE IMPACT RESPONSE OF COMPOSITE PLATES
Robin Olsson Oct. 1991 52 p Sponsored by Swedish Defence Material Administration
(FFA-TN-1991-17; ETN-92-91193) Avail: NTIS HC/MF A04

The impact response of specially orthotropic composite plates under a Hertzian type contact law is addressed for cases where the response is controlled by flexural wave propagation rather than by conditions of fixed boundaries. Such a response is typical for a large class of small mass impacts. Closed form expressions for the plate response are given according to a theory presented recently by the author. The theory is experimentally verified by varying seven parameters of eight that appear to control the impact response. The response is described in terms of transient recordings of the contact force, plate central deflection and principal flexural strains under the impact point. Generally a very good agreement is found between predicted and measured values. ESA

N92-23194*# National Aeronautics and Space Administration. Lewis Research Center, Cleveland, OH.
PROGRESSIVE FRACTURE OF POLYMER MATRIX COMPOSITE STRUCTURES: A NEW APPROACH
C. C. Chamis, P. L. N. Murthy, and L. Minnetyan (Clarkson Univ., Potsdam, NY.) 1992 22 p Presented at the 14th Annual Energy-Sources Technology Conference and Exhibition, Houston, TX, 26-29 Jan. 1992; sponsored by ASME
(NASA-TM-105574; E-6900; NAS 1.15:105574) Avail: NTIS HC/MF A03 CSCL 11D

A new approach independent of stress intensity factors and fracture toughness parameters has been developed and is described for the computational simulation of progressive fracture of polymer matrix composite structures. The damage stages are quantified based on physics via composite mechanics while the degradation of the structural behavior is quantified via the finite element method. The approach account for all types of composite behavior, structures, load conditions, and fracture processes starting from damage initiation, to unstable propagation and to global structural collapse. Results of structural fracture in composite beams, panels, plates, and shells are presented to demonstrate the effectiveness and versatility of this new approach. Parameters and guidelines are identified which can be used as criteria for structural fracture, inspection intervals, and retirement for cause.

Generalization to structures made of monolithic metallic materials are outlined and lessons learned in undertaking the development of new approaches, in general, are summarized. Author

N92-23195*# National Aeronautics and Space Administration. Lewis Research Center, Cleveland, OH.
INFLUENCE OF ENGINEERED INTERFACES ON RESIDUAL STRESSES AND MECHANICAL RESPONSE IN METAL MATRIX COMPOSITES
Steven M. Arnold and Thomas E. Wilt (Toledo Univ., OH.) Mar. 1992 27 p Proposed for presentation at the Fourth International Conference on Composite Interfaces, Cleveland, OH, 26-29 May 1992; sponsored by Case Western Reserve Univ.
(NASA-TM-105438; E-6866; NAS 1.15:105438) Avail: NTIS HC/MF A03 CSCL 11D

Because of the inherent coefficient of thermal expansion (CTE) mismatch between fiber and matrix within metal and intermetallic matrix composite systems, high residual stresses can develop under various thermal loading conditions. These conditions include cooling from processing temperature to room temperature as well as subsequent thermal cycling. As a result of these stresses, within certain composite systems, radial, circumferential, and/or longitudinal cracks have been observed to form at the fiber matrix interface region. A number of potential solutions for reducing this thermally induced residual stress field have been proposed recently. Examples of some potential solutions are high CTE fibers, fiber preheating, thermal anneal treatments, and an engineered interface. Here the focus is on designing an interface (by using a compensating/compliant layer concept) to reduce or eliminate the thermal residual stress field and, therefore, the initiation and propagation of cracks developed during thermal loading. Furthermore, the impact of the engineered interface on the composite's mechanical response when subjected to isothermal mechanical load histories is examined. Author

N92-23256# Argonne National Lab., IL.
THE EFFECT OF PROCESSING ON STRENGTH OF NICALON FIBERS IN NICALON FIBER-SiC MATRIX COMPOSITES
D. Singh and J. P. Singh Dec. 1991 18 p Presented at the 16th Annual Conference on Composites, Materials, and Structures, Coca Beach, FL, 13-16 Jan. 1992
(Contract W-31-109-eng-36)
(DE92-006978; ANL/CP-73895; CONF-920144-1) Avail: NTIS HC/MF A03

Degradation of strength of Nicalon (silicon carbide) fibers during processing of Nicalon fiber-SiC matrix composites was studied. Strength distribution of as-fabricated Nicalon fibers was obtained via bundle tests, whereas strengths of fractured fibers in Nicalon fiber-reinforced SiC matrix composite specimens were estimated by measuring fracture mirror radii. Comparison of fracture probability plots indicates significant differences in the behavior of the as-fabricated fibers and those in the composite. Possible causes leading to these differences are discussed. DOE

N92-23433*# National Aeronautics and Space Administration. Langley Research Center, Hampton, VA.
DAMAGE DEVELOPMENT IN TITANIUM METAL MATRIX COMPOSITES SUBJECTED TO CYCLIC LOADING
W. S. Johnson Apr. 1992 25 p Presented at the Fracture of Inorganic Composites, Cambridge, England, 31 Mar. - 2 Apr. 1992
(NASA-TM-107597; NAS 1.15:107597) Avail: NTIS HC/MF A03 CSCL 11D

Several layups of SCS-6/Ti-15-3 composites were investigated. Fatigue tests were conducted and analyzed for both notched and unnotched specimens at room temperature and elevated temperatures. Thermo-mechanical fatigue results were analyzed. Test results indicated that the stress in the 0 degree fibers is the controlling factor in fatigue life. The static and fatigue strength of these materials is shown to be strongly dependent on the level of residual stresses and the fiber/matrix interfacial strength. Fatigue tests of notched specimens showed that cracks can initiate and grow many fiber spacings in the matrix materials without breaking fibers. Fiber bridging models were applied to characterize the crack growth behavior. The matrix cracks are shown to significantly reduce the residual strength of notched composites. The notch strength of these composites was accurately predicted using a micromechanics based methodology. Author

N92-23434*# National Aeronautics and Space Administration. Langley Research Center, Hampton, VA.
MATRIX DOMINATED STRESS/STRAIN BEHAVIOR IN POLYMERIC COMPOSITES: EFFECTS OF HOLD TIME, NONLINEARITY AND RATE DEPENDENCY
Thomas S. Gates Apr. 1992 23 p Proposed for presentation at the ASTM Symposium on Testing and Design, Pittsburgh, PA, 4 May 1992
(NASA-TM-107595; NAS 1.15:107595) Avail: NTIS HC/MF A03 CSCL 11D

In order to understand matrix dominated behavior in laminated polymer matrix composites, an elastic/viscoplastic constitutive model was developed and used to predict stress strain behavior of off-axis and angle-ply symmetric laminates under in-plane, tensile axial loading. The model was validated for short duration tests at elevated temperatures. Short term stress relaxation and short term creep, strain rate sensitivity, and material nonlinearity were accounted for. The testing times were extended for longer durations, and periods of creep and stress relaxation were used to investigate the ability of the model to account for long term behavior. The model generally underestimated the total change in strain and stress for both long term creep and long term relaxation respectively. Author

N92-23532*# Georgia Inst. of Tech., Atlanta.
ANALYSIS OF DELAMINATION RELATED FRACTURE PROCESSES IN COMPOSITES Semiannual Report
Erian A. Armanios 20 Apr. 1992 49 p
(Grant NAG1-637; GIT Proj. E16-654)
(NASA-CR-190226; NAS 1.26:190226) Avail: NTIS HC/MF A03 CSCL 11D

An anisotropic thin walled closed section beam theory was developed based on an asymptotical analysis of the shell energy functional. The displacement field is not assumed a priori and emerges as a result of the analysis. In addition to the classical out-of-plane torsional warping, two new contributions are identified namely, axial strain and bending warping. A comparison of the derived governing equations confirms the theory developed by Reissner and Tsai. Also, explicit closed form expressions for the beam stiffness coefficients, the stress and displacement fields are provided. The predictions of the present theory were validated by comparison with finite element simulation, other closed form analyses and test data. Author

N92-23585# Allied-Signal Aerospace Co., Kansas City, MO.
HIGH STRENGTH COMPOSITES EVALUATION
S. M. Marten Feb. 1992 24 p
(Contract DE-AC04-76DP-00613)
(DE92-007264; KCP-613-4556) Avail: NTIS HC/MF A03

A high strength, thick section, graphite/epoxy composite was identified. The purpose of this development effort was to evaluate candidate materials and provide LANL with engineering properties. Eight candidate materials (Samples 1000, 1100, 1200, 1300, 1400, 1500, 1600, and 1700) were chosen for evaluation. The Sample 1700 thermoplastic material was the strongest overall. DOE

N92-23693 Utah Univ., Salt Lake City.
THE FRACTURE BEHAVIOR OF CARBON/EPOXY LAMINATES CONTAINING PART THROUGH-THE-THICKNESS FIBER BREAKAGE Ph.D. Thesis
Zhengfei Tian 1991 253 p
Avail: Univ. Microfilms Order No. DA9128091

Part through-the-thickness fiber breakage and delamination are two major types of damage caused by impact loads on composite laminates. The objectives of this investigation were to determine the tensile fracture behavior of laminates when part through-the-thickness fiber breakage is present, and to develop a procedure for predicting laminate tensile residual strength on a

ply-by-ply basis. The investigation was carried out both experimentally and analytically. In the experimental phase, laminate specimens containing internal fiber cuts were manufactured and tested. Residual tensile strengths were measured. Delamination that developed in the specimens during the tensile loading was detected through ultrasonic and microsectioning inspections. In the analytical phase, a three-dimensional finite element analysis was conducted to model the specimens in order to calculate the stress and strain fields. Based on the finite element results, the laminate residual strengths were then evaluated by examining the strain in the fiber direction in principal load carrying plies. This constituted a procedure for predicting residual strength of laminates containing part through-the-thickness fiber cuts. Finally, using literature data of impact damage and residual strength, the residual strength prediction procedure developed from laminates containing internal fiber cuts was verified when applied to laminates containing real impact damage. Dissert. Abstr.

N92-23933# National Research Council of Canada, Boucherville (Quebec). Industrial Materials Research Inst.

COMPOSITES, 1990

1990 392 p Presented at the 9th NRCC/IMI Symposium, Boucherville, Quebec, 20-21 Nov. 1990

(NRC-32603; IMI-90D-000-1063-G; CTN-92-60405) Avail: National Research Council, Montreal Rd, Ottawa, ON K1A 0R6 Canada

High performance composites offer attractive specific strength and rigidity over more conventional materials. The main challenge that engineers and scientists face is development of technology enabling manufacture of high performance materials at high production rates. This symposium was held to promote discussions and exchange of information on the state of the art in the area of mechanical behavior as well as processing and optimization of composites. The theme is composite materials performance and processing. Particular emphasis is given to the damage, fracture, defects, as well as effects of processing on end use performance. For individual titles, see N92-23934 through N92-23949.

N92-23934# Toronto Univ. (Ontario). Dept. of Chemical Engineering.

FAILURE PROCESSES IN THE FIBRE-POLYMER INTERPHASE

M. R. Piggott *In* National Research Council Canada, Composites: 1990 1990 27 p (For primary document see N92-23933 14-24)

Avail: National Research Council, Montreal Rd, Ottawa, ON K1A 0R6 Canada

The nature of the interphase failure process in fiber composites is still not fully understood. Methods used to measure failure properties, such as pull out, microtension, microcompression, and fragmentation test, often give conflicting results. The roles of friction and interphase fracture on the pull out test and the fragmentation test are critically examined. It is shown that it is difficult to obtain results which are untainted by friction and that the different tests probably involve different ratios between friction shears to pure debonding shears. A second difficulty with reported values for debonding shear stress is that they are occasionally much higher than the probable shear strength of the polymer. This is unlikely to be due to constraints arising in the test. Instead, the energy of debonding may be the cause: quite low debonding energies require large shear stresses to overcome them. Fibers studied include: glass fibers, strong carbon, stiff carbon, and Kevlar, all embedded in polyester resin. Author (CISTI)

N92-23935# Universite de Technologie de Compiegne (France). Div. Polymeres et Composites.

MICROSTRUCTURE AND MECHANICAL PROPERTIES OF CARBON FIBRES: RELATIONSHIP WITH THE FIBRE-MATRIX ADHESION IN A CARBON-EPOXY COMPOSITE

M. Guigon *In* National Research Council Canada, Composites: 1990 1990 19 p (For primary document see N92-23933 14-24)

Avail: National Research Council, Montreal Rd, Ottawa, ON K1A 0R6 Canada

Carbon fibers are formed as a set of turbostatic stacks of aromatic layers lying approximately parallel to the fiber axis. The way these fibers are arranged in space, or their microtexture, is responsible for many fiber properties, especially mechanical properties. This paper presents a study of the effect of microstructure on the tensile yield properties of epoxy carbon composites. Selected area x-ray diffraction patterns of several high strength and high modulus fibers were examined. A structural model was developed from these observations. This model indicates that the basic microtextural units are roughly stacked together in high modulus fibers. Any residual defects are probably due to the presence of disclinations, tetrahedral bonds, and crosslinking heteroatoms. As a consequence of heat treatment high modulus fibers are well organized and many defects disappear. The tensile strength of carbon fibers at failure is related to microtextural parameters. In the carbon epoxy composite, the carbon layers in the fiber either exhibit their edge or their surface on the fiber surface. Because edges are very reactive, adhesion between the carbon fiber and the epoxy matrix is strong. Author (CISTI)

N92-23936# National Research Council of Canada, Boucherville (Quebec).

IMPACT-INDUCED DELAMINATION IN (0(5), 90(5), 0(5)) CARBON/PEEK COMPOSITE LAMINATES

H. Wang and T. Vu-Khanh *In its* Composites: 1990 1990 28 p (For primary document see N92-23933 14-24)

Avail: National Research Council, Montreal Rd, Ottawa, ON K1A 0R6 Canada

This paper reports both experimental and analytical investigations on the low-velocity impact delamination in (0(5), 90(5), 0(5)) carbon/peek laminates. The impact force and resulted delamination area are measured respectively by the instrumented impact tester and by x-radiography and thermal deplying techniques. The dynamic response of the laminate was modelled by the real-life impact force and laminate theory using finite element technique. It was found that the impact delamination may result from an interlaminar shear failure mechanism, and the interlaminar shear stress contours can be used to simulate the measured delamination area at every interface. The agreement in trend between numerical results and test data seems to suggest an interlaminar shear stress failure criterion for impact-induced delamination of composite laminates. Author (CISTI)

N92-23937# National Research Council of Canada, Ottawa (Ontario). Structure and Materials Lab.

IMPACT AND COMPRESSION RESPONSE OF COMPOSITE MATERIALS CONTAINING FORTIFIERS

R. F. Scott, S. Lee, C. Poon, and P. C. Gaudert *In its* Composites: 1990 1990 15 p (For primary document see N92-23933 14-24)

Avail: National Research Council, Montreal Rd, Ottawa, ON K1A 0R6 Canada

Additives called 'fortifiers' were developed which improve the tensile strength and modulus of conventional amine-epoxy materials. The addition of fortifiers to neat epoxies resulted in an increase in the tensile strength by 65 percent and the tensile modulus by 40 percent. The effect of adding fortifiers to an epoxy matrix on the response to impact and compression after impact properties of carbon fabric/epoxy laminates was investigated. The experimental work included determining laminate compression strength, absorbed energy from impact, damage area, and compression after impact strength for an impact energy level of 21 joules per centimeter of thickness. All carbon fabric prepreg materials used in this study were easy to process into high quality laminates. The nominal compression strength of the non-impacted carbon fiber reinforced epoxy was found to increase approximately 25 percent with the addition of fortifier while the compression modulus when normalized to a fiber volume of 60 percent showed a minor increase. The addition of fortifier improved the impact resistance of the laminate significantly as both the absorbed energy and damage area were reduced. The addition resulted in an increase of 25 percent in the nominal compression after impact strength and an increase of approximately 17 percent in the net

area strength. The improvement in performance of the laminates with the addition of fortifier appears to be related to changes in the tensile properties of the neat resin. Author (CISTI)

N92-23938# British Columbia Univ., Vancouver. Dept. of Metals and Materials Engineering.
A METHOD TO DETERMINE RESIN FLOW DURING CURING OF COMPOSITE LAMINATES
A. Poursartip, G. Riahi, L. Fredrick, and X. Lin *In* National Research Council Canada, Composites: 1990 1990 21 p (For primary document see N92-23933 14-24)
Avail: National Research Council, Montreal Rd, Ottawa, ON K1A 0R6 Canada

Resin flow modelling is important to the scientific processing of thermoset matrix polymer composites. An experimental method is presented to determine the amount of resin flow within a composite laminate during cure. The method is analogous to the use of radioactive tracers in other applications. Heavier elements such as chlorine and bromine, which may be naturally present in small amounts in epoxy resins, are used to follow resin flow and mixing. The presence and the quantity of these tags is determined using wavelength dispersive x-ray (WDX) analysis in a scanning electron microscope. With the resins in this study, it is shown that it is possible to measure volume fractions of resin with accuracies ranging from plus or minus 0.5 to plus or minus 3 v/o. By using brominated resin in only one layer of a laminate, the degree of mixing of resin from different layers can be followed accurately. The results suggest that there is considerable flow and mixing of resin between layers which is not taken into account in any of the current flow models. WDX analysis of chlorine and bromine content allows the quantitative determination of the final resin volume fraction distribution in an epoxy matrix composite laminate. The amount of tagged resin present in other layers can be determined accurately. Author (CISTI)

N92-23939# Lyon-1 Univ., Villeurbanne (France).
MORPHOLOGY AND MECHANICAL PERFORMANCE OF PPS/CARBON COMPOSITE
L. Caramaro, B. Chabert, J. Chauchard, and T. Vu-Khanh (National Research Council of Canada, Boucherville, Quebec) *In* National Research Council Canada, Composites: 1990 1990 22 p (For primary document see N92-23933 14-24)
Avail: National Research Council, Montreal Rd, Ottawa, ON K1A 0R6 Canada

Work undertaken to correlate the kinetic and thermodynamic aspects of the crystallization of polyphenylene sulfide (PPS), in the presence of carbon fibers, to the global performance of the composite is described. The experiments were first carried out on model samples (PPS powder or film in the presence of carbon fibers). Plates of unidirectional PPS/carbon composite were also molded for the analysis of the mechanical properties. The crystallization of PPS can reversibly take place only for certain melting conditions. The nucleating role of carbon fibers becomes predominant when all the crystalline entities in the PPS matrix are destroyed. In this case a transcrystalline phase around the fibers is observed. When the fibers are close enough to each other, the matrix can consist solely of transcrystalline phase. In the molding process of the samples, it is difficult to accurately reproduce the evolution of the matrix morphology, due to the difficulty of controlling such parameters as thermal inertia, pressure, resident time, etc. However, the variation of the mechanical properties with the molding condition is in good agreement with the results concerning the matrix morphology. Optimum values of shear strength and fracture energy were obtained for melting temperatures between 350 and 380 C. It is therefore possible to optimize some mechanical properties of PPS/carbon composites by adequately controlling the molding conditions and the matrix morphology. Author (CISTI)

N92-23940# National Research Council of Canada, Ottawa (Ontario). Inst. for Environmental Chemistry.
CRYSTALLIZATION BEHAVIOR OF POLY(PHENYLENE SULPHIDE)
Derek R. Budgell and Michael Day *In its* Composites: 1990 1990 24 p (For primary document see N92-23933 14-24)
Avail: National Research Council, Montreal Rd, Ottawa, ON K1A 0R6 Canada

Polyphenylene sulfide (PPS) is a semicrystalline polymer that is widely employed in composites. It has excellent mechanical properties, high chemical resistance, and good thermal stability. Engineering thermoplastics' mechanical properties can be substantially enhanced by the addition of a reinforcement phase. Traditionally, carbon or glass fibers have been employed as additives, but the development of high temperature thermotropic liquid crystal polymers (LCP's) has generated interest in using these materials as blending agents since LCP's can offer several attractive features which include a combination of stiffness, high tensile strength, high impact resistance, chemical resistance, and a low coefficient of thermal expansion. If the liquid crystalline phase formed by the polymer is nematic, then the melts exhibit low viscosity and can aid in the processing of the thermoplastic matrix. The crystallization behavior of PPS was examined by differential scanning calorimetry as a function of melt temperature, residence time in the melt, and the presence of a liquid crystal polymer. The results suggest that the thermal history of the sample plays an important role in determining the crystallization kinetics. Both short residence times at low melt temperatures and high melt temperatures resulted in a low value for the Avrami parameter, eta (the Avrami parameter is related to the time required to reach 50 percent of maximum crystallization). The former effect was ascribed to incomplete melting of the polymer while the latter effect was attributed to thermal degradation. Blending a liquid crystal polymer, Vectra A950, with PPS has only a minor effect on the crystallization behavior. Author (CISTI)

N92-23941# Stuttgart Univ. (Germany, F.R.).
INJECTION MOLDING OF LONG FIBER REINFORCED THERMOPLASTICS: A COMPARISON OF EXTRUDED AND PULTRUDED MATERIALS WITH DIRECT ADDITION OF ROVING STRANDS
F. Truckenmuller and H.-G. Fritz *In* National Research Council Canada, Composites: 1990 1990 43 p (For primary document see N92-23933 14-24)
Avail: National Research Council, Montreal Rd, Ottawa, ON K1A 0R6 Canada

An injection molding process is proposed whereby roving strands are directly incorporated into the polymer melt by using a reciprocating screw plasticating unit. The direct incorporation of continuous fibers (DIF) offers the possibility to substitute for the relatively expensive and limited pultrusion process which is used to produce long fiber pellets. In this preliminary study, experimental investigations on glass fiber reinforced polyamide 6.6 are carried out, starting with short and long fiber pellets in comparison with the direct incorporation of roving strands into the polymer melt. Some special aspects of the processing of long fiber reinforced thermoplastics are discussed. The results of fundamental mechanical and physical investigations are presented. All investigated DIF-materials show exactly the same high level of mechanical/physical properties as their counterparts from pultrusion compounding. Compared to a conventional extrusion compounded short fiber reinforced material, the long fiber reinforced composites showed a very high increase in impact toughness of at least 100 percent, even at low temperatures, as well as a significantly increased shear modulus above the glass transition temperature. The tensile and flexural properties of the short and long fiber reinforced materials were found to be very similar, except that the short fiber reinforced parts exhibit higher values of ultimate tensile strength and strain. The DIF process also provided improved control and uniformity in composite processing. Author (CISTI)

N92-23942# Delaware Univ., Newark. Centre for Composite Materials.

ON THE APPLICATION OF MICROMECHANICS TO THE PREDICTION OF MACROSCOPIC THERMAL RESIDUAL STRESSES IN SHORT-FIBER REINFORCED POLYETHERETHERKETONE (PEEK)

R. F. Eduljee, J. W. Gillespie, Jr., and R. L. McCullough *In* National Research Council Canada, Composites: 1990 1990 21 p (For primary document see N92-23933 14-24)

Avail: National Research Council, Montreal Rd, Ottawa, ON K1A 0R6 Canada

The salient features of a micromechanics model for the prediction of thermoelastic properties of dispersed short fiber systems are discussed. This micromechanics model coupled with a second model for the crystallization of PEEK and the incremental stress analysis model, is used to obtain fundamental insight into the development of thermal residual stresses in neat, semicrystalline PEEK and dispersed, short glass fiber PEEK composites. The temperature history was determined from Fourier's law of heat conduction in one dimension, with convective boundary conditions. The matrix properties as a function of time and the temperature history were determined using the standard linear solid model for semicrystalline matrices. The model parameters for the crystallinity model, the modified standard linear solid (SLS) model, and the thermoelastic properties of the neat PPKk resin were given. Processing shrinkage due to crystallinity is included in the analysis. The model is capable of differentiating between aggregated microstructures of sheet molding compounds and dispersed microstructures typical of injection molded structures. At high cooling rates little crystallinity develops. Under slower cooling conditions crystallinity increased the residual stresses in neat PEEK, but has a much lesser effect on residual stress development in fiber reinforced PEEK. Author (CISTI)

N92-23943# Universite de Technologie de Compiegne (France). Div. Polymeres et Composites.

ON THE TEST OF MODE 1 DELAMINATION AND THE IMPORTANCE OF LAMINATE LAY-UPS

M. L. Benzeggagh, X. J. Gong, A. Laksimi, and J. M. Roelandt *In* National Research Council Canada, Composites: 1990 1990 18 p (For primary document see N92-23933 14-24)

Avail: National Research Council, Montreal Rd, Ottawa, ON K1A 0R6 Canada

Double cantilever beam (DCB) specimens are widely used for determining the critical delamination energy (Glc) under mode 1 testing. Results of pure mode 1 testing using angle ply glass epoxy DCB specimens are presented. The influence of laminate layups on the value of Glc at crack initiation and the critical energy release rate at stable crack propagation (Gslp) were investigated. To bring out problems posed by this test, experimental values were correlated with the results obtained by beam theory models and a finite element analysis. The specimens were also examined microscopically for fracture morphology. The value of Glc of delamination varies with laminate curvature coupling. An empirical model describing this variation is proposed. In addition, it is seen that the critical energy release rates at the initiation of delamination and at stable crack growth are different. Thus, the delamination resistance of a laminated beam can be characterized by two constants, one Glc and one Gslp. The correlation between experimental measurement and analysis on compliance and energy release rate results reveals significant three dimensional effects; hence, two dimensional analysis does not adequately describe the crack initiation process. Author (CISTI)

N92-23944# National Research Council of Canada, Ottawa (Ontario). Inst. for Environmental Chemistry.

APPLICATION OF THE MICROBOND TECHNIQUE: CHARACTERIZATION OF CARBON-EPOXY INTERFACES

D. A. Biro, P. McLean, and Y. Deslandes *In its* Composites: 1990 1990 24 p (For primary document see N92-23933 14-24)

Avail: National Research Council, Montreal Rd, Ottawa, ON K1A 0R6 Canada

The microbond technique provides data on interfacial shear strength, the work of fracture, and frictional components after interphasial adhesion failure. The interfacial shear strengths of carbon fiber/resin composites were determined directly using the microbond technique. This method provides a distribution of values which arise due to small variations on the surface of the carbon fiber surface. The microbond method is suitable for evaluating fiber/matrix interactions using different cure schedules and resin formulations. The effect of cure was determined to have a profound effect on tau of the micro-composite. The interfacial shear strength for a given fiber/epoxy system studied increased three fold from a B-stage to a fully cured material. The addition of a fortifier to the resin formulation increased tau by as much as 74 percent from the host system. Mechanical adhesion arising from residual stress accounted for as much as a quarter of the total of the interfacial shear strength in fortified resin/carbon fiber systems. The microbond method is but one method of determining the interfacial shear strength of a fiber/resin composite. There are limitations as with any technique. Further theoretical work on the fracture mechanics and experimental studies should be continued with this method since it provides a straightforward interpretation of experimental results. Author (CISTI)

N92-23945# Quebec Univ., Trois-Riveres. Centre de Recherche en Pates et Papiers.

INFLUENCE OF MALEIC ANHYDRIDE AS A COUPLING AGENT ON THE PERFORMANCE OF WOOD FIBER: POLYSTYRENE COMPOSITES

D. Maldas and B. V. Kokta *In* National Research Council Canada, Composites: 1990 1990 21 p (For primary document see N92-23933 14-24)

Avail: National Research Council, Montreal Rd, Ottawa, ON K1A 0R6 Canada

The lack of polar groups in thermoplastics, such as polystyrene, provide low adhesion with cellulosic fibers. To improve compatibility between reinforcement and matrix, maleic anhydride (MA) was selected as a coupling agent for wood fiber-filled polystyrene composites. In general, the mechanical properties improved along with the increase in concentrations of MA, initiator (benzoyl peroxide) and wood fiber in the composites up to a certain limit and then decreased at the higher concentrations. The concentrations of MA and fiber which produce maximum improvements in the mechanical properties vary according to wood species, pulping techniques, and type of polystyrene. Moreover, properties were further accelerated when another coupling agent (isocyanate) was used in addition to the MA. Author (CISTI)

N92-23946# Universita degli Studi della Basilicata, Potenza (Italy).

QUANTIFICATION OF SURFACE FUNCTIONAL GROUPS OF CARBON FIBERS BY X RAY PHOTOELECTRON SPECTROSCOPY

G. I. Casella, A. M. Salvi, and E. Desimoni *In* National Research Council Canada, Composites: 1990 1990 23 p (For primary document see N92-23933 14-24)

Avail: National Research Council, Montreal Rd, Ottawa, ON K1A 0R6 Canada

A curve fitting method for the analysis of the C1s region of carbon fibers is described. The identification and quantification of functional groups produced on carbon fiber surfaces by activation (oxidation) treatments presents a real challenge to x-ray photoelectron spectroscopy (XPS). The C1s peak envelope exhibits a pronounced asymmetric tailing towards higher binding energy values. These tails arise partly from intrinsic asymmetry in the graphite peak, and partly from the presence of oxygen containing functional groups. The elucidation of the correct C1s graphitic lineshape is critical in assuring a correct evaluation of surface species. The present paper describes a method using difference spectra to evaluate the lineshape modification caused by ultrahigh vacuum (UHV) annealing. The analysis of the effects of UHV annealing on all the spectral features in the XPS spectra provides evidence of chemical and structural modification of the fibers and permits a reasonably confident lineshape to be obtained for the

C1s graphitic peak for oxygen free fibers. Additional x-ray excited features including Auger peaks and the valence band, can be analyzed for a more complete description of complex samples. A proper cleaning treatment may be necessary in activation studies of carbon fibers as the fibers may exhibit artifacts of UHV storage. Author (CISTI)

N92-23947# Clarkson Univ., Potsdam, NY.
MECHANICAL PROPERTIES OF GLASS BEAD FILLED DUCTILE EPOXY COMPOSITES
R. S. Dave and L. Lorenzo (Dow Chemical Co., Midland, MI.) *In* National Research Council Canada, Composites: 1990 1990 29 p (For primary document see N92-23933 14-24)
Avail: National Research Council, Montreal Rd, Ottawa, ON K1A 0R6 Canada

Degradation in mechanical properties of continuous fiber composite materials is often the result of voids in the part or loss of adhesion to the reinforcing fibers which develop during processing. These voids and loss of adhesion are usually attributed to residual thermal stresses in the part. The basic physics of residual stresses which develop during cooling of thermoplastic matrix materials is analyzed and an analytical model is developed. The residual stress field predicted by the model is compared to observations of the differences in microstructure of polymeric materials with different processing histories. Processing was shown to have a significant effect on the final morphology of compression molded glassy thermoplastics. Rapidly cooled specimens subject to a minimal pressure have approximately an order of magnitude more interior damage, in the form of microvoids, than specimens that were cooled more slowly under a greater pressure. Manipulations of cooling rates and applied pressure are thus effective in counteracting the thermal stresses developed during solidification of molten thermoplastics. The model provides a guide to the magnitude of pressure and cooling rate required to minimize undesirable residual stress. The non-dimensional relaxation parameter indicates how stress relaxation is related to cooling rate. Overall, the two aspects of the modeling provide us with a guide to specification of processing conditions that allow parts to be fabricated rapidly without developing unacceptable levels of residual stress. Author (CISTI)

N92-23948# Quebec Univ., Trois-Riveres. Centre de Recherche en Pates et Papiers.
FILLING HIGH DENSITY POLYETHYLENE WITH CELLULOSIC FIBERS. 1: THE EFFECT OF ADDITIVES ON FIBER DISPERSION
R. G. Raj and B. V. Kokta *In* National Research Council Canada, Composites: 1990 1990 20 p (For primary document see N92-23933 14-24)
Avail: National Research Council, Montreal Rd, Ottawa, ON K1A 0R6 Canada

High density polyethylene (HDPE) was filled with different concentrations (0-40 percent by weight of fiber) of wood flour (aspen). The effects of different additives (stearic acid, mineral oil, maleated ethylene wax, and sodium silicate) on mechanical properties (tensile and impact strength) of the composites were studied. Comparison of tensile properties of the composites showed that the addition of maleated ethylene wax produced a significant increase in tensile strength, with the increase in filler concentration, while tensile modulus remained relatively unaffected. Microscopic studies of the composites indicate a better dispersion of fiber in the polymer matrix when stearic acid was used. Author (CISTI)

N92-23949# Ecole Polytechnique, Montreal (Quebec). Dept. of Mechanical Engineering.
WELDLINE STRENGTH IN INJECTION MOLDED GLASS FIBER REINFORCED POLYPROPYLENE
M. Rahmani and B. Fisa *In* National Research Council Canada, Composites: 1990 1990 30 p (For primary document see N92-23933 14-24)
Avail: National Research Council, Montreal Rd, Ottawa, ON K1A 0R6 Canada

Weldlines are inescapable byproducts of injection molding processes. They represent potentially fatal flaws particularly in multiphase materials. Weldlines in injection molded glass fiber reinforced polypropylene (0-40 weight percent) were studied as a function of cavity shapes and depths. It was found that the weldline is a zone between 2 and 8 mm wide extending throughout the thickness in which the fibers are oriented almost perfectly in a plane parallel to the weldline. Regardless of the mold shape, the weldline strength is that of the matrix reduced by the area occupied by fibers. Since the strength of the moldings without weldlines depends on the mold shape, the strength retention ratio varies with the mold shape. Effects of other variables such as distance of flow, insert diameter, or lateral expansion on the weldline strength is not significant. A simple model based on the assumption of complete debonding of the fiber-matrix interface when failure occurs can be used to predict the strength loss in the weldline.
Author (CISTI)

N92-23981*# National Aeronautics and Space Administration. Langley Research Center, Hampton, VA.
EFFECT OF LOW-SPEED IMPACT DAMAGE AND DAMAGE LOCATION ON BEHAVIOR OF COMPOSITE PANELS
Dawn C. Jegley May 1992 27 p Presented at the 9th DOD/NASA/FAA Conference on Fibrous Composites in Structural Design, Lake Tahoe, NV, 4-7 Nov. 1991
(NASA-TP-3196; L-17031; NAS 1.60:3196) Avail: NTIS HC/MF A03 CSCL 11D

The effect of low speed impact damage on the compression and tension strength of thin and moderately thick composite specimens was investigated. Impact speed ranged from 50 to 550 ft./sec., with corresponding impact energies from 0.25 to 30.7 ft. x lb. Impact locations were near the center of the specimen or near a lateral unloaded edge. In this study, thin specimens with only 90 degree and + or - 45 degree plies that were impacted away from the unloaded edge suffered less reduction in load carrying capability because of impact damage than of the same specimens impacted near the unloaded edge. Failure loads of thicker compression loaded specimens with a similar stacking sequence were independent of impact location. Failure loads of thin tension loaded specimens with 0 degree plies was independent of impact location, whereas failure loads of thicker compression loaded specimens with 0 degree plies were dependent upon impact location. A finite element analysis indicated that high axial strains occurred near the unloaded edges of the postbuckled panels. Thus, impacts near the unloaded edge would significantly affect the behavior of the postbuckled panel. Author

N92-23988# Lawrence Livermore National Lab., CA.
METAL-SEMICONDUCTOR, COMPOSITE RADIATION DETECTORS
W. J. Orvis, J. H. Yee, and D. A. Fuess Dec. 1991 17 p (Contract W-7405-eng-48)
(DE92-008980; UCRL-ID-109159) Avail: NTIS HC/MF A03

In 1989, Naruse and Hatayama of Toshiba published a design for an increased efficiency x-ray detector. The design increased the efficiency of a semiconductor detector by interspersing layers of high-z metal within it. Semiconductors such as silicon make good, high-resolution radiation detectors, but they have low efficiency because they are low-z materials ($z = 14$). High-z metals, on the other hand, are good absorbers of high-energy photons. By interspersing high-z metal layers with semiconductor layers, Naruse and Hatayama combined the high absorption efficiency of the high-z metals with good detection capabilities of a semiconductor. This project is an attempt to use the same design to produce a high-efficiency gamma ray detector. By their nature, gamma rays require thicker metal layers to efficiently absorb them. These thicker layers change the behavior of the detector by reducing the resolution, compared to a solid state detector, and shifting the photopeak by a predictable amount. During the last year, we have modeled parts of the detector and have nearly completed a prototype device. DOE

N92-23996 Rensselaer Polytechnic Inst., Troy, NY.
MODELING AND ANALYSIS OF HIGH-TEMPERATURE INELASTIC DEFORMATION IN METAL MATRIX COMPOSITES Ph.D. Thesis
Rahul S. Shah 1991 409 p
Avail: Univ. Microfilms Order No. DA9202212

Micromechanical analysis of inelastic fibrous metal matrix composites at high temperatures was examined. A small strain unified thermoviscoplasticity theory was developed. This constitutive theory is based on overstress measured from an equilibrium yield surface, and includes hardening and recovery effects. A two surface model is incorporated in the theory to model the quasi-static response. High temperature experimental data on titanium 15-3 are used to illustrate the applicability of this model to the deformation of metals. The microgeometry of the composite used is that of the periodic hexagonal array of Dvorak and Teply. Applications of the constitutive theory and the micromechanical model are presented in the form of a series of numerical studies. One set of simulations is performed at room temperature on boron-aluminum system and compared with experimental observations. These include the evaluation of initial and subsequent yield surfaces, determination of the overall hardening behavior and prediction of plastic strains under multiaxial loading conditions. A study was made to assess the accuracy of available models which base the overall response on averages of the actual nonuniform local fields. Dissert. Abstr.

N92-24012 Carnegie-Mellon Univ., Pittsburgh, PA.
ANALYTICAL AND EXPERIMENTAL INVESTIGATION OF VIBRATORY RESPONSE IN ADHESIVELY BONDED AND COMPOSITE STRUCTURES Ph.D. Thesis
Nam-Eung Kim 1991 147 p
Avail: Univ. Microfilms Order No. DA9207280

The dynamic properties are studied of adhesively bonded and composite beams. A preliminary set of experiments was conducted to qualify the damping in an overlap bonded beam. The results showed inconsistent values of damping and large scatter. Later it was found that damping is sensitive to small predeformation of the beam. To study this behavior, a finite element approach is developed for calculating modal parameters of adhesively bonded and composite beams. This approach uses special elements to represent composite and joint elements, and the modal strain energy method for estimating damping. The special element is derived using a generalization of the shape function method. The resulting element is suited for geometrically complex systems, such as a warped adhesively bonded or a composite beam. The modal strain energy approach for estimating damping is computationally efficient and provides an accurate estimate for lightly damped systems. Results on sandwich beams compare well with published results. This method is good for bonded composite beams with predeformation, and the new approach is used to examine their vibratory characteristics. Predeformation was also found to cause variations in natural frequencies of the beams. Dissert. Abstr.

N92-24013 California Univ., Berkeley.
TRANSVERSE DEFORMATION OF UNIDIRECTIONAL FIBER-REINFORCED METAL MATRIX COMPOSITES Ph.D. Thesis
Bing Kang Yen 1991 155 p
Avail: Univ. Microfilms Order No. DA9203771

The use of forging as a forming or fabrication process for metal matrix composites (MMCs) requires an understanding of the plastic behavior of MMCs during transverse compression. The effects are studied of fiber packing array, fiber volume fraction, aspect ratio, and friction condition at the die/workpiece interface on the debonding and cavity formation at the fiber/matrix interface, which severely limits height reduction of MMCs in forging. Rigid plastic finite element simulation is used to determine the global strain distribution and local interfacial stress distribution in MMCs as a function of various geometric configurations and friction conditions. In order to verify the finite element simulation and study debonding/crack formation around fibers experimentally, MMC specimens with periodic arrays of stainless steel fibers embedded in tin-bismuth alloy are fabricated using a vacuum casting technique developed. MMC samples with various geometric configurations are compressed at different friction conditions to document the debonding/cracking behavior. The results are compared with the finite element simulation to establish the relationship between actual physical debonding/cracking of MMC samples and the stress and strain distributions. Dissert. Abstr.

N92-23652*# Du Pont de Nemours (E. I.) and Co., Deepwater, NJ. Chemicals and Pigments Dept.
ADVANCED MATERIALS CENTER, BATTELLE
Harold Bellis *In* NASA, Washington, Proceedings of the Second Annual Symposium on Industrial Involvement and Successes in Commercial Space 1991 7 p (For primary document see N92-23643 14-12)
Avail: NTIS HC/MF A11 CSCL 06A

N92-23763# Societe Europeenne de Propulsion, Vernon (France).
MATERIALS FOR HIGH LIQUID PROPULSION IN 2010 [LES MATERIAUX DESTINES A LA GROSSE PROPULSION LIQUIDE EN 2010]
Jean-Claude Sylvestre *In* ESA, Launcher Propulsion Towards the Year 2010 Dec. 1991 p 103-116 In FRENCH (For primary document see N92-23750 14-15)
Copyright Avail: NTIS HC/MF A09; ESA, EPD, ESTEC, Noordwijk, Netherlands, HC 50 Dutch guilders

N92-23764# Messerschmitt-Boelkow-Blohm G.m.b.H., Munich (Germany, F.R.).
MATERIALS FOR LIQUID PROPELLANT ENGINES
Wolfgang Keinath and Dietmar Wolf *In* ESA, Launcher Propulsion Towards the Year 2010 Dec. 1991 p 117-131 (For primary document see N92-23750 14-15)
Copyright Avail: NTIS HC/MF A09; ESA, EPD, ESTEC, Noordwijk, Netherlands, HC 50 Dutch guilders

N92-23794# Deutsche Forschungsanstalt fuer Luft- und Raumfahrt, Brunswick (Germany, F.R.). Inst. fuer Strukturmechanik.
CHARACTERIZATION OF INTERLAMINAR MODE 1 AND MODE 2 FRACTURE IN CFRP LAMINATES
Rudolf Prinz and Michael Gaedke *In* ESA, Spacecraft Structures and Mechanical Testing, Volume 1 Oct. 1991 p 97-102 (For primary document see N92-23780 14-18)
Copyright Avail: NTIS HC/MF A21

N92-23806# DNV Ingemansson A.B. (Sweden).
COMPUTER SIMULATION OF MOISTURE PENETRATION IN STRUCTURES
Otto Wilmar *In* ESA, Spacecraft Structures and Mechanical Testing, Volume 1 Oct. 1991 p 175-179 Sponsored by Defence Material Administration (For primary document see N92-23780 14-18)
Copyright Avail: NTIS HC/MF A21

N92-23807# Politecnico di Torino (Italy). Dept. of Aerospace Engineering.
A NEW TEST FACILITY FOR MEASURING THE COEFFICIENT OF MOISTURE EXPANSION OF ADVANCED COMPOSITE MATERIALS
G. Romeo, E. Miraldi, G. Ruscica, F. Bertoglio, and G. Ruvinetti *In* ESA, Spacecraft Structures and Mechanical Testing, Volume 1 Oct. 1991 p 181-185 (For primary document see N92-23780 14-18)
Copyright Avail: NTIS HC/MF A21

N92-23818# Vrije Univ., Brussels (Belgium). Composite Systems and Research Group.
THE TORSIONAL FATIGUE BEHAVIOUR OF THE IN-PLANE AND OUT-OF-PLANE SHEAR MODULI OF COMPOSITE MATERIALS
D. vanHemelrijck, L. Schillemans, F. DeRoey, I. Daerden, F. Boulpaep, J. DeVisscher, and A. Cardon *In* ESA, Spacecraft

Structures and Mechanical Testing, Volume 1 Oct. 1991 p 263-267 (For primary document see N92-23780 14-18)
Copyright Avail: NTIS HC/MF A21

N92-23819# Deutsche Forschungsanstalt fuer Luft- und Raumfahrt, Brunswick (Germany, F.R.). Inst. for Structural Mechanics.
EXPERIMENTAL STUDY OF DELAMINATION GROWTH IN MULTIDIRECTIONAL CFRP-LAMINATES UNDER FATIGUE LOADING
H. C. Goetting *In* ESA, Spacecraft Structures and Mechanical Testing, Volume 1 Oct. 1991 p 269-274 (For primary document see N92-23780 14-18)
Copyright Avail: NTIS HC/MF A21

N92-23831# Avions Marcel Dassault-Breguet Aviation, Saint-Cloud (France).
NON LINEAR STRUCTURAL ANALYSIS OF A THIN SKIN CARBON-CARBON RIGID DECELERATOR
C. Bonnet, J. P. Planas, and M. Rigault *In* ESA, Spacecraft Structures and Mechanical Testing, Volume 1 Oct. 1991 p 359-362 (For primary document see N92-23780 14-18)
Copyright Avail: NTIS HC/MF A21

N92-23832# Vrije Univ., Brussels (Belgium). Composite Systems and Adhesion Group.
DYNAMIC CHARACTERIZATION OF COMPOSITE MATERIALS
I. Daerden, D. vanHemelrijck, L. Schillemans, F. DeRoey, F. Boulpaep, J. DeVisscher, and A. Cardon *In* ESA, Spacecraft Structures and Mechanical Testing, Volume 1 Oct. 1991 p 365-368 (For primary document see N92-23780 14-18)
Copyright Avail: NTIS HC/MF A21

N92-23833# Aerospatiale, Les Mureaux (France).
MECHANICAL BEHAVIOR OF COMPOSITE MATERIALS AND ADHESIVE BONDS AT LOW TEMPERATURES [COMPORTEMENT MECANIQUE DES MATERIAUX COMPOSITES ET ASSEMBLAGES COLLES AUX BASSES TEMPERATURES]
C. Laurent *In* ESA, Spacecraft Structures and Mechanical Testing, Volume 1 Oct. 1991 p 369-373 In FRENCH (For primary document see N92-23780 14-18)
Copyright Avail: NTIS HC/MF A21

N92-23835# Dornier System G.m.b.H., Friedrichshafen (Germany, F.R.). Technology and Mechanics Development Div.
BUCKLING AND FAILURE OF THIN ELLIPTICAL DELAMINATIONS IN COMPOSITES
J. Heitzer *In* ESA, Spacecraft Structures and Mechanical Testing, Volume 1 Oct. 1991 p 383-389 (For primary document see N92-23780 14-18)
Copyright Avail: NTIS HC/MF A21

N92-23839# Deutsche Forschungsanstalt fuer Luft- und Raumfahrt, Brunswick (Germany, F.R.). Inst. for Structural Mechanics.
NOTCHED STRENGTH OF COMPOSITE MATERIALS
A. S. Herrmann *In* ESA, Spacecraft Structures and Mechanical Testing, Volume 1 Oct. 1991 p 415-420 (For primary document see N92-23780 14-18)
Copyright Avail: NTIS HC/MF A21

N92-23840# Messerschmitt-Boelkow-Blohm G.m.b.H., Munich (Germany, F.R.).
STRENGTH AND DEFORMATION BEHAVIOUR OF KEVLAR AND CARBON COMPOSITE SANDWICH STRUCTURES FOR SPACE APPLICATIONS
H. Bansemir and O. Haider *In* ESA, Spacecraft Structures and Mechanical Testing, Volume 1 Oct. 1991 p 421-426 (For primary document see N92-23780 14-18)
Copyright Avail: NTIS HC/MF A21

N92-23841# Alenia Spazio S.p.A., Rome (Italy).
MODELING OF HONEYCOMB CORE FOR SANDWICH CTE PREDICTION
L. Scolamiero *In* ESA, Spacecraft Structures and Mechanical Testing, Volume 1 Oct. 1991 p 427-430 (For primary document see N92-23780 14-18)
Copyright Avail: NTIS HC/MF A21

25 INORGANIC AND PHYSICAL CHEMISTRY

Includes chemical analysis, e.g., chromatography; combustion theory; electrochemistry; and photochemistry.

For related information see also *77 Thermodynamics and Statistical Physics.*.

N92-23181# Sandia National Labs., Livermore, CA.
PROBING PICOSECOND FLAME DYNAMICS WITH TRANSIENT GRATING EXPERIMENTS
J. T. Fourkas, T. R. Brewer, M. D. Fayer, and R. Trebino 1991 7 p Presented at the International Conference on Laser and Applications, San Diego, CA, 8-13 Dec. 1991
(Contract DE-AC04-76DR-00789)
(DE92-003163; SAND-92-8408J; CONF-911296-1) Avail: NTIS HC/MF A02

We describe the results of the first time-resolved transient grating experiments to be performed in flames. Various aspects of the population and transport dynamics of sodium atoms have been investigated in several pre-mixed flames. Measurements include the Na diffusion constant and translational temperature, as well as cross sections for collisions that quench Na excited states, that scatter population between the Na 3P(sub 1/2) and 3P(sub 3/2) excited states, and that scatter population among the ground-state magnetic sublevels. DOE

N92-23199# Brookhaven National Lab., Upton, NY.
APPLICATIONS OF X RAY SYNCHROTRON RADIATION TECHNIQUES TO THE STUDY OF DISPERSED ELECTROCATALYSTS IN HIGH AREA MATERIALS
J. McBreen 1991 18 p Presented at the Workshop on Structural Effects on Electrol Catalysis and Oxygen Electrochemistry, Cleveland, OH, 29 Oct. - 1 Nov. 1991
(Contract DE-AC02-76CH-00016)
(DE92-007458; BNL-45024; CONF-9110242-2) Avail: NTIS HC/MF A03

This report discusses work demonstrating that X-Ray Absorption Spectroscopy is a very powerful technique for the study of electrocatalysts. Results for a prototech catalyst and platinum are presented. DOE

N92-23203# Northwestern Univ., Evanston, IL.
DYNAMIC STRUCTURAL EFFECTS AND ULTRAFAST BIOMOLECULAR KINETICS IN PHOTOINDUCED CHARGE TRANSFER REACTIONS
J. T. Hupp Jan. 1992 6 p
(Contract DE-FG02-87ER-13808)
(DE92-007562; DOE/ER-13808/4) Avail: NTIS HC/MF A02

During the first budget significant progress was made in three areas: (1) assessment of dynamic structural effects accompanying charge transfer, (2) electrochemical assessment of site-to-site electronic coupling in simple inorganic systems, and (3) direct observation of intramolecular electron transfer kinetics in mixed-valence systems. In area 1 the most significant finding was that Franck-Condon parameters for electron transfer (i.e., normal coordinate displacements, vibrational frequencies, and single-mode vibrational reorganizational energy components) could be obtained for weakly interacting (ion-paired) redox systems. Studies in area 3 have yielded results in both the ultrafast (femtosecond/picosecond) time regime and the intermediate (microsecond/millisecond) time regime. DOE

N92-23221# Rensselaer Polytechnic Inst., Troy, NY.
KINETIC MEASUREMENTS ON ELEMENTARY FOSSIL FUEL COMBUSTION REACTIONS OVER WIDE TEMPERATURES RANGES
A. Fontijin Jan. 1992 7 p
(Contract DE-FG02-84ER-13224)
(DE92-007535; DOE/ER-13224/16) Avail: NTIS HC/MF A02

The goals of this work are to provide accurate data on the temperature dependence of the kinetics of elementary combustion reactions (1) for use by combustion modelers, and (2) to gain a better fundamental understanding of, and hence predictive ability for, the chemistry involved. Experimental measurements are made using the pseudo-static HTP (high-temperature photochemistry) technique. This approach allows observations on single reactions in the 300 to 1800 K temperature range to be made. Typical total (bath gas) pressures are in the 100 to 1000 mbar range. Ground-state O and H atoms are produced by flash or excimer laser photolysis of suitable precursors (O2, CO2 SO2, and NH3). The relative atom concentrations are monitored by resonance fluorescence pumped by a CW microwave discharge flow lamp. The molecular reactant-in-excess is introduced through a cooled inlet. Adequate time for mixing, 0.1 to 10 s, between this inlet and the photolysis/observation zone is achieved by using slow flows (typically less than 20 cm s(ezp -1). Results are reported for: O-atom reactions with the four isomeric butenes, H + HCl yields H2 + Cl, and the O-atom 1,3-butadiene reaction. DOE

N92-23332# Rochester Univ., NY.
PHOTOCHEMISTRY AND CHARGE TRANSFER CHEMISTRY OF THE PLATINUM GROUP ELEMENTS
R. Eisenberg Dec. 1991 10 p
(Contract DE-FG02-90ER-14125)
(DE92-007564; DOE/ER-14125/2) Avail: NTIS HC/MF A02

Significant progress has been made on the photochemistry and photophysics of platinum group element dithiolate complexes. The specific systems under investigation are square planar complexes of Pt(II) containing a dithiolate chelate and two other donor groups to complete the coordination sphere. The donor groups may be amines, imines, phosphines, phosphites or olefins, and they can be either monodentate or joined together as part of a chelate ring. DOE

N92-23443# Princeton Univ., NJ. Dept. of Chemistry.
ANALYSIS OF FORWARD AND INVERSE PROBLEMS IN CHEMICAL DYNAMICS AND SPECTROSCOPY
H. Rabitz 1991 8 p
(Contract DE-FG02-86ER-13480)
(DE92-007732; DOE/ER-13480/2) Avail: NTIS HC/MF A02

This research is concerned with the development and application of advanced analysis tools for studying dynamics, kinetics, and spectroscopic phenomena from a forward and inverse perspective. In particular, the forward problem is concerned with understanding how detailed interatomic potential information maps onto a hierarchy of chemical dynamic and kinetic observables. The inverse aspects of the research are concerned with exactly the reverse of this process, whereby we desire to understand how particular measurements project back to yield information regarding the potential surface. Thus, in the latter domain, our research is concerned with the development of theoretically based tools ultimately aimed at applications to the inversion of quality laboratory data for the extraction of microscopic potential information. DOE

N92-23449# California Univ., Berkeley. Lawrence Berkeley Lab.
PROFILING AND MAPPING OF ADVANCED MATERIALS USING SPATIALLY RESOLVED RAMAN SPECTROSCOPY
J. W. Ager, III, D. K. Veirs, H. Q. Lee, and G. M. Rosenblatt Aug. 1991 9 p Presented at the 25th Annual Microbeam Analysis Society Meeting, San Jose, CA, 4-9 Aug. 1991
(Contract DE-AC03-76SF-00098)
(DE92-008304; LBL-30462; CONF-910872-9) Avail: NTIS HC/MF A02

We have developed a technique to profile important physical and chemical properties of materials based upon simultaneous acquisition of Raman spectra along a laser illumination line, coupled with extensive and rapid spectral analysis to extract the desired information. The technique uses a two-dimensional spectroscopic detector and, in contrast to Hadamard techniques, sample movement in one dimension that allows all collected light to be detected. Property maps comprised of the analysis results of more than 10,000 Raman spectra can be built up from successive profiles in a few hours. In order to increase efficiency, the data for one profile are analyzed while the data for the next profile are collected. Two recent applications are discussed: measuring spatial variations in crystalline quality in CVD-grown diamond thin films and mapping transformed zones produced by compressive stress in a bulk sample of phase-stabilized zirconia (PSZ). DOE

N92-23456# New Energy Development Organization, Tokyo (Japan).
SURVEY ON FIXATION AND UTILIZATION OF CARBON DIOXIDE BY CATALYTIC HYDROGENATION
Mar. 1991 197 p In JAPANESE; ENGLISH summary
(DE92-769380; NEDO-ITE-9008) Avail: NTIS HC/MF A09

This paper investigates a chemical method among CO2 fixation technologies. The chemical fixation of CO2 is basically reduction. It is well known that useful chemical intermediates such as methanol, ethanol, low grade hydrocarbon, etc. can be synthesized from CO2 by catalytic hydrogenation. A large amount of energy is required for chemical separation of oxygen from CO2. In the future methanol synthesis from CO2 instead of CO is also expected to be commercialized. CO2 reduction to hydrocarbon requires more hydrogen than CO reduction (Ficher-Tropsch method) but development of its new process hereafter will make fixation of a great deal of CO2 possible. Various studies are made on electrochemical, photochemical and photosynthetical CO2 reduction to hydrocarbon and on CO2 reduction to methane by anaerobic bacteria. For chemical fixation and utilization of CO2, it is not only needed to develop elemental technologies, but to make a comprehensive consideration of volume, energy, environment and economy. DOE

N92-23499# North Carolina Univ., Chapel Hill. Dept. of Chemistry.
REDUCTIVE COUPLING OF CARBON MONOXIDE TO C2 PRODUCTS
J. L. Templeton Aug. 1991 4 p
(Contract DE-FG05-85ER-13430)
(DE92-007529; DOE/ER-13430/T1) Avail: NTIS HC/MF A01

We first prepared Tp(prime)(CO)(sub 2)W(equivalent to)CH from a conversion of the cationic phosphonium carbyne Tp(prime)(CO)(sub 2)W(equivalent to)CPMe(sub 3)+ to a neutral carbene by hydride addition at carbon. Removal of PMe(sub 3) with a Lewis acid trap yielded milligram quantities of the desired terminal carbyne. More recently we have prepared a silylcarbyne precursor which reacts with Bu(sub 4)NF in wet THF to form substantial amounts of the CH carbyne. Dimerization to form an unusual vinylidene bridged complex is a facile decomposition route which consumes the Tp(prime)(CO)(sub 2)M(equivalent to)CH monometer for both M=MO and M=W. Preparation of other carbyne complexes has been achieved using Tp(prime)(CO)(sub 2)W(equivalent to)C-Cl as a reagent. Another carbyne derivative was synthesized from Tp(prime)(CO)(sub 2)M(equivalent to)C-Cl by adding K(CpFe(Co) sub 2) to displace the chloride. Organometallic products formed from the reaction of an electrophilic iron carbene complex with nitrosoarenes or azobenzene reflect net insertion of the ArN-X moiety into the Fe=CHAr bond. Cp(CO)(sub 2)Fe-O-N(Ar(prime)) = CHAr+ and Cp(CO)(sub 2)FeN(Ph)-N(Pha) = CHAr+ have been isolated and spectroscopically characterized. More promising results for long term progress in building electrophilic nitrene complexes have been achieved with Group VI reagents. Simple methods for generating Tp(prime)(CO)(sub 2)W=NHR for R= Ar and Bu(sup t) are encouraging. Furthermore, removal of H(sup minus) from the amido

ligand with either I(sub 2) or 9Ph(sub 3)C (BF(sub 4)) provides access to cationic nitrene complexes. DOE

N92-23572# EG and G Rocky Flats, Inc., Golden, CO.
LIQUID/SUPERCRITICAL FLUID CARBON DIOXIDE CLEANING OF STAINLESS STEEL COMPONENTS
L. M. Bagaasen 25 Nov. 1991 28 p
(Contract DE-AC34-90DP-62349)
(DE92-006947; RFP-4476) Avail: NTIS HC/MF A03

A Development Job Order initiated a study for quantitatively determining effectiveness of Liquid/Supercritical Fluid Carbon Dioxide (LCO2) cleaning for removing hydrocarbons and particulates from full-size stainless steel components. In the first part of the study, full-size bottles were doped with varying amounts of two types of hydrocarbons. After doping, the parts were LCO2 cleaned at 40 C using different pressures (1500 and 3000 psia) and flow rates (10 and 100 cu cm/min). Results of these tests showed that LCO2 effectively removed oil from stainless steel bottles doped to levels as high as 13,000 (mu)g, regardless of the cleaning process parameters. Oil dopant levels of 130,000 (mu)g required higher pressure for effective cleaning. LCO2 cleaning was less effective on the other hydrocarbons. The second part of the study involved coupling ultrasonics and LCO2 processing to determine whether ultrasonics would improve either the particulate or hydrocarbon removal abilities of LCO2. Aluminum foil erosion tests determined that cavitation definitely occurred in the 1200-1500 psia, 40-66 C range. Particulate removal tests showed that this cavitation aided in the removal of loose particulate from two different bottle shapes. Limited testing also showed that ultrasonically induced cavitation improves the ability of LCO2 to remove Trim Sol. DOE

N92-23586# Allied-Signal Aerospace Co., Kansas City, MO.
MEASUREMENT OF SURFACE CLEANLINESS BY AREA-OF-SPREAD
W. B. Harding Feb. 1992 13 p
(Contract DE-AC04-76DP-00613)
(DE92-007265; KCP-613-4626) Avail: NTIS HC/MF A03

The technique of determining the amount of spreading of a small (0.5 to 5 cu mm) drop of water on a surface as a measure of the cleanliness of the surface is described. Calculation of the wetting angle of the drop from the diameter and volume of the drop is explained. Values of wetting angles for several clean and several deliberately contaminated surfaces are presented. Illustrative photomicrographs are included. DOE

N92-23657# Science Applications International Corp., Orlando, FL.
AERODYNAMIC RECTIFIER FOR PULSED COMBUSTORS Final Report, 1 Apr. 1990 - 6 Jan. 1992
J. L. Reed 9 Jan. 1992 46 p
(Contract GRI-5090-260-1970)
(PB92-142587; GRI-91/0401) Avail: NTIS HC/MF A03 CSCL 21B

Exploratory research was conducted to obtain steady and nonsteady flow performance data to determine the feasibility of a suggested 'no-moving-parts' oneway valve for application to pulsating combustors. Such valves offer the opportunity of building arbitrarily large combustors without encountering the difficulties that arise when mechanical 'moving-parts' valves are scaled up in size. The research program produced a valve that exceeded the performance claims of relevant prior art by 100 percent. The valve was also operated in a pulsating combustion environment, and combustion chamber pressure oscillations were recorded in real time. GRA

N92-23685# Pennsylvania State Univ., University Park.
BASIC RESEARCH ON NATURAL GAS COMBUSTION PHENOMENA Annual Report, Sep. 1990 - Aug. 1991
M. Frenklach and W. C. Gardiner 15 Sep. 1991 30 p Prepared in cooperation with Texas Univ., Austin
(Contracts GRI-5086-260-1307; GRI-5086-260-1320)
(PB92-149681; GRI-91/0333) Avail: NTIS HC/MF A03 CSCL 21B

A universal chemical model was sought for the combustion and ignition of methane (and mixtures of methane with other gases, mimicking the composition of natural gas) in terms of elementary chemical reactions with rates specified as functions of temperature and pressure. Rate coefficient expressions for the reactions CO + OH yields CO2 + H and CH3 + O2 yields products were determined. Laser diagnostic techniques for CH3O and OD radical detection were developed. Analysis of OD profiles in D2-O2-Ar mixtures and their interpretation in terms of rate constant theory were completed. Work on reduction of the methane combustion mechanism continued. Author

N92-23715# Lawrence Livermore National Lab., CA.
HIGH-TEMPERATURE IGNITION OF PROPANE WITH MTBE AS AN ADDITIVE: SHOCK-TUBE EXPERIMENTS AND MODELING
J. A. Gray (Sandia National Labs., Livermore, CA.) and C. K. Westbrook 14 Mar. 1991 11 p
(Contracts W-7405-eng-48; DE-AC04-76DP-00789)
(DE92-008557; UCRL-JC-106910; CONF-9103145-3; WSS/CI-91-17) Avail: NTIS HC/MF A03

The ignition delay times for several propane mixtures have been studied in a shock tube and by computational modeling to determine the effect of methyl tert-butyl ether (MTBE) as a fuel additive. Argon mixtures contained oxygen, propane and one of several additives which accounted for up to 25 percent of the fuel. The shock-tube experiments covered a range of temperatures between 1450 and 1800 K, and ignition delays were measured from chemiluminescence at 432 nm due to excited CH radicals. The temperature dependence of the ignition rates was analyzed to yield Arrhenius parameters of E(sub a) approximately 40 kcal/mol and log(A) approximately 9.0 for the overall mechanism. Several reactions involving MTBE and its decomposition products were combined with an established propane mechanism to describe the kinetic interaction of this additive with a typical primary fuel. Experimentally, MTBE and isobutene increased the ignition times by 50 percent at the higher temperatures and had almost no effect at the lower temperatures. The computational model accurately predicts these effects at higher temperatures, but in contrast to the experiments, the model also predicts a 50 percent increase in delay times at lower temperatures. DOE

N92-23904# Lawrence Livermore National Lab., CA.
VITRIMAT2: A MODIFIED MODEL OF VITRINITE MATURATION AND REFLECTANCE
A. K. Burnham Feb. 1992 10 p
(Contract W-7405-eng-48)
(DE92-008987; UCRL-ID-109903) Avail: NTIS HC/MF A02

A faster, modified version of VITRIMAT is presented. The original VITRIMAT model calculates change in vitrinite elemental composition as a function of time and temperature using a system of parallel first-order reactions. The reflectance of light by vitrinite is then calculated via correlations between elemental composition and reflectance. VITRIMAT2 uses a simpler set of parallel second-order reactions and the same correlations to calculate reflectance with one-third the computer time. VITRIMAT2 uses the same kinetic expressions for elimination of H2O and CO2 from the vitrinite structure and neglects the generation of hydrocarbons other than methane. DOE

N92-24038# Illinois Univ., Chicago. Dept. of Chemical Engineering.
KINETICS OF COMBUSTION-RELATED PROCESSES AT HIGH TEMPERATURES
J. H. Kiefer Feb. 1992 10 p
(Contract DE-FG02-85ER-13384)
(DE92-008790; DOE/ER-13384/5) Avail: NTIS HC/MF A02

Again this year, progress is mainly reflected in publications. The following lists titles published, in press, or submitted during late 1990-1991: Tunable Laser Flash Absorption, High Temperature Pyrolyses of Acetylene and Diacetylene Behind Reflected Shock

Waves, Rate of the Retro-Diels-Alder Dissociation of 1,2,3,6-Tetrahydropyridine Over a Wide Temperature Range, The Reaction of C4H2 and H2 Behind Reflected Shock Waves, Thermal Isomerization of Cyclopropanecarbonitrile, The Homogeneous Pyrolysis of Acetylene II, The Importance Of Hindered Rotations and Other Anharmonic Effects in the Thermal Dissociation of Small Unsaturated Molecules, Dissociation Rates of Propyne and Allene at High Temperatures and the Subsequent Formation of Benzene, and The Formaldehyde Decomposition Chain Mechanism. This report consists of the abstracts, titles, and authors for each of these publications. DOE

N92-24064# Lawrence Livermore National Lab., CA.
MODELING OF THE CATALYTIC OXIDATIVE COUPLING OF METHANE
L. M. Hair, W. J. Pitz, M. W. Droege, and C. K. Westbrook Apr. 1992 13 p Presented at the American Chemical Society National Meeting, San Francisco, CA, 5-10 Apr. 1992
(Contract W-7405-eng-48)
(DE92-008554; UCRL-JC-109148; CONF-920444-15) Avail: NTIS HC/MF A03

Catalytic reaction equations describing processes typical of oxidative coupling catalysts were incorporated into a gas-phase, chemical kinetics model. Modeling is used to predict limits in C(sub 2) yield, describe product trends as a function of gas-phase and generalized catalyst behavior and use these results as a guide to catalyst design. The catalytic reaction set included methane activation, hydrocarbon activation and/or product oxidation. A combined hydrodynamic, chemical kinetics and transport model (HCT) utilizing 140 gas-phase reaction equations plus the catalytic set was employed. The model predicts that a highly selective and active catalyst would be capable of yielding adequate C(sub 2) hydrocarbons to justify production. However, a highly selective catalyst with activity characteristic of current oxidative coupling catalysts is predicted to yield no more than 35 percent C(sub 2) hydrocarbons. Any non-selective catalytic reactions lead to unacceptably low yields of C(sub 2) hydrocarbons. A significant finding of this work is the determination of a 'window' of catalyst activity where both thermally-induced and catalytic reactions affect the products. For lower catalyst activities, gas-phase processes determine the outcome; for higher catalyst activities, the selectivity of the catalyst determines the product distribution. DOE

N92-23286*# Boeing Co., Seattle, WA. Defense and Space Group.
PARTICLE TYPES AND SOURCES ASSOCIATED WITH LDEF
E. R. Crutcher and W. W. Wascher *In* NASA. Langley Research Center, LDEF: 69 Months in Space. First Post-Retrieval Symposium, Part 1 Jan. 1992 p 101-119 (For primary document see N92-23280 14-99)
(Contract NAS1-18224)
Avail: NTIS HC/MF A99; 8 functional color pages CSCL 07D

N92-23288*# Boeing Co., Seattle, WA. Defense and Space Group.
QUANTIFICATION OF CONTAMINANTS ASSOCIATED WITH LDEF
E. R. Crutcher, L. S. Nishimura, K. J. Warner, and W. W. Wascher *In* NASA. Langley Research Center, LDEF: 69 Months in Space. First Post-Retrieval Symposium, Part 1 Jan. 1992 p 141-154 (For primary document see N92-23280 14-99)
(Contract NAS1-18224)
Avail: NTIS HC/MF A99; 8 functional color pages CSCL 07D

N92-23299*# Westinghouse Savannah River Co., Aiken, SC.
GAMMA RAY SPECTROMETRY OF LDEF SAMPLES AT SRL
Willard G. Winn *In* NASA. Langley Research Center, LDEF: 69 Months in Space. First Post-Retrieval Symposium, Part 1 Jan. 1992 p 287-300 Sponsored in part by NASA. Marshall Space Flight Center (For primary document see N92-23280 14-99)
(Contract DE-AC09-89SR-18035)
Avail: NTIS HC/MF A99; 8 functional color pages CSCL 07D

N92-23316*# Washington Univ., Saint Louis, MO. Center for the Space Sciences.
SIMS CHEMICAL ANALYSIS OF EXTENDED IMPACT FEATURES FROM THE TRAILING EDGE PORTION OF EXPERIMENT AO187-2
Sachiko Amari, John Foote, Charles Simon, Elmar K. Jessberger, Gundolf Lange, Frank Stadermann (Max-Planck-Inst. fuer Kernphysik, Heidelberg, Germany, F.R.), Pat Swan, Robert M. Walker, and Ernst Zinner *In* NASA. Langley Research Center, LDEF: 69 Months in Space. First Post-Retrieval Symposium, Part 1 Jan. 1992 p 503-516 (For primary document see N92-23280 14-99)
(Contract NAG1-1174; ESTEC-AOP/WK/303284)
Avail: NTIS HC/MF A99; 8 functional color pages CSCL 07D

N92-23337*# Sverdrup Technology, Inc., Cleveland, OH.
THE STUDY OF PDF TURBULENCE MODELS IN COMBUSTION
Andrew T. Hsu *In* NASA. Lewis Research Center, Center for Modeling of Turbulence and Transition (CMOTT). Research Briefs: 1990 Oct. 1991 p 1-3 (For primary document see N92-23336 14-01)
Avail: NTIS HC/MF A08 CSCL 21B

N92-23342*# Vigyan Research Associates, Inc., Hampton, VA.
TURBULENCE MODELING IN SUPERSONIC COMBUSTING FLOWS
Tawit Chitsomboon *In* NASA. Lewis Research Center, Center for Modeling of Turbulence and Transition (CMOTT). Research Briefs: 1990 Oct. 1991 p 19-21 (For primary document see N92-23336 14-01)
Avail: NTIS HC/MF A08 CSCL 21B

N92-23345*# Sverdrup Technology, Inc., Cleveland, OH.
THE STUDY OF PDF TURBULENCE MODELS IN COMBUSTION
Andrew T. Hsu *In* NASA. Lewis Research Center, Center for Modeling of Turbulence and Transition (CMOTT). Research Briefs: 1990 Oct. 1991 p 53-65 Presented at the 9th National Aero-Space Plane Technology Symposium, 1-2 Nov. 1990 (For primary document see N92-23336 14-01)
(Paper-107) Avail: NTIS HC/MF A08 CSCL 21B

N92-23347*# Sverdrup Technology, Inc., Cleveland, OH.
PROGRESS IN THE DEVELOPMENT OF PDF TURBULENCE MODELS FOR COMBUSTION
Andrew T. Hsu *In* NASA. Lewis Research Center, Center for Modeling of Turbulence and Transition (CMOTT). Research Briefs: 1990 Oct. 1991 p 68-76 Presented at the 10th National Aero-Space Plane Technology Symposium, 23-26 Apr. 1991 (For primary document see N92-23336 14-01)
(Contract NAS3-25266)
(Paper-213) Avail: NTIS HC/MF A08 CSCL 21B

N92-23348*# Sverdrup Technology, Inc., Cleveland, OH.
A STUDY OF HYDROGEN DIFFUSION FLAMES USING PDF TURBULENCE MODEL
Andrew T. Hsu *In* NASA. Lewis Research Center, Center for Modeling of Turbulence and Transition (CMOTT). Research Briefs: 1990 Oct. 1991 p 77-86 Previously announced in IAA as A91-45549 (For primary document see N92-23336 14-01)
(Contract NAS2-5266)
Avail: NTIS HC/MF A08 CSCL 21B

26 METALLIC MATERIALS

Includes physical, chemical, and mechanical properties of metals, e.g., corrosion; and metallurgy.

N92-23176# Helsinki Univ. of Technology, Espoo (Finland). Dept. of Mechanical Engineering.
EFFECTS OF IMPURITIES ON THE SOLIDIFICATION AND MECHANICAL BEHAVIOUR OF PRIMARY AND SECONDARY COMMERCIAL PURITY ALUMINIUM AND ALUMINIUM ALLOYS Ph.D. Thesis
J. E. Eklund Jun. 1991 144 p
(PB92-133511; Rept-1/91) Avail: NTIS HC/MF A07 CSCL 11F

The effects of impurities on solidification and mechanical behavior of commercial purity aluminum, aluminum-silicon (7-12 percent), and aluminum-copper (4 percent) alloys were studied. The research work covered the examination of as-cast microstructures, the simulation of the formation of as-cast microstructure, as well as the examination of mechanical behavior of primary and secondary test materials. A comparison viewpoint between primary and secondary materials was adopted in the present study because of the different production methods of these materials. The aim was, accordingly, to determine the usability of secondary casting ingots as raw materials for aluminum castings. The study indicates that the intermetallic impurity rich compounds of AlFeSi, AlMnSi, and AlFeMnSi types possess a tendency to block the intergranular/interdendritic feeding channels of aluminum-silicon casting alloys. Analogous structures for aluminum-copper alloys may be labelled as AlFeCu, AlMgCu, and AlFeMgSi types of intermetallic compounds. The above mentioned harmful impurity compounds favoring the formation of shrinkage porosity do not precipitate until during the solidification of aluminum metals, and therefore may not be eliminated by the ceramic filters. GRA

N92-23178# Helsinki Univ. of Technology, Espoo (Finland). Lab. of Materials Processing and Powder Metallurgy.
PRODUCTION OF METAL POWDERS BY HYDROGEN STRIPPING FROM LOADED ORGANIC EXTRACTANTS
Y. Yang, P. Taskinen, and K. Lilius Oct. 1990 112 p
(PB92-136464; TKK-V-B59; ISBN-951-22-0395-2) Avail: NTIS HC/MF A06 CSCL 11F

The production of metal powders by hydrogen reduction from aqueous systems was begun about 35 years ago. The hydrogen reduction, or hydrogen stripping, of metals from loaded organic extractants to metallic powders is in its infancy, and has not found commercial applications. However, the latter process has several advantages over both 'the aqueous hydrogen reduction' and the conventional 'solvent extraction - acid stripping - electrowinning' processes. The paper will describe the main features of the hydrogen stripping process from both the theoretical and the practical points of view. The main experimental information available is collected and analyzed as much as possible. The physical chemistry, including both thermodynamics and reaction kinetics are discussed according to the different organic systems. The chemical and thermal stabilities of the organic extractants are generalized. The main characteristics, including chemical purity and physical properties, are broadly described. GRA

N92-23179# Helsinki Univ. of Technology, Espoo (Finland). Lab. of Foundry Technology.
CASTING OF SIMPLE-SHAPED SINGLE CRYSTALS OF ALUMINUM
C. Cingi and J. J. Vuorinen 1990 13 p
(PB92-136555; VAL-1/90; ISBN-951-22-0358-8) Avail: NTIS HC/MF A03 CSCL 11F

The Bridgman technique was used to grow simple-shaped single crystals of aluminum. The results show that crystal shape, metal composition, and temperature gradient are the most important factors to be considered. GRA

N92-23197# Brookhaven National Lab., Upton, NY.
IN SITU XANES STUDY OF THE VALENCE STATE OF CHROMIUM DURING ELECTROCHEMICAL POLARIZATION OF AlCr ALLOYS
A. J. Davenport, H. S. Isaacs, G. S. Frankel, A. G. Schrott, C. V. Jahnes, and M. A. Russak (International Business Machines Corp., Yorktown Heights, NY.) 1991 11 p Presented at the 180th Meeting of the Electrochemical Society, Phoenix, AZ, 13-18 Oct. 1991
(Contract DE-AC02-76CH-00016)
(DE92-007452; BNL-47016; CONF-911047-17) Avail: NTIS HC/MF A03

The chemistry of chromium in the passive film on pure chromium and sputtered AlCr thin films was studied in situ in an electrochemical cell under potential control using XANES. Depending on the rate of potential increase, the 6-valent chromium can dissolve from the alloy or be trapped in the passive film where it is electroactive i.e., the valence state can be reversibly switched between the 3- and 6-valent states by switching the applied potential. The kinetics of these processes were investigated. DOE

N92-23198# Brookhaven National Lab., Upton, NY.
APPLICATION OF X RAY ABSORPTION SPECTROSCOPY TO THE STUDY OF CORROSION AND INHIBITION
A. J. Davenport and H. S. Isaacs 1991 17 p Presented at the CORROSION 1991: National Association of Corrosion Engineers (NACE) Conference, Cincinnati, OH, 11-15 Mar. 1991
(Contract DE-AC02-76CH-00016)
(DE92-007456; BNL-45259; CONF-910328-7) Avail: NTIS HC/MF A03

X-ray absorption spectroscopy is a powerful technique for determination of valency and coordination. Measurements can be made in air or in situ under electrochemical control. The technique will be described and its application to the analysis of passive oxide films, corrosion products, and inhibitors will be reviewed. DOE

N92-23210# International Centre for Theoretical Physics, Trieste (Italy).
THEORETICAL MODEL OF THE DENSITY OF STATES OF RANDOM BINARY ALLOYS
N. Zekri and A. Brezini Sep. 1991 20 p
(DE92-617438; IC-91/322) Avail: NTIS HC/MF A03

A theoretical formulation of the density of states for random binary alloys is examined based on a mean field treatment. The present model includes both diagonal and off-diagonal disorder and also short-range order. Extensive results are reported for various concentrations and compared to other calculations. DOE

N92-23211# International Centre for Theoretical Physics, Trieste (Italy).
CHARGED-SOFT-SPHERE POTENTIALS FOR TRIVALENT METAL HALIDES
A. Erbolμkbas, Z. Akdeniz, and M. P. Tosi Sep. 1991 18 p
(DE92-617445; IC-91/279) Avail: NTIS HC/MF A03

Octahedral-type coordination by halogens in the liquid state has been reported for a number of trivalent metal ions from diffraction and Raman scattering experiments on their molten trihalides and from Raman scattering spectroscopy of liquid mixtures of trihalides with alkali halides. We analyze the available data on bond lengths and Raman frequencies by treating an isolated (MX sub 6) (exp 3-) species within a model which adopts charged-soft-sphere interionic potentials supplemented by an account of ionic polarization. The trivalent metal ions that we consider are M = La, Ce, Pr, Nd, Sm, Gd, Dy and Y for X = Cl and M = Al for X = F. The main result of the analysis is the prediction of trends in the soft-sphere repulsive parameters for the trivalent metal ions, leading to estimates of all the vibrational frequencies and the binding energy of such octahedral species. DOE

N92-23263# Japan Atomic Energy Research Inst., Tokyo.
EFFECT OF MINOR ELEMENTS ON HOT WORKABILITY OF Ni-Cr-W SUPERALLOYS
Hirokazu Tsuji, Hajime Nakajima (Japan Atomic Energy Research Inst., Tokai.), Tetsuya Shimizu, and Susumu Isobe Aug. 1991 28 p In JAPANESE; ENGLISH summary
(DE92-750951; JAERI-M-91-116) Avail: NTIS HC/MF A03

Research and development have been carried out on the new Ni-Cr-W superalloys as a component material for high temperature gas-cooled reactors (HTGR) with coolant outlet temperatures of around 1000 C. The basic composition, Ni - 18 to 19 mass percent Cr - 20 to 22 mass percent W, of the experimental alloys was specified in the first step. Applying this new alloy to reactor components, the alloy with stable qualities should be supplied in an industrial scale. From such a viewpoint, the hot workability is one of the most important indices. Thus, in order to examine the effect of addition of Mn, Si, B, Y, Ti, etc. on the hot workability, a series of high-strain-rate high-temperature tension tests, so-called Gleeble tests, was carried out on 21 heats of Ni - 18 to 19 mass percent Cr - 20 to 22 mass percent W alloys at temperatures ranging from 800 to 1300 C at every 50 C for most of the heats, and also at 500, 600 and 700 C for the other heats. Based on the results obtained the following conclusions are drawn: (1) The addition of Mn and Si was extremely harmful to the hot workability. (2) The addition of B was effective to improve the hot workability. (3) The addition of Y was extremely effective to improve the hot workability. The saturation point of the effectiveness was higher than 0.008 mass percent. (4) The addition of Ti was extremely effective to improve the hot workability. Around 0.08 mass percent addition of Ti was enough to exhibit the effectiveness. (5) The addition of Nb, Fe and/or the enrichment of C exhibited no beneficial influence in the aspect of the hot workability substantially. (6) A new Ni-Cr-W superalloy, which shows extremely superior hot workability, has been developed. It will be possible that the new alloy is manufactured in an industrial scale. DOE

N92-23265# Japan Atomic Energy Research Inst., Tokyo.
HYDROGEN ABSORPTION BY ZIRCONIUM ALLOY CLADDING TUBE WITH SURFACE OXIDE FILM
Masaaki Uchida (Japan Atomic Energy Research Inst., Tokai.) Aug. 1991 37 p
(DE92-750962; JAERI-M-91-132) Avail: NTIS HC/MF A03

Hydrogen absorption kinetics of Zircaloy (2 and 4) and Zr-Nb (1 percent and 2.5 percent) cladding tubes were studied by heating in hydrogen gas after oxide film formation in steam, oxygen or air. Hydrogen absorption rate depended on the degree of pre-oxidation. In Zr-Nb, the absorption rate was also sensitive to the atmosphere used for pre-oxidation, whereas in Zircaloy the rate was relatively independent of the kind of oxidant. In all materials, pre-oxidation to the transition point was found to bring about high absorption rate in the subsequent hydriding step. After pre-oxidation to the post-transition region, hydrogen absorption rate by Zircaloy showed constant or slightly decreasing tendency with increasing oxidation level, whereas in Zr-Nb, particularly in Zr-2.5 percent Nb, the rate showed a clearly decreasing tendency depending on the pre-oxidation atmosphere. Different characteristics of Zircaloy and Zr-Nb can partly be explained in terms of different valencies of alloying elements which influence the lattice defect concentrations in the oxide films. DOE

N92-23436*# Case Western Reserve Univ., Cleveland, OH. Dept. of Materials Science and Engineering.
REACTION LAYER FORMATION AT THE GRAPHITE/COPPER-CHROMIUM ALLOY INTERFACE Final Report
Sandra M. DeVincent and Gary M. Michal Mar. 1992 25 p Presented at the 1991 TMS Annual Meeting, New Orleans, LA, 17-21 Feb. 1991
(Contract NCC3-94)
(NASA-CR-189147; E-6961; NAS 1.26:189147) Avail: NTIS HC/MF A03 CSCL 11F

Sessile drop tests were used to obtain information about copper chromium alloys that suitably wet graphite. Characterization of graphite/copper-chromium alloy interfaces subjected to elevated temperatures were conducted using scanning electron micrography, energy dispersive spectroscopy, auger electron spectroscopy, and x ray diffraction analyses. These analyses indicate that during sessile drop tests conducted at 1130 C for one hour, copper alloys containing greater than 0.98 percent chromium form continuous reaction layers of approximately 10 micron thickness. The reaction layers adhere to the graphite surface. The copper wets the reaction layer to form a contact angle of 60 degrees or less. X ray diffraction results indicate that the reaction layer is chromium carbide. The kinetics of reaction layer formation were modelled in terms of bulk diffusion mechanisms. Reaction layer thickness is controlled initially by the diffusion of Cr out of Cu alloy and later by the diffusion of C through chromium carbide. Author

N92-23566*# Florida Univ., Gainesville. Materials Science and Engineering.
THE INFLUENCE OF CHROMIUM ON STRUCTURE AND MECHANICAL PROPERTIES OF B2 NICKEL ALUMINIDE ALLOYS Ph.D. Thesis - Florida Univ., 1991 Final Report
James Dean Cotton Mar. 1992 156 p
(Grant NAG3-1079)
(NASA-CR-189124; NAS 1.26:189124) Avail: NTIS HC/MF A08 CSCL 11F

Major obstacles to the use of NiAl-based alloys and composites are low ductility and toughness. These shortcomings result in part from a lack of sufficient slip systems to accommodate plastic deformation of polycrystalline material (von Mises Criterion). It has been reported that minor additions of chromium to polycrystalline NiAl cause the predominant slip system to shift from the usual. If true, then a major step toward increasing ductility in this compound may be realized. The purpose of the present study was to verify this phenomenon, characterize it with respect to chromium level and Ni to Al ratio, and correlate any change in slip system with microstructure and mechanical properties. Compression and tensile specimens were prepared from alloys containing 0 to 5 percent chromium and 45 to 55 percent aluminum. Following about one percent strain, transmission electron microscopy foils were produced and the slip systems determined using the g x b = 0 invisibility criterion. Contrary to previous results, chromium was found to have no effect on the preferred slip system of any of the alloys studied. Possible reasons for the inconsistency of the current results with previous work are considered. Composition-structure-property relationships are discerned for the alloys, and good correlation are demonstrated in terms of conventional strengthening models for metallic systems. Author

N92-23573# Argonne National Lab., IL.
MELTING OF NICKEL CLUSTERS
I. L. Garzon and J. Jellinek 1991 6 p Presented at the International Symposium on the Physics and Chemistry of Finite Systems, Richmond, VA, 8-12 Oct. 1991
(Contract W-31-109-eng-38)
(DE92-006986; ANL/CP-73727; CONF-911033-5) Avail: NTIS HC/MF A02

The melting-like phenomenon in Ni(sub n), n = 19, 20, 55, clusters is studied using microcanonical molecular dynamics simulations. The interaction between the atoms in the clusters is modelled by a size-dependent Gupta-like potential that incorporates many-body effects. The clusters display the 'usual' stages in their melting-like transition, which characterize also Lennard-Jones (e.g., noble gas) and ionic clusters. In addition, Ni20 passes through a so-called premelting stage found earlier also for Ni14. DOE

N92-23582# International Centre for Theoretical Physics, Trieste (Italy).
AB INITIO PAIR POTENTIALS FOR FCC METALS: AN APPLICATION OF THE METHOD OF MOEBIUS TRANSFORM
A. Mookerjee, Nanxian Chen, V. Kumar, and M. A. Satter Oct. 1991 15 p
(DE92-617440; IC-91/351) Avail: NTIS HC/MF A03

We use the method of Moebius transform introduced by us to obtain pair potentials for face centered cubic (FCC) lattice metals from first principles total energy calculations. The derivation is exact for radial potentials and it converges much faster than the earlier reported method of Carlsson-Gelatt-Ehrenreich. We have tested this formulation for Cu using the tight binding representation of the linear muffin tin orbital method. Our results agree with those obtained by Carlsson et al. and qualitatively with the other Morse-type pair potentials derived from effective medium theories. DOE

N92-23712# Japan Atomic Energy Research Inst., Tokyo.
EFFECT OF MINOR ELEMENTS ON CORROSION BEHAVIOR OF Ni-Cr-W SUPERALLOYS IN HTGR HELIUM
Hirokazu Tsuji, Tomio Suzuki, Takashi Tsukada, and Hajime Nakajima (Japan Atomic Energy Research Inst., Tokai.) Sep. 1991 50 p
(DE92-751006; JAERI-M-91-136) Avail: NTIS HC/MF A03

Research and development have been carried out on the new Ni-Cr-W superalloys as a component material for high temperature gas cooled reactors (HTGCs) with coolant outlet temperatures of around 1000 C. The basic composition, Ni-18 to 19 mass percent Cr-20 to 22 mass percent W, of the experimental alloys was specified in the first step. In order to examine the effect of addition of Mn, Si, B, Y and Ti on corrosion behavior in simulated HTGR helium, corrosion tests were carried out on eight heats of Ni-18 to 19 mass percent Cr-20 to 22 mass percent W alloys at 950 and 1000 C. Thermal cycles were given at intervals of 100 h between room temperature and the each test temperature. The cumulative period of exposure to simulated HTGR helium at the each test temperature was 1000 h. Based on the results obtained the following conclusions are drawn: (1) All the Ni-Cr-W alloys tested showed better resistance to general corrosion than Hastelloy XR, and also indicated better stability of the surface oxide film and less susceptibility to intergranular oxidation than the conventional Ni-Cr-W alloys. (2) The addition of Mn and Si showed no advantage. The alloys containing Mn and Si rather showed inferior corrosion resistance in simulated HTGR helium. (3) The addition of B and Y was effective to improve corrosion resistance in simulated HTGR helium. (4) Although the addition of Ti was harmful to corrosion resistance in simulated HTGR helium, around 0.08 mass percent addition of Ti did not reduce corrosion resistance in the environment. (5) A new Ni-Cr-W superalloy, which shows extremely superior corrosion resistance to conventional Ni-Cr-W superalloys in simulated HTGR helium, has been developed. DOE

N92-23718 Pennsylvania Univ., Philadelphia.
HIGH-TEMPERATURE DEFORMATION BEHAVIOR OF SINGLE CRYSTALLINE A15-TYPE INTERMETALLIC COMPOUNDS Ph.D. Thesis
Chen-Chung Steve Chang 1991 206 p
Avail: Univ. Microfilms Order No. DA9204801

A study of the high temperature deformation behavior of the A15 type intermetallic compound Cr3Si was carried out on single crystalline specimens as part of the effort to develop advanced structural materials. Single crystals of Cr3Si were grown by the containerless float zone method in a double ellipsoidal optical imaging furnace. Compression tests were performed on crystals having various orientations at a constant displacement rate at temperatures between 1200 and 1400 C. Slip traces on the specimen surfaces were observed (the first time they have been observed on any A15 type intermetallic compound) and were used to characterize the slip systems. The temperature and orientation dependence of the critical resolved shear stress (CRSS) was also analyzed. Single crystalline Cr3Si deforms by dislocation glide at a temperature above the ductile to brittle transition (DBTT), which was found to be around 1200 C, but fails in a brittle manner at lower temperatures. The slip system was determined to be of the cube on edge (100)(010) type and the CRSS obeys Schmid's law and no flow stress anomaly was observed. This slip system always results in at least duplex slip. Dissert. Abstr.

N92-23720# Los Alamos National Lab., NM.
HARDENING IN AlN INDUCED BY POINT DEFECTS
H. Suematsu, T. E. Mitchell, T. Iseki, and T. Yano (Tokyo Inst. of Tech., Japan) 1991 7 p Presented at the Annual Fall Meeting of the Materials Research Society, Boston, MA, 2-6 Dec. 1991
(Contract W-7405-eng-36)
(DE92-007717; LA-UR-92-73; CONF-911202-55) Avail: NTIS HC/MF A02

Pressureless-sintered AlN was neutron irradiated and the hardness change was examined by Vickers indentation. The hardness was increased by irradiation. When the samples were annealed at high temperature, the hardness gradually decreased. Length was also found to increase and to change in the same way as the hardness. A considerable density of dislocation loops still remained, even after the hardness completely recovered to the value of the unirradiated sample. Thus, it is concluded that the hardening in AlN is caused by isolated point defects and small clusters of point defects, rather than by dislocation loops. Hardness was found to increase in proportion to the length change. If the length change is assumed to be proportional to the point defect density, then the curve could be fitted qualitatively to that predicted by models of solution hardening in metals. Furthermore, the curves for three samples irradiated at different temperatures and fluences are identical. There should be different kinds of defect clusters in samples irradiated at different conditions, e.g., the fraction of single point defects is the highest in the sample irradiated at the lowest temperature. Thus, hardening is insensitive to the kind of defects remaining in the sample and is influenced only by those which contribute to length change. DOE

N92-23725 Utah Univ., Salt Lake City.
INVESTIGATION OF FRETTING FATIGUE MECHANISMS ON 7075-T6 ALUMINUM ALLOY AND Ti-6Al-4V TITANIUM ALLOY Ph.D. Thesis
Saeed Adibnazari 1991 188 p
Avail: Univ. Microfilms Order No. DA9128100

This research started by hypothesizing that fretting fatigue cracks nucleate after the damage threshold (the amount of fretting damage required to bring a reduction to fatigue life) has been reached. It was hypothesized that there exists a normal pressure threshold as well. In order to verify these hypotheses, fretting fatigue and interrupted fretting fatigue tests were conducted. The results substantiate the existence of a damage threshold. These concepts were found to be dependent on axial fatigue stress, normal pressure, and material. It was discovered that fretting damage was the main cause of crack nucleation. The nucleated cracks initially propagate obliquely to the fretted surface as stage I type cracks, and then change direction and propagate perpendicular to the axial fatigue stress as stage II cracks. The inclination angle and the size of stage I cracks were found to be related to the normal pressure. Dissert. Abstr.

N92-23893# California Univ., Berkeley. Lawrence Berkeley Lab. Materials Science Div.
THE OXIDATION BEHAVIOR OF Co-15WT PERCENT Cr ALLOY CONTAINING DISPERSED OXIDES FORMED BY INTERNAL OXIDATION
P. Y. Hou, Z. R. Shui, and J. Stringer Dec. 1991 32 p Presented at the Corrosion 1992 Conference and Exhibition, Nashville, TN, 27 Apr. - 1 May 1992
(Contract DE-AC03-76SF-00098)
(DE92-008283; LBL-31671; CONF-920458-1) Avail: NTIS HC/MF A03

Internal oxidation pretreatments of Co-15wt percent Cr and Co-15wt percent Cr-1wt percent Ti were carried out using a Rhines pack in quartz, in mullite and in alumina. A dispersion of titanium oxide particles formed in the Ti-containing alloy as a result of the internal oxidation. However, silicon also diffused into all treated specimens when the pretreatments were carried out in quartz or in mullite. The effect of various pretreatments on the subsequent oxidation of these alloys was studied at 1000 C, and compared with that of Co-15wt percent Cr-1wt percent Si alloy. The main

purpose of this study was to determine the relative effectiveness of the dispersed oxide particles and the contaminated silicon on the selective oxidation of chromium. It was found that the oxidation behavior of both treated alloys were strongly affected by the degree of silicon contamination. Selective oxidation of chromium to form a nearly continuous protective Cr2O3 scale was achieved with greater than 0.4wt percent silicon. The presence of dispersed particles reduced initial oxidation rate, but was ineffective in promoting Cr2D3 scale formation. DOE

N92-23984# California Univ., Berkeley. Lawrence Berkeley Lab.
GROUND STATE SEARCHES IN FCC INTERMETALLICS
C. Wolverton, D. deFontaine, G. Ceder, and H. Dreysse (Nancy Univ., France) Dec. 1991 9 p Presented at the Annual Fall Meeting of the Materials Research Society, Boston, MA, 2-6 Dec. 1991
(Contract DE-AC03-76SF-00098)
(DE92-008300; LBL-31831; CONF-911202-61) Avail: NTIS HC/MF A02

A cluster expansion is used to predict the fcc ground states, i.e., the stable phases at zero Kelvin as a function of composition, for alloy systems. The intermetallic structures are not assumed, but derived rigorously by minimizing the configurational energy subject to linear constraints. This ground state search includes pair and multiplet interactions which spatially extend to fourth nearest neighbor. A large number of these concentration-independent interactions are computed by the method of direct configurational averaging using a linearized-muffin-tin orbital Hamiltonian cast into tight binding form (TB-LMTO). The interactions, derived without the use of any adjustable or experimentally obtained parameters, are compared to those calculated via the generalized perturbation method extention of the coherent potential approximation within the context of a KKR Hamiltonian (KKR-CPA-GPM). Agreement with the KKR-CPA-GPM results is quite excellent, as is the comparison of the ground state results with the fcc-based portions of the experimentally-determined phase diagrams under consideration. DOE

N92-24006# Oak Ridge Y-12 Plant, TN.
INVESTIGATION OF PLASMA-SPRAYED LAMINATES FOR HIGH-TEMPERATURE MELTING OPERATIONS
E. L. Bird and C. E. Holcombə, Jr. Dec. 1991 8 p Presented at the 1992 International Thermal Spray Conference, Orlando, FL, 31 May - 5 Jun. 1992
(Contract DE-AC05-84OS-21400)
(DE92-008416; Y/DV-1096; CONF-9205100-1) Avail: NTIS HC/MF A02

Melting of reactive metals, such as zirconium (Zr), is normally accomplished either by vacuum-arc skull melting using consumable electrodes or by vaccum-induction melting, which is limited to small castings using water-cooled copper crucibles. An alternate process is being proposed to vacuum-induction melt large castings in a coated graphite crucible. The laminated coating would consist of plasma-sprayed layers of metal and ceramic that are designed to withstand temperatures approaching 2000 C while maintaining enough integrity to prevent contamination of the melt with carbon (C). This paper describes the selection process, experimental results, and feasibility of using laminated coatings that are plasma sprayed on graphite crucibles for melting Zr. DOE

N92-24014 Arizona Univ., Tucson.
SIMULATION OF FRECKLES DURING VERTICAL SOLIDIFICATION OF BINARY ALLOYS Ph.D. Thesis
Sergio Daniel Felicelli 1991 123 p
Avail: Univ. Microfilms Order No. DA9202077

The formation of channel segregates or freckles during vertical solidification of Pb-Sn alloys is simulated. The simulation is based on a mathematical model of dendritic solidification, in which the solid plus liquid zone is modeled as an anisotropic porous medium of variable porosity. The alloy solidifies from an initial melt and proceeds until the alloy is completely solidified, and the final macrosegregation can be predicted. The growth process is calculated by solving the fully coupled equations of momentum, energy, and solute transport, as well as by maintaining the thermodynamic constraints dictated by the equilibrium phase diagram of the alloy. It is found that the thermosolutal convection that occurs during solidification, under certain growth conditions, can produce localized segregation zones, varying in shape from short streaks or pockets to long and narrow channels or freckles rich in solute. Several numerical examples show how these defects originate and why they subsist or die, depending on whether they face a favorable or adverse convection pattern ahead of the solidification front. Dissert. Abstr.

27 NONMETALLIC MATERIALS

Includes physical, chemical, and mechanical properties of plastics, elastomers, lubricants, polymers, textiles, adhesives, and ceramic materials.

For composite materials see *24 Composite Materials.*

N92-23134# Japan Atomic Energy Research Inst., Tokyo.
RADIATION EFFECTS ON POLYETHYLENE FOAM
Beilin Tang, Kanako Kaji, Motoyoshi Hatada, Iwao Yoshizawa, and Choji Kohara Sep. 1991 53 p In JAPANESE; ENGLISH summary
(DE92-751046; JAERI-M-91-134) Avail: NTIS HC/MF A04

Studies have been carried out on radiation effects on open cell type polyethylene foam. The foam was irradiated with electron beam either in nitrogen atmosphere or in air and changes of strength, elongation, and gel fraction were measured. The gel-percent of the original foam (50 percent) increased by 30 percent after irradiation in nitrogen, while strength measured at room temperature, 70 C, and 100 C did not change by their radiation. However, elongation measured at 70 C and 100 C decreased considerably and dimensional stability above 70 C was also improved. DOE

N92-23165# Technische Univ., Delft (Netherlands).
ON THE KINETICS OF STRUCTURAL RELAXATION IN SOME METALLIC GLASSES Ph.D. Thesis
Gerhardus Wilhelmus Koebrugge 1991 134 p
(PB92-1287272; ETN-92-91142) Avail: NTIS HC/MF A07

The kinetics of structural relaxation in amorphous Fe40Ni40B20 and Pd40Ni40P20 are addressed. Several models are described, of which the most important (for this study) is the mixed model where structural relaxation is considered to consist of two subprocesses: Chemical Short Range Ordering (CSRO) and Topological Short Range Ordering (TSRO). For CSRO an activation energy spectrum model is used. The kinetics of TSRO is described by the free volume model. The effectiveness of this mixed model is demonstrated by experimental data on the structural relaxation in amorphous Fe40Ni40B20. ESA

N92-23185*# National Aeronautics and Space Administration. Lewis Research Center, Cleveland, OH.
AN XPS STUDY OF THE STABILITY OF FOMBLIN Z25 ON THE NATIVE OXIDE OF ALUMINUM
Pilar Herrera-Fierro, Stephen V. Pepper, and William R. Jones Nov. 1991 12 p Presented at the 38th National Symposium of the American Vacuum Society, Seattle WA, 11-15 Nov. 1991
(NASA-TM-105594; E-6926; NAS 1.15:105594) Avail: NTIS HC/MF A03 CSCL 11C

Thin films of Fomblin Z25, a perfluoropolyalkylether lubricant, were vapor deposited onto clean, oxidized aluminum and sapphire surfaces, and their behavior at different temperatures was studied using x ray photoelectron spectroscopy (XPS) and thermal desorption spectroscopy (TDS). It was found that the interfacial fluid molecules decompose on the native oxide at room temperature, and continue to decompose at elevated temperatures, as previous studies had shown to occur on clean metal. TDS indicated that different degradation mechanisms were operative for clean and oxidized aluminum. On sapphire substrates, no

reaction was observed at room temperature. Our conclusion is that the native oxide of aluminum is neither passive nor protective towards Fomblin Z25. At high temperatures (150 C) degradation of the polymer on sapphire produced a debris layer at the interface with a chemical composition similar to the one formed on aluminum oxide. Rubbing a Fomblin film on a single crystal sapphire also induced the decomposition of the lubricant in contact with the interface and the formulation of a debris layer. Author

N92-23192*# National Aeronautics and Space Administration. Lewis Research Center, Cleveland, OH.
ENVIRONMENTAL EFFECTS ON FRICTION AND WEAR OF DIAMOND AND DIAMONDLIKE CARBON COATINGS
Kazuhisa Miyoshi, Richard L. C. Wu, and Alan Garscadden (Wright Lab., Wright-Patterson AFB, OH.) 1992 22 p Presented at the International Conference on Metallurgical Coatings and Thin Films, San Diego, CA, 6-10 Apr. 1992; sponsored by American Vacuum Society
(NASA-TM-105634; E-6977; NAS 1.15:105634) Avail: NTIS HC/MF A03 CSCL 11C

Reciprocating sliding friction experiments were conducted with a natural diamond flat, diamond film, and low and high density diamondlike carbon (DLC) films in contact with pin specimens of natural diamond and silicon nitride (Si3N4) both in humid air and dry air nitrogen. The results indicated that for natural diamond pin contacts the diamond films and the natural diamond flat were not susceptible to moisture but that moisture could increase both the coefficient of friction and the wear factors of the DLC films. The coefficients of friction and wear factors of the diamond films were generally similar to those of the natural diamond flat both in humid air and dry air nitrogen. In dry nitrogen the coefficients of friction of the high density DLC films in contact with pin specimens of both diamond and Si3N4 were generally low (about 0.02) and similar to those of the natural diamond flat and the diamond films. The wear factors of the materials in contact with both natural diamond and Si3N4 were generally in the ascending order of natural diamond flat, diamond film, high density DLC film, and low density DLC film. The moisture in the environment increased the coefficients of friction for Si3N4 pins in contact with all the materials. This increase in friction is due to the silicon oxide film produced on the surface of Si3N4 pins in humid air. Author

N92-23222# Oak Ridge National Lab., TN.
APPLICATIONS OF MULTIPLE-ION IRRADIATIONS TO METALS, CERAMICS, AND POLYMERS
L. K. Mansur, E. H. Lee, M. B. Lewis, and S. J. Zinkle 1991 20 p Presented at the International Conference on Evolution in Beam Applications, Takasaki (Japan), 5-8 Nov. 1991
(Contract DE-AC05-84OR-21400)
(DE92-007686; CONF-911154-2) Avail: NTIS HC/MF A03

The application of ion beams in materials science and engineering has its roots in the development of accelerators and ion sources for nuclear physics research and for the electromagnetic separation of isotopes. Present research at the intersection of materials science and ion beam technology covers the three broadly interrelated fields of ion beam radiation effects, ion beam treatment and ion beam characterization. One area in which exciting new research on radiation effects and on ion beam treatment is being carried out is in the effects in materials of the simultaneous application of multiple ion beams. Work in metallic alloys has been the most extensive and has resulted in detailed mechanistic understanding of such technologically relevant radiation effects phenomena as swelling, microstructural development, effects of gas on radiation response, and radiation affected phase changes. In ceramics, simultaneous anion-cation-helium bombardments permit studies on the fundamentals of displacement damage and helium response, while allowing control of defect behavior induced by departures from stoichiometry. This is particularly relevant for studies of fusion reactor insulator materials. Multiple-beam capability also permits more powerful ion beam treatment studies, because of the essentially unlimited possibilities of tailoring arbitrary combinations of implant species to the materials and processes of interest. For example, recent work on polymeric materials has shown that remarkable improvements in the surface mechanical properties are possible. DOE

N92-23223# Oak Ridge National Lab., TN.
EVALUATION OF THE ELEVATED-TEMPERATURE MECHANICAL RELIABILITY OF A HIPed SILICON NITRIDE
M. K. Ferber and M. G. Jenkins 1991 12 p Presented at the Automotive Technology Development Contractors' Coordination Meeting, Dearborn, MI, 22-25 Oct. 1991
(Contract DE-AC05-84OR-21400)
(DE92-007838; CONF-911050-4) Avail: NTIS HC/MF A03

The long-term mechanical reliability of a commercially-available hot isostatically pressed silicon nitride was evaluated by measuring the tensile creep and fatigue behavior at 1150, 1260, and 1370 C. The stress and temperature sensitivities of the secondary (or minimum) creep rates were used to estimate the stress exponent and activation energy associated with the dominant creep mechanism. The fatigue behavior was examined by allowing individual creep tests to continue until the specimen failed. The applicability of the four-point load geometry to the study of creep behavior was also evaluated by conducting a limited number of flexural creep tests. The tensile fatigue data revealed two distinct failure mechanisms. At 1150 C, failure was controlled by a slow crack growth mechanism. At 1260 and 1370 C, the accumulation of creep damage in the form of grain boundary cavities and cracks dominated the fatigue behavior. In this temperature regime, the fatigue life was controlled by the secondary (or minimum) creep in accordance with the Monkman-Grant relation. DOE

N92-23442# Sandia National Labs., Albuquerque, NM.
OXIDATIVE DEGRADATION OF POLYMERS INDUCED BY IONIZING RADIATION
R. L. Clough and K. T. Gillen 1992 2 p Presented at the 8th International Meeting of the Polymer Processing Society, New Delhi (India), 23-27 Mar. 1992
(Contract DE-AC04-76DP-00789)
(DE92-007657; SAND-92-0236C; CONF-920388-1) Avail: NTIS HC/MF A01

Processing of polymers using ionizing radiation is a rapidly expanding technology. For instance, the use of ionizing radiation is now becoming the preferred method for commercial sterilization of disposable medical equipment. This report briefly discusses the oxidative degradation of polymers by ionizing radiations, primarily gamma and electron beam radiation. DOE

N92-23461*# National Aeronautics and Space Administration. Lewis Research Center, Cleveland, OH.
GUANIDINE BASED VEHICLE/BINDERS FOR USE WITH OXIDES, METALS, AND CERAMICS Patent Application
Warren H. Philipp, inventor (to NASA), Lisa C. Veitch, inventor (to NASA), and Martha H. Jaskowiak, inventor (to NASA) 13 Mar. 1992 14 p
(NASA-Case-LEW-15314-1; NAS 1.71:LEW-15314-1; US-Patent-Appl-SN-842313) Avail: NTIS HC/MF A03 CSCL 11C

The use of guanidine salts of organic fatty acids (guanidine soaps) as vehicles and binders for coating substrate surfaces is disclosed. Being completely organic, the guanidine soaps can be burned off leaving no undesirable residue. Of special interest is the use of guanidine 2-ethyl hexanoate as the vehicle and binder for coating problematic surfaces such as in coating alumina fibers with platinum or zirconia. For this application, the guanidine soap is used as a melt. For applications, the guanidine soap may be use in a solution with a variety of solvents, the solution containing chlorometalates or powdered metals, refractories, or ceramics. NASA

N92-23510# Technische Univ., Delft (Netherlands). Faculty of Industrial Design Engineering.
FAILURE BEHAVIOUR OF HIGH DENSITY POLYETHYLENE PRODUCTS WITH AN EMBRITTLED SURFACE LAYER DUE

TO UV EXPOSURE
J. C. M. deBurijn 14 Jun. 1991 79 p
(PB92-138494; K243) Avail: NTIS HC/MF A05 CSCL 11C

Weathering puts a strong limitation on the useful life of plastic products used outdoors. It can be defined as the change of the physical properties due to the exposure to outdoor conditions, particularly sunlight in the presence of oxygen, but also temperature and humidity. An overview is given of research objectives, procedures, and results of research in the loadability of UV degraded products. The results are mainly concentrated on the samples exposed in the Xenotest 1200. Author

N92-23897# Oak Ridge National Lab., TN.
MULTIFRACTURE OF CERAMIC COMPOSITES
Y. J. Weitsman and H. Zhu (Tennessee Univ., Knoxville.) Mar. 1992 57 p
(Contract DE-AC05-84OR-21400)
(DE92-009630; ORNL-6703) Avail: NTIS HC/MF A04

This work presents a mechanistic model for the multifracture process of uniaxially reinforced fibrous ceramic composites under monotonically increasing tension parallel to the fiber direction. The model employs an energy criterion to account for the progression of matrix cracks, bridged by intact fibers, and Weibull failure statistics to relate the failure of the fibers. Consideration is given to the interactions between the foregoing failure processes as well as to the effects of various material parameters on the response of the composite. DOE

N92-24037# Boston Univ., MA. Dept. of Chemistry.
PHOTOINDUCED ELECTRON TRANSFER IN ORDERED POLYMERS
G. Jones, II Dec. 1991 7 p
(Contract DE-FG02-88ER-13905)
(DE92-008787; DOE/ER-13905/4) Avail: NTIS HC/MF A02

Long range photoinduced electron transfer between electron donor and acceptor groups is of considerable current interest in terms of strategies for artificial photosynthesis and studies regarding the redox properties of proteins. As part of an extensive study of long range electron transfer involving biopolymers, we have carried out this year's investigations of the assembly of electron transfer agents in a system of model short peptides. Also studied is a polyelectrolyte that can adopt a helical conformation when electrostatically complexed with organic dye counter-ions. The principal interest in these systems has to do with the well ordered secondary structures adopted by peptide polymers, and the capabilities for synthetic modification of peptide side chains and end groups with chromophores or electroactive substituents. The present report gives a brief account of the following elements of work related to photochemical electron transfer themes: (1) the synthesis and photochemical characterization of chromophore-bound peptides and amino acid model compounds based on the amino acids, tryptophan and the spacer residue, alanine (Ala); (2) the study of binding of the cationic organic dye to a peptide electrolyte, for which cooperative dye loading and helix formation is important; and (3) completion of the synthesis of a new series of acridinium chromophores that have 'rod-like' arrangements of inked aryl rings for assembly of electron donor-acceptor systems that will exhibit especially long lived charge separation. DOE

N92-24053*# National Aeronautics and Space Administration. Lewis Research Center, Cleveland, OH.
VINYL CAPPED ADDITION POLYIMIDES Patent Application
Raymond D. Vannucci, inventor (to NASA), Diane C. Malarik, inventor (to NASA), and Peter Delvigs, inventor (to NASA) 24 Dec. 1991 15 p
(NASA-Case-LEW-15027-2; NAS 1.71:LEW-15027-2; US-Patent-Appl-SN-824858) Avail: NTIS HC/MF A03 CSCL 11C

Polyimide resins (PMR) are generally useful where high strength and temperature capabilities are required (at temperatures up to about 700 F). Polyimide resins are particularly useful in applications such as jet engine compressor components, for example, blades, vanes, air seals, air splitters, and engine casing parts. Aromatic vinyl capped addition polyimides are obtained by reacting a diamine, an ester of tetracarboxylic acid, and an aromatic vinyl compound. Low void materials with improved oxidative stability when exposed to 700 F air may be fabricated as fiber reinforced high molecular weight capped polyimide composites. The aromatic vinyl capped polyimides are provided with a more aromatic nature and are more thermally stable than highly aliphatic, norbornenyl-type end-capped polyimides employed in PMR resins. The substitution of aromatic vinyl end-caps for norbornenyl end-caps in addition polyimides results in polymers with improved oxidative stability. NASA

N92-24068# Lawrence Livermore National Lab., CA.
FIBER-OPTIC RAMAN SPECTROSCOPY FOR CURE MONITORING OF ADVANCED POLYMER COMPOSITES
M. L. Myrick, S. M. Angel, R. E. Lyon, and T. M. Vess 16 Dec. 1991 12 p Presented at the ANTEC 1992, Detroit, MI, 3-7 May 1992
(Contract W-7405-eng-48)
(DE92-008619; UCRL-JC-109213; CONF-920572-2) Avail: NTIS HC/MF A03

The curing reaction of an epoxy matrix used for wet filament wound composites was monitored using Raman spectroscopy measured over fiber optics. The resin system consists of the diglycidyl ether of bisphenol-A in combination with a polyethertriamine hardener in a 1:1 stoichiometric ratio. The extent of chemical reaction of the epoxy as a function of time was measurable through changes in peak heights of several vibrational modes. A Raman peak associated with a phenyl ring vibration in epoxide component was used as in internal reference to correct for density changes and instrumental variations. Temperature measurements were made over the same fiber optics used to obtain the cure chemistry data by measuring the intensity of anti-Stokes Raman scattering from the epoxy. Both single fiber and dual fiber probes were evaluated. DOE

N92-23805# Deutsche Forschungsanstalt fuer Luft- und Raumfahrt, Brunswick (Germany, F.R.). Inst. for Structural Mechanics.
DAMPING BEHAVIOUR OF UNIDIRECTIONAL FIBRE REINFORCED POLYMERS
Holger Hanselka *In* ESA, Spacecraft Structures and Mechanical Testing, Volume 1 Oct. 1991 p 169-174 (For primary document see N92-23780 14-18)
Copyright Avail: NTIS HC/MF A21

N92-23817# Deutsche Forschungsanstalt fuer Luft- und Raumfahrt, Brunswick (Germany, F.R.). Inst. for Structural Mechanics.
AGING OF POLYMER MATRIX COMPOSITES AT ELEVATED TEMPERATURES
H. Twardy *In* ESA, Spacecraft Structures and Mechanical Testing, Volume 1 Oct. 1991 p 255-261 (For primary document see N92-23780 14-18)
Copyright Avail: NTIS HC/MF A21

N92-23842# Fraunhofer-Inst. fuer Treib- und Explosivstoffe, Pfinztal-Berghausen (Germany, F.R.).
INVESTIGATIONS OF THE DYNAMIC BEHAVIOUR OF COMPOUNDS UNDER PRELOADING
A. Giessler, W. Schmitt, and H. Weber (Karlsruhe Univ., Germany, F.R.) *In* ESA, Spacecraft Structures and Mechanical Testing, Volume 1 Oct. 1991 p 431-433 (For primary document see N92-23780 14-18)
Copyright Avail: NTIS HC/MF A21

28 PROPELLANTS AND FUELS

Includes rocket propellants, igniters, and oxidizers; their storage and handling procedures; and aircraft fuels.

For related information see also *07 Aircraft Propulsion and Power, 20 Spacecraft Propulsion and Power,* and *44 Energy Production and Conversion.*

N92-23555*# Auburn Univ., AL. Dept. of Mechanical Engineering.
CHEMICAL COMPATIBILITY OF CARTRIDGE MATERIALS Final Report
Bryan Ambrose, R. C. Wilcox, and R. H. Zee 1 May 1992 36 p
(Grant NAG8-846)
(NASA-CR-190256; NAS 1.26:190256) Avail: NTIS HC/MF A03 CSCL 07D

The objectives were to determine the chemical compatibility of titanium-zirconium-molybdenum (TZM) with GaAs and CdZnTe, and Inconel with HgCdTe and HgZnTe. At the present time, no other studies regarding the compatibility of these crystal components and their respective cartridge materials have been performed. This study was to identify any possible problems between these materials to insure proper containment of possibly hazardous fumes during crystal growth experiments. In this study, the reaction zone between the materials was studied and the amount of degradation to the system was measured. Detailed results are presented. Author

N92-23756# Bombrini Parodi-Delfino S.p.A., Colleferro (Italy). Coordination Industrielle Activities Spatiales.
MANUFACTURING PROCESS OF THE ARIANE 5 SEGMENTED PROPELLANT CHARGERS [PROCEDE DE FABRICATION DU CHARGEMENT SEGMENTE DES PROPULSEURS D'ARIANE 5]
Roberto Isopi and Michel Vidal (Societe Nationale des Poudres et Explosifs, Saint-Medard-en-Jalles, France) *In* ESA, Launcher Propulsion Towards the Year 2010 Dec. 1991 p 57-66 In FRENCH (For primary document see N92-23750 14-15)
Copyright Avail: NTIS HC/MF A09; ESA, EPD, ESTEC, Noordwijk, Netherlands, HC 50 Dutch guilders

N92-23765# Societe Nationale des Poudres et Explosifs, Vert-Le-Petit (France).
SMALL OR NON POLLUTANT SOLID PROPELLANTS FOR SPACE LAUNCHERS [PROPERGOLS SOLIDES PEU OU NON POLLUANTS POUR LANCEURS SPATIAUX]
Bernard Finck and Christian Perut *In* ESA, Launcher Propulsion Towards the Year 2010 Dec. 1991 p 137-141 In FRENCH (For primary document see N92-23750 14-15)
Copyright Avail: NTIS HC/MF A09; ESA, EPD, ESTEC, Noordwijk, Netherlands, HC 50 Dutch guilders

29 MATERIALS PROCESSING

Includes space-based development of products and processes for commercial applications.

For biological materials see *55 Space Biology.*

N92-23147 Alabama Univ., Huntsville.
MICROGRAVITY DYNAMICAL BEHAVIORS OF CRYOGENIC LIQUID HYDROGEN REORIENTATION AND DRAINING IN SPACE PROPULSION SYSTEM Ph.D. Thesis
Kaun-Long Shyu 1991 293 p
Avail: Univ. Microfilms Order No. DA9203824

Numerical simulation of positive liquid acquisition is attempted by introducing either constant reverse thrust acceleration or impulses reverse thrust acceleration. It shows that there are six dimensionless parameters which hold near constant values through the entire ranges of liquid filled levels, from 30 to 80 pct. Results show that the selection of 1.0 Hz frequency impulsive thrust over the other frequency ranges of impulsive thrust is most proper based on the present study. The characteristics of slosh wave excitation induced by the resettling flow field also were studied. As to the liquid draining, it shows that the liquid residual at the incipience of suction dip increase as the values of gravity decrease, also the residual volume of liquid increase as the flow rates of liquid draining increase. In the slosh wave excitation, it shows that slosh waves are unable to excite for flow fields with lower flow rates of draining and higher restoring force fields of gravity are responsible for the excitation of lower frequencies and higher wave amplitude slosh waves. Dissert. Abstr.

N92-23600*# National Aeronautics and Space Administration. Marshall Space Flight Center, Huntsville, AL.
FIRST INTERNATIONAL MICROGRAVITY LABORATORY EXPERIMENT DESCRIPTIONS
Teresa Y. Miller Feb. 1992 283 p
(NASA-TM-4353; M-681; NAS 1.15:4353) Avail: NTIS HC/MF A13 CSCL 22A

Brief descriptions of the experiments for the First International Microgravity Laboratory (IML-1) which is scheduled for launch from KSC aboard the Orbiter Discovery in early 1992 are presented. For individual titles, see N92-23601 through N92-23642.

N92-23601*# University City Science Center, Philadelphia, PA.
GRAVITROPIC RESPONSES OF PLANTS IN THE ABSENCE OF A COMPLICATING G-FORCE (6-IML-1)
Allan H. Brown *In* NASA. Marshall Space Flight Center, First International Microgravity Laboratory Experiment Descriptions Feb. 1992 p 3-12 Prepared in cooperation with Pennsylvania Univ., Philadelphia (For primary document see N92-23600 14-29)
Avail: NTIS HC/MF A13 CSCL 22A

On the Earth it is patently impossible to measure any tropistic, physiologic, or morphogenic reactions to environmental stimuli without taking into account our planet's gravitational influence on the time course of the test subject's response. It follows that all published reports of quantitative measurements of such responses must have been contaminated by an additional gravity dependent component which probably was not trivial. Our research effort has as its principal scientific objective, the acquisition of experimental data from tests in a microgravity environment that will address a number of basic questions about plants' gravitropic responses to the perception of transversely applied g forces in the hypogravity range, from essentially zero to unit g. Comparable tests on Earth but in the same flight hardware, referred to as the Gravitational Plant Physiology Facility (GPPF), will provide 1 g data for various useful comparisons. Four specific scientific questions are addressed. Author

N92-23602*# University City Science Center, Philadelphia, PA.
A SPACEFLIGHT EXPERIMENT TO INVESTIGATE THE EFFECTS OF A RANGE OF UNILATERAL BLUE LIGHT PHOTOTROPIC STIMULATIONS ON THE MOVEMENTS OF WHEAT COLEOPTILES (6-IML-1)
David G. Heathcote *In* NASA. Marshall Space Flight Center, First International Microgravity Laboratory Experiment Descriptions Feb. 1992 p 13-24 (For primary document see N92-23600 14-29)
Avail: NTIS HC/MF A13 CSCL 22A

In 1978, in response to an announcement of opportunity by NASA, two independent groups proposed related investigations to study the response of seedling plants to photostimulations at microgravity. The spaceflight experiment is known by its NASA acronym, FOTRAN. The scientific objectives behind the experiment are outlined, and a brief description of the spaceflight equipment and the experimental procedures developed to accomplish the aims of the experiment are presented. By reference to the results of ground-based studies, the likely scientific returns of the FOTRAN experiment will be assessed. The experiment is designed to investigate the effects of a range of blue light stimulations on the movements of wheat coleoptiles at zero-g. The seedlings will be dark-grown, and their movements assessed from infrared time-lapse video recordings made during flight. The photostimulus may be expected to modulate circumnutations of the coleoptiles, by synchronizing, initiating or amplifying these rhythmic movements, and to initiate the classic phototropic response. Author

N92-23603*# Jet Propulsion Lab., California Inst. of Tech., Pasadena.
GENETIC AND MOLECULAR DOSIMETRY OF HZE RADIATION (7-IML-1) **c52**
Gregory A. Nelson *In* NASA. Marshall Space Flight Center, First International Microgravity Laboratory Experiment Descriptions Feb. 1992 p 25-31 (For primary document see N92-23600 14-29)
Avail: NTIS HC/MF A13 CSCL 06R

The objectives of the study are to determine the kinetics of production and to characterize the unique aspects of genetic and developmental lesion induced in animal cells by radiation present in the space environment. Special attention is given to heavy charged particles. The organism Caenorhabditis elegans, a simple nematode, is used as a model system for a coordinated set of ground-based and flight experiments. Author

N92-23604*# International Center for Genetic Engineering and Biotechnology, Trieste (Italy).
MICROGRAVITATIONAL EFFECTS ON CHROMOSOME BEHAVIOR (7-IML-1) **c51**
Carlo Bruschi *In* NASA. Marshall Space Flight Center, First International Microgravity Laboratory Experiment Descriptions Feb. 1992 p 33-38 (For primary document see N92-23600 14-29)
Avail: NTIS HC/MF A13 CSCL 06C

The effects of the two major space-related conditions, microgravity and radiation, on the maintenance and transmission of genetic information have been partially documented in many organisms. Specifically, microgravity acts at the chromosomal level, primarily on the structure and segregation of chromosomes, in producing major abberations such as deletions, breaks, nondisjunction, and chromosome loss, and to a lesser degree, cosmic radiation appears to affect the genic level, producing point mutations and DNA damage. To distinguish between the effects from microgravity and from radiation, it is necessary to monitor both mitotic and meiotic genetic damage in the same organism. The yeast Saccharomyces cerevisiae is used to monitor at high resolution the frequency of chromosome loss, nondisjunction, intergenic recombination, and gene mutation in mitotic and meiotic cells, to a degree impossible in other organisms. Because the yeast chromosomes are small, sensitive measurements can be made that can be extrapolated to higher organisms and man. The objectives of the research are: (1) to quantitate the effects of microgravity and its synergism with cosmic radiation on chromosomal integrity and transmission during mitosis and meiosis; (2) to discriminate between chromosomal processes sensitive to microgravity and/or radiation during mitosis and meiosis; and (3) to relate these findings to anomalous mitotic mating type switching and ascosporogenesis following meiosis. Author

N92-23605*# Texas Univ. Health Science Center, Houston. Dental Branch.
CHRONDROGENESIS IN MICROMASS CULTURES OF EMBRYONIC MOUSE LIMB MESENCHYMAL CELLS EXPOSED TO MICROGRAVITY (7-IML-1) **c51**
Jackie Duke *In* NASA. Marshall Space Flight Center, First International Microgravity Laboratory Experiment Descriptions Feb. 1992 p 39-44 (For primary document see N92-23600 14-29)
Avail: NTIS HC/MF A13 CSCL 06C

A basic question of space biology is whether changes in gravity are perceived at the cellular level. Previous studies with a variety of cells have shown that this is the case, but to date the response of skeletal cells has not been examined, even though the skeleton is sensitive to gravitational changes. The objective of the CELLS Experiment is to examine the effect of microgravity in vitro on a skeletal cell known to be sensitive to gravitational changes both in vivo and in vitro - the mammalian chondrocyte. Various aspects of the experiment are discussed. Author

N92-23606*# Vrije Univ., Amsterdam (Netherlands). Dept. of Oral Cell Biology.
EFFECT OF MICROGRAVITY AND MECHANICAL STIMULATION ON THE IN VITRO MINERALIZATION AND RESORPTION OF FETAL MOUSE LONG BONES (7-IML-1) **c51**
J. Paul Veldhuijzen *In* NASA. Marshall Space Flight Center, First International Microgravity Laboratory Experiment Descriptions Feb. 1992 p 45-48 (For primary document see N92-23600 14-29)
Avail: NTIS HC/MF A13 CSCL 06C

Mechanical forces play an important role in the differentiation, growth, and remodeling of skeletal tissues. An increase in the normal loading pattern of the skeleton leads to an increase in bone mass. An overall decrease in the functional load exerted on the skeleton produces mineral loss and osteoporosis. However, the responses of the skeletal tissue cells to various loading conditions are still largely unresolved, as is the mechanism of the cellular response to changed mechanical environment. Using an in vitro approach, we hope to avoid some problems encountered in the use of in vivo animal and man models, which have been extensively used in the past. In a number of experiments we have demonstrated that 16 and 17 day old fetal mouse long bone rudiments (metatarsalia), cultured in a liquid culture medium, are very suitable to study mineralization and resorption, respectively. We have also demonstrated that under hydrostatic compression, mineralization is increased while resorption is decreased. Culture of long bone rudiments under noncompressed control conditions can be regarded as a situation of partial unloading, showing some phenomena of a disuse situation. Under microgravity conditions, responses of osteoblasts and chondrocytes (involved in mineralization) and osteoclasts (involved in mineral resorption), to culture with and without compression, may be much more outspoken. This will have advantages for the study and the interpretation of the role of cellular events in the process of mineralization and resorption of developing skeletal tissues under various loading conditions. The BONES Experiment is carried out in four type I/O and four type I/E containers. Various aspects of the investigation are discussed. Author

N92-23607*# Hubrecht Lab., Utrecht (Netherlands).
EGGS: THE ROLE OF GRAVITY IN THE ESTABLISHMENT OF THE DORSO-VENTRAL AXIS IN THE AMPHIBIAN EMBRYO (7-IML-1) **c51**
Geertje A. Ubbels *In* NASA. Marshall Space Flight Center, First International Microgravity Laboratory Experiment Descriptions Feb. 1992 p 49-53 (For primary document see N92-23600 14-29)
Avail: NTIS HC/MF A13 CSCL 06C

The purpose of this experiment is to fertilize frog (Xenopus laevis) eggs under microgravity, to perform histological fixations at two different programmed times, and after return to Earth, to determine whether timing and pattern of egg cleavages and axis formation are normal. Because of the limited viability of the gametes, this experiment will be the very first to be activated in the Biorack. Various aspects of this investigation are discussed. Author

N92-23608*# Consejo Superior de Investigaciones Cientificas, Madrid (Spain). Dept. of Biochemistry.
THE EFFECT OF SPACE ENVIRONMENT ON THE DEVELOPMENT AND AGING OF DROSOPHILA MELANOGASTER (7-IML-1) **c51**
Roberto Marco *In* NASA. Marshall Space Flight Center, First International Microgravity Laboratory Experiment Descriptions Feb. 1992 p 55-57 (For primary document see N92-23600 14-29)
Avail: NTIS HC/MF A13 CSCL 06C

This experiment involves the study of the development of eggs of the fly, Drosophila, exposed to microgravity. It is presumed that oogenesis, rather than further states of embryonic development, is sensitive to gravity. This hypothesis will be tested by collecting eggs layered at specific times inflight and postflight from flies exposed to 0 and 1 g. This portion of the experiment is a repetition of an earlier experiment flown in Biorack during the Spacelab D1

Mission. An added feature of the experiment for the First International Microgravity Laboratory (IML-1) Mission is to study the effect of microgravity on the life span of Drosophila male flies. Various aspects of the investigation are discussed. Author

N92-23609*# Aarhus Univ. (Denmark).
EFFECT OF MICROGRAVITY ENVIRONMENT ON CELL WALL REGENERATION, CELL DIVISIONS, GROWTH, AND DIFFERENTIATION OF PLANTS FROM PROTOPLASTS (7-IML-1) **c51**
Ole Rasmussen *In* NASA. Marshall Space Flight Center, First International Microgravity Laboratory Experiment Descriptions Feb. 1992 p 59-61 (For primary document see N92-23600 14-29)
Avail: NTIS HC/MF A13 CSCL 06C

The primary goal of this project is to investigate if microgravity has any influence on growth and differentiation of protoplasts. Formation of new cell walls on rapeseed protoplasts takes place within the first 24 hours after isolation. Cell division can be observed after 2-4 days and formation of cell aggregates after 5-7 days. Therefore, it is possible during the 7 day IML-1 Mission to investigate if cell wall formation, cell division, and cell differentiation are influenced by microgravity. Protoplasts of rapeseeds and carrot will be prepared shortly before launch and injected into 0.6 ml polyethylene bags. Eight bags are placed in an aluminum block inside the ESA Type 1 container. The containers are placed at 4 C in PTCU's and transferred to orbiter mid-deck. At 4 C all cell processes are slowed down, including cell wall formation. Latest access to the shuttle will be 12 hours before launch. In orbit the containers will be transferred from the PTC box to the 22 C Biorack incubator. The installation of a 1 g centrifuge in Biorack will make it possible to distinguish between effects of near weightlessness and effects caused by cosmic radiation and other space flight factors including vibrations. Parallel control experiments will be carried out on the ground. Other aspects of the experiment are discussed. Author

N92-23610*# Deutsche Forschungsanstalt fuer Luft- und Raumfahrt, Cologne (Germany, F.R.). Inst. for Aerospace Medicine.
EMBRYOGENESIS AND ORGANOGENESIS OF CARAUSIUS MOROSUS UNDER SPACE FLIGHT CONDITIONS (7-IML-1) **c51**
D. H. Buecker *In* NASA. Marshall Space Flight Center, First International Microgravity Laboratory Experiment Descriptions Feb. 1992 p 63-64 (For primary document see N92-23600 14-29)
Avail: NTIS HC/MF A13 CSCL 06C

The experiment is part of a radiobiological space research program to obtain experimental data on the biological effectiveness of the structured component of cosmic radiation during spaceflight. In this proposed experiment, Carausius morosus embryos of different ages will develop under spaceflight conditions. The experiment is designed to determine the influence of galactic heavy ions of very high energy deposition in microgravity on developmental processes of different radiation sensitivity and regenerative capacity. Layers of Carausius morosus eggs are sandwiched between different track detectors (cellulose nitrate, CR39). This method allows the localization of the trajectory of each heavy ion in the biological layer and the identification of the site of the penetration inside the egg. Author

N92-23611*# Deutsche Forschungsanstalt fuer Luft- und Raumfahrt, Cologne (Germany, F.R.). Inst. for Aerospace Medicine.
DOSIMETRIC MAPPING INSIDE BIORACK (7-IML-1) **c32**
G. Reitz *In* NASA. Marshall Space Flight Center, First International Microgravity Laboratory Experiment Descriptions Feb. 1992 p 65 (For primary document see N92-23600 14-29)
Avail: NTIS HC/MF A13 CSCL 20N

This experiment documents the radiation environment inside Biorack and compares it to theoretical predictions. Other experiments inside Biorack need this information to determine whether changes to samples are caused by radiation or microgravity. Dosimetric stacks, each with 20 to 100 sheets of plastic detector foils (cellulose nitrate, Lexan, and CR39) and nuclear emulsions of different radiation sensitivity are packed together with Thermoluminescence dosimeters (TLD) inside Type 1 containers. Crew members place two stacks in the 37 C incubator and four in the 36 C incubator, two of which are placed on the 1 g centrifuge. Two stacks are located in a stowage position at ambient temperature. After the mission, the plastic detectors are etched and the nuclear emulsions are developed similar to photographic emulsions. The traces resulting from the interaction of heavy ions with matter can then be evaluated under the microscope. The number, charge, and energy of the particles will be determined. From the TLD readings, the absorbed dose of the low LET components will be received. Author

N92-23612*# Johann-Wolfgang-Goethe-Univ., Frankfurt am Main (Germany, F.R.). Inst. of Microbiology.
GROWTH AND SPORULATION OF BACILLUS SUBTILIS UNDER MICROGRAVITY (7-IML-1) **c51**
Horst-Dieter Mennigmann *In* NASA. Marshall Space Flight Center, First International Microgravity Laboratory Experiment Descriptions Feb. 1992 p 67-70 (For primary document see N92-23600 14-29)
Avail: NTIS HC/MF A13 CSCL 06C

The experiment was aimed at measuring the growth and sporulation of Bacillus subtilis under microgravity. The hardware for the experiment consists of a culture chamber (15 ml) made from titanium and closed by a membrane permeable for gases but not for water. Two variants of this basic structure were built which fit into the standard Biorack container types 1 and 2 respectively. Growth of the bacteria will be monitored by continuously measuring the optical density with a built-in miniaturized photometer. Other parameters (viability, sporulation, fine structure, size distribution of cells and spores, growth kinetics, etc.) will be measured on the fixed samples and on those where metabolism was temporarily halted, respectively. Author

N92-23613*# Eidgenoessische Technische Hochschule, Zurich (Switzerland).
FRIEND LEUKEMIA VIRUS TRANSFORMED CELLS EXPOSED TO MICROGRAVITY IN THE PRESENCE OF DMSO (7-IML-1) **c51**
Augusto Cogoli *In* NASA. Marshall Space Flight Center, First International Microgravity Laboratory Experiment Descriptions Feb. 1992 p 71-73 (For primary document see N92-23600 14-29)
Avail: NTIS HC/MF A13 CSCL 06C

The purpose of this experiment is to study the adaptation of living cells to microgravity. The in vitro transformation of Friend cells by Dimethylsufoxide (DMSO) is a good model for the study of cell differentiation and protein biosynthesis. Cultures of cells will be prepared shortly before launch. Once in space, transformation will be induced by injection of DMSO. One set of cultures will be chemically fixed with glutaraldehyde for electron microscope investigations; another set will be preserved for determining the amount of hemogloben produced and the extent of cell proliferation. Author

N92-23614*# Eidgenoessische Technische Hochschule, Zurich (Switzerland). Inst. of Biotechnology.
PROLIFERATION AND PERFORMANCE OF HYBRIDOMA CELLS IN MICROGRAVITY (7-IML-1) **c51**
Augusto Cogoli *In* NASA. Marshall Space Flight Center, First International Microgravity Laboratory Experiment Descriptions Feb. 1992 p 75-77 (For primary document see N92-23600 14-29)
Avail: NTIS HC/MF A13 CSCL 06C

The purpose of this experiment is to study how cell performance (biosynthesis and secretion) is altered by altered gravity conditions. Hybridoma cells are obtained by fusion of an activated B-lymphocyte with a myeloma cell. Activated B-lymphocytes, derived from a human or an animal, carry the information required to produce antibodies of a certain specificity and can survive only a few days in culture. Myeloma cells are tumor cells which can grow indefinitely in culture. Therefore, the product of the fusion is

an immortal cell line capable of producing homogeneous antibodies (monoclonal antibodies). Experimental procedures are explained in some detail. Author

N92-23615*# Eidgenoessische Technische Hochschule, Zurich (Switzerland). Inst. of Biotechnology.
DYNAMIC CELL CULTURE SYSTEM (7-IML-1) **c51**
Augusto Cogoli *In* NASA. Marshall Space Flight Center, First International Microgravity Laboratory Experiment Descriptions Feb. 1992 p 79-80 (For primary document see N92-23600 14-29)
Avail: NTIS HC/MF A13 CSCL 06C

This experiment is one of the Biorack experiments being flown on the International Microgravity Laboratory 1 (MIL-1) mission as part of an investigation studying cell proliferation and performance in space. One of the objectives of this investigation is to assess the potential benefits of bioprocessing in space with the ultimate goal of developing a bioreactor for continuous cell cultures in space. This experiment will test the operation of an automated culture chamber that was designed for use in a Bioreactor in space. The device to be tested is called the Dynamic Cell Culture System (DCCS). It is a simple device in which media are renewed or chemicals are injected automatically, by means of osmotic pumps. This experiment uses four Type I/O experiment containers. One DCCS unit, which contains a culture chamber with renewal of medium and a second chamber without a medium supply fits in each container. Two DCCS units are maintained under zero gravity conditions during the on-orbit period. The other two units are maintained under 1 gh conditions in a 1 g centrifuge. The schedule for incubator transfer is given. Author

N92-23616*# Open Univ. (Scotland).
GROWTH, DIFFERENTIATION AND DEVELOPMENT OF ARABIDOPSIS THALIANA UNDER MICROGRAVITY CONDITIONS (7-IML-1) **c51**
E. P. Maher and L. G. Briarty (Nottingham Univ., England) *In* NASA. Marshall Space Flight Center, First International Microgravity Laboratory Experiment Descriptions Feb. 1992 p 81-87 (For primary document see N92-23600 14-29)
Avail: NTIS HC/MF A13 CSCL 06C

The aim of this set of experiments is to quantify the structural and behavioral changes taking place in germinating seeds of the small plant Arabidopsis thaliana. The protocol to be used will involve germination of the seeds in orbit. Their growth will be followed by fixing and photographing samples of microgravity grown and 1 g control seedlings at intervals over 4 days. The different studies which will then be performed can be classified in relation to the parts of the plants involved. The first study will be an examination of the ultrastructure of the root statocytes, the cells containing gravity sensors, to determine whether their development proceeds normally under microgravity conditions. A second study will examine the differences in root and shoot development and orientation between normal wild type seedlings and those of an agravitropic mutant (aux-1) - one that does not respond normally to gravity. A third set of observations will be made on the structural changes occurring during reserve breakdown and utilization in the cells of the cotyledons, the storage organs of the seed. The fourth part of the work will be an examination of the statocytes present in the shoot and their development in microgravity. The final part of the study will give an answer to the debated question of whether the formation of the hypocotyl hook in seedlings is gravity dependent. Author

N92-23617*# Paris VI Univ. (France).
TRANSMISSION OF GRAVISTIMULUS IN THE STATOCYTE OF THE LENTIL ROOT (7-IML-1) **c51**
Gerald Perbal *In* NASA. Marshall Space Flight Center, First International Microgravity Laboratory Experiment Descriptions Feb. 1992 p 89-91 (For primary document see N92-23600 14-29)
Avail: NTIS HC/MF A13 CSCL 06C

The aim of this Biorack experiment is to determine the presentation time (minimum stimulation period to provoke a slight but significant response) of gravireaction of lentil roots cultivated in microgravity for 27 hours. The location of the statoliths in the statocytes will be analyzed in parallel in order to find the cell structure which can transmit the physical effect of the pressure of the statoliths into a biochemical factor leading to an asymmetrical production or release of the inhibitor which is responsible for the gravitropic response. Seeds of Lens culinaris will be used because of their small size. Details of the experimental procedure are given. Author

N92-23618*# Deutsche Forschungsanstalt fuer Luft- und Raumfahrt, Cologne (Germany, F.R.).
GRAVITY RELATED BEHAVIOR OF THE ACELLULAR SLIME MOLD PHYSARUM POLYCEPHALUM (7-IML-1) **c51**
I. Block *In* NASA. Marshall Space Flight Center, First International Microgravity Laboratory Experiment Descriptions Feb. 1992 p 93-97 (For primary document see N92-23600 14-29)
Avail: NTIS HC/MF A13 CSCL 06C

The objective of the experiment is to investigate the effect of near weightlessness on a single cell. The test object is the acellular slime mold Physarum polycephalum. This cell is composed of a network of protoplastic strands which perform rhythmic contractions in the minute range. These contractions of the strands' ectoplastic walls generate the force to drive the vigorous shuttle streaming of fluid protoplasm inside the strands (hydrostatic pressure flow). A net transport of protoplasm in one direction determines the direction of the cell's locomotion itself. In this way, gravity modifies the contraction rhythm of the strands, the streaming velocity of protoplasm in the strands, and the direction of locomotion of the whole slime mold (geotaxis). The other parts of this experiment will address the major question of how this cell, which does not possess any specialized gravireceptors, gets the information about the direction of the gravity vector. Details of the experimental setup are given. Author

N92-23619*# Toulouse Univ. (France).
STUDIES ON PENETRATION OF ANTIBIOTIC IN BACTERIAL CELLS IN SPACE CONDITIONS (7-IML-1) **c51**
R. Tixador *In* NASA. Marshall Space Flight Center, First International Microgravity Laboratory Experiment Descriptions Feb. 1992 p 99-107 (For primary document see N92-23600 14-29)
Avail: NTIS HC/MF A13 CSCL 06C

The Cytos 2 experiment was performed aboard Salyut 7 in order to test the antibiotic sensitivity of bacteria cultivated in vitro in space. An increase of the Minimal Inhibitory Concentration (MIC) in the inflight cultures (i.e., an increase of the antibiotic resistance) was observed. Complementary studies of the ultrastructure showed a thickening of the cell envelope. In order to confirm the results of the Cytos 2 experiment, we performed the ANTIBIO experiment during the D1 mission to try to differentiate, by means of the 1 g centrifuge in the Biorack, between the biological effects of cosmic rays and those caused by microgravity conditions. The originality of this experiment was in the fact that it was designed to test the antibiotic sensitivity of bacteria cultivated in vitro during the orbital phase of the flight. The results show an increase in resistance to Colistin in in-flight bacteria. The MIC is practically double in the in-flight cultures. A cell count of living bacteria in the cultures containing the different Colistin concentrations showed a significant difference between the cultures developed during space flight and the ground based cultures. The comparison between the 1 g and 0 g in-flight cultures show similar behavior for the two sets. Nevertheless, a small difference between the two sets of ground based control cultures was noted. The cultures developed on the ground centrifuge (1.4 g) present a slight decrease in comparison with the cultures developed in the static rack (1 g). In order to approach the mechanisms of the increase of antibiotic resistance on bacteria cultivated in vitro in space, we have proposed the study on penetration of antibiotics in bacterial cells in space conditions. This experiment was selected for the International Microgravity Laboratory 1 (IML-1) mission. Author

N92-23620*# Calgary Univ. (Alberta).
ENERGY EXPENDITURE IN SPACE FLIGHT (DOUBLY LABELLED WATER METHOD) (8-IML-1) **c52**
Howard G. Parsons *In* NASA. Marshall Space Flight Center,

First International Microgravity Laboratory Experiment Descriptions Feb. 1992 p 111-112 (For primary document see N92-23600 14-29)
Avail: NTIS HC/MF A13 CSCL 06P

The objective of the Energy Expenditure in Space Flight (ESS) experiment is to demonstrate and evaluate the doubly labeled water method of measuring the energy expended by crew members during approximately 7 days in microgravity. The doubly labeled water technique determines carbon dioxide production which is then used to calculate energy expenditure. The method relies on the equilibrium between oxygen in respiratory carbon dioxide and oxygen in body water. Because of this equilibrium, the kinetic of water turnover and respiration are interdependent. Under normal conditions, man contains small but significant amounts of deuterium and oxygen 18. Deuterium is eliminated from the body as water while oxygen 18 is eliminated as water and carbon dioxide. The difference in the turnover rates in the two isotopes is proportional to the carbon dioxide production. Deliberately enriching the total body water with both of these isotopes allows the isotope turnovers to be accurately measured in urine, plasma, or saliva samples. The samples are taken to the laboratory for analysis using an ion-ratio spectrometer. Author

N92-23621*# British Columbia Univ., Vancouver.
PHASE PARTITIONING EXPERIMENT (8-IML-1) **c51**
Donald E. Brooks *In* NASA. Marshall Space Flight Center, First International Microgravity Laboratory Experiment Descriptions Feb. 1992 p 113-116 (For primary document see N92-23600 14-29)
Avail: NTIS HC/MF A13 CSCL 06C

Phase partitioning is a method of separating biological cells and macromolecules via their differential distribution in two phase aqueous polymer solutions. The ultimate goal of the experiment is to test the hypothesis that the efficiency of separation of closely related cell types, by partitioning in immiscible aqueous phases, will be enhanced in the non-convective environment provided by space. Before a cell separation experiment can be performed, the demixing of immiscible aqueous polymer solutions must be understood and controlled in order to optimize the experimental conditions for a cell separation experiment in the future. The present Phase Partitioning Experiment (PPE) is the third in a series, the first two flew on STS 51-D in Apr. 1985 and STS 26 in Oct. 1988. In those experiments the immiscible aqueous phases demixed spontaneously at different rates, the final disposition being one in which the phase which wetted the container wall surrounded the second phase which formed an 'egg yolk' in the center of the chamber. D.R.D.

N92-23622*# British Columbia Univ., Vancouver. University Hospital/Shaughnessy Site.
BACK PAIN IN ASTRONAUTS (8-IML-1) **c52**
P. C. Wing *In* NASA. Marshall Space Flight Center, First International Microgravity Laboratory Experiment Descriptions Feb. 1992 p 117-119 (For primary document see N92-23600 14-29)
Avail: NTIS HC/MF A13 CSCL 06P

As a preliminary study for the International Microgravity Laboratory (IML-1) experiment, a pain diagram was used to elicit information about the incidence and severity of back pain experienced by 20 payload specialists (PS) on 22 shuttle flights from 1983 to 1986. There were 18 responses from 17 PSs (one PS provided information about two missions). Thirteen PSs (72 percent) reported experiencing some degree of back pain, ranging from dull (can be ignored) to severe, making concentration difficult. For the majority, the pain was dull in nature, and did not interfere with work or concentration. For some, the pain abated after only a few minutes; for others, the pain persisted for the entire duration of the flight. D.R.D.

N92-23623*# Canadian Space Agency, Ottawa (Ontario).
MEASUREMENT OF VENOUS COMPLIANCE (8-IML-1) **c52**
R. B. Thirsk *In* NASA. Marshall Space Flight Center, First International Microgravity Laboratory Experiment Descriptions Feb. 1992 p 121-122 (For primary document see N92-23600 14-29)
Avail: NTIS HC/MF A13 CSCL 06P

The prime objective of this International Microgravity Laboratory (IML-1) investigation is to measure the bulk compliance (distensibility) of the veins in the lower leg before, during, and after spaceflight. It is of particular interest whether venous compliance over the range of both positive and negative transmural pressures (various states of venous distention and collapse) changes throughout the duration of spaceflight. Information concerning the occurrence and character of compliance changes could have implications for the design of improved antigravity suits and further the understanding of inflight and postflight venous hemodynamics. Author

N92-23624*# University of Western Ontario, London.
POSITIONAL AND SPONTANEOUS NYSTAGMUS (8-IML-1) **c52**
Joseph McClure *In* NASA. Marshall Space Flight Center, First International Microgravity Laboratory Experiment Descriptions Feb. 1992 p 123-124 (For primary document see N92-23600 14-29)
Avail: NTIS HC/MF A13 CSCL 06P

Nystagmus is an involuntary oscillation of the eyes with a slow eye movement in one direction and a compensatory quick eye movement in the opposite direction to return the eyes to their original position. The slow phase of nystagmus is often generated by asymmetry in the peripheral vestibular system, and generally nystagmus in the horizontal direction dominates although vertical and rotary nystagmus can be seen in certain pathological situations. D.R.D.

N92-23625*# McGill Univ., Montreal (Quebec).
SPACE ADAPTATION SYNDROME EXPERIMENTS (8-IML-1) **c52**
D. Watt *In* NASA. Marshall Space Flight Center, First International Microgravity Laboratory Experiment Descriptions Feb. 1992 p 125-134 (For primary document see N92-23600 14-29)
Avail: NTIS HC/MF A13 CSCL 06P

A set of seven experiments will study adaptation of the human nervous system to weightlessness. Particular emphasis will be placed on the vestibular and proprioceptive systems. The experiments are as follows: the sled/H-reflex; rotation/vestibulo-ocular reflex, the visual stimulator experiment; proprioception (relaxed) experiment; proprioception (active) experiment; proprioception (illusion) experiment; and tactile acuity. D.R.D.

N92-23626*# National Aeronautics and Space Administration. Lyndon B. Johnson Space Center, Houston, TX.
MICROGRAVITY VESTIBULAR INVESTIGATIONS (10-IML-1) **c52**
Millard F. Reschke *In* NASA. Marshall Space Flight Center, First International Microgravity Laboratory Experiment Descriptions Feb. 1992 p 135-180 (For primary document see N92-23600 14-29)
Avail: NTIS HC/MF A13 CSCL 06P

Our perception of how we are oriented in space is dependent on the interaction of virtually every sensory system. For example, to move about in our environment we integrate inputs in our brain from visual, haptic (kinesthetic, proprioceptive, and cutaneous), auditory systems, and labyrinths. In addition to this multimodal system for orientation, our expectations about the direction and speed of our chosen movement are also important. Changes in our environment and the way we interact with the new stimuli will result in a different interpretation by the nervous system of the incoming sensory information. We will adapt to the change in appropriate ways. Because our orientation system is adaptable and complex, it is often difficult to trace a response or change in behavior to any one source of information in this synergistic orientation system. However, with a carefully designed investigation, it is possible to measure signals at the appropriate level of response (both electrophysiological and perceptual) and determine the effect

that stimulus rearrangement has on our sense of orientation. The environment of orbital flight represents the stimulus arrangement that is our immediate concern. The Microgravity Vestibular Investigations (MVI) represent a group of experiments designed to investigate the effects of orbital flight and a return to Earth on our orientation system. Author

N92-23627*# Deutsche Forschungsanstalt fuer Luft- und Raumfahrt, Cologne (Germany, F.R.). Inst. for Aerospace Medicine.
BIOSTACK (14-IML-1) **c93**
H. Buecker *In* NASA. Marshall Space Flight Center, First International Microgravity Laboratory Experiment Descriptions Feb. 1992 p 181-182 (For primary document see N92-23600 14-29)
Avail: NTIS HC/MF A13 CSCL 03B

The Biostack experiments address especially the biological effects of the galactic particles of high atomic number and high energy, called HZE particles. The objective of the experiments is to substantiate the assessment of spaceflight radiation hazards especially regarding these particles. D.R.D.

N92-23628*# Massachusetts Inst. of Tech., Cambridge.
MENTAL WORKLOAD AND PERFORMANCE EXPERIMENT (15-IML-1) **c53**
Harold L. Alexander *In* NASA. Marshall Space Flight Center, First International Microgravity Laboratory Experiment Descriptions Feb. 1992 p 183-187 (For primary document see N92-23600 14-29)
Avail: NTIS HC/MF A13 CSCL 05I

Whether on Earth or in space, people tend to work more productively in settings designed for efficiency and comfort. Because comfortable and stress-free working environments enhance performance and contribute to congenial relationships among co-workers, the living and working arrangements for spacecraft to be used for missions lasting months or years assume particular importance. The Mental Workload and Performance Experiment (MWPE), in part, examines the appropriate design of workstations for performance of various tasks in microgravity, by providing a variable-configuration workstation that may be adjusted by the astronauts. Author

N92-23629*# National Space Development Agency, Tokyo (Japan).
RADIATION MONITORING CONTAINER DEVICE (16-IML-1) **c51**
S. Nagaoka *In* NASA. Marshall Space Flight Center, First International Microgravity Laboratory Experiment Descriptions Feb. 1992 p 189 (For primary document see N92-23600 14-29)
Avail: NTIS HC/MF A13 CSCL 06C

In this experiment, layers of radiation detectors and biological specimens, bacterial spores (Bacillus subtillis), shrimp eggs (Altemia salina), and maize seeds (Zea mays) are sandwiched together in the Radiation Monitoring Container. The detectors, sheets of plastic materials, record the nuclear track of cosmic radiation. The dosimeter package contains conventional detectors made of materials such as lithium fluoride or magnesium-silica-terbium. The thermoluminescent materials (TLD) will, when moderately heated, emit luminescent photons linearly depending upon the dose of radiation received. The experiment, enclosed in a box-like container, is mounted on the aft end cone of the Spacelab, the area where the shielding is somewhat less than other locations. Author

N92-23630*# Alabama A & M Univ., Huntsville.
A STUDY OF SOLUTION CRYSTAL GROWTH IN LOW-g (2-IML-1)
Ravindra B. Lal *In* NASA. Marshall Space Flight Center, First International Microgravity Laboratory Experiment Descriptions Feb. 1992 p 193-201 (For primary document see N92-23600 14-29)
Avail: NTIS HC/MF A13 CSCL 22A

During the International Microgravity Laboratory-1 (IML-1) mission it is planned to grow triglycine sulfate (TGS) crystals from aqueous solution using the modified Fluids Experiment System (FES). A special cooled sting technique will be used for solution crystal growth. The objectives of the experiment are as follows: (1) to grow crystals of TGS using the modified FES; (2) to perform holographic interferometric tomography of the fluid field in three dimensions; (3) to study the fluid motion due to g-jitter by multiple exposure holography of tracer particles; and (4) to study the influence of g-jitter on the growth rate. D.R.D.

N92-23631*# Tennessee Univ. Space Inst., Tullahoma.
AN OPTICAL STUDY OF GRAIN FORMATION: CASTING AND SOLIDIFICATION TECHNOLOGY (2-IML-1)
Mary H. McCay *In* NASA. Marshall Space Flight Center, First International Microgravity Laboratory Experiment Descriptions Feb. 1992 p 203-209 (For primary document see N92-23600 14-29)
Avail: NTIS HC/MF A13 CSCL 22A

By studying the unidirectional growth of a metal-model material in microgravity, an attempt is made to characterize alloy solidification. Using holograms and supporting temperature measurements obtained during processing in the Fluids Experiment System (FES), the solute and thermal fields associated with the dendrite growth front and extraneous nucleation will be measured and compared to a theoretical (computational) model. Ground based supporting experiments include particle tracking to measure the velocity fields, and optical phase shift techniques (confocal optical signal processing, interferometry, and Schlieren) to study thermal and solutal fields. Author

N92-23632*# EG and G Energy Measurements, Inc., Goleta, CA.
VAPOR CRYSTAL GROWTH STUDIES OF SINGLE CRYSTALS OF MERCURIC IODIDE (3-IML-1)
Lodewijk vandenBerg *In* NASA. Marshall Space Flight Center, First International Microgravity Laboratory Experiment Descriptions Feb. 1992 p 211-214 (For primary document see N92-23600 14-29)
Avail: NTIS HC/MF A13 CSCL 22A

A single crystal of mercuric iodide (HgI2) will be grown during the International Microgravity Lab. (IML-1) mission. The crystal growth process takes place by sublimation of HgI2 from an aggregate of purified material, transport of the molecules in the vapor from the source to the crystal, and condensation on the crystal surface. The objectives of the experiment are as follow: to grow a high quality crystal of HgI2 of sufficient size so that its properties can be extensively analyzed; and to study the vapor transport process, specifically the rate of diffusion transport at greatly reduced gravity where convection is minimized. Author

N92-23633*# Clermont-Ferrand Univ. (France).
MERCURY IODIDE NUCLEATION AND CRYSTAL GROWTH IN VAPOR PHASE (4-IML-1)
Robert Cadoret *In* NASA. Marshall Space Flight Center, First International Microgravity Laboratory Experiment Descriptions Feb. 1992 p 215-217 (For primary document see N92-23600 14-29)
Avail: NTIS HC/MF A13 CSCL 22A

The objectives of this experiment are to grow simultaneously three single crystals of mercuric iodide (HgI2) in an imposed temperature profile and to assess the advantages of growth in microgravity on the HgI2 crystal quality. Growth in microgravity should reduce fluctuations in HgI2 concentrations and thus decrease the resultant crystal defects. In order to test this hypothesis, a seeded growth of HgI2 crystals will be performed on International Microgravity Lab. (IML-1). Author

N92-23634*# Alabama Univ., Birmingham.
PROTEIN CRYSTAL GROWTH (5-IML-1)
Charles E. Bugg *In* NASA. Marshall Space Flight Center, First International Microgravity Laboratory Experiment Descriptions Feb. 1992 p 219-224 (For primary document see N92-23600 14-29)
Avail: NTIS HC/MF A13 CSCL 22A

Proteins (enzymes, hormones, immunoglobulins) account for 50 pct. or more of the dry weight of most living systems. A detailed understanding of the structural makeup of a protein is essential to any systematic research pertaining to it. Most macromolecules are extremely difficult to crystallize, and many otherwise exciting projects have terminated at the crystal growth stage. In principle, there are several aspects of microgravity that might be exploited to enhance protein crystal growth. The major factor is the elimination of density driven convective flow. Other factors that can be controlled in the absence of gravity is the sedimentation of growing crystals in a gravitational field, and the potential advantage of doing containerless crystal growth. As a result of these theories and facts, one can readily understand why the microgravity environment of an Earth orbiting vehicle seems to offer unique opportunities for the protein crystallographer. This perception has led to the establishment of the Protein Crystal Growth in a Microgravity Environment (PCG/ME) project. The results of experiments already performed during STS missions have in many cases resulted in large protein crystals which are structurally correct. Thus, the near term objective of the PCG/ME project is to continue to improve the techniques, procedures, and hardware systems used to grow protein crystals in Earth orbit.

Author

N92-23635*# National Space Development Agency, Tokyo (Japan).

ORGANIC CRYSTAL GROWTH EXPERIMENT FACILITY (13-IML-1)

Akio Kanbayashi *In* NASA. Marshall Space Flight Center, First International Microgravity Laboratory Experiment Descriptions Feb. 1992 p 225-229 (For primary document see N92-23600 14-29)

Avail: NTIS HC/MF A13 CSCL 22A

The interesting nature of metal-like organic compounds composed of charge transfer complexes has been recently realized. Crystals of these complexes can usually be grown by the solution crystallization method. It is difficult to grow such organic crystals on Earth, especially from the chemical reactions through diffusion controlled process in the solutions, because of gravitational disturbances, or sedimentation. The International Microgravity Lab. (IML-1) Organic Crystal Growth with G-Gitter Preventive Measure (OCGP) experiment is expected to grow a single crystal large enough to allow its intrinsic physical properties to be measured and its detailed crystal structure to be determined. This experiment also attempts to assess the experimental conditions including the microgravity environment for further study of the fundamental process of solution crystallization, nucleation, and growth from supersaturated phases including chemical reactions. Microgravity disturbances, G-jitter, may be an important environmental factor in the experimental method to assess. The vibration damping effects on organic crystal growth can be carefully studied.

Author

N92-23636*# Deutsche Agentur fuer Raumfahrtangelegenheiten G.m.b.H., Bonn (Germany, F.R.).

CRYOSTAT (18-IML-1) **c31**

In NASA. Marshall Space Flight Center, First International Microgravity Laboratory Experiment Descriptions Feb. 1992 p 231-240 (For primary document see N92-23600 14-29)

Avail: NTIS HC/MF A13 CSCL 13B

The CRYOSTAT is an autonomously working rack mounted equipment. It provides two thermostat chambers, independently controlled by a processor via on/off switching of the current through peltier elements. The temperature profiles of the freezer and stabilizer are subdivided in a common number of steps, each one with a preprogrammable temperature gradient or at constant temperature. Core parameters can be reprogrammed by crew interaction in case of rescheduling the CRYOSTAT operation time due to changed mission requirements or contingency. Actions of the CRYOSTAT (e.g., opening the slide), the steps, actual temperature of the thermostat chambers, experiment time, and the housekeeping data are recorded on a built-in RAM and a tape. In each thermostat chamber, a specific sample container can be inserted which consists of a transparent Plexiglas block accommodating seven crystallization experiments. Author

N92-23637*# National Aeronautics and Space Administration. Marshall Space Flight Center, Huntsville, AL.

THE CRITICAL POINT FACILITY (CPF)

In its First International Microgravity Laboratory Experiment Descriptions Feb. 1992 p 241-249 (For primary document see N92-23600 14-29)

Avail: NTIS HC/MF A13 CSCL 22A

The Critical Point Facility (CPF) is an ESA multiuser facility designed for microgravity research onboard Spacelab. It has been conceived and built to offer investigators opportunities to conduct research on critical point phenomena in microgravity. This facility provides the high precision and stability temperature standards required in this field of research. It has been primarily designed for the purpose of optical investigations of transparent fluids. During a Spacelab mission, the CPF automatically processes several thermostats sequentially, each thermostat corresponding to an experiment. The CPF is now integrated in Spacelab at Kennedy Space Center, in preparation for the International Microgravity Lab. mission. The CPF was designed to submit transparent fluids to an adequate, user defined thermal scenario, and to monitor their behavior by using thermal and optical means. Because they are strongly affected by gravity, a good understanding of critical phenomena in fluids can only be gained in low gravity conditions. Fluids at the critical point become compressed under their own weight. The role played by gravity in the formation of interfaces between distinct phases is not clearly understood. Author

N92-23638*# Commissariat a l'Energie Atomique, Gif-sur-Yvette (France). Service de Physique de l'Etat Condense.

NEAR-CRITICAL POINT PHENOMENA IN FLUIDS (19-IML-1)

D. Beysens *In* NASA. Marshall Space Flight Center, First International Microgravity Laboratory Experiment Descriptions Feb. 1992 p 251-257 (For primary document see N92-23600 14-29)

Avail: NTIS HC/MF A13 CSCL 22A

Understanding the effects of gravity is essential if the behavior of fluids is to be predicted in spacecraft and orbital stations, and, more generally, to give a better understanding of the hydrodynamics in these systems. An understanding is sought of the behavior of fluids in space. What should emerge from the International Microgravity Lab (IML-1) mission is a better understanding of the kinetics of growth in off-critical conditions, in both liquid mixtures and pure fluids. This complex phenomenon is the object of intensive study in physics and materials sciences area. It is also expected that the IML-1 flight will procure key results to provide a better understanding of how a pure fluid can be homogenized without gravity induced convections, and to what extent the 'Piston Effect' is effective in thermalizing the compressible fluids. Author

N92-23639*# Van der Waals Lab., Amsterdam (Netherlands).

STUDY OF DENSITY DISTRIBUTION IN A NEAR-CRITICAL SIMPLE FLUID (19-IML-1)

Teun Michels *In* NASA. Marshall Space Flight Center, First International Microgravity Laboratory Experiment Descriptions Feb. 1992 p 259-260 (For primary document see N92-23600 14-29)

Avail: NTIS HC/MF A13 CSCL 22A

This experiment uses visual observation, interferometry, and light scattering techniques to observe and analyze the density distribution in SF6 above and below the critical temperature. Below the critical temperature, the fluid system is split up into two coexisting phases, liquid and vapor. The spatial separation of these phases on earth, liquid below and vapor above, is not an intrinsic property of the fluid system; it is merely an effect of the action of the gravity field. At a fixed temperature, the density of each of the coexisting phases is in principle fixed. However, near T sub c where the fluid is strongly compressible, gravity induced hydrostatic forces will result in a gradual decrease in density with increasing height in the sample container. This hydrostatic density profile is

even more pronounced in the one phase fluid at temperatures slightly above T sub c. The experiment is set up to study the intrinsic density distributions and equilibration rates of a critical sample in a small container. Interferometry will be used to determine local density and thickness of surface and interface layers. The light scattering data will reveal the size of the density fluctuations on a microscopic scale. Author

N92-23640*# National Aeronautics and Space Administration. Lewis Research Center, Cleveland, OH.
CRITICAL FLUID THERMAL EQUILIBRATION EXPERIMENT (19-IML-1)
R. Allen Wilkinson *In* NASA. Marshall Space Flight Center, First International Microgravity Laboratory Experiment Descriptions Feb. 1992 p 261-263 (For primary document see N92-23600 14-29)
Avail: NTIS HC/MF A13 CSCL 22A

Gravity sometimes blocks all experimental techniques of making a desired measurement. Any pure fluid possesses a liquid-vapor critical point. It is defined by a temperature, pressure, and density state in thermodynamics. The critical issue that this experiment attempts to understand is the time it takes for a sample to reach temperature and density equilibrium as the critical point is approached; is it infinity due to mass and thermal diffusion, or do pressure waves speed up energy transport while mass is still under diffusion control. The objectives are to observe: (1) large phase domain homogenization without and with stirring; (2) time evolution of heat and mass after temperature step is applied to a one phase equilibrium sample; (3) phase evolution and configuration upon going two phase from a one phase equilibrium state; (4) effects of stirring on a low g two phase configuration; (5) two phase to one phase healing dynamics starting from a two phase low g configuration; and (6) effects of shuttle acceleration events on spatially and temporally varying compressible critical fluid dynamics. Author

N92-23641*# IMAX Space Technology, Inc., Houston, TX.
IMAX CAMERA (12-IML-1) **c35**
In NASA. Marshall Space Flight Center, First International Microgravity Laboratory Experiment Descriptions Feb. 1992 p 265-269 (For primary document see N92-23600 14-29)
Avail: NTIS HC/MF A13 CSCL 14E

The IMAX camera system is used to record on-orbit activities of interest to the public. Because of the extremely high resolution of the IMAX camera, projector, and audio systems, the audience is afforded a motion picture experience unlike any other. IMAX and OMNIMAX motion picture systems were designed to create motion picture images of superior quality and audience impact. The IMAX camera is a 65 mm, single lens, reflex viewing design with a 15 perforation per frame horizontal pull across. The frame size is 2.06 x 2.77 inches. Film travels through the camera at a rate of 336 feet per minute when the camera is running at the standard 24 frames/sec. Author

N92-23642*# National Aeronautics and Space Administration. Lewis Research Center, Cleveland, OH.
MICROGRAVITY ACCELERATION MEASUREMENT AND ENVIRONMENT CHARACTERIZATION SCIENCE (17-IML-1)
In NASA. Marshall Space Flight Center, First International Microgravity Laboratory Experiment Descriptions Feb. 1992 p 271-275 (For primary document see N92-23600 14-29)
Avail: NTIS HC/MF A13 CSCL 22A

The Space Acceleration Measurement System (SAMS) is a general purpose instrumentation system designed to measure the accelerations onboard the Shuttle Orbiter and Shuttle/Spacelab vehicles. These measurements are used to support microgravity experiments and investigation into the microgravity environment of the vehicle. Acceleration measurements can be made at locations remote from the SAMS main instrumentation unit by the use of up to three remote triaxial sensor heads. The prime objective for SAMS on the International Microgravity Lab (IML-1) mission will be to measure the accelerations experienced by the Fluid Experiment System (FES). The SAMS acceleration measurements for FES will be complemented by low level, low frequency acceleration measurements made by the Orbital Acceleration Research Experiment (OARE) installed on the shuttle. Secondary objectives for SAMS will be to measure accelerations at several specific locations to enable the acceleration transfer function of the Spacelab module to be analyzed. This analysis effort will be in conjunction with similar measurements analyses on other Spacelab missions. Author

N92-23719 Alabama Univ., Huntsville.
NUMERICAL SIMULATION OF FLUID BEHAVIORS IN MICROGRAVITY ENVIRONMENT Ph.D. Thesis
Chi-Chong Lee 1991 283 p
Avail: Univ. Microfilms Order No. DA9203823

The dynamical behavior is studied of fluids, especially the effect of surface tension on fluids (cryogenic liquid helium and helium vapor) in a partially filled rotating full scale prototype Gravity Probe-B Spacecraft propellant tank and various 10 pct. subscale containers with identical values of similarity parameters such as Bond number, Dynamical Capillary number, Reynolds number, Weber number, and imposed gravity jitters. Case studies of liquid-vapor interface oscillations excitation were numerically simulated. The interface oscillations are caused by various frequencies of gravity jitters under different rotating speeds of the propellant dewar and different levels of background gravity environment. Fluid stress distribution, caused by the excitation of slosh waves and their associated large amplitude disturbances on the liquid-vapor interface, exerted on the outer and inner walls of the rotating dewar container were studied. Results show that fluid stress distribution exerted on the outer and inner walls of the rotating dewar are closely related to the characteristics of slosh waves excited on the liquid-vapor interface in the rotating dewar. Dissert. Abstr.

31 ENGINEERING (GENERAL)

Includes vacuum technology; control engineering; display engineering; cryogenics; and fire prevention.

N92-23708# Joint Publications Research Service, Arlington, VA.
JPRS REPORT: SCIENCE AND TECHNOLOGY. CENTRAL EURASIA: MATERIALS SCIENCE
26 Mar. 1992 54 p Transl. into ENGLISH from various Russian articles
(JPRS-UMS-92-005) Avail: NTIS HC/MF A04

A bibliography of Central Eurasian research in materials science is given. Topics covered include analysis and testing; coatings; composite materials; ferrous and nonferrous alloys, brazes and solders; industrial processes; preparations and metal treatments; and welding, brazing, and soldering. Author

N92-23709# Joint Publications Research Service, Arlington, VA.
JPRS REPORT: SCIENCE AND TECHNOLOGY. CENTRAL EURASIA: MATERIALS SCIENCE
31 Mar. 1992 28 p Transl. into ENGLISH from various Russian articles
(JPRS-UMS-92-006) Avail: NTIS HC/MF A03

A bibliography is given of Central Eurasian research in materials science. Topics covered include analysis and testing; corrosion resistance; ferrous metals; nonferrous alloys, brazes, and solders; heat treatment; welding, brazing, and soldering; and extractive metallurgy. Author

N92-23899# Oak Ridge Y-12 Plant, TN.
ACOUSTIC EMISSION AS A PROCESS MONITOR FOR DIAMOND MACHINING OF METAL OPTICAL COMPONENTS
J. W. Whittaker and A. C. Miller, Jr. Jul. 1991 6 p Presented at the 4th World Meeting on Acoustic Emission, Boston, MA, 16-19 Sep. 1991
(Contract DE-AC05-84OS-21400)
(DE92-008037; Y/DW-1050; CONF-9109348-2) Avail: NTIS HC/MF A02

The results of a study of acoustic emission (AE) produced by diamond machining of 6061 Al mirrors are presented. Workpiece speed, depth of cut, and feed rate were systematically varied to assess their effects on AE production. AE signatures were very repeatable when cuts were made under identical conditions. Results are discussed in light of potential AE generation mechanisms which included material deformation, inclusion fracture, and friction. Detection of tool/workpiece contact by means of AE monitoring was demonstrated. DOE

N92-23901# Allied-Signal Aerospace Co., Kansas City, MO.
FABRICATION OF A HELICAL COIL SHAPE MEMORY ALLOY ACTUATOR
R. E. ODonnell Feb. 1992 23 p
(Contract DE-AC04-76DP-00613)
(DE92-008399; KCP-613-4616) Avail: NTIS HC/MF A03

A fabrication process was developed to form, heat treat, and join NiTi shape memory alloy helical coils for use as mechanical actuators. Tooling and procedures were developed to wind both extension and compression-type coils on a manual lathe. Heat treating fixtures and techniques were used to set the 'memory' of the NiTi alloy to the desired configuration. A swaging process was devised to fasten shape memory alloy extension coils to end fittings for use in actuator testing and for potential attachment to mechanical devices. The strength of this mechanical joint was evaluated. DOE

N92-23989*# National Aeronautics and Space Administration. Langley Research Center, Hampton, VA.
DESIGN CONSIDERATIONS FOR AN AIR CORE MAGNETIC ACTUATOR
Nelson J. Groom Feb. 1992 14 p
(NASA-TM-104229; NAS 1.15:104229) Avail: NTIS HC/MF A03 CSCL 13I

Equations for the force produced by an air core electromagnet on a permanent magnet core as a function of the coil height, coil inner and outer radii, and core displacement are developed. The magnetization vector of the permanent magnet core is assumed to be aligned with the central axis of the electromagnet and the forces which are produced lie along the same axis. Variations in force due to changes in electromagnet parameters and core displacement are investigated and parameter plots which should be useful for coil design are presented. Author

N92-23636*# Deutsche Agentur fuer Raumfahrtangelegenheiten G.m.b.H., Bonn (Germany, F.R.).
CRYOSTAT (18-IML-1)
In NASA. Marshall Space Flight Center, First International Microgravity Laboratory Experiment Descriptions Feb. 1992 p 231-240 (For primary document see N92-23600 14-29)
Avail: NTIS HC/MF A13 CSCL 13B

N92-23966*# Virginia Polytechnic Inst. and State Univ., Blacksburg. Industrial Engineering.
APPLICATIONS OF INDUSTRIAL ENGINEERING Ph.D. Thesis
Walthea V. Yarbrough *In* NASA. Goddard Space Flight Center, Summer Graduate Research Program for Interns in Science and Engineering 24 Mar. 1992 11 p (For primary document see N92-23958 14-99)
Avail: NTIS HC/MF A12 CSCL 13H

32 COMMUNICATIONS AND RADAR

Includes radar; land and global communications; communications theory; and optical communications.

For related information see also *04 Aircraft Communications and Navigation* and *17 Space Communications, Spacecraft Communications, Command and Tracking.* For search and rescue see *03 Air Transportation and Safety,* and *16 Space Transportation.*

N92-23138# Helsinki Univ. of Technology, Espoo (Finland). Electromagnetics Lab.
ELECTROSTATIC IMAGE SOLUTION FOR THE INTERACTION OF TWO DIELECTRIC SPHERES
I. V. Lindell, J. C. E. Sten, and K. I. Nikoskinen Aug. 1991 20 p
(PB92-142199; ISBN-951-22-0756-7; Rept-99) Avail: NTIS HC/MF A03 CSCL 20N

Static image theory for a homogeneous dielectric sphere was recently formulated by one of the authors to account for the reaction of the sphere to the field from any electrostatic charge distribution. The theory is applied here in the analysis of the interaction of two dielectric spheres to find their reaction to external sources. Integral equations for the line image charges are formulated in the general case and a method for their solution is given for the limit case of two conducting spheres. A simple approximative dipole solution for the case of weak interaction between the spheres is also discussed. The theory has potential application in analyzing interactions of closely packed spherical particles suspended in a host medium, in terms of one dimensional integral equations. GRA

N92-23173# National Inst. of Standards and Technology, Boulder, CO. Electromagnetic Fields Div.
AUTOMATIC WAVEFORM ANALYSIS AND MEASUREMENT SYSTEM USER MANUAL
S. M. Chesnut and N. G. Paulter Dec. 1991 323 p Sponsored in part by Army Redstone Arsenal, AL
(PB92-132976; NISTIR-3978) Avail: NTIS HC/MF A14 CSCL 20N

The theory and operation of an upgraded version of the National Institute of Standards and Technology (NIST) Automatic Waveform Analysis and Measurement System (AWAMS) is described. This system, the AWAMS, was commissioned by the Army Primary Standards Laboratory to facilitate measurement comparability with NIST. The AWAMS was installed at the Redstone Arsenal, Alabama. GRA

N92-23180# National Telecommunications and Information Administration, Boulder, CO. Inst. for Telecommunication Sciences.
TABULATIONS OF PROPAGATION DATA OVER IRREGULAR TERRAIN IN THE 75- TO 8400-MHz FREQUENCY RANGE. PART 5: VIRGINIA
G. A. Hufford and F. K. Steele Dec. 1991 306 p
(PB92-137413; NTIA-91-282) Avail: NTIS HC/MF A14 CSCL 20N

This is a supplementary fifth part to a series of reports containing tabulations and graphs of transmission loss data resulting from propagation experiments which have emphasized the UHF band. The first four reports described data taken in various regions of Colorado. Measurements taken at about the same time in the Piedmont region of Virginia and North Carolina are presented. Data are presented for 283 paths varying in length from 0.5 to 120 km. GRA

N92-23245*# Virginia Polytechnic Inst. and State Univ., Blacksburg. Antenna Lab.
FEASIBILITY STUDY OF A SYNTHESIS PROCEDURE FOR ARRAY FEEDS TO IMPROVE RADIATION PERFORMANCE OF LARGE DISTORTED REFLECTOR ANTENNAS Semiannual Status Report
W. L. Stutzman, K. Takamizawa, P. Werntz, J. Lapean, R. Barts, B. Shen, and D. Dunn 10 Apr. 1992 68 p

(Grant NAG1-859)
(NASA-CR-190191; NAS 1.26:190191; SATCOM-92-2) Avail: NTIS HC/MF A04 CSCL 20N

The topics covered include the following: (1) performance analysis of the Gregorian tri-reflector; (2) design and performance of the type 6 reflector antenna; (3) a new spherical main reflector system design; (4) optimization of reflector configurations using physical optics; (5) radiometric array design; and (7) beam efficiency studies. Author

N92-23412*# National Aeronautics and Space Administration. Lewis Research Center, Cleveland, OH.
SOLID STATE TECHNOLOGY BRANCH OF NASA LEWIS RESEARCH CENTER Third Annual Digest, Jun. 1990 - Jun. 1991
1991 153 p
(NASA-TM-105159; E-6447; NAS 1.15:105159) Avail: NTIS HC/MF A08 CSCL 20L

Reprints of one year's production of research publications (June 1990 to June 1991) are presented. These are organized into three major sections: microwave circuits, both hybrid and monolithic microwave integrated circuits (MMICs); materials and device work; and superconductivity. The included papers also cover more specific topics involving waveguides, phase array antennas, dielectrics, and high temperature superconductors. For individual titles, see N92-23413 through N92-23415.

N92-23413*# National Aeronautics and Space Administration. Lewis Research Center, Cleveland, OH.
MICROWAVE RESPONSE OF HIGH TRANSITION TEMPERATURE SUPERCONDUCTING THIN FILMS Abstract Only **c76**
Felix Antonio Miranda *In its* Solid State Technology Branch of NASA Lewis Research Center 1991 p 121-122 (For primary document see N92-23412 14-32)
Avail: NTIS HC/MF A08 CSCL 20L

We have studied the microwave response of YBa2Cu3O(7 - delta), Bi-Sr-Ca-Cu-O, and Tl-Ba-Ca-Cu-O high transition temperature superconducting (HTS) thin films by performing power transmission measurements. These measurements were carried out in the temperature range of 300 K to 20 K and at frequencies within the range of 30 to 40 GHz. Through these measurements we have determined the magnetic penetration depth (lambda), the complex conductivity (sigma(sup *) = sigma(sub 1) - j sigma(sub 2)) and the surface resistance (R(sub s)). An estimate of the intrinsic penetration depth (lambda approx. 121 nm) for the YBa2Cu3O(7 - delta) HTS has been obtained from the film thickness dependence of lambda. This value compares favorably with the best values reported so far (approx. 140 nm) in single crystals and high quality c-axis oriented thin films. Furthermore, it was observed that our technique is sensitive to the intrinsic anisotropy of lambda in this superconductor. Values of lambda are also reported for Bi-based and Tl-based thin films. We observed that for the three types of superconductors, both sigma(sub 1) and sigma(sub 2) increased when cooling the films below their transition temperature. The measured R(sub s) are in good agreement with other R(sub S) values obtained using resonant activity techniques if we assume a quadratic frequency dependence. Our analysis shows that, of the three types of HTS films studied, the YBa2Cu3O(7 - delta) thin film, deposited by laser ablation and off-axis magnetron sputtering are the most promising for microwave applications. Author

N92-23414*# National Aeronautics and Space Administration. Lewis Research Center, Cleveland, OH.
PROPERTIES OF LARGE AREA ErBa2Cu3O(7-x) THIN FILMS DEPOSITED BY IONIZED CLUSTER BEAMS **c76**
L. L. Levenson (Colorado Univ., Colorado Springs.), Mark A. Stan, and Kul B. Bhasin *In its* Solid State Technology Branch of NASA Lewis Research Center 1991 p 127-130 Repr. from Journal of Vacuum Society Science Technology (American Vacuum Society), v. 9, no. 3, May/Jun. 1991 Revised (For primary document see N92-23412 14-32)
Avail: NTIS HC/MF A08 CSCL 20L

ErBa2Cu3O(7-x) films have been produced by simultaneous deposition of Er, Ba, and Cu from three ionized cluster beam (ICB) sources at acceleration voltages of 0.3 to 0.5 kV. Combining ozone oxidation with ICB deposition at 650 C eliminated any need of post annealing processing. The substrates were rotated at 10 rotations per minute during the deposition which took place at a rate of about 3 to 4 nm. Films with areas up to 70 mm in diameter have been made by ICB deposition. These films, 100 nm thick, were deposited on SrTiO3 (100) substrates at 650 C in a mixture of six percent O3 in O2 at a total pressure of 4 x 10(exp -4) Torr. They had T(sub c) ranging from 84.3 K to 86.8 K over a 70 mm diameter and J(sub c) above 10(exp 6) A/sq cm at 77 K. X ray diffraction measurements of the three samples showed preferential c-axis orientation normal to the substrate surface. Scanning electron micrographs (SEM) of the three samples also show some texture dependence on sample position. For the three samples, there is a correlation between SEM texture, full width at half-maximum of rocking curves and J(sub c) versus temperature curves. Author

N92-23415*# National Aeronautics and Space Administration. Lewis Research Center, Cleveland, OH.
DEPENDENCE OF THE CRITICAL TEMPERATURE OF LASER-ABLATED YBa2Cu3O(7-DELTA) THIN FILMS ON LaAlO3 SUBSTRATE GROWTH TECHNIQUE **c76**
Joseph D. Warner, Kul B. Bhasin, and Felix A. Miranda (Case Western Reserve Univ., Cleveland, OH.) *In its* Solid State Technology Branch of NASA Lewis Research Center 1991 p 135-137 Repr. from Supercond. Sci. Technol. (England), v. 3, 1990 p 437-439 (For primary document see N92-23412 14-32)
Avail: NTIS HC/MF A08 CSCL 20L

Samples of LaAlO3 made by flame fusion and Czochralski method were subjected to the same temperature conditions that they have to undergo during the laser ablation deposition of YBa2Cu3O(7 - delta) thin films. After oxygen annealing at 750 C, the LaAlO3 substrate made by two methods experienced surface roughening. The degree of roughening on the substrate made by Czochralski method was three times greater than that on the substrate made by flame fusion. This excessive surface roughening may be the origin of the experimentally observed lowering of the critical temperature of a film deposited by laser ablation on a LaAlO3 substrate made by Czochralski method with respect to its counterpart deposited on LaAlO3 substrates made by flame fusion. Author

N92-23425*# Pennsylvania State Univ., University Park. Dept. of Electrical and Computer Engineering.
USER'S MANUAL FOR THREE DIMENSIONAL FDTD VERSION C CODE FOR SCATTERING FROM FREQUENCY-INDEPENDENT DIELECTRIC AND MAGNETIC MATERIALS
John H. Beggs, Raymond J. Luebbers, and Karl S. Kunz Jan. 1992 26 p
(Grant NAG1-1221)
(NASA-CR-190109; NAS 1.26:190109) Avail: NTIS HC/MF A03 CSCL 20N

The Penn State Finite Difference Time Domain Electromagnetic Scattering Code Version C is a three-dimensional numerical electromagnetic scattering code based on the Finite Difference Time Domain (FDTD) technique. The supplied version of the code is one version of our current three-dimensional FDTD code set. The manual given here provides a description of the code and corresponding results for several scattering problems. The manual is organized into 14 sections: introduction, description of the FDTD method, operation, resource requirements, Version C code capabilities, a brief description of the default scattering geometry, a brief description of each subroutine, a description of the include file (COMMONC.FOR), a section briefly discussing radar cross section computations, a section discussing some scattering results, a new problem checklist, references, and figure titles. Author

N92-23528*# Pennsylvania State Univ., University Park. Dept. of Electrical and Computer Engineering.
WIDEBAND FINITE DIFFERENCE TIME DOMAIN IMPLEMENTATION OF SURFACE IMPEDANCE BOUNDARY CONDITIONS FOR GOOD CONDUCTORS
John H. Beggs, Raymond J. Luebbers, Karl S. Kunz, and Kane S. Yee (Lockheed Missiles and Space Co., Sunnyvale, CA.) 1991 4 p
(Grant NAG1-1221)
(NASA-CR-190098; NAS 1.26:190098) Avail: NTIS HC/MF A01 CSCL 20N

Surface impedance boundary conditions are used to reduce the solution volume during the analysis of scattering from lossy dielectric objects. In a finite difference solution, they also can be used to avoid using small cells, made necessary by shorter wavelengths in conducting media, throughout the solution volume. A one dimensional implementation is presented for a surface impedance boundary condition for good conductors in the Finite Difference Time Domain (FDTD) technique. In order to illustrate the FDTD surface impedance boundary condition, a planar air-lossy dielectric interface is considered. Author

N92-23575# Sandia National Labs., Albuquerque, NM.
SOVIET ARTICLES ON ANTENNA THEORY
K. C. Chen, ed. Jan. 1992 65 p
(Contract DE-AC04-76DP-00789)
(DE92-008452; SAND-91-0720) Avail: NTIS HC/MF A04

Translations of two pioneering Russian papers on antenna theory are presented. The first paper provides a treatise on finite-length dipole antennas; the second paper addresses infinite-length, impedance-loaded transmitting antennas. DOE

N92-23580# International Centre for Theoretical Physics, Trieste (Italy).
MUTUAL SCATTERING OF CARRIERS IN TWO QUANTUM WIRES
Y. M. Sirenko Sep. 1991 17 p
(DE92-616890; IC-91/294) Avail: NTIS HC/MF A03

We have investigated the momentum and energy exchange between two separated quantum wires due to Coulomb mutual scattering. Relevant relaxation frequencies were calculated for all possible combinations of statistics of the gases; dependence of the relaxation frequencies on concentrations, temperature and distance between the gases was analyzed. DOE

N92-23590# Helsinki Univ. of Technology, Espoo (Finland). Electromagnetics Lab.
BIISOTROPIC POLARIZER SHIELD
S. A. Tretyakov and M. I. Oksanen Sep. 1991 16 p
(PB92-141878; ISBN-951-22-0792-3; Rept-102) Avail: NTIS HC/MF A03 CSCL 20N

Reflection and transmission properties of a general biisotropic layer are explored for plane wave excitation at normal incidence. Using the vector circuit theory developed recently for biisotropic layers, explicit formulas for reflection coefficients are given. This enables an analytical study of wave attenuation and polarization rotation of the reflected and transmitted field. Promising application properties of general biisotropic layers are revealed and exemplified by numerical calculations. Author

N92-23591# Helsinki Univ. of Technology, Espoo (Finland). Electromagnetics Lab.
CLOSED PARALLEL-PLATE CHIRAL WAVEGUIDES WITH BOUNDARY IMPEDANCE CONDITIONS
M. I. Oksanen, P. K. Koivisto, and S. A. Tretyakov Feb. 1991 28 p
(PB92-142397; ISBN-951-22-0550-5; Rept-85) Avail: NTIS HC/MF A03 CSCL 20N

Electromagnetic wave propagation is discussed in chiral slab waveguides that are characterized by surface impedances of different types. The method applied makes use of the vector circuit theory and the related tangential field requirements on the slab surfaces. The method forms a coherent and solid approach to waveguide analysis since all cases considered can be solved from the same general eigenvalue equation. There are two parts: the brief derivation of the general equation; and its application to different chiral waveguides. The calculated curves support the theoretical analysis. Author

N92-23661# Helsinki Univ. of Technology, Espoo (Finland). Electromagnetics Lab.
PROPERTIES OF BI-ISOTROPIC FRESNEL REFLECTION COEFFICIENTS
A. H. Sihvola and I. V. Lindell Sep. 1991 10 p
(PB92-141886; ISBN-951-22-0802-4; Rept-103) Avail: NTIS HC/MF A02 CSCL 20N

The Fresnel reflection coefficients R sub 1, R sub 2 for the planar interface between isotropic and generally biisotropic half spaces are studied. The functions (R sub 1 + R sub 2)/(1 + R sub 1(R sub 2)) and (R sub 1 - R sub 2)/(1 - R sub 1(R sub 2)) are seen to be simple functions of the optical material parameters of the media, as has been the case in the corresponding isotropic problem. Also pathological conditions, derived earlier elsewhere for reflection coefficients involving isotropic media, are generalized for the biisotropic (nonreciprocal chiral) case. Furthermore, the special cases of reflection from Pasteur or Tellegen media result from the analysis. Author

N92-23666# Helsinki Univ. of Technology, Espoo (Finland). Electromagnetics Lab.
QUASI-STATIC IMAGE THEORY FOR THE BI-ISOTROPIC (NONRECIPROCAL CHIRAL) SPHERE
I. V. Lindell Dec. 1990 20 p
(PB92-142371; ISBN-951-22-0486-X; Rept-81) Avail: NTIS HC/MF A03 CSCL 20N

Image theory for the static point charge and the conducting sphere, produced by Kelvin's inversion theory, was recently extended to the dielectric sphere by the present author. The objective of the present paper is to further extend the image theory to the bi-isotropic sphere, including the chiral sphere as a special case. Image expressions for the bi-isotropic sphere can be derived in a manner similar to that of the dielectric sphere except that the quasi-static problem now involves both electric and magnetic scalar potentials, coupled through the interface conditions at the spherical surface. The image is a combination of electric and magnetic line charges along the axis connecting the point charge and the center of the sphere, and their expressions are obtained through what can be labeled as finite Mellin transformation. The expressions derived can find application in more complete quasi-static analyses of interaction of dielectric spherical particles in artificial dielectric media. GRA

N92-23667# Helsinki Univ. of Technology, Espoo (Finland). Electromagnetics Lab.
ELECTROSTATIC IMAGE THEORY FOR THE DIELECTRIC SPHERE WITH AN INTERNAL SOURCE
J. C. E. Sten and I. V. Lindell Mar. 1991 20 p
(PB92-142405; ISBN-951-22-0573-4; Rept-88) Avail: NTIS HC/MF A03 CSCL 20N

The well known electrostatic image theory for a point charge next to a conducting sphere, originally discovered by Lord Kelvin, was recently generalized to the dielectric sphere, by one of the present authors, for sources located outside the sphere. The present paper treats the problem of a source located inside the dielectric sphere, thus completing the theory. Image expressions corresponding to potentials both inside and outside the spheres are worked out and their validity is checked with numerous tests. The image expression consists of simple functions easily handled with a pocket calculator. The theory can be straightforwardly transformed to cover direct current problems involving a current source inside a sphere located in a surrounding medium with different conductivity, which can be of interest, for example, to problems of electrocardiography. GRA

N92-23668# Helsinki Univ. of Technology, Espoo (Finland). Electromagnetics Lab.
ELECTROSTATIC IMAGE THEORY FOR THE LAYERED DIELECTRIC SPHERE
I. V. Lindell, M. E. Ermutlu, and A. H. Sihvola Apr. 1991 38 p
(PB92-142413; ISBN-951-22-0610-2; Rept-91) Avail: NTIS HC/MF A03 CSCL 20N

Static image theory for a homogeneous dielectric sphere, recently formulated by one of the present authors is generalized to the problem of a multilayer dielectric sphere in terms of a line image charge. The image line source is seen in this case to be in a relation to the so called static reflection coefficient in what could be labeled as a finite Mellin transformation. The transformation is discussed and a table of corresponding transforming functions is given. The result can be applied in a more complete quasi-static analysis of interactions of layered dielectric spherical particles in artificial dielectric media. More closely, a two layer sphere is considered with special cases of a thin layer, and that of a low contrast between the layers. Finally, numerical results are calculated for the radiowave propagation problem of attenuation due to melting hail particles, assumed to be composed of a spherical ice core with a spherical water shell.
GRA

N92-23676# Technical Univ. of Lisbon (Portugal). Inst. Superior Tecnico.
VARIABLE BIT RATE VIDEO CODING Ph.D. Thesis
F. M. B. Pereira May 1991 420 p
(PB92-134279) Avail: NTIS HC/MF A18 CSCL 17B

The increasing demand for video services, from video telephony and videoconferencing to the more complex high definition TV, are pushing for a new network able to satisfy broadband services demand: the Broadband Integrated Services Digital Network (BISDN) directed to the support of a wide range of services in the same universal network. The network uses the Asynchronous Transfer Mode based in the concept of packet transmission which enables Variable Bit Rate information flows. The application of the variable bit rate capability to video coding, until now constrained to Synchronous Transfer Mode, opened new horizons to video communications. The new capabilities and opportunities offered to video coding by variable bit rate coding is examined. The work is to be integrated in the more general effort of defining the future BISDN services, a fundamental step to its success. Author

N92-23679# Helsinki Univ. of Technology, Espoo (Finland). Electromagnetics Lab.
VECTOR CIRCUIT METHOD APPLIED FOR CHIRAL DIELECTRIC SLAB WAVEGUIDES
M. I. Oksanen, P. K. Koivisto, and S. A. Tretyakov Dec. 1990 26 p
(PB92-142355; ISBN-951-22-0476-2; Rept-79) Avail: NTIS HC/MF A03 CSCL 20N

The analysis makes use of vector circuit modeling of a chiral slab, the method which has been previously applied for calculating reflection and transmission of electromagnetic waves in chiral multilayer structures. After deriving the general eigenvalue equation for the guide and valid for arbitrary boundary impedance conditions on the slab interface, three special cases were analyzed in detail; an open chiral dielectric slab with dielectric half spaces at opposite sides of the slab, a chiral dielectric slab on an ideally conducting surface, and a chiral dielectric slab on an ideal magnetic surface. The theory is supported by calculated dispersion curves indicating the chirality effect on the wave propagation characteristics.
Author

N92-23900# Oak Ridge National Lab., TN.
MODULAR ELECTROMAGNETIC LEVITATOR
C. A. Hahs and R. J. Fox 1992 5 p Presented at the Minerals, Metals, and Materials Society (TMS) Annual Meeting and Exhibition, San Diego, CA, 1-5 Mar. 1992
(Contract DE-AC05-84OR-21400)
(DE92-008278; CONF-920305-6) Avail: NTIS HC/MF A01

A conceptual design of a modular electromagnetic levitator (MEL) is being prepared at Oak Ridge National Laboratory (ORNL) for the National Aeronautics and Space Administration, Marshall Space Flight Center, Alabama. The high-efficiency radio-frequency system developed at ORNL will allow samples of high-temperature metals such as niobium to be levitated and melted in space. The MEL will accommodate multiple samples that can be processed in a vacuum of 10(exp minus 9) torr or in a cover gas. This system is being designed to operate from the power bus of the space shuttle. Flights are being made on the KC-135 at Johnson Space Center to evaluate hardware fabricated for operation in low- and high-gravity environments. DOE

N92-23907# Helsinki Univ. of Technology, Espoo (Finland). Electromagnetics Lab.
APPLICATION OF THE GREEN FUNCTION TECHNIQUE IN THE MICROSTRIP PATCH ANTENNA ANALYSIS
A. Lihtola, K. I. Nikoskinen, and I. V. Lindell Apr. 1991 18 p
Sponsored by Suomen Akatemja, Helsinki
(PB92-142173; ISBN-951-22-0600-5; Rept-90) Avail: NTIS HC/MF A03 CSCL 20N

Microstrip structures are now widely used in microwave systems because of their geometrical simplicity, small size, and ease of fabrication. The microstrip structure is inhomogeneous along several directions, which makes the accurate analysis of the electromagnetic fields very difficult. Hence, the design of microstrip devices is mostly done with approximative and empirical methods of limited accuracy. Green's function is used to analyze rectangular microstrip patches. Scalar Green functions corresponding to the microstrip geometry were derived earlier. With the aid of these functions, surface currents and resonance frequencies of a patch located in the air/dielectric interface can be computed using the method of moments (MOM). To make the implementation of MOM as simple as possible, numerical approximations for scalar Green's functions are developed. These approximations are functions of permittivity, the frequency, and the thickness of the substrate. Examples of computed results for resonance frequencies of a microstrip patch are given.
GRA

N92-24019 University Coll. of North Wales, Bangor.
MUTUAL INTERFERENCE IN MULTICHANNEL FIBRE COMMUNICATION SYSTEMS Ph.D. Thesis
Abdullah Abdulaziz AL-Orainy 1990 185 p
Avail: Univ. Microfilms Order No. BRDX92964

Performance evaluation of multichannel optical fiber communication systems is examined. It is based on comprehensive models of various crosstalk mechanisms encountered in such systems. Special attention was paid to assessment of multichannel direct detection systems since these systems are relatively simple to realize and therefore could satisfy the demand for increased communication capacity at relatively low cost. A tight upper bound on the error probability, the modified Chernoff bound, is used for performance assessment. Its formulation incorporates linear crosstalk impairments in multichannel direct detection systems. Tractable distribution free bounds on the performance are derived for various crosstalk mechanisms where exact evaluations are most difficult. Interchannel crosstalk and transmitted optical power limitations due to fiber nonlinearities in optical networks are studied. The receiver sensitivity degradation due to Raman scattering is obtained. Using performance evaluation and design methods developed, a range of computer programs were produced. Taken together, these represent a substantial software resource for performance assessment of multichannel systems.
Dissert. Abstr.

N92-23611*# Deutsche Forschungsanstalt fuer Luft- und Raumfahrt, Cologne (Germany, F.R.). Inst. for Aerospace Medicine.
DOSIMETRIC MAPPING INSIDE BIORACK (7-IML-1)
G. Reitz *In* NASA. Marshall Space Flight Center, First International Microgravity Laboratory Experiment Descriptions Feb. 1992 p 65 (For primary document see N92-23600 14-29)
Avail: NTIS HC/MF A13 CSCL 20N

N92-23963*# Puerto Rico Univ., Mayaguez.
MODIFICATIONS FOR A COMMUNICATION INTERFACE BOARD
Carlos E. DeJesusLafuente *In* NASA. Goddard Space Flight Center, Summer Graduate Research Program for Interns in Science and Engineering 24 Mar. 1992 39 p (For primary document see N92-23958 14-99)
Avail: NTIS HC/MF A12 CSCL 17B

33 ELECTRONICS AND ELECTRICAL ENGINEERING

Includes test equipment and maintainability; components, e.g., tunnel diodes and transistors; microminiaturization; and integrated circuitry.

For related information see also *60 Computer Operations and Hardware* and *76 Solid-State Physics.*

N92-23140# Michigan Univ., Ann Arbor. Transportation Research Inst.
EVALUATION OF A MECHANICAL BEAM-SWITCHING SYSTEM
P. L. Olson, T. Sato, E. C. Traube, and D. S. Battle Dec. 1991 14 p Sponsored by Stanley Electric Co., Ltd., Tokyo, Japan
(PB92-139773; UMTRI-91-45) Avail: NTIS HC/MF A03 CSCL 09C

An evaluation was conducted of a mechanical beam switching system that may be appropriate for use with high-intensity discharge (HID) lamps. Subjects rated the adequacy of the beam change time at several rates, compared with an electrical beam changing system. The results indicate that subjects rated the mechanical and electrical systems the same, at the shortest change time for the former. Longer change times elicited poorer ratings for the mechanical system. The change from low to high beam was rated better than the change from high to low beam in the mechanical system. This difference was statistically significant at the two slower rates investigated. GRA

N92-23172# Helsinki Univ. of Technology, Espoo (Finland). Radio Lab.
DESIGN AND PERFORMANCE OF 22 GHz COAXIAL LOW NOISE MESFET AND HEMT AMPLIFIERS
J. K. Peltonen Jun. 1990 50 p
(PB92-134071; ISBN-951-22-0334-0; S-186) Avail: NTIS HC/MF A03 CSCL 09C

The report describes the design and construction of low noise, cryogenic 22 GHz metal semiconductor field effect transistor (MESFET) and high electron mobility transistor (HEMT) amplifiers in a coaxial structure. Using packaged, commercially available transistors, experimental one-stage amplifiers were developed. For the amplifier using a HEMT device a gain of 7.4 dB and a noise temperature of 255 K and for the MESFET amplifier 6.4 dB and 315 K were measured at room temperature. A two-stage HEMT amplifier exhibited noise temperature of 300 +/- 20 K and an associated gain of 13.5 dB. GRA

N92-23186# Maryland Univ., College Park.
SCALING STUDY OF PSEUDOSPARK PRODUCED ELECTRON BEAM
K. K. Jain, B. N. Ding, and M. J. Rhee 1991 3 p Presented at the IEEE Particle Accelerator Conference, San Francisco, CA, 6-11 May 1991
(Contract DE-FG05-91ER-40642)
(DE92-003231; CONF-910505-439) Avail: NTIS HC/MF A01

The characteristics of the breakdown voltage of a pseudospark device, the current, and the rms emittance of the electron beam produced in the device are determined. It is found that the breakdown voltage is a function of the product of the gas pressure squared and the anode-cathode gap distance; the electron beam current increases with the breakdown voltage up to 35 kV and then decreases; the rms emittance appears to be nearly constant up to breakdown voltage of 25 kV and then increases. DOE

N92-23193*# National Aeronautics and Space Administration. Lewis Research Center, Cleveland, OH.
A FLEXIBLE CPW PACKAGE FOR A 30 GHz MMIC AMPLIFIER
Rainee N. Simons (Sverdrup Technology, Inc., Brook Park, OH.) and Susan R. Taub 1992 6 p Presented at the Topical Meeting on Electrical Performance of Electronic Packaging, Tucson, AZ, 22-24 Apr. 1992; sponsored by IEEE, MTT, and CHMT
(Contract NAS3-25266)
(NASA-TM-105630; E-6973; NAS 1.15:105630) Avail: NTIS HC/MF A02 CSCL 09A

A novel package, which consists of a carrier housing, has been developed for monolithic-millimeter wave Integrated Circuit amplifiers which operate at 30 giga-Hz. The carrier has coplanar waveguide (CPW) interconnects and provides heat-sinking, tuning, and cascading capabilities. The housing provides electrical isolation, mechanical protection and a feed-thru for biasing. Author

N92-23200# Los Alamos National Lab., NM.
ACTIVELY-STABILIZED PHOTOMULTIPLIER TUBE BASE FOR VACUUM OPERATION
M. A Bryan, C. L. Morris, and G. C. Idzorek Jan. 1992 8 p
(Contract W-7405-eng-36)
(DE92-007528; LA-11623-MS) Avail: NTIS HC/MF A02

An actively stabilized photomultiplier tube (PMT) base design for an Amperex XP-2262B PMT is described. Positive-negative-positive transistors are used as low-impedance current sources to maintain constant voltages on the last three dynodes. This technique results in a highly stable, low-power tube base ideal for use with low-duty-factor beams. Furthermore, because of the low power usage of this large design, these bases can be sealed in a heat-conductive, electrically insulating material and used in a vacuum. DOE

N92-23246# National Aeronautical Lab., Bangalore (India).
AN ALGORITHMIC APPROACH FOR FAULT-MONITORING OF ELECTRICAL ACTUATION SYSTEM FOR ALL ELECTRIC AIRCRAFT
T. V. Rama Murthy, A. Krishnan, and S. Ajay Oct. 1991 20 p
(NAL-PD-AL-9111) Avail: NTIS HC/MF A03

A current trend in fault detection and identification (FDI) is to use a combination of algorithmic procedural methods and artificial intelligence (AI) techniques. A method for monitoring faulty sensors in aircraft electrical actuators is presented. This method is based on static model based fault detection (MBFD) and parameter estimation based on on-line recursive least squares (RLS). Investigations were made of MBFD where measured variables were checked for consistency with those of the model. In the case study, owing to the wide variation of the poles of the overall transfer function, a reduced order model was chosen to model the process. Fault detection is also achieved by estimating the reduced order model parameters in the closed loop by RLS. It is found that RLS is reliable only on the addition of a PRBS dither signal to the input excitation. The combination of the two methods improves the fault detection probability while simultaneously reducing the false alarm probability. This yields a higher confidence level in the fault monitoring, especially in the context of the response of a reduced order model. Author

N92-23326# Fermi National Accelerator Lab., Batavia, IL.
A NEW VME BASED HIGH VOLTAGE POWER SUPPLY FOR LARGE EXPERIMENTS
S. C. Ahn, R. D. Angstadt, T. F. Droege, M. E. Johnson, B. A. MacKinnon, S. E. McNulty, M. F. Shea, R. N. Thompson, M. M. Watson, and P. Franzini Nov. 1991 8 p Presented at the IEEE Nuclear Science Symposium, Santa Fe, NM, 5-9 Nov. 1991
(Contract DE-AC02-76CH-03000)
(DE92-007199; FNAL/C-91/310; CONF-911106-73) Avail: NTIS HC/MF A02

A new VME based high voltage power supply has been developed for the D(O) experiment at Fermilab. There are three types of supplies delivering up to (plus minus)5.6 kV at 1.0 mA or

+2.0 kV at 3.0 mA with a set accuracy of 1.5 V and extremely low voltage ripples. Complete computer control has allowed many special features to be developed for the supply, including user-defined control land monitor groups, variable ramp rates, and advanced histogram and graphic functions. DOE

N92-23430*# Christopher Newport Coll., Newport News, VA.
CHARACTERIZING AND TESTING A THERMALLY ISOLATING SUPERCONDUCTING LINK FOR SAFIRE-LIKE MISSIONS Final Technical Report, Mar. 1991 - Mar. 1992
Raouf L. Selim and Randall Caton Mar. 1992 22 p
(Grant NAG1-1242)
(NASA-CR-190196; NAS 1.26:190196) Avail: NTIS HC/MF A03 CSCL 09C

The recent discovery of high temperature ceramic superconductors with transition temperatures above 90 K has opened the possibilities for new space applications. One application is the fabrication of an electrically conducting and thermally isolating electronic link to connect IR detectors to data acquisition electronics on remote sensing platforms. The Spectroscopy of the Atmosphere using Far Infra-Red Emission (SAFIRE) mission is an example of a platform which employs hybrid dewars and combines both mechanical and cryogenic liquid cooling. This new technology is limited by the heat conducted through sensor array leads that connect the electronics (at approximately 80 K) to the sensors (at approximately 4 K). This link must be made of material that has high electrical conductivity and high thermal resistance. The YBa2Cu3O(x) superconductor with a transition temperature, T(sub c), of 93 K can achieve these conflicting requirements. A link with these characteristics will improve the thermal isolation of IR detectors and will increase the lifetime of the cryogen. A reduction of the thermal load due to the link by a factor of four will increase the lifetime of a seven year mission by about one year. Author

N92-23437*# National Aeronautics and Space Administration. Marshall Space Flight Center, Huntsville, AL.
TESTING AND ANALYSES OF ELECTROCHEMICAL CELLS USING FREQUENCY RESPONSE Final Report, 1 Feb. - 31 Dec. 1991
O. A. Norton, Jr. and D. L. Thomas (Alabama Univ., Huntsville.) Mar. 1992 23 p
(Contract NAS8-36955; Proj. 90-18)
(NASA-TM-103580; NAS 1.15:103580) Avail: NTIS HC/MF A03 CSCL 09C

The feasibility of electrochemical impedance spectroscopy as a method for analyzing battery state of health and state of charge was investigated. Porous silver, zinc, nickel, and cadmium electrodes as well as silver/zinc cells were studied. State of charge could be correlated with impedance data for all but the nickel electrodes. State of health was correlated with impedance data for two silver/zinc cells, one apparently good and the other dead. The experimental data were fit to equivalent circuit models. Author

N92-23462*# National Aeronautics and Space Administration. Goddard Space Flight Center, Greenbelt, MD.
COAXIAL TURNSTILE JUNCTION Patent Application
Robert K. Zimmerman, Jr., inventor (to NASA) 7 Oct. 1991 20 p
(NASA-Case-GSC-13422-1; NAS 1.71:GSC-13422-1; US-Patent-Appl-SN-772741) Avail: NTIS HC/MF A03 CSCL 09C

A microwave turnstile junction is shown consisting of a circular waveguide at the center, four coplanar microwave probes extending into the circular waveguide at one end, and each probe having a coaxial connector affixed at one end and mounted upon the circular waveguide. The circular waveguide has a pair of coaxial sliding plungers mounted at one end. The plungers are capable of extending into the circular waveguide so as to interact with the probes. The novelty is believed to reside in using coaxial cables with coaxial-to-waveguide probes as a replacement for the square waveguide of the prior art turnstiles. NASA

N92-23464*# National Aeronautics and Space Administration. Pasadena Office, CA.
PLANAR VARACTOR FREQUENCY MULTIPLIER DEVICES WITH BLOCKING BARRIER Patent Application
Udo Lieneweg, inventor (to NASA), Margaret A. Frerking, inventor (to NASA), and Joseph Maserian, inventor (to NASA) (Jet Propulsion Lab., California Inst. of Tech., Pasadena.) 26 Feb. 1992 31 p
(Contract NAS7-918)
(NASA-Case-NPO-18428-1-CU; NAS 1.71:NPO-18428-1-CU; US-Patent-Appl-SN-842297) Avail: NTIS HC/MF A03 CSCL 09A

The invention relates to planar varactor frequency multiplier devices with a heterojunction blocking barrier for near millimeter wave radiation of moderate power from a fundamental input wave. The space charge limitation of the submillimeter frequency multiplier devices of the BIN(sup +) type is overcome by a diode structure comprising an n(sup +) doped layer of semiconductor material functioning as a low resistance back contact, a layer of semiconductor material with n-type doping functioning as a drift region grown on the back contact layer, a delta doping sheet forming a positive charge at the interface of the drift region layer with a barrier layer, and a surface metal contact. The layers thus formed on an n(sup +) doped layer may be divided into two isolated back-to-back BNN(sup +) diodes by separately depositing two surface metal contacts. By repeating the sequence of the drift region layer and the barrier layer with the delta doping sheet at the interfaces between the drift and barrier layers, a plurality of stacked diodes is formed. The novelty of the invention resides in providing n-type semiconductor material for the drift region in a GaAs/AlGaAs structure, and in stacking a plurality of such BNN(sup +) diodes stacked for greater output power with and connected back-to-back with the n(sup +) GaAs layer as an internal back contact and separate metal contact over an AlGaAs barrier layer on top of each stack. NASA

N92-23495# Helsinki Univ. of Technology, Espoo (Finland). Inst. of Mathematics.
WAVEFORM RELAXATION ALWAYS CONVERGES FOR RC-CIRCUITS
O. Nevanlinna Feb. 1991 12 p
(PB92-142280; RR-A291; ISBN-951-22-0522-X) Avail: NTIS HC/MF A03 CSCL 09C

It is proved that the waveform relaxation method applied to linear RC circuits always converges. The speed depends strongly on the splitting of the network. Author

N92-23496# Helsinki Univ. of Technology, Espoo (Finland). Lab. of Electromechanics.
ANALYSIS OF A 37 kW CAGE-INDUCTION MOTOR
A. Arkkio 1991 69 p
(PB92-142116; ISBN-951-22-0757-5) Avail: NTIS HC/MF A04 CSCL 09A

An analysis was made of a 37 kW cage induction motor. The operating characteristics of the motor fed by a PWM frequency convertor are studied. Special attention is given to the additional losses caused by the convertor supply and suggestions are made on how to reduce these losses. The calculation of the motor is based on a time stepping, finite element analysis of the electromagnetic field. The field is assumed to be two dimensional. The time dependence of the field and the motion of the rotor are modeled by the Crank-Nicholson method. The nonsinusoidal voltage supplied by the frequency convertor is imposed on the formulation through the circuit equations of the winding. A new rotor specially designed for convertor drives was constructed for the 37 kW motor using the ideas obtained from the analysis. The characteristics measured for the motor equipped with the original rotor are compared with those measured for the new rotor. The new rotor has lower losses and thus produces a smaller temperature rise especially at the low frequency region of operation. Author

N92-23497# Helsinki Univ. of Technology, Espoo (Finland). Electronic Circuit Design Lab.
HIGHER ORDER TEMPERATURE COMPENSATION OF BANDGAP VOLTAGE REFERENCES (I)
O. Salminen and K. Halonen Nov. 1990 34 p
(PB92-142306; ISBN-951-22-0458-4; Rept-18) Avail: NTIS HC/MF A03 CSCL 09C

The higher order temperature compensation is required in CMOS bandgap voltage references to reduce the thermal drift of the reference output voltage. The method introduced uses a nonlinear resistance for compensation. Two circuit topologies are presented. The first one has no additional compensation. The results of the compensated circuits are compared to the traditional ones. Both the simulated and measured results are given for a total of twenty circuits. Author

N92-23535*# National Aeronautics and Space Administration. Lewis Research Center, Cleveland, OH.
NONPLANAR LINEARLY TAPERED SLOT ANTENNA WITH BALANCED MICROSTRIP FEED
Rainee N. Simons, Richard Q. Lee, and Thomas D. Perl (Akron Univ., OH.) 1992 6 p Proposed for presentation at the IEEE-APS International Symposium, Chicago, IL, 18-25 Jul. 1992
(Contract NAS3-25266)
(NASA-TM-105647; E-6754; NAS 1.15:105647) Avail: NTIS HC/MF A02 CSCL 09C

A nonplanar linearly tapered slot antenna (LTSA) has been fabricated and tested at frequencies from 8 to 32 giga-Hz. The LTSA is excited by a broadband balanced microstrip transformer. The measured results include the input term return loss as well as the radiation pattern of the antenna. Author

N92-23538*# Sverdrup Technology, Inc., Brook Park, OH.
CHARACTERIZATION OF POLYBENZIMIDAZOLE (PBI) FILM AT HIGH TEMPERATURES Final Report
Ahmad N. Hammoud and J. L. Suthar (State Univ. of New York, Buffalo.) Apr. 1992 5 p
(Contract NAS3-25266)
(NASA-CR-189174; E-6957; NAS 1.26:189174) Avail: NTIS HC/MF A01 CSCL 09A

Polybenzimidazole, a linear thermoplastic polymer with excellent thermal stability and strength retention over a wide range of temperatures, was evaluated for its potential use as the main dielectric in high temperature capacitors. The film was characterized in terms of its dielectric properties in a frequency range of 50 Hz to 100 kilo-Hz. These properties, which include the dielectric constant and dielectric loss, were also obtained in a temperature range from 20 C to 300 C with an electrical stress of 60 Hz, 50 V/mil present. The alternating and direct current breakdown voltages of silicone oil impregnated films as a function of temperature were also determined. The results obtained indicate that while the film remained relatively stable up to 200 C, it exhibited an increase in its dielectric properties as the temperature was raised to 300 C. It was also found that conditioning of the film by heat treatment at 60 C for six hours tended to improve its dielectric and breakdown properties. The results are discussed and conclusions made concerning the suitability of the film as a high temperature capacitor dielectric. Author

N92-23552*# National Aeronautics and Space Administration. Pasadena Office, CA.
METHOD OF FABRICATING SUPERCONDUCTING DEVICE Patent Application
Marc C. Foote, inventor (to NASA) and Brian D. Hunt, inventor (to NASA) (Jet Propulsion Lab., California Inst. of Tech., Pasadena.) 27 Feb. 1992 21 p
(Contract NAS7-918)
(NASA-Case-NPO-18394-1-CU; NAS 1.71:NPO-18394-1-CU; US-Patent-Appl-SN-849613) Avail: NTIS HC/MF A03 CSCL 09A

An improved method for forming a high temperature superconducting structure is provided. Fabrication is achieved by depositing a high temperature superconductor and a normal metal on a substrate, then annealing the high temperature superconductor/normal metal interface in an oxygen rich environment. By annealing the structure after deposition of the normal metal barrier layer, an improved interface is achieved. Further, the fabrication method is performed in a chamber entirely isolated from air to prevent any degradation of the materials caused by reaction with the air. Specific processing conditions such as temperature and pressure are set forth which help to achieve a high temperature superconducting structure with improved performance characteristics. NASA

N92-23561*# National Aeronautics and Space Administration. Lewis Research Center, Cleveland, OH.
EVALUATION OF HIGH TEMPERATURE CAPACITOR DIELECTRICS
Ahmad N. Hammoud (Sverdrup Technology, Inc., Brook Park, OH.) and Ira T. Myers 1992 8 p Presented at the Conference on Electrical Insulation and Dielectric Phenomena, Leesburg, VA, 29 Oct. - 2 Nov. 1989; sponsored by IEEE
(NASA-TM-105622; E-6960; NAS 1.15:105622) Avail: NTIS HC/MF A02 CSCL 09C

Experiments were carried out to evaluate four candidate materials for high temperature capacitor dielectric applications. The materials investigated were polybenzimidazole polymer and three aramid papers: Voltex 450, Nomex 410, and Nomex M 418, an aramid paper containing 50 percent mica. The samples were heat treated for six hours at 60 C and the direct current and 60 Hz alternating current breakdown voltages of both dry and impregnated samples were obtained in a temperature range of 20 to 250 C. The samples were also characterized in terms of their dielectric constant, dielectric loss, and conductivity over this temperature range with an electrical stress of 60 Hz, 50 V/mil present. Additional measurements are underway to determine the volume resistivity, thermal shrinkage, and weight loss of the materials. Preliminary data indicate that the heat treatment of the films slightly improves the dielectric properties with no influence on their breakdown behavior. Impregnation of the samples leads to significant increases in both alternating and direct current breakdown strength. The results are discussed and conclusions made concerning their suitability as high temperature capacitor dielectrics. Author

N92-23562*# National Aeronautics and Space Administration. Lewis Research Center, Cleveland, OH.
DEFECT BEHAVIOR, CARRIER REMOVAL AND PREDICTED IN-SPACE INJECTION ANNEALING OF InP SOLAR CELLS
I. Weinberg, C. K. Swartz, and P. J. Drevinsky (Phillips Lab., Hanscom AFB, MA.) 1992 6 p Presented at the Fourth International Conference on Indium Phosphide and Related Materials, Newport, RI, 20-24 Apr. 1992; sponsored by IEE and LEOS
(NASA-TM-105624; E-6963; NAS 1.15:105624) Avail: NTIS HC/MF A02 CSCL 10A

Defect behavior, observed by deep level transient spectroscopy (DLTS), is used to predict carrier removal and the effects of simultaneous electron irradiation and injection annealing of the performance of InP solar cells. For carrier removal, the number of holes trapped per defect is obtained from measurements of both carrier concentrations and defect concentrations during an isochronal anneal. In addition, from kinetic considerations, the behavior of the dominant defect during injection annealing is used to estimate the degradation expected from exposure to the ambient electron environment in geostationary orbit. Author

N92-23584# Sandia National Labs., Albuquerque, NM.
PSD COMPUTATIONS USING WELCH'S METHOD
O. M. Solomon, Jr. Dec. 1991 54 p
(Contract DE-AC04-76DP-00789)
(DE92-007419; SAND-91-1533) Avail: NTIS HC/MF A04

This report describes Welch's method for computing Power Spectral Densities (PSDs). We first describe the bandpass filter method which uses filtering, squaring, and averaging operations to estimate a PSD. Second, we delineate the relationship of Welch's method to the bandpass filter method. Third, the frequency domain

signal-to-noise ratio for a sine wave in white noise is derived. This derivation includes the computation of the noise floor due to quantization noise. The signal-to-noise ratio and noise flood depend on the FFT length and window. Fourth, the variance of the Welch's PSD is discussed via chi-square random variables and degrees of freedom. DOE

N92-23678# Helsinki Univ. of Technology, Espoo (Finland). Circuit Theory Lab.
MOSFET LEVEL 1 AND 2 MODELS IN APLAC
A. Kankkunen, M. Andersson, and M. Valtonen 1991 64 p Prepared in cooperation with Technical Research Center of Finland, Espoo
(PB92-143379; ISBN-951-22-0787-7; CT-8) Avail: NTIS HC/MF A04 CSCL 09C

The Analysis Program for Linear Active Circuits (APLAC) implementations are documented of SPICE level 1 and 2 MOS models. First a set of mappings is derived for handling NMOS and PMOS transistors in all operating regions based on the equations of an NMOS transistor with V(ds) = or greater than 0. Then the model equations of the NMOS transistor are presented. Two drain current models are covered. These are SPICE level 1 and SPICE level 2. The documentation consists of all the equations required for the implementation including the substrate diode model, temperature dependencies, and noise equations. The intrinsic charge models presented are the simplified Yang-Chatterjee models and the Ward-Dutton model. Also the extrinsic capacitance model is documented. Author

N92-23735# Oak Ridge National Lab., TN.
EMPIRICAL CHARACTERIZATION OF A HIGH INTENSITY LED PROXIMITY SENSOR
J. E. Baker Nov. 1991 26 p
(Contract DE-AC05-84OR-21400)
(DE91-019074; ORNL/TM-11972; CESAR-91/41) Avail: NTIS HC/MF A03

Many robotic operations require accurate and precise distance measurements to arbitrary targets in an unstructured environment. Such information can be used in path planning, object avoidance, surface following, topological mapping, relative positioning, artifact resolution, etc. Hence, there is a significant need for a non-contact proximity sensor system which is minimally affected by target composition, orientation, color, texture, etc. and to empirically understand its behavior with respect to such target characteristics. This paper describes a most promising sensing technology (high intensity LED triangulation) and presents an empirical analysis of a representative, commercial system. DOE

N92-23902# Lawrence Livermore National Lab., CA.
MONTE CARLO TRANSPORT IN SEMICONDUCTOR
K. J. Wahlstrand and J. H. Yee Sep. 1991 14 p
(Contract W-7405-eng-48)
(DE92-008404; UCRL-ID-108256) Avail: NTIS HC/MF A03

We have developed two Monte Carlo transport codes to investigate transport phenomena in semiconductor materials. The first of these codes uses analytical equations to represent the first conduction band of the material, and is valid only at low electric fields. The other code uses the exact bandstructure of the first conduction band calculated with a pseudopotential energy band code, and includes impact ionization. This code is more accurate for very high transport phenomena. Both codes have been validated for GaAs by comparison with the experimental drift velocity. DOE

N92-23983# Sandia National Labs., Albuquerque, NM.
ELECTRICAL AND OPTICAL PROPERTIES OF HIGH GAIN GaAs SWITCHES
F. J. Zutavern, G. M. Loubriel, D. L. McLaughlin, W. D. Helgeson, and M. W. OMalley 1991 9 p Presented at the Society of Photo-Optical Instrumentation Engineers' International Symposium on Laser Spectroscopy as part of SPIE's Symposium on Optics, Electro-Optics and Laser Applications in Science and Engineering, Los Angeles, CA
(Contract DE-AC04-76DP-00789)
(DE92-008668; SAND-91-1562C; CONF-920124-12) Avail: NTIS HC/MF A02

This paper presents measurements of electrical and optical properties of GaAs photoconductive semiconductor switches (PCSS) operating in a high gain switching mode previously referred to as 'lock-on'. High voltage and high current switching properties are given as motivation for understanding this switching mode. X-ray triggering of these switches is demonstrated, and the sensitivity of high field GaAs devices is discussed. Infrared photoluminescence (PL) images of the switches during the initiation of high gain switching reveal dense filaments of high carrier concentration. Spatial modulation of the optical (532 nm) trigger is shown to control the location and influence the number of filaments. The ability to trigger large lateral GaAs PCSS by focusing the light to a point near either contact is described, and the corresponding rise times and delays to high current switching are shown. The sudden rise of current to several orders of magnitude beyond the space charge limited flow which can come from the contacts demonstrates that initiation of this high gain switching mode cannot be explained solely by carrier injection at the contacts and drift across the 1.5 cm long insulating region. DOE

N92-23985# California Univ., Berkeley. Lawrence Berkeley Lab.
THE EFFECT OF CO-IMPLANTATION ON THE ELECTRICAL ACTIVITY OF IMPLANTED CARBON IN GaAs
A. J. Moll, W. Walukiewicz, K. M. Yu, W. L. Hansen, and E. E. Haller Nov. 1991 6 p Presented at the Annual Fall Meeting of the Materials Research Society, Boston, MA, 2-6 Dec. 1991
(Contract DE-AC03-76SF-00098)
(DE92-008307; LBL-31207; CONF-911202-63) Avail: NTIS HC/MF A02

We have undertaken a systematic study of the effect of co-implantation on the electrical properties of C implanted in GaAs. Two effects have been studied, the additional damage caused by co-implantation and the stoichiometry in the implanted layer. A series of co-implant ions were used: group 3 (B, Al, Ga), group 5 (N, P, As) and noble gases (Ar, Kr). Co-implantation of ions which create an amorphous layer was found to increase the electrical activity of C. Once damage was created, maintaining stoichiometric balance by co-implantation of a group 3 further increased the fraction of electrically active carbon impurities. Co-implantation of Ga and rapid thermal annealing at 950 C for 10s resulted in carbon activation as high as 68 percent, the highest value ever reported. DOE

N92-24025# Oak Ridge National Lab., TN.
AN ANALYSIS OF THE RELATIONSHIP BETWEEN INDUCTION MOTOR CURRENT AND SHAFT SPEED FLUCTUATIONS
C. H. Nowlin 1992 20 p Presented at the 46th Meeting of the Mechanical Failures Prevention Group (MFPG), Virginia Beach, VA, 7-9 Apr. 1992
(Contract DE-AC05-84OR-21400)
(DE92-007234; CONF-920474-1) Avail: NTIS HC/MF A03

For induction motors, motor shaft speed variations accompany motor load torque variations and motor torque variations. Hence, shaft speed fluctuation detection can serve as a warning of undesirable motor load conditions. This paper presents a theoretical foundation for the relationship between motor shaft speed fluctuations and stator current fluctuations when the shaft speed is perturbed by any cause. In addition, it shows that amplitude and frequency demodulation of motor current enhance the observed current fluctuations. The equations presented herein are derived in an as-yet unpublished work. Differential equations and basic electromagnetic equations, rather than phasors, are emphasized in their derivation. Fourier spectra of motor current, amplitude demodulated motor current, and frequency demodulated motor current are given for motor shaft speed modulated simultaneously with 13- and 17-Hz perturbations. We conclude that frequency demodulation is potentially a much better method to detect shaft speed fluctuations than is amplitude demodulation but that better methods of frequency demodulation are needed.

The best presently available methods of frequency demodulation alias interference lines down into the spectra of interest below 60 Hz. There, they mask the valid spectral lines. DOE

N92-24047*# Alabama Univ., Huntsville. Space Systems and Technology Lab.
ADVANCED ELECTRIC MOTOR TECHNOLOGY: FLUX MAPPING Final Technical Report, Apr. 1992
George B. Doane, III, Warren Campbell, Larry W. Brantley, and Garvin Dean 10 Apr. 1992 303 p
(Contract NAS8-36955)
(NASA-CR-184317; NAS 1.26:184317; UAH-5-32640) Avail: NTIS HC/MF A14 CSCL 09C

This report contains the assumptions, mathematical models, design methodology, and design points involved with the design of an electromechanical actuator (EMA) suitable for directing the thrust vector of a large MSFC/NASA launch vehicle. Specifically the design of such an actuator for use on the upcoming liquid fueled National Launch System (NLS) is considered culminating in a point design of both the servo system and the electric motor needed. A major thrust of the work is in selecting spur gear and roller screw reduction ratios to achieve simultaneously wide bandwidth, maximum power transfer, and disturbance rejection while meeting specified horsepower requirements at a given stroking speed as well as a specified maximum stall force. An innovative feedback signal is utilized in meeting these diverse objectives. Author

N92-24063# Sandia National Labs., Albuquerque, NM.
BATTERY TEST FACILITY HARDWARE, SOFTWARE, AND SYSTEM OPERATION
G. P. Rodriguez Sep. 1991 162 p
(Contract DE-AC04-76DP-00789)
(DE92-008455; SAND-91-1059) Avail: NTIS HC/MF A08

Division 2525 Battery Test Laboratory is a fully automated battery testing facility used in evaluating various battery technologies. The results of these tests are used to verify developers' claims, characterize prototypes, and assist in identifying the strengths and weaknesses of each technology. The test facility consists of a central computer and nine remote computer controlled battery test systems. Data acquired during the battery testing process is sent to the central computer system. The test data is then stored in a large database for future analysis. The central computer system is also used in configuring battery tests. These test configurations are then sent to their appropriate remote battery test sites. The battery test facility can perform a variety of battery tests, which include the following: life cycle testing; parametric testing at various temperature levels, cutoff parameters, charge rates, and discharge rates; constant power testing at various power levels; peak power testing at various state-of-charge levels; simplified federal urban driving schedule tests (SFUDS79). The battery test facility is capable of charging a battery either by constant current, constant voltage, step current levels, or any combination of them. Discharge cycles can be by constant current, constant resistance, constant power, step current levels, or also any combination of them. The battery test facility has been configured to provide the flexibility to evaluate a large variety of battery technologies. These technologies include lead-acid, sodium/sulfur, zinc/bromine, nickel/hydrogen, aluminum/air, and nickel/cadmium batteries. DOE

N92-23651*# Johnson Controls, Inc., Butler, WI. Nickel Hydrogen Batteries Div.
CENTER FOR SPACE POWER, TEXAS A AND M UNIVERSITY
Ken Jones *In* NASA, Washington, Proceedings of the Second Annual Symposium on Industrial Involvement and Successes in Commercial Space 1991 5 p (For primary document see N92-23643 14-12)
Avail: NTIS HC/MF A11 CSCL 11D

N92-23654*# Westinghouse Electric Corp., Pittsburgh, PA. Science and Technology Center.
CENTER FOR SPACE POWER AND ADVANCED ELECTRONICS, AUBURN UNIVERSITY
Dan W. Deis and Richard H. Hopkins *In* NASA, Washington, Proceedings of the Second Annual Symposium on Industrial Involvement and Successes in Commercial Space 1991 21 p (For primary document see N92-23643 14-12)
Avail: NTIS HC/MF A11 CSCL 08B

34 FLUID MECHANICS AND HEAT TRANSFER

Includes boundary layers; hydrodynamics; fluidics; mass transfer; and ablation cooling.

For related information see also *02 Aerodynamics* and *77 Thermodynamics and Statistical Physics.*

N92-23146 Cincinnati Univ., OH.
IMPINGING AXISYMMETRIC JET Ph.D. Thesis
Savas Aydore 1991 307 p
Avail: Univ. Microfilms Order No. DA9205395

The characteristics of an axisymmetric air jet with a fully developed pipe flow exit condition impinging vertically onto a flat plate was studied experimentally using hot wire anemometry and flow visualization. The jet to plate spacings ranged from one to five jet diameters and Reynold numbers (based on jet centerline velocity and jet diameter) varied from 40 to 23000. A method for conditional sampling and phase averaging was developed for the education of the large coherent structures in the jet near field. For Re sub D = 13000 and jet to plate spacing of four jet diameters, the phase averaged contour plots are given for vorticity, streamwise and radial velocities, turbulent intensities, Reynold stress, strain rate and turbulence production. The vortex dynamics is studied using the phase averaged quantities and the equations for coherent turbulence and vorticity. The coherent vorticity contour plots suggest that the large structures exist in the middle of the shear layer at about one jet diameter downstream from the jet exit and their largest size is about 0.4 jet diameters. The vortex growth is found to be high on the valleys of coherent shear production and downstream of the peak Reynolds stress region. Dissert. Abstr.

N92-23148 Cincinnati Univ., OH.
AN ADAPTIVE-GRID TECHNIQUE FOR SIMULATION OF COMPLEX UNSTEADY FLOWS Ph.D. Thesis
Hugh Joseph Thornburg 1991 176 p
Avail: Univ. Microfilms Order No. DA9205482

A strongly unsteady flow is simulated. In such flows, regions requiring fine mesh resolution vary with time. A technique was developed to generate a temporally adapting grid in which the adaptation is based on the evolving flow solution. The flow in an axisymmetric constriction was selected as an illustrative problem. The multiple and disparate length scales inherent in this complex flow structure make this flow ideally suited for evaluating the adaptive grid technique. Also, experimental results are available. The vorticity stream function formulation of the unsteady Navier-Stokes equations, written in generalized nonorthogonal time dependent coordinates is used. The vorticity-tranport equation contains grid speed terms which account for the grid movement. Adaption is based on the equidistribution of a weight function, via forcing functions. The significance of this is that the method can be implemented into many existing flow analysis systems with minimal changes. The grid generation equations developed are viewed as grid transport equations. The time dependent control functions perform the role of the driving force or transport mechanism. Dissert. Abstr.

N92-23149 Bristol Univ. (England).
APPLICATIONS OF BOUNDARY INTEGRAL METHODS TO THE STUDY OF STEEP FREE SURFACE WAVES Ph.D. Thesis

A. F. TelesdaSilva 1989 199 p
Avail: Univ. Microfilms Order No. BRDX94110

Boundary Integral Methods are applied to the study of three problems on two dimensional steep surface waves. The first problem is on the propagation of steady waves moving on a shearing flow with constant vorticity. Steady solutions which are either spacially periodic or solitary waves are calculated up to the limiting wave with and angle of 120 deg at its crest. The second problem is on the unsteady development of bores. Bores are studied an an evolution problem starting from an initially smooth wave of elevation. For weaker bores, the growth of undulations is studied in detail; stronger bores are followed until they break. Calculated results are compared with experiments with a general good agreement. The third problem is on the interaction of a submerged cylinder and a free surface flow. The flow produced by an obstacle of finite dimensions fixed in an otherwise uniform stream is calculated for several sizes of the obstacle and different values of the Froude number. Also studied are the disturbances produced on an initially flat water surface by a moving submerged cylinder. Dissert. Abstr.

N92-23154*# National Aeronautics and Space Administration. Lewis Research Center, Cleveland, OH.
COMPARISON OF TWO-DIMENSIONAL AND THREE-DIMENSIONAL DROPLET TRAJECTORY CALCULATIONS IN THE VICINITY OF FINITE WINGS
Stanley R. Mohler, Jr. (Sverdrup Technology, Inc., Brook Park, OH.) and Colin S. Bidwell 1992 34 p Presented at the 30th Aerospace Sciences Meeting, Reno, NV, 6-9 Jan. 1992; sponsored by AIAA Previously announced in IAA as A92-28215
(NASA-TM-105617; E-6806; NAS 1.15:105617; AIAA-92-0645)
Avail: NTIS HC/MF A03 CSCL 20D

Computational predictions of ice accretion on flying aircraft most commonly rely on modeling in two dimensions (2D). These 2D methods treat an aircraft geometry either as wing-like with infinite span, or as an axisymmetric body. Recently, fully three dimensional (3D) methods have been introduced that model an aircrafts true 3D shape. Because 3D methods are more computationally expensive than 2D methods, 2D methods continue to be widely used. However, a 3D method allows us to investigate whether it is valid to continue applying 2D methods to a finite wing. The extent of disagreement between LEWICE, a 2D method, and LEWICE3D, a 3D method, in calculating local collection efficiencies at the leading edge of finite wings is investigated in this paper.
Author

N92-23202# Rensselaer Polytechnic Inst., Troy, NY.
THE CONTINUUM MODELLING OF TWO-PHASE FLOW SYSTEMS
R. T. Lahey, Jr. and D. A. Drew 1992 10 p
(Contract DE-FG02-86ER-13489)
(DE92-007538; DOE/ER-13489/6) Avail: NTIS HC/MF A02

This research program is concerned with the development of self-consistent multidimensional two-fluid models which predict a wide variety of data and satisfy all relevant physical laws and constraints. If successful, these models can revolutionize the way in which two-phase lows are analyzed, since mechanistic, rather than empirical-based predictions should be possible. During this report period the research has focused on understanding the relationships between the interfacial closure laws and the onset of ill-posedness. In particular, it is now known that only the void wave eigenvalues can become complex, thus leading to ill-posedness. As a consequence, a detailed set of void wave data were taken and these data were compared with the two-fluid model we have developed. The kinematic void wave data was well predicted, and, in addition, a much faster void wave was also measured. The faster void wave was associated with bubble clusters which were observed to form due to hydrodynamic effects. Significantly, these clusters were found to be the precursors of Taylor bubble formation (i.e., the bubbly-to-slug flow regime transition). Moreover, it was found that for certain conditions, these void waves were amplified, thus triggering flow regime transition.
DOE

N92-23224*# National Aeronautics and Space Administration. Lewis Research Center, Cleveland, OH.
MODELLING AND EXPERIMENTAL VERIFICATION OF A WATER ALLEVIATION SYSTEM FOR THE NASP
G. James VanFossen 1992 13 p Proposed for presentation at the 92nd National Heat Transfer Conference, San Diego, CA, 9-12 Aug. 1992; sponsored by ASME
(NASA-TM-105661; E-7026; NAS 1.15:105661) Avail: NTIS HC/MF A03 CSCL 20D

One possible low speed propulsion system for the National Aerospace Plane is a liquid air cycle engine (LACE). The LACE system uses the heat sink in the liquid hydrogen propellant to liquefy air in a heat exchanger which is then pumped up to high pressure and used as the oxidizer in a hydrogen liquid air rocket. The inlet airstream must be dehumidified or moisture could freeze on the cryogenic heat exchangers and block them. The main objective of this research has been to develop a computer simulation of the cold tube/antifreeze-spray water alleviation system and to verify the model with experimental data. An experimental facility has been built and humid air tests were conducted on a generic heat exchanger to obtain condensing data for code development. The paper describes the experimental setup, outlines the method of calculation used in the code, and presents comparisons of the calculations and measurements. Cause of discrepancies between the model and data are explained.
Author

N92-23251# Technische Univ., Twente (Netherlands). Faculty of Applied Mathematics.
IMPROVED SHOCK-CAPTURING OF JAMESON'S SCHEME FOR THE EULER EQUATIONS
J. W. vanderBurg, J. G. M. Kuerten, and P. J. Zandbergen Sep. 1991 29 p
(PB92-148758; MEMO-997) Avail: NTIS HC/MF A03 CSCL 20D

It is known that Jameson's scheme is a pseudo-second-order accurate scheme for solving discrete conservation laws. The scheme contains a nonlinear artificial dissipative flux which is designed to capture shocks. It is shown that the shock-capturing of Jameson's scheme for the Euler equations can be improved by replacing the Lax-Friedrichs' type of dissipative flux with Roe's dissipative flux. The replacement is at a moderate expense of the calculation time.
GRA

N92-23253*# Sverdrup Technology, Inc., Brook Park, OH.
A STUDY OF START-UP CHARACTERISTICS OF A POTASSIUM HEAT PIPE FROM THE FROZEN STATE
Jong Hoon Jang Apr. 1992 9 p Proposed for presentation at the 1992 National Heat Transfer Conference, San Diego, CA, 9-12 Aug. 1992; sponsored by ASME
(Contract NAS3-25266)
(NASA-CR-189173; E-7031; NAS 1.26:189173) Avail: NTIS HC/MF A02 CSCL 20D

The start up characteristics of a potassium heat pipe were studied both analytically and experimentally. Using the radiation heat transfer mode the heat pipe was tested in a vacuum chamber. The transition temperature calculated for potassium was then compared with the experimental results of the heat pipe with various heat inputs. These results show that the heat pipe was inactive until it reached the transition temperature. In addition, during the start up period, the evaporator experienced dry-out with a heat input smaller than the capillary limit calculated at the steady state. However, when the working fluid at the condensor was completely melted, the evaporation was rewetted without external aid. The start up period was significantly reduced with a large heat input.
Author

N92-23268*# National Aeronautics and Space Administration. Lewis Research Center, Cleveland, OH.
LIQUID HYDROGEN MASS FLOW THROUGH A MULTIPLE ORIFICE JOULE-THOMSON DEVICE
S. Stephen Papell (Analex Corp., Brook Park, OH.), Ted W. Nyland, and Naseem H. Saiyed 1992 13 p Proposed for presentation

at the 27th Thermophysics Conference, Nashville, TN, 6-8 Jul. 1992; sponsored by AIAA
(NASA-TM-105583; E-6910; NAS 1.15:105583; AIAA-92-2881)
Avail: NTIS HC/MF A03 CSCL 20D

Liquid hydrogen mass flow rate, pressure drop, and temperature drop data were obtained for a number of multiple orifice Joule-Thomas devices known as visco jets. The present investigation continues a study to develop an equation for predicting two phase flow of cryogens through these devices. The test apparatus design allowed isenthalpic expansion of the cryogen through the visco jets. The data covered a range of inlet and outlet operating conditions. The mass flow rate range single phase or two phase was 0.015 to 0.98 lbm/hr. The manufacturer's equation was found to overpredict the single phase hydrogen data by 10 percent and the two phase data by as much as 27 percent. Two modifications of the equation resulted in a data correlation that predicts both the single and two phase flow across the visco jet. The first modification was of a theoretical nature, and the second strictly empirical. The former reduced the spread in the two phase data. It was a multiplication factor of 1 - X applied to the manufacturer's equation. The parameter X is the flow quality downstream of the visco jet based on isenthalpic expansion across the device. The latter modification was a 10 percent correction term that correlated 90 percent of the single and two phase data to within +/- 10 percent scatter band. Author

N92-23516# North Carolina Univ., Chapel Hill. Dept. of Environmental Sciences and Engineering.
NUMERICAL CALCULATION: ASPIRATION EFFICIENCY OF AEROSOLS INTO THIN-WALLED SAMPLING INLETS
K. M. Boyle, T. Kim, M. R. Flynn, and R. W. Wiener Nov. 1991 107 p
(Contract EPA-R-815152)
(PB92-132901; EPA/600/3-91/075) Avail: NTIS HC/MF A06 CSCL 20D

Asperation efficiency of particles from a flowing airstream into a thin-walled sampling inlet is accurately predicted using a numerical model. The model combines the Boundary Integral Equation Method for predicting the velocity field into the inlet with an analytical solution to the particle equations of motion. A two and a three dimensional model are examined. Results for the three dimensional model correlate well with an empirical model of asperation efficiency. The method can be generalized to a wide range of airstream, sampling inlet, and particle conditions.
Author

N92-23542*# National Aeronautics and Space Administration. Lewis Research Center, Cleveland, OH.
RENORMALIZATION GROUP ANALYSIS OF THE REYNOLDS STRESS TRANSPORT EQUATION
R. Rubinstein and J. M. Barton (Sverdrup Technology, Inc., Brook Park, OH.) Mar. 1992 27 p
(Contract NCC3-233)
(NASA-TM-105588; ICOMP-92-06; E-6917; NAS 1.15:105588; CMOTT-92-03) Avail: NTIS HC/MF A03 CSCL 20D

The pressure velocity correlation and return to isotropy term in the Reynolds stress transport equation are analyzed using the Yakhot-Orszag renormalization group. The perturbation series for the relevant correlations, evaluated to lowest order in the epsilon-expansion of the Yakhot-Orszag theory, are infinite series in tensor product powers of the mean velocity gradient and its transpose. Formal lowest order Pade approximations to the sums of these series produce a fast pressure strain model of the form proposed by Launder, Reece, and Rodi, and a return to isotropy model of the form proposed by Rotta. In both cases, the model constant are computed theoretically. The predicted Reynolds stress ratios in simple shear flows are evaluated and compared with experimental data. The possibility is discussed of driving higher order nonlinear models by approximating the sums more accurately. Author

N92-23543*# Old Dominion Univ., Norfolk, VA.
VISCOUS-SHOCK-LAYER ANALYSIS OF HYPERSONIC FLOWS OVER LONG SLENDER VEHICLES Ph.D. Thesis, 1988
Kam-Pui Lee and Roop N. Gupta Mar. 1992 222 p
(Grant NAG1-346)
(NASA-CR-189614; NAS 1.26:189614) Avail: NTIS HC/MF A10 CSCL 20D

An efficient and accurate method for solving the viscous shock layer equations for hypersonic flows over long slender bodies is presented. The two first order equations, continuity and normal momentum, are solved simultaneously as a coupled set. The flow conditions included are from high Reynolds numbers at low altitudes to low Reynolds numbers at high altitudes. For high Reynolds number flows, both chemical nonequilibrium and perfect gas cases are analyzed with surface catalytic effects and different turbulence models, respectively. At low Reynolds number flow conditions, corrected slip models are implemented with perfect gas case. Detailed comparisons are included with other predictions and experimental data. Author

N92-23560*# National Aeronautics and Space Administration. Lewis Research Center, Cleveland, OH.
A TWO-DIMENSIONAL EULER SOLUTION FOR AN UNBLADED JET ENGINE CONFIGURATION
Mark E. M. Stewart Apr. 1992 10 p Presented at the Third Canadian Symposium on Aerodynamics, Toronto (Ontario), 20-21 Nov. 1991; sponsored by the Canadian Aeronautics and Space Inst.
(NASA Order C-99066-G)
(NASA-TM-105329; ICOMP-91-22; E-6691; NAS 1.15:105329)
Avail: NTIS HC/MF A02 CSCL 20D

A two dimensional, nonaxisymmetric Euler solution in a geometry representative of a jet engine configuration without blades is presented. The domain, including internal and external flow, is covered with a multiblock grid. In order to construct this grid, a domain decomposition technique is used to subdivide the domain, and smooth grids are dimensioned and placed in each block. The Euler solution is verified by examining five theoretical properties. The result demonstrates techniques for performing numerical solutions in complex geometries and provides a foundation for complete engine throughflow calculations. Author

N92-23565*# National Aeronautics and Space Administration. Lewis Research Center, Cleveland, OH.
LONG TIME BEHAVIOR OF UNSTEADY FLOW COMPUTATIONS
S. I. Hariharan (Akron Univ., OH.) Mar. 1992 24 p
(Contract NCC3-233; NSF DMS-89-21189)
(NASA-TM-105584; ICOMP-92-04; E-6912; NAS 1.15:105584)
Avail: NTIS HC/MF A03 CSCL 20D

This paper addresses a specific issue of time accuracy in the calculation of external aerodynamic problems. The class of problems discussed consists of inviscid compressible subsonic flows. These problems are governed by a convective equation. A key issue that is not understood is the long time behavior of the solution. This is important if one desires transient calculations of problems governed by the Euler equations or its derivatives such as the small disturbance equations or the potential formulations for the gust problem. Difficulties arise for two dimensional problems where the time rate decay solutions of the wave equation is slow. In concert with the above mentioned problem, exterior flows require proper modeling of the boundary conditions. In particular, this requires the truncation of infinite regions into finite regions with the aid of artificial boundaries. These boundary conditions must be consistent with the physics of the unbounded problem as well as consistent in time and space. Our treatment of the problem is discussed in detail and examples are given to verify the results.
Author

N92-23568*# Alabama Univ., Huntsville. Dept. of Computer Science.
COMPUTATIONAL FLUID DYNAMICS FOR PROPULSION TECHNOLOGY: GEOMETRIC GRID VISUALIZATION IN CFD-BASED PROPULSION TECHNOLOGY RESEARCH Final Report No. 13, 20 Dec. 1990 - 1 Apr. 1992
John P. Ziebarth and Doug Meyer 17 Mar. 1992 44 p
(Contract NAS8-36955)
(NASA-CR-190291; NAS 1.26:190291; CCFD-92-01) Avail: NTIS HC/MF A03 CSCL 20D

The coordination is examined of necessary resources, facilities, and special personnel to provide technical integration activities in the area of computational fluid dynamics applied to propulsion technology. Involved is the coordination of CFD activities between government, industry, and universities. Current geometry modeling, grid generation, and graphical methods are established to use in the analysis of CFD design methodologies. Author

N92-23672 Oxford Univ. (England).
MATHEMATICAL MODELLING AND NUMERICAL APPROXIMATIONS FOR TWO-PHASE FLOW PROBLEMS Ph.D. Thesis
Xin Kai Li 1990 199 p
Avail: Univ. Microfilms Order No. BRD-93063

The study of mathematical modelling and numerical approximations for two-phase flow problems is discussed. This is an important subject from an engineering as well as from a mathematical standpoint. In the first three chapters, we review an averaging procedure to construct a general two-phase flow model based on the conservation laws of mass, momentum, and energy and present four useful two-phase flow models, namely, basic model, two-pressure model, Hancox model, and homogeneous equilibrium model. As an alternative to quasilinear characteristic analysis, an energy analysis for solutions of the basic model with forcing terms is presented in Chapter 4. A two-phase slug flow model is discussed in terms of both mathematical and physical considerations in Chapters 5 and 6. The prediction of the speed of waves plays an important role in two-phase flow systems. Therefore, our study in the last two chapters centers on the prediction of the speed of waves in two-phase flow problems. Dissert. Abstr.

N92-23689 Stanford Univ., CA.
THE KINEMATICS OF TURBULENT BOUNDARY LAYER STRUCTURE Ph.D. Thesis
Stephen Kern Robinson 1991 389 p
Avail: Univ. Microfilms Order No. DA9205711

Research into the internal structure of turbulent boundary layers has not provided a unified picture of the physics responsible for turbulence production and dissipation. The goals of the present research are to: (1) define the current state of boundary layer structure knowledge; and (2) use direct numerical simulation results to help close the unresolved issues identified and to unify the fragmented knowledge of the various coherent motions into a consistent kinematic model of boundary layer structure. The results of the current study show that all classes of coherent motion in the low Reynolds number turbulent boundary layer may be related to vortical structures, but that no single form of vortex is representative of the wide variety of vortical structures observed. In particular, ejection and sweep motions, as well as entrainment from the free stream are shown to have strong spatial and temporal relationships with vortical structures. Distributions of vortex size, location, and intensity show that quasi-streamwise vortices dominate the buffer region, while transverse vortices and vortical arches dominate the wake region. Both types of vortical structure are common in the log region. Dissert. Abstr.

N92-23692 Cranfield Inst. of Tech., Bedford (England).
TOPICS IN NUMERICAL COMPUTATION OF COMPRESSIBLE FLOW Ph.D. Thesis
Hong-Chia Lin 1990 174 p
Avail: Univ. Microfilms Order No. BRDX92928

The development of a multiblock implicit Navier-Stokes code for hypersonic flow applications is discussed. There are three main areas of research: the understanding of basic Riemann solvers; the implementing of the implicit zonal method; and grid adaptation for viscous flow. The problems of Riemann solvers are investigated. The post-shock oscillation problem of slowly moving shocks is examined, especially for Roe's Riemann solver, and possible cures are suggested for both first and second order schemes. The carbuncle phenomenon associated with blunt body calculation is cured by a formula based on pressure gradient, which will not degrade the solutions for viscous calculations too much. Several issues associated with implicit zonal methods are discussed. Several implicit schemes are tested for hypersonic flow. A simple and robust implicit zonal method is demonstrated. The final topic concerns the calculation and grid adaption of viscous flow. The linear advection-diffusion equation is studied. Dissert. Abstr.

N92-23700 Mississippi State Univ., State College.
UNSTEADY THREE-DIMENSIONAL INCOMPRESSIBLE ALGORITHM BASED ON ARTIFICIAL COMPRESSIBILITY Ph.D. Thesis
Lafayette Kenneth Taylor 1991 146 p
Avail: Univ. Microfilms Order No. DA9131250

The development of an implicit finite volume numerical approach for solving the unsteady three dimensional Euler and Navier-Stokes equations is presented. The time dependent equations in Cartesian coordinates are first transformed to a general time dependent curvilinear coordinate system and then artificial compressibility is introduced into the equations. In this cell centered finite volume scheme, the numerical flux at cell faces is calculated using the Roe approximate Riemann solver. Newton's method is the iterative process used to obtain both steady and unsteady solutions. However, the solution matrix operator is new in that it is a discretized Jacobian, whose elements are obtained by using simple finite differences of the flux vectors. Navier-Stokes solutions are simulated through an explicit treatment of the diffusive fluxes. Also, since high Reynolds number flows are of primary interest, the thin layer approximation is applied to the transformed diffusive flux vectors. The turbulence model used is the Baldwin-Lomax algebraic model. Several check cases were studied to test the validity of this approach. Computed results for stationary and dynamic grids were compared with either theoretical or experimental results for both inviscid and viscous, steady and unsteady flows. Dissert. Abstr.

N92-23995 Washington Univ., Seattle.
AN EXPERIMENTAL INVESTIGATION OF ENTRAINMENT AND MIXING IN PULSED AND EXPONENTIAL TRANSVERSE JETS Ph.D. Thesis
Adnan Eroglu 1991 139 p
Avail: Univ. Microfilms Order No. DA9203253

Entrainment in a transverse jet is dominated by two distinct types of large scale vortical structure. These are the shear layer vortices around the jet and the counterrotating longitudinal vortex pair. Water tunnel flow visualization experiments have revealed that the shear layer around the jet contains vortex loops, which are distorted and stretched due to the straining imposed on them by the crossflow. Neighboring vortex loops are forced to merge with each other in an unusual way as a result of this distortion and stretching. In two different experiments, the jet stream was externally forced in order to alter the behavior of both of these vortical structures. The resulting changes in the structure and penetration of the jet were studied by flow visualization techniques. Mixing and flame length behavior was studied with chemically reactive techniques. The effects of periodic forcing was studied of the shear layer vortex loops on the flow. A set of experiments was designed to affect the counterrotating vortex pair by exponentially accelerating the jet stream. Dissert. Abstr.

N92-23997 Virginia Polytechnic Inst. and State Univ., Blacksburg.
NUMERICAL SIMULATIONS OF WAKES, BLADE-VORTEX INTERACTION, FLUTTER, AND FLUTTER SUPPRESSION BY

FEEDBACK CONTROL Ph.D. Thesis
Bonian Dong 1991 191 p
Avail: Univ. Microfilms Order No. DA9204637

A general aerodynamic model for 2-D inviscid flows was developed. This model was used to simulate wakes and blade-vortex interaction. It was also coupled with dynamics and feedback controls to simulate flutter and flutter suppression. The flow was assumed to be attached and incompressible. The model was based on a vorticity panel method coupled with vortex dynamics. The model was used to simulate some actual experiments: wakes generated by oscillating airfoils and blade-vortex interactions in which one airfoil was placed in or near the wake generated by another oscillating airfoil upstream. Flutter was studied by means of numerical simulations. In an incompressible flow, an airfoil was mounted on an elastic support. The airfoil can pitch (rotate) and plunge (translate vertically). The coupled aerodynamic model accurately predicts the critical flutter speed of the freestream, the speed at which the motion of the airfoil grows spontaneously. A feedback control was coupled with aerodynamics to suppress the flutter motion of the airfoil. A flap was added at the trailing edge of the airfoil as a control surface, and its deflection (rotation) about the hinge point was commanded by a feedback control law. Dissert. Abstr.

N92-24018 Mississippi State Univ., State College.
INVESTIGATION OF SOLUTION OPERATORS FOR THE THREE DIMENSIONAL UNSTEADY EULER EQUATIONS Ph.D. Thesis
Francis Allen Mansfield 1991 168 p
Avail: Univ. Microfilms Order No. DA9131218

A method for numerically analyzing the stability of any continuous numerical solution operator for the 2-D and 3-D inviscid Euler equations was developed. Various combinations of the implicit left hand side and explicit right hand side operators were studied in terms of stability bounds and convergence rates for subsonic, transonic, and supersonic flows. The left hand operator consisted of the flux Jacobians and a block solver, while the right hand side operator consisted of the flux terms. The methods considered for evaluating the flux Jacobians on the left hand side included flux vector splitting and Roe's method. With Roe's method, the flux Jacobians were evaluated using an approximate analytical approach and a numerical approach. The only solution method studied for the right hand side flux evaluation was that of Roe, using MUSCL and the flux reconstruction methodologies. Also, some TVD limiters were evaluated to see the effect of higher spatial accuracy. Three different block solvers, tri-diagonal, two pass, and modified two pass were also evaluated. The modified two pass solver was proved to be the best in terms of stability, convergence, and cpu. Dissert. Abstr.

N92-24050*# National Aeronautics and Space Administration. Lewis Research Center, Cleveland, OH.
KOLMOGOROV BEHAVIOR OF NEAR-WALL TURBULENCE AND ITS APPLICATION IN TURBULENCE MODELING
Tsan-Hsing Shih and John L. Lumley (Cornell Univ., Ithaca, NY.) 1992 17 p
(Contract NCC3-233)
(NASA-TM-105663; ICOMP-92-10; NAS 1.15:105663; CMOTT-92-06) Avail: NTIS HC/MF A03 CSCL 20D

The near-wall behavior of turbulence is re-examined in a way different from that proposed by Hanjalic and Launder and followers. It is shown that at a certain distance from the wall, all energetic large eddies will reduce to Kolmogorov eddies (the smallest eddies in turbulence). All the important wall parameters, such as friction velocity, viscous length scale, and mean strain rate at the wall, are characterized by Kolmogorov microscales. According to this Kolmogorov behavior of near-wall turbulence, the turbulence quantities, such as turbulent kinetic energy, dissipation rate, etc. at the location where the large eddies become Kolmogorov eddies, can be estimated by using both direct numerical simulation (DNS) data and asymptotic analysis of near-wall turbulence. This information will provide useful boundary conditions for the turbulent transport equations. As an example, the concept is incorporated in the standard k-epsilon model which is then applied to channel and boundary flows. Using appropriate boundary conditions (based on Kolmogorov behavior of near-wall turbulence), there is no need for any wall-modification to the k-epsilon equations (including model constants). Results compare very well with the DNS and experimental data. Author

N92-24062# Syracuse Univ., NY. Dept. of Chemical Engineering and Materials Science.
NUMERICAL AND PHYSICAL MODELLING OF BUBBLY FLOW PHENOMENA
A. S. Sangani Feb. 1992 16 p
(Contract DE-FG02-90ER-14136)
(DE92-008642; DOE/ER-14136/T1) Avail: NTIS HC/MF A03

The objective of the proposed research is to develop a theoretical framework for analyzing various two-phase flows, with special emphasis on the flows of gas-liquid dispersions. The macroscopic behavior of these flows depends on the details of the microstructure of the dispersion, and these details, in turn, depend on the nature of the flow. Given the very diverse nature of the flows and their complex dependence on the microstructure of the dispersion, it is unlikely that a single set of equations, similar to the Navier-Stokes equations for homogeneous fluids, will apply to all the different situations. What is possible, however, is to develop general methodologies that can be used to examine specific situations and a general understanding about different kinds of macroscopic flows. The aim of the proposed research is to develop efficient numerical techniques for carrying out dynamic simulations of flows of dispersions and to apply them to a carefully selected problems whose solutions would reveal important qualitative as well as quantitative insights into the complex interdependence of the microstructure and macroscopic properties of the flows. These numerical techniques are to be supplemented with the techniques of ensemble averaging and statistical physics to obtain results that could be used in modelling more complicated flows through a set of relatively simple equations. Two classes of macroscopic flows were analyzed in detail during the current funding period. The first is the oscillatory flows, as in the case of acoustic or pressure wave propagation through bubbly liquids, and the second is convective flows as in bubbles rising through a liquid. DOE

N92-23338*# National Aeronautics and Space Administration. Lewis Research Center, Cleveland, OH.
TURBULENCE MODELING
Tsan-Hsing Shih *In its* Center for Modeling of Turbulence and Transition (CMOTT). Research Briefs: 1990 Oct. 1991 p 4-8 Prepared in cooperation with Stanford Univ., CA (For primary document see N92-23336 14-01)
Avail: NTIS HC/MF A08 CSCL 20D

N92-23339*# State Univ. of New York, Buffalo.
EXPERIMENTS AND MODELING
Aamir Shabbir *In* NASA. Lewis Research Center, Center for Modeling of Turbulence and Transition (CMOTT). Research Briefs: 1990 Oct. 1991 p 9-12 (For primary document see N92-23336 14-01)
Avail: NTIS HC/MF A08 CSCL 20D

N92-23340*# National Aeronautics and Space Administration. Lewis Research Center, Cleveland, OH.
MODELING OF COMPRESSIBLE TURBULENT SHEAR FLOWS
William W. Liou *In its* Center for Modeling of Turbulence and Transition (CMOTT). Research Briefs: 1990 Oct. 1991 p 13-15 (For primary document see N92-23336 14-01)
Avail: NTIS HC/MF A08 CSCL 20D

N92-23341*# Cornell Univ., Ithaca, NY.
RNG IN TURBULENCE AND MODELING OF BYPASS TRANSITION
Zhigang Yang *In* NASA. Lewis Research Center, Center for Modeling of Turbulence and Transition (CMOTT). Research Briefs:

1990 Oct. 1991 p 16-18 (For primary document see N92-23336 14-01)
Avail: NTIS HC/MF A08 CSCL 20D

N92-23343*# National Aeronautics and Space Administration. Lewis Research Center, Cleveland, OH.
DEVELOPMENT OF NEW FLUX SPLITTING SCHEMES
Meng-S. Liou and Christopher J. Steffen, Jr. *In its* Center for Modeling of Turbulence and Transition (CMOTT). Research Briefs: 1990 Oct. 1991 p 22-23 (For primary document see N92-23336 14-01)
Avail: NTIS HC/MF A08 CSCL 20D

N92-23344*# Sverdrup Technology, Inc., Cleveland, OH.
PROGRESS OF SIMULATIONS FOR REACTING SHEAR LAYERS
Sheng-Tao Yu *In* NASA. Lewis Research Center, Center for Modeling of Turbulence and Transition (CMOTT). Research Briefs: 1990 Oct. 1991 p 24-25 (For primary document see N92-23336 14-01)
Avail: NTIS HC/MF A08 CSCL 20D

N92-23346*# Sverdrup Technology, Inc., Cleveland, OH.
ON RECONTAMINATION AND DIRECTIONAL-BIAS PROBLEMS IN MONTE CARLO SIMULATION OF PDF TURBULENCE MODELS
Andrew T. Hsu *In* NASA. Lewis Research Center, Center for Modeling of Turbulence and Transition (CMOTT). Research Briefs: 1990 Oct. 1991 p 66-67 (For primary document see N92-23336 14-01)
Avail: NTIS HC/MF A08 CSCL 20D

N92-23349*# Sverdrup Technology, Inc., Cleveland, OH.
AN IMPROVED K-EPSILON MODEL FOR NEAR WALL TURBULENCE
T. H. Shih (National Aeronautics and Space Administration. Lewis Research Center, Cleveland, OH.) and Andrew T. Hsu *In* NASA. Lewis Research Center, Center for Modeling of Turbulence and Transition (CMOTT). Research Briefs: 1990 Oct. 1991 p 87-104 (For primary document see N92-23336 14-01)
Avail: NTIS HC/MF A08 CSCL 21B

N92-23350*# National Aeronautics and Space Administration. Lewis Research Center, Cleveland, OH.
ADVANCEMENTS IN ENGINEERING TURBULENCE MODELING
T.-H. Shih *In its* Center for Modeling of Turbulence and Transition (CMOTT). Research Briefs: 1990 Oct. 1991 p 108-125 Presented at the 9th National Aero-Space Plane Technology Symposium, 1-2 Nov. 1990 (For primary document see N92-23336 14-01)
(Paper-105) Avail: NTIS HC/MF A08 CSCL 20D

N92-23351*# National Aeronautics and Space Administration. Lewis Research Center, Cleveland, OH.
ON THE BASIC EQUATIONS FOR THE SECOND-ORDER MODELING OF COMPRESSIBLE TURBULENCE
William W. Liou and T.-H. Shih *In its* Center for Modeling of Turbulence and Transition (CMOTT). Research Briefs: 1990 Oct. 1991 p 134 (For primary document see N92-23336 14-01)
Avail: NTIS HC/MF A08 CSCL 20D

N92-23352*# National Aeronautics and Space Administration. Lewis Research Center, Cleveland, OH.
DEVELOPMENT OF A NEW FLUX SPLITTING SCHEME
Meng-Sing Liou and Christopher J. Steffen, Jr. *In its* Center for Modeling of Turbulence and Transition (CMOTT). Research Briefs: 1990 Oct. 1991 p 144-145 Previously announced in IAA as A91-40793 (For primary document see N92-23336 14-01)
Avail: NTIS HC/MF A08 CSCL 20D

N92-23353*# National Aeronautics and Space Administration. Lewis Research Center, Cleveland, OH.
HIGH-ORDER POLYNOMIAL EXPANSIONS (HOPE) FOR FLUX-VECTOR SPLITTING
Meng-Sing Liou and Chris J. Steffen, Jr. *In its* Center for Modeling of Turbulence and Transition (CMOTT). Research Briefs: 1990 Oct. 1991 p 146-150 Previously announced as N91-25739 (For primary document see N92-23336 14-01)
Avail: NTIS HC/MF A08 CSCL 20D

N92-23355*# National Aeronautics and Space Administration. Lewis Research Center, Cleveland, OH.
SIMULATIONS OF FREE SHEAR LAYERS USING A COMPRESSIBLE KAPPA-EPSILON MODEL
S. T. Yu (Sverdrup Technology, Inc., Cleveland, OH.), C. T. Chang, and C. J. Marek *In its* Center for Modeling of Turbulence and Transition (CMOTT). Research Briefs: 1990 Oct. 1991 p 152-160 Previously announced in IAA as A91-45778 (For primary document see N92-23336 14-01)
Avail: NTIS HC/MF A08 CSCL 20D

N92-23843# Kreis Consultancies, Pragg-Jenaz (Switzerland).
ON THE ANALYSIS OF LIQUID FILLED FREE-FREE TANKS
Andreas Kreis and Michel Klein (European Space Agency. European Space Research and Technology Center, ESTEC, Noordwijk, Netherlands) *In* ESA, Spacecraft Structures and Mechanical Testing, Volume 1 Oct. 1991 p 437-442 (For primary document see N92-23780 14-18)
Copyright Avail: NTIS HC/MF A21

N92-23844# Industrieanlagen-Betriebsgesellschaft m.b.H., Ottobrunn (Germany, F.R.).
NUMERICAL INVESTIGATION OF FLUID-STRUCTURE-INTERACTION PROBLEMS WITH THE FINITE ELEMENT METHOD
H.-P. Flicke and W. Mohr *In* ESA, Spacecraft Structures and Mechanical Testing, Volume 1 Oct. 1991 p 443-449 (For primary document see N92-23780 14-18)
Copyright Avail: NTIS HC/MF A21

N92-23845# European Space Agency. European Space Research and Technology Center, ESTEC, Noordwijk (Netherlands).
FLUID-STRUCTURE INTERACTION PROBLEMS: DEVELOPMENT OF SPECIAL PROCESSORS
M. Klein and Y. M. Lefevre (MATRA Espace, Toulouse, France) *In its* Spacecraft Structures and Mechanical Testing, Volume 1 Oct. 1991 p 451-455 (For primary document see N92-23780 14-18)
(Contract ESA-6468/86/NL/PH)
Copyright Avail: NTIS HC/MF A21

N92-23846# Universite de Technologie de Compiegne (France). DAVI Centre de Recherche de Royallieu.
A SYMMETRIC COUPLING BETWEEN BEM AND FEM FOR DYNAMICAL ANALYSIS OF SPACECRAFT
A. Omrani and M. A. Hamdi (STRACO S.A., Compiegne, France) *In* ESA, Spacecraft Structures and Mechanical Testing, Volume 1 Oct. 1991 p 457-460 (For primary document see N92-23780 14-18)
Copyright Avail: NTIS HC/MF A21

35 INSTRUMENTATION AND PHOTOGRAPHY

Includes remote sensors; measuring instruments and gages; detectors; cameras and photographic supplies; and holography.

For aerial photography see *43 Earth Resources and Remote Sensing.* For related information see also *06 Aircraft Instrumentation,* and *19 Spacecraft Instrumentation.*

N92-23144 State Univ. of New York, Stony Brook.
X RAY FOURIER TRANSFORM HOLOGRAPHY: BEYOND THE OPTICAL DIFFRACTION LIMIT Ph.D. Thesis

Ian Laurence McNulty 1991 242 p
Avail: Univ. Microfilms Order No. DA9205268

Soft x ray holography is a rapidly developing approach to high resolution imaging of thick, wet, unstained biological specimens. The Fourier transform geometry is especially suited to x ray holographic microscopy with swift turnaround. An experimental test is reviewed of this technique using a holographic x ray microscope. The NSLS Soft X ray Undulator supplied the microscope with coherent soft x radiation. A Fresnel zone plate formed the reference source and provided the specimen illumination. A sensitive CCD camera recorded the holograms. The digitized holograms were reconstructed by computer. This work showed a two dimensional imaging resolution of 60 nm with gold test patterns using 3.4 nm x rays. X ray microscopy and Fourier transform holography are introduced. Theoretical aspects are addressed and zone plates are discussed. The Soft X ray Undulator and X1A beamline are described. CCD detectors and the x ray CCD camera are discussed. The design and use of the microscope is addressed. Experimental results are presented and the performance of the microscope is discussed. Improvements to the source, optics, and detector are addressed, and future extensions are considered. Dissert. Abstr.

N92-23155*# National Aeronautics and Space Administration. Lewis Research Center, Cleveland, OH.
X RAY BASED DISPLACEMENT MEASUREMENT FOR HOSTILE ENVIRONMENTS
Howard A. Canistraro, Eric H. Jordon, Douglas M. Pease (Connecticut Univ., Storrs.), and Gustave C. Fralick Mar. 1992 17 p
(Grant NAG3-1004)
(NASA-TM-105551; E-6872; NAS 1.15:105551) Avail: NTIS HC/MF A03 CSCL 14B

A new method on noncontacting, high temperature extensometry based on the focus and scanning of x rays is currently under development and shows great promise of overcoming limitations associated with available techniques. The chief advantage is the ability to make undisturbed measurements through stratified or flowing gases, smoke, and flame. The system is based on the ability to focus and scan low energy, hard x rays such as those emanating from copper or molybdenum sources. The x rays are focused into a narrow and intense line image which can be scanned onto targets that fluoresce secondary x ray radiation. The final goal of the system is the ability to conduct macroscopic strain measurements in hostile environments by utilizing two or more fluorescing targets. Current work is limited to displacement measurement of a single target with a resolution of 1.25 micro-m and a target temperature of 1200 C, directly through an open flame. The main advantage of the technique lies in the penetrating nature of x rays which are not affected by the presence of refracting gas layers, smoke, flame, or intense thermal radiation, all of which could render conventional extensometry methods inoperative or greatly compromise their performance. Author

N92-23219# International Atomic Energy Agency, Vienna (Austria).
X RAY ANALYSIS SPECTROMETER
J. Pahor Jul. 1991 12 p
(DE92-615124; IAEA-R-5017-F) Avail: NTIS HC/MF A03

A dead time correction module in EUROcard format was designed and assembled. Its circuitry is a further development of the Barnhart approach. The fast discriminator signal from a spectroscopy amplifier is combined with the preamplifier inhibit signal, and with the messages from the analog-to-digital converter. The unit processes this input and produces a coincidence signal for the multichannel analyzer gate. A complete pile-up rejection system is incorporated in the module. DOE

N92-23278# California Univ., Berkeley. Lawrence Berkeley Lab.
A SWITCHED CAPACITOR ARRAY BASED SYSTEM FOR HIGH-SPEED CALORIMETRY
M. Levi, C. Bebek, R. Ely, R. Jared, I. Kipnis, F. Kirsten, S. Kleinfelder, T. Merrick, and O. Milgrome Dec. 1991 5 p Presented at the Calorimetry and High Energy Physics Conference, Capri (Italy), 14-18 Oct. 1991
(Contracts DE-AC03-76SF-00098; DE-AC35-89ER-40486)
(DE92-008288; LBL-31677; CONF-9110281-6) Avail: NTIS HC/MF A01

A sixteen channel analog transient recorder with 256 cells per channel has been fabricated as an integrated circuit. The circuit uses switched capacitor array technology to achieve simultaneous read/write capability and twelve bit dynamic range. Combined with highly parallel analog-to-digital converter and readout control circuitry being developed, this system should satisfy the demanding electronics requirements for calorimeter detectors at the SSC. The system design and test results are presented. DOE

N92-23279# California Univ., Berkeley. Lawrence Berkeley Lab.
TEST BEAM RESULTS FROM THE D0 END ELECTROMAGNETIC CALORIMETER
N. A. Roe Nov. 1991 6 p Presented at the Calorimetry and High Energy Physics Conference, Capri (Italy), 14-18 Oct. 1991
(Contract DE-AC03-76SF-00098)
(DE92-008299; LBL-31497; CONF-9110281-5) Avail: NTIS HC/MF A02

Test beam results are presented for the D0 end electromagnetic calorimeter. Data were taken with electrons and pions ranging in energy from 5 GeV to 150 GeV. Results from the analysis of the test beam data are presented on energy resolution and linearity, stability and uniformity of response, position resolution, and electron-pion separation. DOE

N92-23460*# National Aeronautics and Space Administration. Goddard Space Flight Center, Greenbelt, MD.
SUB-KELVIN RESISTANCE THERMOMETER Patent Application
Stephen H. Castles, inventor (to NASA) 24 Sep. 1991 21 p
(NASA-Case-GSC-13406-1; NAS 1.71:GSC-13406-1; US-Patent-Appl-SN-765070) Avail: NTIS HC/MF A03 CSCL 14B

A device capable of accurate temperature measurement down to 0.01 K of an object whose temperature is to be measured consists of: a heat sink wafer; a first conducting pad bonded near one end of the heat sink wafer; and a second conducting pad bonded near the other end of the heat sink wafer; an oblong doped semiconductor crystal such as germanium; the oblong doped semiconductor crystal has a third conducting pad bonded on its bottom surface with the oblong doped semiconductor crystal bonded to the heat sink wafer by having the fourth conducting pad bonded to the first conducting pad; a wire bonded between the second and third conducting pads; and current and voltage applying wires bonded to the first and second conducting pads whereby the change in resistance of the oblong doped semiconductor crystal indicates the temperature of an object whose temperature is to be measured. NASA

N92-23545*# National Aeronautics and Space Administration. Lyndon B. Johnson Space Center, Houston, TX.
SMART ACCELEROMETER Patent Application
Richard J. Bozeman, Jr., inventor (to NASA) 12 Feb. 1992 16 p
(NASA-Case-MSC-21951-1; NAS 1.71:MSC-21951-1; US-Patent-Appl-SN-834451) Avail: NTIS HC/MF A03 CSCL 14B

The invention discloses methods and apparatus for detecting vibrations from machines which indicate an impending malfunction for the purpose of preventing additional damage and allowing for an orderly shutdown or a change in mode of operation. The method and apparatus is especially suited for reliable operation in providing thruster control data concerning unstable vibration in an electrical environment which is typically noisy and in which unrecognized ground loops may exist. NASA

N92-23594# Helsinki Univ. of Technology, Espoo (Finland). Low Temperature Lab.
MICROSPHERE VISCOMETERS FOR LOW TEMPERATURE APPLICATIONS
K. Gloos, W. Schoepe, J. T. Simola, and J. T. Tuoriniemi 1991 32 p
(PB92-143361; TKK-F-A692) Avail: NTIS HC/MF A03 CSCL 14B

Three types of viscometers using metallic microspheres are described. These microspheres are either electrically charged, or possess a permanent magnetic dipole moment, or both. By different techniques, the spheres can be set into stationary translational motion, vibrational oscillations, or rotation. The observed damping of the motion yields information on the dissipation mechanisms and the viscosity of the medium studied. Author

N92-23283*# National Aeronautics and Space Administration. Marshall Space Flight Center, Huntsville, AL.
PINHOLE CAMERAS AS SENSORS FOR ATOMIC OXYGEN IN ORBIT: APPLICATION TO ATTITUDE DETERMINATION OF THE LDEF
Palmer N. Peters and John C. Gregory *In* NASA. Langley Research Center, LDEF: 69 Months in Space. First Post-Retrieval Symposium, Part 1 Jan. 1992 p 61-67 Previously announced as N92-11078 (For primary document see N92-23280 14-99)
(Contract NAS8-36645; NAGw-812)
Avail: NTIS HC/MF A99; 8 functional color pages CSCL 14E

N92-23641*# IMAX Space Technology, Inc., Houston, TX.
IMAX CAMERA (12-IML-1)
In NASA. Marshall Space Flight Center, First International Microgravity Laboratory Experiment Descriptions Feb. 1992 p 265-269 (For primary document see N92-23600 14-29)
Avail: NTIS HC/MF A13 CSCL 14E

36 LASERS AND MASERS

Includes parametric amplifiers.
For related information see also *76 Solid-State Physics.*

N92-23131# International Centre for Theoretical Physics, Trieste (Italy).
INVESTIGATIONS OF BREAKDOWN OF RARE GASES BY SHORT PULSES OF 1.06(MU)m LASER RADIATION
Y. E. E. D. Gamal and M. S. Shafik Aug. 1991 14 p
(DE92-615399; LAMP-91/6) Avail: NTIS HC/MF A03

An analysis based on a numerical integration of the equation which governs the total growth rate of the electron density due to the combined effect of multiphoton ionization and electron cascade ionization processes is presented. The calculations are carried out for argon and xenon gases in the pressure range 1.0 to 5 x 10(exp 3) Torr illuminated with 10ps pulses of 1.06 mu-m laser radiation. This analysis shows that the two ionization processes (multiphoton and electron cascade) play an important role over the whole pressure regime considered. At low pressures (less than 300 Torr) the breakdown is governed solely by the multiphoton process, indicated by the weak dependence of the threshold intensity on the gas pressure. At higher pressures (less than 760 Torr) however, a strong pressure dependence of the threshold intensity is observed. This is considered as evidence for the domination of the cascade ionization process at these pressures. On the pressure range 200-760 Torr a slight decrease of the threshold intensity is observed for both gases. This is attributed to the minor role played by the cascade ionization process together with the multiphoton ionization process at these pressures. The calculated thresholds for argon and xenon are consistent with those experimentally measured. DOE

N92-23143 Stanford Univ., CA.
LASERS WITHOUT INVERSION: THEORY AND EXPERIMENT Ph.D. Thesis
Atac Imamoglu 1991 161 p
Avail: Univ. Microfilms Order No. DA9206788

The theory of a class of laser systems that do not require atomic population inversion is presented. These laser systems use a quantum interference that is destructive for steady state absorption and constructive for emission, and which is transient in nature. Two types of inversionless laser schemes based on such an interference are described. The first one uses a natural transparency that is created by the interference between two close lying radiatively broadened states. The second one uses a coupling field that creates interfering dressed states. This interference gives nonreciprocal emission and absorption line shapes, with a complete cancellation of absorption at the two photon resonance frequency. Although steady state operation requires the domination of lifetime broadening, lasing without inversion in any atomic basis is possible, provided that there is an inversion in the modes of the pumping radiation field. The cancellation of absorption using a coupling field, which is termed as electromagnetically induced transparency, has applications in other electromagnetic devices. The first demonstration is described of an electromagnetically induced transparency in Sr. Dissert. Abstr.

N92-23557*# National Aeronautics and Space Administration. Langley Research Center, Hampton, VA.
ANALYSIS AND DEVELOPMENT OF DYNAMIC SELECTION OF LASER ARRAY ELEMENTS
M. D. Williams May 1992 11 p
(NASA-TM-4375; L-17043; NAS 1.15:4375) Avail: NTIS HC/MF A03 CSCL 20E

The transmission of large amounts of power in space by laser beam (diode lasers, in particular) requires an array of lasers to increase total power. Concentration of the beam requires some degree of coherence. Temporal coherence can be obtained by locking amplifiers to a master oscillator. However, spatial coherence is not so easily created or maintained. Many mechanical, thermal, and electrical factors oppose it continually. A very simple method is described for creating and maintaining a degree of spatial coherence by simply turning selected diodes ON or OFF. The degree of coherence can be chosen; the greater the coherence, the larger is the number of lasers required for a given power and the longer the lifetime of the array. An experiment for analyzing performance, verifying theory, and evaluating critical parameters is also proposed. Author

N92-23570# Lawrence Livermore National Lab., CA.
LIMITS OF SURVIVABILITY AND DAMAGE FOR OPTICAL COMPONENTS USED IN A HIGH REPETITION RATE VISIBLE LASER
J. R. Taylor, C. J. Stolz, and T. G. Sarginson Oct. 1991 14 p Presented at the SPIE International Society for Optical Engineering Meeting, Boulder, CO, 23-25 Oct. 1991
(Contract W-7405-eng-48)
(DE92-006896; UCRL-JC-108069; CONF-911064-2) Avail: NTIS HC/MF A03

An effort is being made to understand the limits of survivability and damage for optical components exposed to a visible laser operating continuously at a high repetition rate over 4 kHz. Results of this work are reported and related to the materials and manufacturing conditions for coatings and substrates as well as defects seen at the surface under laser illumination. These results were obtained for a variety of optical coatings and conditions using lasers from the Laser Demonstration Facility, part of the Atomic Vapor Laser Isotope Separation (AVLIS) Program at LLNL. Better understanding of the reliability of optical components in this environment could lead to improvements in design and manufacture that would result in reduced size for the laser optical system and correspondingly lower costs for the facilities that can use this technology. DOE

N92-23571# Lawrence Livermore National Lab., CA.
VACUUM MECHATRONIC LASER ALIGNMENT SYSTEM ON THE NOVA LASER
M. Holliday, K. Wong, and R. Shelton Nov. 1991 15 p Presented

at the IEEE Nuclear Science Symposium, Santa Fe, NM, 5-9 Nov. 1991
(Contract W-7405-eng-48)
(DE92-006898; UCRL-JC-108752; CONF-911106-65) Avail: NTIS HC/MF A03

The experiments conducted on NOVA are done to investigate inertially confined laser fusion reactions. To this end, the ten beams of the laser are aligned to within 30 mm. The target chamber employs a vacuum mechatronic based reticle/target positioning system to accomplish this. It is a five degree-of-freedom chamber resident system, known as the Alignment Aids Positioner (AAP). The AAP aids in beam and diagnostic alignment by accurately positioning a reticle at target chamber center to within 7 mm. The AAP system increases target positioning and alignment flexibility and accuracy through the use of a computer controlled multi degree-of-freedom stage assembly. This device uses microstepping DC stepper motors with encoders to achieve closed loop control in a 10(exp -6) torr vacuum. The AAP has two positioning regimes to move the alignment reticle and do beam alignment. One is course positioning in the Y-Z plane that moves a high resolution stage assembly to target chamber center. The other regime is high resolution movement in the X,Y,Z and q directions. DOE

N92-23687 Stanford Univ., CA.
THE PRINCIPLE AND DESIGN OF A HIGH-EFFICIENCY FREE-ELECTRON LASER Ph.D. Thesis
Adrian Hsiu-Tze Ho 1991 169 p
Avail: Univ. Microfilms Order No. DA9205647

Free electron lasers (FELs) are widely tunable sources of coherent radiation in which the radiation is generated by extracting energy from a beam of relativistic electrons. The extraction efficiency of an FEL is defined as the ratio between the generated radiation power and the power on the relativistic electron beam. For practical parameter values, both theory and experiment show that efficiencies are limited to order 1 pct. in standard FELs. A design is proposed to achieve efficiencies far greater than those attainable in standard FELs. In the high efficiency FEL proposed, this problem is overcome by applying an accelerating microwave field to the electrons as they pass through the wiggler, thereby maintaining them at constant energy. A goal is to analyze FEL performance when an accelerating field is compared with the related scheme of using a taper in the wiggler parameters. Another goal is to design a wiggler that not only provides a transverse periodic magnetic field, but is also capable of supporting an accelerating microwave field. Such a structure is proposed and optimized for use in a high efficiency FEL system. Optimization results are given. Author

N92-23723# Allied-Signal Aerospace Co., Kansas City, MO.
IMPROVEMENT OF LASER MACHINING PROCESSES
R. W. Fialko and D. K. Harvey Feb. 1992 15 p
(Contract DE-AC04-76DP-00613)
(DE92-007801; KCP-613-4477) Avail: NTIS HC/MF A03

Laser processing versus steel rule die cutting was evaluated using new fixturing to enhance the processing of flexible and rigid materials. Other enhancements in laser processing reduced carbon deposits from Kapton parts. A special multi-use fixture was designed to enhance laser cutting and save on additional fixturing. This is an example of using different techniques in new ways to improve products. DOE

N92-23891# Rochester Univ., NY. Lab. for Laser Energetics.
ANNUAL REPORT, 1 OCTOBER 1990 - 30 SEPTEMBER 1991
Jan. 1992 233 p
(Contract DE-FC03-85DP-40200)
(DE92-008648; DOE/DP-40200/184) Avail: NTIS HC/MF A11

This report discusses progress in laser fusion; advanced technology developments; national laser users facility news; and a laser system report. DOE

N92-24065# Lawrence Livermore National Lab., CA.
OPTIMIZATION OF THE LASER GLASS COMPOSITION FOR THE NOVA UPGRADE FUSION LASER SYSTEM
M. L. Elder, S. A. Payne, J. H. Campbell, and G. D. Wilke Oct. 1991 6 p Presented at the Advanced Solid-State Lasers Topical Meeting, Santa Fe, NM, 17-19 Feb. 1992
(Contract W-7405-eng-48)
(DE92-008606; UCRL-JC-108475; CONF-920235-2) Avail: NTIS HC/MF A02

The cost and performance of the Nd-doped glass can be optimized with a higher P2O5, lower Al2O3 content, and if certain modifying cations are included in the composition. DOE

N92-24070# Sandia National Labs., Albuquerque, NM.
IN SITU PARTICLE SIZE MEASUREMENTS USING A TWO-COLOR LASER SCATTERING TECHNIQUE
J. C. F. Wang and K. R. Hencken Feb. 1992 21 p Presented at the International Symposium and Workshop on Particulate and Multi-Phase Processes and the 16th Annual Meeting of the Fine Particle Society, Miami Beach, FL, 22-26 Apr. 1985
(Contract DE-AC04-76DR-00789)
(DE92-008634; SAND-85-8869; CONF-850406-15) Avail: NTIS HC/MF A03

We have developed a technique using light scattered from individual particles in the near-forward direction to measure particle size in the range of 10 to 200 microns. This technique uses the Mie scattering theory to relate the measured light intensity to particle size based on calibration techniques employing pinholes and water droplets of known size. We have applied a unique two-color optical arrangement to minimize the edge effect which can cause incorrect size measurements for particles that pass through the edge of the laser beam focal volume. In this paper we describe our experimental technique and the results of size measurements obtained with this technique for water droplets and pulverized coal particles. DOE

N92-23961*# Howard Univ., Washington, DC.
INJECTION SEEDING OF A Q-SWITCHED ALEXANDRITE LASER: STUDY OF FREQUENCY STABILIZATION
Lamarr A. Brown *In* NASA. Goddard Space Flight Center, Summer Graduate Research Program for Interns in Science and Engineering 24 Mar. 1992 19 p (For primary document see N92-23958 14-99)
Avail: NTIS HC/MF A12 CSCL 20E

37 MECHANICAL ENGINEERING

Includes auxiliary systems (nonpower); machine elements and processes; and mechanical equipment.

N92-23152# Helsinki Univ. of Technology, Espoo (Finland). Lab. of Machine Design.
OIL LUBRICATED AND WATER LUBRICATED PIN-ON-DISC WEAR TESTS WITH ENGINEERING CERAMICS
P. Salonen, P. Andersson, and P. Lintula 11 Nov. 1990 71 p Prepared in cooperation with Technical Research Centre of Finland, Espoo; and Tampere Univ. of Technology, Finland
(PB92-136563; ISBN-951-22-0391-X; C-228) Avail: NTIS HC/MF A04 CSCL 13I

Friction and wear tests with ceramics and steels, lubricated with oil and with water, were carried out using a sliding spherical pin-on-disc geometry. In parallel with the sliding tests, the materials of the specimens were characterized by mechanical testing and physical analysis methods. The ceramics studied were aluminas, zirconia toughened alumina (ZTA), MgO - partially stabilized zirconia (PSZ), silicon carbides, and SiAlON. In the oil lubricated tests, the stable coefficient of friction was in the range mu = 0.09 - 0.19 for each of the sliding pairs. The wear rates were generally small and within three orders of magnitude when compared with each other and with steel sliding on steel. For all the material combinations studied, the dominating wear mechanism was a mild polishing of the sliding surfaces. The oil seems to have prevented major chemical interactions from occurring. A minor transfer of steel to alumina and ZTA, and the formation of surface layers on

steel pins slid on silicon-based ceramics were, however, observed. GRA

N92-23158 West Virginia Univ., Morgantown.
AUTOMATED SYNTHESIS OF ROBOT ARM MOTION FOR ROBOT ARM COLLISION AVOIDANCE Ph.D. Thesis
Tak-Lai Daryl Luk 1991 224 p
Avail: Univ. Microfilms Order No. DA9203855

The development is considered of a basic tool for automatic robot motion planning. Research is on the robot arm motion planning for robot arm collision avoidance. A free space generator is developed to generate the Cartesian free space of a two link robot. Given the kinematic parameters and workcell information for a two link revolute robot, the Cartesian free space can be generated with respect to each workcell obstacle. Obstacles can be convex or concave. A final free space is obtained by performing an intersection operation on all the generated free spaces with the use of a 'stack of free spaces' concept. The final free space is then transformed into two graphs: an abstract graph and a free space graph. Graph searching techniques will be used to search for a collision free path from those two graphs. The collision free path can also be optimized, as a user option, to obtain the minimum distance collision free path. A collision avoidance path planner is implemented, which has the computational capability to determine a collision free path and the graphical capability to dynamically simulate a collision free robot motion on the computer screen of a Silicon Graphics Personal IRIS Workstation. Dissert. Abstr.

N92-23177# Allied-Signal Aerospace Co., Kansas City, MO.
Nd: YAG LASER WELDING ALUMINUM ALLOYS
Edgar Jimenez, Jr. Feb. 1992 9 p Presented at the International Conference on Lasers and Applications, San Diego, CA, 8-13 Dec. 1991
(Contract DE-AC04-76DP-00613)
(DE92-003131; KCP-613-4675; CONF-911296-3) Avail: NTIS HC/MF A02

Autogenous Nd:YAG laser welding wrought 4047, 1100, 3003, 2219, 5052, 5086, 5456, and 6061 and cast A356 aluminum alloys to cast A356 aluminum alloy in restrained annular weld joints was investigated. The welds were 12.7 mm (0.375 in.) and 9.5 mm (0.375 in.) diameter with approximately 0.30 mm (0.012 in.) penetration. This investigation determined 4047 aluminum alloy to be the optimum alloy for autogenous Nd:YAG laser welding to cast A356 aluminum alloy. This report describes the investigation and its results. DOE

N92-23226*# National Aeronautics and Space Administration. Lewis Research Center, Cleveland, OH.
NUMERICAL EXPERIMENTS WITH FLOWS OF ELONGATED GRANULES
Harold G. Elrod (Elrod, Harold G., Old Saybrook, CT) and David E. Brewe 1992 10 p Presented at the Leeds-Lyon Symposium, Lyon, France, 3-6 Sep. 1991
(DA Proj. 1L1-61102-AH-45)
(NASA-TM-105567; E-6891; NAS 1.15:105567; AVSCOM-TR-91-C-006) Avail: NTIS HC/MF A02 CSCL 20D

Theory and numerical results are given for a program simulating two dimensional granular flow (1) between two infinite, counter-moving, parallel, roughened walls, and (2) for an infinitely wide slider. Each granule is simulated by a central repulsive force field ratcheted with force restitution factor to introduce dissipation. Transmission of angular momentum between particles occurs via Coulomb friction. The effect of granular hardness is explored. Gaps from 7 to 28 particle diameters are investigated, with solid fractions ranging from 0.2 to 0.9. Among features observed are: slip flow at boundaries, coagulation at high densities, and gross fluctuation in surface stress. A videotape has been prepared to demonstrate the foregoing effects. Author

N92-23377*# National Aeronautics and Space Administration. Goddard Space Flight Center, Greenbelt, MD.
HIGH RELIABILITY ROBOT FRIENDLY ORU INTERFACE Patent Application
George M. Voellmer, inventor (to NASA) 7 Oct. 1991 25 p
(NASA-Case-GSC-13360-1; NAS 1.71:GSC-13360-1; US-Patent-Appl-SN-772200) Avail: NTIS HC/MF A03 CSCL 13I

Presented here is a robot friendly coupling device for an orbital replacement unit (ORU). The invention will provide a coupling that is detached and attached remotely by a robot. The design of the coupling must allow for slight misalignments, over-torque protection, and precision placement. This is accomplished by means of a triangular interface comprising three components. A base plate assembly is located on an attachment surface, such as a satellite. The base plate assembly has a cup member, a slotted member, and a post member. The ORU that the robot attaches to the base plate assembly has an ORU plate assembly with two cone members and a post member which mate to the base plate assembly. As the two plates approach one another, one cone member of the ORU plate assembly has to be placed accurately enough to fall into the cup member of the base plate assembly. The cup member forces alignment until a second cone falls into a slotted member which provides final alignment. A single bolt is used to attach the two plates. Two deflecting plates are attached to the backs of the plates. When pressure is applied to the center of the deflecting plates, the force is distributed preventing the ORU and base plates from deflecting. This accounts for precision in the placement of the article. The novelty is believed to reside in using deflecting plates in conjunction with kinematic mounts to provide distributed forces to the two members. NASA

N92-23378*# National Aeronautics and Space Administration. Goddard Space Flight Center, Greenbelt, MD.
RETRACTABLE TOOL BIT HAVING LATCH TYPE CATCH MECHANISM Patent Application
George Voellmer, inventor (to NASA) 22 Nov. 1991 15 p
(NASA-Case-GSC-13359-1; NAS 1.71:GSC-13359-1; US-Patent-Appl-SN-796496) Avail: NTIS HC/MF A03 CSCL 13I

A retractable tool bit assembly for a tool such as an allen key is presented. The assembly includes one or more spring loaded nestable or telescoping tubular sections together with a catch mechanism for capturing and holding the tool in its retracted position. The catch mechanism consists of a latch mechanism located in a base section and which engages a conically shaped tool head located at the inner end of the tool. The tool head adjoins an eccentric oval type neck portion which extends to a rear lip of the tool head. The latch mechanism releases when the ovular neck portion rotates about the catch members upon actuation of a rotary tool drive motor. When released, all the telescoping sections and the tool extends fully outward to a use position. NASA

N92-23435*# National Aeronautics and Space Administration. Lewis Research Center, Cleveland, OH.
HIGH TEMPERATURE DYNAMIC ENGINE SEAL TECHNOLOGY DEVELOPMENT
Bruce M. Steinetz, Christopher DellaCorte, Michael Machinchick, Rajakkannu Mutharasan, Guang-Wu Du, Frank Ko, Paul J. Sirocky, and Jeffrey H. Miller (Sverdrup Technology, Inc., Brook Park, OH.) 1992 24 p Presented at the National Aerospace Plane Mid-Term Technology Review, Monterey, CA, 20-24 Apr. 1992
(NASA-TM-105641; E-6945; NAS 1.15:105641) Avail: NTIS HC/MF A03 CSCL 13I

Combined cycle ramjet/scramjet engines being designed for advanced hypersonic vehicles, including the National Aerospace Plane (NASP), require innovative high temperature dynamic seals to seal the sliding interfaces of the articulated engine panels. New seals are required that will operate hot (1200 to 2000 F), seal pressures ranging from 0 to 100 psi, remain flexible to accommodate significant sidewall distortions, and resist abrasion over the engine's operational life. This report reviews the recent high temperature durability screening assessments of a new braided rope seal concept, braided of emerging high temperature materials, that shows promise of meeting many of the seal demands of hypersonic engines. The paper presents durability data for: (1)

the fundamental seal building blocks, a range of candidate ceramic fiber tows; and for (2) braided rope seal subelements scrubbed under engine simulated sliding, temperature, and preload conditions. Seal material/architecture attributes and limitations are identified through the investigations performed. The paper summarizes the current seal technology development status and presents areas in which future work will be performed. Author

N92-23459# Oak Ridge National Lab., TN.
DESIGN OF AN OMNIDIRECTIONAL AND HOLONOMIC WHEELED PLATFORM PROTOTYPE
S. M. Killough and F. G. Pin 1991 15 p Presented at the IEEE International Conference on Robotics and Automation, Nice, France, 10-15 May 1992
(Contract DE-AC05-84OR-21400)
(DE92-000046; CONF-920540-7) Avail: NTIS HC/MF A03

This paper presents the concepts for a new family of wheeled platforms which feature full omnidirectionality with simultaneous and independent rotational and translational motion capabilities. We first describe the original 'orthogonal-wheels assembly' on which these platforms are based and discuss how a combination of these assemblies is used to generate an omnidirectional capability. The design and control of a prototype platform developed to test and demonstrate the proposed concepts is then described, and experimental results illustrating the full omnidirectionality of the platform with decoupled rotational and translational degrees of freedom are presented. DOE

N92-23536*# National Aeronautics and Space Administration. Lewis Research Center, Cleveland, OH.
CONTACT STRESSES IN MESHING SPUR GEAR TEETH: USE OF AN INCREMENTAL FINITE ELEMENT PROCEDURE
Chih-Ming Hsieh, Ronald L. Huston (Cincinnati Univ., OH.), and Fred B. Oswald Mar. 1992 22 p
(Grant NSG3-188; DA Proj. 1L1-62211-A-47A)
(NASA-TM-105388; E-6776; NAS 1.15:105388;
AVSCOM-TR-90-C-029) Avail: NTIS HC/MF A03 CSCL 13K

Contact stresses in meshing spur gear teeth are examined. The analysis is based upon an incremental finite element procedure that simultaneously determines the stresses in the contact region between the meshing teeth. The teeth themselves are modeled by two dimensional plain strain elements. Friction effects are included, with the friction forces assumed to obey Coulomb's law. The analysis assumes that the displacements are small and that the tooth materials are linearly elastic. The analysis procedure is validated by comparing its results with those for the classical two contacting semicylinders obtained from the Hertz method. Agreement is excellent. Author

N92-23544*# National Aeronautics and Space Administration. Lyndon B. Johnson Space Center, Houston, TX.
ROBOT-FRIENDLY CONNECTOR Patent Application
George F. Parma, inventor (to NASA), Mark H. Vandeberghe, inventor (to NASA), and Steve C. Ruiz, inventor (to NASA) (Lockheed Corp., Houston, TX.) 26 Nov. 1991 32 p
(NASA-Case-MSC-21864-1; NAS 1.71:MSC-21864-1;
US-Patent-Appl-SN-799460) Avail: NTIS HC/MF A03 CSCL 13I

Robot friendly connectors, which, in one aspect are truss joints with two parts, a receptacle and a joint, the joint having a head which is loosely inserted into the receptacle and is then tightened and aligned; in one aspect, the head is a rounded hammerhead which initially is enclosed in the receptacle with sloppy fit provided by the shape, size and configuration of surfaces on the head and on the receptacle. NASA

N92-23547*# National Aeronautics and Space Administration. Goddard Space Flight Center, Greenbelt, MD.
CLIMBING ROBOT Patent Application
James Kerley, inventor (to NASA), Edward May, inventor (to NASA), and Wayne Ecklund, inventor (to NASA) 10 Feb. 1992 35 p
(NASA-Case-GSC-13442-1; NAS 1.71:GSC-13442-1;
US-Patent-Appl-SN-843861) Avail: NTIS HC/MF A03 CSCL 13I

A mobile robot for traversing any surface consisting of a number of interconnected segments, each interconnected segment having an upper 'U' frame member, a lower 'U' frame member, a compliant joint between the upper 'U' frame member and the lower 'U' frame member, a number of linear actuators between the two frame members acting to provide relative displacement between the frame members, a foot attached to the lower 'U' frame member for adherence of the segment to the surface, an inter-segment attachment attached to the upper 'U' frame member for interconnecting the segments, a power source connected to the linear actuator, and a computer/controller for independently controlling each linear actuator in each interconnected segment such that the mobile robot moves in a caterpillar like fashion. NASA

N92-23548*# National Aeronautics and Space Administration. Goddard Space Flight Center, Greenbelt, MD.
HELIX TRANSLATION DEVICE Patent Application
M. Bruce Milam, inventor (to NASA) and Philip Studer, inventor (to NASA) 4 Sep. 1991 21 p
(NASA-Case-GSC-13141-1; NAS 1.71:GSC-13141-1;
US-Patent-Appl-SN-754875) Avail: NTIS HC/MF A03 CSCL 13I

This invention places a single flat shim, wound into a helical coil, above and below an object to be moved which has a 'transition area' between its upper and lower surface. This 'transition area' allows the helix shim to 'transition' from the top surface of the object to the bottom surface of the object. The 'transition' of the shim is to be accomplished by holding the object steady and rotating the helix shim. When the helix shim is rotated clockwise, the shim will 'transition' from the upper surface of the object to the lower surface of the object at a rate of one shim thickness for every 360 degrees of rotation. The object will then be raised by very fine increments. The invention is a unique rotary to linear motion device capable of continuously variable output displacement and restraint of large loads. The load capacity is large because it relies on compressive rather than shear strength. A continuous rather than incremental output is provided. NASA

N92-23553*# National Aeronautics and Space Administration. Pasadena Office, CA.
CONFIGURATION CONTROL OF SEVEN-DEGREE-OF-FREEDOM ARMS Patent Application
Homayoun Seraji, inventor (to NASA), Mark K. Long, inventor (to NASA), and Thomas S. Lee, inventor (to NASA) (Jet Propulsion Lab., California Inst. of Tech., Pasadena.) 11 Mar. 1992 47 p
(Contract NAS7-918)
(NASA-Case-NPO-18607-1-CU; NAS 1.71:NPO-18607-1-CU;
US-Patent-Appl-SN-849629) Avail: NTIS HC/MF A03 CSCL 13I

A seven degree of freedom robot arm with a six degree of freedom end effector is controlled by a processor employing a 6 by 7 Jacobian matrix for defining location and orientation of the end effector in terms of the rotation angles of the joints, a 1 (or more) by 7 Jacobian matrix for defining 1 (or more) user specified kinematic functions constraining location or movement of selected portions of the arm in terms of the joint angles, the processor combining the two Jacobian matrices to produce an augmented 7 (or more) by 7 Jacobian matrix, the processor effecting control by computing in accordance with forward kinematics from the augmented 7 by 7 Jacobian matrix and from the seven joint angles of the arm a set of seven desired joint angles for transmittal to the joint servo loops of the arm. One of the kinematic functions constraints the orientation of the elbow plane of the arm. Another one of the kinematic functions minimizes a sum of gravitational torques on the joints. Still another kinematic function constrains the location of the arm to perform collision avoidance. Generically, one kinematic function minimizes a sum of selected mechanical parameters of at least some of the joints associated with weighting coefficients which may be changed during arm movement. The

mechanical parameters may be velocity errors or gravity torques associated with individual joints. NASA

N92-23564*# National Aeronautics and Space Administration. Lewis Research Center, Cleveland, OH.
NIST TORSION OSCILLATOR VISCOMETER RESPONSE: PERFORMANCE ON THE LeRC ACTIVE VIBRATION ISOLATION PLATFORM
Robert F. Berg (National Inst. of Standards and Technology, Gaithersburg, MD.) and Carlos M. Grodsinsky Mar. 1992 20 p
(NASA-TM-105571; E-6896; NAS 1.15:105571) Avail: NTIS HC/MF A03 CSCL 20K

Critical point viscosity measurements are limited to their reduced temperature approach to T(sub c) in an Earth bound system, because of density gradients imposed by gravity. Therefore, these classes of experiments have been proposed as good candidates for 'microgravity' science experiments where this limitation is not present. The nature of these viscosity measurements dictate hardware that is sensitive to low frequency excitations. Because of the vibratory acceleration sensitivity of a torsion oscillator viscometer, used to acquire such measurements, a vibration isolation sensitivity test was performed on candidate 'microgravity' hardware to study the possibility of meeting the stringent oscillatory sensitivity requirements of a National Institute of Standards and Technology (NIST) torsion oscillator viscometer. A prototype six degree of freedom active magnetic isolation system, developed at NASA Lewis Research Center, was used as the isolation system. The ambient acceleration levels of the platform were reduced to the noise floor levels of its control sensors, about one microgravity in the 0.1 to 10 Hz bandwidth. Author

N92-23595# Environmental Protection Agency, Ann Arbor, MI. Control Technology and Applications Branch.
EVALUATION OF RESEARCH PROTOTYPE VEHICLES EQUIPPED WITH DIRECT INJECTION 2-STROKE CYCLE ENGINES
K. H. Hellman, G. K. Piotrowski, and R. M. Schaefer Jan. 1992 41 p
(PB92-143692; EPA/AA/CTAB-92/01) Avail: NTIS HC/MF A03 CSCL 13I

The exhaust emissions and fuel economy results are described from two prototype vehicles powered by state-of-the-art two-stroke cycle engines. These vehicles were tested over the Federal Test Procedure (FTP) and Highway Fuel Economy Test (HFET) cycles; the sampling process included the measurement of particulate emissions. A description is included of the test vehicles and engines, the tests and procedures used, future efforts, and appendices containing detailed individual test results for both vehicles. Author

N92-23680# Acurex Corp., Mountain View, CA. Environmental Systems Div.
WHITE PAPER: PRELIMINARY ASSESSMENT OF LNG VEHICLE TECHNOLOGY, ECONOMICS, AND SAFETY ISSUES Topical Report, Apr. - Aug. 1991
C. Powars, D. Luscher, C. Moyer, and L. Browning 6 Nov. 1991 86 p
(Contract GRI-5091-292-2153)
(PB92-137603; GRI-91/0347) Avail: NTIS HC/MF A05 CSCL 13I

The potential is evaluated of Liquid Natural Gas (LNG) as a vehicle fuel, to determine market niches, and to identify needed technology improvements. A preview is presented of the study direction, preliminary conclusions, and initial recommendations. Interim findings relative to LNG vehicle technology, economics, and safety are presented. It is important to decide if heavier hydrocarbons should be allowed in LNG vehicle fuel. Development of suitable refueling couplings and vehicle fuel supply pressure systems are recommended. Initial economics analyses considered transit buses and pickup and delivery trucks fueled via onsite liquifiers and imported LNG. Net user costs were more than (but in some cases close to) those for diesel fuel and gasoline. Lowering the cost of small scale liquefiers would significantly improve the economics of LNG vehicles. New emissions regulations may introduce considerations beyond simple cost comparisons. LNG vehicle safety and available accident data are reviewed. Consistent codes for LNG vehicles and refueling facilities are needed. Author

N92-23690 Georgia Inst. of Tech., Atlanta.
THE DESIGN AND CONTROL OF UNCERTAIN MANIPULATOR ARMS WITH DECOUPLED INERTIA MATRIX Ph.D. Thesis
Xing Zhao 1991 154 p
Avail: Univ. Microfilms Order No. DA9206120

The complexity and nonlinearity of manipulator arm dynamics, as well as the existence of uncertainties during the manufacture and operation of the arms make their control very difficult, especially their on-line control. Three areas of control are examined: structural design, controller design, and a design example. Reducing the model complexity through structural design is a fundamental method. The standard form is introduced of the transmission and the concept of time-invariant transmission. Then, the transmission for n-link spatial arms is designed such that the inertia matrix of their model can be decoupled. Based on this transmission, the necessary and sufficient conditions for the inertia matrix to be decoupled are given. Finally, these results are extended to cover closed loop arms. Feedback linearization technique is extended to deal with uncertain nonlinear model of manipulator arms. The upper bounds for the nonlinear uncertainties are computed based on assumed command trajectories. Since the method to design a mu controller for the uncertain nonlinear model of manipulator arms is a systematic one, a series of steps for such design work are given through two examples which offer mu controllers for an inverted pendulum with uncertain pendulum mass and a 12 link arm with the presence of mass uncertainties of both links. Dissert. Abstr.

N92-23691 Cornell Univ., Ithaca, NY.
THE STATICS, DYNAMICS, AND CONTROL OF THE ELASTICARM: A CONTINUOUS BEAM MANIPULATOR Ph.D. Thesis
Chen-Kee Yuan 1991 174 p
Avail: Univ. Microfilms Order No. DA9204026

In conventional design, robots are usually composed of rigid massive links, and hence have low payload to self weight ratios. A complete study is presented on an innovative robot design idea: the elasticarm, which uses a continuous, flexible beam as the arm of the manipulator. In the static analysis, a thorough discussion on the formulation and solution of the associated elastica problem is presented. Accordingly, the working space of the elasticarm robot is obtained, and the possible configurations of the elasticarm are examined. To study the dynamics of this flexible arm robot, two prototypes were built. In the first, a manually controlled elasticarm is built and an initial experiment is conducted to look into the dynamic behavior of the proposed robot. The equations of motion for small amplitude vibration of a prestressed curved rod are presented. Good agreement between the simulation and experimental results is obtained. Next, a fully computerized elasticarm robot is realized. The dynamics of this robot is carefully studied and a first attempt on the vibration control of this robot is achieved through the implementation of a simple, straightforward constant gain feedback controller. Dissert. Abstr.

N92-23710# Helsinki Univ. of Technology, Espoo (Finland). Inst. of Energy Engineering.
MATHEMATICAL MODEL OF A CONTROL VALVE Ph.D. Thesis
J. Pyoetsiae 8 Nov. 1991 90 p
(PB92-141951; ISBN-951-22-0762-1) Avail: NTIS HC/MF A05 CSCL 13K

The aim was to develop a mathematical model describing a quarter-turn control valve installed into a process pipeline. In forming the model, the main goal was an accurate description of control valve dynamics, paying attention to the construction of the control valve because the main applications of the model are in product development and research work. The core of the work

is a differential equation describing the dynamics of an installed quarter-turn control valve. The differential equation includes the pressures affecting both sides of the actuator piston; the pressures are solved from the mathematical models describing positioner and actuator thermodynamics. The valve load is formed by seat friction, gland packing friction, bearing frictions, and dynamic torque of the valve. To solve these, a mathematical model is needed as a function of valve travel and pressure differential across the valve. Because the pressure differential across the valve changes considerably (especially with great travel changes), a dynamic model for pipeline flow is also needed. A simulation model was formed from the control valve mathematical model and this simulation model was the basis for the C-language simulation program. The simulation program was tested by comparing responses that were measured for one manufacturer's control valve and calculated by the simulation program. Author

N92-23727 Iowa State Univ. of Science and Technology, Ames.
ANALYSIS AND CONTROL OF NONLINEAR FLEXIBLE MANIPULATOR Ph.D. Thesis
Liang Tang 1991 107 p
Avail: Univ. Microfilms Order No. DA9126255

Investigated here are the approximation techniques and instability for nonlinear one-link and two-link flexible manipulators operating in a vertical plane. The flexible components of the arms are modeled by Euler-Bernoulli theory, and the nonlinearity arises due to gravitation and large angle rotation. Two different methods are used for describing the deformation of the flexible members. They are the infinite dimensional coordinates and finite-dimensional coordinates. Variational principle is used to generate the governing differential equations and boundary conditions. The distributed coordinate approach results in partial differential equations, and the Ritz approximation leads to nonlinear ordinary differential equations. The two sets of differential equations are developed in parallel to give a comparison of the static solution and frequency domain characteristics. Furthermore, the full nonlinear ordinary differential equations are integrated forward numerically for the dynamic response to maneuver transient reference inputs.
Dissert. Abstr.

N92-23739 Ohio State Univ., Columbus.
CONCEPTION AND DEVELOPMENT OF IMPROVED ANALYTICAL PREDICTION MODELS FOR FATIGUE INDUCED TOOTH BREAKAGE DUE TO CYCLIC BENDING IN SPUR GEAR TEETH Ph.D. Thesis
Steve Daniewicz 1991 227 p
Avail: Univ. Microfilms Order No. DA9130461

An analytical prediction model for bending fatigue of spur gear teeth which characterizes bending fatigue as a two stage process is considered. The modelling of fatigue crack initiation, the first stage of bending fatigue, is discussed. Modelling of fatigue crack propagation, the second stage of bending fatigue, is performed by employing an elastic-plastic description of a growing fatigue crack. The model considers plasticity induced fatigue crack closure in the presence of residual stress fields, and is based on the Dugdale model, modified to leave plastically deformed material along the crack surfaces as the crack advances. To allow implementation of the model to cracked spur gear teeth under static mesh loading, the effect of a pinion crack on pinion tooth loading is investigated analytically in a static spur gear mesh model which considers contact off the line of action. The stiffness of a cracked spur gear tooth is predicted, and is a function of the mode I and mode II stress intensity factors for the cracked tooth. Stress intensity factors for cracked spur gear teeth are obtained through application of the Bueckner weight function, in conjunction with spur gear tooth stress fields computed through a conformal mapping of the tooth onto an elastic half-plane. Stress intensity factors for cracked spur gear teeth computed using the conformal mapping and weight function compare well with finite element predictions when cracks are small. The elastic-plastic fatigue crack propagation model is used to predict fatigue crack propagation in a carburized and shot peened steel spur gear during a single tooth fatigue test, and comparisons are made with existing experimental data. Dissert. Abstr.

N92-23779# National Aerospace Lab., Tokyo (Japan). Space Technology Research Group.
SLIDING FRICTION TEST OF SELF LUBRICATING POLYMER COMPOSITES FOR ROLLING BEARING RETAINER [KUFT KORO GARI JIKUUKE HOJIKI YO JIKOJUNKATSUSEI KOBUNSHI FU KUGOZAI NO SUBERI MASATSU SHIKEN]
Makoto Nishimura Jun. 1990 17 p In JAPANESE
(NAL-TM-622; ISSN-0452-2982; JTN-92-80310) Avail: NTIS HC/MF A03

Most drive mechanisms onboard artificial satellites are equipped with solid lubricating rolling bearings which use both solid lubricating films and self lubricative composite retainers. In the United States, a combination of PTFE (Poly Tetra FluoroEthylene) polymer composites and molybdenum disulfide sputtered film predominate as rolling bearing materials for aerospace uses. In this paper, sliding friction characteristics of solid lubricative films, such as films of gold, silver, lead, PTFE and molybdenum disulfide were studied. It was proved that lubricative characteristics of molybdenum disulfide sputtered film exhibited the best performance in vacuum. Next, various rolling bearings made from PTFE films, molybdenum disulfide sputtered films and polymer composites were tested. It was shown that a combination of molybdenum disulfide sputtered films and PTFE composites gave the performance of low friction and long life, and had a life of over 10,000 hr at operational speeds of 2,000 rpm. Author (NASDA)

N92-23896# Kansas State Univ., Manhattan.
KANSAS STATE UNIVERSITY ELECTRIC VEHICLE SITE OPERATOR PROGRAM
J. R. Hague, R. A. Steinert, and T. Nissen-Pfrang 1991 19 p
(Contract DE-FC07-91ID-13074)
(DE92-008425; DOE/ID-13074/T2) Avail: NTIS HC/MF A03

Kansas State University is presently working with Grumman Allied and Unique Mobility to establish a working agreement for the research and development of a pure electric postal vehicle. K-State has worked on the design of this vehicle for the past year and is working to establish the appropriate consortium to bring this vehicle to commercial realization. K-State is working to establish infrastructure support for electric vehicles. Presently, a Kansas company is working with K-State to bring its patented low-cost vehicle metering product to market. An anticipated second year DOE project would provide 100 electric metering stations to Southern California for a large scale electric vehicle infrastructure demonstration project. This project would allow a parking lot(s) to be made EV ready. K-State's Site Operator Program continues to get the 'word-out' about electric vehicles. From a personal visit by Senator Bob Dole, to corporate board of director meetings, to school classrooms, to shopping mall demonstrations, K-State Employees are increasing public access and awareness about the electric vehicle industry. As has been shown in this report, K-State's G-Van has logged an average eighteen miles per day while maintaining a full schedule of public relations tours within the state of Kansas and Missouri. K-State has now been contacted by companies in Nebraska and Iowa requesting information and involvement in this program. Kansas and Kansas State will continue its work to contribute to the Site Operator Program effort. With the purchase of two additional electric vehicles and the pending request to purchase two more electric vehicles during the next contractual year, K-States' program will grow. When vehicle development plans and infrastructure requirements are solidified, K-State's program will be ready to participate and be a major contributor to the development and introduction of this technology. DOE

N92-23908# Oak Ridge Y-12 Plant, TN.
REAL-TIME MEASUREMENT OF ELECTRON BEAM WELD PENETRATION IN URANIUM BY ACOUSTIC EMISSION MONITORING
J. W. Whittaker and J. L. Murphy Jul. 1991 7 p Presented at the 4th World Meeting on Acoustic Emission, Boston, MA, 16-19

Sep. 1991
(Contract DE-AC05-84OS-21400)
(DE92-008040; Y/DW-1053; CONF-9109348-1) Avail: NTIS HC/MF A02

High quality electron beam (EB) welds are required in uranium test articles. Acoustic emission (AE) techniques are under development with the goal of measuring weld penetration in real-time. One technique, based on Average Signal Level (ASL) measurement was used to record weld AE signatures. Characteristic AE signatures were recorded for bead-on-plate (BOP) and butt joint (BJ) welds made under varied welding conditions. AE waveforms were sampled to determine what microscopic AE behavior led to the observed macroscopic signature features. Deformation twinning and weld expulsion are two of the main sources of emission. AE behavior was correlated with weld penetration as measured by standard metallographic techniques. The ASL value was found to increase approximately linearly with weld penetration in BJ welds. These results form the basis for a real-time monitoring technique for weld penetration. DOE

N92-24042*# National Aeronautics and Space Administration. Pasadena Office, CA.
CONTROLLING FLEXIBLE ROBOT ARMS USING A HIGH SPEED DYNAMICS PROCESS Patent Application
Abhinandan Jain, inventor (to NASA) and Guillermo Rodriguez, inventor (to NASA) (Jet Propulsion Lab., California Inst. of Tech., Pasadena.) 3 Apr. 1992 65 p
(Contract NAS7-918)
(NASA-Case-NPO-18499-1-CU; NAS 1.71:NPO-18499-1-CU; US-Patent-Appl-SN-862861) Avail: NTIS HC/MF A04 CSCL 13I

Described here is a robot controller for a flexible manipulator arm having plural bodies connected at respective movable hinges, and flexible in plural deformation modes. It is operated by computing articulated body qualities for each of the bodies from the respective modal spatial influence vectors, obtaining specified body forces for each of the bodies, and computing modal deformation accelerations of the nodes and hinge accelerations of the hinges from the specified body forces, from the articulated body quantities and from the modal spatial influence vectors. In one embodiment of the invention, the controller further operates by comparing the accelerations thus computed to desired manipulator motion to determine a motion discrepancy, and correcting the specified body forces so as to reduce the motion discrepancy. The manipulator bodies and hinges are characterized by respective vectors of deformation and hinge configuration variables. Computing modal deformation accelerations and hinge accelerations is carried out for each of the bodies, beginning with the outermost body by computing a residual body force from a residual body force of a previous body, computing a resultant hinge acceleration from the body force, and then, for each one of the bodies beginning with the innermost body, computing a modal body acceleration from a modal body acceleration of a previous body, computing a modal deformation acceleration and hinge acceleration from the resulting hinge acceleration and from the modal body acceleration. NASA

N92-24043*# National Aeronautics and Space Administration. Pasadena Office, CA.
CONTROLLING UNDER-ACTUATED ROBOT ARMS USING A HIGH SPEED DYNAMICS PROCESS Patent Application
Abhinandan Jain, inventor (to NASA) and Guillermo Rodriguez, inventor (to NASA) (Jet Propulsion Lab., California Inst. of Tech., Pasadena.) 3 Apr. 1992 41 p
(Contract NAS8-918)
(NASA-Case-NPO-18498-1-CU; NAS 1.71:NPO-18498-1-CU; US-Patent-Appl-SN-866779) Avail: NTIS HC/MF A03 CSCL 13I

The invention controls an under-actuated manipulator by first obtaining predetermined active joint accelerations of the active joints and the passive joint friction forces of the passive joints, then computing articulated body qualities for each of the joints from the current positions of the links, and finally computing from the articulated body qualities and from the active joint accelerations and the passive joint forces, active joint forces of the active joints. Ultimately, the invention transmits servo commands to the active joint forces thus computed to the respective ones of the joint servos. The computation of the active joint forces is accomplished using a recursive dynamics algorithm. In this computation, an inward recursion is first carried out for each link, beginning with the outermost link in order to compute the residual link force of each link from the active joint acceleration if the corresponding joint is active, or from the known passive joint force if the corresponding joint is passive. Then, an outward recursion is carried out for each link in which the active joint force is computed from the residual link force if the corresponding joint is active or the passive joint acceleration is computed from the residual link force if the corresponding joint is passive. Author

N92-24051*# National Aeronautics and Space Administration. Lyndon B. Johnson Space Center, Houston, TX.
QUICK-CONNECT FASTENERS FOR ASSEMBLING DEVICES IN SPACE Patent Application
Clarence J. Wesselski, inventor (to NASA), Erik E. Evenson, inventor (to NASA), and Steve L. Ruiz, inventor (to NASA) (Lockheed Corp., Houston, TX.) 15 Jan. 1992 27 p
(NASA-Case-MSC-21648-1; NAS 1.71:MSC-21648-1; US-Patent-Appl-SN-824806) Avail: NTIS HC/MF A03 CSCL 13I

A quick-connect fastener of a relatively-simple straightforward design is arranged with a tubular body adapted to be engaged against an attachment fitting in coincidental alignment with an opening in that fitting. A tubular collet having flexible finger projecting from its forward end is arranged in the fastener body to be shifted forwardly by an elongated expander member coaxially arranged within the tubular collet for advancing the collet fingers into the opening in the attachment fitting. Biasing means are arranged between the elongated expander member and a rotatable actuator which is threadedly mounted within the tubular collet so as to be rotated for urging the expander member into engagement with the collet fingers. A first coupling member is arranged on the rotatable actuator to be accessible from outside of the fastener so that a second coupling member on the distal end of a flexible shaft can be introduced into the fastener body and coupled to the first coupling member to enable a typical actuating tool coupled to the shaft outside of the fastener body to be operated for advancing the outwardly-enlarged ends of the collet fingers into the opening in the attachment fitting and thereafter rotating the actuator member to expand the fingers to that attachment fitting. Upon expansion of the collet fingers, the biasing means impose a biasing force on the expander to releasably retain the fingers in their latching positions. NASA

N92-24055*# National Aeronautics and Space Administration. Marshall Space Flight Center, Huntsville, AL.
INDUCTION BOILER Patent Application
Glen A. Robertson, inventor (to NASA) 27 Jan. 1992 13 p
(NASA-Case-MFS-28634-1; NAS 1.71:MFS-28634-1; US-Patent-Appl-SN-825895) Avail: NTIS HC/MF A03 CSCL 13I

The invention is directed to a high temperature boiler which utilizes an inductively heated porous, metallic material in which hot fluids or gasses are produced. The invention utilizes an induction coil surrounding the porous, metallic material, and a chamber which contains both the metallic material and the fluid to be heated. An alternating current is passed through the coil as to establish eddy currents in the porous metallic material. The eddy currents create heat within the porous metallic material. This heat is conducted to the fluid as it passes through the porous metallic material. NASA

N92-24058*# National Aeronautics and Space Administration. Goddard Space Flight Center, Greenbelt, MD.
RETRACTABLE TOOL BIT HAVING SLIDER TYPE CATCH MECHANISM Patent Application
George Voellmer, inventor (to NASA) 24 Sep. 1991 14 p

(NASA-Case-GSC-13358-1; NAS 1.71:GSC-13358-1; US-Patent-Appl-SN-765069) Avail: NTIS HC/MF A03 CSCL 13K

A retractable tool bit assembly utilized in connection with a robotic gripper type end-effector is presented. The apparatus includes one or more spring loaded nestable or telescoping tubular sections together with a catch mechanism for capturing and holding the toll, such as an allen key, in its retracted position. The innermost tubular section includes a threshold cap and engages and holds the tool. The catch mechanism consists of a slider type mechanism located adjacent a relatively larger outer base section and includes means for engaging a conically or mushroom shaped rear end portion of the tool when the telescoping sections are moved to a retracted or parked position. The catch mechanism is released upon actuation of a rotary tool drive motor coupled to a circular mount and which holds the base section. When released all the telescoping sections including the tool extends fully outward to a use position. NASA

N92-24059*# National Aeronautics and Space Administration. Goddard Space Flight Center, Greenbelt, MD.
PAGE TURNING SYSTEM Patent Application
James Kerley, inventor (to NASA) and Wayne Ecklund, inventor (to NASA) 24 Dec. 1991 21 p
(NASA-Case-GSC-13415-1; NAS 1.71:GSC-13415-1; US-Patent-Appl-SN-812932) Avail: NTIS HC/MF A03 CSCL 13K

A device for holding reading materials for use by readers without arm mobility is presented. The device is adapted to hold the reading materials in position for reading with the pages displayed to enable turning by use of a rubber tipped stick that is held in the mouth and has a pair of rectangular frames. The frames are for holding and positioning the reading materials opened in reading posture with the pages displayed at a substantially unobstructed sighting position for reading. The pair of rectangular frames are connected to one another by a hinge so the angle between the frames may be varied thereby varying the inclination of the reading material. A pair of bent spring mounted wires for holding opposing pages of the reading material open for reading without substantial visual interference of the pages is mounted to the base. The wires are also adjustable to the thickness of the reading material and have a variable friction adjustment. This enables the force of the wires against the pages to be varied and permits the reader to manipulate the pages with the stick. Author

N92-24060*# National Aeronautics and Space Administration. Goddard Space Flight Center, Greenbelt, MD.
FLEXIBLE ROBOTIC ARM Patent Application
Israel A. Moya, inventor (to NASA) and Philip A. Studer, inventor (to NASA) 4 Sep. 1991 14 p
(NASA-Case-GSC-13161-1; NAS 1.71:GSC-13161-1; US-Patent-Appl-SN-754828) Avail: NTIS HC/MF A03 CSCL 13I

A plurality of identical modules are serially connected together with each module including a base plate and a top plate interconnected by a ball joint assembly so that the top plate is adapted to pivotally nutate around the base plate to describe a cone in space. An array of twenty-four electromagnets, sequentially energized in sets of three, are arranged in a ring around the periphery of the base plate. Selective energization of the eight sets of electromagnets causes the rim of the top plate to be magnetically attracted to the energized electromagnets. The tilt of the top pivot plate is detected and controlled over a range of 360 degrees, thus permitting a series string of modules to assume any desired elongated configuration. NASA

38 QUALITY ASSURANCE AND RELIABILITY

Includes product sampling procedures and techniques; and quality control.

N92-23189*# National Aeronautics and Space Administration. Lewis Research Center, Cleveland, OH.
DETECTING LAMB WAVES WITH BROAD-BAND ACOUSTO-ULTRASONIC SIGNALS IN COMPOSITE STRUCTURES
Harold E. Kautz Mar. 1992 23 p
(NASA-TM-105557; E-6881; NAS 1.15:105557) Avail: NTIS HC/MF A03 CSCL 14D

Lamb waves can be produced and detected in ceramic matrix composites (CMC) and metal matrix composites (MMC) plates using the acousto-ultrasonic configuration employing broadband transducers. Experimental dispersion curves of lowest symmetric and antisymmetric modes behave in a manner analogous to the graphite/polymer theoretical curves. In this study a basis has been established for analyzing Lamb wave velocities for characterizing composite plates. Lamb wave dispersion curves and group velocities were correlated with variations in axial stiffness and shear stiffness in MMC and CMC. For CMC, interfacial shear strength was also correlated with the first antisymmetric Lamb mode. Author

N92-23258# International Atomic Energy Agency, Vienna (Austria).
TRAINING GUIDELINES IN NON-DESTRUCTIVE TESTING TECHNIQUES
Oct. 1991 274 p In SPANISH
(DE92-615083; IAEA-TECDOC-628/S) Avail: NTIS HC/MF A12

Non-destructive testing methods (NDT), by their very nature, allow components to be fully examined for properties or flaws without interfering with their usefulness. This grouping of inspection methods has grown from a few primitive techniques practiced by artists to a widely known discipline which is an essential part of quality control, largely as a result of the standards demanded by the nuclear and aerospace industries. Recognizing the need for an international publication of NDT training syllabi, the IAEA Consultants Meeting on 'Qualification and Certification of NDT Personnel' (Milan, 20-21 May 1986), recommended that the Agency publish the guidelines developed by Regional Working Group of the Latin America and Caribbean project. It was first issued in English in 1987 and has now been re-edited in English and Spanish and enlarged by the addition of programs for other techniques. DOE

N92-23376*# National Aeronautics and Space Administration. Goddard Space Flight Center, Greenbelt, MD.
METHOD FOR ADVANCED MATERIAL CHARACTERIZATION BY LASER INDUCED EDDY CURRENT IMAGING Patent Application
Engmin J. Chern, inventor (to NASA) 5 Sep. 1991 16 p
(NASA-Case-GSC-13386-1; NAS 1.71:GSC-13386-1; US-Patent-Appl-SN-758977) Avail: NTIS HC/MF A03 CSCL 14D

An improved nondestructive evaluation (NDE) method uses a laser source with modulator and scanning mirror, a pancake shape eddy current detecting coil, a lock-in amplifier, a system controller, and an impedance gain/phase analyzer. The laser is directed by the scanning mirror to a specimen to be analyzed. A very localized or small area of the specimen is impacted directly by the laser beam, creating a thermal or stress wave in the specimen. An impedance gain/phase analyzer is connected to the eddy current detecting coil and to a lock-in amplifier through the system controller. The lock-in amplifier is also synchronized to the laser modulator. The system controller is used to control the lock-in amplifier, scanning mirror, and to process data from the analyzer. Raster scanning of the laser beam across the specimen allows the detection by the coil of the laser generated thermal and elastic

strains induced in the specimen by the laser. The rastering of the laser beam is controlled by the controller by positioning the mirror. NASA

39 STRUCTURAL MECHANICS

Includes structural element design and weight analysis; fatigue; and thermal stress.

For applications see *05 Aircraft Design, Testing and Performance* and *18 Spacecraft Design, Testing and Performance.*

N92-23125 Wisconsin Univ., Milwaukee.
BOUNDARY ELEMENT ANALYSIS OF FRACTURE MECHANICS PROBLEMS Ph.D. Thesis
Jiping Zhang 1991 145 p
Avail: Univ. Microfilms Order No. DA9128018

The application of boundary element analysis and crack surface displacement techniques to fracture mechanics problems is discussed. The material behavior is idealized by elastostatics and elastoplastic models. The analysis is performed using a multidomain boundary element scheme and quadratic quarter point boundary elements for the linear fracture mechanics problems. Combined with the maximum principle stress theory, the crack growth direction is predicted for the mixed mode problems. The boundary element formulation of the governing equations of elastoplasticity developed in this thesis makes use of an initial strain approach in which the incremental solutions are modified by the presence of initial strains. To evaluate the fracture behavior of the mixed mode problems, a displacement technique, called the Crack Surface Relative Displacement (CSRD), is extended to the application of small scale yielding under the mixed loading conditions. The new method is called the Crack Tip Relative Displacement (CTRD). The proposed method eliminates the need for the difficult task of determining the stress field in the vicinity of the crack tip as is normally required. A new fracture control parameter, the crack tip displacement - D, is also proposed for the linear elastic fracture mechanics problems. Dissert. Abstr.

N92-23137# Helsinki Univ. of Technology, Espoo (Finland). Inst. of Mathematics.
PROBLEM OF MEMBRANE LOCKING IN FINITE ELEMENT ANALYSIS OF CYLINDRICAL SHELLS
J. Pitkaeranta Jan. 1991 32 p
(PB92-133941; RR-A290; ISBN-951-22-0485-1) Avail: NTIS HC/MF A03 CSCL 20L

Analyzed is the problem of membrane locking in (h,p) finite element models of a thin hemicylindrical shell roof loaded by a smoothly varying normal pressure distribution. It is shown that in the standard finite element method, locking is severe especially at low values of p and when the finite element grid is not aligned with the axis of the cylinder. A general strategy of avoiding locking by using modified bilinear forms is introduced, and a special implementation of this strategy on aligned rectangular grids is considered. GRA

N92-23159 California Univ., Berkeley.
A DAMAGE MECHANICS MODEL FOR BEAMS Ph.D. Thesis
Boris Krajnc Alves 1991 134 p
Avail: Univ. Microfilms Order No. DA9203478

The objective was to formulate elasto-damage constitutive equations for beams. An attempt was made to formulate damage models in a one dimensional or two dimensional setting appropriate to the description of damage in rods and Cosserat surfaces. Emphasis is given to damage rules that are able to describe with sufficient accuracy the process of damage in a clear phenomenological way. The proposed models are restricted to the description of damage in the Euler-Bernoulli beam. Some difficulties in their extension to rods are discussed. Internal thermodynamic variables are introduced through a partitioning of the cross section and on the basis of simplifying assumptions on the damage loading domain. With those assumptions, a description of the distribution of the elastic degradation over a cross section is obtained. Of importance in that formulation is the identification of the internal variables, describing the phenomenology of damage in a 1-D setting, and the development of evolution laws that lead to the fewest incompatibilities with a 3-D phenomenology. Finally, a novel elasto-damage beam finite element is implemented, showing the capabilities of the proposed model. Dissert. Abstr.

N92-23191*# National Aeronautics and Space Administration. Lewis Research Center, Cleveland, OH.
AEROELASTIC STABILITY ANALYSES OF TWO COUNTER ROTATING PROPFAN DESIGNS FOR A CRUISE MISSILE MODEL
Aparajit J. Mahajan (Toledo Univ., OH.), John M. Lucero, Oral Mehmed, and George L. Stefko Apr. 1992 13 p
(NASA-TM-105268; E-7001; NAS 1.15:105268) Avail: NTIS HC/MF A03 CSCL 20K

Aeroelastic stability analyses were performed to insure structural integrity of two counterrotating propfan blade designs for a NAVY/Air Force/NASA cruise missile model wind tunnel test. This analysis predicted if the propfan designs would be flutter free at the operating conditions of the wind tunnel test. Calculated stability results are presented for the two blade designs with rotational speed and Mach number as the parameters. A aeroelastic analysis code ASTROP2 (Aeroelastic Stability and Response of Propulsion Systems - 2 Dimensional Analysis), developed at LeRC, was used in this project. The aeroelastic analysis is a modal method and uses the combination of a finite element structural model and two dimensional steady and unsteady cascade aerodynamic models. This code was developed to analyze single rotation propfans but was modified and applied to counterrotating propfans for the present work. Modifications were made to transform the geometry and rotation of the aft rotor to the same reference frame as the forward rotor, to input a non-uniform inflow into the rotor being analyzed, and to automatically converge to the least stable aeroelastic mode. Author

N92-23196*# National Aeronautics and Space Administration. Lewis Research Center, Cleveland, OH.
EVALUATION OF MHOST ANALYSIS CAPABILITIES FOR A PLATE ELEMENT
Ho-Jun Lee, Galib H. Abumeri, and Helen C. Brown (Sverdrup Technology, Inc., Brook Park, OH.) Feb. 1992 23 p
(NASA-TM-105387; E-6773; NAS 1.15:105387) Avail: NTIS HC/MF A03 CSCL 20K

Results of the evaluation of the static, buckling, and free vibration analyses capabilities of MHOST for the plate elements are presented. Two large scale, general purpose finite element codes (MARC and MSC/NASTRAN) are used to validate MHOST. Comparisons of MHOST results with those from MARC and MSC/NASTRAN show good agreement and indicate that MHOST can be used with confidence to perform the aforementioned analyses using the plate element. Author

N92-23216# Allied-Signal Aerospace Co., Kansas City, MO.
CRACKING INVESTIGATION OF Nd:YAG LASER WELDED GOLD PLATED GLASS SEALING ALLOYS
P. M. Mizik and E. Jimenez Feb. 1992 7 p Presented at the Lasers 1991, San Diego, CA, Dec. 1991
(Contract DE-AC04-76DP-00613)
(DE92-007971; KCP-613-4687; CONF-911296-4) Avail: NTIS HC/MF A02

Nd:TAG laser butt-lap joint welds were evaluated to determine the maximum gold plating thickness allowable on two glass-sealing alloys without causing weld cracks. The plate thickness was .012 in. Weld penetration ranged from .010 to .015 in. Crack analyses included scanning electron microscope, metallography, scanning Auger, and electron probe micro-analyzer. It was determined that 50 micro-in. of gold plating is an acceptable upper limit. DOE

N92-23267*# National Aeronautics and Space Administration. Lewis Research Center, Cleveland, OH.
COUPLED MULTI-DISCIPLINARY SIMULATION OF COMPOSITE ENGINE STRUCTURES IN PROPULSION ENVIRONMENT
Christos C. Chamis and Surendra N. Singhal (Sverdrup Technology, Inc., Brook Park, OH.) 1992 24 p Proposed for presentation at the International Gas Turbine and Aeroengine Congress and Exposition, Cologne, Fed. Republic of Germany, 1-4 Jun. 1991
(Contract NAS3-25266)
(NASA-TM-105575; E-6901; NAS 1.15:105575) Avail: NTIS HC/MF A03 CSCL 20K

A computational simulation procedure is described for the coupled response of multi-layered multi-material composite engine structural components which are subjected to simultaneous multi-disciplinary thermal, structural, vibration, and acoustic loadings including the effect of hostile environments. The simulation is based on a three dimensional finite element analysis technique in conjunction with structural mechanics codes and with acoustic analysis methods. The composite material behavior is assessed at the various composite scales, i.e., the laminate/ply/constituents (fiber/matrix), via a nonlinear material characterization model. Sample cases exhibiting nonlinear geometrical, material, loading, and environmental behavior of aircraft engine fan blades, are presented. Results for deformed shape, vibration frequency, mode shapes, and acoustic noise emitted from the fan blade, are discussed for their coupled effect in hot and humid environments. Results such as acoustic noise for coupled composite-mechanics/heat transfer/structural/vibration/acoustic analyses demonstrate the effectiveness of coupled multi-disciplinary computational simulation and the various advantages of composite materials compared to metals. Author

N92-23426*# Southwest Research Inst., San Antonio, TX.
PROBABILISTIC STRUCTURAL ANALYSIS METHODS (PSAM) FOR SELECT SPACE PROPULSION SYSTEM COMPONENTS, PART 2 Annual Report No. 6
Nov. 1991 343 p
(Contract NAS3-24389)
(NASA-CR-187200; NAS 1.26:187200) Avail: NTIS HC/MF A15 CSCL 20K

The technical effort and computer code enhancements performed during the sixth year of the Probabilistic Structural Analysis Methods program are summarized. Various capabilities are described to probabilistically combine structural response and structural resistance to compute component reliability. A library of structural resistance models is implemented in the Numerical Evaluations of Stochastic Structures Under Stress (NESSUS) code that included fatigue, fracture, creep, multi-factor interaction, and other important effects. In addition, a user interface was developed for user-defined resistance models. An accurate and efficient reliability method was developed and was successfully implemented in the NESSUS code to compute component reliability based on user-selected response and resistance models. A risk module was developed to compute component risk with respect to cost, performance, or user-defined criteria. The new component risk assessment capabilities were validated and demonstrated using several examples. Various supporting methodologies were also developed in support of component risk assessment. Author

N92-23427*# Virginia Univ., Charlottesville. Dept. of Mechanical and Aerospace Engineering.
THE FREE AND FORCED VIBRATIONS OF STRUCTURES USING THE FINITE DYNAMIC ELEMENT METHOD Ph.D. Thesis, Aug. 1991 Final Report
Neil J. Fergusson 2 Apr. 1992 9 p
(Grant NGT-50343)
(NASA-CR-190184; NAS 1.26:190184) Avail: NTIS HC/MF A02 CSCL 20K

In addition to an extensive review of the literature on exact and corrective displacement based methods of vibration analysis, a few theorems are proven concerning the various structural matrices involved in such analyses. In particular, the consistent mass matrix and the quasi-static mass matrix are shown to be equivalent, in the sense that the terms in their respective Taylor expansions are proportional to one another, and that they both lead to the same dynamic stiffness matrix when used with the appropriate stiffness matrix. Author

N92-23527*# National Aeronautics and Space Administration. Lewis Research Center, Cleveland, OH.
SINGULARITIES IN OPTIMAL STRUCTURAL DESIGN
S. N. Patnaik, J. D. Guptill, and L. Berke Mar. 1992 12 p
(NASA-TM-4365; E-6686; NAS 1.15:4365) Avail: NTIS HC/MF A03 CSCL 20K

Singularity conditions that arise during structural optimization can seriously degrade the performance of the optimizer. The singularities are intrinsic to the formulation of the structural optimization problem and are not associated with the method of analysis. Certain conditions that give rise to singularities have been identified in earlier papers, encompassing the entire structure. Further examination revealed more complex sets of conditions in which singularities occur. Some of these singularities are local in nature, being associated with only a segment of the structure. Moreover, the likelihood that one of these local singularities may arise during an optimization procedure can be much greater than that of the global singularity identified earlier. Examples are provided of these additional forms of singularities. A framework is also given in which these singularities can be recognized. In particular, the singularities can be identified by examination of the stress displacement relations along with the compatibility conditions and/or the displacement stress relations derived in the integrated force method of structural analysis. Author

N92-23549*# National Aeronautics and Space Administration. Goddard Space Flight Center, Greenbelt, MD.
METHOD AND APPARATUS FOR DETERMINATION OF MATERIAL RESIDUAL STRESS Patent Application
Engmin J. Chern, inventor (to NASA) and Yury Flom, inventor (to NASA) 2 Dec. 1991 13 p
(NASA-Case-GSC-13451-1; NAS 1.71:GSC-13451-1; US-Patent-Appl-SN-801141) Avail: NTIS HC/MF A03 CSCL 20K

A device for the determination of residual stress in a material sample consisting of a sensor coil, adjacent to the material sample, whose resistance varies according to the amount of stress within the material sample, a mechanical push-pull machine for imparting a gradually increasing compressional and tensional force on the material sample, and an impedance gain/phase analyzer and personal computer (PC) for sending an input signal to and receiving an input signal from the sensor coil. The PC will measure and record the change in resistance of the sensor coil and the corresponding amount of strain of the sample. The PC will then determine from the measurements of change of resistance and corresponding strain of the sample the point at which the resistance of the sensor coil is at a minimum and the corresponding value and type of strain of the sample at that minimum resistance point thereby enabling a calculation of the residual stress in the sample. NASA

N92-23664# Helsinki Univ. of Technology, Espoo (Finland). Dept. of Structural Engineering.
NONLINEAR FINITE ELEMENT ANALYSIS OF SPACE FRAMES
R. Kouhia 1990 128 p
(PB92-142447; Rept-109) Avail: NTIS HC/MF A07 CSCL 20K

In the study a finite element method for geometrically and materially nonlinear analyses of space frames is developed. The element stiffness matrix and internal force vectors for beams with either solid or thin walled open cross section are derived. Both Timoshenko and Euler-Bernoulli beam theories are considered. The equilibrium equations are formulated using an updated incremental Lagrangian description, where the reference configuration is the previous known equilibrium state. The elements can undergo large displacements and large rotations but the strains are assumed to be small. The linearized incremental displacement assumptions are used and the incremental rotations are also

assumed to be small. The discretized equilibrium equations are solved using the orthogonal trajectory method which allows the determination of the post-buckling regime. Special attention is paid to the detection of singular points and branching onto the secondary equilibrium path. In dynamic cases the time integration method of Newmark family are used. The presented numerical examples have been compared to analytical, experimental, and other numerical solutions found in literature. GRA

N92-23681# Materials Research Lab., Inc., Glenwood, IL.
DEVELOPMENT OF A CRACK ARREST FRACTURE TOUGHNESS MEASUREMENT PROCEDURE FOR QUALITY ASSURANCE OF PLATES AND WELDS USED FOR HYDROCARBON STORAGE TANKS Final Report, Oct. 1986 - Sep. 1991
E. J. Ripling and P. B. Crosley Sep. 1991 79 p
(Contract GRI-5086-254-1363)
(PB92-141753; MRL-7043; GRI-91/0227) Avail: NTIS HC/MF A05 CSCL 20K

A test method was developed for measuring the full thickness crack arrest fracture toughness of steel plates. The method is unique in that it was developed to measure a fracture mechanics parameter for quality control. This was done by designing the test specimen to measure a preselected toughness specimen to measure a preselected toughness value. The method is patterned after an ASTM Standard: E 1221. Full thickness cracks, unlike the cracking described in E 1221, frequently form by tunneling, which means that toughness does not have a single value, but is a function of crack length. The feature is accounted for in the method. Full thickness toughness values are also generally higher than the values measured by ASTM E 1221 so that a plasticity correction is required. Both methods use a static analysis, however, i.e. both methods assume that time dependent affects are negligible. Three plates of nickel steels having different thicknesses and toughnesses were used for developing the test method. Also, tests were made on one carbon-manganese-silicon steel, and a hydrogen charged thick plate. Author

N92-23688 Delaware Univ., Newark.
CRACK PATH PREDICTION NEAR AN ELLIPTICAL INHOMOGENEITY Ph.D. Thesis
Edward Matthew Patton 1991 129 p
Avail: Univ. Microfilms Order No. DA9206379

A new technique is presented which will predict the path of a naturally growing crack near a rigid elliptical inclusion, where the stress field can be modeled as two dimensional. The technique uses a boundary integral approach to the solution of the stress field at the tips of the crack which is in general not straight, and is interacting with a rigid elliptical inclusion. The crack is parameterized as a cubic spline, and the results of both a Green's Function solution to the interaction of a dislocation with an elliptical inclusion, and a first order perturbation solution to account for the generally curvilinear nature of the crack was used. The singular nature of the stresses is accounted for using a numerical technique which describes the distribution of dislocations along the crack as a piecewise quadratic polynomial to transform the problem's resulting integral equations into algebraic equation well suited to a matrix type solution. Results of each step of the analysis were verified with previously published results, and with experimental results of a crack propagating near an open circular hole. New and significant results are also presented as paths of cracks interacting with inclusions of differing ellipticity ratios, and at different orientations with respect to the initial crack.
Dissert. Abstr.

N92-23699 California Univ., Los Angeles.
FREE AND FORCED RESPONSE OF NEARLY PERIODIC MULTI-SPAN BEAMS AND MULTI-BAY TRUSSES Ph.D. Thesis
Steven Dan Lust 1991 245 p
Avail: Univ. Microfilms Order No. DA9129955

The effects are addressed of disorder on the structural dynamic behavior of periodic beams and free-free periodic frames and trusses. It has been shown that disorder can cause spatial confinement of the free vibration response, known as mode localization, and can inhibit the propagation of forced response. Of special interest is the applicability of this research to the behavior of large space structures. The effects of localization are viewed from a modal perspective. Finite element techniques are used to model the ordered and disordered periodic structures. The standard structural dynamics eigenvalue problem is solved to obtain the natural frequencies and mode shapes. The mode summation method is applied to calculate the forced response. Multispan beam structures with progressively increasing complexity are used to study the influence of numerous effects on localization. Monte Carlo analyses for a series of free-free forty span beams are used to determine the variability in the magnitude of localization and to determine the sensitivity of localization to Timoshenko beam effects, coupling strength, imperfection strength, and imperfection type. Results of the research indicate that Timoshenko beam effects, transverse support stiffness, imperfection magnitude, imperfection type, and coupling stiffness are important for the study of mode localization in supported multispan beams.
Dissert. Abstr.

N92-23737 Northwestern Univ., Evanston, IL.
LOCALIZATION OF DEFORMATION AND INELASTIC DEFORMATION OF PRESSURE-SENSITIVE DILATANT MATERIALS Ph.D. Thesis
Kam Tim Chau 1991 210 p
Avail: Univ. Microfilms Order No. DA9128962

The localization of deformation (Part 1) and inelastic of deformation (Part 2) for pressure-sensitive dilatant materials are investigated. In Part 1, bifurcations, including shear band and diffuse geometric modes, are analyzed for rectangular slabs under plane strain deformation and circular cylinders under axisymmetric deformations. For the plane strain analysis, Chapter 2 shows that when the lateral confining stress is zero, the picture of bifurcations is qualitatively similar to that for incompressible materials. For a circular cylinder under axisymmetric deformation, Chapter 3 shows that introduction of transverse anisotropy and non-normality promotes not only localization but also geometric diffuse modes under compression. Numerical solutions of the eigenvalue equation for the elliptic complex regime demonstrate that some geometric diffuse modes with finite wave number, instead of bulging mode, become the first possible bifurcation under compression. Part 2 of the dissertation presents a variation of Costin's microcrack model and its prediction of the yield vertex effect on the effective shear moduli. The response of shearing deformation is found to be highly nonlinear at a yield or damage surface corner. This model provides a preliminary method for incorporating the reduced shear moduli into the constitutive parameters needed for the prediction of the onset of localization. Dissert. Abstr.

N92-23773 California Univ., Davis.
FREE VIBRATION OF THICK ISOTROPIC AND ORTHOTROPIC CYLINDRICAL SHELLS Ph.D. Thesis
Stanley Eugene Bumpas 1991 146 p
Avail: Univ. Microfilms Order No. DA9206213

The vibration of free, thick cylindrical shells that are composed of either isotropic materials or orthotropic materials like modern composite laminates are studied. The formulation starts with an approximate five term displacement field that has been used previously. The subsequent approximate strains, stresses, and force and moment resultants are successively substituted into a variational form of Hamilton's principle to yield the governing vibration equations and boundary condition equations. The two sets of equations are solved simultaneously to obtain dimensionless frequencies. The constitutive law for the material is assumed to be orthogonal with respect to the mid-surface coordinate system. Explicit shear coefficients are assumed for all resultants that have a shear stress in their definition. The computer algorithm that solves the equations is explained along with the exception testing for any found frequency. Results consist mainly of contour plots of the first fundamental frequency for a particular circumferential wave number, n, and symmetric or antisymmetric form. Differences with an accurate series solution for the isotropic case are given.

Through-thickness coefficients are found that would make this formulation agree with the isotropic series solution. A study of higher frequencies is presented and favorably compared to the series solution. Two typical sets of results are presented for orthotropic materials representative of composite laminates that are stiff in the longitudinal and tangential directions. A continuing summary and areas of future work are discussed. Dissert. Abstr.

N92-23990*# National Aeronautics and Space Administration. Langley Research Center, Hampton, VA.
UNDERLYING MODAL DATA ISSUES FOR DETECTING DAMAGE IN TRUSS STRUCTURES
Thomas A-L. Kashangaki, Suzanne Weaver Smith, and Tae W. Lim (Lockheed Engineering and Sciences Co., Hampton, VA.) Feb. 1992 12 p Presented at the 33rd Structures, Structural Dynamics, and Materials Conference, Dallas, TX, 13-17 Apr. 1992
(NASA-TM-107573; NAS 1.15:107573) Avail: NTIS HC/MF A03 CSCL 20K

Independent of the modal identification techniques employed for damage detection, use of measured modal data limits the expectations for damage location. These limitations are examined using the distribution of modal strain energy and the sensitivity of the frequency and mode shapes to structural stiffness changes. For given measured modal information of specific accuracy, this examination reveals the following: (1) damage detection is feasible for members that contribute significantly to the strain energy of the measured modes, (2) the modes which are most effective in detecting damage to certain critical members can be identified, and (3) a relationship can be drawn between the accuracy of the measured modes and frequencies and damage detection feasibility. Author

N92-23992*# National Aeronautics and Space Administration. Langley Research Center, Hampton, VA.
COLLAPSE OF COMPOSITE TUBES UNDER END MOMENTS
Alan E. Stockwell (Lockheed Engineering and Sciences Co., Hampton, VA.) and Paul A. Cooper Apr. 1992 12 p Presented at the 33rd Structures, Structural Dynamics, and Materials Conference, Dallas, TX, 13-17 Apr. 1992
(NASA-TM-107605; NAS 1.15:107605) Avail: NTIS HC/MF A03 CSCL 20K

Cylindrical tubes of moderate wall thickness such as those proposed for the original space station truss, may fail due to the gradual collapse of the tube cross section as it distorts under load. Sometimes referred to as the Brazier instability, it is a nonlinear phenomenon. This paper presents an extension of an approximate closed form solution of the collapse of isotropic tubes subject to end moments developed by Reissner in 1959 to include specially orthotropic material. The closed form solution was verified by an extensive nonlinear finite element analysis of the collapse of long tubes under applied end moments for radius to thickness ratios and composite layups in the range proposed for recent space station truss framework designs. The finite element analysis validated the assumption of inextensional deformation of the cylindrical cross section and the approximation of the material as specially orthotropic. Author

N92-23787# Centre National d'Etudes Spatiales, Toulouse (France).
COUPLED LOAD ANALYSIS: SCATTER RELATED TO MODEL UNCERTAINTIES
P. W. Bousquet, F. Mercier, and M. Klein (European Space Agency. European Space Research and Technology Center, ESTEC, Noordwijk, Netherlands) *In* ESA, Spacecraft Structures and Mechanical Testing, Volume 1 Oct. 1991 p 53-58 (For primary document see N92-23780 14-18)
Copyright Avail: NTIS HC/MF A21

N92-23788# Frazer-Nash Consultancy Ltd., Leatherhead (England).
THE USE OF MODAL SYNTHESIS IN CONJUNCTION WITH NONLINEAR TRANSIENT DYNAMIC ANALYSIS
S. A. Challener and A. J. Vibert *In* ESA, Spacecraft Structures and Mechanical Testing, Volume 1 Oct. 1991 p 59-62 Sponsored in part by Ministry of Defence (For primary document see N92-23780 14-18)
Copyright Avail: NTIS HC/MF A21

N92-23789# MATRA Espace, Toulouse (France). Dept. of Mechanical Engineering.
IMPROVEMENTS FOR INTERPRETATION OF STRUCTURAL DYNAMICS CALCULATION USING EFFECTIVE PARAMETERS FOR SUBSTRUCTURES
T. Berthelon and A. Capitaine *In* ESA, Spacecraft Structures and Mechanical Testing, Volume 1 Oct. 1991 p 63-68 (For primary document see N92-23780 14-18)
Copyright Avail: NTIS HC/MF A21

N92-23793# Cambridge Univ. (England). Dept. of Engineering.
DEVELOPMENT OF FATIGUE DAMAGE MECHANICS FOR APPLICATION TO THE DESIGN OF DAMAGE-TOLERANT COMPOSITE COMPONENTS
P. W. R. Beaumont, S. M. Spearing, and M. T. Kortschot *In* ESA, Spacecraft Structures and Mechanical Testing, Volume 1 Oct. 1991 p 91-96 Sponsored in part by Science Research Council (For primary document see N92-23780 14-18)
Copyright Avail: NTIS HC/MF A21

N92-23795# Framasoft + CSI, Paris (France).
FATIGUE ANALYSIS UNDER RANDOM STRESSES
A. Ricard *In* ESA, Spacecraft Structures and Mechanical Testing, Volume 1 Oct. 1991 p 103-107 Prepared in cooperation with Commission of the European Communities, Brussels, Belgium (For primary document see N92-23780 14-18)
(BRITE Proj. P2381-5)
Copyright Avail: NTIS HC/MF A21

N92-23799# LMS International, Leuven (Belgium).
AN ADVANCED SYSTEM FOR ENVIRONMENTAL SINE TESTING: BASIC PRINCIPLES REVISITED
J. Leuridan, R. Mangelschots, F. Declerq, and G. Bossaert *In* ESA, Spacecraft Structures and Mechanical Testing, Volume 1 Oct. 1991 p 131-134 (For primary document see N92-23780 14-18)
Copyright Avail: NTIS HC/MF A21

N92-23800# Ometron Ltd., London (England).
NON CONTACTING MEASUREMENT OF VIBRATION
A. J. Barker *In* ESA, Spacecraft Structures and Mechanical Testing, Volume 1 Oct. 1991 p 135-138 (For primary document see N92-23780 14-18)
Copyright Avail: NTIS HC/MF A21

N92-23801# Indian Space Research Organization, Bangalore. Mechanical Systems Group.
ON DEVELOPMENT OF AUTOMATED STATIC LOADING SYSTEM FOR SPACECRAFT STRUCTURES
A. V. Patki and R. Samuel *In* ESA, Spacecraft Structures and Mechanical Testing, Volume 1 Oct. 1991 p 139-144 (For primary document see N92-23780 14-18)
Copyright Avail: NTIS HC/MF A21

N92-23802# Veritas Research A.S., Hovik (Norway).
NONLINEAR FINITE-ELEMENT ANALYSIS OF SANDWICH SHELLS
O. Amlid and P. G. Bergan *In* ESA, Spacecraft Structures and Mechanical Testing, Volume 1 Oct. 1991 p 147-152 (For primary document see N92-23780 14-18)
Copyright Avail: NTIS HC/MF A21

N92-23803# Rome Univ. (Italy). Dipartimento Aerospaziale.
INFLUENCE OF THE SUBSTRATE ON THE SOLAR CELLS INTERCONNECTOR: STRESS DISTRIBUTION AND FATIGUE LIFE PREDICTION
S. Tizzi, M. Marchetti, and S. LaTerza *In* ESA, Spacecraft Structures and Mechanical Testing, Volume 1 Oct. 1991 p 153-159 Sponsored by Fabrica Italiana Apparecchiature

Radioelettriche S.p.A. (For primary document see N92-23780 14-18)
Copyright Avail: NTIS HC/MF A21

N92-23804# Politecnico di Torino (Italy). Dept. of Aerospace Engineering.
BUCKLING OF SIMPLY SUPPORTED AND CLAMPED ANISOTROPIC PLATES UNDER COMBINED LOADS
G. Romeo and G. Frulla *In* ESA, Spacecraft Structures and Mechanical Testing, Volume 1 Oct. 1991 p 161-166 Sponsored by Ministry of University (For primary document see N92-23780 14-18)
Copyright Avail: NTIS HC/MF A21

N92-23813# Alenia Spazio S.p.A., Rome (Italy).
ACOUSTIC CAVITY AND FLUID/STRUCTURE INTERACTION MODELS: A METHODOLOGICAL DETERMINISTIC APPROACH AND PROBLEMS ENCOUNTERED
Pietro Carlo Marucchi-Chierro *In* ESA, Spacecraft Structures and Mechanical Testing, Volume 1 Oct. 1991 p 223-232 (For primary document see N92-23780 14-18)
Copyright Avail: NTIS HC/MF A21

N92-23814# IKO Software Service G.m.b.H., Stuttgart (Germany, F.R.).
EMPLOYMENT OF C.B. (CRAIG-BAMPTON) MODELS FOR NONLINEAR DYNAMIC ANALYSIS
P. Deloo and M. R. M. Klein (European Space Agency. European Space Research and Technology Center, ESTEC, Noordwijk, Netherlands) *In* ESA, Spacecraft Structures and Mechanical Testing, Volume 1 Oct. 1991 p 235-240 (For primary document see N92-23780 14-18)
Copyright Avail: NTIS HC/MF A21

N92-23815# Centre National d'Etudes Spatiales, Toulouse (France).
FEASIBILITY OF PAYLOAD SENSITIVITY ANALYSES FOR AR4 DYNAMIC EVENTS
F. Mercier *In* ESA, Spacecraft Structures and Mechanical Testing, Volume 1 Oct. 1991 p 241-246 (For primary document see N92-23780 14-18)
Copyright Avail: NTIS HC/MF A21

N92-23816# Innsbruck Univ. (Austria). Inst. of Engineering Mechanics.
THE RESPONSE SURFACE METHOD: AN EFFICIENT TOOL TO DETERMINE THE FAILURE PROBABILITY OF LARGE STRUCTURAL SYSTEMS
G. I. Schueeller, C. G. Bucher, and H. J. Pradlwarter *In* ESA, Spacecraft Structures and Mechanical Testing, Volume 1 Oct. 1991 p 247-251 (For primary document see N92-23780 14-18)
(Contract FFF-6/546)
Copyright Avail: NTIS HC/MF A21

N92-23826# Messerschmitt-Boelkow-Blohm G.m.b.H., Bremen (Germany, F.R.).
ON THE MODELLING OF A DEPLOYABLE TELESCOPE ELASTIC BEAM-TYPE ELEMENT FOR ON-ORBIT MULTIBODY SIMULATIONS
Bernhard Kotzias *In* ESA, Spacecraft Structures and Mechanical Testing, Volume 1 Oct. 1991 p 323-328 Prepared in cooperation with Erno Raumfahrttechnik G.m.b.H. Bremen, Germany, F.R. (For primary document see N92-23780 14-18)
Copyright Avail: NTIS HC/MF A21

N92-23827# Alenia Spazio S.p.A., Turin (Italy).
DEVELOPMENT AND APPLICATION OF SUBSTRUCTURING TECHNIQUES FOR UNDERSTANDING AND CONTROLLING RESIDUAL VIBRATIONS (MICROGRAVITY ASPECTS)
Daniele Francesconi, Pietro Carlo Marucchi-Chierro, and Roberto Ullio *In* ESA, Spacecraft Structures and Mechanical Testing, Volume 1 Oct. 1991 p 329-338 (For primary document see N92-23780 14-18)
Copyright Avail: NTIS HC/MF A21

N92-23828# Intespace, Toulouse (France).
MINIMIZATION OF VIBRATIONS BY BROADBAND SENSITIVITY APPROACH
A. Girard, J. Chatelain, and N. Roy *In* ESA, Spacecraft Structures and Mechanical Testing, Volume 1 Oct. 1991 p 341-346 Sponsored by Centre d'Etudes et de Recherche sur la Discretion Acoustique des Navires (For primary document see N92-23780 14-18)
Copyright Avail: NTIS HC/MF A21

N92-23829# TeWiSoft G.m.b.H., Soechtenau (Germany, F.R.).
THE CONTINUOUS ELEMENTS METHOD
Peter H. Kulla *In* ESA, Spacecraft Structures and Mechanical Testing, Volume 1 Oct. 1991 p 347-352 (For primary document see N92-23780 14-18)
Copyright Avail: NTIS HC/MF A21

N92-23830# Politecnico di Milano (Italy). Dipartimento di Ingegneria Aerospaziale.
HARMONIC WAVE PROPAGATION IN TWO-DIMENSIONAL PERIODIC LARGE SPACE STRUCTURES
F. Bernelli-Zazzera and F. Ercoli-Finzi *In* ESA, Spacecraft Structures and Mechanical Testing, Volume 1 Oct. 1991 p 353-358 Sponsored by Fondazione Ing. Paolo Foresio (For primary document see N92-23780 14-18)
Copyright Avail: NTIS HC/MF A21

N92-23834# Padua Univ. (Italy). Dipartimento di Ingegneria Meccanica.
MECHANICAL TESTING ON A COMPOSITE FLEXIBLE STRUCTURE
G. Fanti, F. Angrilli, P. Baglioni, and G. Bianchini *In* ESA, Spacecraft Structures and Mechanical Testing, Volume 1 Oct. 1991 p 375-381 Sponsored by Italian Space Agency (For primary document see N92-23780 14-18)
Copyright Avail: NTIS HC/MF A21

N92-23847# Deutsche Forschungsanstalt fuer Luft- und Raumfahrt, Goettingen (Germany, F.R.). Dept. of Structural Dynamics.
OPTIMAL EXCITER PLACEMENT AND FORCE VECTOR TUNING REQUIRED FOR EXPERIMENTAL MODAL ANALYSIS
Norbert Niedbal and Erhard Klusowski *In* ESA, Spacecraft Structures and Mechanical Testing, Volume 1 Oct. 1991 p 463-473 (For primary document see N92-23780 14-18)
Copyright Avail: NTIS HC/MF A21

N92-23848# Besancon Univ. (France). Lab. de Mecanique Appliquee.
MATCHING FINITE ELEMENT MODELS TO MODAL DATA
S. Cogan and G. Lallement *In* ESA, Spacecraft Structures and Mechanical Testing, Volume 1 Oct. 1991 p 475-482 (For primary document see N92-23780 14-18)
(Contract ESTEC-8219/89)
Copyright Avail: NTIS HC/MF A21

N92-23849# Construcciones Aeronauticas S.A., Madrid (Spain). Space Div.
COMPARISON OF MULTI-POINT MODAL TEST METHODS
Kimon Alexiou and Jan R. Wright (Manchester Univ., England) *In* ESA, Spacecraft Structures and Mechanical Testing, Volume 1 Oct. 1991 p 483-490 (For primary document see N92-23780 14-18)
Copyright Avail: NTIS HC/MF A21

N92-23850# Dornier System G.m.b.H., Friedrichshafen (Germany, F.R.).
DESIGN PARAMETER UPDATE OF DYNAMIC MATHEMATICAL MODELS IN PRESENCE OF TEST NOISE AND MODE PAIRING PROBLEMS
B. Caesar, L. Eckert, and A. Hoppe (Stuttgart Univ., Germany,

F.R.) *In* ESA, Spacecraft Structures and Mechanical Testing, Volume 1 Oct. 1991 p 491-499 (For primary document see N92-23780 14-18).
Copyright Avail: NTIS HC/MF A21

42 GEOSCIENCES (GENERAL)

N92-23707# Joint Publications Research Service, Arlington, VA.
JPRS REPORT: SCIENCE AND TECHNOLOGY. USSR: EARTH SCIENCES
19 Aug. 1991 29 p Transl. into ENGLISH from various Russian articles
(JPRS-UES-91-005) Avail: NTIS HC/MF A03

A bibliography of USSR research in earth sciences is given. Topics covered include geology, oceanography, atmospheric physics, and ecology. Author

43 EARTH RESOURCES AND REMOTE SENSING

Includes remote sensing of earth resources by aircraft and spacecraft; photogrammetry; and aerial photography.

For instrumentation see *35 Instrumentation and Photography.*

N92-23145 Miami Univ., Coral Gables, FL.
ATMOSPHERIC CORRECTION OF THE SECOND GENERATION OCEAN COLOR SENSORS Ph.D. Thesis
Menghua Wang 1991 142 p
Avail: Univ. Microfilms Order No. DA9205369

There are two assumptions in the current algorithm for atmospheric correction of Coastal Zone Color Scanner (CZCS) imagery: (1) the sea surface is flat; and (2) the Rayleigh aerosol interaction can be ignored. Simulations are carried out assess the error when the CZCS type algorithm is applied to a realistic ocean in which the surface is roughened by the wind. It is found that both the errors induced by the flat ocean assumption and by ignoring the Rayleigh aerosol interaction can be ignored in CZCS processing because the CZCS does not possess high enough radiometric sensitivity. However, for the new ocean color sensors, these errors can be as much as an order of magnitude larger than the noise equivalent spectral radiance. Therefore, a new algorithm for atmospheric correction was developed, and several viewing scenarios were examined. From the computations, it is found that the error in the retrieved water leaving reflectance in realistic situations is within the allowed limits for the next generation ocean color sensors using the new algorithm. Finally, a possible implementation of the new algorithm is discussed. Dissert. Abstr.

N92-23379# Messerschmitt-Boelkow-Blohm G.m.b.H., Munich (Germany, F.R.). Unternehmensbereich Kommunikationssysteme und Antriebe.
EUROMAR-SEASTARS: A DEFINITION STUDY ON MODULAR MULTISENSOR INSTRUMENTATION FOR AIRBORNE REMOTE SENSING OF THE SEA Final Report [EUROMAR-SEASTARS: DEFINITIONSSTUDIE UEBER MODULARE MULTI-SENSOR-INSTRUMENTIERUNG FUER DIE MEERESFORSCHUNG UND -UEBERWACHUNG. ABSCHLUSSBERICHT]
Aribert P. Wolframm, C. Boesswetter, H. Kuppert, Bernd A. Kunkel, U. Kraft, Hans-Dieter vonBoehm, H. Behrmann, P. Hicks, R. Reuter, and H. Huehnerfuss (Hamburg Univ., Germany, F.R.) et al May 1991 436 p In ENGLISH and GERMAN
(Contract BMFT-MFU-06021; EUREKA Proj. EU-494)
(MBB-UK-0152-91-PUB; ETN-92-91073) Avail: NTIS HC/MF A19

The airborne remote sensing system, Euromar-Seastars, is currently being developed under the EUREKA program with Germany being responsible for the North and Baltic seas. The sensor package comprises active and passive, optical and microwave, imaging and profiling instruments. All instruments are connected through a common bus, and real-time images or data displays show the state of the surrounding sea. The subjects covered are: ocean airborne control, the state of development in Europe, the projected system concept, scientific requirements, single sensor specification, onboard data processing, system consideration, provisional definition of a development program, provisional cost evaluation, and international cooperation. For individual titles, see N92-23380 through N92-23411.

N92-23380# Messerschmitt-Boelkow-Blohm G.m.b.H., Munich (Germany, F.R.).
EUROMAR-SEASTARS: SUMMARY [ZUSAMMENFASSUNG]
C. Boesswetter *In its* Euromar-Seastars: A Definition Study on Modular Multisensor Instrumentation for Airborne Remote Sensing of the Sea May 1991 4 p Sponsored by Bundesministerium fuer Forschung und Technologie (For primary document see N92-23379 14-43)
Avail: NTIS HC/MF A19

The advanced airborne instrumentation for the Euromar-Seastars is described covering: the Synthetic Aperture Radar (SAR), the Forward Looking Airborne Radar (FLAR) which is used as a navigational aid, the Euromar imaging microwave radiometer, the Laser FluoroSensor (LFS) which allows a measurement of the volume of films on the sea surface, and the Euromar Imaging Spectrometer (EURIS) which is a modified derivative of the Reflective Optics System Imaging Spectrometer (ROSIS) airborne version. A scanning laser bathymeter is foreseen, which is to operate with two lasers, a blue green and an infrared one. ESA

N92-23381# Oldenburg Univ. (Germany, F.R.).
INTRODUCTION: OCEAN AIR OBSERVATION [EINLEITUNG: LUFTUEBERWACHUNG DER SEE]
R. Reuter *In* MBB, Euromar-Seastars: A Definition Study on Modular Multisensor Instrumentation for Airborne Remote Sensing of the Sea May 1991 6 p In GERMAN (For primary document see N92-23379 14-43)
Avail: NTIS HC/MF A19

It is shown that coastal waters are to be considered as important regions for oceanographic remote sensing, and that aircraft are particularly suitable for remote sensing, on account of lower costs, with regard to satellite remote sensing. A short review of aircraft remote sensing development status is given. ESA

N92-23382# Oldenburg Univ. (Germany, F.R.).
THE STATE OF THE DEVELOPMENT IN EUROPE [STAND DER ENTWICKLUNG IN EUROPA]
R. Reuter *In* MBB, Euromar-Seastars: A Definition Study on Modular Multisensor Instrumentation for Airborne Remote Sensing of the Sea May 1991 6 p In GERMAN (For primary document see N92-23379 14-43)
Avail: NTIS HC/MF A19

Remote sensing for ocean control is described. The detection and analysis of noxious matters is examined. It is shown that their distribution is obtained by ultraviolet and infrared recording. Sensors for ocean supervision are described and listed, including the radar, the microwave radiometer, the ultraviolet/infrared scanner, the optical multispectral scanner, the laser fluorosensor and the infrared radiometer. The use of operational sensors for several tasks is considered. ESA

N92-23383# Messerschmitt-Boelkow-Blohm G.m.b.H., Munich (Germany, F.R.).
RECOMMENDED SYSTEM CONCEPT [VORGESCHLAGENES SYSTEMKONZEPT]
C. Boesswetter *In its* Euromar-Seastars: A Definition Study on Modular Multisensor Instrumentation for Airborne Remote Sensing of the Sea May 1991 4 p In GERMAN (For primary document see N92-23379 14-43)
Avail: NTIS HC/MF A19

It is shown that microwave sensors are mainly used for the

detection and measurement of surface effects, and that only a multispectral measurement system with several independent sensor principles is able to give a unique interpretation of the phenomena. Such a system is not currently available, either in Germany or in Europe. It should include modular instrumentation on different carrier aircraft, possibilities of integration of sensor systems from the European Euromar countries by standardization, optoelectronic and microwave sensors, and distribution of multisensor data in all interested institutions of Euromar countries. ESA

N92-23384# Oldenburg Univ. (Germany, F.R.).
SENSOR PACKAGE FOR THE NORTH SEA [SENSORPAKET FUER DIE NORDSEE]
R. Reuter *In* MBB, Euromar-Seastars: A Definition Study on Modular Multisensor Instrumentation for Airborne Remote Sensing of the Sea May 1991 30 p In GERMAN (For primary document see N92-23379 14-43)
Avail: NTIS HC/MF A19

A combination of remote sensors are presented for various ocean remote sensing applications. They concern sea noxious matter control and ecological or physical parameters. The structure and physical parameters of water surface are reported. Four sensors are presented: the active microwave process, the multispectral scanner, the infrared radiometer, and the imaging microwave radiometer. The water head parameters are given with three types of sensors: the imaging optical spectrometer, the laser fluorosensor, and the laser bathymeter. ESA

N92-23385# Hamburg Univ. (Germany, F.R.).
GEOPHYSICAL, CHEMICAL AND BIOLOGICAL MEASURING PARAMETERS [GEOPHYSIKALISCHE, CHEMISCHE UND BIOLOGISCHE MESSPARAMETER]
H. Huehnerfuss *In* MBB, Euromar-Seastars: A Definition Study on Modular Multisensor Instrumentation for Airborne Remote Sensing of the Sea May 1991 20 p In GERMAN (For primary document see N92-23379 14-43)
Avail: NTIS HC/MF A19

The organic matters to be found in European coastal waters are characterized. The subdivisions of organic marine substances, with regard to substance classes, are considered. The interactions between organic matters and water, the direct interaction between substance and electromagnetic signal, and boundary layer water are examined. A summarized evaluation of sensor systems and recommendations are given. ESA

N92-23386# Oldenburg Univ. (Germany, F.R.).
THE LASER FLUOROSENSOR [LASER-FLUORO-SENSOR]
R. Reuter *In* MBB, Euromar-Seastars: A Definition Study on Modular Multisensor Instrumentation for Airborne Remote Sensing of the Sea May 1991 25 p In GERMAN (For primary document see N92-23379 14-43)
Avail: NTIS HC/MF A19

It is shown that the laser fluorosensor allows a measurement of the volume of films on the sea surface and a classification of the substance type, so that parameters which are relevant for the evaluation of ecological conditions can be obtained. Particular emphasis is put on the capability for two-dimensional mapping of the sea surface, to allow an optical probing on small geometrical scales. The XeCl laser which is used for the analysis of oil spills is described. A dye laser enables an efficient excitation of chlorophyll fluorescence. The main system parameters are summarized. ESA

N92-23387# Messerschmitt-Boelkow-Blohm G.m.b.H., Munich (Germany, F.R.).
THE IMAGING SPECTROMETER [ABBILDENDES SPEKTROMETER]
B. Kunkel *In its* Euromar-Seastars: A Definition Study of Modular Multisensor Instrumentation for Airborne Remote Sensing of the Sea May 1991 46 p In GERMAN (For primary document see N92-23379 14-43)
Avail: NTIS HC/MF A19

EURIS (Euromar Imaging Spectrometer) is a modified derivative of the ROSIS (Reflective Optics Systems Imaging Spectrometer) airborne version. It is a fully electronic scanning instrument, in both spatial and spectral dimensions, which operates with all reflective objective and spectrometer optics, and allows for a wide spectral range coverage. The main applications are described: biomass determination through chlorophyll absorption and fluorescence measurements; discrimination of algae species; and turbidity and sediment transport determination. The main system parameters are summarized. ESA

N92-23388# Oldenburg Univ. (Germany, F.R.).
THE LASER BATHYMETER [LASER-BATHYMETER]
R. Reuter *In* MBB, Euromar-Seastars: A Definition Study on Modular Multisensor Instrumentation for Airborne Remote Sensing of the Sea May 1991 13 p In GERMAN (For primary document see N92-23379 14-43)
Avail: NTIS HC/MF A19

A scanning laser bathymeter which operates with two lasers, a blue green and an infrared one, is described. The blue green laser is used for determining the bottom topography of shallow water. The infrared laser is used to indicate the instantaneous altitude above the sea level. The information is used to trigger and gate the blue green laser. It is shown that local shoals can be detected this way. The main system parameters are summarized. ESA

N92-23389# Oldenburg Univ. (Germany, F.R.).
SEABORNE LIDAR SYSTEM [SCHIFFSGESTUETZTES LIDAR-SYSTEM]
R. Reuter *In* MBB, Euromar-Seastars: A Definition Study on Modular Multisensor Instrumentation for Airborne Remote Sensing of the Sea May 1991 9 p In GERMAN (For primary document see N92-23379 14-43)
Avail: NTIS HC/MF A19

The theoretical background is described. It is shown that an interpretation of lidar data is essentially carried out, using the hydrographic lidar equation. The seaborne lidar allows measurement with depth probes. The disturbing daylight background is much weaker when using the ship rather than aircraft system because there is no reflection of sunlight from the water surface and the measurement can take place in the shadow of the hull. The selection of excitation wavelengths and detection channels is described. The technical data are summarized. ESA

N92-23390# Messerschmitt-Boelkow-Blohm G.m.b.H., Munich (Germany, F.R.).
THE IMAGING MICROWAVE RADIOMETER [ABBILDENDES MIKROWELLEN-RADIOMETER]
U. Kraft *In its* Euromar-Seastars: A Definition Study on Modular Multisensor Instrumentation for Airborne Remote Sensing of the Sea May 1991 35 p In GERMAN (For primary document see N92-23379 14-43)
Avail: NTIS HC/MF A19

The configuration for the Euromar imaging microwave radiometer consists of two independent modules, the Medium Resolution Module (MRM) and the High Resolution Module (HRM). MRM and HRM tasks, frequencies and technologies are presented. The MRM measures the basic physical parameters of salt content and sea surface temperatures and is used to detect biogenic films. The HRM determines the thickness and volume of the layers which float completely on sea surface and maps and analyzes sea ice. The main system parameters are summarized. ESA

N92-23391# Messerschmitt-Boelkow-Blohm G.m.b.H., Munich (Germany, F.R.).
THE IMAGING RADAR SYSTEM [ABBILDENDE RADAR-SYSTEME]
A. P. Wolframm *In its* Euromar-Seastars: A Definition Study on Modular Multisensor Instrumentation for Airborne Remote Sensing of the Sea May 1991 24 p In GERMAN (For primary document see N92-23379 14-43)
Avail: NTIS HC/MF A19

It is shown that radar instruments can be used under almost

all weather conditions, as compared with optical sensors. Synthetic Aperture Radar (SAR), Side Looking Airborne Radar (SLAR), and Forward Looking Airborne Radar (FLAR) are described. Their missions are presented. Two main operational radar modes are identified. Their specific parameters are given. ESA

N92-23392# Messerschmitt-Boelkow-Blohm G.m.b.H., Munich (Germany, F.R.).
PASSIVE OPTICAL AND IR SENSORS [PASSIVE OPTISCHE UND IR-SENSOREN]
H.-D. v.Boehm and H. Behrmann *In its* Euromar-Seastars: A Definition Study on Modular Multisensor Instrumentation for Airborne Remote Sensing of the Sea May 1991 35 p In GERMAN (For primary document see N92-23379 14-43)
(MBB-UH-HE512) Avail: NTIS HC/MF A19

Forward Looking Infrared (FLIR) sensors are shown to detect the thermal radiation in the medium and far infrared. Passive optical instruments may be added to other sensors to serve as quick look and for archiving purposes. They can help to identify ships causing pollution. Ordinary video cameras with Charge Coupled Device (CCD) are used in normal daylight. At night, Low Level Television (LLTV) cameras with image intensification capability based in Micro Channel Plate (MCP) technology with CCD are used for operation in an aircraft. A FLIR detects the thermal radiation of the object surface and generates images which can be interpreted by the human eye. The main parameters for state-of-the-art systems are given. ESA

N92-23393# Messerschmitt-Boelkow-Blohm G.m.b.H., Munich (Germany, F.R.).
QUICK-LOOK SYSTEM [QUICK-LOOK SYSTEM]
P. Hicks *In its* Euromar-Seastars: A Definition Study on Modular Multisensor Instrumentation for Airborne Remote Sensing of the Sea May 1991 16 p In GERMAN (For primary document see N92-23379 14-43)
Avail: NTIS HC/MF A19

The requirements of the quick look system on board the measuring aircraft are described. Recommendations for the implementation of such a system are given. The functions of the quick look system are presented: sensor checking, sensor mode, control of the flight path, and first collection of measuring results. ESA

N92-23394# Messerschmitt-Boelkow-Blohm G.m.b.H., Munich (Germany, F.R.).
ON BOARD DATA FORMATTING [DATEN-FORMATTIERUNG AN BORD]
P. Hicks *In its* Euromar-Seastars: A Definition Study on Modular Multisensor Instrumentation for Airborne Remote Sensing of the Sea May 1991 4 p In GERMAN (For primary document see N92-23379 14-43)
Avail: NTIS HC/MF A19

Decentralized formatting is provided. It is shown that some sensors do not manage position and time data by data recording. The task is carried out by data formatting. Requirements for formatting and for individual sensors are outlined. Forward Looking Airborne Radar (FLAR), Synthetic Aperture Radar (SAR), radiometer, spectrometer, and fluorosensor applications are covered. ESA

N92-23395# Messerschmitt-Boelkow-Blohm G.m.b.H., Munich (Germany, F.R.).
ON BOARD DATA RECORDING [DATEN-AUFZEICHNUNG AN BORD]
P. Hicks *In its* Euromar-Seastars: A Definition Study on Modular Multisensor Instrumentation for Airborne Remote Sensing of the Sea May 1991 24 p In ENGLISH and GERMAN (For primary document see N92-23379 14-43)
Avail: NTIS HC/MF A19

On board system requirements are outlined. Requirements are detailed for individual sensors: Synthetic Aperture Radar (SAR) recorder, radiometer recorder, spectrometer recorder, fluorosensor recorder, Forward Looking Infrared (FIR) sensor recorder, Low Light Level Television (LLLTV) recorder, magnetic band recorder, and optical disc recorder. ESA

N92-23396# Messerschmitt-Boelkow-Blohm G.m.b.H., Munich (Germany, F.R.).
REAL-TIME RADAR PROCESSOR [ECHTZEIT-RADAR-PROZESSOR]
A. P. Wolframm *In its* Euromar-Seastars: A Definition Study on Modular Multisensor Instrumentation for Airborne Remote Sensing of the Sea May 1991 15 p In GERMAN (For primary document see N92-23379 14-43)
Avail: NTIS HC/MF A19

Only the order of magnitude of the calculating power is evaluated. Two possible system realizations (Synthetic Aperture Radar (SAR) and Forward Looking Airborne Radar (FLAR)) are presented. Computers used as examples are based on the VME bus or the AT bus. ESA

N92-23397# Messerschmitt-Boelkow-Blohm G.m.b.H., Munich (Germany, F.R.).
GROUND STATION [BODENSEGMENT]
P. Hicks *In its* Euromar-Seastars: A Definition Study on Modular Multisensor Instrumentation for Airborne Remote Sensing of the Sea May 1991 13 p In ENGLISH and GERMAN (For primary document see N92-23379 14-43)
Avail: NTIS HC/MF A19

The Euromar-Seastars ground station design is as flexible as possible in order to allow the recording of data in another format, and the combination of various sensor data in a common format for user distribution. General requirements are identified and discussed, with regard to the type of recording medium: data volume, recording data format, data fusion, data preparation and type of data distribution. Ground station implementation is described, and a ground station data flow is shown. ESA

N92-23398# Messerschmitt-Boelkow-Blohm G.m.b.H., Munich (Germany, F.R.).
MULTISENSOR DATA FUSION [MULTI SENSOR DATA FUSION]
T. K. Pike and C. Boesswetter *In its* Euromar-Seastars: A Definition Study on Modular Multisensor Instrumentation for Airborne Remote Sensing of the Sea May 1991 17 p In ENGLISH and GERMAN (For primary document see N92-23379 14-43)
Avail: NTIS HC/MF A19

The present state of development of multisensor data fusion is presented as the MUltiSensor Image Processing (MUSIP) project, which developed a proof of concept software demonstrator for the fusion and analysis of remotely sensed images within a knowledge based environment. The target application is the monitoring of forestry, using a test dataset comprising optical and radar images spanning a twelve year period. The MUSIP system is being implemented on a SUN 4 workstation with selected low level algorithm accelerated by a transputer based processor. ESA

N92-23399# Messerschmitt-Boelkow-Blohm G.m.b.H., Munich (Germany, F.R.).
HARDWARE AND SOFTWARE MODULARITY [MODULARITAET HARDWARE UND SOFTWARE]
P. Hicks *In its* Euromar-Seastars: A Definition Study on Modular Multisensor Instrumentation for Airborne Remote Sensing of the Sea May 1991 5 p In GERMAN (For primary document see N92-23379 14-43)
Avail: NTIS HC/MF A19

It is shown that the interchangeability of sensors is one of the most important factors of the proposed concept. The comparability of sensor requirements is examined in connection with regard to hardware and software. The implementation of the modularity concept is described. ESA

N92-23400# Messerschmitt-Boelkow-Blohm G.m.b.H., Munich (Germany, F.R.).
SENSOR INTERFACES [SENSOR-SCHNITTSTELLEN]
P. Hicks *In its* Euromar-Seastars: A Definition Study on Modular Multisensor Instrumentation for Airborne Remote Sensing of the Sea May 1991 6 p In GERMAN (For primary document see N92-23379 14-43)
Avail: NTIS HC/MF A19

It is shown that most sensor interfaces cannot be detailed enough because sensor development has just started. Information is given on fluorosensor and radiometer interfaces. General information on sensor interface is tabulated. ESA

N92-23401# Messerschmitt-Boelkow-Blohm G.m.b.H., Munich (Germany, F.R.).
TYPES OF OPERATION AND SYSTEM CONTROL [BETRIEBSARTEN- UND SYSTEM-STEUERUNG]
P. Hicks *In its* Euromar-Seastars: A Definition Study on Modular Multisensor Instrumentation for Airborne Remote Sensing of the Sea May 1991 5 p In GERMAN (For primary document see N92-23379 14-43)
Avail: NTIS HC/MF A19

The operational concept is presented. Preflight/mission checks on ground are performed. System initialization, in flight checks, system mode, data recording mode, and post flight checks are examined. Operating functions of sensor control, display selection, and data storage are explained. It is shown that new displays for the operator can be easily implemented. ESA

N92-23402# Deutsche Forschungsanstalt fuer Luft- und Raumfahrt, Cologne (Germany, F.R.).
PRECONSIDERATIONS ON AIRCRAFT INTEGRATION [VORUEBERLEGUNGEN ZUR FLUGZEUG-INTEGRATION]
H. Finkenzeller *In* MBB, Euromar-Seastars: A Definition Study on Modular Multisensor Instrumentation for Airborne Remote Sensing of the Sea May 1991 4 p In GERMAN (For primary document see N92-23379 14-43)
Avail: NTIS HC/MF A19

Preconsiderations were envisaged in the integration of the various sensors and subsystems in the aircraft belonging to the German air and space institution. These preconsiderations could not be carried out because of lack of cooperation in the definition phase. The assembly configuration for the DO 228 LM aircraft is shown as an example. ESA

N92-23403# Messerschmitt-Boelkow-Blohm G.m.b.H., Munich (Germany, F.R.).
SENSOR COMPATIBILITY/OPTIMAL SENSOR COMBINATIONS [SENSOR-VERTRAEGLICHKEIT/OPTIMALE SENSOR-KOMBINATIONEN]
C. Boesswetter *In its* Euromar-Seastars: A Definition Study on Modular Multisensor Instrumentation for Airborne Remote Sensing of the Sea May 1991 2 p In GERMAN (For primary document see N92-23379 14-43)
Avail: NTIS HC/MF A19

It is shown that the sensors considered scan extraordinary wide bandwidth. They cover practically the whole electromagnetic spectrum which is significant for the examination of ocean situation. Sensor compatibility is examined using examples such as the reaction of pilot radiotelephony on simultaneously operating radar or microwave radiometer system. The influence of sensors on the propagation path can be neglected. The most important restrictions result from the limited payload capacity and power consumption of all aircraft carriers considered. ESA

N92-23404# Messerschmitt-Boelkow-Blohm G.m.b.H., Munich (Germany, F.R.).
EVALUATION OF THE SENSOR EFFECTIVENESS [BEWERTUNG DER SENSOR-EFFEKTIVITAET]
C. Boesswetter *In its* Euromar-Seastars: A Definition Study on Modular Multisensor Instrumentation for Airborne Remote Sensing of the Sea May 1991 8 p In GERMAN (For primary document see N92-23379 14-43)
Avail: NTIS HC/MF A19

The quantitative evaluation of the attractiveness of a sensor within a multisensor system, with regard to its effectiveness, is shown as a task which needs to be solved in various fields. To perform the evaluation, it is necessary to determine the single sensor efficiency and the system efficiency in the given operating conditions. The effectiveness of the efficiency model is to be evaluated in relation with the given requirements. The matrix process is presented. A numerical example is given. ESA

N92-23405# Messerschmitt-Boelkow-Blohm G.m.b.H., Munich (Germany, F.R.).
CURRENT DEFINITION OF SOME DEVELOPMENT PROGRAMS [VORLAEUFIGE DEFINITION EINES ENTWICKLUNGS-PROGRAMMS]
C. Boesswetter *In its* Euromar-Seastars: A Definition Study on Modular Multisensor Instrumentation for Airborne Remote Sensing of the Sea May 1991 8 p In GERMAN (For primary document see N92-23379 14-43)
Avail: NTIS HC/MF A19

Partial markets for hardware and software components of onboard systems, ground stations, and for services such as system operations are discussed. Microwave radiometer and radar sensor markets are examined. Local supervision cannot compete with satellite aided systems, but both systems are shown to be complementary. ESA

N92-23406# Messerschmitt-Boelkow-Blohm G.m.b.H., Munich (Germany, F.R.).
REALIZATION AND PROVISIONAL SENSOR DEVELOPMENT PLANNING [REALISIERBARKEIT UND VORLAEUFIGER SENSOR-ENTWICKLUGSPLAN]
C. Boesswetter *In its* Euromar-Seastars: A Definition Study on Modular Multisensor Instrumentation for Airborne Remote Sensing of the Sea May 1991 4 p In GERMAN (For primary document see N92-23379 14-43)
Avail: NTIS HC/MF A19

The Euromar-Seastars development program is discussed. The program is concerned with the following: active and passive optical sensors, imaging radar systems, imaging microwave radiometers, data systems, and real-time radar processors. A seven year development program will be carried out with the cooperation of several European agencies, in particular Italy. ESA

N92-23407# Messerschmitt-Boelkow-Blohm G.m.b.H., Munich (Germany, F.R.).
NATIONAL USER INTERFACES [SCHNITTSTELLE ZU NATIONALEN NUTZERN]
C. Boesswetter *In its* Euromar-Seastars: A Definition Study on Modular Multisensor Instrumentation for Airborne Remote Sensing of the Sea May 1991 4 p In GERMAN (For primary document see N92-23379 14-43)
Avail: NTIS HC/MF A19

Investigations have shown that Euromar-Seastars potential users represent a very heterogeneous group. All currently available national potential user information was examined in a definition study. The potential national users were given a questionnaire and were asked to respond. ESA

N92-23408# Messerschmitt-Boelkow-Blohm G.m.b.H., Munich (Germany, F.R.).
PROVISIONAL COST EVALUATION [VORLAEUFIGE KOSTENSCHAETZUNG]
C. Boesswetter *In its* Euromar-Seastars: A Definition Study on Modular Multisensor Instrumentation for Airborne Remote Sensing of the Sea May 1991 2 p In GERMAN (For primary document see N92-23379 14-43)
Avail: NTIS HC/MF A19

The evaluated costs for all the elements of the implementation phase were estimated, under the assumption that a country, Germany in the this case, is to develop all the elements of the

general program. A total of 47.7 million German Marks is required for a seven year general program. ESA

N92-23409# Messerschmitt-Boelkow-Blohm G.m.b.H., Munich (Germany, F.R.).
INTERNATIONAL COOPERATION [INTERNATIONALE ZUSAMMENARBEIT]
In its Euromar-Seastars: A Definition Study on Modular Multisensor Instrumentation for Airborne Remote Sensing of the Sea May 1991 2 p In GERMAN (For primary document see N92-23379 14-43)
Avail: NTIS HC/MF A19

The agreement for international cooperation is based on two documents: (1) the Euromar-Seastars industrial agreement; and (2) an 18 point catalog of the Euromar-Seastars project. The first document was cooperatively drafted by an Italian company and a German Company. Other countries are expected to sign this agreement. The second document is the official description of the Euromar-Seastars project. ESA

N92-23410# Messerschmitt-Boelkow-Blohm G.m.b.H., Munich (Germany, F.R.).
EUROMAR INDUSTRIAL PARTNERS AGREEMENT
C. Boesswetter *In its* Euromar-Seastars: A Definition Study on Modular Multisensor Instrumentation for Airborne Remote Sensing of the Sea May 1991 6 p (For primary document see N92-23379 14-43)
Avail: NTIS HC/MF A19

Italian, German, and Dutch companies, acting as industrial coordinators of their national industries, committed themselves to begin the project as soon as their respective national administrations can reach an agreement. The total cost of the definition phase is estimated to be 1.1 million ecus. The preliminary cost estimate for the realization phase amounts to 44.8 million ecus over seven years. ESA

N92-23411# Messerschmitt-Boelkow-Blohm G.m.b.H., Munich (Germany, F.R.).
AN 18-POINT CATALOG DESCRIPTION
C. Boesswetter *In its* Euromar-Seastars: A Definition Study on Modular Multisensor Instrumentation for Airborne Remote Sensing of the Sea May 1991 6 p (For primary document see N92-23379 14-43)
Avail: NTIS HC/MF A19

The official description of the Euromar-Seastars project is presented. Its form is the same as for all Euromar projects. The nature of work is defined. The following are reported: participants, preliminary cost estimate, time scale of technological development envisaged, status of agreement between participants, location of development work, and preliminary exploitation of the results. ESA

N92-23441# Helsinki Univ. of Technology, Espoo (Finland). Lab. of Space Technology.
DEVELOPMENT OF A HELICOPTER-BORNE 8-CHANNEL RANGING SCATTEROMETER
J. Hyyppae and M. Hallikainen Jul. 1991 29 p
(PB92-141977; ISBN-951-22-0733-8; Rept-4) Avail: NTIS HC/MF A03 CSCL 14B

A helicopter-borne dual-frequency FM-CW scatterometer (Helsinki University of Technology Scatterometer (HUTSCAT)) is described. The HUTSCAT can measure the backscattering properties of a target with a range resolution of 65 cm. This is accomplished by performing the Fast Fourier Transform (FFT) to the received time-domain signal. The measurement is made simultaneously at eight channels. The scatterometer measures the radar return spectrum for eight channels in 16.6 ms which corresponds to an along-track distance of 0.33 m for the helicopter speed of 20 m/s. GRA

N92-23465# National Space Development Agency, Saitama (Japan). Earth Observation Center.
PROCEEDINGS ON MOS-1 DATA EVALUATION
Korehiro Maeda, ed. and S. Ogawa, ed. Mar. 1990 352 p In ENGLISH and JAPANESE Original contains color illustrations
(HE-90015; JTN-92-80274) Avail: NTIS HC/MF A16

Topics addressed include: Japanese spacecraft, marine observation satellite, satellite observation, spacecraft performance, earth observing system, remote sensing, remote sensors, radiometers, image processing, image analysis, imaging technology, satellite imaging, image reconstruction, signal processing, infrared scanner, microwave radiometers, signal processing, geodetic survey, earth observation, rainfall measurement, snow cover, brightness temperature, antenna radiation patterns, and ice reporting. For individual titles, see N92-23466 through N92-23493.

N92-23466# National Space Development Agency, Saitama (Japan). Earth Observation Center.
OUTLINE OF UTILIZATION RESULTS OF MOS-1 DATA
Korehiro Maeda and Hideo Satoh *In its* Proceedings on MOS-1 Data Evaluation Mar. 1990 p 1-1 (For primary document see N92-23465 14-43)
Avail: NTIS HC/MF A16

Marine Observation Satellite-1 (MOS-1) and MOS-1b were launched in 1987 and 1990, respectively. MOS-1 data are now received by 11 ground stations in the world. National Space Development Agency of Japan (NASDA) conducted the MOS-1 Verification Program (MVP) in collaboration with domestic and foreign investigators in order to evaluate the MOS-1 observation system from various points of view. As a part of MVP, the utility of MOS-1 data in various application fields including earth environment has been evaluated. In this paper, fields of utilization are classified into three categories (ocean, land, and atmosphere). An outline of utilization results are presented. Author (NASDA)

N92-23467# Ministry of Posts and Telecommunications, Tokyo (Japan). Communications Research Lab.
MEASUREMENTS OF RAIN RATE DISTRIBUTION BY MOS-1 MSR
Yuji Ohsaki and Masaharu Fujita *In* NASDA, Proceedings on MOS-1 Data Evaluation Mar. 1990 p 13-16 In JAPANESE; ENGLISH summary (For primary document see N92-23465 14-43)
Avail: NTIS HC/MF A16

An algorithm for estimation of rain rate from Marine Observation Satellite-1 (MOS-1) Microwave Scanning Radiometer (MSR) data was developed. To investigate the performance of this algorithm, the rain rates estimated from MSR were compared with rain rates observed by the weather radar on the top of mount Fuji with the reduction of the effect of the nonuniform distribution of rain in the MSR Field Of View (FOV). The correlation between the MSR and radar rain rates was fairly good, so the availability of the rain observation by MSR could be confirmed. The estimation of rain rate by MSR, however, is limited to the area over the ocean. The measurements of the area over the ocean, but near from the land, is not available because of the effect of the noise from land detected by the MSR antenna sidelobe. So, there is a need to do a comparative study using the rain area over the ocean located far from land. But the accuracy of rain observation by the radar depends on the range of the radar antenna to rain, so the quality on the radar data is not constant by the range. For the next step of the comparative study, it is planned to get the data of Satellite-derived Index (SI) of precipitation intensity. SI is designed to estimate the rain rate from Geostationary Meteorological Satellite (GMS) data. Author (NASDA)

N92-23468# Ministry of Posts and Telecommunications, Tokyo (Japan). Communications Research Lab.
APPLICATION OF GROUND-BASED LASER BEACON FOR EARTH IMAGE CALIBRATION, 3
Masao Takabe, Toshikazu Itabe, and Tadashi Aruga *In* NASDA, Proceedings on MOS-1 Data Evaluation Mar. 1990 p 17-25 In JAPANESE; ENGLISH summary (For primary document see N92-23465 14-43)
Avail: NTIS HC/MF A16

This paper will report some preliminary results of the Marine

Observation Satellite-1 (MOS-1) verification research using a ground-based laser beacon. An earth laser beacon is observed from space as a point similar to a bright star. Thus, the spot image of a laser beacon is very useful for calibration/correction of the earth's surface image taken by optical radiometers or cameras, since it corresponds to an infinitively small land mark whose absolute location and brightness are known precisely. The experiments of tracking the MOS-1 and transmitting a laser beam from a ground station at Communications Research Laboratory (CRL) to the satellite have been conducted. Currently an argon ion laser is used as a beacon, and images taken by the Multispectral Electronic Self Scanning Radiometer (MESSR) are analyzed for this study. As the results of analysis, at first a tendency of the MOS-1 location error obtained from the optical tracking is shown. Then the geometric error of the MESSR earth images and the satellite's attitude estimated from two dimensional coordinates of the laser spot and the scene center, are shown.

Author (NASDA)

N92-23469# Tokai Univ., Tokyo (Japan). Research and Information Center.

ESTIMATION OF MTF OF MOS-1 MESSR IMAGES

Toshibumi Sakata, Haruhisa Shimoda, and Kiyonari Fukue *In* NASDA, Proceedings on MOS-1 Data Evaluation Mar. 1990 p 26-51 In JAPANESE; ENGLISH summary (For primary document see N92-23465 14-43)

Avail: NTIS HC/MF A16

A Modulation Transfer Function (MTF) of Multispectral Electronic Self Scanning Radiometer (MESSR) image was estimated using an edge spectrum ratio method. This method was applied to vertical and horizontal edges in several MESSR images. The Effective Instantaneous Field Of View's (EIFOV) were obtained from the estimated MTF. The average values of obtained EIFOV's are 71-75 m and 77-78 m for tracking and scanning directions, respectively. As the result of evaluation for EIFOV's, the following conclusions were obtained: (1) Seasonal changes of atmospheric condition effects on EIFOV are about 4 m on average and about 10 m as maximum; (2) A difference of EIFOV between the system-1 and 2 is nothing; (3) Atmospheric effects on EIFOV were estimated as 29 m, 24 m, 21 m and 11 m for each channel, respectively; (4) It is estimated, after consideration of the intrinsic performance of MESSR, that the movement of platform increases 14 m (15 percent) of EIFOV. Author (NASDA)

N92-23470# Meteorological Research Inst., Tsukuba (Japan). Oceanographical Research Div.

INVESTIGATIONS ON VERIFICATION OF THE DATA OBSERVED BY THE MESSR AND VTIR, AND ON INTERANNUAL TREND IN THE MSR DATA

Akira Shibata, Yoshio Shinohara, and Kenzo Shuto *In* NASDA, Proceedings on MOS-1 Data Evaluation Mar. 1990 p 52-63 In JAPANESE; ENGLISH summary (For primary document see N92-23465 14-43)

Avail: NTIS HC/MF A16

Performance of the Microwave Scanning Radiometer (MSR) is estimated by using the data in the period May 1987 through November 1989. The difference r.m.s. (root mean square) between the accumulated water vapor content obtained by the MSR and aerological observations is 2.3 kg per sq meter for Chichijima Island, and 2.9 kg per sq meter for Hachijo Island. Those data are excluded in which the accumulated liquid water content observed by the MSR is larger than 0.8 kg per sq meter. In those cases, it becomes difficult for the MSR to estimate the water vapor content accurately, because the microwave is scattered by both rain drops and ice crystals. Several causes for the difference r.m.s. are estimated, including the natural and mechanical ones. Correction coefficients, such as antenna pattern, bias, polarization, and land emission, are shown, which are used in transforming the antenna temperature into the brightness temperature.

Author (NASDA)

N92-23471# Meteorological Research Inst., Tsukuba (Japan). Meteorological Satellite and Observation Research Div.

VERIFICATION OF MESSR AND VTIR, AND TIME VARIATION OF MSR PERFORMANCE

Yozo Takayama, Tsutomu Takashima, Kazuhiko Masuda, and Akio Kurosaki *In* NASDA, Proceedings on MOS-1 Data Evaluation Mar. 1990 p 64-70 In JAPANESE; ENGLISH summary (For primary document see N92-23465 14-43)

Avail: NTIS HC/MF A16

Accuracy in radiation measurement by Visible and Thermal Infrared Radiometer (VTIR) Band 2 was examined by using the relation between water vapor density and observed brightness temperature of the band. In comparison between estimated and observed data, the method could avoid uncertainty in water vapor distribution. The result shows no discrepancy between the predicted relation and the observed one. The relation could apply to analysis of water vapor distribution. For utilization of VTIR sea surface temperature (SST), an image was made and compared with a ten day mean surface temperature map which was based on ship measured SST. The patterns were matched, showing a temperature difference of about 1 C. Author (NASDA)

N92-23472# University of Electro-Communications, Tokyo (Japan).

SIGNAL PROCESSING OF THE DATA OBTAINED BY MOS-1 MSR

Kazuhiko Morita, Ikuo Arai, and Tsutomu Suzuki *In* NASDA, Proceedings on MOS-1 Data Evaluation Mar. 1990 p 71-91 In JAPANESE; ENGLISH summary (For primary document see N92-23465 14-43)

Avail: NTIS HC/MF A16

This paper describes new techniques to improve the accuracy in data from the Marine Observation Satellite-1 (MOS-1) Microwave Scanning Radiometer (MSR). The error correction is processed by an inversion technique to the polarization, side lobes and foot print of the MOS-1 MSR antenna. The error due to unwanted brightness radiation from upper atmosphere is also considered. The result shows that the corrections on the data around Japan are feasible as to the brightness temperatures which are corrected about 20 K and 10 K on the land and sea area, respectively.

Author (NASDA)

N92-23473# Forestry and Forest Products Research Inst., Ibaraki (Japan). Remote Sensing Lab.

EVALUATION OF EFFECTIVE CHARACTERISTIC IN FOREST FIELD

Haruo Sawada, Osamu Nakakita, Kuniko Hasegawa, and Yoshio Awaya *In* NASDA, Proceedings on MOS-1 Data Evaluation Mar. 1990 p 92-99 In JAPANESE; ENGLISH summary (For primary document see N92-23465 14-43)

Avail: NTIS HC/MF A16

Outline of results of evaluation of Marine Observation Satellite-1 (MOS-1) Multispectral Electronic Self Scanning Radiometer (MESSR) for forest resource management in Peninsula Malaysia is presented. Training areas, two hill-forests, swampy forest, and mangrove forest were formed from four images. Their statistics and cluster-classes were calculated. The result was that there were 6 to 11 classes in forestry and the range of visible channel was small. Vegetation indices should be applied (it was discussed in the first report) for tropical forestry of this time. In result, it seems to suggest that vegetation indices show covering ratio of vegetation. Vegetation indices about zoning of forestry were used and satisfactory results were obtained. Author (NASDA)

N92-23474# National Research Center for Disaster Prevention, Tokyo (Japan).

VERIFICATION OF THE EFFECTIVENESS OF MOS-1 MESSR IN THE FIELD OF DISASTER PREVENTION

Shigetsugu Uehara, Kazuro Nakane, Shinobu Yazaki, and Toshikazu Morohoshi *In* NASDA, Proceedings on MOS-1 Data Evaluation Mar. 1990 p 100-108 In JAPANESE; ENGLISH summary (For primary document see N92-23465 14-43)

Avail: NTIS HC/MF A16

This study includes analysis on three different kinds of disasters to verify the effectiveness of Marine Observation Satellite-1 (MOS-1) Multispectral Electronic Self Scanning Radiometer (MESSR). The first is an analysis on the relationship between flooded areas and their geomorphological features to a MESSR image around Dhaka of Bangladesh taken on 17 October 1988. The second is an analysis to delineate the fallen ash covered areas due to the eruptions of Aso Volcano using a MESSR data taken on 18 October 1989. The third is an analysis to make clear the topographical features and patterns of erosion over a MESSR image of Loess Plateau in China. The following results were obtained: (1) A MESSR image around Dhaka was very effective to delineate various micro geomorphological features; (2) The analysis to delineate the fallen ash was fairly difficult; and (3) Topographical features of the erosion of the Loess Plateau were enhanced using differential operator to each of the band images. The near infrared bands are more effective to enhance the features due to thin brightness of vegetation covered areas than visible ones. Author (NASDA)

N92-23475# Meteorological Satellite Center, Tokyo (Japan).
ESTIMATION OF SEA SURFACE TEMPERATURES USING MOS-1, GMS, AND NOAA
Hideyuki Sasaki, Yoshishige Shirakawa, and Yoshiaki Takeuchi *In* NASDA, Proceedings on MOS-1 Data Evaluation Mar. 1990 p 109-118 In JAPANESE; ENGLISH summary (For primary document see N92-23465 14-43)
Avail: NTIS HC/MF A16

Sea Surface Temperatures (SST'S) are estimated by using four regression methods of two satellites, namely two methods using Marine Observation Satellite-1 (MOS-1) Visible and Thermal Infrared Radiometer (VTIR) data and two of NOAA-9 (National Oceanic and Atmospheric Administration-9) Advanced Very High Resolution Radiometer (AVHRR) and Television Infrared Observation Satellite (TIROS) Operational Vertical Sounder (TOVS). The satellite-derived SST are compared with in-situ measured SST. The result shows that (1) Root Mean Square (RMS) errors of four methods are not so different, and (2) bias errors are minus for MOS-1's two methods and plus for NOAA's two methods. The comparison of the calibration of five infrared sensors, MOS-1/VTIR (Band 3 and 4), IR channel of Geostationary Meteorological Satellite-3 (GMS-3) and GMS-4 and NOAA-10/AVHRR shows that VTIR Band 3 and 4 are calibrated with the accuracy of less than 1 C. Author (NASDA)

N92-23476# Maritime Safety Agency, Tokyo (Japan). Hydrographic Dept.
MONITORING OF OCEAN CONDITIONS BY USING MOS-1 DATA
Masataka Hishida, Hiroyuki Yoritaka, Haruo Ishii, Minoru Odamaki, Tooru Tsukamoto, and Satoshi Sato *In* NASDA, Proceedings on MOS-1 Data Evaluation Mar. 1990 p 119-145 In JAPANESE; ENGLISH summary (For primary document see N92-23465 14-43)
Avail: NTIS HC/MF A16

Availability of Marine Observation Satellite-1 (MOS-1) data for mapping of sea surface temperature, transparency, ocean color and discolored water discharged from submarine volcanos was examined. Results of the study are as follows: (1) MOS-1 Multispectral Electronic Self Scanning Radiometer (MESSR) and Visible and Thermal Infrared Radiometer (VTIR) data (black and white film, Computer Compatible Tape (CCT)) were compared with observed ocean conditions (rough pattern of ocean conditions was observed by MESSR data, but fine structure was not. Sea surface temperature was decided from VTIR data with the precision of about + or - 1 C in consequence of comparison with in-situ data, so that only general pattern of sea surface temperature was observed); (2) Discolored water discharged from submarine volcano 'FUKUTOKU OKA NO BA', which was observed from an airplane, was examined using MESSR data (however, it was not detected from color print, but was dimly detected from black and white film (Low Gain Mode); and (3) Accordingly, in a sea area, MESSR should be operated in High Gain Mode, so that its usefulness will be expanded for ocean observation. Author (NASDA)

N92-23477# Japan Fisheries Information Service Center, Tokyo.
STUDY OF MOS-1 MESSR DATA FOR VARIABILITY OF THE BRANCH (WARM STREAMER) FROM WARM EDDY AND FOR FISHING GROUND
Hideo Tameishi, Osamu Honda, Yoshihiro Okada, Toshiyuki Kouguchi, and Keiichi Iwata *In* NASDA, Proceedings on MOS-1 Data Evaluation Mar. 1990 p 146-154 In JAPANESE; ENGLISH summary (For primary document see N92-23465 14-43)
Avail: NTIS HC/MF A16

In the second Symposium on Marine Observation Satellite-1 (MOS-1) Verification Program (MVP), the application of MOS-1 data for forecasting the fishing ground of the Skipjack was reported. Also, in the third Symposium the relationship between the MOS-1 Multispectral Electronic Self Scanning Radiometer (MESSR) Data and Coastal fishing ground was studied. In this study, the relationship between fine structure of warm eddy and fishing ground was investigated by using the MOS-1 Visible and Thermal Infrared Radiometer (VTIR) data with referring aircraft data. The following interesting results were obtained: (1) MOS-1 VTIR imagery can represent the Warm Streamer and it is recognized that the spatial resolution accuracy (2.7 km) is enough to appreciate the fine structure; (2) By use of the simultaneous aircraft data, it is found that the many schools of sardine are distributed at the head of Warm Streamer; and (3) It seems that the Warm Streamer is useful for the transfer of schools toward the north.
Author (NASDA)

N92-23478# Toba Merchant Marine Coll. (Japan).
APPLICABILITY OF MESSR AND VTIR DATA FOR MARINE OBSERVATION Report No. 3
Hiroaki Ochiai *In* NASDA, Proceedings on MOS-1 Data Evaluation Mar. 1990 p 155-161 In JAPANESE; ENGLISH summary (For primary document see N92-23465 14-43)
Avail: NTIS HC/MF A16

Using the data obtained by Marine Observation Satellite-1 (MOS-1), the applicability of Multispectral Electronic Self Scanning Radiometer (MESSR) and Visible and Thermal Infrared Radiometer (VTIR) data for monitoring of marine environment was evaluated and several remarkable results were carried out as follows: (1) The water characteristics in Ise Bay in hottest season is well identified by color sliced imagery produced from Band-1 and Band-4 of MESSR; (2) The sea surface temperature distribution pattern around Kuroshio Current and surrounding area in Kumanonada is recognized as very well in color sliced imagery of Band-4 of VTIR; and (3) In comparison with hydrographical data collected by ship, both MESSR and VTIR data were concluded as very effective for marine observation especially in coastal areas. Author (NASDA)

N92-23479# Chiba Univ. (Japan). Remote Sensing and Image Research Center.
RETRIEVAL OF UPPER PRECIPITABLE WATER PROFILE FROM MOS-1 VTIR WATER VAPOR CHANNEL
Masao Matsumoto, Shigeyuki Takasaki, and Kiyoshi Tsuchiya *In* NASDA, Proceedings on MOS-1 Data Evaluation Mar. 1990 p 162-169 In JAPANESE; ENGLISH summary (For primary document see N92-23465 14-43)
Avail: NTIS HC/MF A16

The retrieval method of precipitable water profile within the range from top of the atmosphere to 500 millibar from Marine Observation Satellite-1 (MOS-1) Visible and Thermal Infrared Radiometer (VTIR) water vapor channel is proposed. The precipitable water profile is retrieved by maximum likelihood solution of linearized radiative transfer equation which represents radiation conservation of layered atmosphere. Up to 35 percent of root mean square error of the estimation occurred. The difference between observed brightness temperature (T sub b) and calculated T sub b through LOWTRAN 7 application of computer program is about 10 K. Computed value is lower than that provided by Earth Observation Satellite (EOS), which difference is the main cause

of estimation error. For more precise analysis, it is necessary to check overall function of VTIR together with absorption characteristics of radiation by H2O in the spectrum of VTIR water vapor channel. Author (NASDA)

N92-23480# National Research Inst. of Fisheries Engineering, Tokyo (Japan). Marine Productivity Div.
UTILIZATION OF SATELLITE IMAGES FOR MARINE RESOURCES
Denzo Inagake and Akira Tomosada *In* NASDA, Proceedings on MOS-1 Data Evaluation Mar. 1990 p 170-174 In JAPANESE; ENGLISH summary (For primary document see N92-23465 14-43)
Avail: NTIS HC/MF A16

A lot of small scale sea surface phenomena are detected by satellite images. Since these phenomena are believed to play important roles in the formation of structures that can be used to determine the concentration, the distribution, and the movement of fish schools, it was tried to identify those structures and their roles for fisheries resources. Marine Observation Satellite-1 (MOS-1) Multispectral Electronic Self Scanning Radiometer (MESSR) high gain data were analyzed to identify the mechanism for the concentration of Shirasu which are the larvae of sardines. The MESSR high gain data show a number of lines on the sea surface at the south of Atsumi peninsula in 25 Aug. 1989. One of these lines has a shape that is similar to the distribution of the Shirasu fishing grounds. Therefore, it is considered that these phenomena, which can be detected by the MOS-1 MESSR, are important for the distribution of Shirasu schools. It is necessary to study the generative mechanism of these lines by oceanographic observation and to make clear the mechanism of the concentration of Shirasu schools using MOS-1 MESSR high gain data.
Author (NASDA)

N92-23481# National Inst. of Polar Research, Tokyo (Japan).
PRELIMINARY REPORT ON THE OBSERVATION OF POLAR ATMOSPHERE AND CRYOSPHERE BY MOS-1 DATA RECEIVED AT SYOWA STATION
Takashi Yamanouchi, Fumihiko Nishio, Makoto Wada, Hiroshi Kanzawa, and Sadao Kawaguchi *In* NASDA, Proceedings on MOS-1 Data Evaluation Mar. 1990 p 175-188 In JAPANESE; ENGLISH summary (For primary document see N92-23465 14-43)
Avail: NTIS HC/MF A16

The multipurpose satellite data receiving system (11m antenna) has received data from the Marine Observation Satellite-1 (MOS-1) since Feb. 1989. The MOS-1 data has enabled the analysis of cloud liquid water content and water vapor amount, derivation of sea ice information and concentration, and monitoring of the ice sheet edge. Using images from the MOS-1 processed data, applicability of the data to the research subject is examined. Multispectral Electronic Self Scanning Radiometer (MESSR) imagery is applicable to the monitoring of the ice sheet edge. The Visible and Thermal Infrared Radiometer (VTIR) supplies important data to observe synoptic and large scale meteorology. However, the detection of clouds over snow and ice surfaces is difficult, especially in polar night. One of the main uses for the Microwave Scanning Radiometer (MSR) data is to survey the condition and distribution of the sea ice. However, the data is affected by the atmospheric liquid water and water vapor, and may result in large estimation errors of the sea ice concentration. It is difficult to derive the liquid water and water vapor concentration from these data over snow or ice covered surfaces.
Author (NASDA)

N92-23482# Hokkaido Inst. of Tech. (Japan).
AVAILABILITY OF MSR DATA FOR SNOW WATER ESTIMATION
Masahiro Suzuki, Masami Sasaki, Kazuo Fujino, and Toshiyuki Kawamura (Hokkaido Univ., Sapporo, Japan) *In* NASDA, Proceedings on MOS-1 Data Evaluation Mar. 1990 p 189-196 In JAPANESE; ENGLISH summary (For primary document see N92-23465 14-43)
Avail: NTIS HC/MF A16

Using the brightness temperature obtained by the Microwave Scanning Radiometer (MSR) onboard the Marine Observation Satellite-1 (MOS-1), at the frequencies of 23.8 and 31.4 GHz, a comparison between data and ground truth data related snowpack parameters in the Hokkaido area was carried out. The availability of MSR data for the estimation of snowpack parameters was discussed, and several factors which had effects on the accuracy of estimation were investigated. The results indicate that, at the present stage, the remote sensing of snowpacks by MOS-1 MSR is useful for the macroscopic estimation of annual snowcover in a region such as Hokkaido, which has a complex configuration of landcover and snow characteristics. Author (NASDA)

N92-23483# Nagaoka Technological Univ., Niigata (Japan).
OBSERVATION OF LINED-UP CUMULUS ROWS UNDER THE WINTER MONSOON SITUATION USING MOS-1 AND RADAR DATA
Toshio Koike, Hiroshi Ueda, and Yasushi Fujiyoshi (Hokkaido Univ., Sapporo, Japan) *In* NASDA, Proceedings on MOS-1 Data Evaluation Mar. 1990 p 197-203 In JAPANESE; ENGLISH summary (For primary document see N92-23465 14-43)
Avail: NTIS HC/MF A16

The distribution of snow clouds in the coastal regions of Hokkaido and Hokuriku was observed by a combination of the Marine Observation Satellite-1 (MOS-1) and radar on 28 Dec. 1988 and 25 Jan. 1990, respectively. In the Hokkaido region, the longitudinal perturbation was in a preferred mode. The cloud top temperature distributions, using VTIR (Visible and Thermal Infrared Radiometer) data, are consistent with the snow fall distribution predicted by radar data. Radar reflectivity was strong in the high cloud top area. In the Hokuriku region, snow clouds were in the transverse mode. The cloud top temperature decreased over land due to the orographic effect. The strong reflectivity area appeared on the windward side of the cloud center. The water vapor and cloud liquid content data, obtained using the Microwave Scanning Radiometer (MSR), cannot be compared with radar reflectivity data due to the strong land radiation effect. Author (NASDA)

N92-23484# Far Seas Fisheries Research Lab., Shimizu (Japan).
THE ACCURACY OF THE DRIFT BUOY POSITIONING BY MOS-1 DCS
Toshiya Kishiro and Satsuki Matsumura *In* NASDA, Proceedings on MOS-1 Data Evaluation Mar. 1990 p 204-214 In JAPANESE; ENGLISH summary (For primary document see N92-23465 14-43)
Avail: NTIS HC/MF A16

The positioning accuracy of the Marine Observation Satellite-1 (MOS-1) Data Collection System (DCS), in the North Pacific Ocean, was examined and compared with the Navy Navigation Satellite System (NNSS) and ARGOS. The differences between the positions of the drift buoy observed by MOS-1 DCS and by NNSS were about 5.4 km in the northward, and about 4.1 km in the eastward, respectively. The positions observed by MOS-1 DCS, NNSS, and ARGOS were distributed randomly within the range of about 5 km of each other. Distances between each position were within the range of systematic error of Doppler effect produced by moving of the Data Collection Platform (DCP).
Author (NASDA)

N92-23485# Tokai Regional Fisheries Research Lab., Tokyo (Japan). Oceanic Fisheries Dept.
RESEARCH PROJECT FOR PRACTICAL USAGE OF MOS-1 DATA COLLECTION SYSTEM
Akira Kuroiwa *In* NASDA, Proceedings on MOS-1 Data Evaluation Mar. 1990 p 215-222 In JAPANESE; ENGLISH summary (For primary document see N92-23465 14-43)
Avail: NTIS HC/MF A16

It is necessary to study oceanographic activity to improve fishery production. The Study and System Evaluation Project of the Marine Observation Satellite-1 (MOS-1) placed a Data Collection Platform

(DCP) onboard a vessel and measured the water temperature at various depths from 1986-1988. The feasibility of collecting, recording, and analyzing real-time data for use in fishing is studied. In addition, the project is further charged with evaluating the performance and practical utilization of the hardware used in the system from 1989-1991. In 1989, study was extended to the development of various sensors for oceanographic observations and to the improvement of compressed data transmission systems. Author (NASDA)

N92-23486# National Research Inst. of Fisheries Engineering, Tokyo (Japan).
STUDY ON DRIFTING-DATA COLLECTION BUOY USING MOS-1: POSITION VERIFICATION IN THE BERING SEA
Koichi Sawada, Yoshimi Takao, Akio Ikeda, and Ei-Ichi Imanari *In* NASDA, Proceedings on MOS-1 Data Evaluation Mar. 1990 p 223-230 In JAPANESE; ENGLISH summary (For primary document see N92-23465 14-43)
Avail: NTIS HC/MF A16

It is useful to monitor the variation of the marine environment for the purpose of managing fisheries operations. Though it is effective to use satellites, it is difficult to obtain vertically distributed marine data, such as water layer temperature or salinity. A data collection buoy, which can collect the vertically distributed water temperature and salinity data, and which can send these data through the Marine Observation Satellite-1 (MOS-1) Data Collection System (DCS) to a land station, was developed. Large amounts of data are sent by dividing them into several sets. This makes it feasible to sample data in a wide area. A position verification experiment in the Bering Sea was performed. A transmitter was installed in a Hokuten trawler. The northern limit of the MOS-1 DCS and the receivable amount of data were examined at the limit. NASDA Earth Observation Center (EOC) estimated positions were compared with positions obtained every four minutes using the Navy Navigation Satellite System (NNSS) and LORAN C. The result is that ten data transmitting occasions per path at N 61 deg (W 175 deg) and five occasions at W 150 deg (N 59 deg) could be obtained. Author (NASDA)

N92-23487# National Oceanic and Atmospheric Administration, Seattle, WA. Office of Research and Applications.
USE OF MARINE OBSERVATION SATELLITE-1 IN APPLIED OCEAN SCIENCE
William G. Pichel and Robert A. Warner *In* NASDA, Proceedings on MOS-1 Data Evaluation Mar. 1990 p 231-245 (For primary document see N92-23465 14-43)
Avail: NTIS HC/MF A16

The Marine Observation Satellite-1 (MOS-1) carries a unique complement of instruments suited for ocean monitoring, particularly for the monitoring of sea ice. Three MOS-1 instruments are examined for their usefulness to ocean applications. Using a personal computer image display workstation, the Microwave Scanning Radiometer (MSR) data are compared to Special Sensor Microwave/Imager (SSM/I) data for ice concentration and ice edge position determination. The response of the MSR 31.4 GHz band is found to be comparable to that of the SSM/I 37 GHz band, and can be used for mapping sea ice under many conditions. The Visible and Thermal Infrared Radiometer (VTIR) and Multispectral Electronic Self Scanning Radiometer (MESSR) instruments are assessed for their utility in measuring sea surface temperature and ocean color, respectively. Author (NASDA)

N92-23488# Universite Catholique de Louvain (Belgium). Remote Sensing Lab.
MULTITEMPORAL AND MULTISENSOR APPROACH WITH MOS DATA TO NATURAL RESOURCES EVALUATION IN DRY TROPICAL AFRICA (BURKINA FASO)
P. Defourny, P. Jacques, and J. Wilmet *In* NASDA, Proceedings on MOS-1 Data Evaluation Mar. 1990 p 246-262 (For primary document see N92-23465 14-43)
Avail: NTIS HC/MF A16

The possibilities offered by the generation of Marine Observation Satellite (MOS) with regard to the study of renewable resources in dry tropical regions are assessed. The first part of the study is devoted to the use of Multispectral Electronic Self Scanning Radiometer (MESSR) data for phenological monitoring and quantitative evaluation of woody vegetation. A comparison of rain and vegetation index distributions would suggest a close relationship between the two types of observation. Despite botanical observations, no correlation between woody vegetation cover and remote sensing information have been found for the end of dry season. Then, a comparison of the MESSR, Multispectral Scanner (MSS), and Thematic Mapper (TM) sensors has revealed that the high resolution of the MOS Satellite is particularly well suited to the study of sudano-sahelian agrarian systems. Finally, the integration of the two sensors MESSR and Visible and Thermal Infrared Radiometer (VTIR) were used for a discussion of methods for simulating coarse resolution data from high resolution data. The performances of VTIR in terms of spatial resolution have turned out to be of the same order as those of the Advanced Very High Resolution Radiometer (AVHRR) sensor.
Author (NASDA)

N92-23489# Indian Space Research Organization, Ahmedabad. Meteorology and Oceanography Div.
A NOTE ON DATA QUALITY: MSR DATA
P. N. Pathak and N. Gautam *In* NASDA, Proceedings on MOS-1 Data Evaluation Mar. 1990 p 263-269 (For primary document see N92-23465 14-43)
Avail: NTIS HC/MF A16

Under Marine Observation Satellite-1 Verification Program-91 (MVP-91), five data tapes containing Microwave Scanning Radiometer (MSR) data recorded at Bangkok were received during April 1989. The quality aspects of these MSR data have been examined in terms of image characteristics and the variations in the MSR radiometric counts. In view of the large variation observed in the basic radiometric counts, no further analysis was considered to be feasible. Author (NASDA)

N92-23490# Indian Space Research Organization, Ahmedabad. Land Resources Div.
COMPARATIVE STUDY OF DIGITAL MOS-1 MESSR, LANDSAT MSS, AND IRS LISS-1 DATA FOR LAND COVER CLASSIFICATION IN SAMBALPUR DISTRICT, INDIA
V. K. Dadhwal and J. S. Parihar *In* NASDA, Proceedings on MOS-1 Data Evaluation Mar. 1990 p 270-276 (For primary document see N92-23465 14-43)
Avail: NTIS HC/MF A16

The study was undertaken for evaluating the performance of the Marine Observation Satellite-1 (MOS-1) Multispectral Electronic Self Scanning Radiometer (MESSR) (4 Oct. 1988), the LANDSAT-5 Multispectral Scanner (MSS) (12 Oct. 1988), and the Indian Remote Sensing Satellite-1A (IRS-1A) Linear Imaging Scanning System-1 (LISS-1) (October 15, 1988) digital data for land cover classification over an intensive test site in Sambalpur district of Orissa State (India). MSS and LISS-1 data were registered on MESSR and subjected to supervised and unsupervised classification. Maximum likelihood (MXL) supervised classification for 27 training classes of eight major land-cover types gave highest overall mapping accuracy for LISS-1. In the unsupervised approach, pixels belonging to vegetation classes (agriculture, forest, and scrub) were clustered using Diday's algorithm with common input parameters. In this test, no sensor had consistently higher accuracy for all the classes. Statistical separability among the clusters of different classes was then compared using average divergence. LISS-1 had the highest separability while MESSR had a higher to similar divergence in comparison to MSS. Author (NASDA)

N92-23491# Indian Space Research Organization, Ahmedabad. Image Processing Systems Div.
DATA QUALITY EVALUATION RESULTS MOS-1 VERIFICATION PROGRAM
S. S. Palsule, Mritunjay, B. S. Shah, Pushpalata, H. S. Bhatt, G. Paswan, H. K. Garg, and C. V. S. Prakash *In* NASDA, Proceedings on MOS-1 Data Evaluation Mar. 1990 p 277-303 (For primary

document see N92-23465 14-43)
Avail: NTIS HC/MF A16

The Marine Observation Satellite-1 (MOS-1) was successfully launched from the Tanegashima Space Center of the National Space Development Agency of Japan (NASDA) by an N-2 Launch Vehicle in Feb. 1987. Study on performance of the Multispectral Electronic Self Scanning Radiometer (MESSR) was done under MOS-1 verification program (MVP). Some results of Data Quality Evaluation on the MOS-1 Computer Compatible Tape (CCT) have been presented, as part of Indian Space Research Organization's (ISRO) participation in MVP. The data acquired by Bangkok station was used in this analysis. Author (NASDA)

N92-23492# Indian Space Research Organization, Ahmedabad. Land Resources Div.
ESTIMATION OF REGIONAL EVAPOTRANSPIRATION WITH MOS-1 VTIR DATA
T. J. Majumdar, S. S. Pokharna, and A. K. Kandya *In* NASDA, Proceedings on MOS-1 Data Evaluation Mar. 1990 p 304-312 (For primary document see N92-23465 14-43)
Avail: NTIS HC/MF A16

A simplified model suggested by Soer (1980) has been used to estimate evapotranspiration (ET) over a part of Eastern India using Marine Observation Satellite-1 (MOS-1) Visible and Thermal Infrared Radiometer (VTIR) data. This data can be used to generate the surface albedo and surface temperature which are essential for the estimation of evaporation of a particular region of interest. Crop surface temperature gives information on the evaporation rate and on soil moisture conditions. Estimation of evaporation on a regional scale is useful in various ways. Firstly, latent heat of evaporation is used for solving energy balance equations and has implications in micrometeorological and agroclimatological studies. Secondly, it is useful in hydrology for estimation of water balances. Comparison of the ET map as obtained from MOS data shows similarity with the agricultural map. Changes in the contribution to evaporation, as one crosses from uncultivated land to an agricultural crop region and from land to water, are observed. Author (NASDA)

N92-23493# Indian Space Research Organization, Ahmedabad. Land Resources Div.
AN ATTEMPT TO DERIVE LAND SURFACE TEMPERATURES FROM MOS-1 VTIR DATA USING SPLIT-WINDOW CHANNEL COMPUTATION TECHNIQUE
T. J. Majumdar *In* NASDA, Proceedings on MOS-1 Data Evaluation Mar. 1990 p 313-324 (For primary document see N92-23465 14-43)
Avail: NTIS HC/MF A16

Marine Observation Satellite-1 (MOS-1) Visible and Thermal Infrared Radiometer (VTIR) multichannel thermal infrared data were utilized to compute the surface temperatures on land in different parts of Eastern India. Two existing models were used to derive surface temperatures. The split-window channel technique employed here avoids the problem due to atmospheric water vapor perturbation. The technique followed here would essentially be valid in a noncloudy region. Author (NASDA)

N92-23521# National Oceanic and Atmospheric Administration, Boulder, CO. Wave Propagation Lab.
FIELD EVALUATION OF REMOTE SENSOR MEASUREMENTS OF WIND, TEMPERATURE, AND MOISTURE FOR ARM INTEGRATED SOUNDING SYSTEM RESEARCH
B. E. Martner, E. R. Westwater, R. G. Strauch, W. L. Ecklund, and J. B. Snider Oct. 1991 117 p
(PB92-140714; NOAA-TM-ERL-211) Avail: NTIS HC/MF A06 CSCL 14B

Remote sensing systems were operated in Colorado in February and March 1991 to obtain detailed profiles of the kinematic and thermodynamic structure of the atmosphere for the U.S. Department of Energy's Atmospheric Radiation Measurement (ARM) research program. The performance of the NOAA remote sensors used in the 1991 field data collection are evaluated. These include five different wind profilers, each equipped with Radio Acoustic Sounding System (RASS) capability for temperature profiling, and microwave radiometers for measurements of path-integrated water vapor and liquid water content. The design and initial testing of a Fourier transform InfraRed Sounder (FIRS) for humidity profiling is also described. The ranges of height coverage and measurement accuracies for each wind profiler/RASS are examined. Specific recommendations for optimizing the design and configuration of similar instruments are made for the ARM Cloud and Radiation Testbed (CART) sites, based on results of the 1991 field work and earlier tests. Author

N92-23659# National Oceanic and Atmospheric Administration, Ann Arbor, MI. Great Lakes Environmental Research Lab.
COMPUTER TUTORIAL AND ANIMATION OF THE NORMAL ICE CYCLE OF THE LAURENTIAN GREAT LAKES OF NORTH AMERICA FOR 1960 - 1979
R. A. Assel and J. M. Ratkos Nov. 1991 35 p
(PB92-129949; NOAA-TM-ERL-GLERL-76) Avail: NTIS HC/MF A03 CSCL 08H

An interactive, menu driven computer tutorial was developed to provide an overview of the annual Great Lakes ice cycle. The tutorial includes an animation to aid in visualizing the seasonal progression and the spatial patterns of ice cover for the base period 1960 to 1979. The computer algorithm was developed from data contained in the NOAA Great Lakes Ice Atlas. The material is presented as a government technical memorandum to make the tutorial available to the public at large for educational purposes. A computer diskette needed to load and run the tutorial (on a Macintosh Plus with at least 2 megabytes of memory) is not included from NTIS. Background information on the ice cover data and methods used to create the tutorial is followed by a description of the spatial and seasonal ice cover distribution patterns as related to lake bathymetry. Author

N92-23686# General Accounting Office, Washington, DC.
EARTH OBSERVING SYSTEM: NASA'S EOSDIS DEVELOPMENT APPROACH IS RISKY
Feb. 1992 37 p Original contains color illustrations
(GAO/IMTEC-92-24; B-247178) Avail: NTIS HC/MF A03; 4 functional color pages

NASA has initiated a program, called the Earth Observing System (EOS), to collect an integrated set of data to study the Earth's atmosphere, biosphere, oceans, and land surfaces as a complete system over a 15 year period. The data from EOS will be processed, archived, and distributed by the EOS Data and Information System (EOSDIS). The House Committee on Science, Space, and Technology asked GAO to examine several key aspects of NASA's development approach, including the extent to which EOSDIS will use prototyping to reduce system development costs and risk, and may require technologies that are beyond the current state of the art. It is concluded that NASA's development strategy does not adequately identify and mitigate the significant technological risks inherent in a project of the size, scope, and technical complexity of EOSDIS. NASA is not devoting enough attention to prototyping key aspects of the EOSDIS concept, nor is it adequately planning for the development and incorporation of critical advanced technologies. NASA's near term EOSDIS prototype projects do not fully address critical areas where technical feasibility is in question nor are they substantial enough to allow users to assess key EOSDIS functions. Author

N92-23703 California Univ., Berkeley.
CONTINUOUS PROFILING OF MAGNETOTELLURIC FIELDS Ph.D. Thesis
Carlos Torres-Verdin 1991 305 p
Avail: Univ. Microfilms Order No. DA9203745

The magnetotelluric (MT) method of mapping ground electrical conductivity is traditionally based on measurements of the surface impedance at widely spaced stations. Because of commonly encountered static effects, inadequate station spacing effectively aliases the electric field measurements and results in distortions that cannot be removed in subsequent processing or modeling. In order to fully exploit the benefits of magnetotellurics in complex

geological situations, closely spaced measurements must be used routinely. An analysis of MT data is taken along continuous profiles and is a first that will allow more encompassing 2-D sampling techniques to become viable in the future. The developments presented are to a large extent motivated by the physical insight gained from low contrast linear solutions to the forward MT problem. These solutions can be simply expressed for 1-D, 2-D, and 3-D resistivity models and hence can be used for a general study of magnetotellurics. Dissert. Abstr.

N92-23724 North Carolina State Univ., Raleigh.
URBAN TEMPERATURE BIAS AS DETERMINED BY POLAR ORBITING SATELLITE DATA Ph.D. Thesis
Gregory Lynn Johnson 1991 163 p
Avail: Univ. Microfilms Order No. DA9202560

A method of determining urban temperature bias from remotely sensed data is developed and successfully tested. First, atmospheric sounding products from NOAA's polar orbiting satellites were used to derive predictive equations of shelter level maximum and minimum temperatures. Sounding data from both winter and summer months were combined with surface data from over 5300 cooperative weather stations in the continental U.S. to develop multiple linear regression equations. Predictive equations were then used to estimate rural temperatures, unaffected by urbanization. Clear and partly cloudy sounding retrievals proved superior to cloudy retrievals. Validation tests showed the models' abilities to predict rural temperatures in different months and in specific climatic regions. Using these equations, estimates of urban temperature bias for 37 cities were made. These estimates compared favorably to ground truth data. Largest differences between observed and predicted bias were found at coastal cities, and those at higher elevations in the western U.S. Mean differences between observed and predicted bias for groups of cities were not significantly different, making the potential application very plausible. Dissert. Abstr.

N92-23367*# National Aeronautics and Space Administration. Goddard Space Flight Center, Greenbelt, MD.
DESIGN OF NEURAL NETWORKS FOR CLASSIFICATION OF REMOTELY SENSED IMAGERY
Samir R. Chettri, Robert F. Cromp, and Mark Birmingham (Princeton Univ., NJ.) *In its* The 1992 Goddard Conference on Space Applications of Artificial Intelligence 1992 p 137-150 (For primary document see N92-23356 14-63)
Avail: NTIS HC/MF A12 CSCL 05B

N92-23368*# Computer Application Systems, Signal Mountain, TN.
IMPROVED IMAGE CLASSIFICATION WITH NEURAL NETWORKS BY FUSING MULTISPECTRAL SIGNATURES WITH TOPOLOGICAL DATA
Craig Harston and Chris Schumacher *In* NASA. Goddard Space Flight Center, The 1992 Goddard Conference on Space Applications of Artificial Intelligence 1992 p 151-158 (For primary document see N92-23356 14-63)
(Contract NAS13-435)
Avail: NTIS HC/MF A12 CSCL 05B

N92-23369*# Loyola Univ., New Orleans, LA. Dept. of Mathematical Sciences.
IMPROVED INTERPRETATION OF SATELLITE ALTIMETER DATA USING GENETIC ALGORITHMS
Kenneth Messa and Matthew Lybanon (Naval Oceanographic and Atmospheric Research Lab., Bay Saint Louis, MS.) *In* NASA. Goddard Space Flight Center, The 1992 Goddard Conference on Space Applications of Artificial Intelligence 1992 p 159-166 Sponsored in part by Navy (For primary document see N92-23356 14-63)
Avail: NTIS HC/MF A12 CSCL 05B

N92-23655*# Intergraph Corp., Reston, VA. International Marketing Div.
CENTER FOR MAPPING, OHIO STATE UNIVERSITY
Lowell Starr *In* NASA, Washington, Proceedings of the Second Annual Symposium on Industrial Involvement and Successes in Commercial Space 1991 17 p (For primary document see N92-23643 14-12)
Avail: NTIS HC/MF A11 CSCL 08B

N92-23914# Politecnico di Milano (Italy). Dipartimento di Ingegneria Idraulica, Ambientale e del Rilevamento.
PROGRESS IN THE SPACEWISE APPROACH TO ARISTOTELES DATA REDUCTION
M. Bassanino, Frederica Migliaccio, and Fernando Sanso *In* ESA, The Solid-Earth Mission Aristoteles Dec. 1991 p 33-43 (For primary document see N92-23910 14-12)
Avail: NTIS HC/MF A06; ESA, EPD, ESTEC, Noordwijk, Netherlands, HC 50 Dutch guilders

N92-23925# Centre National d'Etudes Spatiales, Toulouse (France). Groupe de Recherche de Geodesie Spatiale.
GRAVITY FIELD DATA PRODUCTS FROM THE ARISTOTELES MISSION
Georges Balmino *In* ESA, The Solid-Earth Mission Aristoteles Dec. 1991 p 111-113 (For primary document see N92-23910 14-12)
Avail: NTIS HC/MF A06; ESA, EPD, ESTEC, Noordwijk, Netherlands, HC 50 Dutch guilders

N92-23926# European Space Agency. ESRIN, Frascati (Italy).
DATA DISTRIBUTION AND REDUCTION APPROACHES TO DATA DISTRIBUTION: THE EARTHNET EXPERIENCE
Livio Marelli *In its* The Solid-Earth Mission Aristoteles Dec. 1991 p 115-116 (For primary document see N92-23910 14-12)
Avail: NTIS HC/MF A06; ESA, EPD, ESTEC, Noordwijk, Netherlands, HC 50 Dutch guilders

44 ENERGY PRODUCTION AND CONVERSION

Includes specific energy conversion systems, e.g., fuel cells; global sources of energy; geophysical conversion; and windpower.

For related information see also *07 Aircraft Propulsion and Power, 20 Spacecraft Propulsion and Power,* and *28 Propellants and Fuels.*

N92-23175# Midwest Research Inst., Golden, CO. National Renewable Energy Lab.
GEOTHERMAL ENERGY PROGRAM OVERVIEW
Dec. 1991 14 p
(Contract DE-AC02-83CH-10093)
(DE91-002172; DOE/CH-10093/95) Avail: NTIS HC/MF A03

The mission of the Geothermal Energy Program is to develop the science and technology necessary for tapping our nation's tremendous heat energy sources contained within the Earth. Geothermal energy is a domestic energy source that can produce clean, reliable, cost-effective heat and electricity for our nation's energy needs. Geothermal energy - the heat of the Earth - is one of our nation's most abundant energy resources. In fact, geothermal energy represents nearly 40 percent of the total U.S. energy resource base and already provides an important contribution to our nation's energy needs. Geothermal energy systems can provide clean, reliable, cost-effective energy for our nation's industries, businesses, and homes in the form of heat and electricity. The U.S. Department of Energy's (DOE) Geothermal Energy Program sponsors research aimed at developing the science and technology necessary for utilizing this resource more fully. Geothermal energy originates from the Earth's interior. The hottest fluids and rocks at accessible depths are associated with recent volcanic activity in the western states. In some places, heat comes to the surface as natural hot water or steam, which have been used since prehistoric times for cooking and bathing. Today, wells convey the heat from deep in the Earth to electric generators, factories,

farms, and homes. The competitiveness of power generation with lower quality hydrothermal fluids, geopressured brines, hot dry rock, and magma (the four types of geothermal energy), still depends on the technical advancements sought by DOE's Geothermal Energy Program. DOE

N92-23463*# National Aeronautics and Space Administration. Goddard Space Flight Center, Greenbelt, MD.
MICROPROCESSOR CONTROL OF MULTIPLE PEAK POWER TRACKING DC/DC CONVERTERS FOR USE WITH SOLAR CELL ARRAYS Patent Application
Martin E. Frederick, inventor (to NASA) and Joel Jermakian, inventor (to NASA) 5 Nov. 1991 21 p
(NASA-Case-GSC-13450-1; NAS 1.71:GSC-13450-1; US-Patent-Appl-SN-787993) Avail: NTIS HC/MF A03 CSCL 10A

A method and an apparatus is provided for efficiently controlling the power output of a solar cell array string or a plurality of solar cell array strings to achieve a maximum amount of output power from the strings under varying conditions of use. Maximum power output from a solar array string is achieved through control of a pulse width modulated DC/DC buck converter which transfers power from a solar array to a load or battery bus. The input voltage from the solar array to the converter is controlled by a pulse width modulation duty cycle, which in turn is controlled by a differential signal controller. By periodically adjusting the control voltage up or down by a small amount and comparing the power on the load or bus with that generated at different voltage values a maximum power output voltage may be obtained. The system is totally modular and additional solar array strings may be added to the system simply by adding converter boards to the system and changing some constants in the controller's control routines. NASA

N92-23509# International Fuel Cells Corp., South Windsor, CT.
DEMONSTRATION OF FUEL CELLS TO RECOVER ENERGY FROM LANDFILL GAS: CONCEPTUAL STUDY Final Report, Jan. - Sep. 1991
G. J. Sandelli Jan. 1992 86 p
(Contract EPA-68-D1-0008)
(PB92-137520; FCR-11900A; EPA/600/R-92/007) Avail: NTIS HC/MF A05 CSCL 10A

Discussed here are the results of a conceptual design, cost, and evaluation study of energy recovery from landfill gas using a commercial phosphoric acid fuel cell power plant. The conceptual design of the fuel cell energy recovery system is described, and its economic and environmental feasibility is projected. A conceptual design of the project demonstration was established from the commercial system conceptual design. Key demonstration issues facing commercialization of the concept are addressed. Candidate demonstration sites were evaluated, which led to selection and EPA approval of the demonstration site. A plan is discussed for the construction and testing of a landfill gas pretreatment system which will render landfill gas suitable for use in the fuel cell. The final phase of the study will be a demonstration of the energy recovery concept. Author

N92-23569*# Jet Propulsion Lab., California Inst. of Tech., Pasadena.
DIRECT CONVERSION TECHNOLOGY
P. F. Massier, L. H. Back, M. A. Ryan, and G. Fabris Jan. 1992 29 p
(Contract DE-AI01-86CE-90237)
(NASA-CR-190188; JPL-D-9263; NAS 1.26:190188; DE92-006868) Avail: NTIS HC/MF A03 CSCL 10A

The overall objective of the Direct Conversion Technology task is to develop an experimentally verified technology base for promising direct conversion systems that have potential application for energy conservation in the end-use sectors. This report contains progress of research on the Alkali Metal Thermal-to-Electric Converter (AMTEC) and on the Two-Phase Liquid-Metal MHD Electrical Generator (LMMHD) for the period 1 Jan. 1991 - 31 Dec. 1991. Research on AMTEC and on LMMHD was initiated during Oct. 1987. Reports prepared on previous occasions contain descriptive and performance discussions of the following direct conversion concepts: thermoelectric, pyroelectric, thermionic, thermophotovoltaic, thermoacoustic, thermomagnetic, thermoelastic (Nitionol heat engine); and also, more complete descriptive discussions of AMTEC and LMMHD systems. DOE

N92-23592# Helsinki Univ. of Technology, Espoo (Finland). Dept. of Technical Physics.
COMPARISON OF ANALYTICAL AND NUMERICAL MODELLING APPROACHES FOR SIZING OF SEASONAL STORAGE SOLAR HEATING SYSTEMS
S. S. Peltola and P. D. Lund Jan. 1991 25 p
(PB92-141829; TKK-F-A675; ISBN-951-22-0583-1) Avail: NTIS HC/MF A03 CSCL 10A

Analytical and numerical approaches for the predesign of Central Solar Heating Plants with Seasonal Storage (CSHPSS) systems are compared. The results indicate that the analytical approach used in SOLCHIPS predesign tool is significantly faster and more powerful than the traditional numerical methods for predesign of high solar fraction seasonal storage solar heating systems. Author

N92-23683# Helsinki Univ. of Technology, Espoo (Finland). Dept. of Technical Physics.
PHOTO: A COMPUTER SIMULATION PROGRAM FOR PHOTOVOLTAIC AND HYBRID ENERGY SYSTEMS. DOCUMENT AND USER'S GUIDE
L. M. Manninen, P. D. Lund, and A. Virkkula 27 Nov. 1990 138 p
(PB92-141928; TKK-F-A670; ISBN-951-22-0465-7) Avail: NTIS HC/MF A07 CSCL 10A

The version 3.0 is described of the program package PHOTO for the simulation and sizing of hybrid power systems (photovoltaic and wind power plants) on IBM PC, XT, AT, PS/2 and compatibles. The minimum memory requirement is 260 kB. Graphical output is created with HALO'88 graphics subroutine library. In the simulation model, special attention is given to the battery storage unit. A backup generator can also be included in the system configuration. The dynamic method developed uses accurate system component models accounting for component interactions and losses in e.g. wiring and diodes. The photovoltaic array can operate in a maximum power mode or in a clamped voltage mode together with the other subsystems. Various control strategies can also be considered. Individual subsystem models were verified against real measurements. Illustrative simulation example is also discussed. The presented model can be used to simulate various system configurations accurately and evaluate system performance, such as energy flows and power losses in photovoltaic array, wind generator, backup generator, wiring, diodes, maximum power point tracking device, inverter and battery. Energy cost is also an important consideration. Author

N92-23684# New Energy Development Organization, Tokyo (Japan).
INVESTIGATION ON EFFECTIVE PROMOTION OF GEOTHERMAL ENERGY DEVELOPMENT
Mar. 1991 125 p
(DE92-783370; NEDO-P-9009) Avail: NTIS HC/MF A06

Efficient and effective measures for promoting geothermal energy development are studied considering the present status and the problems of the geothermal energy development in Japan. To promote it smoothly, solutions to technical and socioeconomic problems are needed: There are many unclear points about the location and amount of geothermal resources. For geothermal energy development, it is necessary to establish a consensus of procedures for surveying the development and settlement of selling prices, and risk sharing in the development. It is indispensable to consider an adjustment with natural parks and hot springs for the development. Troubles in making an adjustment are seen in many cases, and it is necessary to make efforts for that understanding. Improvement of economical efficiency of geothermal power generation is an important subject. From the above mentioned

studies, the conclusion is obtained that it is most effective to make rules for development and to expand and strengthen resource prospecting by the government. If the rules are made, reduction of the development cost and shortening of the development period are planned, and the future of the geothermal energy business is expected to be promising. DOE

N92-23998 Arkansas Univ., Fayetteville.
RAPID RECRYSTALLIZATION OF SEMICONDUCTOR THIN FILMS FOR PHOTOVOLTAIC APPLICATIONS Ph.D. Thesis
George David Mooney 1990 218 p
Avail: Univ. Microfilms Order No. DA9204728

Photovoltaics promise to be an important energy source of the future. One promising material for use in photovoltaic devices is thin film polycrystalline CuInSe2. This material holds the current energy conversion efficiency record for a polycrystalline thin film material. The techniques used to produce these devices have features undesirable for mass production such as highly toxic gases and lengthy thermal anneals. New, safe methods are explored to fabricate device quality CuInSe2. Fundamental characterization techniques showed the properties of the codeposited films subjected to Rapid Thermal Processing (RTP) to be comparable to films grown by other methods. Characterization included structural and phase studies by x ray diffraction analysis, study of optical properties and electronic band structures by reflection and transmission spectroscopy, studies of composition and modeling the dynamics of film growth during the process by electron probe for microanalysis, and the effects of the process of grain growth and morphology by scanning electron microscopy. RTP of vacuum codeposited Cu, In, and Se subjects films to a heating by radiation. This method was used to fabricate device quality CuInSe2. Dissert. Abstr.

N92-24030# Oregon Inst. of Tech., Klamath Falls. Geo-Heat Center.
GEOTHERMAL DIRECT USE ENGINEERING AND DESIGN GUIDEBOOK
P. J. Lienau, ed. and B. C. Lunis, ed. 1991 445 p
(Contracts DE-FG07-90ID-13040; DE-AC07-76ID-01570)
(DE92-008686; DOE/ID-13040/T3) Avail: NTIS HC/MF A19

The Geothermal Direct Use Engineering and Design Guidebook is designed to be a comprehensive, thoroughly practical reference guide for engineers and designers of direct heat projects. These projects could include the conversion of geothermal energy into space heating and cooling of buildings, district heating, greenhouse heating, aquaculture and industrial processing. The Guidebook is directed at understanding the nature of geothermal resources and the exploration of the resources, fluid sampling techniques, drilling, and completion of geothermal wells through well testing, and reservoir evaluation. It presents information useful to engineers on the specification of equipment including well pumps, piping, heat exchangers, space heating equipment, heat pumps and absorption refrigeration. A compilation of current information about greenhouse aquaculture and industrial applications is included together with a discussion of engineering cost analysis, regulation requirements, and environmental consideration. The purpose of the Guidebook is to provide an integrated view for the development of direct use projects for which there is a very large potential in the United States. DOE

N92-24054*# National Aeronautics and Space Administration. Lewis Research Center, Cleveland, OH.
A DUAL ANODE NICKEL-HYDROGEN CELL Patent Application
Randall F. Gahn, inventor (to NASA) and Timothy P. Ryan, inventor (to NASA) 18 Feb. 1992 23 p
(NASA-Case-LEW-15212-1; NAS 1.71:LEW-15212-1;
US-Patent-Appl-SN-836490) Avail: NTIS HC/MF A03 CSCL 10A

A dual anode cell with decreased polarization effects provides improved performance characteristics, such as voltage characteristics and depth-of-discharge characteristics. A hydrogen electrode is placed on both sides of a nickel electrode. An electrolyte saturated separator is placed between each hydrogen electrode and the nickel electrode. The electrolyte saturated separator can be a layered-type separator consisting of one layer of zirconia knit cloth next to the hydrogen electrode and a layer of radiation-grafted polyethylene film next to the nickel electrode. These layers of the electrochemical cell are cut in a pineapple-slice configuration. Both hydrogen electrodes are connected in parallel to form a single electrical node. The electrochemical cell is placed in a vessel pressurized with hydrogen and saturated with a potassium hydroxide electrolyte. A gas screen is placed on the outer surface of each of the hydrogen electrodes. NASA

N92-24057*# National Aeronautics and Space Administration. Lewis Research Center, Cleveland, OH.
SELF-DEPLOYING PHOTOVOLTAIC POWER SYSTEM Patent Application
Anthony J. Colozza, inventor (to NASA) 2 Apr. 1992 19 p
(NASA-Case-LEW-15308-1; NAS 1.71:LEW-15308-1;
US-Patent-Appl-SN-862113) Avail: NTIS HC/MF A03 CSCL 10A

A lightweight flexible photovoltaic (PV) blanket is attached to a support structure of initially stowed telescoping members. The deployment mechanism comprises a series of extendable and rotatable columns. As these columns are extended the PV blanket is deployed to its proper configuration. NASA

45 ENVIRONMENT POLLUTION

Includes atmospheric, noise, thermal, and water pollution.

N92-23123# Lawrence Livermore National Lab., CA.
SCIENTIFIC DEVELOPMENT OF THE ADVANCED PARALLEL CHEMISTRY (APACHE) CLIMATE MODEL
D. J. Wuebbles and D. A. Rotman 16 Dec. 1991 7 p
(Contract W-7405-eng-48)
(DE92-006657; UCRL-ID-109264) Avail: NTIS HC/MF A02

Modeling of atmospheric chemistry and constituent transport is an important requirement for meeting the CHAMMP goal of exploring the limits of climate predictability and of simulating the time-dependent behavior of climatic changes on scales from regional to global. This report discusses the results obtained by the CHAMMP Pilot Project on atmospheric chemistry started at Lawrence Livermore National Laboratory (LLNL) in Apr. 1990. This project had the long-term goal of contributing to the development of the chemical-transport modeling capabilities for CHAMMP with the initial efforts aimed at defining some of the important design criteria for the modeling development needed for the advanced climate model. Primary efforts have branched into three distinct areas. First, to gain the necessary understanding of the challenges and opportunities of computing on a massively parallel computer an existing version of the LLNL two-dimensional chemical-radiative-transport code was transferred to a massively parallel computer. Second, the present LLNL two-dimensional chemical-radiative-transport code was used as a test bed in the study of advanced numerical methods needed to solve the stiff equations associated with chemistry, atmospheric dynamics, and higher order transport algorithms. Third, in order to prepare for development of the future three-dimensional chemical-transport model, an existing state-of-the-art three-dimensional tracer transport code was obtained and evaluated. This code has helped us push the model development forward by providing a head start on the three-dimensional model structure and formulation. DOE

N92-23160 Pennsylvania State Univ., University Park.
MONSOON-ENSO RELATIONSHIPS Ph.D. Thesis
Ilana Elazari Kein C Wainer 1991 232 p
Avail: Univ. Microfilms Order No. DA9204311

A coupled ocean-atmosphere model is used to study the equatorial Indian Ocean response to the seasonally varying monsoon winds and the relationship between monsoon variability and the El Nino South Oscillation (ENSO) phenomena in the Pacific

Ocean. The atmosphere is modeled using a simple shallow water model coupled to a nonlinear zonally symmetric model, which provides a zonally averaged annual cycle. The model domain includes an Indian and Pacific Ocean. The Indian Ocean is surrounded by an 'Asian' land mass to the north and an 'African' land mass to the west. The two oceans are separated by a solid boundary. The model extends laterally between 41N and 41S. The asymmetric atmospheric model is driven by a mass source/sink term that is proportional to the sea surface temperature (SST) over the oceans, and the heat balance over land. The ocean is modeled using the Anderson and McCreary reduced gravity, transport model which includes a prognostic equation for the SST. The coupled system is driven by the annual cycle manifested through zonally symmetric and asymmetric land and ocean heating. The ocean is driven by the atmospheric wind stress forcing and a parameterized heat flux. Dissert. Abstr.

N92-23204# Department of Energy, Washington, DC. Office of Environmental Analysis.

LIMITING NET GREENHOUSE GAS EMISSIONS IN THE UNITED STATES, VOLUME 1

R. A. Bradley, ed., E. C. Watts, ed., and E. R. Williams, ed. Sep. 1991 368 p

(DE92-007593; DOE/PE-0101-Vol-1) Avail: NTIS HC/MF A16

In 1988 the Congress requested DOE produce a study on carbon dioxide inventory and policy to provide an inventory of emissions sources and to analyze policies to achieve a 20 percent reduction in carbon dioxide emissions in 5 to 10 years and a 50 percent reduction in 15 to 20 years. This report presents the results of that study. Energy and environmental technology data were analyzed using computational analysis models. This information was then evaluated, drawing on current scientific understanding of global climate change, the possible consequences of anthropogenic climate change (change caused by human activity), and the relationship between energy production and use and the emission of radiactively important gases. Topics discussed include energy and environmental technology to reduce greenhouse gas emissions, fossil energy production and electricity generation technologies, nuclear energy technology, renewable energy technologies, energy storage, transmission and distribution technology, transportation technology, industrial technology, residential and commercial building technology, greenhouse gas removal technology, and approaches to restructuring the demand for energy. DOE

N92-23333# Department of Energy, Washington, DC. Office of Environmental Analysis.

LIMITING NET GREENHOUSE GAS EMISSIONS IN THE UNITED STATES, VOLUME 2

R. A. Bradley, ed., E. C. Watts, ed., and E. R. Williams, ed. Sep. 1991 529 p

(DE92-007592; DOE/PE-0101-Vol-2) Avail: NTIS HC/MF A23

In 1988, Congress requested that DOE produce a study on carbon dioxide inventory and policy to provide an inventory of emissions sources and to analyze policies to achieve a 20 percent reduction in carbon dioxide emissions in 5 to 10 years and a 50 percent reduction in 15 to 20 years. Energy and environmental technology data were analyzed using computational analysis models. This information was then evaluated, drawing on current scientific understanding of global climate change, the possible consequences of anthropogenic climate change (change caused by human activity) and the relationship between energy production and use and the emission of radiatively important gases. Topics discussed include the state of the science in estimating atmosphere/climate change relationships, the potential consequences of atmosphere/climate change, US greenhouse emissions past and present, an approach to analyzing the technical potential and cost of reducing US energy-related greenhouse gas emissions, current policy base and National Energy Strategy actions, fiscal instruments, regulatory instruments, combined strategies and instruments, macroeconomic impacts, carbon taxation and international trade, and a comparison to other studies. DOE

N92-23454# New Energy Development Organization, Tokyo (Japan).

PROMOTION OF INDUSTRIAL TECHNOLOGIES ON THE GLOBAL ENVIRONMENT

Mar. 1991 173 p In JAPANESE; ENGLISH summary

(DE92-769377; NEDO-ITE-9002-5) Avail: NTIS HC/MF A08

A global recycling system is proposed which controls CO2 and also transports natural energy existing in a remote place. In terms of resource volume, the sun is the most feasible for a direct use as a non-fossil energy source which aims at a complete substitution of fossil fuels, especially as a renewable natural energy source. The desert is a place suitable for use of the sun because it is unused land and is rich in solar energy. For transportation of solar energy, it is effective to convert hydrogen to hydride for transport by tanker, in view of storage, initial capacity investment, maintenance and safety. For this, methanol is the most suitable as an energy carrier in terms of its hydrogen content and energy volume. Hydrogen is produced by electrolysis of water using electric power obtained from solar energy. Moreover, this system produces methanol by reducing CO2 with this hydrogen and transports it by tanker. This system will succeed technically. DOE

N92-23455# New Energy Development Organization, Tokyo (Japan).

SURVEY ON SUBTERRANEAN DISPOSAL AND STORAGE TECHNOLOGY OF CO2

Mar. 1991 97 p In JAPANESE; ENGLISH summary

(DE92-769378; NEDO-ITE-9006) Avail: NTIS HC/MF A05

This paper makes a feasibility study mainly on subterranean disposal and storage technology of CO2 recovered from exhaust gas, etc. As for use of subterranean caves or spaces, the capacity is too small for long term storage and disposal. The use of subterranean strata is feasible, but detailed study is needed on site selection, environmental effects and CO2 behaviors in the subterranean stratum. Regarding the use of subterranean water, a considerable amount of CO2 disposal or storage is possible because CO2 can be dissolved easily in subterranean water, if any feasible site is found. The use of subterranean water in water soluble gas fields, especially, is significant in consideration of the ground subsidence problem. Concerning geothermal power stations, CO2 utilization to protect scaling is feasible, but a large amount of CO2 disposal is not expected. Oil and gas fields are already utilized as a miscible flooding in enhanced oil recovery, but the problem is that in Japan there are few feasible sites and the disposal capacity is limited. Further studies should be made on subterranean behaviors of CO2, evaluation of applicability to Japan and abroad and demonstration tests. DOE

N92-23512# Commission of the European Communities (Luxembourg).

METHODS FOR THE DETECTION OF MICROORGANISMS IN THE ENVIRONMENT

22 Jan. 1992 122 p

(PB92-137454) Avail: NTIS HC/MF A06 CSCL 13B

Presented here is an overview and summary of the increasing variety of methods used for detecting and monitoring microorganisms in the environment. A general overview of detection methods which surveys a variety of techniques is provided for readers with a general interest in the topic of microbial detection methods. Another section provides a more detailed examination of individual techniques. The techniques discussed include those based on direct detection, on culturing, and on nucleic acid hybridization. This work is intended to be used as a reference document for regulatory officials, scientists, and others interested in microbial biotechnology. Author

N92-23515# Council on Environmental Quality, Washington, DC.

NATIONAL ACID PRECIPITATION ASSESSMENT PROGRAM: MISSION, GOALS, AND PROGRAM PLAN POST 1990. PUBLIC REVIEW DRAFT

Nov. 1991 72 p

(PB92-128248) Avail: NTIS HC/MF A04 CSCL 13B

The Acid Precipitation Act of 1980 and its re-authorization in 1990 mandates a comprehensive national program of policy oriented research to assess the causes and consequences of acidic deposition and the effectiveness of the recently legislated acid rain controls. The National Acid Precipitation Program (NAPAP) is directed towards providing technical input for decision making in the areas of energy production, natural resource management, pollution abatement, and environmental policy. The program not only links the efforts of the federal agencies, but also coordinates them with the research and monitoring activities of the private sector and state and local governments, and fosters cooperation with the international community. Author

N92-23517# Environmental Protection Agency, Research Triangle Park, NC. Office of Air Quality Planning and Standards.
NATIONAL AIR QUALITY AND EMISSIONS TRENDS REPORT, 1990
T. Curran, R. Faoro, T. Fitz-Simons, N. Frank, and W. Freas Nov. 1991 135 p
(PB92-141555; EPA/450/4-91/023) Avail: NTIS HC/MF A07 CSCL 13B

National and regional trends in air quality from 1981 through 1990 for particulate matter, sulfur dioxide, carbon monoxide, nitrogen dioxide, ozone, and lead are discussed. Air quality trends are presented for 15 metropolitan areas. National air quality trends are also presented for both the National Air Monitoring Sites (NAMS) and other site categories. In addition to ambient air quality, trends are also presented for annual nationwide emissions. These emissions are estimated using the best available engineering calculations; the ambient levels presented are averages of direct measurements. Air quality statistics are presented for each of the pollutants for all Metropolitan Statistical Areas (MSAs) with data in 1990. Author

N92-23593# Council on Environmental Quality, Washington, DC.
NATIONAL ACID PRECIPITATION ASSESSMENT PROGRAM: 1990 INTEGRATED ASSESSMENT REPORT
Nov. 1991 546 p
(PB92-100346) Avail: NTIS HC/MF A23 CSCL 13B

A summary is presented of the causes and effects of acidic deposition and a comparison of the costs and effectiveness of alternative emission control scenarios. In developing the Integrated Assessment (IA), it was NAPAP's goal to produce a structured compilation of policy relevant technical information. The IA is based on findings and data from a series of 27 State-of-Science Technology Reports (SOST) on acidic deposition published by NAPAP in 1990. The scope includes: (1) emissions, atmospheric processes, and deposition; (2) effects on surface waters, forests, agricultural crops, exposed materials, human health, and visibility; and (3) control technologies, future emissions, and effects valuation. Author

N92-23733# New Energy Development Organization, Tokyo (Japan).
PROMOTION OF INDUSTRIAL TECHNOLOGIES ON THE GLOBAL ENVIRONMENT
Mar. 1991 128 p In JAPANESE; ENGLISH summary
(DE92-769374; NEDO-ITE-9002-1) Avail: NTIS HC/MF A07

The development is studied of a method for a systematic estimation of the aggregate CO2 emission by linking together CO2 estimated from the industry-related analysis and that emitted from each industrial sector. Use of this method aims at pointing out a new industrial system. Calculating unit requirement (per unit amount of production) of CO2 from each industrial sector, cash flow obtained from industrial relation and CO2 emitted from each industrial sector are linked. This method enables quantitative evaluation of changes of CO2 emission due to changes in the industrial structure in each area and at the same time the method is effective in studying the spread to other areas and the whole Japan. Changes of the aggregate CO2 emission nationwide can also be estimated. Energy substitution in each industrial sector and degree of contribution to energy conservation can be evaluated. The possibility of applying it to international industry relation is foreseen in the future. It is necessary to enhance accuracy by integrating CO2 to enhance accuracy by integrating CO2 emitted from the process itself which uses no energy, CO2 emission caused by waste disposal and effects of resources recycling into the method. DOE

N92-23734# New Energy Development Organization, Tokyo (Japan).
PROMOTION OF INDUSTRIAL TECHNOLOGIES ON THE GLOBAL ENVIRONMENT
Mar. 1991 267 p In JAPANESE; ENGLISH summary
(DE92-769375; NEDO-ITE-9002-2) Avail: NTIS HC/MF A12

An evaluation method similar to the industry relation analysis is first proposed, aimed at establishing a quantitative evaluation method of CO2 emission control effects of various CO2 control technologies. A concept of an accumulated CO2 emission unit (phi) is used as an evaluation index. The premise of this concept is that input-output flow relations of materials can be expressed linearly in each unit of the process, a combination form in each unit is already known, and phi values for raw materials, energy, costs of utility, equipment, labor and management are already known as initial conditions. If such conditions are satisfied, accumulated CO2 per product unit amount can be calculated in the actual process by this method, and effects of CO2 control technology can be evaluated quantitatively by comparing sizes of phi for the identical product. This method is applied to electric power, iron and steel, oil refinery and cement industries, and the present status is described. In the 1991 FY analysis, however, phi values for costs of equipment, labor and management are not set as initial conditions. DOE

N92-23740# Lawrence Livermore National Lab., CA.
ON THE GLOBAL WARMING POTENTIALS OF CANDIDATE GASEOUS DIFFUSION PLANT COOLANTS
D. J. Wuebbles 21 Nov. 1991 6 p
(Contract W-7405-eng-48)
(DE92-006640; UCRL-ID-109227) Avail: NTIS HC/MF A02

CFC-114 has been used in large quantities as a coolant in gaseous diffusion plants for some time. International and national policy actions related to protection of the ozone layer now call for the elimination of the production of several chlorofluorocarbons, including CF2ClCF2Cl, termed CFC-114, by the end of this decade. Atmospheric researchers have played major roles in the research and atmospheric modeling studies that led to the development of these policies. In a recent 1991 report for the U.S. Department of Energy (DOE), Lee Trowbridge of the Uranium Enrichment Organization makes a preliminary analysis of the potential environmental effects of compounds being considered as replacements for CFC-114 as coolants in the processing of uranium in gaseous diffusion plants. This report evaluates the findings of the Trowbridge report in relationship to the current understanding of atmospheric chemical, physical and climatic processes. DOE

N92-23898*# Bionetics Corp., Cocoa Beach, FL.
ACID RAIN MONITORING IN EAST-CENTRAL FLORIDA FROM 1977 TO PRESENT Final Report, 22-24 Oct. 1990
B. C. Madsen, T. Kheoh (Parke-Davis Pharmaceutical Co., Ann Arbor, MI.), C. R. Hinkle, and T. W. Dreschel 1990 22 p Presented at the Florida Acidic Deposition Conference, Tampa, Fl, 22-24 Oct. 1990
(Contracts NAS10-8986; NAS10-9841; NAS10-10285)
(NASA-CR-190152; NAS 1.26:190152) Avail: NTIS HC/MF A03 CSCL 13B

Rainfall has been collected on the University of Central Florida campus and at the Kennedy Space Center over a 12 year period. The chemical composition has been determined and summarized by monthly, annual periods, and for the entire 12 year period at both locations. The weighted average pH at each site is 4.58; however, annual weighted average pH has been equal to or above the 12 year average during six of the past eight years. Nitrate concentrations have increased slightly during recent years while excess sulfate concentrations have remained below the 12 year

weighted average during six of the past seven years. Stepwise regression suggests that sulfate, nitrate, ammonium ion and calcium play major roles in the description of rainwater acidity. Annual acid deposition and annual rainfall have varied from 20 to 50 meg/(m(exp 2) year) and 100 to 180 cm/year, respectively. Sea salt comprises at least 25 percent of the total ionic composition.
Author

N92-24003# National Park Service, Denver, CO. Air Quality Div.
ACID RAIN AND AIR POLLUTION IN DESERT PARK AREAS. PROCEEDINGS OF A WORKSHOP: MANAGEMENT RECOMMENDATIONS
D. Mangis, J. Baron, and K. Stolte Nov. 1991 136 p Workshop held in Tucson, AZ, 16-18 May 1988
(PB92-140532; NPS/NRAQD/NRTR-91/02) Avail: NTIS HC/MF A07 CSCL 13B

The National Park Service sponsored a workshop in Tucson, Arizona in May 1988 to discuss issues associated with the effects of acid deposition and air pollution on desert ecosystems. There were 12 papers delivered on aspects of research and monitoring in park units in Southwest deserts. Subjects covered include current levels of acid rain, dry deposition, and gaseous air pollutants; the sensitivity of desert ecosystems to air pollution; and the sensitivity of cultural resources to air pollution. The discussion includes some management recommendations for Federal Land Managers on attempts to control the effects of air pollutants on desert parks and reserves.
Author

N92-24023# New Energy Development Organization, Tokyo (Japan).
PROMOTION OF INDUSTRIAL TECHNOLOGIES ON THE GLOBAL ENVIRONMENT
Mar. 1991 196 p In JAPANESE; ENGLISH summary
(DE92-769376; NEDO-ITE-9002-4) Avail: NTIS HC/MF A09

The paper examines the technological trend mainly in elemental technologies for CO2 reduction from a standpoint of chemical technology, and makes an assessment and an analysis based on the global balance of materials and energy. As for chemical CO2 reduction measures, those on a long term basis are: development of solar energy utilization technology, chemical and electrochemical fixation technology to be combinedly used therewith. Measures on a short- to medium-term basis are: further promotion of energy saving related technology (utilization of low temperature waste heat, improvement of utilization efficiency, highly selective synthesis technique), technology of effective chemical conversion to high convenient energy mediums, promotion of chemical technologies for environment protection such as measures against acid rain, use of clean fuels, measures against greenhouse effect gases other than CO2. It is necessary to promote in well balance development of elemental technologies on the short-, medium- and long-term basis as well as the overall application of various measures. The important subject studied is to secure primary energy sources except fossil fuels and to develop energy conservation technology.
DOE

N92-24024# New Energy Development Organization, Tokyo (Japan).
SURVEY ON OPTIMIZATION OF CO2 DISPOSAL SYSTEM AND CARBON UTILIZATION TECHNOLOGY
Mar. 1991 101 p In JAPANESE
(DE92-769381; NEDO-ITE-9003) Avail: NTIS HC/MF A06

Studies were made on the possibility of combining a technology for extracting carbon materials from fossil fuels and a CO2 fixation and utilization system and also on effects of CO2 emission control. Carbon materials which attract attention hereafter are carbon fiber, vitreous carbon, graphite intercalnation compounds and new diamond, etc. Pitch based carbon fiber, in particular, is the most promising because of its potential and wide field of application. The present technical problems were studied of pitch based carbon fiber. HP-grade carbon fiber is used, and its present price and future target price are set at 20,000 and 5,000 yen/kg, respectively. The price of oil pitch as fuel is set at 20,000 yen/kl, the same as that of heavy oil. In view of an economic use per CO2 emission volume, it is much more effective to use oil pitch as carbon fiber with high-value added than to use it as fuel. If a unit price of hundreds yen/kg is realized, carbon fiber is expected to be used also in the concrete reinforced fiber market which has a production of 2.9 million tons/year. This will contribute to CO2 emission control.
DOE

N92-23965*# Temple Univ., Philadelphia, PA. Dept. of Physics.
USE OF THE MAXIMUM ENTROPY METHOD TO RETRIEVE THE VERTICAL ATMOSPHERIC OZONE PROFILE AND PREDICT ATMOSPHERIC OZONE CONTENT
B. Curtis Turner *In* NASA. Goddard Space Flight Center, Summer Graduate Research Program for Interns in Science and Engineering 24 Mar. 1992 19 p (For primary document see N92-23958 14-99)
Avail: NTIS HC/MF A12 CSCL 13B

46 GEOPHYSICS

Includes aeronomy; upper and lower atmosphere studies; ionospheric and magnetospheric physics; and geomagnetism.

For space radiation see *93 Space Radiation.*

N92-23142 Houston Univ., TX.
THE SUBIONOSPHERIC ELECTROMAGNETIC RESPONSE TO MAGNETOPAUSE PROCESSES Ph.D. Thesis
Zhongmin Lin 1991 254 p
Avail: Univ. Microfilms Order No. DA9205008

The correlation between high latitude impulsive events, the interplanetary magnetic field, and solar wind plasma properties was studied based on the data acquired from the 1985 to 86 Balloon Campaign at South Pole Station. An independent cylindrical current model in the ionosphere was studied analytically to calculate balloon altitude electric field and ground magnetic field perturbations. The monopole term of the general series expansion of any cylindrical current model produces a single convection vortex pattern on the ground that is consistent with the FTE model suggested by Lanzerotti et al. The dipole term of the general series expansion produces a twin vortex model in the ionosphere. Model studies show that the horizontal electric field in the ionosphere maps down to approx. 30 km with little attenuation. Statistics and detailed case studies show that high latitude impulsive events may come from magnetic field reconnection or solar wind pressure variations. Study also reveal the hydrodynamic reason for the motion of magnetic flux ropes in the ionosphere. Solar wind plasma flow pushes a magnetic flux tube to move westward in the morning and to move eastward in the afternoon.
Dissert. Abstr.

N92-23262# National Inst. for Fusion Science, Nagoya (Japan).
DEVELOPMENT OF 3-DIMENSIONAL COMPACT MAGNETIC DOSIMETER FOR ENVIRONMENTAL MAGNETIC FIELD MONITORING
Yusuke Kubota, Haruo Obayashi, Akira Miyahara, Kazuko Ohno, Kouichi Nakamura, and Kenzi Horii Jul. 1991 48 p In JAPANESE; ENGLISH summary
(DE92-750825; NIFS-MEMO-2) Avail: NTIS HC/MF A03

A computer-driven, three-dimensional magnetic fluxmeter to be used for magnetic field dosimetry has been developed. A magnetic monitor applicable to this object should be measurable to an absolute value of local magnetic field strength and also be able to record its time integration as a measure of exposed dose to the magnetic field. The present fluxmeter consists of signal amplifiers, rectifiers, an A/D converter, and a pocket computer (PC). The signal outputs from the sensors are processed with the PC to compose an absolute strength of magnetic flux density and its time-integrated value. The whole system is driven by a battery and is quite compact in size to be used as a handy portable system. Further details of the design, idea, construction, specification, and testing result of the fluxmeter are described.

The measurable range are from 0.4G to 20,000G in normal mode and 8mG to 400G in high-sensitivity AC mode, and the sensitivity is well independent of the magnetic field direction. These measured data are displayed in real time on the LCD panel of the PC and memorized in RAM files. Possible application of the fluxmeter is discussed with special attention to the search of the leakage and/or disturbing error fields around LHD (Large Helical Device) and other magnetic systems, the individual dose control to the workers in strong magnetic fields, and the evaluation of the effects of long irradiation of magnetic fields. DOE

N92-23522# National Center for Atmospheric Research, Boulder, CO. Atmospheric Chemistry Div.
GENLN2: A GENERAL LINE-BY-LINE ATMOSPHERIC TRANSMITTANCE AND RADIANCE MODEL. VERSION 3.0: DESCRIPTION AND USERS GUIDE
D. P. Edwards Jan. 1992 157 p
(PB92-148543; NCAR/TN-376+STR) Avail: NTIS HC/MF A08 CSCL 04A

This is the latest documentation for Version 3.0 of the GENLN2 suite of programs as of November 1991. This is intended to be a working document for those using GENLN2. A separate section is devoted to each of the programs that comprise the GENLN2 suite. A brief overview is given of the purpose of each program and the physics involved. A detailed description is given of the code structure, required input, and code implementation. The input and output for two example calculations are given. Author

N92-23540*# Texas Univ., Austin. Center for Space Research.
DETERMINATION OF CRUSTAL MOTIONS USING SATELLITE LASER RANGING Final Report, 15 Feb. 1989 - 31 Dec. 1991
31 Dec. 1991 55 p
(Grant NAG5-1118)
(NASA-CR-190246; NAS 1.26:190246) Avail: NTIS HC/MF A04 CSCL 08G

Satellite laser ranging has matured over the last decade into one of the essential space geodesy techniques. It has demonstrated centimeter site positioning and millimeter per year velocity determinations in a frame tied dynamically to the mass center of the solid Earth hydrosphere atmosphere system. Such a coordinate system is a requirement for studying long term eustatic sea level rise and other global change phenomena. Earth orientation parameters determined with the coordinate system have been produced in near real time operationally since 1983, at a relatively modest cost. The SLR ranging to Lageos has also provided a rich spectrum of results based upon the analysis of Lageos orbital dynamics. These include significant improvements in the knowledge of the mean and variable components of the Earth's gravity field and the Earth's gravitational parameter. The ability to measure the time variations of the Earth's gravity field has opened as exciting area of study in relating global processes, including meteorologically derived mass transport through changes in the satellite dynamics. New confirmation of general relativity was obtained using the Lageos SLR data. Author

N92-23558*# Massachusetts Inst. of Tech., Cambridge. Earth Resources Lab.
THE INTERPRETATION OF CRUSTAL DYNAMICS DATA IN TERMS OF PLATE INTERACTIONS AND ACTIVE TECTONICS OF THE ANATOLIAN PLATE AND SURROUNDING REGIONS IN THE MIDDLE EAST Final Report
M. Nafi Toksoz and Robert Reilinger 1 May 1992 58 p
(Grant NAG5-753)
(NASA-CR-188466; NAS 1.26:188466) Avail: NTIS HC/MF A04 CSCL 08G

A detailed study was made of the consequences of the Arabian plate convergence against Eurasia and its effects on the tectonics of Anatolia and surrounding regions of the eastern Mediterranean. A primary source of information is time rates of change of baseline lengths and relative heights determined by repeated SLR measurements. These SLR observations are augmented by a network of GPS stations in Anatolia, Aegea, and Greece, established and twice surveyed since 1988. The existing SLR and GPS networks provide the spatial resolution necessary to reveal the details of ongoing tectonic processes in this area of continental collision. The effort has involved examining the state of stress in the lithosphere and relative plate motions as revealed by these space based geodetic measurements, seismicity, and earthquake mechanisms as well as the aseismic deformations of the plates from conventional geodetic data and geological evidence. These observations are used to constrain theoretical calculations of the relative effects of: (1) the push of the Arabian plate; (2) high topography of Eastern Anatolia; (3) the geometry and properties of African-Eurasian plate boundary; (4) subduction under the Hellenic Arc and southwestern Turkey; and (5) internal deformation and rotation of the Anatolian plate. Author

N92-23702 Cornell Univ., Ithaca, NY.
RADAR OBSERVATIONS AND DYNAMICS OF THE POLAR SUMMER MESOSPHERE Ph.D. Thesis
Timothy Mather Hall 1991 257 p
Avail: Univ. Microfilms Order No. DA9204092

The lowest temperatures and the highest clouds on Earth, complex ion chemistry, large amplitude waves, and intense radar scatter make the summer polar mesosphere a fascinating atmospheric region. Two aspects of the region related to radar echoing and detection are addressed: the role of the Stokes drift in measurements of the seasonal circulation, and the extension of the electron density variance spectrum to length scales smaller than those of the driving turbulence. Although the mass flux rate at the summer polar mesopause must be about 1 cm/s upward to be consistent with the temperature, radars measure 20 to 30 cm/s downward. This surprising result was verified with four years of radar data. After discussing the Stokes drift in detail, the calculation is generalized to include a wave spectrum. The results indicate that the Stokes drift is not large enough to explain the radar measurements. As an alternative, it is suggested that the radar is detecting the fall speed of charge aerosols. Structuring of the polar summer mesospheric electron density at scales shorter than the inner scale of turbulence is necessary to explain the intensity of VHF radar echoes. Dissert. Abstr.

N92-23741# Pacific Northwest Lab., Richland, WA.
CLOUDS AND RADIATION TESTBED DATA ENVIRONMENT: SITE DATA SYSTEM AND EXPERIMENT CENTER
R. B. Melton, S. F. Bobrowski, A. Peter Campbell, Jonathan M. Corbet (National Center for Atmospheric Research, Boulder, CO.), and D Edwards Jan. 1992 7 p Presented at the 8th International Conference on Interactive Information and Processing Systems for Meteorology, Oceanography, and Hydrology, Atlanta, GA, 5-10 Jan. 1992
(Contract DE-AC06-76RL-01830)
(DE92-006732; PNL-SA-19880; CONF-920163-1) Avail: NTIS HC/MF A02

The Department of Energy (DOE) has initiated the Atmospheric Radiation Measurement (ARM) program as a research effort to reduce the uncertainties found in general circulation and other models due to the effects of clouds and solar radiation (DOE 1990, Patrinos, et al. 1990). This program will provide an experimental testbed for the study of important atmospheric effects, particularly cloud and radiative processes, and testing of parameterizations of the processes for use in atmospheric models. The design of the testbed, known as the Clouds and Radiation Testbed (CART), calls for five long-term field data collection sites as well as a mobile set of instrumentation to be used in short-term field campaigns. The first of the sites is expected to begin operation in April of 1992. Within the ARM Program, an experiment has been defined as the prospective test of a model, i.e., the test of a model's predictive capability. An experiment is specified by identifying the model or models to be tested, the model input requirements, the measurements needed for comparison to model outputs, and the measurements needed to diagnose model performance. The identification of required measurements includes the specification of data fusion or other techniques to be used in converting the basic instrument observations into the required set of measurements. The CART Data Environment (CDE) is the

element of the testbed which acquires the basic observations from the instruments and processes them to meet the measurement requirements of ARM experiments. DOE

N92-23772 Maryland Univ., College Park.
ANALYSIS OF GRAVITY AND TOPOGRAPHY ON EARTH AND VENUS: COMPARISONS OF LITHOSPHERIC AND SUBLITHOSPHERIC PROCESSES Ph.D. Thesis
Martin Thomas Black 1991 148 p
Avail: Univ. Microfilms Order No. DA9205032

Cross-spectral analysis was used to study the relationship between mean sea surface height (geoid) and bathymetry in 16 deg x 16 deg blocks in the oceans. The admittances (spectral transfer functions) obtained from this analysis were compared with thermomechanical models of the lithosphere and sublithosphere to determine modes of topographic compensation in different parts of the oceans. Peak admittances at short wavelengths indicate that loads are supported by the mechanical strength of the lithosphere, while peak admittances at long wavelengths are indicative of lithospheric cooling or dynamic sublithospheric processes. Models of upper mantle convection predict higher admittances at long wavelengths than do models of lithospheric cooling. In most areas the observed admittances can be explained by models of the thermomechanical properties of the lithosphere, but in the eastern Pacific Ocean, the northern Indian Ocean, and the Cape Verde Rise high long-wavelength admittances are evidence for upper mantle convection. Observed Pioneer Venus orbiter gravity profiles over Aphrodite Terra were compared to profiles predicted from models of thermal isostasy, mantle convection, and Airy compensation using finite impulse response filters. Dissert. Abstr.

N92-23913# Ohio State Univ., Columbus. Dept. of Geodetic Science and Surveying.
THE EARTH'S GRAVITY FIELD FROM SATELLITE GEODESY: A 30 YEAR ADVENTURE
Richard H. Rapp *In* ESA, The Solid-Earth Mission Aristoteles Dec. 1991 p 29-32 (For primary document see N92-23910 14-12)
Avail: NTIS HC/MF A06; ESA, EPD, ESTEC, Noordwijk, Netherlands, HC 50 Dutch guilders

N92-23915*# National Aeronautics and Space Administration. Goddard Space Flight Center, Greenbelt, MD.
THE GEOPHYSICAL IMPACT OF THE ARISTOTELES MISSION
Allen Joel Anderson, E. Klingele, R. Sabadini, S. Tinti, and Suzanna Zerbini (Bologna Univ., Italy) *In* ESA, The Solid-Earth Mission Aristoteles Dec. 1991 p 45-50 (For primary document see N92-23910 14-12)
Avail: NTIS HC/MF A06; ESA, EPD, ESTEC, Noordwijk, Netherlands, HC 50 Dutch guilders CSCL 08G

N92-23916# European Space Agency. European Space Research and Technology Center, ESTEC, Noordwijk (Netherlands).
INTRODUCTORY REMARKS TO THE MISSION AND SYSTEM ASPECTS SESSION
Rene Bonnefoy and M. Schuyer *In its* The Solid-Earth Mission Aristoteles Dec. 1991 p 53-5 (For primary document see N92-23910 14-12)
Avail: NTIS HC/MF A06; ESA, EPD, ESTEC, Noordwijk, Netherlands, HC 50 Dutch guilders

N92-23927# Observatoire de la Cote d'Azur, Nice (France).
POSSIBLE ATMOSPHERIC RESEARCH WITH ARISTOTELES
Francois Barlier *In* ESA, The Solid-Earth Mission Aristoteles Dec. 1991 p 135-137 (For primary document see N92-23910 14-12)
Avail: NTIS HC/MF A06; ESA, EPD, ESTEC, Noordwijk, Netherlands, HC 50 Dutch guilders

N92-23960*# Jackson State Coll., MS.
FAST AURORA ZONE ANALYSIS
Mattie Booker *In* NASA. Goddard Space Flight Center, Summer Graduate Research Program for Interns in Science and Engineering 24 Mar. 1992 19 p (For primary document see N92-23958 14-99)
Avail: NTIS HC/MF A12 CSCL 04A

47 METEOROLOGY AND CLIMATOLOGY

Includes weather forecasting and modification.

N92-23121 California Univ., Los Angeles.
AN OBSERVATIONAL STUDY OF THE INTERNAL STRUCTURE OF AIR-MASS THUNDERSTORMS Ph.D. Thesis
David Edmund Kingsmill 1991 139 p
Avail: Univ. Microfilms Order No. DA9207741

The internal structure of air mass thunderstorms is examined with Doppler and dual polarization radar, photographic, and rawinsonde data from the 1986 MIST project. A kinematic, dynamic, and thermodynamic analysis of one well documented case shows a life cycle which closely resembles the Byers and Braham model for airmass storms. Other less detailed cases, examined to supplement this analysis, largely confirm these findings. However, several phenomena never documented for this storm type are discussed. One of these is a midlevel inflow, which in one case caused a visible constriction in a storm cloud. This inflow appears to arise from the mass compensation required when a strong updraft driven by buoyancy from glaciation forms above a weaker updraft loaded down by the precipitation core. A downdraft at midlevels with an associated 'weak echo' trench is also observed. Its origin appears related to a shear induced wake entrainment process. Also, microbursts intensity surface outflows are observed. The downdrafts responsible for these events appear to be restricted to low levels and to separate from the midlevel downdraft. One case shows this type of downdraft to be initiated by precipitation loading and intensified by negative thermal buoyancy. Dissert. Abstr.

N92-23150 Ohio State Univ., Columbus.
ENERGY CYCLES IN THE SUMMER TROPICAL ATMOSPHERE OVER THE NORTH ATLANTIC OCEAN Ph.D. Thesis
Jianfu Pan 1991 256 p
Avail: Univ. Microfilms Order No. DA9201733

To study tropical energetics and their intraseasonal fluctuations in relation to tropical cyclogenesis, energies and conversions are calculated on a daily basis over North America during the summer of 1979. It was found that the available potential energy is only about 21 pct. as large as the kinetic energy and is mainly stored in eddy form. Conversions show that the upper troposphere is essentially barotropic. Strong low frequency peaks are found in energies at 32 to 43 days, 18 days, and 1 to 2 weeks. Cyclone development is observed during LFO minima at times of significant conversion from AE to KE throughout the troposphere. Dissert. Abstr.

N92-23257# Colorado State Univ., Fort Collins. Dept. of Atmospheric Science.
QUASI-THREE-DIMENSIONAL SIMULATIONS OF DEEP CONVECTION
R. F. A. Hertenstein, W. R. Cotton, and M. J. Weissbluth 1991 4 p Presented at the 5th Conference on Mesoscale Processes, Atlanta, GA, 5-10 Jan. 1992
(Contract DE-FG02-90ER-61066)
(DE92-007204; DOE/ER-61066/3; CONF-920174-1) Avail: NTIS HC/MF A01

Simulations of deep convection along the Florida sea-breeze front have previously been carried out in two dimensions using the Colorado State University Regional Atmospheric Modeling System. These experiments were in good agreement with observations, capturing the propagation of the sea-breeze fronts and the associated convection as well as the eventual collision of the two sea-breeze fronts from opposite shores, leading to more fully developed deep convection. We have extended this simulation by adding enough points in the third dimension to capture the

three-dimensional convective cells. We have two goals with this work. First we will use this experiment as a step towards fully three-dimensional simulations of Mesoscale Convective Systems in which interactive-grid nests are used to explicitly simulate convective processes. A second goal is to use the results of these simulations as a synthetic data set. We can then run simulations of the same case using a convective parameterization scheme, compare the results of the parameterization run to the synthetic data set, and use diagnostic analyses to refine the parameterization scheme. DOE

N92-23431*# District of Columbia Univ., Washington, DC.
CLOUDS, SURFACE TEMPERATURE, AND THE TROPICAL AND SUBTROPICAL RADIATION BUDGET
Harbans L. Dhuria and H. Lee Kyle (National Aeronautics and Space Administration. Goddard Space Flight Center, Greenbelt, MD.) May 1980 13 p
(Grant NAG5-1012)
Avail: NTIS HC/MF A03 CSCL 04B

Solar energy drives both the Earth's climate and biosphere, but the absorbed energy is unevenly distributed over the Earth. The tropical regions receive excess energy which is then transported by atmospheric and ocean currents to the higher latitudes. All regions at a given latitude receive the same top of the atmosphere solar irradiance (insolation). However, the net radiation received from the Sun in the tropics and subtropics varies greatly from one region to another depending on local conditions. Over land, variations in surface albedo are important. Over both land and ocean, surface temperature, cloud amount, and cloud type are also important. The Nimbus-7 cloud and Earth radiation budget (ERB) data sets are used to examine the affect of these parameters. D.R.D.

N92-23439# National Weather Service, Silver Spring, MD.
FUNCTIONAL PRECISION OF NATIONAL WEATHER SERVICE UPPER-AIR MEASUREMENTS USING VIZ MANUFACTURING CO. A RADIOSONDE (MODEL 1492-510)
P. Ahnert, M. Gelman, and M. Lukes Oct. 1991 47 p Prepared in cooperation with National Meteorological Center, Washington, DC
(PB92-137850; NOAA-TR-NWS-44) Avail: NTIS HC/MF A03 CSCL 04B

The functional precision of VIZ model 1492-510 (VIZA) radiosonde was determined using the National Weather Service functional analysis test package. The comparisons were made from 35 flights of paired radiosondes suspended from the same balloon. Functional precision is given by the root mean square of the differences between measurements made by two sensors of the same type exposed to the same environment. Results are summarized for simultaneous measurements at one minute intervals as well as measurements at a predefined set of pressure levels. The tests were conducted in conjunction with acceptance testing of replacement radiosondes and results are reported for use by the meteorological community in specifying the characteristics of this radiosonde, which was used operationally from 1986 to 1989. GRA

N92-23494# National Weather Service, Silver Spring, MD.
FUNCTIONAL PRECISION OF NATIONAL WEATHER SERVICE UPPER-AIR MEASUREMENTS USING VIZ MANUFACTURING CO. B RADIOSONDE (MODEL 1492-520)
P. Ahnert, M. Gelman, and M. Lukes Oct. 1991 46 p Prepared in cooperation with National Meteorological Center, Washington, DC
(PB92-137868; NOAA-TR-NWS-45) Avail: NTIS HC/MF A03 CSCL 04B

The functional precision of VIZ Model 1492-520 (VIZB) radiosonde was determined using the National Weather Service functional analysis test package. The comparisons were made from 33 flights of paired radiosondes suspended from the same balloon. Functional precision is given by the root mean square of the differences between measurements made by two sensors of the same type exposed to the same environment. Results are summarized for simultaneous measurements at one minute intervals as well as measurements at a predefined set of pressure levels. These tests were conducted for the acceptance of contract production samples and results are reported for use by the meteorological community in specifying the characteristics of this radiosonde, which operational use started in 1989. Author

N92-23520# Nevada Univ., Las Vegas. Desert Research Inst.
CLIMATE
M. R. Rose, M. Boehm, and R. K. Olson 1992 27 p Prepared in cooperation with ManTech Environmental Technology, Inc., Corvallis, OR Sponsored in part by Corvallis Environmental Research Lab. Submitted for publication
(PB92-150457; EPA/600/A-92/023) Avail: NTIS HC/MF A03 CSCL 04B

Since analysis of trends in annual growth increments of forests are central to the regional air pollution effects studies, an understanding of the general patterns and variability of climate in the western United States is necessary for interpreting results of forest studies. Here, the general patterns and causes of climate over the western United States are described. More detailed climatic descriptions are then presented for the five regions of the western United States. The regions discussed are Northwestern Washington, the Colorado Front Range, Arizona and New Mexico, Sierra Nevada, and Southern California. Mean seasonal temperature and precipitation are characterized for selected climatic divisions within the regions. The Palmer Drought Severity Index is used to discuss temporal variability in the climate of these regions. Author

N92-23587# National Center for Atmospheric Research, Boulder, CO. Atmospheric Technology Div.
INTERNATIONAL WORKSHOP ON THE AIRBORNE MEASUREMENT OF WIND, TURBULENCE, AND POSITION
H. P. Fimpel, D. Baumgardner, and A. M. Jochum Jan. 1992 92 p Workshop held in Oberpfaffenhofen, Fed. Republic of Germany, 26-28 Jul. 1989 Sponsored by NSF
(PB92-139963; NCAR/TN-365+PROC) Avail: NTIS HC/MF A05 CSCL 04B

The goal of the workshop was three-fold: (1) to exchange information on measurement technology, calibration techniques, and analysis methods; (2) to discuss possible areas where standardization is beneficial, such as calibrations, data processing procedures, and possible future collaborations, in particular, the development of new sensors, the assessment of uncertainty, and the exchanges of personnel between facilities. GRA

N92-23656*# National Center for Atmospheric Research, Boulder, CO.
INVESTIGATION OF THE ARCHEAN CLIMATE USING THE NCAR CCM Ph.D. Thesis
G. S. Jenkins 1991 168 p Prepared in cooperation with Michigan Univ., Ann Arbor
(Grants NGT-70120; NSF ATM-87-09659)
(NASA-CR-189878; NAS 1.26:189878; NCAR/CT-132) Avail: NTIS HC/MF A08 CSCL 04B

The Archean (2.5 to 3.8 billion years ago) is of interest climatically because of the 'Faint Young Sun's Paradox,' which can be characterized by the Sun's reduced energy output. The lower energy output leads to a frozen planet if the climate existed as it does today, but the geological record shows that water was flowing at the earth's surface 3.8 b.y. ago. Energy balance models predict a frozen planet for this time period, unless CO_2 concentrations exist in the Archean atmosphere. The thesis explores the Archean climate with the Community Climate Model. A series of sensitivity simulations were undertaken which first explores individual factors that may be important for the Archean. They include rotation rate, lower solar luminosity, and land fraction. Then these climatic factors, along with higher CO_2 concentrations, are combined into a set of experiments. The conclusions are (1) that large CO_2 concentrations in the Archean atmosphere are not necessary to obtain an equitable climate, (2) that a faster rotation

rate causes a large reduction in clouds, and (3) that atmospheric dynamics are large components of the climate system and cannot be ignored. Author

N92-23660# National Oceanic and Atmospheric Administration, Boulder, CO. Climate Monitoring and Diagnostics Lab.
DIFFERENCES WITHIN AND AMONG SURFACE MARINE DATASETS
S. D. Woodruff, S. J. Lubker, R. G. Quayle, U. Radok, and E. D. Doggett Oct. 1991 221 p
(PB92-135326) Avail: NTIS HC/MF A10 CSCL 04B

Comparisons of global real time surface marine data for Dec. 1986 and Jun. 1988 are presented. Three data sets are compared: one obtained from the National Meteorological Center (NMC); one from the U.S. Navy Fleet Numerical Oceanography Center; and a third from U.S. Air Force Global Weather Central. In addition to the full data set obtained from NMC, subsets obtained from different observational platforms and during daytime and nighttime hours are also considered. The data (primarily in the form of monthly averages for 2 deg. latitude x 2 deg longitude boxes) are analyzed before and following uniform quality control procedures used for the Comprehensive Ocean-Atmosphere Data Set, including identification and removal of duplicate reports and of statistical outliers (trimming). Author

N92-23677# World Meteorological Organization, Geneva (Switzerland). World Climate Data and Monitoring Program.
CLIMATE SYSTEM MONITORING (CSM). EL NINO/SOUTHERN OSCILLATION (ENSO) DIAGNOSTIC ADVISORY, SPECIAL ISSUE
Jan. 1992 16 p
Avail: NTIS MF A01; print copy available at WMO, Geneva, Switzerland

In this special issue of the Climate System Monitoring Bulletin analyses from three climate centers have been compiled under a single cover. The first analysis is from the Climate Analysis Center, National Weather Service of the U.S.A., the second is from the Darwin Regional/Specialized Meteorological Center (RSMC), Australia and the third includes a portion of the first issue of the South Pacific Climate Monitor, from New Zealand, National Climate Center. H.A.

N92-23682# National Oceanic and Atmospheric Administration, Seattle, WA. Pacific Marine Environmental Lab.
WIND, CURRENT AND TEMPERATURE DATA AT 0 DEG, 165 DEG E: JANUARY 1986 TO MARCH 1991
F. Yue, H. P. Freitag, M. J. McPhaden, and A. J. Shepherd Dec. 1991 57 p
(PB92-143080; NOAA-DR-ERL-PMEL-36) Avail: NTIS HC/MF A04 CSCL 04B

The data presented were collected from a current meter mooring nominally located at 0 deg, 165 deg E as part of the U.S./People's Republic of China Bilateral Air-Sea Interaction Program. The field phase of the program consisted of 8 approx. semi-annual research cruises to the western equatorial Pacific between Jan. 1986 and Jul. 1990. The purpose of the US/PRC Bilateral was to study air-sea interaction in the western equatorial Pacific warm pool on time scales of relevance to the El Nino/Southern Oscillation phenomenon. Bilateral activities were conducted within the overall framework of the International Tropical Ocean-Global Atmosphere (TOGA) program. Portions of the data discussed have appeared in several recent publications dealing with the dynamics and thermodynamics of the western equatorial Pacific Ocean. Author

N92-23746# National Weather Service, Silver Spring, MD.
FUNCTIONAL PRECISION OF NATIONAL WEATHER SERVICE UPPER-AIR MEASUREMENTS USING SPACE DATA DIVISION RADIOSONDE (MODEL 909-10-01)
P. Ahnert, M. Gelman, and M. Lukes Oct. 1991 49 p Prepared in cooperation with National Meteorological Center, Washington, DC
(PB92-137843; NOAA-TR-NWS-46) Avail: NTIS HC/MF A03 CSCL 04B

The functional precision of Space Data Corporation Model 909-10-01 (SDC) radiosonde was determined using the National Weather Service functional analysis test package. The comparisons were made from 45 flights of paired radiosondes suspended from the same balloon. The two sondes were vertically separated by about 10 meters and functional precision is given by the standard deviation of the differences (sigma-D) between measurements made by two sensors of the same type exposed to the same environment. Results are summarized for simultaneous measurements at one minute intervals as well as measurements at a predefined set of pressure levels. These tests were conducted for the acceptance of contract production samples, and results are reported for use by the meteorological community in specifying the characteristics of this radiosonde which began operational use in Feb. 1989. GRA

N92-23771 Delaware Univ., Newark.
EVALUATION OF TERRESTRIAL CLIMATE VARIABILITY USING A MOISTURE INDEX Ph.D. Thesis
Johannes Jan Feddema 1990 163 p
Avail: Univ. Microfilms Order No. DA9206297

A geographically dense station network of precipitation and temperature observations is used to evaluate global patterns of climate variation over the twenty-year period from Jan. 1951 to Dec. 1970. Selection of this particular time period is based on an analysis of the spatial representativeness of available monthly climate records from 1880 to 1987. This analysis illustrates the errors associated with varying station distributions through time. However, neither temperature nor precipitation alone is adequate for a comprehensive analysis of climate change. A modified form of Thornthwaite's moisture index, showing the relative moistness or dryness of a climate, is therefore evaluated since it represents a more active or integrative factor in climate. The twenty-year time series of mean terrestrial moisture index values shows that moisture demand exceeds moisture supply by about 20 percent. There does not seem to be a consistent relationship between annual values of the mean moisture index values of the two hemispheres. Analysis of climate variation included the mapping and analysis of moisture indices on a 2 deg of latitude by 2 deg of longitude grid. A composite scenario of El Nino events was created from the six years of known El Nino events in the Pacific Ocean. Further spatial analysis involved the clustering of similar yearly moisture index distributions into six composites.
Dissert. Abstr.

N92-23906# National Weather Service, Fort Worth, TX.
TORNADIC SUPERCELL OVER DADE AND BROWARD COUNTIES (FLORIDA) ON JANUARY 15, 1991
R. Edwards Jan. 1992 30 p
(PB92-134444; NOAA-TM-NWS-SR-140) Avail: NTIS HC/MF A03 CSCL 04B

On the afternoon of 15 Jan. 1991, a supercell thunderstorm developed over southern Dade County and moved north-northeastward across populous urban areas of northeastern Dade and southern Broward counties. The associated mesocyclone produced four confirmed tornadoes, injuring five persons and causing several million dollars in damage. Another thunderstorm, following a parallel track several miles west of the tornadic supercell, contained a weaker mesocyclone which spawned no tornadoes. Observations and descriptions of the event are presented, along with largely qualitative investigation into those mechanisms likely to have contributed to this rare supercell event for southern Florida. In addition, forecast implications are discussed, and the concept of helicity is presented as a useful forecast tool for such events. GRA

N92-23994# National Hurricane Center, Coral Gables, FL.
DIAGNOSTIC REPORT OF THE NATIONAL HURRICANE CENTER: JUNE AND JULY 1991. VOLUME 4, NUMBER 1
C. J. McAdie and E. N. Rappaport 1991 48 p
(PB92-134501) Avail: NTIS HC/MF A03 CSCL 04B

An overview is given of tropical activity for June and July 1991. Topics covered include the mean flow patterns for the Atlantic

and Eastern Pacific basins; a tropical wave and tropical cyclone summary; tropical cyclone activity in the Atlantic basin; tropical cyclone activity in the Pacific basin; and official forecast performance. Much of the information is given in the form of graphs and charts. Author

48 OCEANOGRAPHY

Includes biological, dynamic, and physical oceanography; and marine resources.

For related information see also *43 Earth Resources and Remote Sensing.*

N92-23519# National Marine Fisheries Service, Seattle, WA.
OUR LIVING OCEANS: THE FIRST ANNUAL REPORT ON THE STATUS OF US LIVING MARINE RESOURCES
Nov. 1991 130 p
(PB92-145689; NOAA-TM-NMFS-F/SPO-1) Avail: NTIS HC/MF A07 CSCL 08C

This is a comprehensive summary of the status of living marine resources. Information is given on the health and abundance of most marine and anadromous fish species, as well as shellfish, marine mammals, sea turtles, and corals that have commercial, recreational, or ecological significance. Detailed scientific data is given on recent, current, and long-term potential yields of each species. Author

N92-23669# National Oceanic and Atmospheric Administration, Boulder, CO. Wave Propagation Lab.
OCEAN ACOUSTIC TOMOGRAPHY INVERSION IN THE ADIABATIC-INVARIANT APPROXIMATION
R. M. Jones, T. M. Georges, L. Nesbitt, and A. Weickmann Dec. 1991 244 p
(PB92-140466; NOAA-TM-ERL-WPL-217) Avail: NTIS HC/MF A11 CSCL 08C

Inversion of vertical-slice, ocean acoustic tomography (travel-time) measurements, in which they use the adiabatic-invariant approximation to convert multi-loop measurements to single-loop ray properties before using an Abel transform is discussed. For a range-dependent sound channel, the method yields a range average of the symmetric part of the sound channel and the antisymmetric part of the sound channel at the source and receiver if the symmetric part of the sound channel at the source and receiver can be determined. For a uniform sound channel, the inversion recovers both the symmetric and antisymmetric parts of the sound channel, including the vertical displacement of the sound-channel axis. The inversion is demonstrated by applying it to a simulated pulse-arrival sequence for a uniform sound channel (generated by ray tracing), and compare the recovered sound-speed profile with that used for the simulation. GRA

N92-23732# National Oceanic and Atmospheric Administration, Miami, FL. Atlantic Oceanographic and Meteorological Labs.
CODAR IN THE STRAITS OF FLORIDA Final Report
W. McLeish and G. A. Maul Aug. 1991 53 p
(PB92-129964; NOAA-TR-ERL-447-AOML-35) Avail: NTIS HC/MF A04 CSCL 08C

The Atlantic Oceanographic and Meteorological Lab (AOML) operated a Coastal Ocean Dynamics Applications Radar (CODAR) in a project to measure ocean surface currents near Miami and produce a series of maps of ocean surface current vectors. The project also evaluated the feasibility and value of routine operational use of the HF radar system. The CODAR system produced many maps that showed the west and central portions of the Florida Current. The core speed of the rapid flow, its distance offshore, and the often sharp decrease in speed nearshore were apparent. Also, the maps showed at times a band of water nearshore that was moving slowly southward along the coast and sometimes a cyclonic eddy about 15 km in diameter that was centered in a nearly fixed location 20 km northeast of Miami. However, on the whole, the CODAR system could not be used as the project planned. The system required excessively frequent maintenance to remain on line. The maps produced were inadequate for the intended uses and too many maps were missing. The concept of a fully automatic system to produce valid CODAR results was not realized in the version of CODAR system that the project evaluated. Author

N92-23769 Columbia Univ., New York, NY.
RECONSTRUCTING THE TROPICAL ATLANTIC SEASONAL THERMOCLINE USING PLANKTONIC FORAMINIFERA Ph.D. Thesis
Ana Christina Ravelo 1991 179 p
Avail: Univ. Microfilms Order No. DA9202734

Abundances of planktonic foraminifera from vertically stratified plankton tows from the east equatorial Atlantic Ocean are compared to hydrographic conditions of the water from which they were collected (generally down to 100 meters below the sea surface). These data demonstrate that different species proliferate at the water column depth where their ecological habitats are found. Some spinose species are found in greatest abundance close to the surface in the relatively nutrient depleted mixed layer. Some spinose and non-spinose species are found in greatest abundance at the depth of the maximum in primary productivity. Because of the tow results, sediment planktonic foraminifera assemblages and isotopic values can be understood as reflecting the hydrography overlying the core tops. Dissert. Abstr.

51 LIFE SCIENCES (GENERAL)

N92-23518# Oak Ridge National Lab., TN.
NUCLEAR MEDICINE PROGRAM Progress Report, quarter ending 30 Sep. 1991
F. F. Knapp, Jr., K. R. Ambrose, A. P. Callahan, D. W. McPherson, S. Mirzadeh, P. C. Srivastava, A. Hasan, C. R. Lambert, S. J. Lambert, and D. E. Rice Feb. 1992 14 p
(Contract DE-AC05-84OR-21400)
(DE92-006979; ORNL/TM-11992) Avail: NTIS HC/MF A03

Rat tissue distribution properties of 'IQNP', a new radioiodinated cholinergic-muscarinic receptor antagonist, are described. IQNP is the acronym for 1-azabicyclo(2.2.2)oct-3-yl alpha-hydroxy alpha-phenyl alpha (1-idio-1 propen-30yl) acetate, which is an analogue of the QNB muscarinic antagonist in which the p-iodophenyl moiety has been replaced with the 1-iodo-1-propen-3-yl moiety. The radioiodinated IQNP analogue is easier to prepare in much higher yields than QNB and is thus a candidate for the evaluation of muscarinic receptors by external imaging techniques. Studies in rats demonstrated that IQNP shows high uptake in those cerebral regions rich in muscarinic receptors. QNB-treatment of rats either 1 h before (pre) or 2 h after (post) administration of radioiodinated IQNP resulted in significant displacement or blocking of cerebral specific IQNP uptake (percent dose/gm) in the cortex and striatum. These studies demonstrate that IQNP has specificity for the cholinergic-muscarinic receptor and is a good candidate for further studies. Also during this period, several agents developed in the ORNL Nuclear Medicine Program were supplied to Medical Cooperative Programs for collaborative studies including the iodine-125-labeled BMIPP and DMIPP fatty acid analogues and the IPM antibody labeling agent. Tin-117m and gold-199 were produced in the ORNL High Flux Isotope Reactor (HFIR) and supplied to the OHER-supported program in the Medical Department at Brookhaven National Laboratory to aid in their research until the re-start of the High Flux Brookhaven Reactor. DOE

N92-23706# Joint Publications Research Service, Arlington, VA.
JPRS REPORT: SCIENCE AND TECHNOLOGY. CENTRAL EURASIA: LIFE SCIENCES
26 Mar. 1992 46 p Transl. into ENGLISH from various Russian articles
(JPRS-ULS-92-010) Avail: NTIS HC/MF A03

A bibliography is given of Central Eurasian research in life sciences. Topics covered include biochemistry, biophysics, biotechnology, the Earth environment, radiation effects, genetics, immunology, clinical medicine, microbiology, pharmacology, toxicology, physiology, public health, psychology, radiation biology, veterinary medicine, and virology. Author

N92-24052*# National Aeronautics and Space Administration. Lyndon B. Johnson Space Center, Houston, TX.
THREE-DIMENSIONAL CULTURED GLIOMA CELL LINES Patent Application
Steve R. Gonda, inventor (to NASA) and Garry M. Marley, inventor (to NASA) (Krug International, Houston, TX.) 9 Dec. 1991 28 p
(NASA-Case-MSC-21843-1-NP; NAS 1.71:MSC-21843-1-NP; US-Patent-Appl-SN-803828) Avail: NTIS HC/MF A03 CSCL 06C

Three-dimensional glioma spheroids were produced in vitro with size and histological differentiation previously unattained. The spheroids were grown in liquid media suspension in a Johnson Space Center (JSC) Rotating Wall Bioreactor without using support matrices such as microcarrier beads. Spheroid volumes of greater than 3.5 cu mm and diameters of 2.5 mm were achieved with a viable external layer or rim of proliferating cells, a transitional layer beneath the external layer with histological differentiation, and a degenerative central region with a hypoxic necrotic core. Cell debris was evident in the degenerative central region. The necrotics centers of some of the spheroids had hyaline droplets. Granular bodies were detected predominantly in the necrotic center. NASA

N92-23604*# International Center for Genetic Engineering and Biotechnology, Trieste (Italy).
MICROGRAVITATIONAL EFFECTS ON CHROMOSOME BEHAVIOR (7-IML-1)
Carlo Bruschi *In* NASA. Marshall Space Flight Center, First International Microgravity Laboratory Experiment Descriptions Feb. 1992 p 33-38 (For primary document see N92-23600 14-29)
Avail: NTIS HC/MF A13 CSCL 06C

N92-23605*# Texas Univ. Health Science Center, Houston. Dental Branch.
CHRONDROGENESIS IN MICROMASS CULTURES OF EMBRYONIC MOUSE LIMB MESENCHYMAL CELLS EXPOSED TO MICROGRAVITY (7-IML-1)
Jackie Duke *In* NASA. Marshall Space Flight Center, First International Microgravity Laboratory Experiment Descriptions Feb. 1992 p 39-44 (For primary document see N92-23600 14-29)
Avail: NTIS HC/MF A13 CSCL 06C

N92-23606*# Vrije Univ., Amsterdam (Netherlands). Dept. of Oral Cell Biology.
EFFECT OF MICROGRAVITY AND MECHANICAL STIMULATION ON THE IN VITRO MINERALIZATION AND RESORPTION OF FETAL MOUSE LONG BONES (7-IML-1)
J. Paul Veldhuijzen *In* NASA. Marshall Space Flight Center, First International Microgravity Laboratory Experiment Descriptions Feb. 1992 p 45-48 (For primary document see N92-23600 14-29)
Avail: NTIS HC/MF A13 CSCL 06C

N92-23607*# Hubrecht Lab., Utrecht (Netherlands).
EGGS: THE ROLE OF GRAVITY IN THE ESTABLISHMENT OF THE DORSO-VENTRAL AXIS IN THE AMPHIBIAN EMBRYO (7-IML-1)
Geertje A. Ubbels *In* NASA. Marshall Space Flight Center, First International Microgravity Laboratory Experiment Descriptions Feb. 1992 p 49-53 (For primary document see N92-23600 14-29)
Avail: NTIS HC/MF A13 CSCL 06C

N92-23608*# Consejo Superior de Investigaciones Cientificas, Madrid (Spain). Dept. of Biochemistry.
THE EFFECT OF SPACE ENVIRONMENT ON THE DEVELOPMENT AND AGING OF DROSOPHILA MELANOGASTER (7-IML-1)
Roberto Marco *In* NASA. Marshall Space Flight Center, First International Microgravity Laboratory Experiment Descriptions Feb. 1992 p 55-57 (For primary document see N92-23600 14-29)
Avail: NTIS HC/MF A13 CSCL 06C

N92-23609*# Aarhus Univ. (Denmark).
EFFECT OF MICROGRAVITY ENVIRONMENT ON CELL WALL REGENERATION, CELL DIVISIONS, GROWTH, AND DIFFERENTIATION OF PLANTS FROM PROTOPLASTS (7-IML-1)
Ole Rasmussen *In* NASA. Marshall Space Flight Center, First International Microgravity Laboratory Experiment Descriptions Feb. 1992 p 59-61 (For primary document see N92-23600 14-29)
Avail: NTIS HC/MF A13 CSCL 06C

N92-23610*# Deutsche Forschungsanstalt fuer Luft- und Raumfahrt, Cologne (Germany, F.R.). Inst. for Aerospace Medicine.
EMBRYOGENESIS AND ORGANOGENESIS OF CARAUSIUS MOROSUS UNDER SPACE FLIGHT CONDITIONS (7-IML-1)
D. H. Buecker *In* NASA. Marshall Space Flight Center, First International Microgravity Laboratory Experiment Descriptions Feb. 1992 p 63-64 (For primary document see N92-23600 14-29)
Avail: NTIS HC/MF A13 CSCL 06C

N92-23612*# Johann-Wolfgang-Goethe-Univ., Frankfurt am Main (Germany, F.R.). Inst. of Microbiology.
GROWTH AND SPORULATION OF BACILLUS SUBTILIS UNDER MICROGRAVITY (7-IML-1)
Horst-Dieter Mennigmann *In* NASA. Marshall Space Flight Center, First International Microgravity Laboratory Experiment Descriptions Feb. 1992 p 67-70 (For primary document see N92-23600 14-29)
Avail: NTIS HC/MF A13 CSCL 06C

N92-23613*# Eidgenoessische Technische Hochschule, Zurich (Switzerland).
FRIEND LEUKEMIA VIRUS TRANSFORMED CELLS EXPOSED TO MICROGRAVITY IN THE PRESENCE OF DMSO (7-IML-1)
Augusto Cogoli *In* NASA. Marshall Space Flight Center, First International Microgravity Laboratory Experiment Descriptions Feb. 1992 p 71-73 (For primary document see N92-23600 14-29)
Avail: NTIS HC/MF A13 CSCL 06C

N92-23614*# Eidgenoessische Technische Hochschule, Zurich (Switzerland). Inst. of Biotechnology.
PROLIFERATION AND PERFORMANCE OF HYBRIDOMA CELLS IN MICROGRAVITY (7-IML-1)
Augusto Cogoli *In* NASA. Marshall Space Flight Center, First International Microgravity Laboratory Experiment Descriptions Feb. 1992 p 75-77 (For primary document see N92-23600 14-29)
Avail: NTIS HC/MF A13 CSCL 06C

N92-23615*# Eidgenoessische Technische Hochschule, Zurich (Switzerland). Inst. of Biotechnology.
DYNAMIC CELL CULTURE SYSTEM (7-IML-1)
Augusto Cogoli *In* NASA. Marshall Space Flight Center, First International Microgravity Laboratory Experiment Descriptions Feb. 1992 p 79-80 (For primary document see N92-23600 14-29)
Avail: NTIS HC/MF A13 CSCL 06C

N92-23616*# Open Univ. (Scotland).
GROWTH, DIFFERENTIATION AND DEVELOPMENT OF ARABIDOPSIS THALIANA UNDER MICROGRAVITY CONDITIONS (7-IML-1)
E. P. Maher and L. G. Briarty (Nottingham Univ., England) *In* NASA. Marshall Space Flight Center, First International Microgravity Laboratory Experiment Descriptions Feb. 1992 p 81-87 (For

primary document see N92-23600 14-29)
Avail: NTIS HC/MF A13 CSCL 06C

N92-23617*# Paris VI Univ. (France).
TRANSMISSION OF GRAVISTIMULUS IN THE STATOCYTE OF THE LENTIL ROOT (7-IML-1)
Gerald Perbal *In* NASA. Marshall Space Flight Center, First International Microgravity Laboratory Experiment Descriptions Feb. 1992 p 89-91 (For primary document see N92-23600 14-29)
Avail: NTIS HC/MF A13 CSCL 06C

N92-23618*# Deutsche Forschungsanstalt fuer Luft- und Raumfahrt, Cologne (Germany, F.R.).
GRAVITY RELATED BEHAVIOR OF THE ACELLULAR SLIME MOLD PHYSARUM POLYCEPHALUM (7-IML-1)
I. Block *In* NASA. Marshall Space Flight Center, First International Microgravity Laboratory Experiment Descriptions Feb. 1992 p 93-97 (For primary document see N92-23600 14-29)
Avail: NTIS HC/MF A13 CSCL 06C

N92-23619*# Toulouse Univ. (France).
STUDIES ON PENETRATION OF ANTIBIOTIC IN BACTERIAL CELLS IN SPACE CONDITIONS (7-IML-1)
R. Tixador *In* NASA. Marshall Space Flight Center, First International Microgravity Laboratory Experiment Descriptions Feb. 1992 p 99-107 (For primary document see N92-23600 14-29)
Avail: NTIS HC/MF A13 CSCL 06C

N92-23621*# British Columbia Univ., Vancouver.
PHASE PARTITIONING EXPERIMENT (8-IML-1)
Donald E. Brooks *In* NASA. Marshall Space Flight Center, First International Microgravity Laboratory Experiment Descriptions Feb. 1992 p 113-116 (For primary document see N92-23600 14-29)
Avail: NTIS HC/MF A13 CSCL 06C

N92-23629*# National Space Development Agency, Tokyo (Japan).
RADIATION MONITORING CONTAINER DEVICE (16-IML-1)
S. Nagaoka *In* NASA. Marshall Space Flight Center, First International Microgravity Laboratory Experiment Descriptions Feb. 1992 p 189 (For primary document see N92-23600 14-29)
Avail: NTIS HC/MF A13 CSCL 06C

N92-23653*# Genetech, Inc., San Francisco, CA. Endocrine Research Div.
CENTER FOR CELL RESEARCH, PENNSYLVANIA STATE UNIVERSITY
Mike Cronin *In* NASA, Washington, Proceedings of the Second Annual Symposium on Industrial Involvement and Successes in Commercial Space 1991 11 p (For primary document see N92-23643 14-12)
Avail: NTIS HC/MF A11 CSCL 10B

52 AEROSPACE MEDICINE

Includes physiological factors; biological effects of radiation; and effects of weightlessness on man and animals.

N92-23139# Civil Aeromedical Inst., Oklahoma City, OK.
RADIATION EXPOSURE OF AIR CARRIER CREWMEMBERS 2 Final Report
W. Friedberg, L. Snyder, D. N. Faulkner, E. B. Darden, and K. OBrien Jan. 1992 21 p Prepared in cooperation with Oak Ridge Associated Universities, Inc., TN; and Univ. of Northern Arizona, Flagstaff Sponsored by FAA
(PB92-140037; DOT/FAA-AM-92/2) Avail: NTIS HC/MF A03 CSCL 06R

The cosmic radiation environment at air carrier flight altitudes is described and estimates given of the amounts of galactic cosmic radiation received on a wide variety of routes to and from, and within the contiguous United States. Radiation exposure from radioactive air cargo is also considered. Methods are provided to assess health risks from exposure to galactic radiation. On the flights studied, the highest dose of galactic radiation received annually by a crewmember who worked as many as 1000 block hours a year would be less than half the annual limit recommended by the International Commission on Radiological Protection for a nonpregnant occupationally exposed adult. The radiation exposure for a pregnant crewmember who worked 70 block hours a month for five months would exceed the recommended 2-millisievert pregnancy limit on about one-third of the flights. GRA

N92-23424*# National Aeronautics and Space Administration. Ames Research Center, Moffett Field, CA.
SKELETAL RESPONSES TO SPACEFLIGHT
Emily Morey-Holton and Sara B. Arnaud Dec. 1991 35 p
(NASA-TM-103890; A-91232; NAS 1.15:103890) Avail: NTIS HC/MF A03 CSCL 06P

The role of gravity in the determination of bone structure is elucidated by observations in adult humans and juvenile animals during spaceflight. The primary response of bone tissue to microgravity is at the interface of the mineral and matrix in the process of biomineralization. This response is manifested by demineralization or retarded growth in some regions of the skeleton and hypermineralization in others. The most pronounced effects are seen in the heelbone and skull, the most distally located bones relative to the heart. Ground based flight simulation models that focus on changes in bone structure at the molecular, organ, and whole body levels are described and compared to flight results. On Earth, the morphologic and compositional changes in the unloaded bones are very similar to changes during flight; however, the ground based changes appear to be more transient. In addition, a redistribution of bone mineral in gravity-dependent bones occurs both in space and during head down positioning on Earth. Longitudinal data provided considerable information on the influence of endocrine and muscular changes on bone structure after unloading. Author

N92-24033# Columbia Univ., New York, NY.
LOW DOSE NEUTRON LATE EFFECTS: CATARACTOGENESIS
B. V. Worgul Dec. 1991 6 p
(Contract DE-FG02-90ER-61009)
(DE92-005539; DOE/ER-61009/2) Avail: NTIS HC/MF A02

The work is formulated to resolve the uncertainty regarding the relative biological effectiveness (RBE) of low dose neutron radiation. The study exploits the fact that cataractogenesis is sensitive to the inverse dose-rate effect as has been observed with heavy ions and was an endpoint considered in the follow-up of the A-bomb survivors. The neutron radiations were initiated at the Radiological Research Accelerator Facility (RARAF) of the Nevis Laboratory of Columbia University. Four week old (plus or minus 1 day) rats were divided into eight dose groups each receiving single or fractionated total doses of 0.2, 1.0, 5.0 and 25.0 cGy of monoenergetic 435 KeV neutrons. Special restraining jigs insured that the eye, at the midpoint of the lens, received the appropriate energy and dose with a relative error of plus or minus 5 percent. The fractionation regimen consisted of four exposures, each administered at three hour (plus minus) intervals. The neutron irradiated groups are being compared to rats irradiated with 250 kVp x-rays in doses ranging from 0.5 to 7 Gy. The animals are being examined on a biweekly basis utilizing conventional slit-lamp biomicroscopy and the Scheimpflug Slit Lamp Imaging System (Zeiss). The follow-ups, entering their second year, will continue throughout the life-span of the animals. This is essential inasmuch as given the extremely low doses which are being utilized, clinically detectable opacities were not anticipated until a significant fraction of the life span has lapsed. Current data support this contention. At this juncture, cataracts in the irradiated groups are beginning to exceed control levels. DOE

N92-23603*# Jet Propulsion Lab., California Inst. of Tech., Pasadena.
GENETIC AND MOLECULAR DOSIMETRY OF HZE RADIATION (7-IML-1)
Gregory A. Nelson *In* NASA. Marshall Space Flight Center,

First International Microgravity Laboratory Experiment Descriptions Feb. 1992 p 25-31 (For primary document see N92-23600 14-29)
Avail: NTIS HC/MF A13 CSCL 06R

N92-23620*# Calgary Univ. (Alberta).
ENERGY EXPENDITURE IN SPACE FLIGHT (DOUBLY LABELLED WATER METHOD) (8-IML-1)
Howard G. Parsons *In* NASA. Marshall Space Flight Center, First International Microgravity Laboratory Experiment Descriptions Feb. 1992 p 111-112 (For primary document see N92-23600 14-29)
Avail: NTIS HC/MF A13 CSCL 06P

N92-23622*# British Columbia Univ., Vancouver. University Hospital/Shaughnessy Site.
BACK PAIN IN ASTRONAUTS (8-IML-1)
P. C. Wing *In* NASA. Marshall Space Flight Center, First International Microgravity Laboratory Experiment Descriptions Feb. 1992 p 117-119 (For primary document see N92-23600 14-29)
Avail: NTIS HC/MF A13 CSCL 06P

N92-23623*# Canadian Space Agency, Ottawa (Ontario).
MEASUREMENT OF VENOUS COMPLIANCE (8-IML-1)
R. B. Thirsk *In* NASA. Marshall Space Flight Center, First International Microgravity Laboratory Experiment Descriptions Feb. 1992 p 121-122 (For primary document see N92-23600 14-29)
Avail: NTIS HC/MF A13 CSCL 06P

N92-23624*# University of Western Ontario, London.
POSITIONAL AND SPONTANEOUS NYSTAGMUS (8-IML-1)
Joseph McClure *In* NASA. Marshall Space Flight Center, First International Microgravity Laboratory Experiment Descriptions Feb. 1992 p 123-124 (For primary document see N92-23600 14-29)
Avail: NTIS HC/MF A13 CSCL 06P

N92-23625*# McGill Univ., Montreal (Quebec).
SPACE ADAPTATION SYNDROME EXPERIMENTS (8-IML-1)
D. Watt *In* NASA. Marshall Space Flight Center, First International Microgravity Laboratory Experiment Descriptions Feb. 1992 p 125-134 (For primary document see N92-23600 14-29)
Avail: NTIS HC/MF A13 CSCL 06P

N92-23626*# National Aeronautics and Space Administration. Lyndon B. Johnson Space Center, Houston, TX.
MICROGRAVITY VESTIBULAR INVESTIGATIONS (10-IML-1)
Millard F. Reschke *In* NASA. Marshall Space Flight Center, First International Microgravity Laboratory Experiment Descriptions Feb. 1992 p 135-180 (For primary document see N92-23600 14-29)
Avail: NTIS HC/MF A13 CSCL 06P

53 BEHAVIORAL SCIENCES

Includes psychological factors; individual and group behavior; crew training and evaluation; and psychiatric research.

N92-23628*# Massachusetts Inst. of Tech., Cambridge.
MENTAL WORKLOAD AND PERFORMANCE EXPERIMENT (15-IML-1)
Harold L. Alexander *In* NASA. Marshall Space Flight Center, First International Microgravity Laboratory Experiment Descriptions Feb. 1992 p 183-187 (For primary document see N92-23600 14-29)
Avail: NTIS HC/MF A13 CSCL 05I

54 MAN/SYSTEM TECHNOLOGY AND LIFE SUPPORT

Includes human engineering; biotechnology; and space suits and protective clothing.

For related information see also *16 Space Transportation.*

N92-23218# Joint Food and Agriculture Organization - International Atomic Energy Agency, Vienna (Austria). Div. of Nuclear Techniques in Food and Agriculture.
FOOD IRRADIATION NEWSLETTER, VOLUME 15, NUMBER 2
Oct. 1991 62 p
(DE92-614951; INIS-MF-13047-Vol-15-No-2) Avail: NTIS HC/MF A04

This newsletter contains brief summaries of three coordinated research meetings held in 1991: irradiation in combination with other processes for improving food quality; application of irradiation technique for food processing in Africa; and food irradiation programme for Middle East and European countries. The first Workshop on Public Information on Food Irradiation is summarized, and a Coordinated Research Programme on Irradiation as a Quarantine Treatment of Mites, Nematodes, and Insects other than Fruit Fly is announced. This issue also contains a report on the status of food irradiation in China, and a supplement lists clearances of irradiated foods. DOE

N92-23513# Maryland Univ., Baltimore.
STRESS EFFECTS OF HUMAN-COMPUTER INTERACTIONS Final Report
H. H. Emurian Oct. 1991 60 p Sponsored in part by National Inst. for Occupational Safety and Health, Cincinnati, OH
(Grant PHS-OH-02614-01A1)
(PB92-136001) Avail: NTIS HC/MF A04 CSCL 05H

Experiments were carried out to investigate the effects of human/computer interactions on indicators of stress. Men solved 50 database queries consecutively presented on a video display terminal (VDT). Each query required solution within 45 seconds of its initial presentation to avoid a reduction in potential earnings. A solution required the correct selection of three successive hypertext indices hierarchically structured from the query to the data answer. In a second study, 16 men and 16 women solved 80 database queries under conditions of high or low work density. The results indicated that motivated time pressure work at a VDT will produce tonic elevations over a resting baseline in blood pressure, heart rate, and masseter electromyogram (EMG) activity in men and women who are experienced computer users. A relationship exists between the personality of the computer user and the magnitude of systolic blood pressure. Under conditions of 8 second constant and 8 second variable system response times (SRTs) in men, the constant and variable SRTs did not differentially affect physiological responses. Men and women showed higher systolic blood pressure during high density work than during low density work. Females showed reliably greater masseter EMG activity during high density work than during low density work. Author

N92-24022# Food and Agriculture Organization of the United Nations, Rome (Italy).
IRRADIATION OF SPICES, HERBS, AND OTHER VEGETABLE SEASONINGS: A COMPILATION OF TECHNICAL DATA FOR ITS AUTHORIZATION AND CONTROL
Feb. 1992 52 p Prepared in cooperation with International Atomic Energy Agency, Vienna, Austria and World Health Organization, Geneva, Switzerland
(DE92-619064; IAEA-TECDOC-639) Avail: NTIS HC/MF A04

This publication contains a compilation of all available scientific and technical data on the irradiation of spices, herbs and other vegetable seasonings. It is intended to assist governments in considering the authorization of this particular application of radiation processing of food and in ensuring its control in the facility and the control of irradiated food products moving in trade. The Compilation was prepared in response to the requirement of the Codex General Standard for Irradiated Foods and associated

Code that radiation treatment of food be justified on the basis of a technological need or of a need to improve the hygienic quality of the food. It was prepared also in response to the recommendations of the FAO/IAEA/WHO/ITC-UNCTAD/GATT International Conference on the Acceptance, Control of and Trade in Irradiated Food (Geneva, 1989) concerning the need for regulatory control of radiation processing of food. It is hoped that the information contained in this publication will assist governments in considering requests for the approval of radiation treatment of spices, herbs and other vegetable seasonings, or requests for authorization to import such irradiated products. DOE

N92-24044*# National Aeronautics and Space Administration. Marshall Space Flight Center, Huntsville, AL.
PROSTHETIC HELPING HAND Patent Application
Thomas W. Vest, inventor (to NASA) (MSI Electronics, Inc., Woodside, NY.), James R. Carden, inventor (to NASA), William E. Norton, inventor (to NASA), and Jewell G. Belcher, inventor (to NASA) 7 Feb. 1992 12 p
(NASA-Case-MFS-28430-1; NAS 1.71:MFS-28430-1; US-Patent-Appl-SN-832569) Avail: NTIS HC/MF A03 CSCL 06C

A prosthetic device for below-the-elbow amputees, having a C-shaped clamping mechanism for grasping cylindrical objects, is described. The clamping mechanism is pivotally mounted to a cuff that fits on the amputee's lower arm. The present invention is utilized by placing an arm that has been amputated below the elbow into the cuff. The clamping mechanism then serves as a hand whenever it becomes necessary for the amputee to grasp a cylindrical object such as a handle, a bar, a rod, etc. To grasp the cylindrical object, the object is jammed against the opening in the C-shaped spring, causing the spring to open, the object to pass to the center of the spring, and the spring to snap shut behind the object. Various sizes of clamping mechanisms can be provided and easily interchanged to accommodate a variety of diameters. With the extension that pivots and rotates, the clamping mechanism can be used in a variety of orientations. Thus, this invention provides the amputee with a clamping mechanism that can be used to perform a number of tasks. NASA

N92-24056*# National Aeronautics and Space Administration. Marshall Space Flight Center, Huntsville, AL.
BAR-HOLDING PROSTHETIC LIMB Patent Application
Thomas W. Vest, inventor (to NASA) (MSI Electronics, Inc., Woodside, NY.), William E. Norton, inventor (to NASA), Jewell G. Belcher, inventor (to NASA), and James R. Carden, inventor (to NASA) 15 Apr. 1992 11 p
(NASA-Case-MFS-28481-1; NAS 1.71:MFS-28481-1; US-Patent-Appl-SN-873931) Avail: NTIS HC/MF A03 CSCL 06C

A prosthetic device for below-the-elbow amputees is disclosed. The device has a removable effector, which is attached to the end of an arm cuff. The effector is comprised of a pair of C-shaped members that are oriented so as to face each other. Working in concert, the C-shaped members are able to hold a bar such as a chainsaw handle. A flat spring is fitted around the C-shaped members to hold them together. NASA

55 SPACE BIOLOGY

Includes exobiology; planetary biology; and extraterrestrial life.

N92-23429*# National Aeronautics and Space Administration, Washington, DC.
PUBLICATIONS OF THE EXOBIOLOGY PROGRAM FOR 1990: A SPECIAL BIBLIOGRAPHY
Mar. 1992 54 p Prepared in cooperation with George Washington Univ., Washington, DC
(Contract NASw-4324)
(NASA-TM-4364; NAS 1.15:4364) Avail: NTIS HC/MF A04 CSCL 06A

The Exobiology Program is an integrated program designed to investigate and understand those processes related to the origin, evolution, and distribution of life in the universe. The Exobiology Program is broad in scope, covering the following subject areas: cosmic evolution of biogenic compounds; prebiotic evolution; early evolution of life; evolution of advanced life; solar system exploration; search for extraterrestrial intelligence; planetary protection; and advanced programs in biological systems research. A listing of the 1990 publications resulting from research supported by the Exobiology Program is presented. D.R.D.

59 MATHEMATICAL AND COMPUTER SCIENCES (GENERAL)

N92-23559*# National Aeronautics and Space Administration. Langley Research Center, Hampton, VA.
A VERIFIED DESIGN OF A FAULT-TOLERANT CLOCK SYNCHRONIZATION CIRCUIT: PRELIMINARY INVESTIGATIONS
Paul S. Miner Mar. 1992 100 p
(NASA-TM-107568; NAS 1.15:107568) Avail: NTIS HC/MF A05 CSCL 12A

Schneider demonstrates that many fault tolerant clock synchronization algorithms can be represented as refinements of a single proven correct paradigm. Shankar provides mechanical proof that Schneider's schema achieves Byzantine fault tolerant clock synchronization provided that 11 constraints are satisfied. Some of the constraints are assumptions about physical properties of the system and cannot be established formally. Proofs are given that the fault tolerant midpoint convergence function satisfies three of the constraints. A hardware design is presented, implementing the fault tolerant midpoint function, which is shown to satisfy the remaining constraints. The synchronization circuit will recover completely from transient faults provided the maximum fault assumption is not violated. The initialization protocol for the circuit also provides a recovery mechanism from total system failure caused by correlated transient faults. Author

60 COMPUTER OPERATIONS AND HARDWARE

Includes hardware for computer graphics, firmware, and data processing.

For components see *33 Electronics and Electrical Engineering.*

N92-23546*# National Aeronautics and Space Administration. Pasadena Office, CA.
OPTICAL INNER PRODUCT NEURAL ASSOCIATIVE MEMORY Patent Application
Hua-Kuang Liu, inventor (to NASA) (Jet Propulsion Lab., California Inst. of Tech., Pasadena.) 26 Nov. 1991 20 p
(Contract NAS7-918)
(NASA-Case-NPO-18491-1-CU; NAS 1.71:NPO-18491-1-CU; US-Patent-Appl-SN-880210) Avail: NTIS HC/MF A03 CSCL 09B

An optical implementation of an inner-product neural associative memory is realized with a first spatial light modulator for entering an initial two dimensional n-tuple vector and for entering a threshold output vector image after each iteration until convergence is reached, and a second spatial light modulator for entering M weighted vectors of inner-product scalars multiplied with each of the M stored vectors, where the inner-product scalars are produced by multiplication of the initial input vector in the first iterative cycle (and threshold vectors in subsequent iterative cycles) with each of the M stored vectors, and the weighted vectors are produced by multiplication of the scalars with corresponding ones of the stored vectors. A Hughes liquid crystal light valve is used for the

dual function of summing the weighted vectors and thresholding the sum vector. The threshold vector is then entered through the first spatial light modulator for reiteration of the process cycle until convergence is reached. NASA

61 COMPUTER PROGRAMMING AND SOFTWARE

Includes computer programs, routines, alogorithms, and specific applications, e.g., CAD/CAM.

N92-23255# Lawrence Livermore National Lab., CA.
A SIGNAL AND IMAGE PROCESSING OBJECT-BASED SYSTEM USING CLOS
J. E. Hernandez, Shin-Yee Lu, R. J. Sherwood, G. A. Clark, and B. S. Lawver Sep. 1991 9 p Presented at the 1st Annual LISP Users and Vendors Conference, Gaithersburg, MD, 18 Oct. - 1 Nov. 1991
(Contract W-7405-eng-48)
(DE92-006826; UCRL-JC-108409; CONF-9110323-1) Avail: NTIS HC/MF A02

This paper presents a LISP based system for signal and image processing. Using an object based approach, the system integrates signal and image processing algorithms, supervised and unsupervised neural network algorithms, and mild-level computer vision capabilities, into a cohesive framework. This framework is suitable for prototyping complex algorithms dealing with multiple classes of data. The system, known as VISION, is currently used as a prototyping environment for wide range of scientific applications internal to LLNL. This paper highlights some of the capabilities of VISION, and how they were implemented using the Common LISP Object System, CLOS. DOE

N92-23266# Tokyo Univ., Tanashi (Japan). Inst. for Nuclear Study.
THE 7TH INS SCIENTIFIC COMPUTATIONAL PROGRAMS
Jul. 1991 83 p In JAPANESE; ENGLISH summary
(DE92-750967; INS-T-503) Avail: NTIS HC/MF A05

Nineteen groups were accepted at the 7th INS Scientific Computational Programs (ISCP). This ISCP can use full resources of the INS central computer without an operational limitation. The 7th ISCP started on June 11, 1991 and ended on March 30, 1991. Some results were already published in journals or appeared in physical meetings. This is a sum of the used statistics of the 7th ISCP and reports presented by groups performed the 7th ISCP. DOE

N92-23416*# Nebraska Univ., Lincoln.
[DESIGN OF JOINT SOURCE/CHANNEL CODERS]
1991 128 p
(Grant NAG5-916)
(NASA-CR-189960; NAS 1.26:189960) Avail: NTIS HC/MF A07 CSCL 09B

The need to transmit large amounts of data over a band limited channel has led to the development of various data compression schemes. Many of these schemes function by attempting to remove redundancy from the data stream. An unwanted side effect of this approach is to make the information transfer process more vulnerable to channel noise. Efforts at protecting against errors involve the reinsertion of redundancy and an increase in bandwidth requirements. The papers presented within this document attempt to deal with these problems from a number of different approaches. For individual titles, see N92-23417 through N92-23423.

N92-23417*# Nebraska Univ., Lincoln. Dept. of Electrical Engineering.
MAXIMUM APOSTERIORI JOINT SOURCE/CHANNEL CODING
Khalid Sayood and Jerry D. Gibson *In its* Design of Joint Source/Channel Coders 1991 12 p Presented at the 22nd Annual Conference on Information Science and Systems, Princeton, NJ, Mar. 1988 (For primary document see N92-23416 14-61)
(Grants NAG5-916; NAG3-806)
Avail: NTIS HC/MF A07 CSCL 09B

A maximum aposteriori probability (MAP) approach to joint source/channel coder design is presented in this paper. This method attempts to explore a technique for designing joint source/channel codes, rather than ways of distributing bits between source coders and channel coders. For a nonideal source coder, MAP arguments are used to design a decoder which takes advantage of redundancy in the source coder output to perform error correction. Once the decoder is obtained, it is analyzed with the purpose of obtaining 'desirable properties' of the channel input sequence for improving overall system performance. Finally, an encoder design which incorporates these properties is proposed. H.A.

N92-23418*# Nebraska Univ., Lincoln.
A JOINT SOURCE/CHANNEL CODER DESIGN
Fuling Liu, Khalid Sayood, and Jerry D. Gibson (Stanford Univ., CA.) *In its* Design of Joint Source/Channel Coders 1991 6 p Presented at the 25th Asilomar Conference on Signals, Systems, and Computers Prepared in cooperation with Texas A&M Univ., College Station (For primary document see N92-23416 14-61)
(Grants NAG5-916; NAG3-806)
Avail: NTIS HC/MF A07 CSCL 09B

Source coders and channel coders are generally designed without reference to each other. This approach is justified by a famous result of Shannon's. However, there are many situations in practice in which the assumptions upon which this result is based are violated. Specifically, we examine the situation where there is residual redundancy at the source coder output. We have previously shown that this residual redundancy can be used to provide error correction using a viterbi decoder. In this paper, we present the second half of this design; the design of encoders for this situation. We show through simulation results that the proposed coders consistently outperform conventional source/channel coder pairs with gains of up to 12 dB at high probability of error. Author

N92-23419*# Nebraska Univ., Lincoln. Dept. of Electrical Engineering.
AN EDGE PRESERVING DIFFERENTIAL IMAGE CODING SCHEME
Martin C. Rost (Sandia National Labs., Albuquerque, NM.) and Khalid Sayood *In its* Design of Joint Source/Channel Coders 1991 8 p (For primary document see N92-23416 14-61)
(Grant NAG5-916)
Avail: NTIS HC/MF A07 CSCL 09B

Differential encoding techniques are fast and easy to implement. However, a major problem with the use of differential encoding for images is the rapid edge degradation encountered when using such systems. This makes differential encoding techniques of limited utility especially when coding medical or scientific images, where edge preservation is of utmost importance. We present a simple, easy to implement differential image coding system with excellent edge preservation properties. The coding system can be used over variable rate channels which makes it especially attractive for use in the packet network environment. Author

N92-23420*# Nebraska Univ., Lincoln. Dept. of Electrical Engineering.
A ROBUST LOW-RATE CODING SCHEME FOR PACKET VIDEO
Y. C. Chen, Khalid Sayood, D. J. Nelson, and E. Arikan, ed. *In its* Design of Joint Source/Channel Coders 1991 6 p (For primary document see N92-23416 14-61)
Avail: NTIS HC/MF A07 CSCL 09B

Due to the rapidly evolving field of image processing and networking, video information promises to be an important part of telecommunication systems. Although up to now video transmission has been transported mainly over circuit-switched networks, it is likely that packet-switched networks will dominate the

communication world in the near future. Asynchronous transfer mode (ATM) techniques in broadband-ISDN can provide a flexible, independent and high performance environment for video communication. For this paper, the network simulator was used only as a channel in this simulation. Mixture blocking coding with progressive transmission (MBCPT) has been investigated for use over packet networks and has been found to provide high compression rate with good visual performance, robustness to packet loss, tractable integration with network mechanics and simplicity in parallel implementation. H.A.

N92-23421*# Nebraska Univ., Lincoln.
A HYBRID LBG/LATTICE VECTOR QUANTIZER FOR HIGH QUALITY IMAGE CODING
V. Ramamoorthy (Technology Resources, Inc., Saint Louis, MO.), K. Sayood, and E. Arikan, ed. *In its* Design of Joint Source/Channel Coders 1991 1 p Repr. from Communication, Control, and Signal Processing, Elsevier Science Publishers B. V., 1990 (For primary document see N92-23416 14-61)
Avail: NTIS HC/MF A07 CSCL 09B

It is well known that a vector quantizer is an efficient coder offering a good trade-off between quantization distortion and bit rate. The performance of a vector quantizer asymptotically approaches the optimum bound with increasing dimensionality. A vector quantized image suffers from the following types of degradations: (1) edge regions in the coded image contain staircase effects, (2) quasi-constant or slowly varying regions suffer from contouring effects, and (3) textured regions lose details and suffer from granular noise. All three of these degradations are due to the finite size of the code book, the distortion measures used in the design, and due to the finite training procedure involved in the construction of the code book. In this paper, we present an adaptive technique which attempts to ameliorate the edge distortion and contouring effects. Author

N92-23422*# Nebraska Univ., Lincoln. Dept. of Electrical Engineering.
A ROBUST CODING SCHEME FOR PACKET VIDEO
Y. C. Chen, Khalid Sayood, and D. J. Nelson *In its* Design of Joint Source/Channel Coders 1991 30 p Submitted for publication (For primary document see N92-23416 14-61)
(Grant NAG5-916)
Avail: NTIS HC/MF A07 CSCL 09B

We present a layered packet video coding algorithm based on a progressive transmission scheme. The algorithm provides good compression and can handle significant packet loss with graceful degradation in the reconstruction sequence. Simulation results for various conditions are presented. Author

N92-23423*# Nebraska Univ., Lincoln. Dept. of Electrical Engineering.
A PROGRESSIVE DATA COMPRESSION SCHEME BASED UPON ADAPTIVE TRANSFORM CODING: MIXTURE BLOCK CODING OF NATURAL IMAGES
Martin C. Rost and Khalid Sayood *In its* Design of Joint Source/Channel Coders 1991 4 p (For primary document see N92-23416 14-61)
(Grant NAG5-916)
Avail: NTIS HC/MF A07 CSCL 09B

A method for efficiently coding natural images using a vector-quantized variable-blocksized transform source coder is presented. The method, mixture block coding (MBC), incorporates variable-rate coding by using a mixture of discrete cosine transform (DCT) source coders. Which coders are selected to code any given image region is made through a threshold driven distortion criterion. In this paper, MBC is used in two different applications. The base method is concerned with single-pass low-rate image data compression. The second is a natural extension of the base method which allows for low-rate progressive transmission (PT). Since the base method adapts easily to progressive coding, it offers the aesthetic advantage of progressive coding without incorporating extensive channel overhead. Image compression rates of approximately 0.5 bit/pel are demonstrated for both monochrome and color images. Author

N92-23432*# National Aeronautics and Space Administration. Marshall Space Flight Center, Huntsville, AL.
TECHNIQUE TO ELIMINATE COMPUTATIONAL INSTABILITY IN MULTIBODY SIMULATIONS EMPLOYING THE LAGRANGE MULTIPLIER
G. Watts Apr. 1992 30 p
(NASA-TP-3220; M-687; NAS 1.60:3220) Avail: NTIS HC/MF A03 CSCL 09B

A programming technique to eliminate computational instability in multibody simulations that use the Lagrange multiplier is presented. The computational instability occurs when the attached bodies drift apart and violate the constraints. The programming technique uses the constraint equation, instead of integration, to determine the coordinates that are not independent. Although the equations of motion are unchanged, a complete derivation of the incorporation of the Lagrange multiplier into the equation of motion for two bodies is presented. A listing of a digital computer program which uses the programming technique to eliminate computational instability is also presented. The computer program simulates a solid rocket booster and parachute connected by a frictionless swivel. Author

N92-23507# Technische Univ., Twente (Netherlands). Faculty of Applied Mathematics.
HIERARCHICAL SETS IN MATHEMATICAL PROGRAMMING MODELING LANGUAGES
J. J. Bisschop and C. A. C. Kuip Aug. 1991 24 p
(PB92-148683; Memo-990) Avail: NTIS HC/MF A03 CSCL 09B

The mathematical notation commonly applied for the formulation of mathematical programming models is extended to include hierarchical structures. The proposed notation is related to hierarchical set concepts in the languages UIMP, AMPL, and LPL. With the proposed notation, it is possible to aggregate and disaggregate over hierarchical structures. In addition, views are introduced to permit the use of hierarchical substructures and to create new hierarchies out of existing ones. The proposed notation for hierarchical sets and views is illustrated by applying it to the representation and estimation of social accounting matrices (SAMs). Author

N92-23554*# Research Inst. for Computing and Information Systems, Houston, TX.
FRAMEWORK PROGRAMMABLE PLATFORM FOR THE ADVANCED SOFTWARE DEVELOPMENT WORKSTATION: FRAMEWORK PROCESSOR DESIGN DOCUMENT
Richard J. Mayer, Thomas M. Blinn, Paula S. D. Mayer, Keith A. Ackley, Wes Crump, and Les Sanders (Knowledge Based Systems, Inc. College Station, TX.) 20 Sep. 1991 84 p
(Contract NCC9-16; RICIS Proj. SE-37)
(NASA-CR-190173; NAS 1.26:190173) Avail: NTIS HC/MF A05 CSCL 09B

The design of the Framework Processor (FP) component of the Framework Programmable Software Development Platform (FFP) is described. The FFP is a project aimed at combining effective tool and data integration mechanisms with a model of the software development process in an intelligent integrated software development environment. Guided by the model, this Framework Processor will take advantage of an integrated operating environment to provide automated support for the management and control of the software development process so that costly mistakes during the development phase can be eliminated. Author

N92-23851# CASA-RI/SME, Tel Aviv (Israel).
PROCEEDINGS OF THE INTERNATIONAL CONFERENCE ON CAD/CAM AND AMT. VOLUME 1: GENERAL SESSIONS
14 Dec. 1989 215 p Conference held in Jerusalem, Israel, 11-14 Dec. 1989 Sponsored by Israel Ministry of Defense, Israel Ministry of Science and Technology, Rafael, and Daisy/Cadnetix

(DASIX) Prepared in cooperation with the Israel Society for CAD/CAM, Tel Aviv
(ITN-92-85127) Avail: NTIS HC/MF A10

This is the first of four volumes of papers presented at the conference on CAD/CAM (computer aided design/computer aided manufacturing). The included papers cover design automation, testing, very large scale integration, design and production line planning. For individual titles, see N92-23852 through N92-23889.

N92-23852# Virginia Univ., Charlottesville. School of Engineering and Applied Science.
THE NEED FOR STANDARDS IN DESIGN AUTOMATION
Ronald Waxman *In* CASA RI/SME, Proceedings of the International Conference on CAD/CAM and AMT. Volume 1: General Sessions 14 Dec. 1989 4 p (For primary document see N92-23851 14-61)
(P-1-1) Avail: NTIS HC/MF A10

Creating and maintaining complex electronic systems are dependent on the ability to communicate design details between disciplines and to integrate various data types. The VHSIC Hardware Description Language (VHDL) and the Electronic Design Interchange Format (EDIF) are two standards that may help to streamline the process. A conceptual schema for shared product data may be used to relate the electrical design environment to the mechanical design and fabrication environment. This paper explores the potential effect of design automation standards on the design process and product transition from design to production. ISA

N92-23853# Israel Aircraft Industries Ltd., Ben-Gurion Airport.
FORMAL METHODS FOR THE EVALUATION OF CORPORATE CAD/CAM UTILIZATION
Lawrence Odess, Janet Seltzer, and Avigdor Laserson *In* CASA RI/SME, Proceedings of the International Conference on CAD/CAM and AMT. Volume 1: General Sessions 14 Dec. 1989 7 p (For primary document see N92-23851 14-61)
(Rept-1.1.1) Avail: NTIS HC/MF A10

There is a clear need for methods to evaluate the utilization of CAD/CAM (computer aided design/computer aided manufacturing) tools in the user's environment, to identify problems, and to guide future corporate decisions. This need is described here, together with two formal methods of evaluation which were recently developed. In the first method (the statistical method) quantitative data on the utilization of CAD/CAM are gathered from the users on the basis of disciplines, sub-disciplines, and user facilities. These data are then analyzed, in order to obtain normalized measures of utilization, which permit comparison among the various facilities, and comparison with typical utilization throughout industry. These normalized data are presented in a form that permits easy identification of abnormal or suspect data, as well as indicating averages and trends. In order to complement the statistical results and to overcome limitations of the statistical method, a second method (the empirical method) was also developed. The data acquired by this method can be analyzed by simulation, so as to obtain total costs (or total cycle times) and their sensitivities to individual operations, which in turn aids in defining investment priorities. ISA

N92-23854# Politecnico di Milano (Italy). Dept. of Electronics.
FAPES: AN EXPERT SYSTEM FOR DESIGNING AND OPTIMISING FAULT-TOLERANT ARITHMETIC ARRAY PROCESSORS
Vicenzo Piuri *In* CASA RI/SME, Proceedings of the International Conference on CAD/CAM and AMT. Volume 1: General Sessions 14 Dec. 1989 7 p (For primary document see N92-23851 14-61)
(Rept-1.1.2) Avail: NTIS HC/MF A10

Design of efficient array processors with fault-tolerant capabilities is a complex task, which involves an accurate optimization to produce effective, low-cost architectures. This paper presents the expert system FAPES; it is a computer aided design (CAD) tool which incorporates the knowledge and the skill of an expert designer to choose automatically the optimum design methodology for a fault-tolerant architecture. At the moment, FAPES considers array processors dedicated to arithmetic applications. Different techniques and structures are considered and evaluated by the expert system to introduce the degree of fault tolerance defined by the user, i.e., error detection, error correction, fault localization and reconfiguration. ISA

N92-23855# State Univ. of New York, Stony Brook. Dept. of Computer Science.
VOXEL-BASED SOLID MODELING
Arie Kaufman *In* CASA RI/SME, Proceedings of the International Conference on CAD/CAM and AMT. Volume 1: General Sessions 14 Dec. 1989 3 p (For primary document see N92-23851 14-61)
(Grants NSF DCR-86-03603; NSF MIP-88-05130)
(Rept-1.1.3) Avail: NTIS HC/MF A10

Representation of 3-dimensional volumetric objects can be achieved by sampling and discretizing an intrinsically continuous scene and storing it in a cubic frame buffer of numerically coded volume elements or voxels. Current applications of voxel representation include computer tomography, magnetic resonance imaging, seismic measurements and positron emission tomography. Potential applications include computer aided design (CAD), flight simulation, astrophysics and fluid flow. The system described here enables the computerized model to be overlaid with or compared with experimental data. A nomenclature and theory of 3-dimensional discrete topology have been developed which enable synthetic objects to be classified according to their connectivity, lack of tunnels and lack of cavities. Three-dimensional scan-conversion algorithms are described, which convert a continuous representation of a geometric object into a set of voxels in the discrete voxel-image space that best models the original object. The 3-dimensional scan algorithm was implemented on Sun 4, Silicon Graphics Iris 4D and HP 370 Turbo SRX workstations, as part of the Cube system, which is a general-purpose, voxel-based system. A volume editor was developed for generating, manipulating and viewing sampled and/or synthetic volumetric objects; it facilitates image reconstruction, density segmentation, arbitrary slicing, translucency control, measurements, discrete projection and discrete shading. ISA

N92-23856# Israel Aircraft Industries Ltd., Yehud. Artificial Intelligence Lab.
MBT-WIRE: INTELLIGENT CAD IN WIRING DESIGN
Yakov Grinbaum, Ester Podolak, Tal Raz, and Amiel Turnheim *In* CASA RI/SME, Proceedings of the International Conference on CAD/CAM and AMT. Volume 1: General Sessions 14 Dec. 1989 5 p (For primary document see N92-23851 14-61)
(Rept-1.1.4) Avail: NTIS HC/MF A10

An advanced editor is presented, which enables wiring diagrams for wiring harnesses to be produced automatically from the wiring lists. The editor is based on intelligent CAD (computer aided design) software, which includes data on electronic circuit elements, and which can perform simulations and testing. Among the information items included in the wiring lists are the individual wire specifications and connection points, wire grouping specifications, and details of other relevant components. The basic editor is mouse-driven; it includes standard editing features, and graphic elements for standard wiring symbols. The assembly is drawn on the screen and, simultaneously, FORTRAN-like code is generated, to be run on a remote VAX computer with graphic output to a remote Versatex plotter. Diagrams which the output can generate include plug diagrams of the units interconnected by the harness; signal-flow diagrams, which illustrate the flow of signals among the various plugs of the harness; and a functional diagram, still under development, which will display the signal flow among the elements of the system, through the wiring harnesses connecting them. Intelligent features to be added to the editor, based on users' concepts and expert knowledge, include error checking; a macro-facility for compound instructions, which will provide automatic data insertion; and automatic length and gauge calculations. ISA

N92-23857# Ohri (Edith), Tel Aviv (Israel).
GROUP TECHNOLOGY, RCO: ROUGH-CUT OPTIMIZER. THE KEY TO INTEGRATION OF PLANT OPERATIONS c81
Edith Ohri *In* CASA RI/SME, Proceedings of the International Conference on CAD/CAM and AMT. Volume 1: General Sessions 14 Dec. 1989 3 p (For primary document see N92-23851 14-61)
(Rept-1.1.6) Avail: NTIS HC/MF A10

The RCO (Rough-Cut Optimizer) provides a system for integrating the operations of an industrial plant which comprises a number of specialized departments, which supply varied products or services to varied and changing outlets. The RCO develops a nested structure to accommodate different groups of items, classified according to their intrinsic qualities and to their use throughout the manufacturing process. The system crosses interdepartmental boundaries. It aids decision making, based on minimal information, and allows each level of management to make its decisions without overlapping other levels. It can tolerate some inaccuracy in item description and is sufficiently simple to enable integration to be handled by human rather than computer intelligence. RCO was shown to have advantages over established production control methods, e.g., the decision tree and statistical correlation. RCO enables non-productive elements to be eliminated from the lead-time for various input items, in setting delivery dates. It gathers orders of different sizes into groups, enabling the fluctuations in required capacity to be smoothed statistically. By grouping products according to shared processing requirements, RCO enables work cells to be established, which comprise groups of machines involved in compatible operations. Overall, RCO enables production rates in the various departments to be matched. ISA

N92-23858# Rafael Armament Development Authority, Haifa (Israel).
DYNAMIC AGGREGATE MODELS FOR GROUP TECHNOLOGY MANUFACTURING ENVIRONMENT
Michael Mizrach *In* CASA RI/SME, Proceedings of the International Conference on CAD/CAM and AMT. Volume 1: General Sessions 14 Dec. 1989 3 p (For primary document see N92-23851 14-61)
(Rept-1.1.7) Avail: NTIS HC/MF A10

Good production schedules attempt to achieve high utilization rates of scarce and expensive facilities. It is easier to fulfil this goal in the stable production line than in the volatile job shop. Among other benefits of Group Technology, is that it serves as a way to smooth production planning in job-shop-like environments, by permanent allocation of resources to groups of products. (Resources are usually arranged in 'production cells'). However, it is possible to utilize resources more efficiently and still keep the scheduling manageable, by allocating resources to groups of products dynamically. By grouping similar products, the size of long-term scheduling problems can be reduced substantially; otherwise, they could have been too large for optimization. The focus of our discussion will be on models which produce optimal, capacity-constrained production schedules, in which activities of the same groups of products will be aggregated. This approach can be used for various problems, including the 'minimal span of production' (given capacity), or 'resource smoothing' (given delivery schedule). ISA

N92-23859# Center for Technology, Holon (Israel).
CREATIVE SEARCH SYSTEMS AS SPECIFIC EXPERT SYSTEMS
V. Bachmutsky and A. Shenkman *In* CASA RI/SME, Proceedings of the International Conference on CAD/CAM and AMT. Volume 1: General Sessions 14 Dec. 1989 2 p (For primary document see N92-23851 14-61)
(Rept-1.1.8) Avail: NTIS HC/MF A10

Different aspects of Creative Search Systems (CSS) as specific expert systems, including terms coordination in expert systems and problem solving fields, are discussed. The importance of intersubject approach and generalization on the problem definition and solving stages is shown. The full CSS, and its subsystem and module structures are defined and illustrated. The main features of CSS are described. They include separate presentation of data and operation bases; the separate presentation of intersubject-oriented operation and result estimation modules; the hierarchical presentation of TS (Technical Solutions) structures and, correspondingly, the hierarchical presentation of data and operations; and the inclusion of new blocks and modules for data handling. ISA

N92-23860# Instituto Superior Tecnico, Lisbon (Portugal).
FAST SIMULATION OF MOS DIGITAL NETWORKS USING A PHYSICAL MACROMODELLING APPROACH
I. M. C. Teixeira, J. P. C. Teixeira, and H. C. Neto *In* CASA RI/SME, Proceedings of the International Conference on CAD/CAM and AMT. Volume 1: General Sessions 14 Dec. 1989 5 p Sponsored by Commission of the European Communities (For primary document see N92-23851 14-61)
(Rept-1.2.1) Avail: NTIS HC/MF A10

Fast, yet accurate simulation of MOS (metal oxide semiconductor) digital networks is a must in the design activity. In this paper, a physical macromodelling procedure, used in the development of electric and logic macromodels, is presented. The resulting macromodels are implemented in the multi-level simulator CINNAMON, as resident models, and are used in the evaluation of complex networks composed of series or parallels of MOS transistors. The results obtained, even when logic models are used, show that the overall circuit behavior is well captured and that significant gains in computer resources can be achieved with this approach. ISA

N92-23861# Southampton Univ. (England). Dept. of Electronics and Computer Science.
DESIGN FOR TESTABILITY: WHERE ARE THE GOALPOSTS?
B. R. Wilkins and C. Shi *In* CASA RI/SME, Proceedings of the International Conference on CAD/CAM and AMT. Volume 1: General Sessions 14 Dec. 1989 6 p (For primary document see N92-23851 14-61)
(Rept-1.2.2) Avail: NTIS HC/MF A10

The paper discusses the need for providing circuit designers with an assessment tool that can give guidance about testability at the earliest stages of the design process. The implications of this requirement are discussed in detail, and a framework for testability measurement is set out. The need to incorporate an assessment of the effects of using particular DFT (design for testability) techniques is also discussed, leading on to a description of early experiments, based on analysis of standard benchmark circuits, aimed at establishing statistical relationships between test costs and externally observable circuit parameters. ISA

N92-23862# IMS/Valid International, Slough (England).
AN INTEGRATED TEST SOLUTION TO ADDRESS SCAN TECHNIQUES
Nigel Crawley *In* CASA RI/SME, Proceedings of the International Conference on CAD/CAM and AMT. Volume 1: General Sessions 14 Dec. 1989 4 p (For primary document see N92-23851 14-61)
(Rept-1.2.3) Avail: NTIS HC/MF A10

There is currently a move by the IC (integrated circuit) vendors and semiconductor houses towards using scan design methods. Certainly there is becoming a greater awareness towards the use of Boundary Scan Techniques since the emergence of JTAG (Joint Testing Action Group), and the current IEEE P1149.1 Proposal to standardize Boundary Scan. This new awareness has resulted in multiple techniques for embedded scan at the component level. Consequently there is now a need for a flexible test solution which can be applied to general scan design verification. The paper discusses an integrated scan test approach to verify and test compact and board designs that incorporate scan methodology. The key to this method is a user friendly interface to control hardware features while maintaining the flexibility to offer a general solution. ISA

N92-23863# SIFU-Elektronik, Stockholm (Sweden).
AN EXHAUSTIVE SELF-TEST DESIGN METHODOLOGY FOR SYNCHRONOUS STATE MACHINES
Peter S. H. Wahlfridsson *In* CASA RI/SME, Proceedings of the International Conference on CAD/CAM and AMT. Volume 1: General Sessions 14 Dec. 1989 5 p (For primary document see N92-23851 14-61)
(Rept-1.2.4) Avail: NTIS HC/MF A10

The problem of how to know if produced samples of digital circuits are working functionally correctly or not, with a minimum waste of time, may be solved through a number of design considerations. These are usually referred to as Design for Test Methods. This paper will show and prove a different methodology that can be applied to synchronous finite state machines which, with a minimum of logic overhead and design effort, may be controlled and observed in a way that makes an exhaustive self-test possible. The test may be used for a GO/NO-GO decision or, if the objective is to raise production yield for a design, to point out from where the fault may stem. ISA

N92-23864# Siemens A.G., Munich (Germany, F.R.). Corporate Labs for Information Technology.
USING RANGE ANALYSIS TO SUPPORT HIERARCHICAL TEST PATTERN GENERATION
H. Hofestaedt and M. Vogt *In* CASA RI/SME, Proceedings of the International Conference on CAD/CAM and AMT. Volume 1: General Sessions 14 Dec. 1989 6 p (For primary document see N92-23851 14-61)
(Rept-1.2.5) Avail: NTIS HC/MF A10

Range analysis is a method of exploiting the designer's expertise in design hierarchy. Essentially, each subcircuit can be regarded as being isolated from its circuit environment during test pattern generation. Thus, smaller solution spaces have to be searched. The efficiency of this approach is demonstrated for combinatorial circuits using range analysis together with the FAN-algorithm. ISA

N92-23865# Instituto Superior Tecnico, Lisbon (Portugal).
TEST PREPARATION FOR MOS DIGITAL CIRCUITS USING HEURISTICS FOR RELIABLE FAULT SIMULATION
J. P. C. Teixeira, I. M. C. Teixeira, C. F. B. Almeida, A. Oliveira, and F. Goncalves *In* CASA RI/SME, Proceedings of the International Conference on CAD/CAM and AMT. Volume 1: General Sessions 14 Dec. 1989 6 p (For primary document see N92-23851 14-61)
(Rept-1.2.6) Avail: NTIS HC/MF A10

The production of complex digital VLSI (very large scale integration) circuits requires a reliable and cost-effective testing procedure, allowing the release of chips with a very low defect level. For MOS (metal oxide semiconductor) VLSI circuits, test preparation, which has to be carried out by the IC (integrated circuit) designer, needs to take into account, with reasonable computer costs, the possible occurrence of faults which are not detected by test patterns derived for stuck-at-fault detection. In this paper, a bottom-up test preparation methodology is reviewed, together with the set of software tools that implement it, which allows the generation of switch-level realistic fault lists, fault analysis and accurate test pattern validation, and paves the way to testability enhancements, at layout level, by LLDFT (Layout-Level Design for Testability) techniques. Simulation results are presented, ascertaining the features of the software package and its applications. The possibility of increasing the accuracy and reliability of switch-level fault coverage statistics, by using heuristics that introduce circuit knowledge in fault simulation, is demonstrated. ISA

N92-23866# Politecnico di Torino (Italy). Dept. of Automation and Information.
EXACT PROBABILISTIC TESTABILITY MEASURES FOR MULTI-OUTPUT CIRCUITS
P. Camurati, P. Prinetto, and M. SonzaReorda *In* CASA RI/SME, Proceedings of the International Conference on CAD/CAM and AMT. Volume 1: General Sessions 14 Dec. 1989 6 p (For primary document see N92-23851 14-61)
(Rept-1.2.7) Avail: NTIS HC/MF A10

The computation of probabilistic Testability Measures is increasingly important and some methods have been proposed to cope with this need, although the exact solution of the problem has been shown to be np-hard. Referring to an analytical method presented by S.C. Seth, B.B. Bhattacharya and V.D. Agrawal, this paper presents its formulation and its extension to multi-output combinational circuits. ISA

N92-23867# Philips Telecommunication Industries, Hilversum (Netherlands).
CHANGE IN TEST-TECHNOLOGY
H. Bleeker *In* CASA RI/SME, Proceedings of the International Conference on CAD/CAM and AMT. Volume 1: General Sessions 14 Dec. 1989 4 p (For primary document see N92-23851 14-61)
(Rept-1.2.8) Avail: NTIS HC/MF A10

The price/performance ratio of today's electronic products is continuously eroding. The process of improving this ratio is driven by enhancements within a particular technology or often by changing the technology used to realize the products. The test technology has to cope with these processes. Timely reaction by both technical and managerial resources is required. The JTAG (Joint Test Action Group) industry-wide standardization on test methodology has evolved as a result of such an awareness. In this paper the historical background and a short technical introduction to JTAG are presented. ISA

N92-23868# Carnegie-Mellon Univ., Pittsburgh, PA.
A FRAMEWORK FOR THE SUPPORT OF VLSI (VERY LARGE SCALE INTEGRATION) DESIGN FOR MANUFACTURE
Stephen W. Director and Jim Daniell *In* CASA RI/SME, Proceedings of the International Conference on CAD/CAM and AMT. Volume 1: General Sessions 14 Dec. 1989 4 p Sponsored by NSF and Semiconductor Research Corp. (For primary document see N92-23851 14-61)
(Rept-1.3.1) Avail: NTIS HC/MF A10

Previous attempts at the creation of a design framework have led us to re-examine the way we approach the central issue of CAD (Computer Aided Design) tool control. Towards this end, we have developed a general mechanism for decentralized control based on an object oriented view of CAD tools. This approach has been implemented in the Cadweld design framework. The Cadweld framework includes an interactive user interface, interprocessor communication, intelligent CAD tool argument modeling, an object editor and a backtracking system. Use of CAD tool objects means that the designer need not deal with the minute details associated with CAD tool execution, in addition to the CAD tasks. By organizing the CAD tools to work with a more powerful design representation and allowing them to be automatically executed when necessary, the designer is freed from the more tedious aspects of design. ISA

N92-23869# IBM Israel Scientific Center, Haifa.
ON GENERATING TWO DIMENSIONAL CMOS CELLS
Jack A. Feldman and Israel Koren (Massachusetts Univ., Amherst.) *In* CASA RI/SME, Proceedings of the International Conference on CAD/CAM and AMT. Volume 1: General Sessions 14 Dec. 1989 10 p (For primary document see N92-23851 14-61)
(Rept-1.3.2) Avail: NTIS HC/MF A10

Most standard cell generators for CMOS (complementary metal oxide semiconductor) circuits follow the single-row (of transistor pairs) layout style. Multi-row layouts are then obtained by placing and interconnecting basic cells which were generated in the single-row style. In this paper we present an algorithm for generating two-dimensional layouts. The number of rows (of transistor pairs) can be imposed by the user. This aspect ratio is selected so as to either minimize the total cell area or meet some height or width requirements. We illustrate our algorithm through a set of examples, ranging from simple CMOS circuits to

complex ones. We then compare the generated multi-row layouts to single-row layouts of the same circuits. This comparison demonstrates the advantage of the two-dimensional style over the single-row style, especially for more complex CMOS circuits.
ISA

N92-23870# IBM Israel Scientific Center, Haifa.
BREATHING MAZE ROUTER FOR ANALOG VLSI CELL GENERATION
Esther Solel and Shmuel Wimmer *In* CASA RI/SME, Proceedings of the International Conference on CAD/CAM and AMT. Volume 1: General Sessions 14 Dec. 1989 7 p (For primary document see N92-23851 14-61)
(Rept-1.3.3) Avail: NTIS HC/MF A10

An improvement of the maze routing algorithm which was developed as a part of a generator to design analog VLSI (very large scale integration) CMOS (complementary metal oxide semiconductor) cells is presented. The inability of the Lee algorithm to guarantee completion and the quality of the routing, which degrades as more and more nets are being routed, have been studied in many papers. Although an impressive improvement of the original Lee algorithm has been achieved, and many layout systems employ maze routers successfully, there are inherent problems that cannot be resolved by any of the methods proposed so far. We present an algorithm that overcomes the above problems by maintaining enough room all over the maze matrix throughout the routing procedure, thus, allowing the wires to take short routes, without frequent obstacle avoidance and layer changes. This in turn reduces the number of contacts, which is an important factor in VLSI cell generation. The virtual area which is introduced during the routing procedure is eliminated later in a compaction phase, which is afforded in the environment of analog VLSI cell generation. Although it was developed for VLSI technology, the breathing algorithm is applicable to PCB (printed circuit board) layouts, where the location of the elements is not stiff and they can move apart.
ISA

N92-23871# Carnegie-Mellon Univ., Pittsburgh, PA. Dept. of Electrical and Computer Engineering.
STATISTICAL PROCESS CONTROL SYSTEM FOR VLSI FABRICATION Abstract only
Andrzej J. Strojwas *In* CASA RI/SME, Proceedings of the International Conference on CAD/CAM and AMT. Volume 1: General Sessions 14 Dec. 1989 1 p (For primary document see N92-23851 14-61)
(Rept-1.3.4) Avail: NTIS HC/MF A10

The CMU-CAM system for statistical process control of VLSI (very large scale integration) manufacturing is described. It is a software system which can perform statistical quality control and feed-forward control rescheduling on line, and process diagnosis off line. In predicting the yield of a batch of wafers, as a basis for deciding to reject or rework them after a certain processing step, the CMU-CAM system takes account of multivariate distributions of in-lines. Precise algorithms, that evaluate probabilistic distance measures, are employed. If the process can be brought back to its desired trajectory by manipulating controls of the subsequent process steps, the feed-forward procedures are invoked. The CMU-CAM system also contains a diagnostic module based on statistical pattern recognition algorithms. This allows for identification of reasons for yield drop, and so, prevents the subsequent wafers or entire batches from being affected by these effects. If, however, significant yield problems are encountered, it may be necessary to reschedule the batches to meet the demand for the IC's (integrated circuits) in production. A re-scheduler is then employed to change the sequence of batches to maximize the profit from the fabrication line. All of these software modules are integrated and have been applied to a number of industrial examples. Some of these practical applications are demonstrated.
ISA

N92-23872# Technion - Israel Inst. of Tech., Haifa. Dept. of Electrical Engineering.
STATISTICAL OPTIMIZATION OF INTEGRATED CIRCUITS IN ORDER TO REDUCE THE SENSITIVITY TO VARIATIONS IN PROCESS PARAMETERS AND ENVIRONMENTAL CONDITIONS
E. Maayan and D. Lubzens *In* CASA RI/SME, Proceedings of the International Conference on CAD/CAM and AMT. Volume 1: General Sessions 14 Dec. 1989 4 p (For primary document see N92-23851 14-61)
(Rept-1.3.6) Avail: NTIS HC/MF A10

A method for the analysis of an integrated circuit design is presented. This method derives simple models of the integrated circuit performance using experimental design and regression analysis. These models allow the designer to analyze the circuit performance and its sensitivity to variations in process parameters and environmental conditions. Using these models, the cost of the design and optimization stages is reduced.
ISA

N92-23873# National Semiconductor (IC) Ltd., Herzliya (Israel).
FUNCTIONAL DESIGN VERIFICATION OF ULSI COMPONENTS
Coby Hanoch *In* CASA RI/SME, Proceedings of the International Conference on CAD/CAM and AMT. Volume 1: General Sessions 14 Dec. 1989 5 p (For primary document see N92-23851 14-61)
(Rept-1.3.7) Avail: NTIS HC/MF A10

An overview of the currently used FDV (Functional Design Verification) methods is presented, with a focus on their applicability to ULSI (ultra large scale integration) component design. An emphasis is placed on a new method, CAFTG (Controllable Automatic Functional Test Generation), which was conceived as an answer to the weaknesses of the older tools in the ULSI FDV. CAFTG is presented along with a tool, FTG (Functional Test Generator), which implements it.
ISA

N92-23874# Aristotle Univ. of Thessaloniki (Greece). Lab. for Machine Tool and Machine Dynamic.
OPTIMUM CUTTING CONDITIONS DETERMINATION FOR THE NC-MILLING **c63**
K.-D. Bouzakis, K. Efstathiou, and R. Paraskevopoulou *In* CASA RI/SME, Proceedings of the International Conference on CAD/CAM and AMT. Volume 1: General Sessions 14 Dec. 1989 6 p (For primary document see N92-23851 14-61)
(Rept-2.1.2) Avail: NTIS HC/MF A10

A procedure to optimize the feedrate and the cutting tool speed in numerically controlled milling is introduced. The corresponding optimization algorithms are conducted in all successive tool path regions, which are defined considering the actual workpiece contour and the tool kinematics. On the basis of developed computer programs to describe the penetrations between tool and workpiece, significant process parameters, such as the cutting force and the tool wear, may be defined. With their help, using as criteria the maximum machine power, machine control limitations, the manufacturing cost or time, etc., optimum values for the feedrate and for the cutting speed for each of the introduced tool path regions are calculated. The developed method is demonstrated for a particular example of rough and finished milling of a workpiece.
ISA

N92-23875# Ohri (Edith), Tel Aviv (Israel).
CONTROLLING OPERATIONS THROUGH PROCEDURES: APE (AUTOMATED PROCEDURE EDITOR) **c63**
Edith Ohri *In* CASA RI/SME, Proceedings of the International Conference on CAD/CAM and AMT. Volume 1: General Sessions 14 Dec. 1989 2 p (For primary document see N92-23851 14-61)
(Rept-2.2.1) Avail: NTIS HC/MF A10

The APE (Automated Procedure Editor) aims to incorporate workshop manual material into the computerized machine control system, to provide automatic on-the-job guidance, when needed. The system also automatically updates the documentation and analyzes textual changes. Use of APE should improve: (1) procedures through modularization; (2) management and control

of changes, through automatic record keeping; (3) efficiency by helping systems analysts to identify all procedures affected by a given change; and (4) management and maintenance of procedures. Implementation of APE requires: definition of relevant parameters; characterization of every new procedure; checking and, if necessary, adjusting of each of the procedures involved; and recording and printing out all the changes. ISA

N92-23876# Israel Aircraft Industries Ltd., Lod.
SHOP FLOOR SCHEDULING THROUGH A SIMULATION BASED SCHEDULER **c81**
Z. Feuer and E. M. Dar-El *In* CASA RI/SME, Proceedings of the International Conference on CAD/CAM and AMT. Volume 1: General Sessions 14 Dec. 1989 8 p (For primary document see N92-23851 14-61)
(Rept-2.3.3) Avail: NTIS HC/MF A10

The problem of finite capacity, short-term scheduling concerns the lowest level of scheduling practiced in a factory. A simulation-based scheduler, which was developed to assist a shop foreman in planning operation sequences, was proven successful. Higher levels of scheduling, to which the simulation technique might be adapted, are aggregate production planning, which involves overall planning of all aspects of a company's operations and is usually performed through linear programming, and master production scheduling, which establishes production delivery schedules according to anticipated demands. A case study involved the application of the new scheduler to Israel Aircraft Industries' (IAI) new numerically controlled machine shop, where six 5-axis, 3-head SNK profilers are used for normal production, while a 7th machine is used only for numerical control file prove-out. Production costs for some 200 different parts are estimated at $150-200 per hour. Application of the scheduler improved machine utilization from 45 to 71 percent, reduced the time to complete a one-month production order by 27.45 percent, and reduced lead times by 33 percent. Planned future developments of the scheduler include improvement of its interfaces with humans and with systems, and the development of a set of software tools to enable it to be rapidly adapted to a variety of manufacturing processes. ISA

N92-23877# Rochester Univ., NY. Graduate School of Business Administration.
ADVANCES IN PROCESSING RATES OPTIMIZATION FOR FLEXIBLE MANUFACTURING SYSTEMS **c63**
Abraham Seidmann and Paul J. Schweitzer *In* CASA RI/SME, Proceedings of the International Conference on CAD/CAM and AMT. Volume 1: General Sessions 14 Dec. 1989 4 p Sponsored in part by IBM (For primary document see N92-23851 14-61)
(Rept-2.3.4) Avail: NTIS HC/MF A10

A performance optimization methodology is given to optimize processing rates (tool speeds, tool feed rates, and tool choices) in FMS (flexible manufacturing systems). Our goal is to minimize the variable production costs subject to constraints on throughput, WIP (pallets), parts routes, transporter delays, and information on tool lives as functions of tool speeds. Case studies indicate that considerable cost savings (factor of 2-3 reduction in tool costs) are possible in metal cutting operations, with significant impact on production planning practice in a CIM (computer integrated manufacturing) environment. ISA

N92-23878# Tel-Aviv Univ. (Israel).
FLEXIBLE DESIGN ENVIRONMENT (FDE) FOR OPERATION SYSTEMS DESIGN
Ron Gur *In* CASA RI/SME, Proceedings of the International Conference on CAD/CAM and AMT. Volume 1: General Sessions 14 Dec. 1989 6 p (For primary document see N92-23851 14-61)
(Rept-2.3.5) Avail: NTIS HC/MF A10

Computerized design and engineering tools are well established for the engineering and design of products via CAE/CAD/CAM (Computer Aided Engineering/Computer Aided Design/Computer Aided Manufacturing) technologies. The great advances in computer technologies, especially high-speed CPU (Central Processing Unit) microcomputers, high-resolution color graphics, and new approaches in AI (Artificial Intelligence) ES (Expert Systems) and simulation languages, are making it feasible to construct a normative framework that integrates all these tools into a flexible environment for the design and effective management of operational systems. The state-of-the-art is that all the components needed are at hand, but are without a frame to integrate them into a comprehensive design environment. This would allow for the amplification of design capabilities. It would support better communication among design team members along the various stages of an operational system life cycle. The various components available to construct a normative framework for their integration into an FDE (Flexible Design Environment) are reviewed. ISA

N92-23879# TADIRAN Israel Electronics Industries Ltd., Givat-Shmuel.
WRITING A SIMULATION OF A COMMUNICATIONS NETWORK USING SIMSCRIPT/DISS
Mitchell Snyder and Smadar Lipetz *In* CASA RI/SME, Proceedings of the International Conference on CAD/CAM and AMT. Volume 1: General Sessions 14 Dec. 1989 3 p (For primary document see N92-23851 14-61)
(Rept-2.3.6) Avail: NTIS HC/MF A10

In designing telecommunications equipment, system simulations are used to fix specifications. An event-driven approach is used for these simulations, rather than the classical object-driven approach. The SIMSCRIPT language used for the simulations includes commands for both event-driven and object-driven programming; it is used in conjunction with its DISS (Distributed System Simulation) macro extension. In object-driven programming, all queues (buffers) are automatically managed by the language, which also schedules all events, e.g., wait, work, and delay. For the current application, these advantages are outweighed by the advantages of event-driven programming: the engineers, for whom the system is being designed, think in terms of computer behavior and not message behavior; and the real-time code to be written for the product being simulated will be event-driven. ISA

N92-23880# Israel Aircraft Industries Ltd., Ben-Gurion Airport.
COMBINING A CAD/CAM SYSTEM WITH AN ADVANCED DATABASE ARCHITECTURE
Stewart A. Bresler *In* CASA RI/SME, Proceedings of the International Conference on CAD/CAM and AMT. Volume 1: General Sessions 14 Dec. 1989 8 p (For primary document see N92-23851 14-61)
(Rept-3.1.5) Avail: NTIS HC/MF A10

Previous generations of CAD/CAM (Computer Aided Design/Computer Aided Manufacturing) systems relied on the 2-D (2-dimensional) drawing as a master description of a designed part. This configuration presented the user and the CAD/CAM system designer with serious bottlenecks in passing from 2-D design to 3-D (3-dimensional) analysis and manufacturing. As a result, CAD/CAM systems are now storing the master design in its 3-D form (as wireframe, surface, or solid) and the remaining portions of the design process are derived from it. Although this has removed bottlenecks associated with analysis and manufacturing, it has created an information management problem for controlling, integrating and maintaining the massive amount of information which can be directly attached to the 3-D master design. Previous generation CAD/CAM databases were ill-equipped to tackle this problem. To fulfill this need, next generation systems are now incorporating the architecture of associative and relational style databases into CAD/CAM databases to effectively manage the mass of information which is linked to and dependent on the 3-D master design. UNICORN is a CAD/CAM system which is based on 3-D master designs and uses an advanced database architecture. ISA

N92-23881# Israel Aircraft Industries Ltd., Ben-Gurion Airport.
FROM IGES TO STEP
Jean-Pierre Stroweis *In* CASA RI/SME, Proceedings of the International Conference on CAD/CAM and AMT. Volume 1:

General Sessions 14 Dec. 1989 6 p (For primary document see N92-23851 14-61)
(Rept-3.1.6) Avail: NTIS HC/MF A10

This paper describes some of the new concepts of the STEP (Standard for Exchange of Product Model Data), an ongoing international effort to define a high-level neutral data interface between different CAD/CAM systems. The evolution of computer-generated data transfer is placed into the CAD/CAM historical perspective. STEP notions on geometry, presentation, topology, form features, and tolerances are presented. Comparison with the IGES (Initial Graphics Exchange Specification) is drawn. ISA

N92-23882# Israel Military Industries, Ramat-Hasharon (Israel).
IGES: APPLICATION GENERATOR IN DISGUISE
Yoram Retter *In* CASA RI/SME, Proceedings of the International Conference on CAD/CAM and AMT. Volume 1: General Sessions 14 Dec. 1989 3 p (For primary document see N92-23851 14-61)
(Rept-3.1.7) Avail: NTIS HC/MF A10

An attempt to transfer product definition data with the IGES (Initial Graphics Exchange Specification) may not be an instant success. More commonly, such an attempt will result in partial data transfer. Examination of the translators used by sending and receiving CAD/CAM systems and of the IGES file may show that the problem is in the wide scope of IGES. A given datum may be translated using more than one valid IGES format, resulting in loss of information during translation. A manual attempt to correct an IGES file while in transfer is not practical for non-trivial cases, owing to the complexity of the file structure. A group of FORTRAN subroutines was written for this purpose. Making the subroutines general solved the problem of correcting IGES files in transfer with the additional benefit of creating an effective 'IGES Application Generator' for a CAD/CAM environment. ISA

N92-23883# Waterloo Univ. (Ontario). Centre for Integrated Manufacturing.
COMPUTER INTEGRATED ENTERPRISE: THE NEXT STEP IN CIM EVOLUTION
David M. Dilts *In* CASA RI/SME, Proceedings of the International Conference on CAD/CAM and AMT. Volume 1: General Sessions 14 Dec. 1989 4 p (For primary document see N92-23851 14-61)
(Rept-3.2.2) Avail: NTIS HC/MF A10

The Computer Integrated Enterprise (CIE) extends the idea of Computer Integrated Manufacturing (CIM) to include all aspects of company management and operation. The development of CIM is reviewed and the technologies involved in its evolution into CIE are indicated. Delays in implementing automation are attributed to differences in emphasis on the parts of engineers and managers, who are concerned, respectively, with fabrication of parts and with assembly of previously fabricated parts and components. Among the requirements for successful implementation of CIE are a company's ability to respond to changes, flexibility in the manufacturing processes, clear definition of functions, and strong attention to punctuality. ISA

N92-23884# TADIRAN Israel Electronics Industries Ltd., Tel Aviv.
CIM IMPLEMENTATION AT CVALIM, D.T.C. DIVISION, BET-SHEAN, ISRAEL
Gad Vitner *In* CASA RI/SME, Proceedings of the International Conference on CAD/CAM and AMT. Volume 1: General Sessions 14 Dec. 1989 2 p (For primary document see N92-23851 14-61)
(Rept-3.2.4) Avail: NTIS HC/MF A10

CVALIM, D.T.C. Division is a manufacturer of telecommunication cables and fiber optics. In order to increase the operational efficiency of the division, a decision was made to install a CIM (Computer Integrated Manufacturing) system to control and monitor the machines in the production line. At present, there are 40 machines on the floor, all of them linked to the system. The plant manager knows the real-time status of work done on the floor via a monitor on his desk. Work orders are transmitted to the operator terminal, enabling the operator to choose the next job to be performed. The system continuously monitors the operational parameters via sensors and the data collection center. ISA

N92-23885# Technion - Israel Inst. of Tech., Haifa.
CIM: THE FUTURE TECHNOLOGY
Gideon Halevi *In* CASA RI/SME, Proceedings of the International Conference on CAD/CAM and AMT. Volume 1: General Sessions 14 Dec. 1989 7 p (For primary document see N92-23851 14-61)
(Rept-3.3.1) Avail: NTIS HC/MF A10

CIM (Computer Integrated Manufacturing) is a logical development and a natural evolution of the computer aided era. One day, it will be the dominating technology and control the factory of the future. However, there is a danger that by rushing things the logic-gap phenomenon will impede if not halt the natural course of development. Technologically we are not ready yet for the integration. There are missing links that cannot be overlooked. CIM should be a target and a research topic today and not a working system. Different approaches should be carefully studied, filling the technological gaps, and only then should CIM be implemented. ISA

N92-23886# Ben Gurion Univ. of the Negev, Beersheva (Israel). Dept. of Industrial Engineering and Management.
GROUP SCHEDULING USING GROUP TECHNOLOGY CONCEPTS **c81**
D. Ben-Arieh and M. Dror *In* CASA RI/SME, Proceedings of the International Conference on CAD/CAM and AMT. Volume 1: General Sessions 14 Dec. 1989 5 p (For primary document see N92-23851 14-61)
(Rept-3.3.2) Avail: NTIS HC/MF A10

GT (Group Technology) is a manufacturing concept aimed at alleviating the production problems of a proliferation of products with decreasing life expectancy and improved quality. This approach takes advantage of part similarities. Parts can be grouped together based on designs or manufacturing properties. One aspect that is currently missing from GT classification is grouping parts according to their behavioral parameters. Even parts that share the same group of machines can have diverse properties that suggest different scheduling and routing techniques. This paper highlights the need for a different classification approach that categorizes parts according to similarity in control measures. This approach is used to construct a GT-based scheduling. The GT-based scheduling is demonstrated for an open shop environment and includes the clustering analysis, scheduling algorithms, and results. ISA

N92-23887# Daisy/Cadnetix Israel Ltd., Herzliya.
THE USE OF EDIF AT DAISY/CADNETIX
Avi Bivas *In* CASA RI/SME, Proceedings of the International Conference on CAD/CAM and AMT. Volume 1: General Sessions 14 Dec. 1989 7 p (For primary document see N92-23851 14-61)
(Rept-4.2.1) Avail: NTIS HC/MF A10

EDIF (Electronic Design Interchange Format) has become the major means of transferring designs between computer aided design systems, particularly for schematic and netlist files. EDIF is a public domain format which provides a means of transferring schematic, symbolic, physical layout, interconnection, and textual information related to digital and analog circuit designs. An EDIF file is a character stream organized in LISP-like format. The file comprises a structured collection of cells, each of which defines a circuit feature, e.g., a component. Cell specifications may embody three levels of complexity and can include a variety of views, related to various aspects of design. Daisy/Cadnetix has completed the ENR (EDIF Netlist Reader), ENW (EDIF Netlist Writer), and ESR (EDIF Schematic Reader), and is developing the ESW (EDIF Schematic Writer) and EDIF PCBLayout (Reader and Writer). ISA

N92-23888# Israel Defense Forces, Tel Aviv.
INFRASTRUCTURE AND TRAINING OF MANPOWER FOR CAD/CAM SYSTEMS
R. Aharony *In* CASA RI/SME, Proceedings of the International Conference on CAD/CAM and AMT. Volume 1: General Sessions 14 Dec. 1989 2 p (For primary document see N92-23851 14-61)
(Rept-4.2.2) Avail: NTIS HC/MF A10

The smooth introduction of a CADD (Computer Aided Design and Drawing) system is aided by prior attention to personnel selection and training, computer hardware and software, and ancillary facilities. The choice and training of the system supervisor is particularly important, since that person is responsible for maintaining and updating the system, and for ensuring its efficient use by the workers. Software choice must involve close cooperation between the system users and the software supplier, to ensure that it matches the CADD system requirements. Ancillary facilities include lighting, furnishing, electricity supplies, communications, and working environment, all of which must be chosen or designed to match the needs of the system. ISA

N92-23889# Elta Electronics Industries, Ashdod (Israel).
DELETING PADS IN MULTI-LAYERED PRINTED CIRCUITS
Brenda Delano *In* CASA RI/SME, Proceedings of the International Conference on CAD/CAM and AMT. Volume 1: General Sessions 14 Dec. 1989 5 p (For primary document see N92-23851 14-61)
(Rept-4.2.3) Avail: NTIS HC/MF A10

A method of mathematical physics is applied to solve a long-standing problem, familiar to users of the SCICARDS utility, to delete pads which are not connected to any line segment in each layer of a multi-layered printed circuit. Parameters for the calculation include the dimensions, shape and center coordinates of the pads, thickness of the lines, the coordinates of the line points which define the positions of line segments, and tolerance (the maximum separation from a line for a 'connected' pad.) For SCICARDS users, the universal file 'UNV' contains all the above information, with the exception of the tolerance, which was chosen appropriately to the user's accuracy requirements. The application described here generates a new universal file with the unnecessary pads deleted. There is no limit to the number of layers which may be included in the file. The calculation is completely general, with no restrictions on the relative orientation of lines and pads, and accuracy is retained to one ten-thousandth of an inch. The attached plots show: (1) layers before being processed; and (2) the same layers after processing by the program using the algorithm. ISA

N92-23991*# MCAT Inst., San Jose, CA.
USER INTERFACE USER'S GUIDE FOR HYPGEN Annual Report
Ing-Tsau Chiu Apr. 1992 21 p
(Contract NCC2-692)
(NASA-CR-190304; NAS 1.26:190304; Rept-92-008) Avail: NTIS HC/MF A03 CSCL 09B

The user interface (UI) of HYPGEN is developed using Panel Library to shorten the learning curve for new users and provide easier ways to run HYPGEN for casual users as well as for advanced users. Menus, buttons, sliders, and type-in fields are used extensively in UI to allow users to point and click with a mouse to choose various available options or to change values of parameters. On-line help is provided to give users information on using UI without consulting the manual. Default values are set for most parameters and boundary conditions are determined by UI to further reduce the effort needed to run HYPGEN; however, users are free to make any changes and save it in a file for later use. A hook to PLOT3D is built in to allow graphics manipulation. The viewpoint and min/max box for PLOT3D windows are computed by UI and saved in a PLOT3D journal file. For large grids which take a long time to generate on workstations, the grid generator (HYPGEN) can be run on faster computers such as Crays, while UI stays at the workstation. Author

N92-24035# Oak Ridge Y-12 Plant, TN.
THE USE OF STEP IN AN INTEGRATED MANUFACTURING ENVIRONMENT
W. D. Cain 1992 10 p Presented at the CAD and Engineering Workstations 1992, Anaheim, CA, 9-12 Mar. 1992
(Contract DE-AC05-84OS-21400)
(DE92-008417; Y/EN-4562; CONF-920392-1) Avail: NTIS HC/MF A02

The ability to exchange and share product data between and within enterprises is essential for implementing the concepts of concurrent engineering. An international standard, the Standard for the Exchange of Product Model Data (STEP), is currently being developed within the International Organization for Standardization (ISO) to provide a comprehensive and reliable product data exchange/sharing mechanism for industry. The purpose of STEP is to prescribe a neutral mechanism capable of completely representing product data throughout the life cycle of a product. Application Protocols (APs) which define the context for the use of product data and specify the use of STEP to satisfy an industrial need are being developed and have become an integral part of STEP. This paper discusses the work being done to develop a suite of interoperable APs for STEP for the exchange and sharing of product and process information in an integrated design and manufacturing environment. DOE

N92-24041# Sandia National Labs., Albuquerque, NM.
CEPXS/ONELD: A ONE-DIMENSIONAL COUPLED ELECTRON-PHOTON DISCRETE ORDINATES CODE PACKAGE
L. J. Lorence, Jr. and J. E. Morel (Los Alamos National Lab., NM.) 1992 12 p Presented at the Deterministic Methods Seminar and TORT Workshop, Oak Ridge, TN, 4-6 Feb. 1992
(Contract DE-AC04-76DP-00789)
(DE92-003146; SAND-92-0261C; CONF-920277-1) Avail: NTIS HC/MF A03

CEPXS/ONELD is a discrete ordinates transport code package that can model the electron-photon cascade from 100 MeV to 1 keV. The CEPXS code generates fully-coupled multigroup-Legendre cross section data. This data is used by the general purpose discrete ordinates code, ONELD, which is derived from the Los Alamos ONEDANT and ONETRAN codes. Version 1.0 of CEPXS/ONELD was released in 1989 and has been primarily used to analyze the effect of radiation environments on electronics. Version 2.0 is under development and will include user-friendly features such as the automatic selection of group structure, spatial mesh structure, and S(sub N) order. DOE

N92-23959*# North Carolina Agricultural and Technical State Univ., Greensboro.
USING MICROSOFT EXCEL APPLICATIONS IN THE GRADUATE INTERN PROGRAM AT GODDARD SPACE FLIGHT CENTER M.S. Thesis
Lisa Antoine *In* NASA. Goddard Space Flight Center, Summer Graduate Research Program for Interns in Science and Engineering 24 Mar. 1992 10 p (For primary document see N92-23958 14-99)
Avail: NTIS HC/MF A12 CSCL 09B

62 COMPUTER SYSTEMS

Includes computer networks and special application computer systems.

N92-23583*# Research Inst. for Computing and Information Systems, Houston, TX.
ARCHITECTURAL IMPACT OF FDDI NETWORK ON SCHEDULING HARD REAL-TIME TRAFFIC
Gopal Agrawal, Baio Chen, Wei Zhao, and Sadegh Davari (Houston Univ., Clear Lake, TX.) Dec. 1991 8 p
(Contract NCC9-16)
(NASA-CR-190272; NAS 1.26:190272) Avail: NTIS HC/MF A02 CSCL 09B

The architectural impact on guaranteeing synchronous message deadlines in FDDI (Fiber Distributed Data Interface) token ring networks is examined. The FDDI network does not have facility to support (global) priority arbitration which is a useful facility for scheduling hard real time activities. As a result, it was found that the worst case utilization of synchronous traffic in an FDDI network can be far less than that in a centralized single processor system. Nevertheless, it is proposed and analyzed that a scheduling method can guarantee deadlines of synchronous messages having traffic utilization up to 33 pct., the highest to date. Author

N92-24045*# National Aeronautics and Space Administration. Pasadena Office, CA.
SYNCHRONOUS PARALLEL SYSTEM FOR EMULATION AND DISCRETE EVENT SIMULATION Patent Application
Jeffrey S. Steinman, inventor (to NASA) (Jet Propulsion Lab., California Inst. of Tech., Pasadena.) 21 Jan. 1992 52 p
(Contract NAS7-918)
(NASA-Case-NPO-18414-1-CU; NAS 1.71:NPO-18414-1-CU; US-Patent-Appl-SN-880211) Avail: NTIS HC/MF A04 CSCL 09B

A synchronous parallel system for emulation and discrete event simulation having parallel nodes responds to received messages at each node by generating event objects having individual time stamps, stores only the changes to state variables of the simulation object attributable to the event object, and produces corresponding messages. The system refrains from transmitting the messages and changing the state variables while it determines whether the changes are superseded, and then stores the unchanged state variables in the event object for later restoral to the simulation object if called for. This determination preferably includes sensing the time stamp of each new event object and determining which new event object has the earliest time stamp as the local event horizon, determining the earliest local event horizon of the nodes as the global event horizon, and ignoring the events whose time stamps are less than the global event horizon. Host processing between the system and external terminals enables such a terminal to query, monitor, command or participate with a simulation object during the simulation process. NASA

63 CYBERNETICS

Includes feedback and control theory, artificial intelligence, robotics and expert systems.

For related information see also *54 Man/System Technology and Life Support.*

N92-23356*# National Aeronautics and Space Administration. Goddard Space Flight Center, Greenbelt, MD.
THE 1992 GODDARD CONFERENCE ON SPACE APPLICATIONS OF ARTIFICIAL INTELLIGENCE
James L. Rash, ed. Washington 1992 251 p Conference held in Greenbelt, MD, 5-6 May 1992
(NASA-CP-3141; Rept-92B00045; NAS 1.55:3141) Avail: NTIS HC/MF A12 CSCL 09B

The purpose of this conference is to provide a forum in which current research and development directed at space applications of artificial intelligence can be presented and discussed. The papers fall into the following areas: planning and scheduling, control, fault monitoring/diagnosis and recovery, information management, tools, neural networks, and miscellaneous applications. For individual titles, see N92-23357 through N92-23375.

N92-23357*# Jet Propulsion Lab., California Inst. of Tech., Pasadena.
ARTIFICIAL INTELLIGENCE APPROACH TO PLANNING THE ROBOTIC ASSEMBLY OF LARGE TETRAHEDRAL TRUSS STRUCTURES
Luiz S. HomemdeMello *In* NASA. Goddard Space Flight Center, The 1992 Goddard Conference on Space Applications of Artificial Intelligence 1992 p 3-12 (For primary document see N92-23356 14-63)
Avail: NTIS HC/MF A12 CSCL 09B

An assembly planner for tetrahedral truss structures is presented. To overcome the difficulties due to the large number of parts, the planner exploits the simplicity and uniformity of the shapes of the parts and the regularity of their interconnection. The planning automation is based on the computational formalism known as production system. The global data base consists of a hexagonal grid representation of the truss structure. This representation captures the regularity of tetrahedral truss structures and their multiple hierarchies. It maps into quadratic grids and can be implemented in a computer by using a two-dimensional array data structure. By maintaining the multiple hierarchies explicitly in the model, the choice of a particular hierarchy is only made when needed, thus allowing a more informed decision. Furthermore, testing the preconditions of the production rules is simple because the patterned way in which the struts are interconnected is incorporated into the topology of the hexagonal grid. A directed graph representation of assembly sequences allows the use of both graph search and backtracking control strategies. Author

N92-23358*# National Taiwan Univ., Taipei. Dept. of Computer Science and Information Engineering.
SLS-PLAN-IT: A KNOWLEDGE-BASED BLACKBOARD SCHEDULING SYSTEM FOR SPACELAB LIFE SCIENCES MISSIONS
Cheng-Yan Kao and Seok-Hua Lee (General Electric Co., Houston, TX.) *In* NASA. Goddard Space Flight Center, The 1992 Goddard Conference on Space Applications of Artificial Intelligence 1992 p 13-27 (For primary document see N92-23356 14-63)
(Contract NAS9-17884)
Avail: NTIS HC/MF A12 CSCL 09B

The primary scheduling tool in use during the Spacelab Life Science (SLS-1) planning phase was the operations research (OR) based, tabular form Experiment Scheduling System (ESS) developed by NASA Marshall. PLAN-IT is an artificial intelligence based interactive graphic timeline editor for ESS developed by JPL. The PLAN-IT software was enhanced for use in the scheduling of Spacelab experiments to support the SLS missions. The enhanced software SLS-PLAN-IT System was used to support the real-time reactive scheduling task during the SLS-1 mission. SLS-PLAN-IT is a frame-based blackboard scheduling shell which, from scheduling input, creates resource-requiring event duration objects and resource-usage duration objects. The blackboard structure is to keep track of the effects of event duration objects on the resource usage objects. Various scheduling heuristics are coded in procedural form and can be invoked any time at the user's request. The system architecture is described along with what has been learned with the SLS-PLAN-IT project. Author

N92-23359*# Space Telescope Science Inst., Baltimore, MD.
DETECTING OPPORTUNITIES FOR PARALLEL OBSERVATIONS ON THE HUBBLE SPACE TELESCOPE c89
Michael Lucks *In* NASA. Goddard Space Flight Center, The 1992 Goddard Conference on Space Applications of Artificial Intelligence 1992 p 29-44 (For primary document see N92-23356 14-63)
Avail: NTIS HC/MF A12 CSCL 03A

The presence of multiple scientific instruments aboard the Hubble Space Telescope provides opportunities for parallel science, i.e., the simultaneous use of different instruments for different observations. Determining whether candidate observations are suitable for parallel execution depends on numerous criteria (some involving quantitative tradeoffs) that may change frequently. A knowledge based approach is presented for constructing a scoring function to rank candidate pairs of observations for parallel science. In the Parallel Observation Matching System (POMS), spacecraft knowledge and schedulers' preferences are represented using a uniform set of mappings, or knowledge functions. Assessment of parallel science opportunities is achieved via composition of the knowledge functions in a prescribed manner. The knowledge

acquisition, and explanation facilities of the system are presented. The methodology is applicable to many other multiple criteria assessment problems. Author

N92-23360*# Symbiotics, Inc., Cambridge, MA.
COORDINATING COMPLEX PROBLEM-SOLVING AMONG DISTRIBUTED INTELLIGENT AGENTS
Richard M. Adler *In* NASA. Goddard Space Flight Center, The 1992 Goddard Conference on Space Applications of Artificial Intelligence 1992 p 47-57 (For primary document see N92-23356 14-63)
(Contracts NAS10-11606; NAS10-11763)
Avail: NTIS HC/MF A12 CSCL 09B

A process-oriented control model is described for distributed problem solving. The model coordinates the transfer and manipulation of information across independent networked applications, both intelligent and conventional. The model was implemented using SOCIAL, a set of object-oriented tools for distributing computing. Complex sequences of distributed tasks are specified in terms of high level scripts. Scripts are executed by SOCIAL objects called Manager Agents, which realize an intelligent coordination model that routes individual tasks to suitable server applications across the network. These tools are illustrated in a prototype distributed system for decision support of ground operations for NASA's Space Shuttle fleet. Author

N92-23361*# Naval Research Lab., Washington, DC. Interface and Control Systems.
DISTRIBUTED EXPERT SYSTEMS FOR GROUND AND SPACE APPLICATIONS
Brian Buckley and Louis Wheatcraft (Barrios Technology, Inc., Houston, TX.) *In* NASA. Goddard Space Flight Center, The 1992 Goddard Conference on Space Applications of Artificial Intelligence 1992 p 59-70 (For primary document see N92-23356 14-63)
Avail: NTIS HC/MF A12 CSCL 09B

Presented here is the Spacecraft Command Language (SCL) concept of the unification of ground and space operations using a distributed approach. SCL is a hybrid software environment borrowing from expert system technology, fifth generation language development, and multitasking operating system environments. Examples of potential uses for the system and current distributed applications of SCL are given. Author

N92-23362*# Jet Propulsion Lab., California Inst. of Tech., Pasadena.
EVALUATING MODEL ACCURACY FOR MODEL-BASED REASONING
Steve Chien and Joseph Roden *In* NASA. Goddard Space Flight Center, The 1992 Goddard Conference on Space Applications of Artificial Intelligence 1992 p 71-76 (For primary document see N92-23356 14-63)
Avail: NTIS HC/MF A12 CSCL 09B

Described here is an approach to automatically assessing the accuracy of various components of a model. In this approach, actual data from the operation of a target system is used to drive statistical measures to evaluate the prediction accuracy of various portions of the model. We describe how these statistical measures of model accuracy can be used in model-based reasoning for monitoring and design. We then describe the application of these techniques to the monitoring and design of the water recovery system of the Environmental Control and Life Support System (ECLSS) of Space Station Freedom. Author

N92-23363*# Loral AeroSys, Seabrook, MD.
AN ARCHITECTURE FOR THE DEVELOPMENT OF REAL-TIME FAULT DIAGNOSIS SYSTEMS USING MODEL-BASED REASONING
Gardiner A. Hall, James Schuetzle, David LaVallee, and Uday Gupta *In* NASA. Goddard Space Flight Center, The 1992 Goddard Conference on Space Applications of Artificial Intelligence 1992 p 77-86 (For primary document see N92-23356 14-63)
Avail: NTIS HC/MF A12 CSCL 09B

Presented here is an architecture for implementing real-time telemetry based diagnostic systems using model-based reasoning. First, we describe Paragon, a knowledge acquisition tool for offline entry and validation of physical system models. Paragon provides domain experts with a structured editing capability to capture the physical component's structure, behavior, and causal relationships. We next describe the architecture of the run time diagnostic system. The diagnostic system, written entirely in Ada, uses the behavioral model developed offline by Paragon to simulate expected component states as reflected in the telemetry stream. The diagnostic algorithm traces causal relationships contained within the model to isolate system faults. Since the diagnostic process relies exclusively on the behavioral model and is implemented without the use of heuristic rules, it can be used to isolate unpredicted faults in a wide variety of systems. Finally, we discuss the implementation of a prototype system constructed using this technique for diagnosing faults in a science instrument. The prototype demonstrates the use of model-based reasoning to develop maintainable systems with greater diagnostic capabilities at a lower cost. Author

N92-23364*# General Electric Co., Philadelphia, PA. Military and Data Systems Organization.
THE ACHIEVEMENT OF SPACECRAFT AUTONOMY THROUGH THE THEMATIC APPLICATION OF MULTIPLE COOPERATING INTELLIGENT AGENTS
Philip J. Rossomando *In* NASA. Goddard Space Flight Center, The 1992 Goddard Conference on Space Applications of Artificial Intelligence 1992 p 87-103 (For primary document see N92-23356 14-63)
Avail: NTIS HC/MF A12 CSCL 09B

A description is given of UNICORN, a prototype system developed for the purpose of investigating artificial intelligence (AI) concepts supporting spacecraft autonomy. UNICORN employs thematic reasoning, of the type first described by Rodger Schank of Northwestern University, to allow the context-sensitive control of multiple intelligent agents within a blackboard based environment. In its domain of application, UNICORN demonstrates the ability to reason teleologically with focused knowledge. Also presented are some of the lessons learned as a result of this effort. These lessons apply to any effort wherein system level autonomy is the objective. Author

N92-23365*# National Aeronautics and Space Administration. Lewis Research Center, Cleveland, OH.
INTELLIGENT FAULT ISOLATION AND DIAGNOSIS FOR COMMUNICATION SATELLITE SYSTEMS
Donald P. Tallo, John Durkin (Akron Univ., OH.), and Edward J. Petrik *In* NASA. Goddard Space Flight Center, The 1992 Goddard Conference on Space Applications of Artificial Intelligence 1992 p 105-120 (For primary document see N92-23356 14-63)
Avail: NTIS HC/MF A12 CSCL 09B

Discussed here is a prototype diagnosis expert system to provide the Advanced Communication Technology Satellite (ACTS) System with autonomous diagnosis capability. The system, the Fault Isolation and Diagnosis EXpert (FIDEX) system, is a frame-based system that uses hierarchical structures to represent such items as the satellite's subsystems, components, sensors, and fault states. This overall frame architecture integrates the hierarchical structures into a lattice that provides a flexible representation scheme and facilitates system maintenance. FIDEX uses an inexact reasoning technique based on the incrementally acquired evidence approach developed by Shortliffe. The system is designed with a primitive learning ability through which it maintains a record of past diagnosis studies. Author

N92-23366*# Colorado Univ., Colorado Springs. Dept. of Computer Science.
FEATURE DETECTION IN SATELLITE IMAGES USING NEURAL NETWORK TECHNOLOGY
Marijke F. Augusteijn and Arturo S. Dimalanta *In* NASA. Goddard Space Flight Center, The 1992 Goddard Conference on Space Applications of Artificial Intelligence 1992 p 123-136 Sponsored

in part by CTA, Inc. (For primary document see N92-23356 14-63)
Avail: NTIS HC/MF A12 CSCL 09B

A feasibility study of automated classification of satellite images is described. Satellite images were characterized by the textures they contain. In particular, the detection of cloud textures was investigated. The method of second-order gray level statistics, using co-occurrence matrices, was applied to extract feature vectors from image segments. Neural network technology was employed to classify these feature vectors. The cascade-correlation architecture was successfully used as a classifier. The use of a Kohonen network was also investigated but this architecture could not reliably classify the feature vectors due to the complicated structure of the classification problem. The best results were obtained when data from different spectral bands were fused.
Author

N92-23367*# National Aeronautics and Space Administration. Goddard Space Flight Center, Greenbelt, MD.
DESIGN OF NEURAL NETWORKS FOR CLASSIFICATION OF REMOTELY SENSED IMAGERY **c43**
Samir R. Chettri, Robert F. Cromp, and Mark Birmingham (Princeton Univ., NJ.) *In its* The 1992 Goddard Conference on Space Applications of Artificial Intelligence 1992 p 137-150 (For primary document see N92-23356 14-63)
Avail: NTIS HC/MF A12 CSCL 05B

Classification accuracies of a backpropagation neural network are discussed and compared with a maximum likelihood classifier (MLC) with multivariate normal class models. We have found that, because of its nonparametric nature, the neural network outperforms the MLC in this area. In addition, we discuss techniques for constructing optimal neural nets on parallel hardware like the MasPar MP-1 currently at GSFC. Other important discussions are centered around training and classification times of the two methods, and sensitivity to the training data. Finally, we discuss future work in the area of classification and neural nets. Author

N92-23368*# Computer Application Systems, Signal Mountain, TN.
IMPROVED IMAGE CLASSIFICATION WITH NEURAL NETWORKS BY FUSING MULTISPECTRAL SIGNATURES WITH TOPOLOGICAL DATA **c43**
Craig Harston and Chris Schumacher *In* NASA. Goddard Space Flight Center, The 1992 Goddard Conference on Space Applications of Artificial Intelligence 1992 p 151-158 (For primary document see N92-23356 14-63)
(Contract NAS13-435)
Avail: NTIS HC/MF A12 CSCL 05B

Automated schemes are needed to classify multispectral remotely sensed data. Human intelligence is often required to correctly interpret images from satellites and aircraft. Humans suceed because they use various types of cues about a scene to accurately define the contents of the image. Consequently, it follows that computer techniques that integrate and use different types of information would perform better than single source approaches. This research illustrated that multispectral signatures and topographical information could be used in concert. Significantly, this dual source tactic classified a remotely sensed image better than the multispectral classification alone. These classifications were accomplished by fusing spectral signatures with topographical information using neural network technology. A neural network was trained to classify Landsat mulitspectral signatures. A file of georeferenced ground truth classifications were used as the training criterion. The network was trained to classify urban, agriculture, range, and forest with an accuracy of 65.7 percent. Another neural network was programmed and trained to fuse these multispectral signature results with a file of georeferenced altitude data. This topological file contained 10 levels of elevations. When this nonspectral elevation information was fused with the spectral signatures, the classifications were improved to 73.7 and 75.7 percent.
Author

N92-23369*# Loyola Univ., New Orleans, LA. Dept. of Mathematical Sciences.
IMPROVED INTERPRETATION OF SATELLITE ALTIMETER DATA USING GENETIC ALGORITHMS **c43**
Kenneth Messa and Matthew Lybanon (Naval Oceanographic and Atmospheric Research Lab., Bay Saint Louis, MS.) *In* NASA. Goddard Space Flight Center, The 1992 Goddard Conference on Space Applications of Artificial Intelligence 1992 p 159-166 Sponsored in part by Navy (For primary document see N92-23356 14-63)
Avail: NTIS HC/MF A12 CSCL 05B

Genetic algorithms (GA) are optimization techniques that are based on the mechanics of evolution and natural selection. They take advantage of the power of cumulative selection, in which successive incremental improvements in a solution structure become the basis for continued development. A GA is an iterative procedure that maintains a 'population' of 'organisms' (candidate solutions). Through successive 'generations' (iterations) the population as a whole improves in simulation of Darwin's 'survival of the fittest'. GA's have been shown to be successful where noise significantly reduces the ability of other search techniques to work effectively. Satellite altimetry provides useful information about oceanographic phenomena. It provides rapid global coverage of the oceans and is not as severely hampered by cloud cover as infrared imagery. Despite these and other benefits, several factors lead to significant difficulty in interpretation. The GA approach to the improved interpretation of satellite data involves the representation of the ocean surface model as a string of parameters or coefficients from the model. The GA searches in parallel, a population of such representations (organisms) to obtain the individual that is best suited to 'survive', that is, the fittest as measured with respect to some 'fitness' function. The fittest organism is the one that best represents the ocean surface model with respect to the altimeter data.
Author

N92-23370*# Teledyne Brown Engineering, Huntsville, AL. Space Operations Dept.
THE USE OF ARTIFICIAL INTELLIGENCE TECHNIQUES TO IMPROVE THE MULTIPLE PAYLOAD INTEGRATION PROCESS
Dannie E. Cutts and Brian K. Widgren *In* NASA. Goddard Space Flight Center, The 1992 Goddard Conference on Space Applications of Artificial Intelligence 1992 p 169-179 (For primary document see N92-23356 14-63)
Avail: NTIS HC/MF A12 CSCL 09B

A maximum return of science and products with a minimum expenditure of time and resources is a major goal of mission payload integration. A critical component then, in successful mission payload integration is the acquisition and analysis of experiment requirements from the principal investigator and payload element developer teams. One effort to use artificial intelligence techniques to improve the acquisition and analysis of experiment requirements within the payload integration process is described.
Author

N92-23371*# George Mason Univ., Fairfax, VA. Dept. of Information and Software Systems Engineering.
KNOWLEDGE-BASED APPROACH FOR GENERATING TARGET SYSTEM SPECIFICATIONS FROM A DOMAIN MODEL
Hassan Gomaa, Larry Kerschberg, and Vijayan Sugumaran *In* NASA. Goddard Space Flight Center, The 1992 Goddard Conference on Space Applications of Artificial Intelligence 1992 p 181-194 (For primary document see N92-23356 14-63)
Avail: NTIS HC/MF A12 CSCL 09B

Several institutions in industry and academia are pursuing research efforts in domain modeling to address unresolved issues in software reuse. To demonstrate the concepts of domain modeling and software reuse, a prototype software engineering environment is being developed at George Mason University to support the creation of domain models and the generation of target system specifications. This prototype environment, which is application domain independent, consists of an integrated set of commercial off-the-shelf software tools and custom-developed

software tools. This paper describes the knowledge-based tool that was developed as part of the environment to generate target system specifications from a domain model. Author

N92-23372*# University of Central Florida, Orlando. Dept. of Computer Science.
COMBINING FACTUAL AND HEURISTIC KNOWLEDGE IN KNOWLEDGE ACQUISITION
Fernando Gomez, Richard Hull, Clark Karr, Bruce Hosken, and William Verhagen (Grumman Aerospace Corp., Bethpage, NY.) *In* NASA. Goddard Space Flight Center, The 1992 Goddard Conference on Space Applications of Artificial Intelligence 1992 p 195-209 (For primary document see N92-23356 14-63)
(Grant NAG10-0058)
Avail: NTIS HC/MF A12 CSCL 09B

A knowledge acquisition technique that combines heuristic and factual knowledge represented as two hierarchies is described. These ideas were applied to the construction of a knowledge acquisition interface to the Expert System Analyst (OPERA). The goal of OPERA is to improve the operations support of the computer network in the space shuttle launch processing system. The knowledge acquisition bottleneck lies in gathering knowledge from human experts and transferring it to OPERA. OPERA's knowledge acquisition problem is approached as a classification problem-solving task, combining this approach with the use of factual knowledge about the domain. The interface was implemented in a Symbolics workstation making heavy use of windows, pull-down menus, and other user-friendly devices.
Author

N92-23373*# National Aeronautics and Space Administration. Goddard Space Flight Center, Greenbelt, MD.
A SPATIAL DATA HANDLING SYSTEM FOR RETRIEVAL OF IMAGES BY UNRESTRICTED REGIONS OF USER INTEREST **c82**
Erik Dorfman (Hughes STX, Inc., Greenbelt, MD.) and Robert F. Cromp *In its* The 1992 Goddard Conference on Space Applications of Artificial Intelligence 1992 p 213-230 (For primary document see N92-23356 14-63)
Avail: NTIS HC/MF A12 CSCL 05B

The Intelligent Data Management (IDM) project at NASA/Goddard Space Flight Center has prototyped an Intelligent Information Fusion System (IIFS), which automatically ingests metadata from remote sensor observations into a large catalog which is directly queryable by end-users. The greatest challenge in the implementation of this catalog was supporting spatially-driven searches, where the user has a possible complex region of interest and wishes to recover those images that overlap all or simply a part of that region. A spatial data management system is described, which is capable of storing and retrieving records of image data regardless of their source. This system was designed and implemented as part of the IIFS catalog. A new data structure, called a hypercylinder, is central to the design. The hypercylinder is specifically tailored for data distributed over the surface of a sphere, such as satellite observations of the Earth or space. Operations on the hypercylinder are regulated by two expert systems. The first governs the ingest of new metadata records, and maintains the efficiency of the data structure as it grows. The second translates, plans, and executes users' spatial queries, performing incremental optimization as partial query results are returned. Author

N92-23374*# Argonne National Lab., IL. Environmental Assessment and Information Sciences Div.
DATA EXPLORATION SYSTEMS FOR DATABASES **c82**
Richard J. Greene and Christopher Hield *In* NASA. Goddard Space Flight Center, The 1992 Goddard Conference on Space Applications of Artificial Intelligence 1992 p 231-244 (For primary document see N92-23356 14-63)
Avail: NTIS HC/MF A12 CSCL 05B

Data exploration systems apply machine learning techniques, multivariate statistical methods, information theory, and database theory to databases to identify significant relationships among the data and summarize information. The result of applying data exploration systems should be a better understanding of the structure of the data and a perspective of the data enabling an analyst to form hypotheses for interpreting the data. This paper argues that data exploration systems need a minimum amount of domain knowledge to guide both the statistical strategy and the interpretation of the resulting patterns discovered by these systems. Author

N92-23375*# Loyola Univ., New Orleans, LA. Mathematical Sciences.
LOGIC PROGRAMMING AND METADATA SPECIFICATIONS
Antonio M. Lopez, Jr. and Marguerite E. Saacks (Xavier Univ. of Louisiana, New Orleans.) *In* NASA. Goddard Space Flight Center, The 1992 Goddard Conference on Space Applications of Artificial Intelligence 1992 p 245-253 Sponsored by NASA. Stennis Space Center (For primary document see N92-23356 14-63)
Avail: NTIS HC/MF A12 CSCL 09B

Artificial intelligence (AI) ideas and techniques are critical to the development of intelligent information systems that will be used to collect, manipulate, and retrieve the vast amounts of space data produced by 'Missions to Planet Earth.' Natural language processing, inference, and expert systems are at the core of this space application of AI. This paper presents logic programming as an AI tool that can support inference (the ability to draw conclusions from a set of complicated and interrelated facts). It reports on the use of logic programming in the study of metadata specifications for a small problem domain of airborne sensors, and the dataset characteristics and pointers that are needed for data access. Author

N92-23438*# Research Inst. for Computing and Information Systems, Houston, TX.
SUMMARY REPORT: A PRELIMINARY INVESTIGATION INTO THE USE OF FUZZY LOGIC FOR THE CONTROL OF REDUNDANT MANIPULATORS
John B. Cheatham, Jr. and Kevin N. Magee (Rice Univ., Houston, TX.) Dec. 1991 44 p
(Contract NCC9-16; RICIS Proj. AI-02)
(NASA-CR-190277; NAS 1.26:190277) Avail: NTIS HC/MF A03 CSCL 09B

The Rice University Department of Mechanical Engineering and Materials Sciences' Robotics Group designed and built an eight degree of freedom redundant manipulator. Fuzzy logic was proposed as a control scheme for tasks not directly controlled by a human operator. In preliminary work, fuzzy logic control was implemented for a camera tracking system and a six degree of freedom manipulator. Both preliminary systems use real time vision data as input to fuzzy controllers. Related projects include integration of tactile sensing and fuzzy control of a redundant snake-like arm that is under construction. Author

N92-23457# Oak Ridge National Lab., TN.
ON MOTION PLANNING AMIDST TRANSIENT OBSTACLES
Kikuo Fujimura 1992 28 p Presented at the IEEE International Conference on Robotics and Automation, Nice, France, 10-15 May 1992
(Contract DE-AC05-84OR-21400)
(DE91-018939; CONF-920540-1) Avail: NTIS HC/MF A03

Motion planning in the presence of time-dependent obstacles is studied. Much of the prior approaches assumes that the obstacles always exist in the environment whether they are stationary or in motion. In this paper, we consider the case that the environment contains obstacles whose existing periods are dependent on time, i.e., they may disappear and reappear in the environment. This formulation enables us to model a variety of time-varying situations that can arise in some application domains. For example, one can plan a motion in an environment where another agent rearranges the environment by picking up an object and placing it back at another location in the same environment. A concept similar to that of visibility is used to solve the problem. An algorithm is presented to generate a motion in such a dynamic domain and

its time-minimality is proved. The algorithm runs in O(n(sup 3) log n) time, where n is the total number of vertices in the environment. DOE

N92-23458# Sandia National Labs., Albuquerque, NM.
DYNAMIC ANALYSIS OF PLANAR MANIPULATION TASKS
R. C. Brost 1991 7 p Presented at the IEEE International Conference on Robotics and Automation, Nice, France, 10-15 May 1992
(Contract DE-AC04-76DP-00789)
(DE91-019060; SAND-91-2041C; CONF-920540-4) Avail: NTIS HC/MF A02

This paper presents two algorithms that construct a set of initial (x, y, (theta)) configurations from which a given action will reliably accomplish a planar manipulation task. The first algorithm applies energy arguments to construct a conservative set of successful initial configurations, while the second algorithm performs numerical integration to construct a set that is much less conservative. The algorithms may be applied to a variety of tasks, including pushing, placing-by-dropping, and force-controlled assembly tasks. Both algorithms consider the task geometry and mechanics, and allow uncertainty in every task parameter except for the object shapes. Experimental results are presented which demonstrate the validity of the algorithms' output for two example manipulation tasks. DOE

N92-23506# Technische Univ., Twente (Netherlands). Faculty of Applied Mathematics.
CONTROL PROBLEM FOR A MULTI SERVER LOSS SYSTEM
W. M. Nawijn Aug. 1991 16 p
(PB92-148675; Memo-989) Avail: NTIS HC/MF A03 CSCL 09B

A stationary break-in policy is discussed that controls a multi-server loss system. The policy allows the removal of a job from the system in favor of an arriving job. The decision epochs coincide with arrival epochs and the state space is comprised of service time information of jobs present at these epochs. It is shown that the proposed policy attains the maximal possible fraction of completed jobs in the long run given perfect information over the future of the underlying processes. A derivation of the optimal fraction for the system GI/G/1/0 is given. Author

N92-23508# Tilburg Univ. (Netherlands). Dept. of Econometrics.
OPTIMIZING FLOW RATES IN A QUEUEING NETWORK WITH SIDE CONSTRAINTS
B. Pourbabai, J. P. C. Blanc, and F. A. vanderDuynSchouten 1992 21 p Prepared in cooperation with Maryland Univ., College Park
(PB92-149996; FEW-511) Avail: NTIS HC/MF A03 CSCL 09B

Modified versions of the classical deterministic maximum flow and minimum cost network flow problems are presented in a stochastic queueing environment. In the maximum flow network model, the throughout rate in the network is maximized such that for each arc of the network, the resulting probability of finding congestion along that arc in excess of a desirable threshold does not exceed an acceptable value. In the minimum cost network flow model, the minimum cost routing of a flow of given magnitude is determined under the same type of constraints on the arcs. After proper transformation, these models are solved by Ford and Fulkerson's labeling algorithm and 'out of kilter' algorithm, respectively. Author

N92-24011 Stanford Univ., CA.
OPTIMAL CONTROL OF CLOSED CHAIN ROBOTIC SYSTEMS Ph.D. Thesis
Rhonda Ann Slattery 1991 167 p
Avail: Univ. of Microfilms Order No. DA9205725

A system of rigid bodies which are connected to form a closed ring has more complicated dynamic interactions than a simple chain. Such a system arises when two robot arms grasp a common payload. The advantages of a two arm manipulator over a one arm manipulator are in moving large or awkward loads, and in increased stability due to two contact points on the payload. A disadvantage is the more complicated dynamics arising from the closed kinematic chain structure. By studying motions which minimize some cost functions, feed forward logic was determined for several tasks. A method for deriving the equations of motion of a closed ring system is presented which is related to two arm force control. This method has the advantages of emphasizing the payload and not being specific to one of the two arms. A simplification of this derivation is also given which can be used under special circumstances. The equations of motion are used to determine minimum time and fastest throw paths for two closed chain robotic systems. The two systems studied consist of two planar two link robot arms grasping a point mass or finite payload. For both robotic systems all actuators have bounded torques. The minimum time solution is usually bang-bang in all control.
Dissert. Abstr.

N92-24032# Oak Ridge National Lab., TN.
TIME OPTIMAL TRAJECTORIES FOR A 2-WHEELED ROBOT
D. B. Reister and F. G. Pin 1991 31 p Presented at the IEEE International Conference on Robotics and Automation, Nice, France, 10-15 May 1992
(Contract DE-AC05-84OR-21400)
(DE92-000069; CONF-920540-8) Avail: NTIS HC/MF A03

This paper addresses the problem of time-optimal motions for a mobile platform in a 2-D planar environment. The platform is assumed to be of the skid-steer type, with two non-steerable independently driven wheels. The overall mission of the robot is expressed in terms of a sequence of via points at which the platform must be at rest in a given configuration (position and orientation). The objective is to plan time-optimal trajectories between these configurations assuming an unobstructed environment. Using Pontryagin's maximum principle, we formally demonstrate that the time optimal motions of the platform are bang-bang (at each instant, the acceleration on each wheel is either at the upper or lower limit). The optimal trajectories can be characterized by a set of unique parameters corresponding to the switch times (the times at which the wheel accelerations change sign). We show numerically that trajectories with three switch times (two on one wheel, one on the other) can reach any position, while trajectories with four switch times can reach any configuration. Given the desired final configuration of the platform, we can search the parameter space and find the switch times that will produce particular paths to the configuration. We show numerically that a uniquely defined subset of these paths are time optimal by calculating the dual variables required by the maximum principle.
DOE

N92-24066# Lawrence Livermore National Lab., CA.
A SELF-NAVIGATING MOBILE ROBOT
D. T. Gavel and R. Legrand (Rice Univ., Houston, TX.) Oct. 1991 13 p Presented at the 1992 IEEE International Conference on Robotics and Automation, Nice, France, 10-15 May 1992
(Contract W-7405-eng-48)
(DE92-008612; UCRL-JC-108592; CONF-920540-15) Avail: NTIS HC/MF A03

Mobile robots can go places where it is undesirable or unsafe for humans to go. With only a modest amount of on-board computer capability, a robot can accomplish important tasks without the intervention of a human operator. We have constructed a small robot that has autonomous navigation and steering capabilities. The technology developed and tested here will find eventual application on robots that must enter hazardous environments.
DOE

N92-23874# Aristotle Univ. of Thessaloniki (Greece). Lab. for Machine Tool and Machine Dynamic.
OPTIMUM CUTTING CONDITIONS DETERMINATION FOR THE NC-MILLING
K.-D. Bouzakis, K. Efstathiou, and R. Paraskevopoulou *In* CASA RI/SME, Proceedings of the International Conference on CAD/CAM and AMT. Volume 1: General Sessions 14 Dec.

1989 6 p (For primary document see N92-23851 14-61)
(Rept-2.1.2) Avail: NTIS HC/MF A10

N92-23875# Ohri (Edith), Tel Aviv (Israel).
CONTROLLING OPERATIONS THROUGH PROCEDURES: APE (AUTOMATED PROCEDURE EDITOR)
Edith Ohri *In* CASA RI/SME, Proceedings of the International Conference on CAD/CAM and AMT. Volume 1: General Sessions 14 Dec. 1989 2 p (For primary document see N92-23851 14-61)
(Rept-2.2.1) Avail: NTIS HC/MF A10

N92-23877# Rochester Univ., NY. Graduate School of Business Administration.
ADVANCES IN PROCESSING RATES OPTIMIZATION FOR FLEXIBLE MANUFACTURING SYSTEMS
Abraham Seidmann and Paul J. Schweitzer *In* CASA RI/SME, Proceedings of the International Conference on CAD/CAM and AMT. Volume 1: General Sessions 14 Dec. 1989 4 p Sponsored in part by IBM (For primary document see N92-23851 14-61)
(Rept-2.3.4) Avail: NTIS HC/MF A10

64 NUMERICAL ANALYSIS

Includes iteration, difference equations, and numerical approximation.

N92-23128# International Centre for Theoretical Physics, Trieste (Italy).
EUCLIDEAN-ISOTOPIC SYMMETRIES
R. M. Santilli Sep. 1991 8 p
(DE92-615260; IC-91/262) Avail: NTIS HC/MF A02

In this note we introduce the largest possible nonlinear and nonlocal symmetries of the separation (r(sub ia)-r(sub ib))G(sub ij)(r,dr/dt,d(sup 2)r/dt(sup 2))(r(sub ja)-r(sub jb)), ij = 1,2,3, a,b = 1,2, ... ,N, in a Euclidean-isotopic space E(r,G,A) with isometric G; we identify their Lie-isotopic structure E(3), here called Euclidean-isotopic symmetries; and we show that they are all locally isomorphic to the conventional Euclidean symmetry E(3) under the condition of positive-definiteness of the isometric. DOE

N92-23129# International Centre for Theoretical Physics, Trieste (Italy).
GALILEI-ISOTOPIC SYMMETRIES
R. M. Santilli Sep. 1991 14 p
(DE92-615261; IC-91/263) Avail: NTIS HC/MF A03

We construct the most general known classical, nonlinear and nonlocal generalization of the conventional Galilei transformations, as well as the corresponding classical realization of the infinite family of Galilei-isotopic symmetries G(3.1) proposed in preceding works, under the condition that they result to be all locally isomorphic to the conventional Galilei symmetry. The symmetries G(3.1) are then used to characterize the largest possible class of nonlinear, nonlocal and nonhamiltonian Newtonian systems which still verify the conservation laws of all ten, total, physical quantities, as preparatory grounds for subsequent operator studies for the hadronic structure. The method for the explicit construction of the space-time isosymmetries G(3.1) from given Galilei-noninvariant equations of motion is outlined. DOE

N92-23182# Technische Univ., Twente (Netherlands). Faculty of Applied Mathematics.
GEOMETRY OF DIFFERENTIAL DIFFERENCE EQUATIONS
G. F. Helminck and G. F. Post Sep. 1991 38 p
(PB92-148774; MEMO-999) Avail: NTIS HC/MF A03 CSCL 12A

To each maximal commuting subalgebra h of g(l sub m)(c) is associated a system of differential difference equations, generalizing several known systems. Starting from a Grassmann manifold, solutions are constructed, their properties are discussed, and the relation with other systems is given. Finally, how to express these solutions in r-functions is shown. GRA

N92-23184# Institut des Hautes Etudes Scientifiques, Bures-sur-Yvette (France).
NON-COMMUTATIVE DIFFERENTIAL GEOMETRY AND YANG-BAXTER EQUATION
D. Gurevich, A. Radul, and V. Rubtsov Dec. 1991 19 p
(PB92-149459; IHES/M/91/88) Avail: NTIS HC/MF A03 CSCL 12A

Basic objects of differential geometry (differential forms, vector fields, manifolds, etc) for noncommutative rings, associated with an involutive solution S of Yang-Baxter equation are defined. GRA

N92-23201# Sandia National Labs., Livermore, CA.
A COMPARATIVE STUDY OF PRECONDITIONED LANCZOS METHODS FOR NONSYMMETRIC LINEAR SYSTEMS
C. H. Tong Jan. 1992 34 p
(Contract DE-AC04-76DR-00789)
(DE92-007530; SAND-91-8240) Avail: NTIS HC/MF A03

In this report, numerical results for Lanczos methods for the solution of nonsymmetric linear systems are presented and compared. Numerical examples with varying degrees of difficulty are used. The examples range from convection-diffusion equations to the Harwell-Boeing problem set. Some interesting observations are gathered and a few conclusions are drawn based on these observations. DOE

N92-23248# Vrije Univ., Amsterdam (Netherlands). Subfaculteit Wiskunde en Informatica.
SOME TOPOLOGICAL PROBLEMS I MET
M. Husek Mar. 1991 14 p
(PB92-149327; WS-378) Avail: NTIS HC/MF A03 CSCL 12A

Ten topological problems that I have considered over the years are presented. Problems 3, 4, 5, 9, and 10 are connected to so called categorical topology; they are related to categorical notions like reflectivity, injectivity, simplicity, etc. However, one may completely forget such relations as the basic nature of the problems is purely topological; the categorical lookmay of course help to find a solution. In fact, the well-known topological problem 2 is 'categorical' because it deals with products of reflections. GRA

N92-23249# Vrije Univ., Amsterdam (Netherlands). Subfaculteit Wiskunde en Informatica.
ISOMETRIC EMBEDDING OF MEDIAN ALGEBRAS INTO L1 (mu) SPACES
M. vandeVel and E. Verheul Sep. 1991 14 p
(PB92-149343; WS-384) Avail: NTIS HC/MF A03 CSCL 12A

The class of median metric spaces is known to include examples ranging from L(sub 1)(mu) spaces and K(sub 1)(mu) spaces to valuated lattices and collapsible polyhedra. It is shown that the first-named types are universal in the sense that each median metric space can be isometrically embedded into one of that type. Moreover, if a median metric space can be embedded in l(sub 1)(n) as a median subalgebra, then it embeds isometrically into l(sub 1)(n). GRA

N92-23250# Vrije Univ., Amsterdam (Netherlands). Subfaculteit Wiskunde en Informatica.
SMALL SOLUTIONS AND COMPLETENESS FOR LINEAR FUNCTIONAL DIFFERENTIAL EQUATIONS
S. M. Verduyn Lunel Aug. 1991 24 p Prepared in cooperation with Georgia Inst. of Tech., Atlanta
(PB92-149350; WS-383) Avail: NTIS HC/MF A03 CSCL 12A

A class of unbounded operators is presented that, in particular, contains the generator for functional differential equations. It is possible for this class of operators to state necessary and sufficient conditions in order to have a complete system of eigenfunctions and generalized eigenfunctions. As an illustration of the abstract result, both autonomous and periodic functional differential equations are considered. In particular, if the delays are integer multiples of the period, the necessary and sufficient conditions are presented in order to have a complete system of Floquet solutions. GRA

N92-23329# Brookhaven National Lab., Upton, NY.
A MULTILEVEL PRECONDITIONER FOR DOMAIN DECOMPOSITION BOUNDARY SYSTEMS
J. H. Bramble, J. E. Pasciak, and Jinchao Xu 11 Dec. 1991 12 p Presented at the 10th International Conference on Computing Methods in Applied Sciences and Engineering, Paris (France), 11-14 Feb. 1992
(Contract DE-AC02-76CH-00016)
(DE92-008055; BNL-46984; CONF-920213-1) Avail: NTIS HC/MF A03

In this note, we consider multilevel preconditioning of the reduced boundary systems which arise in nonoverlapping domain decomposition methods. It is shown that the resulting preconditioned systems have condition numbers which are bounded in the case of multilevel spaces on the whole domain and grow most proportional to the number of levels in the case of multilevel boundary spaces without multilevel extensions into the interior. DOE

N92-23331# International Centre for Theoretical Physics, Trieste (Italy).
SHEAVES OF SCHWARTZ DISTRIBUTIONS
B. P. Damyanov Sep. 1991 29 p
(DE92-615217; IC-91/272) Avail: NTIS HC/MF A03

The theory of sheaves is a relevant mathematical language for describing the localization principle, known to be valid for the Schwartz distributions (generalized functions). After introducing some fundamentals of sheaves and the basic facts about distribution spaces, the distribution sheaf D(sub (Omega)) of topological C-vector spaces over an open set (Omega) in R(sup n) is systematically studied. A sheaf D(sub M) of distributions on a C(sup infinity) manifold M is then introduced, following a definition of Hoermander's for its particular elements. Further, a general definition of sheaves on a manifold, that are locally isomorphic to (or, modelled on) a sheaf on R(sup n), in proposed. The sheaf properties of D(sub M) are studied and this sheaf is shown to be locally isomorphic to D(sub Omega), as a sheaf of topological vector spaces. DOE

N92-23335# International Centre for Theoretical Physics, Trieste (Italy).
ON THE STONE-WEIERSTRASS THEOREM FOR SCALAR AND VECTOR VALUED FUNCTIONS
L. A. Khan Sep. 1991 5 p
(DE92-616916; IC-91/257) Avail: NTIS HC/MF A01

In this paper we discuss the formulation of the Stone-Weierstrass approximation theorem for vector-valued functions and then determine whether the classical Stone-Weierstrass theorem for scalar-valued functions can be deduced from the above one. We also state some open problems in this area. DOE

N92-23440# Helsinki Univ. of Technology, Espoo (Finland). Digital Systems Lab.
COMPOSITIONALITY AND ANALYSIS OF ALGEBRAIC HIGH-LEVEL NETS
J. Lilius Oct. 1991 83 p
(PB92-143551; ISBN-951-22-0828-8; SER-A-16) Avail: NTIS HC/MF A05 CSCL 12A

Three aspects of net theory are discussed: compositionality of nets, analysis of nets, and high-level nets. Net theory has often been criticized for the difficulty of giving a compositional semantics to a net. The problem from a category theoretic point of view is discussed. In category theory, compositionality is represented by colimits. How a high-level net can be mapped into a low-level net that represents its behavior is shown. The construction is functorial and preserves colimits, giving a compositional reasoning with high-level nets. Linear logic is a recently discovered logic that has many interesting properties. From a net theoretic point of view, its interest lies in the fact that it is able to express resources in an analogous manner to nets. Several interpretations of Petri nets in terms of linear logic exist. A model theoretic interpretation where the behavior of the net gives a model of linear logic is studied. The construction is extended to cover the algebraic high-level nets defined in the work. GRA

N92-23502# International Centre for Theoretical Physics, Trieste (Italy).
ON SOME TYPES OF RIEMANNIAN V(SUB N) WITH ZERO RICCI CURVATURE
M. S. Rahman Sep. 1991 8 p
(DE92-616917; IC-91/312) Avail: NTIS HC/MF A02

A Riemannian V(sub n) with zero Ricci curvature is characterized and the reason why the V(sub 2) and V(sub 3) are excluded from the class of spaces is explained. The case for a V(sub n) to be a space of zero Ricci curvature is studied. The conditions that cause a V(sub n) of zero Ricci curvature to be flat are found. A few results on the space satisfying some other curvature conditions are then derived. DOE

N92-23511# National Inst. of Standards and Technology, Gaithersburg, MD. Applied and Computational Mathematics Div.
CONFIDENCE INTERVALS FOR DISCRETE APPROXIMATIONS TO ILL-POSED PROBLEMS
B. W. Rust and D. P. OLeary Jan. 1992 41 p
(PB92-143742; NISTIR-4720) Avail: NTIS HC/MF A03 CSCL 12A

The authors consider the linear regression model obtained by discretizing a system of first kind integral equations with random measurement errors in the right hand side. The errors are assumed to have zero means and known variances. The authors consider the problem of estimating confidence intervals for linear functions of a solution vector. For such problems, the least squares solution is a highly unstable function of the measurements, and the classical confidence intervals are too wide to be useful. The solution can often be stabilized by imposing physically motivated, a priori nonnegativity constraints on the solution. It is shown how to extend the classical confidence interval estimation procedure to accommodate these nonnegativity constraints in order to obtain improved confidence intervals. The technique defines valid confidence intervals even for problems with fewer measurements than unknowns. Author

N92-23514# Technische Univ., Delft (Netherlands). Faculty of Geodetic Engineering.
ANALYSIS OF ORDERING SCHEME FOR THE UNKNOWNS DURING THE SOLVING OF GEODETIC LEAST SQUARES SYSTEMS
P. J. deJonge Jul. 1991 87 p
(PB92-137355; Rept-91-4) Avail: NTIS HC/MF A05 CSCL 12A

The order in which the unknowns are treated during a Choleski factorization, for instance during the solving of geodetic least squares systems, is an important performance parameter for sparse systems. Here, a number of schemes, or algorithms, to derive a 'good' ordering are investigated. The ordering schemes can be divided into two groups: those that try to minimize the number of new nonzero elements in the Choleski factor, and those that try to minimize the size of the envelope of this factor. Examples of the first category are the minimum degree and the nested dissection schemes. Envelope minimizing schemes which have been analyzed are the reverse Cuthill-McKee and banker's schemes. These ordering schemes are described and the results of their application to some normal matrices of geodetic least squares adjustments are given. The authors have applied them to normal matrices of the adjustment of 2D geodetic terrestrial networks, normal matrices of photogrammetric bundle-block adjustments, and a normal matrix of a photogrammetric adjustment with independent models. For the ordering of the normal matrix of an adjustment of a 2D geodetic terrestrial network, some strategies have been developed which use a priori information to reduce the time needed for the ordering. Author

N92-23579# Fermi National Accelerator Lab., Batavia, IL.
GENERAL P-T FIT CONSTRUCTION FOR He, N2, Ar, H2 AND Ne VPT USED AT FERMILAB
M. Geynisman and J. Makara Jan. 1992 9 p
(Contract DE-AC02-76CH-03000)
(DE92-008851; FNAL-TM-1767) Avail: NTIS HC/MF A02

Polynomial fits are constructed for Fermilab Tevatron vapor pressure thermometers (VPT) for use with ACNET database. Fit coefficients and P-T graphs are included. Fits cover the VPT saturation region and the gas region. The thermodynamic analysis of VPT bulb is used to define transition points for each cryogenic VPT with given geometry and 'charge' conditions. The methodology is described to repeat fit construction calculations for any geometry and 'charge' conditions if required. DOE

N92-23589# Helsinki Univ. of Technology, Espoo (Finland). Inst. of Mathematics.
THEORY FOR ITERATIVE SOLUTION OF LARGE DYNAMICAL SYSTEMS USING PARALLEL COMPUTATION Ph.D. Thesis
U. Miekkala Nov. 1991 130 p Sponsored by Suomen Akatemja, Helsinki
(PB92-143304; RR-A304; ISBN-951-22-0846-6) Avail: NTIS HC/MF A07 CSCL 12A

The development of parallel computers has increased interest on iterative methods for solving large systems of differential equations. Such methods are extensions of the classical Picard-Lindelof iteration, and they are also known as waveform relaxation or dynamic iteration methods. Convergence studies of Picard-Lindelof type iteration methods are summarized. GRA

N92-23599# Institut des Hautes Etudes Scientifiques, Bures-sur-Yvette (France).
EXISTENCE OF CLOSED GEODESICS ON 2-SPHERES
V. Bangert Dec. 1991 16 p
(PB92-149434; IHES/M/91/92) Avail: NTIS HC/MF A03 CSCL 12A

Previously, J. Franks proves the existence of infinitely many closed geodesics for every Riemannian metric on S sup 2 which satisfies the following condition: there exists a simple closed geodesic for which Birkhoff's annulus map is defined. In particular, all metrics with positive Gaussian curvature have this property. Here, the existence is proved of infinitely many closed geodesics for every Riemannian metric on S sup 2 which has a simple closed geodesic for which Birkhoff's annulus map is not defined. Combining this with J. Franks' result and with the fact that every Riemannian metric on S sup 2 has a simple closed geodesic, one obtains the existence of infinitely many closed geodesics for every Riemannian metric on S sup 2. Author

N92-23658# Helsinki Univ. of Technology, Espoo (Finland). Inst. of Mathematics.
SENSITIVITY I(SUP 1) MINIMIZATION WITH BOUNDARY ZEROS OR POLES
O. J. Staffans Oct. 1991 17 p Prepared in cooperation with Virginia Polytechnic Inst. and State Univ., Blacksburg
(PB92-141803; RR-A301; ISBN-951-22-0803-2) Avail: NTIS HC/MF A03 CSCL 12A

The linear programming approach to the solution of a discrete-time mixed sensitivity minimization problem in the l(sup 1)-norm is discussed. It is shown that in the presence of boundary zeros or poles, the minimization of a weighted combination of the norms of S and I-S does not lead to a satisfactory system response function. A natural alternative approach when there are boundary zeros or poles is to take also CS or PS, respectively, into account. In particular, they show that if the full system transfer matrix is included in the minimization process, then no discrete interpolation conditions are needed, and an optimal solution always exists. Moreover, the dual solution method for the resulting linear programming system can be implemented in a very straightforward way. GRA

N92-23670# Institut des Hautes Etudes Scientifiques, Bures-sur-Yvette (France).
FAMILY OF POISSON STRUCTURES ON COMPACT HERMITIAN SYMMETRIC SPACES
S. Khoroshkin, A. Radul, and V. Rubtsov Dec. 1991 19 p Prepared in cooperation with Academy of Sciences (USSR), Moscow
(PB92-149442; IHES/M/91/91) Avail: NTIS HC/MF A03 CSCL 12A

The work is the first part of a program devoted to obtaining a better understanding of the interrelations between the geometry of a Poisson manifold and both classical and quantum symmetries of field theoretical models. By a well-known prescription of Kirillov-Kostant-Souriau, coadjoint orbits O of a compact semi-simple Lie group G have a natural symplectic structure and hence are Poisson manifolds. The developments of the Poisson-Lie group theory make it possible to introduce another Poisson structure on O which is introduced from the Poisson-Lie structure on the compact semi-simple Lie group G. These structures are denoted by pi(sub Kir) and pi(sub G) respectively. The main result is to show that pi(sub Kir) and pi(sub G) are coordinated (or compatible) on the orbit O if O is a hermitian compact symmetric space occurring in the Cartan list. GRA

N92-23738 Washington Univ., Seattle.
THE DISCONTINUOUS FINITE ELEMENT METHOD WITH THE TAYLOR-GALERKIN APPROACH FOR NONLINEAR HYPERBOLIC CONSERVATION LAWS Ph.D. Thesis
Kyu Yearl Choe 1991 206 p
Avail: Univ. Microfilms Order No. DA9131624

A one step, explicit finite element scheme which is second order accurate in both time and space is developed for the computation of weak solutions of nonlinear hyperbolic conservation laws. The scheme is an improved version of the discontinuous finite element (Discontinuous Galerkin) method using the Taylor-Galerkin procedure. It is linearly stable under a fixed Courant-Friedrichs-Lewy (CFL) number up to nearly 0.4 (or 1/2 for the alternative two step explicit scheme also developed here) and TVDM which guarantees convergence to a weak solution in nonlinear problems when the flux limiter is applied with the CFL number up to 0.366 (or 1/2 for the two step scheme) in one dimension. The scheme is easily extended to multi-dimensions by approximating the two-dimensional Riemann problem and using the extended flux limiter. No special treatment is required for the refined elements when using an adaptive finite element method. Numerical experimentation demonstrates the overall improvement in solution quality and the convergence of the solution to the entropy one even for non-convex flux cases. The scheme captures stationary discontinuities perfectly. Dissert. Abstr.

N92-23745# International Centre for Theoretical Physics, Trieste (Italy).
LIE-ADMISSIBLE STRUCTURE OF HAMILTON'S ORIGINAL EQUATIONS WITH EXTERNAL TERMS
R. M. Santilli Sep. 1991 13 p
(DE92-615216; IC-91/266) Avail: NTIS HC/MF A03

As a necessary additional step in preparation of our operator studies of closed nonhamiltonian systems, in this note we consider the algebraic structure of the original equations proposed by Lagrange and Hamilton, those with external terms representing precisely the contact nonpotential forces of the interior dynamical problem. We show that the brackets of the theory violate the conditions to characterize any algebra. Nevertheless, when properly written, they characterize a covering of the Lie-isotopic algebras called Lie-admissible algebras. It is indicated that a similar occurrence exists for conventional operator treatments, e.g. for nonconservative nuclear cases characterized by nonhermitean Hamiltonians. This occurrence then prevents a rigorous treatment of basic notions, such as that of angular momentum and spin spin, which are centrally dependent on the existence of a consistent algebraic structure. The emergence of the Lie-admissible algebras is therefore expected to be unavoidable for any rigorous operator

treatment of open systems with nonlinear, nonlocal and nonhamiltonian external forces. DOE

N92-24039# International Centre for Theoretical Physics, Trieste (Italy).
CLOSED SYSTEMS WITH NONHAMILTONIAN INTERNAL FORCES
R. M. Santilli Sep. 1991 16 p
(DE92-619234; IC-91/259) Avail: NTIS HC/MF A03

In a preceding paper, we have treated the inequivalence between the exterior (local, potential and selfadjoint) problem, and the interior (nonlocal, nonhamiltonian and nonselfadjoint) problem. In this note, we treat their compatibility via the notion of closed nonselfadjoint systems, i.e. systems which verify all conventional total conservation laws when isolated from the rest of the Universe; yet their interior structure is nonlinear, nonlocal and nonhamiltonian. The generalized analytic, algebraic and geometrical formulations needed for their treatment are identified, jointly with their direct universality for the case of nonlinear and nonhamiltonian internal forces in local approximation. This allows the technical identification of the open problems for subsequent consideration. DOE

N92-24061# Institut des Hautes Etudes Scientifiques, Bures-sur-Yvette (France).
SPHERE PACKINGS CENTERED AT S-UNITS OF ALGEBRAIC TORI
Boris E. Kunyavskii (Saratov Inst. for Mechanization in Agriculture, USSR) Oct. 1991 18 p
(PB92-136373; IHES/M/91/70) Avail: NTIS HC/MF A03
CSCL 12A

This is inspired by a series of articles introducing several new explicit constructions of dense sphere packings in R(sup n) which have good asymptotic properties while n tends to infinity. A generalization of these constructions is presented. The main idea is to consider the group of S-units of an algebraic torus defined over a global field and to embed the torsion-free component of this finitely generated group into R(sup n) with the help of the logarithmic map (in the case of a number ground field), or the divisorial map (in the case of a function field). For the trivial torus T = G(sub m) it is nothing but a construction of (R/Ts). The resulting lattice in R(sup n) generates a sphere packing whose parameters can be estimated while investigating arithmetical properties of algebraic tori. The key points are the (generalized) Dirichlet unit theorem valid for S-units of algebraic tori and some class number relations. GRA

N92-23964*# Temple Univ., Philadelphia, PA. Dept. of Mathematics.
MATHEMATICAL ANALYSIS TECHNIQUES FOR MODELING THE SPACE NETWORK ACTIVITIES
Lisa M. Foster *In* NASA. Goddard Space Flight Center, Summer Graduate Research Program for Interns in Science and Engineering 24 Mar. 1992 23 p (For primary document see N92-23958 14-99)
Avail: NTIS HC/MF A12 CSCL 12A

65 STATISTICS AND PROBABILITY

Includes data sampling and smoothing; Monte Carlo method; and stochastic processes.

N92-23731# Tilburg Univ. (Netherlands).
DENSITY OF THE F-STATISTIC IN THE LINEAR MODEL WITH ARBITRARILY NORMAL DISTRIBUTED ERRORS
B. B. vanderGenugten 1992 20 p
(PB92-128792; FEW-500) Avail: NTIS HC/MF A03 CSCL 12A

The density is examined of the F-statistic in the context of a linear model with normal distributed errors. The covariance matrix of the errors is arbitrary. The result is useful in the study of robustness of the F-test with respect to errors of the first and second kind. An explicit expression for this density is given in the form of a proper Riemann integral on a finite interval, suitable for numerical calculation. Author

N92-23777 North Carolina State Univ., Raleigh.
ANALYSIS OF TIME SERIES WITH MISSING VALUES Ph.D. Thesis
Michael Edward Wisniewski 1991 144 p
Avail: Univ. Microfilms Order No. DA9130602

The purpose of this research is to evaluate imputation with interpolated values as a solution to the problem of estimating the spectral density for time series with missing values. This solution produces asymptotically biased estimates of the spectral density; however, the solution is easy to implement. Also, these estimates of the spectral density are positive, a property that the alternatives lack, which is crucial for application of the spectral density in certain interpolation and projection procedures. Imputation procedures are evaluated by simulation. Results indicate that imputation using linearly interpolated values produces an acceptable estimate of the spectral density. It is recommended for use because of its ease of implementation. Also, other interpolation procedures, such as thin plate spline and minimum mean square linear interpolation, are evaluated. These methods do not produce better results and are more difficult to implement. United States unemployment data from 1948 to 1969 are used as an example to illustrate the results. These methods are extended for spatial series with periodic missing values. Also, the classical method developed by Jones and Parzen is extended for spatial series. The uniformity trial data of Mercer and Hall (1911) is used to illustrate these procedures. Linear interpolation is also recommended for use in spatial series because it is easy to apply. Dissert. Abstr.

N92-24008 ESDU International Ltd., London (England).
THE STATISTICAL ANALYSIS OF DATA FROM NORMAL DISTRIBUTIONS, WITH PARTICULAR REFERENCE TO SMALL SAMPLES
Dec. 1991 29 p Supersedes ESDU-68014; ESDU-68016; ESDU-68017
(ESDU-91041; ESDU-68014; ESDU-68016; ESDU-68017; ISBN-0-85679-803-7; ISSN-0141-4089; ISSN-9058-0379; ISSN-0141-4097) Avail: ESDU

ESDU 91041 explains the analysis of samples of less than 30 to predict the behavior of the population. The analysis includes the prediction of mean values, standard deviations, percentiles, and coefficients of variation. Also included is a method for comparison of samples which is particularly useful if it can be used to show two small samples may be combined into one larger sample so improving the accuracy of the predictions. It is also useful when comparing the influence of design changes. Tables of the required statistics are included and equations are provided that allow less commonly used statistics to be estimated to an acceptable engineering accuracy. A fully worked example illustrates the major facets of the analysis of small samples. ESDU

66 SYSTEMS ANALYSIS

Includes mathematical modeling; network analysis; and operations research.

N92-23505# Technische Univ., Twente (Netherlands). Faculty of Applied Mathematics.
STOCHASTIC GAMES WITH AVERAGE PAYOFF CRITERION
M. K. Ghosh and A. Bagchi Jul. 1991 28 p
(PB92-148634; Memo-985) Avail: NTIS HC/MF A03 CSCL 12B

Two person stochastic games were studied on a Polish state and compact action spaces and with average payoff criterion action under a certain ergodicity condition. For a zero sum game, the existence is established of a value and stationary optimal strategies for both players. For a nonzero sum case, the existence of Nash

equilibrium in stationary strategies is established under certain separability conditions. Author

67 THEORETICAL MATHEMATICS

Includes topology and number theory.

N92-23207# International Centre for Theoretical Physics, Trieste (Italy).
AN EXCEPTIONAL N=8 SUPERCONFORMAL ALGEBRA IN TWO DIMENSIONS ASSOCIATED WITH F(4)
E. S. Fradkin and V. Ya. Linetsky Oct. 1991 9 p
(DE92-616991; IC-91/348) Avail: NTIS HC/MF A02

An exceptional N=8 superconformal algebra in two dimensions is constructed. It includes a multiplet of Kac-Moody currents in the adjoint representation of Spin(7) and a multiplet of supercurrents in the spinor representation of Spin(7), besides the energy-momentum tensor. It involves both central terms and quadratically non-linear terms in the supercommutators. The Moebius subsuperalgebra is reduced to F(4). The existence of the entire construction is accounted for by the remarkable properties of octonions. DOE

70 PHYSICS (GENERAL)

For precision time and time interval (PTTI) see *35 Instrumentation and Photography;* for geophysics, astrophysics or solar physics see *46 Geophysics, 90 Astrophysics,* or *92 Solar Physics.*

N92-23220# International Centre for Theoretical Physics, Trieste (Italy).
A PROBABILISTIC MECHANISM HIDDEN BEHIND THE UNIVERSAL POWER LAW FOR DIELECTRIC RELAXATION. PART 1: GENERAL RELAXATION EQUATION
K. Weron Aug. 1991 24 p
(DE92-615484; IC-91/246) Avail: NTIS HC/MF A03

A new model for the explanation of the universal dielectric response law is proposed. It differs significantly from all previous works on the subject. The presented model is based on the assumption that individual dipoles and their environment do not remain independent during the process of relaxation. Therefore, the time, theta(sub i), needed for the regression to equilibrium of polarization fluctuations in a random variable which depends for each relaxing dipole on two other random variables: the waiting time, eta(sub i), and the dissipation rate, beta(sub i). As a consequence, we derive a general relaxation equation which gives the universal dielectric response in the power law form (as a special case the stretched exponential form is obtained). DOE

N92-23556*# Lehigh Univ., Bethlehem, PA.
A STUDY OF ALUMINUM-LITHIUM ALLOY SOLIDIFICATION USING ACOUSTIC EMISSION TECHNIQUES Ph.D. Thesis, 1991
Daniel P. Henkel Washington NASA. Langley Research Center Apr. 1992 206 p
(Grant NGT-50417)
(NASA-CR-4437; NAS 1.26:4437) Avail: NTIS HC/MF A10 CSCL 20C

Physical phenomena associated with the solidification of an aluminum lithium alloy was characterized using acoustic emission (AE) techniques. It is shown that repeatable patterns of AE activity may be correlated to microstructural changes that occur during solidification. The influence of the experimental system on generated signals was examined in the time and frequency domains. The analysis was used to show how an AE signal from solidifying aluminum is changed by each component in the detection system to produce a complex waveform. Conventional AE analysis has shown that a period of high AE activity occurs in pure aluminum, an Al-Cu alloy, and the Al-Li alloy, as the last fraction of solid forms. A model attributes this to the internal stresses of grain boundary formation. An additional period of activity occurs as the last fraction of solid forms, but only in the two alloys. A model attributes this to the formation of interdendritic porosity which was not present in the pure aluminum. The AE waveforms were dominated by resonant effects of the waveguide and the transducer. Author

N92-23598# International Centre for Theoretical Physics, Trieste (Italy).
A PROBABILISTIC MECHANISM HIDDEN BEHIND THE UNIVERSAL POWER LAW FOR DIELECTRIC RELAXATION. PART 2: DISCUSSION OF THE RESPONSE FUNCTION
K. Weron Aug. 1991 19 p
(DE92-615485; IC-91/247) Avail: NTIS HC/MF A03

This paper is a continuation of our previous work, where the new probabilistic model based directly on the reaction picture of relaxation was introduced and a general relaxation equation was derived. Here we show the universal character of distributions of damping rates and waiting times used in this model. Moreover, we discuss in detail a physical significance of the response function derived as a solution of the general relaxation equation. DOE

N92-23665# Helsinki Univ. of Technology, Espoo (Finland). Low Temperature Lab.
ULTRASONIC INVESTIGATION OF (3)He-A VORTICES IN LOW MAGNETIC FIELDS
K. Torizuka, J. P. Pekola, and A. J. Manninen 8 Aug. 1991 60 p Sponsored in part by Suomen Akatemja, Helsinki; and Akad. Nauk SSSR, Moscow
(PB92-142256; TKK-F-A691) Avail: NTIS HC/MF A04 CSCL 20C

The authors report ultrasonic measurements on rotating (3)He-A at 26.7 bar pressure and at magnetic fields below 12.0 mT. They observed two distinct types of vortices: the attenuation of zero sound by vortices which were created at small fields is higher than the attenuation by vortices created at high fields. The first order transition between the two vortex states was observed at H(sub c) approximately H(sub D) (approx. = 3 mT). The low field structure can be identified with type-1 vortices proposed by Fujita et al. and the high field one with that of Seppala and Volovik and initially discovered in nuclear magnetic resonance (NMR) experiments. The structural change may be viewed as a topological transition, because the d-vector distribution is different for the dipole locked vortices in low fields from that for the dipole unlocked vortices in high fields. In addition, a continuous change between coreless vortices and vortices with a well defined core was observed at low enough fields H' much less than H(sub c). The vortices in (3)He-A can, therefore, be characterized by three magnetic fields: H', H(sub c), and H(sub c1). The last is the catastrophic field at which the dipole locked vortices become unstable. GRA

71 ACOUSTICS

Includes sound generation, transmission and attenuation. For noise pollution see *45 Environmental Pollution.*

N92-23170# Southampton Univ. (England). Inst. of Sound and Vibration Research.
A FREQUENCY DOMAIN LEAST SQUARES METHOD FOR MODELLING ACOUSTIC FIELDS
M. Anciant, P. A. Nelson, and J. K. Hammond Jul. 1991 74 p
(ISVR-TR-196; ETN-92-91196) Avail: NTIS HC/MF A04

The reduction of the noise around the cap of Ariane 4 and more especially inside the cap is a critical problem when the rocket is launched. At this moment, the external noise level which is generated by the propulsor engines reaches nearly 150 dB. The satellites placed inside of the cap are then exposed to an intensive acoustic field which can be the source of unsuitable and dangerous vibrations for the material on board. The contribution of the airborne sound to the vibrations of the satellites is as significant as the one directly transmitted by the structure. The least squares method, used to estimate the linear and nonlinear

parameters of a deterministic acoustic source model, in the frequency domain is introduced and discussed. The linear parameters of the sources are their strength, since the nonlinear parameters may be, for example, the angles of arrival of plane waves or the spatial location of point sources. Two types of model are considered, one with plane waves (1, 2, and more...), and the other with one point source. A series of cost functions depending on the nonlinear parameters are presented, assuming in each case, that the data are produced by a pure tone source (without noise) of the same type as the model considered. The effect of the number of sensors, the sensor location and the frequency on the cost function is studied. From an optimization point of view, it is useful to get a smoothly varying cost function, preferably with no local minima. In this respect, the estimation of parameters common to one band of frequency is investigated for the single point source model. With regard to a multiple plane wave model, some properties of the cost function in N dimensional space are presented, and some ambiguities which can appear in the calculation of the cost function are shown. ESA

N92-23588# National Aerospace Lab., Amsterdam (Netherlands).
EVALUATION OF THE APPLICABILITY OF HELMHOLTZ RESONATORS FOR LOW FREQUENCY ACOUSTIC LINERS
J. M. M. vanderWal 19 Sep. 1988 39 p
(PB92-138544; NLR-TR-88148-U) Avail: NTIS HC/MF A03 CSCL 20A

A literature study was performed on the acoustic behavior of those Helmholtz resonator type liners which are most promising for low frequency sound absorption in aero-engine applications. The equations for the acoustic impedance of various types of Helmholtz resonators were analyzed as well as the conditions for the validity of these equations. An experimental program is defined for a further analysis of various types of resonators. GRA

N92-23726 Pennsylvania State Univ., University Park.
EXPERIMENTAL STUDY OF THE MECHANISM OF SOUND GENERATION BY ROTATING STALL IN CENTRIFUGAL TURBOMACHINES Ph.D. Thesis
Luc Mongeau 1991 258 p
Avail: Univ. Microfilms Order No. DA9127385

Experiments were conducted in order to investigate the aerodynamic sound generating mechanisms in centrifugal turbomachines. A facility consisting of a centrifugal water pump impeller with a variable discharge configuration and an inlet duct was designed and built for the experiments. Air is used as the fluid medium. The inlet duct provides a controlled, quiet inflow to the impeller. Measurements of the acoustic noise radiated in the pump surroundings were made in parallel with fluid dynamic measurements in order to establish correlations. The most significant conclusion reached is that a form of rotating stall dominates the voice signature in various configurations with no outlet diffuser or casing. The sequence of experiments that led to this finding is analyzed and presented in detail. Dissert. Abstr.

N92-23790# Intespace, Toulouse (France).
ACOUSTIC ABSORPTION DUE TO SPECIMEN IN TEST IN A REVERBERANT CHAMBER
A. Girard and C. Blanchard *In* ESA, Spacecraft Structures and Mechanical Testing, Volume 1 Oct. 1991 p 71-75 (For primary document see N92-23780 14-18)
(Contract ESA-7821/88)
Copyright Avail: NTIS HC/MF A21

N92-23791# MATRA Espace, Toulouse (France). Dept. of Mechanical Engineering.
MAXIMAL MODAL ENERGY METHOD: AN OVERVALUING TOOL FOR LOW FREQUENCY PREDICTION OF STRUCTURE ACOUSTIC RESPONSE
B. Laviron, P. Herman, and S. DeZotti *In* ESA, Spacecraft Structures and Mechanical Testing, Volume 1 Oct. 1991 p 77-82 (For primary document see N92-23780 14-18)
Copyright Avail: NTIS HC/MF A21

N92-23792# Industrieanlagen-Betriebsgesellschaft m.b.H., Ottobrunn (Germany, F.R.).
NUMERICAL AND EXPERIMENTAL STUDY OF NOISE GENERATED BY A VIBRATING PLATE
O. vonEstorff, A. Homm, and F. Bartels (Fraunhofer-Forschungsgruppe fuer Hydroakustik, Ottobrunn, Germany, F.R.) *In* ESA, Spacecraft Structures and Mechanical Testing, Volume 1 Oct. 1991 p 83-87 (For primary document see N92-23780 14-18)
Copyright Avail: NTIS HC/MF A21

72 ATOMIC AND MOLECULAR PHYSICS

Includes atomic structure, electron properties, and molecular spectra.

N92-23217# Colorado Univ., Boulder. Dept. of Astrophysical, Planetary, and Atmospheric Sciences.
PARTICLE DYNAMICS IN A WAVE WITH VARIABLE AMPLITUDE
J. R. Cary Jan. 1992 57 p
(Contract DE-FG02-86ER-40302)
(DE92-008340; DOE/ER-40302/6) Avail: NTIS HC/MF A04

Our past research efforts led to the derivation of the adiabatic invariant in spatially varying accelerator structures, to the calculation of the loss of the invariant due to trapping, and to a method for determining transverse invariants using a nonperturbative approach to the Hamilton-Jacobi equation. These research efforts resulted in the training of two graduate students who are now working in the area of accelerator physics. DOE

N92-23274# Gosudarstvennyi Komitet po Ispolzovaniyu Atomnoi Energii, Serpukhov (USSR). Inst. Fiziki Vysokikh Ehnergij.
THRESHOLDS OF LONGITUDINAL INSTABILITY OF BUNCHED BEAM IN THE PRESENCE OF DOMINANT INDUCTIVE IMPEDANCE
V. I. Balbekov and S. V. Ivanov 1991 24 p
(DE92-617992; IHEP-OUNK-91-14; IFVE-OUNK-91-14) Avail: NTIS HC/MF A03

The paper studied thresholds of multipole instability of a bunch under the assumption that all its oscillation eigen-modes are completely determined by a dominating low-frequency inductance of the vacuum chamber. The acceptable value of its impedance is found to coincide through stability of microwave oscillations multiplied by the value of the relative inside-the-bunch spread of synchrotron frequencies. The effect of stationary space charge self-fields is also estimated. DOE

N92-23277# Oak Ridge National Lab., TN.
STATIC MULTIPOLE DEFORMATIONS IN NUCLEI
W. Nazarewicz 1991 29 p Presented at the International School of Nuclear Physics on 4Pi High Resolution Gamma-Ray, Erice (Italy), 20-28 Sep. 1991
(Contract DE-AC05-84OR-21400)
(DE92-008250; CONF-9109332-3) Avail: NTIS HC/MF A03

The physics of static multipole deformations in nuclei is reviewed. Nuclear static moments result from the delicate balance between the vibronic Jahn-Teller interaction (particle-vibration coupling) and the residual interaction (pairing force). Examples of various permanent nuclear deformations are discussed. DOE

N92-23327# Stanford Linear Accelerator Center, CA.
RECENT RESULTS ON K(OMEGA) AND (PI)(PI) SYSTEMS FROM LASS
D. Aston, T. Bienz, F. Bird, W. Dunwoodie, W. B. Johnson, P. Kunz, Y. Kwon, D. W. G. S. Leith, L. Levinson, and B. N. Ratcliff et al Dec. 1991 2 p Presented at the 4th International Conference on Hadron Spectroscopy, College Park, MD, 12-16 Aug. 1991
(Contract DE-AC03-76SF-00515)
(DE92-007389; SU-SLAC-PUB-5722; CONF-910864-10) Avail: NTIS HC/MF A01

Preliminary results from ongoing analyses of the K(exp minus) omega and the hypercharge exchange produced pi (exp -) pi (exp +) systems are presented. The data described are taken from a 4.1 event/nb exposure of the LASS spectrometer to an 11 GeV/cK(exp -) beam. DOE

N92-23328# Argonne National Lab., IL. High Energy Physics Div.

SEARCH FOR ATMOSPHERIC NEUTRINO OSCILLATIONS WITH THE SOUDAN 2 DETECTOR

D. M. Roback (Minnesota Univ., Minneapolis.) 20 Jan. 1992 6 p Presented at the Workshop on Long-Baseline Neutrino Oscillations, Batavia, IL, 17-20 Nov. 1991

(Contract W-31-109-eng-38)

(DE92-007397; ANL-HEP-CP-92-03; CONF-9111141-3) Avail: NTIS HC/MF A02

Underground proton decay detectors record a sizeable number of atmospheric neutrino-induced events. These neutrinos come primarily from the decay of pions and muons produced in cosmic ray showers in the earth's atmosphere. The expected flux ratio of muon neutrinos to electron neutrinos traversing an underground detector, nu sub mu/nu sub e, is about 2. The combined nuclear cross section differences between nu sub mu and nu sub e interactions typically reduce the measured nu sub mu/nu sub e event ratio to about 1. Over the last decade, both the Kamioka detector in Japan and the IMB detector in the United States have made high-statistics measurements of the atmospheric neutrino event ratio. Both groups have presented strong experimental evidence that the underground nu sub mu/nu sub e event ratio is substantially smaller than predicted. In both cases, a statistically significant deficit of muon neutrino-induced events is measured. One possible explanation of the muon neutrino deficit is that these neutrinos are undergoing flavor oscillations between their production points in the atmosphere and their interaction points in underground detectors. An MSW effect interpretation of solar neutrino experiments implies a nu sub e yields nu sub mu oscillation region in delta m(exp 2)-sin(exp 2)(2 theta) space at least two orders of magnitude lower in delta m(exp 2) than the best fit point of the Kamioka result. It is therefore usually assumed that the relevant flavor oscillation for atmospheric muon neutrinos would be nu sub mu yields nu sub r. The Soudan 2 nucleon decay detector is now approaching completion and collecting data. It will be able to make low-background measurements of atmospheric neutrinos in the next few years to check the possibility that atmospheric neutrinos undergo detectable flavor oscillations. DOE

N92-23330# California Univ., Irvine.

INELASTIC ELECTRON SCATTERING FROM SURFACES

S. Y. Tong (Wisconsin Univ., Milwaukee.) and D. L. Mills 1992 10 p

(Contract DE-FG03-84ER-45083)

(DE92-008129; DOE/ER-45083/T1) Avail: NTIS HC/MF A02

This report contains highlights of accomplishments of the past year, for the University of California, Irvine and the University of Wisconsin, Milwaukee collaboration on surface excitations, and their interactions with low energy electrons. In addition, we present a summary of future research to be carried out in the coming grant year. DOE

N92-23448# Toledo Univ., OH. Dept. of Physics and Astronomy.

SEMIEMPIRICAL STUDIES OF ATOMIC STRUCTURE

L. J. Curtis 1992 3 p

(Contract DE-FG05-88ER-13958)

(DE92-008143; DOE/ER-13958/28) Avail: NTIS HC/MF A01

The energy level structure, transition probabilities, and general spectroscopic properties of highly-ionized many-electron systems are studied through the combined use of sensitive semiempirical data systematizations, selected precision experimental measurements, and specialized theoretical computations. Measurements are made primarily through the use of fast ion beam excitation methods, which are combined with available data from laser- and tokamak-produced plasmas, astrophysical sources, and conventional light sources. The experimental studies are strengthened through large scale ab initio calculations. Large blocks of data are predictively systematized and parameterized along isoelectric, homologous, isoionic, Rydberg, and yrast series, to provide a comprehensive and reliable data base. DOE

N92-23450# California Univ., Berkeley. Lawrence Berkeley Lab.

POTENTIAL ENERGY SURFACES AND REACTION DYNAMICS OF POLYATOMIC MOLECULES Ph.D. Thesis

Yan-Tyng Chang Nov. 1991 168 p

(Contract DE-AC03-76SF-00098)

(DE92-008314; LBL-31622) Avail: NTIS HC/MF A08

A simple empirical valence bond (EVB) model approach is suggested for constructing global potential energy surfaces for reactions of polyatomic molecular systems. This approach produces smooth and continuous potential surfaces which can be directly utilized in a dynamical study. Two types of reactions are of special interest, the unimolecular dissociation and the unimolecular isomerization. For the first type, the molecular dissociation dynamics of formaldehyde on the ground eiectronic surface is investigated through classical trajectory calculations on EVB surfaces. The product state distributions and vector correlations obtained from this study suggest very similar behaviors seen in the experiments. The intramolecular hydrogen atom transfer in the formic acid dimer is an example of the isomerization reaction. High level ab initio quantum chemistry calculations are performed to obtain optimized equilibrium and transition state dimer geometries and also the harmonic frequencies. DOE

N92-23577# North Carolina State Univ., Raleigh. Dept. of Physics.

THEORETICAL NUCLEAR REACTION AND STRUCTURE STUDIES USING HYPERONS AND PHOTONS

S. R. Cotanch 1991 6 p

(Contract DE-FG05-88ER-40461)

(DE92-008587; DOE/ER-40461/4) Avail: NTIS HC/MF A02

This report details research progress and results obtained during the 12 month period from January 1991 through 31 December 1991. The research project, entitled 'Theoretical Nuclear Reaction and Structure Studies Using Hyperons and Photons,' is supported by grant DE-FG05-88ER40461 between North Carolina State University and the United States Department of Energy. In compliance with grant requirements the Principal Investigator, Professor Stephen R. Cotanch, has conducted a research program addressing theoretical investigations of reactions involving hyperons and photons. The new, significant research results are briefly summarized in the following sections. DOE

N92-23674 Oxford Univ. (England).

A STUDY OF UNDERGROUND MUONS IN THE SOUDAN 2 DETECTOR Ph.D. Thesis

Lucy Mary Kirby-Gallagher 1990 232 p

Avail: Univ. Microfilms Order No. BRD-93051

An 1100 ton fine grained tracking calorimeter, designed by the Soudan II collaboration, is being constructed in a purpose-built underground laboratory in northern Minnesota, U.S.A. The experiment is situated at a depth of 2090 meters of water equivalent, latitude 47 deg 78 min N and longitude 92 deg 20 min W. During the period from Mar. - Aug. 1989, an equivalent live-time of 0.221 years, the completed 350 tons of the detector was used to collect a sample of 1,222 cosmic ray data runs. Fast track reconstruction software was developed, which determines underground muon trajectories to approximately +/- 1.0 deg. The strict quality control of data imposed prior to a physics analysis is described. After data reduction, the sample to be analyzed contained 452,708 reconstructed single muon tracks. This sample was used to investigate the possibility that the astronomical point source, Cygnus X-3, is an emitter of high energy muons. The integrated excess muon flux was determined by using the data to calculate the expected muon rate from the source direction. A 2.1(sigma) overall excess was observed within a 3 deg half-angle

cone centered on the source, which corresponds to a 90 percent confidence level upper limit on the integrated excess flux of (2.3 +/- 0.1)(10)(exp -11)/sq cm-s. Enhancements of 2.0(sigma) and 2.1(sigma) were also observed in two a priori selected phase bands. Cygnus X-3 underwent two giant radio outbursts in Jun. and Jul. 1989. Evidence was found for a 3.18(sigma) increase in the muon rate, within the two chosen phase bands, subsequent to the initial activity in the radio region. Dissert. Abstr.

N92-23714# Los Alamos National Lab., NM.
FROM GROUND STATE TO FISSION FRAGMENTS: A COMPLEX, MULTI-DIMENSIONAL MULTI-PATH PROBLEM
P. Moeller, J. R. Nix, and W. J. Swiatecki (California Univ., Berkeley. Lawrence Berkeley Lab.) 1992 61 p Presented at the Specialists' Meeting on Physics and Engineering of Fission, Osaka, Japan, 7 Jan. 1991
(Contract W-7405-eng-36)
(DE92-008488; LA-UR-92-578; CONF-920192-1) Avail: NTIS HC/MF A04

Experimental results on the fission properties of nuclei close to Fm-264 show sudden and large changes with a change of only one or two neutrons or protons. The nucleus Fm-258, for instance, undergoes symmetric fission with a half-life of about 0.4 ms and a kinetic-energy distribution peaked at about 235 MeV whereas Fm-256 undergoes asymmetric fission with a half-life of about 3 h and a kinetic-energy distribution peaked at about 200 MeV. Qualitatively, these sudden changes have been postulated to be due to the emergence of fragment shells in symmetric-fission products close to Sn-132. Here we present a quantitative calculation that shows where high-kinetic-energy symmetric fusion occurs and why it is associated with a sudden and large decrease in fission half-lives. We base our study on calculations of potential-energy surfaces in the macroscopic-microscopic model and a semi-empirical model for the nuclear inertia. We use the three-quadratic-surface parameterization to generate the shapes for which the potential-energy surfaces are calculated. The use of this parameterization and the use of the finite-range macroscopic model allows for the study of two touching spheres and similar shapes. Since these shapes are thought to correspond to the scission shapes for the high-kinetic-energy events, it is of crucial importance that a continuous sequence of shapes leading from the nuclear ground state to these configurations can be studied within the framework of the model. We present the results of the calculations in terms of potential-energy surfaces and fission half-lives for heavy even nuclei. The surfaces are displayed in the form of contour diagrams as functions of two moments of the shape. They clearly show the appearance of a second fission valley, which leads to scission configurations close to tow touching spheres, for fissioning systems in the vicinity of Fm-264. DOE

N92-23744# International Centre for Theoretical Physics, Trieste (Italy).
THE NOTION OF NONRELATIVISTIC ISOPARTICLE
R. M. Santilli Sep. 1991 19 p
(DE92-615215; IC-91/265) Avail: NTIS HC/MF A03

We introduce the notion of nonrelativistic isoparticle as a representation of a Galilei-isotopic symmetry studied in preceding works or, equivalently, as the generalization of the conventional notion of particle characterized by the isotopic liftings of the unit. We show that the lifting represents the transition from massive points moving in vacuum to extended-deformable particles moving within physical media. As explicit examples, we work out the cases of an extended-deformable particle: (1) in free conditions; (2) under external 'potential selfadjoint' interactions; and (3) under external 'potential selfadjoint' and 'nonhamiltonian nonselfadjoint' interactions. The emerging methods are applied to a first classical and nonrelativistic treatment of Rauch's experiments on the spinorial symmetry of thermal neutrons under external (magnetic and) nuclear fields. The notion nonrelativistic isoquark is submitted as a conceivable classical basis for future operator studies. DOE

N92-23747# Los Alamos National Lab., NM.
RESULTS FROM THE SOVIET-AMERICAN GALLIUM EXPERIMENT
A. I. Abazov, O. L. Anosov, E. L. Faizov, V. N. Gavrin, A. V. Kalikhov, T. V. Knodel, I. I. Knyshenko, V. N. Kornoukhov, S. A. Mezentseva, and I. N. Mirmov et al 1991 18 p Presented at the International Workshop on Electroweak Physics beyond the Standard Model, Valencia (Spain), 2-5 Oct. 1991
(Contract W-7405-eng-36)
(DE92-007414; LA-UR-92-338; CONF-9110332-1) Avail: NTIS HC/MF A03

A radiochemical (71)Ga-(71)Ge experiment to determine the primary flux of neutrinos from the Sun has begun operation at the Baksan Neutrino Observatory. The number of Ge-71 atoms extracted from thirty tons of gallium was measured in five runs during the period of January to July 1990. Assuming that the extraction efficiency for Ge-71 atoms produced by solar neutrinos is the same as from natural Ge carrier, we observed the capture rate to be 20 + 15/-20 (stat) (+ or -) 32 (syst) SNU, resulting in a limit of less than 79 SNU (90 pct. CL). This is to be compared with 132 SNU predicted by the Standard Solar Model. DOE

N92-23894# Sandia National Labs., Albuquerque, NM.
MOLECULAR DESIGN OF SUBSTRATE BINDING SITES
J. A. Shelnutt and J. D. Hobbs 1991 8 p Presented at the American Chemical Society National Meeting, San Francisco, CA, 5-10 Apr. 1992
(Contract DE-AC04-76DP-00789)
(DE92-008331; SAND-91-2921C; CONF-920444-14) Avail: NTIS HC/MF A02

Computer-aided molecular design methods were used to tailor binding sites for small substrate molecules, including CO2 and methane. The goal is to design a cavity, adjacent to a catalytic metal center, into which the substrate will selectively bind through only non-bonding interactions with the groups lining the binding pocket. Porphyrins are used as a basic molecular structure, with various substituents added to construct the binding pocket. The conformations of these highly-substituted porphyrins are predicted using molecular mechanics calculations with a force field that gives accurate predictions for metalloporphyrins. Dynamics and energy-minimization calculations of substrate molecules bound to the cavity indicate high substrate binding affinity. The size, shape and charge-distribution of groups surrounding the cavity provide molecular selectivity. Specifically, calculated binding energies of methane, benzene, dichloromethane, CO2 and chloroform vary by about 10 kcal/mol for metal octaethyl-tetraphenylporphyrins (OETPPs) with chloroform, dichloromethane, and CO2 having the lowest. Significantly, a solvent molecule is found in the cavity in the X-ray structures of Co- and CuOETPP crystals obtained from dichloromethane. DOE

N92-23895# Kansas State Univ., Manhattan. Dept. of Physics.
ATOMIC PHYSICS OF STRONGLY CORRELATED SYSTEMS
C. D. Lin 1991 4 p Presented at the DOE/Office of Basic Energy Sciences (BES) Atomic Physics Contractors' Meeting, Manhattan, KS, 15-16 Oct. 1991
(Contract DE-FG02-86ER-13596)
(DE92-008356; DOE/ER-13596/25; CONF-9110335-1-Extd-Abst) Avail: NTIS HC/MF A01

This report discusses the study of coulombic 3-body systems in hyperspherical coordinates; further studies of electron correlations in doubly excited states of atoms; and theoretical studies of ion-atom collisions. DOE

N92-23903# Lawrence Livermore National Lab., CA.
MULTI-PHOTON OPTICAL EXCITATION OF POSITRONIUM
R. H. Howell, K. P. Ziock, F. Magnotta, C. D. Dermer, R. A. Failor, and K. M. Jones 20 Aug. 1991 6 p Presented at the 9th International Conference on Positron Annihilation, Szombathely, Hungary, 26-31 Aug. 1991
(Contract W-7405-eng-48)
(DE92-008567; UCRL-JC-107010; CONF-9108150-7) Avail: NTIS HC/MF A02

We have performed the first resonant excitation of high n states of positronium using two resonantly excited transitions 1S to 2P and 2P to nL. Magnetic and electric fields in the chamber mixed the high n states so that all 1 sublevels were populated in the high n state. Values for the line centroid and widths were quantitatively determined and compared well with calculated predictions. Qualitative reproduction of the n(sub minus 3) scaling of the relative transition rates was also observed. DOE

N92-24005# Lawrence Livermore National Lab., CA.
THE ALL PARTICLE METHOD Status Report, 1991
D. E. Cullen, C. T. Ballinger, and S. T. Perkins Jul. 1991 28 p Presented at the ENFIR Brazilian Meeting on Reactor Physics and Thermal Hydraulics, Sao Paulo, Brazil, 17-20 Sep. 1991
(Contract W-7405-eng-48)
(DE92-008357; UCRL-JC-108061; CONF-910983-3) Avail: NTIS HC/MF A03

At the present time a Monte Carlo transport computer code is being designed and implemented at Lawrence Livermore National Laboratory to include the transport of neutrons, photons, electrons and light charged particles as well as the coupling between all species of particles, e.g. photon induced electron emission. Since this code is being designed to handle all particles, this approach is called the 'All Particle Method'. This paper describes the current design philosophy and status of the Monte Carlo transport code and its supporting data bases. The treatment of neutrons and photons used by the All Particle Method code is conventional and as such this topic will not be discussed in this paper. Here emphasis is on discussion of our recent work to extend our ability to perform electron transport, as well as photon transport, as it is affected by coupling to electron transport, and atomic relaxation. First we discuss our new extended photon and electron interaction and atomic relaxation data bases. Next we illustrate the extended capabilities that these new data bases provide by presenting the results of several Monte Carlo transport calculations. DOE

N92-24026# Oak Ridge National Lab., TN.
RESONANT TRANSFER EXCITATION: INTERFERENCE EFFECTS
S. M. Shafroth and M. Benhenni (North Carolina Univ., Chapel Hill.) 1991 9 p Presented at the NATO Workshop on Recombination of Atomic Ions, Belfast (Ireland), 6-9 Oct. 1991
(Contract DE-AC05-84OR-21400)
(DE92-007240; CONF-9110313-5) Avail: NTIS HC/MF A02

Interference effects in RTE (Resonant Transfer Excitation) can be studied for low Z projectiles via Auger electrons emitted from highly ionized fast moving projectile ions following collisions with low Z targets. RTE in ion-atom collisions is closely related to dielectronic recombination. In the latter case which is of practical interest to the fusion power program an electron with the proper velocity incident on a highly charged ion is resonantly captured and simultaneously interacts with an inner shell electron to excite it, thus forming a doubly excited state which may decay predominantly by x ray emission for higher Z ions or by Auger electron decay for lower Z ions. The resonant velocity is that of the Auger electron emitted by the ion in the doubly excited state. In RTE the electrons to be captured are in low Z atomic (typically He) or molecular (typically H2) targets and the ions are produced by accelerators in highly charged states with the appropriate resonant velocity. The resonance is much broadened by the velocity distribution of the target electrons. Thus the resonance width as a function of projectile energy is determined by folding the Compton profile of the target electrons with the dielectronic recombination cross sections. A weaker effect and more speculative is Two Electron Transfer Excitation. Here one target electron excites the projectile 1s electron to the 2p shell for example and the other target electron is captured to an excited state of the projectile. This effect becomes more important at projectile energies higher than the energy where the RTE cross section has its maximum value. The electron-electron interaction has been beautifully demonstrated by Zouros et al. Finally, there might be interference with shakeup. This paper will present angular distribution measurements of Auger lines so that the effects of interference between these various processes can be studied. DOE

N92-24031# Florida State Univ., Tallahassee. Dept. of Physics.
PULSED ELECTRON BEAM PRECHARGER
W. C. Finney, ed. 1991 75 p
(Contract DE-FG22-89PC-89768)
(DE92-008693; DOE/PC-89768/T3) Avail: NTIS HC/MF A04

Electron beam precharging of a high resistivity aerosol was successfully demonstrated during this reporting period (Quarters Five and Six). The initial E-beam particle precharging experiments completed this term were designed to confirm and extend some of the work performed under the previous contract. There are several reasons for doing this: (1) to re-establish a baseline performance criterion for comparison to other runs, (2) to test several recently upgraded or repaired subsystems, and (3) to improve upon the collection efficiency of the electron beam precipitator when testing precharging effectiveness with a very high resistivity, moderate-to-high concentration dust load. In addition, these shakedown runs were used to determine a set of suitable operational parameters for the wind tunnel, the electrostatic collecting sections, and the MINACC E-beam accelerator. These parameters will generally be held constant while the precharging parameters are varied to produce an optimum particle charge. DOE

N92-23289*# Boeing Co., Seattle, WA. Defense and Space Group.
MOLECULAR FILMS ASSOCIATED WITH LDEF
E. R. Crutcher and K. J. Warner *In* NASA. Langley Research Center, LDEF: 69 Months in Space. First Post-Retrieval Symposium, Part 1 Jan. 1992 p 155-177 (For primary document see N92-23280 14-99)
(Contract NAS1-18224)
Avail: NTIS HC/MF A99; 8 functional color pages CSCL 20H

N92-23291*# National Aeronautics and Space Administration. Marshall Space Flight Center, Huntsville, AL.
SUMMARY OF IONIZING RADIATION ANALYSIS ON THE LONG DURATION EXPOSURE FACILITY
T. A. Parnell *In* NASA. Langley Research Center, LDEF: 69 Months in Space. First Post-Retrieval Symposium, Part 1 Jan. 1992 p 199-212 (For primary document see N92-23280 14-99)
Avail: NTIS HC/MF A99; 8 functional color pages CSCL 20H

N92-23292*# National Aeronautics and Space Administration. Marshall Space Flight Center, Huntsville, AL.
PREDICTION OF LDEF IONIZING RADIATION ENVIRONMENT
John W. Watts, T. A. Parnell, James H. Derrickson, T. W. Armstrong, and E. V. Benton (San Francisco Univ., CA.) *In* NASA. Langley Research Center, LDEF: 69 Months in Space. First Post-Retrieval Symposium, Part 1 Jan. 1992 p 213-224 (For primary document see N92-23280 14-99)
Avail: NTIS HC/MF A99; 8 functional color pages CSCL 20H

N92-23295*# Royal Aircraft Establishment, Farnborough (England). Space Dept.
SURFACE ACTIVATION OF CONCORDE BY Be-7
P. R. Truscott, C. S. Dyer, and J. C. Flatman *In* NASA. Langley Research Center, LDEF: 69 Months in Space. First Post-Retrieval Symposium, Part 1 Jan. 1992 p 249-254 (For primary document see N92-23280 14-99)
Avail: NTIS HC/MF A99; 8 functional color pages CSCL 20H

N92-23296*# Massachusetts Inst. of Tech., Cambridge. Nuclear Reactor Lab.
CHARGED PARTICLE ACTIVATION STUDIES ON THE SURFACE OF LDEF SPACECRAFT Abstract Only
Ilhan Olmez, Forrest Burns, and Paul Sagalyn (Army Materials Technology Lab., Watertown, MA.) *In* NASA. Langley Research Center, LDEF: 69 Months in Space. First Post-Retrieval Symposium, Part 1 Jan. 1992 p 255 (For primary document see N92-23280

14-99)
Avail: NTIS HC/MF A99; 8 functional color pages CSCL 20H

N92-23297*# California Univ., Berkeley. Lawrence Berkeley Lab. Engineering Div.
RADIOACTIVITIES OF LONG DURATION EXPOSURE FACILITY (LDEF) MATERIALS: BAGGAGE AND BONANZAS
Alan R. Smith and Donna L. Hurley *In* NASA. Langley Research Center, LDEF: 69 Months in Space. First Post-Retrieval Symposium, Part 1 Jan. 1992 p 257-270 (For primary document see N92-23280 14-99)
(Contract NASA Order H-06815-D; DE-AC03-76SF-00098)
Avail: NTIS HC/MF A99; 8 functional color pages CSCL 20H

N92-23298*# Los Alamos National Lab., NM. Space Science and Technology Div.
MEASUREMENTS OF INDUCED RADIOACTIVITY IN SOME LDEF SAMPLES
C. E. Moss and R. C. Reedy *In* NASA. Langley Research Center, LDEF: 69 Months in Space. First Post-Retrieval Symposium, Part 1 Jan. 1992 p 271-285 Previously announced as N91-32882 Sponsored in part by NASA and DOE (For primary document see N92-23280 14-99)
Avail: NTIS HC/MF A99; 8 functional color pages CSCL 20H

N92-23300*# National Aeronautics and Space Administration. Marshall Space Flight Center, Huntsville, AL.
INDUCED RADIOACTIVITY IN LDEF COMPONENTS
B. A. Harmon, G. J. Fishman, T. A. Parnell, and C. E. Laird (University of Eastern Kentucky, Richmond.) *In* NASA. Langley Research Center, LDEF: 69 Months in Space. First Post-Retrieval Symposium, Part 1 Jan. 1992 p 301-311 (For primary document see N92-23280 14-99)
Avail: NTIS HC/MF A99; 8 functional color pages CSCL 20H

N92-23303*# National Aeronautics and Space Administration. Marshall Space Flight Center, Huntsville, AL.
CHARGED PARTICLE LET-SPECTRA MEASUREMENTS ABOARD LDEF
I. Csige, E. V. Benton, A. L. Frank, L. A. Frigo, E. R. Benton (San Francisco Univ., CA.), T. A. Parnell, and J. W. Watts, Jr. *In* NASA. Langley Research Center, LDEF: 69 Months in Space. First Post-Retrieval Symposium, Part 1 Jan. 1992 p 339-346 (For primary document see N92-23280 14-99)
(Grant NAG8-168)
Avail: NTIS HC/MF A99; 8 functional color pages CSCL 20H

N92-23304*# National Aeronautics and Space Administration. Marshall Space Flight Center, Huntsville, AL.
IONIZING RADIATION CALCULATIONS AND COMPARISONS WITH LDEF DATA
T. W. Armstrong, B. L. Colborn (Science Applications International Corp., Prospect, TN.), and J. W. Watts, Jr. *In* NASA. Langley Research Center, LDEF: 69 Months in Space. First Post-Retrieval Symposium, Part 1 Jan. 1992 p 347-359 (For primary document see N92-23280 14-99)
(Contract NAS8-38566)
Avail: NTIS HC/MF A99; 8 functional color pages CSCL 20H

N92-23305*# Science Applications International Corp., San Diego, CA.
LDEF GEOMETRY/MASS MODEL FOR RADIATION ANALYSES
B. L. Colborn and T. W. Armstrong *In* NASA. Langley Research Center, LDEF: 69 Months in Space. First Post-Retrieval Symposium, Part 1 Jan. 1992 p 361-365 (For primary document see N92-23280 14-99)
(Contract NAS8-35866)
Avail: NTIS HC/MF A99; 8 functional color pages CSCL 20H

N92-23308*# Kiel Univ. (Germany, F.R.). Inst. fuer Reine und Angewandte Kernphysik.
HEAVY ION MEASUREMENT ON LDEF
R. Beaujean, D. Jonathal, and W. Enge *In* NASA. Langley Research Center, LDEF: 69 Months in Space. First Post-Retrieval Symposium, Part 1 Jan. 1992 p 393-397 Previously announced in IAA as A92-20919 (For primary document see N92-23280 14-99)
Avail: NTIS HC/MF A99; 8 functional color pages CSCL 20H

73 NUCLEAR AND HIGH-ENERGY PHYSICS

Includes elementary and nuclear particles; and reactor theory.

For space radiation see *93 Space Radiation.*

N92-23130# International Atomic Energy Agency, Vienna (Austria).
NEUTRON INDUCED GAMMA-RAY PRODUCTION DATA
Yukun Ho Nov. 1991 10 p
(DE92-615322; IAEA-R-5234-F) Avail: NTIS HC/MF A02

The capture reaction mechanisms are classified according to the hierarchy of quasiparticle numbers in the capture configurations - one quasiparticle (channel capture), three quasiparticles (doorway mechanism) and five or more quasiparticles (statistical processes). The nonstatistical effects in the 2 P and 3 S size resonance region of neutron strength function were systematically studied and the mass, shell and even-odd effects were explored. Two computer codes, GRS and GNASH-M, were developed and used for the calculations of neutron-induced photon production data in C-12, O-16, Al-27, Si-28, Fe-56, Cu-63-65, Au-197, and Pb-208 at the neutron energy region from thermal to 20 MeV. DOE

N92-23214# Northwestern Univ., Evanston, IL.
RESEARCH IN HIGH ENERGY PHYSICS
26 Jan. 1992 43 p
(Contract DE-AC02-76ER-02289)
(DE92-007967; DOE/ER-02289/3) Avail: NTIS HC/MF A03

This report discusses research being conducted in high energy physics in the following areas: quantum chromodynamics; drift chambers; proton-antiproton interactions; particle decays; particle production; polarimeters; quark-gluon plasma; and conformal field theory. DOE

N92-23215# Northwestern Univ., Evanston, IL.
RESEARCH IN HIGH ENERGY PHYSICS
26 Jan. 1992 43 p
(Contract DE-AC02-76ER-02289)
(DE92-007968; DOE/ER-02289/4) Avail: NTIS HC/MF A03

This report discusses research being conducted in high energy physics in the following areas: quantum chromodynamics; drift chambers; proton-antiproton interactions; particle decays; particle production; polarimeters; quark-gluon plasma; and conformed field theory. DOE

N92-23276# Tennessee Technological Univ., Cookeville. Dept. of Physics.
STUDIES OF FLUCTUATION PROCESSES IN NUCLEAR COLLISIONS
S. Ayik Feb. 1992 18 p
(Contract DE-FG05-89ER-40530)
(DE92-008144; DOE/ER-40530/3) Avail: NTIS HC/MF A03

This report discusses the following topics: Relativistic Boltzmann-Langevin model for heavy-ion collision; K+ production far below free neucleon-nucleon threshold; and damping of collective vibrations in a memory-dependent transport model. DOE

N92-23334# Texas A&M Univ., College Station.
NEW TECHNOLOGY FOR LINEAR COLLIDERS
P. M. McIntyre 1991 47 p
(Contract DE-AC02-85ER-40236)
(DE92-007912; DOE/ER-40236/T2) Avail: NTIS HC/MF A03

The purpose of this contract is to develop and evaluate new technology for future e(sup +)e(sup -) linear colliders. TeV linac colliders require major technology advances in a number of areas

in order to become feasible. The work of this contract focuses on the development of an efficient microwave driver having the performance required for such linacs. Three years ago we invented gigatron, a new design for microwave power amplifiers. The gigatron design concept is described in Section 2. A key component of gigatron is a cathode employing a gated field-emitter array (FEA) to produce fully modulated electron beam directly into vacuum. During the past 18 months our research has focused on the fabrication and testing of FEA cathodes, and the development of an improved cathode design which can provide the performance required for gigatron. During the first half of 1990 we have achieved important milestones of successful cathode fabrication and modeling of cathode operation. Section 3 describes the accomplishments of our program during the past six months.
DOE

N92-23445# Oak Ridge National Lab., TN.
THE CASE FOR EXOTIC BEAMS AT THE HOLIFIELD HEAVY ION RESEARCH FACILITY
J. D. Garrett 1991 19 p Presented at the International Symposium on Reflections and Directions in Low Energy Heavy Ion Physics, Oak Ridge, TN, 14-15 Oct. 1991
(Contract DE-AC05-84OR-21400)
(DE92-008003; CONF-9110289-4) Avail: NTIS HC/MF A03

The case is presented for modifying the Holifield Heavy Ion Research Facility at Oak Ridge National Laboratory to provide beams of proton-rich exotic isotopes, that do not occur terrestrially. A program of nuclear structure studies for light- and medium-mass, nearly self-conjugate nuclei and for heavy, proton-rich, quasibound nuclei is outlined, as are studies of hydrogen-burning reactions that occur in nucleosynthetic processes. Such a scientific program will provide a unique future for nuclear physics research at ORNL consistent with the long standing tradition of this laboratory.
DOE

N92-23500# Northwestern Univ., Evanston, IL.
RESEARCH IN HIGH ENERGY PHYSICS
26 Jan. 1992 58 p
(Contract DE-AC02-76ER-02289)
(DE92-007966; DOE/ER-02289/2) Avail: NTIS HC/MF A04

This report discusses research being conducted in high energy physics in the following areas: quantum chromodynamics; drift chambers; proton-antiproton interactions; particle decays; particle production; polarimeters; quark-gluon plasma; and conformed field theory.
DOE

N92-23576# California Inst. of Tech., Pasadena. Dept. of Physics.
HIGH ENERGY PHYSICS: REPORT OF RESEARCH ACCOMPLISHMENTS AND FUTURE GOALS, FY 1992
Sep. 1991 353 p
(Contract DE-AC03-81ER-40050)
(DE92-008543; DOE/ER-40050/T7) Avail: NTIS HC/MF A16

This report discusses high energy physics research in the following areas: research in theoretical physics; phenomenology; experimental computer facility at Caltech; Beijing BES; MACRO; CLEO II; SLD; L3 at LEP; the B Factory Research and Development Program; Superconducting Super Collider (SSC) GEM Detector; and a high resolution barium fluoride calorimeter for the SSC.
DOE

N92-23713# National Lab. for High Energy Physics, Tsukuba (Japan).
REPORT FROM ORBIT SUB-GROUP OF TASK FORCE FOR MR SYNCHROTRON RADIATION PROJECT
M. Kobayashi, ed. Jul. 1991 133 p In JAPANESE; ENGLISH summary
(DE92-751024; KEK-91-5) Avail: NTIS HC/MF A07

This report includes feasibility studies for a new synchrotron radiation source using TRISTAN Main Ring (MR) of KEK now being used as an electron and positron collider. A task force for the feasibility study started in the spring of 1990, and a sub-group was organized to study and discuss the problems related to the lattice of MR. The main subject in this report is how to realize both very small emittance and large dynamic aperture in a new lattice. Two long straight sections in the present lattice called 'Nikko' and 'Oho' must be modified like a gable roof, 1) to get free space for insertion devices, 2) to extract their synchrotron radiation to the experimental hutches which will be set in the ring tunnel in those sections and 3) to add a radiation shielding wall between the ring and the beam channel for the synchrotron radiation. The other two long straight sections called 'Fuji' and 'Tsukuba' will be used for injection, RF cavities and damping wigglers necessary for the very low emittance. The ultimate emittance will be 1.6 nm rad with the horizontal dynamic aperture of 36 x 10(sup -6) m rad that is about half the aperture experienced at the present MR.
DOE

74 OPTICS

Includes light phenomena; and optical devices.
For lasers see *36 Lasers and Masers.*

N92-23161 Princeton Univ., NJ.
AN INSTRUMENT TO SEARCH FOR SMALL-SCALE ANISOTROPY IN THE COSMIC MICROWAVE BACKGROUND AT 90 GHz Ph.D. Thesis
Gregory Sheridan Tucker 1991 65 p
Avail: Univ. Microfilms Order No. DA9202523

An instrument is described which measures spatial anisotropies of the cosmic microwave background (CMB) at an angular scale of approx. 15 min and a center frequency of 90 GHz. The detection of anisotropy or an upper limit on Delta(T)/T provides a probe of density fluctuations in the early universe at the time of the decoupling of radiation from matter. A fully steerable conical scan Cassegrain telescope, constructed for this experiment, is used to compare the temperature between four spots on the sky. Observations are carried out from the South Pole to minimize systematic effects from ground radiation and the atmosphere. The detector, an adiabatic demagnetization refrigerator cooled single-mode waveguide composite bolometer, developed especially for this experiment allows the instrument to reach a sensitivity of Delta(T) sub rms = 500 mK/sq rt of Hz (raw detector sensitivity). If the noise integrates down as 1/sq rt of r then a Delta(T)/T less than 1 x 10(exp -5) measurement can be expected in 24 hrs of integration on four independent spots on the sky. Dissert. Abstr.

N92-23166# Technische Univ., Delft (Netherlands).
INTEGRATED OPTICS IN SILICON-BASED ALUMINUM OXIDE Ph.D. Thesis
Meint Koert Smit 1991 383 p
(ISBN-90-9004261-X; ETN-92-91143) Copyright Avail: NTIS HC/MF A17

Work on the (silicon based) aluminum oxide waveguide system is presented. Technological research, device modeling and experiments, measurement technique and fiber coupling are handled. Although the aluminum oxide waveguide system is of limited interest for commercial applications (because of its high index contrast) it is very attractive for component research because of the good reproducibility of the fabrication process (better than 0.001 for the effective index), and because of its easy and reproducible optical accessibility for characterization of devices and circuits. An additional advantage is the fact that the effective wavelength of visible He-Ne light inside the waveguide material (0.4 micrometers) equals that of 1.3 micrometers radiation in InGaAsP waveguides. Furthermore, the index contrasts are comparable so that aluminum oxide may be used for prototyping InGaAsP components with visible light. As such, it has proven to be of great value.
ESA

N92-23525*# National Aeronautics and Space Administration. Goddard Space Flight Center, Greenbelt, MD.
WAMDII: THE WIDE ANGLE MICHELSON DOPPLER IMAGING INTERFEROMETER
1992 36 p Prepared in cooperation with OAO Corp., Greenbelt,

MD and National Research Council of Canada, Ottawa (Ontario)
Original contains color illustrations
(NASA-TM-105526; NAS 1.15:105526) Avail: NTIS HC/MF A03; 30 functional color pages CSCL 20F

As part of an effort to learn more about the upper atmosphere and how it is linked to the weather experienced each day, NASA and NRCC are jointly sponsoring the Wide Angle Michelson Doppler Imaging Interferometer (WAMDII) Mission. WAMDII will measure atmospheric temperature and wind speed in the upper atmosphere. In addition to providing data on the upper atmosphere, the wind speed and temperature readings WAMDII takes will also be highly useful in developing and updating computer simulated models of the upper atmosphere. These models are used in the design and testing of equipment and software for Shuttles, satellites, and reentry vehicles. In making its wind speed and temperature measurements, WAMDII examines the Earth's airglow, a faint photochemical luminescence caused by the influx of solar ultraviolet energy into the upper atmosphere. During periods of high solar flare activity, the amount of this UV energy entering the upper atmosphere increases, and this increase may effect airglow emissions. Author

N92-23551*# National Aeronautics and Space Administration. Pasadena Office, CA.
ELECTRO-OPTIC RESONANT PHASE MODULATOR Patent Application
Chien-Chung Chen, inventor (to NASA), Hamid Hemmati, inventor (to NASA), and Deborah L. Robinson, inventor (to NASA) (Jet Propulsion Lab., California Inst. of Tech., Pasadena.) 26 Feb. 1992 37 p
(Contract NAS7-918)
(NASA-Case-NPO-18702-1-CU; NAS 1.71:NPO-18702-1-CU; US-Patent-Appl-SN-842300) Avail: NTIS HC/MF A03 CSCL 20F

An electro-optic resonant cavity is used to achieve phase modulation with lower driving voltages. Laser damage thresholds are inherently higher than with previously used integrated optics due to the utilization of bulk optics. Phase modulation is achieved at higher speeds with lower driving voltages than previously obtained with non-resonant electro-optic phase modulators. The instant scheme uses a data locking dither approach as opposed to the conventional sinusoidal locking schemes. In accordance with a disclosed embodiment, a resonant cavity modulator has been designed to operate at a data rate in excess of 100 megabits per sec. By carefully choosing the cavity finesse and its dimension, it is possible to control the pulse switching time to within 4 nano-sec. and to limit the required switching voltage to within 10 V. This cavity locking scheme can be applied by using only the random data sequence, and without the need of dithering of the cavity. Compared to waveguide modulators, the resonant cavity has a comparable modulating voltage requirement. Because of its bulk geometry, the resonant cavity modulator has the potential of accommodating higher throughput power. Mode matching into the bulk device is easier and typically can be achieved with higher efficiency. An additional control loop is incorporated into the modulator to maintain the cavity on resonance. NASA

N92-23567*# California Univ., Los Angeles. Dept. of Electrical Engineering.
APPLICATION OF OPTICAL DISTRIBUTED SENSING AND COMPUTATION TO CONTROL OF LARGE SPACE STRUCTURES Final Technical Report
A. V. Balakrishnan May 1992 35 p
(Grant NAG1-1074)
(NASA-CR-190293; NAS 1.26:190293) Avail: NTIS HC/MF A03 CSCL 20F

A real time holographic sensing technique is introduced and its advantages are investigated from the filtering and control point of view. A feature of holographic sensing is its capability to make distributed measurements of the position and velocity of moving objects, such as a vibrating flexible space structure. This work is based upon the distributed parameter models of linear time invariant systems, particularly including the linear oscillator equations describing the vibration of large flexible space structures. The general conclusion is that application of optical distributed sensors bring gains in the situation where Kalman filtering is necessary for state estimation. In this case, both steady state and transient filtering error covariance become smaller. This in turn results in smaller cost in the LQG problem. Author

N92-23662# Helsinki Univ. of Technology, Espoo (Finland). Dept. of Technical Physics.
BINARY SURFACE-RELIEF GRATINGS FOR ARRAY ILLUMINATION IN DIGITAL OPTICS
A. Vasara, M. R. Taghizadeh, J. Turunen, J. Westerholm, and E. Noponen 1991 56 p Prepared in cooperation with Heriot-Watt Univ., Edinburgh (Scotland)
(PB92-143585; TKK-F-A690; ISBN-951-22-0741-9) Avail: NTIS HC/MF A04 CSCL 20F

Separable binary phase array illuminators for fan out up to 1024 x 1024 and about 65 pct. 2-D efficiency are designed using simulated annealing with constraints to maximize the minimum feature size. A new nonseparable trapezoidal coding technique is introduced and applied to design high efficiency (about 75 to 80 pct.) array generators for fan out up to 16 x 16. Rigorous electromagnetic diffraction theory is used to evaluate the range of validity of the scalar designs (both grating period and input angle are considered), to analyze fabrication errors (slanted groove walls and undercutting), and to design binary resonance domain 1-D array generators with 90 to 100 pct. efficiency. Trapezoidal gratings for low fan out (8x8), separable gratings for high fan out (up to 64x64), and a 1x5 resonance domain (100 pct. efficient) reflection grating are demonstrated experimentally. Author

N92-23748# Sandia National Labs., Albuquerque, NM.
VERSATILE BISTABLE OPTICAL SWITCHES AND LATCHING OPTICAL LOGIC USING INTEGRATED PHOTOTHYRISTORS AND SURFACE-EMITTING LASERS
Ping Zhou, Julian Cheng, C. F. Schaus, S. Z. Sun, D. R. Myers, and G. A. Vawter 1991 5 p Presented at the International Electron Devices Meeting, Washington, DC, 8-11 Dec. 1991
(Contract DE-AC04-76DP-00789)
(DE92-008677; SAND-91-1584C; CONF-911221-1) Avail: NTIS HC/MF A01

We describe a new family of versatile, cascadable, optical switches with different functional characteristics - latching, non-latching, and bistable - using a single epitaxial structure based on the monolithic integration of photothyristors and surface-emitting layers. High performance optical switching characteristics have been achieved for all three switch archetypes. We also demonstrate the AND, OR, NAND, NOR, and INVERT optical logic functions using monolithic switch structures. DOE

N92-23999 Arkansas Univ., Fayetteville.
STRONGLY COUPLED CAVITY QED Ph.D. Thesis
Paul Martin Alsing 1991 281 p
Avail: Univ. Microfilms Order No. DA9204674

A single atom strongly coupled to a quantized mode of an electromagnetic cavity driven by an external coherent field was studied. Dissipation is included in the model via cavity transmission losses and atomic fluorescence out the sides of the cavity. The strong coupling limit is defined by the condition that the atom field coupling constant is much larger than the dissipative rates. The system is explored for a range of driving field strengths which vary from small to large with respect to the atom field coupling constant. Numerical calculations of the steady state field inside the cavity, and the transmitted and fluorescent spectra, are performed. For large driving fields, a phase bimodality in the steady state field is observed. This field is shown to be intimately related to the state of the atom which is maximally polarized. The spontaneous emission spectrum reveals a Mollow-like spectrum with a very narrow central peak and Rabi sidebands with linewidths on the order of twice the atom field coupling constant. A quantum mechanical model is constructed to explain the features above. The semiclassical steady states of the system are explored in the limit of zero spontaneous emission. Dissert. Abstr.

N92-24029# International Centre for Theoretical Physics, Trieste (Italy).
OPTICAL PROPERTIES OF METALLIC MULTI-LAYER FILMS
R. Dimmich Sep. 1991 24 p
(DE92-615486; IC-91/276) Avail: NTIS HC/MF A03

Optical properties of multi-layer films consisting of alternating layers of two different metals are studied on the basis of the Maxwell equations and the Boltzmann transport theory. The influence of free-electron scattering at the film external surface and at the interfaces is taken into account and considered as a function of the electromagnetic field frequency and the structure modulation wavelength. Derived formulas for optical coefficients are valid at low frequencies, where the skin effect is nearly classical, as well as in the near-infrared, visible and ultraviolet spectral ranges, where the skin effect has the anomalous nature. It is shown that the obtained results are apparently dependent on the values of the scattering parameters. What is more, the oscillatory nature of analyzed spectra is observed, where the two oscillation periods may appear on certain conditions. The oscillations result from the electron surface and interface scattering and their amplitudes and periods depend on the boundary conditions for free-electron scattering. Finally, the application of the interference phenomenon in dielectric layers is proposed to obtain the enhancement of the nondistinct details which can appear in optical spectra of metallic films. DOE

N92-24049# Lawrence Livermore National Lab., CA.
HIGH-PERFORMANCE MULTILAYER MIRRORS FOR SOFT X RAY PROJECTION LITHOGRAPHY
D. G. Stearns, R. S. Rosen, and S. P. Vernon 17 Sep. 1991 14 p Presented at the Society of Photo-Optical Instrumentation Engineers Meeting, San Diego, CA, 21-26 Jul. 1991
(Contract W-7405-eng-48)
(DE92-008615; UCRL-JC-108299; CONF-9107115-71) Avail: NTIS HC/MF A03

We present a comparative study of three metal-Si multilayer coatings, Mo-Si, Ru-Si and Rh-Si, designed for optimum normal incidence reflectivity at x-ray wavelengths near 130 A. The multilayer (ML) structures are characterized using x-ray diffraction and high-resolution electron microscopy, and the results are correlated with the normal incidence reflectivity measured using synchrotron radiation. It is found that interlayers of mixed composition are formed to various degrees in the as-deposited structures for all three material compositions. The thinnest interlayers are observed in Mo-Si and the most intermixing occurs in Rh-Si, where the pure Rh layers are completely consumed. The stoichiometry of the interlayers in all cases is most consistent with the formation of the Si-rich silicide. The highest peak normal incidence reflectivity of 61 percent at approximately 130 A is achieved with Mo-Si, whereas the highest integrated reflectivity of 4.4 A is achieved with the Ru-Si. In a separate study, the formation of the interlayers in as-deposited Mo-Si multilayer coatings is investigated by systematically varying the thickness of either the Mo or Si layers. We observe a contraction of the multilayer period which is consistent with formation of MoSi2 at the interfaces. The presence of MoSi2 interlayers decreases the normal incidence reflectivity, thereby limiting the x-ray throughput in soft x-ray projection lithography applications. DOE

75 PLASMA PHYSICS

Includes magnetohydrodynamics and plasma fusion.

For ionospheric plasmas see *46 Geophysics*. For space plasmas see *90 Astrophysics*.

N92-23132# Japan Atomic Energy Research Inst., Tokyo.
CONCEPTUAL DESIGN OF FUSION EXPERIMENTAL REACTOR
Yasushi Seki, Hideyuki Takatsu (Japan Atomic Energy Research Inst., Naka.), and Hiromasa Iida Aug. 1991 522 p In JAPANESE; ENGLISH summary
(DE92-751036; JAERI-M-91-126) Avail: NTIS HC/MF A22

Safety analysis and evaluation have been made for the FER (Fusion Experimental Reactor) as well as for the ITER (International Thermonuclear Experimental Reactor) which are basically the same in terms of safety. This report describes the results obtained in fiscal years 1988 - 1990, in addition to a summary of the results obtained prior to 1988. The report shows the philosophy of the safety design, safety analysis and evaluation for each of the operation conditions, namely, normal operation, repair and maintenance, and accident. Considerations for safety regulations and standards are also added. DOE

N92-23133# Japan Atomic Energy Research Inst., Tokyo.
FUSION GAIN DUE TO HIGH ENERGY IONS ACCELERATED BY ADDITIONAL HEATING
Kiyotaka Hamamatsu, Masafumi Azumi, and Atsushi Fukuyama (Japan Atomic Energy Research Inst., Naka.) Oct. 1991 21 p In JAPANESE; ENGLISH summary
(DE92-751038; JAERI-M-91-156) Avail: NTIS HC/MF A03

In order to investigate a gain of fusion reaction caused by high energy ions, the ICRF wave propagation equation and the Fokker-Planck equation with the effects of particle acceleration due to the RF-electric field are numerically analyzed in a self-consistent manner. In the ICRF and NBI heated plasmas, the input power dependences of fusion output power of D-D, D-(sup 3)He and D-T reactions are calculated and compared with each other. As for the ICRF heating conditions, the higher harmonic resonance up to the third one and phase control of antenna currents are taken into account. To optimize the NBI heating condition on a fusion reaction, the beam energy needs to be exceeded the energy where the fusion cross section is maximum. In the case of ICRF heating, fast ions are accelerated beyond the several MeV by the velocity diffusion coefficient due to the RF-electric field in the Fokker-Planck equation. The ICRF heating condition does not affect the fusion output so seriously from this standpoint. As for the D-D reaction, however, the third harmonic resonance heating is more effective than the second one. Because, the fusion cross-section of D-D reaction has a maximum value at high energy range (3 to approximately 4 MeV) and the third harmonic resonance heating accelerates higher energy particles than the second one. On the other hand, in order to avoid the direct power loss by electron Landau damping in the wave propagation process, the phase difference of antenna currents needs to be inphase. DOE

N92-23135# Japan Atomic Energy Research Inst., Tokyo.
EVOLUTION OF MAGNETIC MOMENT DUE TO THE CYCLOTRON RESONANCE WITH FIELD RIPPLES IN A TOKAMAK
Masatoshi Tanaka (Japan Atomic Energy Research Inst., Naka.) Oct. 1991 31 p In JAPANESE; ENGLISH summary
(DE92-751058; JAERI-M-91-168) Avail: NTIS HC/MF A03

Toroidal field ripples of tokamaks resonate under certain conditions with the cyclotron motion of charged particles streaming along the magnetic field lines. This resonance may yield the evolution of the magnetic moment, a good adiabatic invariant of the motion in magnetic fields. The equation of motion for the magnetic moment is discretized to a mapping which describes the evolution of the magnetic moment across the successive resonances. On the basis of the mapping, derived is the linear stability of the motion in the phase space and the diffusion constant of the magnetic moment when the motion becomes stochastic. DOE

N92-23208# International Centre for Theoretical Physics, Trieste (Italy).
THE STRUCTURE OF MFD SHOCK WAVES FOR RECTILINEAR MOTION IN SOME MODEL OF PLASMA
M. Hesaaraki Aug. 1991 34 p
(DE92-617386; IC-91/226) Avail: NTIS HC/MF A03

The mathematical question of the existence of structure for 'fast', 'slow', and 'intermediate' MFD shock waves in the case of rectilinear motion in some model of plasma has been described, and a proof of existence for some cases of neglecting viscosity

and heat conduction for fast and slow shocks has been given. This question is stated in terms of a six-dimensional system of ordinary differential equations, which depends on five viscosity parameters. In this article we shall show that this system is gradient-like. Then by using the Conley theory, we prove that the fast and the slow shocks always possess structure. Moreover, the intermediate shocks do not admit structure. Some limiting cases for singular viscosities are investigated. In particular, we show how the general results in the classical one fluid MHD theory are obtained when 'the plasma viscosities' beta and chi tend to zero. DOE

N92-23209# International Centre for Theoretical Physics, Trieste (Italy).
LOW FREQUENCY ELECTROSTATIC MODES IN A MAGNETIZED DUSTY PLASMA
M. Salimullah and M. H. A. Hassan Sep. 1991 12 p
(DE92-617387; IC-91/318) Avail: NTIS HC/MF A03

The dispersion properties of low frequency electrostatic modes in a dusty plasma in the presence of a static homogeneous magnetic field are examined. It is found that the presence of the dust particles and the static magnetic field have significant effects on the dispersion relations. For the parallel propagation, the electrostatic mode is slightly modified by the magnetic field for the ion acoustic branch. A new longitudinal mode arises at the extreme low frequency limit, which is unaffected by the magnetic field for the parallel propagation. For the transverse propagation, the ion acoustic mode is not affected by the magnetic field. However, the undamped extreme low frequency mode is significantly modified by the presence of the magnetic field for the propagation transverse to the direction of the magnetic field. DOE

N92-23261# National Inst. for Fusion Science, Nagoya (Japan).
FEEDBACK CONTROL OF PLASMA EQUILIBRIUM WITH CONTROL SYSTEM AIDED BY PERSONAL COMPUTER ON THE JIPP T-IIU TOKAMAK
T. Tsuzuki, K. Toi, and K. Matsuura Apr. 1991 35 p In JAPANESE; ENGLISH summary
(DE92-750824; NIFS-MEMO-1) Avail: NTIS HC/MF A03

A feedback control system aided by a personal computer is developed to maintain plasma position on the required position in the JIPP T-IIU tokamak. The personal computer enables adjustment of control parameters easily. In this control system, a control demand for driving the power supply of feedback controlled vertical field coils is composed to be proportional to a total plasma current. This system has been successfully employed throughout the discharge where the plasma current substantially changes from zero to hundreds of kiloamperes, because the feedback control can be done, being independent of the plasma current. The analysis of this feedback control system taken into account of digital sampling agrees well with the experimental results. DOE

N92-23264# Japan Atomic Energy Research Inst., Tokyo.
EVALUATION OF MODE PURITY OF ORDINARY AND EXTRAORDINARY MODES BY FIXED ELLIPTICALLY POLARIZED WAVE FOR ECH AND ECCD
Mikio Saigusa (Japan Atomic Energy Research Inst., Naka.) Aug. 1991 20 p
(DE92-750961; JAERI-M-91-131) Avail: NTIS HC/MF A03

Mode separation ratio from an arbitrary elliptically polarized electromagnetic wave to an ordinary and an extraordinary modes on a plasma surface for oblique launch is evaluated quantitatively for designing an electron cyclotron current drive (ECCD) antenna. An optimized elliptical polarization for the wide range of injection angles and magnetic fields is firstly investigated for ECCD and ECH experiments. DOE

N92-23446# General Atomic Co., San Diego, CA.
FAST WAVE CURRENT DRIVE ANTENNA PERFORMANCE ON D3-D
M. J. Mayberry, R. I. Pinsker, C. C. Petty, S. C. Chiu, G. L. Jackson, S. I. Lippmann, R. Prater, and M. Porkolab (Massachusetts Inst. of Tech., Cambridge.) Oct. 1991 5 p Presented at the 9th Topical Conference on Radio Frequency Power in Plasmas, Charleston, SC, 19-21 Aug. 1991
(Contracts DE-AC03-89ER-51114; DE-AC05-84OR-21400)
(DE92-008052; GA-A-20694; CONF-910869-27) Avail: NTIS HC/MF A01

Fast wave current drive (FWCD) experiments at 60 MHz are being performed on the D3-D tokamak for the first time in high electron temperature, high (beta) target plasmas. A four-element phased-array antenna is used to launch a directional wave spectrum with the peak n(sub parallel) value (approximately = 7) optimized for strong single-pass electron absorption due to electron Landau damping. For this experiment, high power FW injection (2 MW) must be accomplished without voltage breakdown in the transmission lines or antenna, and without significant impurity influx. In addition, there is the technological challenge of impedance matching a four-element antenna while maintaining equal currents and the correct phasing (90 degrees) in each of the straps for a directional spectrum. We describe the performance of the D3-D FWCD antenna during initial FW electron heating and current drive experiments in terms of these requirements. DOE

N92-23523# Lawrence Livermore National Lab., CA.
AN X RAY DIAGNOSTIC OF ELECTRON POWER LOSS
D. Ress, B. W. Rice, and R. D. Horton (TRW, Inc., Redondo Beach, CA.) 1992 11 p Presented at the 8th Topical Conference on High-Temperature Plasma Diagnostics, Hyannis, MA, 6-10 May 1990
(Contract W-7405-eng-48)
(DE92-008599; UCRL-JC-103284; CONF-900557-34) Avail: NTIS HC/MF A03

A significant fraction of the power lost from a confined plasma can be carried by energetic electrons. When such electrons are incident on a probe or limiting surface, they produce thick-target x rays. It is shown that a properly filtered measurement of this x ray flux is proportional to the electron-power loss, with little dependence on the electron loss mechanism and velocity-space distribution. The diagnostic was successfully implemented to study the radial loss of hot electrons in the Tandem Mirror Experiment-Upgrade. The method provides a very fast measurement of electron loss processes, and could therefore be useful in other areas of plasma research such as magnetic confinement in tokamaks, and inertial-confinement fusion. DOE

N92-23663# Helsinki Univ. of Technology, Espoo (Finland). Dept. of Technical Physics.
THEORY STUDY ON FAST WAVE ABSORPTION AT THE PLASMA EDGE
M. J. Alava and J. A. Heikkinen 1991 47 p
(PB92-141936; TKK-F-A678; ISBN-951-22-0526-2) Avail: NTIS HC/MF A03 CSCL 20I

Mode conversion and absorption of the magnetosonic wave at the peripheral plasma is studied for ion cyclotron heating on tokamaks. Analytical and numerical methods to evaluate the conversion rate are developed and applied for relevant heating scenarios in the Joint European Tokamak (JET). The relation of the conversion rate to the local field and plasma parameters at the resonance is studied and the effect of the gradients and boundary conditions on the conversion is studied in detail. A strong absorption of the fast wave at the Alfven resonance is predicted for first harmonic heating of tritium in a DT plasma. The heating scenario could be simulated in an inactive phase by first harmonic heating of He-3 in a (3)HeH plasma. At the lower hybrid resonance, large radial electric fields are found which may contribute to impurity probiems in Ion Cyclotron Resonance Heating (ICRH). A novel antenna configuration is proposed which could be used alternatively for fast wave or ion Bernstein wave heating on tokamaks by controlling the conversion by the poloidal phasing of the antenna. Author

N92-23711# Japan Atomic Energy Research Inst., Tokyo.
CONCEPTUAL DESIGN OF FUSION EXPERIMENTAL REACTOR (FER/ITER)

Haruyuki Kimura, Mikio Saigusa (Japan Atomic Energy Research Inst., Naka.), and Yasushi Saitoh Jun. 1991 99 p
(DE92-750949; JAERI-M-91-094) Avail: NTIS HC/MF A05

Conceptual design of the Ion Cyclotron Wave (ICW) system for the FER and the Japanese contribution to the conceptual design of the International Thermonuclear Experimental Reactor (ITER) Ion Cyclotron Wave (ICW) system are presented. A frequency range of the FER ICW system is 50-85 MHz, which covers 2 omega (sub cT) heating, current drive by transit time magnetic pumping (TTMP) and 2 omega (sub cD) heating. Physics analyses show that the FER and the ITER ICW systems are suitable for the central ion heating and the burn control. The launching systems of the FER ICW system and the ITER high frequency ICW system are characterized by in-port plug and ridged-waveguide-fed 5x4 phased loop array. Merits of those systems are (1) a ceramic support is not necessary inside the cryostat and (2) remote maintenance of the front end part of the launcher is relatively easy. Overall structure of the launching system is consistent with radiation shielding, cooling, pumping, tritium safety and remote maintenance. The launcher has injection capability of 20 MW in the frequency range of 50-85 MHz with the separatrix-antenna distance of 15 cm and steep scrape-off density profile of H-mode. The shape of the ridged waveguide is optimized to provide desired frequency range and power handling capability with a finite element method. Matching between the current strap and the ridged waveguide is satisfactorily good. Thermal analysis of the Faraday shield shows that high electric conductivity low Z material such as beryllium should be chosen for a protection tile of the Faraday shield. A thick Faraday shield is necessary to tolerate electromagnetic force during disruptions. R and D needs for the ITER/FER ICW systems are identified and gain from JT-60/60U ICRF experiments and operations are indicated in connection with them. DOE

N92-23749# Sandia National Labs., Albuquerque, NM.
A SIMPLE UNFOLD METHOD FOR RUTHERFORD-SCATTERING, INTENSE ION-BEAM SPECTROGRAPHS
D. L. Fehl, R. J. Leeper, and R. P. Kensek 1992 6 p Presented at the 9th Topical Conference on High-Temperature Plasma Diagnostics, Santa Fe, NM, 15-19 Mar. 1992
(Contract DE-AC04-76DP-00789)
(DE92-008678; SAND-92-0064C; CONF-920362-3) Avail: NTIS HC/MF A02

Elastic Rutherford scattering with subsequent analysis has become a powerful tool for analyzing intense, pulsed light-ion beams for Inertial Confinement Fusion (ICF) studies. The ion spectrum is obtained by mathematical inversion of the data. This paper reports a product-integration solution to the inverse problem which is readily adapted to rapid data analysis and is simpler in form than reported previously. While this approach introduces some unphysical (negative) components into the solution, these are often negligible. Discussed here is the unfold method together with its accuracy and precision. DOE

N92-23905# Allied-Signal Aerospace Co., Kansas City, MO.
REPLACEMENT OF HYDROGEN PEROXIDE CLEANING WITH OXYGEN PLASMA
B. E. Adams Mar. 1992 48 p
(Contract DE-AC04-76DP-00613)
(DE92-009020; KCP-613-4653) Avail: NTIS HC/MF A03

Comparison between the standard peroxide cleaning method and an oxygen plasma modified version was run on thin film bond monitors. The plasma modified version substituted oxygen plasma for the peroxide cleaning step in the process and reduced the DI rinse water temperature from 75 C to 25 C. A direct surface cleanliness comparison was made between the two cleaning methods using Auger spectroscopy. A beam lead and ribbon bonding experiment was also run on plasma-cleaned networks. Results of both experiments indicate that plasma cleaning is superior to peroxide cleaning and that reliable bonding can be done on plasma-cleaned thin film networks. DOE

N92-23987# Lawrence Livermore National Lab., CA.
COMPACT FUSION ADVANCED RANKINE (CFAR2) POWER CYCLE
B. G. Logan 23 Aug. 1991 11 p Presented at the 6th International Conference on Emerging Nuclear Energy Systems, Monterey, CA, 16-21 Jun. 1991
(Contract W-7405-eng-48)
(DE92-008577; UCRL-JC-106407; CONF-910626-15) Avail: NTIS HC/MF A03

The Compact Fusion Advanced Rankine (CFARII) power cycle is a direct plasma energy conversion scheme for inertial fusion (ICF) and magnetically-insulated, inertially confined fusion (MICF) reactors utilizing (1) conversion of plasma thermal ionization and thermal energy into kinetic energy of a supersonic plasma jet, (2) conversion of the plasma jet kinetic energy into DC electricity by slowing down in an 'impulse' type of magnetohydrodynamic (MHD) generator, and (3) condensation and heat rejection of the exhaust plasma on droplets of recirculating condensate ('raindrop' condensor). A preliminary evaluation of a particular reference case, CFARII Balance-of-Plant (BoP), is found sufficiently attractive (52 percent gross cycle efficiency, 40 million 1991 $ BoP for 1 GWe gross electric) to warrant further work on several design issues. DOE

N92-24020# Lawrence Livermore National Lab., CA.
STEADY STATE ADVANCED TOKAMAK (SSAT): THE MISSION AND THE MACHINE
K. Thomassen, R. Goldston, B. Nevins, H. Neilson, T. Shannon, and B. Montgomery Mar. 1992 85 p
(Contract W-7405-eng-48)
(DE92-008983; UCRL-ID-109807) Avail: NTIS HC/MF A05

Extending the tokamak concept to the steady state regime and pursuing advances in tokamak physics are important and complementary steps for the magnetic fusion energy program. The required transition away from inductive current drive will provide exciting opportunities for advances in tokamak physics, as well as important impetus to drive advances in fusion technology. Recognizing this, the Fusion Policy Advisory Committee and the U.S. National Energy Strategy identified the development of steady state tokamak physics and technology, and improvements in the tokamak concept, as vital elements in the magnetic fusion energy development plan. Both called for the construction of a steady state tokamak facility to address these plan elements. Advances in physics that produce better confinement and higher pressure limits are required for a similar unit size reactor. Regimes with largely self-driven plasma current are required to permit a steady-state tokamak reactor with acceptable recirculating power. Reliable techniques of disruption control will be needed to achieve the availability goals of an economic reactor. Thus the central role of this new tokamak facility is to point the way to a more attractive demonstration reactor (DEMO) than the present data base would support. To meet the challenges, we propose a new 'Steady State Advanced Tokamak' (SSAT) facility that would develop and demonstrate optimized steady state tokamak operating mode. While other tokamaks in the world program employ superconducting toroidal field coils, SSAT would be the first major tokamak to operate with a fully superconducting coil set in the elongated, divertor geometry planned for ITER and DEMO. DOE

N92-24021# Argonne National Lab., IL. Fusion Power Program.
TRANSPORT CALCULATIONS OF CHEMICALLY SPUTTERED CARBON NEAR A PLASMA DIVERTOR SURFACE
J. N. Brooks Jan. 1992 15 p
(Contract W-31-109-eng-38)
(DE92-009022; ANL/FPP/TM-259) Avail: NTIS HC/MF A03

The transport of chemically sputtered carbon near a tokamak divertor surface has been analyzed with the Monte Carlo code WBC. The code follows the motion of sputtered methane atoms and the resulting carbon and hydrocarbon derivatives. Ion transport due to the magnetic field, sheath electric field, and collisions with the plasma is computed. Redeposition fractions, impinging species type, charge state, and velocity have been analyzed. For plasma temperatures greater than or equal to 10 eV, and for typical divertor

plasma densities, local redeposition of chemically sputtered carbon approaches 100 percent. Redeposition fractions are lower (approximately 80 percent) for lower temperatures and/or lower density. Physical sputtering of carbon due to redeposition of chemically sputtered material is low, but a hydrocarbon reflection cascade due to redeposition may be high. DOE

N92-24067# Lawrence Livermore National Lab., CA.
ION MICROTOMOGRAPHY (IMT) AND PARTICLE-INDUCED X RAY EMISSION (PIXE) ANALYSIS DIRECT DRIVE OF INERTIAL CONFINEMENT FUSION (ICF) TARGETS
A. J. Antolak, A. E. Pontau, D. H. Morse (Sandia National Labs., Livermore, CA.), D. L. Weirup, D. W. Heikkinen, R. S. Hornady, M. Cholewa, G. S. Bench, and G. J Legge 20 Nov. 1991 15 p Presented at the 38th National Symposium of the American Vacuum Society, Seattle, WA, 11-15 Nov. 1991
(Contract W-7405-eng-48)
(DE92-008614; UCRL-JC-109030; CONF-911132-21) Avail: NTIS HC/MF A03

The complementary techniques of ion microtomography (IMT) and particle-induced x-ray emission (PIXE) are used to provide micro-characterization of inertial confinement fusion (ICF) targets for density uniformity, sphericity, and trace element spatial distributions. ICF target quality control in the laser fusion program is important to ensure that the energy deposition from the lasers results in uniform compression and minimization of Taylor-Rayleigh instabilities. We obtain 1 percent density determinations using IMT with spatial resolution approaching two microns. Utilizing PIXE, we can map out dopant and impurity distributions with elemental detection sensitivities on the order of a few ppm. We present examples of IMT and PIXE analyses performed on several ICF targets. DOE

76 SOLID-STATE PHYSICS

Includes superconductivity.

For related information, see also *33 Electronics and Electrical Engineering* and *36 Lasers and Masers.*

N92-23205# Virginia Univ., Charlottesville. Dept. of Physics.
SUPERCONDUCTING MATERIALS
J. Ruvalds 1992 25 p
(Contract DE-FG05-84ER-45113)
(DE92-007748; DOE/ER-45113/T3) Avail: NTIS HC/MF A03

Our research on high temperatures superconductors has produced novel insights for the normal state properties of copper oxides that have been discovered in the last few years. Advances in materials preparation have produced single crystal samples, and sophisticated surface cleavage techniques have unveiled truly metallic behavior in many respects. Thus, the recent confirmation of a Fermi surface in several cuprate superconductors by photoemission spectroscopy has aroused interest in experimental features which heretofore were in apparent contrast to the expectations for a conventional Fermi Liquid. Our group has discovered that 'nested' nearly parallel sections of the electron orbits yield anomalous responses which influence the electrical resistivity, optical reflectance, Raman spectrum, and neutron scattering cross section. Our analysis has provided an explanation for seemingly disparate experimental features of high temperature superconductors using consistent values for the electron-electron coupling and the plasma frequency. Our results include the following properties of high temperature superconductors: Nested Fermi Liquid Response in High Temperature Superconductors, Optical Reflectivity and Electron Energy Loss Data, Raman Spectra, Neutron Scattering Cross Section and Scaling, and Prospects for New Superconductors. DOE

N92-23213# Carnegie-Mellon Univ., Pittsburgh, PA.
THE ROLE OF MICROSTRUCTURAL PHENOMENA IN MAGNETIC THIN FILMS
D. E. Laughlin and D. N. Lambeth 1991 8 p
(Contract DE-FG02-90ER-45423)
(DE92-007960; DOE/ER-45423/2) Avail: NTIS HC/MF A02

We have pursued two lines of research during the first year and a half of this work. In the main portion of the project, we have performed fundamental investigations of the microstructure and crystallographic texture of Co based alloys deposited on Cr underlayers. This has included atomic resolution electron microscopy of the cross-sections of CoNiCr on Cr thin films, as well as studies of the microstructures and properties of magnetic thin films produced with interlayers of Cr. The other portion of our work has centered on understanding the crystallography and crystal structure of CoSm/Cr thin films. These CoSm films have the potential of being utilized as high density media, but their structure is not yet understood. DOE

N92-23259# International Centre for Theoretical Physics, Trieste (Italy).
MONTE CARLO SIMULATION OF THE 3-STATE VECTOR POTTS MODEL ON A 3-DIMENSIONAL RANDOM LATTICE
Jianbo Zhang and Heping Ying (Bern Univ., Switzerland) Sep. 1991 12 p
(DE92-615489; IC-91/288) Avail: NTIS HC/MF A03

We have performed a numerical simulation of the three-state vector Potts model on a three-dimensional random lattice. The averages of energy density, magnetization, specific heat and susceptibility of the system in the N(exp 3)(N = 8,10,12) lattices were calculated. The results show that a first order nature of the Z(3) symmetry breaking transition appears to be characterized by a thermal hysterisis in the energy density as well as an abrupt drop of magnetization sharpness and discontinuous with increasing of volume in the cross-over region. The results obtained on the random lattice were consistent with those obtained on the three-dimensional cubic lattice. DOE

N92-23260# International Centre for Theoretical Physics, Trieste (Italy).
NONEQUILIBRIUM STATISTICAL OPERATOR IN HOT-ELECTRON TRANSPORT THEORY
D. Y. Xing and M. Liu Sep. 1991 22 p
(DE92-615517; IC-91/277) Avail: NTIS HC/MF A03

The Nonequilibrium Statistical Operator method developed by Zubarev is generalized and applied to the study of hot-electron transport in semiconductors. The steady-state balance equations for momentum and energy are derived to the lowest order in the electron-lattice coupling. We show that the derived balance equations are exactly the same as those obtained by Lei and Ting. This equivalence stems from the fact that to the linear order in the electron-lattice coupling, two statistical density matrices have identical effect when they are used to calculate the average value of a dynamical operator. The application to the steady-state and transient hot-electron transport in multivalley semiconductors is also discussed. DOE

N92-23270# International Centre for Theoretical Physics, Trieste (Italy).
Cu CHARGE FLUCTUATIONS AND ANOMALOUS BEHAVIOUR IN THE PHONON SPECTRUM OF La2CuO4
A. Dobry, A. Greco, R. Migoni, and M. Stachiotti Sep. 1991 8 p
(DE92-617446; IC-91/281) Avail: NTIS HC/MF A02

The additional excitation observed in the phonon spectrum of La2CuO4 is shown to arise from Cu charge fluctuations. A nonlinear breathing shell model is formulated for the coupling of these fluctuations with the lattice. The harmonic dynamics and exact nonlinear solutions are studied in a 2-D model of the CuO2 planes. A molecular dynamics simulation shows an additional peak of nonphononic character originated by the nonlinear lattice dynamics. DOE

N92-23271# International Centre for Theoretical Physics, Trieste (Italy).
SOLITARY EXCITATIONS IN GYROTROPIC CRYSTALS

M. T. Primatarowa and K. T. Stoychev (Bulgarian Academy of Sciences, Sofia.) Sep. 1991 15 p
(DE92-617447; IC-91/293) Avail: NTIS HC/MF A03

Nonlinear effects caused by the exciton-exciton interaction in gyrotropic molecular crystals are investigated when the system consists of mechanical excitons and when the excitons interact with the light field. It is found that in both cases bell solitons and kink excitations can appear. The parameters of the solitary excitations (energy, length, velocity) are obtained. DOE

N92-23272# International Centre for Theoretical Physics, Trieste (Italy).
ELECTRON POLARIZATION IN MODULATION DOPED HETEROSTRUCTURES
M. I. El-Kawni, K. F. Ilaiwi (Middle East Technical Univ., Ankara, Turkey), and M. Tomak Oct. 1991 16 p
(DE92-617490; IC-91/297) Avail: NTIS HC/MF A03

Self-consistent energy levels of electrons in modulation doped GaAs-Ga(1-x)Al(x)As heterostructures are presented and their dependence on various device parameters are examined. The results of calculation of the subband electron polarization under an external electric field are presented. DOE

N92-23273# International Centre for Theoretical Physics, Trieste (Italy).
ON THE ELECTRONEGATIVITY OF THE HIGH-T(SUB c) OXIDE SUPERCONDUCTOR
Zhang Liyuan Aug. 1991 5 p
(DE92-617537; IC-91/289) Avail: NTIS HC/MF A01

We employ a very useful quantity, the electronegativity, to classify the superconductor. The value of the group average electronegativity to separate the superconductor into two categories is 2. Each category has unique chemical bond features. The high-T(sub c) oxide superconductor belongs to the second category with group average electronegativity being larger than 2. Their unusual bond nature also gives new insight into some essential factors beneficial to enhance superconductivity. DOE

N92-23275# California Inst. of Tech., Pasadena.
FUNDAMENTAL ELECTRON TRANSFER PROCESSES AT THE SINGLE CRYSTAL SEMICONDUCTOR/LIQUID INTERFACE
N. S. Lewis 1991 8 p
(Contract DE-FG03-88ER-13932)
(DE92-008132; DOE/ER-13932/T1) Avail: NTIS HC/MF A02

The last year's work has focused on several aspects of the fundamental chemistry and physics semiconductor/liquid junction behavior. These projects have been directed primarily towards GaAs/liquid contacts, because GaAs/liquid systems provide high energy conversion efficiencies and offer an opportunity to gain mechanistic understanding of the factors that are important to control in an efficient photoelectrochemical energy conversion system. DOE

N92-23444# Oak Ridge National Lab., TN.
SPECTRAL EFFECTS IN RADIATION EMBRITTLEMENT
K. Farrell and L. K. Mansur 1991 2 p Presented at the Annual Meeting of the International Group on Radiation Damage Mechanisms in Pressure Vessel Steels, Raleigh, NC, 22-26 Apr. 1991
(Contract DE-AC05-84OR-21400)
(DE92-007837; CONF-9104333-1-Extd-Abst) Avail: NTIS HC/MF A01

It has long been suspected that radiation effects such as embrittlement might depend not only on the total neutron exposure and temperature but also on the neutron flux and the neutron spectrum. This paper describes two different effects of neutron spectra. DOE

N92-23447# Oak Ridge National Lab., TN.
TEMPERATURE-DEPENDENT EVOLUTION OF CHEMISORBED DIGERMANE IN Ge THIN FILM GROWTH
D. Eres and J. W. Sharp (Tennessee Univ., Knoxville.) Jan. 1992 6 p Presented at the Annual Fall Meeting of the Materials Research Society, Boston, MA, 2-6 Dec. 1991
(Contract DE-AC05-84OR-21400)
(DE92-008098; CONF-911202-59) Avail: NTIS HC/MF A02

The formation and evolution of chemisorbed digermane layers in context with germanium thin film growth was investigated by time-resolved surface reflectometry. Modulation of the source gas supply made possible the separation and independent study of the temperature dependence of the adsorption and desorption processes. The regeneration of active sites by molecular hydrogen desorption was identified as the rate-limiting step at low substrate temperatures. A dynamic method of thin film growth was demonstrated by repetitively replenishing the active film growth sites regenerated between two successive source gas pulses. The film growth rate was shown to be related to the substrate temperature and the delay time between successive source gas pulses. DOE

N92-23451# Sandia National Labs., Albuquerque, NM.
THE ELECTRONIC STRUCTURE OF ICOSAHEDRAL BORON CLUSTERS
A. C. Switendick 1991 8 p Presented at the International Symposium on the Physics and Chemistry of Finite Systems: From Clusters To Crystals, Richmond, VA, 8-12 Oct. 1991
(Contract DE-AC04-76DP-00789)
(DE92-008336; SAND-91-1196C; CONF-911033-6) Avail: NTIS HC/MF A02

The one-electron energy levels of icosahedral boron clusters have been calculated as a function of intericosahedral spacing maintaining the intraicosahedral spacing of (alpha)-boron. For crystalline lattice constants greater than 1.25 times the equilibrium one, band overlap occurs with concomitant metallic behavior. At smaller lattice constants, orbitals (bands) associated with bonds to adjacent icosahedra are lowered and orbitals (bands) associated with 'antibonds' are raised. Four bands which were three quarters full become empty, while three bands which were empty become filled. This leads to an energy gap between the filled states and the empty states which accounts for the experimentally observed insulating behavior of this elemental material with three valence electrons per atom. DOE

N92-23452# International Centre for Theoretical Physics, Trieste (Italy).
MAGNETIC FLUCTUATIONS AND NORMAL STATE PROPERTIES OF THE t-J MODEL AT FINITE DOPINGS
Y. M. Li, L. Yu, D. N. Sheng, and Z. B. Su (Academia Sinica, Beijing, China) Sep. 1991 16 p
(DE92-617538; IC-91/317) Avail: NTIS HC/MF A03

A loop expansion beyond the mean field approximation is developed to study the effects of magnetic fluctuations on normal state properties of the t-J model at finite dopings, using the Schwinger boson approach. The calculated conductivity consists of a Drude peak and a broad band, while the electron density of states is linear in omega at the scale of J, in consistency with experiments on oxide superconductors. The antiferromagnetic nature of fluctuations is found to be essential for these properties. DOE

N92-23453# International Centre for Theoretical Physics, Trieste (Italy).
MANY-BODY PROBLEMS IN HIGH TEMPERATURE SUPERCONDUCTIVITY
Yu Lu Oct. 1991 26 p
(DE92-617539; IC-91/339) Avail: NTIS HC/MF A03

The basic experimental facts about high T(sub c) superconductors are outlined. The superconducting properties of these superconductors are not very different from those of the ordinary superconductors. However, their normal state properties cannot be described by the standard Fermi liquid (FL) theory. Our current understanding of the strongly correlated models is summarized. In one dimension these systems behave like a 'Luttinger liquid', very much distinct from the FL. In spite of the enormous efforts made in two-dimensional studies, the question of FL vs non-FL behavior is still open. The numerical results as

well as various approximation schemes are discussed. Both the single hole problem in a quantum antiferromagnet and finite doping regime are considered. DOE

N92-23498# Helsinki Univ. of Technology, Espoo (Finland). Electron Physics Lab.
SEMICLASSICAL MODEL AND PROPERTIES OF RESONANT TUNNELING DIODE Ph.D. Thesis
H. Sheng 12 Dec. 1991 94 p
(PB92-143320; ISBN-951-22-0854-7) Avail: NTIS HC/MF A05 CSCL 20L

A semiclassical model involving the semiclassical transport theory is developed for the double barrier resonant tunneling diode (RTD). In the transport theory, a correlation function which accounts for the phase coherence is introduced. By means of a simple multiple scattering theory, the correlation function can be analytically expressed. Based on the semiclassical transport theory, the DC and AC small signal models are built. DC properties, such as current, quantum well charge density, voltage distribution, accumulation layer current, capacitance as well as conductance are analyzed and calculated in detail. Fabrication and measurement of RTD are also carried out and the experimental and the theoretical results agree well. An improved design, the graded spacer layer resonant tunneling diode, is proposed. This new design promises to greatly increase the peak-to-valley current ratio. In the AC small signal model, the cutoff frequency is calculated and an expression for the recently found inductance in the equivalent circuit is derived. Also the high frequency oscillations associated with the transit time resonance are obtained. Also, this infrared resonance property is analyzed by a quantum model. Author

N92-23504# International Centre for Theoretical Physics, Trieste (Italy).
IMPROVED SPIN WAVE THEORY: AN APPLICATION TO THE SPIN-1/2 ANTIFERROMAGNETIC HEISENBERG MODEL ON A SQUARE LATTICE
Ruibao Tao Sep. 1991 11 p
(DE92-617436; IC-91/315) Avail: NTIS HC/MF A03

A method is developed to make a Bose transformation which is restricted in proper space. A self-consistent independent spin wave representation (SCISWR) is found for two dimensional isotropic antiferromagnets of Heisenberg square lattices. In the SCISWR, we have successfully done the renormalization from both the dynamic and kinematic interaction and calculated the corrections from the correlations of the nearest neighbor and next nearest neighbor sites. An anisotropic excitation energy of a spin wave in improper space is found self-consistently and has a gap. The difficulty of divergence appearing from higher order perturbation terms in the conventional spin wave theory has been overcome, and the convergence in our approach seems quite good. We find the energy of ground state E approx. -0.659 in low order approximation and the magnetization of sublattice M(sup z) = 0.430 x (N/2) for system with spin 1/2. It is also proved that a physical spin excitation restricted in proper space is still isotropic and has no gap. DOE

N92-23574# Argonne National Lab., IL.
TEM STUDY OF FLUX PINNING DEFECTS IN YBa2Cu3O7-DELTA PRODUCED BY 580 MeV Sn ION IRRADIATION
R. Wheeler, M. A. Kirk, R. Brown, A. D. Marwick, L. Civale, and F. H. Holtzberg 1991 7 p Presented at the Annual Fall Meeting of the Materials Research Society, Boston, MA, 2-6 Dec. 1991
(Contract W-31-109-eng-38)
(DE92-006991; ANL/CP-73627; CONF-911202-49) Avail: NTIS HC/MF A02

Recent studies of high T(sub c) superconductors irradiated with high energy heavy ions have indicated that a defect structure is produced which is extremely effective in pinning magnetic flux lines. In attempting to develop models to account for these observations, it is imperative to have a complete characterization of the defects responsible for the property enhancements. Hence, the defect microstructure produced in single crystal YBCO by 580 MeV Sn(sup 30+) irradiation, recently demonstrated to provide highly effective flux pinning at high fields and temperatures, was investigated by conventional transmission electron microscopy. This irradiation condition is shown to produce linear, yet segmented, tracks of damaged material, approximately aligned with the incident irradiation direction, throughout the entire crystal thickness of 22 microns. The cross sectional density of damage tracks is in close agreement with the ion fluence. Two specific characteristics of the track morphology were studied, namely, their continuity and angular spread. The continuity of the tracks does not appear to follow threshold-like behavior within the electronic loss range studied here and the angular distribution of the defect track directions is only approximated by the Monte Carlo calculations of TRIM. DOE

N92-23581# International Centre for Theoretical Physics, Trieste (Italy).
EFFECTIVE MASS THEORY FOR ABRUPT HETEROJUNCTIONS
A. Brezini and N. Zekri Sep. 1991 15 p
(DE92-617439; IC-91/323) Avail: NTIS HC/MF A03

For an abrupt heterojunction between two otherwise homogeneous semiconductors in one dimension we study the effective mass Hamiltonian H = -1/2 x h(sup 2) x (m(z)(sup alpha) x (d/ds)m(z)(sup beta) x (d/ds)m(z)(sup alpha)) + E(sub c)(z) with 2 x alpha + beta = -1, where m(z) is the position dependent effective mass and E(sub c)(z) the position dependent conduction band edge. Through exact model calculations on heterostructures, we find when the effective mass theory is valid the parameters alpha and beta are 0 and -1, respectively. This conclusion is obtained in the asymptotic limit of the energy near the band edge and holds for equal lattice parameter. Results are also compared to other theories and possible extension is suggested for strained heterostructures. DOE

N92-23721# Virginia Univ., Charlottesville. Dept. of Physics.
SURFACE STRUCTURE AND ANALYSIS WITH SCANNING TUNNELING MICROSCOPY AND ELECTRON TUNNELING SPECTROSCOPY
R. V. Coleman 1992 11 p
(Contract DE-FG05-84ER-45072)
(DE92-007747; DOE/ER-45072/50) Avail: NTIS HC/MF A03

The following topics are discussed: charge-density waves in layer structures; charge-density waves in linear chain compounds; spectroscopy with the STM; STM studies of oxides; and development of atomic force microscopy. DOE

N92-23774 California Univ., San Diego.
HIGH-TEMPERATURE SUPERCONDUCTIVITY: ELECTRON-DOPED CUPRATES AND COMPOSITES FROM ALLOY PRECURSORS Ph.D. Thesis
Edward Allen Early 1991 215 p
Avail: Univ. Microfilms Order No. DA9131789

An interesting aspect of electron-doped cuprate superconductors is the variation of the superconducting transition temperature T(sub c) with host and dopant element. The series Sm(2-x)Ce(x)CuO(4-y), Eu(2-x)Ce(x)CuO(4-y), and Sm(2-x) Th(x)CuO(4-y) for 0.12 less than or equal to x less than or equal to 0.20 were carefully prepared and characterized to investigate the compositional dependence of superconductivity in these compounds. The series Sm(2-x)Ce(x)CuO(4-y) has an anomalous double resistive superconducting transition which from the results of resistivity and magnetization measurements, is not caused by either bulk phase separation or coupling between superconducting grains. Instead, the results are best explained by the presence of a phase with Ce dopant concentration x approximately equal to 0.15 at the grain boundaries. The cause of low T(sub c)'s in the other two series of compounds is possible due to competition between superconductivity and Cu antiferromagnetism. This interpretation is supported by the finding that T(sub c) is not a maximum for x = 0.15, as it is for other series with T(sub c) approximately 20 K at this dopant

concentration, but rather increases for x greater than 0.15. A significant obstacle to the widespread application of high temperature superconductors is the poor mechanical properties of these oxides. A novel processing technique was investigated which attempts to circumvent this problem using ductile alloy precursors to superconducting composites. Dissert. Abstr.

N92-23775 Stevens Inst. of Tech., Hoboken, NJ.
MAGNETOTRANSPORT AND RESPONSES OF SEMICONDUCTOR MICROSTRUCTURES Ph.D. Thesis
Vassilios Fessatidis 1991 262 p
Avail: Univ. Microfilms Order No. DA9130106

Quantum theory of carrier transport in bulk semiconductors is considered through the use of the Lei-Ting nonlinear balance equation. The longitudinal magnetoresistivity due to impurity scatterers is examined in the linear limit, for both degenerate and non-degenerate statistics, and for all magnetic field strengths. In addition, the effect of various phonon scattering mechanisms is considered for both the linear and nonlinear magnetoresistivity. Response phenomena of a density modulated 2D electron gas are examined. The magnetoplasma spectrum of such a system is shown to exhibit unusual oscillatory behavior. Such oscillations arise from the commensurability of the length scales of the system (period of modulation and cyclotron orbit radius at the Fermi level). A hydrodynamic theory of linear response is developed to examine the dielectric properties and the collective charge density oscillations of the system. In addition to the usual principal magnetoplasmon, a new mode appears as a result of the resonance drift of the cyclotron orbit center, periodic in 1/B. Both 1D and 2D modulated potentials are considered and the respective dielectric tensors and magnetoplasma modes are examined.
Dissert. Abstr.

N92-23776# Ohio State Univ., Columbus.
NUMERICAL STUDY OF THE MAGNETIC ORDERING AND SUPERCONDUCTING STATE OF HIGH-TEMPERATURE SUPERCONDUCTOR Ph.D. Thesis
Eunsook Kim 1991 172 p
Avail: Univ. Microfilms Order No. DA9120675

The three dimensional (3D) La(2-x)Sr(x)CuO(4-y) structure is studied in terms of frustration. Using an Ising model, various thermal and magnetic properties, including the two dimensional (2D) and 3D staggered magnetic moment were calculated. The 2D staggered magnetic moment corresponds to the 2D antiferromagnetic (AF) ordering within CuO2 planes which is found in all copper oxide high temperature superconducting materials. In the tetragonal structure, the system is fully frustrated and only 2D ordering is observed. The 3D ordering is achieved when frustration from two competing AF exchange interactions between Cu02 planes is removed by a tetragonal-orthorhombic structural transition. The disappearance of 3D AF order by doping is explained by introducing effective ferromagnetic (FM) bonds within the Cu02 planes, resulting in a new type of interplanar frustration. The 2D AF order within the CuO2 planes is disturbed hence 3D AF order also disappears as the material is doped. In the second part of this dissertation, the 2D CuO2 plane is studied because it is generally accepted that the CuO2 plane plays an important role in copper oxide high temperature superconducting materials. The model consists of two overlapping lattices, the lattice of spins on Cu sites and the lattice of holes on oxygen sites between the Cu sites. Dissert. Abstr.

N92-23890*# National Aeronautics and Space Administration. Lewis Research Center, Cleveland, OH.
PHASE TRANSFORMATIONS IN SrAl2Si2O8 GLASS
Charles H. Drummond, III (Ohio State Univ., Columbus.) and Narottam P. Bansal 1992 12 p Proposed for presentation at the 16th International Congress on Glass, Madrid, Spain, 4-9 Oct. 1992
(NASA-TM-105657; E-7021; NAS 1.15:105657) Avail: NTIS HC/MF A03 CSCL 20L

Bulk glass of SrAl2Si2O8 composition crystallized at temperatures below 1000 C into hexacelsian, a hexagonal phase which undergoes a reversible, rapid transformation to an orthorhombic phase at 758 C, and at higher temperatures crystallized as celsian, a monoclinic phase. The glass transition temperature and crystallization onset temperature were determined to be 883 C and 1086 C, respectively, from DSC at a heating rate of 20 C/min. Thermal expansion of the various phases and density and bend strengths of cold isostatically pressed glass powder bars, sintered at various temperatures, were measured. The kinetics of the hexacelsian-to-celsian transformation for SrAl2Si2O8 were studied. Hexacelsian flakes were isothermally heat treated at temperatures from 1025-1200 C for various times. Avrami plots were determined by quantitatively measuring the amount of monoclinic celsian formed at various times using x ray diffraction. The Avrami constant was determined to be 1.1, suggesting a diffusionless, one dimensional transformation mechanism. The activation energy was determined from an Arrhenius plot of 1n k vs. 1/T to be 125 kilocal/mole. This value is consistent with a mechanism which transforms the layered hexacelsian structure to a three dimensional framework celsian structure and involves the breaking of Si-O bonds. Author

N92-23892# Ames Lab., IA.
MAGNETIC FLUX MOTION AND FLUX PINNING SUPERCONDUCTORS Ph.D. Thesis
S. C. Sanders 28 Jan. 1992 122 p
(Contract W-7405-eng-82)
(DE92-008243; IS-T-1604) Avail: NTIS HC/MF A06

Magnetization measurements on the two high-temperature superconductors Nd(sub 1.85)Ce(sub 0.15)CuO(sub 4 minus y) and Ba(sub 0.6)K(sub 0.4)BiO3 have been undertaken in order to study the reversible and irreversible magnetic behavior and compare these two different materials with other high-temperature superconducutors (HTSC). While the other HTSC are known to have hole carriers and layers of CuO2 planes in anisotropic crystal structures, Nd(sub 1.85)Ce(sub 0.15)CuO(sub 4 minus y) (NCCO) has electron carriers as well as hole carriers, and Ba(sub 0.6)K(sub 0.4)BiO3 (BKBO) has an isotropic crystal structure with no CuO2 layers. For NCCO, the field-dependence of the specific heat derived from the reversible magnetization, C(sub o)-C(sub H), exhibited peak broadening with increasing field and a field-independent onset temperature, both of which are observed in YBa2Cu3O7(minus delta). The value at the highest available field, C(sub o)-C(sub 2T) = 1.2 mJ/cm(exp 3)K, establishes a lower limit of the calorimetric specific heat just Delta C(sub p). Flux creep and hysteresis data were parameterized in terms of a single effective pinning potential U(sub eff) in order to study the crossover from reversible to flux-pinning behavior in NCCO. There is a band in the H-T plane below H(sub irr)(T) where U(sub eff)/kT gradually rises from 2 to 20. The position of the U(sub eff)/kT lines for NCCO are in approximately the same location as those for the hole carrier Tl(2223), when a reduced temperature scale is used.
DOE

N92-23986# Lawrence Livermore National Lab., CA.
ELECTRONIC STRUCTURE IN HIGH TEMPERATURE SUPERCONDUCTING OXIDES
R. H. Howell, P. Sterne, F. Solal, M. J. Fluss, J. Tobin, J. OBrien, H. B. Radousky, H. Haghighi, J. H. Kaiser, and S. L. Rayner et al 20 Aug. 1991 10 p Presented at the 9th International Conference on Positron Annihilation, Szombathely, Hungary, 26-31 Aug. 1991
(Contract W-7405-eng-48)
(DE92-008566; UCRL-JC-108266; CONF-9108150-8) Avail: NTIS HC/MF A02

We have performed measurements on entwined single crystals of YBCO using both photoemission and positron angular correlation of annihilation radiation and on single crystals of LSCO using only angular correlation. Fermi surface features in good agreement with band theory were found and identified in all of the measurements. In photoemission, the Fermi momentum was fixed for several points and the band dispersion below the Fermi energy was mapped. In positron angular correlation measurements, the shape of the Fermi surface was mapped for the CuO chains (YBCO) and the CuO

planes (LSCO). Demonstration of the existence of Fermi surfaces in the HTSC materials points a direction for future theoretical considerations. DOE

N92-24007# Lawrence Livermore National Lab., CA.
THE ELECTRON-POSITRON MOMENTUM DENSITY AND FERMI SURFACE OF YBa2Cu3O(7-x)
H. Haghighi, J. H. Kaiser, S. Rayner, R. N. West, J. Z. Liu, R. Shelton (California Univ., Davis.), R. H. Howell, F. Solal, P. A. Sterne, and M. J. Fluss 11 Oct. 1991 9 p Presented at the 9th International Conference on Positron Annihilation, Szombathely, Hungary, 26-31 Aug. 1991
(Contract W-7405-eng-48)
(DE92-008605; UCRL-JC-108674; CONF-9108150-9) Avail: NTIS HC/MF A02

The search for evidence of Fermi surface in the cuprate high temperature superconductors has provided the greatest challenge for the 2D ACAR technique thus far in its relatively short history. Much of the effort in both theory and experiment has focused on the yttrium compound where the small size of samples, twinning and structural oxygen defects have made the experiments difficult, complicated the interpretation of results and led to some confusion. With the advent of good twin-free crystals that confusion has now been resolved. In this paper we shall briefly review the earlier experiments on twinned crystals and then describe in more detail, and in the context of the contemporary bandstructure theory, our recent clear resolution of a major Fermi surface section in untwinned crystals of YBa2Cu3O(sub 7-x). DOE

N92-24034# Sandia National Labs., Albuquerque, NM.
FERMI LEVEL EFFECTS ON DISLOCATION FORMATION IN InAs(1-x)Sb(x) GROWN BY MOCVD
R. M. Biefeld and T. J. Drummond 1991 6 p Presented at the Annual Fall Meeting of the Materials Research Society, Boston, MA, 2-6 Dec. 1991
(Contract DE-AC04-76DP-00789)
(DE92-008332; SAND-91-1561C; CONF-911202-64) Avail: NTIS HC/MF A02

Dislocation formation in InAs(sub 1-x)Sb(sub x) buffer layers grown by metal-organic chemical vapor deposition is shown to be reproducibly enhanced by p-type doping at levels greater than or equal to the intrinsic carrier concentration at the growth temperature. To achieve a carrier concentration greater than 2 times 10(exp 18) cm(exp minus 3), the intrinsic carrier concentration of InSb at 475 C, p-type doping with diethylzinc was used. Carrier concentrations up to 6 times 10(exp 18) cm(exp minus 3) were obtained. The zinc doped buffer layers have proven to be reproducibly crack free for InAs(sub 1-x)Sb(sub x) step graded buffer layers with a final composition of x = 0.12 and a strained layer superlattice with an average composition of x = 0.09. These buffer layers have been used to prepare SLS infrared photodiodes. The details of the buffer layer growth, an explanation for the observed Fermi level effect and the growth and characterization of an infrared photodiode are discussed. DOE

N92-24036# Los Alamos National Lab., NM.
NQR INVESTIGATION OF PRESSURE-INDUCED CHARGE TRANSFER IN OXYGEN-DEFICIENT YBa2Cu3O(7-DELTA) (DELTA = 0.38)
A. P. Reyes, E. T. Ahrens, P. C. Hammel, R. H. Heffner, and M. Takigawa (IBM Watson Research Center, Yorktown Heights, NY.) 1992 7 p Presented at the Lattice Effects in High (Tc) Superconductors, Santa Fe, NM, 13-15 Jan. 1992
(Contract W-7405-eng-36)
(DE92-008441; LA-UR-92-429; CONF-920141-2) Avail: NTIS HC/MF A02

Measurements of the pressure dependence of Cu-63 nuclear quadrupole frequency in YBa2Cu3O(sub 6.62) from ambient pressure up to 1.5 GPa at 4k have been performed. (Tc) was found to increase with pressure: d(Tc)/dp (approximately) 5 K/GPa. All observed NQR lines are linear in pressure: dln(nu)(sub Q)/dp = z. We found positive z for the empty chain sites, consistent with ionic (Cu exp 1+) configuration in which the atom simply fills a squeezing lattice. Planar coppers close to the empty chains have positive z, while those that are close to full chains have z approximately 0. We present an analysis of the NQR result on the basis of the charge transfer model in which the mobile charges migrate from the chain to the plane sites. We deduced that a transfer of 0.021 holes to the O(2,3) sites would explain the result in YBa2Cu3O(sub 6.62), whereas only 0.007 holes transfer in fully oxygenated YBa2Cu3O7. DOE

N92-24069# Lawrence Livermore National Lab., CA.
WORKING GAS PRESSURE AND FLOW EFFECTS ON REACTIVELY SPUTTERED MOLYBDENUM-OXIDE THIN FILMS
A. F. Jankowski and L. R. Schrawyer Apr. 1992 24 p Presented at the International Conference on Metallurgical Coatings and Thin Films, San Diego, CA, 6-10 Apr. 1992
(Contract W-7405-eng-48)
(DE92-008624; UCRL-JC-108620; CONF-920439-1) Avail: NTIS HC/MF A03

The microstructure and composition of reactively sputtered, molybdenum-oxide thin films are found to be especially sensitive to the working gas pressure and flow conditions. The variations in composition and crystallographic texture of nominal Mo2O3 films are studied, as formed at low pressure (less than 5 mTorr) and flow (less than 25 sccm) conditions, using Auger electron spectroscopy and x-ray diffraction. The structure and composition of the Mo2O3 films are categorized as part of a continuous series of molybdenum-oxide compounds based on a body centered tetragonal unit cell. DOE

N92-23413*# National Aeronautics and Space Administration. Lewis Research Center, Cleveland, OH.
MICROWAVE RESPONSE OF HIGH TRANSITION TEMPERATURE SUPERCONDUCTING THIN FILMS Abstract Only
Felix Antonio Miranda *In its* Solid State Technology Branch of NASA Lewis Research Center 1991 p 121-122 (For primary document see N92-23412 14-32)
Avail: NTIS HC/MF A08 CSCL 20L

N92-23414*# National Aeronautics and Space Administration. Lewis Research Center, Cleveland, OH.
PROPERTIES OF LARGE AREA ErBa2Cu3O(7-x) THIN FILMS DEPOSITED BY IONIZED CLUSTER BEAMS
L. L. Levenson (Colorado Univ., Colorado Springs.), Mark A. Stan, and Kul B. Bhasin *In its* Solid State Technology Branch of NASA Lewis Research Center 1991 p 127-130 Repr. from Journal of Vacuum Society Science Technology (American Vacuum Society), v. 9, no. 3, May/Jun. 1991 Revised (For primary document see N92-23412 14-32)
Avail: NTIS HC/MF A08 CSCL 20L

N92-23415*# National Aeronautics and Space Administration. Lewis Research Center, Cleveland, OH.
DEPENDENCE OF THE CRITICAL TEMPERATURE OF LASER-ABLATED YBa2Cu3O(7-DELTA) THIN FILMS ON LaAlO3 SUBSTRATE GROWTH TECHNIQUE
Joseph D. Warner, Kul B. Bhasin, and Felix A. Miranda (Case Western Reserve Univ., Cleveland, OH.) *In its* Solid State Technology Branch of NASA Lewis Research Center 1991 p 135-137 Repr. from Supercond. Sci. Technol. (England), v. 3, 1990 p 437-439 (For primary document see N92-23412 14-32)
Avail: NTIS HC/MF A08 CSCL 20L

77 THERMODYNAMICS AND STATISTICAL PHYSICS

Includes quantum mechanics; theoretical physics; and Bose and Fermi statistics.

For related information see also *25 Inorganic and Physical Chemistry* and *34 Fluid Mechanics and Heat Transfer.*

N92-23136# Helsinki Univ. of Technology, Espoo (Finland). Lab. of Thermal Engineering.
USE OF CONTROL THEORY FOR ANALYZING STABILITY OF STATES IN CONTINUUM THERMODYNAMICS
M. J. Lampinen and U. Pursiheimo 1992 11 p Prepared in cooperation with Turku Univ., Finland
(PB92-136571; Rept-46) Avail: NTIS HC/MF A03 CSCL 20M

The necessary condition was studied for the stable equilibrium state in continuous media. The new element in this analysis is the use of mathematical control theory. Using the control function as one state variable, it was derived by the variational method the necessary condition for the thermodynamic field quantities so that the entropy of the isolated continuous body is maximized. They also show that the condition is equivalent to two other stability problems. Author

N92-23206# International Centre for Theoretical Physics, Trieste (Italy).
BEYOND CONVENTIONAL QUANTUM MECHANICS
C. Ghirardi Oct. 1991 30 p
(DE92-616892; IC-91/336) Avail: NTIS HC/MF A03

The author reviews some recent attempts to overcome the conceptual difficulties encountered by trying to interpret quantum mechanics as giving a complete, objective and unified description of natural phenomena. DOE

N92-23501# International Centre for Theoretical Physics, Trieste (Italy).
THE JORDAN-SCHWINGER REALIZATION OF TWO-PARAMETRIC QUANTUM GROUP SI(SUB Q,S)(2)
Sicong Jing Oct. 1991 8 p
(DE92-616891; IC-91/335) Avail: NTIS HC/MF A02

In order to construct the Jordan-Schwinger realization for two-parametric quantum group SI(sub q,s)(2), two independent q,s-deformed harmonic oscillators are defined in this paper and the Heisenberg commutation relations of the q,s-deformed oscillator are also derived by Schwinger's contraction procedure. DOE

N92-23503# International Centre for Theoretical Physics, Trieste (Italy).
CONSTANT CURVATURE AND NON-PERTURBATIVE W(SUB 3) GRAVITY
N. Mohammedi Sep. 1991 10 p
(DE92-616919; IC-91/310) Avail: NTIS HC/MF A02

We show that the new classical action for two dimensional gravity (the Jackiw-Teitelboim model) possesses a W(sub 3) algebra. We quantise the resulting W(sub 3) gravity in the presence of matter fields with arbitrary central charges and obtain the critical exponents. The auxiliary field of the model, expressing the constancy of the scalar curvature, can be interpreted as one of the physical degrees of freedom of the W(sub 3) gravity. Our expressions are corrections to some previously published results for this model where the W(sub 3) symmetry was not accounted for. DOE

N92-23578# New York Univ., New York. Dept. of Physics.
IMPROVED NUMERICAL METHODS FOR QUANTUM FIELD THEORY (OUTSTANDING JUNIOR INVESTIGATOR AWARD)
A. D. Sokal 10 Jan. 1992 5 p
(Contract DE-FG02-90ER-40581)
(DE92-008730; DOE/ER-40581/2) Avail: NTIS HC/MF A01

We are developing new and more efficient numerical methods for problems in quantum field theory. Our principal goal is to achieve radical reductions in critical slowing-down. We are concentrating at present on three new families of algorithms: multi-grid Monte Carlo, Swendsen-Wang, and generalized Wolff-type embedding algorithms. In addition, we are making a high-precision numerical study of the hyperscaling conjecture for the self-avoiding walk, which is closely related to the triviality problem for phi(sup 4) quantum field theory. DOE

N92-23743# International Centre for Theoretical Physics, Trieste (Italy).
INEQUIVALENCE OF INTERIOR AND EXTERIOR DYNAMICAL PROBLEMS
R. M. Santilli Sep. 1991 14 p
(DE92-615214; IC-91/258) Avail: NTIS HC/MF A03

We begin a series of notes with the review of the historical distinction by Lagrange, Hamilton, Jacobi and other Founding Fathers of analytic dynamics, between the exterior dynamical problem, consisting of motion in vacuum under action-at-a-distance interactions, and the interior dynamical problem, consisting of motion within a resistive medium with the additional presence of contact, nonlinear, nonlocal and nonhamiltonian internal forces. After recalling some of the historical reasons that led to the contemporary, virtually complete restriction of research to the exterior problem, we show that the interior dynamical problem cannot be reduced to the exterior one. This establishes the open character of the central objective of these notes: the identification of the space-time symmetries and relativities that are applicable to interior, nonlinear, nonlocal and nonhamiltonian systems. DOE

N92-24040# Florida Univ., Gainesville. Inst. for Fundamental Theory.
SEMIRIGID CONSTRUCTION OF TOPOLOGICAL SUPERGRAVITIES
S. Govindarajan, P. Nelson (Pennsylvania Univ., Philadelphia.), and Soo-Jong Rey May 1991 20 p
(Contracts DE-FG05-86ER-40272; DE-AC02-76ER-03071)
(DE92-008772; DOE/ER-40272/129; UFIFT-HEP-91-10; UPR-0472T) Avail: NTIS HC/MF A03

We show how to construct topological N = 1 and 2 supergravity theories from appropriately constrained N = 3 and 4 ghost plus matter systems. In particular, N = 4 susy is not needed to obtain the N = 1 topological theory. We give a description of the relevant supermoduli spaces which must be integrated to obtain the amplitudes of these theories, as well as explicit formulas for the ingredients entering the integrands; in particular, the various supercurrents with their inhomogeneous terms. DOE

80 SOCIAL SCIENCES (GENERAL)

Includes educational matters.

No abstracts in this category.

81 ADMINISTRATION AND MANAGEMENT

Includes management planning and research.

N92-23247# Assistant Secretary of Defense (Comptroller), Washington, DC.
RESEARCH, DEVELOPMENT, TEST AND EVALUATION (R, D, T, AND E) PROGRAMS (R-1), DEPARTMENT OF DEFENSE BUDGET FOR FISCAL YEAR 1993
29 Jan. 1992 70 p
(PB92-127745) Avail: NTIS HC/MF A04 CSCL 05A

The Research, Development, Test, and Evaluation (RDT and E) Programs budget from the Department of Defense (DoD) is outlined for FY 1993. Program budgets are given for the Army, Navy, Air Force, and Defense Agencies. GRA

N92-23928# Messerschmitt-Boelkow-Blohm G.m.b.H., Munich (Germany, F.R.). Unternehmensbereich Energie- und Industrietechnik.
SYMPOSIUM ON MARKETING FOR TECHNOLOGICAL PRODUCTS [SYMPOSIUM MARKETING FUER TECHNNOLOGIEPRODUKTE]
1990 84 p In GERMAN Symposium held in Munich, Fed. Republic of Germany, 27 Mar. 1990
(MBB-UE-0014-90-PUB; ETN-92-91074) Avail: NTIS HC/MF A05

Subjects covered were: market directed thinking in a technological operation, marketing qualification as a requirement for operational success, marketing as a necessary condition for the successful development and commercialization of technological products, and requirements for the training profile of the engineer and definition of his role. For individual titles, see N92-23929 through N92-23932.

N92-23929# Messerschmitt-Boelkow-Blohm G.m.b.H., Munich (Germany, F.R.).
MARKET DIRECTED THINKING IN A TECHNOLOGICAL OPERATION [MARKTORIENTIERTES DENKEN IN EINEM TECHNOLOGIEUNTERNEHMEN]
Walter Komann *In its* Symposium on Marketing for Technological Products 1990 3 p In GERMAN (For primary document see N92-23928 14-81)
Avail: NTIS HC/MF A05

The main themes to be dealt with in the symposium are presented. Market directed thinking is to take a predominant part in all industrial activities, including aircraft navigation, space navigation, and defense technique in particular as defense activities are decreasing. ESA

N92-23930# Messerschmitt-Boelkow-Blohm G.m.b.H., Munich (Germany, F.R.).
MARKETING QUALIFICATION AS A REQUIREMENT FOR OPERATING SUCCESS [MARKETING-QUALIFIZIERUNG ALS VORAUSSETZUNG FUER DEN UNTERNEHMENSERFOLG]
Willibald Spaeth *In its* Symposium on Marketing for Technological Products 1990 5 p In GERMAN (For primary document see N92-23928 14-81)
Avail: NTIS HC/MF A05

The difficult market situation and the behavior of offer and demand people, in particular within the market of investment products, make it necessary to become marketing conscious. It is no longer necessary to think of what one does but of the market requirements. All workers in a firm are to follow a qualification process with regard to markets and customers. ESA

N92-23931# Kassel Univ. (Germany, F.R.). Management and Marketing.
MARKETING AS A NECESSARY CONDITION FOR THE SUCCESSFUL DEVELOPMENT AND COMMERCIALIZATION OF TECHNOLOGICAL PRODUCTS [MARKETING ALS NOTWENDIGE VORAUSSETZUNG FUER DIE ERFOLGREICHE ENTWICKLUNG UND VERMARKTUNG VON TECHNOLOGIEPRODUKTEN]
Armin Teopfer *In* MBB, Symposium on Marketing for Technological Products 1990 47 p In GERMAN (For primary document see N92-23928 14-81)
Avail: NTIS HC/MF A05

Marketing is defined and its weight for technological products is considered on the basis of examples taken in large firms and also in medium size businesses. Marketing strategies and milestones are reported. The measures to be taken for improving marketing qualifications are emphasized. ESA

N92-23932# Kassel Univ. (Germany, F.R.). Arbeitswissenschaften.
REQUIREMENTS FOR THE ENGINEER TRAINING PROFILE AND DEFINITION OF HIS ROLE [ANFORDERUNGEN AN DAS AUSBILDUNGSPROFIL UND ROLLENVERSTAENDNIS DES INGENIEURS]
Helmut Noelker *In* MBB, Symposium on Marketing for Technological Products 1990 10 p In GERMAN (For primary document see N92-23928 14-81)
Avail: NTIS HC/MF A05

The plurality of roles of the engineer in industrial activities is described. Difficulties and changes in marketing qualifications for engineers are emphasized. A plea for better training and further education of the engineer is given. A customer engineer dialogue in the field of personal computer sales is reported as an example. ESA

N92-23857# Ohri (Edith), Tel Aviv (Israel).
GROUP TECHNOLOGY, RCO: ROUGH-CUT OPTIMIZER. THE KEY TO INTEGRATION OF PLANT OPERATIONS
Edith Ohri *In* CASA RI/SME, Proceedings of the International Conference on CAD/CAM and AMT. Volume 1: General Sessions 14 Dec. 1989 3 p (For primary document see N92-23851 14-61)
(Rept-1.1.6) Avail: NTIS HC/MF A10

N92-23876# Israel Aircraft Industries Ltd., Lod.
SHOP FLOOR SCHEDULING THROUGH A SIMULATION BASED SCHEDULER
Z. Feuer and E. M. Dar-El *In* CASA RI/SME, Proceedings of the International Conference on CAD/CAM and AMT. Volume 1: General Sessions 14 Dec. 1989 8 p (For primary document see N92-23851 14-61)
(Rept-2.3.3) Avail: NTIS HC/MF A10

N92-23886# Ben Gurion Univ. of the Negev, Beersheva (Israel). Dept. of Industrial Engineering and Management.
GROUP SCHEDULING USING GROUP TECHNOLOGY CONCEPTS
D. Ben-Arieh and M. Dror *In* CASA RI/SME, Proceedings of the International Conference on CAD/CAM and AMT. Volume 1: General Sessions 14 Dec. 1989 5 p (For primary document see N92-23851 14-61)
(Rept-3.3.2) Avail: NTIS HC/MF A10

82 DOCUMENTATION AND INFORMATION SCIENCE

Includes information management; information storage and retrieval technology; technical writing; graphic arts; and micrography.

For computer documentation see *61 Computer Programming and Software.*

N92-23156 Louisiana State Univ., Baton Rouge.
MODELING OF PHYSICAL DATABASE DESIGN AND PERFORMANCE ANALYSIS WITH EMPHASIS ON VSAM FILES Ph.D. Thesis
Sung-Eon Kim 1991 115 p
Avail: Univ. Microfilms Order No. DA9207514

Growth in the size of a database is reflected in deterioration of database performance. Since deterioration is related to the structure of the file, the performance efficiency involves the design of a physical database and the proper management of it. This research addresses a modeling procedure of a physical database design considering both records insertions and deletions. The model describes the behavior of a physical database in a Virtual Storage Access Method (VSAM) file environment, and is extended to the issue of database reorganization through a cost analysis. The cost of accessing the database increases due to the physical disorganization of the database caused by records updates and insertions. A cost function that describes this excess cost is defined. As a remedy of the performance deterioration, database reorganization is required. Optimum reorganization points are obtained as a trade-off between the excessive costs and the reorganization cost. Numerical examples based on the characteristics of IBM 3380 are given. Dissert. Abstr.

N92-23183# Allied-Signal Aerospace Co., Kansas City, MO.
PROCEDURE IMPROVEMENT ENTERPRISES
P. L. Davis Jan. 1992 24 p Presented at the Pro SIG Trade Conference, St. Petersburg, FL, 18-20 Nov. 1991
(Contract DE-AC04-76DP-00613)
(DE92-003222; KCP-613-4758; CONF-9111183-1) Avail: NTIS HC/MF A03

At Allied-Signal's Kansas City Division (KCD), we recognize the importance of clear, concise and timely procedures for sharing information, promoting consistency and documenting the way we do business. For these reasons, the KCD has gathered a team of employees to analyze the process we currently use to publish procedures, identify the procedure needs of KCD employees, and design a system that meets or exceeds the requirements and expectations of DOE. The name of our group is the Procedure Improvement Enterprise Critical Process Team, or PIE CPT. The mission statement of Procedure Improvement Enterprise is to develop and implement within the Kansas City Division an effective, flexible procedure system that will establish a model of excellence, will emphasize team work and open communication, and will ensure compliance with corporate/government requirements. DOE

N92-23188# Pacific Northwest Lab., Richland, WA.
HEIS: AN INTEGRATED INFORMATION SYSTEM FOR ENVIRONMENTAL RESTORATION AND MONITORING AT HANFORD
S. Tzemos and B. Kissinger Nov. 1991 5 p Presented at the Winter Meeting of the ANS, San Francisco, CA, 10-15 Nov. 1991
(Contract DE-AC06-76RL-01830)
(DE92-006467; PNL-SA-19800; CONF-911107-54) Avail: NTIS HC/MF A01

The US Department of Energy's Hanford Site has about 1500 waste sites that contain a complex mixture of chemical and radioactive contaminants. After many years of environmental monitoring to assess the impact of Hanford operations to the environment, the Site's mission is shifting to environmental restoration. The Hanford Environmental Information System (HEIS) is being developed to provide advanced tools to (1) support environmental restoration and routine site-wide monitoring, and (2) aid the scientists in understanding and conducting the restoration efforts. This paper describes some of the highlights and distinctive features of HEIS. DOE

N92-23212# Fermi National Accelerator Lab., Batavia, IL.
MODELING OF THE DZero DATA ACQUISITION SYSTEM
R. Angstadt, M. Johnson, I. L. Manning, and J. A. Wightman Dec. 1991 8 p Presented at the IEEE Nuclear Science Symposium, Santa Fe, NM, 5-9 Nov. 1991
(Contract DE-AC02-76CH-03000)
(DE92-007913; FNAL/C-91/351; CONF-911106-80) Avail: NTIS HC/MF A02

A queuing theory model was used in the initial design of the D0 data acquisition system. It was mainly used for the front end electronic systems. Since then the model has been extended to include the entire data path for the tracking system. The tracking system generates the most data so we expect this system to determine the overall transfer rate. The model was developed using both analytical and simulation methods for solving a series of single server queues. We describe the model and the methods used to develop it. We also present results from the original models, updated calculations representing the system as built, and comparisons with measurements made with the hardware in place for the cosmic ray test run. DOE

N92-23550*# National Aeronautics and Space Administration. John C. Stennis Space Center, Bay Saint Louis, MS.
DIGITAL DATA REGISTRATION AND DIFFERENCING COMPRESSION SYSTEM Patent Application
Gary A. Ransford, inventor (to NASA) and Vivien J. Cambridge, inventor (to NASA) (Sverdrup Technology, Inc., Bay Saint Louis, MS.) 28 Feb. 1992 46 p
(NASA-Case-SSC-00010-2; NAS 1.71:SSC-00010-2; US-Patent-Appl-SN-842956) Avail: NTIS HC/MF A03 CSCL 05B

A process for x ray registration and differencing results in more efficient compression is discussed. Differencing of registered modeled subject image with a modeled reference image forms a differential image for compression with conventional compression algorithms. Obtention of a modeled reference image includes modeling a relatively unrelated standard reference image upon a three dimensional model, which three dimensional model is also used to model the subject image for obtaining the modeled subject image. The registration process of the modeled subject image and modeled reference image translationally correlates such modeled images for resulting correlation thereof in spatial and spectral dimensions. Prior to compression, a portion of the image falling outside a designated area of interest may be eliminated, for subsequent replenishment with a standard reference image. The compressed differenced image may be subsequently transmitted and/or stored, for subsequent decompression and addition to a standard reference image so as to form a reconstituted or approximated subject image at either remote location and/or at a later moment in time. Overall effective compression ratios of 100:1 are possible for thoracic x ray digital images. NASA

N92-23728 Texas A&M Univ., College Station.
THE MARKET FOR COMPUTER READABLE INFORMATION Ph.D. Thesis
Lawrence Alarie West, Jr. 1991 337 p
Avail: Univ. Microfilms Order No. DA9134021

The market for computer readable information (CRI) is the exchange of machine readable data between organizations when no other transaction between the organizations is supported by the exchange. Modeled here are the cost and revenue (benefit) structures of the market participants, including users, distributers (vendors), producers, and government agencies. This effort draws on industrial organization research to explain how cost structures have determined market structure and behavior. The existence of long run average costs for database management systems accounts for much of the structure of the market, as well as for the wave of mergers and acquisitions observed. Changing technology and competitive/contestable pressures are shown to account for changes in price and service levels and structures observed in the industry. Extensive nonprice competition by participants is explained as a competitive response, but also as a way of creating tying arrangements which reduce the public good problem. Overall, the research concludes that the participants are behaving rationally given their respective cost structures and market conditions. Disclosure of the determinants of industry structure and behavior also clarifies important design issues. Specific implications for designers of producing, distributing, and using systems are drawn from the conclusions. Dissert. Abstr.

N92-23730 Case Western Reserve Univ., Cleveland, OH.
TRAINING USERS OF A FLEXIBLE DECISION SUPPORT SYSTEM: THE EFFECTS OF TRAINING CONTENT AND USER ABILITY Ph.D. Thesis
Suzanne Marie Rodriguez 1991 529 p
Avail: Univ. Microfilms Order No. DA9202258

Two forms of training are contrasted: operations training, and strategy training. Operations training provides information concerning how to operate the features of the Decision Support System (DSS). Operations trained subjects have sole responsibility for the development of a decision strategy. Strategy trained subjects need not develop their own strategy for using the DSS. The dimension of user ability selected for study was cognitive restructuring ability (CRA) as measured by the Group Embedded Figures Test. CRA is used in the strategy formulation activities of selecting, organizing, and reorganizing information. CRA was expected to interact with the form of training in determining performance because the training treatments provided different levels of support to the strategy formulation process. Forty-two MBA students participated in a lab experiment based on a job sequencing task. Computer logs, questionnaire responses and concurrent verbal protocols were analyzed. Strategy training

resulted in higher performance, regardless of CRA. For operations trained subjects, high CRA individuals performed better than low CRA individuals. The relationship with CRA was reversed for strategy trained subjects. Dissert. Abstr.

N92-23742# International Atomic Energy Agency, Vienna (Austria). International Nuclear Data Committee.
METHOD FOR EVALUATING NON-CONSISTENT DATA USING TWO STATISTICAL CRITERIA
Yu. F. Yaborov Nov. 1991 10 p Transl. into ENGLISH from Yadernye Konstanty (USSR), 1989
(DE92-615195; INDC(CCP)-343/L) Avail: NTIS HC/MF A02

The paper presents methods of identifying mismatched data and finding possible causes of their being mismatched by using a statistical criterion which highlights abnormal extreme values. Processing methods for systems of non-consistent data are suggested. DOE

N92-24016 Harvard Univ., Cambridge, MA.
EXPERT SYSTEMS: A MAPPING BETWEEN SYMBOL SUSCEPTIBLE TASKS AND SOFTWARE TOOLS Ph.D. Thesis
Thomas Grandon Gill 1991 523 p
Avail: Univ. Microfilms Order No. DA9132184

Described here is an exploratory investigation into the relationship between task characteristics and commercially available software tools for the development of expert systems. The primary objective is to propose a conceptual structure for characterizing tasks suited for expert systems which can be used to help manage the processes of opportunity identification, feasibility determination and systems analysis in the early stages of expert system development processes. The empirical portion of the research describes a field study of 16 different commercial expert systems, conducted to explore the task-tool model. The investigator classified tasks using the dimensions of the task-tool model, and identified the corresponding set of tool features that were used. A pattern matching approach was used to contrast these actual features with those predicted by the model. An extremely high level of correspondence was observed between predicted and actual features, leading to the proposing of hypotheses relating to what types of tasks are performed by expert system tools in general, how tasks can be shared between human and expert systems, and how specific task attributes map to specific expert system tool features. Dissert. Abstr.

N92-23313*# National Aeronautics and Space Administration. Lyndon B. Johnson Space Center, Houston, TX.
METEOROID AND DEBRIS SPECIAL INVESTIGATION GROUP DATA ACQUISITION PROCEDURES
Thomas H. See, Martha K. Allbrooks, Dale R. Atkinson, Clyde A. Sapp, Charles G. Simon (Institute for Space Science and Technology, Inc., Gainesville, FL.), and Mike E. Zolensky *In* NASA. Langley Research Center, LDEF: 69 Months in Space. First Post-Retrieval Symposium, Part 1 Jan. 1992 p 459-475 (For primary document see N92-23280 14-99)
Avail: NTIS HC/MF A99; 8 functional color pages CSCL 05B

N92-23373*# National Aeronautics and Space Administration. Goddard Space Flight Center, Greenbelt, MD.
A SPATIAL DATA HANDLING SYSTEM FOR RETRIEVAL OF IMAGES BY UNRESTRICTED REGIONS OF USER INTEREST
Erik Dorfman (Hughes STX, Inc., Greenbelt, MD.) and Robert F. Cromp *In its* The 1992 Goddard Conference on Space Applications of Artificial Intelligence 1992 p 213-230 (For primary document see N92-23356 14-63)
Avail: NTIS HC/MF A12 CSCL 05B

N92-23374*# Argonne National Lab., IL. Environmental Assessment and Information Sciences Div.
DATA EXPLORATION SYSTEMS FOR DATABASES
Richard J. Greene and Christopher Hield *In* NASA. Goddard Space Flight Center, The 1992 Goddard Conference on Space Applications of Artificial Intelligence 1992 p 231-244 (For primary document see N92-23356 14-63)
Avail: NTIS HC/MF A12 CSCL 05B

83 ECONOMICS AND COST ANALYSIS

Includes cost effectiveness studies.

No abstracts in this category.

84 LAW, POLITICAL SCIENCE AND SPACE POLICY

Includes NASA appropriation hearings; aviation law; space law and policy; international law; international cooperation; and patent policy.

No abstracts in this category.

85 URBAN TECHNOLOGY AND TRANSPORTATION

Includes applications of space technology to urban problems; technology transfer; technology assessment; and surface and mass transportation.

For related information see also *03 Air Transportation and Safety, 16 Space Transportation,* and *44 Energy Production and Conversion.*

No abstracts in this category.

88 SPACE SCIENCES (GENERAL)

No abstracts in this category.

89 ASTRONOMY

Includes radio, gamma-ray, and infrared astronomy, and astrometry.

N92-23428*# New Mexico Univ., Albuquerque. Dept. of Physics and Astronomy.
ANNUAL PROGRESS REPORT
Nebojsa Duric 2 Apr. 1992 31 p
(Grant NAG5-1239)
(NASA-CR-190197; NAS 1.26:190197) Avail: NTIS HC/MF A03 CSCL 03A

The emission components of spiral galaxies between 12 microns and 90 cm are identified. Additionally, an attempt to understand the relationships between them was made. The specific goal was to gain some understanding on the nature of the radio-infrared correlation. The results are summarized. Author

N92-23673 Oxford Univ. (England).
OBSERVATIONS OF ACCRETION DISCS IN INTERACTING BINARIES Ph.D. Thesis

William Bruce Honey 1989 246 p
Avail: Univ. Microfilms Order No. BRD-93069

Cataclysmic and X-ray binaries (CV and LMXB) are considered, and new observations of both types of source are considered. Chapter 1 gives an introduction to the subject and presents a study of the evolution and period relationships of these objects. Chapter 2 studies the superoutburst of a system. The observational data presented in the Chapter are used to place constraints on the geometry of the system, and also upon the theoretical models examined; only eccentric disc models are found to be acceptable. A tidally dominated eccentric accretion disc is considered, and good agreement between the observations and a tidally distorted disc simulation is achieved. In Chapter 3, a search for the superhump phenomenon is conducted. No such superhump behavior was found. These observations support the ideas first raised in Chapter 2 of the importance of tidal behavior in dwarf novae. Chapter 4 reviews observations of black hole candidates, and lists the generally expected 'fingerprint' thought to be associated with black holes in binary systems. Chapter 5 reports on observations of the LMXB GX339-4 and the discovery of the period for the system. Constraints on the system parameters are given and a model is presented that is compatible with the observations. Chapter 6 reviews the work done and considers other important observational evidence that is to be found in the literature and is pertinent to the work in this thesis.
Dissert. Abstr.

N92-23675 California Univ., Berkeley.
HIGH RESOLUTION STUDIES OF NGC 1275 AND THE GALACTIC CENTER Ph.D. Thesis
Jonathan Michael Marr 1990 214 p
Avail: Univ. Microfilms Order No. DA9126690

Radio studies of the parsec-scale structure in the centers of NGC 1275 and the Milky Way galaxy are presented. The nucleus of NGC 1275 was observed with Very Long Baseline Interferometry (VLBI) at 1.3 cm twice per year for three years, with a resolution of 0.3 milliarcseconds, corresponding to approximately 0.1 pc. The galactic center was observed in the J = 1 approaches 0 transition lines of H-13(CN) and HCO(+) with the Berkeley-Illinois-Maryland Array (BIMA) at the Hat Creek Radio Observatory, with a spatial resolution that corresponded to 0.2 pc, and spectral resolution of 4 km s(exp -1). The H-13(CN) and HCO(+) data, which were seen in emission from the 2 pc galactocentric ring and in absorption from galactic line-of-sight features, were compared with published H-12(CN) observations. The VLBI maps of NGC 1275 reveal that intensity flares are associated with the ejection of knots of emission moving at velocities approximately 0.5 h(exp -1) c, while a slowly evolving outburst is associated with the emergence of diffuse emission expanding in a cone at a velocity approximately 0.33 h(exp -1) pc. The core emission has a roughly constant and complex morphology with a number of ridges extending out radially from the emission peak and an inner jet at PA 210 deg. The galactic center observations are also used to study previously identified foreground features that appear in absorption by HCO(+) and HCN. Opacity maps suggest either that Sgr A* is at least 3 pc in front of the ionized gas bar or that 'the high velocity gas' is very clumpy and has a window at the position of Sgr A*.
Dissert. Abstr.

N92-23695 California Univ., Riverside.
GAMMA RAYS FROM SN1987A WITH THE UCR DOUBLE-COMPTON TELESCOPE Ph.D. Thesis
Farid Ait-Ouamer 1991 195 p
Avail: Univ. Microfilms Order No. DA9133871

Results are presented for gamma rays from SN1987A observed on a flight of the UCR double Compton telescope from Alice-Springs, Australia, 15 to 16 April 1988, some 418 days after SN1987A explosion. The calibrations before the flight gave energy resolutions of 13 pct. FWHM at 1.35 MeV and 10 pct. FWHM at 2.75 MeV and an angular resolution of 11 deg FWHM. The wide field of view provides Compton ring imaging of gamma rays from 1 to 30 MeV with about 10 deg FWHM resolution. A significant excess of gamma rays was observed from the direction of SN1987A in the energy range of 1 to 2.5 MeV. Two features at 1.2 and 1.9 MeV are attributed to the 1.238 MeV and combined 1.771, 2.035, and 2.051 MeV line emissions from the decay of Co-56 in the expanding ejecta with fluxes of (3.2 + or - 1.0 + or - 0.6) x 10(exp -4) gamma/sq cm/s and (2.7 + or - 0.8 + or - 1.1) x 10(exp -4) gamma/sq cm/s, respectively. The first error is statistical and the second systematic. The energy resolution of 11 pct. did not permit a definite separation of the 1.771 MeV line from the two other lines at 2.051 and 2.035 MeV that form the group at 1.9 MeV.
Dissert. Abstr.

N92-24001 Princeton Univ., NJ.
OBSERVING MILLISECOND AND BINARY PULSARS Ph.D. Thesis
Stephen Erik Thorsett 1991 125 p
Avail: Univ. Microfilms Order No. DA9202541

The spin up of a slowly rotating neutron star by mass accretion from a companion object creates more than just a fast pulsar. The so-called 'recycled' pulsars, a class including millisecond pulsars and most if not all pulsars in binary systems and globular clusters, differ in a number of interesting and important ways from their slower cousins. Typical pulsars are young objects, thousands to tens of millions of years old, whereas billion year old recycled pulsars are the living fossils of the galaxy. The magnetic fields of recycled pulsars are often a thousand times weaker than those of young pulsars. A time system was installed at the Very Large Array, primarily to observe recycled pulsars. Preliminary observations were made on a number of fast pulsars. Long term timing of an array of millisecond pulsars can set strong limits on the cosmological background of very low frequency gravitational radiation, predicted by several models of the early universe, and allows very precise astrometrical and metrological measurements. Observations were made of the eclipsing binary pulsar in Terzan 5, at both the VLA and Green Bank, to study the mechanism by which a pulsar may evaporate a companion star. Dissert. Abstr.

N92-24002 Rice Inst., Houston, TX.
AN ANALYSIS OF THE WN SHELL NEBULA NGC 6888 USING CCD IMAGERY AND SPECTROPHOTOMETRY Ph.D. Thesis
Patralekha Mitra 1991 181 p
Avail: Univ. Microfilms Order No. DA9136049

A model is presented which describes the morphology and physical processes in NGC 6888, a 'wind blown' nebula around the WN6 star HD192163. CCD imagery with the Palomar 1.5 m revealed distinct morphological features that were further probed with spectrophotometry using the KPNO #2 telescope + Intensified Reticon Scanner. Distinctions in morphology in (O III) compared to H(alpha) led to a parameterization into two physical systems: (1) An inner ionized shell observable in all the emission lines, with (N II) T sub e = 8000 K, (O III) T sub e = 14000 K and (S II) N sub e = 400/cu cm, and (2) The (O III) bubble and rim, visible only in (O III) and characterized by a higher (O III) T sub e = 50000 K. The nebula is found to have 5 to 10 solar mass of ionized mass. An extrapolation of (O III) lambda 5007 fluxes to IR emission line intensities led to revised values of neutral mass approx. 40 solar mass for the nebula. Of this 3 to 6 solar mass is found to be enriched mass, 0.5 solar mass contributed by stellar wind mass loss and wind swept ISM mass is determined to be approx. 20 to 60 solar mass. Photoionization models show that the shell is enriched in N and He and depleted in O compared to galactic H II regions.
Dissert. Abstr.

N92-24027# Los Alamos National Lab., NM.
THE ALEXIS DATA PROCESSING PACKAGE: AN IDL-BASED SYSTEM
J. J. Bloch, B. W. Smith, and B. C. Edwards 1991 4 p Presented at the Astronomical Data Analysis Software and Systems Conference, Tucson, AZ, 6-8 Nov. 1991
(Contract W-7405-eng-36)
(DE92-007429; LA-UR-91-4163; CONF-9111185-1) Avail: NTIS HC/MF A01

The ALEXIS experiment is a mini-satellite containing six wide angle EUV/ultrasoft x ray telescopes. Its purpose is to map out

the sky in three narrow (5 pct.) bandpasses around 66, 71, and 93 eV. The 66 and 71 eV bandpasses are centered on intense Fe emission lines which are characteristic of million-degree plasmas such as the one thought to produce the soft x ray background. The 93 eV bandpass is not near any strong emission lines and is more sensitive to continuum sources. The emission will be launched on the Pegasus Air-Launched Vehicle in the first quarter of 1992 into a 400-nautical-mile, high inclination orbit and will be controlled entirely from a small ground station located at Los Alamos. The six telescopes are arranged in three pairs. As the satellite spins twice a minute they scan the entire anti-solar hemisphere. Each f/1 telescope consists of a spherical, multilayer coated mirror with a curved, microchannel plate detector located at the prime focus. The multilayer coatings determine the bandpasses of the telescopes. The field of each telescope is 30 degrees with a spatial resolution of 0.5 degree, limited by spherical aberration. The data processing requirements for ALEXIS are large. Each event in one of the six telescopes is telemetered to the ground with its time of arrival and position on the detector. This information must be folded with the aspect solution for the satellite to reconstruct the direction on the sky from which the photon came. Because of the way the six telescopes scan the sky, the effective exposure calculations is also very compute-intensive. ALEXIS may generate up to 100 megabytes of raw data per day, which are converted into a gigabyte per day of processed data. The entire analysis system is built on a set of SPARC station platforms.

DOE

N92-23359*# Space Telescope Science Inst., Baltimore, MD.
DETECTING OPPORTUNITIES FOR PARALLEL OBSERVATIONS ON THE HUBBLE SPACE TELESCOPE
Michael Lucks *In* NASA. Goddard Space Flight Center, The 1992 Goddard Conference on Space Applications of Artificial Intelligence 1992 p 29-44 (For primary document see N92-23356 14-63)
Avail: NTIS HC/MF A12 CSCL 03A

N92-23962*# Howard Univ., Washington, DC.
THE USE OF HIGH TEMPERATURE SUPERCONDUCTORS TO LEVITATE LUNAR TELESCOPE
Beth A. Brown *In* NASA. Goddard Space Flight Center, Summer Graduate Research Program for Interns in Science and Engineering 24 Mar. 1992 10 p (For primary document see N92-23958 14-99)
Avail: NTIS HC/MF A12 CSCL 03A

90 ASTROPHYSICS

Includes cosmology; celestial mechanics; space plasmas; and interstellar and interplanetary gases and dust.

For related information see also *75 Plasma Physics*.

N92-23126 California Univ., Berkeley.
CONSTRUCTING A PULSAR TIMING ARRAY Ph.D. Thesis
Roger Sherman Foster, III 1990 195 p
Avail: Univ. Microfilms Order No. DA9126561

Several millisecond pulsars separated by large angles on the sky are used to construct a spatial Pulsar Timing Array (PTA). Correlations in the pulsar timing residuals can be caused by the following: (1) reference clock wandering; (2) uncorrected perturbations in the Earth's orbit; (3) local deviations in the space-time metric; and (4) dispersion measure fluctuations. The PTA concept, with regard to a timing program established at the National Radio Astronomy Observatory's 43 m telescope in Green Bank, is explored. Currently there are four pulsars included in the timing array: PSR's 1620-26, 1821-24, 1855+09, and 1937+21. The influences of global parameters - clock, Earth, and metric perturbations - on the data are discussed. Results from two pulsar timing programs conducted at the National Radio Astronomy Observatory in Green Bank, West Virginia are presented. The first program covers observations between Jul. 1987 and Jun. 1989, while the second program covers observations between Aug. 1989 and Sep. 1990. The hardware used to collect the data are described. Estimates of the flux density and spectral indices of the four millisecond period radio pulsars are presented, including a derived analytic pulse template model based on a multi-frequency observing campaign conducted in Aug. 1989. An assessment of the sources of uncertainty in the data is given, along with methods for improving data quality and array performance through future upgrades. Finally, a proposal is made for linking together pulsar data sets from different observatories by properly referencing pulse arrival times to a proper fiducial point. Dissert. Abstr.

N92-23127 Connecticut Univ., Storrs.
ROTATING, RADIATING MASS IMBEDDED IN A DE SITTER UNIVERSE Ph.D. Thesis
Robert Harrison Hadley 1991 160 p
Avail: Univ. Microfilms Order No. DA9128847

A new solution to the Einstein field equations for a rotating, radiating mass imbedded in a de Sitter universe, the Kerr de Sitter-Vaidya (KDV) line element, is presented. Solutions are presented which were precursers to the new solution. One of these, the Vaidya-Mallett (VM) metric is used as a starting point to derive the KDV metric by a method called 'complexification.' The mathematical framework for the KDV metric is the Newman-Penrose formalism, a powerful tool which provides insight into the various properties of the spacetime geometry and optical properties of the radiation field. Using this formalism, the metric can be expressed in tetrad form and the Newman-Penrose spin-coefficient equations solved for tetrad components of the tracefree Ricci tensor, Ricci scalar, Maxwell tensor, and Weyl tensor. Using the tetrad components of the Weyl tensor, the Petrov type for the gravitational and electromagnetic fields are found. The new solution is shown to be a solution to the Einstein-Maxwell equations for a particular choice of energy-momentum tensor which is studied in detail. The motion of spinning test particles in the KDV metric are found using the equations of A. Papapetrou. The particular case of the path of a light ray in the KDV metric is analyzed in detail to a particular order. Dissert. Abstr.

N92-23153# California Univ., Berkeley. Lawrence Berkeley Lab.
PARTICLE PHYSICS AND COSMOLOGY
L. J. Hall Jan. 1992 8 p Presented at the International Workshop on Electroweak Symmetry Breaking, Hiroshima (Japan), 12-15 Nov. 1991
(Contract DE-AC03-76SF-00098)
(DE92-008301; LBL-31678; CONF-9111182-3; UCB-PTH-92/01)
Avail: NTIS HC/MF A02

I give a brief review of the cosmological implications for new particle physics, the search for dark matter and the general nature of dark matter. DOE

N92-23164 Johns Hopkins Univ., Baltimore, MD.
SEARCH FOR COSMOLOGICAL DUST Ph.D. Thesis
Yichuan C. Pei 1991 212 p
Avail: Univ. Microfilms Order No. DA9132706

A search was made for dust in the damped Ly alpha absorption systems, which are discovered in the spectra of distant quasars and generally thought to be the high redshift analogs or progenitors of present day galactic disks. The method is based on a reddening test for differences in the spectra of quasars with and without damped Ly alpha systems in the foreground. The detection of dust in the damped Ly alpha systems is reported for the first time, based on the data available in literature. It is concluded that the typical dust to gas ratio in damped Ly alpha systems at red shifts between about two and three is 5 to 20 pct. of that in the Milky Way and the shape of the extinction curve in the damped Ly alpha systems resembles that in the Small or Large Magellanic Cloud rather than that in the Milky Way. Some of the implications of the results are discussed. In particular, it is suggested that the dust in damped Ly alpha systems provides important clues to the chemical enrichment of galaxies, possibly affects searches for primeval galaxies, and probably produces significant obscuration

on quasars and other objects at cosmological distances. It is concluded that the possible obscuration of quasars by dust in an intergalactic medium cannot be ruled out. Dissert. Abstr.

N92-23696 Georgia State Univ., Atlanta. Coll. of Arts and Sciences.
ON THE LIMITING ASTROMETRIC ACCURACY OF BINARY STAR SPECKLE INTERFEROMETRY Ph.D. Thesis
Ali Mohammad S. A. Al-Shukri 1991 334 p
Avail: Univ. Microfilms Order No. DA9134202

The presence or absence is examined of matter collected in mass ranges encompassing the low mass stars, brown dwarfs, and the Jovian planets. Observational selection effects lead to a gap between the masses of the heaviest planets and lightest stars known. Speckle interferometry has great potential for high resolution imaging in astronomy and which has applications to the problem of detecting low mass objects in the Universe. It works by freezing the fluctuations in the atmosphere, using snapshots that contain spatial structure down to the theoretical resolving limit of a telescope. The very extensive series of speckle observations are used to evaluate the limiting accuracy of these data and to make the first study of the detectability of unseen companions in the data. It is possible in principle to not only detect low mass companions bound in orbits about one component of the resolved binary, but it may also be possible to provide new statistical information on the spectrum of planetary to stellar masses. Among the 70 binary systems analyzed, six systems showed some indications of significant submotions.
Dissert. Abstr.

N92-23698 Virginia Univ., Charlottesville.
THE THROES OF STAR FORMATION: A STUDY OF THE ORION-KL AND DR21(OH) MOLECULAR CLOUDS Ph.D. Thesis
Jeffrey Gary Mangum 1990 268 p
Avail: Univ. Microfilms Order No. DA9131571

An interferometric and single antenna molecular spectral line study is presented of the Orion-KL and DR21(OH) star forming regions. New observations are used to study the physical properties of star formation over spatial scales from 0.01 to 0.1 pc. In a study of the larger spatial scales in the Orion-KL molecular cloud, a multitransition, multiisotopomer H2CO data set was used in conjunction with a large velocity gradient model of the radiative transfer to derive the spatial density in the Orion-KL compact ridge component. An analysis of the H2CO abundance in the subsources which comprise Orion-KL indicates that there is no evidence for substantial variation in the H2CO abundances, but that H2CO is approx. an order of magnitude more abundant in the warmer Orion-KL subsources than it is in other molecular clouds. In the study of DR21(OH) molecular cloud, many similarities were found to the Orion-KL star forming region. The (18)CO and millimeter continuum observations have shown that within a region approx. 45000 AU in extent, several of the early phases of star formation were seen. Regions in DR21(OH) possess the same size and luminosity as Orion-KL, indicating that DR21(OH) may be a massive star forming region. Dissert. Abstr.

N92-23716 California Univ., Los Angeles.
NUCLEAR WINDS IN ACTIVE GALAXIES Ph.D. Thesis
Steven Joseph Smith 1991 164 p
Avail: Univ. Microfilms Order No. DA9129961

The consequences of nuclear winds in active galaxies are investigated. Nuclear winds are defined to be any supersonic wind generated by the active nucleus; starburst winds could be similar. A review of theory and observation relevant to nuclear winds is presented, and the range of possible wind parameters is defined. A detailed analysis of the interaction of a nuclear wind with the hot interstellar medium (ISM) of a host elliptical galaxy is performed. The hot ISM in elliptical galaxies shortens the timescale of the interaction and generally prevents a dense, wind driven shell from forming. Nuclear winds will have a profound effect on the host galaxy, replacing some or all of the ISM. Nuclear winds can also shut off normal star formation in the galaxy as well as that due to cooling flows. The effect of mass loading of the nuclear wind by stellar wind mass loss is investigated. An ideal hydrodynamic analysis finds that stellar winds are unlikely to mass load the nuclear wind unless instabilities act very rapidly to mix the stellar wind material into the nuclear wind. Observational signatures of the nuclear wind are presented, the most striking of which is the alteration of the x-ray profile of the host galaxy. A powerful nuclear wind will eject the hot component of the ISM from its host galaxy, which will not show the extended x-ray halo normally seen in large elliptical galaxies. Instead, only the central nuclear and stellar x-ray sources will be seen. The shape of the radial ionization parameter profile is also a signature of the nuclear wind, and will indicate the presence of stellar wind mass loading. The relationship between the nuclear wind and emission-line clouds is discussed, including cloud properties and dynamics. The narrow-line clouds are capable of mass loading the nuclear wind and may be the source of the inferred ionization gradients. A stable zone may exist in the stellar core of the host galaxy. Emission-line clouds could survive in this zone for a comparatively long time. Finally, a parameter space for nuclear winds is presented. Nuclear winds are likely to be fast and at least moderately efficient.
Dissert. Abstr.

N92-23770 Brown Univ., Providence, RI.
THE METEORITE RECORD AS CLUES TO ASTEROIDAL REGOLITH PROCESSES Ph.D. Thesis
Daniel Turner Britt, III 1991 320 p
Avail: Univ. Microfilms Order No. DA9204833

A major question in asteroid science is the identification of the asteroidal source of ordinary chondrite meteorites. Although ordinary chondrites account for approximately 80 percent of meteorite falls, so far remote spectral observations have failed to unequivocally identify any main asteroid belt parent bodies for this most abundant meteorite type. This thesis reports the results of intensive laboratory work on the petrological and spectral properties of black and gas-rich ordinary chondrite parent bodies. Black and gas-rich ordinary chondrites sample the spectral effects of regolith and regolith-like (such as shock) processes in the space environment. Shock processes can alter the optical properties of ordinary chondrite material by redistributing the metal and troilite fraction into micron-sized blobs. This produces a dark, flat spectrum similar to that of carbonaceous chondrite meteorites. The optically altered black and gas-rich ordinary chondrites are relatively abundant in the population of ordinary chondrites, accounting for 16.7 percent of observed falls. The implications of this work suggest that the large ordinary chondrite parent bodies may have an optically thick regolith of shock-darkened material. This darkened regolith would have spectral characteristics similar to the low-albedo C-class asteroids, suggesting that the parent asteroids of ordinary chondrite meteorites are 'hiding' among the C-class population. Although the spectral features of black and gas-rich ordinary chondrites are similar to other low-reflectance meteorites, there are subtle diagnostic features that can be used to identify ordinary chondrite parent bodies. These features include subtle absorption bands near 1.0 and 2.0 microns, and the lack of hydration features at 3.0 microns. Dissert. Abstr.

N92-24000 Columbia Univ., New York, NY.
MAGNETIC RECONNECTION IN MAGNETOTAIL AND SOLAR PLASMAS Ph.D. Thesis
Xiaogang Wang 1991 125 p
Avail: Univ. Microfilms Order No. DA9202784

The formation of current sheets which dominates the heating of the solar corona and the onset of substorms due to collisionless tearing instability in the magnetotail are studied in the context of magnetic field line reconnection in space plasmas. The collisionless tearing instability and current disruption of the magnetotail are considered. The linear collisionless tearing instability, with wavelengths of the order of 10 R sub E, and with a growth rate of gamma approx. = 10(exp -2)/sec, is identified as a possible mechanism for the growth phase of a substorm. The linear analysis was carried out in the presence of an equilibrium B sub y field, neglected in other theories. From the evolution equations for

electromagnetic field perturbations, a nonlinear growth rate was derived by generalizing the boundary layer techniques of linear theory. It is shown that current sheets can be formed in Parker's model of the solar corona in the presence of smooth photospheric flows, despite van Ballegooijen and Field's proof that in an ideal plasma current sheets do not occur unless the boundary velocity field is discontinuous. The rapid reconnection involved in the formation of current sheets justifies the helicity conservation.
Dissert. Abstr.

N92-24015 Toledo Univ., OH.
LINE PROFILE ASYMMETRIES IN CHROMOSPHERICALLY ACTIVE STARS Ph.D. Thesis
Robert C. Dempsey 1991 197 p
Avail: Univ. Microfilms Order No. DA9203226

A new application of cross correlation is reported. Chromospherically active stars are correlated with inactive, normal stars to obtain information about surface inhomogeneities contained in the absorption line profiles. This technique presents a considerable improvement over Doppler imaging in that S/N and resolution requirements are much less stringent. Results for 16 F-K stars with 10 less than visni less than or = 80 km/s are reported. High resolution observations of the Ca II lambda 8542 line, obtained simultaneously with the correlation spectra, give additional information on surface inhomogeneities producing profile asymmetries. Almost all of the program stars possess some degree of emission creating abnormally shallow Ca II profiles. Spectra of several stars exhibit well defined emission reversals. In the case of HR 8703, the reversal is present during photometric minima and absent otherwise. Periodic variations in the Ca II emission in sigma Gem are discussed. Detailed modeling is applied to sigma Gem. Profile asymmetries for this star are fitted by two high latitude spots covering a little over 5 pct. of the stellar surface. The derived temperature of 3400 K is lower than found previously.
Dissert. Abstr.

N92-24017 California Univ., Santa Cruz.
TYPE Ib SUPERNOVAE AND A NEW RADIATION HYDRODYNAMICS CODE Ph.D. Thesis
Lisa Marie Ensman 1991 215 p
Avail: Univ. Microfilms Order No. DA9135898

Two issues are addressed. First, the hypothesis that the progenitors of the peculiar Type I supernovae, SNIb, are massive stars which have lost their hydrogen envelopes is examined. The stellar evolution/explosion code KEPLER of Weaver and Woosley was used to model explosions of such stars, and the resulting theoretical light curves are compared to observations. The width of the peak in the light curves implies that the masses of Type Ib progenitors lie in the range of 4 to 8 solar mass. Other aspects of the massive star progenitor hypothesis of SNIb are also discussed. Next, a new radiation hydrodynamics code, which will be used to calculate supernova light curves, was developed and tested. This code solves the full frequency integrated moments of the radiative transfer equation to order v/c. All terms in the moments equations are retained, so the solution is valid in both optically thick and thin regimes. In addition, the matter and the radiation are allowed to decouple (different temperatures), and the decoupling between the radiation field and the matter is treated self consistently. Finally, the preliminary results of a test SNIb calculation are discussed.
Dissert. Abstr.

N92-24028# Los Alamos National Lab., NM.
INTERCEPTION OF COMETS AND ASTEROIDS ON COLLISION COURSE WITH EARTH
J. C. Solem 1992 24 p Presented at the Workshop on Near Earth Objects, Los Alamos, NM, 14-26 Jan. 1992
(Contract W-7405-eng-36)
(DE92-007431; LA-UR-92-231; CONF-920180-1) Avail: NTIS HC/MF A03

I derive expressions for the weight and range of applicability of interceptors capable of deflecting a comet or asteroid on collision course with Earth. The expressions use a fairly general relationship between the energy deposited and the mass of material blown off the astral assailant. To assess the probability that the astral assailant will fracture, I also calculate the fraction of the astral assailant's mass that will be blown off. The interaction is calculated for both kinetic energy deflection and nuclear explosive deflection. In the nuclear explosive case, I calculate the interceptor mass and cratering effect for detonations above the surface and below the surface as well as directly on the surface of the astral assailant. Because of the wide range of densities and material properties that the astral assailant may possess, the principal value of this work is to show the relationships among the salient parameters of the problem.
DOE

N92-23310*# Office National d'Etudes et de Recherches Aerospatiales, Toulouse (France). Space Technology Dept.
STUDY OF COSMIC DUST PARTICLES ON BOARD LDEF: THE FRECOPA EXPERIMENTS AO138-1 AND AO138-2
J. C. Mandeville and Janet Borg (Centre National de la Recherche Scientifique, Orsay, France) *In* NASA. Langley Research Center, LDEF: 69 Months in Space. First Post-Retrieval Symposium, Part 1 Jan. 1992 p 419-434 Previously announced in IAA as A92-18664 (For primary document see N92-23280 14-99)
Avail: NTIS HC/MF A99; 8 functional color pages CSCL 03B

N92-23315*# National Aeronautics and Space Administration. Lyndon B. Johnson Space Center, Houston, TX.
PRELIMINARY ANALYSIS OF LDEF INSTRUMENT A0187-1: CHEMISTRY OF MICROMETEOROIDS EXPERIMENT
Friedrich Hoerz, Ronald P. Bernhard, Jack Warren, Thomas H. See, Donald E. Brownlee, Mark R. Laurance, Scott Messenger, and Robert B. Peterson (Peterson, Robert B., Houston, TX) *In* NASA. Langley Research Center, LDEF: 69 Months in Space. First Post-Retrieval Symposium, Part 1 Jan. 1992 p 487-501 (For primary document see N92-23280 14-99)
Avail: NTIS HC/MF A99; 8 functional color pages CSCL 03B

N92-23317*# National Aeronautics and Space Administration. Langley Research Center, Hampton, VA.
IDE SPATIO-TEMPORAL IMPACT FLUXES AND HIGH TIME-RESOLUTION STUDIES OF MULTI-IMPACT EVENTS AND LONG-LIVED DEBRIS CLOUDS
J. Derral Mulholland, S. Fred Singer, John P. Oliver, Jerry L. Weinberg, William J. Cooke, Nancy L. Montague, Jim J. Wortman (North Carolina State Univ., Raleigh.), Phillip C. Kassel, and William H. Kinard *In its* LDEF: 69 Months in Space. First Post-Retrieval Symposium, Part 1 Jan. 1992 p 517-527 (For primary document see N92-23280 14-99)
(Contract NAS1-16550; NAG1-1218)
Avail: NTIS HC/MF A99; 8 functional color pages CSCL 03B

N92-23318*# Institute for Space Science and Technology, Inc., Gainesville, FL.
ION MICROPROBE ELEMENTAL ANALYSES OF IMPACT FEATURES ON INTERPLANETARY DUST EXPERIMENT SENSOR SURFACES
Charles G. Simon, Jerry L. Hunter, Jim J. Wortman, and Dieter P. Griffis (North Carolina State Univ., Raleigh.) *In* NASA. Langley Research Center, LDEF: 69 Months in Space. First Post-Retrieval Symposium, Part 1 Jan. 1992 p 529-548 (For primary document see N92-23280 14-99)
(Grants NAG1-1214; NAG1-1218)
Avail: NTIS HC/MF A99; 8 functional color pages CSCL 03B

N92-23320*# Kent Univ., Canterbury (England). Unit for Space Sciences.
DYNAMIC (COMPUTER) MODELLING OF THE PARTICULATE ENVIRONMENT: TRANSFORMATIONS FROM THE LDEF REFERENCE FRAME TO DECODE GEOCENTRIC AND INTERPLANETARY POPULATIONS Abstract Only
J. A. M. McDonnell and K. Sullivan *In* NASA. Langley Research Center, LDEF: 69 Months in Space. First Post-Retrieval Symposium, Part 1 Jan. 1992 p 565 Previously announced as N91-25010 (For primary document see N92-23280 14-99)
Avail: NTIS HC/MF A99; 8 functional color pages CSCL 03B

N92-23322*# National Aeronautics and Space Administration. Lyndon B. Johnson Space Center, Houston, TX.
DERIVING THE VELOCITY DISTRIBUTION OF METEOROIDS FROM THE MEASURED METEOROID IMPACT DIRECTIONALITY ON THE VARIOUS LDEF SURFACES
Herbert A. Zook *In* NASA. Langley Research Center, LDEF: 69 Months in Space. First Post-Retrieval Symposium, Part 1 Jan. 1992 p 569-579 (For primary document see N92-23280 14-99)
Avail: NTIS HC/MF A99; 8 functional color pages CSCL 03B

N92-23325*# Utah State Univ., Logan.
THE INTERSTELLAR GAS EXPERIMENT
D. L. Lind, J. Geiss, F. Buehler, and O. Eugster (Bern Univ., Switzerland) *In* NASA. Langley Research Center, LDEF: 69 Months in Space. First Post-Retrieval Symposium, Part 1 Jan. 1992 p 585-594 Sponsored in part by the Swiss National Science Foundation (For primary document see N92-23280 14-99)
(Grant NAGw-2066)
Avail: NTIS HC/MF A99; 8 functional color pages CSCL 03B

91 LUNAR AND PLANETARY EXPLORATION

Includes planetology; and manned and unmanned flights.
For spacecraft design or space stations see *18 Spacecraft Design, Testing and Performance.*

N92-23124# Pacific Northwest Lab., Richland, WA.
POWER BEAMING: MISSION ENABLING FOR LUNAR EXPLORATION
J. A. Bamberger Jan. 1992 7 p Presented at the 9th Symposium on Space Nuclear Power Systems, Albuquerque, NM, 13-16 Jan. 1992
(Contract DE-AC06-76RL-01830)
(DE92-006727; PNL-SA-19713; CONF-920104-27) Avail: NTIS HC/MF A02

This paper explores several beam power concepts proposed for powering either lunar base or rover vehicles. At present, power requirements to support lunar exploration activity are met by integral self-contained power system designs. To provide requisite energy flexibility for human expansion into space, an innovative approach to replace on-board self-contained power systems is needed. Power beaming provides an alternative approach to supplying power that would ensure increased mission flexibility while reducing total mass launched into space. Providing power to the moon presents significant design challenges because of the duration of the lunar night. Power beaming provides an alternative to solar photovoltaic systems coupled with battery storage, radioisotope thermoelectric generation, and surface nuclear power. The Synthesis Group describes power beaming as a technology supporting lunar exploration. In this analysis beam power designs are compared to conventional power generation methods. DOE

N92-23704 Washington Univ., Seattle.
A MODEL OF LARGE-SCALE INSTABILITIES IN THE JOVIAN TROPOSPHERE Ph.D. Thesis
Yvan Joseph Orsolini 1991 222 p
Avail: Univ. Microfilms Order No. DA9203291

The cloud top circulation of Jupiter is characterized by latitudinal cloud bands and near steady jets which decay with height. A quasi-geostrophic midlatitude beta plane was developed to study whether the jet decay and meridional circulations are driven by large scale instabilities of a deep zonal flow extending upward into the troposphere of Jupiter. Linear barotropic and baroclinic instabilities of simple analytic zonal flows thought to be representative of the Jovian tropospheric circulation are studied. A quasi-linear model was used to study how an initially barotropically unstable flow develops a steady shear zone in the lower scale heights as a result of the action of the eddy fluxes. The instabilities are then acting as a vertical drag term and the jets decay to a non-zero barotropic component. A Rayleigh drag is introduced, forcing the mean flow back to its unstable state, while the eddies are damped radiatively. When the forcing time scale is the same as the radiatively damping time, an asymmetric life cycle type of behavior was found, with the eddy energy growing quickly to saturation and decaying slowly. Dissert. Abstr.

92 SOLAR PHYSICS

Includes solar activity, solar flares, solar radiation and sunspots.
For related information see *93 Space Radiation.*

N92-23171 Pennsylvania State Univ., University Park.
TESTING THE SOLAR PARADIGM FOR CHROMOSPHERIC ACTIVITY IN RS CVN BINARIES: MODERATE RESOLUTION SPECTROSCOPY OF SOLAR ACTIVE REGIONS Ph.D. Thesis
Margaret McMath Chester 1991 245 p
Avail: Univ. Microfilms Order No. DA9204179

Low spatial resolution observations in the range 3900A to 9000A of solar active regions were compared to similar observations of the active components of three RS CVn binaries. The solar observations were obtained in 1989 with a solar echelle spectrograph and charge-coupled device (CCD) camera on the 6-inch guide telescope at Penn State's Black Moshannon Observatory. The stellar observations were obtained in 1987 and 1988 with the fiber optic echelle (FOE) spectrograph and CCD on the coude feed at Kitt Peak National Observatory. Excess emission profiles of H alpha, H beta, and the 8498A and 8542A lines of the Ca II infrared triplet were analyzed. The ratio of the energy emitted in H alpha and H beta is much smaller in solar plages then in RS CVn active subgiants. The character of the infrared triplet emission is also different. Analysis of these differences and the phase behavior of the Balmer and infrared triplet lines in the RS CVns suggests that the Balmer emission originates from different emitting structures than the infrared triplet. In agreement with Buzasi (1989), the Balmer emission is produced primarily in prominence-like extended material. The Ca II infrared triplet emission appears to be largely plage related. Emission in the far wings of the Balmer lines may also arise in plages.
Dissert. Abstr.

N92-23697 Saint Andrew's Univ. (Scotland).
THE EFFECTS OF MAGNETIC FIELDS ON OSCILLATIONS IN THE SOLAR ATMOSPHERE Ph.D. Thesis
David J. Evans 1990 212 p
Avail: Univ. Microfilms Order No. BRDX93496

A study was made of wave propagation in two regions of the solar atmosphere in which magnetic forces are significant. Sunspot observations indicate a rich variety of characteristic modes of oscillation roughly divided into three categories: three minute umbral oscillations; five minute umbral oscillations; and penumbral waves. Outside of intense magnetic flux concentrations, the oscillation spectrum is dominated by the five minute period. These waves are trapped in a cavity whose upper boundary may be affected by the magnetism of the chromosphere. A sunspot was modeled by a uniform cylindrical flux tube. The allowable modes of oscillation are found to vary as the atmospheric parameter change with depth. The magnetic structure of the chromosphere was modeled as an isothermal atmosphere permeated by a uniform and horizontal magnetic field. A dispersion relation for the trapped waves below such an atmosphere was derived and both asymptotic and numerical solutions found. The effect of a uniform magnetic field is to increase the frequency of the trapped modes. A physical explanation for these changes in frequency was put forward. Observational evidence may indicate that such effects are indeed seen. Dissert. Abstr.

N92-23701# National Geophysical Data Center, Boulder, CO.
SOLAR-GEOPHYSICAL DATA NUMBER 564, AUGUST 1991. PART 2 (COMPREHENSIVE REPORTS): DATA FOR FEBRUARY 1991 AND MISCELLANEOUS

H. E. Coffey Aug. 1991 116 p
(PB92-111699; SGD-564-Pt-2) Avail: NTIS HC/MF A06 CSCL 03B

Data is given in tabular form for February 1991 on solar flares, solar radio bursts at fixed frequencies, interplanetary solar particles and plasma, solar x-ray radiation from the GOES satellite, mass ejections from the Sun, active solar prominences, and solar filaments. Miscellaneous data is given on interplanetary solar particles and plasma from the IMP 8 solar wind observations of October 1990 to January 1991, and total solar irradiance from NIMBUS observations of November 1978 to April 1991. Author

N92-23909# International Centre for Theoretical Physics, Trieste (Italy).
A NEW APPROACH TO ESTIMATE ANGSTROM COEFFICIENTS
M. AbdelWahab Sep. 1991 11 p
(DE92-619048; IC-91/298) Avail: NTIS HC/MF A03

A simple quadratic equation to estimate global solar radiation with coefficients depending on some physical atmospheric parameters is presented. The importance of the second order and sensitivity to some climatic variations is discussed. DOE

N92-23993# National Geophysical Data Center, Boulder, CO.
SOLAR-GEOPHYSICAL DATA NUMBER 566, OCTOBER 1991. PART 2 (COMPREHENSIVE REPORTS): DATA FOR APRIL 1991 AND MISCELLANEOUS
H. E. Coffey Oct. 1991 90 p
(PB92-129402; SGD-566-Pt-2) Avail: NTIS HC/MF A05 CSCL 03B

A detailed index of data for 1991 is given. Data for April 1991 include solar flares, solar radio bursts at fixed frequencies, solar x ray radiation from the GOES satellite, interplanetary solar particles and plasma, mass ejections from the Sun, active prominences and filaments, and solar irradiance. Miscellaneous data include the NOAA 9 solar ultraviolet data for May 1986 to December 1988. Author

93 SPACE RADIATION

Includes cosmic radiation; and inner and outer earth's radiation belts.

For biological effects of radiation see *52 Aerospace Medicine*. For theory see *73 Nuclear and High-Energy Physics*.

N92-23141 Harvard Univ., Cambridge, MA.
THE ORIGINS OF THE COSMIC X RAY AND GAMMA RAY BACKGROUNDS Ph.D. Thesis
Robert Derward Rogers 1991 190 p
Avail: Univ. Microfilms Order No. DA9132028

We explore models for the diffuse cosmic X-ray and gamma ray backgrounds. We show that hot gas (T approx. equals 4 x 10(exp 8 K) cannot explain the X-ray background, whether it is smoothly distributed or confined in clumps, because of its effects on the cosmic microwave background and on the images of quasars. We show that active galactic nuclei (AGN), whose X-ray spectra are reproduced by Compton reflection from cold gas within the 1- to 100 Schwarzschild radii from the central object, can explain the X-ray background. Further, we show that when inverse Compton scattering of the X-ray spectrum is taken into account, the model can explain the gamma ray background spectrum as well. We show that, because of a relativistic effect, a large fraction (greater than 50 percent) of the X-rays emitted in the AGN will be reprocessed if the cold gas is contained in a thin accretion disk. Finally, we calculate the probability that a gamma ray and an X-ray emitted by an AGN will interact to produce an electron-positron pair. We stress the implications of our results for the evolution of AGN, and discuss the possibility of observing such sources. Author

N92-23162 Cornell Univ., Ithaca, NY.
INFRARED EMISSION LINES FROM HIGHLY IONIZED REGIONS Ph.D. Thesis
Neil Rowlands 1991 126 p
Avail: Univ. Microfilms Order No. DA9204053

Infrared and ultraviolet emission lines are used to determine the physical conditions in the important, but infrequently studied, highly ionized (HeIII) regions of planetary nebulae. Observational techniques in both wavelength ranges are discussed, with emphasis on the use of an infrared detector array in a cooled grating spectrometer and on the use of a tilting filter ultraviolet spectrometer. The planetary nebulae emission line ratios indicate that the HeIII region electron densities are similar to those found in the low excitation regions. In contrast, HeIII region electron temperatures are, in most cases, considerably higher than those found in the low excitation regions. To some extent, this is expected due to the lack of ions with strong collisionally excited emission lines in this region. However, the wide variation in HeIII region electron temperatures found among the observed planetary nebulae was not expected. This variation is shown to be a consequence of substantial differences in the abundances of carbon and nitrogen, whose emission lines cool this highly ionized region, among the observed planetary nebulae. Dissert. Abstr.

N92-23163 Indiana Univ., Bloomington.
THE ISOTOPIC COMPOSITION OF COSMIC RAY HELIUM FROM 500 TO 1100 MeV PER NUCLEON Ph.D. Thesis
Scott Lowry Nutter 1991 172 p
Avail: Univ. Microfilms Order No. DA9134820

The isotopic composition of cosmic ray Helium was measured during a period of solar maximum in a particle kinetic energy range from 100 to 1100 MeV/nucleon with the SMILI (Superconducting Magnet Instrument for Light Isotopes) magnetic spectrometer. Presented here is a description of the SMILI instrument, with a focus on the Cerenkov detector and its velocity resolution, including the addition to the resolution from knock-on electrons. Also, three data points using the data from the Cerenkov detector are presented for the important secondary to primary abundance ratio He-3/He-4 in the kinetic energy range 500 to 1100 MeV/nucleon. The data indicate a flatter energy dependence of the ratio than typical propagation predictions based on fits to the cosmic ray Boron to Carbon abundance ratio. Dissert. Abstr.

N92-23736 Durham Univ. (England).
TeV GAMMA RAY EMISSION FROM ACCRETING BINARY PULSARS Ph.D. Thesis
Vincent Mannings 1990 414 p
Avail: Univ. Microfilms Order No. BRD-93525

The high mass X ray binary SMC X-1 was observed during the interval 1986 to 1989 at a threshold gamma ray energy of 0.4 TeV using a Mark III air Cerenkov telescope. The Cerenkov arrival time series recorded during these observations were tested for periodicity at the contemporary pulse period of the SMC X-1 X ray pulsar. This period analysis was performed using a new technique, herein presented, which is designed for TeV gamma ray source candidates in binary systems and which simultaneously seeks evidence for pulsed TeV gamma ray emission and information on the location of the emission site within the binary. Results are also presented from the period analysis of data accumulated during observations of the low mass X ray binaries X0021.8-7221 and GX 1 + 4. X ray binaries as a class of TeV gamma ray source are considered and their properties compared. Previous models which invoke the interaction of beams of high energy particles with material within the environment of a binary system are discussed. One of these models is adapted herein in order to propose a simple explanation of the narrow TeV gamma ray orbital light curve observed for the high mass binary Centaurus X-3. Dissert. Abstr.

N92-23293*# Naval Research Lab., Washington, DC.
GAMMA RADIATION SURVEY OF THE LDEF SPACECRAFT
G. W. Phillips, S. E. King, R. A. August, J. C. Ritter, J. H. Cutchin, P. S. Haskins, J. E. McKisson, D. W. Ely, A. G. Weisenberger,

and R. B. Piercey (Mississippi State Univ., Mississippi State.) et al *In* NASA. Langley Research Center, LDEF: 69 Months in Space. First Post-Retrieval Symposium, Part 1 Jan. 1992 p 225-236 (For primary document see N92-23280 14-99)
Avail: NTIS HC/MF A99; 8 functional color pages CSCL 03B

N92-23294*# National Aeronautics and Space Administration. Marshall Space Flight Center, Huntsville, AL.
THE INTERACTIONS OF ATMOSPHERIC COSMOGENIC RADIONUCLIDES WITH SPACECRAFT SURFACES
J. C. Gregory (Alabama Univ., Huntsville.), G. J. Fishman, B. A. Harmon, and T. A. Parnell *In* NASA. Langley Research Center, LDEF: 69 Months in Space. First Post-Retrieval Symposium, Part 1 Jan. 1992 p 237-247 Previously announced as N92-11075 (For primary document see N92-23280 14-99)
Avail: NTIS HC/MF A99; 8 functional color pages CSCL 03B

N92-23301*# Grumman Aerospace Corp., Bethpage, NY.
THERMOLUMINESCENT DOSIMETRY FOR LDEF EXPERIMENT M0006
J. Y. Chang, D. Giangano, T. Kantorcik, M. Stauber, and L. Snead (Brookhaven National Lab., Upton, NY.) *In* NASA. Langley Research Center, LDEF: 69 Months in Space. First Post-Retrieval Symposium, Part 1 Jan. 1992 p 313-324 (For primary document see N92-23280 14-99)
Avail: NTIS HC/MF A99; 8 functional color pages CSCL 03B

N92-23302*# National Aeronautics and Space Administration. Marshall Space Flight Center, Huntsville, AL.
RADIATION EXPOSURE OF LDEF: INITIAL RESULTS
E. V. Benton, A. L. Frank, E. R. Benton, I. Csige (San Francisco Univ., CA.), T. A. Parnell, and J. W. Watts, Jr. *In* NASA. Langley Research Center, LDEF: 69 Months in Space. First Post-Retrieval Symposium, Part 1 Jan. 1992 p 325-337 (For primary document see N92-23280 14-99)
(Grant NAG8-168)
Avail: NTIS HC/MF A99; 8 functional color pages CSCL 03B

N92-23306*# Dublin Inst. for Advanced Studies (Ireland).
THE LDEF ULTRA HEAVY COSMIC RAY EXPERIMENT
D. OSullivan, A. Thompson, J. Bosch, R. Keegan, K.-P. Wenzel, A. Smit, and C. Domingo (Barcelona Univ., Spain) *In* NASA. Langley Research Center, LDEF: 69 Months in Space. First Post-Retrieval Symposium, Part 1 Jan. 1992 p 367-375 (For primary document see N92-23280 14-99)
Avail: NTIS HC/MF A99; 8 functional color pages CSCL 03B

N92-23307*# Naval Research Lab., Washington, DC. Center for Space Research.
PRELIMINARY RESULTS FROM THE HEAVY IONS IN SPACE EXPERIMENT
James H. Adams, Jr., Lorraine P. Beahm, and Allan J. Tylka *In* NASA. Langley Research Center, LDEF: 69 Months in Space. First Post-Retrieval Symposium, Part 1 Jan. 1992 p 377-391 (For primary document see N92-23280 14-99)
Avail: NTIS HC/MF A99; 8 functional color pages CSCL 03B

N92-23627*# Deutsche Forschungsanstalt fuer Luft- und Raumfahrt, Cologne (Germany, F.R.). Inst. for Aerospace Medicine.
BIOSTACK (14-IML-1)
H. Buecker *In* NASA. Marshall Space Flight Center, First International Microgravity Laboratory Experiment Descriptions Feb. 1992 p 181-182 (For primary document see N92-23600 14-29)
Avail: NTIS HC/MF A13 CSCL 03B

N92-23975# European Space Agency. European Space Operations Center, Darmstadt (Germany, F.R.). Spacecraft Trajectory Branch.
PREDICTION OF SOLAR AND GEOMAGNETIC ACTIVITY FOR ESA LOW-FLYING SPACECRAFT
R. Mugellesi and D. J. Kerridge (Natural Environmental Research Council, Edinburgh, Scotland) *In its* The Reentry of Salyut-7/Kosmos-1686 Aug. 1991 p 63-7 (For primary document see N92-23967 14-18)
Copyright Avail: NTIS HC/MF A05

99 GENERAL

N92-23280*# National Aeronautics and Space Administration. Langley Research Center, Hampton, VA.
LDEF: 69 MONTHS IN SPACE. FIRST POST-RETRIEVAL SYMPOSIUM, PART 1
Arlene S. Levine, ed. Jan. 1992 603 p Symposium held in Kissimmee, FL, 2-8 Jun. 1991; sponsored by NASA, Washington Original contains color illustrations
(NASA-CP-3134-Pt-1; L-17042-Pt-1; NAS 1.55:3134-Pt-1) Avail: NTIS HC/MF A99; 8 functional color pages CSCL 22A

A compilation of papers from the symposium is presented. The papers represent the preliminary data analysis of the 57 experiments flown on the Long Duration Exposure Facility (LDEF). The experiments include materials, coatings, thermal systems, power and propulsion, science (cosmic ray, interstellar gas, heavy ions, and micrometeoroids), electronics, optics, and life sciences. For individual titles, see N92-23281 through N92-23325.

N92-23281*# National Aeronautics and Space Administration. Langley Research Center, Hampton, VA.
LONG DURATION EXPOSURE FACILITY: A GENERAL OVERVIEW **c18**
Robert L. ONeal and E. Burton Lightner *In its* LDEF: 69 Months in Space. First Post-Retrieval Symposium, Part 1 Jan. 1992 p 3-48 (For primary document see N92-23280 14-99)
Avail: NTIS HC/MF A99; 8 functional color pages CSCL 22B

The Long Duration Exposure Facility (LDEF) is a large, low-cost, reusable, unmanned, free-flying spacecraft which accommodates technology, science, and applications experiments for long-term exposure to the space environment. The LDEF was designed and built by the NASA Langley Research Center (LaRC) for NASA's Office of Aeronautics and Space Technology. Specifically, the LDEF was designed to transport experiments into space via the Space Shuttle, to free fly in Earth orbit for an extended period, and be retrieved on a later Space Shuttle flight allowing experiments to be returned to Earth for postflight analysis in the laboratory. The LDEF with a full complement of experiments was placed in Earth orbit in April 1984 by Challenger and retrieved from orbit in January 1990 by Columbia. A general overview of the LDEF, its mission, systems, experiments, and operations is presented. Excerpts from various NASA documents are extensively used. K.S.

N92-23282*# National Aeronautics and Space Administration. Langley Research Center, Hampton, VA.
LONG DURATION EXPOSURE FACILITY (LDEF) SPACE ENVIRONMENTS OVERVIEW **c18**
William H. Kinard and Glenna D. Martin *In its* LDEF: 69 Months in Space. First Post-Retrieval Symposium, Part 1 Jan. 1992 p 49-60 (For primary document see N92-23280 14-99)
Avail: NTIS HC/MF A99; 8 functional color pages CSCL 22B

The Long Duration Exposure Facility (LDEF) was retrieved from Earth orbit in January 1990 after spending almost six years in space. It had flown in a near-circular orbit with an inclination of 28.5 degrees. Initially, the orbit altitude was approximately 257 nautical miles; however, when the LDEF was retrieved the orbit altitude had decayed to approximately 179 nautical miles. The LDEF was passively stabilized about three axes while in free flight, making it an ideal platform for exposing experiments which were measuring the environments of near-Earth space and investigating the long-term effects of these environments on spacecraft. A brief overview of the encountered environments that were of most interest to the LDEF investigators is presented. K.S.

N92-23283*# National Aeronautics and Space Administration. Marshall Space Flight Center, Huntsville, AL.

PINHOLE CAMERAS AS SENSORS FOR ATOMIC OXYGEN IN ORBIT: APPLICATION TO ATTITUDE DETERMINATION OF THE LDEF **c35**

Palmer N. Peters and John C. Gregory *In* NASA. Langley Research Center, LDEF: 69 Months in Space. First Post-Retrieval Symposium, Part 1 Jan. 1992 p 61-67 Previously announced as N92-11078 (For primary document see N92-23280 14-99)
(Contract NAS8-36645; NAGw-812)
Avail: NTIS HC/MF A99; 8 functional color pages CSCL 14E

Images produced by pinhole cameras using film sensitive to atomic oxygen provide information on the ratio of spacecraft orbital velocity to the most probable thermal speed of oxygen atoms, provided the spacecraft orientation is maintained stable relative to the orbital direction. Alternatively, information on the spacecraft attitude relative to the orbital velocity can be obtained, provided that corrections are properly made for thermal spreading and a corotating atmosphere. The Long Duration Exposure Facility (LDEF) orientation, uncorrected for a corotating atmosphere, was determined to be yawed 8.0 +/- 0.4 degrees from its nominal attitude, with an estimated +/- 0.35 degree oscillation in yaw. The integrated effect of inclined orbit and corotating atmosphere produces an apparent oscillation in the observed yaw direction, suggesting that the LDEF attitude measurement will indicate even better stability when corrected for a corotating atmosphere. The measured thermal spreading is consistent with major exposure occurring during high solar activity, which occurred late during the LDEF mission. K.S.

N92-23284*# National Aeronautics and Space Administration. Langley Research Center, Hampton, VA.

USE OF THE LONG DURATION EXPOSURE FACILITY'S THERMAL MEASUREMENT SYSTEM FOR THE VERIFICATION OF THERMAL MODELS **c19**

William M. Berrios *In its* LDEF: 69 Months in Space. First Post-Retrieval Symposium, Part 1 Jan. 1992 p 69-83 (For primary document see N92-23280 14-99)
Avail: NTIS HC/MF A99; 8 functional color pages CSCL 14B

The Long Duration Exposure Facility (LDEF) postflight thermal model predicted temperatures were matched to flight temperature data recorded by the Thermal Measurement System (THERM), LDEF experiment P0003. Flight temperatures, recorded at intervals of approximately 112 minutes for the first 390 days of LDEF's 2105 day mission were compared with predictions using the thermal mathematical model (TMM). This model was unverified prior to flight. The postflight analysis has reduced the thermal model uncertainty at the temperature sensor locations from +/- 40 F to +/- 18 F. The improved temperature predictions will be used by the LDEF's principal investigators to calculate improved flight temperatures experienced by 57 experiments located on 86 trays of the facility. K.S.

N92-23285*# Science Applications International Corp., Glendora, CA.

MEASURED SPACE ENVIRONMENTAL EFFECTS TO LDEF DURING RETRIEVAL **c18**

Carl R. Maag and W. Kelly Linder (Air Force Systems Command, Houston, TX.) *In its* LDEF: 69 Months in Space. First Post-Retrieval Symposium, Part 1 Jan. 1992 p 85-99 (For primary document see N92-23280 14-99)
Avail: NTIS HC/MF A99; 8 functional color pages CSCL 22B

On the STS-32 shuttle mission, a space flight experiment provided an understanding of the effects of the space environment on the Long Duration Exposure Facility (LDEF) from rendezvous with the shuttle until removal from the payload bay at the Orbiter Processing Facility (OPF) at KSC. The Interim Operational Contamination Monitor (IOCM) is an attached shuttle payload that has been used on two earlier flights (STS 51C and STS 28) to quantify the contamination deposited during the course of the mission. The IOCM can characterize by direct measurement, the deposition of molecular and particulate contamination during any phase of flight. In addition to these principal measurements, the IOCM actively measures the thermophysical properties of thermal control surfaces by calorimetry, the flux of the ambient atomic oxygen environment, the incident solar flux, and the absolute ambient pressure in the payload bay. The IOCM also provides a structure and sample holders for the exposure of passive material samples to the space environment, e.g. thermal cycling, atomic oxygen, and micrometeoroids and/or orbital debris, etc. One of the more salient results from the STS-32 flight suggests that the LDEF emitted a large number of particulates after berthing into the shuttle. The mission atomic oxygen fluence was also calculated. Although the fluence was low by normal standards, the Kapton passive samples exhibited the onset of erosion. Orbital debris and micrometeoroid impacts also occurred during the retrieval mission. The average perforation diameter was approximately 12.5 microns. The largest perforation diameter was measured at 65 microns. Author

N92-23286*# Boeing Co., Seattle, WA. Defense and Space Group.

PARTICLE TYPES AND SOURCES ASSOCIATED WITH LDEF **c25**

E. R. Crutcher and W. W. Wascher *In* NASA. Langley Research Center, LDEF: 69 Months in Space. First Post-Retrieval Symposium, Part 1 Jan. 1992 p 101-119 (For primary document see N92-23280 14-99)
(Contract NAS1-18224)
Avail: NTIS HC/MF A99; 8 functional color pages CSCL 07D

The particulate contamination history of the Long Duration Exposure Facility (LDEF) can be resolved by careful analysis of particle types, the LDEF time line, evidence of the relationship between particles and the surface of the LDEF, and a consideration of probable sources. This work is far from complete but was initiated as part of the characterization of the condition of experimental trays that were returned to principle investigators for their analysis. The work presented in this photo-essay is continuing and will be updated in subsequent reports to NASA and at future technical meetings. Author

N92-23287*# Boeing Co., Seattle, WA. Defense and Space Group.

MIGRATION AND GENERATION OF CONTAMINANTS FROM LAUNCH THROUGH RECOVERY: LDEF CASE HISTORY **c18**

E. R. Crutcher, L. S. Nishimura, K. J. Warner, and W. W. Wascher *In* NASA. Langley Research Center, LDEF: 69 Months in Space. First Post-Retrieval Symposium, Part 1 Jan. 1992 p 121-140 (For primary document see N92-23280 14-99)
(Contract NAS1-18224)
Avail: NTIS HC/MF A99; 8 functional color pages CSCL 22B

It is possible to recreate the contamination history of the Long Duration Exposure Facility (LDEF) through an analysis of its contaminants and selective samples that were collected from surfaces with better documented exposure histories. This data was then used to compare estimates based on monitoring methods that were selected for the purpose of tracking LDEF's exposure to contaminants. The LDEF experienced much more contamination than would have been assumed based on the monitors. Work is still in progress but much of what was learned so far is already being used in the selection of materials and in the design of systems for space. Now experiments are being prepared for flight to resolve questions created by the discoveries on the LDEF. A summary of what was learned about LDEF contaminants over the first year since recovery and deintegration is presented. Over 35 specific conclusions in 5 contamination related categories are listed. Author

N92-23288*# Boeing Co., Seattle, WA. Defense and Space Group.

QUANTIFICATION OF CONTAMINANTS ASSOCIATED WITH LDEF **c25**

E. R. Crutcher, L. S. Nishimura, K. J. Warner, and W. W. Wascher *In* NASA. Langley Research Center, LDEF: 69 Months in Space. First Post-Retrieval Symposium, Part 1 Jan. 1992

p 141-154 (For primary document see N92-23280 14-99)
(Contract NAS1-18224)
Avail: NTIS HC/MF A99; 8 functional color pages CSCL 07D

The quantification of contaminants on the Long Duration Exposure Facility (LDEF) and associated hardware or tools is addressed. The purpose of this study was to provide a background data base for the evaluation of the surface of the LDEF and the effects of orbital exposure on that surface. This study necessarily discusses the change in the distribution of contaminants on the LDEF with time and environmental exposure. Much of this information may be of value for the improvement of contamination control procedures during ground based operations. The particulate data represents the results of NASA contractor monitoring as well as the results of samples collected and analyzed by the authors. The data from the tapelifts collected in the Space Shuttle Bay at Edwards Air Force Base and KSC are also presented. The amount of molecular film distributed over the surface of the LDEF is estimated based on measurements made at specific locations and extrapolated over the surface area of the LDEF. Some consideration of total amount of volatile-condensible materials available to form the resultant deposit is also presented. All assumptions underlying these estimates are presented along with the rationale for the conclusions. Each section is presented in a subsection for particles and another for molecular films. Author

N92-23289*# Boeing Co., Seattle, WA. Defense and Space Group.
MOLECULAR FILMS ASSOCIATED WITH LDEF c72
E. R. Crutcher and K. J. Warner *In* NASA. Langley Research Center, LDEF: 69 Months in Space. First Post-Retrieval Symposium, Part 1 Jan. 1992 p 155-177 (For primary document see N92-23280 14-99)
(Contract NAS1-18224)
Avail: NTIS HC/MF A99; 8 functional color pages CSCL 20H

The molecular films deposited on the surface of the Long Duration Exposure Facility (LDEF) originated from the paints and room-temperature-vulcanized (RTV) silicone materials intentionally used on the satellite and not from residual contaminants. The high silicone content of most of the films and the uniformity of the films indicates a homogenization process in the molecular deposition and suggests a chemically most favored composition for the final film. The deposition on interior surfaces and vents indicated multiple bounce trajectories or repeated deposition-reemission cycles. Exterior surface deposits indicated a significant return flux. Ultraviolet light exposure was required to fix the deposited film as is indicated by the distribution of the films on interior surfaces and the thickness of films at the vent locations. Thermal conditions at the time of exposure to ultraviolet light seems to be an important factor in the thickness of the deposit. Sunrise facing (ram direction) surfaces always had the thicker film. These were the coldest surfaces at the time of their exposure to ultraviolet light. The films have a layered structure suggesting cyclic deposition. As many as 34 distinct layers were seen in the films. The cyclic nature of the deposition and the chemical uniformity of the film one layer to the next suggest an early deposition of the films though there is evidence for the deposition of molecular films throughout the nearly six year exposure of the satellite. A final 'spray' of an organic material associated with water soluble salts occurred very late in the mission. This may have been the result of one of the shuttle dump activities. Author

N92-23290*# National Aeronautics and Space Administration. Langley Research Center, Hampton, VA.
ORGANIC CONTAMINATION OF LDEF c23
Gale A. Harvey *In its* LDEF: 69 Months in Space. First Post-Retrieval Symposium, Part 1 Jan. 1992 p 179-197 (For primary document see N92-23280 14-99)
Avail: NTIS HC/MF A99; 8 functional color pages CSCL 07A

A brown stain of varying thickness was present on most of the exterior surface of the retrieved Long Duration Exposure Facility (LDEF). Tape lifts of Earth-end LDEF surfaces taken in Feb. 1990 showed that the surface particle cleanliness immediately after retrieval was very good, but faint footprints of the tape strips on the tested surfaces indicated a very faint film was removed by the tape. Solvent wipes of these surfaces showed that the stain was not amenable to standard organic solvent removal. Infrared spectra of optical windows from tray E5 and scrapings indicate that the film is primarily of organic composition, but is not similar to the oil that seeped from tray C12. Very dark and heavy deposits of the stain are present at openings and vents to the interior of the LDEF. Heavy brown and blue-green deposits are present in the interior of LDEF where sunlight penetrated through cracks and vent openings. Photographs of the deintegrated LDEF graphically show the stain distribution. The exterior of the LDEF had significant areas painted with a white polyurethane paint for thermal control, and almost all of the interior was painted with a black polyurethane paint for thermal control. The brown staining of the LDEF is consistent with long-term outgassing of hydrocarbons from these paints followed by rapid solar-ultraviolet-induced polymerization of the outgassed hydrocarbons when the outgassed molecules stuck to surfaces exposed to sunlight. Author

N92-23291*# National Aeronautics and Space Administration. Marshall Space Flight Center, Huntsville, AL.
SUMMARY OF IONIZING RADIATION ANALYSIS ON THE LONG DURATION EXPOSURE FACILITY c72
T. A. Parnell *In* NASA. Langley Research Center, LDEF: 69 Months in Space. First Post-Retrieval Symposium, Part 1 Jan. 1992 p 199-212 (For primary document see N92-23280 14-99)
Avail: NTIS HC/MF A99; 8 functional color pages CSCL 20H

The ionizing radiation measurements flown on the Long Duration Exposure Facility (LDEF) were contained in 15 experiments which utilized passive detectors to pursue objectives in astrophysics and to measure the radiation environment and dosimetric quantities. The spacecraft structure became sufficiently radioactive to permit additional important studies. The induced activity allows extensive radiation mapping in the structure, and independent comparison with experiment dosimetric techniques, and significant studies of secondary effects. The long exposure time, attitude stability, and number and types of measurements produced a unique and critical set of data for low Earth orbit that will not be duplicated for more than a decade. The data allow an unprecedented test, and improvement if required, of models of the radiation environment and the radiation transport methods that are used to calculate the internal radiation and its effects in spacecraft. Results of measurements in the experiments, as well as from radioactivity in the structure, have clearly shown effects from the directional properties of the radiation environment, and progress was made in the dosimetric mapping of LDEF. These measurements have already influenced some Space Station Freedom design requirements. Preliminary results from experiments, reported at this symposium and in earlier papers, show that the 5.8 years exposure considerably enhanced the scientific return of the radiation measurements. The early results give confidence that the experiments will make significant advances in the knowledge of ultra heavy cosmic rays, anomalous cosmic rays, and heavy ions trapped in the radiation belts. Unexpected phenomena were observed, which require explanation. These include stopping iron group ions between the energy ranges anticipated for anomalous and galactic cosmic rays in the LDEF orbit. A surprising concentration of the Be-7 nuclide was discovered on the 'front' surface of LDEF, apparently transported up from the stratosphere with exceptional efficiency. Author

N92-23292*# National Aeronautics and Space Administration. Marshall Space Flight Center, Huntsville, AL.
PREDICTION OF LDEF IONIZING RADIATION ENVIRONMENT c72
John W. Watts, T. A. Parnell, James H. Derrickson, T. W. Armstrong, and E. V. Benton (San Francisco Univ., CA.) *In* NASA. Langley Research Center, LDEF: 69 Months in Space. First Post-Retrieval Symposium, Part 1 Jan. 1992 p 213-224 (For primary document

see N92-23280 14-99)
Avail: NTIS HC/MF A99; 8 functional color pages CSCL 20H

The Long Duration Exposure Facility (LDEF) spacecraft flew in a 28.5 deg inclination circular orbit with an altitude in the range from 172 to 258.5 nautical miles. For this orbital altitude and inclination two components contribute most of the penetrating charge particle radiation encountered - the galactic cosmic rays and the geomagnetically trapped Van Allen protons. Where shielding is less than 1.0 g/sq cm geomagnetically trapped electrons make a significant contribution. The 'Vette' models together with the associated magnetic filed models were used to obtain the trapped electron and proton fluences. The mission proton doses were obtained from the fluence using the Burrell proton dose program. For the electron and bremsstrahlung dose we used the Marshall Space Flight Center (MSFC) electron dose program. The predicted doses were in general agreement with those measured with on-board thermoluminescent detector (TLD) dosimeters. The NRL package of programs, Cosmic Ray Effects on MicroElectronics (CREME), was used to calculate the linear energy transfer (LET) spectrum due to galactic cosmic rays (GCR) and trapped protons for comparison with LDEF measurements. D.R.D.

N92-23293*# Naval Research Lab., Washington, DC.
GAMMA RADIATION SURVEY OF THE LDEF SPACECRAFT **c93**

G. W. Phillips, S. E. King, R. A. August, J. C. Ritter, J. H. Cutchin, P. S. Haskins, J. E. McKisson, D. W. Ely, A. G. Weisenberger, and R. B. Piercey (Mississippi State Univ., Mississippi State.) et al *In* NASA. Langley Research Center, LDEF: 69 Months in Space. First Post-Retrieval Symposium, Part 1 Jan. 1992 p 225-236 (For primary document see N92-23280 14-99)
Avail: NTIS HC/MF A99; 8 functional color pages CSCL 03B

The retrieval of the Long Duration Exposure Facility spacecraft in January 1990 after nearly six years in orbit offered a unique opportunity to study the long term buildup of induced radioactivity in the variety of materials on board. We conducted the first complete gamma-ray survey of a large spacecraft on LDEF shortly after its return to earth. A surprising observation was the Be-7 activity which was seen primarily on the leading edge of the satellite, implying that it was picked up by LDEF in orbit. This is the first known evidence for accretion of a radioactive isotope onto an orbiting spacecraft. Other isotopes observed during the survey, the strongest being Na-22, are all attributed to activation of spacecraft components. Be-7 is a spallation product of cosmic rays on nitrogen and oxygen in the upper atmosphere. However, the observed density is much greater than expected due to cosmic-ray production in situ. This implies transport of Be-7 from much lower altitudes up to the LDEF orbit. D.R.D.

N92-23294*# National Aeronautics and Space Administration. Marshall Space Flight Center, Huntsville, AL.
THE INTERACTIONS OF ATMOSPHERIC COSMOGENIC RADIONUCLIDES WITH SPACECRAFT SURFACES **c93**

J. C. Gregory (Alabama Univ., Huntsville.), G. J. Fishman, B. A. Harmon, and T. A. Parnell *In* NASA. Langley Research Center, LDEF: 69 Months in Space. First Post-Retrieval Symposium, Part 1 Jan. 1992 p 237-247 Previously announced as N92-11075 (For primary document see N92-23280 14-99)
Avail: NTIS HC/MF A99; 8 functional color pages CSCL 03B

The discovery of the cosmogenic radionuclide Be-7 on the front surface of the Long Duration Exposure Facility (LDEF) spacecraft has opened opportunities to investigate new phenomena in several disciplines of space science. The experiments performed for this work show that the Be-7 results only if the source of the isotope is the atmosphere through which the spacecraft passed. We should expect that the uptake of beryllium in such circumstances will depend on the chemical form of the Be and the chemical nature of the substrate. It was found that the observed concentration of Be-7 does, in fact, differ between metal surfaces and organic surfaces such as PTFE (teflon). It is noted, however, that: (1) organic surfaces, even PTFE, are etched by the atomic oxygen found under these orbital conditions, and (2) the relative velocity of the species is 8 km(exp -1)s relative to the surface and the interaction chemistry and physics may differ from the norm. The Be-7 is formed by spallation of O and N nuclei under cosmic ray proton bombardment. The principal source region is at altitudes of 12-15 km. While very small quantities are produced above 300 km, the amount measured on the LDEF was 3 to 4 orders of magnitude higher than expected from production at orbital altitude. The most reasonable explanation is that Be-7 is rapidly transported from low altitudes by some unknown mechanism. The process must take place on a time scale similar to the half-life of the isotope (53 days). Many other isotopes are produced by cosmic ray reactions, and some of these are suited to measurement by the extremely sensitive methods of accelerator mass spectrometry. A program was initiated to search for these isotopes and it is hoped that such studies will provide new methods for studying mixing in the upper atmosphere. Author

N92-23295*# Royal Aircraft Establishment, Farnborough (England). Space Dept.
SURFACE ACTIVATION OF CONCORDE BY Be-7 **c72**

P. R. Truscott, C. S. Dyer, and J. C. Flatman *In* NASA. Langley Research Center, LDEF: 69 Months in Space. First Post-Retrieval Symposium, Part 1 Jan. 1992 p 249-254 (For primary document see N92-23280 14-99)
Avail: NTIS HC/MF A99; 8 functional color pages CSCL 20H

Activation analysis of two airframe components from the Concorde aircraft has identified the presence of Be-7, a nuclide found by other investigators that was deposited on the forward edge of the Long Duration Exposure Facility (LDEF) structure. The results of the Concorde analysis indicate that this phenomenon is very much a surface effect, and that the areal densities of the Be-7 are comparable to those found for LDEF. The collection of Be-7 by the aircraft must be greater than in the case of LDEF (since duration for which Concorde is accumulating the nuclide is shorter) and is of the order of 1.2 to 41 nuclei/sq cm(-)s(exp -1) depending upon assumptions made regarding the altitude at which collection becomes appreciable, and the efficiency of the process which removes the radionuclide. D.R.D.

N92-23296*# Massachusetts Inst. of Tech., Cambridge. Nuclear Reactor Lab.
CHARGED PARTICLE ACTIVATION STUDIES ON THE SURFACE OF LDEF SPACECRAFT Abstract Only **c72**

Ilhan Olmez, Forrest Burns, and Paul Sagalyn (Army Materials Technology Lab., Watertown, MA.) *In* NASA. Langley Research Center, LDEF: 69 Months in Space. First Post-Retrieval Symposium, Part 1 Jan. 1992 p 255 (For primary document see N92-23280 14-99)
Avail: NTIS HC/MF A99; 8 functional color pages CSCL 20H

High energy proton induced nuclear reaction products are examined using seven elements, namely: aluminum, silicon, nickel, copper, zirconium, tantalum, and tungsten. We detected activities due to Na-22 from Al, Co-56 and Co-57 from Ni, Co-58 from Cu, and Y-88 from Zr targets. No induced activity was observed in Si, Ta, and W, most probably due to the long cooling times. Only the Zr sample contained a weak Be-7 peak, although Ta and W were also located at the leading edge of the spacecraft. Gamma-rays of individual isotopes were measured using a high-resolution Ge(Li) solid state detector coupled to a 4096-multichannel analyzer. Activities were calculated for Co-56 (846 keV) and Co-57 (122 and 136 keV's) at the time of the entry of the spacecraft and found to be 0.014 +/- 0.005 c/s-g, 0.018 +/- 0.002 c/s-g, and 0.0024 +/- 0.0007 c/s-g, respectively. Author

N92-23297*# California Univ., Berkeley. Lawrence Berkeley Lab. Engineering Div.
RADIOACTIVITIES OF LONG DURATION EXPOSURE FACILITY (LDEF) MATERIALS: BAGGAGE AND BONANZAS **c72**

Alan R. Smith and Donna L. Hurley *In* NASA. Langley Research Center, LDEF: 69 Months in Space. First Post-Retrieval Symposium, Part 1 Jan. 1992 p 257-270 (For primary document see

N92-23280 14-99)
(Contract NASA Order H-06815-D; DE-AC03-76SF-00098)
Avail: NTIS HC/MF A99; 8 functional color pages CSCL 20H

Radioactivities in materials onboard the returned Long Duration Exposure Facility (LDEF) satellite were studied by a variety of techniques. Among the most powerful is low-background Ge-semiconductor detector gamma-ray spectrometry, illustrated here by results obtained at the Lawrence Berkeley Laboratory's (LBL) Low Background Facilities. The observed radioactivities are of two origins: those radionuclides produced by nuclear reactions with the radiation field in orbit, and radionuclides present initially as 'contaminants' in materials used for construction of the spacecraft and experimental assemblies. In the first category are experiment-related monitor foils and tomato seeds, and such spacecraft materials as aluminum, stainless steel, and titanium. In the second category are aluminum, beryllium, titanium, vanadium, and some special glasses. Author

N92-23298*# Los Alamos National Lab., NM. Space Science and Technology Div.
MEASUREMENTS OF INDUCED RADIOACTIVITY IN SOME LDEF SAMPLES c72
C. E. Moss and R. C. Reedy *In* NASA. Langley Research Center, LDEF: 69 Months in Space. First Post-Retrieval Symposium, Part 1 Jan. 1992 p 271-285 Previously announced as N91-32882 Sponsored in part by NASA and DOE (For primary document see N92-23280 14-99)
Avail: NTIS HC/MF A99; 8 functional color pages CSCL 20H

Twenty-six stainless steel trunnion samples, five aluminum end support retainer plate samples, two aluminum keel plate samples, and two titanium clips were analyzed. The shielded high purity germanium detectors used had efficiencies of 33, 54, and 80 percent at 1332 keV. Detector efficiencies as a function of energy and corrections for self-absorption in the samples were determined with calibrated sources and unactivated control samples. Several measurements were made on most samples. In the trunnion samples, Mn-54 and Co-57 were seen and limits were obtained for other isotopes. The results agree well with 1-D activation calculations for an anisotropic trapped proton model. In the aluminum and titanium samples, Na-22 was detected. Other results are presented. Author

N92-23299*# Westinghouse Savannah River Co., Aiken, SC.
GAMMA RAY SPECTROMETRY OF LDEF SAMPLES AT SRL c25
Willard G. Winn *In* NASA. Langley Research Center, LDEF: 69 Months in Space. First Post-Retrieval Symposium, Part 1 Jan. 1992 p 287-300 Sponsored in part by NASA. Marshall Space Flight Center (For primary document see N92-23280 14-99)
(Contract DE-AC09-89SR-18035)
Avail: NTIS HC/MF A99; 8 functional color pages CSCL 07D

A total of 31 samples from the Long Duration Exposure Facility (LDEF), including materials of aluminum, vanadium, and steel trunnions were analyzed by ultra-low-level gamma spectrometry. The study quantified particle induced activations of Na-22, Sc-46, Cr-51, Mn-54, Co-56, Co-57, Co-58, and Co-60. The samples of trunnion sections exhibited increasing activity toward the outer end of the trunnion and decreasing activity toward its radial center. The trunnion sections did not include end pieces, which were reported to collect noticeable Be-7 on their leading surfaces. No significant Be-7 was detected in the samples analyzed. D.R.D.

N92-23300*# National Aeronautics and Space Administration. Marshall Space Flight Center, Huntsville, AL.
INDUCED RADIOACTIVITY IN LDEF COMPONENTS c72
B. A. Harmon, G. J. Fishman, T. A. Parnell, and C. E. Laird (University of Eastern Kentucky, Richmond.) *In* NASA. Langley Research Center, LDEF: 69 Months in Space. First Post-Retrieval Symposium, Part 1 Jan. 1992 p 301-311 (For primary document see N92-23280 14-99)
Avail: NTIS HC/MF A99; 8 functional color pages CSCL 20H

A systematic study of the induced radioactivity of the Long Duration Exposure Facility (LDEF) is being carried out in order to gather information about the low earth orbit radiation environment and its effects on materials. The large mass of the LDEF spacecraft, its stabilized configuration, and long mission duration have presented an opportunity to determine space radiation-induced radioactivities with a precision not possible before. Data presented include preliminary activities for steel and aluminum structural samples, and activation subexperiment foils. Effects seen in the data show a clear indication of the trapped proton anisotropy in the South Atlantic Anomaly and suggest contributions from different sources of external radiation fluxes. D.R.D.

N92-23301*# Grumman Aerospace Corp., Bethpage, NY.
THERMOLUMINESCENT DOSIMETRY FOR LDEF EXPERIMENT M0006 c93
J. Y. Chang, D. Giangano, T. Kantorcik, M. Stauber, and L. Snead (Brookhaven National Lab., Upton, NY.) *In* NASA. Langley Research Center, LDEF: 69 Months in Space. First Post-Retrieval Symposium, Part 1 Jan. 1992 p 313-324 (For primary document see N92-23280 14-99)
Avail: NTIS HC/MF A99; 8 functional color pages CSCL 03B

Experiment M0006 on the Long Duration Exposure Facility had as its objective the investigation of space radiation effects on various electronic and optical components, as well as on seed germination. The Grumman Corporate Research Center provided the radiation dosimetric measurements for M0006, comprising the preparation of thermoluminescent dosimeters (TLD) and the subsequent measurement and analysis of flight exposed and control samples. In addition, various laboratory exposures of TLD's with gamma rays and protons were performed to obtain a better understanding of the flight exposures. D.R.D.

N92-23302*# National Aeronautics and Space Administration. Marshall Space Flight Center, Huntsville, AL.
RADIATION EXPOSURE OF LDEF: INITIAL RESULTS c93
E. V. Benton, A. L. Frank, E. R. Benton, I. Csige (San Francisco Univ., CA.), T. A. Parnell, and J. W. Watts, Jr. *In* NASA. Langley Research Center, LDEF: 69 Months in Space. First Post-Retrieval Symposium, Part 1 Jan. 1992 p 325-337 (For primary document see N92-23280 14-99)
(Grant NAG8-168)
Avail: NTIS HC/MF A99; 8 functional color pages CSCL 03B

Initial results from LDEF include radiation detector measurements from four experiments, P0006, P0004, M0004, and A0015. The detectors were located on both the leading and trailing edges of the orbiter and also on the Earthside end. This allowed the directional dependence of the incoming radiation to be measured. Total absorbed doses from thermoluminescent detectors (TLDs) verified the predicted spatial east-west dose ratio dependence of a factor approx. 2.5, due to trapped proton anisotropy in the South Atlantic Anomaly. On the trailing edge of the orbiter a range of doses from 6.64 to 2.91 Gy were measured under Al equivalent shielding of 0.42 to 1.11 g/sq cm. A second set of detectors near this location yielded doses of 6.48 to 2.66 Gy under Al equivalent shielding of 0.48 to 15.4 g/sq cm. On the leading edge, doses of 2.58 to 2.10 Gy were found under Al equivalent shielding of 1.37 to 2.90 g/sq cm. Initial charged particle LET (linear energy transfer) spectra, fluxes, doses and dose equivalents, for LET in H2O greater than or = 8 keV/micron, were measured with plastic nuclear track detectors (PNTDs) located in two experiments. Also preliminary data on low energy neutrons were obtained from detectors containing (6)LiF foils. Author

N92-23303*# National Aeronautics and Space Administration. Marshall Space Flight Center, Huntsville, AL.
CHARGED PARTICLE LET-SPECTRA MEASUREMENTS ABOARD LDEF c72
I. Csige, E. V. Benton, A. L. Frank, L. A. Frigo, E. R. Benton (San Francisco Univ., CA.), T. A. Parnell, and J. W. Watts, Jr. *In* NASA. Langley Research Center, LDEF: 69 Months in Space. First Post-Retrieval Symposium, Part 1 Jan. 1992 p 339-346 (For primary document see N92-23280 14-99)
(Grant NAG8-168)
Avail: NTIS HC/MF A99; 8 functional color pages CSCL 20H

The linear energy transfer (LET) spectra of charged particles was measured in the 5 to 250 keV/micron (water) interval with CR-39 and in the 500 to 1500 keV/micron (water) interval with polycarbonate plastic nuclear track detectors (PNTDs) under different shielding depths in the P0006 experiment. The optimal processing conditions were determined for both PNTDs in relation to the relatively high track densities due to the long term exposure in space. The total track density was measured over the selected samples, and tracks in coincidence on the facing surfaces of two detector sheets were selected for measuring at the same position on each sheet. The short range (SR) and Galactic Cosmic Ray (GCR) components were measured separately with CR-39 PNTDs and the integral dose and dose rate spectra of charged particles were also determined. The high LET portion of the LET spectra was measured with polycarbonate PNTDs with high statistical accuracy. This is a unique result of this exposure due to the low flux of these types of particles for typical spaceflight durations. The directional dependence of the charged particles at the position of the P0006 experiment was also studied by four small side stacks which surrounded the main stack and by analyzing the dip angle and polar angle distributions of the measured SR and GCR particle tracks in the main stack. Author

N92-23304*# National Aeronautics and Space Administration. Marshall Space Flight Center, Huntsville, AL.

IONIZING RADIATION CALCULATIONS AND COMPARISONS WITH LDEF DATA **c72**

T. W. Armstrong, B. L. Colborn (Science Applications International Corp., Prospect, TN.), and J. W. Watts, Jr. *In* NASA. Langley Research Center, LDEF: 69 Months in Space. First Post-Retrieval Symposium, Part 1 Jan. 1992 p 347-359 (For primary document see N92-23280 14-99)

(Contract NAS8-38566)

Avail: NTIS HC/MF A99; 8 functional color pages CSCL 20H

In conjunction with the analysis of LDEF ionizing radiation dosimetry data, a calculational program is in progress to aid in data interpretation and to assess the accuracy of current radiation models for future mission applications. To estimate the ionizing radiation environment at the LDEF dosimeter locations, scoping calculations for a simplified (one dimensional) LDEF mass model were made of the primary and secondary radiations produced as a function of shielding thickness due to trapped proton, galactic proton, and atmospheric (neutron and proton cosmic ray albedo) exposures. Preliminary comparisons of predictions with LDEF induced radioactivity and dose measurements were made to test a recently developed model of trapped proton anisotropy. Author

N92-23305*# Science Applications International Corp., San Diego, CA.

LDEF GEOMETRY/MASS MODEL FOR RADIATION ANALYSES **c72**

B. L. Colborn and T. W. Armstrong *In* NASA. Langley Research Center, LDEF: 69 Months in Space. First Post-Retrieval Symposium, Part 1 Jan. 1992 p 361-365 (For primary document see N92-23280 14-99)

(Contract NAS8-35866)

Avail: NTIS HC/MF A99; 8 functional color pages CSCL 20H

A three-dimensional geometry/mass model of LDEF is under development for ionizing radiation analyses. This model, together with ray tracing algorithms, is being programmed for use both as a stand alone code in determining three-dimensional shielding distributions at dosimetry locations and as a geometry module that can be interfaced with radiation transport codes. Author

N92-23306*# Dublin Inst. for Advanced Studies (Ireland).

THE LDEF ULTRA HEAVY COSMIC RAY EXPERIMENT **c93**

D. OSullivan, A. Thompson, J. Bosch, R. Keegan, K.-P. Wenzel, A. Smit, and C. Domingo (Barcelona Univ., Spain) *In* NASA. Langley Research Center, LDEF: 69 Months in Space. First Post-Retrieval Symposium, Part 1 Jan. 1992 p 367-375 (For primary document see N92-23280 14-99)

Avail: NTIS HC/MF A99; 8 functional color pages CSCL 03B

The LDEF Ultra Heavy Cosmic Ray Experiment (UHCRE) used 16 side viewing LDEF trays giving a total geometry factor for high energy cosmic rays of 30 sq m sr. The total exposure factor was 170 sq m sr y. The experiment is based on a modular array of 192 solid state nuclear track detector stacks, mounted in sets of four in 48 pressure vessels. The extended duration of the LDEF mission has resulted in a greatly enhanced potential scientific yield from the UHCRE. Initial scanning results indicate that at least 1800 cosmic ray nuclei with Z greater than 65 were collected, including the world's first statistically significant sample of actinides. Post flight work to date and the current status of the experiment are reviewed. Author

N92-23307*# Naval Research Lab., Washington, DC. Center for Space Research.

PRELIMINARY RESULTS FROM THE HEAVY IONS IN SPACE EXPERIMENT **c93**

James H. Adams, Jr., Lorraine P. Beahm, and Allan J. Tylka *In* NASA. Langley Research Center, LDEF: 69 Months in Space. First Post-Retrieval Symposium, Part 1 Jan. 1992 p 377-391 (For primary document see N92-23280 14-99)

Avail: NTIS HC/MF A99; 8 functional color pages CSCL 03B

The Heavy Ions In Space (HIIS) experiment has two primary objectives: (1) to measure the elemental composition of ultraheavy galactic cosmic rays, beginning in the tin-barium region of the periodic table; and (2) to study heavy ions which arrive at LDEF below the geomagnetic cutoff, either because they are not fully stripped of electrons or because their source is within the magnetosphere. Both of these objectives have practical as well as astrophysical consequences. In particular, the high atomic number of the ultraheavy galactic cosmic rays puts them among the most intensely ionizing particles in Nature. They are therefore capable of upsetting electronic components normally considered immune to such effects. The below cutoff heavy ions are intensely ionizing because of their low velocity. They can be a significant source of microelectronic anomalies in low inclination orbits, where Earth's magnetic field protects satellites from most particles from interplanetary space. The HIIS results will lead to significantly improved estimates of the intensely ionizing radiation environment. Author

N92-23308*# Kiel Univ. (Germany, F.R.). Inst. fuer Reine und Angewandte Kernphysik.

HEAVY ION MEASUREMENT ON LDEF **c72**

R. Beaujean, D. Jonathal, and W. Enge *In* NASA. Langley Research Center, LDEF: 69 Months in Space. First Post-Retrieval Symposium, Part 1 Jan. 1992 p 393-397 Previously announced in IAA as A92-20919 (For primary document see N92-23280 14-99)

Avail: NTIS HC/MF A99; 8 functional color pages CSCL 20H

A stack of CR-39 and Kodak CN track detectors was exposed on the NASA satellite LDEF and recovered after almost six years in space. The quick look analysis yielded heavy ion tracks on a background of low energy secondaries from proton interaction. The detected heavy ions show a steep energy spectrum which indicates a radiation belt origin. Author

N92-23309*# National Aeronautics and Space Administration. Langley Research Center, Hampton, VA.

LARGE CRATERS ON THE METEOROID AND SPACE DEBRIS IMPACT EXPERIMENT **c18**

Donald H. Humes *In its* LDEF: 69 Months in Space. First Post-Retrieval Symposium, Part 1 Jan. 1992 p 399-418 (For primary document see N92-23280 14-99)

Avail: NTIS HC/MF A99; 8 functional color pages CSCL 22B

Examination of 29.37 sq m of thick aluminum plates from the LDEF, which were exposed to the meteoroid and man-made orbital debris environments for 5.8 years, revealed 606 craters that were 0.5 mm in diameter or larger. Most were nearly hemispherical. There was a large variation in the number density of craters around the three axis gravity gradient stabilized spacecraft. A new model of the near-Earth meteoroid environment gives good agreement with the crater fluxes measured on the fourteen faces of the LDEF.

The man-made orbital debris model of Kessler, which predicts that 16 pct. of the craters would be caused by man-made debris, is plausible. No chemical analyses of impactor residue that will distinguish between meteoroids and man-made debris is yet available. Author

N92-23310*# Office National d'Etudes et de Recherches Aerospatiales, Toulouse (France). Space Technology Dept.
STUDY OF COSMIC DUST PARTICLES ON BOARD LDEF: THE FRECOPA EXPERIMENTS AO138-1 AND AO138-2 c90
J. C. Mandeville and Janet Borg (Centre National de la Recherche Scientifique, Orsay, France) *In* NASA. Langley Research Center, LDEF: 69 Months in Space. First Post-Retrieval Symposium, Part 1 Jan. 1992 p 419-434 Previously announced in IAA as A92-18664 (For primary document see N92-23280 14-99)
Avail: NTIS HC/MF A99; 8 functional color pages CSCL 03B

Two experiments, within the French Cooperative Payload (FRECOPA) and devoted to the detection of cosmic dust, were flown on the LDEF. A variety of sensors and collecting devices have made possible the study of impact processes on materials of technological interest. Preliminary examination of hypervelocity impact features gives valuable data on size distribution and nature of interplanetary dust particles in low earth orbit, within the 0.5 to 300 micrometer size range. Most of the events detected on the trailing face of LDEF are expected to be the result of impacts of meteoritic particles only. So far, chemical analysis of craters by EDS clearly shows evidence of elements (Na, Mg, Si, S, Ca, and Fe) consistent with cosmic origin. Systematic occurrence of C and O in crater residues is an important result, to be compared with the existence of CHON particles detected in P-Halley comet nucleus. Crater size distribution is in good agreement with results from other dust experiments flown on LDEF. However, no crater smaller than 1.5 micron was observed, thus suggesting a cutoff in the near earth particle distribution. Possible origin and orbital evolution of micrometeoroids is discussed. Author

N92-23311*# National Aeronautics and Space Administration. Marshall Space Flight Center, Huntsville, AL.
METEOROID/SPACE DEBRIS IMPACTS ON MSFC LDEF EXPERIMENTS c18
Miria Finckenor *In* NASA. Langley Research Center, LDEF: 69 Months in Space. First Post-Retrieval Symposium, Part 1 Jan. 1992 p 435-442 (For primary document see N92-23280 14-99)
Avail: NTIS HC/MF A99; 8 functional color pages CSCL 22B

The many meteoroid and space debris impacts found on A0171, A0034, S1005, and other MSFC experiments are considered. In addition to those impacts found by the meteoroid and debris studies, numerous impacts less than 0.5 mm were found and photographed. The flux and size distribution of impacts is presented as well as EDS analysis of impact residue. Emphasis is on morphology of impacts in the various materials, including graphite/epoxy composites, polymeric materials, optical coatings, thin films, and solar cells. Author

N92-23312*# Kent Univ., Canterbury (England). Physics Lab.
HYPERVELOCITY IMPACT MICROFOIL PERFORATIONS IN THE LEO SPACE ENVIRONMENT (LDEF, MAP AO-023 EXPERIMENT) c18
J. A. M. McDonnell and T. J. Stevenson *In* NASA. Langley Research Center, LDEF: 69 Months in Space. First Post-Retrieval Symposium, Part 1 Jan. 1992 p 443-458 (For primary document see N92-23280 14-99)
Avail: NTIS HC/MF A99; 8 functional color pages CSCL 22B

The Microabrasion Foil Experiment comprises arrays of frames, each supporting two layers of closely spaced metallic foils and a back-stop plate. The arrays, deploying aluminum and brass foil ranging from 1.5 to some 30 microns were exposed for 5.78 years on NASA's LDEF at a mean altitude of 458 km. They were deployed on the North, South, East, West, and Space pointing faces; results presented comprise the perforation rates for each location as a function of foil thickness. Initial results refer primarily to aluminum of 5 microns thickness or greater. This penetration distribution, comprising 2,342 perforations in total, shows significantly differing characteristics for each detector face. The anisotropy confirms, incorporating the dynamics of particulate orbital mechanics, the dominance of incorporating extraterrestrial particulates penetrating thicknesses greater than 20 microns in Al foil, yielding fluxes compatible with hyperbolic geocentric velocities. For thinner foils, a disproportionate increase in flux of particles on the East, North, and South faces shows the presence of orbital particulates which exceed the extraterrestrial component perforation rate at 5 micron foil thickness by a factor of approx. 4. Author

N92-23313*# National Aeronautics and Space Administration. Lyndon B. Johnson Space Center, Houston, TX.
METEOROID AND DEBRIS SPECIAL INVESTIGATION GROUP DATA ACQUISITION PROCEDURES c82
Thomas H. See, Martha K. Allbrooks, Dale R. Atkinson, Clyde A. Sapp, Charles G. Simon (Institute for Space Science and Technology, Inc., Gainesville, FL.), and Mike E. Zolensky *In* NASA. Langley Research Center, LDEF: 69 Months in Space. First Post-Retrieval Symposium, Part 1 Jan. 1992 p 459-475 (For primary document see N92-23280 14-99)
Avail: NTIS HC/MF A99; 8 functional color pages CSCL 05B

The entire LDEF spacecraft was examined by M&D SIG for impact (i.e., craters greater than or = 0.5 mm and penetrations greater than or = 0.3 mm in diameter) and related features (e.g., debris, secondaries). During the various detailed surveys conducted at NASA Kennedy, approx. 5,000 impact related features were photodocumented, and their locations measured and recorded; an additional approx. 30,000 smaller features were counted. The equipment and techniques used by the M&D SIG permitted the determination and recording of the locations and diameters of the 5,000 imaged features. A variety of experimental and LDEF structural hardware was acquired by the M&D SIG and is presently being examined and curated at NASA Johnson. Author

N92-23314*# National Aeronautics and Space Administration. Lyndon B. Johnson Space Center, Houston, TX.
METEOROID, AND DEBRIS SPECIAL INVESTIGATION GROUP PRELIMINARY RESULTS: SIZE-FREQUENCY DISTRIBUTION AND SPATIAL DENSITY OF LARGE IMPACT FEATURES ON LDEF c18
Thomas H. See, Friedrich Hoerz, Michael E. Zolensky, Martha K. Allbrooks, Dale R. Atkinson, and Charles G. Simon (Institute for Space Science and Technology, Inc., Gainesville, FL.) *In* NASA. Langley Research Center, LDEF: 69 Months in Space. First Post-Retrieval Symposium, Part 1 Jan. 1992 p 477-486 (For primary document see N92-23280 14-99)
Avail: NTIS HC/MF A99; 8 functional color pages CSCL 22B

All craters greater than or equal to 500 microns and penetration holes greater than or equal to 300 microns in diameter on the entire Long Duration Exposure Facility (LDEF) were documented. Summarized here are the observations on the LDEF frame, which exposed aluminum 6061-T6 in 26 specific directions relative to LDEF's velocity vector. In addition, the opportunity arose to characterize the penetration holes in the A0178 thermal blankets, which pointed in nine directions. For each of the 26 directions, LDEF provided time-area products that approach those afforded by all previous space-retrieved materials combined. The objective here is to provide a factual database pertaining to the largest collisional events on the entire LDEF spacecraft with a minimum of interpretation. This database may serve to encourage and guide more interpretative efforts and modeling attempts. Author

N92-23315*# National Aeronautics and Space Administration. Lyndon B. Johnson Space Center, Houston, TX.
PRELIMINARY ANALYSIS OF LDEF INSTRUMENT A0187-1: CHEMISTRY OF MICROMETEOROIDS EXPERIMENT c90
Friedrich Hoerz, Ronald P. Bernhard, Jack Warren, Thomas H. See, Donald E. Brownlee, Mark R. Laurance, Scott Messenger, and Robert B. Peterson (Peterson, Robert B., Houston, TX) *In* NASA. Langley Research Center, LDEF: 69 Months in Space. First Post-Retrieval Symposium, Part 1 Jan. 1992 p 487-501

(For primary document see N92-23280 14-99)
Avail: NTIS HC/MF A99; 8 functional color pages CSCL 03B

The Chemistry of Micrometeoroids Experiment (CME) exposed approximately 0.8 sq. m of gold on the Long Duration Exposure Facility's (LDEF's) trailing edge (location A03) and approximately 1.1 sq. m of aluminum in the forward-facing A11 location. The most significant results to date relate to the discovery of unmelted pyroxene and olivine fragments associated with natural cosmic dust impacts. The latter are sufficiently large for detailed phase studies, and they serve to demonstrate that recovery of unmelted dust fragments is a realistic prospect for further dust experiments that will employ more advanced collector media. We also discovered that man-made debris impacts occur on the LDEF's trailing edge with substantially higher frequency than expected, suggesting that orbital debris in highly elliptical orbits may have been somewhat underestimated. Author

N92-23316*# Washington Univ., Saint Louis, MO. Center for the Space Sciences.

SIMS CHEMICAL ANALYSIS OF EXTENDED IMPACT FEATURES FROM THE TRAILING EDGE PORTION OF EXPERIMENT AO187-2 **c25**

Sachiko Amari, John Foote, Charles Simon, Elmar K. Jessberger, Gundolf Lange, Frank Stadermann (Max-Planck-Inst. fuer Kernphysik, Heidelberg, Germany, F.R.), Pat Swan, Robert M. Walker, and Ernst Zinner *In* NASA. Langley Research Center, LDEF: 69 Months in Space. First Post-Retrieval Symposium, Part 1 Jan. 1992 p 503-516 (For primary document see N92-23280 14-99)
(Contract NAG1-1174; ESTEC-AOP/WK/303284)
Avail: NTIS HC/MF A99; 8 functional color pages CSCL 07D

One hundred capture cells from the trailing edge, which had lost their cover foils during flight, were optically scanned for extended impact features caused by high velocity projectiles impinging on the cells while the foils were still intact. Of the 53 candidates, 24 impacts were analyzed by secondary ion mass spectroscopy for the chemical composition of the deposits. Projectile material was found in all impacts, and at least 75 percent of them appear to be caused by interplanetary dust particles. Elemental ratios are fractionated, with refractory elements enriched in the impacts relative to interplanetary dust particles collected in the stratosphere. Although this could be due to systematic differences in the compositions, a more likely explanation is volatility fractionation during the impact process. Author

N92-23317*# National Aeronautics and Space Administration. Langley Research Center, Hampton, VA.

IDE SPATIO-TEMPORAL IMPACT FLUXES AND HIGH TIME-RESOLUTION STUDIES OF MULTI-IMPACT EVENTS AND LONG-LIVED DEBRIS CLOUDS **c90**

J. Derral Mulholland, S. Fred Singer, John P. Oliver, Jerry L. Weinberg, William J. Cooke, Nancy L. Montague, Jim J. Wortman (North Carolina State Univ., Raleigh.), Phillip C. Kassel, and William H. Kinard *In its* LDEF: 69 Months in Space. First Post-Retrieval Symposium, Part 1 Jan. 1992 p 517-527 (For primary document see N92-23280 14-99)
(Contract NAS1-16550; NAG1-1218)
Avail: NTIS HC/MF A99; 8 functional color pages CSCL 03B

The purpose of the Interplanetary Dust Experiment (IDE) on the Long Duration Exposure Facility (LDEF) was to sample the cosmic dust environment and to use the spatio-temporal aspect of the experiment to distinguish between the various components of the environment: zodiacal cloud, beta meteoroids, meteor streams, interstellar dust, and orbital debris. It was found that the introduction of precise time and even rudimentary directionality as co-lateral observables in sampling the particulate environment in near-Earth space produces an enormous qualitative improvement in the information content of the impact data. The orbital debris population is extremely clumpy, being dominated by persistent clouds in which the fluxes may rise orders of magnitude above the background. The IDE data suggest a strategy to minimize the damage to sensitive spacecraft components, using the observed characteristics of cloud encounters. Author

N92-23318*# Institute for Space Science and Technology, Inc., Gainesville, FL.

ION MICROPROBE ELEMENTAL ANALYSES OF IMPACT FEATURES ON INTERPLANETARY DUST EXPERIMENT SENSOR SURFACES **c90**

Charles G. Simon, Jerry L. Hunter, Jim J. Wortman, and Dieter P. Griffis (North Carolina State Univ., Raleigh.) *In* NASA. Langley Research Center, LDEF: 69 Months in Space. First Post-Retrieval Symposium, Part 1 Jan. 1992 p 529-548 (For primary document see N92-23280 14-99)
(Grants NAG1-1214; NAG1-1218)
Avail: NTIS HC/MF A99; 8 functional color pages CSCL 03B

Hypervelocity impact features from very small particles (less than 3 microns in diameter) on several of the electro-active dust sensors used in the Interplanetary Dust Experiment (IDE) were subjected to elemental analysis using an ion microscope. The same analytical techniques were applied to impact and containment features on a set of ultra-pure, highly polished single crystal germanium wafer witness plates that were mounted on tray B12. Very little unambiguously identifiable impactor debris was found in the central craters or shatter zones of small impacts in this crystalline surface. The surface contamination, ubiquitous on the surface of the Long Duration Exposure Facility, has greatly complicated data collection and interpretation from microparticle impacts on all surfaces. Author

N92-23319*# National Aeronautics and Space Administration. Ames Research Center, Moffett Field, CA.

LDEF IMPACT CRATERS FORMED BY CARBON-RICH IMPACTORS: A PRELIMINARY REPORT **c18**

T. E. Bunch, F. Radicati diBrozolo, Ronald H. Fleming, David W. Harris, Don Brownlee, and Terrence W. Reilly (Hitachi Scientific Instruments, Mountain View, CA.) *In* NASA. Langley Research Center, LDEF: 69 Months in Space. First Post-Retrieval Symposium, Part 1 Jan. 1992 p 549-564 (For primary document see N92-23280 14-99)
Avail: NTIS HC/MF A99; 8 functional color pages CSCL 22B

Two impact craters found in Al from the Long Duration Exposure Facility (LDEF) experiment tray have residues concentrated in the bottoms, along the walls, and on top of overturned rims. Analyses indicate a 'chondritic' compositional signature (Si, S, Ca, Fe, Mg, and Ni) for the bulk residue. In one crater (number 74), round to irregular silicate grains are overlain by carbon. In addition, carbon also partially covers the crater walls, the top of the raised overturned rim, and extends outward from the crater. The second crater (number 31) also contains carbon with similar distribution in and about the crater, although the silicate residue appears to be glassy. Silver, I, K, and F (possibly some of the Ca, S, and Cl) appear to be contaminants as well as analyzed aromatic carbonaceous species associated with the raised rim and the area surrounding the crater. The origin of the impactors is assumed to be extraterrestrial. The existence of impactor residue in two craters implies impact velocities less than or equal to 6 km, based on experimental hypervelocity studies. Author

N92-23320*# Kent Univ., Canterbury (England). Unit for Space Sciences.

DYNAMIC (COMPUTER) MODELLING OF THE PARTICULATE ENVIRONMENT: TRANSFORMATIONS FROM THE LDEF REFERENCE FRAME TO DECODE GEOCENTRIC AND INTERPLANETARY POPULATIONS Abstract Only **c90**

J. A. M. McDonnell and K. Sullivan *In* NASA. Langley Research Center, LDEF: 69 Months in Space. First Post-Retrieval Symposium, Part 1 Jan. 1992 p 565 Previously announced as N91-25010 (For primary document see N92-23280 14-99)
Avail: NTIS HC/MF A99; 8 functional color pages CSCL 03B

The Long Duration Exposure Facility (LDEF) impact signature record and the size frequency distribution of craters and perforations offers a unique record of environmental data referenced conveniently to the geocentric reference frame. Chemical analysis of residues can offer only limited assistance. Hence, flux modeling has been developed to transform both geocentric orbital distributions and geocentrically unbounded

interplanetary source distributions. This is applied to the foil and crater penetration records in the Ram (E), Trailing (W), and Space Pointing directions to offer the means of decoding the records. It shows that the mix of the components is size dependent. Parametric forms of the modeling transformations are presented for the orbital and unbounded populations. Author

N92-23321*# POD Associates, Inc., Albuquerque, NM.
LDEF DATA CORRELATION TO EXISTING NASA DEBRIS ENVIRONMENT MODELS Abstract Only c18
Dale R. Atkinson, Martha K. Allbrooks, and Alan J. Watts *In* NASA. Langley Research Center, LDEF: 69 Months in Space. First Post-Retrieval Symposium, Part 1 Jan. 1992 p 567 (For primary document see N92-23280 14-99)
Avail: NTIS HC/MF A99; 8 functional color pages CSCL 22B

The Long Duration Exposure Facility (LDEF) was recovered in January 1990, following 5.75 years exposure of about 130 sq. m to low-Earth orbit. About 25 sq. m of this surface area was aluminum 6061 T-6 exposed in every direction. In addition, about 17 sq. m of Scheldahl G411500 silver-Teflon thermal control blankets were exposed in 9 of the 12 directions. Since the LDEF was gravity gradient stabilized and did not rotate, the directional dependence of the flux can be easily distinguished. During the disintegration of the LDEF, all impact features larger than 0.5 mm into aluminum were documented for diameters and locations. In addition, the diameters and locations of all impact features larger than 0.3 mm into Scheldahl G411500 thermal control blankets were also documented. This data, along with additional information collected from LDEF materials will be compared with current meteoroid and debris models. This comparison will provide a validation of the models and will identify discrepancies between the models and the data. Author

N92-23322*# National Aeronautics and Space Administration. Lyndon B. Johnson Space Center, Houston, TX.
DERIVING THE VELOCITY DISTRIBUTION OF METEOROIDS FROM THE MEASURED METEOROID IMPACT DIRECTIONALITY ON THE VARIOUS LDEF SURFACES c90
Herbert A. Zook *In* NASA. Langley Research Center, LDEF: 69 Months in Space. First Post-Retrieval Symposium, Part 1 Jan. 1992 p 569-579 (For primary document see N92-23280 14-99)
Avail: NTIS HC/MF A99; 8 functional color pages CSCL 03B

Because of spacecraft orbital motion about the Earth, a much higher flux of meteoroids is expected to strike spacecraft surfaces that face in the direction of spacecraft motion (apex direction) than would strike apex facing or trailing edge surfaces. Impact velocities are also higher on apex facing surfaces compared to antapex facing surfaces which futher increases the apex/antapex ratio of spatial density of impact craters of a given size. Measurements of the areal densities of impact craters on the different LDEF surfaces should give important clues about the velocity distribution, and therefore the origins, of meteoroids. Preliminary results appear to support the meteoroid velocity distributions derived by Erickson and by Kessler, which would lead to a mean impact velocity on the LDEF spacecraft of about 19 km/s. Author

N92-23323*# National Aeronautics and Space Administration. Lyndon B. Johnson Space Center, Houston, TX.
M AND D SIG PROGRESS REPORT: LABORATORY SIMULATIONS OF LDEF IMPACT FEATURES Abstract Only c18
Friedrich Horz, R. P. Bernhard, T. H. See, D. Atkinson, and M. Allbrooks (POD Associates, Inc., Albuquerque, NM.) *In* NASA. Langley Research Center, LDEF: 69 Months in Space. First Post-Retrieval Symposium, Part 1 Jan. 1992 p 581 (For primary document see N92-23280 14-99)
Avail: NTIS HC/MF A99; 8 functional color pages CSCL 22B

Laboratory impact experiments are needed to understand the relationship between a measured penetration hole diameter and associated projectile dimension in the thermal blankets of experiment A0178, which occupied some 16 sq. m. These blankets are composed of 125 micron thick Teflon that has an Ag/enconel second mirror surface, backed by organic binder and Chemglaze paint for a total thickness of some 170 microns. While dedicated experiments are required to understand the penetration behavior of this compound target in detail, we report here on impact simulations sponsored by other projects into pure Teflon and aluminum targets. These experiments will allow first order interpretations of impact features on the Long Duration Exposure Facility (LDEF), and they will serve as guides for dedicated experiments that employ the real LDEF blankets, both exposed and unexposed, for a refined understanding of the LDEF's collisional environment. We employed a light gas gun to launch soda-lime glass spheres from 50 to 3200 microns in diameter that impacted targets of variable thickness. Penetration measurements are given. Author

N92-23324*# National Aeronautics and Space Administration. Lyndon B. Johnson Space Center, Houston, TX.
PRELIMINARY MICROMETEOROID AND DEBRIS EFFECTS ON LDEF THERMAL CONTROL SURFACES Abstract Only c18
Martha K. Allbrooks, Dale R. Atkinson, Thomas See (Lockheed Engineering and Sciences Co., Houston, TX.), and Fred Horz *In* NASA. Langley Research Center, LDEF: 69 Months in Space. First Post-Retrieval Symposium, Part 1 Jan. 1992 p 583 (For primary document see N92-23280 14-99)
Avail: NTIS HC/MF A99; 8 functional color pages CSCL 22B

Thermal control surfaces returned from space exhibited synergistic effects of simultaneous exposure to various natural environments. The thermal control surfaces of the Long Duration Exposure Facility (LDEF) were exposed to 5.75 years of low Earth orbit environments. Since LDEF was gravity-gradient stabilized and directionally stable (i.e., no rotation), the effects of each of the environments (meteoroid and space debris impacts, thermal cycling, atomic oxygen, and ultraviolet light exposure) can be distinguished via changes in material responses to hypervelocity impacts. The extent of these impacts are being visually and microscopically characterized using thermal control surfaces archived at NASA Johnson Space Center (JSC) in order to determine the relationship between environment exposure and resulting ring sizes, delamination areas, and penetration diameters. The characterization of these affected areas will provide spacecraft system designers with the information they require to determine degradation of thermal control systems during satellite lifetimes.
Author

N92-23325*# Utah State Univ., Logan.
THE INTERSTELLAR GAS EXPERIMENT c90
D. L. Lind, J. Geiss, F. Buehler, and O. Eugster (Bern Univ., Switzerland) *In* NASA. Langley Research Center, LDEF: 69 Months in Space. First Post-Retrieval Symposium, Part 1 Jan. 1992 p 585-594 Sponsored in part by the Swiss National Science Foundation (For primary document see N92-23280 14-99)
(Grant NAGw-2066)
Avail: NTIS HC/MF A99; 8 functional color pages CSCL 03B

The Interstellar Gas Experiment (IGE) exposed thin metallic foils to collect neutral interstellar gas particles. These particles penetrate the solar system due to their motion relative to the sun. Thus, it is possible to entrap them in the collecting foils along with precipitating magnetospheric and perhaps some ambient atmospheric particles. For the entire duration of the Long Duration Exposure Facility (LDEF) mission, seven of these foils collected particles arriving from seven different directions as seen from the spacecraft. In the mass spectroscopic analysis of the noble gas component of these particles, we have detected the isotopes of He-3, He-4, Ne-20, and Ne-22. In the foil analyses carried out so far, we find a distribution of particle arrival directions which shows that a significant part of the trapped particles are indeed interstellar atoms. The analysis needed to subtract the competing fluxes of magnetospheric and atmospheric particles is still in progress.
Author

N92-23958*# National Aeronautics and Space Administration. Goddard Space Flight Center, Greenbelt, MD.
SUMMER GRADUATE RESEARCH PROGRAM FOR INTERNS IN SCIENCE AND ENGINEERING Final Report
Clinton B. Lee 24 Mar. 1992 267 p Sponsored in cooperation with North Carolina Agricultural and Technical State Univ.
(Grant NAG1-956)
(NASA-TM-107813; NAS 1.15:107813) Avail: NTIS HC/MF A12 CSCL 05B

The goal of the 10 week graduate intern program was to increase the source of candidates for positions in science and engineering at the Goddard Space Flight Center. Students participating in this program submitted papers on the work they performed over the 10 week period and also filled out questionnaires on the program's effectiveness, their own performance, and suggestions on improvements. The topics covered by the student's papers include: microsoft excel applications; fast aurora zone analysis; injection seeding of a Q-switched alexandrite laser; use of high temperature superconductors; modifications on a communication interface board; modeling of space network activities; prediction of atmospheric ozone content; and applications of industrial engineering. For individual titles, see N92-23959 through N92-23966.

N92-23959*# North Carolina Agricultural and Technical State Univ., Greensboro.
USING MICROSOFT EXCEL APPLICATIONS IN THE GRADUATE INTERN PROGRAM AT GODDARD SPACE FLIGHT CENTER M.S. Thesis **c61**
Lisa Antoine *In* NASA. Goddard Space Flight Center, Summer Graduate Research Program for Interns in Science and Engineering 24 Mar. 1992 10 p (For primary document see N92-23958 14-99)
Avail: NTIS HC/MF A12 CSCL 09B

An outline of the Project Operations Branch at Goddard Space Flight Center is presented that describes the management of the division and each subgroup's responsibility. The paper further describes the development of software tools for the Macintosh personal computer, and their impending implementation. A detailed step by step procedure is given for using these software tools.
H.A.

N92-23960*# Jackson State Coll., MS.
FAST AURORA ZONE ANALYSIS **c46**
Mattie Booker *In* NASA. Goddard Space Flight Center, Summer Graduate Research Program for Interns in Science and Engineering 24 Mar. 1992 19 p (For primary document see N92-23958 14-99)
Avail: NTIS HC/MF A12 CSCL 04A

The Flight Dynamics Facility (FDF) of the Flight Dynamics Division (FDD), of the Goddard Space Flight Center provides acquisition data to tracking stations and orbit and attitude services to scientists and mission support personnel. The following paper explains how a method was determined that found spacecraft entry and exit times of the aurora zone. H.A.

N92-23961*# Howard Univ., Washington, DC.
INJECTION SEEDING OF A Q-SWITCHED ALEXANDRITE LASER: STUDY OF FREQUENCY STABILIZATION **c36**
Lamarr A. Brown *In* NASA. Goddard Space Flight Center, Summer Graduate Research Program for Interns in Science and Engineering 24 Mar. 1992 19 p (For primary document see N92-23958 14-99)
Avail: NTIS HC/MF A12 CSCL 20E

AlGaAs diode lasers were used to injection seed a pulsed Q-switched alexandrite laser which produces a narrowband of radiation. Injection seeding is a method for achieving linewidths of less than 500 mega-Hz in the output of the broadband, tunable solid state laser. When the laser was set at a current of 59.8 milli-A and a temperature of 14.04 C, the wavelength was 767.6 nano-m. The Q-switched alexandrite laser was injection seeded and frequency stabilization was studied. The linewidth requirement was met, but the stability requirement was not due to drifting in the feedback voltage. Improvements on injection seeding should focus on increasing the feedback voltage to the laser diode, filtering the laser diode by using temperature controlled narrowband filters, and the use of diamond (SiC) grating placed inside the alexandrite laser's resonator cavity. Author

N92-23962*# Howard Univ., Washington, DC.
THE USE OF HIGH TEMPERATURE SUPERCONDUCTORS TO LEVITATE LUNAR TELESCOPE **c89**
Beth A. Brown *In* NASA. Goddard Space Flight Center, Summer Graduate Research Program for Interns in Science and Engineering 24 Mar. 1992 10 p (For primary document see N92-23958 14-99)
Avail: NTIS HC/MF A12 CSCL 03A

The objective of this paper was to assist in the construction of a lunar telescope mirror model by conducting research on composite materials and other lightweight, rigid materials, and by determining how much weight can be levitated by available superconductors. It is believed that with the construction of four magnets suspended over four bulk superconductors (or vice versa), there should be no problems lifting a model mirror and stabilizing it at different positions. It may be necessary to increase the size and quality of the superconductors and/or magnets in order to achieve this. H.A.

N92-23963*# Puerto Rico Univ., Mayaguez.
MODIFICATIONS FOR A COMMUNICATION INTERFACE BOARD **c32**
Carlos E. DeJesusLafuente *In* NASA. Goddard Space Flight Center, Summer Graduate Research Program for Interns in Science and Engineering 24 Mar. 1992 39 p (For primary document see N92-23958 14-99)
Avail: NTIS HC/MF A12 CSCL 17B

The objectives of this report had three sections. First, it is to modify a communication interface board by using erasable programmable logic devices to replace around SSI and MSI logic. Second, it is to simulate selected portions of the schematics using Altera Maxplus 1990 and Maxplus 2 1991 CAD programs. Third, it is to replace a first input first output (FIFO) device as well as serial to parallel and parallel to serial converters with new FIFO's that have internal converters. H.A.

N92-23964*# Temple Univ., Philadelphia, PA. Dept. of Mathematics.
MATHEMATICAL ANALYSIS TECHNIQUES FOR MODELING THE SPACE NETWORK ACTIVITIES **c64**
Lisa M. Foster *In* NASA. Goddard Space Flight Center, Summer Graduate Research Program for Interns in Science and Engineering 24 Mar. 1992 23 p (For primary document see N92-23958 14-99)
Avail: NTIS HC/MF A12 CSCL 12A

The objective of the present work was to explore and identify mathematical analysis techniques, and in particular, the use of linear programming. This topic was then applied to the Tracking and Data Relay Satellite System (TDRSS) in order to understand the space network better. Finally, a small scale version of the system was modeled, variables were identified, data was gathered, and comparisons were made between actual and theoretical data. H.A.

N92-23965*# Temple Univ., Philadelphia, PA. Dept. of Physics.
USE OF THE MAXIMUM ENTROPY METHOD TO RETRIEVE THE VERTICAL ATMOSPHERIC OZONE PROFILE AND PREDICT ATMOSPHERIC OZONE CONTENT **c45**
B. Curtis Turner *In* NASA. Goddard Space Flight Center, Summer Graduate Research Program for Interns in Science and Engineering 24 Mar. 1992 19 p (For primary document see N92-23958 14-99)
Avail: NTIS HC/MF A12 CSCL 13B

A method is developed for prediction of ozone levels in planetary atmospheres. This method is formulated in terms of error covariance matrices, and is associated with both direct

measurements, a priori first guess profiles, and a weighting function matrix. This is described by the following linearized equation: y = A(matrix) x X + eta, where A is the weighting matrix and eta is noise. The problems to this approach are: (1) the A matrix is near singularity; (2) the number of unknowns in the profile exceeds the number of data points, therefore, the solution may not be unique; and (3) even if a unique solution exists, eta may cause the solution to be ill conditioned. H.A.

N92-23966*# Virginia Polytechnic Inst. and State Univ., Blacksburg. Industrial Engineering.

APPLICATIONS OF INDUSTRIAL ENGINEERING Ph.D. Thesis

c31

Walthea V. Yarbrough *In* NASA. Goddard Space Flight Center, Summer Graduate Research Program for Interns in Science and Engineering 24 Mar. 1992 11 p (For primary document see N92-23958 14-99)

Avail: NTIS HC/MF A12 CSCL 13H

Two separate and distinctly different projects are described within this paper: the stepping motion bearing tester, and the memo search and find project. The objective of the first project was to program the JSI Digital Servo Controller to control the motor using the stepping pattern prescribed by the AMSU-U2 Scan Profile. The objective of the second project was to develop a dBASE 3 Plus program that would allow the user to gain the necessary information to retrieve the memo(s) being sought upon supplying a word or group of words possibly found in the keyword list or upon supplying the author's name. H.A.

Typical Subject Index Listing

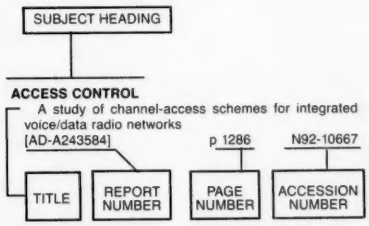

The subject heading is a key to the subject content of the document. Titles, report numbers, and accession numbers of pertinent documents are provided under each subject heading. When the title is insufficiently descriptive of the document content, a title extension has been added, separated from the title by three hyphens. The report number helps to indicate the type of document cited (e.g., NASA report, NASA translation, NASA contractor report). The accession number is the number by which the document abstracts are arranged in this journal and by which the document is sold or requested. The page number helps you locate the the citation in the abstract section. The titles, with title extensions if present, are arranged under each subject heading in ascending accession number order. The subject headings have been selected from the latest revision of the *NASA Thesaurus*.

A

ABILITIES
Training users of a flexible decision support system: The effects of training content and user ability p 2453 N92-23730

ABSORBERS (MATERIALS)
Evaluation of the applicability of Helmholtz resonators for low frequency acoustic liners [PB92-138544] p 2436 N92-23588

ABSORPTION SPECTRA
Retrieval of upper precipitable water profile from MOS-1 VTIR water vapor channel p 2398 N92-23479
The meteorite record as clues to asteroidal regolith processes p 2457 N92-23770

ABSORPTION SPECTROSCOPY
Application of x ray absorption spectroscopy to the study of corrosion and inhibition [DE92-007456] p 2350 N92-23198
Applications of x ray synchrotron radiation techniques to the study of dispersed electrocatalysts in high area materials [DE92-007458] p 2346 N92-23199

ABSORPTIVITY
Acoustic absorption due to specimen in test in a reverberant chamber p 2324 N92-23790

ABUNDANCE
Infrared emission lines from highly ionized regions p 2460 N92-23162
The throes of star formation: A study of the Orion-KL and DR21(OH) molecular clouds p 2457 N92-23698

ACCELERATION (PHYSICS)
Microgravity acceleration measurement and environment characterization science (17-IML-1) p 2363 N92-23642

ACCELEROMETERS
Smart accelerometer --- vibration damage detection [NASA-CASE-MSC-21951-1] p 2378 N92-23545
The GRADIOmeter payload p 2315 N92-23917
The GRADIO accelerometer: Design and development status p 2316 N92-23918

ACCESS TIME
Modeling of physical database design and performance analysis with emphasis on VSAM files p 2452 N92-23156

ACCRETION DISKS
The origins of the cosmic x ray and gamma ray backgrounds p 2460 N92-23141
Observations of accretion discs in interacting binaries p 2454 N92-23673

ACCURACY
Experiments and modeling p 2301 N92-23339

ACETATES
Nuclear medicine program [DE92-006979] p 2412 N92-23518

ACID RAIN
National acid precipitation assessment program: Mission, goals, and program plan post 1990. Public review draft [PB92-126248] p 2405 N92-23515
National acid precipitation assessment program: 1990 integrated assessment report [PB92-100346] p 2406 N92-23593
Acid rain monitoring in East-Central Florida from 1977 to present [NASA-CR-190152] p 2406 N92-23898
Acid rain and air pollution in desert park areas. Proceedings of a workshop: Management recommendations [PB92-140532] p 2407 N92-24003

ACIDITY
National acid precipitation assessment program: Mission, goals, and program plan post 1990. Public review draft [PB92-126248] p 2405 N92-23515

ACOUSTIC EMISSION
A study of aluminum-lithium alloy solidification using acoustic emission techniques [NASA-CR-4437] p 2435 N92-23556
Acoustic emission as a process monitor for diamond machining of metal optical components [DE92-008037] p 2363 N92-23899
Real-time measurement of electron beam weld penetration in uranium by acoustic emission monitoring [DE92-008040] p 2384 N92-23908

ACOUSTIC FREQUENCIES
A frequency domain least squares method for modelling acoustic fields [ISVR-TR-196] p 2435 N92-23170

ACOUSTIC IMPEDANCE
Evaluation of the applicability of Helmholtz resonators for low frequency acoustic liners [PB92-138544] p 2436 N92-23588

ACOUSTIC MEASUREMENT
Acoustic emission as a process monitor for diamond machining of metal optical components [DE92-008037] p 2363 N92-23899
Real-time measurement of electron beam weld penetration in uranium by acoustic emission monitoring [DE92-008040] p 2384 N92-23908

ACOUSTIC SIMULATION
Acoustic absorption due to specimen in test in a reverberant chamber p 2324 N92-23790

ACOUSTIC SOUNDING
Field evaluation of remote sensor measurements of wind, temperature, and moisture for ARM integrated sounding system research [PB92-140714] p 2401 N92-23521

ACOUSTIC VELOCITY
Ocean acoustic tomography inversion in the adiabatic-invariant approximation [PB92-140466] p 2412 N92-23669

ACOUSTICS
Maximal modal energy method: An overvaluing tool for low frequency prediction of structure acoustic response p 2324 N92-23791
Numerical and experimental study of noise generated by a vibrating plate p 2324 N92-23792
Ariane 4 internal acoustic environment: Interpretation of flight data with a vibroacoustic model of the upper part of the launcher p 2321 N92-23811
Acoustic prediction on satellite structure p 2327 N92-23812
Acoustic cavity and fluid/structure interaction models: A methodological deterministic approach and problems encountered p 2327 N92-23813

ACTIVATION ANALYSIS
Surface activation of Concorde by Be-7 p 2439 N92-23295
Charged particle activation studies on the surface of LDEF spacecraft p 2439 N92-23296

ACTIVATION ENERGY
Phase transformations in SrAl2Si2O8 glass [NASA-TM-105657] p 2449 N92-23890

ACTIVE CONTROL
Simulation of Space Station loads with active control systems p 2329 N92-23824

ACTIVE GALACTIC NUCLEI
The origins of the cosmic x ray and gamma ray backgrounds p 2460 N92-23141

ACTIVE GALAXIES
Nuclear winds in active galaxies p 2457 N92-23716

ACTS
Intelligent fault isolation and diagnosis for communication satellite systems p 2427 N92-23365

ACTUATORS
An algorithmic approach for fault-monitoring of electrical actuation system for all electric aircraft [NAL-PD-AL-9111] p 2368 N92-23246
Climbing robot --- caterpillar design [NASA-CASE-GSC-13442-1] p 2382 N92-23547
Fabrication of a helical coil shape memory alloy actuator [DE92-008399] p 2364 N92-23901
Design considerations for an air core magnetic actuator [NASA-TM-104229] p 2364 N92-23989
Advanced electric motor technology: Flux mapping [NASA-CR-184317] p 2372 N92-24047
Quick-connect fasteners for assembling devices in space [NASA-CASE-MSC-21648-1] p 2385 N92-24051

ADDITION RESINS
Vinyl capped addition polyimides [NASA-CASE-LEW-15027-2] p 2355 N92-24053

ADDITIVES
Effect of minor elements on hot workability of Ni-Cr-W superalloys [DE92-750951] p 2351 N92-23263
The influence of chromium on structure and mechanical properties of B2 nickel aluminide alloys [NASA-CR-189124] p 2351 N92-23566
High-temperature ignition of propane with MTBE as an additive: Shock-tube experiments and modeling [DE92-008557] p 2348 N92-23715
Impact and compression response of composite materials containing fortifiers p 2341 N92-23937
Influence of maleic anhydride as a coupling agent on the performance of wood fiber: Polystyrene composites p 2343 N92-23945
Filling high density polyethylene with cellulosic fibers. 1: The effect of additives on fiber dispersion p 2344 N92-23948
Fermi level effects on dislocation formation in InAs(1-x)Sb(x) grown by MOCVD [DE92-008332] p 2450 N92-24034
Optimization of the laser glass composition for the Nova upgrade fusion laser system [DE92-008606] p 2380 N92-24065

ADHESION
Characterization of organic coatings with impedance measurements: A study of coating structure, adhesion and underfilm corrosion [PB92-133479] p 2339 N92-23174
Deposition of adherent Ag-Ti duplex films on ceramics in a multiple-cathode sputter deposition system [NASA-TM-105586] p 2311 N92-23225

ADHESIVE BONDING
Mechanical behavior of composite materials and adhesive bonds at low temperatures p 2330 N92-23633

Microstructure and mechanical properties of carbon fibres: Relationship with the fibre-matrix adhesion in a carbon-epoxy composite p 2341 N92-23935
Analytical and experimental investigation of vibratory response in adhesively bonded and composite structures p 2345 N92-24012

ADHESIVES
Mechanical behavior of composite materials and adhesive bonds at low temperatures p 2330 N92-23833

ADIABATIC CONDITIONS
Evolution of magnetic moment due to the cyclotron resonance with field ripples in a tokamak
[DE92-751058] p 2443 N92-23135
An instrument to search for small-scale anisotropy in the cosmic microwave background at 90 GHz p 2441 N92-23161
Particle dynamics in a wave with variable amplitude
[DE92-008340] p 2436 N92-23217

ADIABATIC EQUATIONS
Ocean acoustic tomography inversion in the adiabatic-invariant approximation
[PB92-140466] p 2412 N92-23669

ADSORPTION
Hydrogen absorption by zirconium alloy cladding tube with surface oxide film
[DE92-750962] p 2351 N92-23265

ADVECTION
Development of a new flux splitting scheme p 2303 N92-23352

AERIAL RUDDERS
Design of a fighter aircraft vertical tail enhanced buffet environment survivability p 2307 N92-23235

AEROACOUSTICS
Experimental study of the mechanism of sound generation by rotating stall in centrifugal turbomachines p 2436 N92-23726

AEROASSIST
Nonlinear feedback guidance law for aero-assisted orbit transfer maneuvers
[NASA-CR-190129] p 2317 N92-23529

AERODYNAMIC BRAKES
Stretched skin concept for the entry aerodynamic decelerator system of planetary probes p 2331 N92-23836

AERODYNAMIC CHARACTERISTICS
First approach to an integrated fin design p 2308 N92-23236
Introduction to Special Course on Engineering Methods in Aerodynamic Analysis and Design of Aircraft p 2308 N92-23951
Configuration development --- preliminary aircraft design p 2309 N92-23953
Panel methods for aerodynamic analysis and design p 2309 N92-23955
Aircraft drag analysis methods p 2309 N92-23957

AERODYNAMIC DRAG
Aircraft drag analysis methods p 2309 N92-23957

AERODYNAMIC FORCES
Modelling of aerodynamic forces and heat transfer for orbital decay and reentry calculations p 2334 N92-23974

AERODYNAMIC HEAT TRANSFER
Modelling of aerodynamic forces and heat transfer for orbital decay and reentry calculations p 2334 N92-23974

AERODYNAMIC INTERFERENCE
Survey of experimental techniques for performance prediction p 2309 N92-23954

AERODYNAMIC LOADS
Development of Japanese experiment module p 2323 N92-23781
Adaptive active flutter suppression of wings in subsonic and transonic flight regimes p 2310 N92-24010

AERODYNAMIC NOISE
Experimental study of the mechanism of sound generation by rotating stall in centrifugal turbomachines p 2436 N92-23726

AERODYNAMIC STABILITY
Aeroelastic stability analyses of two counter rotating propfan designs for a cruise missile model
[NASA-TM-105268] p 2387 N92-23191

AERODYNAMIC STALLING
High angle of attack: Aerodynamics p 2305 N92-23956

AERODYNAMICS
Integrated Design Analysis and Optimisation of Aircraft Structures
[AGARD-R-784] p 2306 N92-23227
JPRS report: Science and technology. Central Eurasia: Space
[JPRS-USP-92-002] p 2314 N92-23705
Special Course on Engineering Methods in Aerodynamic Analysis and Design of Aircraft
[AGARD-R-783] p 2308 N92-23950
Configuration development --- preliminary aircraft design p 2309 N92-23953
High angle of attack: Aerodynamics p 2305 N92-23956

AEROELASTICITY
Aeroelastic stability analyses of two counter rotating propfan designs for a cruise missile model
[NASA-TM-105268] p 2387 N92-23191
Integrated Design Analysis and Optimisation of Aircraft Structures
[AGARD-R-784] p 2306 N92-23227
Sensitivity analysis of dynamic aeroelastic responses p 2306 N92-23229
Application of analytical and design tools for fighter wing aeroelastic tailoring p 2307 N92-23231
The structural optimization system OPTSYS: Current status and applications p 2307 N92-23232
Application of an automated multidisciplinary analysis and optimisation system to the design of aircraft structures p 2307 N92-23233
Multidisciplinary optimization studies using ASTROS p 2307 N92-23234

AEROSOLS
Numerical calculation: Aspiration efficiency of aerosols into thin-walled sampling inlets
[PB92-132901] p 2374 N92-23516

AEROSPACE ENGINEERING
The 1992 Goddard Conference on Space Applications of Artificial Intelligence
[NASA-CP-3141] p 2426 N92-23356
JPRS report: Science and technology. Central Eurasia: Space
[JPRS-USP-92-002] p 2314 N92-23705

AEROSPACE INDUSTRY
Center for Space Power, Texas A and M University p 2313 N92-23651

AEROSPACE PLANES
Conceptional design to heat-resistant airframe of HOPE p 2328 N92-23820
Large thin composite thermostructural parts p 2329 N92-23821
Design challenges for the National Aero-Space Plane p 2310 N92-23822

AEROSPACE SAFETY
Mission safety evaluation report for STS-43, postflight edition
[NASA-TM-107801] p 2312 N92-23240
Mission safety evaluation report for STS-32, postflight edition
[NASA-TM-107775] p 2312 N92-23243
Mission safety evaluation report for STS-36, postflight edition
[NASA-TM-107780] p 2312 N92-23244

AEROSPACE SYSTEMS
A system approach to aircraft optimization p 2306 N92-23228
The achievement of spacecraft autonomy through the thematic application of multiple cooperating intelligent agents p 2427 N92-23364
Systems for COMET p 2313 N92-23646

AGING (BIOLOGY)
The effect of space environment on the development and aging of Drosophila Melanogaster (7-IML-1) p 2357 N92-23608

AGING (MATERIALS)
Aging of polymer matrix composites at elevated temperatures p 2328 N92-23817

AGREEMENTS
Euromar industrial partners agreement p 2396 N92-23410

AIR CONDITIONING
Geothermal direct use engineering and design guidebook
[DE92-008686] p 2404 N92-24030

AIR DEFENSE
Market directed thinking in a technological operation p 2452 N92-23929

AIR FLOW
Numerical calculation: Aspiration efficiency of aerosols into thin-walled sampling inlets
[PB92-132901] p 2374 N92-23516

AIR JETS
Impinging axisymmetric jet p 2372 N92-23146

AIR MASSES
An observational study of the internal structure of air-mass thunderstorms p 2409 N92-23121

AIR NAVIGATION
Market directed thinking in a technological operation p 2452 N92-23929

AIR POLLUTION
Limiting net greenhouse gas emissions in the United States, volume 2
[DE92-007592] p 2405 N92-23333
Acid rain monitoring in East-Central Florida from 1977 to present
[NASA-CR-190152] p 2406 N92-23898
Acid rain and air pollution in desert park areas. Proceedings of a workshop: Management recommendations
[PB92-140532] p 2407 N92-24003

AIR QUALITY
National air quality and emissions trends report, 1990
[PB92-141555] p 2406 N92-23517

AIR TRAFFIC CONTROL
Aircraft accident report: Runway collision of USAir Flight 1493, Boeing 737 and Skywest Flight 5569 Fairchild Metroliner, Los Angeles International Airport, Los Angeles, CA, February 1, 1991
[PB91-910409] p 2305 N92-23596

AIR TRANSPORTATION
Radiation exposure of air carrier crewmembers 2
[PB92-140037] p 2414 N92-23139

AIR WATER INTERACTIONS
Atmospheric correction of the second generation ocean color sensors p 2392 N92-23145
Monsoon-ENSO relationships p 2404 N92-23160
Differences within and among surface marine datasets
[PB92-135326] p 2411 N92-23660
Wind, current and temperature data at 0 deg, 165 deg E: January 1986 to March 1991
[PB92-143080] p 2411 N92-23682

AIRBORNE EQUIPMENT
Euromar-Seastars: A definition study on modular multisensor instrumentation for airborne remote sensing of the sea
[MBB-UK-0152-91-PUB] p 2392 N92-23379
Introduction: Ocean air observation p 2392 N92-23381
The imaging spectrometer p 2393 N92-23387
Quick-look system p 2394 N92-23393
On board data recording p 2394 N92-23395
Realization and provisional sensor development planning p 2395 N92-23406
International cooperation p 2396 N92-23409
Euromar industrial partners agreement p 2396 N92-23410
An 18-point catalog description p 2396 N92-23411
Development of a helicopter-borne 8-channel ranging scatterometer
[PB92-141977] p 2396 N92-23441
International workshop on the airborne measurement of wind, turbulence, and position
[PB92-139963] p 2410 N92-23587

AIRCRAFT ACCIDENT INVESTIGATION
Aircraft accident report: Runway collision of USAir Flight 1493, Boeing 737 and Skywest Flight 5569 Fairchild Metroliner, Los Angeles International Airport, Los Angeles, CA, February 1, 1991
[PB91-910409] p 2305 N92-23596
Aircraft accident report: Ryan International Airlines DC-9-15, N565PC, loss of control on takeoff, Cleveland-Hopkins International Airport, Cleveland, Ohio, February 17, 1991
[PB91-910410] p 2305 N92-23597

AIRCRAFT ACCIDENTS
Aircraft accident report: Runway collision of USAir Flight 1493, Boeing 737 and Skywest Flight 5569 Fairchild Metroliner, Los Angeles International Airport, Los Angeles, CA, February 1, 1991
[PB91-910409] p 2305 N92-23596
Aircraft accident report: Ryan International Airlines DC-9-15, N565PC, loss of control on takeoff, Cleveland-Hopkins International Airport, Cleveland, Ohio, February 17, 1991
[PB91-910410] p 2305 N92-23597

AIRCRAFT CONFIGURATIONS
Preconsiderations on aircraft integration p 2395 N92-23402
Configuration development --- preliminary aircraft design p 2309 N92-23953
Panel methods for aerodynamic analysis and design p 2309 N92-23955
Aircraft drag analysis methods p 2309 N92-23957

AIRCRAFT CONSTRUCTION MATERIALS
Conceptional design to heat-resistant airframe of HOPE p 2328 N92-23820

AIRCRAFT CONTROL
Configuration development --- preliminary aircraft design p 2309 N92-23953

AIRCRAFT DESIGN
A system approach to aircraft optimization p 2306 N92-23228
Sensitivity analysis of dynamic aeroelastic responses p 2306 N92-23229
Application of multidisciplinary optimization methods to the design of a supersonic transport p 2307 N92-23230
Application of analytical and design tools for fighter wing aeroelastic tailoring p 2307 N92-23231
Application of an automated multidisciplinary analysis and optimisation system to the design of aircraft structures p 2307 N92-23233

Design of a fighter aircraft vertical tail enhanced buffet environment survivability p 2307 N92-23235
Efficient and robust design optimization of transonic airfoils p 2305 N92-23717
Special Course on Engineering Methods in Aerodynamic Analysis and Design of Aircraft [AGARD-R-783] p 2308 N92-23950
Introduction to Special Course on Engineering Methods in Aerodynamic Analysis and Design of Aircraft p 2308 N92-23951
Computational procedures for preliminary design p 2309 N92-23952
Configuration development --- preliminary aircraft design p 2309 N92-23953
Panel methods for aerodynamic analysis and design p 2309 N92-23955
High angle of attack: Aerodynamics p 2305 N92-23956
Aircraft drag analysis methods p 2309 N92-23957

AIRCRAFT ENGINES
Coupled multi-disciplinary simulation of composite engine structures in propulsion environment [NASA-TM-105575] p 2388 N92-23267
Evaluation of the applicability of Helmholtz resonators for low frequency acoustic liners [PB92-138544] p 2436 N92-23588

AIRCRAFT ICING
Comparison of two-dimensional and three-dimensional droplet trajectory calculations in the vicinity of finite wings [NASA-TM-105617] p 2373 N92-23154
Aircraft accident report: Ryan International Airlines DC-9-15, N565PC, loss of control on takeoff, Cleveland-Hopkins International Airport, Cleveland, Ohio, February 17, 1991 [PB91-910410] p 2305 N92-23597

AIRCRAFT INSTRUMENTS
Introduction: Ocean air observation p 2392 N92-23381
Recommended system concept p 2392 N92-23383
The imaging spectrometer p 2393 N92-23387
The laser bathymeter p 2393 N92-23388
Quick-look system p 2394 N92-23393
Preconsiderations on aircraft integration p 2395 N92-23402

AIRCRAFT PERFORMANCE
Survey of experimental techniques for performance prediction p 2309 N92-23954

AIRCRAFT PRODUCTION
From IGES to STEP [REPT-3.1.6] p 2423 N92-23881

AIRCRAFT STRUCTURES
Integrated Design Analysis and Optimisation of Aircraft Structures [AGARD-R-784] p 2306 N92-23227
Application of an automated multidisciplinary analysis and optimisation system to the design of aircraft structures p 2307 N92-23233
First approach to an integrated fin design p 2308 N92-23236
A fin optimisation study p 2308 N92-23237
Structural optimization of aircraft practice and trends p 2308 N92-23239

AIRFOIL PROFILES
Grid generation and flow solution method for Euler equations on unstructured grids [NASA-TM-4295] p 2305 N92-23533

AIRFOILS
Improved shock-capturing of Jameson's scheme for the Euler equations [PB92-148758] p 2373 N92-23251
Efficient and robust design optimization of transonic airfoils p 2305 N92-23717

AIRFRAME MATERIALS
Conceptional design to heat-resistant airframe of HOPE p 2328 N92-23820

AIRFRAMES
Conceptional design to heat-resistant airframe of HOPE p 2328 N92-23820

AIRGLOW
WAMDII: The Wide Angle Michelson Doppler Imaging Interferometer [NASA-TM-105526] p 2441 N92-23525

AIRLINE OPERATIONS
Aircraft accident report: Ryan International Airlines DC-9-15, N565PC, loss of control on takeoff, Cleveland-Hopkins International Airport, Cleveland, Ohio, February 17, 1991 [PB91-910410] p 2305 N92-23597

ALANINE
Photoinduced electron transfer in ordered polymers [DE92-008787] p 2355 N92-24037

ALGEBRA
An exceptional N=8 superconformal algebra in two dimensions associated with F(4) [DE92-616991] p 2435 N92-23207
Sheaves of Schwartz distributions [DE92-615217] p 2432 N92-23331
On the Stone-Weierstrass theorem for scalar and vector valued functions [DE92-616916] p 2432 N92-23335
Lie-admissible structure of Hamilton's original equations with external terms [DE92-615216] p 2433 N92-23745
Sphere packings centered at S-units of algebraic tori [PB92-136373] p 2434 N92-24061

ALGORITHMS
Atmospheric correction of the second generation ocean color sensors p 2392 N92-23145
An algorithmic approach for fault-monitoring of electrical actuation system for all electric aircraft [NAL-PD-AL-9111] p 2368 N92-23246
A signal and image processing object-based system using CLOS [DE92-006826] p 2417 N92-23255
LDEF geometry/mass model for radiation analyses p 2440 N92-23305
Turbulence modeling in supersonic combusting flows p 2302 N92-23342
Development of new flux splitting schemes p 2302 N92-23343
On recontamination and directional-bias problems in Monte Carlo simulation of PDF turbulence models p 2302 N92-23346
Improved interpretation of satellite altimeter data using genetic algorithms p 2402 N92-23369
Optimizing flow rates in a queueing network with side constraints [PB92-149996] p 2430 N92-23508
Analysis of ordering scheme for the unknowns during the solving of geodetic least squares systems [PB92-137355] p 2432 N92-23514
Grid generation and flow solution method for Euler equations on unstructured grids [NASA-TM-4295] p 2305 N92-23533
A verified design of a fault-tolerant clock synchronization circuit: Preliminary investigations [NASA-TM-107568] p 2416 N92-23559
Computations of unsteady multistage turbomachinery flows p 2311 N92-23671
Unsteady three-dimensional incompressible algorithm based on artificial compressibility p 2375 N92-23700
Method for evaluating non-consistent data using two statistical criteria [DE92-615195] p 2454 N92-23742
Voxel-based solid modeling [REPT-1.1.3] p 2419 N92-23855
On generating two dimensional CMOS cells [REPT-1.3.2] p 2421 N92-23869
Breathing maze router for analog VLSI cell generation [REPT-1.3.3] p 2422 N92-23870
Adaptive active flutter suppression of wings in subsonic and transonic flight regimes p 2310 N92-24010

ALIGNMENT
High reliability robot friendly ORU interface [NASA-CASE-GSC-13360-1] p 2381 N92-23377
Vacuum mechatronic laser alignment system on the NOVA laser [DE92-006898] p 2379 N92-23571

ALKALI METALS
Theoretical model of the density of states of random binary alloys [DE92-617438] p 2350 N92-23210

ALLOCATIONS
Research, Development, Test and Evaluation (R, D, T, and E) Programs (R-1), Department of Defense budget for fiscal year 1993 [PB92-127745] p 2451 N92-23247

ALLOYS
Applications of multiple-ion irradiations to metals, ceramics, and polymers [DE92-007686] p 2354 N92-23222
An optical study of grain formation: Casting and solidification technology (2-IML-1) p 2361 N92-23631

ALUMINIDES
The influence of chromium on structure and mechanical properties of B2 nickel aluminide alloys [NASA-CR-189124] p 2351 N92-23566

ALUMINUM
Casting of simple-shaped single crystals of aluminum [PB92-136555] p 2350 N92-23179
An XPS study of the stability of Fomblin Z25 on the native oxide of aluminum --- x ray photoelectron spectroscopy [NASA-TM-105594] p 2353 N92-23185
M and D SIG progress report: Laboratory simulations of LDEF impact features p 2336 N92-23323

ALUMINUM ALLOYS
Effects of impurities on the solidification and mechanical behaviour of primary and secondary commercial purity aluminium and aluminium alloys [PB92-133511] p 2350 N92-23176
Nd: YAG laser welding aluminum alloys [DE92-003131] p 2381 N92-23177
In situ XANES study of the valence state of chromium during electrochemical polarization of AlCr alloys [DE92-007452] p 2350 N92-23197

ALUMINUM GALLIUM ARSENIDE LASERS
Injection seeding of a Q-switched alexandrite laser: Study of frequency stabilization p 2380 N92-23961

ALUMINUM GALLIUM ARSENIDES
Electron polarization in modulation doped heterostructures [DE92-617490] p 2447 N92-23272
Planar varactor frequency multiplier devices with blocking barrier [NASA-CASE-NPO-18428-1-CU] p 2369 N92-23464
Semiclassical model and properties of resonant tunneling diode [PB92-143320] p 2448 N92-23498

ALUMINUM NITRIDES
Hardening in AlN induced by point defects [DE92-007717] p 2352 N92-23720

ALUMINUM OXIDES
Integrated optics in silicon-based aluminum oxide [ISBN-90-9004261-X] p 2441 N92-23166
Tribological evaluation of an Al2O3-SiO2 ceramic fiber candidate for high temperature sliding seals [NASA-TM-105611] p 2339 N92-23190
Guanidine based vehicle/binders for use with oxides, metals, and ceramics [NASA-CASE-LEW-15314-1] p 2354 N92-23461
Optimization of the laser glass composition for the Nova upgrade fusion laser system [DE92-008606] p 2380 N92-24065

ALUMINUM-LITHIUM ALLOYS
A study of aluminum-lithium alloy solidification using acoustic emission techniques [NASA-CR-4437] p 2435 N92-23556

AMINO ACIDS
Photoinduced electron transfer in ordered polymers [DE92-008787] p 2355 N92-24037

AMPLIFIERS
A flexible CPW package for a 30 GHz MMIC amplifier --- coplanar waveguide [NASA-TM-105630] p 2368 N92-23193

ANALOG TO DIGITAL CONVERTERS
A switched capacitor array based system for high-speed calorimetry [DE92-008288] p 2378 N92-23278

ANALYSIS (MATHEMATICS)
Constant curvature and non-perturbative W(sub 3) gravity [DE92-616919] p 2451 N92-23503

ANGLE OF ATTACK
High angle of attack: Aerodynamics p 2305 N92-23956
Normal force of low aspect ratio wing-body combinations up to high angles of attack at supersonic speeds [ESDU-91042] p 2309 N92-24009

ANGULAR DISTRIBUTION
Inelastic electron scattering from surfaces [DE92-008129] p 2437 N92-23330

ANGULAR RESOLUTION
Gamma rays from SN1987A with the UCR double-Compton telescope p 2455 N92-23695

ANGULAR VELOCITY
An analysis of the relationship between induction motor current and shaft speed fluctuations [DE92-007234] p 2371 N92-24025

ANIMALS
Nuclear medicine program [DE92-006979] p 2412 N92-23518

ANISOTROPY
An instrument to search for small-scale anisotropy in the cosmic microwave background at 90 GHz p 2441 N92-23161
Localization of deformation and inelastic deformation of pressure-sensitive dilatant materials p 2389 N92-23737

ANNEALING
Dependence of the critical temperature of laser-ablated YBa2Cu3O(7-delta) thin films on LaAlO3 substrate growth technique p 2365 N92-23415
Method of fabricating superconducting device [NASA-CASE-NPO-18394-1-CU] p 2370 N92-23552
Defect behavior, carrier removal and predicted in-space injection annealing of InP solar cells [NASA-TM-105624] p 2370 N92-23562
Binary surface-relief gratings for array illumination in digital optics [PB92-143585] p 2442 N92-23682

ANNUAL VARIATIONS
Possible atmospheric research with Aristoteles p 2317 N92-23927

ANTENNA ARRAYS
Feasibility study of a synthesis procedure for array feeds to improve radiation performance of large distorted reflector antennas
[NASA-CR-190191] p 2364 N92-23245
Solid State Technology Branch of NASA Lewis Research Center
[NASA-TM-105159] p 2365 N92-23412
Fast wave current drive antenna performance on D3-D
[DE92-008052] p 2444 N92-23446

ANTENNA DESIGN
Feasibility study of a synthesis procedure for array feeds to improve radiation performance of large distorted reflector antennas
[NASA-CR-190191] p 2364 N92-23245
Nonplanar linearly tapered slot antenna with balanced microstrip feed
[NASA-TM-105647] p 2370 N92-23535
Application of the Green function technique in the microstrip patch antenna analysis
[PB92-142173] p 2367 N92-23907

ANTENNA FEEDS
Feasibility study of a synthesis procedure for array feeds to improve radiation performance of large distorted reflector antennas
[NASA-CR-190191] p 2364 N92-23245

ANTENNA RADIATION PATTERNS
Feasibility study of a synthesis procedure for array feeds to improve radiation performance of large distorted reflector antennas
[NASA-CR-190191] p 2364 N92-23245
Application of the Green function technique in the microstrip patch antenna analysis
[PB92-142173] p 2367 N92-23907

ANTIBIOTICS
Studies on penetration of antibiotic in bacterial cells in space conditions (7-IML-1) p 2359 N92-23619

ANTIFERROMAGNETISM
Magnetic fluctuations and normal state properties of the t-J model at finite dopings
[DE92-617538] p 2447 N92-23452
Many-body problems in high temperature superconductivity
[DE92-617539] p 2447 N92-23453
Improved spin wave theory: An application to the spin-1/2 antiferromagnetic Heisenberg model on a square lattice
[DE92-617436] p 2448 N92-23504
High-temperature superconductivity: Electron-doped cuprates and composites from alloy precursors p 2448 N92-23774
Numerical study of the magnetic ordering and superconducting state of high-temperature superconductor p 2449 N92-23776

ANTIPROTONS
Research in high energy physics
[DE92-007966] p 2441 N92-23500

ANTIREFLECTION COATINGS
Limits of survivability and damage for optical components used in a high repetition rate visible laser
[DE92-006896] p 2379 N92-23570

APPLICATIONS OF MATHEMATICS
Mathematical analysis techniques for modeling the space network activities p 2434 N92-23964

APPLICATIONS PROGRAMS (COMPUTERS)
Multidisciplinary optimization studies using ASTROS p 2307 N92-23234
Using microsoft excel applications in the graduate intern program at Goddard Space Flight Center p 2425 N92-23959
User interface user's guide for HYPGEN
[NASA-CR-190304] p 2425 N92-23991
CEPXS/ONELD: A one-dimensional coupled electron-photon discrete ordinates code package
[DE92-003146] p 2425 N92-24041

APPROXIMATION
Confidence intervals for discrete approximations to ill-posed problems
[PB92-143742] p 2432 N92-23511
Ocean acoustic tomography inversion in the adiabatic-invariant approximation
[PB92-140466] p 2412 N92-23669
Mathematical modelling and numerical approximations for two-phase flow problems p 2375 N92-23672
Efficient and robust design optimization of transonic airfoils p 2305 N92-23717
Feasibility of payload sensitivity analyses for AR4 dynamic events p 2328 N92-23815

AQUEOUS SOLUTIONS
Phase partitioning experiment (8-IML-1) p 2360 N92-23621
A study of solution crystal growth in LOW-g (2-IML-1) p 2361 N92-23630

ARC SPRAYING
Investigation of plasma-sprayed laminates for high-temperature melting operations
[DE92-008416] p 2353 N92-24006

ARCHITECTURE (COMPUTERS)
A signal and image processing object-based system using CLOS
[DE92-006826] p 2417 N92-23255
A new VME based high voltage power supply for large experiments
[DE92-007199] p 2368 N92-23326
SLS-PLAN-IT: A knowledge-based blackboard scheduling system for Spacelab life sciences missions p 2426 N92-23358
An architecture for the development of real-time fault diagnosis systems using model-based reasoning p 2427 N92-23363
Feature detection in satellite images using neural network technology p 2427 N92-23366
Optical inner product neural associative memory
[NASA-CASE-NPO-18491-1-CU] p 2416 N92-23546
Architectural impact of FDDI network on scheduling hard real-time traffic
[NASA-CR-190272] p 2425 N92-23583
Combining a CAD/CAM system with an advanced database architecture
[REPT-3.1.5] p 2423 N92-23880

ARGON
Investigations of breakdown of rare gases by short pulses of 1.06(mu)m laser radiation
[DE92-615399] p 2379 N92-23131

ARIANE LAUNCH VEHICLE
Ariane technology: From today into the next century p 2318 N92-23751
Development status of the Ariane 5 solid propellant engine p 2319 N92-23755
Manufacturing process of the Ariane 5 segmented propellant chargers p 2319 N92-23756
Development status of the cryotechnical principal stage p 2319 N92-23758
Development status of the Vulcain engine p 2319 N92-23759
Reusable launchers: New concepts and technological advances for the manufacturing of cryogenic tanks p 2319 N92-23760
Materials for high liquid propulsion in 2010 p 2320 N92-23763
Materials for liquid propellant engines p 2320 N92-23764
Future launchers: Large size solid propellant monolithic booster p 2320 N92-23766
Dynamic load cases on Ariane 5 p 2321 N92-23797
Multi parameter optimization on Ariane 5 p 2321 N92-23798
Ariane 5 structural definition of the upper composite p 2321 N92-23808
Advanced numerical analyses for the optimisation of the structural behaviour of the intersegment connection for the Ariane 5 booster case p 2327 N92-23809
Brief history of the development of the EPS-structure p 2321 N92-23810
Ariane 4 internal acoustic environment: Interpretation of flight data with a vibroacoustic model of the upper part of the launcher p 2321 N92-23811
Feasibility of payload sensitivity analyses for AR4 dynamic events p 2328 N92-23815

ARITHMETIC AND LOGIC UNITS
FAPES: An expert system for designing and optimising fault-tolerant arithmetic array processors
[REPT-1.1.2] p 2419 N92-23854

ARM (ANATOMY)
Bar-holding prosthetic limb
[NASA-CASE-MFS-28481-1] p 2416 N92-24056

ARMED FORCES (UNITED STATES)
Research, Development, Test and Evaluation (R, D, T, and E) Programs (R-1), Department of Defense budget for fiscal year 1993
[PB92-127745] p 2451 N92-23247

ARSENIC COMPOUNDS
Fermi level effects on dislocation formation in InAs(1-x)Sb(x) grown by MOCVD
[DE92-008332] p 2450 N92-24034

ARTIFICIAL INTELLIGENCE
An algorithmic approach for fault-monitoring of electrical actuation system for all electric aircraft
[NAL-PD-AL-9111] p 2368 N92-23246
The 1992 Goddard Conference on Space Applications of Artificial Intelligence
[NASA-CP-3141] p 2426 N92-23356
Artificial intelligence approach to planning the robotic assembly of large tetrahedral truss structures p 2426 N92-23357
Detecting opportunities for parallel observations on the Hubble Space Telescope p 2426 N92-23359
Coordinating complex problem-solving among distributed intelligent agents p 2427 N92-23360
An architecture for the development of real-time fault diagnosis systems using model-based reasoning p 2427 N92-23363
Improved image classification with neural networks by fusing multispectral signatures with topological data p 2402 N92-23368
The use of artificial intelligence techniques to improve the multiple payload integration process p 2428 N92-23370
Logic programming and metadata specifications p 2429 N92-23375
MBT-WIRE: Intelligent CAD in wiring design
[REPT-1.1.4] p 2419 N92-23856

ARTIFICIAL SATELLITES
Prediction of solar and geomagnetic activity for ESA low-flying spacecraft p 2334 N92-23975

ASTEROIDS
The meteorite record as clues to asteroidal regolith processes p 2457 N92-23770
Interception of comets and asteroids on collision course with Earth
[DE92-007431] p 2458 N92-24028

ASTRONAUTS
Back pain in astronauts (8-IML-1) p 2360 N92-23622

ASTRONOMICAL MAPS
The ALEXIS data processing package: An IDL-based system
[DE92-007429] p 2455 N92-24027

ASTRONOMICAL MODELS
Observations of accretion discs in interacting binaries p 2454 N92-23673
Observing millisecond and binary pulsars p 2455 N92-24001

ASTRONOMICAL SPECTROSCOPY
Testing the solar paradigm for chromospheric activity in RS CVN binaries: Moderate resolution spectroscopy of solar active regions p 2459 N92-23171

ASYMMETRY
Line profile asymmetries in chromospherically active stars p 2458 N92-24015

ASYMPTOTIC METHODS
Turbulence modeling p 2301 N92-23338
An improved k-epsilon model for near wall turbulence p 2303 N92-23349

ATLANTIS (ORBITER)
Mission safety evaluation report for STS-43, postflight edition
[NASA-TM-107801] p 2312 N92-23240
Mission safety evaluation report for STS-30, postflight edition
[NASA-TM-107774] p 2312 N92-23242
Mission safety evaluation report for STS-36, postflight edition
[NASA-TM-107780] p 2312 N92-23244

ATMOSPHERIC CHEMISTRY
Scientific development of the Advanced Parallel Chemistry (APACHE) climate model
[DE92-006657] p 2404 N92-23123
Radar observations and dynamics of the polar summer mesosphere p 2408 N92-23702

ATMOSPHERIC CIRCULATION
Quasi-three-dimensional simulations of deep convection
[DE92-007204] p 2409 N92-23257
A model of large-scale instabilities in the Jovian troposphere p 2459 N92-23704

ATMOSPHERIC COMPOSITION
Use of the maximum entropy method to retrieve the vertical atmospheric ozone profile and predict atmospheric ozone content p 2407 N92-23965

ATMOSPHERIC CORRECTION
Atmospheric correction of the second generation ocean color sensors p 2392 N92-23145

ATMOSPHERIC MODELS
Scientific development of the Advanced Parallel Chemistry (APACHE) climate model
[DE92-006657] p 2404 N92-23123
Monsoon-ENSO relationships p 2404 N92-23160
Quasi-three-dimensional simulations of deep convection
[DE92-007204] p 2409 N92-23257
GENLN2: A general line-by-line atmospheric transmittance and radiance model. Version 3.0: Description and users guide
[PB92-148543] p 2408 N92-23522
WAMDII: The Wide Angle Michelson Doppler Imaging Interferometer
[NASA-TM-105526] p 2441 N92-23525
Investigation of the Archean climate using the NCAR CCM
[NASA-CR-189878] p 2410 N92-23656
A model of large-scale instabilities in the Jovian troposphere p 2459 N92-23704

On the global warming potentials of candidate gaseous diffusion plant coolants
[DE92-006640] p 2406 N92-23740
Clouds and radiation testbed data environment: Site data system and experiment center
[DE92-006732] p 2408 N92-23741

ATMOSPHERIC MOISTURE
Investigations on verification of the data observed by the MESSR and VTIR, and on interannual trend in the MSR data p 2397 N92-23470
Verification of MESSR and VTIR, and time variation of MSR performance p 2397 N92-23471
Preliminary report on the observation of polar atmosphere and cryosphere by MOS-1 data received at Syowa Station p 2399 N92-23481
Observation of lined-up cumulus rows under the winter monsoon situation using MOS-1 and radar data p 2399 N92-23483

ATMOSPHERIC PHYSICS
Scientific development of the Advanced Parallel Chemistry (APACHE) climate model
[DE92-006657] p 2404 N92-23123
JPRS report: Science and technology. USSR: Earth sciences
[JPRS-UES-91-005] p 2392 N92-23707
A new approach to estimate Angstrom coefficients
[DE92-619048] p 2460 N92-23909

ATMOSPHERIC PRESSURE
Functional precision of National Weather Service upper-air measurements using VIZ Manufacturing Co. B radiosonde (model 1492-520)
[PB92-137868] p 2410 N92-23494

ATMOSPHERIC RADIATION
Field evaluation of remote sensor measurements of wind, temperature, and moisture for ARM integrated sounding system research
[PB92-140714] p 2401 N92-23521

ATMOSPHERIC SOUNDING
Functional precision of National Weather Service upper-air measurements using VIZ Manufacturing Co. A radiosonde (model 1492-510)
[PB92-137850] p 2410 N92-23439
Proceedings on MOS-1 data evaluation
[HE-90015] p 2396 N92-23465
Field evaluation of remote sensor measurements of wind, temperature, and moisture for ARM integrated sounding system research
[PB92-140714] p 2401 N92-23521
International workshop on the airborne measurement of wind, turbulence, and position
[PB92-139963] p 2410 N92-23587
Urban temperature bias as determined by polar orbiting satellite data p 2402 N92-23724
Functional precision of National Weather Service upper-air measurements using space data division radiosonde (model 909-10-01)
[PB92-137843] p 2411 N92-23746
Possible atmospheric research with Aristoteles p 2317 N92-23927

ATMOSPHERIC STRATIFICATION
Radar observations and dynamics of the polar summer mesosphere p 2408 N92-23702

ATMOSPHERIC TEMPERATURE
Functional precision of National Weather Service upper-air measurements using VIZ Manufacturing Co. B radiosonde (model 1492-520)
[PB92-137868] p 2410 N92-23494
WAMDII: The Wide Angle Michelson Doppler Imaging Interferometer
[NASA-TM-105526] p 2441 N92-23525
Urban temperature bias as determined by polar orbiting satellite data p 2402 N92-23724
Possible atmospheric research with Aristoteles p 2317 N92-23927

ATMOSPHERIC TURBULENCE
International workshop on the airborne measurement of wind, turbulence, and position
[PB92-139963] p 2410 N92-23587

ATOMIC PHYSICS
Atomic physics of strongly correlated systems
[DE92-008356] p 2438 N92-23895

ATOMIC STRUCTURE
On the kinetics of structural relaxation in some metallic glasses
[PB92-1287272] p 2353 N92-23165
Superconducting materials
[DE92-007748] p 2446 N92-23205
Semiempirical studies of atomic structure
[DE92-008143] p 2437 N92-23448
The electronic structure of icosahedral boron clusters
[DE92-008336] p 2447 N92-23451
Effective mass theory for abrupt heterojunctions
[DE92-617439] p 2448 N92-23581
Ground state searches in FCC intermetallics
[DE92-008300] p 2353 N92-23984
Electronic structure in high temperature superconducting oxides
[DE92-008566] p 2449 N92-23986

ATOMS
Lasers without inversion: Theory and experiment p 2379 N92-23143

ATTITUDE INDICATORS
Pinhole cameras as sensors for atomic oxygen in orbit: Application to attitude determination of the LDEF p 2379 N92-23283

AUGER EFFECT
Inelastic electron scattering from surfaces
[DE92-008129] p 2437 N92-23330
Resonant transfer excitation: Interference effects
[DE92-007240] p 2439 N92-24026

AUGER SPECTROSCOPY
Deposition of adherent Ag-Ti duplex films on ceramics in a multiple-cathode sputter deposition system
[NASA-TM-105586] p 2311 N92-23225

AURORAL ZONES
Fast aurora zone analysis p 2409 N92-23960

AUTOMATIC CONTROL
Controlling operations through procedures: APE (automated procedure editor)
[REPT-2.2.1] p 2422 N92-23875
Distributed computer system in the large scale low speed wind tunnel
[NAL-TM-629] p 2312 N92-23979

AUTOMATIC TEST EQUIPMENT
On development of automated static loading system for spacecraft structures p 2326 N92-23801

AUTOMATION
Computer integrated enterprise: The next step in CIM evolution
[REPT-3.2.2] p 2424 N92-23883
A self-navigating mobile robot
[DE92-008612] p 2430 N92-24066

AUTOMOBILE FUELS
High-temperature ignition of propane with MTBE as an additive: Shock-tube experiments and modeling
[DE92-008557] p 2348 N92-23715

AUTOMOBILES
Evaluation of research prototype vehicles equipped with direct injection 2-stroke cycle engines
[PB92-143692] p 2383 N92-23595
Center for Space Power, Texas A and M University p 2313 N92-23651

AUTONOMOUS NAVIGATION
On motion planning amidst transient obstacles
[DE91-018939] p 2429 N92-23457

AUTONOMY
The achievement of spacecraft autonomy through the thematic application of multiple cooperating intelligent agents p 2427 N92-23364

AUXILIARY PROPULSION
Derated ion thruster design issues
[NASA-TM-105576] p 2337 N92-23534

AXIAL LOADS
Dynamic characterization of composite materials p 2330 N92-23832
Notched strength of composite materials p 2331 N92-23839
Transverse deformation of unidirectional fiber-reinforced metal matrix composites p 2345 N92-24013

AXIAL STRAIN
Analysis of delamination related fracture processes in composites
[NASA-CR-190226] p 2340 N92-23532
Localization of deformation and inelastic deformation of pressure-sensitive dilatant materials p 2389 N92-23737

AXIAL STRESS
Investigation of fretting fatigue mechanisms on 7075-T6 aluminum alloy and Ti-6Al-4V titanium alloy p 2352 N92-23725

AXISYMMETRIC BODIES
Comparison of two-dimensional and three-dimensional droplet trajectory calculations in the vicinity of finite wings
[NASA-TM-105617] p 2373 N92-23154
Normal force of low aspect ratio wing-body combinations up to high angles of attack at supersonic speeds
[ESDU-91042] p 2309 N92-24009

B

BACILLUS
Growth and sporulation of Bacillus subtilis under microgravity (7-IML-1) p 2358 N92-23612

BACKGROUND RADIATION
The origins of the cosmic x ray and gamma ray backgrounds p 2460 N92-23141
An instrument to search for small-scale anisotropy in the cosmic microwave background at 90 GHz p 2441 N92-23161

BACKSCATTERING
Development of a helicopter-borne 8-channel ranging scatterometer
[PB92-141977] p 2396 N92-23441

BACTERIA
Growth and sporulation of Bacillus subtilis under microgravity (7-IML-1) p 2358 N92-23612
Studies on penetration of antibiotic in bacterial cells in space conditions (7-IML-1) p 2359 N92-23619

BALLOON SOUNDING
Functional precision of National Weather Service upper-air measurements using VIZ Manufacturing Co. A radiosonde (model 1492-510)
[PB92-137850] p 2410 N92-23439
Functional precision of National Weather Service upper-air measurements using space data division radiosonde (model 909-10-01)
[PB92-137843] p 2411 N92-23746

BALLOON-BORNE INSTRUMENTS
Functional precision of National Weather Service upper-air measurements using VIZ Manufacturing Co. A radiosonde (model 1492-510)
[PB92-137850] p 2410 N92-23439
Functional precision of National Weather Service upper-air measurements using space data division radiosonde (model 909-10-01)
[PB92-137843] p 2411 N92-23746

BALLS
Flexible robotic arm
[NASA-CASE-GSC-13161-1] p 2386 N92-24060

BANACH SPACE
Isometric embedding of median algebras into L1 (mu) spaces
[PB92-149343] p 2431 N92-23249

BAND STRUCTURE OF SOLIDS
The electronic structure of icosahedral boron clusters
[DE92-008336] p 2447 N92-23451
Effective mass theory for abrupt heterojunctions
[DE92-617439] p 2448 N92-23581
Ab initio pair potentials for FCC metals: An application of the method of Moebius transform
[DE92-617440] p 2351 N92-23582
The electron-positron momentum density and Fermi surface of YBa2Cu3O(7-x)
[DE92-008605] p 2450 N92-24007

BANDPASS FILTERS
PSD computations using Welch's method
[DE92-007419] p 2370 N92-23584

BANDWIDTH
Control of a helicopter engine in low altitude flight p 2310 N92-23122
Sensor compatibility/optimal sensor combinations p 2395 N92-23403

BARIUM OXIDES
Electronic structure in high temperature superconducting oxides
[DE92-008566] p 2449 N92-23986
NQR investigation of pressure-induced charge transfer in oxygen-deficient YBa2Cu3O(7-delta) (delta = 0.38)
[DE92-008441] p 2450 N92-24036

BAROCLINIC INSTABILITY
A model of large-scale instabilities in the Jovian troposphere p 2459 N92-23704

BARRIER LAYERS
Planar varactor frequency multiplier devices with blocking barrier
[NASA-CASE-NPO-18428-1-CU] p 2369 N92-23464
Method of fabricating superconducting device
[NASA-CASE-NPO-18394-1-CU] p 2370 N92-23552

BARS
Bar-holding prosthetic limb
[NASA-CASE-MFS-28481-1] p 2416 N92-24056

BATHYMETERS
The laser bathymeter p 2393 N92-23388
Computer tutorial and animation of the normal ice cycle of the Laurentian Great Lakes of North America for 1960 - 1979
[PB92-129949] p 2401 N92-23659

BAYS (STRUCTURAL UNITS)
Measured space environmental effects to LDEF during retrieval p 2335 N92-23285

BEACONS
Application of ground-based laser beacon for Earth image calibration, 3 p 2396 N92-23468

BEAM INJECTION
Fusion gain due to high energy ions accelerated by additional heating
[DE92-751038] p 2443 N92-23133
Report from orbit sub-group of task force for MR synchrotron radiation project
[DE92-751024] p 2441 N92-23713

BEAM INTERACTIONS
High energy physics: Report of research accomplishments and future goals, FY 1992
[DE92-008543] p 2441 N92-23576

BEAM SWITCHING
Evaluation of a mechanical beam-switching system [PB92-139773] p 2368 N92-23140
BEAMS (RADIATION)
Test beam results from the D0 end electromagnetic calorimeter [DE92-008299] p 2378 N92-23279
Research in high energy physics [DE92-007966] p 2441 N92-23500
BEAMS (SUPPORTS)
A damage mechanics model for beams p 2387 N92-23159
On the modelling of a deployable telescope elastic beam-type element for on-orbit multibody simulations p 2329 N92-23826
Analytical and experimental investigation of vibratory response in adhesively bonded and composite structures p 2345 N92-24012
BEARINGS
Applications of industrial engineering p 2364 N92-23966
BEND TESTS
On the test of mode 1 delamination and the importance of laminate lay-ups p 2343 N92-23943
BENDING FATIGUE
Conception and development of improved analytical prediction models for fatigue induced tooth breakage due to cyclic bending in spur gear teeth p 2384 N92-23739
BERYLLIUM
Beryllium-thermal protection technology p 2331 N92-23837
BERYLLIUM ISOTOPES
Gamma radiation survey of the LDEF spacecraft p 2460 N92-23293
The interactions of atmospheric cosmogenic radionuclides with spacecraft surfaces p 2461 N92-23294
Surface activation of Concorde by Be-7 p 2439 N92-23295
Gamma ray spectrometry of LDEF samples at SRL p 2349 N92-23299
BIAS
Urban temperature bias as determined by polar orbiting satellite data p 2402 N92-23724
Analysis of time series with missing values p 2434 N92-23777
BIBLIOGRAPHIES
Publications of the exobiology program for 1990: A special bibliography [NASA-TM-4364] p 2416 N92-23429
JPRS report: Science and technology. Central Eurasia: Space [JPRS-USP-92-002] p 2314 N92-23705
JPRS report: Science and technology. Central Eurasia: Life sciences [JPRS-ULS-92-010] p 2412 N92-23706
JPRS report: Science and technology. USSR: Earth sciences [JPRS-UES-91-005] p 2392 N92-23707
JPRS report: Science and technology. Central Eurasia: Materials science [JPRS-UMS-92-005] p 2363 N92-23708
JPRS report: Science and technology. Central Eurasia: Materials science [JPRS-UMS-92-006] p 2363 N92-23709
BIG BANG COSMOLOGY
Particle physics and cosmology [DE92-008301] p 2456 N92-23153
BINARY ALLOYS
Theoretical model of the density of states of random binary alloys [DE92-617438] p 2350 N92-23210
Simulation of freckles during vertical solidification of binary alloys p 2353 N92-24014
BINARY DATA
Binary surface-relief gratings for array illumination in digital optics [PB92-143585] p 2442 N92-23662
BINARY STARS
Discovery of orbital decay in SMC X-1 [NASA-CR-190214] p 2317 N92-23531
On the limiting astrometric accuracy of binary star speckle interferometry p 2457 N92-23696
BINDERS (MATERIALS)
Guanidine based vehicle/binders for use with oxides, metals, and ceramics [NASA-CASE-LEW-15314-1] p 2354 N92-23461
BIOCHEMISTRY
JPRS report: Science and technology. Central Eurasia: Life sciences [JPRS-ULS-92-010] p 2412 N92-23706
BIOLOGICAL EFFECTS
Radiation exposure of air carrier crewmembers 2 [PB92-140037] p 2414 N92-23139
Development of 3-dimensional compact magnetic dosimeter for environmental magnetic field monitoring [DE92-750825] p 2407 N92-23262
Embryogenesis and organogenesis of Carausius morosus under space flight conditions (7-IML-1) p 2358 N92-23610
Studies on penetration of antibiotic in bacterial cells in space conditions (7-IML-1) p 2359 N92-23619
Biostack (14-IML-1) p 2361 N92-23627
Promotion of industrial technologies on the global environment [DE92-769375] p 2406 N92-23734
Low dose neutron late effects: Cataractogenesis [DE92-005539] p 2414 N92-24033
BIOLOGICAL EVOLUTION
Publications of the exobiology program for 1990: A special bibliography [NASA-TM-4364] p 2416 N92-23429
BIOPHYSICS
JPRS report: Science and technology. Central Eurasia: Life sciences [JPRS-ULS-92-010] p 2412 N92-23706
BIOPROCESSING
Dynamic cell culture system (7-IML-1) p 2359 N92-23615
Suborbital missions: The Joust p 2313 N92-23644
BIOREACTORS
Dynamic cell culture system (7-IML-1) p 2359 N92-23615
Three-dimensional cultured glioma cell lines [NASA-CASE-MSC-21843-1-NP] p 2413 N92-24052
BIOSPHERE
Earth observing system: NASA's EOSDIS development approach is risky [GAO/IMTEC-92-24] p 2401 N92-23686
BIOSYNTHESIS
Friend leukemia virus transformed cells exposed to microgravity in the presence of DMSO (7-IML-1) p 2358 N92-23613
Proliferation and performance of hybridoma cells in microgravity (7-IML-1) p 2358 N92-23614
BIOTECHNOLOGY
JPRS report: Science and technology. Central Eurasia: Life sciences [JPRS-ULS-92-010] p 2412 N92-23706
BLACK HOLES (ASTRONOMY)
Observations of accretion discs in interacting binaries p 2454 N92-23673
BLADE-VORTEX INTERACTION
Numerical simulations of wakes, blade-vortex interaction, flutter, and flutter suppression by feedback control p 2375 N92-23997
BLAST LOADS
Dynamic load cases on Ariane 5 p 2321 N92-23797
BLOOD PRESSURE
Stress effects of human-computer interactions [PB92-136001] p 2415 N92-23513
BLUNT BODIES
Hypersonic laminar flow computations over a blunt leading edged delta wing at three different chord Reynolds numbers [FFA-TN-1991-40] p 2304 N92-23168
Topics in numerical computation of compressible flow p 2375 N92-23692
BODY FLUIDS
Energy expenditure in space flight (doubly labelled water method) (8-IML-1) p 2359 N92-23620
BODY-WING CONFIGURATIONS
Normal force of low aspect ratio wing-body combinations up to high angles of attack at supersonic speeds [ESDU-91042] p 2309 N92-24009
BOILERS
Induction boiler [NASA-CASE-MFS-28634-1] p 2385 N92-24055
BOILING
The continuum modelling of two-phase flow systems [DE92-007538] p 2373 N92-23202
BOLTED JOINTS
Robot-friendly connector --- space truss structures [NASA-CASE-MSC-21864-1] p 2382 N92-23544
BOLTS
High reliability robot friendly ORU interface [NASA-CASE-GSC-13360-1] p 2381 N92-23377
BOLTZMANN TRANSPORT EQUATION
CEPXS/ONELD: A one-dimensional coupled electron-photon discrete ordinates code package [DE92-003146] p 2425 N92-24041
BONE DEMINERALIZATION
Skeletal responses to spaceflight [NASA-TM-103890] p 2414 N92-23424
Effect of microgravity and mechanical stimulation on the in vitro mineralization and resorption of fetal mouse long bones (7-IML-1) p 2357 N92-23606
BONE MINERAL CONTENT
Effect of microgravity and mechanical stimulation on the in vitro mineralization and resorption of fetal mouse long bones (7-IML-1) p 2357 N92-23606
BONES
Skeletal responses to spaceflight [NASA-TM-103890] p 2414 N92-23424
Effect of microgravity and mechanical stimulation on the in vitro mineralization and resorption of fetal mouse long bones (7-IML-1) p 2357 N92-23606
Center for Cell Research, Pennsylvania State University p 2314 N92-23653
BOOLEAN ALGEBRA
Isometric embedding of median algebras into L1 (mu) spaces [PB92-149343] p 2431 N92-23249
BOOSTER ROCKET ENGINES
Future launchers: Large size solid propellant monolithic booster p 2320 N92-23766
Development of solid propellant booster p 2320 N92-23767
Advanced numerical analyses for the optimisation of the structural behaviour of the intersegment connection for the Ariane 5 booster case p 2327 N92-23809
BORON
The electronic structure of icosahedral boron clusters [DE92-008336] p 2447 N92-23451
BOSONS
Magnetic fluctuations and normal state properties of the t-J model at finite dopings [DE92-617538] p 2447 N92-23452
BOUNDARIES
Sensitivity l(sup 1) minimization with boundary zeros or poles [PB92-141803] p 2433 N92-23658
BOUNDARY CONDITIONS
Wideband finite difference time domain implementation of surface impedance boundary conditions for good conductors [NASA-CR-190098] p 2366 N92-23528
Long time behavior of unsteady flow computations [NASA-TM-105584] p 2374 N92-23565
BOUNDARY ELEMENT METHOD
Boundary element analysis of fracture mechanics problems p 2387 N92-23125
Numerical and experimental study of noise generated by a vibrating plate p 2324 N92-23792
On the analysis of liquid filled free-free tanks p 2332 N92-23843
BOUNDARY INTEGRAL METHOD
Applications of boundary integral methods to the study of steep free surface waves p 2372 N92-23149
Numerical calculation: Aspiration efficiency of aerosols into thin-walled sampling inlets [PB92-132901] p 2374 N92-23516
BOUNDARY LAYER FLOW
Turbulence modeling p 2301 N92-23338
Development of new flux splitting schemes p 2302 N92-23343
BOUNDARY LAYER TRANSITION
Center for Modeling of Turbulence and Transition (CMOTT). Research briefs: 1990 [NASA-TM-105243] p 2301 N92-23336
RNG in turbulence and modeling of bypass transition p 2301 N92-23341
BOUNDARY VALUE PROBLEMS
A multilevel preconditioner for domain decomposition boundary systems [DE92-008055] p 2432 N92-23329
The discontinuous finite element method with the Taylor-Galerkin approach for nonlinear hyperbolic conservation laws p 2433 N92-23738
Progress in the spacewise approach to Aristoteles data reduction p 2315 N92-23914
BOX BEAMS
Nonlinear finite element analysis of space frames [PB92-142447] p 2388 N92-23664
BRAIN
Microgravity vestibular investigations (10-IML-1) p 2360 N92-23626
BRAKES (FOR ARRESTING MOTION)
Non linear structural analysis of a thin skin carbon-carbon rigid decelerator p 2330 N92-23831
BRAZING
JPRS report: Science and technology. Central Eurasia: Materials science [JPRS-UMS-92-005] p 2363 N92-23708
JPRS report: Science and technology. Central Eurasia: Materials science [JPRS-UMS-92-006] p 2363 N92-23709
BRIDGMAN METHOD
Casting of simple-shaped single crystals of aluminum [PB92-136555] p 2350 N92-23179
BRIGHTNESS TEMPERATURE
Verification of MESSR and VTIR, and time variation of MSR performance p 2397 N92-23471

Signal processing of the data obtained by MOS-1 MSR p 2397 N92-23472
Retrieval of upper precipitable water profile from MOS-1 VTIR water vapor channel p 2398 N92-23479
Availability of MSR data for snow water estimation p 2399 N92-23482

BRINES
Geothermal energy program overview [DE91-002172] p 2402 N92-23175

BROADBAND
Detecting Lamb waves with broad-band acousto-ultrasonic signals in composite structures [NASA-TM-105557] p 2386 N92-23189
Wideband finite difference time domain implementation of surface impedance boundary conditions for good conductors [NASA-CR-190098] p 2366 N92-23528
Variable bit rate video coding [PB92-134279] p 2367 N92-23676

BUBBLES
Numerical and physical modelling of bubbly flow phenomena [DE92-008642] p 2376 N92-24062

BUCKLING
Evaluation of MHOST analysis capabilities for a plate element --- finite element modeling [NASA-TM-105387] p 2387 N92-23196
Buckling of simply supported and clamped anisotropic plates under combined loads p 2326 N92-23804
Non linear structural analysis of a thin skin carbon-carbon rigid decelerator p 2330 N92-23831
Buckling and failure of thin elliptical delaminations in composites p 2331 N92-23835
Effect of low-speed impact damage and damage location on behavior of composite panels [NASA-TP-3196] p 2344 N92-23981
Collapse of composite tubes under end moments [NASA-TM-107605] p 2390 N92-23992

BUFFETING
Design of a fighter aircraft vertical tail enhanced buffet environment survivability p 2307 N92-23235

BULGING
Localization of deformation and inelastic deformation of pressure-sensitive dilatant materials p 2389 N92-23737

BUOYS
The accuracy of the drift buoy positioning by MOS-1 DCS p 2399 N92-23484
Study on drifting-data collection buoy using MOS-1: Position verification in the Bering Sea p 2400 N92-23486

BUTENES
High-temperature ignition of propane with MTBE as an additive: Shock-tube experiments and modeling [DE92-008557] p 2348 N92-23715

BYPASSES
Turbulence modeling p 2301 N92-23338

C

CALCIFICATION
Skeletal responses to spaceflight [NASA-TM-103890] p 2414 N92-23424

CALCULUS OF VARIATIONS
The Jordan-Schwinger realization of two-parametric quantum group SI(sub q,s)(2) [DE92-616891] p 2451 N92-23501

CALIBRATING
Application of ground-based laser beacon for Earth image calibration, 3 p 2396 N92-23468
Investigations on verification of the data observed by the MESSR and VTIR, and on interannual trend in the MSR data p 2397 N92-23470
International workshop on the airborne measurement of wind, turbulence, and position [PB92-139963] p 2410 N92-23587

CALIFORNIA
Climate [PB92-150457] p 2410 N92-23520

CALORIMETERS
Test beam results from the D0 end electromagnetic calorimeter [DE92-008299] p 2378 N92-23279
A study of underground muons in the Soudan 2 detector p 2437 N92-23674

CAMERAS
Testing the solar paradigm for chromospheric activity in RS CVN binaries: Moderate resolution spectroscopy of solar active regions p 2459 N92-23171
IMAX camera (12-IML-1) p 2363 N92-23641

CANTILEVER PLATES
The continuous elements method p 2330 N92-23829

CAPACITORS
A switched capacitor array based system for high-speed calorimetry [DE92-008288] p 2378 N92-23278
Characterization of polybenzimidazole (PBI) film at high temperatures [NASA-CR-189174] p 2370 N92-23538
Evaluation of high temperature capacitor dielectrics [NASA-TM-105622] p 2370 N92-23561

CARBON
Environmental effects on friction and wear of diamond and diamondlike carbon coatings [NASA-TM-105634] p 2354 N92-23192
LDEF impact craters formed by carbon-rich impactors: A preliminary report p 2336 N92-23319
Proceedings: Nozzle Initiative Industry Advisory Committee on Standardization of Carbon-Phenolic Test Methods and Specifications [NASA-CR-190203] p 2337 N92-23539
Improvement of laser machining processes [DE92-007801] p 2380 N92-23723
The effect of co-implantation on the electrical activity of implanted carbon in GaAs [DE92-008307] p 2371 N92-23985
Transport calculations of chemically sputtered carbon near a plasma divertor surface [DE92-009022] p 2445 N92-24021
Survey on optimization of CO2 disposal system and carbon utilization technology [DE92-769381] p 2407 N92-24024

CARBON DIOXIDE
Limiting net greenhouse gas emissions in the United States, volume 1 [DE92-007593] p 2405 N92-23204
Limiting net greenhouse gas emissions in the United States, volume 2 [DE92-007592] p 2405 N92-23333
Promotion of industrial technologies on the global environment [DE92-769377] p 2405 N92-23454
Survey on subterranean disposal and storage technology of CO2 [DE92-769378] p 2405 N92-23455
Survey on fixation and utilization of carbon dioxide by catalytic hydrogenation [DE92-769380] p 2347 N92-23456
Liquid/supercritical fluid carbon dioxide cleaning of stainless steel components [DE92-006947] p 2348 N92-23572
Energy expenditure in space flight (doubly labelled water method) (8-IML-1) p 2359 N92-23620
Promotion of industrial technologies on the global environment [DE92-769374] p 2406 N92-23733
Promotion of industrial technologies on the global environment [DE92-769375] p 2406 N92-23734
Molecular design of substrate binding sites [DE92-008331] p 2438 N92-23894
Promotion of industrial technologies on the global environment [DE92-769376] p 2407 N92-24023
Survey on optimization of CO2 disposal system and carbon utilization technology [DE92-769381] p 2407 N92-24024

CARBON DIOXIDE CONCENTRATION
Investigation of the Archean climate using the NCAR CCM [NASA-CR-189878] p 2410 N92-23656

CARBON FIBER REINFORCED PLASTICS
The effect of fatigue-induced damage on the mechanical properties of CFRP composites p 2339 N92-23157
Characterization of interlaminar mode 1 and mode 2 fracture in CFRP laminates p 2325 N92-23794
Experimental study of delamination growth in multidirectional CFRP-laminates under fatigue loading p 2328 N92-23819
Conceptional design to heat-resistant airframe of HOPE p 2328 N92-23820
Microstructure and mechanical properties of carbon fibres: Relationship with the fibre-matrix adhesion in a carbon-epoxy composite p 2341 N92-23935
Impact-induced delamination in (0(5), 90(5), 0(5)) carbon/peek composite laminates p 2341 N92-23936
Impact and compression response of composite materials containing fortifiers p 2341 N92-23937
Morphology and mechanical performance of PPS/carbon composite p 2342 N92-23939
Application of the microbond technique: Characterization of carbon-epoxy interfaces p 2343 N92-23944

CARBON FIBERS
Proceedings: Nozzle Initiative Industry Advisory Committee on Standardization of Carbon-Phenolic Test Methods and Specifications [NASA-CR-190203] p 2337 N92-23539
The fracture behavior of carbon/epoxy laminates containing part through-the-thickness fiber breakage p 2340 N92-23693
Stretched skin concept for the entry aerodynamic decelerator system of planetary probes p 2331 N92-23836
Microstructure and mechanical properties of carbon fibres: Relationship with the fibre-matrix adhesion in a carbon-epoxy composite p 2341 N92-23935
Quantification of surface functional groups of carbon fibers by x ray photoelectron spectroscopy p 2343 N92-23946
Survey on optimization of CO2 disposal system and carbon utilization technology [DE92-769381] p 2407 N92-24024

CARBON MONOXIDE
Reductive coupling of carbon monoxide to C2 products [DE92-007529] p 2347 N92-23499

CARBON 12
Studies of fluctuation processes in nuclear collisions [DE92-008144] p 2440 N92-23276

CARBON 13
Reductive coupling of carbon monoxide to C2 products [DE92-007529] p 2347 N92-23499

CARBON-CARBON COMPOSITES
Large thin composite thermostructural parts p 2329 N92-23821
Non linear structural analysis of a thin skin carbon-carbon rigid decelerator p 2330 N92-23831

CARBONACEOUS CHONDRITES
The meteorite record as clues to asteroidal regolith processes p 2457 N92-23770

CARGO SPACECRAFT
Solar-electric-propulsion cargo vehicles for split/sprint Mars mission [NASA-CR-189983] p 2322 N92-23526

CARRIER DENSITY (SOLID STATE)
Defect behavior, carrier removal and predicted in-space injection annealing of InP solar cells [NASA-TM-105624] p 2370 N92-23562

CARTRIDGES
Chemical compatibility of cartridge materials [NASA-CR-190256] p 2356 N92-23555

CASE HISTORIES
Migration and generation of contaminants from launch through recovery: LDEF case history p 2335 N92-23287

CASSEGRAIN OPTICS
An instrument to search for small-scale anisotropy in the cosmic microwave background at 90 GHz p 2441 N92-23161

CAST ALLOYS
Effects of impurities on the solidification and mechanical behaviour of primary and secondary commercial purity aluminium and aluminium alloys [PB92-133511] p 2350 N92-23176

CASTING
Casting of simple-shaped single crystals of aluminum [PB92-136555] p 2350 N92-23179
An optical study of grain formation: Casting and solidification technology (2-IML-1) p 2361 N92-23631

CASTINGS
Effects of impurities on the solidification and mechanical behaviour of primary and secondary commercial purity aluminium and aluminium alloys [PB92-133511] p 2350 N92-23176
Investigation of plasma-sprayed laminates for high-temperature melting operations [DE92-008416] p 2353 N92-24006

CATACLYSMIC VARIABLES
Observations of accretion discs in interacting binaries p 2454 N92-23673

CATALYSIS
Survey on fixation and utilization of carbon dioxide by catalytic hydrogenation [DE92-769380] p 2347 N92-23456
Advanced Materials Center, Battelle p 2314 N92-23652

CATALYSTS
Advanced Materials Center, Battelle p 2314 N92-23652
Modeling of the catalytic oxidative coupling of methane [DE92-008554] p 2349 N92-24064

CATARACTS
Low dose neutron late effects: Cataractogenesis [DE92-005539] p 2414 N92-24033

CATHODES
New technology for linear colliders [DE92-007912] p 2440 N92-23334

CAVITATION FLOW
Liquid/supercritical fluid carbon dioxide cleaning of stainless steel components [DE92-006947] p 2348 N92-23572

CAVITIES
Strongly coupled cavity QED p 2442 N92-23999
CAVITY RESONATORS
Electro-optic resonant phase modulator
[NASA-CASE-NPO-18702-1-CU] p 2442 N92-23551
CELL ANODES
A dual anode nickel-hydrogen cell
[NASA-CASE-LEW-15212-1] p 2404 N92-24054
CELL DIVISION
Microgravitational effects on chromosome behavior (7-IML-1) p 2357 N92-23604
Effect of microgravity environment on cell wall regeneration, cell divisions, growth, and differentiation of plants from protoplasts (7-IML-1) p 2358 N92-23609
CELL MEMBRANES (BIOLOGY)
Effect of microgravity environment on cell wall regeneration, cell divisions, growth, and differentiation of plants from protoplasts (7-IML-1) p 2358 N92-23609
CELLS (BIOLOGY)
First International Microgravity Laboratory experiment descriptions
[NASA-TM-4353] p 2356 N92-23600
Chrondrogenesis in micromass cultures of embryonic mouse limb mesenchymal cells exposed to microgravity (7-IML-1) p 2357 N92-23605
Effect of microgravity environment on cell wall regeneration, cell divisions, growth, and differentiation of plants from protoplasts (7-IML-1) p 2358 N92-23609
Friend leukemia virus transformed cells exposed to microgravity in the presence of DMSO (7-IML-1) p 2358 N92-23613
Dynamic cell culture system (7-IML-1) p 2359 N92-23615
Studies on penetration of antibiotic in bacterial cells in space conditions (7-IML-1) p 2359 N92-23619
Phase partitioning experiment (8-IML-1) p 2360 N92-23621
Three-dimensional cultured glioma cell lines
[NASA-CASE-MSC-21843-1-NP] p 2413 N92-24052
CELLULOSE
Influence of maleic anhydride as a coupling agent on the performance of wood fiber: Polystyrene composites p 2343 N92-23945
CENTRAL PROCESSING UNITS
Real-time radar processor p 2394 N92-23396
Provisional cost evaluation p 2395 N92-23408
Functional design verification of ULSI components
[REPT-1.3.7] p 2422 N92-23873
CENTRIFUGAL FORCE
Experimental study of the mechanism of sound generation by rotating stall in centrifugal turbomachines p 2436 N92-23726
CENTRIFUGAL PUMPS
Experimental study of the mechanism of sound generation by rotating stall in centrifugal turbomachines p 2436 N92-23726
CERAMIC FIBERS
Tribological evaluation of an Al2O3-SiO2 ceramic fiber candidate for high temperature sliding seals
[NASA-TM-105611] p 2339 N92-23190
High temperature dynamic engine seal technology development
[NASA-TM-105641] p 2381 N92-23435
Multifracture of ceramic composites
[DE92-009630] p 2355 N92-23897
CERAMIC MATRIX COMPOSITES
Detecting Lamb waves with broad-band acousto-ultrasonic signals in composite structures
[NASA-TM-105557] p 2386 N92-23189
Materials for high liquid propulsion in 2010 p 2320 N92-23763
CNSR Rosetta: Earth return capsule p 2331 N92-23838
Multifracture of ceramic composites
[DE92-009630] p 2355 N92-23897
CERAMICS
Oil lubricated and water lubricated pin-on-disc wear tests with engineering ceramics
[PB92-136563] p 2380 N92-23152
Applications of multiple-ion irradiations to metals, ceramics, and polymers
[DE92-007686] p 2354 N92-23222
Evaluation of the elevated-temperature mechanical reliability of a HIPed silicon nitride
[DE92-007838] p 2354 N92-23223
Deposition of adherent Ag-Ti duplex films on ceramics in a multiple-cathode sputter deposition system
[NASA-TM-105586] p 2311 N92-23225
Characterizing and testing a thermally isolating superconducting link for SAFIRE-like missions
[NASA-CR-190196] p 2369 N92-23430
Guanidine based vehicle/binders for use with oxides, metals, and ceramics
[NASA-CASE-LEW-15314-1] p 2354 N92-23461
CEREBELLUM
Nuclear medicine program
[DE92-006979] p 2412 N92-23518
CERENKOV RADIATION
The isotopic composition of cosmic ray helium from 500 to 1100 MeV per nucleon p 2460 N92-23163
TeV gamma ray emission from accreting binary pulsars p 2460 N92-23736
CHANNEL FLOW
Turbulence modeling p 2301 N92-23338
An improved k-epsilon model for near wall turbulence p 2303 N92-23349
Advancements in engineering turbulence modeling
[PAPER-105] p 2303 N92-23350
CHANNELS (DATA TRANSMISSION)
Design of joint source/channel coders
[NASA-CR-189960] p 2417 N92-23416
Maximum aposteriori joint source/channel coding p 2417 N92-23417
A joint source/channel coder design p 2417 N92-23418
An edge preserving differential image coding scheme p 2417 N92-23419
A robust low-rate coding scheme for packet video p 2417 N92-23420
A hybrid LBG/lattice vector quantizer for high quality image coding p 2418 N92-23421
A robust coding scheme for packet video p 2418 N92-23422
A progressive data compression scheme based upon adaptive transform coding: Mixture block coding of natural images p 2418 N92-23423
CHARACTERIZATION
Characterization of organic coatings with impedance measurements: A study of coating structure, adhesion and underfilm corrosion
[PB92-133479] p 2339 N92-23174
CHARGE CARRIERS
Mutual scattering of carriers in two quantum wires
[DE92-616890] p 2366 N92-23580
CHARGE COUPLED DEVICES
Testing the solar paradigm for chromospheric activity in RS CVN binaries: Moderate resolution spectroscopy of solar active regions p 2459 N92-23171
CHARGE DISTRIBUTION
Cu charge fluctuations and anomalous behaviour in the phonon spectrum of La2CuO4
[DE92-617446] p 2446 N92-23270
Surface structure and analysis with scanning tunneling microscopy and electron tunneling spectroscopy
[DE92-007747] p 2448 N92-23721
CHARGE TRANSFER
Dynamic structural effects and ultrafast biomolecular kinetics in photoinduced charge transfer reactions
[DE92-007562] p 2346 N92-23203
Photochemistry and charge transfer chemistry of the platinum group elements
[DE92-007564] p 2347 N92-23332
Monte Carlo transport in semiconductor
[DE92-008404] p 2371 N92-23902
NQR investigation of pressure-induced charge transfer in oxygen-deficient YBa2Cu3O(7-delta) (delta = 0.38)
[DE92-008441] p 2450 N92-24036
CHARGED PARTICLES
Charged particle activation studies on the surface of LDEF spacecraft p 2439 N92-23296
Charged particle LET-spectra measurements aboard LDEF p 2440 N92-23303
Pulsed electron beam precharger
[DE92-008693] p 2439 N92-24031
CHARM (PARTICLE PHYSICS)
Particle physics and cosmology
[DE92-008301] p 2456 N92-23153
Research in high energy physics
[DE92-007966] p 2441 N92-23500
CHEMICAL ANALYSIS
SIMS chemical analysis of extended impact features from the trailing edge portion of experiment AO187-2 p 2349 N92-23316
Ion microprobe elemental analyses of impact features on interplanetary dust experiment sensor surfaces p 2458 N92-23318
Dynamic (computer) modelling of the particulate environment: Transformations from the LDEF reference frame to decode geocentric and interplanetary populations p 2458 N92-23320
CHEMICAL BONDS
Potential energy surfaces and reaction dynamics of polyatomic molecules
[DE92-008314] p 2437 N92-23450
Nuclear medicine program
[DE92-006979] p 2412 N92-23518
Molecular design of substrate binding sites
[DE92-008331] p 2438 N92-23894
CHEMICAL COMPOSITION
The isotopic composition of cosmic ray helium from 500 to 1100 MeV per nucleon p 2460 N92-23163
SIMS chemical analysis of extended impact features from the trailing edge portion of experiment AO187-2 p 2349 N92-23316
Characterization of rocket propellant combustion products
[DE92-007799] p 2337 N92-23722
Acid rain monitoring in East-Central Florida from 1977 to present
[NASA-CR-190152] p 2406 N92-23898
CHEMICAL EFFECTS
Radiation effects on polyethylene foam
[DE92-751046] p 2353 N92-23134
Oxidative degradation of polymers induced by ionizing radiation
[DE92-007657] p 2354 N92-23442
CHEMICAL EQUILIBRIUM
Effects of chemical equilibrium on turbine engine performance for various fuels and combustor temperatures
[NASA-TM-105399] p 2311 N92-23254
CHEMICAL EVOLUTION
Publications of the exobiology program for 1990: A special bibliography
[NASA-TM-4364] p 2416 N92-23429
CHEMICAL PROPERTIES
Production of metal powders by hydrogen stripping from loaded organic extractants
[PB92-136464] p 2350 N92-23178
Profiling and mapping of advanced materials using spatially resolved Raman spectroscopy
[DE92-008304] p 2347 N92-23449
CHEMICAL REACTIONS
Dynamic structural effects and ultrafast biomolecular kinetics in photoinduced charge transfer reactions
[DE92-007562] p 2346 N92-23203
Hydrogen absorption by zirconium alloy cladding tube with surface oxide film
[DE92-750962] p 2351 N92-23265
The study of PDF turbulence models in combustion p 2301 N92-23337
Progress of simulations for reacting shear layers p 2302 N92-23344
The study of PDF turbulence models in combustion
[PAPER-107] p 2302 N92-23345
Progress in the development of PDF turbulence models for combustion
[PAPER-213] p 2303 N92-23347
Center for Macromolecular Crystallography, University of Alabama in Birmingham p 2313 N92-23650
The oxidation behavior of Co-15wt percent Cr alloy containing dispersed oxides formed by internal oxidation
[DE92-008283] p 2352 N92-23893
VITRIMAT2: A modified model of vitrinite maturation and reflectance
[DE92-008987] p 2348 N92-23904
Kinetics of combustion-related processes at high temperatures
[DE92-008790] p 2348 N92-24038
Modeling of the catalytic oxidative coupling of methane
[DE92-008554] p 2349 N92-24064
CHEMISORPTION
Hydrogen absorption by zirconium alloy cladding tube with surface oxide film
[DE92-750962] p 2351 N92-23265
Temperature-dependent evolution of chemisorbed digermane in Ge thin film growth
[DE92-008098] p 2447 N92-23447
CHIPS (ELECTRONICS)
Test preparation for MOS digital circuits using heuristics for reliable fault simulation
[REPT-1.2.6] p 2421 N92-23865
CHIRAL DYNAMICS
Closed parallel-plate chiral waveguides with boundary impedance conditions
[PB92-142397] p 2366 N92-23591
CHLOROFLUOROCARBONS
On the global warming potentials of candidate gaseous diffusion plant coolants
[DE92-006640] p 2406 N92-23740
CHONDRITES
LDEF impact craters formed by carbon-rich impactors: A preliminary report p 2336 N92-23319
CHROMIUM
The influence of chromium on structure and mechanical properties of B2 nickel aluminide alloys
[NASA-CR-189124] p 2351 N92-23566
CHROMIUM ALLOYS
In situ XANES study of the valence state of chromium during electrochemical polarization of AlCr alloys
[DE92-007452] p 2350 N92-23197

Effect of minor elements on hot workability of Ni-Cr-W superalloys
[DE92-750951] p 2351 N92-23263
Reaction layer formation at the graphite/copper-chromium alloy interface
[NASA-CR-189147] p 2351 N92-23436
Effect of minor elements on corrosion behavior of Ni-Cr-W superalloys in HTGR helium
[DE92-751006] p 2352 N92-23712

CHROMIUM OXIDES
The oxidation behavior of Co-15wt percent Cr alloy containing dispersed oxides formed by internal oxidation
[DE92-008283] p 2352 N92-23893

CHROMOSOMES
Microgravitational effects on chromosome behavior (7-IML-1) p 2357 N92-23604

CHROMOSPHERE
Testing the solar paradigm for chromospheric activity in RS CVN binaries: Moderate resolution spectroscopy of solar active regions p 2459 N92-23171
Line profile asymmetries in chromospherically active stars p 2458 N92-24015

CIRCUIT BOARDS
An integrated test solution to address scan techniques
[REPT-1.2.3] p 2420 N92-23862
Breathing maze router for analog VLSI cell generation
[REPT-1.3.3] p 2422 N92-23870
Deleting pads in multi-layered printed circuits
[REPT-4.2.3] p 2425 N92-23889

CIRCUIT DIAGRAMS
MBT-WIRE: Intelligent CAD in wiring design
[REPT-1.1.4] p 2419 N92-23856
The use of EDIF at Daisy/Cadnetix
[REPT-4.2.1] p 2424 N92-23887

CIRCUIT RELIABILITY
Test preparation for MOS digital circuits using heuristics for reliable fault simulation
[REPT-1.2.6] p 2421 N92-23865

CIRCUITS
A verified design of a fault-tolerant clock synchronization circuit: Preliminary investigations
[NASA-TM-107568] p 2416 N92-23559
Vector circuit method applied for chiral dielectric slab waveguides
[PB92-142355] p 2367 N92-23679

CIRCULAR TUBES
Tubular copper thrust chamber design study
[NASA-CR-187206] p 2337 N92-23982

CITIES
National air quality and emissions trends report, 1990
[PB92-141555] p 2406 N92-23517
Urban temperature bias as determined by polar orbiting satellite data p 2402 N92-23724

CIVIL AVIATION
Symposium on Marketing for Technological Products
[MBB-UE-0014-90-PUB] p 2452 N92-23928

CLADDING
Hydrogen absorption by zirconium alloy cladding tube with surface oxide film
[DE92-750962] p 2351 N92-23265

CLASSICAL MECHANICS
Inequivalence of interior and exterior dynamical problems
[DE92-615214] p 2451 N92-23743
Lie-admissible structure of Hamilton's original equations with external terms
[DE92-615216] p 2433 N92-23745

CLASSIFICATIONS
Improved image classification with neural networks by fusing multispectral signatures with topological data p 2402 N92-23368
Combining factual and heuristic knowledge in knowledge acquisition p 2429 N92-23372

CLASSIFIERS
Feature detection in satellite images using neural network technology p 2427 N92-23366

CLEAN ENERGY
Investigation on effective promotion of geothermal energy development
[DE92-783370] p 2403 N92-23684

CLEANING
Liquid/supercritical fluid carbon dioxide cleaning of stainless steel components
[DE92-006947] p 2348 N92-23572
Replacement of hydrogen peroxide cleaning with oxygen plasma
[DE92-009020] p 2445 N92-23905

CLEANLINESS
Measurement of surface cleanliness by area-of-spread
[DE92-007265] p 2348 N92-23586

CLIMATE
Clouds, surface temperature, and the tropical and subtropical radiation budget p 2410 N92-23431
Climate
[PB92-150457] p 2410 N92-23520
Evaluation of terrestrial climate variability using a moisture index p 2411 N92-23771
A new approach to estimate Angstrom coefficients
[DE92-619048] p 2460 N92-23909

CLIMATE CHANGE
National acid precipitation assessment program: 1990 integrated assessment report
[PB92-100346] p 2406 N92-23593
Climate System Monitoring (CSM). El Nino/Southern Oscillation (ENSO) diagnostic advisory, special issue p 2411 N92-23677
Evaluation of terrestrial climate variability using a moisture index p 2411 N92-23771

CLIMATOLOGY
Scientific development of the Advanced Parallel Chemistry (APACHE) climate model
[DE92-006657] p 2404 N92-23123
Climate
[PB92-150457] p 2410 N92-23520
National acid precipitation assessment program: 1990 integrated assessment report
[PB92-100346] p 2406 N92-23593
Investigation of the Archean climate using the NCAR CCM
[NASA-CR-189878] p 2410 N92-23656
Evaluation of terrestrial climate variability using a moisture index p 2411 N92-23771

CLOCKS
A verified design of a fault-tolerant clock synchronization circuit: Preliminary investigations
[NASA-TM-107568] p 2416 N92-23559

CLOUDS
Clouds and radiation testbed data environment: Site data system and experiment center
[DE92-006732] p 2408 N92-23741

CLOUDS (METEOROLOGY)
Clouds, surface temperature, and the tropical and subtropical radiation budget p 2410 N92-23431
Observation of lined-up cumulus rows under the winter monsoon situation using MOS-1 and radar data p 2399 N92-23483

CLUSTER ANALYSIS
Comparative study of digital MOS-1 MESSR, LANDSAT MSS, and IRS LISS-1 data for land cover classification in Sambalpur district, India p 2400 N92-23490
Group scheduling using group technology concepts
[REPT-3.3.2] p 2424 N92-23886

CLUSTERS
Melting of nickel clusters
[DE92-006986] p 2351 N92-23573

CMOS
Higher order temperature compensation of bandgap voltage references (I)
[PB92-142306] p 2370 N92-23497
On generating two dimensional CMOS cells
[REPT-1.3.2] p 2421 N92-23869
Breathing maze router for analog VLSI cell generation
[REPT-1.3.3] p 2422 N92-23870

COASTAL WATER
Introduction: Ocean air observation p 2392 N92-23381
Geophysical, chemical and biological measuring parameters p 2393 N92-23385
The laser bathymeter p 2393 N92-23388
CODAR in the Straits of Florida
[PB92-129964] p 2412 N92-23732

COASTAL ZONE COLOR SCANNER
Atmospheric correction of the second generation ocean color sensors p 2392 N92-23145

COATINGS
High-performance multilayer mirrors for soft x ray projection lithography
[DE92-008615] p 2443 N92-24049

COAXIAL CABLES
Coaxial turnstile junction
[NASA-CASE-GSC-13422-1] p 2369 N92-23462

COBALT ALLOYS
The oxidation behavior of Co-15wt percent Cr alloy containing dispersed oxides formed by internal oxidation
[DE92-008283] p 2352 N92-23893

CODERS
Design of joint source/channel coders
[NASA-CR-189960] p 2417 N92-23416
Maximum aposteriori joint source/channel coding p 2417 N92-23417
A joint source/channel coder design p 2417 N92-23418
An edge preserving differential image coding scheme p 2417 N92-23419

CODING
Maximum aposteriori joint source/channel coding p 2417 N92-23417
A robust low-rate coding scheme for packet video p 2417 N92-23420
A hybrid LBG/lattice vector quantizer for high quality image coding p 2418 N92-23421
A robust coding scheme for packet video p 2418 N92-23422
A progressive data compression scheme based upon adaptive transform coding: Mixture block coding of natural images p 2418 N92-23423
Variable bit rate video coding
[PB92-134279] p 2367 N92-23676

COEFFICIENTS
A new test facility for measuring the coefficient of moisture expansion of advanced composite materials p 2326 N92-23807
Modeling of honeycomb core for sandwich CTE prediction p 2332 N92-23841
A new approach to estimate Angstrom coefficients
[DE92-619048] p 2460 N92-23909

COHERENT RADIATION
X ray Fourier transform holography: Beyond the optical diffraction limit p 2377 N92-23144
The principle and design of a high-efficiency free-electron laser p 2380 N92-23687

COLLAPSE
Collapse of composite tubes under end moments
[NASA-TM-107605] p 2390 N92-23992

COLLECTION
The interstellar gas experiment p 2459 N92-23325

COLLISION AVOIDANCE
Automated synthesis of robot arm motion for robot arm collision avoidance p 2381 N92-23158
On motion planning amidst transient obstacles
[DE91-018939] p 2429 N92-23457
Interception of comets and asteroids on collision course with Earth
[DE92-007431] p 2458 N92-24028

COLLISIONS
Aircraft accident report: Runway collision of USAir Flight 1493, Boeing 737 and Skywest Flight 5569 Fairchild Metroliner, Los Angeles International Airport, Los Angeles, CA, February 1, 1991
[PB91-910409] p 2305 N92-23596

COLUMBIA (ORBITER)
Mission safety evaluation report for STS-32, postflight edition
[NASA-TM-107775] p 2312 N92-23243

COLUMBUS SPACE STATION
The Columbus Free Flying Laboratory: Mechanical design aspects p 2323 N92-23782
Structural assessment of the Space Station Freedom's pressurized elements p 2323 N92-23783

COMBINATORIAL ANALYSIS
Optimal exciter placement and force vector tuning required for experimental modal analysis p 2333 N92-23847

COMBUSTIBLE FLOW
Turbulence modeling in supersonic combusting flows p 2302 N92-23342
Progress in the development of PDF turbulence models for combustion
[PAPER-213] p 2303 N92-23347
A study of hydrogen diffusion flames using PDF turbulence model p 2303 N92-23348

COMBUSTION
Probing picosecond flame dynamics with transient grating experiments
[DE92-003163] p 2346 N92-23181
Kinetic measurements on elementary fossil fuel combustion reactions over wide temperatures ranges
[DE92-007535] p 2347 N92-23221
The study of PDF turbulence models in combustion p 2301 N92-23337
The study of PDF turbulence models in combustion
[PAPER-107] p 2302 N92-23345
Kinetics of combustion-related processes at high temperatures
[DE92-008790] p 2348 N92-24038

COMBUSTION CHAMBERS
Effects of chemical equilibrium on turbine engine performance for various fuels and combustor temperatures
[NASA-TM-105399] p 2311 N92-23254
Three-dimensional calculations of supersonic reacting flows using an LU scheme p 2304 N92-23354
Aerodynamic rectifier for pulsed combustors
[PB92-142587] p 2348 N92-23657
Materials for high liquid propulsion in 2010 p 2320 N92-23763
Materials for liquid propellant engines p 2320 N92-23764
Tubular copper thrust chamber design study
[NASA-CR-187206] p 2337 N92-23982

COMBUSTION PHYSICS
Basic research on natural gas combustion phenomena
[PB92-149681] p 2348 N92-23685
Kinetics of combustion-related processes at high temperatures
[DE92-008790] p 2348 N92-24038

COMBUSTION PRODUCTS
Characterization of rocket propellant combustion products
[DE92-007799] p 2337 N92-23722
COMBUSTION STABILITY
A study of hydrogen diffusion flames using PDF turbulence model p 2303 N92-23348
COMBUSTION TEMPERATURE
Kinetic measurements on elementary fossil fuel combustion reactions over wide temperatures ranges
[DE92-007535] p 2347 N92-23221
COMETS
Interception of comets and asteroids on collision course with Earth
[DE92-007431] p 2458 N92-24028
COMFORT
Infrastructure and training of manpower for CAD/CAM systems
[REPT-4.2.2] p 2425 N92-23888
COMMAND LANGUAGES
Distributed expert systems for ground and space applications p 2427 N92-23361
COMMERCE
Launch vehicle for orbital missions: COMET
p 2313 N92-23645
Marketing as a necessary condition for the successful development and commercialization of technological products p 2452 N92-23931
COMMERCIAL AIRCRAFT
Effects of turbine cooling assumptions on performance and sizing of high-speed civil transport
[NASA-TM-105610] p 2311 N92-23537
COMMUNICATION CABLES
CIM implementation at CVALIM, D.T.C. Division, Bet-Shean, Israel
[REPT-3.2.4] p 2424 N92-23884
COMMUNICATION EQUIPMENT
Modifications for a communication interface board
p 2368 N92-23963
COMMUNICATION NETWORKS
Achieving spectrum conservation for the minimum-span and minimum-order frequency assignment problems
[NASA-TM-105649] p 2322 N92-23187
Design of neural networks for classification of remotely sensed imagery p 2402 N92-23367
Variable bit rate video coding
[PB92-134279] p 2367 N92-23676
Writing a simulation of a communications network using SIMSCRIPT/DISS
[REPT-2.3.6] p 2423 N92-23879
COMMUNICATION SATELLITES
Interim Service ISDN Satellite (ISIS) hardware experiment development for advanced ISDN satellite designs and experiments
[NASA-CR-190257] p 2335 N92-24046
COMPARISON
Comparison of multi-point modal test methods
p 2333 N92-23849
COMPLEX COMPOUNDS
Organic crystal growth experiment facility (13-IML-1)
p 2362 N92-23635
COMPONENT RELIABILITY
Probabilistic Structural Analysis Methods (PSAM) for select space propulsion system components, part 2
[NASA-CR-187200] p 2388 N92-23426
Statistical optimization of integrated circuits in order to reduce the sensitivity to variations in process parameters and environmental conditions
[REPT-1.3.6] p 2422 N92-23872
COMPONENTS
Group scheduling using group technology concepts
[REPT-3.3.2] p 2424 N92-23886
COMPOSITE MATERIALS
The effect of processing on strength of Nicalon fibers in Nicalon fiber-SiC matrix composites
[DE92-006978] p 2340 N92-23256
Analysis of delamination related fracture processes in composites
[NASA-CR-190226] p 2340 N92-23532
Biisotropic polarizer shield
[PB92-141878] p 2366 N92-23590
JPRS report: Science and technology. Central Eurasia: Materials science
[JPRS-UMS-92-005] p 2363 N92-23708
Influence of the substrate on the solar cells interconnector: Stress distribution and fatigue life prediction p 2326 N92-23803
Damping behaviour of unidirectional fibre reinforced polymers p 2326 N92-23805
The torsional fatigue behaviour of the in-plane and out-of-plane shear moduli of composite materials
p 2328 N92-23818
The challenge of the Hermes TPS shingles
p 2322 N92-23823
Buckling and failure of thin elliptical delaminations in composites p 2331 N92-23835
Notched strength of composite materials
p 2331 N92-23839
Strength and deformation behaviour of Keviar and carbon composite sandwich structures for space applications p 2332 N92-23840
Phase transformations in SrAl2Si2O8 glass
[NASA-TM-105657] p 2449 N92-23890
Metal-semiconductor, composite radiation detectors
[DE92-008980] p 2344 N92-23988
Fiber-optic Raman spectroscopy for cure monitoring of advanced polymer composites
[DE92-008619] p 2355 N92-24068
COMPOSITE STRUCTURES
Experimental verification of a theory for the impact response of composite plates
[FFA-TN-1991-17] p 2339 N92-23167
Detecting Lamb waves with broad-band acousto-ultrasonic signals in composite structures
[NASA-TM-105557] p 2386 N92-23189
Progressive fracture of polymer matrix composite structures: A new approach
[NASA-TM-105574] p 2339 N92-23194
Coupled multi-disciplinary simulation of composite engine structures in propulsion environment
[NASA-TM-105575] p 2388 N92-23267
Method of fabricating superconducting device
[NASA-CASE-NPO-18394-1-CU] p 2370 N92-23552
Non linear structural analysis of a thin skin carbon-carbon rigid decelerator p 2330 N92-23831
Mechanical testing on a composite flexible structure
p 2331 N92-23834
Collapse of composite tubes under end moments
[NASA-TM-107605] p 2390 N92-23992
COMPOSITION (PROPERTY)
Filling high density polyethylene with cellulosic fibers. 1: The effect of additives on fiber dispersion
p 2344 N92-23948
COMPRESSIBILITY EFFECTS
Modeling of compressible turbulent shear flows
p 2301 N92-23340
Progress of simulations for reacting shear layers
p 2302 N92-23344
On the basic equations for the second-order modeling of compressible turbulence p 2303 N92-23351
COMPRESSIBLE FLOW
Center for Modeling of Turbulence and Transition (CMOTT). Research briefs: 1990
[NASA-TM-105243] p 2301 N92-23336
On the basic equations for the second-order modeling of compressible turbulence p 2303 N92-23351
Simulations of free shear layers using a compressible kappa-epsilon model p 2304 N92-23355
Long time behavior of unsteady flow computations
[NASA-TM-105584] p 2374 N92-23565
Topics in numerical computation of compressible flow
p 2375 N92-23692
COMPRESSIBLE FLUIDS
Critical fluid thermal equilibration experiment (19-IML-1) p 2363 N92-23640
COMPRESSION TESTS
High-temperature deformation behavior of single crystalline A15-type intermetallic compounds
p 2352 N92-23718
Buckling of simply supported and clamped anisotropic plates under combined loads p 2326 N92-23804
COMPRESSIVE STRENGTH
Impact and compression response of composite materials containing fortifiers p 2341 N92-23937
COMPUTATION
The 7th INS Scientific Computational Programs
[DE92-750967] p 2417 N92-23266
The study of PDF turbulence models in combustion
p 2301 N92-23337
Theory for iterative solution of large dynamical systems using parallel computation
[PB92-143304] p 2433 N92-23589
Special Course on Engineering Methods in Aerodynamic Analysis and Design of Aircraft
[AGARD-R-783] p 2308 N92-23950
Computational procedures for preliminary design
p 2309 N92-23952
COMPUTATIONAL FLUID DYNAMICS
Center for Modeling of Turbulence and Transition (CMOTT). Research briefs: 1990
[NASA-TM-105243] p 2301 N92-23336
Turbulence modeling p 2301 N92-23338
Modeling of compressible turbulent shear flows
p 2301 N92-23340
Advancements in engineering turbulence modeling
[PAPER-105] p 2303 N92-23350
A two-dimensional Euler solution for an unbladed jet engine configuration
[NASA-TM-105329] p 2374 N92-23560
Interactive solution-adaptive grid generation procedure
[NASA-TM-105432] p 2305 N92-23563
Computational fluid dynamics for propulsion technology: Geometric grid visualization in CFD-based propulsion technology research
[NASA-CR-190291] p 2375 N92-23568
COMPUTATIONAL GRIDS
Problem of membrane locking in finite element analysis of cylindrical shells
[PB92-133941] p 2387 N92-23137
An adaptive-grid technique for simulation of complex unsteady flows p 2372 N92-23148
A multilevel preconditioner for domain decomposition boundary systems
[DE92-008055] p 2432 N92-23329
On recontamination and directional-bias problems in Monte Carlo simulation of PDF turbulence models
p 2302 N92-23346
Artificial intelligence approach to planning the robotic assembly of large tetrahedral truss structures
p 2426 N92-23357
Grid generation and flow solution method for Euler equations on unstructured grids
[NASA-TM-4295] p 2305 N92-23533
Interactive solution-adaptive grid generation procedure
[NASA-TM-105432] p 2305 N92-23563
User interface user's guide for HYPGEN
[NASA-CR-190304] p 2425 N92-23991
COMPUTER AIDED DESIGN
Multidisciplinary optimization studies using ASTROS
p 2307 N92-23234
First approach to an integrated fin design
p 2308 N92-23236
Simultaneous stress and flutter optimization for the wing of a transport aircraft equipped with four engines
p 2308 N92-23238
Structural optimization of aircraft practice and trends
p 2308 N92-23239
Framework Programmable Platform for the advanced software development workstation: Framework processor design document
[NASA-CR-190173] p 2418 N92-23554
The challenge of the Hermes TPS shingles
p 2322 N92-23823
Proceedings of the International Conference on CAD/CAM and AMT. Volume 1: General sessions
[ITN-92-85127] p 2418 N92-23851
Formal methods for the evaluation of corporate CAD/CAM utilization
[REPT-1.1.1] p 2419 N92-23853
FAPES: An expert system for designing and optimising fault-tolerant arithmetic array processors
[REPT-1.1.2] p 2419 N92-23854
Voxel-based solid modeling
[REPT-1.1.3] p 2419 N92-23855
MBT-WIRE: Intelligent CAD in wiring design
[REPT-1.1.4] p 2419 N92-23856
Group technology, RCO: Rough-Cut Optimizer. The key to integration of plant operations
[REPT-1.1.6] p 2420 N92-23857
Creative search systems as specific expert systems
[REPT-1.1.8] p 2420 N92-23859
Design for testability: Where are the goalposts?
[REPT-1.2.2] p 2420 N92-23861
An integrated test solution to address scan techniques
[REPT-1.2.3] p 2420 N92-23862
An exhaustive self-test design methodology for synchronous state machines
[REPT-1.2.4] p 2421 N92-23863
Using range analysis to support hierarchical test pattern generation
[REPT-1.2.5] p 2421 N92-23864
A framework for the support of VLSI (very large scale integration) design for manufacture
[REPT-1.3.1] p 2421 N92-23868
On generating two dimensional CMOS cells
[REPT-1.3.2] p 2421 N92-23869
Breathing maze router for analog VLSI cell generation
[REPT-1.3.3] p 2422 N92-23870
Statistical optimization of integrated circuits in order to reduce the sensitivity to variations in process parameters and environmental conditions
[REPT-1.3.6] p 2422 N92-23872
Flexible Design Environment (FDE) for operation systems design
[REPT-2.3.5] p 2423 N92-23878
Writing a simulation of a communications network using SIMSCRIPT/DISS
[REPT-2.3.6] p 2423 N92-23879
Combining a CAD/CAM system with an advanced database architecture
[REPT-3.1.5] p 2423 N92-23880
From IGES to STEP
[REPT-3.1.6] p 2423 N92-23881
IGES: Application generator in disguise
[REPT-3.1.7] p 2424 N92-23882

Computer integrated enterprise: The next step in CIM evolution
[REPT-3.2.2] p 2424 N92-23883
CIM: The future technology
[REPT-3.3.1] p 2424 N92-23885
The use of EDIF at Daisy/Cadnetix
[REPT-4.2.1] p 2424 N92-23887
Infrastructure and training of manpower for CAD/CAM systems
[REPT-4.2.2] p 2425 N92-23888
Deleting pads in multi-layered printed circuits
[REPT-4.2.3] p 2425 N92-23889
Molecular design of substrate binding sites
[DE92-008331] p 2438 N92-23894

COMPUTER AIDED MANUFACTURING
The challenge of the Hermes TPS shingles
p 2322 N92-23823
Proceedings of the International Conference on CAD/CAM and AMT. Volume 1: General sessions
[ITN-92-85127] p 2418 N92-23851
The need for standards in design automation
[P-1-1] p 2419 N92-23852
Formal methods for the evaluation of corporate CAD/CAM utilization
[REPT-1.1.1] p 2419 N92-23853
Group technology, RCO: Rough-Cut Optimizer. The key to integration of plant operations
[REPT-1.1.6] p 2420 N92-23857
Statistical process control system for VLSI fabrication
[REPT-1.3.4] p 2422 N92-23871
Optimum cutting conditions determination for the NC-milling
[REPT-2.1.2] p 2422 N92-23874
Controlling operations through procedures: APE (automated procedure editor)
[REPT-2.2.1] p 2422 N92-23875
Shop floor scheduling through a simulation based scheduler
[REPT-2.3.3] p 2423 N92-23876
Advances in processing rates optimization for flexible manufacturing systems
[REPT-2.3.4] p 2423 N92-23877
Flexible Design Environment (FDE) for operation systems design
[REPT-2.3.5] p 2423 N92-23878
Writing a simulation of a communications network using SIMSCRIPT/DISS
[REPT-2.3.6] p 2423 N92-23879
Combining a CAD/CAM system with an advanced database architecture
[REPT-3.1.5] p 2423 N92-23880
From IGES to STEP
[REPT-3.1.6] p 2423 N92-23881
IGES: Application generator in disguise
[REPT-3.1.7] p 2424 N92-23882
Computer integrated enterprise: The next step in CIM evolution
[REPT-3.2.2] p 2424 N92-23883
CIM implementation at CVALIM, D.T.C. Division, Bet-Shean, Israel
[REPT-3.2.4] p 2424 N92-23884
CIM: The future technology
[REPT-3.3.1] p 2424 N92-23885
Group scheduling using group technology concepts
[REPT-3.3.2] p 2424 N92-23886
The use of EDIF at Daisy/Cadnetix
[REPT-4.2.1] p 2424 N92-23887
Infrastructure and training of manpower for CAD/CAM systems
[REPT-4.2.2] p 2425 N92-23888
Deleting pads in multi-layered printed circuits
[REPT-4.2.3] p 2425 N92-23889
The use of STEP in an integrated manufacturing environment
[DE92-008417] p 2425 N92-24035

COMPUTER AIDED MAPPING
Center for Mapping, Ohio State University
p 2314 N92-23655

COMPUTER AIDED TOMOGRAPHY
Ion Microtomography (IMT) and Particle-Induced X ray Emission (PIXE) analysis direct drive of Inertial Confinement Fusion (ICF) targets
[DE92-008614] p 2446 N92-24067

COMPUTER ANIMATION
Computer tutorial and animation of the normal ice cycle of the Laurentian Great Lakes of North America for 1960 - 1979
[PB92-129949] p 2401 N92-23659

COMPUTER GRAPHICS
Voxel-based solid modeling
[REPT-1.1.3] p 2419 N92-23855
From IGES to STEP
[REPT-3.1.6] p 2423 N92-23881
IGES: Application generator in disguise
[REPT-3.1.7] p 2424 N92-23882

COMPUTER NETWORKS
Feature detection in satellite images using neural network technology p 2427 N92-23366
Multisensor data fusion p 2394 N92-23398
Architectural impact of FDDI network on scheduling hard real-time traffic
[NASA-CR-190272] p 2425 N92-23583
Interim Service ISDN Satellite (ISIS) hardware experiment development for advanced ISDN satellite designs and experiments
[NASA-CR-190257] p 2335 N92-24046

COMPUTER PROGRAMMING
Knowledge-based approach for generating target system specifications from a domain model
p 2428 N92-23371
Framework Programmable Platform for the advanced software development workstation: Framework processor design document
[NASA-CR-190173] p 2418 N92-23554

COMPUTER PROGRAMS
Automated synthesis of robot arm motion for robot arm collision avoidance p 2381 N92-23158
Evaluation of MHOST analysis capabilities for a plate element --- finite element modeling
[NASA-TM-105387] p 2387 N92-23196
Effects of chemical equilibrium on turbine engine performance for various fuels and combustor temperatures
[NASA-TM-105399] p 2311 N92-23254
Detecting opportunities for parallel observations on the Hubble Space Telescope p 2426 N92-23359
Coordinating complex problem-solving among distributed intelligent agents p 2427 N92-23360
Distributed expert systems for ground and space applications p 2427 N92-23361
Multisensor data fusion p 2394 N92-23398
Hardware and software modularity
p 2394 N92-23399
Current definition of some development programs
p 2395 N92-23405
Probabilistic Structural Analysis Methods (PSAM) for select space propulsion system components, part 2
[NASA-CR-187200] p 2388 N92-23426
GENLN2: A general line-by-line atmospheric transmittance and radiance model. Version 3.0: Description and users guide
[PB92-148543] p 2408 N92-23522
Computational fluid dynamics for propulsion technology: Geometric grid visualization in CFD-based propulsion technology research
[NASA-CR-190291] p 2375 N92-23568
PSD computations using Welch's method
[DE92-007419] p 2370 N92-23584
PHOTO: A computer simulation program for photovoltaic and hybrid energy systems. Document and user's guide
[PB92-141928] p 2403 N92-23683
Clouds and radiation testbed data environment: Site data system and experiment center
[DE92-006732] p 2408 N92-23741
The use of modal synthesis in conjunction with nonlinear transient dynamic analysis p 2324 N92-23788
Multi parameter optimization on Ariane 5
p 2321 N92-23798
Computer simulation of moisture penetration in structures p 2326 N92-23806
Type Ib supernovae and a new radiation hydrodynamics code p 2458 N92-24017
Mutual interference in multichannel fibre communication systems p 2367 N92-24019
The ALEXIS data processing package: An IDL-based system
[DE92-007429] p 2455 N92-24027

COMPUTER SYSTEMS DESIGN
An advanced system for environmental sine testing: Basic principles revisited p 2325 N92-23799
Distributed computer system in the large scale low speed wind tunnel
[NAL-TM-629] p 2312 N92-23979

COMPUTER SYSTEMS PERFORMANCE
Ground station p 2394 N92-23397
Hardware and software modularity
p 2394 N92-23399
Types of operation and system control
p 2395 N92-23401

COMPUTER TECHNIQUES
Technique to eliminate computational instability in multibody simulations employing the Lagrange multiplier
[NASA-TP-3220] p 2418 N92-23432
Aircraft drag analysis methods p 2309 N92-23957

COMPUTERIZED SIMULATION
Numerical experiments with flows of elongated granules
[NASA-TM-105567] p 2381 N92-23226
Application of analytical and design tools for fighter wing aeroelastic tailoring p 2307 N92-23231
Quasi-three-dimensional simulations of deep convection
[DE92-007204] p 2409 N92-23257
The 7th INS Scientific Computational Programs
[DE92-750967] p 2417 N92-23266
Coupled multi-disciplinary simulation of composite engine structures in propulsion environment
[NASA-TM-105575] p 2388 N92-23267
Dynamic (computer) modelling of the particulate environment: Transformations from the LDEF reference frame to decode geocentric and interplanetary populations p 2458 N92-23320
Technique to eliminate computational instability in multibody simulations employing the Lagrange multiplier
[NASA-TP-3220] p 2418 N92-23432
Proceedings: Nozzle Initiative Industry Advisory Committee on Standardization of Carbon-Phenolic Test Methods and Specifications
[NASA-CR-190203] p 2337 N92-23539
Comparison of analytical and numerical modelling approaches for sizing of seasonal storage solar heating systems
[PB92-141829] p 2403 N92-23592
PHOTO: A computer simulation program for photovoltaic and hybrid energy systems. Document and user's guide
[PB92-141928] p 2403 N92-23683
Fast simulation of MOS digital networks using a physical macromodelling approach
[REPT-1.2.1] p 2420 N92-23860
VITRIMAT2: A modified model of vitrinite maturation and reflectance
[DE92-008987] p 2348 N92-23904
Introduction to Special Course on Engineering Methods in Aerodynamic Analysis and Design of Aircraft
p 2308 N92-23951
Metal-semiconductor, composite radiation detectors
[DE92-008980] p 2344 N92-23988

COMPUTERS
The 7th INS Scientific Computational Programs
[DE92-750967] p 2417 N92-23266
Battery test facility hardware, software, and system operation
[DE92-008455] p 2372 N92-24063

CONCORDE AIRCRAFT
Surface activation of Concorde by Be-7
p 2439 N92-23295

CONDENSERS (LIQUEFIERS)
White paper: Preliminary assessment of LNG vehicle technology, economics, and safety issues
[PB92-137603] p 2383 N92-23680

CONDENSING
Modelling and experimental verification of a water alleviation system for the NASP --- National Aerospace Plane
[NASA-TM-105661] p 2373 N92-23224

CONES
Fast aurora zone analysis p 2409 N92-23960

CONFERENCES
Integrated Design Analysis and Optimisation of Aircraft Structures
[AGARD-R-784] p 2306 N92-23227
LDEF: 69 Months in Space. First Post-Retrieval Symposium, part 1
[NASA-CP-3134-PT-1] p 2461 N92-23280
Launcher Propulsion Towards the Year 2010
[ESA-SP-327] p 2318 N92-23750
Proceedings of the International Conference on CAD/CAM and AMT. Volume 1: General sessions
[ITN-92-85127] p 2418 N92-23851
Composites, 1990
[NRC-32603] p 2341 N92-23933
Acid rain and air pollution in desert park areas. Proceedings of a workshop: Management recommendations
[PB92-140532] p 2407 N92-24003

CONFIDENCE LIMITS
A study of underground muons in the Soudan 2 detector p 2437 N92-23674

CONFORMAL MAPPING
Semigid construction of topological supergravities
[DE92-008772] p 2451 N92-24040

CONICAL FLOW
High-Order Polynomial Expansions (HOPE) for flux-vector splitting p 2304 N92-23353

CONNECTORS
Robot-friendly connector --- space truss structures
[NASA-CASE-MSC-21864-1] p 2382 N92-23544
Advanced numerical analyses for the optimisation of the structural behaviour of the intersegment connection for the Ariane 5 booster case p 2327 N92-23809

CONSERVATION
Achieving spectrum conservation for the minimum-span and minimum-order frequency assignment problems
[NASA-TM-105649] p 2322 N92-23187

CONSERVATION LAWS
Improved shock-capturing of Jameson's scheme for the Euler equations
[PB92-148758] p 2373 N92-23251
Mathematical modelling and numerical approximations for two-phase flow problems p 2375 N92-23672
The discontinuous finite element method with the Taylor-Galerkin approach for nonlinear hyperbolic conservation laws p 2433 N92-23738
Closed systems with nonHamiltonian internal forces
[DE92-619234] p 2434 N92-24039

CONSTRAINTS
Application of an automated multidisciplinary analysis and optimisation system to the design of aircraft structures p 2307 N92-23233
A fin optimisation study p 2308 N92-23237

CONSTRUCTION
The use of high temperature superconductors to levitate lunar telescope p 2456 N92-23962

CONSUMERS
Marketing qualification as a requirement for operating success p 2452 N92-23930

CONTACT LOADS
Contact stresses in meshing spur gear teeth: Use of an incremental finite element procedure
[NASA-TM-105388] p 2382 N92-23536

CONTAMINANTS
Particle types and sources associated with LDEF p 2349 N92-23286
Migration and generation of contaminants from launch through recovery: LDEF case history p 2335 N92-23287
Quantification of contaminants associated with LDEF p 2349 N92-23288
Molecular films associated with LDEF p 2439 N92-23289
Radioactivities of Long Duration Exposure Facility (LDEF) materials: Baggage and bonanzas p 2440 N92-23297
LDEF impact craters formed by carbon-rich impactors: A preliminary report p 2336 N92-23319
The state of the development in Europe p 2392 N92-23382
National air quality and emissions trends report, 1990
[PB92-141555] p 2406 N92-23517

CONTAMINATION
Ion microprobe elemental analyses of impact features on interplanetary dust experiment sensor surfaces p 2458 N92-23318

CONTINENTAL DRIFT
The interpretation of crustal dynamics data in terms of plate interactions and active tectonics of the Anatolian plate and surrounding regions in the Middle East
[NASA-CR-188466] p 2408 N92-23558

CONTINUITY
The continuous elements method p 2330 N92-23829

CONTINUUM MECHANICS
Use of control theory for analyzing stability of states in continuum thermodynamics
[PB92-136571] p 2451 N92-23136

CONTINUUM MODELING
The continuum modelling of two-phase flow systems
[DE92-007538] p 2373 N92-23202

CONTROL SYSTEMS DESIGN
The design and control of uncertain manipulator arms with decoupled inertia matrix p 2383 N92-23690
Simulation of Space Station loads with active control systems p 2329 N92-23824

CONTROL THEORY
Use of control theory for analyzing stability of states in continuum thermodynamics
[PB92-136571] p 2451 N92-23136

CONTROL VALVES
Mathematical model of a control valve
[PB92-141951] p 2383 N92-23710

CONTROLLERS
Method for advanced material characterization by laser induced eddy current imaging
[NASA-CASE-GSC-13386-1] p 2386 N92-23376
Summary report: A preliminary investigation into the use of fuzzy logic for the control of redundant manipulators
[NASA-CR-190277] p 2429 N92-23438
Controlling flexible robot arms using a high speed dynamics process
[NASA-CASE-NPO-18499-1-CU] p 2385 N92-24042
Controlling under-actuated robot arms using a high speed dynamics process
[NASA-CASE-NPO-18498-1-CU] p 2385 N92-24043

CONVECTION
Quasi-three-dimensional simulations of deep convection
[DE92-007204] p 2409 N92-23257

CONVECTIVE FLOW
Development of a new flux splitting scheme p 2303 N92-23352
Protein crystal growth (5-IML-1) p 2361 N92-23634

CONVERGENCE
A comparative study of preconditioned Lanczos methods for nonsymmetric linear systems
[DE92-007530] p 2431 N92-23201
Waveform relaxation always converges for RC-circuits
[PB92-142280] p 2369 N92-23495

CONVOLUTION INTEGRALS
Automatic waveform analysis and measurement system user manual
[PB92-132976] p 2364 N92-23173

COOLANTS
On the global warming potentials of candidate gaseous diffusion plant coolants
[DE92-006640] p 2406 N92-23740

COOLING
Effects of turbine cooling assumptions on performance and sizing of high-speed civil transport
[NASA-TM-105610] p 2311 N92-23537
Analysis of gravity and topography on Earth and Venus: Comparisons of lithospheric and sublithospheric processes p 2409 N92-23772

COPPER
Ab initio pair potentials for FCC metals: An application of the method of Moebius transform
[DE92-617440] p 2351 N92-23582
Tubular copper thrust chamber design study
[NASA-CR-187206] p 2337 N92-23982

COPPER ALLOYS
Reaction layer formation at the graphite/copper-chromium alloy interface
[NASA-CR-189147] p 2351 N92-23436

COPPER ISOTOPES
NQR investigation of pressure-induced charge transfer in oxygen-deficient YBa2Cu3O(7-delta) (delta = 0.38)
[DE92-008441] p 2450 N92-24036

COPPER OXIDES
Electronic structure in high temperature superconducting oxides
[DE92-008566] p 2449 N92-23986
NQR investigation of pressure-induced charge transfer in oxygen-deficient YBa2Cu3O(7-delta) (delta = 0.38)
[DE92-008441] p 2450 N92-24036

COPPER SELENIDES
Rapid recrystallization of semiconductor thin films for photovoltaic applications p 2404 N92-23998

CORRELATION
Semiclassical model and properties of resonant tunneling diode
[PB92-143320] p 2448 N92-23498

CORROSION
Effect of minor elements on corrosion behavior of Ni-Cr-W superalloys in HTGR helium
[DE92-751006] p 2352 N92-23712

CORROSION RESISTANCE
Hydrogen absorption by zirconium alloy cladding tube with surface oxide film
[DE92-750962] p 2351 N92-23265
JPRS report: Science and technology. Central Eurasia: Materials science
[JPRS-UMS-92-006] p 2363 N92-23709
Effect of minor elements on corrosion behavior of Ni-Cr-W superalloys in HTGR helium
[DE92-751006] p 2352 N92-23712

COSMIC DUST
Search for cosmological dust p 2456 N92-23164
Study of cosmic dust particles on board LDEF: The FRECOPA experiments AO138-1 and AO138-2 p 2458 N92-23310
Preliminary analysis of LDEF instrument A0187-1: Chemistry of Micrometeoroids Experiment p 2458 N92-23315

COSMIC RAY ALBEDO
Ionizing radiation calculations and comparisons with LDEF data p 2440 N92-23304

COSMIC RAY SHOWERS
A study of underground muons in the Soudan 2 detector p 2437 N92-23674

COSMIC RAYS
The isotopic composition of cosmic ray helium from 500 to 1100 MeV per nucleon p 2460 N92-23163
Modeling of the DZero data acquisition system
[DE92-007913] p 2453 N92-23212
Gamma radiation survey of the LDEF spacecraft p 2460 N92-23293
The interactions of atmospheric cosmogenic radionuclides with spacecraft surfaces p 2461 N92-23294
Surface activation of Concorde by Be-7 p 2439 N92-23295
The LDEF ultra heavy cosmic ray experiment p 2461 N92-23306
Microgravitational effects on chromosome behavior (7-IML-1) p 2357 N92-23604
Embryogenesis and organogenesis of Carausius morosus under space flight conditions (7-IML-1) p 2358 N92-23610
Radiation monitoring container device (16-IML-1) p 2361 N92-23629

COSMIC X RAYS
The ALEXIS data processing package: An IDL-based system
[DE92-007429] p 2455 N92-24027

COSSERAT SURFACES
A damage mechanics model for beams p 2387 N92-23159

COST EFFECTIVENESS
Special Course on Engineering Methods in Aerodynamic Analysis and Design of Aircraft
[AGARD-R-783] p 2308 N92-23950

COST ESTIMATES
Provisional cost evaluation p 2395 N92-23408
Euromar industrial partners agreement p 2396 N92-23410
Mathematical analysis techniques for modeling the space network activities p 2434 N92-23964

COSTS
The market for computer readable information p 2453 N92-23728

COULOMB POTENTIAL
Mutual scattering of carriers in two quantum wires
[DE92-616890] p 2366 N92-23580

COUNTER ROTATION
Aeroelastic stability analyses of two counter rotating propfan designs for a cruise missile model
[NASA-TM-105268] p 2387 N92-23191

COUNTERS
A hybrid LBG/lattice vector quantizer for high quality image coding p 2418 N92-23421

COUPLED MODES
Coupled load analysis: Scatter related to model uncertainties p 2324 N92-23787
Strongly coupled cavity QED p 2442 N92-23999

COUPLERS
High reliability robot friendly ORU interface
[NASA-CASE-GSC-13360-1] p 2381 N92-23377

COUPLING
Dynamic load cases on Ariane 5 p 2321 N92-23797
Feasibility of payload sensitivity analyses for AR4 dynamic events p 2328 N92-23815
On the analysis of liquid filled free-free tanks p 2332 N92-23843

COVARIANCE
Density of the F-statistic in the linear model with arbitrarily normal distributed errors
[PB92-128792] p 2434 N92-23731

CRACK ARREST
Development of a crack arrest fracture toughness measurement procedure for quality assurance of plates and welds used for hydrocarbon storage tanks
[PB92-141753] p 2389 N92-23681

CRACK GEOMETRY
Crack path prediction near an elliptical inhomogeneity p 2389 N92-23688

CRACK INITIATION
Conception and development of improved analytical prediction models for fatigue induced tooth breakage due to cyclic bending in spur gear teeth p 2384 N92-23739
Fatigue analysis under random stresses p 2325 N92-23795
On the test of mode 1 delamination and the importance of laminate lay-ups p 2343 N92-23943

CRACK PROPAGATION
Boundary element analysis of fracture mechanics problems p 2387 N92-23125
Damage development in titanium metal matrix composites subjected to cyclic loading
[NASA-TM-107597] p 2340 N92-23433
Development of a crack arrest fracture toughness measurement procedure for quality assurance of plates and welds used for hydrocarbon storage tanks
[PB92-141753] p 2389 N92-23681
Crack path prediction near an elliptical inhomogeneity p 2389 N92-23688
Conception and development of improved analytical prediction models for fatigue induced tooth breakage due to cyclic bending in spur gear teeth p 2384 N92-23739
On the test of mode 1 delamination and the importance of laminate lay-ups p 2343 N92-23943

CRACK TIPS
Boundary element analysis of fracture mechanics problems p 2387 N92-23125
Crack path prediction near an elliptical inhomogeneity p 2389 N92-23688

CRACKS
Cracking investigation of Nd:YAG laser welded gold plated glass sealing alloys
[DE92-007971] p 2387 N92-23216
Investigation of fretting fatigue mechanisms on 7075-T6 aluminum alloy and Ti-6Al-4V titanium alloy
p 2352 N92-23725
Multifracture of ceramic composites
[DE92-009630] p 2355 N92-23897

CRASHES
Aircraft accident report: Ryan International Airlines DC-9-15, N565PC, loss of control on takeoff, Cleveland-Hopkins International Airport, Cleveland, Ohio, February 17, 1991
[PB91-910410] p 2305 N92-23597

CRATERING
Study of cosmic dust particles on board LDEF: The FRECOPA experiments AO138-1 and AO138-2
p 2458 N92-23310

CRATERS
Large craters on the meteoroid and space debris impact experiment p 2335 N92-23309
Meteoroid and debris special investigation group data acquisition procedures p 2454 N92-23313
Meteoroid, and debris special investigation group preliminary results: Size-frequency distribution and spatial density of large impact features on LDEF
p 2336 N92-23314
Ion microprobe elemental analyses of impact features on interplanetary dust experiment sensor surfaces
p 2458 N92-23318
LDEF impact craters formed by carbon-rich impactors: A preliminary report p 2336 N92-23319
Dynamic (computer) modelling of the particulate environment: Transformations from the LDEF reference frame to decode geocentric and interplanetary populations p 2458 N92-23320
Deriving the velocity distribution of meteoroids from the measured meteoroid impact directionality on the various LDEF surfaces p 2459 N92-23322
M and D SIG progress report: Laboratory simulations of LDEF impact features p 2336 N92-23323

CREEP PROPERTIES
Matrix dominated stress/strain behavior in polymeric composites: Effects of hold time, nonlinearity and rate dependency
[NASA-TM-107595] p 2340 N92-23434

CRITICAL LOADING
High-temperature deformation behavior of single crystalline A15-type intermetallic compounds
p 2352 N92-23718

CRITICAL POINT
The Critical Point Facility (CPF) p 2362 N92-23637
Near-critical point phenomena in fluids (19-IML-1)
p 2362 N92-23638
Critical fluid thermal equilibration experiment (19-IML-1) p 2363 N92-23640

CRITICAL TEMPERATURE
Dependence of the critical temperature of laser-ablated YBa2Cu3O(7-delta) thin films on LaAlO3 substrate growth technique p 2365 N92-23415
Study of density distribution in a near-critical simple fluid (19-IML-1) p 2362 N92-23639

CROP IDENTIFICATION
Estimation of regional evapotranspiration with MOS-1 VTIR data p 2401 N92-23492

CROP VIGOR
Estimation of regional evapotranspiration with MOS-1 VTIR data p 2401 N92-23492

CROSS CORRELATION
Line profile asymmetries in chromospherically active stars p 2458 N92-24015

CROSSTALK
Mutual interference in multichannel fibre communication systems p 2367 N92-24019

CRUCIBLES
Investigation of plasma-sprayed laminates for high-temperature melting operations
[DE92-008416] p 2353 N92-24006

CRUISE MISSILES
Aeroelastic stability analyses of two counter rotating propfan designs for a cruise missile model
[NASA-TM-105268] p 2387 N92-23191

CRYOGENIC COOLING
Characterizing and testing a thermally isolating superconducting link for SAFIRE-like missions
[NASA-CR-190196] p 2369 N92-23430

CRYOGENIC EQUIPMENT
Microsphere viscometers for low temperature applications
[PB92-143361] p 2379 N92-23594

CRYOGENIC FLUIDS
Microgravity dynamical behaviors of cryogenic liquid hydrogen reorientation and draining in space propulsion system p 2356 N92-23147
Liquid hydrogen mass flow through a multiple orifice Joule-Thomson device
[NASA-TM-105583] p 2373 N92-23268
General P-T fit construction for He, N2, Ar, H2 and Ne VPT used at Fermilab
[DE92-008851] p 2433 N92-23579

CRYOGENICS
Experience of the Chemical Automatics Design Bureau in creation of RD-0120 LOX/LH2 liquid rocket engine with thrust of 2 mn for Energia launcher
p 2319 N92-23757
Development status of the cryotechnical principal stage p 2319 N92-23758
Development status of the Vulcain engine
p 2319 N92-23759
Reusable launchers: New concepts and technological advances for the manufacturing of cryogenic tanks
p 2319 N92-23760

CRYOSTATS
CRYOSTAT (18-IML-1) p 2362 N92-23636

CRYSTAL DEFECTS
TEM study of flux pinning defects in YBa2Cu3O7-delta produced by 580 MeV Sn ion irradiation
[DE92-006991] p 2448 N92-23574
Fermi level effects on dislocation formation in InAs(1-x)Sb(x) grown by MOCVD
[DE92-008332] p 2450 N92-24034

CRYSTAL DISLOCATIONS
High-temperature deformation behavior of single crystalline A15-type intermetallic compounds
p 2352 N92-23718

CRYSTAL GROWTH
Casting of simple-shaped single crystals of aluminum
[PB92-136555] p 2350 N92-23179
Temperature-dependent evolution of chemisorbed digermane in Ge thin film growth
[DE92-008098] p 2447 N92-23447
Chemical compatibility of cartridge materials
[NASA-CR-190256] p 2356 N92-23555
A study of solution crystal growth in LOW-g (2-IML-1)
p 2361 N92-23630
Vapor crystal growth studies of single crystals of mercuric iodide (3-IML-1) p 2361 N92-23632
Mercury iodide nucleation and crystal growth in vapor phase (4-IML-1) p 2361 N92-23633
Organic crystal growth experiment facility (13-IML-1)
p 2362 N92-23635
Center for Macromolecular Crystallography, University of Alabama in Birmingham p 2313 N92-23650
Center for Space Power and Advanced Electronics, Auburn University p 2314 N92-23654

CRYSTAL LATTICES
Monte Carlo simulation of the 3-state vector Potts model on a 3-dimensional random lattice
[DE92-615489] p 2446 N92-23259
Improved spin wave theory: An application to the spin-1/2 antiferromagnetic Heisenberg model on a square lattice
[DE92-617436] p 2448 N92-23504

CRYSTAL OPTICS
Solitary excitations in gyrotropic crystals
[DE92-617447] p 2446 N92-23271

CRYSTAL STRUCTURE
The role of microstructural phenomena in magnetic thin films
[DE92-007960] p 2446 N92-23213
Organic crystal growth experiment facility (13-IML-1)
p 2362 N92-23635

CRYSTALLIZATION
CRYOSTAT (18-IML-1) p 2362 N92-23636
Phase transformations in SrAl2Si2O8 glass
[NASA-TM-105657] p 2449 N92-23890
Morphology and mechanical performance of PPS/carbon composite p 2342 N92-23939
Crystallization behavior of poly(phenylene sulphide)
p 2342 N92-23940

CRYSTALLOGRAPHY
The role of microstructural phenomena in magnetic thin films
[DE92-007960] p 2446 N92-23213
Center for Macromolecular Crystallography, University of Alabama in Birmingham p 2313 N92-23650

CRYSTALS
Solitary excitations in gyrotropic crystals
[DE92-617447] p 2446 N92-23271
The electron-positron momentum density and Fermi surface of YBa2Cu3O(7-x)
[DE92-008605] p 2450 N92-24007

CUFFS
Bar-holding prosthetic limb
[NASA-CASE-MFS-28481-1] p 2416 N92-24056

CULTURE TECHNIQUES
Proliferation and performance of hybridoma cells in microgravity (7-IML-1) p 2358 N92-23614
Dynamic cell culture system (7-IML-1)
p 2359 N92-23615

CUMULATIVE DAMAGE
Progressive fracture of polymer matrix composite structures: A new approach
[NASA-TM-105574] p 2339 N92-23194

CURING
A method to determine resin flow during curing of composite laminates p 2342 N92-23938
Fiber-optic Raman spectroscopy for cure monitoring of advanced polymer composites
[DE92-008619] p 2355 N92-24068

CURRENT DENSITY
Semiclassical model and properties of resonant tunneling diode
[PB92-143320] p 2448 N92-23498
An x ray diagnostic of electron power loss
[DE92-008599] p 2444 N92-23523

CURRENT SHEETS
Magnetic reconnection in magnetotail and solar plasmas p 2457 N92-24000

CURVATURE
On some types of Riemannian V(sub n) with zero Ricci curvature
[DE92-616917] p 2432 N92-23502
Constant curvature and non-perturbative W(sub 3) gravity
[DE92-616919] p 2451 N92-23503

CUTTING
Improvement of laser machining processes
[DE92-007801] p 2380 N92-23723

CYCLES
Energy cycles in the summer tropical atmosphere over the North Atlantic Ocean p 2409 N92-23150

CYCLOGENESIS
Energy cycles in the summer tropical atmosphere over the North Atlantic Ocean p 2409 N92-23150

CYCLOTRON RESONANCE
Evolution of magnetic moment due to the cyclotron resonance with field ripples in a tokamak
[DE92-751058] p 2443 N92-23135
Evaluation of mode purity of ordinary and extraordinary modes by fixed elliptically polarized wave for ECH and ECCD
[DE92-750961] p 2444 N92-23264
Theory study on fast wave absorption at the plasma edge
[PB92-141936] p 2444 N92-23663

CYLINDRICAL SHELLS
Problem of membrane locking in finite element analysis of cylindrical shells
[PB92-133941] p 2387 N92-23137
Free vibration of thick isotropic and orthotropic cylindrical shells p 2389 N92-23773

D

DAMAGE
A damage mechanics model for beams
p 2387 N92-23159
Damage development in titanium metal matrix composites subjected to cyclic loading
[NASA-TM-107597] p 2340 N92-23433
Limits of survivability and damage for optical components used in a high repetition rate visible laser
[DE92-006896] p 2379 N92-23570
Investigation of fretting fatigue mechanisms on 7075-T6 aluminum alloy and Ti-6Al-4V titanium alloy
p 2352 N92-23725
Development of fatigue damage mechanics for application to the design of damage-tolerant composite components p 2324 N92-23793
Fatigue analysis under random stresses
p 2325 N92-23795
Experimental study of delamination growth in multidirectional CFRP-laminates under fatigue loading
p 2328 N92-23819

DAMAGE ASSESSMENT
Smart accelerometer --- vibration damage detection
[NASA-CASE-MSC-21951-1] p 2378 N92-23545
Underlying modal data issues for detecting damage in truss structures
[NASA-TM-107573] p 2390 N92-23990

DAMPING
Damping behaviour of unidirectional fibre reinforced polymers p 2326 N92-23805

DARK MATTER
Particle physics and cosmology
[DE92-008301] p 2456 N92-23153

DATA ACQUISITION
Modeling of the DZero data acquisition system
[DE92-007913] p 2453 N92-23212
Battery test facility hardware, software, and system operation
[DE92-008455] p 2372 N92-24063

DATA BASE MANAGEMENT SYSTEMS
Modeling of physical database design and performance analysis with emphasis on VSAM files p 2452 N92-23156
Differences within and among surface marine datasets [PB92-135326] p 2411 N92-23660
The market for computer readable information p 2453 N92-23728

DATA BASES
Modeling of physical database design and performance analysis with emphasis on VSAM files p 2452 N92-23156
Data exploration systems for databases p 2429 N92-23374
Multisensor data fusion p 2394 N92-23398
Semiempirical studies of atomic structure [DE92-008143] p 2437 N92-23448

DATA COLLECTION PLATFORMS
Research project for practical usage of MOS-1 data collection system p 2399 N92-23485

DATA COMPRESSION
Design of joint source/channel coders [NASA-CR-189960] p 2417 N92-23416
Maximum aposteriori joint source/channel coding p 2417 N92-23417
A joint source/channel coder design p 2417 N92-23418
An edge preserving differential image coding scheme p 2417 N92-23419
A robust low-rate coding scheme for packet video p 2417 N92-23420
A hybrid LBG/lattice vector quantizer for high quality image coding p 2418 N92-23421
A robust coding scheme for packet video p 2418 N92-23422
A progressive data compression scheme based upon adaptive transform coding: Mixture block coding of natural images p 2418 N92-23423
Digital data registration and differencing compression system [NASA-CASE-SSC-00010-2] p 2453 N92-23550

DATA CONVERTERS
Modifications for a communication interface board p 2368 N92-23963

DATA CORRELATION
LDEF data correlation to existing NASA debris environment models p 2336 N92-23321

DATA INTEGRATION
Framework Programmable Platform for the advanced software development workstation: Framework processor design document [NASA-CR-190173] p 2418 N92-23554

DATA MANAGEMENT
Design of neural networks for classification of remotely sensed imagery p 2402 N92-23367
The use of artificial intelligence techniques to improve the multiple payload integration process p 2428 N92-23370
A spatial data handling system for retrieval of images by unrestricted regions of user interest p 2429 N92-23373
Data exploration systems for databases p 2429 N92-23374
Logic programming and metadata specifications p 2429 N92-23375
The need for standards in design automation [P-1-1] p 2419 N92-23852
CIM: The future technology [REPT-3.3.1] p 2424 N92-23885

DATA PROCESSING
Improved interpretation of satellite altimeter data using genetic algorithms p 2402 N92-23369
Digital data registration and differencing compression system [NASA-CASE-SSC-00010-2] p 2453 N92-23550
International workshop on the airborne measurement of wind, turbulence, and position [PB92-139963] p 2410 N92-23587
Dynamic positioning by GPS p 2306 N92-23729
The statistical analysis of data from normal distributions, with particular reference to small samples [ESDU-91041] p 2434 N92-24008
The ALEXIS data processing package: An IDL-based system [DE92-007429] p 2455 N92-24027

DATA RECORDERS
On board data recording p 2394 N92-23395

DATA RECORDING
On board data recording p 2394 N92-23395
Ground station p 2394 N92-23397
Distributed computer system in the large scale low speed wind tunnel [NAL-TM-629] p 2312 N92-23979

DATA REDUCTION
An advanced system for environmental sine testing: Basic principles revisited p 2325 N92-23799
Employment of C.B. (Craig-Bampton) models for nonlinear dynamic analysis p 2327 N92-23814

DATA SAMPLING
Distributed computer system in the large scale low speed wind tunnel [NAL-TM-629] p 2312 N92-23979

DATA STORAGE
Types of operation and system control p 2395 N92-23401

DATA STRUCTURES
A spatial data handling system for retrieval of images by unrestricted regions of user interest p 2429 N92-23373
Combining a CAD/CAM system with an advanced database architecture [REPT-3.1.5] p 2423 N92-23880

DATA SYSTEMS
A spatial data handling system for retrieval of images by unrestricted regions of user interest p 2429 N92-23373
Data exploration systems for databases p 2429 N92-23374

DATA TRANSFER (COMPUTERS)
From IGES to STEP [REPT-3.1.6] p 2423 N92-23881
IGES: Application generator in disguise [REPT-3.1.7] p 2424 N92-23882
The use of EDIF at Daisy/Cadnetix [REPT-4.2.1] p 2424 N92-23887
Infrastructure and training of manpower for CAD/CAM systems [REPT-4.2.2] p 2425 N92-23888

DATA TRANSMISSION
A signal and image processing object-based system using CLOS [DE92-006826] p 2417 N92-23255
Data distribution and reduction approaches to data distribution: The Earthnet experience p 2317 N92-23926
The use of STEP in an integrated manufacturing environment [DE92-008417] p 2425 N92-24035

DEBRIS
Meteoroid, and debris special investigation group preliminary results: Size-frequency distribution and spatial density of large impact features on LDEF p 2336 N92-23314

DECISION MAKING
Dynamic aggregate models for group technology manufacturing environment [REPT-1.1.7] p 2420 N92-23858

DECISION THEORY
Training users of a flexible decision support system: The effects of training content and user ability p 2453 N92-23730

DECODERS
Maximum aposteriori joint source/channel coding p 2417 N92-23417

DECODING
Dynamic (computer) modelling of the particulate environment: Transformations from the LDEF reference frame to decode geocentric and interplanetary populations p 2458 N92-23320

DECOMPOSITION
On the basic equations for the second-order modeling of compressible turbulence p 2303 N92-23351

DECONDITIONING
Measurement of venous compliance (8-IML-1) p 2360 N92-23623

DEFECTS
Defect behavior, carrier removal and predicted in-space injection annealing of InP solar cells [NASA-TM-105624] p 2370 N92-23562

DEFENSE PROGRAM
Research, Development, Test and Evaluation (R, D, T, and E) Programs (R-1), Department of Defense budget for fiscal year 1993 [PB92-127745] p 2451 N92-23247

DEFORMATION
The effect of processing on strength of Nicalon fibers in Nicalon fiber-SiC matrix composites [DE92-006978] p 2340 N92-23256
Analysis of delamination related fracture processes in composites [NASA-CR-190226] p 2340 N92-23532
High-temperature deformation behavior of single crystalline A15-type intermetallic compounds p 2352 N92-23718
Localization of deformation and inelastic deformation of pressure-sensitive dilatant materials p 2389 N92-23737
Modeling and analysis of high-temperature inelastic deformation in metal matrix composites p 2345 N92-23996
Analytical and experimental investigation of vibratory response in adhesively bonded and composite structures p 2345 N92-24012
Transverse deformation of unidirectional fiber-reinforced metal matrix composites p 2345 N92-24013

DEGRADATION
Preliminary micrometeoroid and debris effects on LDEF thermal control surfaces p 2336 N92-23324
Oxidative degradation of polymers induced by ionizing radiation [DE92-007657] p 2354 N92-23442

DEGREES OF FREEDOM
Design of an omnidirectional and holonomic wheeled platform prototype [DE92-000046] p 2382 N92-23459
Configuration control of seven-degree-of-freedom arms [NASA-CASE-NPO-18607-1-CU] p 2382 N92-23553
Vacuum mechatronic laser alignment system on the NOVA laser [DE92-006898] p 2379 N92-23571
On the analysis of liquid filled free-free tanks p 2332 N92-23843

DELAMINATING
Progressive fracture of polymer matrix composite structures: A new approach [NASA-TM-105574] p 2339 N92-23194
Analysis of delamination related fracture processes in composites [NASA-CR-190226] p 2340 N92-23532
The fracture behavior of carbon/epoxy laminates containing part through-the-thickness fiber breakage p 2340 N92-23693
Characterization of interlaminar mode 1 and mode 2 fracture in CFRP laminates p 2325 N92-23794
Experimental study of delamination growth in multidirectional CFRP-laminates under fatigue loading p 2328 N92-23819
Buckling and failure of thin elliptical delaminations in composites p 2331 N92-23835
Impact-induced delamination in (0(5), 90(5), 0(5)) carbon/peek composite laminates p 2341 N92-23936
On the test of mode 1 delamination and the importance of laminate lay-ups p 2343 N92-23943

DELIVERY
Dynamic aggregate models for group technology manufacturing environment [REPT-1.1.7] p 2420 N92-23858

DELTA LAUNCH VEHICLE
Rocket propulsion for NASA's Earth to orbit launchers p 2319 N92-23754
The Delta 2 launcher p 2316 N92-23921

DELTA WINGS
Hypersonic laminar flow computations over a blunt leading edged delta wing at three different chord Reynolds numbers [FFA-TN-1991-40] p 2304 N92-23168
Normal force of low aspect ratio wing-body combinations up to high angles of attack at supersonic speeds [ESDU-91042] p 2309 N92-24009

DEMAGNETIZATION
An instrument to search for small-scale anisotropy in the cosmic microwave background at 90 GHz p 2441 N92-23161

DEMAND (ECONOMICS)
Marketing qualification as a requirement for operating success p 2452 N92-23930

DENSITY DISTRIBUTION
Study of density distribution in a near-critical simple fluid (19-IML-1) p 2362 N92-23639

DEOXYRIBONUCLEIC ACID
Microgravitational effects on chromosome behavior (7-IML-1) p 2357 N92-23604

DEPLOYMENT
Self-deploying photovoltaic power system [NASA-CASE-LEW-15308-1] p 2404 N92-24057

DEPOSITION
Hydrogen absorption by zirconium alloy cladding tube with surface oxide film [DE92-750962] p 2351 N92-23265
Properties of large area ErBa2Cu3O(7-x) thin films deposited by ionized cluster beams p 2365 N92-23414
National acid precipitation assessment program: Mission, goals, and program plan post 1990. Public review draft [PB92-126248] p 2405 N92-23515
Transport calculations of chemically sputtered carbon near a plasma divertor surface [DE92-009022] p 2445 N92-24021
High-performance multilayer mirrors for soft x ray projection lithography [DE92-008615] p 2443 N92-24049
Working gas pressure and flow effects on reactively sputtered molybdenum-oxide thin films [DE92-008624] p 2450 N92-24069

DEPOSITS
SIMS chemical analysis of extended impact features from the trailing edge portion of experiment AO187-2
p 2349 N92-23316
DEPTH MEASUREMENT
Seaborne lidar system p 2393 N92-23389
DESCENT TRAJECTORIES
Modelling of aerodynamic forces and heat transfer for orbital decay and reentry calculations
p 2334 N92-23974
DESCRIPTIONS
An 18-point catalog description p 2396 N92-23411
DESERTS
Acid rain and air pollution in desert park areas. Proceedings of a workshop: Management recommendations
[PB92-140532] p 2407 N92-24003
DESIGN ANALYSIS
Conceptual design of Fusion Experimental Reactor
[DE92-751036] p 2443 N92-23132
A flexible CPW package for a 30 GHz MMIC amplifier --- coplanar waveguide
[NASA-TM-105630] p 2368 N92-23193
Integrated Design Analysis and Optimisation of Aircraft Structures
[AGARD-R-784] p 2306 N92-23227
Application of multidisciplinary optimization methods to the design of a supersonic transport
p 2307 N92-23230
Application of analytical and design tools for fighter wing aeroelastic tailoring p 2307 N92-23231
The structural optimization system OPTSYS: Current status and applications p 2307 N92-23232
First approach to an integrated fin design
p 2308 N92-23236
Structural optimization of aircraft practice and trends
p 2308 N92-23239
Design of joint source/channel coders
[NASA-CR-189960] p 2417 N92-23416
Maximum aposteriori joint source/channel coding
p 2417 N92-23417
A joint source/channel coder design
p 2417 N92-23418
Efficient and robust design optimization of transonic airfoils p 2305 N92-23717
The need for standards in design automation
[P-1-1] p 2419 N92-23852
Design for testability: Where are the goalposts?
[REPT-1.2.2] p 2420 N92-23861
Application of the Green function technique in the microstrip patch antenna analysis
[PB92-142173] p 2367 N92-23907
Special Course on Engineering Methods in Aerodynamic Analysis and Design of Aircraft
[AGARD-R-783] p 2308 N92-23950
Introduction to Special Course on Engineering Methods in Aerodynamic Analysis and Design of Aircraft
p 2308 N92-23951
Computational procedures for preliminary design
p 2309 N92-23952
Panel methods for aerodynamic analysis and design
p 2309 N92-23955
Aircraft drag analysis methods p 2309 N92-23957
Tubular copper thrust chamber design study
[NASA-CR-187206] p 2337 N92-23982
Advanced electric motor technology: Flux mapping
[NASA-CR-184317] p 2372 N92-24047
DESORPTION
Temperature-dependent evolution of chemisorbed digermane in Ge thin film growth
[DE92-008098] p 2447 N92-23447
DESTRUCTIVE TESTS
Application of the microbond technique: Characterization of carbon-epoxy interfaces
p 2343 N92-23944
DETECTION
Search for atmospheric neutrino oscillations with the Soudan 2 detector
[DE92-007397] p 2437 N92-23328
Methods for the detection of microorganisms in the environment
[PB92-137454] p 2405 N92-23512
Underlying modal data issues for detecting damage in truss structures
[NASA-TM-107573] p 2390 N92-23990
DETERIORATION
Modeling of physical database design and performance analysis with emphasis on VSAM files
p 2452 N92-23156
DEUTERIUM
Energy expenditure in space flight (doubly labelled water method) (8-IML-1) p 2359 N92-23620
DIAMINES
Vinyl capped addition polyimides
[NASA-CASE-LEW-15027-2] p 2355 N92-24053
DIAMOND FILMS
Environmental effects on friction and wear of diamond and diamondlike carbon coatings
[NASA-TM-105634] p 2354 N92-23192
Profiling and mapping of advanced materials using spatially resolved Raman spectroscopy
[DE92-008304] p 2347 N92-23449
DIAMONDS
Environmental effects on friction and wear of diamond and diamondlike carbon coatings
[NASA-TM-105634] p 2354 N92-23192
DIELECTRIC POLARIZATION
Mutual scattering of carriers in two quantum wires
[DE92-616890] p 2366 N92-23580
DIELECTRIC PROPERTIES
A probabilistic mechanism hidden behind the universal power law for dielectric relaxation. Part 1: General relaxation equation
[DE92-615484] p 2435 N92-23220
Characterization of polybenzimidazole (PBI) film at high temperatures
[NASA-CR-189174] p 2370 N92-23538
Evaluation of high temperature capacitor dielectrics
[NASA-TM-105622] p 2370 N92-23561
A probabilistic mechanism hidden behind the universal power law for dielectric relaxation. Part 2: Discussion of the response function
[DE92-615485] p 2435 N92-23598
DIELECTRICS
Electrostatic image solution for the interaction of two dielectric spheres
[PB92-142199] p 2364 N92-23138
A probabilistic mechanism hidden behind the universal power law for dielectric relaxation. Part 1: General relaxation equation
[DE92-615484] p 2435 N92-23220
User's manual for three dimensional FDTD version C code for scattering from frequency-independent dielectric and magnetic materials
[NASA-CR-190109] p 2365 N92-23425
Characterization of polybenzimidazole (PBI) film at high temperatures
[NASA-CR-189174] p 2370 N92-23538
Evaluation of high temperature capacitor dielectrics
[NASA-TM-105622] p 2370 N92-23561
Quasi-static image theory for the bi-isotropic (nonreciprocal chiral) sphere
[PB92-142371] p 2366 N92-23666
Electrostatic image theory for the dielectric sphere with an internal source
[PB92-142405] p 2366 N92-23667
Electrostatic image theory for the layered dielectric sphere
[PB92-142413] p 2367 N92-23668
Vector circuit method applied for chiral dielectric slab waveguides
[PB92-142355] p 2367 N92-23679
DIFFERENCE EQUATIONS
Geometry of differential difference equations
[PB92-148774] p 2431 N92-23182
DIFFERENTIAL EQUATIONS
Geometry of differential difference equations
[PB92-148774] p 2431 N92-23182
Small solutions and completeness for linear functional differential equations
[PB92-149350] p 2431 N92-23250
Improved shock-capturing of Jameson's scheme for the Euler equations
[PB92-148758] p 2373 N92-23251
Experiments and modeling p 2301 N92-23339
Grid generation and flow solution method for Euler equations on unstructured grids
[NASA-TM-4295] p 2305 N92-23533
Soviet articles on antenna theory
[DE92-008452] p 2366 N92-23575
Theory for iterative solution of large dynamical systems using parallel computation
[PB92-143304] p 2433 N92-23589
Mathematical model of a control valve
[PB92-141951] p 2383 N92-23710
DIFFERENTIAL GEOMETRY
Geometry of differential difference equations
[PB92-148774] p 2431 N92-23182
Non-commutative differential geometry and Yang-Baxter equation
[PB92-149459] p 2431 N92-23184
DIFFRACTION
Center for Macromolecular Crystallography, University of Alabama in Birmingham p 2313 N92-23650
DIFFRACTION PATTERNS
X ray Fourier transform holography: Beyond the optical diffraction limit p 2377 N92-23144
DIFFUSION
Probing picosecond flame dynamics with transient grating experiments
[DE92-003163] p 2346 N92-23181
Reaction layer formation at the graphite/copper-chromium alloy interface
[NASA-CR-189147] p 2351 N92-23436
DIFFUSION FLAMES
A study of hydrogen diffusion flames using PDF turbulence model p 2303 N92-23348
DIFFUSION WAVES
Critical fluid thermal equilibration experiment (19-IML-1) p 2363 N92-23640
DIFFUSIVITY
Unsteady three-dimensional incompressible algorithm based on artificial compressibility p 2375 N92-23700
DIGITAL COMPUTERS
Distributed computer system in the large scale low speed wind tunnel
[NAL-TM-629] p 2312 N92-23979
DIGITAL DATA
Digital data registration and differencing compression system
[NASA-CASE-SSC-00010-2] p 2453 N92-23550
DIGITAL ELECTRONICS
Fast simulation of MOS digital networks using a physical macromodelling approach
[REPT-1.2.1] p 2420 N92-23860
An exhaustive self-test design methodology for synchronous state machines
[REPT-1.2.4] p 2421 N92-23863
Test preparation for MOS digital circuits using heuristics for reliable fault simulation
[REPT-1.2.6] p 2421 N92-23865
DIGITAL SIMULATION
The validation of hydrocodes for orbital debris impact simulation p 2323 N92-23784
Computer simulation of moisture penetration in structures p 2326 N92-23806
Ariane 4 internal acoustic environment: Interpretation of flight data with a vibroacoustic model of the upper part of the launcher p 2321 N92-23811
DIGITAL SYSTEMS
Applications of industrial engineering
p 2364 N92-23966
DIMENSIONAL ANALYSIS
An exceptional N=8 superconformal algebra in two dimensions associated with F(4)
[DE92-616991] p 2435 N92-23207
Time optimal trajectories for a 2-wheeled robot
[DE92-000069] p 2430 N92-24032
DIMERS
Potential energy surfaces and reaction dynamics of polyatomic molecules
[DE92-008314] p 2437 N92-23450
DIODES
Semiclassical model and properties of resonant tunneling diode
[PB92-143320] p 2448 N92-23498
MOSFET level 1 and 2 models in APLAC
[PB92-143379] p 2371 N92-23678
DIPOLE ANTENNAS
Soviet articles on antenna theory
[DE92-008452] p 2366 N92-23575
DIRECTIONAL SOLIDIFICATION (CRYSTALS)
Casting of simple-shaped single crystals of aluminum
[PB92-136555] p 2350 N92-23179
DIRECTIVITY
Numerical and experimental study of noise generated by a vibrating plate p 2324 N92-23792
DISASTERS
Verification of the effectiveness of MOS-1 MESSR in the field of disaster prevention p 2397 N92-23474
DISCOVERY (ORBITER)
Mission safety evaluation report for STS-29, postflight edition
[NASA-TM-107773] p 2312 N92-23241
DISKS (SHAPES)
Oil lubricated and water lubricated pin-on-disc wear tests with engineering ceramics
[PB92-136563] p 2380 N92-23152
DISPERSIONS
Numerical and physical modelling of bubbly flow phenomena
[DE92-008642] p 2376 N92-24062
DISPLACEMENT
Analysis of delamination related fracture processes in composites
[NASA-CR-190226] p 2340 N92-23532
Helix translation device --- shim for precision displacements
[NASA-CASE-GSC-13141-1] p 2382 N92-23548
DISPLACEMENT MEASUREMENT
X ray based displacement measurement for hostile environments
[NASA-TM-105551] p 2378 N92-23155
DISPLAY DEVICES
Quick-look system p 2394 N92-23393
Stress effects of human-computer interactions
[PB92-136001] p 2415 N92-23513

DISSOCIATION
Potential energy surfaces and reaction dynamics of polyatomic molecules
[DE92-008314] p 2437 N92-23450
DISTRIBUTED PROCESSING
Coordinating complex problem-solving among distributed intelligent agents p 2427 N92-23360
Distributed expert systems for ground and space applications p 2427 N92-23361
Architectural impact of FDDI network on scheduling hard real-time traffic
[NASA-CR-190272] p 2425 N92-23583
DISTRIBUTION (PROPERTY)
Meteoroid, and debris special investigation group preliminary results: Size-frequency distribution and spatial density of large impact features on LDEF
p 2336 N92-23314
Filling high density polyethylene with cellulosic fibers. 1: The effect of additives on fiber dispersion
p 2344 N92-23948
DOCUMENTS
Publications of the exobiology program for 1990: A special bibliography
[NASA-TM-4364] p 2416 N92-23429
DOPED CRYSTALS
Electron polarization in modulation doped heterostructures
[DE92-617490] p 2447 N92-23272
Magnetic fluctuations and normal state properties of the t-J model at finite dopings
[DE92-617538] p 2447 N92-23452
Sub-Kelvin resistance thermometer
[NASA-CASE-GSC-13406-1] p 2378 N92-23460
Numerical study of the magnetic ordering and superconducting state of high-temperature superconductor p 2449 N92-23776
DOPPLER EFFECT
Non contacting measurement of vibration
p 2325 N92-23800
DOPPLER RADAR
An observational study of the internal structure of air-mass thunderstorms p 2409 N92-23121
WAMDII: The Wide Angle Michelson Doppler Imaging Interferometer
[NASA-TM-105526] p 2441 N92-23525
CODAR in the Straits of Florida
[PB92-129964] p 2412 N92-23732
DORNIER AIRCRAFT
Preconsiderations on aircraft integration
p 2395 N92-23402
DOSIMETERS
Development of 3-dimensional compact magnetic dosimeter for environmental magnetic field monitoring
[DE92-750825] p 2407 N92-23262
Summary of ionizing radiation analysis on the Long Duration Exposure Facility p 2439 N92-23291
Prediction of LDEF ionizing radiation environment
p 2439 N92-23292
Thermoluminescent dosimetry for LDEF experiment M0006 p 2461 N92-23301
Dosimetric mapping inside biorack (7-IML-1)
p 2358 N92-23611
Radiation monitoring container device (16-IML-1)
p 2361 N92-23629
DRAG
Salyut-7/Kosmos-1686 reentry predictions for the Italian Civil Defence Authority p 2334 N92-23972
DRAINAGE
Microgravity dynamical behaviors of cryogenic liquid hydrogen reorientation and draining in space propulsion system p 2356 N92-23147
DRILL BITS
Retractable tool bit having latch type catch mechanism
[NASA-CASE-GSC-13359-1] p 2381 N92-23378
Retractable tool bit having slider type catch mechanism
[NASA-CASE-GSC-13358-1] p 2385 N92-24058
DROPS (LIQUIDS)
Comparison of two-dimensional and three-dimensional droplet trajectory calculations in the vicinity of finite wings
[NASA-TM-105617] p 2373 N92-23154
DROSOPHILA
The effect of space environment on the development and aging of Drosophila Melanogaster (7-IML-1)
p 2357 N92-23608
DURABILITY
High temperature dynamic engine seal technology development
[NASA-TM-105641] p 2381 N92-23435
DWARF NOVAE
Observations of accretion discs in interacting binaries
p 2454 N92-23673
DYADICS
Closed parallel-plate chiral waveguides with boundary impedance conditions
[PB92-142397] p 2366 N92-23591
DYE LASERS
Probing picosecond flame dynamics with transient grating experiments
[DE92-003163] p 2346 N92-23181
DYNAMIC CHARACTERISTICS
Cu charge fluctuations and anomalous behaviour in the phonon spectrum of La2CuO4
[DE92-617446] p 2446 N92-23270
Analysis of forward and inverse problems in chemical dynamics and spectroscopy
[DE92-007732] p 2347 N92-23443
Dynamic characterization of composite materials
p 2330 N92-23832
DYNAMIC CONTROL
Nonlinear feedback guidance law for aero-assisted orbit transfer maneuvers
[NASA-CR-190129] p 2317 N92-23529
DYNAMIC LOADS
A review of Space Shuttle payload-bay lift-off flight data and analysis comparisons p 2322 N92-23796
Dynamic load cases on Ariane 5
p 2321 N92-23797
Buckling of simply supported and clamped anisotropic plates under combined loads p 2326 N92-23804
Ariane 5 structural definition of the upper composite
p 2321 N92-23808
Feasibility of payload sensitivity analyses for AR4 dynamic events p 2328 N92-23815
The response surface method: An efficient tool to determine the failure probability of large structural systems p 2328 N92-23816
Simulation of Space Station loads with active control systems p 2329 N92-23824
DYNAMIC MODELS
Mathematical model of a control valve
[PB92-141951] p 2383 N92-23710
DYNAMIC MODULUS OF ELASTICITY
Damping behaviour of unidirectional fibre reinforced polymers p 2326 N92-23805
DYNAMIC RESPONSE
Sensitivity analysis of dynamic aeroelastic responses
p 2306 N92-23229
A probabilistic mechanism hidden behind the universal power law for dielectric relaxation. Part 2: Discussion of the response function
[DE92-615485] p 2435 N92-23598
Analysis and control of nonlinear flexible manipulator
p 2384 N92-23727
The use of modal synthesis in conjunction with nonlinear transient dynamic analysis p 2324 N92-23788
Dynamic load cases on Ariane 5
p 2321 N92-23797
Simulation of Space Station loads with active control systems p 2329 N92-23824
Minimization of vibrations by broadband sensitivity approach p 2330 N92-23828
Harmonic wave propagation in two-dimensional periodic large space structures p 2330 N92-23830
Investigations of the dynamic behaviour of compounds under preloading p 2332 N92-23842
DYNAMIC STRUCTURAL ANALYSIS
The free and forced vibrations of structures using the finite dynamic element method
[NASA-CR-190184] p 2388 N92-23427
Free and forced response of nearly periodic multi-span beams and multi-bay trusses p 2389 N92-23699
Spacecraft Structures and Mechanical Testing, volume 1
[ESA-SP-321-VOL-1] p 2322 N92-23780
The Columbus Free Flying Laboratory: Mechanical design aspects p 2323 N92-23782
Structural assessment of the Space Station Freedom's pressurized elements p 2323 N92-23783
Coupled load analysis: Scatter related to model uncertainties p 2324 N92-23787
The use of modal synthesis in conjunction with nonlinear transient dynamic analysis p 2324 N92-23788
Improvements for interpretation of structural dynamics calculation using effective parameters for substructures
p 2324 N92-23789
A review of Space Shuttle payload-bay lift-off flight data and analysis comparisons p 2322 N92-23796
Nonlinear finite-element analysis of sandwich shells
p 2326 N92-23802
Damping behaviour of unidirectional fibre reinforced polymers p 2326 N92-23805
Ariane 5 structural definition of the upper composite
p 2321 N92-23808
Advanced numerical analyses for the optimisation of the structural behaviour of the intersegment connection for the Ariane 5 booster case p 2327 N92-23809
Brief history of the development of the EPS-structure
p 2321 N92-23810
Acoustic cavity and fluid/structure interaction models: A methodological deterministic approach and problems encountered p 2327 N92-23813
Employment of C.B. (Craig-Bampton) models for nonlinear dynamic analysis p 2327 N92-23814
Feasibility of payload sensitivity analyses for AR4 dynamic events p 2328 N92-23815
The response surface method: An efficient tool to determine the failure probability of large structural systems p 2328 N92-23816
Design challenges for the National Aero-Space Plane
p 2310 N92-23822
Simulation of Space Station loads with active control systems p 2329 N92-23824
Influence of microvibrations on spacecraft performances p 2329 N92-23825
Development and application of substructuring techniques for understanding and controlling residual vibrations (microgravity aspects) p 2330 N92-23827
Minimization of vibrations by broadband sensitivity approach p 2330 N92-23828
The continuous elements method
p 2330 N92-23829
Harmonic wave propagation in two-dimensional periodic large space structures p 2330 N92-23830
Non linear structural analysis of a thin skin carbon-carbon rigid decelerator p 2330 N92-23831
Stretched skin concept for the entry aerodynamic decelerator system of planetary probes
p 2331 N92-23836
Strength and deformation behaviour of Kevlar and carbon composite sandwich structures for space applications p 2332 N92-23840
On the analysis of liquid filled free-free tanks
p 2332 N92-23843
Numerical investigation of fluid-structure-interaction problems with the finite element method
p 2332 N92-23844
Fluid-structure interaction problems: Development of special processors p 2332 N92-23845
A symmetric coupling between BEM and FEM for dynamical analysis of spacecraft p 2332 N92-23846
Optimal exciter placement and force vector tuning required for experimental modal analysis
p 2333 N92-23847
Matching finite element models to modal data
p 2333 N92-23848
Design parameter update of dynamic mathematical models in presence of test noise and mode pairing problems p 2333 N92-23850
DYNAMICAL SYSTEMS
Technique to eliminate computational instability in multibody simulations employing the Lagrange multiplier
[NASA-TP-3220] p 2418 N92-23432
Theory for iterative solution of large dynamical systems using parallel computation
[PB92-143304] p 2433 N92-23589
DYNODES
Actively-stabilized photomultiplier tube base for vacuum operation
[DE92-007528] p 2368 N92-23200

E

EARTH (PLANET)
Interception of comets and asteroids on collision course with Earth
[DE92-007431] p 2458 N92-24028
EARTH ATMOSPHERE
Limiting net greenhouse gas emissions in the United States, volume 2
[DE92-007592] p 2405 N92-23333
Earth observing system: NASA's EOSDIS development approach is risky
[GAO/IMTEC-92-24] p 2401 N92-23686
EARTH CRUST
Determination of crustal motions using satellite laser ranging
[NASA-CR-190246] p 2408 N92-23540
The interpretation of crustal dynamics data in terms of plate interactions and active tectonics of the Anatolian plate and surrounding regions in the Middle East
[NASA-CR-188466] p 2408 N92-23558
EARTH ENVIRONMENT
JPRS report: Science and technology. Central Eurasia: Life sciences
[JPRS-ULS-92-010] p 2412 N92-23706
EARTH GRAVITATION
The Earth's gravity field from satellite geodesy: A 30 year adventure p 2315 N92-23913
Progress in the spacewise approach to Aristoteles data reduction p 2315 N92-23914

Introductory remarks to the mission and system aspects session p 2315 N92-23916

EARTH MOVEMENTS
Determination of crustal motions using satellite laser ranging
[NASA-CR-190246] p 2408 N92-23540

EARTH OBSERVATIONS (FROM SPACE)
Evaluation of effective characteristic in forest field p 2397 N92-23473
Verification of the effectiveness of MOS-1 MESSR in the field of disaster prevention p 2397 N92-23474
Estimation of sea surface temperatures using MOS-1, GMS, and NOAA p 2398 N92-23475
Monitoring of ocean conditions by using MOS-1 data p 2398 N92-23476
Study of MOS-1 MESSR data for variability of the branch (Warm Streamer) from warm eddy and for fishing ground p 2398 N92-23477
Applicability of MESSR and VTIR data for marine observation p 2398 N92-23478
The geophysical impact of the Aristoteles mission p 2315 N92-23915

EARTH OBSERVING SYSTEM (EOS)
Proceedings on MOS-1 data evaluation
[HE-90015] p 2396 N92-23465
Outline of utilization results of MOS-1 data p 2396 N92-23466
Measurements of rain rate distribution by MOS-1 MSR p 2396 N92-23467
Application of ground-based laser beacon for Earth image calibration, 3 p 2396 N92-23468
Estimation of MTF of MOS-1 MESSR images p 2397 N92-23469
Investigations on verification of the data observed by the MESSR and VTIR, and on interannual trend in the MSR data p 2397 N92-23470
Verification of MESSR and VTIR, and time variation of MSR performance p 2397 N92-23471
Signal processing of the data obtained by MOS-1 MSR p 2397 N92-23472
Retrieval of upper precipitable water profile from MOS-1 VTIR water vapor channel p 2398 N92-23479
Earth observing system: NASA's EOSDIS development approach is risky
[GAO/IMTEC-92-24] p 2401 N92-23686

EARTH ORBITAL ENVIRONMENTS
Measured space environmental effects to LDEF during retrieval p 2335 N92-23285
Hypervelocity impact microfoil perforations in the LEO space environment (LDEF, MAP AO-023 experiment) p 2336 N92-23312

EARTH ORBITS
Induced radioactivity in LDEF components p 2440 N92-23300
Preliminary micrometeoroid and debris effects on LDEF thermal control surfaces p 2336 N92-23324
STS investigators' guide
[NASA-TM-105523] p 2321 N92-23524
From Earth to orbit --- assessment of transportation options
[NASA-CR-190216] p 2321 N92-23980

EARTH ORIENTATION
Determination of crustal motions using satellite laser ranging
[NASA-CR-190246] p 2408 N92-23540

EARTH PLANETARY STRUCTURE
On the principle of Aristoteles p 2314 N92-23911
Mission objectives and scientific rationale for the magnetometer mission p 2315 N92-23912

EARTH RADIATION BUDGET
Clouds, surface temperature, and the tropical and subtropical radiation budget p 2410 N92-23431

EARTH SCIENCES
JPRS report: Science and technology. USSR: Earth sciences
[JPRS-UES-91-005] p 2392 N92-23707

EARTHNET
Data distribution and reduction approaches to data distribution: The Earthnet experience p 2317 N92-23926

ECLIPSING BINARY STARS
Testing the solar paradigm for chromospheric activity in RS CVN binaries: Moderate resolution spectroscopy of solar active regions p 2459 N92-23171

ECOLOGY
JPRS report: Science and technology. USSR: Earth sciences
[JPRS-UES-91-005] p 2392 N92-23707

ECONOMIC ANALYSIS
Investigation on effective promotion of geothermal energy development
[DE92-783370] p 2403 N92-23684

ECONOMICS
Proceedings of the Second Annual Symposium on Industrial Involvement and Successes in Commercial Space
[NASA-TM-107812] p 2312 N92-23643
White paper: Preliminary assessment of LNG vehicle technology, economics, and safety issues
[PB92-137603] p 2383 N92-23680

ECOSYSTEMS
Acid rain and air pollution in desert park areas. Proceedings of a workshop: Management recommendations
[PB92-140532] p 2407 N92-24003

EDDY CURRENTS
Method for advanced material characterization by laser induced eddy current imaging
[NASA-CASE-GSC-13386-1] p 2386 N92-23376

EDDY VISCOSITY
Turbulence modeling p 2301 N92-23338
An improved k-epsilon model for near wall turbulence p 2303 N92-23349

EDGE DISLOCATIONS
The influence of chromium on structure and mechanical properties of B2 nickel aluminide alloys
[NASA-CR-189124] p 2351 N92-23566

EDGES
An edge preserving differential image coding scheme p 2417 N92-23419

EDITING
IGES: Application generator in disguise
[REPT-3.1.7] p 2424 N92-23882

EDITING ROUTINES (COMPUTERS)
MBT-WIRE: Intelligent CAD in wiring design
[REPT-1.1.4] p 2419 N92-23856
Controlling operations through procedures: APE (automated procedure editor)
[REPT-2.2.1] p 2422 N92-23875

EDUCATION
Training guidelines in non-destructive testing techniques
[DE92-615083] p 2386 N92-23258
Training users of a flexible decision support system: The effects of training content and user ability p 2453 N92-23730
Infrastructure and training of manpower for CAD/CAM systems
[REPT-4.2.2] p 2425 N92-23688
Symposium on Marketing for Technological Products
[MBB-UE-0014-90-PUB] p 2452 N92-23928
Requirements for the engineer training profile and definition of his role p 2452 N92-23932
Summer graduate research program for interns in science and engineering
[NASA-TM-107813] p 2470 N92-23958
Using microsoft excel applications in the graduate intern program at Goddard Space Flight Center p 2425 N92-23959
Fast aurora zone analysis p 2409 N92-23960

EFFICIENCY
The principle and design of a high-efficiency free-electron laser p 2380 N92-23687

EGGS
Eggs: The role of gravity in the establishment of the dorso-ventral axis in the amphibian embryo (7-IML-1) p 2357 N92-23607
The effect of space environment on the development and aging of Drosophila Melanogaster (7-IML-1) p 2357 N92-23608
Embryogenesis and organogenesis of Carausius morosus under space flight conditions (7-IML-1) p 2358 N92-23610
Biostack (14-IML-1) p 2361 N92-23627

EIGENVALUES
Numerical investigation of fluid-structure-interaction problems with the finite element method p 2332 N92-23844
Matching finite element models to modal data p 2333 N92-23848

EIGENVECTORS
Small solutions and completeness for linear functional differential equations
[PB92-149350] p 2431 N92-23250

EINSTEIN EQUATIONS
Rotating, radiating mass imbedded in a de Sitter universe p 2456 N92-23127

EJECTA
Gamma rays from SN1987A with the UCR double-Compton telescope p 2455 N92-23695

EL NINO
Climate System Monitoring (CSM). El Nino/Southern Oscillation (ENSO) diagnostic advisory, special issue p 2411 N92-23677
Wind, current and temperature data at 0 deg, 165 deg E: January 1986 to March 1991
[PB92-143080] p 2411 N92-23682

ELASTIC DEFORMATION
Contact stresses in meshing spur gear teeth: Use of an incremental finite element procedure
[NASA-TM-105388] p 2382 N92-23536

ELASTIC PROPERTIES
A damage mechanics model for beams p 2387 N92-23159
The statics, dynamics, and control of the elasticarm: A continuous beam manipulator p 2383 N92-23691
Maximal modal energy method: An overvaluing tool for low frequency prediction of structure acoustic response p 2324 N92-23791
Notched strength of composite materials p 2331 N92-23839

ELASTIC SCATTERING
A simple unfold method for Rutherford-scattering, intense ion-beam spectrographs
[DE92-008678] p 2445 N92-23749
CEPXS/ONELD: A one-dimensional coupled electron-photon discrete ordinates code package
[DE92-003146] p 2425 N92-24041

ELASTODYNAMICS
On the modelling of a deployable telescope elastic beam-type element for on-orbit multibody simulations p 2329 N92-23826

ELECTRIC BATTERIES
PHOTO: A computer simulation program for photovoltaic and hybrid energy systems. Document and user's guide
[PB92-141928] p 2403 N92-23683
Kansas State University electric vehicle site operator program
[DE92-008425] p 2384 N92-23896
Battery test facility hardware, software, and system operation
[DE92-008455] p 2372 N92-24063

ELECTRIC CHARGE
Monte Carlo transport in semiconductor
[DE92-008404] p 2371 N92-23902
NQR investigation of pressure-induced charge transfer in oxygen-deficient YBa2Cu3O(7-delta) (delta = 0.38)
[DE92-008441] p 2450 N92-24036

ELECTRIC CURRENT
Electrical and optical properties of high gain GaAs switches
[DE92-008668] p 2371 N92-23983

ELECTRIC DISCHARGES
Scaling study of pseudospark produced electron beam
[DE92-003231] p 2368 N92-23186

ELECTRIC FIELDS
Electrostatic image solution for the interaction of two dielectric spheres
[PB92-142199] p 2364 N92-23138
The subionospheric electromagnetic response to magnetopause processes p 2407 N92-23142
Theory study on fast wave absorption at the plasma edge
[PB92-141936] p 2444 N92-23663
Continuous profiling of magnetotelluric fields p 2401 N92-23703
Monte Carlo transport in semiconductor
[DE92-008404] p 2371 N92-23902

ELECTRIC GENERATORS
Limiting net greenhouse gas emissions in the United States, volume 1
[DE92-007593] p 2405 N92-23204

ELECTRIC MOTOR VEHICLES
Power beaming: Mission enabling for lunar exploration
[DE92-006727] p 2459 N92-23124
Kansas State University electric vehicle site operator program
[DE92-008425] p 2384 N92-23896

ELECTRIC MOTORS
Advanced electric motor technology: Flux mapping
[NASA-CR-184317] p 2372 N92-24047

ELECTRIC POTENTIAL
Analysis of a 37 kW cage-induction motor
[PB92-142116] p 2369 N92-23496
Injection seeding of a Q-switched alexandrite laser: Study of frequency stabilization p 2380 N92-23961
A dual anode nickel-hydrogen cell
[NASA-CASE-LEW-15212-1] p 2404 N92-24054

ELECTRIC POWER PLANTS
Geothermal energy program overview
[DE91-002172] p 2402 N92-23175

ELECTRIC POWER SUPPLIES
Power beaming: Mission enabling for lunar exploration
[DE92-006727] p 2459 N92-23124
A new VME based high voltage power supply for large experiments
[DE92-007199] p 2368 N92-23326
Compact Fusion Advanced Rankine (CFAR2) power cycle
[DE92-008577] p 2445 N92-23987
Self-deploying photovoltaic power system
[NASA-CASE-LEW-15308-1] p 2404 N92-24057

ELECTRICAL FAULTS
An algorithmic approach for fault-monitoring of electrical actuation system for all electric aircraft
[NAL-PD-AL-9111] p 2368 N92-23246
ELECTRICAL IMPEDANCE
Characterization of organic coatings with impedance measurements: A study of coating structure, adhesion and underfilm corrosion
[PB92-133479] p 2339 N92-23174
Thresholds of longitudinal instability of bunched beam in the presence of dominant inductive impedance
[DE92-617992] p 2436 N92-23274
Testing and analyses of electrochemical cells using frequency response
[NASA-TM-103580] p 2369 N92-23437
Wideband finite difference time domain implementation of surface impedance boundary conditions for good conductors
[NASA-CR-190098] p 2366 N92-23528
Closed parallel-plate chiral waveguides with boundary impedance conditions
[PB92-142397] p 2366 N92-23591
Continuous profiling of magnetotelluric fields p 2401 N92-23703
ELECTRICAL INSULATION
Evaluation of high temperature capacitor dielectrics
[NASA-TM-105622] p 2370 N92-23561
ELECTRICAL PROPERTIES
Electrical and optical properties of high gain GaAs switches
[DE92-008668] p 2371 N92-23983
The effect of co-implantation on the electrical activity of implanted carbon in GaAs
[DE92-008307] p 2371 N92-23985
ELECTRICAL RESISTIVITY
Continuous profiling of magnetotelluric fields p 2401 N92-23703
High-temperature superconductivity: Electron-doped cuprates and composites from alloy precursors p 2448 N92-23774
ELECTRO-OPTICS
Electro-optic resonant phase modulator
[NASA-CASE-NPO-18702-1-CU] p 2442 N92-23551
ELECTROCATALYSTS
Applications of x ray synchrotron radiation techniques to the study of dispersed electrocatalysts in high area materials
[DE92-007458] p 2346 N92-23199
ELECTROCHEMICAL CELLS
Fundamental electron transfer processes at the single crystal semiconductor/liquid interface
[DE92-008132] p 2447 N92-23275
ELECTROCHEMICAL CORROSION
In situ XANES study of the valence state of chromium during electrochemical polarization of AlCr alloys
[DE92-007452] p 2350 N92-23197
Application of x ray absorption spectroscopy to the study of corrosion and inhibition
[DE92-007456] p 2350 N92-23198
ELECTROCHEMISTRY
Dynamic structural effects and ultrafast biomolecular kinetics in photoinduced charge transfer reactions
[DE92-007562] p 2346 N92-23203
ELECTROLYSIS
Promotion of industrial technologies on the global environment
[DE92-769377] p 2405 N92-23454
ELECTROLYTES
Photoinduced electron transfer in ordered polymers
[DE92-008787] p 2355 N92-24037
ELECTROMAGNETIC FIELDS
Rotating, radiating mass imbedded in a de Sitter universe p 2456 N92-23127
Analysis of a 37 kW cage-induction motor
[PB92-142116] p 2369 N92-23496
Soviet articles on antenna theory
[DE92-008452] p 2366 N92-23575
Modular electromagnetic levitator
[DE92-008278] p 2367 N92-23900
ELECTROMAGNETIC INTERACTIONS
Test beam results from the D0 end electromagnetic calorimeter
[DE92-008299] p 2378 N92-23279
The electron-positron momentum density and Fermi surface of YBa2Cu3O(7-x)
[DE92-008605] p 2450 N92-24007
ELECTROMAGNETIC INTERFERENCE
Resonant transfer excitation: Interference effects
[DE92-007240] p 2439 N92-24026
ELECTROMAGNETIC RADIATION
Evaluation of mode purity of ordinary and extraordinary modes by fixed elliptically polarized wave for ECH and ECCD
[DE92-750961] p 2444 N92-23264
Soviet articles on antenna theory
[DE92-008452] p 2366 N92-23575
Vector circuit method applied for chiral dielectric slab waveguides
[PB92-142355] p 2367 N92-23679
ELECTROMAGNETIC SCATTERING
User's manual for three dimensional FDTD version C code for scattering from frequency-independent dielectric and magnetic materials
[NASA-CR-190109] p 2365 N92-23425
ELECTROMAGNETIC SPECTRA
Sensor compatibility/optimal sensor combinations p 2395 N92-23403
Optical properties of metallic multi-layer films
[DE92-615486] p 2443 N92-24029
ELECTROMAGNETIC WAVE TRANSMISSION
Biisotropic polarizer shield
[PB92-141878] p 2366 N92-23590
Closed parallel-plate chiral waveguides with boundary impedance conditions
[PB92-142397] p 2366 N92-23591
Vector circuit method applied for chiral dielectric slab waveguides
[PB92-142355] p 2367 N92-23679
ELECTROMAGNETS
Design considerations for an air core magnetic actuator
[NASA-TM-104229] p 2364 N92-23989
ELECTROMECHANICAL DEVICES
Advanced electric motor technology: Flux mapping
[NASA-CR-184317] p 2372 N92-24047
ELECTROMYOGRAPHY
Stress effects of human-computer interactions
[PB92-136001] p 2415 N92-23513
ELECTRON BEAM WELDING
Real-time measurement of electron beam weld penetration in uranium by acoustic emission monitoring
[DE92-008040] p 2384 N92-23908
ELECTRON BEAMS
Scaling study of pseudospark produced electron beam
[DE92-003231] p 2368 N92-23186
Oxidative degradation of polymers induced by ionizing radiation
[DE92-007657] p 2354 N92-23442
Real-time measurement of electron beam weld penetration in uranium by acoustic emission monitoring
[DE92-008040] p 2384 N92-23908
Pulsed electron beam precharger
[DE92-008693] p 2439 N92-24031
ELECTRON CYCLOTRON HEATING
Evaluation of mode purity of ordinary and extraordinary modes by fixed elliptically polarized wave for ECH and ECCD
[DE92-750961] p 2444 N92-23264
ELECTRON DENSITY (CONCENTRATION)
Investigations of breakdown of rare gases by short pulses of 1.06(mu)m laser radiation
[DE92-615399] p 2379 N92-23131
Infrared emission lines from highly ionized regions p 2460 N92-23162
Magnetic fluctuations and normal state properties of the t-J model at finite dopings
[DE92-617538] p 2447 N92-23452
Center for Macromolecular Crystallography, University of Alabama in Birmingham p 2313 N92-23650
Radar observations and dynamics of the polar summer mesosphere p 2408 N92-23702
ELECTRON ENERGY
Infrared emission lines from highly ionized regions p 2460 N92-23162
Reaction layer formation at the graphite/copper-chromium alloy interface
[NASA-CR-189147] p 2351 N92-23436
Fast wave current drive antenna performance on D3-D
[DE92-008052] p 2444 N92-23446
ELECTRON IRRADIATION
Defect behavior, carrier removal and predicted in-space injection annealing of InP solar cells
[NASA-TM-105624] p 2370 N92-23562
ELECTRON MICROSCOPY
The role of microstructural phenomena in magnetic thin films
[DE92-007960] p 2446 N92-23213
Surface structure and analysis with scanning tunneling microscopy and electron tunneling spectroscopy
[DE92-007747] p 2448 N92-23721
A method to determine resin flow during curing of composite laminates p 2342 N92-23938
ELECTRON MOBILITY
Nonequilibrium statistical operator in hot-electron transport theory
[DE92-615517] p 2446 N92-23260
ELECTRON PARAMAGNETIC RESONANCE
Resonant transfer excitation: Interference effects
[DE92-007240] p 2439 N92-24026
ELECTRON PHOTON CASCADES
CEPXS/ONELD: A one-dimensional coupled electron-photon discrete ordinates code package
[DE92-003146] p 2425 N92-24041
ELECTRON SCATTERING
Inelastic electron scattering from surfaces
[DE92-008129] p 2437 N92-23330
Optical properties of metallic multi-layer films
[DE92-615486] p 2443 N92-24029
ELECTRON SOURCES
Scaling study of pseudospark produced electron beam
[DE92-003231] p 2368 N92-23186
ELECTRON SPECTROSCOPY
Surface structure and analysis with scanning tunneling microscopy and electron tunneling spectroscopy
[DE92-007747] p 2448 N92-23721
ELECTRON TRANSFER
Dynamic structural effects and ultrafast biomolecular kinetics in photoinduced charge transfer reactions
[DE92-007562] p 2346 N92-23203
Fundamental electron transfer processes at the single crystal semiconductor/liquid interface
[DE92-008132] p 2447 N92-23275
Resonant transfer excitation: Interference effects
[DE92-007240] p 2439 N92-24026
Photoinduced electron transfer in ordered polymers
[DE92-008787] p 2355 N92-24037
ELECTRON TRANSITIONS
Probing picosecond flame dynamics with transient grating experiments
[DE92-003163] p 2346 N92-23181
ELECTRON TUNNELING
Surface structure and analysis with scanning tunneling microscopy and electron tunneling spectroscopy
[DE92-007747] p 2448 N92-23721
ELECTRONIC EQUIPMENT TESTS
Design for testability: Where are the goalposts?
[REPT-1.2.2] p 2420 N92-23861
Change in test-technology
[REPT-1.2.8] p 2421 N92-23867
ELECTRONIC SPECTRA
Resonant transfer excitation: Interference effects
[DE92-007240] p 2439 N92-24026
ELECTRONS
The electron-positron momentum density and Fermi surface of YBa2Cu3O(7-x)
[DE92-008605] p 2450 N92-24007
CEPXS/ONELD: A one-dimensional coupled electron-photon discrete ordinates code package
[DE92-003146] p 2425 N92-24041
ELECTROSTATIC PRECIPITATORS
Pulsed electron beam precharger
[DE92-008693] p 2439 N92-24031
ELECTROSTATICS
Electrostatic image solution for the interaction of two dielectric spheres
[PB92-142199] p 2364 N92-23138
Low frequency electrostatic modes in a magnetized dusty plasma
[DE92-617387] p 2444 N92-23209
Quasi-static image theory for the bi-isotropic (nonreciprocal chiral) sphere
[PB92-142371] p 2366 N92-23666
Electrostatic image theory for the dielectric sphere with an internal source
[PB92-142405] p 2366 N92-23667
Electrostatic image theory for the layered dielectric sphere
[PB92-142413] p 2367 N92-23668
ELEMENTARY EXCITATIONS
Solitary excitations in gyrotropic crystals
[DE92-617447] p 2446 N92-23271
ELEMENTARY PARTICLE INTERACTIONS
Research in high energy physics
[DE92-007967] p 2440 N92-23214
Research in high energy physics
[DE92-007968] p 2440 N92-23215
Solitary excitations in gyrotropic crystals
[DE92-617447] p 2446 N92-23271
Static multipole deformations in nuclei
[DE92-008250] p 2436 N92-23277
ELEMENTARY PARTICLES
Particle physics and cosmology
[DE92-008301] p 2456 N92-23153
High energy physics: Report of research accomplishments and future goals, FY 1992
[DE92-008543] p 2441 N92-23576
The notion of nonrelativistic isoparticle
[DE92-615215] p 2438 N92-23744
ELEVATION ANGLE
Fast aurora zone analysis p 2409 N92-23960
ELLIPTICAL GALAXIES
Nuclear winds in active galaxies p 2457 N92-23716

ELLIPTICAL ORBITS
Preliminary analysis of LDEF instrument A0187-1: Chemistry of Micrometeoroids Experiment
p 2458 N92-23315

EMBEDDING
Isometric embedding of median algebras into L1 (mu) spaces
[PB92-149343] p 2431 N92-23249

EMBRITTLEMENT
Spectral effects in radiation embrittlement
[DE92-007837] p 2447 N92-23444
Failure behaviour of high density polyethylene products with an embrittled surface layer due to UV exposure
[PB92-138494] p 2354 N92-23510

EMBRYOLOGY
Embryogenesis and organogenesis of Carausius morosus under space flight conditions (7-IML-1)
p 2358 N92-23610

EMBRYOS
Chrondrogenesis in micromass cultures of embryonic mouse limb mesenchymal cells exposed to microgravity (7-IML-1) p 2357 N92-23605
Eggs: The role of gravity in the establishment of the dorso-ventral axis in the amphibian embryo (7-IML-1)
p 2357 N92-23607
Embryogenesis and organogenesis of Carausius morosus under space flight conditions (7-IML-1)
p 2358 N92-23610

EMISSION
Limiting net greenhouse gas emissions in the United States, volume 2
[DE92-007592] p 2405 N92-23333
Promotion of industrial technologies on the global environment
[DE92-769374] p 2406 N92-23733

EMISSION SPECTRA
Infrared emission lines from highly ionized regions
p 2460 N92-23162
Strongly coupled cavity QED p 2442 N92-23999
An analysis of the WN shell nebula NGC 6888 using CCD imagery and spectrophotometry
p 2455 N92-24002
Line profile asymmetries in chromospherically active stars p 2458 N92-24015
The ALEXIS data processing package: An IDL-based system
[DE92-007429] p 2455 N92-24027

EMITTANCE
Testing the solar paradigm for chromospheric activity in RS CVN binaries: Moderate resolution spectroscopy of solar active regions p 2459 N92-23171
Scaling study of pseudospark produced electron beam
[DE92-003231] p 2368 N92-23186
Report from orbit sub-group of task force for MR synchrotron radiation project
[DE92-751024] p 2441 N92-23713

END EFFECTORS
Configuration control of seven-degree-of-freedom arms
[NASA-CASE-NPO-18607-1-CU] p 2382 N92-23553
Bar-holding prosthetic limb
[NASA-CASE-MFS-28481-1] p 2416 N92-24056
Retractable tool bit having slider type catch mechanism
[NASA-CASE-GSC-13358-1] p 2385 N92-24058

ENERGETIC PARTICLES
Biostack (14-IML-1) p 2361 N92-23627

ENERGY CONSERVATION
Promotion of industrial technologies on the global environment
[DE92-769374] p 2406 N92-23733
Promotion of industrial technologies on the global environment
[DE92-769376] p 2407 N92-24023

ENERGY CONVERSION
Direct conversion technology
[NASA-CR-190188] p 2403 N92-23569

ENERGY CONVERSION EFFICIENCY
Fundamental electron transfer processes at the single crystal semiconductor/liquid interface
[DE92-008132] p 2447 N92-23275
Direct conversion technology
[NASA-CR-190188] p 2403 N92-23569

ENERGY DISSIPATION
An x ray diagnostic of electron power loss
[DE92-008599] p 2444 N92-23523
Energy expenditure in space flight (doubly labelled water method) (8-IML-1) p 2359 N92-23620

ENERGY GAPS (SOLID STATE)
The electronic structure of icosahedral boron clusters
[DE92-008336] p 2447 N92-23451
Higher order temperature compensation of bandgap voltage references (I)
[PB92-142306] p 2370 N92-23497

ENERGY LEVELS
Semiempirical studies of atomic structure
[DE92-008143] p 2437 N92-23448
The electronic structure of icosahedral boron clusters
[DE92-008336] p 2447 N92-23451

ENERGY METHODS
Maximal modal energy method: An overvaluing tool for low frequency prediction of structure acoustic response
p 2324 N92-23791

ENERGY POLICY
National acid precipitation assessment program: Mission, goals, and program plan post 1990. Public review draft
[PB92-128248] p 2405 N92-23515
Investigation on effective promotion of geothermal energy development
[DE92-783370] p 2403 N92-23684

ENERGY SPECTRA
Cu charge fluctuations and anomalous behaviour in the phonon spectrum of La2CuO4
[DE92-617446] p 2446 N92-23270
The LDEF ultra heavy cosmic ray experiment
p 2461 N92-23306
Heavy ion measurement on LDEF
p 2440 N92-23308
PSD computations using Welch's method
[DE92-007419] p 2370 N92-23584
Gamma rays from SN1987A with the UCR double-Compton telescope p 2455 N92-23695

ENERGY STORAGE
Limiting net greenhouse gas emissions in the United States, volume 1
[DE92-007593] p 2405 N92-23204
Comparison of analytical and numerical modelling approaches for sizing of seasonal storage solar heating systems
[PB92-141829] p 2403 N92-23592

ENERGY TECHNOLOGY
Promotion of industrial technologies on the global environment
[DE92-769374] p 2406 N92-23733
Promotion of industrial technologies on the global environment
[DE92-769375] p 2406 N92-23734
Promotion of industrial technologies on the global environment
[DE92-769376] p 2407 N92-24023

ENERGY TRANSFER
Mutual scattering of carriers in two quantum wires
[DE92-616890] p 2366 N92-23580
Buckling and failure of thin elliptical delaminations in composites p 2331 N92-23835

ENGINE CONTROL
Control of a helicopter engine in low altitude flight
p 2310 N92-23122

ENGINE DESIGN
Effects of turbine cooling assumptions on performance and sizing of high-speed civil transport
[NASA-TM-105610] p 2311 N92-23537

ENGINE FAILURE
Health monitoring of reusable rocket engines
p 2320 N92-23762

ENGINE PARTS
Coupled multi-disciplinary simulation of composite engine structures in propulsion environment
[NASA-TM-105575] p 2388 N92-23267

ENGINE TESTS
Evaluation of research prototype vehicles equipped with direct injection 2-stroke cycle engines
[PB92-143692] p 2383 N92-23595

ENGINEERING
Summer graduate research program for interns in science and engineering
[NASA-TM-107813] p 2470 N92-23958
Applications of industrial engineering
p 2364 N92-23966

ENGINEERING DRAWINGS
Combining a CAD/CAM system with an advanced database architecture
[REPT-3.1.5] p 2423 N92-23880

ENTRAINMENT
An experimental investigation of entrainment and mixing in pulsed and exponential transverse jets
p 2375 N92-23995

ENTROPY
Use of control theory for analyzing stability of states in continuum thermodynamics
[PB92-136571] p 2451 N92-23136

ENVIRONMENT EFFECTS
Environmental effects on friction and wear of diamond and diamondlike carbon coatings
[NASA-TM-105634] p 2354 N92-23192
Development of 3-dimensional compact magnetic dosimeter for environmental magnetic field monitoring
[DE92-750825] p 2407 N92-23262
JPRS report: Science and technology. Central Eurasia: Life sciences
[JPRS-ULS-92-010] p 2412 N92-23706
Computer simulation of moisture penetration in structures p 2326 N92-23806
Acid rain and air pollution in desert park areas. Proceedings of a workshop: Management recommendations
[PB92-140532] p 2407 N92-24003

ENVIRONMENT MANAGEMENT
National acid precipitation assessment program: Mission, goals, and program plan post 1990. Public review draft
[PB92-128248] p 2405 N92-23515

ENVIRONMENT MODELS
LDEF data correlation to existing NASA debris environment models p 2336 N92-23321

ENVIRONMENT POLLUTION
Small or non pollutant solid propellants for space launchers p 2320 N92-23765

ENVIRONMENTAL CONTROL
Evaluating model accuracy for model-based reasoning
p 2427 N92-23362
Spacehab p 2313 N92-23647

ENVIRONMENTAL MONITORING
Development of 3-dimensional compact magnetic dosimeter for environmental magnetic field monitoring
[DE92-750825] p 2407 N92-23262
National air quality and emissions trends report, 1990
[PB92-141555] p 2406 N92-23517

ENVIRONMENTAL TESTS
Measured space environmental effects to LDEF during retrieval p 2335 N92-23285

ENZYME ACTIVITY
Center for Macromolecular Crystallography, University of Alabama in Birmingham p 2313 N92-23650

EPHEMERIDES
Precision GPS ephemerides and baselines
[NASA-CR-190247] p 2306 N92-23541

EPOXY MATRIX COMPOSITES
The effect of fatigue-induced damage on the mechanical properties of CFRP composites p 2339 N92-23157
The fracture behavior of carbon/epoxy laminates containing part through-the-thickness fiber breakage
p 2340 N92-23693
Microstructure and mechanical properties of carbon fibres: Relationship with the fibre-matrix adhesion in a carbon-epoxy composite p 2341 N92-23935
Impact and compression response of composite materials containing fortifiers p 2341 N92-23937
A method to determine resin flow during curing of composite laminates p 2342 N92-23938

EPOXY RESINS
A method to determine resin flow during curing of composite laminates p 2342 N92-23938

EQUATIONS OF MOTION
Galilei-isotopic symmetries
[DE92-615261] p 2431 N92-23129

EQUIVALENT CIRCUITS
MOSFET level 1 and 2 models in APLAC
[PB92-143379] p 2371 N92-23678

ERGODIC PROCESS
Stochastic games with average payoff criterion
[PB92-148634] p 2434 N92-23505

ERROR ANALYSIS
An architecture for the development of real-time fault diagnosis systems using model-based reasoning
p 2427 N92-23363
Intelligent fault isolation and diagnosis for communication satellite systems p 2427 N92-23365

ERROR CORRECTING CODES
Design of joint source/channel coders
[NASA-CR-189960] p 2417 N92-23416
Maximum aposteriori joint source/channel coding
p 2417 N92-23417
A joint source/channel coder design
p 2417 N92-23418
An edge preserving differential image coding scheme
p 2417 N92-23419
FAPES: An expert system for designing and optimising fault-tolerant arithmetic array processors
[REPT-1.1.2] p 2419 N92-23854

ERROR DETECTION CODES
FAPES: An expert system for designing and optimising fault-tolerant arithmetic array processors
[REPT-1.1.2] p 2419 N92-23854

ERRORS
Density of the F-statistic in the linear model with arbitrarily normal distributed errors
[PB92-128792] p 2434 N92-23731

ESTERS
Nuclear medicine program
[DE92-006979] p 2412 N92-23518
Vinyl capped addition polyimides
[NASA-CASE-LEW-15027-2] p 2355 N92-24053

ETHERS
High-temperature ignition of propane with MTBE as an additive: Shock-tube experiments and modeling
[DE92-008557] p 2348 N92-23715
EUCLIDEAN GEOMETRY
Euclidean-isotopic symmetries
[DE92-615260] p 2431 N92-23128
Galilei-isotopic symmetries
[DE92-615261] p 2431 N92-23129
EULER EQUATIONS OF MOTION
Improved shock-capturing of Jameson's scheme for the Euler equations
[PB92-148758] p 2373 N92-23251
A two-dimensional Euler solution for an unbladed jet engine configuration
[NASA-TM-105329] p 2374 N92-23560
EUROPEAN SPACE PROGRAMS
Ariane technology: From today into the next century
p 2318 N92-23751
The Solid-Earth Mission Aristoteles
[ESA-SP-329] p 2314 N92-23910
Introductory remarks to the mission and system aspects session p 2315 N92-23916
EVALUATION
Evaluation of a mechanical beam-switching system
[PB92-139773] p 2368 N92-23140
Research, Development, Test and Evaluation (R, D, T, and E) Programs (R-1), Department of Defense budget for fiscal year 1993
[PB92-127745] p 2451 N92-23247
Evaluation of the sensor effectiveness
p 2395 N92-23404
EVAPOTRANSPIRATION
Estimation of regional evapotranspiration with MOS-1 VTIR data p 2401 N92-23492
EVENT HORIZON
Synchronous parallel system for emulation and discrete event simulation
[NASA-CASE-NPO-18414-1-CU] p 2426 N92-24045
EXCITATION
The flip-flop nozzle extended to supersonic flows
[NASA-TM-105570] p 2304 N92-23269
Atomic physics of strongly correlated systems
[DE92-008356] p 2438 N92-23895
Multi-photon optical excitation of positronium
[DE92-008567] p 2438 N92-23903
EXCITONS
Solitary excitations in gyrotropic crystals
[DE92-617447] p 2446 N92-23271
EXHAUST EMISSION
Evaluation of research prototype vehicles equipped with direct injection 2-stroke cycle engines
[PB92-143692] p 2383 N92-23595
Survey on optimization of CO2 disposal system and carbon utilization technology
[DE92-769381] p 2407 N92-24024
EXHAUST GASES
Limiting net greenhouse gas emissions in the United States, volume 1
[DE92-007593] p 2405 N92-23204
Limiting net greenhouse gas emissions in the United States, volume 2
[DE92-007592] p 2405 N92-23333
Orbital Maneuvering Vehicle (OMV) plume and plume effects study
[NASA-CR-184292] p 2322 N92-23530
Characterization of rocket propellant combustion products
[DE92-007799] p 2337 N92-23722
EXOBIOLOGY
Publications of the exobiology program for 1990: A special bibliography
[NASA-TM-4364] p 2416 N92-23429
First International Microgravity Laboratory experiment descriptions
[NASA-TM-4353] p 2356 N92-23600
Genetic and molecular dosimetry of HZE radiation (7-IML-1) p 2357 N92-23603
EXPANDABLE STRUCTURES
Isometric embedding of median algebras into L1 (mu) spaces
[PB92-149343] p 2431 N92-23249
EXPANSION
A new test facility for measuring the coefficient of moisture expansion of advanced composite materials
p 2326 N92-23807
EXPERIMENT DESIGN
STS investigators' guide
[NASA-TM-105523] p 2321 N92-23524
First International Microgravity Laboratory experiment descriptions
[NASA-TM-4353] p 2356 N92-23600
Gravitropic responses of plants in the absence of a complicating G-force (6-IML-1) p 2356 N92-23601
A spaceflight experiment to investigate the effects of a range of unilateral blue light phototropic stimulations on the movements of wheat coleoptiles (6-IML-1)
p 2356 N92-23602
Genetic and molecular dosimetry of HZE radiation (7-IML-1) p 2357 N92-23603
Microgravitational effects on chromosome behavior (7-IML-1) p 2357 N92-23604
Chrondrogenesis in micromass cultures of embryonic mouse limb mesenchymal cells exposed to microgravity (7-IML-1) p 2357 N92-23605
Effect of microgravity and mechanical stimulation on the in vitro mineralization and resorption of fetal mouse long bones (7-IML-1) p 2357 N92-23606
Eggs: The role of gravity in the establishment of the dorso-ventral axis in the amphibian embryo (7-IML-1)
p 2357 N92-23607
The effect of space environment on the development and aging of Drosophila Melanogaster (7-IML-1)
p 2357 N92-23608
Effect of microgravity environment on cell wall regeneration, cell divisions, growth, and differentiation of plants from protoplasts (7-IML-1) p 2358 N92-23609
CRYOSTAT (18-IML-1) p 2362 N92-23636
EXPERT SYSTEMS
SLS-PLAN-IT: A knowledge-based blackboard scheduling system for Spacelab life sciences missions
p 2426 N92-23358
Distributed expert systems for ground and space applications p 2427 N92-23361
The achievement of spacecraft autonomy through the thematic application of multiple cooperating intelligent agents p 2427 N92-23364
Intelligent fault isolation and diagnosis for communication satellite systems p 2427 N92-23365
The use of artificial intelligence techniques to improve the multiple payload integration process
p 2428 N92-23370
Combining factual and heuristic knowledge in knowledge acquisition p 2429 N92-23372
A spatial data handling system for retrieval of images by unrestricted regions of user interest
p 2429 N92-23373
Multisensor data fusion p 2394 N92-23398
Evaluation of the sensor effectiveness
p 2395 N92-23404
FAPES: An expert system for designing and optimising fault-tolerant arithmetic array processors
[REPT-1.1.2] p 2419 N92-23854
Creative search systems as specific expert systems
[REPT-1.1.8] p 2420 N92-23859
Flexible Design Environment (FDE) for operation systems design
[REPT-2.3.5] p 2423 N92-23878
Expert systems: A mapping between symbol susceptible tasks and software tools p 2454 N92-24016
EXPOSURE
Preliminary analysis of LDEF instrument A0187-1: Chemistry of Micrometeoroids Experiment
p 2458 N92-23315
LDEF data correlation to existing NASA debris environment models p 2336 N92-23321
Preliminary micrometeoroid and debris effects on LDEF thermal control surfaces p 2336 N92-23324
Failure behaviour of high density polyethylene products with an embrittled surface layer due to UV exposure
[PB92-138494] p 2354 N92-23510
EXTRATERRESTRIAL RADIATION
Preliminary results from the heavy ions in space experiment p 2461 N92-23307
EYE (ANATOMY)
Low dose neutron late effects: Cataractogenesis
[DE92-005539] p 2414 N92-24033

F

FABRICATION
The effect of processing on strength of Nicalon fibers in Nicalon fiber-SiC matrix composites
[DE92-006978] p 2340 N92-23256
Method of fabricating superconducting device
[NASA-CASE-NPO-18394-1-CU] p 2370 N92-23552
Fabrication of a helical coil shape memory alloy actuator
[DE92-008399] p 2364 N92-23901
Crystallization behavior of poly(phenylene sulphide)
p 2342 N92-23940
FACE CENTERED CUBIC LATTICES
Ab initio pair potentials for FCC metals: An application of the method of Moebius transform
[DE92-617440] p 2351 N92-23582
FACTORIZATION
Analysis of ordering scheme for the unknowns during the solving of geodetic least squares systems
[PB92-137355] p 2432 N92-23514
FAILURE
Failure behaviour of high density polyethylene products with an embrittled surface layer due to UV exposure
[PB92-138494] p 2354 N92-23510
Fatigue analysis under random stresses
p 2325 N92-23795
An analysis of the relationship between induction motor current and shaft speed fluctuations
[DE92-007234] p 2371 N92-24025
FAILURE ANALYSIS
An algorithmic approach for fault-monitoring of electrical actuation system for all electric aircraft
[NAL-PD-AL-9111] p 2368 N92-23246
Experimental study of delamination growth in multidirectional CFRP-laminates under fatigue loading
p 2328 N92-23819
Buckling and failure of thin elliptical delaminations in composites p 2331 N92-23835
Test preparation for MOS digital circuits using heuristics for reliable fault simulation
[REPT-1.2.6] p 2421 N92-23865
Exact probabilistic testability measures for multi-output circuits
[REPT-1.2.7] p 2421 N92-23866
FAILURE MODES
Impact-induced delamination in (0(5), 90(5), 0(5)) carbon/peek composite laminates p 2341 N92-23936
FAN BLADES
Coupled multi-disciplinary simulation of composite engine structures in propulsion environment
[NASA-TM-105575] p 2388 N92-23267
FARM CROPS
National acid precipitation assessment program: 1990 integrated assessment report
[PB92-100346] p 2406 N92-23593
FASTENERS
Quick-connect fasteners for assembling devices in space
[NASA-CASE-MSC-21648-1] p 2385 N92-24051
FATIGUE (MATERIALS)
Evaluation of the elevated-temperature mechanical reliability of a HIPed silicon nitride
[DE92-007838] p 2354 N92-23223
Fatigue analysis under random stresses
p 2325 N92-23795
Experimental study of delamination growth in multidirectional CFRP-laminates under fatigue loading
p 2328 N92-23819
Dynamic characterization of composite materials
p 2330 N92-23832
FATIGUE LIFE
Damage development in titanium metal matrix composites subjected to cyclic loading
[NASA-TM-107597] p 2340 N92-23433
Investigation of fretting fatigue mechanisms on 7075-T6 aluminum alloy and Ti-6Al-4V titanium alloy
p 2352 N92-23725
Development of fatigue damage mechanics for application to the design of damage-tolerant composite components p 2324 N92-23793
Influence of the substrate on the solar cells interconnector: Stress distribution and fatigue life prediction p 2326 N92-23803
FATIGUE TESTS
Damage development in titanium metal matrix composites subjected to cyclic loading
[NASA-TM-107597] p 2340 N92-23433
High temperature dynamic engine seal technology development
[NASA-TM-105641] p 2381 N92-23435
Investigation of fretting fatigue mechanisms on 7075-T6 aluminum alloy and Ti-6Al-4V titanium alloy
p 2352 N92-23725
Characterization of interlaminar mode 1 and mode 2 fracture in CFRP laminates p 2325 N92-23794
The torsional fatigue behaviour of the in-plane and out-of-plane shear moduli of composite materials
p 2328 N92-23818
FAULT TOLERANCE
The 1992 Goddard Conference on Space Applications of Artificial Intelligence
[NASA-CP-3141] p 2426 N92-23356
A verified design of a fault-tolerant clock synchronization circuit: Preliminary investigations
[NASA-TM-107568] p 2416 N92-23559
FAPES: An expert system for designing and optimising fault-tolerant arithmetic array processors
[REPT-1.1.2] p 2419 N92-23854
Test preparation for MOS digital circuits using heuristics for reliable fault simulation
[REPT-1.2.6] p 2421 N92-23865
FAULTS
Intelligent fault isolation and diagnosis for communication satellite systems p 2427 N92-23365

FEASIBILITY ANALYSIS
Feasibility study of a synthesis procedure for array feeds to improve radiation performance of large distorted reflector antennas
[NASA-CR-190191] p 2364 N92-23245
Feasibility of payload sensitivity analyses for AR4 dynamic events p 2328 N92-23815
From Earth to orbit --- assessment of transportation options
[NASA-CR-190216] p 2321 N92-23980
Advanced electric motor technology: Flux mapping
[NASA-CR-184317] p 2372 N92-24047
FEDERAL BUDGETS
Research, Development, Test and Evaluation (R, D, T, and E) Programs (R-1), Department of Defense budget for fiscal year 1993
[PB92-127745] p 2451 N92-23247
FEEDBACK
Injection seeding of a Q-switched alexandrite laser: Study of frequency stabilization p 2380 N92-23961
FEEDBACK CONTROL
An algorithmic approach for fault-monitoring of electrical actuation system for all electric aircraft
[NAL-PD-AL-9111] p 2368 N92-23246
Feedback control of plasma equilibrium with control system aided by personal computer on the JIPP T-IIU tokamak
[DE92-750824] p 2444 N92-23261
Sensitivity l(sup 1) minimization with boundary zeros or poles
[PB92-141803] p 2433 N92-23658
The design and control of uncertain manipulator arms with decoupled inertia matrix p 2383 N92-23690
Analysis and control of nonlinear flexible manipulator p 2384 N92-23727
An advanced system for environmental sine testing: Basic principles revisited p 2325 N92-23799
Numerical simulations of wakes, blade-vortex interaction, flutter, and flutter suppression by feedback control p 2375 N92-23997
FEEDFORWARD CONTROL
Statistical process control system for VLSI fabrication
[REPT-1.3.4] p 2422 N92-23871
FEMALES
Stress effects of human-computer interactions
[PB92-136001] p 2415 N92-23513
FERMI LIQUIDS
Many-body problems in high temperature superconductivity
[DE92-617539] p 2447 N92-23453
FERMI SURFACES
The electron-positron momentum density and Fermi surface of YBa2Cu3O(7-x)
[DE92-008605] p 2450 N92-24007
FERMIUM
From ground state to fission fragments: A complex, multi-dimensional multi-path problem
[DE92-008488] p 2438 N92-23714
FERROMAGNETIC MATERIALS
Numerical study of the magnetic ordering and superconducting state of high-temperature superconductor p 2449 N92-23776
FERROUS METALS
JPRS report: Science and technology. Central Eurasia: Materials science
[JPRS-UMS-92-006] p 2363 N92-23709
FERTILIZATION
Eggs: The role of gravity in the establishment of the dorso-ventral axis in the amphibian embryo (7-IML-1) p 2357 N92-23607
FIBER COMPOSITES
The effect of fatigue-induced damage on the mechanical properties of CFRP composites p 2339 N92-23157
Development of fatigue damage mechanics for application to the design of damage-tolerant composite components p 2324 N92-23793
Damping behaviour of unidirectional fibre reinforced polymers p 2326 N92-23805
A new test facility for measuring the coefficient of moisture expansion of advanced composite materials p 2326 N92-23807
Dynamic characterization of composite materials p 2330 N92-23832
Mechanical behavior of composite materials and adhesive bonds at low temperatures p 2330 N92-23833
Composites, 1990
[NRC-32603] p 2341 N92-23933
Failure processes in the fibre-polymer interphase p 2341 N92-23934
On the application of micromechanics to the prediction of macroscopic thermal residual stresses in short-fiber reinforced Polyetheretherketone (PEEK) p 2343 N92-23942
Influence of maleic anhydride as a coupling agent on the performance of wood fiber: Polystyrene composites p 2343 N92-23945
Mechanical properties of glass bead filled ductile epoxy composites p 2344 N92-23947
Filling high density polyethylene with cellulosic fibers. 1: The effect of additives on fiber dispersion p 2344 N92-23948
Modeling and analysis of high-temperature inelastic deformation in metal matrix composites p 2345 N92-23996
Transverse deformation of unidirectional fiber-reinforced metal matrix composites p 2345 N92-24013
Vinyl capped addition polyimides
[NASA-CASE-LEW-15027-2] p 2355 N92-24053
FIBER OPTICS
Application of optical distributed sensing and computation to control of large space structures
[NASA-CR-190293] p 2442 N92-23567
Architectural impact of FDDI network on scheduling hard real-time traffic
[NASA-CR-190272] p 2425 N92-23583
Fiber-optic Raman spectroscopy for cure monitoring of advanced polymer composites
[DE92-008619] p 2355 N92-24068
FIBER ORIENTATION
On the test of mode 1 delamination and the importance of laminate lay-ups p 2343 N92-23943
Weldline strength in injection molded glass fiber reinforced polypropylene p 2344 N92-23949
FIBER RELEASE
Failure processes in the fibre-polymer interphase p 2341 N92-23934
Application of the microbond technique: Characterization of carbon-epoxy interfaces p 2343 N92-23944
FIBER STRENGTH
Strength and deformation behaviour of Kevlar and carbon composite sandwich structures for space applications p 2332 N92-23840
Microstructure and mechanical properties of carbon fibres: Relationship with the fibre-matrix adhesion in a carbon-epoxy composite p 2341 N92-23935
FIBERS
Filling high density polyethylene with cellulosic fibers. 1: The effect of additives on fiber dispersion p 2344 N92-23948
Mutual interference in multichannel fibre communication systems p 2367 N92-24019
FIELD EFFECT TRANSISTORS
Design and performance of 22 GHz coaxial low noise MESFET and HEMT amplifiers
[PB92-134071] p 2368 N92-23172
Higher order temperature compensation of bandgap voltage references (I)
[PB92-142306] p 2370 N92-23497
MOSFET level 1 and 2 models in APLAC
[PB92-143379] p 2371 N92-23678
FIELD STRENGTH
Strongly coupled cavity QED p 2442 N92-23999
FIELD THEORY (PHYSICS)
Theoretical model of the density of states of random binary alloys
[DE92-617438] p 2350 N92-23210
Research in high energy physics
[DE92-007967] p 2440 N92-23214
Research in high energy physics
[DE92-007968] p 2440 N92-23215
The 7th INS Scientific Computational Programs
[DE92-750967] p 2417 N92-23266
On the Stone-Weierstrass theorem for scalar and vector valued functions
[DE92-616916] p 2432 N92-23335
Constant curvature and non-perturbative W(sub 3) gravity
[DE92-616919] p 2451 N92-23503
Improved numerical methods for quantum field theory (outstanding junior investigator award)
[DE92-008730] p 2451 N92-23578
Family of Poisson structures on compact hermitian symmetric spaces
[PB92-149442] p 2433 N92-23670
Inequivalence of interior and exterior dynamical problems
[DE92-615214] p 2451 N92-23743
FIGHTER AIRCRAFT
Application of analytical and design tools for fighter wing aeroelastic tailoring p 2307 N92-23231
Design of a fighter aircraft vertical tail enhanced buffet environment survivability p 2307 N92-23235
FILAMENT WINDING
Fiber-optic Raman spectroscopy for cure monitoring of advanced polymer composites
[DE92-008619] p 2355 N92-24068
FILE MAINTENANCE (COMPUTERS)
The use of EDIF at Daisy/Cadnetix
[REPT-4.2.1] p 2424 N92-23887
Deleting pads in multi-layered printed circuits
[REPT-4.2.3] p 2425 N92-23889
FILM THICKNESS
Organic contamination of LDEF p 2339 N92-23290
Hypervelocity impact microfoil perforations in the LEO space environment (LDEF, MAP AO-023 experiment) p 2336 N92-23312
FINE STRUCTURE
Study of MOS-1 MESSR data for variability of the branch (Warm Streamer) from warm eddy and for fishing ground p 2398 N92-23477
FINITE DIFFERENCE THEORY
User's manual for three dimensional FDTD version C code for scattering from frequency-independent dielectric and magnetic materials
[NASA-CR-190109] p 2365 N92-23425
Wideband finite difference time domain implementation of surface impedance boundary conditions for good conductors
[NASA-CR-190098] p 2366 N92-23528
FINITE ELEMENT METHOD
Problem of membrane locking in finite element analysis of cylindrical shells
[PB92-133941] p 2387 N92-23137
Evaluation of MHOST analysis capabilities for a plate element --- finite element modeling
[NASA-TM-105387] p 2387 N92-23196
Contact stresses in meshing spur gear teeth: Use of an incremental finite element procedure
[NASA-TM-105388] p 2382 N92-23536
Nonlinear finite element analysis of space frames
[PB92-142447] p 2388 N92-23664
The discontinuous finite element method with the Taylor-Galerkin approach for nonlinear hyperbolic conservation laws p 2433 N92-23738
The use of modal synthesis in conjunction with nonlinear transient dynamic analysis p 2324 N92-23788
Improvements for interpretation of structural dynamics calculation using effective parameters for substructures p 2324 N92-23789
Nonlinear finite-element analysis of sandwich shells p 2326 N92-23802
Computer simulation of moisture penetration in structures p 2326 N92-23806
Acoustic cavity and fluid/structure interaction models: A methodological deterministic approach and problems encountered p 2327 N92-23813
Influence of microvibrations on spacecraft performances p 2329 N92-23825
The continuous elements method p 2330 N92-23829
Fluid-structure interaction problems: Development of special processors p 2332 N92-23845
Matching finite element models to modal data p 2333 N92-23848
Design parameter update of dynamic mathematical models in presence of test noise and mode pairing problems p 2333 N92-23850
Collapse of composite tubes under end moments
[NASA-TM-107605] p 2390 N92-23992
FINS
First approach to an integrated fin design p 2308 N92-23236
A fin optimisation study p 2308 N92-23237
FISHERIES
Utilization of satellite images for marine resources p 2399 N92-23480
Research project for practical usage of MOS-1 data collection system p 2399 N92-23485
FISHES
Study of MOS-1 MESSR data for variability of the branch (Warm Streamer) from warm eddy and for fishing ground p 2398 N92-23477
Our living oceans: The first annual report on the status of US living marine resources
[PB92-145689] p 2412 N92-23519
FISSION
From ground state to fission fragments: A complex, multi-dimensional multi-path problem
[DE92-008488] p 2438 N92-23714
FISSION PRODUCTS
From ground state to fission fragments: A complex, multi-dimensional multi-path problem
[DE92-008488] p 2438 N92-23714
FITTING
Quick-connect fasteners for assembling devices in space
[NASA-CASE-MSC-21648-1] p 2385 N92-24051
FLAME PROPAGATION
A study of hydrogen diffusion flames using PDF turbulence model p 2303 N92-23348

FLAMES
Probing picosecond flame dynamics with transient grating experiments
[DE92-003163] p 2346 N92-23181
FLAMMABILITY
Material considerations for habitable areas of manned spacecraft p 2323 N92-23785
FLAVOR (PARTICLE PHYSICS)
Search for atmospheric neutrino oscillations with the Soudan 2 detector
[DE92-007397] p 2437 N92-23328
FLEXIBLE BODIES
Technique to eliminate computational instability in multibody simulations employing the Lagrange multiplier
[NASA-TP-3220] p 2418 N92-23432
Application of optical distributed sensing and computation to control of large space structures
[NASA-CR-190293] p 2442 N92-23567
Mechanical testing on a composite flexible structure p 2331 N92-23834
On the analysis of liquid filled free-free tanks p 2332 N92-23843
Quick-connect fasteners for assembling devices in space
[NASA-CASE-MSC-21648-1] p 2385 N92-24051
Flexible robotic arm
[NASA-CASE-GSC-13161-1] p 2386 N92-24060
FLIGHT CHARACTERISTICS
Ariane 4 internal acoustic environment: Interpretation of flight data with a vibroacoustic model of the upper part of the launcher p 2321 N92-23811
The Delta 2 launcher p 2316 N92-23921
FLIGHT CONDITIONS
Embryogenesis and organogenesis of Carausius morosus under space flight conditions (7-IML-1) p 2358 N92-23610
FLIGHT CREWS
Radiation exposure of air carrier crewmembers 2
[PB92-140037] p 2414 N92-23139
FLIR DETECTORS
Passive optical and IR sensors
[MBB-UH-HE512] p 2394 N92-23392
Real-time radar processor p 2394 N92-23396
FLOOD DAMAGE
Verification of the effectiveness of MOS-1 MESSR in the field of disaster prevention p 2397 N92-23474
FLOQUET THEOREM
Small solutions and completeness for linear functional differential equations
[PB92-149350] p 2431 N92-23250
FLORIDA
Acid rain monitoring in East-Central Florida from 1977 to present
[NASA-CR-190152] p 2406 N92-23898
Tornadic supercell over Dade and Broward Counties (Florida) on January 15, 1991
[PB92-134444] p 2411 N92-23906
FLOW CHARACTERISTICS
Three-dimensional calculations of supersonic reacting flows using an LU scheme p 2304 N92-23354
A method to determine resin flow during curing of composite laminates p 2342 N92-23938
Distributed computer system in the large scale low speed wind tunnel
[NAL-TM-629] p 2312 N92-23979
FLOW DISTRIBUTION
Impinging axisymmetric jet p 2372 N92-23146
Microgravity dynamical behaviors of cryogenic liquid hydrogen reorientation and draining in space propulsion system p 2356 N92-23147
An adaptive-grid technique for simulation of complex unsteady flows p 2372 N92-23148
Applications of boundary integral methods to the study of steep free surface waves p 2372 N92-23149
The flip-flop nozzle extended to supersonic flows
[NASA-TM-105570] p 2304 N92-23269
RNG in turbulence and modeling of bypass transition p 2301 N92-23341
Turbulence modeling in supersonic combusting flows p 2302 N92-23342
Development of new flux splitting schemes p 2302 N92-23343
Progress of simulations for reacting shear layers p 2302 N92-23344
The study of PDF turbulence models in combustion
[PAPER-107] p 2302 N92-23345
Orbital Maneuvering Vehicle (OMV) plume and plume effects study
[NASA-CR-184292] p 2322 N92-23530
Grid generation and flow solution method for Euler equations on unstructured grids
[NASA-TM-4295] p 2305 N92-23533
Viscous-shock-layer analysis of hypersonic flows over long slender vehicles
[NASA-CR-189614] p 2374 N92-23543
Computations of unsteady multistage turbomachinery flows p 2311 N92-23671
An experimental investigation of entrainment and mixing in pulsed and exponential transverse jets p 2375 N92-23995
Numerical simulations of wakes, blade-vortex interaction, flutter, and flutter suppression by feedback control p 2375 N92-23997
FLOW VELOCITY
Optimizing flow rates in a queueing network with side constraints
[PB92-149996] p 2430 N92-23508
Mathematical modelling and numerical approximations for two-phase flow problems p 2375 N92-23672
Working gas pressure and flow effects on reactively sputtered molybdenum-oxide thin films
[DE92-008624] p 2450 N92-24069
FLOW VISUALIZATION
Numerical experiments with flows of elongated granules
[NASA-TM-105567] p 2381 N92-23226
The flip-flop nozzle extended to supersonic flows
[NASA-TM-105570] p 2304 N92-23269
An experimental investigation of entrainment and mixing in pulsed and exponential transverse jets p 2375 N92-23995
FLUE GASES
Pulsed electron beam precharger
[DE92-008693] p 2439 N92-24031
FLUENCE
Magnetic flux motion and flux pinning superconductors
[DE92-008243] p 2449 N92-23892
FLUID DYNAMICS
Experiments and modeling p 2301 N92-23339
The Critical Point Facility (CPF) p 2362 N92-23637
Acoustic cavity and fluid/structure interaction models: A methodological deterministic approach and problems encountered p 2327 N92-23813
Panel methods for aerodynamic analysis and design p 2309 N92-23955
FLUID MANAGEMENT
Microgravity dynamical behaviors of cryogenic liquid hydrogen reorientation and draining in space propulsion system p 2356 N92-23147
FLUID-SOLID INTERACTIONS
Numerical investigation of fluid-structure-interaction problems with the finite element method p 2332 N92-23844
Fluid-structure interaction problems: Development of special processors p 2332 N92-23845
A symmetric coupling between BEM and FEM for dynamical analysis of spacecraft p 2332 N92-23846
FLUORESCENCE
On board data formatting p 2394 N92-23394
Sensor interfaces p 2395 N92-23400
FLUTTER ANALYSIS
Aeroelastic stability analyses of two counter rotating propfan designs for a cruise missile model
[NASA-TM-105268] p 2387 N92-23191
Sensitivity analysis of dynamic aeroelastic responses p 2306 N92-23229
Multidisciplinary optimization studies using ASTROS p 2307 N92-23234
Simultaneous stress and flutter optimization for the wing of a transport aircraft equipped with four engines p 2308 N92-23238
FLUX DENSITY
Constructing a pulsar timing array p 2456 N92-23126
Advanced electric motor technology: Flux mapping
[NASA-CR-184317] p 2372 N92-24047
FLUX PINNING
TEM study of flux pinning defects in YBa2Cu3O7-delta produced by 580 MeV Sn ion irradiation
[DE92-006991] p 2448 N92-23574
Magnetic flux motion and flux pinning superconductors
[DE92-008243] p 2449 N92-23892
FLUX VECTOR SPLITTING
Development of new flux splitting schemes p 2302 N92-23343
Development of a new flux splitting scheme p 2303 N92-23352
High-Order Polynomial Expansions (HOPE) for flux-vector splitting p 2304 N92-23353
FOAMS
Radiation effects on polyethylene foam
[DE92-751046] p 2353 N92-23134
FOOD PROCESSING
Food Irradiation Newsletter, volume 15, number 2
[DE92-614951] p 2415 N92-23218
FORCE DISTRIBUTION
Comparison of multi-point modal test methods p 2333 N92-23849
Normal force of low aspect ratio wing-body combinations up to high angles of attack at supersonic speeds
[ESDU-91042] p 2309 N92-24009
FORCED VIBRATION
The free and forced vibrations of structures using the finite dynamic element method
[NASA-CR-190184] p 2388 N92-23427
FOREARM
Prosthetic helping hand
[NASA-CASE-MFS-28430-1] p 2416 N92-24044
FOREST MANAGEMENT
Evaluation of effective characteristic in forest field p 2397 N92-23473
FORESTS
Evaluation of effective characteristic in forest field p 2397 N92-23473
Climate
[PB92-150457] p 2410 N92-23520
National acid precipitation assessment program: 1990 integrated assessment report
[PB92-100346] p 2406 N92-23593
FORMALDEHYDE
The throes of star formation: A study of the Orion-KL and DR21(OH) molecular clouds p 2457 N92-23698
FORMAT
On board data formatting p 2394 N92-23394
Ground station p 2394 N92-23397
IGES: Application generator in disguise
[REPT-3.1.7] p 2424 N92-23882
FORMULATIONS
Nonlinear finite-element analysis of sandwich shells p 2326 N92-23802
FOSSIL FUELS
Limiting net greenhouse gas emissions in the United States, volume 1
[DE92-007593] p 2405 N92-23204
Kinetic measurements on elementary fossil fuel combustion reactions over wide temperatures ranges
[DE92-007535] p 2347 N92-23221
FOURIER TRANSFORMATION
X ray Fourier transform holography: Beyond the optical diffraction limit p 2377 N92-23144
FRACTURE MECHANICS
Boundary element analysis of fracture mechanics problems p 2387 N92-23125
Development of a crack arrest fracture toughness measurement procedure for quality assurance of plates and welds used for hydrocarbon storage tanks
[PB92-141753] p 2389 N92-23681
The fracture behavior of carbon/epoxy laminates containing part through-the-thickness fiber breakage p 2340 N92-23693
Localization of deformation and inelastic deformation of pressure-sensitive dilatant materials p 2389 N92-23737
Failure processes in the fibre-polymer interphase p 2341 N92-23934
Impact-induced delamination in (0(5), 90(5), 0(5)) carbon/peek composite laminates p 2341 N92-23936
On the test of mode 1 delamination and the importance of laminate lay-ups p 2343 N92-23943
Application of the microbond technique: Characterization of carbon-epoxy interfaces p 2343 N92-23944
FRACTURE STRENGTH
Development of a crack arrest fracture toughness measurement procedure for quality assurance of plates and welds used for hydrocarbon storage tanks
[PB92-141753] p 2389 N92-23681
Characterization of interlaminar mode 1 and mode 2 fracture in CFRP laminates p 2325 N92-23794
Morphology and mechanical performance of PPS/carbon composite p 2342 N92-23939
FRACTURES (MATERIALS)
Failure processes in the fibre-polymer interphase p 2341 N92-23934
FRACTURING
Boundary element analysis of fracture mechanics problems p 2387 N92-23125
Progressive fracture of polymer matrix composite structures: A new approach
[NASA-TM-105574] p 2339 N92-23194
Analysis of delamination related fracture processes in composites
[NASA-CR-190226] p 2340 N92-23532
FRAGMENTS
From ground state to fission fragments: A complex, multi-dimensional multi-path problem
[DE92-008488] p 2438 N92-23714
FRAMES
Nonlinear finite element analysis of space frames
[PB92-142447] p 2388 N92-23664
Page turning system
[NASA-CASE-GSC-13415-1] p 2386 N92-24059
FRANCK-CONDON PRINCIPLE
Dynamic structural effects and ultrafast biomolecular kinetics in photoinduced charge transfer reactions
[DE92-007562] p 2346 N92-23203

FREE CONVECTION
Analysis of gravity and topography on Earth and Venus: Comparisons of lithospheric and sublithospheric processes p 2409 N92-23772
FREE ELECTRON LASERS
Particle dynamics in a wave with variable amplitude [DE92-008340] p 2436 N92-23217
The principle and design of a high-efficiency free-electron laser p 2380 N92-23687
FREE VIBRATION
Evaluation of MHOST analysis capabilities for a plate element --- finite element modeling [NASA-TM-105387] p 2387 N92-23196
The free and forced vibrations of structures using the finite dynamic element method [NASA-CR-190184] p 2388 N92-23427
Free and forced response of nearly periodic multi-span beams and multi-bay trusses p 2389 N92-23699
Free vibration of thick isotropic and orthotropic cylindrical shells p 2389 N92-23773
FREQUENCIES
Free vibration of thick isotropic and orthotropic cylindrical shells p 2389 N92-23773
FREQUENCY ASSIGNMENT
Achieving spectrum conservation for the minimum-span and minimum-order frequency assignment problems [NASA-TM-105649] p 2322 N92-23187
FREQUENCY DISTRIBUTION
A frequency domain least squares method for modelling acoustic fields [ISVR-TR-196] p 2435 N92-23170
FREQUENCY MULTIPLIERS
Planar varactor frequency multiplier devices with blocking barrier [NASA-CASE-NPO-18428-1-CU] p 2369 N92-23464
FREQUENCY RANGES
Tabulations of propagation data over irregular terrain in the 75- to 8400-MHz frequency range. Part 5: Virginia [PB92-137413] p 2364 N92-23180
Minimization of vibrations by broadband sensitivity approach p 2330 N92-23828
FREQUENCY RESPONSE
Testing and analyses of electrochemical cells using frequency response [NASA-TM-103580] p 2369 N92-23437
FREQUENCY STABILITY
Injection seeding of a Q-switched alexandrite laser: Study of frequency stabilization p 2380 N92-23961
FRESNEL REFLECTORS
Properties of bi-isotropic Fresnel reflection coefficients [PB92-141886] p 2366 N92-23661
FRETTING
Investigation of fretting fatigue mechanisms on 7075-T6 aluminum alloy and Ti-6Al-4V titanium alloy p 2352 N92-23725
FRICTION
Environmental effects on friction and wear of diamond and diamondlike carbon coatings [NASA-TM-105634] p 2354 N92-23192
Employment of C.B. (Craig-Bampton) models for nonlinear dynamic analysis p 2327 N92-23814
FRICTIONLESS ENVIRONMENTS
The use of high temperature superconductors to levitate lunar telescope p 2456 N92-23962
FROGS
Eggs: The role of gravity in the establishment of the dorso-ventral axis in the amphibian embryo (7-IML-1) p 2357 N92-23607
FRUSTRATION
Numerical study of the magnetic ordering and superconducting state of high-temperature superconductor p 2449 N92-23776
FUEL CELLS
Demonstration of fuel cells to recover energy from landfill gas: Conceptual study [PB92-137520] p 2403 N92-23509
FUEL COMBUSTION
Kinetic measurements on elementary fossil fuel combustion reactions over wide temperatures ranges [DE92-007535] p 2347 N92-23221
A study of hydrogen diffusion flames using PDF turbulence model p 2303 N92-23348
FUEL CONSUMPTION
Evaluation of research prototype vehicles equipped with direct injection 2-stroke cycle engines [PB92-143692] p 2383 N92-23595
FUEL SYSTEMS
White paper: Preliminary assessment of LNG vehicle technology, economics, and safety issues [PB92-137603] p 2383 N92-23680
FUEL TANKS
Reusable launchers: New concepts and technological advances for the manufacturing of cryogenic tanks p 2319 N92-23760
FUEL TESTS
Effects of chemical equilibrium on turbine engine performance for various fuels and combustor temperatures [NASA-TM-105399] p 2311 N92-23254
Evaluation of research prototype vehicles equipped with direct injection 2-stroke cycle engines [PB92-143692] p 2383 N92-23595
FUNCTION SPACE
Sheaves of Schwartz distributions [DE92-615217] p 2432 N92-23331
On the Stone-Weierstrass theorem for scalar and vector valued functions [DE92-616916] p 2432 N92-23335
FUNCTIONAL ANALYSIS
Functional precision of National Weather Service upper-air measurements using VIZ Manufacturing Co. A radiosonde (model 1492-510) [PB92-137850] p 2410 N92-23439
FUNCTIONAL DESIGN SPECIFICATIONS
Functional design verification of ULSI components [REPT-1.3.7] p 2422 N92-23873
FUNCTIONS (MATHEMATICS)
Geometry of differential difference equations [PB92-148774] p 2431 N92-23182
FUSION
Fusion gain due to high energy ions accelerated by additional heating [DE92-751038] p 2443 N92-23133
FUSION (MELTING)
Melting of nickel clusters [DE92-006986] p 2351 N92-23573
FUSION REACTORS
Conceptual design of Fusion Experimental Reactor [DE92-751036] p 2443 N92-23132
Conceptual design of fusion experimental reactor (FER/ITER) [DE92-750949] p 2444 N92-23711
Annual report, 1 October 1990 - 30 September 1991 [DE92-008648] p 2380 N92-23891
Steady State Advanced Tokamak (SSAT): The mission and the machine [DE92-008983] p 2445 N92-24020
FUZZY SYSTEMS
Summary report: A preliminary investigation into the use of fuzzy logic for the control of redundant manipulators [NASA-CR-190277] p 2429 N92-23438

G

GALACTIC COSMIC RAYS
Radiation exposure of air carrier crewmembers 2 [PB92-140037] p 2414 N92-23139
Prediction of LDEF ionizing radiation environment p 2439 N92-23292
Charged particle LET-spectra measurements aboard LDEF p 2440 N92-23303
Preliminary results from the heavy ions in space experiment p 2461 N92-23307
GALERKIN METHOD
The discontinuous finite element method with the Taylor-Galerkin approach for nonlinear hyperbolic conservation laws p 2433 N92-23738
GALLIUM ARSENIDES
Electron polarization in modulation doped heterostructures [DE92-617490] p 2447 N92-23272
Fundamental electron transfer processes at the single crystal semiconductor/liquid interface [DE92-008132] p 2447 N92-23275
Chemical compatibility of cartridge materials [NASA-CR-190256] p 2356 N92-23555
Monte Carlo transport in semiconductor [DE92-008404] p 2371 N92-23902
Electrical and optical properties of high gain GaAs switches [DE92-008668] p 2371 N92-23983
The effect of co-implantation on the electrical activity of implanted carbon in GaAs [DE92-008307] p 2371 N92-23985
GALLIUM ISOTOPES
Results from the Soviet-American gallium experiment [DE92-007414] p 2438 N92-23747
GAME THEORY
Stochastic games with average payoff criterion [PB92-148634] p 2434 N92-23505
GAMMA RAY SPECTRA
Gamma ray spectrometry of LDEF samples at SRL p 2349 N92-23299
Induced radioactivity in LDEF components p 2440 N92-23300
Gamma rays from SN1987A with the UCR double-Compton telescope p 2455 N92-23695
GAMMA RAY SPECTROMETERS
Radioactivities of Long Duration Exposure Facility (LDEF) materials: Baggage and bonanzas p 2440 N92-23297
Gamma ray spectrometry of LDEF samples at SRL p 2349 N92-23299
GAMMA RAYS
Neutron induced gamma-ray production data [DE92-615322] p 2440 N92-23130
The origins of the cosmic x ray and gamma ray backgrounds p 2460 N92-23141
Gamma radiation survey of the LDEF spacecraft p 2460 N92-23293
Thermoluminescent dosimetry for LDEF experiment M0006 p 2461 N92-23301
Oxidative degradation of polymers induced by ionizing radiation [DE92-007657] p 2354 N92-23442
GAPS
Advanced numerical analyses for the optimisation of the structural behaviour of the intersegment connection for the Ariane 5 booster case p 2327 N92-23809
GAS CHROMATOGRAPHY
Characterization of rocket propellant combustion products [DE92-007799] p 2337 N92-23722
GAS COMPOSITION
Basic research on natural gas combustion phenomena [PB92-149681] p 2348 N92-23685
GAS COOLED REACTORS
Effect of minor elements on hot workability of Ni-Cr-W superalloys [DE92-750951] p 2351 N92-23263
GAS GENERATORS
Advanced ramjet systems for the propulsion of guided weapons [ETN-92-91195] p 2310 N92-23169
GAS IONIZATION
Investigations of breakdown of rare gases by short pulses of 1.06(mu)m laser radiation [DE92-615399] p 2379 N92-23131
GAS JETS
Three-dimensional calculations of supersonic reacting flows using an LU scheme p 2304 N92-23354
GAS PRESSURE
Working gas pressure and flow effects on reactively sputtered molybdenum-oxide thin films [DE92-008624] p 2450 N92-24069
GAS RECOVERY
Demonstration of fuel cells to recover energy from landfill gas: Conceptual study [PB92-137520] p 2403 N92-23509
GEAR TEETH
Contact stresses in meshing spur gear teeth: Use of an incremental finite element procedure [NASA-TM-105388] p 2382 N92-23536
Conception and development of improved analytical prediction models for fatigue induced tooth breakage due to cyclic bending in spur gear teeth p 2384 N92-23739
GENETICS
Improved interpretation of satellite altimeter data using genetic algorithms p 2402 N92-23369
Genetic and molecular dosimetry of HZE radiation (7-IML-1) p 2357 N92-23603
GEODESIC LINES
Existence of closed geodesics on 2-spheres [PB92-149434] p 2433 N92-23599
GEODESY
Analysis of ordering scheme for the unknowns during the solving of geodetic least squares systems [PB92-137355] p 2432 N92-23514
Determination of crustal motions using satellite laser ranging [NASA-CR-190246] p 2408 N92-23540
Analysis of gravity and topography on Earth and Venus: Comparisons of lithospheric and sublithospheric processes p 2409 N92-23772
On the principle of Aristoteles p 2314 N92-23911
Mission objectives and scientific rationale for the magnetometer mission p 2315 N92-23912
The geophysical impact of the Aristoteles mission p 2315 N92-23915
The GRADIOmeter payload p 2315 N92-23917
Aristoteles ground segment: Operational concept p 2316 N92-23923
Possible atmospheric research with Aristoteles p 2317 N92-23927
GEODETIC ACCURACY
A note on data quality: MSR data p 2400 N92-23489
The Earth's gravity field from satellite geodesy: A 30 year adventure p 2315 N92-23913
The potential use of fiducial ground networks p 2316 N92-23924

GEODETIC SATELLITES
The Solid-Earth Mission Aristoteles
[ESA-SP-329] p 2314 N92-23910
The Earth's gravity field from satellite geodesy: A 30 year adventure p 2315 N92-23913
The potential use of fiducial ground networks p 2316 N92-23924

GEODETIC SURVEYS
The interpretation of crustal dynamics data in terms of plate interactions and active tectonics of the Anatolian plate and surrounding regions in the Middle East
[NASA-CR-188466] p 2408 N92-23558

GEODYNAMICS
The interpretation of crustal dynamics data in terms of plate interactions and active tectonics of the Anatolian plate and surrounding regions in the Middle East
[NASA-CR-188466] p 2408 N92-23558
The geophysical impact of the Aristoteles mission p 2315 N92-23915

GEOGRAPHIC INFORMATION SYSTEMS
Center for Mapping, Ohio State University p 2314 N92-23655

GEOGRAPHY
A note on data quality: MSR data p 2400 N92-23489
Comparative study of digital MOS-1 MESSR, LANDSAT MSS, and IRS LISS-1 data for land cover classification in Sambalpur district, India p 2400 N92-23490

GEOIDS
Analysis of gravity and topography on Earth and Venus: Comparisons of lithospheric and sublithospheric processes p 2409 N92-23772

GEOLOGY
JPRS report: Science and technology. USSR: Earth sciences
[JPRS-UES-91-005] p 2392 N92-23707

GEOMAGNETISM
Continuous profiling of magnetotelluric fields p 2401 N92-23703
Prediction of solar and geomagnetic activity for ESA low-flying spacecraft p 2334 N92-23975

GEOMORPHOLOGY
Verification of the effectiveness of MOS-1 MESSR in the field of disaster prevention p 2397 N92-23474

GEOPHYSICS
Geophysical, chemical and biological measuring parameters p 2393 N92-23385
Solar-geophysical data Number 564, August 1991. Part 2 (comprehensive reports): Data for February 1991 and miscellaneous
[PB92-111699] p 2459 N92-23701
Continuous profiling of magnetotelluric fields p 2401 N92-23703
The geophysical impact of the Aristoteles mission p 2315 N92-23915
Solar-geophysical data Number 566, October 1991. Part 2 (comprehensive reports): Data for April 1991 and miscellaneous
[PB92-129402] p 2460 N92-23993

GEOPOTENTIAL
The Earth's gravity field from satellite geodesy: A 30 year adventure p 2315 N92-23913
Introductory remarks to the mission and system aspects session p 2315 N92-23916

GEOSTROPHIC WIND
A model of large-scale instabilities in the Jovian troposphere p 2459 N92-23704

GEOTHERMAL ENERGY CONVERSION
Geothermal energy program overview
[DE91-002172] p 2402 N92-23175
Investigation on effective promotion of geothermal energy development
[DE92-783370] p 2403 N92-23684
Geothermal direct use engineering and design guidebook
[DE92-008686] p 2404 N92-24030

GEOTHERMAL ENERGY UTILIZATION
Geothermal energy program overview
[DE91-002172] p 2402 N92-23175
Investigation on effective promotion of geothermal energy development
[DE92-783370] p 2403 N92-23684
Geothermal direct use engineering and design guidebook
[DE92-008686] p 2404 N92-24030

GEOTHERMAL RESOURCES
Geothermal energy program overview
[DE91-002172] p 2402 N92-23175
Investigation on effective promotion of geothermal energy development
[DE92-783370] p 2403 N92-23684
Geothermal direct use engineering and design guidebook
[DE92-008686] p 2404 N92-24030

GEOTHERMAL TECHNOLOGY
Geothermal energy program overview
[DE91-002172] p 2402 N92-23175
Geothermal direct use engineering and design guidebook
[DE92-008686] p 2404 N92-24030

GERMANIUM
Measurements of induced radioactivity in some LDEF samples p 2440 N92-23298
Temperature-dependent evolution of chemisorbed digermane in Ge thin film growth
[DE92-008098] p 2447 N92-23447

GERMANIUM ISOTOPES
Static multipole deformations in nuclei
[DE92-008250] p 2436 N92-23277
Results from the Soviet-American gallium experiment
[DE92-007414] p 2438 N92-23747

GERMINATION
Growth, differentiation and development of Arabidopsis thaliana under microgravity conditions (7-IML-1) p 2359 N92-23616

GLASS
Cracking investigation of Nd:YAG laser welded gold plated glass sealing alloys
[DE92-007971] p 2387 N92-23216
Phase transformations in SrAl2Si2O8 glass
[NASA-TM-105657] p 2449 N92-23890
Optimization of the laser glass composition for the Nova upgrade fusion laser system
[DE92-008606] p 2380 N92-24065

GLASS FIBER REINFORCED PLASTICS
Sliding friction test of self lubricating polymer composites for rolling bearing retainer
[NAL-TM-622] p 2384 N92-23779
Injection molding of long fiber reinforced thermoplastics: A comparison of extruded and pultruded materials with direct addition of roving strands p 2342 N92-23941
Weldline strength in injection molded glass fiber reinforced polypropylene p 2344 N92-23949

GLASS FIBERS
Injection molding of long fiber reinforced thermoplastics: A comparison of extruded and pultruded materials with direct addition of roving strands p 2342 N92-23941

GLASS LASERS
Annual report, 1 October 1990 - 30 September 1991
[DE92-008648] p 2380 N92-23891

GLOBAL POSITIONING SYSTEM
Precision GPS ephemerides and baselines
[NASA-CR-190247] p 2306 N92-23541
Dynamic positioning by GPS p 2306 N92-23729
On the principle of Aristoteles p 2314 N92-23911
Progress in the spacewise approach to Aristoteles data reduction p 2315 N92-23914
NASA's GPS tracking system for Aristoteles p 2316 N92-23919
Data distribution and reduction approaches to data distribution: The Earthnet experience p 2317 N92-23926

GLOBAL WARMING
On the global warming potentials of candidate gaseous diffusion plant coolants
[DE92-006640] p 2406 N92-23740

GLOBULAR CLUSTERS
Observing millisecond and binary pulsars p 2455 N92-24001

GLYCINE
A study of solution crystal growth in LOW-g (2-IML-1) p 2361 N92-23630

GOLD
Method of fabricating superconducting device
[NASA-CASE-NPO-18394-1-CU] p 2370 N92-23552

GOLD COATINGS
Cracking investigation of Nd:YAG laser welded gold plated glass sealing alloys
[DE92-007971] p 2387 N92-23216

GOLD ISOTOPES
Static multipole deformations in nuclei
[DE92-008250] p 2436 N92-23277

GOVERNMENT/INDUSTRY RELATIONS
Euromar industrial partners agreement p 2396 N92-23410

GRAIN BOUNDARIES
A study of aluminum-lithium alloy solidification using acoustic emission techniques
[NASA-CR-4437] p 2435 N92-23556

GRANULAR MATERIALS
Numerical experiments with flows of elongated granules
[NASA-TM-105567] p 2381 N92-23226

GRAPH THEORY
Control problem for a multi server loss system
[PB92-148675] p 2430 N92-23506

GRAPHITE
Reaction layer formation at the graphite/copper-chromium alloy interface
[NASA-CR-189147] p 2351 N92-23436
Investigation of plasma-sprayed laminates for high-temperature melting operations
[DE92-008416] p 2353 N92-24006

GRAPHITE-EPOXY COMPOSITES
High strength composites evaluation
[DE92-007264] p 2340 N92-23585
Effect of low-speed impact damage and damage location on behavior of composite panels
[NASA-TP-3196] p 2344 N92-23981

GRATINGS (SPECTRA)
Binary surface-relief gratings for array illumination in digital optics
[PB92-143585] p 2442 N92-23662

GRAVIRECEPTORS
Gravity related behavior of the acellular slime mold Physarum polycephalum (7-IML-1) p 2359 N92-23618

GRAVITATION
Constant curvature and non-perturbative W(sub 3) gravity
[DE92-616919] p 2451 N92-23503
Critical fluid thermal equilibration experiment (19-IML-1) p 2363 N92-23640

GRAVITATIONAL EFFECTS
Skeletal responses to spaceflight
[NASA-TM-103890] p 2414 N92-23424
Gravitropic responses of plants in the absence of a complicating G-force (6-IML-1) p 2356 N92-23601
Proliferation and performance of hybridoma cells in microgravity (7-IML-1) p 2358 N92-23614
Growth, differentiation and development of Arabidopsis thaliana under microgravity conditions (7-IML-1) p 2359 N92-23616
Transmission of gravistimulus in the statocyte of the lentil root (7-IML-1) p 2359 N92-23617
Gravity related behavior of the acellular slime mold Physarum polycephalum (7-IML-1) p 2359 N92-23618
Studies on penetration of antibiotic in bacterial cells in space conditions (7-IML-1) p 2359 N92-23619
Back pain in astronauts (8-IML-1) p 2360 N92-23622
The Critical Point Facility (CPF) p 2362 N92-23637
Near-critical point phenomena in fluids (19-IML-1) p 2362 N92-23638
Study of density distribution in a near-critical simple fluid (19-IML-1) p 2362 N92-23639
Microgravity acceleration measurement and environment characterization science (17-IML-1) p 2363 N92-23642
Spacehab p 2313 N92-23647

GRAVITATIONAL FIELDS
Rotating, radiating mass imbedded in a de Sitter universe p 2456 N92-23127
Determination of crustal motions using satellite laser ranging
[NASA-CR-190246] p 2408 N92-23540
Protein crystal growth (5-IML-1) p 2361 N92-23634
Study of density distribution in a near-critical simple fluid (19-IML-1) p 2362 N92-23639
Introductory remarks to the mission and system aspects session p 2315 N92-23916
Gravity field data products from the Aristoteles mission p 2317 N92-23925

GRAVITATIONAL PHYSIOLOGY
First International Microgravity Laboratory experiment descriptions
[NASA-TM-4353] p 2356 N92-23600
Gravitropic responses of plants in the absence of a complicating G-force (6-IML-1) p 2356 N92-23601
A spaceflight experiment to investigate the effects of a range of unilateral blue light phototropic stimulations on the movements of wheat coleoptiles (6-IML-1) p 2356 N92-23602
Microgravitational effects on chromosome behavior (7-IML-1) p 2357 N92-23604
Chrondrogenesis in micromass cultures of embryonic mouse limb mesenchymal cells exposed to microgravity (7-IML-1) p 2357 N92-23605
Effect of microgravity and mechanical stimulation on the in vitro mineralization and resorption of fetal mouse long bones (7-IML-1) p 2357 N92-23606
Eggs: The role of gravity in the establishment of the dorso-ventral axis in the amphibian embryo (7-IML-1) p 2357 N92-23607
The effect of space environment on the development and aging of Drosophila Melanogaster (7-IML-1) p 2357 N92-23608
Effect of microgravity environment on cell wall regeneration, cell divisions, growth, and differentiation of plants from protoplasts (7-IML-1) p 2358 N92-23609
Measurement of venous compliance (8-IML-1) p 2360 N92-23623
Positional and spontaneous nystagmus (8-IML-1) p 2360 N92-23624
Microgravity vestibular investigations (10-IML-1) p 2360 N92-23626

Center for Cell Research, Pennsylvania State University p 2314 N92-23653

GRAVITATIONAL WAVES
Observing millisecond and binary pulsars p 2455 N92-24001

GRAVITROPISM
Gravitropic responses of plants in the absence of a complicating G-force (6-IML-1) p 2356 N92-23601
Transmission of gravistimulus in the statocyte of the lentil root (7-IML-1) p 2359 N92-23617

GRAVITY GRADIOMETERS
On the principle of Aristoteles p 2314 N92-23911
The geophysical impact of the Aristoteles mission p 2315 N92-23915
The GRADIOmeter payload p 2315 N92-23917
The GRADIO accelerometer: Design and development status p 2316 N92-23918
Gravity field data products from the Aristoteles mission p 2317 N92-23925

GREEN'S FUNCTIONS
Application of the Green function technique in the microstrip patch antenna analysis
[PB92-142173] p 2367 N92-23907

GREENHOUSE EFFECT
Limiting net greenhouse gas emissions in the United States, volume 1
[DE92-007593] p 2405 N92-23204
Limiting net greenhouse gas emissions in the United States, volume 2
[DE92-007592] p 2405 N92-23333
On the global warming potentials of candidate gaseous diffusion plant coolants
[DE92-006640] p 2406 N92-23740

GREGORIAN ANTENNAS
Feasibility study of a synthesis procedure for array feeds to improve radiation performance of large distorted reflector antennas
[NASA-CR-190191] p 2364 N92-23245

GRID GENERATION (MATHEMATICS)
An adaptive-grid technique for simulation of complex unsteady flows p 2372 N92-23148
Grid generation and flow solution method for Euler equations on unstructured grids
[NASA-TM-4295] p 2305 N92-23533
A two-dimensional Euler solution for an unbladed jet engine configuration
[NASA-TM-105329] p 2374 N92-23560
Interactive solution-adaptive grid generation procedure
[NASA-TM-105432] p 2305 N92-23563
Computational fluid dynamics for propulsion technology: Geometric grid visualization in CFD-based propulsion technology research
[NASA-CR-190291] p 2375 N92-23568
Topics in numerical computation of compressible flow p 2375 N92-23692
User interface user's guide for HYPGEN
[NASA-CR-190304] p 2425 N92-23991
Semirigid construction of topological supergravities
[DE92-008772] p 2451 N92-24040

GROUND OPERATIONAL SUPPORT SYSTEM
Distributed expert systems for ground and space applications p 2427 N92-23361

GROUND STATE
Improved spin wave theory: An application to the spin-1/2 antiferromagnetic Heisenberg model on a square lattice
[DE92-617436] p 2448 N92-23504
Ground state searches in FCC intermetallics
[DE92-008300] p 2353 N92-23984

GROUND STATIONS
Ground station p 2394 N92-23397
Current definition of some development programs p 2395 N92-23405
NASA's GPS tracking system for Aristoteles p 2316 N92-23919
The potential use of fiducial ground networks p 2316 N92-23924

GROUND SUPPORT SYSTEMS
Aristoteles ground segment: Operational concept p 2316 N92-23923

GROUND WATER
Survey on subterranean disposal and storage technology of CO2
[DE92-769378] p 2405 N92-23455

GROUP THEORY
Family of Poisson structures on compact hermitian symmetric spaces
[PB92-149442] p 2433 N92-23670

GROWTH
Effect of microgravity environment on cell wall regeneration, cell divisions, growth, and differentiation of plants from protoplasts (7-IML-1) p 2358 N92-23609

GUANIDINES
Guanidine based vehicle/binders for use with oxides, metals, and ceramics
[NASA-CASE-LEW-15314-1] p 2354 N92-23461

GYROTROPISM
Solitary excitations in gyrotropic crystals
[DE92-617447] p 2446 N92-23271

H

HABITABILITY
Material considerations for habitable areas of manned spacecraft p 2323 N92-23785

HALF LIFE
Method for evaluating non-consistent data using two statistical criteria
[DE92-615195] p 2454 N92-23742

HALF SPACES
Properties of bi-isotropic Fresnel reflection coefficients
[PB92-141886] p 2366 N92-23661
Vector circuit method applied for chiral dielectric slab waveguides
[PB92-142355] p 2367 N92-23679

HALOGENATION
Nuclear medicine program
[DE92-006979] p 2412 N92-23518

HAMILTON-JACOBI EQUATION
Particle dynamics in a wave with variable amplitude
[DE92-008340] p 2436 N92-23217

HAMILTONIAN FUNCTIONS
Improved spin wave theory: An application to the spin-1/2 antiferromagnetic Heisenberg model on a square lattice
[DE92-617436] p 2448 N92-23504
Effective mass theory for abrupt heterojunctions
[DE92-617439] p 2448 N92-23581
Lie-admissible structure of Hamilton's original equations with external terms
[DE92-615216] p 2433 N92-23745
Closed systems with nonHamiltonian internal forces
[DE92-619234] p 2434 N92-24039

HAND (ANATOMY)
Bar-holding prosthetic limb
[NASA-CASE-MFS-28481-1] p 2416 N92-24056

HANFORD REACTORS
HEIS: An integrated information system for environmental restoration and monitoring at Hanford
[DE92-006467] p 2453 N92-23188

HARDNESS
Hardening in AlN induced by point defects
[DE92-007717] p 2352 N92-23720

HARDWARE
Hardware and software modularity p 2394 N92-23399
Current definition of some development programs p 2395 N92-23405
Battery test facility hardware, software, and system operation
[DE92-008455] p 2372 N92-24063

HARMONIC ANALYSIS
Harmonic wave propagation in two-dimensional periodic large space structures p 2330 N92-23830

HARMONIC OSCILLATORS
The Jordan-Schwinger realization of two-parametric quantum group Sl(sub q,s)(2)
[DE92-616891] p 2451 N92-23501

HEAD MOVEMENT
Positional and spontaneous nystagmus (8-IML-1) p 2360 N92-23624

HEART RATE
Stress effects of human-computer interactions
[PB92-136001] p 2415 N92-23513

HEAT BALANCE
Monsoon-ENSO relationships p 2404 N92-23160

HEAT EXCHANGERS
Modelling and experimental verification of a water alleviation system for the NASP --- National Aerospace Plane
[NASA-TM-105661] p 2373 N92-23224
Direct conversion technology
[NASA-CR-190188] p 2403 N92-23569

HEAT MEASUREMENT
A switched capacitor array basad system for high-speed calorimetry
[DE92-008288] p 2378 N92-23278

HEAT PIPES
A study of start-up characteristics of a potassium heat pipe from the frozen state
[NASA-CR-189173] p 2373 N92-23253

HEAT PUMPS
Comparison of analytical and numerical modelling approaches for sizing of seasonal storage solar heating systems
[PB92-141829] p 2403 N92-23592
Geothermal direct use engineering and design guidebook
[DE92-008686] p 2404 N92-24030

HEAT RESISTANT ALLOYS
Effect of minor elements on hot workability of Ni-Cr-W superalloys
[DE92-750951] p 2351 N92-23263
Effect of minor elements on corrosion behavior of Ni-Cr-W superalloys in HTGR helium
[DE92-751006] p 2352 N92-23712

HEAT SOURCES
A study of start-up characteristics of a potassium heat pipe from the frozen state
[NASA-CR-189173] p 2373 N92-23253

HEAT TRANSFER
The continuum modelling of two-phase flow systems
[DE92-007538] p 2373 N92-23202
Modelling and experimental verification of a water alleviation system for the NASP --- National Aerospace Plane
[NASA-TM-105661] p 2373 N92-23224
A study of start-up characteristics of a potassium heat pipe from the frozen state
[NASA-CR-189173] p 2373 N92-23253

HEAT TREATMENT
JPRS report: Science and technology. Central Eurasia: Materials science
[JPRS-UMS-92-005] p 2363 N92-23708
JPRS report: Science and technology. Central Eurasia: Materials science
[JPRS-UMS-92-006] p 2363 N92-23709
Fabrication of a helical coil shape memory alloy actuator
[DE92-008399] p 2364 N92-23901

HEATING
Geothermal direct use engineering and design guidebook
[DE92-008686] p 2404 N92-24030

HEAVY IONS
Studies of fluctuation processes in nuclear collisions
[DE92-008144] p 2440 N92-23276
Preliminary results from the heavy ions in space experiment p 2461 N92-23307
Heavy ion measurement on LDEF p 2440 N92-23308
The case for exotic beams at the Holifield Heavy Ion Research Facility
[DE92-008003] p 2441 N92-23445
TEM study of flux pinning defects in YBa2Cu3O7-delta produced by 580 MeV Sn ion irradiation
[DE92-006991] p 2448 N92-23574
Embryogenesis and organogenesis of Carausius morosus under space flight conditions (7-IML-1) p 2358 N92-23610
Dosimetric mapping inside biorack (7-IML-1) p 2358 N92-23611
Low dose neutron late effects: Cataractogenesis
[DE92-005539] p 2414 N92-24033

HEAVY NUCLEI
The LDEF ultra heavy cosmic ray experiment p 2461 N92-23306
The case for exotic beams at the Holifield Heavy Ion Research Facility
[DE92-008003] p 2441 N92-23445

HELICAL WINDINGS
Fabrication of a helical coil shape memory alloy actuator
[DE92-008399] p 2364 N92-23901

HELICES
Helix translation device --- shim for precision displacements
[NASA-CASE-GSC-13141-1] p 2382 N92-23548

HELICOPTER CONTROL
Control of a helicopter engine in low altitude flight p 2310 N92-23122

HELICOPTER ENGINES
Control of a helicopter engine in low altitude flight p 2310 N92-23122

HELICOPTER PERFORMANCE
Control of a helicopter engine in low altitude flight p 2310 N92-23122

HELICOPTERS
Development of a helicopter-borne 8-channel ranging scatterometer
[PB92-141977] p 2396 N92-23441

HELIUM
Effect of minor elements on corrosion behavior of Ni-Cr-W superalloys in HTGR helium
[DE92-751006] p 2352 N92-23712

HELIUM ISOTOPES
The isotopic composition of cosmic ray helium from 500 to 1100 MeV per nucleon p 2460 N92-23163
Ultrasonic investigation of (3)He-A vortices in low magnetic fields
[PB92-142256] p 2435 N92-23665

HELMHOLTZ RESONATORS
Evaluation of the applicability of Helmholtz resonators for low frequency acoustic liners
[PB92-138544] p 2436 N92-23588

HEMODYNAMIC RESPONSES
Measurement of venous compliance (8-IML-1) p 2360 N92-23623
HERMES MANNED SPACEPLANE
The challenge of the Hermes TPS shingles p 2322 N92-23823
HETEROJUNCTIONS
Electron polarization in modulation doped heterostructures [DE92-617490] p 2447 N92-23272
Planar varactor frequency multiplier devices with blocking barrier [NASA-CASE-NPO-18428-1-CU] p 2369 N92-23464
Effective mass theory for abrupt heterojunctions [DE92-617439] p 2448 N92-23581
Versatile bistable optical switches and latching optical logic using integrated photothyristors and surface-emitting lasers [DE92-008677] p 2442 N92-23748
HEURISTIC METHODS
SLS-PLAN-IT: A knowledge-based blackboard scheduling system for Spacelab life sciences missions p 2426 N92-23358
An architecture for the development of real-time fault diagnosis systems using model-based reasoning p 2427 N92-23363
Combining factual and heuristic knowledge in knowledge acquisition p 2429 N92-23372
HIERARCHIES
Combining factual and heuristic knowledge in knowledge acquisition p 2429 N92-23372
Using range analysis to support hierarchical test pattern generation [REPT-1.2.5] p 2421 N92-23864
HIGH ELECTRON MOBILITY TRANSISTORS
Design and performance of 22 GHz coaxial low noise MESFET and HEMT amplifiers [PB92-134071] p 2368 N92-23172
HIGH ENERGY ELECTRONS
Test beam results from the D0 end electromagnetic calorimeter [DE92-008299] p 2378 N92-23279
HIGH ENERGY INTERACTIONS
Fusion gain due to high energy ions accelerated by additional heating [DE92-751038] p 2443 N92-23133
Research in high energy physics [DE92-007967] p 2440 N92-23214
Research in high energy physics [DE92-007968] p 2440 N92-23215
Research in high energy physics [DE92-007966] p 2441 N92-23500
High energy physics: Report of research accomplishments and future goals, FY 1992 [DE92-008543] p 2441 N92-23576
A study of underground muons in the Soudan 2 detector p 2437 N92-23674
HIGH RESOLUTION
High resolution studies of NGC 1275 and the galactic center p 2455 N92-23675
HIGH SPEED
Controlling flexible robot arms using a high speed dynamics process [NASA-CASE-NPO-18499-1-CU] p 2385 N92-24042
Controlling under-actuated robot arms using a high speed dynamics process [NASA-CASE-NPO-18498-1-CU] p 2385 N92-24043
HIGH TEMPERATURE
Effects of chemical equilibrium on turbine engine performance for various fuels and combustor temperatures [NASA-TM-105399] p 2311 N92-23254
High temperature dynamic engine seal technology development [NASA-TM-105641] p 2381 N92-23435
Evaluation of high temperature capacitor dielectrics [NASA-TM-105622] p 2370 N92-23561
HIGH TEMPERATURE GAS COOLED REACTORS
Effect of minor elements on corrosion behavior of Ni-Cr-W superalloys in HTGR helium [DE92-751006] p 2352 N92-23712
HIGH TEMPERATURE GASES
The origins of the cosmic x ray and gamma ray backgrounds p 2460 N92-23141
HIGH TEMPERATURE SUPERCONDUCTORS
Cu charge fluctuations and anomalous behaviour in the phonon spectrum of La2CuO4 [DE92-617446] p 2446 N92-23270
On the electronegativity of the high-T(sub c) oxide superconductor [DE92-617537] p 2447 N92-23273
Solid State Technology Branch of NASA Lewis Research Center [NASA-TM-105159] p 2365 N92-23412
Microwave response of high transition temperature superconducting thin films p 2365 N92-23413
Properties of large area ErBa2Cu3O(7-x) thin films deposited by ionized cluster beams p 2365 N92-23414
Dependence of the critical temperature of laser-ablated YBa2Cu3O(7-delta) thin films on LaAlO3 substrate growth technique p 2365 N92-23415
Characterizing and testing a thermally isolating superconducting link for SAFIRE-like missions [NASA-CR-190196] p 2369 N92-23430
Many-body problems in high temperature superconductivity [DE92-617539] p 2447 N92-23453
Method of fabricating superconducting device [NASA-CASE-NPO-18394-1-CU] p 2370 N92-23552
TEM study of flux pinning defects in YBa2Cu3O7-delta produced by 580 MeV Sn ion irradiation [DE92-006991] p 2448 N92-23574
High-temperature superconductivity: Electron-doped cuprates and composites from alloy precursors p 2448 N92-23774
Numerical study of the magnetic ordering and superconducting state of high-temperature superconductor p 2449 N92-23776
The use of high temperature superconductors to levitate lunar telescope p 2456 N92-23962
Electronic structure in high temperature superconducting oxides [DE92-008566] p 2449 N92-23986
The electron-positron momentum density and Fermi surface of YBa2Cu3O(7-x) [DE92-008605] p 2450 N92-24007
HIGH TEMPERATURE TESTS
X ray based displacement measurement for hostile environments [NASA-TM-105551] p 2378 N92-23155
Tribological evaluation of an Al2O3-SiO2 ceramic fiber candidate for high temperature sliding seals [NASA-TM-105611] p 2339 N92-23190
A study of start-up characteristics of a potassium heat pipe from the frozen state [NASA-CR-189173] p 2373 N92-23253
Reaction layer formation at the graphite/copper-chromium alloy interface [NASA-CR-189147] p 2351 N92-23436
Characterization of polybenzimidazole (PBI) film at high temperatures [NASA-CR-189174] p 2370 N92-23538
Phase transformations in SrAl2Si2O8 glass [NASA-TM-105657] p 2449 N92-23890
HIGH VOLTAGES
A new VME based high voltage power supply for large experiments [DE92-007199] p 2368 N92-23326
HILBERT SPACE
Geometry of differential difference equations [PB92-148774] p 2431 N92-23182
HISTOLOGY
Three-dimensional cultured glioma cell lines [NASA-CASE-MSC-21843-1-NP] p 2413 N92-24052
HOLE GEOMETRY (MECHANICS)
M and D SIG progress report: Laboratory simulations of LDEF impact features p 2336 N92-23323
HOLES (ELECTRON DEFICIENCIES)
Defect behavior, carrier removal and predicted in-space injection annealing of InP solar cells [NASA-TM-105624] p 2370 N92-23562
NQR investigation of pressure-induced charge transfer in oxygen-deficient YBa2Cu3O(7-delta) (delta = 0.38) [DE92-008441] p 2450 N92-24036
HOLES (MECHANICS)
M and D SIG progress report: Laboratory simulations of LDEF impact features p 2336 N92-23323
Crack path prediction near an elliptical inhomogeneity p 2389 N92-23688
HOLOGRAPHY
X ray Fourier transform holography: Beyond the optical diffraction limit p 2377 N92-23144
Application of optical distributed sensing and computation to control of large space structures [NASA-CR-190293] p 2442 N92-23567
HOMOTROPY
Existence of closed geodesics on 2-spheres [PB92-149434] p 2433 N92-23599
HONEYCOMB CORES
Modeling of honeycomb core for sandwich CTE prediction p 2332 N92-23841
HOT ELECTRONS
Nonequilibrium statistical operator in hot-electron transport theory [DE92-615517] p 2446 N92-23260
HOT ISOSTATIC PRESSING
Evaluation of the elevated-temperature mechanical reliability of a HIPed silicon nitride [DE92-007838] p 2354 N92-23223
HOT WORKING
Effect of minor elements on hot workability of Ni-Cr-W superalloys [DE92-750951] p 2351 N92-23263
HOUSINGS
A flexible CPW package for a 30 GHz MMIC amplifier --- coplanar waveguide [NASA-TM-105630] p 2368 N92-23193
HUBBLE SPACE TELESCOPE
Detecting opportunities for parallel observations on the Hubble Space Telescope p 2426 N92-23359
HUMAN RESOURCES
Infrastructure and training of manpower for CAD/CAM systems [REPT-4.2.2] p 2425 N92-23888
HUMIDITY
Functional precision of National Weather Service upper-air measurements using VIZ Manufacturing Co. B radiosonde (model 1492-520) [PB92-137868] p 2410 N92-23494
HURRICANES
Diagnostic report of the National Hurricane Center: June and July 1991. Volume 4, number 1 [PB92-134501] p 2411 N92-23994
HYBRID PROPULSION
What future for hybrid rocket propulsion? p 2321 N92-23768
HYDROCARBONS
Liquid/supercritical fluid carbon dioxide cleaning of stainless steel components [DE92-006947] p 2348 N92-23572
HYDROCHLORIC ACID
Small or non pollutant solid propellants for space launchers p 2320 N92-23765
HYDRODYNAMICS
Near-critical point phenomena in fluids (19-IML-1) p 2362 N92-23638
Nuclear winds in active galaxies p 2457 N92-23716
Magnetotransport and responses of semiconductor microstructures p 2449 N92-23775
Type Ib supernovae and a new radiation hydrodynamics code p 2458 N92-24017
HYDROELASTICITY
A symmetric coupling between BEM and FEM for dynamical analysis of spacecraft p 2332 N92-23846
HYDROGEN
Production of metal powders by hydrogen stripping from loaded organic extractants [PB92-136464] p 2350 N92-23178
Hydrogen absorption by zirconium alloy cladding tube with surface oxide film [DE92-750962] p 2351 N92-23265
HYDROGEN FUELS
A study of hydrogen diffusion flames using PDF turbulence model p 2303 N92-23348
HYDROGEN PEROXIDE
Replacement of hydrogen peroxide cleaning with oxygen plasma [DE92-009020] p 2445 N92-23905
HYDROGEN PRODUCTION
Promotion of industrial technologies on the global environment [DE92-769377] p 2405 N92-23454
HYDROGENATION
Survey on fixation and utilization of carbon dioxide by catalytic hydrogenation [DE92-769380] p 2347 N92-23456
HYDROGRAPHY
Seaborne lidar system p 2393 N92-23389
Reconstructing the tropical Atlantic seasonal thermocline using planktonic foraminifera p 2412 N92-23769
HYDROMETALLURGY
Production of metal powders by hydrogen stripping from loaded organic extractants [PB92-136464] p 2350 N92-23178
HYDROSTATICS
Gravity related behavior of the acellular slime mold Physarum polycephalum (7-IML-1) p 2359 N92-23618
HYDROTHERMAL SYSTEMS
Geothermal energy program overview [DE91-002172] p 2402 N92-23175
HYPERONS
Theoretical nuclear reaction and structure studies using hyperons and photons [DE92-008587] p 2437 N92-23577
HYPERSONIC FLIGHT
Design challenges for the National Aero-Space Plane p 2310 N92-23822
Stretched skin concept for the entry aerodynamic decelerator system of planetary probes p 2331 N92-23836

HYPERSONIC FLOW
Hypersonic laminar flow computations over a blunt leading edged delta wing at three different chord Reynolds numbers
[FFA-TN-1991-40] p 2304 N92-23168
Development of a new flux splitting scheme p 2303 N92-23352
High-Order Polynomial Expansions (HOPE) for flux-vector splitting p 2304 N92-23353
Viscous-shock-layer analysis of hypersonic flows over long slender vehicles
[NASA-CR-189614] p 2374 N92-23543
Topics in numerical computation of compressible flow p 2375 N92-23692

HYPERSONIC VEHICLES
Modeling of compressible turbulent shear flows p 2301 N92-23340

HYPERVELOCITY IMPACT
Large craters on the meteoroid and space debris impact experiment p 2335 N92-23309
Study of cosmic dust particles on board LDEF: The FRECOPA experiments AO138-1 and AO138-2 p 2458 N92-23310
Meteoroid/space debris impacts on MSFC LDEF experiments p 2335 N92-23311
Hypervelocity impact microfoil perforations in the LEO space environment (LDEF, MAP AO-023 experiment) p 2336 N92-23312
Ion microprobe elemental analyses of impact features on interplanetary dust experiment sensor surfaces p 2458 N92-23318
Deriving the velocity distribution of meteoroids from the measured meteoroid impact directionality on the various LDEF surfaces p 2459 N92-23322
Preliminary micrometeoroid and debris effects on LDEF thermal control surfaces p 2336 N92-23324
The validation of hydrocodes for orbital debris impact simulation p 2323 N92-23784
Protection of spacecraft against meteroid/orbital debris impacts p 2323 N92-23786

HYSTERESIS
Mechanical testing on a composite flexible structure p 2331 N92-23834

I

ICE ENVIRONMENTS
Preliminary report on the observation of polar atmosphere and cryosphere by MOS-1 data received at Syowa Station p 2399 N92-23481

ICE FORMATION
Comparison of two-dimensional and three-dimensional droplet trajectory calculations in the vicinity of finite wings
[NASA-TM-105617] p 2373 N92-23154

ICE MAPPING
Preliminary report on the observation of polar atmosphere and cryosphere by MOS-1 data received at Syowa Station p 2399 N92-23481
Use of Marine Observation Satellite-1 in applied ocean science p 2400 N92-23487
Computer tutorial and animation of the normal ice cycle of the Laurentian Great Lakes of North America for 1960 - 1979
[PB92-129949] p 2401 N92-23659

ICE REPORTING
Use of Marine Observation Satellite-1 in applied ocean science p 2400 N92-23487

IGNITION
Basic research on natural gas combustion phenomena
[PB92-149681] p 2348 N92-23685
High-temperature ignition of propane with MTBE as an additive: Shock-tube experiments and modeling
[DE92-008557] p 2348 N92-23715

ILLUMINATORS
Binary surface-relief gratings for array illumination in digital optics
[PB92-143585] p 2442 N92-23662

IMAGE ANALYSIS
Feature detection in satellite images using neural network technology p 2427 N92-23366
Design of neural networks for classification of remotely sensed imagery p 2402 N92-23367
Proceedings on MOS-1 data evaluation
[HE-90015] p 2396 N92-23465
Estimation of MTF of MOS-1 MESSR images p 2397 N92-23469
Availability of MSR data for snow water estimation p 2399 N92-23482
Use of Marine Observation Satellite-1 in applied ocean science p 2400 N92-23487
A note on data quality: MSR data p 2400 N92-23489
Comparative study of digital MOS-1 MESSR, LANDSAT MSS, and IRS LISS-1 data for land cover classification in Sambalpur district, India p 2400 N92-23490
Data quality evaluation results MOS-1 verification program p 2400 N92-23491
Estimation of regional evapotranspiration with MOS-1 VTIR data p 2401 N92-23492

IMAGE CORRELATORS
Improved image classification with neural networks by fusing multispectral signatures with topological data p 2402 N92-23368

IMAGE PROCESSING
A signal and image processing object-based system using CLOS
[DE92-006826] p 2417 N92-23255
Feature detection in satellite images using neural network technology p 2427 N92-23366
Design of neural networks for classification of remotely sensed imagery p 2402 N92-23367
Improved image classification with neural networks by fusing multispectral signatures with topological data p 2402 N92-23368
Multisensor data fusion p 2394 N92-23398
An edge preserving differential image coding scheme p 2417 N92-23419
A robust low-rate coding scheme for packet video p 2417 N92-23420
A hybrid LBG/lattice vector quantizer for high quality image coding p 2418 N92-23421
A robust coding scheme for packet video p 2418 N92-23422
A progressive data compression scheme based upon adaptive transform coding: Mixture block coding of natural images p 2418 N92-23423
Proceedings on MOS-1 data evaluation
[HE-90015] p 2396 N92-23465
Application of ground-based laser beacon for Earth image calibration, 3 p 2396 N92-23468
Estimation of MTF of MOS-1 MESSR images p 2397 N92-23469
Multitemporal and multisensor approach with MOS data to natural resources evaluation in dry tropical Africa (Burkina Faso) p 2400 N92-23488
A note on data quality: MSR data p 2400 N92-23489
Comparative study of digital MOS-1 MESSR, LANDSAT MSS, and IRS LISS-1 data for land cover classification in Sambalpur district, India p 2400 N92-23490
Data quality evaluation results MOS-1 verification program p 2400 N92-23491
Estimation of regional evapotranspiration with MOS-1 VTIR data p 2401 N92-23492
Digital data registration and differencing compression system
[NASA-CASE-SSC-00010-2] p 2453 N92-23550

IMAGERY
Electrostatic image solution for the interaction of two dielectric spheres
[PB92-142199] p 2364 N92-23138
Quasi-static image theory for the bi-isotropic (nonreciprocal chiral) sphere
[PB92-142371] p 2366 N92-23666
Electrostatic image theory for the dielectric sphere with an internal source
[PB92-142405] p 2366 N92-23667
Electrostatic image theory for the layered dielectric sphere
[PB92-142413] p 2367 N92-23668
Voxel-based solid modeling
[REPT-1.1.3] p 2419 N92-23855

IMAGING RADAR
Euromar-Seastars: Summary p 2392 N92-23380
Provisional cost evaluation p 2395 N92-23408

IMAGING SPECTROMETERS
The imaging spectrometer p 2393 N92-23387

IMAGING TECHNIQUES
Method for advanced material characterization by laser induced eddy current imaging
[NASA-CASE-GSC-13386-1] p 2386 N92-23376
Sensor package for the North Sea p 2393 N92-23384
The imaging microwave radiometer p 2393 N92-23390
The imaging radar system p 2393 N92-23391

IMPACT DAMAGE
Experimental verification of a theory for the impact response of composite plates
[FFA-TN-1991-17] p 2339 N92-23167
Meteoroid, and debris special investigation group preliminary results: Size-frequency distribution and spatial density of large impact features on LDEF p 2336 N92-23314
SIMS chemical analysis of extended impact features from the trailing edge portion of experiment AO187-2 p 2349 N92-23316
IDE spatio-temporal impact fluxes and high time-resolution studies of multi-impact events and long-lived debris clouds p 2458 N92-23317
M and D SIG progress report: Laboratory simulations of LDEF impact features p 2336 N92-23323
Effect of low-speed impact damage and damage location on behavior of composite panels
[NASA-TP-3196] p 2344 N92-23981

IMPACT LOADS
The fracture behavior of carbon/epoxy laminates containing part through-the-thickness fiber breakage p 2340 N92-23693
The validation of hydrocodes for orbital debris impact simulation p 2323 N92-23784

IMPACT PREDICTION
The validation of hydrocodes for orbital debris impact simulation p 2323 N92-23784

IMPACT TESTS
Impact-induced delamination in (0(5), 90(5), 0(5)) carbon/peek composite laminates p 2341 N92-23936
Impact and compression response of composite materials containing fortifiers p 2341 N92-23937
Effect of low-speed impact damage and damage location on behavior of composite panels
[NASA-TP-3196] p 2344 N92-23981

IMPACTORS
LDEF impact craters formed by carbon-rich impactors: A preliminary report p 2336 N92-23319

IMPEDANCE MEASUREMENT
Characterization of organic coatings with impedance measurements: A study of coating structure, adhesion and underfilm corrosion
[PB92-133479] p 2339 N92-23174

IMPROVEMENT
Procedure improvement enterprises
[DE92-003222] p 2453 N92-23183
Development of solid propellant booster p 2320 N92-23767

IMPURITIES
Effects of impurities on the solidification and mechanical behaviour of primary and secondary commercial purity aluminium and aluminium alloys
[PB92-133511] p 2350 N92-23176
Transport calculations of chemically sputtered carbon near a plasma divertor surface
[DE92-009022] p 2445 N92-24021

INCLUSIONS
Crack path prediction near an elliptical inhomogeneity p 2389 N92-23688

INCOMPRESSIBLE FLOW
Center for Modeling of Turbulence and Transition (CMOTT). Research briefs: 1990
[NASA-TM-105243] p 2301 N92-23336
Unsteady three-dimensional incompressible algorithm based on artificial compressibility p 2375 N92-23700

INCONEL (TRADEMARK)
Chemical compatibility of cartridge materials
[NASA-CR-190256] p 2356 N92-23555

INDEPENDENT VARIABLES
Geophysical, chemical and biological measuring parameters p 2393 N92-23385

INDIUM ANTIMONIDES
Fermi level effects on dislocation formation in InAs(1-x)Sb(x) grown by MOCVD
[DE92-008332] p 2450 N92-24034

INDIUM COMPOUNDS
Rapid recrystallization of semiconductor thin films for photovoltaic applications p 2404 N92-23998

INDIUM PHOSPHIDES
Defect behavior, carrier removal and predicted in-space injection annealing of InP solar cells
[NASA-TM-105624] p 2370 N92-23562

INDUCTANCE
Thresholds of longitudinal instability of bunched beam in the presence of dominant inductive impedance
[DE92-617992] p 2436 N92-23274

INDUCTION HEATING
Induction boiler
[NASA-CASE-MFS-28634-1] p 2385 N92-24055

INDUCTION MOTORS
Analysis of a 37 kW cage-induction motor
[PB92-142116] p 2369 N92-23496
An analysis of the relationship between induction motor current and shaft speed fluctuations
[DE92-007234] p 2371 N92-24025

INDUSTRIAL MANAGEMENT
Procedure improvement enterprises
[DE92-003222] p 2453 N92-23183
The market for computer readable information p 2453 N92-23728
Formal methods for the evaluation of corporate CAD/CAM utilization
[REPT-1.1.1] p 2419 N92-23853
Computer integrated enterprise: The next step in CIM evolution
[REPT-3.2.2] p 2424 N92-23883

INDUSTRIAL PLANTS
Group technology, RCO: Rough-Cut Optimizer. The key to integration of plant operations
[REPT-1.1.6] p 2420 N92-23857
Computer integrated enterprise: The next step in CIM evolution
[REPT-3.2.2] p 2424 N92-23883

INDUSTRIES
Symposium on Marketing for Technological Products
[MBB-UE-0014-90-PUB] p 2452 N92-23928
Market directed thinking in a technological operation p 2452 N92-23929
Marketing qualification as a requirement for operating success p 2452 N92-23930
Marketing as a necessary condition for the successful development and commercialization of technological products p 2452 N92-23931
Requirements for the engineer training profile and definition of his role p 2452 N92-23932
Applications of industrial engineering p 2364 N92-23966
The use of STEP in an integrated manufacturing environment
[DE92-008417] p 2425 N92-24035

INELASTIC SCATTERING
Inelastic electron scattering from surfaces
[DE92-008129] p 2437 N92-23330
Mutual scattering of carriers in two quantum wires
[DE92-616890] p 2366 N92-23580

INERTIA
On the modelling of a deployable telescope elastic beam-type element for on-orbit multibody simulations p 2329 N92-23826

INERTIAL CONFINEMENT FUSION
A simple unfold method for Rutherford-scattering, intense ion-beam spectrographs
[DE92-008678] p 2445 N92-23749
Compact Fusion Advanced Rankine (CFAR2) power cycle
[DE92-008577] p 2445 N92-23987
Ion Microtomography (IMT) and Particle-Induced X ray Emission (PIXE) analysis direct drive of Inertial Confinement Fusion (ICF) targets
[DE92-008614] p 2446 N92-24067

INFERENCE
Logic programming and metadata specifications p 2429 N92-23375
Analysis of time series with missing values p 2434 N92-23777

INFORMATION RETRIEVAL
Creative search systems as specific expert systems
[REPT-1.1.8] p 2420 N92-23859

INFORMATION SYSTEMS
HEIS: An integrated information system for environmental restoration and monitoring at Hanford
[DE92-006467] p 2453 N92-23188
A spatial data handling system for retrieval of images by unrestricted regions of user interest p 2429 N92-23373
Earth observing system: NASA's EOSDIS development approach is risky
[GAO/IMTEC-92-24] p 2401 N92-23686
The use of STEP in an integrated manufacturing environment
[DE92-008417] p 2425 N92-24035

INFORMATION TRANSFER
Coordinating complex problem-solving among distributed intelligent agents p 2427 N92-23360
Design of joint source/channel coders
[NASA-CR-189960] p 2417 N92-23416

INFRARED ASTRONOMY
Annual progress report
[NASA-CR-190197] p 2454 N92-23428

INFRARED DETECTORS
The state of the development in Europe p 2392 N92-23382
Passive optical and IR sensors
[MBB-UH-HE512] p 2394 N92-23392
Characterizing and testing a thermally isolating superconducting link for SAFIRE-like missions
[NASA-CR-190196] p 2369 N92-23430

INFRARED INSTRUMENTS
Field evaluation of remote sensor measurements of wind, temperature, and moisture for ARM integrated sounding system research
[PB92-140714] p 2401 N92-23521

INFRARED LASERS
The laser bathymeter p 2393 N92-23388

INFRARED RADIATION
Infrared emission lines from highly ionized regions p 2460 N92-23162

INFRARED RADIOMETERS
Sensor package for the North Sea p 2393 N92-23384
Verification of the effectiveness of MOS-1 MESSR in the field of disaster prevention p 2397 N92-23474
Estimation of sea surface temperatures using MOS-1, GMS, and NOAA p 2398 N92-23475
Monitoring of ocean conditions by using MOS-1 data p 2398 N92-23476
Study of MOS-1 MESSR data for variability of the branch (Warm Streamer) from warm eddy and for fishing ground p 2398 N92-23477
Applicability of MESSR and VTIR data for marine observation p 2398 N92-23478
Retrieval of upper precipitable water profile from MOS-1 VTIR water vapor channel p 2398 N92-23479
Utilization of satellite images for marine resources p 2399 N92-23480
Preliminary report on the observation of polar atmosphere and cryosphere by MOS-1 data received at Syowa Station p 2399 N92-23481

INFRARED SCANNERS
Verification of MESSR and VTIR, and time variation of MSR performance p 2397 N92-23471

INFRARED SOURCES (ASTRONOMY)
Annual progress report
[NASA-CR-190197] p 2454 N92-23428

INFRARED SPECTROSCOPY
Characterizing and testing a thermally isolating superconducting link for SAFIRE-like missions
[NASA-CR-190196] p 2369 N92-23430

INHIBITORS
Transmission of gravistimulus in the statocyte of the lentil root (7-IML-1) p 2359 N92-23617

INHOMOGENEITY
Crack path prediction near an elliptical inhomogeneity p 2389 N92-23688

INJECTION LASERS
Injection seeding of a Q-switched alexandrite laser: Study of frequency stabilization p 2380 N92-23961

INJECTION MOLDING
Injection molding of long fiber reinforced thermoplastics: A comparison of extruded and pultruded materials with direct addition of roving strands p 2342 N92-23941
Mechanical properties of glass bead filled ductile epoxy composites p 2344 N92-23947

INLET FLOW
Control of a helicopter engine in low altitude flight p 2310 N92-23122

INPUT/OUTPUT ROUTINES
The use of EDIF at Daisy/Cadnetix
[REPT-4.2.1] p 2424 N92-23887

INSECTS
Food Irradiation Newsletter, volume 15, number 2
[DE92-614951] p 2415 N92-23218

INSERTION
Modeling of physical database design and performance analysis with emphasis on VSAM files p 2452 N92-23156

INSOLATION
Clouds, surface temperature, and the tropical and subtropical radiation budget p 2410 N92-23431

INSPECTION
Training guidelines in non-destructive testing techniques
[DE92-615083] p 2386 N92-23258

INSTRUMENT COMPENSATION
Investigations on verification of the data observed by the MESSR and VTIR, and on interannual trend in the MSR data p 2397 N92-23470
Signal processing of the data obtained by MOS-1 MSR p 2397 N92-23472

INTEGRAL EQUATIONS
Confidence intervals for discrete approximations to ill-posed problems
[PB92-143742] p 2432 N92-23511
Soviet articles on antenna theory
[DE92-008452] p 2366 N92-23575

INTEGRALS
Constant curvature and non-perturbative W(sub 3) gravity
[DE92-616919] p 2451 N92-23503

INTEGRATED CIRCUITS
A flexible CPW package for a 30 GHz MMIC amplifier --- coplanar waveguide
[NASA-TM-105630] p 2368 N92-23193
A switched capacitor array based system for high-speed calorimetry
[DE92-008288] p 2378 N92-23278
Solid State Technology Branch of NASA Lewis Research Center
[NASA-TM-105159] p 2365 N92-23412
An integrated test solution to address scan techniques
[REPT-1.2.3] p 2420 N92-23862
Test preparation for MOS digital circuits using heuristics for reliable fault simulation
[REPT-1.2.6] p 2421 N92-23865
Change in test-technology
[REPT-1.2.8] p 2421 N92-23867
Statistical process control system for VLSI fabrication
[REPT-1.3.4] p 2422 N92-23871
Statistical optimization of integrated circuits in order to reduce the sensitivity to variations in process parameters and environmental conditions
[REPT-1.3.6] p 2422 N92-23872

INTEGRATED OPTICS
Integrated optics in silicon-based aluminum oxide
[ISBN-90-9004261-X] p 2441 N92-23166
Electro-optic resonant phase modulator
[NASA-CASE-NPO-18702-1-CU] p 2442 N92-23551

INTERATOMIC FORCES
Analysis of forward and inverse problems in chemical dynamics and spectroscopy
[DE92-007732] p 2347 N92-23443
Ab initio pair potentials for FCC metals: An application of the method of Moebius transform
[DE92-617440] p 2351 N92-23582

INTERCEPTION
Interception of comets and asteroids on collision course with Earth
[DE92-007431] p 2458 N92-24028

INTERFACES
Influence of engineered interfaces on residual stresses and mechanical response in metal matrix composites
[NASA-TM-105438] p 2340 N92-23195
Sensor interfaces p 2395 N92-23400
National user interfaces p 2395 N92-23407
Reaction layer formation at the graphite/copper-chromium alloy interface
[NASA-CR-189147] p 2351 N92-23436
Properties of bi-isotropic Fresnel reflection coefficients
[PB92-141886] p 2366 N92-23661
The use of EDIF at Daisy/Cadnetix
[REPT-4.2.1] p 2424 N92-23887
Modifications for a communication interface board p 2368 N92-23963

INTERFACIAL ENERGY
Application of the microbond technique: Characterization of carbon-epoxy interfaces p 2343 N92-23944

INTERFACIAL TENSION
Numerical simulation of fluid behaviors in microgravity environment p 2363 N92-23719

INTERFEROMETRY
Study of density distribution in a near-critical simple fluid (19-IML-1) p 2362 N92-23639

INTERMETALLICS
Ground state searches in FCC intermetallics
[DE92-008300] p 2353 N92-23984

INTERNATIONAL COOPERATION
International cooperation p 2396 N92-23409
Euromar industrial partners agreement p 2396 N92-23410

INTERPLANETARY DUST
Study of cosmic dust particles on board LDEF: The FRECOPA experiments AO138-1 and AO138-2 p 2458 N92-23310
SIMS chemical analysis of extended impact features from the trailing edge portion of experiment AO187-2 p 2349 N92-23316
IDE spatio-temporal impact fluxes and high time-resolution studies of multi-impact events and long-lived debris clouds p 2458 N92-23317
Ion microprobe elemental analyses of impact features on interplanetary dust experiment sensor surfaces p 2458 N92-23318
JPRS report: Science and technology. Central Eurasia: Space
[JPRS-USP-92-002] p 2314 N92-23705

INTERPLANETARY MAGNETIC FIELDS
The subionospheric electromagnetic response to magnetopause processes p 2407 N92-23142

INTERPLANETARY SPACECRAFT
Synergistic use of high and low thrust propulsion systems for piloted missions to Mars
[NASA-CR-189138] p 2338 N92-24004

INTERPOLATION
Sensitivity l(sup 1) minimization with boundary zeros or poles
[PB92-141803] p 2433 N92-23658
Analysis of time series with missing values p 2434 N92-23777

INTERPROCESSOR COMMUNICATION
A framework for the support of VLSI (very large scale integration) design for manufacture
[REPT-1.3.1] p 2421 N92-23868

INTERSTELLAR GAS
The interstellar gas experiment p 2459 N92-23325

INTERSTELLAR MATTER
Nuclear winds in active galaxies p 2457 N92-23716

INVARIANCE
Beyond conventional quantum mechanics
[DE92-616892] p 2451 N92-23206
An exceptional N=8 superconformal algebra in two dimensions associated with F(4)
[DE92-616991] p 2435 N92-23207

Particle dynamics in a wave with variable amplitude
[DE92-008340] p 2436 N92-23217
Constant curvature and non-perturbative W(sub 3) gravity
[DE92-616919] p 2451 N92-23503
Ocean acoustic tomography inversion in the adiabatic-invariant approximation
[PB92-140466] p 2412 N92-23669

INVERSIONS
Ocean acoustic tomography inversion in the adiabatic-invariant approximation
[PB92-140466] p 2412 N92-23669

INVISCID FLOW
Improved shock-capturing of Jameson's scheme for the Euler equations
[PB92-148758] p 2373 N92-23251
Long time behavior of unsteady flow computations
[NASA-TM-105584] p 2374 N92-23565
Computations of unsteady multistage turbomachinery flows p 2311 N92-23671
Unsteady three-dimensional incompressible algorithm based on artificial compressibility p 2375 N92-23700
Numerical simulations of wakes, blade-vortex interaction, flutter, and flutter suppression by feedback control p 2375 N92-23997
Investigation of solution operators for the three dimensional unsteady Euler equations p 2376 N92-24018

IODIDES
Vapor crystal growth studies of single crystals of mercuric iodide (3-IML-1) p 2361 N92-23632
Mercury iodide nucleation and crystal growth in vapor phase (4-IML-1) p 2361 N92-23633

ION ACCELERATORS
The case for exotic beams at the Holifield Heavy Ion Research Facility
[DE92-008003] p 2441 N92-23445

ION ATOM INTERACTIONS
Atomic physics of strongly correlated systems
[DE92-008356] p 2438 N92-23895
Resonant transfer excitation: Interference effects
[DE92-007240] p 2439 N92-24026

ION BEAMS
Applications of multiple-ion irradiations to metals, ceramics, and polymers
[DE92-007686] p 2354 N92-23222
The case for exotic beams at the Holifield Heavy Ion Research Facility
[DE92-008003] p 2441 N92-23445
Semiempirical studies of atomic structure
[DE92-008143] p 2437 N92-23448
A simple unfold method for Rutherford-scattering, intense ion-beam spectrographs
[DE92-008678] p 2445 N92-23749

ION CYCLOTRON RADIATION
Theory study on fast wave absorption at the plasma edge
[PB92-141936] p 2444 N92-23663

ION EMISSION
Ion Microtomography (IMT) and Particle-Induced X ray Emission (PIXE) analysis direct drive of Inertial Confinement Fusion (ICF) targets
[DE92-008614] p 2446 N92-24067

ION ENGINES
Derated ion thruster design issues
[NASA-TM-105576] p 2337 N92-23534

ION IMPLANTATION
The effect of co-implantation on the electrical activity of implanted carbon in GaAs
[DE92-008307] p 2371 N92-23985

ION IRRADIATION
TEM study of flux pinning defects in YBa2Cu3O7-delta produced by 580 MeV Sn ion irradiation
[DE92-006991] p 2448 N92-23574

ION MICROSCOPES
Ion microprobe elemental analyses of impact features on interplanetary dust experiment sensor surfaces p 2458 N92-23318

ION PROBES
Ion microprobe elemental analyses of impact features on interplanetary dust experiment sensor surfaces p 2458 N92-23318

ION PROPULSION
Derated ion thruster design issues
[NASA-TM-105576] p 2337 N92-23534

IONIC COLLISIONS
Atomic physics of strongly correlated systems
[DE92-008356] p 2438 N92-23895

IONIC REACTIONS
Radar observations and dynamics of the polar summer mesosphere p 2408 N92-23702

IONIZED GASES
Investigations of breakdown of rare gases by short pulses of 1.06(mu)m laser radiation
[DE92-615399] p 2379 N92-23131

IONIZING RADIATION
Summary of ionizing radiation analysis on the Long Duration Exposure Facility p 2439 N92-23291
Prediction of LDEF ionizing radiation environment p 2439 N92-23292
Ionizing radiation calculations and comparisons with LDEF data p 2440 N92-23304
LDEF geometry/mass model for radiation analyses p 2440 N92-23305
Preliminary results from the heavy ions in space experiment p 2461 N92-23307
Oxidative degradation of polymers induced by ionizing radiation
[DE92-007657] p 2354 N92-23442

IONS
Fusion gain due to high energy ions accelerated by additional heating
[DE92-751038] p 2443 N92-23133
Atomic physics of strongly correlated systems
[DE92-008356] p 2438 N92-23895

IRRADIATION
Food Irradiation Newsletter, volume 15, number 2
[DE92-614951] p 2415 N92-23218
Oxidative degradation of polymers induced by ionizing radiation
[DE92-007657] p 2354 N92-23442
Irradiation of spices, herbs, and other vegetable seasonings: A compilation of technical data for its authorization and control
[DE92-619064] p 2415 N92-24022
Low dose neutron late effects: Cataractogenesis
[DE92-005539] p 2414 N92-24033

ISING MODEL
Numerical study of the magnetic ordering and superconducting state of high-temperature superconductor p 2449 N92-23776

ISOMERIZATION
Potential energy surfaces and reaction dynamics of polyatomic molecules
[DE92-008314] p 2437 N92-23450

ISOMORPHISM
Euclidean-isotopic symmetries
[DE92-615260] p 2431 N92-23128

ISOTHERMAL PROCESSES
Aging of polymer matrix composites at elevated temperatures p 2328 N92-23817

ISOTOPES
The case for exotic beams at the Holifield Heavy Ion Research Facility
[DE92-008003] p 2441 N92-23445

ISOTROPIC MEDIA
Quasi-static image theory for the bi-isotropic (nonreciprocal chiral) sphere
[PB92-142371] p 2366 N92-23666

ISOTROPY
Properties of bi-isotropic Fresnel reflection coefficients
[PB92-141886] p 2366 N92-23661
Free vibration of thick isotropic and orthotropic cylindrical shells p 2389 N92-23773

ITERATION
Improved interpretation of satellite altimeter data using genetic algorithms p 2402 N92-23369
Theory for iterative solution of large dynamical systems using parallel computation
[PB92-143304] p 2433 N92-23589
Efficient and robust design optimization of transonic airfoils p 2305 N92-23717

ITERATIVE SOLUTION
A comparative study of preconditioned Lanczos methods for nonsymmetric linear systems
[DE92-007530] p 2431 N92-23201
A multilevel preconditioner for domain decomposition boundary systems
[DE92-008055] p 2432 N92-23329
Theory for iterative solution of large dynamical systems using parallel computation
[PB92-143304] p 2433 N92-23589

J

JACOBI MATRIX METHOD
Configuration control of seven-degree-of-freedom arms
[NASA-CASE-NPO-18607-1-CU] p 2382 N92-23553

JAHN-TELLER EFFECT
Static multipole deformations in nuclei
[DE92-008250] p 2436 N92-23277

JAPANESE SPACE PROGRAM
Development of Japanese experiment module p 2323 N92-23781

JAPANESE SPACECRAFT
Proceedings on MOS-1 data evaluation
[HE-90015] p 2396 N92-23465
Outline of utilization results of MOS-1 data p 2396 N92-23466
Application of ground-based laser beacon for Earth image calibration, 3 p 2396 N92-23468
Estimation of MTF of MOS-1 MESSR images p 2397 N92-23469
Investigations on verification of the data observed by the MESSR and VTIR, and on interannual trend in the MSR data p 2397 N92-23470
Verification of MESSR and VTIR, and time variation of MSR performance p 2397 N92-23471
Signal processing of the data obtained by MOS-1 MSR p 2397 N92-23472

JET ENGINES
A two-dimensional Euler solution for an unbladed jet engine configuration
[NASA-TM-105329] p 2374 N92-23560

JET FLOW
An experimental investigation of entrainment and mixing in pulsed and exponential transverse jets p 2375 N92-23995

JET IMPINGEMENT
Impinging axisymmetric jet p 2372 N92-23146

JETS
Liquid hydrogen mass flow through a multiple orifice Joule-Thomson device
[NASA-TM-105583] p 2373 N92-23268

JOINING
Advanced numerical analyses for the optimisation of the structural behaviour of the intersegment connection for the Ariane 5 booster case p 2327 N92-23809

JOINTS (JUNCTIONS)
Analytical and experimental investigation of vibratory response in adhesively bonded and composite structures p 2345 N92-24012
Flexible robotic arm
[NASA-CASE-GSC-13161-1] p 2386 N92-24060

JOULE-THOMSON EFFECT
Liquid hydrogen mass flow through a multiple orifice Joule-Thomson device
[NASA-TM-105583] p 2373 N92-23268

JUPITER ATMOSPHERE
A model of large-scale instabilities in the Jovian troposphere p 2459 N92-23704

K

K-EPSILON TURBULENCE MODEL
Turbulence modeling in supersonic combusting flows p 2302 N92-23342
Progress of simulations for reacting shear layers p 2302 N92-23344
An improved k-epsilon model for near wall turbulence p 2303 N92-23349
Advancements in engineering turbulence modeling
[PAPER-105] p 2303 N92-23350
Simulations of free shear layers using a compressible kappa-epsilon model p 2304 N92-23355
Renormalization group analysis of the Reynolds stress transport equation
[NASA-TM-105588] p 2374 N92-23542
Kolmogorov behavior of near-wall turbulence and its application in turbulence modeling
[NASA-TM-105663] p 2376 N92-24050

KALMAN FILTERS
Application of optical distributed sensing and computation to control of large space structures
[NASA-CR-190293] p 2442 N92-23567

KEROSENE
Oxygen-kerosene liquid rocket engines with postburning generator gas and high pressure in combustion chamber p 2320 N92-23761

KINEMATICS
Precision GPS ephemerides and baselines
[NASA-CR-190247] p 2306 N92-23541
Configuration control of seven-degree-of-freedom arms
[NASA-CASE-NPO-18607-1-CU] p 2382 N92-23553
The kinematics of turbulent boundary layer structure p 2375 N92-23689
Ariane 5 structural definition of the upper composite p 2321 N92-23808

KINETIC ENERGY
Energy cycles in the summer tropical atmosphere over the North Atlantic Ocean p 2409 N92-23150

KINETIC EQUATIONS
Numerical experiments with flows of elongated granules
[NASA-TM-105567] p 2381 N92-23226

KINETICS
Near-critical point phenomena in fluids (19-IML-1) p 2362 N92-23638
Kinetics of combustion-related processes at high temperatures
[DE92-008790] p 2348 N92-24038

KNOWLEDGE BASES (ARTIFICIAL INTELLIGENCE)
Detecting opportunities for parallel observations on the Hubble Space Telescope p 2426 N92-23359
Multisensor data fusion p 2394 N92-23398
KNOWLEDGE REPRESENTATION
Combining factual and heuristic knowledge in knowledge acquisition p 2429 N92-23372
Creative search systems as specific expert systems [REPT-1.1.8] p 2420 N92-23859
KOLMOGOROFF THEORY
Kolmogorov behavior of near-wall turbulence and its application in turbulence modeling [NASA-TM-105663] p 2376 N92-24050

L

LAGRANGE MULTIPLIERS
Technique to eliminate computational instability in multibody simulations employing the Lagrange multiplier [NASA-TP-3220] p 2418 N92-23432
LAKE ICE
Computer tutorial and animation of the normal ice cycle of the Laurentian Great Lakes of North America for 1960 - 1979 [PB92-129949] p 2401 N92-23659
LAMB WAVES
Detecting Lamb waves with broad-band acousto-ultrasonic signals in composite structures [NASA-TM-105557] p 2386 N92-23189
LAMINAR BOUNDARY LAYER
RNG in turbulence and modeling of bypass transition p 2301 N92-23341
LAMINAR FLOW
Hypersonic laminar flow computations over a blunt leading edged delta wing at three different chord Reynolds numbers [FFA-TN-1991-40] p 2304 N92-23168
LAMINATES
Matrix dominated stress/strain behavior in polymeric composites: Effects of hold time, nonlinearity and rate dependency [NASA-TM-107595] p 2340 N92-23434
Free vibration of thick isotropic and orthotropic cylindrical shells p 2389 N92-23773
Characterization of interlaminar mode 1 and mode 2 fracture in CFRP laminates p 2325 N92-23794
Experimental study of delamination growth in multidirectional CFRP-laminates under fatigue loading p 2328 N92-23819
On the test of mode 1 delamination and the importance of laminate lay-ups p 2343 N92-23943
Effect of low-speed impact damage and damage location on behavior of composite panels [NASA-TP-3196] p 2344 N92-23981
Investigation of plasma-sprayed laminates for high-temperature melting operations [DE92-008416] p 2353 N92-24006
LANDFILLS
Demonstration of fuel cells to recover energy from landfill gas: Conceptual study [PB92-137520] p 2403 N92-23509
LARGE SPACE STRUCTURES
Artificial intelligence approach to planning the robotic assembly of large tetrahedral truss structures p 2426 N92-23357
Application of optical distributed sensing and computation to control of large space structures [NASA-CR-190293] p 2442 N92-23567
Free and forced response of nearly periodic multi-span beams and multi-bay trusses p 2389 N92-23699
The response surface method: An efficient tool to determine the failure probability of large structural systems p 2328 N92-23816
Minimization of vibrations by broadband sensitivity approach p 2330 N92-23828
Harmonic wave propagation in two-dimensional periodic large space structures p 2330 N92-23830
LASER APPLICATIONS
The laser bathymeter p 2393 N92-23386
Profiling and mapping of advanced materials using spatially resolved Raman spectroscopy [DE92-008304] p 2347 N92-23449
LASER ARRAYS
Analysis and development of dynamic selection of laser array elements [NASA-TM-4375] p 2379 N92-23557
LASER BEAMS
Investigations of breakdown of rare gases by short pulses of 1.06(mu)m laser radiation [DE92-615399] p 2379 N92-23131
Method for advanced material characterization by laser induced eddy current imaging [NASA-CASE-GSC-13386-1] p 2386 N92-23376
Analysis and development of dynamic selection of laser array elements [NASA-TM-4375] p 2379 N92-23557
LASER CUTTING
Improvement of laser machining processes [DE92-007801] p 2380 N92-23723
LASER FUSION
Annual report, 1 October 1990 - 30 September 1991 [DE92-008648] p 2380 N92-23891
Optimization of the laser glass composition for the Nova upgrade fusion laser system [DE92-008606] p 2380 N92-24065
LASER INDUCED FLUORESCENCE
The laser fluorosensor p 2393 N92-23386
LASER INTERFEROMETRY
Non contacting measurement of vibration p 2325 N92-23800
LASER MATERIALS
Limits of survivability and damage for optical components used in a high repetition rate visible laser [DE92-006896] p 2379 N92-23570
LASER OUTPUTS
Method for advanced material characterization by laser induced eddy current imaging [NASA-CASE-GSC-13386-1] p 2386 N92-23376
Multi-photon optical excitation of positronium [DE92-008567] p 2438 N92-23903
In situ particle size measurements using a two-color laser scattering technique [DE92-008634] p 2380 N92-24070
LASER PLASMAS
Annual report, 1 October 1990 - 30 September 1991 [DE92-008648] p 2380 N92-23891
LASER POWER BEAMING
Power beaming: Mission enabling for lunar exploration [DE92-006727] p 2459 N92-23124
LASER RANGE FINDERS
Determination of crustal motions using satellite laser ranging [NASA-CR-190246] p 2408 N92-23540
LASER TARGETS
Vacuum mechatronic laser alignment system on the NOVA laser [DE92-006898] p 2379 N92-23571
LASER WELDING
Nd: YAG laser welding aluminum alloys [DE92-003131] p 2381 N92-23177
Cracking investigation of Nd:YAG laser welded gold plated glass sealing alloys [DE92-007971] p 2387 N92-23216
LASERS
Lasers without inversion: Theory and experiment p 2379 N92-23143
Method for advanced material characterization by laser induced eddy current imaging [NASA-CASE-GSC-13386-1] p 2386 N92-23376
Improvement of laser machining processes [DE92-007801] p 2380 N92-23723
Versatile bistable optical switches and latching optical logic using integrated photothyristors and surface-emitting lasers [DE92-008677] p 2442 N92-23748
LATCHES
Retractable tool bit having latch type catch mechanism [NASA-CASE-GSC-13359-1] p 2381 N92-23378
Retractable tool bit having slider type catch mechanism [NASA-CASE-GSC-13358-1] p 2385 N92-24058
LATTICE VIBRATIONS
Cu charge fluctuations and anomalous behaviour in the phonon spectrum of La2CuO4 [DE92-617446] p 2446 N92-23270
LATTICES (MATHEMATICS)
Sphere packings centered at S-units of algebraic tori [PB92-136373] p 2434 N92-24061
LAUNCH DATES
The Aristoteles mission profile p 2316 N92-23922
LAUNCH VEHICLE CONFIGURATIONS
Brief history of the development of the EPS-structure p 2321 N92-23810
LAUNCH VEHICLES
Launch vehicle for orbital missions: COMET p 2313 N92-23645
Launcher Propulsion Towards the Year 2010 [ESA-SP-327] p 2318 N92-23750
Launch systems for future NASA missions p 2318 N92-23752
The USSR launchers programme p 2319 N92-23753
Space transfer concepts and analyses for exploration missions: Technical directive 10 [NASA-CR-184309] p 2317 N92-24048
LAUNCHERS
Launch systems for future NASA missions p 2318 N92-23752
Experience of the Chemical Automatics Design Bureau in creation of RD-0120 LOX/LH2 liquid rocket engine with thrust of 2 mn for Energia launcher p 2319 N92-23757
Ariane 5 structural definition of the upper composite p 2321 N92-23808
LAW (JURISPRUDENCE)
Irradiation of spices, herbs, and other vegetable seasonings: A compilation of technical data for its authorization and control [DE92-619064] p 2415 N92-24022
LAY-UP
On the test of mode 1 delamination and the importance of laminate lay-ups p 2343 N92-23943
LAYERS
Electrostatic image theory for the layered dielectric sphere [PB92-142413] p 2367 N92-23668
LEADING EDGES
Hypersonic laminar flow computations over a blunt leading edged delta wing at three different chord Reynolds numbers [FFA-TN-1991-40] p 2304 N92-23168
Radiation exposure of LDEF: Initial results p 2461 N92-23302
LEAST SQUARES METHOD
A frequency domain least squares method for modelling acoustic fields [ISVR-TR-196] p 2435 N92-23170
Analysis of ordering scheme for the unknowns during the solving of geodetic least squares systems [PB92-137355] p 2432 N92-23514
General P-T fit construction for He, N2, Ar, H2 and Ne VPT used at Fermilab [DE92-008851] p 2433 N92-23579
Progress in the spacewise approach to Aristoteles data reduction p 2315 N92-23914
LEAVES
A spaceflight experiment to investigate the effects of a range of unilateral blue light phototropic stimulations on the movements of wheat coleoptiles (6-IML-1) p 2356 N92-23602
LENNARD-JONES POTENTIAL
Melting of nickel clusters [DE92-006986] p 2351 N92-23573
LENS DESIGN
IMAX camera (12-IML-1) p 2363 N92-23641
LESIONS
Genetic and molecular dosimetry of HZE radiation (7-IML-1) p 2357 N92-23603
LEUKEMIAS
Friend leukemia virus transformed cells exposed to microgravity in the presence of DMSO (7-IML-1) p 2358 N92-23613
LEVITATION
Modular electromagnetic levitator [DE92-008278] p 2367 N92-23900
The use of high temperature superconductors to levitate lunar telescope p 2456 N92-23962
LIE GROUPS
Euclidean-isotopic symmetries [DE92-615260] p 2431 N92-23128
Galilei-isotopic symmetries [DE92-615261] p 2431 N92-23129
An exceptional N=8 superconformal algebra in two dimensions associated with F(4) [DE92-616991] p 2435 N92-23207
Family of Poisson structures on compact hermitian symmetric spaces [PB92-149442] p 2433 N92-23670
Lie-admissible structure of Hamilton's original equations with external terms [DE92-615216] p 2433 N92-23745
Closed systems with nonHamiltonian internal forces [DE92-619234] p 2434 N92-24039
LIFE (DURABILITY)
Reusable launchers: New concepts and technological advances for the manufacturing of cryogenic tanks p 2319 N92-23760
LIFE SCIENCES
JPRS report: Science and technology. Central Eurasia: Life sciences [JPRS-ULS-92-010] p 2412 N92-23706
LIFE SPAN
Low dose neutron late effects: Cataractogenesis [DE92-005539] p 2414 N92-24033
LIFE SUPPORT SYSTEMS
Evaluating model accuracy for model-based reasoning p 2427 N92-23362
LIFT
A review of Space Shuttle payload-bay lift-off flight data and analysis comparisons p 2322 N92-23796
LIGANDS
Nuclear medicine program [DE92-006979] p 2412 N92-23518

LIGHT BEAMS
Report from orbit sub-group of task force for MR synchrotron radiation project
[DE92-751024] p 2441 N92-23713
LIGHT EMITTING DIODES
Empirical characterization of a high intensity LED proximity sensor
[DE91-019074] p 2371 N92-23735
Versatile bistable optical switches and latching optical logic using integrated photothyristors and surface-emitting lasers
[DE92-008677] p 2442 N92-23748
LIGHT GAS GUNS
M and D SIG progress report: Laboratory simulations of LDEF impact features p 2336 N92-23323
LIGHT MODULATION
Optical inner product neural associative memory
[NASA-CASE-NPO-18491-1-CU] p 2416 N92-23546
LIGHT SCATTERING
Study of density distribution in a near-critical simple fluid (19-IML-1) p 2362 N92-23639
In situ particle size measurements using a two-color laser scattering technique
[DE92-008634] p 2380 N92-24070
LIMBS (ANATOMY)
Chrondrogenesis in micromass cultures of embryonic mouse limb mesenchymal cells exposed to microgravity (7-IML-1) p 2357 N92-23605
LIMITERS (FUSION REACTORS)
An x ray diagnostic of electron power loss
[DE92-008599] p 2444 N92-23523
LINE SPECTRA
Lasers without inversion: Theory and experiment p 2379 N92-23143
Gamma rays from SN1987A with the UCR double-Compton telescope p 2455 N92-23695
The throes of star formation: A study of the Orion-KL and DR21(OH) molecular clouds p 2457 N92-23698
Line profile asymmetries in chromospherically active stars p 2458 N92-24015
An analysis of the relationship between induction motor current and shaft speed fluctuations
[DE92-007234] p 2371 N92-24025
The ALEXIS data processing package: An IDL-based system
[DE92-007429] p 2455 N92-24027
LINEAR ACCELERATORS
Recent results on K(omega) and (pi)(pi) systems from LASS
[DE92-007389] p 2436 N92-23327
New technology for linear colliders
[DE92-007912] p 2440 N92-23334
LINEAR CIRCUITS
MOSFET level 1 and 2 models in APLAC
[PB92-143379] p 2371 N92-23678
LINEAR ENERGY TRANSFER (LET)
Prediction of LDEF ionizing radiation environment p 2439 N92-23292
Radiation exposure of LDEF: Initial results p 2461 N92-23302
Charged particle LET-spectra measurements aboard LDEF p 2440 N92-23303
LINEAR EQUATIONS
Small solutions and completeness for linear functional differential equations
[PB92-149350] p 2431 N92-23250
LINEAR PROGRAMMING
Sensitivity l(sup 1) minimization with boundary zeros or poles
[PB92-141803] p 2433 N92-23658
Mathematical analysis techniques for modeling the space network activities p 2434 N92-23964
LINEAR QUADRATIC GAUSSIAN CONTROL
Application of optical distributed sensing and computation to control of large space structures
[NASA-CR-190293] p 2442 N92-23567
LINEAR SYSTEMS
A comparative study of preconditioned Lanczos methods for nonsymmetric linear systems
[DE92-007530] p 2431 N92-23201
Compositionality and analysis of algebraic high-level nets
[PB92-143551] p 2432 N92-23440
LININGS
Evaluation of the applicability of Helmholtz resonators for low frequency acoustic liners
[PB92-138544] p 2436 N92-23588
Materials for liquid propellant engines p 2320 N92-23764
LIQUEFIED NATURAL GAS
White paper: Preliminary assessment of LNG vehicle technology, economics, and safety issues
[PB92-137603] p 2383 N92-23680
LIQUID COOLING
Characterizing and testing a thermally isolating superconducting link for SAFIRE-like missions
[NASA-CR-190196] p 2369 N92-23430
LIQUID CRYSTALS
Crystallization behavior of poly(phenylene sulphide) p 2342 N92-23940
LIQUID FILLED SHELLS
Fluid-structure interaction problems: Development of special processors p 2332 N92-23845
LIQUID FLOW
A method to determine resin flow during curing of composite laminates p 2342 N92-23938
LIQUID HELIUM
Ultrasonic investigation of (3)He-A vortices in low magnetic fields
[PB92-142256] p 2435 N92-23665
Numerical simulation of fluid behaviors in microgravity environment p 2363 N92-23719
LIQUID HYDROGEN
Microgravity dynamical behaviors of cryogenic liquid hydrogen reorientation and draining in space propulsion system p 2356 N92-23147
Liquid hydrogen mass flow through a multiple orifice Joule-Thomson device
[NASA-TM-105583] p 2373 N92-23268
Experience of the Chemical Automatics Design Bureau in creation of RD-0120 LOX/LH2 liquid rocket engine with thrust of 2 mn for Energia launcher p 2319 N92-23757
LIQUID OXYGEN
Oxygen-kerosene liquid rocket engines with postburning generator gas and high pressure in combustion chamber p 2320 N92-23761
LIQUID PROPELLANT ROCKET ENGINES
Launcher Propulsion Towards the Year 2010
[ESA-SP-327] p 2318 N92-23750
Experience of the Chemical Automatics Design Bureau in creation of RD-0120 LOX/LH2 liquid rocket engine with thrust of 2 mn for Energia launcher p 2319 N92-23757
Development status of the Vulcain engine p 2319 N92-23759
Oxygen-kerosene liquid rocket engines with postburning generator gas and high pressure in combustion chamber p 2320 N92-23761
Health monitoring of reusable rocket engines p 2320 N92-23762
Materials for high liquid propulsion in 2010 p 2320 N92-23763
Materials for liquid propellant engines p 2320 N92-23764
LIQUID SLOSHING
Numerical investigation of fluid-structure-interaction problems with the finite element method p 2332 N92-23844
Fluid-structure interaction problems: Development of special processors p 2332 N92-23845
A symmetric coupling between BEM and FEM for dynamical analysis of spacecraft p 2332 N92-23846
LIQUID-SOLID INTERFACES
Fundamental electron transfer processes at the single crystal semiconductor/liquid interface
[DE92-008132] p 2447 N92-23275
Numerical investigation of fluid-structure-interaction problems with the finite element method p 2332 N92-23844
Fluid-structure interaction problems: Development of special processors p 2332 N92-23845
LIQUID-VAPOR INTERFACES
Numerical simulation of fluid behaviors in microgravity environment p 2363 N92-23719
LIQUIDS
Numerical and physical modelling of bubbly flow phenomena
[DE92-008642] p 2376 N92-24062
LISTS
MBT-WIRE: Intelligent CAD in wiring design
[REPT-1.1.4] p 2419 N92-23856
LITHIUM FLUORIDES
Radiation monitoring container device (16-IML-1) p 2361 N92-23629
LITHOGRAPHY
High-performance multilayer mirrors for soft x ray projection lithography
[DE92-008615] p 2443 N92-24049
LITHOSPHERE
Analysis of gravity and topography on Earth and Venus: Comparisons of lithospheric and sublithospheric processes p 2409 N92-23772
LOAD TESTS
On development of automated static loading system for spacecraft structures p 2326 N92-23801
LOADING MOMENTS
Collapse of composite tubes under end moments
[NASA-TM-107605] p 2390 N92-23992
LOCKING
Problem of membrane locking in finite element analysis of cylindrical shells
[PB92-133941] p 2387 N92-23137
LOCOMOTION
Gravity related behavior of the acellular slime mold Physarum polycephalum (7-IML-1) p 2359 N92-23618
LOGIC CIRCUITS
Versatile bistable optical switches and latching optical logic using integrated photothyristors and surface-emitting lasers
[DE92-008677] p 2442 N92-23748
LOGIC PROGRAMMING
Logic programming and metadata specifications p 2429 N92-23375
LONG DURATION EXPOSURE FACILITY
LDEF: 69 Months in Space. First Post-Retrieval Symposium, part 1
[NASA-CP-3134-PT-1] p 2461 N92-23280
Long Duration Exposure Facility: A general overview p 2335 N92-23281
Long Duration Exposure Facility (LDEF) space environments overview p 2335 N92-23282
Pinhole cameras as sensors for atomic oxygen in orbit: Application to attitude determination of the LDEF p 2379 N92-23283
Use of the Long Duration Exposure Facility's thermal measurement system for the verification of thermal models p 2336 N92-23284
Measured space environmental effects to LDEF during retrieval p 2335 N92-23285
Particle types and sources associated with LDEF p 2349 N92-23286
Migration and generation of contaminants from launch through recovery: LDEF case history p 2335 N92-23287
Quantification of contaminants associated with LDEF p 2349 N92-23288
Molecular films associated with LDEF p 2439 N92-23289
Organic contamination of LDEF p 2339 N92-23290
Summary of ionizing radiation analysis on the Long Duration Exposure Facility p 2439 N92-23291
Prediction of LDEF ionizing radiation environment p 2439 N92-23292
Gamma radiation survey of the LDEF spacecraft p 2460 N92-23293
The interactions of atmospheric cosmogenic radionuclides with spacecraft surfaces p 2461 N92-23294
Charged particle activation studies on the surface of LDEF spacecraft p 2439 N92-23296
Radioactivities of Long Duration Exposure Facility (LDEF) materials: Baggage and bonanzas p 2440 N92-23297
Measurements of induced radioactivity in some LDEF samples p 2440 N92-23298
Gamma ray spectrometry of LDEF samples at SRL p 2349 N92-23299
Induced radioactivity in LDEF components p 2440 N92-23300
Thermoluminescent dosimetry for LDEF experiment M0006 p 2461 N92-23301
Radiation exposure of LDEF: Initial results p 2461 N92-23302
Charged particle LET-spectra measurements aboard LDEF p 2440 N92-23303
Ionizing radiation calculations and comparisons with LDEF data p 2440 N92-23304
LDEF geometry/mass model for radiation analyses p 2440 N92-23305
The LDEF ultra heavy cosmic ray experiment p 2461 N92-23306
Preliminary results from the heavy ions in space experiment p 2461 N92-23307
Heavy ion measurement on LDEF p 2440 N92-23308
Large craters on the meteoroid and space debris impact experiment p 2335 N92-23309
Study of cosmic dust particles on board LDEF: The FRECOPA experiments AO138-1 and AO138-2 p 2458 N92-23310
Meteoroid/space debris impacts on MSFC LDEF experiments p 2335 N92-23311
Hypervelocity impact microfoil perforations in the LEO space environment (LDEF, MAP AO-023 experiment) p 2336 N92-23312
Meteoroid and debris special investigation group data acquisition procedures p 2454 N92-23313
Meteoroid, and debris special investigation group preliminary results: Size-frequency distribution and spatial density of large impact features on LDEF p 2336 N92-23314
Preliminary analysis of LDEF instrument A0187-1: Chemistry of Micrometeoroids Experiment p 2458 N92-23315

SIMS chemical analysis of extended impact features from the trailing edge portion of experiment AO187-2 p 2349 N92-23316
IDE spatio-temporal impact fluxes and high time-resolution studies of multi-impact events and long-lived debris clouds p 2458 N92-23317
Ion microprobe elemental analyses of impact features on interplanetary dust experiment sensor surfaces p 2458 N92-23318
LDEF impact craters formed by carbon-rich impactors: A preliminary report p 2336 N92-23319
Dynamic (computer) modelling of the particulate environment: Transformations from the LDEF reference frame to decode geocentric and interplanetary populations p 2458 N92-23320
LDEF data correlation to existing NASA debris environment models p 2336 N92-23321
Deriving the velocity distribution of meteoroids from the measured meteoroid impact directionality on the various LDEF surfaces p 2459 N92-23322
M and D SIG progress report: Laboratory simulations of LDEF impact features p 2336 N92-23323
Preliminary micrometeoroid and debris effects on LDEF thermal control surfaces p 2336 N92-23324
The interstellar gas experiment p 2459 N92-23325

LONG DURATION SPACE FLIGHT
Measurement of venous compliance (8-IML-1) p 2360 N92-23623
Mental workload and performance experiment (15-IML-1) p 2361 N92-23628

LOW ASPECT RATIO
Normal force of low aspect ratio wing-body combinations up to high angles of attack at supersonic speeds [ESDU-91042] p 2309 N92-24009

LOW FREQUENCIES
Acoustic prediction on satellite structure p 2327 N92-23812

LOW NOISE
Design and performance of 22 GHz coaxial low noise MESFET and HEMT amplifiers [PB92-134071] p 2368 N92-23172

LOW REYNOLDS NUMBER
An improved k-epsilon model for near wall turbulence p 2303 N92-23349
Advancements in engineering turbulence modeling [PAPER-105] p 2303 N92-23350
The kinematics of turbulent boundary layer structure p 2375 N92-23689

LOW SPEED
Effect of low-speed impact damage and damage location on behavior of composite panels [NASA-TP-3196] p 2344 N92-23981

LOW SPEED WIND TUNNELS
Distributed computer system in the large scale low speed wind tunnel [NAL-TM-629] p 2312 N92-23979

LOW TEMPERATURE
Sub-Kelvin resistance thermometer [NASA-CASE-GSC-13406-1] p 2378 N92-23460

LOW TEMPERATURE TESTS
Mechanical behavior of composite materials and adhesive bonds at low temperatures p 2330 N92-23833

LOW THRUST PROPULSION
Low thrust propulsion literature survey [NASA-CR-190179] p 2337 N92-23151

LUBRICATING OILS
Oil lubricated and water lubricated pin-on-disc wear tests with engineering ceramics [PB92-136563] p 2380 N92-23152

LUMINAIRES
Evaluation of a mechanical beam-switching system [PB92-139773] p 2368 N92-23140

LUNAR BASED EQUIPMENT
The use of high temperature superconductors to levitate lunar telescope p 2456 N92-23962

LUNAR BASES
Power beaming: Mission enabling for lunar exploration [DE92-006727] p 2459 N92-23124

LUNAR EXPLORATION
Power beaming: Mission enabling for lunar exploration [DE92-006727] p 2459 N92-23124
Space transfer concepts and analyses for exploration missions: Technical directive 10 [NASA-CR-184309] p 2317 N92-24048

LYMAN ALPHA RADIATION
Search for cosmological dust p 2456 N92-23164

LYMPHOCYTES
Proliferation and performance of hybridoma cells in microgravity (7-IML-1) p 2358 N92-23614

M

MACHINE LEARNING
Data exploration systems for databases p 2429 N92-23374

MACHINING
Improvement of laser machining processes [DE92-007801] p 2380 N92-23723
Optimum cutting conditions determination for the NC-milling [REPT-2.1.2] p 2422 N92-23874
Advances in processing rates optimization for flexible manufacturing systems [REPT-2.3.4] p 2423 N92-23877
Acoustic emission as a process monitor for diamond machining of metal optical components [DE92-008037] p 2363 N92-23899

MAGNETIC ANOMALIES
The Earth's gravity field from satellite geodesy: A 30 year adventure p 2315 N92-23913

MAGNETIC COILS
Design considerations for an air core magnetic actuator [NASA-TM-104229] p 2364 N92-23989
Steady State Advanced Tokamak (SSAT): The mission and the machine [DE92-008983] p 2445 N92-24020

MAGNETIC CORES
Design considerations for an air core magnetic actuator [NASA-TM-104229] p 2364 N92-23989

MAGNETIC DIPOLES
Microsphere viscometers for low temperature applications [PB92-143361] p 2379 N92-23594

MAGNETIC EFFECTS
The effects of magnetic fields on oscillations in the solar atmosphere p 2459 N92-23697

MAGNETIC FIELD CONFIGURATIONS
The effects of magnetic fields on oscillations in the solar atmosphere p 2459 N92-23697

MAGNETIC FIELD RECONNECTION
The subionospheric electromagnetic response to magnetopause processes p 2407 N92-23142
Magnetic reconnection in magnetotail and solar plasmas p 2457 N92-24000

MAGNETIC FIELDS
Evolution of magnetic moment due to the cyclotron resonance with field ripples in a tokamak [DE92-751058] p 2443 N92-23135
An instrument to search for small-scale anisotropy in the cosmic microwave background at 90 GHz p 2441 N92-23161
Low frequency electrostatic modes in a magnetized dusty plasma [DE92-617387] p 2444 N92-23209
Feedback control of plasma equilibrium with control system aided by personal computer on the JIPP T-IIU tokamak [DE92-750824] p 2444 N92-23261
Development of 3-dimensional compact magnetic dosimeter for environmental magnetic field monitoring [DE92-750825] p 2407 N92-23262
Ultrasonic investigation of (3)He-A vortices in low magnetic fields [PB92-142256] p 2435 N92-23665
Observing millisecond and binary pulsars p 2455 N92-24001

MAGNETIC FILMS
The role of microstructural phenomena in magnetic thin films [DE92-007960] p 2446 N92-23213

MAGNETIC FLUX
TEM study of flux pinning defects in YBa2Cu3O7-delta produced by 580 MeV Sn ion irradiation [DE92-006991] p 2448 N92-23574
Magnetic flux motion and flux pinning superconductors [DE92-008243] p 2449 N92-23892

MAGNETIC MATERIALS
User's manual for three dimensional FDTD version C code for scattering from frequency-independent dielectric and magnetic materials [NASA-CR-190109] p 2365 N92-23425

MAGNETIC MEASUREMENT
Aristoteles magnetometer system p 2316 N92-23920

MAGNETIC MOMENTS
Evolution of magnetic moment due to the cyclotron resonance with field ripples in a tokamak [DE92-751058] p 2443 N92-23135

MAGNETIC PERMEABILITY
Monte Carlo simulation of the 3-state vector Potts model on a 3-dimensional random lattice [DE92-615489] p 2446 N92-23259

MAGNETIC PROPERTIES
Magnetic flux motion and flux pinning superconductors [DE92-008243] p 2449 N92-23892

MAGNETIC SPECTROSCOPY
The isotopic composition of cosmic ray helium from 500 to 1100 MeV per nucleon p 2460 N92-23163

MAGNETIC STORMS
JPRS report: Science and technology. Central Eurasia: Space [JPRS-USP-92-002] p 2314 N92-23705

MAGNETIC SURVEYS
Continuous profiling of magnetotelluric fields p 2401 N92-23703

MAGNETIC SUSPENSION
Design considerations for an air core magnetic actuator [NASA-TM-104229] p 2364 N92-23989

MAGNETIC VARIATIONS
Magnetic fluctuations and normal state properties of the t-J model at finite dopings [DE92-617538] p 2447 N92-23452

MAGNETIZATION
Monte Carlo simulation of the 3-state vector Potts model on a 3-dimensional random lattice [DE92-615489] p 2446 N92-23259
High-temperature superconductivity: Electron-doped cuprates and composites from alloy precursors p 2448 N92-23774
Magnetic flux motion and flux pinning superconductors [DE92-008243] p 2449 N92-23892

MAGNETOHYDRODYNAMIC GENERATORS
Direct conversion technology [NASA-CR-190188] p 2403 N92-23569
Compact Fusion Advanced Rankine (CFAR2) power cycle [DE92-008577] p 2445 N92-23987

MAGNETOHYDRODYNAMIC STABILITY
Feedback control of plasma equilibrium with control system aided by personal computer on the JIPP T-IIU tokamak [DE92-750824] p 2444 N92-23261

MAGNETOHYDRODYNAMICS
The structure of MFD shock waves for rectilinear motion in some model of plasma [DE92-617386] p 2443 N92-23208

MAGNETOMETERS
Mission objectives and scientific rationale for the magnetometer mission p 2315 N92-23912
The geophysical impact of the Aristoteles mission p 2315 N92-23915
Aristoteles magnetometer system p 2316 N92-23920

MAGNETOPAUSE
The subionospheric electromagnetic response to magnetopause processes p 2407 N92-23142

MAGNETORESISTIVITY
Magnetotransport and responses of semiconductor microstructures p 2449 N92-23775

MAGNETOSPHERE-IONOSPHERE COUPLING
Mission objectives and scientific rationale for the magnetometer mission p 2315 N92-23912

MAGNONS
Improved spin wave theory: An application to the spin-1/2 antiferromagnetic Heisenberg model on a square lattice [DE92-617436] p 2448 N92-23504

MALES
Stress effects of human-computer interactions [PB92-136001] p 2415 N92-23513

MAN TENDED FREE FLYERS
The Columbus Free Flying Laboratory: Mechanical design aspects p 2323 N92-23782

MAN-COMPUTER INTERFACE
Stress effects of human-computer interactions [PB92-136001] p 2415 N92-23513
A framework for the support of VLSI (very large scale integration) design for manufacture [REPT-1.3.1] p 2421 N92-23868
User interface user's guide for HYPGEN [NASA-CR-190304] p 2425 N92-23991

MANAGEMENT METHODS
Procedure improvement enterprises [DE92-003222] p 2453 N92-23183

MANAGEMENT PLANNING
Realization and provisional sensor development planning p 2395 N92-23406
National user interfaces p 2395 N92-23407
Provisional cost evaluation p 2395 N92-23408
Group technology, RCO: Rough-Cut Optimizer. The key to integration of plant operations [REPT-1.1.6] p 2420 N92-23857

MANAGEMENT SYSTEMS
Design of neural networks for classification of remotely sensed imagery p 2402 N92-23367

The use of artificial intelligence techniques to improve the multiple payload integration process p 2428 N92-23370

MANIFOLDS (MATHEMATICS)
Geometry of differential difference equations [PB92-148774] p 2431 N92-23182
Non-commutative differential geometry and Yang-Baxter equation [PB92-149459] p 2431 N92-23184
Family of Poisson structures on compact hermitian symmetric spaces [PB92-149442] p 2433 N92-23670

MANIPULATORS
Summary report: A preliminary investigation into the use of fuzzy logic for the control of redundant manipulators [NASA-CR-190277] p 2429 N92-23438
Dynamic analysis of planar manipulation tasks [DE91-019060] p 2430 N92-23458
The design and control of uncertain manipulator arms with decoupled inertia matrix p 2383 N92-23690
The statics, dynamics, and control of the elasticarm: A continuous beam manipulator p 2383 N92-23691
Analysis and control of nonlinear flexible manipulator p 2384 N92-23727
Optimal control of closed chain robotic systems p 2430 N92-24011
Controlling flexible robot arms using a high speed dynamics process [NASA-CASE-NPO-18499-1-CU] p 2385 N92-24042
Controlling under-actuated robot arms using a high speed dynamics process [NASA-CASE-NPO-18498-1-CU] p 2385 N92-24043
Page turning system [NASA-CASE-GSC-13415-1] p 2386 N92-24059

MANNED MARS MISSIONS
Synergistic use of high and low thrust propulsion systems for piloted missions to Mars [NASA-CR-189138] p 2338 N92-24004
Space transfer concepts and analyses for exploration missions: Technical directive 10 [NASA-CR-184309] p 2317 N92-24048

MANNED SPACE FLIGHT
Space transfer concepts and analyses for exploration missions: Technical directive 10 [NASA-CR-184309] p 2317 N92-24048

MANNED SPACECRAFT
Material considerations for habitable areas of manned spacecraft p 2323 N92-23785

MANUALS
Controlling operations through procedures: APE (automated procedure editor) [REPT-2.2.1] p 2422 N92-23675

MANUFACTURING
Center for Space Power, Texas A and M University p 2313 N92-23651
Manufacturing process of the Ariane 5 segmented propellant chargers p 2319 N92-23756
Crystallization behavior of poly(phenylene sulphide) p 2342 N92-23940

MANY BODY PROBLEM
Many-body problems in high temperature superconductivity [DE92-617539] p 2447 N92-23453
Melting of nickel clusters [DE92-006986] p 2351 N92-23573

MANY ELECTRON EFFECTS
Semiempirical studies of atomic structure [DE92-008143] p 2437 N92-23448

MAPPING
The laser fluorosensor p 2393 N92-23386

MARINE BIOLOGY
Geophysical, chemical and biological measuring parameters p 2393 N92-23385
Our living oceans: The first annual report on the status of US living marine resources [PB92-145689] p 2412 N92-23519
Reconstructing the tropical Atlantic seasonal thermocline using planktonic foraminifera p 2412 N92-23769

MARINE CHEMISTRY
Geophysical, chemical and biological measuring parameters p 2393 N92-23385

MARINE MAMMALS
Our living oceans: The first annual report on the status of US living marine resources [PB92-145689] p 2412 N92-23519

MARINE METEOROLOGY
Differences within and among surface marine datasets [PB92-135326] p 2411 N92-23660

MARINE RESOURCES
Proceedings on MOS-1 data evaluation [HE-90015] p 2396 N92-23465
Our living oceans: The first annual report on the status of US living marine resources [PB92-145689] p 2412 N92-23519

MARKETING
Current definition of some development programs p 2395 N92-23405
The market for computer readable information p 2453 N92-23728
Kansas State University electric vehicle site operator program [DE92-008425] p 2384 N92-23896
Symposium on Marketing for Technological Products [MBB-UE-0014-90-PUB] p 2452 N92-23928
Market directed thinking in a technological operation p 2452 N92-23929
Marketing qualification as a requirement for operating success p 2452 N92-23930
Marketing as a necessary condition for the successful development and commercialization of technological products p 2452 N92-23931
Requirements for the engineer training profile and definition of his role p 2452 N92-23932

MARS PROBES
Solar-electric-propulsion cargo vehicles for split/sprint Mars mission [NASA-CR-189983] p 2322 N92-23526

MARTENSITIC TRANSFORMATION
Fabrication of a helical coil shape memory alloy actuator [DE92-008399] p 2364 N92-23901

MASS
Effective mass theory for abrupt heterojunctions [DE92-617439] p 2448 N92-23581

MASS DISTRIBUTION
Multi parameter optimization on Ariane 5 p 2321 N92-23798

MASS FLOW
Liquid hydrogen mass flow through a multiple orifice Joule-Thomson device [NASA-TM-105583] p 2373 N92-23268

MASS SPECTROSCOPY
The interactions of atmospheric cosmogenic radionuclides with spacecraft surfaces p 2461 N92-23294
Characterization of rocket propellant combustion products [DE92-007799] p 2337 N92-23722

MASS TRANSFER
Modelling and experimental verification of a water alleviation system for the NASP --- National Aerospace Plane [NASA-TM-105661] p 2373 N92-23224
Promotion of industrial technologies on the global environment [DE92-769375] p 2406 N92-23734

MATERIALS HANDLING
A self-navigating mobile robot [DE92-008612] p 2430 N92-24066

MATERIALS TESTS
Radiation effects on polyethylene foam [DE92-751046] p 2353 N92-23134

MATHEMATICAL LOGIC
Compositionality and analysis of algebraic high-level nets [PB92-143551] p 2432 N92-23440

MATHEMATICAL MODELS
Neutron induced gamma-ray production data [DE92-615322] p 2440 N92-23130
Investigations of breakdown of rare gases by short pulses of 1.06(mu)m laser radiation [DE92-615399] p 2379 N92-23131
Fusion gain due to high energy ions accelerated by additional heating [DE92-751038] p 2443 N92-23133
Use of control theory for analyzing stability of states in continuum thermodynamics [PB92-136571] p 2451 N92-23136
Electrostatic image solution for the interaction of two dielectric spheres [PB92-142199] p 2364 N92-23138
Comparison of two-dimensional and three-dimensional droplet trajectory calculations in the vicinity of finite wings [NASA-TM-105617] p 2373 N92-23154
A damage mechanics model for beams p 2387 N92-23159
Hypersonic laminar flow computations over a blunt leading edged delta wing at three different chord Reynolds numbers [FFA-TN-1991-40] p 2304 N92-23168
Achieving spectrum conservation for the minimum-span and minimum-order frequency assignment problems [NASA-TM-105649] p 2322 N92-23187
Aeroelastic stability analyses of two counter rotating propfan designs for a cruise missile model [NASA-TM-105268] p 2387 N92-23191
Progressive fracture of polymer matrix composite structures: A new approach [NASA-TM-105574] p 2339 N92-23194
Theoretical model of the density of states of random binary alloys [DE92-617438] p 2350 N92-23210
Modeling of the DZero data acquisition system [DE92-007913] p 2453 N92-23212
Sensitivity analysis of dynamic aeroelastic responses p 2306 N92-23229
Application of analytical and design tools for fighter wing aeroelastic tailoring p 2307 N92-23231
The structural optimization system OPTSYS: Current status and applications p 2307 N92-23232
Multidisciplinary optimization studies using ASTROS p 2307 N92-23234
Design of a fighter aircraft vertical tail enhanced buffet environment survivability p 2307 N92-23235
A fin optimisation study p 2308 N92-23237
Simultaneous stress and flutter optimization for the wing of a transport aircraft equipped with four engines p 2308 N92-23238
Structural optimization of aircraft practice and trends p 2308 N92-23239
A study of start-up characteristics of a potassium heat pipe from the frozen state [NASA-CR-189173] p 2373 N92-23253
Coupled multi-disciplinary simulation of composite engine structures in propulsion environment [NASA-TM-105575] p 2388 N92-23267
Liquid hydrogen mass flow through a multiple orifice Joule-Thomson device [NASA-TM-105583] p 2373 N92-23268
Use of the Long Duration Exposure Facility's thermal measurement system for the verification of thermal models p 2336 N92-23284
Turbulence modeling in supersonic combusting flows p 2302 N92-23342
Evaluating model accuracy for model-based reasoning p 2427 N92-23362
Testing and analyses of electrochemical cells using frequency response [NASA-TM-103580] p 2369 N92-23437
Magnetic fluctuations and normal state properties of the t-J model at finite dopings [DE92-617538] p 2447 N92-23452
On motion planning amidst transient obstacles [DE91-018939] p 2429 N92-23457
Analysis of a 37 kW cage-induction motor [PB92-142116] p 2369 N92-23496
Hierarchical sets in mathematical programming modeling languages [PB92-148683] p 2418 N92-23507
Optimizing flow rates in a queueing network with side constraints [PB92-149996] p 2430 N92-23508
A two-dimensional Euler solution for an unbladed jet engine configuration [NASA-TM-105329] p 2374 N92-23560
Long time behavior of unsteady flow computations [NASA-TM-105584] p 2374 N92-23565
Soviet articles on antenna theory [DE92-008452] p 2366 N92-23575
Improved numerical methods for quantum field theory (outstanding junior investigator award) [DE92-008730] p 2451 N92-23578
General P-T fit construction for He, N2, Ar, H2 and Ne VPT used at Fermilab [DE92-008851] p 2433 N92-23579
Effective mass theory for abrupt heterojunctions [DE92-617439] p 2448 N92-23581
Comparison of analytical and numerical modelling approaches for sizing of seasonal storage solar heating systems [PB92-141829] p 2403 N92-23592
Ultrasonic investigation of (3)He-A vortices in low magnetic fields [PB92-142256] p 2435 N92-23665
Quasi-static image theory for the bi-isotropic (nonreciprocal chiral) sphere [PB92-142371] p 2366 N92-23666
Electrostatic image theory for the dielectric sphere with an internal source [PB92-142405] p 2366 N92-23667
Electrostatic image theory for the layered dielectric sphere [PB92-142413] p 2367 N92-23668
Family of Poisson structures on compact hermitian symmetric spaces [PB92-149442] p 2433 N92-23670
Mathematical modelling and numerical approximations for two-phase flow problems p 2375 N92-23672
MOSFET level 1 and 2 models in APLAC [PB92-143379] p 2371 N92-23678
Mathematical model of a control valve [PB92-141951] p 2383 N92-23710
Characterization of rocket propellant combustion products [DE92-007799] p 2337 N92-23722

Density of the F-statistic in the linear model with arbitrarily normal distributed errors
[PB92-128792] p 2434 N92-23731
Improvements for interpretation of structural dynamics calculation using effective parameters for substructures p 2324 N92-23789
Maximal modal energy method: An overvaluing tool for low frequency prediction of structure acoustic response p 2324 N92-23791
Acoustic cavity and fluid/structure interaction models: A methodological deterministic approach and problems encountered p 2327 N92-23813
Employment of C.B. (Craig-Bampton) models for nonlinear dynamic analysis p 2327 N92-23814
On the modelling of a deployable telescope elastic beam-type element for on-orbit multibody simulations p 2329 N92-23826
Notched strength of composite materials p 2331 N92-23839
Voxel-based solid modeling
[REPT-1.1.3] p 2419 N92-23855
Fast simulation of MOS digital networks using a physical macromodelling approach
[REPT-1.2.1] p 2420 N92-23860
Flexible Design Environment (FDE) for operation systems design
[REPT-2.3.5] p 2423 N92-23878
Gravity field data products from the Aristoteles mission p 2317 N92-23925
Impact-induced delamination in (0(5), 90(5), 0(5)) carbon/peek composite laminates p 2341 N92-23936
On the application of micromechanics to the prediction of macroscopic thermal residual stresses in short-fiber reinforced Polyetheretherketone (PEEK) p 2343 N92-23942
On the test of mode 1 delamination and the importance of laminate lay-ups p 2343 N92-23943
Mechanical properties of glass bead filled ductile epoxy composites p 2344 N92-23947
Computational procedures for preliminary design p 2309 N92-23952
Panel methods for aerodynamic analysis and design p 2309 N92-23955
Mathematical analysis techniques for modeling the space network activities p 2434 N92-23964
Modelling of aerodynamic forces and heat transfer for orbital decay and reentry calculations p 2334 N92-23974
Design considerations for an air core magnetic actuator
[NASA-TM-104229] p 2364 N92-23989
Underlying modal data issues for detecting damage in truss structures
[NASA-TM-107573] p 2390 N92-23990
Modeling and analysis of high-temperature inelastic deformation in metal matrix composites p 2345 N92-23996
Adaptive active flutter suppression of wings in subsonic and transonic flight regimes p 2310 N92-24010
Simulation of freckles during vertical solidification of binary alloys p 2353 N92-24014
CEPXS/ONELD: A one-dimensional coupled electron-photon discrete ordinates code package
[DE92-003146] p 2425 N92-24041
Advanced electric motor technology: Flux mapping
[NASA-CR-184317] p 2372 N92-24047
Numerical and physical modelling of bubbly flow phenomena
[DE92-008642] p 2376 N92-24062
Modeling of the catalytic oxidative coupling of methane
[DE92-008554] p 2349 N92-24064

MATHEMATICAL PROGRAMMING
The structural optimization system OPTSYS: Current status and applications p 2307 N92-23232
Hierarchical sets in mathematical programming modeling languages
[PB92-148683] p 2418 N92-23507

MATRICES (MATHEMATICS)
Hierarchical sets in mathematical programming modeling languages
[PB92-148683] p 2418 N92-23507

MATRIX MATERIALS
The effect of processing on strength of Nicalon fibers in Nicalon fiber-SiC matrix composites
[DE92-006978] p 2340 N92-23256

MAXIMUM ENTROPY METHOD
Use of the maximum entropy method to retrieve the vertical atmospheric ozone profile and predict atmospheric ozone content p 2407 N92-23965

MAXWELL EQUATION
Optical properties of metallic multi-layer films
[DE92-615486] p 2443 N92-24029

MAZE LEARNING
Breathing maze router for analog VLSI cell generation
[REPT-1.3.3] p 2422 N92-23870

MEAN SQUARE VALUES
Functional precision of National Weather Service upper-air measurements using VIZ Manufacturing Co. A radiosonde (model 1492-510)
[PB92-137850] p 2410 N92-23439

MEASURING INSTRUMENTS
X ray based displacement measurement for hostile environments
[NASA-TM-105551] p 2378 N92-23155
Euromar-Seastars: A definition study on modular multisensor instrumentation for airborne remote sensing of the sea
[MBB-UK-0152-91-PUB] p 2392 N92-23379
Euromar-Seastars: Summary p 2392 N92-23380
Geophysical, chemical and biological measuring parameters p 2393 N92-23385
Method and apparatus for determination of material residual stress
[NASA-CASE-GSC-13451-1] p 2388 N92-23549

MECHANICAL DEVICES
Evaluation of a mechanical beam-switching system
[PB92-139773] p 2368 N92-23140
Helix translation device --- shim for precision displacements
[NASA-CASE-GSC-13141-1] p 2382 N92-23548

MECHANICAL DRIVES
Retractable tool bit having latch type catch mechanism
[NASA-CASE-GSC-13359-1] p 2381 N92-23378
Retractable tool bit having slider type catch mechanism
[NASA-CASE-GSC-13358-1] p 2385 N92-24058

MECHANICAL ENGINEERING
Spacecraft Structures and Mechanical Testing, volume 1
[ESA-SP-321-VOL-1] p 2322 N92-23780
The Columbus Free Flying Laboratory: Mechanical design aspects p 2323 N92-23782
Brief history of the development of the EPS-structure p 2321 N92-23810

MECHANICAL MEASUREMENT
Failure processes in the fibre-polymer interphase p 2341 N92-23934

MECHANICAL PROPERTIES
Effects of impurities on the solidification and mechanical behaviour of primary and secondary commercial purity aluminium and aluminium alloys
[PB92-133511] p 2350 N92-23176
Detecting Lamb waves with broad-band acousto-ultrasonic signals in composite structures
[NASA-TM-105557] p 2386 N92-23189
Evaluation of the elevated-temperature mechanical reliability of a HiPed silicon nitride
[DE92-007838] p 2354 N92-23223
The effect of processing on strength of Nicalon fibers in Nicalon fiber-SiC matrix composites
[DE92-006978] p 2340 N92-23256
The influence of chromium on structure and mechanical properties of B2 nickel aluminide alloys
[NASA-CR-189124] p 2351 N92-23566
Aging of polymer matrix composites at elevated temperatures p 2328 N92-23817
Mechanical behavior of composite materials and adhesive bonds at low temperatures p 2330 N92-23833
Mechanical testing on a composite flexible structure p 2331 N92-23834
Modeling of honeycomb core for sandwich CTE prediction p 2332 N92-23841
Optimization of the laser glass composition for the Nova upgrade fusion laser system
[DE92-008606] p 2380 N92-24065

MEDICAL SCIENCE
Prosthetic helping hand
[NASA-CASE-MFS-28430-1] p 2416 N92-24044

MELTING
Investigation of plasma-sprayed laminates for high-temperature melting operations
[DE92-008416] p 2353 N92-24006

MEMBRANE STRUCTURES
Problem of membrane locking in finite element analysis of cylindrical shells
[PB92-133941] p 2387 N92-23137

MEMBRANES
Growth and sporulation of Bacillus subtilis under microgravity (7-IML-1) p 2358 N92-23612
Suborbital missions: The Joust p 2313 N92-23644

MEMORY (COMPUTERS)
Optical inner product neural associative memory
[NASA-CASE-NPO-18491-1-CU] p 2416 N92-23546

MENTAL PERFORMANCE
Mental workload and performance experiment (15-IML-1) p 2361 N92-23628
Training users of a flexible decision support system: The effects of training content and user ability p 2453 N92-23730

MERCURY CADMIUM TELLURIDES
Chemical compatibility of cartridge materials
[NASA-CR-190256] p 2356 N92-23555

MERCURY COMPOUNDS
Vapor crystal growth studies of single crystals of mercuric iodide (3-IML-1) p 2361 N92-23632
Mercury iodide nucleation and crystal growth in vapor phase (4-IML-1) p 2361 N92-23633

MESOMETEOROLOGY
Tornadic supercell over Dade and Broward Counties (Florida) on January 15, 1991
[PB92-134444] p 2411 N92-23906

MESOSCALE PHENOMENA
Tornadic supercell over Dade and Broward Counties (Florida) on January 15, 1991
[PB92-134444] p 2411 N92-23906

MESOSPHERE
Radar observations and dynamics of the polar summer mesosphere p 2408 N92-23702

MESSAGE PROCESSING
Architectural impact of FDDI network on scheduling hard real-time traffic
[NASA-CR-190272] p 2425 N92-23583

MESSAGES
Synchronous parallel system for emulation and discrete event simulation
[NASA-CASE-NPO-18414-1-CU] p 2426 N92-24045

METABOLISM
Growth and sporulation of Bacillus subtilis under microgravity (7-IML-1) p 2358 N92-23612

METAL COATINGS
Deposition of adherent Ag-Ti duplex films on ceramics in a multiple-cathode sputter deposition system
[NASA-TM-105586] p 2311 N92-23225

METAL CUTTING
Optimum cutting conditions determination for the NC-milling
[REPT-2.1.2] p 2422 N92-23874
Advances in processing rates optimization for flexible manufacturing systems
[REPT-2.3.4] p 2423 N92-23877

METAL FATIGUE
Investigation of fretting fatigue mechanisms on 7075-T6 aluminum alloy and Ti-6Al-4V titanium alloy p 2352 N92-23725

METAL FILMS
Optical properties of metallic multi-layer films
[DE92-615486] p 2443 N92-24029

METAL FOILS
Hypervelocity impact microfoil perforations in the LEO space environment (LDEF, MAP AO-023 experiment) p 2336 N92-23312
The interstellar gas experiment p 2459 N92-23325

METAL HALIDES
Charged-soft-sphere potentials for trivalent metal halides
[DE92-617445] p 2350 N92-23211

METAL MATRIX COMPOSITES
Detecting Lamb waves with broad-band acousto-ultrasonic signals in composite structures
[NASA-TM-105557] p 2386 N92-23189
Influence of engineered interfaces on residual stresses and mechanical response in metal matrix composites
[NASA-TM-105438] p 2340 N92-23195
Damage development in titanium metal matrix composites subjected to cyclic loading
[NASA-TM-107597] p 2340 N92-23433
Modeling and analysis of high-temperature inelastic deformation in metal matrix composites p 2345 N92-23996
Transverse deformation of unidirectional fiber-reinforced metal matrix composites p 2345 N92-24013

METAL OXIDE SEMICONDUCTORS
MOSFET level 1 and 2 models in APLAC
[PB92-143379] p 2371 N92-23678
Fast simulation of MOS digital networks using a physical macromodelling approach
[REPT-1.2.1] p 2420 N92-23860
Test preparation for MOS digital circuits using heuristics for reliable fault simulation
[REPT-1.2.6] p 2421 N92-23865

METAL PLATES
Large craters on the meteoroid and space debris impact experiment p 2335 N92-23309
Development of a crack arrest fracture toughness measurement procedure for quality assurance of plates and welds used for hydrocarbon storage tanks
[PB92-141753] p 2389 N92-23681

METAL POWDER
Production of metal powders by hydrogen stripping from loaded organic extractants
[PB92-136464] p 2350 N92-23178

METAL SURFACES
Hydrogen absorption by zirconium alloy cladding tube with surface oxide film
[DE92-750962] p 2351 N92-23265

The interactions of atmospheric cosmogenic radionuclides with spacecraft surfaces p 2461 N92-23294

METAL VAPOR LASERS
Limits of survivability and damage for optical components used in a high repetition rate visible laser [DE92-006896] p 2379 N92-23570

METALLIC GLASSES
On the kinetics of structural relaxation in some metallic glasses [PB92-1287272] p 2353 N92-23165
Cracking investigation of Nd:YAG laser welded gold plated glass sealing alloys [DE92-007971] p 2387 N92-23216

METALLURGY
JPRS report: Science and technology. Central Eurasia: Materials science [JPRS-UMS-92-006] p 2363 N92-23709

METALORGANIC CHEMICAL VAPOR DEPOSITION
Fermi level effects on dislocation formation in InAs(1-x)Sb(x) grown by MOCVD [DE92-008332] p 2450 N92-24034

METALS
Modular electromagnetic levitator [DE92-008278] p 2367 N92-23900

METEORITE COLLISIONS
Large craters on the meteoroid and space debris impact experiment p 2335 N92-23309
Meteoroid/space debris impacts on MSFC LDEF experiments p 2335 N92-23311
Deriving the velocity distribution of meteoroids from the measured meteoroid impact directionality on the various LDEF surfaces p 2459 N92-23322
Preliminary micrometeoroid and debris effects on LDEF thermal control surfaces p 2336 N92-23324
Interception of comets and asteroids on collision course with Earth [DE92-007431] p 2458 N92-24028

METEORITES
The meteorite record as clues to asteroidal regolith processes p 2457 N92-23770

METEOROID CONCENTRATION
Large craters on the meteoroid and space debris impact experiment p 2335 N92-23309
Deriving the velocity distribution of meteoroids from the measured meteoroid impact directionality on the various LDEF surfaces p 2459 N92-23322

METEOROID PROTECTION
Protection of spacecraft against meteroid/orbital debris impacts p 2323 N92-23786

METEOROIDS
Meteoroid and debris special investigation group data acquisition procedures p 2454 N92-23313
Meteoroid, and debris special investigation group preliminary results: Size-frequency distribution and spatial density of large impact features on LDEF p 2336 N92-23314
IDE spatio-temporal impact fluxes and high time-resolution studies of multi-impact events and long-lived debris clouds p 2458 N92-23317
LDEF data correlation to existing NASA debris environment models p 2336 N92-23321
Deriving the velocity distribution of meteoroids from the measured meteoroid impact directionality on the various LDEF surfaces p 2459 N92-23322

METEOROLOGICAL RADAR
Observation of lined-up cumulus rows under the winter monsoon situation using MOS-1 and radar data p 2399 N92-23483

METEOROLOGICAL SATELLITES
Measurements of rain rate distribution by MOS-1 MSR p 2396 N92-23467

METEOROLOGICAL SERVICES
Functional precision of National Weather Service upper-air measurements using VIZ Manufacturing Co. B radiosonde (model 1492-520) [PB92-137868] p 2410 N92-23494
Climate System Monitoring (CSM). El Nino/Southern Oscillation (ENSO) diagnostic advisory, special issue p 2411 N92-23677
Functional precision of National Weather Service upper-air measurements using space data division radiosonde (model 909-10-01) [PB92-137843] p 2411 N92-23746

METEOROLOGY
Measurements of rain rate distribution by MOS-1 MSR p 2396 N92-23467
Functional precision of National Weather Service upper-air measurements using space data division radiosonde (model 909-10-01) [PB92-137843] p 2411 N92-23746

METHANE
Basic research on natural gas combustion phenomena [PB92-149681] p 2348 N92-23685
Molecular design of substrate binding sites [DE92-008331] p 2438 N92-23894
Modeling of the catalytic oxidative coupling of methane [DE92-008554] p 2349 N92-24064

METHOD OF MOMENTS
Application of the Green function technique in the microstrip patch antenna analysis [PB92-142173] p 2367 N92-23907

METHYL ALCOHOL
Promotion of industrial technologies on the global environment [DE92-769377] p 2405 N92-23454
Survey on fixation and utilization of carbon dioxide by catalytic hydrogenation [DE92-769380] p 2347 N92-23456

METRIC SPACE
Constructing a pulsar timing array p 2456 N92-23126
Some topological problems I met [PB92-149327] p 2431 N92-23248
Isometric embedding of median algebras into L1 (mu) spaces [PB92-149343] p 2431 N92-23249
On some types of Riemannian V(sub n) with zero Ricci curvature [DE92-616917] p 2432 N92-23502
Constant curvature and non-perturbative W(sub 3) gravity [DE92-616919] p 2451 N92-23503
Existence of closed geodesics on 2-spheres [PB92-149434] p 2433 N92-23599

MICE
Chrondrogenesis in micromass cultures of embryonic mouse limb mesenchymal cells exposed to microgravity (7-IML-1) p 2357 N92-23605
Effect of microgravity and mechanical stimulation on the in vitro mineralization and resorption of fetal mouse long bones (7-IML-1) p 2357 N92-23606

MICHELSON INTERFEROMETERS
WAMDII: The Wide Angle Michelson Doppler Imaging Interferometer [NASA-TM-105526] p 2441 N92-23525

MICROELECTRONICS
Preliminary results from the heavy ions in space experiment p 2461 N92-23307

MICROGRAVITY APPLICATIONS
Phase partitioning experiment (8-IML-1) p 2360 N92-23621
Center for Macromolecular Crystallography, University of Alabama in Birmingham p 2313 N92-23650
Advanced Materials Center, Battelle p 2314 N92-23652

MICROMECHANICS
Damage development in titanium metal matrix composites subjected to cyclic loading [NASA-TM-107597] p 2340 N92-23433
Development of fatigue damage mechanics for application to the design of damage-tolerant composite components p 2324 N92-23793
Modeling and analysis of high-temperature inelastic deformation in metal matrix composites p 2345 N92-23996

MICROMETEOROIDS
Preliminary analysis of LDEF instrument A0187-1: Chemistry of Micrometeoroids Experiment p 2458 N92-23315
Preliminary micrometeoroid and debris effects on LDEF thermal control surfaces p 2336 N92-23324

MICROORGANISMS
Methods for the detection of microorganisms in the environment [PB92-137454] p 2405 N92-23512

MICROPARTICLES
Ion microprobe elemental analyses of impact features on interplanetary dust experiment sensor surfaces p 2458 N92-23318
Microsphere viscometers for low temperature applications [PB92-143361] p 2379 N92-23594

MICROPROCESSORS
Microprocessor control of multiple peak power tracking DC/DC converters for use with solar cell arrays [NASA-CASE-GSC-13450-1] p 2403 N92-23463

MICROSCOPY
X ray Fourier transform holography: Beyond the optical diffraction limit p 2377 N92-23144

MICROSTRIP ANTENNAS
Nonplanar linearly tapered slot antenna with balanced microstrip feed [NASA-TM-105647] p 2370 N92-23535
Vector circuit method applied for chiral dielectric slab waveguides [PB92-142355] p 2367 N92-23679
Application of the Green function technique in the microstrip patch antenna analysis [PB92-142173] p 2367 N92-23907

MICROSTRUCTURE
The effect of fatigue-induced damage on the mechanical properties of CFRP composites p 2339 N92-23157
Effects of impurities on the solidification and mechanical behaviour of primary and secondary commercial purity aluminium and aluminium alloys [PB92-133511] p 2350 N92-23176
The role of microstructural phenomena in magnetic thin films [DE92-007960] p 2446 N92-23213
A study of aluminum-lithium alloy solidification using acoustic emission techniques [NASA-CR-4437] p 2435 N92-23556
The influence of chromium on structure and mechanical properties of B2 nickel aluminide alloys [NASA-CR-189124] p 2351 N92-23566
TEM study of flux pinning defects in YBa2Cu3O7-delta produced by 580 MeV Sn ion irradiation [DE92-006991] p 2448 N92-23574
Surface structure and analysis with scanning tunneling microscopy and electron tunneling spectroscopy [DE92-007747] p 2448 N92-23721
Magnetotransport and responses of semiconductor microstructures p 2449 N92-23775
Development of fatigue damage mechanics for application to the design of damage-tolerant composite components p 2324 N92-23793
Microstructure and mechanical properties of carbon fibres: Relationship with the fibre-matrix adhesion in a carbon-epoxy composite p 2341 N92-23935
High-performance multilayer mirrors for soft x ray projection lithography [DE92-008615] p 2443 N92-24049

MICROWAVE AMPLIFIERS
Design and performance of 22 GHz coaxial low noise MESFET and HEMT amplifiers [PB92-134071] p 2368 N92-23172
New technology for linear colliders [DE92-007912] p 2440 N92-23334

MICROWAVE CIRCUITS
Solid State Technology Branch of NASA Lewis Research Center [NASA-TM-105159] p 2365 N92-23412

MICROWAVE EQUIPMENT
Recommended system concept p 2392 N92-23383

MICROWAVE IMAGERY
Availability of MSR data for snow water estimation p 2399 N92-23482

MICROWAVE OSCILLATORS
Thresholds of longitudinal instability of bunched beam in the presence of dominant inductive impedance [DE92-617992] p 2436 N92-23274

MICROWAVE PROBES
Coaxial turnstile junction [NASA-CASE-GSC-13422-1] p 2369 N92-23462

MICROWAVE RADIOMETERS
Euromar-Seastars: Summary p 2392 N92-23380
The imaging microwave radiometer p 2393 N92-23390
Provisional cost evaluation p 2395 N92-23408
Measurements of rain rate distribution by MOS-1 MSR p 2396 N92-23467
Estimation of MTF of MOS-1 MESSR images p 2397 N92-23469
Investigations on verification of the data observed by the MESSR and VTIR, and on interannual trend in the MSR data p 2397 N92-23470
Signal processing of the data obtained by MOS-1 MSR p 2397 N92-23472
Availability of MSR data for snow water estimation p 2399 N92-23482
Observation of lined-up cumulus rows under the winter monsoon situation using MOS-1 and radar data p 2399 N92-23483
Field evaluation of remote sensor measurements of wind, temperature, and moisture for ARM integrated sounding system research [PB92-140714] p 2401 N92-23521

MICROWAVE SENSORS
Sensor package for the North Sea p 2393 N92-23384

MICROWAVES
The origins of the cosmic x ray and gamma ray backgrounds p 2460 N92-23141
An instrument to search for small-scale anisotropy in the cosmic microwave background at 90 GHz p 2441 N92-23161
Microwave response of high transition temperature superconducting thin films p 2365 N92-23413
Coaxial turnstile junction [NASA-CASE-GSC-13422-1] p 2369 N92-23462
Analysis of solar and microwave thermal propulsion systems p 2337 N92-23694

MIE SCATTERING
In situ particle size measurements using a two-color laser scattering technique
[DE92-008634] p 2380 N92-24070
MILKY WAY GALAXY
High resolution studies of NGC 1275 and the galactic center p 2455 N92-23675
MILLIMETER WAVES
A flexible CPW package for a 30 GHz MMIC amplifier --- coplanar waveguide
[NASA-TM-105630] p 2368 N92-23193
Planar varactor frequency multiplier devices with blocking barrier
[NASA-CASE-NPO-18428-1-CU] p 2369 N92-23464
MILLING MACHINES
Optimum cutting conditions determination for the NC-milling
[REPT-2.1.2] p 2422 N92-23874
MIRRORS
Method for advanced material characterization by laser induced eddy current imaging
[NASA-CASE-GSC-13386-1] p 2386 N92-23376
Acoustic emission as a process monitor for diamond machining of metal optical components
[DE92-008037] p 2363 N92-23899
High-performance multilayer mirrors for soft x ray projection lithography
[DE92-008615] p 2443 N92-24049
MISSION PLANNING
CRYOSTAT (18-IML-1) p 2362 N92-23636
Suborbital missions: The Joust p 2313 N92-23644
The Solid-Earth Mission Aristoteles
[ESA-SP-329] p 2314 N92-23910
The GRADIOmeter payload p 2315 N92-23917
The Delta 2 launcher p 2316 N92-23921
The Aristoteles mission profile p 2316 N92-23922
Prediction of solar and geomagnetic activity for ESA low-flying spacecraft p 2334 N92-23975
Space transfer concepts and analyses for exploration missions: Technical directive 10
[NASA-CR-184309] p 2317 N92-24048
MIXED OXIDES
Advanced Materials Center, Battelle
p 2314 N92-23652
MIXING
A method to determine resin flow during curing of composite laminates p 2342 N92-23938
MIXING LENGTH FLOW THEORY
An experimental investigation of entrainment and mixing in pulsed and exponential transverse jets
p 2375 N92-23995
MODAL RESPONSE
The use of modal synthesis in conjunction with nonlinear transient dynamic analysis p 2324 N92-23788
Improvements for interpretation of structural dynamics calculation using effective parameters for substructures
p 2324 N92-23789
Acoustic cavity and fluid/structure interaction models: A methodological deterministic approach and problems encountered p 2327 N92-23813
Feasibility of payload sensitivity analyses for AR4 dynamic events p 2328 N92-23815
Development and application of substructuring techniques for understanding and controlling residual vibrations (microgravity aspects) p 2330 N92-23827
Numerical investigation of fluid-structure-interaction problems with the finite element method
p 2332 N92-23844
Optimal exciter placement and force vector tuning required for experimental modal analysis
p 2333 N92-23847
Matching finite element models to modal data
p 2333 N92-23848
Comparison of multi-point modal test methods
p 2333 N92-23849
Design parameter update of dynamic mathematical models in presence of test noise and mode pairing problems p 2333 N92-23850
Underlying modal data issues for detecting damage in truss structures
[NASA-TM-107573] p 2390 N92-23990
MODULARITY
Euromar-Seastars: A definition study on modular multisensor instrumentation for airborne remote sensing of the sea
[MBB-UK-0152-91-PUB] p 2392 N92-23379
Recommended system concept p 2392 N92-23383
Hardware and software modularity
p 2394 N92-23399
MODULATION DOPING
Electron polarization in modulation doped heterostructures
[DE92-617490] p 2447 N92-23272
MODULATORS
Method for advanced material characterization by laser induced eddy current imaging
[NASA-CASE-GSC-13386-1] p 2386 N92-23376
Electro-optic resonant phase modulator
[NASA-CASE-NPO-18702-1-CU] p 2442 N92-23551
MODULES
The imaging microwave radiometer
p 2393 N92-23390
Spacehab p 2313 N92-23647
MOISTURE
Field evaluation of remote sensor measurements of wind, temperature, and moisture for ARM integrated sounding system research
[PB92-140714] p 2401 N92-23521
Computer simulation of moisture penetration in structures p 2326 N92-23806
A new test facility for measuring the coefficient of moisture expansion of advanced composite materials
p 2326 N92-23807
MOISTURE CONTENT
Preliminary report on the observation of polar atmosphere and cryosphere by MOS-1 data received at Syowa Station p 2399 N92-23481
Field evaluation of remote sensor measurements of wind, temperature, and moisture for ARM integrated sounding system research
[PB92-140714] p 2401 N92-23521
Evaluation of terrestrial climate variability using a moisture index p 2411 N92-23771
MOLDS
Gravity related behavior of the acellular slime mold Physarum polycephalum (7-IML-1) p 2359 N92-23618
MOLECULAR CLOUDS
The throes of star formation: A study of the Orion-KL and DR21(OH) molecular clouds p 2457 N92-23698
MOLECULAR ENERGY LEVELS
Charged-soft-sphere potentials for trivalent metal halides
[DE92-617445] p 2350 N92-23211
MOLECULAR EXCITATION
Cu charge fluctuations and anomalous behaviour in the phonon spectrum of La2CuO4
[DE92-617446] p 2446 N92-23270
MOLECULAR PHYSICS
Cu charge fluctuations and anomalous behaviour in the phonon spectrum of La2CuO4
[DE92-617446] p 2446 N92-23270
MOLECULAR RELAXATION
On the kinetics of structural relaxation in some metallic glasses
[PB92-1287272] p 2353 N92-23165
MOLECULAR SPECTRA
High resolution studies of NGC 1275 and the galactic center p 2455 N92-23675
MOLECULAR STRUCTURE
The influence of chromium on structure and mechanical properties of B2 nickel aluminide alloys
[NASA-CR-189124] p 2351 N92-23566
Characterization of rocket propellant combustion products
[DE92-007799] p 2337 N92-23722
Molecular design of substrate binding sites
[DE92-008331] p 2438 N92-23894
MOLECULAR WEIGHT
Vinyl capped addition polyimides
[NASA-CASE-LEW-15027-2] p 2355 N92-24053
MOLECULES
Phase partitioning experiment (8-IML-1)
p 2360 N92-23621
Protein crystal growth (5-IML-1) p 2361 N92-23634
MOLYBDENUM ALLOYS
Chemical compatibility of cartridge materials
[NASA-CR-190256] p 2356 N92-23555
MOLYBDENUM OXIDES
Working gas pressure and flow effects on reactively sputtered molybdenum-oxide thin films
[DE92-008624] p 2450 N92-24069
MOMENTUM
The electron-positron momentum density and Fermi surface of YBa2Cu3O(7-x)
[DE92-008605] p 2450 N92-24007
MOMENTUM TRANSFER
Mutual scattering of carriers in two quantum wires
[DE92-616890] p 2366 N92-23580
MONITORS
Health monitoring of reusable rocket engines
p 2320 N92-23762
Acoustic emission as a process monitor for diamond machining of metal optical components
[DE92-008037] p 2363 N92-23899
MONOMOLECULAR FILMS
Quantification of contaminants associated with LDEF
p 2349 N92-23288
Molecular films associated with LDEF
p 2439 N92-23289
Organic contamination of LDEF p 2339 N92-23290
MONSOONS
Monsoon-ENSO relationships p 2404 N92-23160
MONTE CARLO METHOD
Monte Carlo simulation of the 3-state vector Potts model on a 3-dimensional random lattice
[DE92-615489] p 2446 N92-23259
Search for atmospheric neutrino oscillations with the Soudan 2 detector
[DE92-007397] p 2437 N92-23328
The study of PDF turbulence models in combustion
[PAPER-107] p 2302 N92-23345
On recontamination and directional-bias problems in Monte Carlo simulation of PDF turbulence models
p 2302 N92-23346
Progress in the development of PDF turbulence models for combustion
[PAPER-213] p 2303 N92-23347
A study of hydrogen diffusion flames using PDF turbulence model p 2303 N92-23348
Coupled load analysis: Scatter related to model uncertainties p 2324 N92-23787
Monte Carlo transport in semiconductor
[DE92-008404] p 2371 N92-23902
Metal-semiconductor, composite radiation detectors
[DE92-008980] p 2344 N92-23988
The all particle method
[DE92-008357] p 2439 N92-24005
MORPHOLOGY
Mechanical properties of glass bead filled ductile epoxy composites p 2344 N92-23947
An analysis of the WN shell nebula NGC 6888 using CCD imagery and spectrophotometry
p 2455 N92-24002
MORSE POTENTIAL
Ab initio pair potentials for FCC metals: An application of the method of Moebius transform
[DE92-617440] p 2351 N92-23582
MOTOR VEHICLES
Evaluation of a mechanical beam-switching system
[PB92-139773] p 2368 N92-23140
MOUTH
Page turning system
[NASA-CASE-GSC-13415-1] p 2386 N92-24059
MULTICHANNEL COMMUNICATION
Mutual interference in multichannel fibre communication systems p 2367 N92-24019
MULTIGRID METHODS
Improved shock-capturing of Jameson's scheme for the Euler equations
[PB92-148758] p 2373 N92-23251
MULTIPHOTON ABSORPTION
Multi-photon optical excitation of positronium
[DE92-008567] p 2438 N92-23903
MULTIPOLES
Thresholds of longitudinal instability of bunched beam in the presence of dominant inductive impedance
[DE92-617992] p 2436 N92-23274
Static multipole deformations in nuclei
[DE92-008250] p 2436 N92-23277
MULTISENSOR APPLICATIONS
Euromar-Seastars: A definition study on modular multisensor instrumentation for airborne remote sensing of the sea
[MBB-UK-0152-91-PUB] p 2392 N92-23379
Introduction: Ocean air observation
p 2392 N92-23381
Recommended system concept p 2392 N92-23383
Seaborne lidar system p 2393 N92-23389
Multisensor data fusion p 2394 N92-23398
Evaluation of the sensor effectiveness
p 2395 N92-23404
National user interfaces p 2395 N92-23407
MULTISPECTRAL RADAR
Recommended system concept p 2392 N92-23383
Sensor package for the North Sea
p 2393 N92-23384
MUONS
A study of underground muons in the Soudan 2 detector p 2437 N92-23674
MUSCLES
Center for Cell Research, Pennsylvania State University p 2314 N92-23653
MUSCULAR FUNCTION
Center for Cell Research, Pennsylvania State University p 2314 N92-23653

N

NASA PROGRAMS
Publications of the exobiology program for 1990: A special bibliography
[NASA-TM-4364] p 2416 N92-23429
Center for Space Power, Texas A and M University
p 2313 N92-23651

NASA SPACE PROGRAMS
Launch systems for future NASA missions
p 2318 N92-23752
Rocket propulsion for NASA's Earth to orbit launchers
p 2319 N92-23754
The Solid-Earth Mission Aristoteles
[ESA-SP-329] p 2314 N92-23910
NASCOM NETWORK
Mathematical analysis techniques for modeling the space network activities p 2434 N92-23964
NATIONAL AEROSPACE PLANE PROGRAM
Modelling and experimental verification of a water alleviation system for the NASP --- National Aerospace Plane
[NASA-TM-105661] p 2373 N92-23224
High temperature dynamic engine seal technology development
[NASA-TM-105641] p 2381 N92-23435
Design challenges for the National Aero-Space Plane
p 2310 N92-23822
NATIONAL PARKS
Acid rain and air pollution in desert park areas. Proceedings of a workshop: Management recommendations
[PB92-140532] p 2407 N92-24003
NATURAL GAS
Survey on subterranean disposal and storage technology of CO2
[DE92-769378] p 2405 N92-23455
Basic research on natural gas combustion phenomena
[PB92-149681] p 2348 N92-23685
NATURAL LANGUAGE (COMPUTERS)
Logic programming and metadata specifications
p 2429 N92-23375
NAVIER-STOKES EQUATION
Development of new flux splitting schemes
p 2302 N92-23343
NAVIGATION
Time optimal trajectories for a 2-wheeled robot
[DE92-000069] p 2430 N92-24032
A self-navigating mobile robot
[DE92-008612] p 2430 N92-24066
NAVIGATION AIDS
The accuracy of the drift buoy positioning by MOS-1 DCS p 2399 N92-23484
Study on drifting-data collection buoy using MOS-1: Position verification in the Bering Sea
p 2400 N92-23486
NAVIGATION INSTRUMENTS
A self-navigating mobile robot
[DE92-008612] p 2430 N92-24066
NAVIGATION SATELLITES
The accuracy of the drift buoy positioning by MOS-1 DCS p 2399 N92-23484
Precision GPS ephemerides and baselines
[NASA-CR-190247] p 2306 N92-23541
NEBULAE
An analysis of the WN shell nebula NGC 6888 using CCD imagery and spectrophotometry
p 2455 N92-24002
NEGATIVE ELECTRON AFFINITY
On the electronegativity of the high-T(sub c) oxide superconductor
[DE92-617537] p 2447 N92-23273
NEODYMIUM
Optimization of the laser glass composition for the Nova upgrade fusion laser system
[DE92-008606] p 2380 N92-24065
NEODYMIUM LASERS
Cracking investigation of Nd:YAG laser welded gold plated glass sealing alloys
[DE92-007971] p 2387 N92-23216
Photoinduced electron transfer in ordered polymers
[DE92-008787] p 2355 N92-24037
NERVOUS SYSTEM
Space adaptation syndrome experiments (8-IML-1)
p 2360 N92-23625
NETWORK ANALYSIS
Compositionality and analysis of algebraic high-level nets
[PB92-143551] p 2432 N92-23440
Optimizing flow rates in a queueing network with side constraints
[PB92-149996] p 2430 N92-23508
Fast simulation of MOS digital networks using a physical macromodelling approach
[REPT-1.2.1] p 2420 N92-23860
Design for testability: Where are the goalposts?
[REPT-1.2.2] p 2420 N92-23861
NETWORK CONTROL
Writing a simulation of a communications network using SIMSCRIPT/DISS
[REPT-2.3.6] p 2423 N92-23879
NEURAL NETS
The 1992 Goddard Conference on Space Applications of Artificial Intelligence
[NASA-CP-3141] p 2426 N92-23356
Feature detection in satellite images using neural network technology p 2427 N92-23366
Design of neural networks for classification of remotely sensed imagery p 2402 N92-23367
Improved image classification with neural networks by fusing multispectral signatures with topological data
p 2402 N92-23368
Optical inner product neural associative memory
[NASA-CASE-NPO-18491-1-CU] p 2416 N92-23546
NEUTRAL GASES
The interstellar gas experiment p 2459 N92-23325
NEUTRINOS
Search for atmospheric neutrino oscillations with the Soudan 2 detector
[DE92-007397] p 2437 N92-23328
NEUTRON FLUX DENSITY
Spectral effects in radiation embrittlement
[DE92-007837] p 2447 N92-23444
Magnetic flux motion and flux pinning superconductors
[DE92-008243] p 2449 N92-23892
NEUTRON IRRADIATION
Hardening in AlN induced by point defects
[DE92-007717] p 2352 N92-23720
NEUTRON SPECTRA
Spectral effects in radiation embrittlement
[DE92-007837] p 2447 N92-23444
NEUTRON STARS
Discovery of orbital decay in SMC X-1
[NASA-CR-190214] p 2317 N92-23531
Observing millisecond and binary pulsars
p 2455 N92-24001
NEUTRONS
Neutron induced gamma-ray production data
[DE92-615322] p 2440 N92-23130
The notion of nonrelativistic isoparticle
[DE92-615215] p 2438 N92-23744
Low dose neutron late effects: Cataractogenesis
[DE92-005539] p 2414 N92-24033
NICKEL ALLOYS
On the kinetics of structural relaxation in some metallic glasses
[PB92-1287272] p 2353 N92-23165
The influence of chromium on structure and mechanical properties of B2 nickel aluminide alloys
[NASA-CR-189124] p 2351 N92-23566
NICKEL CADMIUM BATTERIES
Testing and analyses of electrochemical cells using frequency response
[NASA-TM-103580] p 2369 N92-23437
NICKEL COMPOUNDS
Melting of nickel clusters
[DE92-006986] p 2351 N92-23573
NICKEL HYDROGEN BATTERIES
Center for Space Power, Texas A and M University
p 2313 N92-23651
A dual anode nickel-hydrogen cell
[NASA-CASE-LEW-15212-1] p 2404 N92-24054
NICKEL STEELS
Development of a crack arrest fracture toughness measurement procedure for quality assurance of plates and welds used for hydrocarbon storage tanks
[PB92-141753] p 2389 N92-23681
NITROGEN
Orbital Maneuvering Vehicle (OMV) plume and plume effects study
[NASA-CR-184292] p 2322 N92-23530
NOISE (SOUND)
Experimental study of the mechanism of sound generation by rotating stall in centrifugal turbomachines
p 2436 N92-23726
NOISE REDUCTION
A frequency domain least squares method for modelling acoustic fields
[ISVR-TR-196] p 2435 N92-23170
NOISE TEMPERATURE
Design and performance of 22 GHz coaxial low noise MESFET and HEMT amplifiers
[PB92-134071] p 2368 N92-23172
NONDESTRUCTIVE TESTS
Detecting Lamb waves with broad-band acousto-ultrasonic signals in composite structures
[NASA-TM-105557] p 2386 N92-23189
Training guidelines in non-destructive testing techniques
[DE92-615083] p 2386 N92-23258
Method for advanced material characterization by laser induced eddy current imaging
[NASA-CASE-GSC-13386-1] p 2386 N92-23376
Method and apparatus for determination of material residual stress
[NASA-CASE-GSC-13451-1] p 2388 N92-23549
Non contacting measurement of vibration
p 2325 N92-23800
Underlying modal data issues for detecting damage in truss structures
[NASA-TM-107573] p 2390 N92-23990
Ion Microtomography (IMT) and Particle-Induced X ray Emission (PIXE) analysis direct drive of Inertial Confinement Fusion (ICF) targets
[DE92-008614] p 2446 N92-24067
NONLINEAR EQUATIONS
Euclidean-isotopic symmetries
[DE92-615260] p 2431 N92-23128
Galilei-isotopic symmetries
[DE92-615261] p 2431 N92-23129
NONLINEAR FEEDBACK
Nonlinear feedback guidance law for aero-assisted orbit transfer maneuvers
[NASA-CR-190129] p 2317 N92-23529
NONLINEAR SYSTEMS
The discontinuous finite element method with the Taylor-Galerkin approach for nonlinear hyperbolic conservation laws p 2433 N92-23738
Magnetotransport and responses of semiconductor microstructures p 2449 N92-23775
Closed systems with nonHamiltonian internal forces
[DE92-619234] p 2434 N92-24039
NONLINEARITY
Matrix dominated stress/strain behavior in polymeric composites: Effects of hold time, nonlinearity and rate dependency
[NASA-TM-107595] p 2340 N92-23434
Nonlinear feedback guidance law for aero-assisted orbit transfer maneuvers
[NASA-CR-190129] p 2317 N92-23529
Nonlinear finite element analysis of space frames
[PB92-142447] p 2388 N92-23664
Analysis and control of nonlinear flexible manipulator
p 2384 N92-23727
Employment of C.B. (Craig-Bampton) models for nonlinear dynamic analysis p 2327 N92-23814
Non linear structural analysis of a thin skin carbon-carbon rigid decelerator p 2330 N92-23831
Investigations of the dynamic behaviour of compounds under preloading p 2332 N92-23842
NORMAL DENSITY FUNCTIONS
The statistical analysis of data from normal distributions, with particular reference to small samples
[ESDU-91041] p 2434 N92-24008
NORTH SEA
Euromar-Seastars: A definition study on modular multisensor instrumentation for airborne remote sensing of the sea
[MBB-UK-0152-91-PUB] p 2392 N92-23379
Sensor package for the North Sea
p 2393 N92-23384
NOTCH STRENGTH
Development of fatigue damage mechanics for application to the design of damage-tolerant composite components p 2324 N92-23793
Notched strength of composite materials
p 2331 N92-23839
NOVA LASER SYSTEM
Vacuum mechatronic laser alignment system on the NOVA laser
[DE92-006898] p 2379 N92-23571
Optimization of the laser glass composition for the Nova upgrade fusion laser system
[DE92-008606] p 2380 N92-24065
NOZZLE DESIGN
Progress of simulations for reacting shear layers
p 2302 N92-23344
NOZZLE FLOW
The flip-flop nozzle extended to supersonic flows
[NASA-TM-105570] p 2304 N92-23269
NOZZLE GEOMETRY
The flip-flop nozzle extended to supersonic flows
[NASA-TM-105570] p 2304 N92-23269
NUCLEAR CAPTURE
Neutron induced gamma-ray production data
[DE92-615322] p 2440 N92-23130
NUCLEAR DEFORMATION
Static multipole deformations in nuclei
[DE92-008250] p 2436 N92-23277
From ground state to fission fragments: A complex, multi-dimensional multi-path problem
[DE92-008488] p 2438 N92-23714
NUCLEAR DEVICES
An x ray diagnostic of electron power loss
[DE92-008599] p 2444 N92-23523
NUCLEAR ELECTRIC PROPULSION
Blazing the trailway: Nuclear electric propulsion and its technology program plans
[NASA-TM-105605] p 2337 N92-23252
NUCLEAR EMULSIONS
Dosimetric mapping inside biorack (7-IML-1)
p 2358 N92-23611

NUCLEAR ENERGY
Limiting net greenhouse gas emissions in the United States, volume 1
[DE92-007593] p 2405 N92-23204
NUCLEAR FUSION
The case for exotic beams at the Holifield Heavy Ion Research Facility
[DE92-008003] p 2441 N92-23445
NUCLEAR MAGNETIC RESONANCE
Reductive coupling of carbon monoxide to C2 products
[DE92-007529] p 2347 N92-23499
NUCLEAR MEDICINE
Nuclear medicine program
[DE92-006979] p 2412 N92-23518
JPRS report: Science and technology. Central Eurasia: Life sciences
[JPRS-ULS-92-010] p 2412 N92-23706
NUCLEAR METEOROLOGY
Nuclear winds in active galaxies p 2457 N92-23716
NUCLEAR PHYSICS
The all particle method
[DE92-008357] p 2439 N92-24005
NUCLEAR QUADRUPOLE RESONANCE
NQR investigation of pressure-induced charge transfer in oxygen-deficient YBa2Cu3O(7-delta) (delta = 0.38)
[DE92-008441] p 2450 N92-24036
NUCLEAR REACTIONS
Neutron induced gamma-ray production data
[DE92-615322] p 2440 N92-23130
Studies of fluctuation processes in nuclear collisions
[DE92-008144] p 2440 N92-23276
Charged particle activation studies on the surface of LDEF spacecraft p 2439 N92-23296
Radioactivities of Long Duration Exposure Facility (LDEF) materials: Baggage and bonanzas
p 2440 N92-23297
Theoretical nuclear reaction and structure studies using hyperons and photons
[DE92-008587] p 2437 N92-23577
NUCLEAR REACTOR CONTROL
Conceptual design of Fusion Experimental Reactor
[DE92-751036] p 2443 N92-23132
NUCLEAR REACTORS
Fusion gain due to high energy ions accelerated by additional heating
[DE92-751038] p 2443 N92-23133
A simple unfold method for Rutherford-scattering, intense ion-beam spectrographs
[DE92-008678] p 2445 N92-23749
Transport calculations of chemically sputtered carbon near a plasma divertor surface
[DE92-009022] p 2445 N92-24021
NUCLEAR STRUCTURE
The case for exotic beams at the Holifield Heavy Ion Research Facility
[DE92-008003] p 2441 N92-23445
Theoretical nuclear reaction and structure studies using hyperons and photons
[DE92-008587] p 2437 N92-23577
NUCLEATION
Mercury iodide nucleation and crystal growth in vapor phase (4-IML-1) p 2361 N92-23633
Investigation of fretting fatigue mechanisms on 7075-T6 aluminum alloy and Ti-6Al-4V titanium alloy
p 2352 N92-23725
NUCLEIC ACIDS
Methods for the detection of microorganisms in the environment
[PB92-137454] p 2405 N92-23512
NUCLEON-NUCLEON INTERACTIONS
Studies of fluctuation processes in nuclear collisions
[DE92-008144] p 2440 N92-23276
NUCLIDES
Surface activation of Concorde by Be-7
p 2439 N92-23295
NUMERICAL ANALYSIS
Electrostatic image solution for the interaction of two dielectric spheres
[PB92-142199] p 2364 N92-23138
A comparative study of preconditioned Lanczos methods for nonsymmetric linear systems
[DE92-007530] p 2431 N92-23201
Charged-soft-sphere potentials for trivalent metal halides
[DE92-617445] p 2350 N92-23211
Numerical experiments with flows of elongated granules
[NASA-TM-105567] p 2381 N92-23226
Improved numerical methods for quantum field theory (outstanding junior investigator award)
[DE92-008730] p 2451 N92-23578
Mathematical modelling and numerical approximations for two-phase flow problems p 2375 N92-23672
Introduction to Special Course on Engineering Methods in Aerodynamic Analysis and Design of Aircraft
p 2308 N92-23951
NUMERICAL CONTROL
A new VME based high voltage power supply for large experiments
[DE92-007199] p 2368 N92-23326
On motion planning amidst transient obstacles
[DE91-018939] p 2429 N92-23457
Microprocessor control of multiple peak power tracking DC/DC converters for use with solar cell arrays
[NASA-CASE-GSC-13450-1] p 2403 N92-23463
Optimum cutting conditions determination for the NC-milling
[REPT-2.1.2] p 2422 N92-23874
Shop floor scheduling through a simulation based scheduler
[REPT-2.3.3] p 2423 N92-23876
From IGES to STEP
[REPT-3.1.6] p 2423 N92-23881
Time optimal trajectories for a 2-wheeled robot
[DE92-000069] p 2430 N92-24032
NUMERICAL STABILITY
Investigation of solution operators for the three dimensional unsteady Euler equations
p 2376 N92-24018
NUMERICAL WEATHER FORECASTING
Scientific development of the Advanced Parallel Chemistry (APACHE) climate model
[DE92-006657] p 2404 N92-23123
NYSTAGMUS
Positional and spontaneous nystagmus (8-IML-1)
p 2360 N92-23624

O

OBJECT-ORIENTED PROGRAMMING
Coordinating complex problem-solving among distributed intelligent agents p 2427 N92-23360
OCEAN COLOR SCANNER
Utilization of satellite images for marine resources
p 2399 N92-23480
OCEAN CURRENTS
Applicability of MESSR and VTIR data for marine observation p 2398 N92-23478
Wind, current and temperature data at 0 deg, 165 deg E: January 1986 to March 1991
[PB92-143080] p 2411 N92-23682
CODAR in the Straits of Florida
[PB92-129964] p 2412 N92-23732
OCEAN DATA ACQUISITIONS SYSTEMS
Euromar-Seastars: A definition study on modular multisensor instrumentation for airborne remote sensing of the sea
[MBB-UK-0152-91-PUB] p 2392 N92-23379
Euromar-Seastars: Summary p 2392 N92-23380
Proceedings on MOS-1 data evaluation
[HE-90015] p 2396 N92-23465
Outline of utilization results of MOS-1 data
p 2396 N92-23466
OCEAN MODELS
Monsoon-ENSO relationships p 2404 N92-23160
Improved interpretation of satellite altimeter data using genetic algorithms p 2402 N92-23369
OCEAN SURFACE
Improved interpretation of satellite altimeter data using genetic algorithms p 2402 N92-23369
Sensor package for the North Sea
p 2393 N92-23384
The laser fluorosensor p 2393 N92-23386
CODAR in the Straits of Florida
[PB92-129964] p 2412 N92-23732
Reconstructing the tropical Atlantic seasonal thermocline using planktonic foraminifera
p 2412 N92-23769
Analysis of gravity and topography on Earth and Venus: Comparisons of lithospheric and sublithospheric processes p 2409 N92-23772
OCEAN TEMPERATURE
Study of MOS-1 MESSR data for variability of the branch (Warm Streamer) from warm eddy and for fishing ground
p 2398 N92-23477
Wind, current and temperature data at 0 deg, 165 deg E: January 1986 to March 1991
[PB92-143080] p 2411 N92-23682
OCEANOGRAPHIC PARAMETERS
Geophysical, chemical and biological measuring parameters p 2393 N92-23385
Wind, current and temperature data at 0 deg, 165 deg E: January 1986 to March 1991
[PB92-143080] p 2411 N92-23682
On the principle of Aristoteles p 2314 N92-23911
OCEANOGRAPHY
Euromar-Seastars: A definition study on modular multisensor instrumentation for airborne remote sensing of the sea
[MBB-UK-0152-91-PUB] p 2392 N92-23379
International cooperation p 2396 N92-23409
Euromar industrial partners agreement
p 2396 N92-23410
An 18-point catalog description p 2396 N92-23411
Research project for practical usage of MOS-1 data collection system p 2399 N92-23485
JPRS report: Science and technology. USSR: Earth sciences
[JPRS-UES-91-005] p 2392 N92-23707
Gravity field data products from the Aristoteles mission p 2317 N92-23925
OCEANS
Introduction: Ocean air observation
p 2392 N92-23381
The state of the development in Europe
p 2392 N92-23382
Our living oceans: The first annual report on the status of US living marine resources
[PB92-145689] p 2412 N92-23519
Ocean acoustic tomography inversion in the adiabatic-invariant approximation
[PB92-140466] p 2412 N92-23669
Earth observing system: NASA's EOSDIS development approach is risky
[GAO/IMTEC-92-24] p 2401 N92-23686
OCTAVES
Acoustic prediction on satellite structure
p 2327 N92-23812
OIL SLICKS
The laser fluorosensor p 2393 N92-23386
OILS
Liquid/supercritical fluid carbon dioxide cleaning of stainless steel components
[DE92-006947] p 2348 N92-23572
OLIVINE
Preliminary analysis of LDEF instrument A0187-1: Chemistry of Micrometeoroids Experiment
p 2458 N92-23315
ON-LINE SYSTEMS
Feedback control of plasma equilibrium with control system aided by personal computer on the JIPP T-IIU tokamak
[DE92-750824] p 2444 N92-23261
The design and control of uncertain manipulator arms with decoupled inertia matrix p 2383 N92-23690
User interface user's guide for HYPGEN
[NASA-CR-190304] p 2425 N92-23991
ONBOARD DATA PROCESSING
Quick-look system p 2394 N92-23393
On board data formatting p 2394 N92-23394
On board data recording p 2394 N92-23395
Real-time radar processor p 2394 N92-23396
Ground station p 2394 N92-23397
Sensor interfaces p 2395 N92-23400
ONBOARD EQUIPMENT
Types of operation and system control
p 2395 N92-23401
Current definition of some development programs
p 2395 N92-23405
Realization and provisional sensor development planning p 2395 N92-23406
OPERATING COSTS
Change in test-technology
[REPT-1.2.8] p 2421 N92-23867
Advances in processing rates optimization for flexible manufacturing systems
[REPT-2.3.4] p 2423 N92-23877
OPERATIONAL PROBLEMS
Types of operation and system control
p 2395 N92-23401
OPERATIONS RESEARCH
SLS-PLAN-IT: A knowledge-based blackboard scheduling system for Spacelab life sciences missions
p 2426 N92-23358
OPERATOR PERFORMANCE
Training users of a flexible decision support system: The effects of training content and user ability
p 2453 N92-23730
OPERATORS (MATHEMATICS)
Small solutions and completeness for linear functional differential equations
[PB92-149350] p 2431 N92-23250
Nonequilibrium statistical operator in hot-electron transport theory
[DE92-615517] p 2446 N92-23260
The Jordan-Schwinger realization of two-parametric quantum group SI(sub q,s)(2)
[DE92-616891] p 2451 N92-23501
Lie-admissible structure of Hamilton's original equations with external terms
[DE92-615216] p 2433 N92-23745

Investigation of solution operators for the three dimensional unsteady Euler equations p 2376 N92-24018

OPTICAL COMMUNICATION
Electro-optic resonant phase modulator [NASA-CASE-NPO-18702-1-CU] p 2442 N92-23551

OPTICAL EQUIPMENT
Thermoluminescent dosimetry for LDEF experiment M0006 p 2461 N92-23301
In situ particle size measurements using a two-color laser scattering technique [DE92-008634] p 2380 N92-24070

OPTICAL FIBERS
Integrated optics in silicon-based aluminum oxide [ISBN-90-9004261-X] p 2441 N92-23166
CIM implementation at CVALIM, D.T.C. Division, Bet-Shean, Israel [REPT-3.2.4] p 2424 N92-23884
Mutual interference in multichannel fibre communication systems p 2367 N92-24019

OPTICAL MEASUREMENT
An optical study of grain formation: Casting and solidification technology (2-IML-1) p 2361 N92-23631

OPTICAL MEASURING INSTRUMENTS
Realization and provisional sensor development planning p 2395 N92-23406
Provisional cost evaluation p 2395 N92-23408
Limits of survivability and damage for optical components used in a high repetition rate visible laser [DE92-006896] p 2379 N92-23570

OPTICAL MEMORY (DATA STORAGE)
Optical inner product neural associative memory [NASA-CASE-NPO-18491-1-CU] p 2416 N92-23546

OPTICAL PROPERTIES
Superconducting materials [DE92-007748] p 2446 N92-23205
Meteoroid/space debris impacts on MSFC LDEF experiments p 2335 N92-23311
Electrical and optical properties of high gain GaAs switches [DE92-008668] p 2371 N92-23983
Optical properties of metallic multi-layer films [DE92-615486] p 2443 N92-24029

OPTICAL RADAR
Seaborne lidar system p 2393 N92-23389

OPTICAL WAVEGUIDES
Integrated optics in silicon-based aluminum oxide [ISBN-90-9004261-X] p 2441 N92-23166

OPTIMAL CONTROL
Sensor compatibility/optimal sensor combinations p 2395 N92-23403
Control problem for a multi server loss system [PB92-148675] p 2430 N92-23506
Sensitivity l(sup 1) minimization with boundary zeros or poles [PB92-141803] p 2433 N92-23658
Optimal control of closed chain robotic systems p 2430 N92-24011

OPTIMIZATION
Integrated Design Analysis and Optimisation of Aircraft Structures [AGARD-R-784] p 2306 N92-23227
A system approach to aircraft optimization p 2306 N92-23228
Application of multidisciplinary optimization methods to the design of a supersonic transport p 2307 N92-23230
Application of an automated multidisciplinary analysis and optimisation system to the design of aircraft structures p 2307 N92-23233
Multidisciplinary optimization studies using ASTROS p 2307 N92-23234
A fin optimisation study p 2308 N92-23237
Structural optimization of aircraft practice and trends p 2308 N92-23239
Singularities in optimal structural design [NASA-TM-4365] p 2388 N92-23527
Efficient and robust design optimization of transonic airfoils p 2305 N92-23717
Multi parameter optimization on Ariane 5 p 2321 N92-23798
Advanced numerical analyses for the optimisation of the structural behaviour of the intersegment connection for the Ariane 5 booster case p 2327 N92-23809
Minimization of vibrations by broadband sensitivity approach p 2330 N92-23828
Optimal exciter placement and force vector tuning required for experimental modal analysis p 2333 N92-23847
Statistical optimization of integrated circuits in order to reduce the sensitivity to variations in process parameters and environmental conditions [REPT-1.3.6] p 2422 N92-23872
Advances in processing rates optimization for flexible manufacturing systems [REPT-2.3.4] p 2423 N92-23877
The GRADIO accelerometer: Design and development status p 2316 N92-23918
Impact and compression response of composite materials containing fortifiers p 2341 N92-23937

ORBIT CALCULATION
The Aristoteles mission profile p 2316 N92-23922
Salyut-7/Kosmos-1686 reentry predictions for the Italian Civil Defence Authority p 2334 N92-23972
Debris reentry prediction: Salyut-7/Kosmos-1686 p 2318 N92-23973
Salyut-7/Kosmos-1686 orbit determination from radar data p 2318 N92-23976
Orbital decay and reentry of the Salyut-7 orbital complex p 2335 N92-23978

ORBIT DECAY
Discovery of orbital decay in SMC X-1 [NASA-CR-190214] p 2317 N92-23531
The Reentry of Salyut-7/Kosmos-1686 [ESA-SP-345] p 2333 N92-23967
Salyut-7/Kosmos-1686 reentry predictions for the Italian Civil Defence Authority p 2334 N92-23972
Orbital decay and reentry of the Salyut-7 orbital complex p 2335 N92-23978

ORBIT PERTURBATION
Constructing a pulsar timing array p 2456 N92-23126
Precision GPS ephemerides and baselines [NASA-CR-190247] p 2306 N92-23541

ORBIT TRANSFER VEHICLES
Nonlinear feedback guidance law for aero-assisted orbit transfer maneuvers [NASA-CR-190129] p 2317 N92-23529

ORBITAL ASSEMBLY
Artificial intelligence approach to planning the robotic assembly of large tetrahedral truss structures p 2426 N92-23357
High reliability robot friendly ORU interface [NASA-CASE-GSC-13360-1] p 2381 N92-23377
Robot-friendly connector --- space truss structures [NASA-CASE-MSC-21864-1] p 2382 N92-23544

ORBITAL LAUNCHING
From Earth to orbit --- assessment of transportation options [NASA-CR-190216] p 2321 N92-23980

ORBITAL MANEUVERING VEHICLES
Orbital Maneuvering Vehicle (OMV) plume and plume effects study [NASA-CR-184292] p 2322 N92-23530

ORBITAL MECHANICS
Salyut-7/Kosmos-1686 reentry predictions for the Italian Civil Defence Authority p 2334 N92-23972
Salyut-7/Kosmos-1686 orbit determination from radar data p 2318 N92-23976

ORBITAL POSITION ESTIMATION
Application of ground-based laser beacon for Earth image calibration, 3 p 2396 N92-23468
Prediction of solar and geomagnetic activity for ESA low-flying spacecraft p 2334 N92-23975

ORGANIC COMPOUNDS
Organic crystal growth experiment facility (13-IML-1) p 2362 N92-23635

ORGANIC MATERIALS
Characterization of organic coatings with impedance measurements: A study of coating structure, adhesion and underfilm corrosion [PB92-133479] p 2339 N92-23174

ORGANOMETALLIC COMPOUNDS
Reductive coupling of carbon monoxide to C2 products [DE92-007529] p 2347 N92-23499

ORTHOTROPIC PLATES
Experimental verification of a theory for the impact response of composite plates [FFA-TN-1991-17] p 2339 N92-23167

ORTHOTROPIC SHELLS
Free vibration of thick isotropic and orthotropic cylindrical shells p 2389 N92-23773

OSCILLATING FLOW
The flip-flop nozzle extended to supersonic flows [NASA-TM-105570] p 2304 N92-23269

OSCILLATIONS
Thresholds of longitudinal instability of bunched beam in the presence of dominant inductive impedance [DE92-617992] p 2436 N92-23274

OSCILLATORS
NIST torsion oscillator viscometer response: Performance on the LeRC active vibration isolation platform [NASA-TM-105571] p 2383 N92-23564
Application of optical distributed sensing and computation to control of large space structures [NASA-CR-190293] p 2442 N92-23567

OSTEOPOROSIS
Effect of microgravity and mechanical stimulation on the in vitro mineralization and resorption of fetal mouse long bones (7-IML-1) p 2357 N92-23606

OXIDATION
Hydrogen absorption by zirconium alloy cladding tube with surface oxide film [DE92-750962] p 2351 N92-23265
Oxidative degradation of polymers induced by ionizing radiation [DE92-007657] p 2354 N92-23442
The oxidation behavior of Co-15wt percent Cr alloy containing dispersed oxides formed by internal oxidation [DE92-008283] p 2352 N92-23893
Modeling of the catalytic oxidative coupling of methane [DE92-008554] p 2349 N92-24064

OXIDATION RESISTANCE
Large thin composite thermostructural parts p 2329 N92-23821

OXIDE FILMS
Hydrogen absorption by zirconium alloy cladding tube with surface oxide film [DE92-750962] p 2351 N92-23265

OXIDES
An XPS study of the stability of Fomblin Z25 on the native oxide of aluminum --- x ray photoelectron spectroscopy [NASA-TM-105594] p 2353 N92-23185
Magnetic fluctuations and normal state properties of the t-J model at finite dopings [DE92-617538] p 2447 N92-23452

OXYGEN
Energy expenditure in space flight (doubly labelled water method) (8-IML-1) p 2359 N92-23620

OXYGEN ATOMS
Pinhole cameras as sensors for atomic oxygen in orbit: Application to attitude determination of the LDEF p 2379 N92-23283

OXYGEN IONS
Resonant transfer excitation: Interference effects [DE92-007240] p 2439 N92-24026

OXYGEN PLASMA
Replacement of hydrogen peroxide cleaning with oxygen plasma [DE92-009020] p 2445 N92-23905

OXYGEN 18
Energy expenditure in space flight (doubly labelled water method) (8-IML-1) p 2359 N92-23620

OZONE
Use of the maximum entropy method to retrieve the vertical atmospheric ozone profile and predict atmospheric ozone content p 2407 N92-23965

OZONOSPHERE
On the global warming potentials of candidate gaseous diffusion plant coolants [DE92-006640] p 2406 N92-23740

P

PACKET TRANSMISSION
Design of joint source/channel coders [NASA-CR-189960] p 2417 N92-23416
A robust low-rate coding scheme for packet video p 2417 N92-23420
A robust coding scheme for packet video p 2418 N92-23422
Variable bit rate video coding [PB92-134279] p 2367 N92-23676

PACKETS (COMMUNICATION)
Design of joint source/channel coders [NASA-CR-189960] p 2417 N92-23416
A robust low-rate coding scheme for packet video p 2417 N92-23420
A robust coding scheme for packet video p 2418 N92-23422

PACKING DENSITY
Sphere packings centered at S-units of algebraic tori [PB92-136373] p 2434 N92-24061

PAIN
Back pain in astronauts (8-IML-1) p 2360 N92-23622

PAINTS
Molecular films associated with LDEF p 2439 N92-23289
Organic contamination of LDEF p 2339 N92-23290

PANEL METHOD (FLUID DYNAMICS)
Panel methods for aerodynamic analysis and design p 2309 N92-23955

PARALLEL COMPUTERS
Theory for iterative solution of large dynamical systems using parallel computation [PB92-143304] p 2433 N92-23589

PARALLEL PLATES
Closed parallel-plate chiral waveguides with boundary impedance conditions [PB92-142397] p 2366 N92-23591

PARALLEL PROCESSING (COMPUTERS)
Scientific development of the Advanced Parallel Chemistry (APACHE) climate model
[DE92-006657] p 2404 N92-23123
Synchronous parallel system for emulation and discrete event simulation
[NASA-CASE-NPO-18414-1-CU] p 2426 N92-24045
PARAMETER IDENTIFICATION
Matching finite element models to modal data
p 2333 N92-23848
Design parameter update of dynamic mathematical models in presence of test noise and mode pairing problems p 2333 N92-23850
PARTIAL DIFFERENTIAL EQUATIONS
Euclidean-isotopic symmetries
[DE92-615260] p 2431 N92-23128
Studies of fluctuation processes in nuclear collisions
[DE92-008144] p 2440 N92-23276
PARTICLE ACCELERATOR TARGETS
Neutron induced gamma-ray production data
[DE92-615322] p 2440 N92-23130
Studies of fluctuation processes in nuclear collisions
[DE92-008144] p 2440 N92-23276
Results from the Soviet-American gallium experiment
[DE92-007414] p 2438 N92-23747
PARTICLE ACCELERATORS
Actively-stabilized photomultiplier tube base for vacuum operation
[DE92-007528] p 2368 N92-23200
Particle dynamics in a wave with variable amplitude
[DE92-008340] p 2436 N92-23217
PARTICLE COLLISIONS
Studies of fluctuation processes in nuclear collisions
[DE92-008144] p 2440 N92-23276
PARTICLE ENERGY
The isotopic composition of cosmic ray helium from 500 to 1100 MeV per nucleon p 2460 N92-23163
PARTICLE INTERACTIONS
Heavy ion measurement on LDEF
p 2440 N92-23308
Recent results on K(omega) and (pi)(pi) systems from LASS
[DE92-007389] p 2436 N92-23327
Research in high energy physics
[DE92-007966] p 2441 N92-23500
PARTICLE MOTION
Probing picosecond flame dynamics with transient grating experiments
[DE92-003163] p 2346 N92-23181
Particle dynamics in a wave with variable amplitude
[DE92-008340] p 2436 N92-23217
Potential energy surfaces and reaction dynamics of polyatomic molecules
[DE92-008314] p 2437 N92-23450
Numerical calculation: Aspiration efficiency of aerosols into thin-walled sampling inlets
[PB92-132901] p 2374 N92-23516
Inequivalence of interior and exterior dynamical problems
[DE92-615214] p 2451 N92-23743
Numerical and physical modelling of bubbly flow phenomena
[DE92-008642] p 2376 N92-24062
PARTICLE PRODUCTION
Research in high energy physics
[DE92-007967] p 2440 N92-23214
Research in high energy physics
[DE92-007968] p 2440 N92-23215
Studies of fluctuation processes in nuclear collisions
[DE92-008144] p 2440 N92-23276
PARTICLE SIZE DISTRIBUTION
Quantification of contaminants associated with LDEF
p 2349 N92-23288
In situ particle size measurements using a two-color laser scattering technique
[DE92-008634] p 2380 N92-24070
PARTICLE THEORY
Research in high energy physics
[DE92-007966] p 2441 N92-23500
PARTICLE TRACKS
Heavy ion measurement on LDEF
p 2440 N92-23308
PARTICLE TRAJECTORIES
A study of underground muons in the Soudan 2 detector p 2437 N92-23674
PARTICULATES
Numerical experiments with flows of elongated granules
[NASA-TM-105567] p 2381 N92-23226
Particle types and sources associated with LDEF
p 2349 N92-23286
Quantification of contaminants associated with LDEF
p 2349 N92-23288
Dynamic (computer) modelling of the particulate environment: Transformations from the LDEF reference frame to decode geocentric and interplanetary populations p 2458 N92-23320
PATTERN RECOGNITION
Feature detection in satellite images using neural network technology p 2427 N92-23366
PAYLOAD INTEGRATION
The use of artificial intelligence techniques to improve the multiple payload integration process
p 2428 N92-23370
Suborbital missions: The Joust p 2313 N92-23644
Introductory remarks to the mission and system aspects session p 2315 N92-23916
PAYLOADS
The use of artificial intelligence techniques to improve the multiple payload integration process
p 2428 N92-23370
Spacehab p 2313 N92-23647
Space Station Freedom p 2313 N92-23649
Ariane 5 structural definition of the upper composite
p 2321 N92-23808
Feasibility of payload sensitivity analyses for AR4 dynamic events p 2328 N92-23815
PEEK
Impact-induced delamination in (0(5), 90(5), 0(5)) carbon/peek composite laminates p 2341 N92-23936
On the application of micromechanics to the prediction of macroscopic thermal residual stresses in short-fiber reinforced Polyetheretherketone (PEEK)
p 2343 N92-23942
PENETRATION
Hypervelocity impact microfoil perforations in the LEO space environment (LDEF, MAP AO-023 experiment)
p 2336 N92-23312
Meteoroid and debris special investigation group data acquisition procedures p 2454 N92-23313
Meteoroid, and debris special investigation group preliminary results: Size-frequency distribution and spatial density of large impact features on LDEF
p 2336 N92-23314
Dynamic (computer) modelling of the particulate environment: Transformations from the LDEF reference frame to decode geocentric and interplanetary populations p 2458 N92-23320
M and D SIG progress report: Laboratory simulations of LDEF impact features p 2336 N92-23323
Preliminary micrometeoroid and debris effects on LDEF thermal control surfaces p 2336 N92-23324
The interstellar gas experiment p 2459 N92-23325
Computer simulation of moisture penetration in structures p 2326 N92-23806
Real-time measurement of electron beam weld penetration in uranium by acoustic emission monitoring
[DE92-008040] p 2384 N92-23908
PEPTIDES
Photoinduced electron transfer in ordered polymers
[DE92-008787] p 2355 N92-24037
PERFLUORO COMPOUNDS
An XPS study of the stability of Fomblin Z25 on the native oxide of aluminum --- x ray photoelectron spectroscopy
[NASA-TM-105594] p 2353 N92-23185
PERFORMANCE PREDICTION
Effects of chemical equilibrium on turbine engine performance for various fuels and combustor temperatures
[NASA-TM-105399] p 2311 N92-23254
Derated ion thruster design issues
[NASA-TM-105576] p 2337 N92-23534
Nonplanar linearly tapered slot antenna with balanced microstrip feed
[NASA-TM-105647] p 2370 N92-23535
Influence of microvibrations on spacecraft performances p 2329 N92-23825
Aristoteles magnetometer system
p 2316 N92-23920
Special Course on Engineering Methods in Aerodynamic Analysis and Design of Aircraft
[AGARD-R-783] p 2308 N92-23950
Introduction to Special Course on Engineering Methods in Aerodynamic Analysis and Design of Aircraft
p 2308 N92-23951
Survey of experimental techniques for performance prediction p 2309 N92-23954
Aircraft drag analysis methods p 2309 N92-23957
Modelling of aerodynamic forces and heat transfer for orbital decay and reentry calculations
p 2334 N92-23974
PERFORMANCE TESTS
Evaluation of MHOST analysis capabilities for a plate element --- finite element modeling
[NASA-TM-105387] p 2387 N92-23196
Fast wave current drive antenna performance on D3-D
[DE92-008052] p 2444 N92-23446
Spacecraft Structures and Mechanical Testing, volume 1
[ESA-SP-321-VOL-1] p 2322 N92-23780
Change in test-technology
[REPT-1.2.8] p 2421 N92-23867
PERIODIC FUNCTIONS
Harmonic wave propagation in two-dimensional periodic large space structures p 2330 N92-23830
PERIODIC VARIATIONS
Climate System Monitoring (CSM). El Nino/Southern Oscillation (ENSO) diagnostic advisory, special issue
p 2411 N92-23677
PERMANENT MAGNETS
Design considerations for an air core magnetic actuator
[NASA-TM-104229] p 2364 N92-23989
PERSONAL COMPUTERS
Feedback control of plasma equilibrium with control system aided by personal computer on the JIPP T-IIU tokamak
[DE92-750824] p 2444 N92-23261
PERSONNEL
Requirements for the engineer training profile and definition of his role p 2452 N92-23932
PETRI NETS
Compositionality and analysis of algebraic high-level nets
[PB92-143551] p 2432 N92-23440
PH
Acid rain monitoring in East-Central Florida from 1977 to present
[NASA-CR-190152] p 2406 N92-23898
PHASE COHERENCE
Semiclassical model and properties of resonant tunneling diode
[PB92-143320] p 2448 N92-23498
PHASE DIAGRAMS
Simulation of freckles during vertical solidification of binary alloys p 2353 N92-24014
PHASE MODULATION
Electro-optic resonant phase modulator
[NASA-CASE-NPO-18702-1-CU] p 2442 N92-23551
PHASE TRANSFORMATIONS
Monte Carlo simulation of the 3-state vector Potts model on a 3-dimensional random lattice
[DE92-615489] p 2446 N92-23259
Melting of nickel clusters
[DE92-006986] p 2351 N92-23573
Near-critical point phenomena in fluids (19-IML-1)
p 2362 N92-23638
Critical fluid thermal equilibration experiment (19-IML-1) p 2363 N92-23640
Phase transformations in SrAl2Si2O8 glass
[NASA-TM-105657] p 2449 N92-23890
Morphology and mechanical performance of PPS/carbon composite p 2342 N92-23939
Crystallization behavior of poly(phenylene sulphide)
p 2342 N92-23940
PHASED ARRAYS
Fast wave current drive antenna performance on D3-D
[DE92-008052] p 2444 N92-23446
Analysis and development of dynamic selection of laser array elements
[NASA-TM-4375] p 2379 N92-23557
Binary surface-relief gratings for array illumination in digital optics
[PB92-143585] p 2442 N92-23662
PHENOLIC RESINS
Proceedings: Nozzle Initiative Industry Advisory Committee on Standardization of Carbon-Phenolic Test Methods and Specifications
[NASA-CR-190203] p 2337 N92-23539
PHONONS
Cu charge fluctuations and anomalous behaviour in the phonon spectrum of La2CuO4
[DE92-617446] p 2446 N92-23270
Inelastic electron scattering from surfaces
[DE92-008129] p 2437 N92-23330
PHOSPHORIC ACID FUEL CELLS
Demonstration of fuel cells to recover energy from landfill gas: Conceptual study
[PB92-137520] p 2403 N92-23509
PHOSPHORUS OXIDES
Optimization of the laser glass composition for the Nova upgrade fusion laser system
[DE92-008606] p 2380 N92-24065
PHOTOCHEMICAL REACTIONS
Fundamental electron transfer processes at the single crystal semiconductor/liquid interface
[DE92-008132] p 2447 N92-23275
Photochemistry and charge transfer chemistry of the platinum group elements
[DE92-007564] p 2347 N92-23332
Survey on fixation and utilization of carbon dioxide by catalytic hydrogenation
[DE92-769380] p 2347 N92-23456

PHOTOELECTROCHEMISTRY
Fundamental electron transfer processes at the single crystal semiconductor/liquid interface
[DE92-008132] p 2447 N92-23275
PHOTOELECTRON SPECTROSCOPY
An XPS study of the stability of Fomblin Z25 on the native oxide of aluminum — x ray photoelectron spectroscopy
[NASA-TM-105594] p 2353 N92-23185
PHOTOGRAPHIC FILM
IMAX camera (12-IML-1) p 2363 N92-23641
PHOTOLUMINESCENCE
Electrical and optical properties of high gain GaAs switches
[DE92-008668] p 2371 N92-23983
PHOTOLYSIS
Kinetic measurements on elementary fossil fuel combustion reactions over wide temperatures ranges
[DE92-007535] p 2347 N92-23221
Photoinduced electron transfer in ordered polymers
[DE92-008787] p 2355 N92-24037
PHOTOMETERS
Growth and sporulation of Bacillus subtilis under microgravity (7-IML-1) p 2358 N92-23612
PHOTOMETRY
Line profile asymmetries in chromospherically active stars p 2458 N92-24015
PHOTOMULTIPLIER TUBES
Actively-stabilized photomultiplier tube base for vacuum operation
[DE92-007528] p 2368 N92-23200
PHOTONS
Theoretical nuclear reaction and structure studies using hyperons and photons
[DE92-008587] p 2437 N92-23577
CEPXS/ONELD: A one-dimensional coupled electron-photon discrete ordinates code package
[DE92-003146] p 2425 N92-24041
PHOTOPRODUCTION
Research in high energy physics
[DE92-007966] p 2441 N92-23500
PHOTOSYNTHESIS
Survey on fixation and utilization of carbon dioxide by catalytic hydrogenation
[DE92-769380] p 2347 N92-23456
PHOTOTRANSISTORS
Versatile bistable optical switches and latching optical logic using integrated photothyristors and surface-emitting lasers
[DE92-008677] p 2442 N92-23748
PHOTOTROPISM
A spaceflight experiment to investigate the effects of a range of unilateral blue light phototropic stimulations on the movements of wheat coleoptiles (6-IML-1)
p 2356 N92-23602
PHOTOVOLTAIC CELLS
PHOTO: A computer simulation program for photovoltaic and hybrid energy systems. Document and user's guide
[PB92-141928] p 2403 N92-23683
Self-deploying photovoltaic power system
[NASA-CASE-LEW-15308-1] p 2404 N92-24057
PHOTOVOLTAIC CONVERSION
Rapid recrystallization of semiconductor thin films for photovoltaic applications p 2404 N92-23998
PHYSICAL OPTICS
Report from orbit sub-group of task force for MR synchrotron radiation project
[DE92-751024] p 2441 N92-23713
PHYSIOLOGICAL EFFECTS
Skeletal responses to spaceflight
[NASA-TM-103890] p 2414 N92-23424
First International Microgravity Laboratory experiment descriptions
[NASA-TM-4353] p 2356 N92-23600
Genetic and molecular dosimetry of HZE radiation (7-IML-1) p 2357 N92-23603
Measurement of venous compliance (8-IML-1)
p 2360 N92-23623
PHYSIOLOGICAL RESPONSES
Stress effects of human-computer interactions
[PB92-136001] p 2415 N92-23513
Gravitropic responses of plants in the absence of a complicating G-force (6-IML-1) p 2356 N92-23601
A spaceflight experiment to investigate the effects of a range of unilateral blue light phototropic stimulations on the movements of wheat coleoptiles (6-IML-1)
p 2356 N92-23602
Chrondrogenesis in micromass cultures of embryonic mouse limb mesenchymal cells exposed to microgravity (7-IML-1) p 2357 N92-23605
Effect of microgravity and mechanical stimulation on the in vitro mineralization and resorption of fetal mouse long bones (7-IML-1) p 2357 N92-23606
Eggs: The role of gravity in the establishment of the dorso-ventral axis in the amphibian embryo (7-IML-1)
p 2357 N92-23607
The effect of space environment on the development and aging of Drosophila Melanogaster (7-IML-1)
p 2357 N92-23608
Positional and spontaneous nystagmus (8-IML-1)
p 2360 N92-23624
Space adaptation syndrome experiments (8-IML-1)
p 2360 N92-23625
Microgravity vestibular investigations (10-IML-1)
p 2360 N92-23626
Center for Cell Research, Pennsylvania State University p 2314 N92-23653
PINHOLE CAMERAS
Pinhole cameras as sensors for atomic oxygen in orbit: Application to attitude determination of the LDEF
p 2379 N92-23283
PINS
Oil lubricated and water lubricated pin-on-disc wear tests with engineering ceramics
[PB92-136563] p 2380 N92-23152
PIONS
Test beam results from the D0 end electromagnetic calorimeter
[DE92-008299] p 2378 N92-23279
PIPE FLOW
Impinging axisymmetric jet p 2372 N92-23146
PIPELINES
Mathematical model of a control valve
[PB92-141951] p 2383 N92-23710
PIPES (TUBES)
Collapse of composite tubes under end moments
[NASA-TM-107605] p 2390 N92-23992
PITCH (MATERIAL)
Survey on optimization of CO2 disposal system and carbon utilization technology
[DE92-769381] p 2407 N92-24024
PIVOTS
Flexible robotic arm
[NASA-CASE-GSC-13161-1] p 2386 N92-24060
PLANAR STRUCTURES
Coaxial turnstile junction
[NASA-CASE-GSC-13422-1] p 2369 N92-23462
PLANE STRAIN
Localization of deformation and inelastic deformation of pressure-sensitive dilatant materials
p 2389 N92-23737
PLANE STRESS
Notched strength of composite materials
p 2331 N92-23839
PLANE WAVES
A frequency domain least squares method for modelling acoustic fields
[ISVR-TR-196] p 2435 N92-23170
Biisotropic polarizer shield
[PB92-141878] p 2366 N92-23590
PLANETARY ATMOSPHERES
Use of the maximum entropy method to retrieve the vertical atmospheric ozone profile and predict atmospheric ozone content p 2407 N92-23965
PLANETARY EVOLUTION
Publications of the exobiology program for 1990: A special bibliography
[NASA-TM-4364] p 2416 N92-23429
PLANETARY NEBULAE
Infrared emission lines from highly ionized regions
p 2460 N92-23162
PLANETARY SYSTEMS
JPRS report: Science and technology. Central Eurasia: Space
[JPRS-USP-92-002] p 2314 N92-23705
PLANKTON
Reconstructing the tropical Atlantic seasonal thermocline using planktonic foraminifera
p 2412 N92-23769
PLANT ROOTS
Transmission of gravistimulus in the statocyte of the lentil root (7-IML-1) p 2359 N92-23617
PLANTS (BOTANY)
Gravitropic responses of plants in the absence of a complicating G-force (6-IML-1) p 2356 N92-23601
Growth, differentiation and development of Arabidopsis thaliana under microgravity conditions (7-IML-1)
p 2359 N92-23616
PLASMA COMPOSITION
Transport calculations of chemically sputtered carbon near a plasma divertor surface
[DE92-009022] p 2445 N92-24021
PLASMA CURRENTS
Fast wave current drive antenna performance on D3-D
[DE92-008052] p 2444 N92-23446
Magnetic reconnection in magnetotail and solar plasmas p 2457 N92-24000
PLASMA DIAGNOSTICS
An x ray diagnostic of electron power loss
[DE92-008599] p 2444 N92-23523
PLASMA EQUILIBRIUM
Feedback control of plasma equilibrium with control system aided by personal computer on the JIPP T-IIU tokamak
[DE92-750824] p 2444 N92-23261
PLASMA HEATING
Fusion gain due to high energy ions accelerated by additional heating
[DE92-751038] p 2443 N92-23133
Fast wave current drive antenna performance on D3-D
[DE92-008052] p 2444 N92-23446
Theory study on fast wave absorption at the plasma edge
[PB92-141936] p 2444 N92-23663
Conceptual design of fusion experimental reactor (FER/ITER)
[DE92-750949] p 2444 N92-23711
PLASMA INTERACTIONS
The subionospheric electromagnetic response to magnetopause processes p 2407 N92-23142
PLASMA RESONANCE
Theory study on fast wave absorption at the plasma edge
[PB92-141936] p 2444 N92-23663
PLASMA-PARTICLE INTERACTIONS
Semiempirical studies of atomic structure
[DE92-008143] p 2437 N92-23448
PLASMAS (PHYSICS)
The structure of MFD shock waves for rectilinear motion in some model of plasma
[DE92-617386] p 2443 N92-23208
Low frequency electrostatic modes in a magnetized dusty plasma
[DE92-617387] p 2444 N92-23209
Research in high energy physics
[DE92-007967] p 2440 N92-23214
Research in high energy physics
[DE92-007968] p 2440 N92-23215
Feedback control of plasma equilibrium with control system aided by personal computer on the JIPP T-IIU tokamak
[DE92-750824] p 2444 N92-23261
Analysis of solar and microwave thermal propulsion systems p 2337 N92-23694
A simple unfold method for Rutherford-scattering, intense ion-beam spectrographs
[DE92-008678] p 2445 N92-23749
Annual report, 1 October 1990 - 30 September 1991
[DE92-008648] p 2380 N92-23891
Compact Fusion Advanced Rankine (CFAR2) power cycle
[DE92-008577] p 2445 N92-23987
Transport calculations of chemically sputtered carbon near a plasma divertor surface
[DE92-009022] p 2445 N92-24021
PLASTIC DEFORMATION
Conception and development of improved analytical prediction models for fatigue induced tooth breakage due to cyclic bending in spur gear teeth
p 2384 N92-23739
PLASTIC PROPERTIES
Conception and development of improved analytical prediction models for fatigue induced tooth breakage due to cyclic bending in spur gear teeth
p 2384 N92-23739
PLATES (STRUCTURAL MEMBERS)
Nd: YAG laser welding aluminum alloys
[DE92-003131] p 2381 N92-23177
Buckling of simply supported and clamped anisotropic plates under combined loads p 2326 N92-23804
PLATES (TECTONICS)
The interpretation of crustal dynamics data in terms of plate interactions and active tectonics of the Anatolian plate and surrounding regions in the Middle East
[NASA-CR-188466] p 2408 N92-23558
PLATFORMS
Design of an omnidirectional and holonomic wheeled platform prototype
[DE92-000046] p 2382 N92-23459
PLATINUM
Guanidine based vehicle/binders for use with oxides, metals, and ceramics
[NASA-CASE-LEW-15314-1] p 2354 N92-23461
PLATINUM COMPOUNDS
Photochemistry and charge transfer chemistry of the platinum group elements
[DE92-007564] p 2347 N92-23332
PLUMES
Orbital Maneuvering Vehicle (OMV) plume and plume effects study
[NASA-CR-184292] p 2322 N92-23530
POINT DEFECTS
Spectral effects in radiation embrittlement
[DE92-007837] p 2447 N92-23444
Hardening in AlN induced by point defects
[DE92-007717] p 2352 N92-23720

POINT SOURCES
Electrostatic image theory for the dielectric sphere with an internal source
[PB92-142405] p 2366 N92-23667
POINTING CONTROL SYSTEMS
Influence of microvibrations on spacecraft performances p 2329 N92-23825
POLARIMETERS
Research in high energy physics
[DE92-007967] p 2440 N92-23214
Research in high energy physics
[DE92-007968] p 2440 N92-23215
POLARIZATION (CHARGE SEPARATION)
Electron polarization in modulation doped heterostructures
[DE92-617490] p 2447 N92-23272
POLARIZATION (WAVES)
Evaluation of mode purity of ordinary and extraordinary modes by fixed elliptically polarized wave for ECH and ECCD
[DE92-750961] p 2444 N92-23264
Properties of bi-isotropic Fresnel reflection coefficients
[PB92-141886] p 2366 N92-23661
POLARIZATION CHARACTERISTICS
In situ XANES study of the valence state of chromium during electrochemical polarization of AlCr alloys
[DE92-007452] p 2350 N92-23197
POLARIZED RADIATION
Research in high energy physics
[DE92-007966] p 2441 N92-23500
POLARIZERS
Biisotropic polarizer shield
[PB92-141878] p 2366 N92-23590
POLICIES
National acid precipitation assessment program: Mission, goals, and program plan post 1990. Public review draft
[PB92-128248] p 2405 N92-23515
POLLUTION CONTROL
Promotion of industrial technologies on the global environment
[DE92-769375] p 2406 N92-23734
Small or non pollutant solid propellants for space launchers p 2320 N92-23765
Promotion of industrial technologies on the global environment
[DE92-769376] p 2407 N92-24023
Survey on optimization of CO2 disposal system and carbon utilization technology
[DE92-769381] p 2407 N92-24024
Pulsed electron beam precharger
[DE92-008693] p 2439 N92-24031
POLYATOMIC MOLECULES
Potential energy surfaces and reaction dynamics of polyatomic molecules
[DE92-008314] p 2437 N92-23450
Melting of nickel clusters
[DE92-006986] p 2351 N92-23573
POLYBENZIMIDAZOLE
Characterization of polybenzimidazole (PBI) film at high temperatures
[NASA-CR-189174] p 2370 N92-23538
Evaluation of high temperature capacitor dielectrics
[NASA-TM-105622] p 2370 N92-23561
POLYCARBONATES
Charged particle LET-spectra measurements aboard LDEF p 2440 N92-23303
POLYETHER RESINS
An XPS study of the stability of Fomblin Z25 on the native oxide of aluminum --- x ray photoelectron spectroscopy
[NASA-TM-105594] p 2353 N92-23185
POLYETHYLENES
Radiation effects on polyethylene foam
[DE92-751046] p 2353 N92-23134
Failure behaviour of high density polyethylene products with an embrittled surface layer due to UV exposure
[PB92-138494] p 2354 N92-23510
POLYIMIDE RESINS
Vinyl capped addition polyimides
[NASA-CASE-LEW-15027-2] p 2355 N92-24053
POLYMER CHEMISTRY
Phase partitioning experiment (8-IML-1)
p 2360 N92-23621
POLYMER MATRIX COMPOSITES
Progressive fracture of polymer matrix composite structures: A new approach
[NASA-TM-105574] p 2339 N92-23194
Matrix dominated stress/strain behavior in polymeric composites: Effects of hold time, nonlinearity and rate dependency
[NASA-TM-107595] p 2340 N92-23434
Aging of polymer matrix composites at elevated temperatures p 2328 N92-23817
Investigations of the dynamic behaviour of compounds under preloading p 2332 N92-23842
Composites, 1990
[NRC-32603] p 2341 N92-23933
Morphology and mechanical performance of PPS/carbon composite p 2342 N92-23939
Crystallization behavior of poly(phenylene sulphide) p 2342 N92-23940
Injection molding of long fiber reinforced thermoplastics: A comparison of extruded and pultruded materials with direct addition of roving strands p 2342 N92-23941
On the application of micromechanics to the prediction of macroscopic thermal residual stresses in short-fiber reinforced Polyetheretherketone (PEEK) p 2343 N92-23942
Influence of maleic anhydride as a coupling agent on the performance of wood fiber: Polystyrene composites p 2343 N92-23945
Mechanical properties of glass bead filled ductile epoxy composites p 2344 N92-23947
Filling high density polyethylene with cellulosic fibers. 1: The effect of additives on fiber dispersion p 2344 N92-23948
POLYMER PHYSICS
On the application of micromechanics to the prediction of macroscopic thermal residual stresses in short-fiber reinforced Polyetheretherketone (PEEK) p 2343 N92-23942
POLYMERIZATION
Radiation effects on polyethylene foam
[DE92-751046] p 2353 N92-23134
Mechanical behavior of composite materials and adhesive bonds at low temperatures p 2330 N92-23833
POLYMERS
Oxidative degradation of polymers induced by ionizing radiation
[DE92-007657] p 2354 N92-23442
POLYNOMIALS
High-Order Polynomial Expansions (HOPE) for flux-vector splitting p 2304 N92-23353
On the modelling of a deployable telescope elastic beam-type element for on-orbit multibody simulations p 2329 N92-23826
POLYPROPYLENE
Weldline strength in injection molded glass fiber reinforced polypropylene p 2344 N92-23949
POLYSTYRENE
Influence of maleic anhydride as a coupling agent on the performance of wood fiber: Polystyrene composites p 2343 N92-23945
POLYURETHANE RESINS
Organic contamination of LDEF p 2339 N92-23290
POPULATION INVERSION
Lasers without inversion: Theory and experiment p 2379 N92-23143
POROSITY
A study of aluminum-lithium alloy solidification using acoustic emission techniques
[NASA-CR-4437] p 2435 N92-23556
PORPHYRINS
Molecular design of substrate binding sites
[DE92-008331] p 2438 N92-23894
POSITION (LOCATION)
Positional and spontaneous nystagmus (8-IML-1) p 2360 N92-23624
POSITION ERRORS
The accuracy of the drift buoy positioning by MOS-1 DCS p 2399 N92-23484
Study on drifting-data collection buoy using MOS-1: Position verification in the Bering Sea p 2400 N92-23486
Data quality evaluation results MOS-1 verification program p 2400 N92-23491
POSITION SENSING
The accuracy of the drift buoy positioning by MOS-1 DCS p 2399 N92-23484
Study on drifting-data collection buoy using MOS-1: Position verification in the Bering Sea p 2400 N92-23486
Data quality evaluation results MOS-1 verification program p 2400 N92-23491
POSITIONING
Skeletal responses to spaceflight
[NASA-TM-103890] p 2414 N92-23424
Determination of crustal motions using satellite laser ranging
[NASA-CR-190246] p 2408 N92-23540
Vacuum mechatronic laser alignment system on the NOVA laser
[DE92-006898] p 2379 N92-23571
Dynamic positioning by GPS p 2306 N92-23729
POSITIONING DEVICES (MACHINERY)
Page turning system
[NASA-CASE-GSC-13415-1] p 2386 N92-24059
POSITRONIUM
Multi-photon optical excitation of positronium
[DE92-008567] p 2438 N92-23903
POSITRONS
The electron-positron momentum density and Fermi surface of YBa2Cu3O(7-x)
[DE92-008605] p 2450 N92-24007
POSTFLIGHT ANALYSIS
Mission safety evaluation report for STS-43, postflight edition
[NASA-TM-107801] p 2312 N92-23240
Mission safety evaluation report for STS-29, postflight edition
[NASA-TM-107773] p 2312 N92-23241
Mission safety evaluation report for STS-30, postflight edition
[NASA-TM-107774] p 2312 N92-23242
Mission safety evaluation report for STS-32, postflight edition
[NASA-TM-107775] p 2312 N92-23243
Mission safety evaluation report for STS-36, postflight edition
[NASA-TM-107780] p 2312 N92-23244
LDEF: 69 Months in Space. First Post-Retrieval Symposium, part 1
[NASA-CP-3134-PT-1] p 2461 N92-23280
Long Duration Exposure Facility: A general overview p 2335 N92-23281
Use of the Long Duration Exposure Facility's thermal measurement system for the verification of thermal models p 2336 N92-23284
POTASSIUM
A study of start-up characteristics of a potassium heat pipe from the frozen state
[NASA-CR-189173] p 2373 N92-23253
POTENTIAL ENERGY
Energy cycles in the summer tropical atmosphere over the North Atlantic Ocean p 2409 N92-23150
Potential energy surfaces and reaction dynamics of polyatomic molecules
[DE92-008314] p 2437 N92-23450
POTENTIAL THEORY
Quasi-static image theory for the bi-isotropic (nonreciprocal chiral) sphere
[PB92-142371] p 2366 N92-23666
POWDER METALLURGY
Production of metal powders by hydrogen stripping from loaded organic extractants
[PB92-136464] p 2350 N92-23178
POWER CONVERTERS
Microprocessor control of multiple peak power tracking DC/DC converters for use with solar cell arrays
[NASA-CASE-GSC-13450-1] p 2403 N92-23463
POWER SERIES
A probabilistic mechanism hidden behind the universal power law for dielectric relaxation. Part 1: General relaxation equation
[DE92-615484] p 2435 N92-23220
POWER SPECTRA
PSD computations using Welch's method
[DE92-007419] p 2370 N92-23584
POWER TRANSMISSION
Power beaming: Mission enabling for lunar exploration
[DE92-006727] p 2459 N92-23124
PRECAMBRIAN PERIOD
Investigation of the Archean climate using the NCAR CCM
[NASA-CR-189878] p 2410 N92-23656
PRECIPITATION (METEOROLOGY)
Quasi-three-dimensional simulations of deep convection
[DE92-007204] p 2409 N92-23257
PRECONDITIONING
A multilevel preconditioner for domain decomposition boundary systems
[DE92-008055] p 2432 N92-23329
PREDICTION ANALYSIS TECHNIQUES
Use of the Long Duration Exposure Facility's thermal measurement system for the verification of thermal models p 2336 N92-23284
Prediction of LDEF ionizing radiation environment p 2439 N92-23292
Advancements in engineering turbulence modeling
[PAPER-105] p 2303 N92-23350
Evaluating model accuracy for model-based reasoning p 2427 N92-23362
Determination and prediction of satellite motion at the end of the lifetime p 2334 N92-23971
Prediction of solar and geomagnetic activity for ESA low-flying spacecraft p 2334 N92-23975
Salyut-7/Kosmos-1686 orbit determination from radar data p 2318 N92-23976
Lifetime of objects in geostationary transfer orbit p 2318 N92-23977
PREDICTIONS
Acoustic prediction on satellite structure p 2327 N92-23812

Use of the maximum entropy method to retrieve the vertical atmospheric ozone profile and predict atmospheric ozone content p 2407 N92-23965
The Reentry of Salyut-7/Kosmos-1686 [ESA-SP-345] p 2333 N92-23967
Orbit analysis and lifetime prediction using radar data by reentry of Salyut-7/Kosmos-1686 p 2318 N92-23969
Salyut-7/Kosmos-1686 reentry prediction activities at ESOC p 2334 N92-23970
Salyut-7/Kosmos-1686 reentry predictions for the Italian Civil Defence Authority p 2334 N92-23972
Debris reentry prediction: Salyut-7/Kosmos-1686 p 2318 N92-23973
Orbital decay and reentry of the Salyut-7 orbital complex p 2335 N92-23978
The statistical analysis of data from normal distributions, with particular reference to small samples [ESDU-91041] p 2434 N92-24008

PREFIRING TESTS
Development status of the cryotechnical principal stage p 2319 N92-23758

PREGNANCY
Radiation exposure of air carrier crewmembers 2 [PB92-140037] p 2414 N92-23139

PRESSURE
Experiments and modeling p 2301 N92-23339

PRESSURE DEPENDENCE
Liquid/supercritical fluid carbon dioxide cleaning of stainless steel components [DE92-006947] p 2348 N92-23572
General P-T fit construction for He, N2, Ar, H2 and Ne VPT used at Fermilab [DE92-008851] p 2433 N92-23579
Working gas pressure and flow effects on reactively sputtered molybdenum-oxide thin films [DE92-008624] p 2450 N92-24069

PRESSURE DISTRIBUTION
Orbital Maneuvering Vehicle (OMV) plume and plume effects study [NASA-CR-184292] p 2322 N92-23530
Renormalization group analysis of the Reynolds stress transport equation [NASA-TM-105588] p 2374 N92-23542
Development of wall pressure measuring apparatus for an existing transonic wind tunnel test section [NAL-TM-565] p 2312 N92-23778

PRESSURE EFFECTS
Mechanical properties of glass bead filled ductile epoxy composites p 2344 N92-23947
Working gas pressure and flow effects on reactively sputtered molybdenum-oxide thin films [DE92-008624] p 2450 N92-24069

PRESSURE GRADIENTS
Topics in numerical computation of compressible flow p 2375 N92-23692

PRESSURE MEASUREMENT
Development of wall pressure measuring apparatus for an existing transonic wind tunnel test section [NAL-TM-565] p 2312 N92-23778

PRESSURE OSCILLATIONS
Aerodynamic rectifier for pulsed combustors [PB92-142587] p 2348 N92-23657

PRESSURE VESSELS
Spectral effects in radiation embrittlement [DE92-007837] p 2447 N92-23444

PRESSURIZED CABINS
Structural assessment of the Space Station Freedom's pressurized elements p 2323 N92-23783
Material considerations for habitable areas of manned spacecraft p 2323 N92-23785

PRESTRESSING
Investigations of the dynamic behaviour of compounds under preloading p 2332 N92-23842

PRINTED CIRCUITS
An integrated test solution to address scan techniques [REPT-1.2.3] p 2420 N92-23862
Change in test-technology [REPT-1.2.8] p 2421 N92-23867
Breathing maze router for analog VLSI cell generation [REPT-1.3.3] p 2422 N92-23870
Deleting pads in multi-layered printed circuits [REPT-4.2.3] p 2425 N92-23889
Replacement of hydrogen peroxide cleaning with oxygen plasma [DE92-009020] p 2445 N92-23905

PROBABILITY DENSITY FUNCTIONS
The study of PDF turbulence models in combustion p 2301 N92-23337
The study of PDF turbulence models in combustion [PAPER-107] p 2302 N92-23345
On recontamination and directional-bias problems in Monte Carlo simulation of PDF turbulence models p 2302 N92-23346
Progress in the development of PDF turbulence models for combustion [PAPER-213] p 2303 N92-23347
A study of hydrogen diffusion flames using PDF turbulence model p 2303 N92-23348

PROBABILITY DISTRIBUTION FUNCTIONS
The response surface method: An efficient tool to determine the failure probability of large structural systems p 2328 N92-23816

PROBABILITY THEORY
A probabilistic mechanism hidden behind the universal power law for dielectric relaxation. Part 1: General relaxation equation [DE92-615484] p 2435 N92-23220
An algorithmic approach for fault-monitoring of electrical actuation system for all electric aircraft [NAL-PD-AL-9111] p 2368 N92-23246
The study of PDF turbulence models in combustion p 2301 N92-23337
Probabilistic Structural Analysis Methods (PSAM) for select space propulsion system components, part 2 [NASA-CR-187200] p 2388 N92-23426
Control problem for a multi server loss system [PB92-148675] p 2430 N92-23506
A probabilistic mechanism hidden behind the universal power law for dielectric relaxation. Part 2: Discussion of the response function [DE92-615485] p 2435 N92-23598
Clouds and radiation testbed data environment: Site data system and experiment center [DE92-006732] p 2408 N92-23741

PROBLEM SOLVING
Combining factual and heuristic knowledge in knowledge acquisition p 2429 N92-23372

PROCEDURES
Procedure improvement enterprises [DE92-003222] p 2453 N92-23183

PROCESS CONTROL (INDUSTRY)
A framework for the support of VLSI (very large scale integration) design for manufacture [REPT-1.3.1] p 2421 N92-23868
Statistical process control system for VLSI fabrication [REPT-1.3.4] p 2422 N92-23871
Statistical optimization of integrated circuits in order to reduce the sensitivity to variations in process parameters and environmental conditions [REPT-1.3.6] p 2422 N92-23872
CIM implementation at CVALIM, D.T.C. Division, Bet-Shean, Israel [REPT-3.2.4] p 2424 N92-23884
The use of STEP in an integrated manufacturing environment [DE92-008417] p 2425 N92-24035

PRODUCT DEVELOPMENT
Realization and provisional sensor development planning p 2395 N92-23406
The Wake Shield Facility: A space experiment platform p 2313 N92-23648
Center for Space Power and Advanced Electronics, Auburn University p 2314 N92-23654
Center for Mapping, Ohio State University p 2314 N92-23655

PRODUCTION COSTS
Advances in processing rates optimization for flexible manufacturing systems [REPT-2.3.4] p 2423 N92-23877

PRODUCTION ENGINEERING
Proceedings of the International Conference on CAD/CAM and AMT. Volume 1: General sessions [ITN-92-85127] p 2418 N92-23851
Group technology, RCO: Rough-Cut Optimizer. The key to integration of plant operations [REPT-1.1.6] p 2420 N92-23857
From IGES to STEP [REPT-3.1.6] p 2423 N92-23881
Computer integrated enterprise: The next step in CIM evolution [REPT-3.2.2] p 2424 N92-23883
CIM: The future technology [REPT-3.3.1] p 2424 N92-23885
Symposium on Marketing for Technological Products [MBB-UE-0014-90-PUB] p 2452 N92-23928
Marketing as a necessary condition for the successful development and commercialization of technological products p 2452 N92-23931

PRODUCTION MANAGEMENT
Formal methods for the evaluation of corporate CAD/CAM utilization [REPT-1.1.1] p 2419 N92-23853
Dynamic aggregate models for group technology manufacturing environment [REPT-1.1.7] p 2420 N92-23858
Statistical process control system for VLSI fabrication [REPT-1.3.4] p 2422 N92-23871
Controlling operations through procedures: APE (automated procedure editor) [REPT-2.2.1] p 2422 N92-23875
CIM implementation at CVALIM, D.T.C. Division, Bet-Shean, Israel [REPT-3.2.4] p 2424 N92-23884
CIM: The future technology [REPT-3.3.1] p 2424 N92-23885
Group scheduling using group technology concepts [REPT-3.3.2] p 2424 N92-23886

PRODUCTION PLANNING
Group technology, RCO: Rough-Cut Optimizer. The key to integration of plant operations [REPT-1.1.6] p 2420 N92-23857
Dynamic aggregate models for group technology manufacturing environment [REPT-1.1.7] p 2420 N92-23858
Controlling operations through procedures: APE (automated procedure editor) [REPT-2.2.1] p 2422 N92-23875
Shop floor scheduling through a simulation based scheduler [REPT-2.3.3] p 2423 N92-23876
CIM implementation at CVALIM, D.T.C. Division, Bet-Shean, Israel [REPT-3.2.4] p 2424 N92-23884
CIM: The future technology [REPT-3.3.1] p 2424 N92-23885
Marketing as a necessary condition for the successful development and commercialization of technological products p 2452 N92-23931

PRODUCTIVITY
Mental workload and performance experiment (15-IML-1) p 2361 N92-23628
Shop floor scheduling through a simulation based scheduler [REPT-2.3.3] p 2423 N92-23876

PROGRAMMING LANGUAGES
Hierarchical sets in mathematical programming modeling languages [PB92-148883] p 2418 N92-23507

PROJECT MANAGEMENT
International cooperation p 2396 N92-23409
An 18-point catalog description p 2396 N92-23411
Computational procedures for preliminary design p 2309 N92-23952

PROJECT PLANNING
International cooperation p 2396 N92-23409
An 18-point catalog description p 2396 N92-23411

PROJECTILES
M and D SIG progress report: Laboratory simulations of LDEF impact features p 2336 N92-23323

PROJECTORS
IMAX camera (12-IML-1) p 2363 N92-23641

PROPANE
High-temperature ignition of propane with MTBE as an additive: Shock-tube experiments and modeling [DE92-008557] p 2348 N92-23715

PROPELLANT TANKS
Numerical simulation of fluid behaviors in microgravity environment p 2363 N92-23719

PROPELLER FANS
Aeroelastic stability analyses of two counter rotating propfan designs for a cruise missile model [NASA-TM-105268] p 2387 N92-23191

PROPRIOCEPTION
Space adaptation syndrome experiments (8-IML-1) p 2360 N92-23625

PROPULSION
Computational fluid dynamics for propulsion technology: Geometric grid visualization in CFD-based propulsion technology research [NASA-CR-190291] p 2375 N92-23568

PROPULSION SYSTEM CONFIGURATIONS
Low thrust propulsion literature survey [NASA-CR-190179] p 2337 N92-23151
Modelling and experimental verification of a water alleviation system for the NASP --- National Aerospace Plane [NASA-TM-105661] p 2373 N92-23224
Solar-electric-propulsion cargo vehicles for split/sprint Mars mission [NASA-CR-189983] p 2322 N92-23526
Analysis of solar and microwave thermal propulsion systems p 2337 N92-23694
Configuration development --- preliminary aircraft design p 2309 N92-23953
Synergistic use of high and low thrust propulsion systems for piloted missions to Mars [NASA-CR-189138] p 2338 N92-24004

PROPULSION SYSTEM PERFORMANCE
Low thrust propulsion literature survey [NASA-CR-190179] p 2337 N92-23151
Advanced ramjet systems for the propulsion of guided weapons [ETN-92-91195] p 2310 N92-23169

Analysis of solar and microwave thermal propulsion systems p 2337 N92-23694
Synergistic use of high and low thrust propulsion systems for piloted missions to Mars
[NASA-CR-189138] p 2338 N92-24004

PROPULSIVE EFFICIENCY
Advanced ramjet systems for the propulsion of guided weapons
[ETN-92-91195] p 2310 N92-23169

PROSTHETIC DEVICES
Prosthetic helping hand
[NASA-CASE-MFS-28430-1] p 2416 N92-24044
Bar-holding prosthetic limb
[NASA-CASE-MFS-28481-1] p 2416 N92-24056

PROTECTIVE COATINGS
Characterization of organic coatings with impedance measurements: A study of coating structure, adhesion and underfilm corrosion
[PB92-133479] p 2339 N92-23174

PROTEIN CRYSTAL GROWTH
Protein crystal growth (5-IML-1) p 2361 N92-23634

PROTEINS
Center for Cell Research, Pennsylvania State University p 2314 N92-23653

PROTOCOL (COMPUTERS)
Training users of a flexible decision support system: The effects of training content and user ability p 2453 N92-23730
Interim Service ISDN Satellite (ISIS) hardware experiment development for advanced ISDN satellite designs and experiments
[NASA-CR-190257] p 2335 N92-24046

PROTON BEAMS
Thresholds of longitudinal instability of bunched beam in the presence of dominant inductive impedance
[DE92-617992] p 2436 N92-23274

PROTONS
Induced radioactivity in LDEF components p 2440 N92-23300

PROTOPLASM
Gravity related behavior of the acellular slime mold Physarum polycephalum (7-IML-1) p 2359 N92-23618

PROTOTYPES
Knowledge-based approach for generating target system specifications from a domain model p 2428 N92-23371
NIST torsion oscillator viscometer response: Performance on the LeRC active vibration isolation platform
[NASA-TM-105571] p 2383 N92-23564

PROVING
Functional design verification of ULSI components
[REPT-1.3.7] p 2422 N92-23873

PROXIMITY
Empirical characterization of a high intensity LED proximity sensor
[DE91-019074] p 2371 N92-23735

PUBLIC HEALTH
JPRS report: Science and technology. Central Eurasia: Life sciences
[JPRS-ULS-92-010] p 2412 N92-23706

PULSARS
Constructing a pulsar timing array p 2456 N92-23126
Discovery of orbital decay in SMC X-1
[NASA-CR-190214] p 2317 N92-23531
TeV gamma ray emission from accreting binary pulsars p 2460 N92-23736
Observing millisecond and binary pulsars p 2455 N92-24001

PULSED LASERS
Limits of survivability and damage for optical components used in a high repetition rate visible laser
[DE92-006896] p 2379 N92-23570

PUMP IMPELLERS
Experimental study of the mechanism of sound generation by rotating stall in centrifugal turbomachines p 2436 N92-23726

PURITY
Effects of impurities on the solidification and mechanical behaviour of primary and secondary commercial purity aluminium and aluminium alloys
[PB92-133511] p 2350 N92-23176

PYRENES
Photoinduced electron transfer in ordered polymers
[DE92-008787] p 2355 N92-24037

PYROLYSIS
Kinetics of combustion-related processes at high temperatures
[DE92-008790] p 2348 N92-24038

Q

Q SWITCHED LASERS
Injection seeding of a Q-switched alexandrite laser: Study of frequency stabilization p 2380 N92-23961

QUADRATIC EQUATIONS
A new approach to estimate Angstrom coefficients
[DE92-619048] p 2460 N92-23909

QUADRATIC PROGRAMMING
Simultaneous stress and flutter optimization for the wing of a transport aircraft equipped with four engines p 2308 N92-23238

QUALIFICATIONS
On development of automated static loading system for spacecraft structures p 2326 N92-23801
Marketing qualification as a requirement for operating success p 2452 N92-23930

QUALITY CONTROL
Food Irradiation Newsletter, volume 15, number 2
[DE92-614951] p 2415 N92-23218
Training guidelines in non-destructive testing techniques
[DE92-615083] p 2386 N92-23258
Development of a crack arrest fracture toughness measurement procedure for quality assurance of plates and welds used for hydrocarbon storage tanks
[PB92-141753] p 2389 N92-23681
Statistical process control system for VLSI fabrication
[REPT-1.3.4] p 2422 N92-23871
Statistical optimization of integrated circuits in order to reduce the sensitivity to variations in process parameters and environmental conditions
[REPT-1.3.6] p 2422 N92-23872

QUANTITATIVE ANALYSIS
Evaluation of the sensor effectiveness p 2395 N92-23404

QUANTUM CHROMODYNAMICS
Research in high energy physics
[DE92-007967] p 2440 N92-23214
Research in high energy physics
[DE92-007968] p 2440 N92-23215
On the Stone-Weierstrass theorem for scalar and vector valued functions
[DE92-616916] p 2432 N92-23335
Research in high energy physics
[DE92-007966] p 2441 N92-23500
High energy physics: Report of research accomplishments and future goals, FY 1992
[DE92-008543] p 2441 N92-23576

QUANTUM MECHANICS
Beyond conventional quantum mechanics
[DE92-616892] p 2451 N92-23206
Nonequilibrium statistical operator in hot-electron transport theory
[DE92-615517] p 2446 N92-23260
The Jordan-Schwinger realization of two-parametric quantum group SI(sub q,s)(2)
[DE92-616891] p 2451 N92-23501
Mutual scattering of carriers in two quantum wires
[DE92-616890] p 2366 N92-23580
Inequivalence of interior and exterior dynamical problems
[DE92-615214] p 2451 N92-23743

QUANTUM THEORY
Non-commutative differential geometry and Yang-Baxter equation
[PB92-149459] p 2431 N92-23184
Low frequency electrostatic modes in a magnetized dusty plasma
[DE92-617387] p 2444 N92-23209
The 7th INS Scientific Computational Programs
[DE92-750967] p 2417 N92-23266
Static multipole deformations in nuclei
[DE92-008250] p 2436 N92-23277
On the Stone-Weierstrass theorem for scalar and vector valued functions
[DE92-616916] p 2432 N92-23335
Constant curvature and non-perturbative W(sub 3) gravity
[DE92-616919] p 2451 N92-23503
Improved numerical methods for quantum field theory (outstanding junior investigator award)
[DE92-008730] p 2451 N92-23578
Family of Poisson structures on compact hermitian symmetric spaces
[PB92-149442] p 2433 N92-23670
Inequivalence of interior and exterior dynamical problems
[DE92-615214] p 2451 N92-23743
Magnetotransport and responses of semiconductor microstructures p 2449 N92-23775

QUARKS
Research in high energy physics
[DE92-007966] p 2441 N92-23500
The notion of nonrelativistic isoparticle
[DE92-615215] p 2438 N92-23744

QUASARS
The origins of the cosmic x ray and gamma ray backgrounds p 2460 N92-23141
Search for cosmological dust p 2456 N92-23164

QUEUEING THEORY
Modeling of the DZero data acquisition system
[DE92-007913] p 2453 N92-23212
Control problem for a multi server loss system
[PB92-148675] p 2430 N92-23506
Optimizing flow rates in a queueing network with side constraints
[PB92-149996] p 2430 N92-23508

R

RADAR DATA
An observational study of the internal structure of air-mass thunderstorms p 2409 N92-23121

RADAR IMAGERY
The imaging radar system p 2393 N92-23391

RADAR MAPS
CODAR in the Straits of Florida
[PB92-129964] p 2412 N92-23732

RADAR SCATTERING
Development of a helicopter-borne 8-channel ranging scatterometer
[PB92-141977] p 2396 N92-23441
Radar observations and dynamics of the polar summer mesosphere p 2408 N92-23702

RADAR TARGETS
Development of a helicopter-borne 8-channel ranging scatterometer
[PB92-141977] p 2396 N92-23441

RADAR TRACKING
The Reentry of Salyut-7/Kosmos-1686
[ESA-SP-345] p 2333 N92-23967
Radar tracking and observation of noncooperative space objects by reentry of Salyut-7/Kosmos-1686 p 2333 N92-23968
Orbit analysis and lifetime prediction using radar data by reentry of Salyut-7/Kosmos-1686 p 2318 N92-23969
Salyut-7/Kosmos-1686 orbit determination from radar data p 2318 N92-23976

RADIAL VELOCITY
Impinging axisymmetric jet p 2372 N92-23146

RADIANCE
GENLN2: A general line-by-line atmospheric transmittance and radiance model. Version 3.0: Description and users guide
[PB92-148543] p 2408 N92-23522

RADIATION ABSORPTION
Analysis of solar and microwave thermal propulsion systems p 2337 N92-23694

RADIATION BELTS
Summary of ionizing radiation analysis on the Long Duration Exposure Facility p 2439 N92-23291
Prediction of LDEF ionizing radiation environment p 2439 N92-23292
JPRS report: Science and technology. Central Eurasia: Space
[JPRS-USP-92-002] p 2314 N92-23705

RADIATION COUNTERS
Metal-semiconductor, composite radiation detectors
[DE92-008980] p 2344 N92-23988

RADIATION DAMAGE
Applications of multiple-ion irradiations to metals, ceramics, and polymers
[DE92-007686] p 2354 N92-23222
Low dose neutron late effects: Cataractogenesis
[DE92-005539] p 2414 N92-24033

RADIATION DETECTORS
A switched capacitor array based system for high-speed calorimetry
[DE92-008288] p 2378 N92-23278
Test beam results from the D0 end electromagnetic calorimeter
[DE92-008299] p 2378 N92-23279
Measurements of induced radioactivity in some LDEF samples p 2440 N92-23298
Radiation exposure of LDEF: Initial results p 2461 N92-23302
Search for atmospheric neutrino oscillations with the Soudan 2 detector
[DE92-007397] p 2437 N92-23328
An x ray diagnostic of electron power loss
[DE92-008599] p 2444 N92-23523
Radiation monitoring container device (16-IML-1) p 2361 N92-23629
A study of underground muons in the Soudan 2 detector p 2437 N92-23674
Metal-semiconductor, composite radiation detectors
[DE92-008980] p 2344 N92-23988

RADIATION DISTRIBUTION
Rotating, radiating mass imbedded in a de Sitter universe p 2456 N92-23127
Lasers without inversion: Theory and experiment p 2379 N92-23143
Radioactivities of Long Duration Exposure Facility (LDEF) materials: Baggage and bonanzas p 2440 N92-23297
Type Ib supernovae and a new radiation hydrodynamics code p 2458 N92-24017

RADIATION DOSAGE
Radiation exposure of air carrier crewmembers 2 [PB92-140037] p 2414 N92-23139
Development of 3-dimensional compact magnetic dosimeter for environmental magnetic field monitoring [DE92-750825] p 2407 N92-23262
Radiation exposure of LDEF: Initial results p 2461 N92-23302
Charged particle LET-spectra measurements aboard LDEF p 2440 N92-23303
Ionizing radiation calculations and comparisons with LDEF data p 2440 N92-23304
Dosimetric mapping inside biorack (7-IML-1) p 2358 N92-23611
Radiation monitoring container device (16-IML-1) p 2361 N92-23629
Irradiation of spices, herbs, and other vegetable seasonings: A compilation of technical data for its authorization and control [DE92-619064] p 2415 N92-24022
Low dose neutron late effects: Cataractogenesis [DE92-005539] p 2414 N92-24033

RADIATION EFFECTS
Radiation effects on polyethylene foam [DE92-751046] p 2353 N92-23134
Thermoluminescent dosimetry for LDEF experiment M0006 p 2461 N92-23301
Preliminary results from the heavy ions in space experiment p 2461 N92-23307
Oxidative degradation of polymers induced by ionizing radiation [DE92-007657] p 2354 N92-23442
Spectral effects in radiation embrittlement [DE92-007837] p 2447 N92-23444
Genetic and molecular dosimetry of HZE radiation (7-IML-1) p 2357 N92-23603
Embryogenesis and organogenesis of Carausius morosus under space flight conditions (7-IML-1) p 2358 N92-23610
Dosimetric mapping inside biorack (7-IML-1) p 2358 N92-23611
Radiation monitoring container device (16-IML-1) p 2361 N92-23629
JPRS report: Science and technology. Central Eurasia: Life sciences [JPRS-ULS-92-010] p 2412 N92-23706
Magnetic flux motion and flux pinning superconductors [DE92-008243] p 2449 N92-23892

RADIATION HARDENING
Hardening in AlN induced by point defects [DE92-007717] p 2352 N92-23720

RADIATION HAZARDS
Radiation exposure of air carrier crewmembers 2 [PB92-140037] p 2414 N92-23139
Biostack (14-IML-1) p 2361 N92-23627

RADIATION MEASUREMENT
Ionizing radiation calculations and comparisons with LDEF data p 2440 N92-23304
Search for atmospheric neutrino oscillations with the Soudan 2 detector [DE92-007397] p 2437 N92-23328
Field evaluation of remote sensor measurements of wind, temperature, and moisture for ARM integrated sounding system research [PB92-140714] p 2401 N92-23521
Clouds and radiation testbed data environment: Site data system and experiment center [DE92-006732] p 2408 N92-23741

RADIATION SHIELDING
LDEF geometry/mass model for radiation analyses p 2440 N92-23305

RADIATION SOURCES
The throes of star formation: A study of the Orion-KL and DR21(OH) molecular clouds p 2457 N92-23698
The ALEXIS data processing package: An IDL-based system [DE92-007429] p 2455 N92-24027

RADIATION TRANSPORT
Summary of ionizing radiation analysis on the Long Duration Exposure Facility p 2439 N92-23291
LDEF geometry/mass model for radiation analyses p 2440 N92-23305
The all particle method [DE92-008357] p 2439 N92-24005

RADICALS
Reductive coupling of carbon monoxide to C2 products [DE92-007529] p 2347 N92-23499

RADIO ASTRONOMY
Annual progress report [NASA-CR-190197] p 2454 N92-23428

RADIO ATTENUATION
Electrostatic image theory for the layered dielectric sphere [PB92-142413] p 2367 N92-23668

RADIO GALAXIES
Annual progress report [NASA-CR-190197] p 2454 N92-23428

RADIO TELESCOPES
Constructing a pulsar timing array p 2456 N92-23126

RADIO TRANSMISSION
Tabulations of propagation data over irregular terrain in the 75- to 8400-MHz frequency range. Part 5: Virginia [PB92-137413] p 2364 N92-23180

RADIOACTIVE DECAY
Research in high energy physics [DE92-007967] p 2440 N92-23214
Research in high energy physics [DE92-007968] p 2440 N92-23215

RADIOACTIVE ISOTOPES
Charged particle activation studies on the surface of LDEF spacecraft p 2439 N92-23296
Radioactivities of Long Duration Exposure Facility (LDEF) materials: Baggage and bonanzas p 2440 N92-23297

RADIOACTIVE WASTES
HEIS: An integrated information system for environmental restoration and monitoring at Hanford [DE92-006467] p 2453 N92-23188

RADIOACTIVITY
Summary of ionizing radiation analysis on the Long Duration Exposure Facility p 2439 N92-23291
Gamma radiation survey of the LDEF spacecraft p 2460 N92-23293
Measurements of induced radioactivity in some LDEF samples p 2440 N92-23298
Induced radioactivity in LDEF components p 2440 N92-23300

RADIOBIOLOGY
Embryogenesis and organogenesis of Carausius morosus under space flight conditions (7-IML-1) p 2358 N92-23610
Biostack (14-IML-1) p 2361 N92-23627
Radiation monitoring container device (16-IML-1) p 2361 N92-23629

RADIOLOGY
Low dose neutron late effects: Cataractogenesis [DE92-005539] p 2414 N92-24033

RADIOMETERS
On board data formatting p 2394 N92-23394
Sensor interfaces p 2395 N92-23400
Verification of MESSR and VTIR, and time variation of MSR performance p 2397 N92-23471
Evaluation of effective characteristic in forest field p 2397 N92-23473

RADIOSONDES
Functional precision of National Weather Service upper-air measurements using VIZ Manufacturing Co. A radiosonde (model 1492-510) [PB92-137850] p 2410 N92-23439
Functional precision of National Weather Service upper-air measurements using VIZ Manufacturing Co. B radiosonde (model 1492-520) [PB92-137868] p 2410 N92-23494
Functional precision of National Weather Service upper-air measurements using space data division radiosonde (model 909-10-01) [PB92-137843] p 2411 N92-23746

RAIN
Measurements of rain rate distribution by MOS-1 MSR p 2396 N92-23467
Multitemporal and multisensor approach with MOS data to natural resources evaluation in dry tropical Africa (Burkina Faso) p 2400 N92-23488

RAMAN SPECTRA
Dynamic structural effects and ultrafast biomolecular kinetics in photoinduced charge transfer reactions [DE92-007562] p 2346 N92-23203
Superconducting materials [DE92-007748] p 2446 N92-23205
Charged-soft-sphere potentials for trivalent metal halides [DE92-617445] p 2350 N92-23211
Profiling and mapping of advanced materials using spatially resolved Raman spectroscopy [DE92-008304] p 2347 N92-23449

RAMAN SPECTROSCOPY
Profiling and mapping of advanced materials using spatially resolved Raman spectroscopy [DE92-008304] p 2347 N92-23449
Fiber-optic Raman spectroscopy for cure monitoring of advanced polymer composites [DE92-008619] p 2355 N92-24068

RAMJET ENGINES
Advanced ramjet systems for the propulsion of guided weapons [ETN-92-91195] p 2310 N92-23169

RAMJET MISSILES
Advanced ramjet systems for the propulsion of guided weapons [ETN-92-91195] p 2310 N92-23169

RANDOM ERRORS
Confidence intervals for discrete approximations to ill-posed problems [PB92-143742] p 2432 N92-23511

RANDOM PROCESSES
Fatigue analysis under random stresses p 2325 N92-23795

RANGE (EXTREMES)
Using range analysis to support hierarchical test pattern generation [REPT-1.2.5] p 2421 N92-23864

RANGEFINDING
Development of a helicopter-borne 8-channel ranging scatterometer [PB92-141977] p 2396 N92-23441
Determination of crustal motions using satellite laser ranging [NASA-CR-190246] p 2408 N92-23540

RANKINE CYCLE
Compact Fusion Advanced Rankine (CFAR2) power cycle [DE92-008577] p 2445 N92-23987

RASTER SCANNING
Method for advanced material characterization by laser induced eddy current imaging [NASA-CASE-GSC-13386-1] p 2386 N92-23376

RATS
Nuclear medicine program [DE92-006979] p 2412 N92-23518
Low dose neutron late effects: Cataractogenesis [DE92-005539] p 2414 N92-24033

RAY TRACING
LDEF geometry/mass model for radiation analyses p 2440 N92-23305
Ocean acoustic tomography inversion in the adiabatic-invariant approximation [PB92-140466] p 2412 N92-23689

RAYON
Proceedings: Nozzle Initiative Industry Advisory Committee on Standardization of Carbon-Phenolic Test Methods and Specifications [NASA-CR-190203] p 2337 N92-23539

RC CIRCUITS
Waveform relaxation always converges for RC-circuits [PB92-142280] p 2369 N92-23495

REACTING FLOW
Three-dimensional calculations of supersonic reacting flows using an LU scheme p 2304 N92-23354

REACTION BONDING
Reaction layer formation at the graphite/copper-chromium alloy interface [NASA-CR-189147] p 2351 N92-23436

REACTION KINETICS
Dynamic structural effects and ultrafast biomolecular kinetics in photoinduced charge transfer reactions [DE92-007562] p 2346 N92-23203
Kinetic measurements on elementary fossil fuel combustion reactions over wide temperatures ranges [DE92-007535] p 2347 N92-23221
Hydrogen absorption by zirconium alloy cladding tube with surface oxide film [DE92-750962] p 2351 N92-23265
The study of PDF turbulence models in combustion p 2301 N92-23337
On recontamination and directional-bias problems in Monte Carlo simulation of PDF turbulence models p 2302 N92-23346
Progress in the development of PDF turbulence models for combustion [PAPER-213] p 2303 N92-23347
Analysis of forward and inverse problems in chemical dynamics and spectroscopy [DE92-007732] p 2347 N92-23443
Temperature-dependent evolution of chemisorbed digermane in Ge thin film growth [DE92-008098] p 2447 N92-23447
Basic research on natural gas combustion phenomena [PB92-149681] p 2348 N92-23685
Phase transformations in SrAl2Si2O8 glass [NASA-TM-105657] p 2449 N92-23890

The oxidation behavior of Co-15wt percent Cr alloy containing dispersed oxides formed by internal oxidation
[DE92-008283] p 2352 N92-23893
VITRIMAT2: A modified model of vitrinite maturation and reflectance
[DE92-008987] p 2348 N92-23904
Kinetics of combustion-related processes at high temperatures
[DE92-008790] p 2348 N92-24038
Modeling of the catalytic oxidative coupling of methane
[DE92-008554] p 2349 N92-24064

REACTION PRODUCTS
Charged particle activation studies on the surface of LDEF spacecraft p 2439 N92-23296

REACTOR DESIGN
Conceptual design of fusion experimental reactor (FER/ITER)
[DE92-750949] p 2444 N92-23711
Steady State Advanced Tokamak (SSAT): The mission and the machine
[DE92-008983] p 2445 N92-24020

REACTOR MATERIALS
Effect of minor elements on corrosion behavior of Ni-Cr-W superalloys in HTGR helium
[DE92-751006] p 2352 N92-23712

REACTOR SAFETY
Conceptual design of Fusion Experimental Reactor
[DE92-751036] p 2443 N92-23132

READING
Page turning system
[NASA-CASE-GSC-13415-1] p 2386 N92-24059

REAL TIME OPERATION
An architecture for the development of real-time fault diagnosis systems using model-based reasoning p 2427 N92-23363
Real-time radar processor p 2394 N92-23396
Summary report: A preliminary investigation into the use of fuzzy logic for the control of redundant manipulators
[NASA-CR-190277] p 2429 N92-23438
Research project for practical usage of MOS-1 data collection system p 2399 N92-23485
Application of optical distributed sensing and computation to control of large space structures
[NASA-CR-190293] p 2442 N92-23567
Architectural impact of FDDI network on scheduling hard real-time traffic
[NASA-CR-190272] p 2425 N92-23583
NASA's GPS tracking system for Aristoteles p 2316 N92-23919

RECLAMATION
HEIS: An integrated information system for environmental restoration and monitoring at Hanford
[DE92-006467] p 2453 N92-23188

RECOMBINATION REACTIONS
Spectral effects in radiation embrittlement
[DE92-007837] p 2447 N92-23444

RECRYSTALLIZATION
Rapid recrystallization of semiconductor thin films for photovoltaic applications p 2404 N92-23998

RECTANGULAR WINGS
Normal force of low aspect ratio wing-body combinations up to high angles of attack at supersonic speeds
[ESDU-91042] p 2309 N92-24009

RED SHIFT
Search for cosmological dust p 2456 N92-23164

REDUCED GRAVITY
Microgravity dynamical behaviors of cryogenic liquid hydrogen reorientation and draining in space propulsion system p 2356 N92-23147
Skeletal responses to spaceflight
[NASA-TM-103890] p 2414 N92-23424
NIST torsion oscillator viscometer response: Performance on the LeRC active vibration isolation platform
[NASA-TM-105571] p 2383 N92-23564
First International Microgravity Laboratory experiment descriptions
[NASA-TM-4353] p 2356 N92-23600
Gravitropic responses of plants in the absence of a complicating G-force (6-IML-1) p 2356 N92-23601
A spaceflight experiment to investigate the effects of a range of unilateral blue light phototropic stimulations on the movements of wheat coleoptiles (6-IML-1) p 2356 N92-23602
Microgravitational effects on chromosome behavior (7-IML-1) p 2357 N92-23604
Chrondrogenesis in micromass cultures of embryonic mouse limb mesenchymal cells exposed to microgravity (7-IML-1) p 2357 N92-23605
Effect of microgravity and mechanical stimulation on the in vitro mineralization and resorption of fetal mouse long bones (7-IML-1) p 2357 N92-23606
Eggs: The role of gravity in the establishment of the dorso-ventral axis in the amphibian embryo (7-IML-1) p 2357 N92-23607
The effect of space environment on the development and aging of Drosophila Melanogaster (7-IML-1) p 2357 N92-23608
Effect of microgravity environment on cell wall regeneration, cell divisions, growth, and differentiation of plants from protoplasts (7-IML-1) p 2358 N92-23609
Embryogenesis and organogenesis of Carausius morosus under space flight conditions (7-IML-1) p 2358 N92-23610
Dosimetric mapping inside biorack (7-IML-1) p 2358 N92-23611
Growth and sporulation of Bacillus subtilis under microgravity (7-IML-1) p 2358 N92-23612
Friend leukemia virus transformed cells exposed to microgravity in the presence of DMSO (7-IML-1) p 2358 N92-23613
Proliferation and performance of hybridoma cells in microgravity (7-IML-1) p 2358 N92-23614
Dynamic cell culture system (7-IML-1) p 2359 N92-23615
Growth, differentiation and development of Arabidopsis thaliana under microgravity conditions (7-IML-1) p 2359 N92-23616
Transmission of gravistimulus in the statocyte of the lentil root (7-IML-1) p 2359 N92-23617
Studies on penetration of antibiotic in bacterial cells in space conditions (7-IML-1) p 2359 N92-23619
Energy expenditure in space flight (doubly labelled water method) (8-IML-1) p 2359 N92-23620
Back pain in astronauts (8-IML-1) p 2360 N92-23622
Measurement of venous compliance (8-IML-1) p 2360 N92-23623
Microgravity vestibular investigations (10-IML-1) p 2360 N92-23626
Mental workload and performance experiment (15-IML-1) p 2361 N92-23628
A study of solution crystal growth in LOW-g (2-IML-1) p 2361 N92-23630
An optical study of grain formation: Casting and solidification technology (2-IML-1) p 2361 N92-23631
Vapor crystal growth studies of single crystals of mercuric iodide (3-IML-1) p 2361 N92-23632
Mercury iodide nucleation and crystal growth in vapor phase (4-IML-1) p 2361 N92-23633
Protein crystal growth (5-IML-1) p 2361 N92-23634
Organic crystal growth experiment facility (13-IML-1) p 2362 N92-23635
CRYOSTAT (18-IML-1) p 2362 N92-23636
The Critical Point Facility (CPF) p 2362 N92-23637
Near-critical point phenomena in fluids (19-IML-1) p 2362 N92-23638
Study of density distribution in a near-critical simple fluid (19-IML-1) p 2362 N92-23639
Microgravity acceleration measurement and environment characterization science (17-IML-1) p 2363 N92-23642
Suborbital missions: The Joust p 2313 N92-23644
Spacehab p 2313 N92-23647
The Wake Shield Facility: A space experiment platform p 2313 N92-23648
Center for Macromolecular Crystallography, University of Alabama in Birmingham p 2313 N92-23650
Center for Cell Research, Pennsylvania State University p 2314 N92-23653
Numerical simulation of fluid behaviors in microgravity environment p 2363 N92-23719
The Columbus Free Flying Laboratory: Mechanical design aspects p 2323 N92-23782
Development and application of substructuring techniques for understanding and controlling residual vibrations (microgravity aspects) p 2330 N92-23827

REDUCTION (CHEMISTRY)
Survey on fixation and utilization of carbon dioxide by catalytic hydrogenation
[DE92-769380] p 2347 N92-23456

REDUNDANCY ENCODING
Design of joint source/channel coders
[NASA-CR-189960] p 2417 N92-23416

REENTRY
Large thin composite thermostructural parts p 2329 N92-23821
Stretched skin concept for the entry aerodynamic decelerator system of planetary probes p 2331 N92-23836
Beryllium-thermal protection technology p 2331 N92-23837
CNSR Rosetta: Earth return capsule p 2331 N92-23838

REENTRY TRAJECTORIES
Determination and prediction of satellite motion at the end of the lifetime p 2334 N92-23971

REFLECTANCE
Properties of bi-isotropic Fresnel reflection coefficients
[PB92-141886] p 2366 N92-23661
VITRIMAT2: A modified model of vitrinite maturation and reflectance
[DE92-008987] p 2348 N92-23904

REFLECTOR ANTENNAS
Feasibility study of a synthesis procedure for array feeds to improve radiation performance of large distorted reflector antennas
[NASA-CR-190191] p 2364 N92-23245

REGENERATION
Temperature-dependent evolution of chemisorbed digermane in Ge thin film growth
[DE92-008098] p 2447 N92-23447

REGOLITH
The meteorite record as clues to asteroidal regolith processes p 2457 N92-23770

REGRESSION ANALYSIS
Estimation of sea surface temperatures using MOS-1, GMS, and NOAA p 2398 N92-23475
Confidence intervals for discrete approximations to ill-posed problems
[PB92-143742] p 2432 N92-23511

REGULATIONS
Irradiation of spices, herbs, and other vegetable seasonings: A compilation of technical data for its authorization and control
[DE92-619064] p 2415 N92-24022

REINFORCING MATERIALS
Crystallization behavior of poly(phenylene sulphide) p 2342 N92-23940

RELATIVISTIC ELECTRON BEAMS
The principle and design of a high-efficiency free-electron laser p 2380 N92-23687

RELATIVISTIC PARTICLES
The notion of nonrelativistic isoparticle
[DE92-615215] p 2438 N92-23744

RELATIVISTIC VELOCITY
Beyond conventional quantum mechanics
[DE92-616892] p 2451 N92-23206

RELAXATION (MECHANICS)
On the kinetics of structural relaxation in some metallic glasses
[PB92-1287272] p 2353 N92-23165
A probabilistic mechanism hidden behind the universal power law for dielectric relaxation. Part 1: General relaxation equation
[DE92-615484] p 2435 N92-23220
A probabilistic mechanism hidden behind the universal power law for dielectric relaxation. Part 2: Discussion of the response function
[DE92-615485] p 2435 N92-23598

RELAXATION METHOD (MATHEMATICS)
Waveform relaxation always converges for RC-circuits
[PB92-142280] p 2369 N92-23495

RELIABILITY
Determination and prediction of satellite motion at the end of the lifetime p 2334 N92-23971

RELIABILITY ANALYSIS
The Delta 2 launcher p 2316 N92-23921

RELIABILITY ENGINEERING
Exact probabilistic testability measures for multi-output circuits
[REPT-1.2.7] p 2421 N92-23866

REMOTE CONTROL
Analysis and control of nonlinear flexible manipulator p 2384 N92-23727

REMOTE SENSING
X ray based displacement measurement for hostile environments
[NASA-TM-105551] p 2378 N92-23155
Design of neural networks for classification of remotely sensed imagery p 2402 N92-23367
Improved image classification with neural networks by fusing multispectral signatures with topological data p 2402 N92-23368
Euromar-Seastars: A definition study on modular multisensor instrumentation for airborne remote sensing of the sea
[MBB-UK-0152-91-PUB] p 2392 N92-23379
The state of the development in Europe p 2392 N92-23382
Recommended system concept p 2392 N92-23383
Sensor package for the North Sea p 2393 N92-23384
Geophysical, chemical and biological measuring parameters p 2393 N92-23385
The laser fluorosensor p 2393 N92-23386
Hardware and software modularity p 2394 N92-23399
Types of operation and system control p 2395 N92-23401
Current definition of some development programs p 2395 N92-23405
Realization and provisional sensor development planning p 2395 N92-23406
National user interfaces p 2395 N92-23407
Provisional cost evaluation p 2395 N92-23408

International cooperation p 2396 N92-23409
Euromar industrial partners agreement p 2396 N92-23410
An 18-point catalog description p 2396 N92-23411
Proceedings on MOS-1 data evaluation [HE-90015] p 2396 N92-23465
Outline of utilization results of MOS-1 data p 2396 N92-23466
Measurements of rain rate distribution by MOS-1 MSR p 2396 N92-23467
Application of ground-based laser beacon for Earth image calibration, 3 p 2396 N92-23468
Estimation of MTF of MOS-1 MESSR images p 2397 N92-23469
Investigations on verification of the data observed by the MESSR and VTIR, and on interannual trend in the MSR data p 2397 N92-23470
Verification of MESSR and VTIR, and time variation of MSR performance p 2397 N92-23471
Signal processing of the data obtained by MOS-1 MSR p 2397 N92-23472
Use of Marine Observation Satellite-1 in applied ocean science p 2400 N92-23487
Multitemporal and multisensor approach with MOS data to natural resources evaluation in dry tropical Africa (Burkina Faso) p 2400 N92-23488
A note on data quality: MSR data p 2400 N92-23489
Comparative study of digital MOS-1 MESSR, LANDSAT MSS, and IRS LISS-1 data for land cover classification in Sambalpur district, India p 2400 N92-23490
Data quality evaluation results MOS-1 verification program p 2400 N92-23491
Estimation of regional evapotranspiration with MOS-1 VTIR data p 2401 N92-23492
An attempt to derive land surface temperatures from MOS-1 VTIR data using split-window channel computation technique p 2401 N92-23493
Field evaluation of remote sensor measurements of wind, temperature, and moisture for ARM integrated sounding system research [PB92-140714] p 2401 N92-23521
Center for Mapping, Ohio State University p 2314 N92-23655
Empirical characterization of a high intensity LED proximity sensor [DE91-019074] p 2371 N92-23735
Acoustic emission as a process monitor for diamond machining of metal optical components [DE92-008037] p 2363 N92-23899
Fiber-optic Raman spectroscopy for cure monitoring of advanced polymer composites [DE92-008619] p 2355 N92-24068

REMOTE SENSORS
A spatial data handling system for retrieval of images by unrestricted regions of user interest p 2429 N92-23373
Introduction: Ocean air observation p 2392 N92-23381
Sensor interfaces p 2395 N92-23400
Preconsiderations on aircraft integration p 2395 N92-23402
Sensor compatibility/optimal sensor combinations p 2395 N92-23403
Proceedings on MOS-1 data evaluation [HE-90015] p 2396 N92-23465
Outline of utilization results of MOS-1 data p 2396 N92-23466
Measurements of rain rate distribution by MOS-1 MSR p 2396 N92-23467
Application of ground-based laser beacon for Earth image calibration, 3 p 2396 N92-23468
Estimation of MTF of MOS-1 MESSR images p 2397 N92-23469
Investigations on verification of the data observed by the MESSR and VTIR, and on interannual trend in the MSR data p 2397 N92-23470
Verification of MESSR and VTIR, and time variation of MSR performance p 2397 N92-23471
Signal processing of the data obtained by MOS-1 MSR p 2397 N92-23472
Field evaluation of remote sensor measurements of wind, temperature, and moisture for ARM integrated sounding system research [PB92-140714] p 2401 N92-23521
Microgravity acceleration measurement and environment characterization science (17-IML-1) p 2363 N92-23642

RENORMALIZATION GROUP METHODS
Renormalization group analysis of the Reynolds stress transport equation [NASA-TM-105588] p 2374 N92-23542

REPLACING
High reliability robot friendly ORU interface [NASA-CASE-GSC-13360-1] p 2381 N92-23377

REPRODUCTION (BIOLOGY)
Embryogenesis and organogenesis of Carausius morosus under space flight conditions (7-IML-1) p 2358 N92-23610

REQUIREMENTS
The challenge of the Hermes TPS shingles p 2322 N92-23823

RESEARCH
Summer graduate research program for interns in science and engineering [NASA-TM-107813] p 2470 N92-23958

RESEARCH AND DEVELOPMENT
Research, Development, Test and Evaluation (R, D, T, and E) Programs (R-1), Department of Defense budget for fiscal year 1993 [PB92-127745] p 2451 N92-23247
High energy physics: Report of research accomplishments and future goals, FY 1992 [DE92-008543] p 2441 N92-23576
What future for hybrid rocket propulsion? p 2321 N92-23768

RESEARCH FACILITIES
Conceptual design of Fusion Experimental Reactor [DE92-751036] p 2443 N92-23132
Annual report, 1 October 1990 - 30 September 1991 [DE92-008648] p 2380 N92-23891

RESEARCH MANAGEMENT
Conceptual design of Fusion Experimental Reactor [DE92-751036] p 2443 N92-23132

RESIDENTIAL AREAS
Limiting net greenhouse gas emissions in the United States, volume 1 [DE92-007593] p 2405 N92-23204

RESIDUAL STRENGTH
The fracture behavior of carbon/epoxy laminates containing part through-the-thickness fiber breakage p 2340 N92-23693

RESIDUAL STRESS
Influence of engineered interfaces on residual stresses and mechanical response in metal matrix composites [NASA-TM-105438] p 2340 N92-23195
Damage development in titanium metal matrix composites subjected to cyclic loading [NASA-TM-107597] p 2340 N92-23433
Method and apparatus for determination of material residual stress [NASA-CASE-GSC-13451-1] p 2388 N92-23549
Conception and development of improved analytical prediction models for fatigue induced tooth breakage due to cyclic bending in spur gear teeth p 2384 N92-23739
On the application of micromechanics to the prediction of macroscopic thermal residual stresses in short-fiber reinforced Polyetheretherketone (PEEK) p 2343 N92-23942
Mechanical properties of glass bead filled ductile epoxy composites p 2344 N92-23947

RESIDUES
LDEF impact craters formed by carbon-rich impactors: A preliminary report p 2336 N92-23319
Dynamic (computer) modelling of the particulate environment: Transformations from the LDEF reference frame to decode geocentric and interplanetary populations p 2458 N92-23320

RESIN BONDING
Application of the microbond technique: Characterization of carbon-epoxy interfaces p 2343 N92-23944

RESIN MATRIX COMPOSITES
The effect of fatigue-induced damage on the mechanical properties of CFRP composites p 2339 N92-23157
Proceedings: Nozzle Initiative Industry Advisory Committee on Standardization of Carbon-Phenolic Test Methods and Specifications [NASA-CR-190203] p 2337 N92-23539
Composites, 1990 [NRC-32603] p 2341 N92-23933

RESISTANCE THERMOMETERS
Sub-Kelvin resistance thermometer [NASA-CASE-GSC-13406-1] p 2378 N92-23460

RESOLUTION
The imaging microwave radiometer p 2393 N92-23390

RESONANT FREQUENCIES
A fin optimisation study p 2308 N92-23237
Free and forced response of nearly periodic multi-span beams and multi-bay trusses p 2389 N92-23699
Numerical investigation of fluid-structure-interaction problems with the finite element method p 2332 N92-23844
Analytical and experimental investigation of vibratory response in adhesively bonded and composite structures p 2345 N92-24012

RESONANT TUNNELING
Semiclassical model and properties of resonant tunneling diode [PB92-143320] p 2448 N92-23498

RESONANT VIBRATION
The torsional fatigue behaviour of the in-plane and out-of-plane shear moduli of composite materials p 2328 N92-23818
Dynamic characterization of composite materials p 2330 N92-23832
Comparison of multi-point modal test methods p 2333 N92-23849

RESOURCE ALLOCATION
Dynamic aggregate models for group technology manufacturing environment [REPT-1.1.7] p 2420 N92-23858

RESOURCES MANAGEMENT
National acid precipitation assessment program: Mission, goals, and program plan post 1990. Public review draft [PB92-128248] p 2405 N92-23515

RETRACTABLE EQUIPMENT
Retractable tool bit having latch type catch mechanism [NASA-CASE-GSC-13359-1] p 2381 N92-23378

REUSABLE ROCKET ENGINES
Health monitoring of reusable rocket engines p 2320 N92-23762

REVENUE
Launch vehicle for orbital missions: COMET p 2313 N92-23645
The market for computer readable information p 2453 N92-23728

REVERBERATION CHAMBERS
Acoustic absorption due to specimen in test in a reverberant chamber p 2324 N92-23790

REVISIONS
Modifications for a communication interface board p 2368 N92-23963

REYNOLDS NUMBER
Hypersonic laminar flow computations over a blunt leading edged delta wing at three different chord Reynolds numbers [FFA-TN-1991-40] p 2304 N92-23168

REYNOLDS STRESS
On the basic equations for the second-order modeling of compressible turbulence p 2303 N92-23351
Renormalization group analysis of the Reynolds stress transport equation [NASA-TM-105588] p 2374 N92-23542

RIEMANN MANIFOLD
On some types of Riemannian V(sub n) with zero Ricci curvature [DE92-616917] p 2432 N92-23502
Existence of closed geodesics on 2-spheres [PB92-149434] p 2433 N92-23599

RIGID STRUCTURES
On the analysis of liquid filled free-free tanks p 2332 N92-23843
Optimal control of closed chain robotic systems p 2430 N92-24011

RIPPLES
Evolution of magnetic moment due to the cyclotron resonance with field ripples in a tokamak [DE92-751058] p 2443 N92-23135

ROBOT ARMS
Automated synthesis of robot arm motion for robot arm collision avoidance p 2381 N92-23158
Configuration control of seven-degree-of-freedom arms [NASA-CASE-NPO-18607-1-CU] p 2382 N92-23553
The design and control of uncertain manipulator arms with decoupled inertia matrix p 2383 N92-23690
The statics, dynamics, and control of the elasticarm: A continuous beam manipulator p 2383 N92-23691
Optimal control of closed chain robotic systems p 2430 N92-24011
Controlling flexible robot arms using a high speed dynamics process [NASA-CASE-NPO-18499-1-CU] p 2385 N92-24042
Controlling under-actuated robot arms using a high speed dynamics process [NASA-CASE-NPO-18498-1-CU] p 2385 N92-24043
Flexible robotic arm [NASA-CASE-GSC-13161-1] p 2386 N92-24060

ROBOT CONTROL
Dynamic analysis of planar manipulation tasks [DE91-019060] p 2430 N92-23458
Climbing robot --- caterpillar design [NASA-CASE-GSC-13442-1] p 2382 N92-23547
The statics, dynamics, and control of the elasticarm: A continuous beam manipulator p 2383 N92-23691

ROBOT DYNAMICS
Automated synthesis of robot arm motion for robot arm collision avoidance p 2381 N92-23158

On motion planning amidst transient obstacles
[DE91-018939] p 2429 N92-23457
Dynamic analysis of planar manipulation tasks
[DE91-019060] p 2430 N92-23458
Climbing robot --- caterpillar design
[NASA-CASE-GSC-13442-1] p 2382 N92-23547
The design and control of uncertain manipulator arms with decoupled inertia matrix p 2383 N92-23690
The statics, dynamics, and control of the elasticarm: A continuous beam manipulator p 2383 N92-23691
Flexible robotic arm
[NASA-CASE-GSC-13161-1] p 2386 N92-24060

ROBOTICS
Artificial intelligence approach to planning the robotic assembly of large tetrahedral truss structures p 2426 N92-23357
Summary report: A preliminary investigation into the use of fuzzy logic for the control of redundant manipulators
[NASA-CR-190277] p 2429 N92-23438
Group scheduling using group technology concepts
[REPT-3.3.2] p 2424 N92-23886
Optimal control of closed chain robotic systems p 2430 N92-24011
Time optimal trajectories for a 2-wheeled robot
[DE92-000069] p 2430 N92-24032
Controlling flexible robot arms using a high speed dynamics process
[NASA-CASE-NPO-18499-1-CU] p 2385 N92-24042
Controlling under-actuated robot arms using a high speed dynamics process
[NASA-CASE-NPO-18498-1-CU] p 2385 N92-24043

ROBOTS
High reliability robot friendly ORU interface
[NASA-CASE-GSC-13360-1] p 2381 N92-23377
Climbing robot --- caterpillar design
[NASA-CASE-GSC-13442-1] p 2382 N92-23547
Empirical characterization of a high intensity LED proximity sensor
[DE91-019074] p 2371 N92-23735
Time optimal trajectories for a 2-wheeled robot
[DE92-000069] p 2430 N92-24032
Controlling flexible robot arms using a high speed dynamics process
[NASA-CASE-NPO-18499-1-CU] p 2385 N92-24042
Controlling under-actuated robot arms using a high speed dynamics process
[NASA-CASE-NPO-18498-1-CU] p 2385 N92-24043
A self-navigating mobile robot
[DE92-008612] p 2430 N92-24066

ROBUSTNESS (MATHEMATICS)
Density of the F-statistic in the linear model with arbitrarily normal distributed errors
[PB92-128792] p 2434 N92-23731

ROCKET ENGINE DESIGN
Blazing the trailway: Nuclear electric propulsion and its technology program plans
[NASA-TM-105605] p 2337 N92-23252
Derated ion thruster design issues
[NASA-TM-105576] p 2337 N92-23534

ROCKET ENGINES
Advanced ramjet systems for the propulsion of guided weapons
[ETN-92-91195] p 2310 N92-23169
What future for hybrid rocket propulsion? p 2321 N92-23768
Tubular copper thrust chamber design study
[NASA-CR-187206] p 2337 N92-23982

ROCKET LAUNCHERS
Rocket propulsion for NASA's Earth to orbit launchers p 2319 N92-23754

ROCKET LAUNCHING
Dynamic load cases on Ariane 5 p 2321 N92-23797

RODS
A damage mechanics model for beams p 2387 N92-23159

ROLLER BEARINGS
Sliding friction test of self lubricating polymer composites for rolling bearing retainer
[NAL-TM-622] p 2384 N92-23779

ROTATING BODIES
Design of an omnidirectional and holonomic wheeled platform prototype
[DE92-000046] p 2382 N92-23459
Quick-connect fasteners for assembling devices in space
[NASA-CASE-MSC-21648-1] p 2385 N92-24051

ROTATING FLUIDS
Ultrasonic investigation of (3)He-A vortices in low magnetic fields
[PB92-142256] p 2435 N92-23665
Numerical simulation of fluid behaviors in microgravity environment p 2363 N92-23719

ROTATING SPHERES
Microsphere viscometers for low temperature applications
[PB92-143361] p 2379 N92-23594

ROTATING STALLS
Experimental study of the mechanism of sound generation by rotating stall in centrifugal turbomachines p 2436 N92-23726

ROTATION
Rotating, radiating mass imbedded in a de Sitter universe p 2456 N92-23127
Helix translation device --- shim for precision displacements
[NASA-CASE-GSC-13141-1] p 2382 N92-23548

ROTOR SPEED
Control of a helicopter engine in low altitude flight p 2310 N92-23122

ROTORS
Analysis of a 37 kW cage-induction motor
[PB92-142116] p 2369 N92-23496
Computations of unsteady multistage turbomachinery flows p 2311 N92-23671

RUNGE-KUTTA METHOD
Improved shock-capturing of Jameson's scheme for the Euler equations
[PB92-148758] p 2373 N92-23251

S

SACCHAROMYCES
Microgravitational effects on chromosome behavior (7-IML-1) p 2357 N92-23604

SADDLE POINTS (GAME THEORY)
Stochastic games with average payoff criterion
[PB92-148634] p 2434 N92-23505

SAFETY
White paper: Preliminary assessment of LNG vehicle technology, economics, and safety issues
[PB92-137603] p 2383 N92-23680

SAFETY FACTORS
Mission safety evaluation report for STS-43, postflight edition
[NASA-TM-107801] p 2312 N92-23240
Mission safety evaluation report for STS-29, postflight edition
[NASA-TM-107773] p 2312 N92-23241
Mission safety evaluation report for STS-30, postflight edition
[NASA-TM-107774] p 2312 N92-23242
Mission safety evaluation report for STS-32, postflight edition
[NASA-TM-107775] p 2312 N92-23243
Mission safety evaluation report for STS-36, postflight edition
[NASA-TM-107780] p 2312 N92-23244

SAFETY MANAGEMENT
Mission safety evaluation report for STS-43, postflight edition
[NASA-TM-107801] p 2312 N92-23240
Mission safety evaluation report for STS-29, postflight edition
[NASA-TM-107773] p 2312 N92-23241
Mission safety evaluation report for STS-30, postflight edition
[NASA-TM-107774] p 2312 N92-23242
Mission safety evaluation report for STS-32, postflight edition
[NASA-TM-107775] p 2312 N92-23243
Mission safety evaluation report for STS-36, postflight edition
[NASA-TM-107780] p 2312 N92-23244

SALYUT SPACE STATION
The Reentry of Salyut-7/Kosmos-1686
[ESA-SP-345] p 2333 N92-23967
Radar tracking and observation of noncooperative space objects by reentry of Salyut-7/Kosmos-1686 p 2333 N92-23968
Orbit analysis and lifetime prediction using radar data by reentry of Salyut-7/Kosmos-1686 p 2318 N92-23969
Salyut-7/Kosmos-1686 reentry prediction activities at ESOC p 2334 N92-23970
Salyut-7/Kosmos-1686 reentry predictions for the Italian Civil Defence Authority p 2334 N92-23972
Debris reentry prediction: Salyut-7/Kosmos-1686 p 2318 N92-23973
Salyut-7/Kosmos-1686 orbit determination from radar data p 2318 N92-23976
Orbital decay and reentry of the Salyut-7 orbital complex p 2335 N92-23978

SAMPLES
An exhaustive self-test design methodology for synchronous state machines
[REPT-1.2.4] p 2421 N92-23863
The statistical analysis of data from normal distributions, with particular reference to small samples
[ESDU-91041] p 2434 N92-24008

SAMPLING
Numerical calculation: Aspiration efficiency of aerosols into thin-walled sampling inlets
[PB92-132901] p 2374 N92-23516

SANDWICH STRUCTURES
Nonlinear finite-element analysis of sandwich shells p 2326 N92-23802
Strength and deformation behaviour of Kevlar and carbon composite sandwich structures for space applications p 2332 N92-23840
Modeling of honeycomb core for sandwich CTE prediction p 2332 N92-23841

SATELLITE ALTIMETRY
Improved interpretation of satellite altimeter data using genetic algorithms p 2402 N92-23369

SATELLITE ATTITUDE CONTROL
Progress in the spacewise approach to Aristoteles data reduction p 2315 N92-23914

SATELLITE COMMUNICATION
Design of neural networks for classification of remotely sensed imagery p 2402 N92-23367
Interim Service ISDN Satellite (ISIS) hardware experiment development for advanced ISDN satellite designs and experiments
[NASA-CR-190257] p 2335 N92-24046

SATELLITE CONFIGURATIONS
Acoustic prediction on satellite structure p 2327 N92-23812

SATELLITE DESIGN
Interim Service ISDN Satellite (ISIS) hardware experiment development for advanced ISDN satellite designs and experiments
[NASA-CR-190257] p 2335 N92-24046

SATELLITE GROUND SUPPORT
Aristoteles ground segment: Operational concept p 2316 N92-23923

SATELLITE GROUND TRACKS
Aristoteles ground segment: Operational concept p 2316 N92-23923

SATELLITE IMAGERY
Feature detection in satellite images using neural network technology p 2427 N92-23366
Design of neural networks for classification of remotely sensed imagery p 2402 N92-23367
Improved image classification with neural networks by fusing multispectral signatures with topological data p 2402 N92-23368
Proceedings on MOS-1 data evaluation
[HE-90015] p 2396 N92-23465
Availability of MSR data for snow water estimation p 2399 N92-23482
Multitemporal and multisensor approach with MOS data to natural resources evaluation in dry tropical Africa (Burkina Faso) p 2400 N92-23488

SATELLITE INSTRUMENTS
Pinhole cameras as sensors for atomic oxygen in orbit: Application to attitude determination of the LDEF p 2379 N92-23283

SATELLITE LIFETIME
The Reentry of Salyut-7/Kosmos-1686
[ESA-SP-345] p 2333 N92-23967
Determination and prediction of satellite motion at the end of the lifetime p 2334 N92-23971
Debris reentry prediction: Salyut-7/Kosmos-1686 p 2318 N92-23973
Lifetime of objects in geostationary transfer orbit p 2318 N92-23977

SATELLITE NAVIGATION SYSTEMS
NASA's GPS tracking system for Aristoteles p 2316 N92-23919

SATELLITE OBSERVATION
Detecting opportunities for parallel observations on the Hubble Space Telescope p 2426 N92-23359
Proceedings on MOS-1 data evaluation
[HE-90015] p 2396 N92-23465
Outline of utilization results of MOS-1 data p 2396 N92-23466
Measurements of rain rate distribution by MOS-1 MSR p 2396 N92-23467
Application of ground-based laser beacon for Earth image calibration, 3 p 2396 N92-23468
Estimation of MTF of MOS-1 MESSR images p 2397 N92-23469
Investigations on verification of the data observed by the MESSR and VTIR, and on interannual trend in the MSR data p 2397 N92-23470
Verification of MESSR and VTIR, and time variation of MSR performance p 2397 N92-23471
Signal processing of the data obtained by MOS-1 MSR p 2397 N92-23472
Evaluation of effective characteristic in forest field p 2397 N92-23473

Verification of the effectiveness of MOS-1 MESSR in the field of disaster prevention p 2397 N92-23474
Estimation of sea surface temperatures using MOS-1, GMS, and NOAA p 2398 N92-23475
Monitoring of ocean conditions by using MOS-1 data p 2398 N92-23476
Applicability of MESSR and VTIR data for marine observation p 2398 N92-23478
Utilization of satellite images for marine resources p 2399 N92-23480
Preliminary report on the observation of polar atmosphere and cryosphere by MOS-1 data received at Syowa Station p 2399 N92-23481
Observation of lined-up cumulus rows under the winter monsoon situation using MOS-1 and radar data p 2399 N92-23483
The accuracy of the drift buoy positioning by MOS-1 DCS p 2399 N92-23484
Research project for practical usage of MOS-1 data collection system p 2399 N92-23485
Study on drifting-data collection buoy using MOS-1: Position verification in the Bering Sea p 2400 N92-23486
Use of Marine Observation Satellite-1 in applied ocean science p 2400 N92-23487
Multitemporal and multisensor approach with MOS data to natural resources evaluation in dry tropical Africa (Burkina Faso) p 2400 N92-23488
A note on data quality: MSR data p 2400 N92-23489
Comparative study of digital MOS-1 MESSR, LANDSAT MSS, and IRS LISS-1 data for land cover classification in Sambalpur district, India p 2400 N92-23490
Data quality evaluation results MOS-1 verification program p 2400 N92-23491
Estimation of regional evapotranspiration with MOS-1 VTIR data p 2401 N92-23492
An attempt to derive land surface temperatures from MOS-1 VTIR data using split-window channel computation technique p 2401 N92-23493
Urban temperature bias as determined by polar orbiting satellite data p 2402 N92-23724

SATELLITE ORIENTATION
Pinhole cameras as sensors for atomic oxygen in orbit: Application to attitude determination of the LDEF p 2379 N92-23283

SATELLITE SOUNDING
Possible atmospheric research with Aristoteles p 2317 N92-23927

SATELLITE TRACKING
Application of ground-based laser beacon for Earth image calibration, 3 p 2396 N92-23468
NASA's GPS tracking system for Aristoteles p 2316 N92-23919

SATELLITE TRANSMISSION
Aristoteles ground segment: Operational concept p 2316 N92-23923
Interim Service ISDN Satellite (ISIS) hardware experiment development for advanced ISDN satellite designs and experiments [NASA-CR-190257] p 2335 N92-24046

SATELLITE-BORNE INSTRUMENTS
The GRADIOmeter payload p 2315 N92-23917
The GRADIO accelerometer: Design and development status p 2316 N92-23918
Aristoteles magnetometer system p 2316 N92-23920

SCALE MODELS
Aeroelastic stability analyses of two counter rotating propfan designs for a cruise missile model [NASA-TM-105268] p 2387 N92-23191
Survey of experimental techniques for performance prediction p 2309 N92-23954
A self-navigating mobile robot [DE92-008612] p 2430 N92-24066

SCALING LAWS
Scaling study of pseudospark produced electron beam [DE92-003231] p 2368 N92-23186

SCANNERS
Applications of industrial engineering p 2364 N92-23966

SCANNING TUNNELING MICROSCOPY
Surface structure and analysis with scanning tunneling microscopy and electron tunneling spectroscopy [DE92-007747] p 2448 N92-23721

SCATTERING
Superconducting materials [DE92-007748] p 2446 N92-23205
Feasibility of payload sensitivity analyses for AR4 dynamic events p 2328 N92-23815
A new approach to estimate Angstrom coefficients [DE92-619048] p 2460 N92-23909

SCATTERING AMPLITUDE
Inelastic electron scattering from surfaces [DE92-008129] p 2437 N92-23330

SCATTERING FUNCTIONS
Semiclassical model and properties of resonant tunneling diode [PB92-143320] p 2448 N92-23498

SCATTEROMETERS
Development of a helicopter-borne 8-channel ranging scatterometer [PB92-141977] p 2396 N92-23441

SCHEDULES
Shop floor scheduling through a simulation based scheduler [REPT-2.3.3] p 2423 N92-23876

SCHEDULING
SLS-PLAN-IT: A knowledge-based blackboard scheduling system for Spacelab life sciences missions p 2426 N92-23358
Detecting opportunities for parallel observations on the Hubble Space Telescope p 2426 N92-23359
Control problem for a multi server loss system [PB92-148675] p 2430 N92-23506
Architectural impact of FDDI network on scheduling hard real-time traffic [NASA-CR-190272] p 2425 N92-23583
Dynamic aggregate models for group technology manufacturing environment [REPT-1.1.7] p 2420 N92-23858
Group scheduling using group technology concepts [REPT-3.3.2] p 2424 N92-23886
The Aristoteles mission profile p 2316 N92-23922

SCHOOLS (FISH)
Utilization of satellite images for marine resources p 2399 N92-23480

SCHROEDINGER EQUATION
Beyond conventional quantum mechanics [DE92-616892] p 2451 N92-23206

SCIENCE
Summer graduate research program for interns in science and engineering [NASA-TM-107813] p 2470 N92-23958

SCIENTIFIC SATELLITES
Proceedings on MOS-1 data evaluation [HE-90015] p 2396 N92-23465
Outline of utilization results of MOS-1 data p 2396 N92-23466
Application of ground-based laser beacon for Earth image calibration, 3 p 2396 N92-23468
Estimation of MTF of MOS-1 MESSR images p 2397 N92-23469
Investigations on verification of the data observed by the MESSR and VTIR, and on interannual trend in the MSR data p 2397 N92-23470
Verification of MESSR and VTIR, and time variation of MSR performance p 2397 N92-23471
Signal processing of the data obtained by MOS-1 MSR p 2397 N92-23472
Study on drifting-data collection buoy using MOS-1: Position verification in the Bering Sea p 2400 N92-23486
Use of Marine Observation Satellite-1 in applied ocean science p 2400 N92-23487
Multitemporal and multisensor approach with MOS data to natural resources evaluation in dry tropical Africa (Burkina Faso) p 2400 N92-23488
A note on data quality: MSR data p 2400 N92-23489
Comparative study of digital MOS-1 MESSR, LANDSAT MSS, and IRS LISS-1 data for land cover classification in Sambalpur district, India p 2400 N92-23490
Data quality evaluation results MOS-1 verification program p 2400 N92-23491
Estimation of regional evapotranspiration with MOS-1 VTIR data p 2401 N92-23492
An attempt to derive land surface temperatures from MOS-1 VTIR data using split-window channel computation technique p 2401 N92-23493
The Solid-Earth Mission Aristoteles [ESA-SP-329] p 2314 N92-23910
On the principle of Aristoteles p 2314 N92-23911
Mission objectives and scientific rationale for the magnetometer mission p 2315 N92-23912
The Earth's gravity field from satellite geodesy: A 30 year adventure p 2315 N92-23913
The geophysical impact of the Aristoteles mission p 2315 N92-23915
Introductory remarks to the mission and system aspects session p 2315 N92-23916
The GRADIOmeter payload p 2315 N92-23917
The GRADIO accelerometer: Design and development status p 2316 N92-23918
NASA's GPS tracking system for Aristoteles p 2316 N92-23919
Aristoteles magnetometer system p 2316 N92-23920
The Delta 2 launcher p 2316 N92-23921
The Aristoteles mission profile p 2316 N92-23922
Aristoteles ground segment: Operational concept p 2316 N92-23923
The potential use of fiducial ground networks p 2316 N92-23924
Gravity field data products from the Aristoteles mission p 2317 N92-23925
Data distribution and reduction approaches to data distribution: The Earthnet experience p 2317 N92-23926
Possible atmospheric research with Aristoteles p 2317 N92-23927

SEA ICE
Use of Marine Observation Satellite-1 in applied ocean science p 2400 N92-23487

SEA SURFACE TEMPERATURE
Monsoon-ENSO relationships p 2404 N92-23160
Clouds, surface temperature, and the tropical and subtropical radiation budget p 2410 N92-23431
Signal processing of the data obtained by MOS-1 MSR p 2397 N92-23472
Estimation of sea surface temperatures using MOS-1, GMS, and NOAA p 2398 N92-23475
Monitoring of ocean conditions by using MOS-1 data p 2398 N92-23476
Applicability of MESSR and VTIR data for marine observation p 2398 N92-23478
Use of Marine Observation Satellite-1 in applied ocean science p 2400 N92-23487

SEA WATER
The laser fluorosensor p 2393 N92-23386

SEALING
Cracking investigation of Nd:YAG laser welded gold plated glass sealing alloys [DE92-007971] p 2387 N92-23216

SEALS (STOPPERS)
Tribological evaluation of an Al2O3-SiO2 ceramic fiber candidate for high temperature sliding seals [NASA-TM-105611] p 2339 N92-23190
High temperature dynamic engine seal technology development [NASA-TM-105641] p 2381 N92-23435

SEARCH PROFILES
Creative search systems as specific expert systems [REPT-1.1.8] p 2420 N92-23859

SEDIMENTS
Reconstructing the tropical Atlantic seasonal thermocline using planktonic foraminifera p 2412 N92-23769

SEEDS
Thermoluminescent dosimetry for LDEF experiment M0006 p 2461 N92-23301
Transmission of gravistimulus in the statocyte of the lentil root (7-IML-1) p 2359 N92-23617

SELF ERECTING DEVICES
Self-deploying photovoltaic power system [NASA-CASE-LEW-15308-1] p 2404 N92-24057

SELF LUBRICATING MATERIALS
Sliding friction test of self lubricating polymer composites for rolling bearing retainer [NAL-TM-622] p 2384 N92-23779

SELF TESTS
An exhaustive self-test design methodology for synchronous state machines [REPT-1.2.4] p 2421 N92-23863

SEMICONDUCTOR DEVICES
Measurements of induced radioactivity in some LDEF samples p 2440 N92-23298
Versatile bistable optical switches and latching optical logic using integrated photothyristors and surface-emitting lasers [DE92-008677] p 2442 N92-23748
Magnetotransport and responses of semiconductor microstructures p 2449 N92-23775
Fast simulation of MOS digital networks using a physical macromodelling approach [REPT-1.2.1] p 2420 N92-23860
Electrical and optical properties of high gain GaAs switches [DE92-008668] p 2371 N92-23983
Metal-semiconductor, composite radiation detectors [DE92-008980] p 2344 N92-23988

SEMICONDUCTOR LASERS
Analysis and development of dynamic selection of laser array elements [NASA-TM-4375] p 2379 N92-23557

SEMICONDUCTORS (MATERIALS)
Electron polarization in modulation doped heterostructures [DE92-617490] p 2447 N92-23272
Fundamental electron transfer processes at the single crystal semiconductor/liquid interface [DE92-008132] p 2447 N92-23275
Sub-Kelvin resistance thermometer [NASA-CASE-GSC-13406-1] p 2378 N92-23460
Center for Space Power and Advanced Electronics, Auburn University p 2314 N92-23654

Magnetotransport and responses of semiconductor microstructures p 2449 N92-23775
Monte Carlo transport in semiconductor [DE92-008404] p 2371 N92-23902
Rapid recrystallization of semiconductor thin films for photovoltaic applications p 2404 N92-23998
Fermi level effects on dislocation formation in InAs(1-x)Sb(x) grown by MOCVD [DE92-008332] p 2450 N92-24034

SENSITIVITY
Integrated Design Analysis and Optimisation of Aircraft Structures [AGARD-R-784] p 2306 N92-23227
A system approach to aircraft optimization p 2306 N92-23228
Sensitivity analysis of dynamic aeroelastic responses p 2306 N92-23229
Sensitivity l(sup 1) minimization with boundary zeros or poles [PB92-141803] p 2433 N92-23658
Feasibility of payload sensitivity analyses for AR4 dynamic events p 2328 N92-23815

SENSORS
Method and apparatus for determination of material residual stress [NASA-CASE-GSC-13451-1] p 2388 N92-23549

SEPARATED FLOW
Hypersonic laminar flow computations over a blunt leading edged delta wing at three different chord Reynolds numbers [FFA-TN-1991-40] p 2304 N92-23168
Three-dimensional calculations of supersonic reacting flows using an LU scheme p 2304 N92-23354
High angle of attack: Aerodynamics p 2305 N92-23956

SEPARATION
Phase partitioning experiment (8-IML-1) p 2360 N92-23621

SEQUENCING
Coordinating complex problem-solving among distributed intelligent agents p 2427 N92-23360

SERVOMECHANISMS
Applications of industrial engineering p 2364 N92-23966
Controlling under-actuated robot arms using a high speed dynamics process [NASA-CASE-NPO-18498-1-CU] p 2385 N92-24043

SET THEORY
Some topological problems I met [PB92-149327] p 2431 N92-23248
Hierarchical sets in mathematical programming modeling languages [PB92-148683] p 2418 N92-23507

SHAFTS (MACHINE ELEMENTS)
Gamma ray spectrometry of LDEF samples at SRL p 2349 N92-23299
An analysis of the relationship between induction motor current and shaft speed fluctuations [DE92-007234] p 2371 N92-24025
Quick-connect fasteners for assembling devices in space [NASA-CASE-MSC-21648-1] p 2385 N92-24051

SHAPE MEMORY ALLOYS
Fabrication of a helical coil shape memory alloy actuator [DE92-008399] p 2364 N92-23901

SHAPES
Casting of simple-shaped single crystals of aluminum [PB92-136555] p 2350 N92-23179

SHEAR FLOW
Numerical experiments with flows of elongated granules [NASA-TM-105567] p 2381 N92-23226
Experiments and modeling p 2301 N92-23339
Modeling of compressible turbulent shear flows p 2301 N92-23340
Renormalization group analysis of the Reynolds stress transport equation [NASA-TM-105588] p 2374 N92-23542

SHEAR LAYERS
Progress of simulations for reacting shear layers p 2302 N92-23344
Simulations of free shear layers using a compressible kappa-epsilon model p 2304 N92-23355
An experimental investigation of entrainment and mixing in pulsed and exponential transverse jets p 2375 N92-23995

SHEAR STRAIN
The torsional fatigue behaviour of the in-plane and out-of-plane shear moduli of composite materials p 2328 N92-23818

SHEAR STRENGTH
High strength composites evaluation [DE92-007264] p 2340 N92-23585
Morphology and mechanical performance of PPS/carbon composite p 2342 N92-23939
Application of the microbond technique: Characterization of carbon-epoxy interfaces p 2343 N92-23944

SHEAR STRESS
High-temperature deformation behavior of single crystalline A15-type intermetallic compounds p 2352 N92-23718
Free vibration of thick isotropic and orthotropic cylindrical shells p 2389 N92-23773
Buckling of simply supported and clamped anisotropic plates under combined loads p 2326 N92-23804

SHEARING
Localization of deformation and inelastic deformation of pressure-sensitive dilatant materials p 2389 N92-23737

SHIPS
Seaborne lidar system p 2393 N92-23389

SHOCK LAYERS
Viscous-shock-layer analysis of hypersonic flows over long slender vehicles [NASA-CR-189614] p 2374 N92-23543

SHOCK SPECTRA
Coupled load analysis: Scatter related to model uncertainties p 2324 N92-23787

SHOCK TUBES
High-temperature ignition of propane with MTBE as an additive: Shock-tube experiments and modeling [DE92-008557] p 2348 N92-23715

SHOCK WAVE INTERACTION
Development of a new flux splitting scheme p 2303 N92-23352

SHOCK WAVES
The structure of MFD shock waves for rectilinear motion in some model of plasma [DE92-617386] p 2443 N92-23208
Improved shock-capturing of Jameson's scheme for the Euler equations [PB92-148758] p 2373 N92-23251

SIDE-LOOKING RADAR
The imaging radar system p 2393 N92-23391

SIERRA NEVADA MOUNTAINS (CA)
Climate [PB92-150457] p 2410 N92-23520

SIGNAL ANALYSIS
Quick-look system p 2394 N92-23393

SIGNAL ENCODING
A joint source/channel coder design p 2417 N92-23418

SIGNAL PROCESSING
Automatic waveform analysis and measurement system user manual [PB92-132976] p 2364 N92-23173
A signal and image processing object-based system using CLOS [DE92-006826] p 2417 N92-23255
Real-time radar processor p 2394 N92-23396
Proceedings on MOS-1 data evaluation [HE-90015] p 2396 N92-23465
Signal processing of the data obtained by MOS-1 MSR p 2397 N92-23472

SIGNAL TO NOISE RATIOS
PSD computations using Welch's method [DE92-007419] p 2370 N92-23584

SIGNATURES
LDEF impact craters formed by carbon-rich impactors: A preliminary report p 2336 N92-23319

SILICON
Integrated optics in silicon-based aluminum oxide [ISBN-90-9004261-X] p 2441 N92-23166
Molecular films associated with LDEF p 2439 N92-23289
High-performance multilayer mirrors for soft x ray projection lithography [DE92-008615] p 2443 N92-24049

SILICON CARBIDES
The effect of processing on strength of Nicalon fibers in Nicalon fiber-SiC matrix composites [DE92-006978] p 2340 N92-23256
Center for Space Power and Advanced Electronics, Auburn University p 2314 N92-23654

SILICON NITRIDES
Evaluation of the elevated-temperature mechanical reliability of a HIPed silicon nitride [DE92-007838] p 2354 N92-23223

SILICON OXIDES
Tribological evaluation of an Al2O3-SiO2 ceramic fiber candidate for high temperature sliding seals [NASA-TM-105611] p 2339 N92-23190

SILICONES
Molecular films associated with LDEF p 2439 N92-23289

SILVER ZINC BATTERIES
Testing and analyses of electrochemical cells using frequency response [NASA-TM-103580] p 2369 N92-23437

SIMULATION
M and D SIG progress report: Laboratory simulations of LDEF impact features p 2336 N92-23323
Simulation of freckles during vertical solidification of binary alloys p 2353 N92-24014
Synchronous parallel system for emulation and discrete event simulation [NASA-CASE-NPO-18414-1-CU] p 2426 N92-24045

SINE WAVES
An advanced system for environmental sine testing: Basic principles revisited p 2325 N92-23799

SINGLE CRYSTALS
Casting of simple-shaped single crystals of aluminum [PB92-136555] p 2350 N92-23179
Fundamental electron transfer processes at the single crystal semiconductor/liquid interface [DE92-008132] p 2447 N92-23275
Dependence of the critical temperature of laser-ablated YBa2Cu3O(7-delta) thin films on LaAlO3 substrate growth technique p 2365 N92-23415
Vapor crystal growth studies of single crystals of mercuric iodide (3-IML-1) p 2361 N92-23632
Mercury iodide nucleation and crystal growth in vapor phase (4-IML-1) p 2361 N92-23633
Organic crystal growth experiment facility (13-IML-1) p 2362 N92-23635
High-temperature deformation behavior of single crystalline A15-type intermetallic compounds p 2352 N92-23718

SINGLE STAGE TO ORBIT VEHICLES
Design challenges for the National Aero-Space Plane p 2310 N92-23822

SINGULARITY (MATHEMATICS)
Singularities in optimal structural design [NASA-TM-4365] p 2388 N92-23527

SIZE DETERMINATION
In situ particle size measurements using a two-color laser scattering technique [DE92-008634] p 2380 N92-24070

SIZE DISTRIBUTION
Study of cosmic dust particles on board LDEF: The FRECOPA experiments AO138-1 and AO138-2 p 2458 N92-23310
Meteoroid/space debris impacts on MSFC LDEF experiments p 2335 N92-23311
Dynamic (computer) modelling of the particulate environment: Transformations from the LDEF reference frame to decode geocentric and interplanetary populations p 2458 N92-23320

SKIN (STRUCTURAL MEMBER)
Non linear structural analysis of a thin skin carbon-carbon rigid decelerator p 2330 N92-23831
Stretched skin concept for the entry aerodynamic decelerator system of planetary probes p 2331 N92-23836

SLENDER BODIES
Viscous-shock-layer analysis of hypersonic flows over long slender vehicles [NASA-CR-189614] p 2374 N92-23543

SLIDING
Mechanical testing on a composite flexible structure p 2331 N92-23834

SLIDING CONTACT
Oil lubricated and water lubricated pin-on-disc wear tests with engineering ceramics [PB92-136563] p 2380 N92-23152

SLIDING FRICTION
Environmental effects on friction and wear of diamond and diamondlike carbon coatings [NASA-TM-105634] p 2354 N92-23192

SLOT ANTENNAS
Nonplanar linearly tapered slot antenna with balanced microstrip feed [NASA-TM-105647] p 2370 N92-23535

SNOW
Availability of MSR data for snow water estimation p 2399 N92-23482
Observation of lined-up cumulus rows under the winter monsoon situation using MOS-1 and radar data p 2399 N92-23483

SNOW COVER
Preliminary report on the observation of polar atmosphere and cryosphere by MOS-1 data received at Syowa Station p 2399 N92-23481
Availability of MSR data for snow water estimation p 2399 N92-23482

SOAPS
Guanidine based vehicle/binders for use with oxides, metals, and ceramics [NASA-CASE-LEW-15314-1] p 2354 N92-23461

SOFTWARE ENGINEERING
Knowledge-based approach for generating target system specifications from a domain model p 2428 N92-23371

Framework Programmable Platform for the advanced software development workstation: Framework processor design document
[NASA-CR-190173] p 2418 N92-23554

SOFTWARE TOOLS
Knowledge-based approach for generating target system specifications from a domain model
p 2428 N92-23371
Maximal modal energy method: An overvaluing tool for low frequency prediction of structure acoustic response
p 2324 N92-23791
Multi parameter optimization on Ariane 5
p 2321 N92-23798
Ariane 4 internal acoustic environment: Interpretation of flight data with a vibroacoustic model of the upper part of the launcher p 2321 N92-23811
Acoustic prediction on satellite structure
p 2327 N92-23812
The response surface method: An efficient tool to determine the failure probability of large structural systems p 2328 N92-23816
The challenge of the Hermes TPS shingles
p 2322 N92-23823
The need for standards in design automation
[P-1-1] p 2419 N92-23852
A framework for the support of VLSI (very large scale integration) design for manufacture
[REPT-1.3.1] p 2421 N92-23868
Shop floor scheduling through a simulation based scheduler
[REPT-2.3.3] p 2423 N92-23876
Infrastructure and training of manpower for CAD/CAM systems
[REPT-4.2.2] p 2425 N92-23888
High angle of attack: Aerodynamics
p 2305 N92-23956
Using microsoft excel applications in the graduate intern program at Goddard Space Flight Center
p 2425 N92-23959
Expert systems: A mapping between symbol susceptible tasks and software tools p 2454 N92-24016
Battery test facility hardware, software, and system operation
[DE92-008455] p 2372 N92-24063

SOLAR ACTIVITY
Testing the solar paradigm for chromospheric activity in RS CVN binaries: Moderate resolution spectroscopy of solar active regions p 2459 N92-23171

SOLAR ACTIVITY EFFECTS
The isotopic composition of cosmic ray helium from 500 to 1100 MeV per nucleon p 2460 N92-23163
Prediction of solar and geomagnetic activity for ESA low-flying spacecraft p 2334 N92-23975

SOLAR ARRAYS
Microprocessor control of multiple peak power tracking DC/DC converters for use with solar cell arrays
[NASA-CASE-GSC-13450-1] p 2403 N92-23463
PHOTO: A computer simulation program for photovoltaic and hybrid energy systems. Document and user's guide
[PB92-141928] p 2403 N92-23683
Strength and deformation behaviour of Kevlar and carbon composite sandwich structures for space applications p 2332 N92-23840
Self-deploying photovoltaic power system
[NASA-CASE-LEW-15308-1] p 2404 N92-24057

SOLAR ATMOSPHERE
The effects of magnetic fields on oscillations in the solar atmosphere p 2459 N92-23697

SOLAR BLANKETS
Self-deploying photovoltaic power system
[NASA-CASE-LEW-15308-1] p 2404 N92-24057

SOLAR CELLS
Microprocessor control of multiple peak power tracking DC/DC converters for use with solar cell arrays
[NASA-CASE-GSC-13450-1] p 2403 N92-23463
Solar-electric-propulsion cargo vehicles for split/sprint Mars mission
[NASA-CR-189983] p 2322 N92-23526
Defect behavior, carrier removal and predicted in-space injection annealing of InP solar cells
[NASA-TM-105624] p 2370 N92-23562
Influence of the substrate on the solar cells interconnector: Stress distribution and fatigue life prediction p 2326 N92-23803

SOLAR CORONA
Magnetic reconnection in magnetotail and solar plasmas p 2457 N92-24000

SOLAR ELECTRIC PROPULSION
Solar-electric-propulsion cargo vehicles for split/sprint Mars mission
[NASA-CR-189983] p 2322 N92-23526

SOLAR ENERGY CONVERSION
Promotion of industrial technologies on the global environment
[DE92-769377] p 2405 N92-23454
Promotion of industrial technologies on the global environment
[DE92-769376] p 2407 N92-24023

SOLAR FLARES
Solar-geophysical data Number 564, August 1991. Part 2 (comprehensive reports): Data for February 1991 and miscellaneous
[PB92-111699] p 2459 N92-23701
Solar-geophysical data Number 566, October 1991. Part 2 (comprehensive reports): Data for April 1991 and miscellaneous
[PB92-129402] p 2460 N92-23993

SOLAR HEATING
Comparison of analytical and numerical modelling approaches for sizing of seasonal storage solar heating systems
[PB92-141829] p 2403 N92-23592

SOLAR MAGNETIC FIELD
The effects of magnetic fields on oscillations in the solar atmosphere p 2459 N92-23697

SOLAR NEUTRINOS
Results from the Soviet-American gallium experiment
[DE92-007414] p 2438 N92-23747

SOLAR ORBITS
Constructing a pulsar timing array
p 2456 N92-23126

SOLAR OSCILLATIONS
The effects of magnetic fields on oscillations in the solar atmosphere p 2459 N92-23697

SOLAR PHYSICS
Solar-geophysical data Number 564, August 1991. Part 2 (comprehensive reports): Data for February 1991 and miscellaneous
[PB92-111699] p 2459 N92-23701
Solar-geophysical data Number 566, October 1991. Part 2 (comprehensive reports): Data for April 1991 and miscellaneous
[PB92-129402] p 2460 N92-23993

SOLAR PROMINENCES
Solar-geophysical data Number 564, August 1991. Part 2 (comprehensive reports): Data for February 1991 and miscellaneous
[PB92-111699] p 2459 N92-23701
Solar-geophysical data Number 566, October 1991. Part 2 (comprehensive reports): Data for April 1991 and miscellaneous
[PB92-129402] p 2460 N92-23993

SOLAR RADIATION
Clouds, surface temperature, and the tropical and subtropical radiation budget p 2410 N92-23431
Investigation of the Archean climate using the NCAR CCM
[NASA-CR-189878] p 2410 N92-23656
Analysis of solar and microwave thermal propulsion systems p 2337 N92-23694
Solar-geophysical data Number 564, August 1991. Part 2 (comprehensive reports): Data for February 1991 and miscellaneous
[PB92-111699] p 2459 N92-23701
Clouds and radiation testbed data environment: Site data system and experiment center
[DE92-006732] p 2408 N92-23741
A new approach to estimate Angstrom coefficients
[DE92-619048] p 2460 N92-23909

SOLAR RADIO BURSTS
Solar-geophysical data Number 564, August 1991. Part 2 (comprehensive reports): Data for February 1991 and miscellaneous
[PB92-111699] p 2459 N92-23701
Solar-geophysical data Number 566, October 1991. Part 2 (comprehensive reports): Data for April 1991 and miscellaneous
[PB92-129402] p 2460 N92-23993

SOLAR SAILS
JPRS report: Science and technology. Central Eurasia: Space
[JPRS-USP-92-002] p 2314 N92-23705

SOLAR WIND
The subionospheric electromagnetic response to magnetopause processes p 2407 N92-23142
Solar-geophysical data Number 564, August 1991. Part 2 (comprehensive reports): Data for February 1991 and miscellaneous
[PB92-111699] p 2459 N92-23701

SOLAR X-RAYS
Solar-geophysical data Number 564, August 1991. Part 2 (comprehensive reports): Data for February 1991 and miscellaneous
[PB92-111699] p 2459 N92-23701
Solar-geophysical data Number 566, October 1991. Part 2 (comprehensive reports): Data for April 1991 and miscellaneous
[PB92-129402] p 2460 N92-23993

SOLDERING
JPRS report: Science and technology. Central Eurasia: Materials science
[JPRS-UMS-92-005] p 2363 N92-23708
JPRS report: Science and technology. Central Eurasia: Materials science
[JPRS-UMS-92-006] p 2363 N92-23709

SOLDERS
JPRS report: Science and technology. Central Eurasia: Materials science
[JPRS-UMS-92-005] p 2363 N92-23708
JPRS report: Science and technology. Central Eurasia: Materials science
[JPRS-UMS-92-006] p 2363 N92-23709

SOLID LUBRICANTS
Tribological evaluation of an Al2O3-SiO2 ceramic fiber candidate for high temperature sliding seals
[NASA-TM-105611] p 2339 N92-23190
Sliding friction test of self lubricating polymer composites for rolling bearing retainer
[NAL-TM-622] p 2384 N92-23779

SOLID PROPELLANT IGNITION
Manufacturing process of the Ariane 5 segmented propellant chargers p 2319 N92-23756

SOLID PROPELLANT ROCKET ENGINES
Launcher Propulsion Towards the Year 2010
[ESA-SP-327] p 2318 N92-23750
Development status of the Ariane 5 solid propellant engine p 2319 N92-23755
Future launchers: Large size solid propellant monolithic booster p 2320 N92-23766
Development of solid propellant booster
p 2320 N92-23767

SOLID PROPELLANTS
Small or non pollutant solid propellants for space launchers p 2320 N92-23765

SOLID STATE
Solid State Technology Branch of NASA Lewis Research Center
[NASA-TM-105159] p 2365 N92-23412

SOLID STATE DEVICES
The LDEF ultra heavy cosmic ray experiment
p 2461 N92-23306

SOLID SURFACES
Grid generation and flow solution method for Euler equations on unstructured grids
[NASA-TM-4295] p 2305 N92-23533

SOLID-SOLID INTERFACES
Failure processes in the fibre-polymer interphase
p 2341 N92-23934
Application of the microbond technique: Characterization of carbon-epoxy interfaces
p 2343 N92-23944
Influence of maleic anhydride as a coupling agent on the performance of wood fiber: Polystyrene composites
p 2343 N92-23945

SOLIDIFICATION
Effects of impurities on the solidification and mechanical behaviour of primary and secondary commercial purity aluminium and aluminium alloys
[PB92-133511] p 2350 N92-23176
A study of aluminum-lithium alloy solidification using acoustic emission techniques
[NASA-CR-4437] p 2435 N92-23556
An optical study of grain formation: Casting and solidification technology (2-IML-1) p 2361 N92-23631
Simulation of freckles during vertical solidification of binary alloys p 2353 N92-24014

SOLITARY WAVES
Applications of boundary integral methods to the study of steep free surface waves p 2372 N92-23149
Solitary excitations in gyrotropic crystals
[DE92-617447] p 2446 N92-23271

SOLVENT EXTRACTION
Production of metal powders by hydrogen stripping from loaded organic extractants
[PB92-136464] p 2350 N92-23178

SONDES
Seaborne lidar system p 2393 N92-23389

SOUND FIELDS
A frequency domain least squares method for modelling acoustic fields
[ISVR-TR-196] p 2435 N92-23170

SOUND GENERATORS
Experimental study of the mechanism of sound generation by rotating stall in centrifugal turbomachines
p 2436 N92-23726
Numerical and experimental study of noise generated by a vibrating plate p 2324 N92-23792

SOUND PRESSURE
Acoustic absorption due to specimen in test in a reverberant chamber p 2324 N92-23790

SOUND WAVES
Evaluation of the applicability of Helmholtz resonators for low frequency acoustic liners
[PB92-138544] p 2436 N92-23588

Acoustic absorption due to specimen in test in a reverberant chamber p 2324 N92-23790
Maximal modal energy method: An overvaluing tool for low frequency prediction of structure acoustic response p 2324 N92-23791
Numerical and experimental study of noise generated by a vibrating plate p 2324 N92-23792
Ariane 4 internal acoustic environment: Interpretation of flight data with a vibroacoustic model of the upper part of the launcher p 2321 N92-23811

SOYUZ SPACECRAFT
The USSR launchers programme p 2319 N92-23753

SPACE ADAPTATION SYNDROME
Space adaptation syndrome experiments (8-IML-1) p 2360 N92-23625

SPACE CAPSULES
CNSR Rosetta: Earth return capsule p 2331 N92-23838

SPACE COMMERCIALIZATION
Proceedings of the Second Annual Symposium on Industrial Involvement and Successes in Commercial Space
[NASA-TM-107812] p 2312 N92-23643
Launch vehicle for orbital missions: COMET p 2313 N92-23645
Systems for COMET p 2313 N92-23646
Space Station Freedom p 2313 N92-23649
Center for Space Power and Advanced Electronics, Auburn University p 2314 N92-23654
Center for Mapping, Ohio State University p 2314 N92-23655

SPACE DEBRIS
Large craters on the meteoroid and space debris impact experiment p 2335 N92-23309
Meteoroid/space debris impacts on MSFC LDEF experiments p 2335 N92-23311
Meteoroid and debris special investigation group data acquisition procedures p 2454 N92-23313
Preliminary analysis of LDEF instrument A0187-1: Chemistry of Micrometeoroids Experiment p 2458 N92-23315
IDE spatio-temporal impact fluxes and high time-resolution studies of multi-impact events and long-lived debris clouds p 2458 N92-23317
Ion microprobe elemental analyses of impact features on interplanetary dust experiment sensor surfaces p 2458 N92-23318
LDEF data correlation to existing NASA debris environment models p 2336 N92-23321
Preliminary micrometeoroid and debris effects on LDEF thermal control surfaces p 2336 N92-23324
The validation of hydrocodes for orbital debris impact simulation p 2323 N92-23784
Protection of spacecraft against meteroid/orbital debris impacts p 2323 N92-23786
Radar tracking and observation of noncooperative space objects by reentry of Salyut-7/Kosmos-1686 p 2333 N92-23968
Debris reentry prediction: Salyut-7/Kosmos-1686 p 2318 N92-23973

SPACE ERECTABLE STRUCTURES
Robot-friendly connector --- space truss structures
[NASA-CASE-MSC-21864-1] p 2382 N92-23544
On the modelling of a deployable telescope elastic beam-type element for on-orbit multibody simulations p 2329 N92-23826

SPACE FLIGHT
Skeletal responses to spaceflight
[NASA-TM-103890] p 2414 N92-23424
Embryogenesis and organogenesis of Carausius morosus under space flight conditions (7-IML-1) p 2358 N92-23610

SPACE LABORATORIES
Development of Japanese experiment module p 2323 N92-23781

SPACE MANUFACTURING
Proceedings of the Second Annual Symposium on Industrial Involvement and Successes in Commercial Space
[NASA-TM-107812] p 2312 N92-23643
Launch vehicle for orbital missions: COMET p 2313 N92-23645
Systems for COMET p 2313 N92-23646
The Wake Shield Facility: A space experiment platform p 2313 N92-23648
Space Station Freedom p 2313 N92-23649

SPACE MISSIONS
The achievement of spacecraft autonomy through the thematic application of multiple cooperating intelligent agents p 2427 N92-23364

SPACE NAVIGATION
Low thrust propulsion literature survey
[NASA-CR-190179] p 2337 N92-23151
Market directed thinking in a technological operation p 2452 N92-23929

SPACE PLASMAS
Solar-geophysical data Number 564, August 1991. Part 2 (comprehensive reports): Data for February 1991 and miscellaneous
[PB92-111699] p 2459 N92-23701
Solar-geophysical data Number 566, October 1991. Part 2 (comprehensive reports): Data for April 1991 and miscellaneous
[PB92-129402] p 2460 N92-23993
Magnetic reconnection in magnetotail and solar plasmas p 2457 N92-24000

SPACE PROBES
Non linear structural analysis of a thin skin carbon-carbon rigid decelerator p 2330 N92-23831
Beryllium-thermal protection technology p 2331 N92-23837

SPACE PROCESSING
Advanced Materials Center, Battelle p 2314 N92-23652

SPACE PROGRAMS
Launcher Propulsion Towards the Year 2010
[ESA-SP-327] p 2318 N92-23750
From Earth to orbit --- assessment of transportation options
[NASA-CR-190216] p 2321 N92-23980

SPACE SHUTTLE MISSIONS
Mission safety evaluation report for STS-43, postflight edition
[NASA-TM-107801] p 2312 N92-23240
Mission safety evaluation report for STS-29, postflight edition
[NASA-TM-107773] p 2312 N92-23241
Mission safety evaluation report for STS-30, postflight edition
[NASA-TM-107774] p 2312 N92-23242
Mission safety evaluation report for STS-32, postflight edition
[NASA-TM-107775] p 2312 N92-23243
Mission safety evaluation report for STS-36, postflight edition
[NASA-TM-107780] p 2312 N92-23244

SPACE SHUTTLE ORBITERS
Measured space environmental effects to LDEF during retrieval p 2335 N92-23285
STS investigators' guide
[NASA-TM-105523] p 2321 N92-23524

SPACE SHUTTLE PAYLOADS
A review of Space Shuttle payload-bay lift-off flight data and analysis comparisons p 2322 N92-23796

SPACE SHUTTLES
Spacehab p 2313 N92-23647

SPACE STATION FREEDOM
Evaluating model accuracy for model-based reasoning p 2427 N92-23362
Proceedings of the Second Annual Symposium on Industrial Involvement and Successes in Commercial Space
[NASA-TM-107812] p 2312 N92-23643
Space Station Freedom p 2313 N92-23649

SPACE STATIONS
High reliability robot friendly ORU interface
[NASA-CASE-GSC-13360-1] p 2381 N92-23377
Development of Japanese experiment module p 2323 N92-23781
Simulation of Space Station loads with active control systems p 2329 N92-23824

SPACE TRANSPORTATION
From Earth to orbit --- assessment of transportation options
[NASA-CR-190216] p 2321 N92-23980

SPACE TRANSPORTATION SYSTEM
STS investigators' guide
[NASA-TM-105523] p 2321 N92-23524
Ariane technology: From today into the next century p 2318 N92-23751

SPACE TRANSPORTATION SYSTEM FLIGHTS
Mission safety evaluation report for STS-43, postflight edition
[NASA-TM-107801] p 2312 N92-23240
Mission safety evaluation report for STS-29, postflight edition
[NASA-TM-107773] p 2312 N92-23241
Mission safety evaluation report for STS-30, postflight edition
[NASA-TM-107774] p 2312 N92-23242
Mission safety evaluation report for STS-32, postflight edition
[NASA-TM-107775] p 2312 N92-23243
Mission safety evaluation report for STS-36, postflight edition
[NASA-TM-107780] p 2312 N92-23244
A review of Space Shuttle payload-bay lift-off flight data and analysis comparisons p 2322 N92-23796

SPACE-TIME FUNCTIONS
Rotating, radiating mass imbedded in a de Sitter universe p 2456 N92-23127
Inequivalence of interior and exterior dynamical problems
[DE92-615214] p 2451 N92-23743

SPACEBORNE EXPERIMENTS
LDEF: 69 Months in Space. First Post-Retrieval Symposium, part 1
[NASA-CP-3134-PT-1] p 2461 N92-23280
Long Duration Exposure Facility: A general overview p 2335 N92-23281
Long Duration Exposure Facility (LDEF) space environments overview p 2335 N92-23282
Use of the Long Duration Exposure Facility's thermal measurement system for the verification of thermal models p 2336 N92-23284
Measured space environmental effects to LDEF during retrieval p 2335 N92-23285
Preliminary results from the heavy ions in space experiment p 2461 N92-23307
The use of artificial intelligence techniques to improve the multiple payload integration process p 2428 N92-23370
NIST torsion oscillator viscometer response: Performance on the LeRC active vibration isolation platform
[NASA-TM-105571] p 2383 N92-23564
First International Microgravity Laboratory experiment descriptions
[NASA-TM-4353] p 2356 N92-23600
Gravitropic responses of plants in the absence of a complicating G-force (6-IML-1) p 2356 N92-23601
A spaceflight experiment to investigate the effects of a range of unilateral blue light phototropic stimulations on the movements of wheat coleoptiles (6-IML-1) p 2356 N92-23602
Genetic and molecular dosimetry of HZE radiation (7-IML-1) p 2357 N92-23603
Microgravitational effects on chromosome behavior (7-IML-1) p 2357 N92-23604
Chrondrogenesis in micromass cultures of embryonic mouse limb mesenchymal cells exposed to microgravity (7-IML-1) p 2357 N92-23605
Effect of microgravity and mechanical stimulation on the in vitro mineralization and resorption of fetal mouse long bones (7-IML-1) p 2357 N92-23606
Eggs: The role of gravity in the establishment of the dorso-ventral axis in the amphibian embryo (7-IML-1) p 2357 N92-23607
The effect of space environment on the development and aging of Drosophila Melanogaster (7-IML-1) p 2357 N92-23608
Effect of microgravity environment on cell wall regeneration, cell divisions, growth, and differentiation of plants from protoplasts (7-IML-1) p 2358 N92-23609
Embryogenesis and organogenesis of Carausius morosus under space flight conditions (7-IML-1) p 2358 N92-23610
Dosimetric mapping inside biorack (7-IML-1) p 2358 N92-23611
Growth and sporulation of Bacillus subtilis under microgravity (7-IML-1) p 2358 N92-23612
Friend leukemia virus transformed cells exposed to microgravity in the presence of DMSO (7-IML-1) p 2358 N92-23613
Proliferation and performance of hybridoma cells in microgravity (7-IML-1) p 2358 N92-23614
Dynamic cell culture system (7-IML-1) p 2359 N92-23615
Growth, differentiation and development of Arabidopsis thaliana under microgravity conditions (7-IML-1) p 2359 N92-23616
Transmission of gravistimulus in the statocyte of the lentil root (7-IML-1) p 2359 N92-23617
Gravity related behavior of the acellular slime mold Physarum polycephalum (7-IML-1) p 2359 N92-23618
Studies on penetration of antibiotic in bacterial cells in space conditions (7-IML-1) p 2359 N92-23619
Energy expenditure in space flight (doubly labelled water method) (8-IML-1) p 2359 N92-23620
The Wake Shield Facility: A space experiment platform p 2313 N92-23648
Center for Macromolecular Crystallography, University of Alabama in Birmingham p 2313 N92-23650
The Columbus Free Flying Laboratory: Mechanical design aspects p 2323 N92-23782

SPACEBORNE LASERS
Analysis and development of dynamic selection of laser array elements
[NASA-TM-4375] p 2379 N92-23557

SPACEBORNE PHOTOGRAPHY
Pinhole cameras as sensors for atomic oxygen in orbit: Application to attitude determination of the LDEF p 2379 N92-23283

SPACEBORNE TELESCOPES
On the modelling of a deployable telescope elastic beam-type element for on-orbit multibody simulations p 2329 N92-23826

SPACECRAFT ANTENNAS
Feasibility study of a synthesis procedure for array feeds to improve radiation performance of large distorted reflector antennas
[NASA-CR-190191] p 2364 N92-23245
SPACECRAFT BREAKUP
Radar tracking and observation of noncooperative space objects by reentry of Salyut-7/Kosmos-1686
p 2333 N92-23968
Orbit analysis and lifetime prediction using radar data by reentry of Salyut-7/Kosmos-1686
p 2318 N92-23969
Salyut-7/Kosmos-1686 reentry prediction activities at ESOC p 2334 N92-23970
SPACECRAFT COMPONENTS
Gamma radiation survey of the LDEF spacecraft
p 2460 N92-23293
High reliability robot friendly ORU interface
[NASA-CASE-GSC-13360-1] p 2381 N92-23377
Sliding friction test of self lubricating polymer composites for rolling bearing retainer
[NAL-TM-622] p 2384 N92-23779
SPACECRAFT CONSTRUCTION MATERIALS
Induced radioactivity in LDEF components
p 2440 N92-23300
Meteoroid, and debris special investigation group preliminary results: Size-frequency distribution and spatial density of large impact features on LDEF
p 2336 N92-23314
Materials for liquid propellant engines
p 2320 N92-23764
Spacecraft Structures and Mechanical Testing, volume 1
[ESA-SP-321-VOL-1] p 2322 N92-23780
Material considerations for habitable areas of manned spacecraft p 2323 N92-23785
Large thin composite thermostructural parts
p 2329 N92-23821
Design challenges for the National Aero-Space Plane
p 2310 N92-23822
The challenge of the Hermes TPS shingles
p 2322 N92-23823
Beryllium-thermal protection technology
p 2331 N92-23837
CNSR Rosetta: Earth return capsule
p 2331 N92-23838
SPACECRAFT CONTAMINATION
Measured space environmental effects to LDEF during retrieval p 2335 N92-23285
Particle types and sources associated with LDEF
p 2349 N92-23286
Migration and generation of contaminants from launch through recovery: LDEF case history
p 2335 N92-23287
Quantification of contaminants associated with LDEF
p 2349 N92-23288
Molecular films associated with LDEF
p 2439 N92-23289
Organic contamination of LDEF p 2339 N92-23290
SPACECRAFT CONTROL
Distributed expert systems for ground and space applications p 2427 N92-23361
Simulation of Space Station loads with active control systems p 2329 N92-23824
Influence of microvibrations on spacecraft performances p 2329 N92-23825
SPACECRAFT DESIGN
Conceptional design to heat-resistant airframe of HOPE p 2328 N92-23820
Large thin composite thermostructural parts
p 2329 N92-23821
Design challenges for the National Aero-Space Plane
p 2310 N92-23822
SPACECRAFT GUIDANCE
Nonlinear feedback guidance law for aero-assisted orbit transfer maneuvers
[NASA-CR-190129] p 2317 N92-23529
SPACECRAFT LAUNCHING
A review of Space Shuttle payload-bay lift-off flight data and analysis comparisons p 2322 N92-23796
The Delta 2 launcher p 2316 N92-23921
SPACECRAFT MOTION
Deriving the velocity distribution of meteoroids from the measured meteoroid impact directionality on the various LDEF surfaces p 2459 N92-23322
SPACECRAFT PERFORMANCE
Influence of microvibrations on spacecraft performances p 2329 N92-23825
SPACECRAFT POWER SUPPLIES
Center for Space Power, Texas A and M University
p 2313 N92-23651
SPACECRAFT PROPULSION
Low thrust propulsion literature survey
[NASA-CR-190179] p 2337 N92-23151
Blazing the trailway: Nuclear electric propulsion and its technology program plans
[NASA-TM-105805] p 2337 N92-23252
Probabilistic Structural Analysis Methods (PSAM) for select space propulsion system components, part 2
[NASA-CR-187200] p 2388 N92-23426
Launcher Propulsion Towards the Year 2010
[ESA-SP-327] p 2318 N92-23750
Launch systems for future NASA missions
p 2318 N92-23752
Rocket propulsion for NASA's Earth to orbit launchers
p 2319 N92-23754
Materials for high liquid propulsion in 2010
p 2320 N92-23763
Small or non pollutant solid propellants for space launchers p 2320 N92-23765
Space transfer concepts and analyses for exploration missions: Technical directive 10
[NASA-CR-184309] p 2317 N92-24048
SPACECRAFT RECOVERY
Measured space environmental effects to LDEF during retrieval p 2335 N92-23285
SPACECRAFT SHIELDING
Protection of spacecraft against meteroid/orbital debris impacts p 2323 N92-23786
SPACECRAFT STRUCTURES
Summary of ionizing radiation analysis on the Long Duration Exposure Facility p 2439 N92-23291
Application of optical distributed sensing and computation to control of large space structures
[NASA-CR-190293] p 2442 N92-23567
Nonlinear finite element analysis of space frames
[PB92-142447] p 2388 N92-23664
Spacecraft Structures and Mechanical Testing, volume 1
[ESA-SP-321-VOL-1] p 2322 N92-23780
Improvements for interpretation of structural dynamics calculation using effective parameters for substructures
p 2324 N92-23789
On development of automated static loading system for spacecraft structures p 2326 N92-23801
Acoustic prediction on satellite structure
p 2327 N92-23812
Large thin composite thermostructural parts
p 2329 N92-23821
Influence of microvibrations on spacecraft performances p 2329 N92-23825
Development and application of substructuring techniques for understanding and controlling residual vibrations (microgravity aspects) p 2330 N92-23827
Non linear structural analysis of a thin skin carbon-carbon rigid decelerator p 2330 N92-23831
Strength and deformation behaviour of Kevlar and carbon composite sandwich structures for space applications p 2332 N92-23840
Optimal exciter placement and force vector tuning required for experimental modal analysis
p 2333 N92-23847
SPACECREWS
Center for Cell Research, Pennsylvania State University p 2314 N92-23653
SPACELAB
Microgravity acceleration measurement and environment characterization science (17-IML-1)
p 2363 N92-23642
SPACELAB PAYLOADS
First International Microgravity Laboratory experiment descriptions
[NASA-TM-4353] p 2356 N92-23600
Genetic and molecular dosimetry of HZE radiation (7-IML-1) p 2357 N92-23603
Embryogenesis and organogenesis of Carausius morosus under space flight conditions (7-IML-1)
p 2358 N92-23610
Dosimetric mapping inside biorack (7-IML-1)
p 2358 N92-23611
Growth and sporulation of Bacillus subtilis under microgravity (7-IML-1) p 2358 N92-23612
Friend leukemia virus transformed cells exposed to microgravity in the presence of DMSO (7-IML-1)
p 2358 N92-23613
Proliferation and performance of hybridoma cells in microgravity (7-IML-1) p 2358 N92-23614
Dynamic cell culture system (7-IML-1)
p 2359 N92-23615
Growth, differentiation and development of Arabidopsis thaliana under microgravity conditions (7-IML-1)
p 2359 N92-23616
Transmission of gravistimulus in the statocyte of the lentil root (7-IML-1) p 2359 N92-23617
Gravity related behavior of the acellular slime mold Physarum polycephalum (7-IML-1) p 2359 N92-23618
Studies on penetration of antibiotic in bacterial cells in space conditions (7-IML-1) p 2359 N92-23619
Energy expenditure in space flight (doubly labelled water method) (8-IML-1) p 2359 N92-23620
SPALLATION
Gamma radiation survey of the LDEF spacecraft
p 2460 N92-23293
The interactions of atmospheric cosmogenic radionuclides with spacecraft surfaces
p 2461 N92-23294
SPATIAL RESOLUTION
Study of MOS-1 MESSR data for variability of the branch (Warm Streamer) from warm eddy and for fishing ground
p 2398 N92-23477
High resolution studies of NGC 1275 and the galactic center p 2455 N92-23675
SPECIFIC IMPULSE
Analysis of solar and microwave thermal propulsion systems p 2337 N92-23694
SPECIFICATIONS
Knowledge-based approach for generating target system specifications from a domain model
p 2428 N92-23371
SPECKLE INTERFEROMETRY
On the limiting astrometric accuracy of binary star speckle interferometry p 2457 N92-23696
SPECTRA
Achieving spectrum conservation for the minimum-span and minimum-order frequency assignment problems
[NASA-TM-105649] p 2322 N92-23187
SPECTRAL RECONNAISSANCE
The imaging spectrometer p 2393 N92-23387
SPECTRAL RESOLUTION
High resolution studies of NGC 1275 and the galactic center p 2455 N92-23675
On the limiting astrometric accuracy of binary star speckle interferometry p 2457 N92-23696
SPECTRAL SIGNATURES
Improved image classification with neural networks by fusing multispectral signatures with topological data
p 2402 N92-23368
SPECTROGRAPHS
Testing the solar paradigm for chromospheric activity in RS CVN binaries: Moderate resolution spectroscopy of solar active regions p 2459 N92-23171
A simple unfold method for Rutherford-scattering, intense ion-beam spectrographs
[DE92-008678] p 2445 N92-23749
SPECTROMETERS
X ray analysis spectrometer
[DE92-615124] p 2378 N92-23219
Recent results on K(omega) and (pi)(pi) systems from LASS
[DE92-007389] p 2436 N92-23327
On board data formatting p 2394 N92-23394
SPECTROPHOTOMETRY
An analysis of the WN shell nebula NGC 6888 using CCD imagery and spectrophotometry
p 2455 N92-24002
SPECTROSCOPIC ANALYSIS
The interstellar gas experiment p 2459 N92-23325
Analysis of forward and inverse problems in chemical dynamics and spectroscopy
[DE92-007732] p 2347 N92-23443
Quantification of surface functional groups of carbon fibers by x ray photoelectron spectroscopy
p 2343 N92-23946
SPECTROSCOPY
Testing and analyses of electrochemical cells using frequency response
[NASA-TM-103580] p 2369 N92-23437
Analysis of forward and inverse problems in chemical dynamics and spectroscopy
[DE92-007732] p 2347 N92-23443
Semiempirical studies of atomic structure
[DE92-008143] p 2437 N92-23448
Replacement of hydrogen peroxide cleaning with oxygen plasma
[DE92-009020] p 2445 N92-23905
SPECTRUM ANALYSIS
Profiling and mapping of advanced materials using spatially resolved Raman spectroscopy
[DE92-008304] p 2347 N92-23449
The meteorite record as clues to asteroidal regolith processes p 2457 N92-23770
Analysis of gravity and topography on Earth and Venus: Comparisons of lithospheric and sublithospheric processes p 2409 N92-23772
Acoustic prediction on satellite structure
p 2327 N92-23812
SPHERES
Electrostatic image solution for the interaction of two dielectric spheres
[PB92-142199] p 2364 N92-23138
Quasi-static image theory for the bi-isotropic (nonreciprocal chiral) sphere
[PB92-142371] p 2366 N92-23666
Electrostatic image theory for the dielectric sphere with an internal source
[PB92-142405] p 2366 N92-23667

Sphere packings centered at S-units of algebraic tori [PB92-136373] p 2434 N92-24061

SPHERICAL SHELLS
Electrostatic image theory for the layered dielectric sphere [PB92-142413] p 2367 N92-23668

SPHEROIDS
Three-dimensional cultured glioma cell lines [NASA-CASE-MSC-21843-1-NP] p 2413 N92-24052

SPINE
Back pain in astronauts (8-IML-1) p 2360 N92-23622

SPIRAL GALAXIES
Annual progress report [NASA-CR-190197] p 2454 N92-23428

SPONTANEOUS EMISSION
Strongly coupled cavity QED p 2442 N92-23999

SPORES
Growth and sporulation of Bacillus subtilis under microgravity (7-IML-1) p 2358 N92-23612

SPRAYED COATINGS
Investigation of plasma-sprayed laminates for high-temperature melting operations [DE92-008416] p 2353 N92-24006

SPREADING
Measurement of surface cleanliness by area-of-spread [DE92-007265] p 2348 N92-23586

SPUTTERING
Deposition of adherent Ag-Ti duplex films on ceramics in a multiple-cathode sputter deposition system [NASA-TM-105586] p 2311 N92-23225
Transport calculations of chemically sputtered carbon near a plasma divertor surface [DE92-009022] p 2445 N92-24021
Working gas pressure and flow effects on reactively sputtered molybdenum-oxide thin films [DE92-008624] p 2450 N92-24069

STABILITY
An XPS study of the stability of Fomblin Z25 on the native oxide of aluminum --- x ray photoelectron spectroscopy [NASA-TM-105594] p 2353 N92-23185

STAINING
Organic contamination of LDEF p 2339 N92-23290

STAINLESS STEELS
Liquid/supercritical fluid carbon dioxide cleaning of stainless steel components [DE92-006947] p 2348 N92-23572

STANDARDIZATION
International workshop on the airborne measurement of wind, turbulence, and position [PB92-139963] p 2410 N92-23587
The need for standards in design automation [P-1-1] p 2419 N92-23852
Group technology, RCO: Rough-Cut Optimizer. The key to integration of plant operations [REPT-1.1.6] p 2420 N92-23857
Change in test-technology [REPT-1.2.8] p 2421 N92-23867

STANDARDS
From IGES to STEP [REPT-3.1.6] p 2423 N92-23881

STAR FORMATION
The throes of star formation: A study of the Orion-KL and DR21(OH) molecular clouds p 2457 N92-23698
Nuclear winds in active galaxies p 2457 N92-23716

STATE ESTIMATION
Application of optical distributed sensing and computation to control of large space structures [NASA-CR-190293] p 2442 N92-23567

STATIC DEFORMATION
Static multipole deformations in nuclei [DE92-008250] p 2436 N92-23277

STATIC LOADS
On development of automated static loading system for spacecraft structures p 2326 N92-23801
Investigations of the dynamic behaviour of compounds under preloading p 2332 N92-23842

STATIC MODELS
An algorithmic approach for fault-monitoring of electrical actuation system for all electric aircraft [NAL-PD-AL-9111] p 2368 N92-23246

STATIC PRESSURE
Development of wall pressure measuring apparatus for an existing transonic wind tunnel test section [NAL-TM-565] p 2312 N92-23778

STATIC TESTS
The statics, dynamics, and control of the elasticarm: A continuous beam manipulator p 2383 N92-23691

STATISTICAL ANALYSIS
Nonequilibrium statistical operator in hot-electron transport theory [DE92-615517] p 2446 N92-23260
Data exploration systems for databases p 2429 N92-23374
Data quality evaluation results MOS-1 verification program p 2400 N92-23491
Estimation of regional evapotranspiration with MOS-1 VTIR data p 2401 N92-23492
Analysis of time series with missing values p 2434 N92-23777
Development and application of substructuring techniques for understanding and controlling residual vibrations (microgravity aspects) p 2330 N92-23827
Formal methods for the evaluation of corporate CAD/CAM utilization [REPT-1.1.1] p 2419 N92-23853
Statistical optimization of integrated circuits in order to reduce the sensitivity to variations in process parameters and environmental conditions [REPT-1.3.6] p 2422 N92-23872
Multifracture of ceramic composites [DE92-009630] p 2355 N92-23897

STATISTICAL DISTRIBUTIONS
Sheaves of Schwartz distributions [DE92-615217] p 2432 N92-23331
Coupled load analysis: Scatter related to model uncertainties p 2324 N92-23787
The statistical analysis of data from normal distributions, with particular reference to small samples [ESDU-91041] p 2434 N92-24008

STATISTICAL MECHANICS
Numerical and physical modelling of bubbly flow phenomena [DE92-008642] p 2376 N92-24062

STATISTICAL TESTS
Density of the F-statistic in the linear model with arbitrarily normal distributed errors [PB92-128792] p 2434 N92-23731
Method for evaluating non-consistent data using two statistical criteria [DE92-615195] p 2454 N92-23742
Exact probabilistic testability measures for multi-output circuits [REPT-1.2.7] p 2421 N92-23866
Statistical process control system for VLSI fabrication [REPT-1.3.4] p 2422 N92-23871

STATORS
Computations of unsteady multistage turbomachinery flows p 2311 N92-23671

STEADY FLOW
Aerodynamic rectifier for pulsed combustors [PB92-142587] p 2348 N92-23657

STEADY STATE
Use of control theory for analyzing stability of states in continuum thermodynamics [PB92-136571] p 2451 N92-23136

STEELS
Oil lubricated and water lubricated pin-on-disc wear tests with engineering ceramics [PB92-136563] p 2380 N92-23152
Spectral effects in radiation embrittlement [DE92-007837] p 2447 N92-23444

STELLAR ENVELOPES
High resolution studies of NGC 1275 and the galactic center p 2455 N92-23675

STELLAR EVOLUTION
JPRS report: Science and technology. Central Eurasia: Space [JPRS-USP-92-002] p 2314 N92-23705
Type Ib supernovae and a new radiation hydrodynamics code p 2458 N92-24017

STELLAR LUMINOSITY
Search for cosmological dust p 2456 N92-23164
The throes of star formation: A study of the Orion-KL and DR21(OH) molecular clouds p 2457 N92-23698

STELLAR MASS
On the limiting astrometric accuracy of binary star speckle interferometry p 2457 N92-23696
An analysis of the WN shell nebula NGC 6888 using CCD imagery and spectrophotometry p 2455 N92-24002
Type Ib supernovae and a new radiation hydrodynamics code p 2458 N92-24017

STELLAR MASS ACCRETION
TeV gamma ray emission from accreting binary pulsars p 2460 N92-23736

STELLAR MODELS
Type Ib supernovae and a new radiation hydrodynamics code p 2458 N92-24017

STELLAR ROTATION
Observing millisecond and binary pulsars p 2455 N92-24001

STELLAR SPECTRA
Search for cosmological dust p 2456 N92-23164
Gamma rays from SN1987A with the UCR double-Compton telescope p 2455 N92-23695
On the limiting astrometric accuracy of binary star speckle interferometry p 2457 N92-23696
Strongly coupled cavity QED p 2442 N92-23999
Observing millisecond and binary pulsars p 2455 N92-24001
An analysis of the WN shell nebula NGC 6888 using CCD imagery and spectrophotometry p 2455 N92-24002
Line profile asymmetries in chromospherically active stars p 2458 N92-24015

STELLAR WINDS
Nuclear winds in active galaxies p 2457 N92-23716
An analysis of the WN shell nebula NGC 6888 using CCD imagery and spectrophotometry p 2455 N92-24002

STIFFNESS
Aging of polymer matrix composites at elevated temperatures p 2328 N92-23817

STIFFNESS MATRIX
The free and forced vibrations of structures using the finite dynamic element method [NASA-CR-190184] p 2388 N92-23427

STIMULATION
Transmission of gravistimulus in the statocyte of the lentil root (7-IML-1) p 2359 N92-23617

STOCHASTIC PROCESSES
Probabilistic Structural Analysis Methods (PSAM) for select space propulsion system components, part 2 [NASA-CR-187200] p 2388 N92-23426
Stochastic games with average payoff criterion [PB92-148634] p 2434 N92-23505
Optimizing flow rates in a queueing network with side constraints [PB92-149996] p 2430 N92-23508

STORAGE RINGS (PARTICLE ACCELERATORS)
Report from orbit sub-group of task force for MR synchrotron radiation project [DE92-751024] p 2441 N92-23713

STRAIN DISTRIBUTION
Analysis of delamination related fracture processes in composites [NASA-CR-190226] p 2340 N92-23532
Transverse deformation of unidirectional fiber-reinforced metal matrix composites p 2345 N92-24013

STRAIN ENERGY RELEASE RATE
Characterization of interlaminar mode 1 and mode 2 fracture in CFRP laminates p 2325 N92-23794

STRAIN RATE
Matrix dominated stress/strain behavior in polymeric composites: Effects of hold time, nonlinearity and rate dependency [NASA-TM-107595] p 2340 N92-23434

STRAITS
CODAR in the Straits of Florida [PB92-129964] p 2412 N92-23732

STRESS (PHYSIOLOGY)
Stress effects of human-computer interactions [PB92-136001] p 2415 N92-23513

STRESS ANALYSIS
Influence of engineered interfaces on residual stresses and mechanical response in metal matrix composites [NASA-TM-105438] p 2340 N92-23195
Simultaneous stress and flutter optimization for the wing of a transport aircraft equipped with four engines p 2308 N92-23238
Contact stresses in meshing spur gear teeth: Use of an incremental finite element procedure [NASA-TM-105388] p 2382 N92-23536
Renormalization group analysis of the Reynolds stress transport equation [NASA-TM-105588] p 2374 N92-23542
Method and apparatus for determination of material residual stress [NASA-CASE-GSC-13451-1] p 2388 N92-23549
Development of fatigue damage mechanics for application to the design of damage-tolerant composite components p 2324 N92-23793
Fatigue analysis under random stresses p 2325 N92-23795
On the modelling of a deployable telescope elastic beam-type element for on-orbit multibody simulations p 2329 N92-23826

STRESS CYCLES
Mechanical testing on a composite flexible structure p 2331 N92-23834

STRESS DISTRIBUTION
Boundary element analysis of fracture mechanics problems p 2387 N92-23125
Singularities in optimal structural design [NASA-TM-4365] p 2388 N92-23527
Analysis of delamination related fracture processes in composites [NASA-CR-190226] p 2340 N92-23532
Crack path prediction near an elliptical inhomogeneity p 2389 N92-23688
Influence of the substrate on the solar cells interconnector: Stress distribution and fatigue life prediction p 2326 N92-23803

Transverse deformation of unidirectional fiber-reinforced metal matrix composites p 2345 N92-24013

STRESS RELAXATION

Matrix dominated stress/strain behavior in polymeric composites: Effects of hold time, nonlinearity and rate dependency
[NASA-TM-107595] p 2340 N92-23434

Mechanical properties of glass bead filled ductile epoxy composites p 2344 N92-23947

STRESS WAVES

Method for advanced material characterization by laser induced eddy current imaging
[NASA-CASE-GSC-13386-1] p 2386 N92-23376

STRESS-STRAIN RELATIONSHIPS

Matrix dominated stress/strain behavior in polymeric composites: Effects of hold time, nonlinearity and rate dependency
[NASA-TM-107595] p 2340 N92-23434

Materials for liquid propellant engines p 2320 N92-23764

Buckling and failure of thin elliptical delaminations in composites p 2331 N92-23835

STRESSES

The effect of processing on strength of Nicalon fibers in Nicalon fiber-SiC matrix composites
[DE92-006978] p 2340 N92-23256

Stretched skin concept for the entry aerodynamic decelerator system of planetary probes p 2331 N92-23836

STRING THEORY

Research in high energy physics
[DE92-007966] p 2441 N92-23500

STRIP TRANSMISSION LINES

Nonplanar linearly tapered slot antenna with balanced microstrip feed
[NASA-TM-105647] p 2370 N92-23535

STRONGLY COUPLED PLASMAS

Ion Microtomography (IMT) and Particle-Induced X ray Emission (PIXE) analysis direct drive of Inertial Confinement Fusion (ICF) targets
[DE92-008614] p 2446 N92-24067

STRUCTURAL ANALYSIS

Progressive fracture of polymer matrix composite structures: A new approach
[NASA-TM-105574] p 2339 N92-23194

Evaluation of MHOST analysis capabilities for a plate element --- finite element modeling
[NASA-TM-105387] p 2387 N92-23196

Integrated Design Analysis and Optimisation of Aircraft Structures
[AGARD-R-784] p 2306 N92-23227

The structural optimization system OPTSYS: Current status and applications p 2307 N92-23232

Application of an automated multidisciplinary analysis and optimisation system to the design of aircraft structures p 2307 N92-23233

Design of a fighter aircraft vertical tail enhanced buffet environment survivability p 2307 N92-23235

First approach to an integrated fin design p 2308 N92-23236

A fin optimisation study p 2308 N92-23237

Structural optimization of aircraft practice and trends p 2308 N92-23239

Coupled multi-disciplinary simulation of composite engine structures in propulsion environment
[NASA-TM-105575] p 2388 N92-23267

Probabilistic Structural Analysis Methods (PSAM) for select space propulsion system components, part 2
[NASA-CR-187200] p 2388 N92-23426

Singularities in optimal structural design
[NASA-TM-4365] p 2388 N92-23527

Nonlinear finite element analysis of space frames
[PB92-142447] p 2388 N92-23664

STRUCTURAL DESIGN

Multidisciplinary optimization studies using ASTROS p 2307 N92-23234

Design of a fighter aircraft vertical tail enhanced buffet environment survivability p 2307 N92-23235

First approach to an integrated fin design p 2308 N92-23236

Simultaneous stress and flutter optimization for the wing of a transport aircraft equipped with four engines p 2308 N92-23238

Singularities in optimal structural design
[NASA-TM-4365] p 2388 N92-23527

Spacecraft Structures and Mechanical Testing, volume 1
[ESA-SP-321-VOL-1] p 2322 N92-23780

Development of Japanese experiment module p 2323 N92-23781

Structural assessment of the Space Station Freedom's pressurized elements p 2323 N92-23783

Brief history of the development of the EPS-structure p 2321 N92-23810

Conceptional design to heat-resistant airframe of HOPE p 2328 N92-23820

Design challenges for the National Aero-Space Plane p 2310 N92-23822

Design parameter update of dynamic mathematical models in presence of test noise and mode pairing problems p 2333 N92-23850

STRUCTURAL FAILURE

The response surface method: An efficient tool to determine the failure probability of large structural systems p 2328 N92-23816

STRUCTURAL RELIABILITY

Probabilistic Structural Analysis Methods (PSAM) for select space propulsion system components, part 2
[NASA-CR-187200] p 2388 N92-23426

STRUCTURAL STRAIN

The effect of fatigue-induced damage on the mechanical properties of CFRP composites p 2339 N92-23157

STRUCTURAL VIBRATION

Influence of microvibrations on spacecraft performances p 2329 N92-23825

Development and application of substructuring techniques for understanding and controlling residual vibrations (microgravity aspects) p 2330 N92-23827

Minimization of vibrations by broadband sensitivity approach p 2330 N92-23828

STRUCTURAL WEIGHT

Protection of spacecraft against meteroid/orbital debris impacts p 2323 N92-23786

STUDENTS

Summer graduate research program for interns in science and engineering
[NASA-TM-107813] p 2470 N92-23958

Using microsoft excel applications in the graduate intern program at Goddard Space Flight Center p 2425 N92-23959

Fast aurora zone analysis p 2409 N92-23960

SUBDUCTION (GEOLOGY)

The interpretation of crustal dynamics data in terms of plate interactions and active tectonics of the Anatolian plate and surrounding regions in the Middle East
[NASA-CR-188466] p 2408 N92-23558

SUBGIANT STARS

Testing the solar paradigm for chromospheric activity in RS CVN binaries: Moderate resolution spectroscopy of solar active regions p 2459 N92-23171

SUBORBITAL FLIGHT

Suborbital missions: The Joust p 2313 N92-23644

SUBSONIC FLOW

Long time behavior of unsteady flow computations
[NASA-TM-105584] p 2374 N92-23565

Adaptive active flutter suppression of wings in subsonic and transonic flight regimes p 2310 N92-24010

Investigation of solution operators for the three dimensional unsteady Euler equations p 2376 N92-24018

SUBSTRATES

Properties of large area ErBa2Cu3O(7-x) thin films deposited by ionized cluster beams p 2365 N92-23414

Dependence of the critical temperature of laser-ablated YBa2Cu3O(7-delta) thin films on LaAlO3 substrate growth technique p 2365 N92-23415

Temperature-dependent evolution of chemisorbed digermane in Ge thin film growth
[DE92-008098] p 2447 N92-23447

Influence of the substrate on the solar cells interconnector: Stress distribution and fatigue life prediction p 2326 N92-23803

SULFATES

A study of solution crystal growth in LOW-g (2-IML-1) p 2361 N92-23630

SUMMER

Energy cycles in the summer tropical atmosphere over the North Atlantic Ocean p 2409 N92-23150

Radar observations and dynamics of the polar summer mesosphere p 2408 N92-23702

Summer graduate research program for interns in science and engineering
[NASA-TM-107813] p 2470 N92-23958

Using microsoft excel applications in the graduate intern program at Goddard Space Flight Center p 2425 N92-23959

Fast aurora zone analysis p 2409 N92-23960

SUN

Solar-geophysical data Number 564, August 1991. Part 2 (comprehensive reports): Data for February 1991 and miscellaneous
[PB92-111699] p 2459 N92-23701

Solar-geophysical data Number 566, October 1991. Part 2 (comprehensive reports): Data for April 1991 and miscellaneous
[PB92-129402] p 2460 N92-23993

SUPERCOMPUTERS

The 7th INS Scientific Computational Programs
[DE92-750967] p 2417 N92-23266

SUPERCONDUCTING FILMS

Microwave response of high transition temperature superconducting thin films p 2365 N92-23413

Properties of large area ErBa2Cu3O(7-x) thin films deposited by ionized cluster beams p 2365 N92-23414

Dependence of the critical temperature of laser-ablated YBa2Cu3O(7-delta) thin films on LaAlO3 substrate growth technique p 2365 N92-23415

SUPERCONDUCTING SUPER COLLIDER

A switched capacitor array based system for high-speed calorimetry
[DE92-008288] p 2378 N92-23278

High energy physics: Report of research accomplishments and future goals, FY 1992
[DE92-008543] p 2441 N92-23576

SUPERCONDUCTIVITY

On the electronegativity of the high-T(sub c) oxide superconductor
[DE92-617537] p 2447 N92-23273

Numerical study of the magnetic ordering and superconducting state of high-temperature superconductor p 2449 N92-23776

SUPERCONDUCTORS

Superconducting materials
[DE92-007748] p 2446 N92-23205

Magnetic fluctuations and normal state properties of the t-J model at finite dopings
[DE92-617538] p 2447 N92-23452

Magnetic flux motion and flux pinning superconductors
[DE92-008243] p 2449 N92-23892

Steady State Advanced Tokamak (SSAT): The mission and the machine
[DE92-008983] p 2445 N92-24020

SUPERFLUIDITY

Ultrasonic investigation of (3)He-A vortices in low magnetic fields
[PB92-142256] p 2435 N92-23665

SUPERGRAVITY

Semirigid construction of topological supergravities
[DE92-008772] p 2451 N92-24040

SUPERLATTICES

Fermi level effects on dislocation formation in InAs(1-x)Sb(x) grown by MOCVD
[DE92-008332] p 2450 N92-24034

SUPERNOVA 1987A

Gamma rays from SN1987A with the UCR double-Compton telescope p 2455 N92-23695

SUPERNOVAE

Type Ib supernovae and a new radiation hydrodynamics code p 2458 N92-24017

SUPERSONIC BOUNDARY LAYERS

High-Order Polynomial Expansions (HOPE) for flux-vector splitting p 2304 N92-23353

SUPERSONIC COMBUSTION RAMJET ENGINES

High temperature dynamic engine seal technology development
[NASA-TM-105641] p 2381 N92-23435

SUPERSONIC FLOW

Turbulence modeling in supersonic combusting flows p 2302 N92-23342

Development of a new flux splitting scheme p 2303 N92-23352

Three-dimensional calculations of supersonic reacting flows using an LU scheme p 2304 N92-23354

Development of wall pressure measuring apparatus for an existing transonic wind tunnel test section
[NAL-TM-565] p 2312 N92-23778

Investigation of solution operators for the three dimensional unsteady Euler equations p 2376 N92-24018

SUPERSONIC INLETS

Interactive solution-adaptive grid generation procedure
[NASA-TM-105432] p 2305 N92-23563

SUPERSONIC JET FLOW

The flip-flop nozzle extended to supersonic flows
[NASA-TM-105570] p 2304 N92-23269

SUPERSONIC NOZZLES

Progress of simulations for reacting shear layers p 2302 N92-23344

SUPERSONIC SPEED

The flip-flop nozzle extended to supersonic flows
[NASA-TM-105570] p 2304 N92-23269

Effects of turbine cooling assumptions on performance and sizing of high-speed civil transport
[NASA-TM-105610] p 2311 N92-23537

Normal force of low aspect ratio wing-body combinations up to high angles of attack at supersonic speeds
[ESDU-91042] p 2309 N92-24009

SUPERSONIC TEST APPARATUS

Development of wall pressure measuring apparatus for an existing transonic wind tunnel test section
[NAL-TM-565] p 2312 N92-23778

SUPERSONIC TRANSPORTS
Application of multidisciplinary optimization methods to the design of a supersonic transport p 2307 N92-23230
SUPERSYMMETRY
Semirigid construction of topological supergravities [DE92-008772] p 2451 N92-24040
SUPPORTS
High reliability robot friendly ORU interface [NASA-CASE-GSC-13360-1] p 2381 N92-23377
SURFACE FINISHING
Acoustic emission as a process monitor for diamond machining of metal optical components [DE92-008037] p 2363 N92-23899
SURFACE PROPERTIES
Quantification of contaminants associated with LDEF p 2349 N92-23288
Wideband finite difference time domain implementation of surface impedance boundary conditions for good conductors [NASA-CR-190098] p 2366 N92-23528
Measurement of surface cleanliness by area-of-spread [DE92-007265] p 2348 N92-23586
Surface structure and analysis with scanning tunneling microscopy and electron tunneling spectroscopy [DE92-007747] p 2448 N92-23721
Quantification of surface functional groups of carbon fibers by x ray photoelectron spectroscopy p 2343 N92-23946
SURFACE REACTIONS
The interactions of atmospheric cosmogenic radionuclides with spacecraft surfaces p 2461 N92-23294
Potential energy surfaces and reaction dynamics of polyatomic molecules [DE92-008314] p 2437 N92-23450
SURFACE TEMPERATURE
Clouds, surface temperature, and the tropical and subtropical radiation budget p 2410 N92-23431
An attempt to derive land surface temperatures from MOS-1 VTIR data using split-window channel computation technique p 2401 N92-23493
SURFACE WATER
National acid precipitation assessment program: 1990 integrated assessment report [PB92-100346] p 2406 N92-23593
SURFACE WAVES
Applications of boundary integral methods to the study of steep free surface waves p 2372 N92-23149
SURVEYS
Low thrust propulsion literature survey [NASA-CR-190179] p 2337 N92-23151
Dynamic positioning by GPS p 2306 N92-23729
SUSPENSION SYSTEMS (VEHICLES)
The structural optimization system OPTSYS: Current status and applications p 2307 N92-23232
SWITCHES
Versatile bistable optical switches and latching optical logic using integrated photothyristors and surface-emitting lasers [DE92-008677] p 2442 N92-23748
Electrical and optical properties of high gain GaAs switches [DE92-008668] p 2371 N92-23983
SWITCHING CIRCUITS
A switched capacitor array based system for high-speed calorimetry [DE92-008288] p 2378 N92-23278
Using range analysis to support hierarchical test pattern generation [REPT-1.2.5] p 2421 N92-23864
Exact probabilistic testability measures for multi-output circuits [REPT-1.2.7] p 2421 N92-23866
SYMBOLS
Expert systems: A mapping between symbol susceptible tasks and software tools p 2454 N92-24016
SYNCHRONISM
A verified design of a fault-tolerant clock synchronization circuit: Preliminary investigations [NASA-TM-107568] p 2416 N92-23559
SYNCHROTRON RADIATION
Applications of x ray synchrotron radiation techniques to the study of dispersed electrocatalysts in high area materials [DE92-007458] p 2346 N92-23199
Report from orbit sub-group of task force for MR synchrotron radiation project [DE92-751024] p 2441 N92-23713
SYNCHROTRONS
Thresholds of longitudinal instability of bunched beam in the presence of dominant inductive impedance [DE92-617992] p 2436 N92-23274
Research in high energy physics [DE92-007966] p 2441 N92-23500
General P-T fit construction for He, N2, Ar, H2 and Ne VPT used at Fermilab [DE92-008851] p 2433 N92-23579
SYNTHESIS (CHEMISTRY)
The case for exotic beams at the Holifield Heavy Ion Research Facility [DE92-008003] p 2441 N92-23445
Reductive coupling of carbon monoxide to C2 products [DE92-007529] p 2347 N92-23499
Advanced Materials Center, Battelle p 2314 N92-23652
SYNTHETIC APERTURE RADAR
Euromar-Seastars: Summary p 2392 N92-23380
The imaging radar system p 2393 N92-23391
On board data formatting p 2394 N92-23394
Real-time radar processor p 2394 N92-23396
SYNTHETIC FIBERS
Crystallization behavior of poly(phenylene sulphide) p 2342 N92-23940
SYSTEM EFFECTIVENESS
Evaluation of the sensor effectiveness p 2395 N92-23404
SYSTEMS ANALYSIS
A system approach to aircraft optimization p 2306 N92-23228
Promotion of industrial technologies on the global environment [DE92-769374] p 2406 N92-23733
Expert systems: A mapping between symbol susceptible tasks and software tools p 2454 N92-24016
SYSTEMS ENGINEERING
A system approach to aircraft optimization p 2306 N92-23228
Evaluating model accuracy for model-based reasoning p 2427 N92-23362
The achievement of spacecraft autonomy through the thematic application of multiple cooperating intelligent agents p 2427 N92-23364
Sensor compatibility/optimal sensor combinations p 2395 N92-23403
Steady State Advanced Tokamak (SSAT): The mission and the machine [DE92-008983] p 2445 N92-24020
SYSTEMS INTEGRATION
A system approach to aircraft optimization p 2306 N92-23228
Application of multidisciplinary optimization methods to the design of a supersonic transport p 2307 N92-23230
Application of an automated multidisciplinary analysis and optimisation system to the design of aircraft structures p 2307 N92-23233
First approach to an integrated fin design p 2308 N92-23236
Structural optimization of aircraft practice and trends p 2308 N92-23239
Preconsiderations on aircraft integration p 2395 N92-23402
Flexible Design Environment (FDE) for operation systems design [REPT-2.3.5] p 2423 N92-23878
SYSTEMS MANAGEMENT
CIM: The future technology [REPT-3.3.1] p 2424 N92-23885
SYSTEMS SIMULATION
Simulation of Space Station loads with active control systems p 2329 N92-23824
SYSTEMS STABILITY
Thresholds of longitudinal instability of bunched beam in the presence of dominant inductive impedance [DE92-617992] p 2436 N92-23274

T

TABLES (DATA)
Solar-geophysical data Number 564, August 1991. Part 2 (comprehensive reports): Data for February 1991 and miscellaneous [PB92-111699] p 2459 N92-23701
TAIL ASSEMBLIES
Design of a fighter aircraft vertical tail enhanced buffet environment survivability p 2307 N92-23235
TAKEOFF
Aircraft accident report: Runway collision of USAir Flight 1493, Boeing 737 and Skywest Flight 5569 Fairchild Metroliner, Los Angeles International Airport, Los Angeles, CA, February 1, 1991 [PB91-910409] p 2305 N92-23596
Aircraft accident report: Ryan International Airlines DC-9-15, N565PC, loss of control on takeoff, Cleveland-Hopkins International Airport, Cleveland, Ohio, February 17, 1991 [PB91-910410] p 2305 N92-23597
TANKS (CONTAINERS)
On the analysis of liquid filled free-free tanks p 2332 N92-23843
Fluid-structure interaction problems: Development of special processors p 2332 N92-23845
A symmetric coupling between BEM and FEM for dynamical analysis of spacecraft p 2332 N92-23846
TARGETS
Fast wave current drive antenna performance on D3-D [DE92-008052] p 2444 N92-23446
TASK PLANNING (ROBOTICS)
Dynamic analysis of planar manipulation tasks [DE91-019060] p 2430 N92-23458
TASKS
Expert systems: A mapping between symbol susceptible tasks and software tools p 2454 N92-24016
TDR SATELLITES
Mathematical analysis techniques for modeling the space network activities p 2434 N92-23964
TEARING MODES (PLASMAS)
Magnetic reconnection in magnetotail and solar plasmas p 2457 N92-24000
TECHNOLOGIES
Symposium on Marketing for Technological Products [MBB-UE-0014-90-PUB] p 2452 N92-23928
Market directed thinking in a technological operation p 2452 N92-23929
Marketing as a necessary condition for the successful development and commercialization of technological products p 2452 N92-23931
TECHNOLOGY ASSESSMENT
Limiting net greenhouse gas emissions in the United States, volume 1 [DE92-007593] p 2405 N92-23204
Blazing the trailway: Nuclear electric propulsion and its technology program plans [NASA-TM-105605] p 2337 N92-23252
High temperature dynamic engine seal technology development [NASA-TM-105641] p 2381 N92-23435
Launcher Propulsion Towards the Year 2010 [ESA-SP-327] p 2318 N92-23750
Rocket propulsion for NASA's Earth to orbit launchers p 2319 N92-23754
Development status of the Ariane 5 solid propellant engine p 2319 N92-23755
What future for hybrid rocket propulsion? p 2321 N92-23768
From Earth to orbit --- assessment of transportation options [NASA-CR-190216] p 2321 N92-23980
TECHNOLOGY UTILIZATION
Center for Space Power, Texas A and M University p 2313 N92-23651
TECTONICS
The interpretation of crustal dynamics data in terms of plate interactions and active tectonics of the Anatolian plate and surrounding regions in the Middle East [NASA-CR-188466] p 2408 N92-23558
TEFLON (TRADEMARK)
M and D SIG progress report: Laboratory simulations of LDEF impact features p 2336 N92-23323
TELECOMMUNICATION
Writing a simulation of a communications network using SIMSCRIPT/DISS [REPT-2.3.6] p 2423 N92-23879
Modifications for a communication interface board p 2368 N92-23963
TELECONFERENCING
Variable bit rate video coding [PB92-134279] p 2367 N92-23676
TELEMETRY
An architecture for the development of real-time fault diagnosis systems using model-based reasoning p 2427 N92-23363
TELESCOPES
Testing the solar paradigm for chromospheric activity in RS CVN binaries: Moderate resolution spectroscopy of solar active regions p 2459 N92-23171
The use of high temperature superconductors to levitate lunar telescope p 2456 N92-23962
TELLURIUM ALLOYS
TeV gamma ray emission from accreting binary pulsars p 2460 N92-23736
TEMPERATURE COMPENSATION
Verification of MESSR and VTIR, and time variation of MSR performance p 2397 N92-23471
Higher order temperature compensation of bandgap voltage references (I) [PB92-142306] p 2370 N92-23497
TEMPERATURE DEPENDENCE
Kinetic measurements on elementary fossil fuel combustion reactions over wide temperatures ranges [DE92-007535] p 2347 N92-23221
The LDEF ultra heavy cosmic ray experiment p 2461 N92-23306

Temperature-dependent evolution of chemisorbed digermane in Ge thin film growth
[DE92-008098] p 2447 N92-23447
Higher order temperature compensation of bandgap voltage references (i)
[PB92-142306] p 2370 N92-23497
General P-T fit construction for He, N2, Ar, H2 and Ne VPT used at Fermilab
[DE92-008851] p 2433 N92-23579
VITRIMAT2: A modified model of vitrinite maturation and reflectance
[DE92-008987] p 2348 N92-23904

TEMPERATURE DISTRIBUTION
Use of the Long Duration Exposure Facility's thermal measurement system for the verification of thermal models p 2336 N92-23284
Monitoring of ocean conditions by using MOS-1 data p 2398 N92-23476
Observation of lined-up cumulus rows under the winter monsoon situation using MOS-1 and radar data p 2399 N92-23483

TEMPERATURE EFFECTS
Influence of engineered interfaces on residual stresses and mechanical response in metal matrix composites
[NASA-TM-105438] p 2340 N92-23195
The Critical Point Facility (CPF) p 2362 N92-23637
High-temperature deformation behavior of single crystalline A15-type intermetallic compounds p 2352 N92-23718
Hardening in AlN induced by point defects
[DE92-007717] p 2352 N92-23720
Crystallization behavior of poly(phenylene sulphide) p 2342 N92-23940

TEMPERATURE GRADIENTS
Experiments and modeling p 2301 N92-23339
Urban temperature bias as determined by polar orbiting satellite data p 2402 N92-23724

TEMPERATURE MEASUREMENT
Use of the Long Duration Exposure Facility's thermal measurement system for the verification of thermal models p 2336 N92-23284
Sub-Kelvin resistance thermometer
[NASA-CASE-GSC-13406-1] p 2378 N92-23460
Functional precision of National Weather Service upper-air measurements using VIZ Manufacturing Co. B radiosonde (model 1492-520)
[PB92-137868] p 2410 N92-23494
Field evaluation of remote sensor measurements of wind, temperature, and moisture for ARM integrated sounding system research
[PB92-140714] p 2401 N92-23521
An optical study of grain formation: Casting and solidification technology (2-IML-1) p 2361 N92-23631
Fiber-optic Raman spectroscopy for cure monitoring of advanced polymer composites
[DE92-008619] p 2355 N92-24068

TEMPERATURE PROFILES
CRYOSTAT (18-IML-1) p 2362 N92-23636

TENSILE PROPERTIES
Application of the microbond technique: Characterization of carbon-epoxy interfaces p 2343 N92-23944

TENSILE STRENGTH
High strength composites evaluation
[DE92-007264] p 2340 N92-23585
Microstructure and mechanical properties of carbon fibres: Relationship with the fibre-matrix adhesion in a carbon-epoxy composite p 2341 N92-23935

TENSILE STRESS
Notched strength of composite materials p 2331 N92-23839

TERRADYNAMICS
Mission objectives and scientific rationale for the magnetometer mission p 2315 N92-23912

TERRAIN
Tabulations of propagation data over irregular terrain in the 75- to 8400-MHz frequency range. Part 5: Virginia
[PB92-137413] p 2364 N92-23180

TEST FACILITIES
Buckling of simply supported and clamped anisotropic plates under combined loads p 2326 N92-23804
A new test facility for measuring the coefficient of moisture expansion of advanced composite materials p 2326 N92-23807
Battery test facility hardware, software, and system operation
[DE92-008455] p 2372 N92-24063

TEST PATTERN GENERATORS
Using range analysis to support hierarchical test pattern generation
[REPT-1.2.5] p 2421 N92-23864

TESTS
Modelling and experimental verification of a water alleviation system for the NASP --- National Aerospace Plane
[NASA-TM-105661] p 2373 N92-23224
Research, Development, Test and Evaluation (R, D, T, and E) Programs (R-1), Department of Defense budget for fiscal year 1993
[PB92-127745] p 2451 N92-23247
Liquid hydrogen mass flow through a multiple orifice Joule-Thomson device
[NASA-TM-105583] p 2373 N92-23268
Testing and analyses of electrochemical cells using frequency response
[NASA-TM-103580] p 2369 N92-23437
An integrated test solution to address scan techniques
[REPT-1.2.3] p 2420 N92-23862
Battery test facility hardware, software, and system operation
[DE92-008455] p 2372 N92-24063
In situ particle size measurements using a two-color laser scattering technique
[DE92-008634] p 2380 N92-24070

TETHERED SATELLITES
Mechanical testing on a composite flexible structure p 2331 N92-23834

TETRAD THEORY
Rotating, radiating mass imbedded in a de Sitter universe p 2456 N92-23127

TEXTURES
Feature detection in satellite images using neural network technology p 2427 N92-23366

THEOREM PROVING
Experimental verification of a theory for the impact response of composite plates
[FFA-TN-1991-17] p 2339 N92-23167

THEORETICAL PHYSICS
Particle physics and cosmology
[DE92-008301] p 2456 N92-23153
High energy physics: Report of research accomplishments and future goals, FY 1992
[DE92-008543] p 2441 N92-23576
Theoretical nuclear reaction and structure studies using hyperons and photons
[DE92-008587] p 2437 N92-23577

THERMAL CONTROL COATINGS
Organic contamination of LDEF p 2339 N92-23290

THERMAL CYCLING TESTS
Effect of minor elements on corrosion behavior of Ni-Cr-W superalloys in HTGR helium
[DE92-751006] p 2352 N92-23712

THERMAL DIFFUSION
Critical fluid thermal equilibration experiment (19-IML-1) p 2363 N92-23640

THERMAL ENERGY
Comparison of analytical and numerical modelling approaches for sizing of seasonal storage solar heating systems
[PB92-141829] p 2403 N92-23592

THERMAL EXPANSION
Influence of engineered interfaces on residual stresses and mechanical response in metal matrix composites
[NASA-TM-105438] p 2340 N92-23195
Modeling of honeycomb core for sandwich CTE prediction p 2332 N92-23841

THERMAL INSULATION
M and D SIG progress report: Laboratory simulations of LDEF impact features p 2336 N92-23323
Preliminary micrometeoroid and debris effects on LDEF thermal control surfaces p 2336 N92-23324

THERMAL POLLUTION
Pulsed electron beam precharger
[DE92-008693] p 2439 N92-24031

THERMAL PROTECTION
The challenge of the Hermes TPS shingles p 2322 N92-23823
Beryllium-thermal protection technology p 2331 N92-23837
CNSR Rosetta: Earth return capsule p 2331 N92-23838

THERMAL RADIATION
Passive optical and IR sensors
[MBB-UH-HE512] p 2394 N92-23392

THERMAL RESISTANCE
Characterizing and testing a thermally isolating superconducting link for SAFIRE-like missions
[NASA-CR-190196] p 2369 N92-23430
Conceptional design to heat-resistant airframe of HOPE p 2328 N92-23820
Large thin composite thermostructural parts p 2329 N92-23821

THERMAL STABILITY
Production of metal powders by hydrogen stripping from loaded organic extractants
[PB92-136464] p 2350 N92-23178
Strength and deformation behaviour of Kevlar and carbon composite sandwich structures for space applications p 2332 N92-23840
Vinyl capped addition polyimides
[NASA-CASE-LEW-15027-2] p 2355 N92-24053

THERMAL STRESSES
Influence of engineered interfaces on residual stresses and mechanical response in metal matrix composites
[NASA-TM-105438] p 2340 N92-23195
Method for advanced material characterization by laser induced eddy current imaging
[NASA-CASE-GSC-13386-1] p 2386 N92-23376
Aging of polymer matrix composites at elevated temperatures p 2328 N92-23817
Mechanical properties of glass bead filled ductile epoxy composites p 2344 N92-23947

THERMOCLINES
Reconstructing the tropical Atlantic seasonal thermocline using planktonic foraminifera p 2412 N92-23769

THERMODYNAMIC EQUILIBRIUM
Critical fluid thermal equilibration experiment (19-IML-1) p 2363 N92-23640

THERMODYNAMICS
An observational study of the internal structure of air-mass thunderstorms p 2409 N92-23121
Use of control theory for analyzing stability of states in continuum thermodynamics
[PB92-136571] p 2451 N92-23136
Damage development in titanium metal matrix composites subjected to cyclic loading
[NASA-TM-107597] p 2340 N92-23433
Field evaluation of remote sensor measurements of wind, temperature, and moisture for ARM integrated sounding system research
[PB92-140714] p 2401 N92-23521
Mathematical model of a control valve
[PB92-141951] p 2383 N92-23710

THERMOELASTICITY
Direct conversion technology
[NASA-CR-190188] p 2403 N92-23569
Modeling of honeycomb core for sandwich CTE prediction p 2332 N92-23841
On the application of micromechanics to the prediction of macroscopic thermal residual stresses in short-fiber reinforced Polyetheretherketone (PEEK) p 2343 N92-23942

THERMOELECTRIC GENERATORS
Direct conversion technology
[NASA-CR-190188] p 2403 N92-23569

THERMOLUMINESCENCE
Dosimetric mapping inside biorack (7-IML-1) p 2358 N92-23611
Radiation monitoring container device (16-IML-1) p 2361 N92-23629

THERMOMETERS
General P-T fit construction for He, N2, Ar, H2 and Ne VPT used at Fermilab
[DE92-008851] p 2433 N92-23579

THERMONUCLEAR REACTIONS
The case for exotic beams at the Holifield Heavy Ion Research Facility
[DE92-008003] p 2441 N92-23445
A simple unfold method for Rutherford-scattering, intense ion-beam spectrographs
[DE92-008678] p 2445 N92-23749

THERMOPLASTIC RESINS
High strength composites evaluation
[DE92-007264] p 2340 N92-23585
Morphology and mechanical performance of PPS/carbon composite p 2342 N92-23939
Crystallization behavior of poly(phenylene sulphide) p 2342 N92-23940
Injection molding of long fiber reinforced thermoplastics: A comparison of extruded and pultruded materials with direct addition of roving strands p 2342 N92-23941
Influence of maleic anhydride as a coupling agent on the performance of wood fiber: Polystyrene composites p 2343 N92-23945
Mechanical properties of glass bead filled ductile epoxy composites p 2344 N92-23947

THIN FILMS
An XPS study of the stability of Fomblin Z25 on the native oxide of aluminum --- x ray photoelectron spectroscopy
[NASA-TM-105594] p 2353 N92-23185
Environmental effects on friction and wear of diamond and diamondlike carbon coatings
[NASA-TM-105634] p 2354 N92-23192
In situ XANES study of the valence state of chromium during electrochemical polarization of AlCr alloys
[DE92-007452] p 2350 N92-23197
The role of microstructural phenomena in magnetic thin films
[DE92-007960] p 2446 N92-23213
Deposition of adherent Ag-Ti duplex films on ceramics in a multiple-cathode sputter deposition system
[NASA-TM-105586] p 2311 N92-23225
Inelastic electron scattering from surfaces
[DE92-008129] p 2437 N92-23330

Microwave response of high transition temperature superconducting thin films p 2365 N92-23413
Properties of large area ErBa2Cu3O(7-x) thin films deposited by ionized cluster beams p 2365 N92-23414
Dependence of the critical temperature of laser-ablated YBa2Cu3O(7-delta) thin films on LaAlO3 substrate growth technique p 2365 N92-23415
Temperature-dependent evolution of chemisorbed digermane in Ge thin film growth [DE92-008098] p 2447 N92-23447
Profiling and mapping of advanced materials using spatially resolved Raman spectroscopy [DE92-008304] p 2347 N92-23449
Characterization of polybenzimidazole (PBI) film at high temperatures [NASA-CR-189174] p 2370 N92-23538
Suborbital missions: The Joust p 2313 N92-23644
Buckling and failure of thin elliptical delaminations in composites p 2331 N92-23835
Rapid recrystallization of semiconductor thin films for photovoltaic applications p 2404 N92-23998
Working gas pressure and flow effects on reactively sputtered molybdenum-oxide thin films [DE92-008624] p 2450 N92-24069

THIN WALLED SHELLS
Nonlinear finite element analysis of space frames [PB92-142447] p 2388 N92-23664

THIN WALLS
Numerical calculation: Aspiration efficiency of aerosols into thin-walled sampling inlets [PB92-132901] p 2374 N92-23516

THREE DIMENSIONAL BODIES
Voxel-based solid modeling [REPT-1.1.3] p 2419 N92-23855

THREE DIMENSIONAL MODELS
Scientific development of the Advanced Parallel Chemistry (APACHE) climate model [DE92-008657] p 2404 N92-23123
Comparison of two-dimensional and three-dimensional droplet trajectory calculations in the vicinity of finite wings [NASA-TM-105617] p 2373 N92-23154
Coupled multi-disciplinary simulation of composite engine structures in propulsion environment [NASA-TM-105575] p 2388 N92-23267
LDEF geometry/mass model for radiation analyses p 2440 N92-23305
Three-dimensional calculations of supersonic reacting flows using an LU scheme p 2304 N92-23354
Numerical calculation: Aspiration efficiency of aerosols into thin-walled sampling inlets [PB92-132901] p 2374 N92-23516
Digital data registration and differencing compression system [NASA-CASE-SSC-00010-2] p 2453 N92-23550
Computational procedures for preliminary design p 2309 N92-23952

THREE DIMENSIONAL MOTION
Quasi-three-dimensional simulations of deep convection [DE92-007204] p 2409 N92-23257
Monte Carlo simulation of the 3-state vector Potts model on a 3-dimensional random lattice [DE92-615489] p 2446 N92-23259

THRUST CHAMBERS
Tubular copper thrust chamber design study [NASA-CR-187206] p 2337 N92-23982

THRUST REVERSAL
Microgravity dynamical behaviors of cryogenic liquid hydrogen reorientation and draining in space propulsion system p 2356 N92-23147

THRUST VECTOR CONTROL
Advanced electric motor technology: Flux mapping [NASA-CR-184317] p 2372 N92-24047

THUNDERSTORMS
An observational study of the internal structure of air-mass thunderstorms p 2409 N92-23121
Tornadic supercell over Dade and Broward Counties (Florida) on January 15, 1991 [PB92-134444] p 2411 N92-23906

THYRISTORS
Versatile bistable optical switches and latching optical logic using integrated photothyristors and surface-emitting lasers [DE92-008677] p 2442 N92-23748

TILES
The challenge of the Hermes TPS shingles p 2322 N92-23823

TIME DEPENDENCE
Matrix dominated stress/strain behavior in polymeric composites: Effects of hold time, nonlinearity and rate dependency [NASA-TM-107595] p 2340 N92-23434
On motion planning amidst transient obstacles [DE91-018939] p 2429 N92-23457
VITRIMAT2: A modified model of vitrinite maturation and reflectance [DE92-008987] p 2348 N92-23904

TIME DIVISION MULTIPLE ACCESS
Interim Service ISDN Satellite (ISIS) hardware experiment development for advanced ISDN satellite designs and experiments [NASA-CR-190257] p 2335 N92-24046

TIME MEASUREMENT
Constructing a pulsar timing array p 2456 N92-23126
Control problem for a multi server loss system [PB92-148675] p 2430 N92-23506

TIME OF FLIGHT SPECTROMETERS
Kinetics of combustion-related processes at high temperatures [DE92-008790] p 2348 N92-24038

TIME SERIES ANALYSIS
TeV gamma ray emission from accreting binary pulsars p 2460 N92-23736
Evaluation of terrestrial climate variability using a moisture index p 2411 N92-23771
Analysis of time series with missing values p 2434 N92-23777

TISSUES (BIOLOGY)
Nuclear medicine program [DE92-006979] p 2412 N92-23518

TITAN LAUNCH VEHICLES
Rocket propulsion for NASA's Earth to orbit launchers p 2319 N92-23754
Future launchers: Large size solid propellant monolithic booster p 2320 N92-23766

TITANIUM
Damage development in titanium metal matrix composites subjected to cyclic loading [NASA-TM-107597] p 2340 N92-23433
Modeling and analysis of high-temperature inelastic deformation in metal matrix composites p 2345 N92-23996

TOKAMAK DEVICES
Evolution of magnetic moment due to the cyclotron resonance with field ripples in a tokamak [DE92-751058] p 2443 N92-23135
Feedback control of plasma equilibrium with control system aided by personal computer on the JIPP T-IIU tokamak [DE92-750824] p 2444 N92-23261
Fast wave current drive antenna performance on D3-D [DE92-008052] p 2444 N92-23446
Theory study on fast wave absorption at the plasma edge [PB92-141936] p 2444 N92-23663
Conceptual design of fusion experimental reactor (FER/ITER) [DE92-750949] p 2444 N92-23711
Steady State Advanced Tokamak (SSAT): The mission and the machine [DE92-008983] p 2445 N92-24020
Transport calculations of chemically sputtered carbon near a plasma divertor surface [DE92-009022] p 2445 N92-24021

TOLLMIEN-SCHLICHTING WAVES
RNG in turbulence and modeling of bypass transition p 2301 N92-23341

TOMOGRAPHY
Ocean acoustic tomography inversion in the adiabatic-invariant approximation [PB92-140466] p 2412 N92-23669

TOPOGRAPHY
Comparative study of digital MOS-1 MESSR, LANDSAT MSS, and IRS LISS-1 data for land cover classification in Sambalpur district, India p 2400 N92-23490

TOPOLOGY
Some topological problems I met [PB92-149327] p 2431 N92-23248
Sheaves of Schwartz distributions [DE92-615217] p 2432 N92-23331
On the Stone-Weierstrass theorem for scalar and vector valued functions [DE92-616916] p 2432 N92-23335
Improved image classification with neural networks by fusing multispectral signatures with topological data p 2402 N92-23368
Voxel-based solid modeling [REPT-1.1.3] p 2419 N92-23855
Semirigid construction of topological supergravities [DE92-008772] p 2451 N92-24040

TORNADOES
Tornadic supercell over Dade and Broward Counties (Florida) on January 15, 1991 [PB92-134444] p 2411 N92-23906

TOROIDAL PLASMAS
Fast wave current drive antenna performance on D3-D [DE92-008052] p 2444 N92-23446

TORQUE
An analysis of the relationship between induction motor current and shaft speed fluctuations [DE92-007234] p 2371 N92-24025

TORSION
NIST torsion oscillator viscometer response: Performance on the LeRC active vibration isolation platform [NASA-TM-105571] p 2383 N92-23564

TORSIONAL STRESS
Dynamic characterization of composite materials p 2330 N92-23832

TORSIONAL VIBRATION
The torsional fatigue behaviour of the in-plane and out-of-plane shear moduli of composite materials p 2328 N92-23818

TORUSES
Sphere packings centered at S-units of algebraic tori [PB92-135373] p 2434 N92-24061

TOXICITY
Material considerations for habitable areas of manned spacecraft p 2323 N92-23785

TOXICOLOGY
JPRS report: Science and technology. Central Eurasia: Life sciences [JPRS-ULS-92-010] p 2412 N92-23706

TRACKING NETWORKS
The potential use of fiducial ground networks p 2316 N92-23924
Data distribution and reduction approaches to data distribution: The Earthnet experience p 2317 N92-23926

TRACKING STATIONS
Distributed expert systems for ground and space applications p 2427 N92-23361

TRAILING EDGES
Radiation exposure of LDEF: Initial results p 2461 N92-23302
Preliminary analysis of LDEF instrument A0187-1: Chemistry of Micrometeoroids Experiment p 2458 N92-23315

TRAJECTORIES
Time optimal trajectories for a 2-wheeled robot [DE92-000069] p 2430 N92-24032

TRAJECTORY ANALYSIS
Solar-electric-propulsion cargo vehicles for split/sprint Mars mission [NASA-CR-189983] p 2322 N92-23526

TRAJECTORY CONTROL
Automated synthesis of robot arm motion for robot arm collision avoidance p 2381 N92-23158
On motion planning amidst transient obstacles [DE91-018939] p 2429 N92-23457
The design and control of uncertain manipulator arms with decoupled inertia matrix p 2383 N92-23690

TRAJECTORY MEASUREMENT
Comparison of two-dimensional and three-dimensional droplet trajectory calculations in the vicinity of finite wings [NASA-TM-105617] p 2373 N92-23154

TRAJECTORY PLANNING
On motion planning amidst transient obstacles [DE91-018939] p 2429 N92-23457

TRANSDUCERS
Smart accelerometer — vibration damage detection [NASA-CASE-MSC-21951-1] p 2378 N92-23545

TRANSFER FUNCTIONS
Microgravity acceleration measurement and environment characterization science (17-IML-1) p 2363 N92-23642
Sensitivity I(sup 1) minimization with boundary zeros or poles [PB92-141803] p 2433 N92-23658
Analysis of gravity and topography on Earth and Venus: Comparisons of lithospheric and sublithospheric processes p 2409 N92-23772

TRANSFER ORBITS
Lifetime of objects in geostationary transfer orbit p 2318 N92-23977

TRANSFORMATIONS (MATHEMATICS)
Galilei-isotopic symmetries [DE92-615261] p 2431 N92-23129
The 7th INS Scientific Computational Programs [DE92-750967] p 2417 N92-23266

TRANSIENT LOADS
Coupled load analysis: Scatter related to model uncertainties p 2324 N92-23787

TRANSISTOR AMPLIFIERS
Design and performance of 22 GHz coaxial low noise MESFET and HEMT amplifiers [PB92-134071] p 2368 N92-23172

TRANSISTOR CIRCUITS
Fast simulation of MOS digital networks using a physical macromodelling approach [REPT-1.2.1] p 2420 N92-23860

On generating two dimensional CMOS cells
[REPT-1.3.2] p 2421 N92-23869

TRANSISTORS
Actively-stabilized photomultiplier tube base for vacuum operation
[DE92-007528] p 2368 N92-23200
Center for Space Power and Advanced Electronics, Auburn University p 2314 N92-23654

TRANSITION PROBABILITIES
Semiempirical studies of atomic structure
[DE92-008143] p 2437 N92-23448

TRANSITION TEMPERATURE
A study of start-up characteristics of a potassium heat pipe from the frozen state
[NASA-CR-189173] p 2373 N92-23253
Microwave response of high transition temperature superconducting thin films p 2365 N92-23413
Properties of large area ErBa2Cu3O(7-x) thin films deposited by ionized cluster beams
p 2365 N92-23414
High-temperature superconductivity: Electron-doped cuprates and composites from alloy precursors
p 2448 N92-23774

TRANSLATING
IGES: Application generator in disguise
[REPT-3.1.7] p 2424 N92-23882

TRANSLATIONAL MOTION
Design of an omnidirectional and holonomic wheeled platform prototype
[DE92-000046] p 2382 N92-23459
Helix translation device --- shim for precision displacements
[NASA-CASE-GSC-13141-1] p 2382 N92-23548

TRANSMISSION LOSS
Tabulations of propagation data over irregular terrain in the 75- to 8400-MHz frequency range. Part 5: Virginia
[PB92-137413] p 2364 N92-23180

TRANSMITTANCE
GENLN2: A general line-by-line atmospheric transmittance and radiance model. Version 3.0: Description and users guide
[PB92-148543] p 2408 N92-23522

TRANSONIC FLIGHT
Adaptive active flutter suppression of wings in subsonic and transonic flight regimes p 2310 N92-24010

TRANSONIC FLOW
Efficient and robust design optimization of transonic airfoils p 2305 N92-23717
Adaptive active flutter suppression of wings in subsonic and transonic flight regimes p 2310 N92-24010
Investigation of solution operators for the three dimensional unsteady Euler equations
p 2376 N92-24018

TRANSONIC WIND TUNNELS
Development of wall pressure measuring apparatus for an existing transonic wind tunnel test section
[NAL-TM-565] p 2312 N92-23778

TRANSPARENCE
The Critical Point Facility (CPF) p 2362 N92-23637

TRANSPORT AIRCRAFT
Simultaneous stress and flutter optimization for the wing of a transport aircraft equipped with four engines
p 2308 N92-23238
Effects of turbine cooling assumptions on performance and sizing of high-speed civil transport
[NASA-TM-105610] p 2311 N92-23537

TRANSPORT PROPERTIES
Particle dynamics in a wave with variable amplitude
[DE92-008340] p 2436 N92-23217
RNG in turbulence and modeling of bypass transition
p 2301 N92-23341

TRANSPORT THEORY
Nonequilibrium statistical operator in hot-electron transport theory
[DE92-615517] p 2446 N92-23260
Studies of fluctuation processes in nuclear collisions
[DE92-008144] p 2440 N92-23276
Semiclassical model and properties of resonant tunneling diode
[PB92-143320] p 2448 N92-23498
The all particle method
[DE92-008357] p 2439 N92-24005
Optical properties of metallic multi-layer films
[DE92-615486] p 2443 N92-24029

TRANSPORTER
Proceedings of the Second Annual Symposium on Industrial Involvement and Successes in Commercial Space
[NASA-TM-107812] p 2312 N92-23643
Systems for COMET p 2313 N92-23646

TRAPPED PARTICLES
Particle dynamics in a wave with variable amplitude
[DE92-008340] p 2436 N92-23217

TRENDS
National air quality and emissions trends report, 1990
[PB92-141555] p 2406 N92-23517
Climate
[PB92-150457] p 2410 N92-23520

TRIANGULATION
Grid generation and flow solution method for Euler equations on unstructured grids
[NASA-TM-4295] p 2305 N92-23533

TRIBOLOGY
Tribological evaluation of an Al2O3-SiO2 ceramic fiber candidate for high temperature sliding seals
[NASA-TM-105611] p 2339 N92-23190

TROPICAL METEOROLOGY
Climate System Monitoring (CSM). El Nino/Southern Oscillation (ENSO) diagnostic advisory, special issue
p 2411 N92-23677
Wind, current and temperature data at 0 deg, 165 deg E: January 1986 to March 1991
[PB92-143080] p 2411 N92-23682
Diagnostic report of the National Hurricane Center: June and July 1991. Volume 4, number 1
[PB92-134501] p 2411 N92-23994

TROPICAL REGIONS
Energy cycles in the summer tropical atmosphere over the North Atlantic Ocean p 2409 N92-23150
Clouds, surface temperature, and the tropical and subtropical radiation budget p 2410 N92-23431
Reconstructing the tropical Atlantic seasonal thermocline using planktonic foraminifera
p 2412 N92-23769
Diagnostic report of the National Hurricane Center: June and July 1991. Volume 4, number 1
[PB92-134501] p 2411 N92-23994

TROPOSPHERE
Energy cycles in the summer tropical atmosphere over the North Atlantic Ocean p 2409 N92-23150
A model of large-scale instabilities in the Jovian troposphere p 2459 N92-23704

TRUCKS
White paper: Preliminary assessment of LNG vehicle technology, economics, and safety issues
[PB92-137603] p 2383 N92-23680

TRUSSES
Artificial intelligence approach to planning the robotic assembly of large tetrahedral truss structures
p 2426 N92-23357
Robot-friendly connector --- space truss structures
[NASA-CASE-MSC-21864-1] p 2382 N92-23544
Free and forced response of nearly periodic multi-span beams and multi-bay trusses p 2389 N92-23699
Minimization of vibrations by broadband sensitivity approach p 2330 N92-23828
Underlying modal data issues for detecting damage in truss structures
[NASA-TM-107573] p 2390 N92-23990

TRYPTOPHAN
Photoinduced electron transfer in ordered polymers
[DE92-008787] p 2355 N92-24037

TUNABLE LASERS
Injection seeding of a Q-switched alexandrite laser: Study of frequency stabilization p 2380 N92-23961

TUNGSTEN ALLOYS
Effect of minor elements on hot workability of Ni-Cr-W superalloys
[DE92-750951] p 2351 N92-23263

TUNGSTEN COMPOUNDS
Reductive coupling of carbon monoxide to C2 products
[DE92-007529] p 2347 N92-23499

TURBINES
Effects of turbine cooling assumptions on performance and sizing of high-speed civil transport
[NASA-TM-105610] p 2311 N92-23537

TURBOFAN ENGINES
Effects of chemical equilibrium on turbine engine performance for various fuels and combustor temperatures
[NASA-TM-105399] p 2311 N92-23254

TURBOMACHINERY
Computations of unsteady multistage turbomachinery flows p 2311 N92-23671
Experimental study of the mechanism of sound generation by rotating stall in centrifugal turbomachines
p 2436 N92-23726

TURBULENCE
Center for Modeling of Turbulence and Transition (CMOTT). Research briefs: 1990
[NASA-TM-105243] p 2301 N92-23336
The study of PDF turbulence models in combustion
p 2301 N92-23337
Turbulence modeling p 2301 N92-23338
Modeling of compressible turbulent shear flows
p 2301 N92-23340
An improved k-epsilon model for near wall turbulence
p 2303 N92-23349
Advancements in engineering turbulence modeling
[PAPER-105] p 2303 N92-23350
On the basic equations for the second-order modeling of compressible turbulence p 2303 N92-23351
Kolmogorov behavior of near-wall turbulence and its application in turbulence modeling
[NASA-TM-105663] p 2376 N92-24050

TURBULENCE EFFECTS
The kinematics of turbulent boundary layer structure
p 2375 N92-23689

TURBULENCE MODELS
The study of PDF turbulence models in combustion
p 2301 N92-23337
Turbulence modeling p 2301 N92-23338
Experiments and modeling p 2301 N92-23339
RNG in turbulence and modeling of bypass transition
p 2301 N92-23341
Development of new flux splitting schemes
p 2302 N92-23343
The study of PDF turbulence models in combustion
[PAPER-107] p 2302 N92-23345
On recontamination and directional-bias problems in Monte Carlo simulation of PDF turbulence models
p 2302 N92-23346
Progress in the development of PDF turbulence models for combustion
[PAPER-213] p 2303 N92-23347
A study of hydrogen diffusion flames using PDF turbulence model p 2303 N92-23348
Viscous-shock-layer analysis of hypersonic flows over long slender vehicles
[NASA-CR-189614] p 2374 N92-23543
Unsteady three-dimensional incompressible algorithm based on artificial compressibility p 2375 N92-23700

TURBULENT BOUNDARY LAYER
An improved k-epsilon model for near wall turbulence
p 2303 N92-23349
The kinematics of turbulent boundary layer structure
p 2375 N92-23689

TURBULENT FLOW
Turbulence modeling p 2301 N92-23338
Modeling of compressible turbulent shear flows
p 2301 N92-23340
Progress in the development of PDF turbulence models for combustion
[PAPER-213] p 2303 N92-23347
An improved k-epsilon model for near wall turbulence
p 2303 N92-23349
Advancements in engineering turbulence modeling
[PAPER-105] p 2303 N92-23350
On the basic equations for the second-order modeling of compressible turbulence p 2303 N92-23351
Simulations of free shear layers using a compressible kappa-epsilon model p 2304 N92-23355
Kolmogorov behavior of near-wall turbulence and its application in turbulence modeling
[NASA-TM-105663] p 2376 N92-24050

TWINNING
The electron-positron momentum density and Fermi surface of YBa2Cu3O(7-x)
[DE92-008605] p 2450 N92-24007

TWO DIMENSIONAL FLOW
Numerical experiments with flows of elongated granules
[NASA-TM-105567] p 2381 N92-23226
Improved shock-capturing of Jameson's scheme for the Euler equations
[PB92-148758] p 2373 N92-23251
Simulations of free shear layers using a compressible kappa-epsilon model p 2304 N92-23355

TWO DIMENSIONAL MODELS
Aeroelastic stability analyses of two counter rotating propfan designs for a cruise missile model
[NASA-TM-105268] p 2387 N92-23191
Contact stresses in meshing spur gear teeth: Use of an incremental finite element procedure
[NASA-TM-105388] p 2382 N92-23536
A two-dimensional Euler solution for an unbladed jet engine configuration
[NASA-TM-105329] p 2374 N92-23560
Interactive solution-adaptive grid generation procedure
[NASA-TM-105432] p 2305 N92-23563
Improved numerical methods for quantum field theory (outstanding junior investigator award)
[DE92-008730] p 2451 N92-23578
The continuous elements method
p 2330 N92-23829
Numerical simulations of wakes, blade-vortex interaction, flutter, and flutter suppression by feedback control p 2375 N92-23997

TWO PHASE FLOW
The continuum modelling of two-phase flow systems
[DE92-007538] p 2373 N92-23202
Liquid hydrogen mass flow through a multiple orifice Joule-Thomson device
[NASA-TM-105583] p 2373 N92-23268
Critical fluid thermal equilibration experiment (19-IML-1) p 2363 N92-23640

Mathematical modelling and numerical approximations for two-phase flow problems p 2375 N92-23672
Numerical and physical modelling of bubbly flow phenomena
[DE92-008642] p 2376 N92-24062

U

U.S.S.R.
JPRS report: Science and technology. USSR: Earth sciences
[JPRS-UES-91-005] p 2392 N92-23707
U.S.S.R. SPACE PROGRAM
The USSR launchers programme p 2319 N92-23753
Oxygen-kerosene liquid rocket engines with postburning generator gas and high pressure in combustion chamber p 2320 N92-23761
ULTRAHIGH FREQUENCIES
Tabulations of propagation data over irregular terrain in the 75- to 8400-MHz frequency range. Part 5: Virginia
[PB92-137413] p 2364 N92-23180
ULTRASONIC TESTS
Detecting Lamb waves with broad-band acousto-ultrasonic signals in composite structures
[NASA-TM-105557] p 2386 N92-23189
Training guidelines in non-destructive testing techniques
[DE92-615083] p 2386 N92-23258
Ultrasonic investigation of (3)He-A vortices in low magnetic fields
[PB92-142256] p 2435 N92-23665
ULTRAVIOLET DETECTORS
The state of the development in Europe p 2392 N92-23382
ULTRAVIOLET EMISSION
Infrared emission lines from highly ionized regions p 2460 N92-23162
UNCONTROLLED REENTRY (SPACECRAFT)
The Reentry of Salyut-7/Kosmos-1686
[ESA-SP-345] p 2333 N92-23967
Radar tracking and observation of noncooperative space objects by reentry of Salyut-7/Kosmos-1686 p 2333 N92-23968
Orbit analysis and lifetime prediction using radar data by reentry of Salyut-7/Kosmos-1686 p 2318 N92-23969
Salyut-7/Kosmos-1686 reentry prediction activities at ESOC p 2334 N92-23970
Determination and prediction of satellite motion at the end of the lifetime p 2334 N92-23971
Salyut-7/Kosmos-1686 reentry predictions for the Italian Civil Defence Authority p 2334 N92-23972
Debris reentry prediction: Salyut-7/Kosmos-1686 p 2318 N92-23973
Modelling of aerodynamic forces and heat transfer for orbital decay and reentry calculations p 2334 N92-23974
Lifetime of objects in geostationary transfer orbit p 2318 N92-23977
Orbital decay and reentry of the Salyut-7 orbital complex p 2335 N92-23978
UNDERGROUND STRUCTURES
Survey on subterranean disposal and storage technology of CO2
[DE92-769378] p 2405 N92-23455
UNDERWATER ACOUSTICS
Ocean acoustic tomography inversion in the adiabatic-invariant approximation
[PB92-140466] p 2412 N92-23669
UNITED STATES
Limiting net greenhouse gas emissions in the United States, volume 2
[DE92-007592] p 2405 N92-23333
Acid rain and air pollution in desert park areas. Proceedings of a workshop: Management recommendations
[PB92-140532] p 2407 N92-24003
UNSTEADY FLOW
An adaptive-grid technique for simulation of complex unsteady flows p 2372 N92-23148
Discovery of orbital decay in SMC X-1
[NASA-CR-190214] p 2317 N92-23531
Long time behavior of unsteady flow computations
[NASA-TM-105584] p 2374 N92-23565
Aerodynamic rectifier for pulsed combustors
[PB92-142587] p 2348 N92-23657
Computations of unsteady multistage turbomachinery flows p 2311 N92-23671
Unsteady three-dimensional incompressible algorithm based on artificial compressibility p 2375 N92-23700
Survey of experimental techniques for performance prediction p 2309 N92-23954
UPPER ATMOSPHERE
WAMDII: The Wide Angle Michelson Doppler Imaging Interferometer
[NASA-TM-105526] p 2441 N92-23525
URINE
Energy expenditure in space flight (doubly labelled water method) (8-IML-1) p 2359 N92-23620
USER MANUALS (COMPUTER PROGRAMS)
Automatic waveform analysis and measurement system user manual
[PB92-132976] p 2364 N92-23173
User's manual for three dimensional FDTD version C code for scattering from frequency-independent dielectric and magnetic materials
[NASA-CR-190109] p 2365 N92-23425
User interface user's guide for HYPGEN
[NASA-CR-190304] p 2425 N92-23991
USER REQUIREMENTS
National user interfaces p 2395 N92-23407

V

VACUUM
Actively-stabilized photomultiplier tube base for vacuum operation
[DE92-007528] p 2368 N92-23200
Vacuum mechatronic laser alignment system on the NOVA laser
[DE92-006898] p 2379 N92-23571
VACUUM MELTING
Modular electromagnetic levitator
[DE92-008278] p 2367 N92-23900
VACUUM SYSTEMS
Vacuum mechatronic laser alignment system on the NOVA laser
[DE92-006898] p 2379 N92-23571
VALENCE
In situ XANES study of the valence state of chromium during electrochemical polarization of AlCr alloys
[DE92-007452] p 2350 N92-23197
Application of x ray absorption spectroscopy to the study of corrosion and inhibition
[DE92-007456] p 2350 N92-23198
Potential energy surfaces and reaction dynamics of polyatomic molecules
[DE92-008314] p 2437 N92-23450
The electronic structure of icosahedral boron clusters
[DE92-008336] p 2447 N92-23451
VALVES
Aerodynamic rectifier for pulsed combustors
[PB92-142587] p 2348 N92-23657
VANADIUM ALLOYS
TeV gamma ray emission from accreting binary pulsars p 2460 N92-23736
VAPOR DEPOSITION
An XPS study of the stability of Fomblin Z25 on the native oxide of aluminum — x ray photoelectron spectroscopy
[NASA-TM-105594] p 2353 N92-23185
Deposition of adherent Ag-Ti duplex films on ceramics in a multiple-cathode sputter deposition system
[NASA-TM-105586] p 2311 N92-23225
Vapor crystal growth studies of single crystals of mercuric iodide (3-IML-1) p 2361 N92-23632
VAPOR PHASES
Mercury iodide nucleation and crystal growth in vapor phase (4-IML-1) p 2361 N92-23633
VAPOR PRESSURE
General P-T fit construction for He, N2, Ar, H2 and Ne VPT used at Fermilab
[DE92-008851] p 2433 N92-23579
VARACTOR DIODES
Planar varactor frequency multiplier devices with blocking barrier
[NASA-CASE-NPO-18428-1-CU] p 2369 N92-23464
VARIABILITY
Climate
[PB92-150457] p 2410 N92-23520
Evaluation of terrestrial climate variability using a moisture index p 2411 N92-23771
VARIABLE CYCLE ENGINES
Effects of turbine cooling assumptions on performance and sizing of high-speed civil transport
[NASA-TM-105610] p 2311 N92-23537
VARIATIONAL PRINCIPLES
Analysis and control of nonlinear flexible manipulator p 2384 N92-23727
Free vibration of thick isotropic and orthotropic cylindrical shells p 2389 N92-23773
VARIATIONS
Cu charge fluctuations and anomalous behaviour in the phonon spectrum of La2CuO4
[DE92-617446] p 2446 N92-23270
VECTOR SPACES
Family of Poisson structures on compact hermitian symmetric spaces
[PB92-149442] p 2433 N92-23670
VECTORS (MATHEMATICS)
An exceptional N=8 superconformal algebra in two dimensions associated with F(4)
[DE92-616991] p 2435 N92-23207
Vector circuit method applied for chiral dielectric slab waveguides
[PB92-142355] p 2367 N92-23679
VEGETABLES
Irradiation of spices, herbs, and other vegetable seasonings: A compilation of technical data for its authorization and control
[DE92-619064] p 2415 N92-24022
VEGETATION
Multitemporal and multisensor approach with MOS data to natural resources evaluation in dry tropical Africa (Burkina Faso) p 2400 N92-23488
Comparative study of digital MOS-1 MESSR, LANDSAT MSS, and IRS LISS-1 data for land cover classification in Sambalpur district, India p 2400 N92-23490
VEGETATION GROWTH
Multitemporal and multisensor approach with MOS data to natural resources evaluation in dry tropical Africa (Burkina Faso) p 2400 N92-23488
VEGETATIVE INDEX
Evaluation of effective characteristic in forest field p 2397 N92-23473
Multitemporal and multisensor approach with MOS data to natural resources evaluation in dry tropical Africa (Burkina Faso) p 2400 N92-23488
VEINS
Measurement of venous compliance (8-IML-1) p 2360 N92-23623
VELOCITY DISTRIBUTION
Deriving the velocity distribution of meteoroids from the measured meteoroid impact directionality on the various LDEF surfaces p 2459 N92-23322
Numerical calculation: Aspiration efficiency of aerosols into thin-walled sampling inlets
[PB92-132901] p 2374 N92-23516
Renormalization group analysis of the Reynolds stress transport equation
[NASA-TM-105588] p 2374 N92-23542
VENUS SURFACE
Analysis of gravity and topography on Earth and Venus: Comparisons of lithospheric and sublithospheric processes p 2409 N92-23772
VERBAL COMMUNICATION
Training users of a flexible decision support system: The effects of training content and user ability p 2453 N92-23730
VERTEBRAE
Back pain in astronauts (8-IML-1) p 2360 N92-23622
VERTICAL AIR CURRENTS
An observational study of the internal structure of air-mass thunderstorms p 2409 N92-23121
VERY LARGE SCALE INTEGRATION
Proceedings of the International Conference on CAD/CAM and AMT. Volume 1: General sessions
[ITN-92-85127] p 2418 N92-23851
Fast simulation of MOS digital networks using a physical macromodelling approach
[REPT-1.2.1] p 2420 N92-23860
Design for testability: Where are the goalposts?
[REPT-1.2.2] p 2420 N92-23861
Test preparation for MOS digital circuits using heuristics for reliable fault simulation
[REPT-1.2.6] p 2421 N92-23865
A framework for the support of VLSI (very large scale integration) design for manufacture
[REPT-1.3.1] p 2421 N92-23868
Breathing maze router for analog VLSI cell generation
[REPT-1.3.3] p 2422 N92-23870
Statistical process control system for VLSI fabrication
[REPT-1.3.4] p 2422 N92-23871
Functional design verification of ULSI components
[REPT-1.3.7] p 2422 N92-23873
VERY LONG BASE INTERFEROMETRY
High resolution studies of NGC 1275 and the galactic center p 2455 N92-23675
Data distribution and reduction approaches to data distribution: The Earthnet experience p 2317 N92-23926
VESTIBULAR TESTS
Positional and spontaneous nystagmus (8-IML-1) p 2360 N92-23624
Microgravity vestibular investigations (10-IML-1) p 2360 N92-23626
VESTIBULES
Space adaptation syndrome experiments (8-IML-1) p 2360 N92-23625

VHSIC (CIRCUITS)
The need for standards in design automation
[P-1-1] p 2419 N92-23852
VIBRATION
Control of a helicopter engine in low altitude flight
p 2310 N92-23122
Automatic waveform analysis and measurement system user manual
[PB92-132976] p 2364 N92-23173
Application of optical distributed sensing and computation to control of large space structures
[NASA-CR-190293] p 2442 N92-23567
An advanced system for environmental sine testing: Basic principles revisited p 2325 N92-23799
Ariane 4 internal acoustic environment: Interpretation of flight data with a vibroacoustic model of the upper part of the launcher p 2321 N92-23811
VIBRATION DAMPING
Microsphere viscometers for low temperature applications
[PB92-143361] p 2379 N92-23594
The statics, dynamics, and control of the elasticarm: A continuous beam manipulator p 2383 N92-23691
Influence of microvibrations on spacecraft performances p 2329 N92-23825
Dynamic characterization of composite materials
p 2330 N92-23832
Numerical simulations of wakes, blade-vortex interaction, flutter, and flutter suppression by feedback control p 2375 N92-23997
Adaptive active flutter suppression of wings in subsonic and transonic flight regimes p 2310 N92-24010
Analytical and experimental investigation of vibratory response in adhesively bonded and composite structures p 2345 N92-24012
VIBRATION EFFECTS
Analytical and experimental investigation of vibratory response in adhesively bonded and composite structures p 2345 N92-24012
VIBRATION MEASUREMENT
Smart accelerometer --- vibration damage detection
[NASA-CASE-MSC-21951-1] p 2378 N92-23545
Non contacting measurement of vibration
p 2325 N92-23800
VIBRATION METERS
Smart accelerometer --- vibration damage detection
[NASA-CASE-MSC-21951-1] p 2378 N92-23545
VIBRATION MODE
Free and forced response of nearly periodic multi-span beams and multi-bay trusses p 2389 N92-23699
Underlying modal data issues for detecting damage in truss structures
[NASA-TM-107573] p 2390 N92-23990
VIBRATION TESTS
NIST torsion oscillator viscometer response: Performance on the LeRC active vibration isolation platform
[NASA-TM-105571] p 2383 N92-23564
VIDEO COMMUNICATION
A robust low-rate coding scheme for packet video
p 2417 N92-23420
VIDEO DATA
A robust coding scheme for packet video
p 2418 N92-23422
A progressive data compression scheme based upon adaptive transform coding: Mixture block coding of natural images p 2418 N92-23423
VIRGINIA
Tabulations of propagation data over irregular terrain in the 75- to 8400-MHz frequency range. Part 5: Virginia
[PB92-137413] p 2364 N92-23180
VIRUSES
Friend leukemia virus transformed cells exposed to microgravity in the presence of DMSO (7-IML-1)
p 2358 N92-23613
VISCOELASTIC DAMPING
Analysis and control of nonlinear flexible manipulator
p 2384 N92-23727
VISCOMETERS
NIST torsion oscillator viscometer response: Performance on the LeRC active vibration isolation platform
[NASA-TM-105571] p 2383 N92-23564
VISCOSITY
The structure of MFD shock waves for rectilinear motion in some model of plasma
[DE92-617386] p 2443 N92-23208
Microsphere viscometers for low temperature applications
[PB92-143361] p 2379 N92-23594
VISCOUS FLOW
High-Order Polynomial Expansions (HOPE) for flux-vector splitting p 2304 N92-23353
Viscous-shock-layer analysis of hypersonic flows over long slender vehicles
[NASA-CR-189614] p 2374 N92-23543
Topics in numerical computation of compressible flow
p 2375 N92-23692
Unsteady three-dimensional incompressible algorithm based on artificial compressibility p 2375 N92-23700
VISUAL OBSERVATION
Study of density distribution in a near-critical simple fluid (19-IML-1) p 2362 N92-23639
VITERBI DECODERS
A joint source/channel coder design
p 2417 N92-23418
VOLTAGE CONVERTERS (DC TO DC)
Microprocessor control of multiple peak power tracking DC/DC converters for use with solar cell arrays
[NASA-CASE-GSC-13450-1] p 2403 N92-23463
VORTICES
Ultrasonic investigation of (3)He-A vortices in low magnetic fields
[PB92-142256] p 2435 N92-23665
The kinematics of turbulent boundary layer structure
p 2375 N92-23689
High angle of attack: Aerodynamics
p 2305 N92-23956
An experimental investigation of entrainment and mixing in pulsed and exponential transverse jets
p 2375 N92-23995
Kolmogorov behavior of near-wall turbulence and its application in turbulence modeling
[NASA-TM-105663] p 2376 N92-24050
VORTICITY
An adaptive-grid technique for simulation of complex unsteady flows p 2372 N92-23148
Applications of boundary integral methods to the study of steep free surface waves p 2372 N92-23149
VOSTOK SPACECRAFT
The USSR launchers programme
p 2319 N92-23753

W

WAFERS
Statistical process control system for VLSI fabrication
[REPT-1.3.4] p 2422 N92-23871
WAKES
Numerical simulations of wakes, blade-vortex interaction, flutter, and flutter suppression by feedback control p 2375 N92-23997
WALL FLOW
An improved k-epsilon model for near wall turbulence
p 2303 N92-23349
Advancements in engineering turbulence modeling
[PAPER-105] p 2303 N92-23350
Kolmogorov behavior of near-wall turbulence and its application in turbulence modeling
[NASA-TM-105663] p 2376 N92-24050
WALLS
Turbulence modeling p 2301 N92-23338
WASHINGTON
Climate
[PB92-150457] p 2410 N92-23520
WASTE DISPOSAL
HEIS: An integrated information system for environmental restoration and monitoring at Hanford
[DE92-006467] p 2453 N92-23188
Survey on subterranean disposal and storage technology of CO2
[DE92-769378] p 2405 N92-23455
A self-navigating mobile robot
[DE92-008612] p 2430 N92-24066
WATER
Oil lubricated and water lubricated pin-on-disc wear tests with engineering ceramics
[PB92-136563] p 2380 N92-23152
Modelling and experimental verification of a water alleviation system for the NASP --- National Aerospace Plane
[NASA-TM-105661] p 2373 N92-23224
Measurement of surface cleanliness by area-of-spread
[DE92-007265] p 2348 N92-23586
Energy expenditure in space flight (doubly labelled water method) (8-IML-1) p 2359 N92-23620
Investigation of the Archean climate using the NCAR CCM
[NASA-CR-189878] p 2410 N92-23656
WATER COLOR
Atmospheric correction of the second generation ocean color sensors p 2392 N92-23145
Monitoring of ocean conditions by using MOS-1 data
p 2398 N92-23476
Applicability of MESSR and VTIR data for marine observation p 2398 N92-23478
Utilization of satellite images for marine resources
p 2399 N92-23480
Use of Marine Observation Satellite-1 in applied ocean science p 2400 N92-23487
WATER DEPTH
Computer tutorial and animation of the normal ice cycle of the Laurentian Great Lakes of North America for 1960 - 1979
[PB92-129949] p 2401 N92-23659
WATER POLLUTION
The state of the development in Europe
p 2392 N92-23382
The laser fluorosensor p 2393 N92-23386
WATER TEMPERATURE
Research project for practical usage of MOS-1 data collection system p 2399 N92-23485
WATER VAPOR
Investigations on verification of the data observed by the MESSR and VTIR, and on interannual trend in the MSR data p 2397 N92-23470
Retrieval of upper precipitable water profile from MOS-1 VTIR water vapor channel p 2398 N92-23479
Preliminary report on the observation of polar atmosphere and cryosphere by MOS-1 data received at Syowa Station p 2399 N92-23481
Field evaluation of remote sensor measurements of wind, temperature, and moisture for ARM integrated sounding system research
[PB92-140714] p 2401 N92-23521
WAVE ATTENUATION
Biisotropic polarizer shield
[PB92-141878] p 2366 N92-23590
WAVE DIFFRACTION
Binary surface-relief gratings for array illumination in digital optics
[PB92-143585] p 2442 N92-23662
WAVE DRAG
Efficient and robust design optimization of transonic airfoils p 2305 N92-23717
WAVE EQUATIONS
Long time behavior of unsteady flow computations
[NASA-TM-105584] p 2374 N92-23565
WAVE FUNCTIONS
Beyond conventional quantum mechanics
[DE92-616892] p 2451 N92-23206
WAVE PROPAGATION
Applications of boundary integral methods to the study of steep free surface waves p 2372 N92-23149
Experimental verification of a theory for the impact response of composite plates
[FFA-TN-1991-17] p 2339 N92-23167
Evaluation of mode purity of ordinary and extraordinary modes by fixed elliptically polarized wave for ECH and ECCD
[DE92-750961] p 2444 N92-23264
Solitary excitations in gyrotropic crystals
[DE92-617447] p 2446 N92-23271
Soviet articles on antenna theory
[DE92-008452] p 2366 N92-23575
The effects of magnetic fields on oscillations in the solar atmosphere p 2459 N92-23697
Harmonic wave propagation in two-dimensional periodic large space structures p 2330 N92-23830
WAVE REFLECTION
Biisotropic polarizer shield
[PB92-141878] p 2366 N92-23590
WAVEFORMS
Automatic waveform analysis and measurement system user manual
[PB92-132976] p 2364 N92-23173
Waveform relaxation always converges for RC-circuits
[PB92-142280] p 2369 N92-23495
WAVEGUIDES
A flexible CPW package for a 30 GHz MMIC amplifier --- coplanar waveguide
[NASA-TM-105630] p 2368 N92-23193
Solid State Technology Branch of NASA Lewis Research Center
[NASA-TM-105159] p 2365 N92-23412
Coaxial turnstile junction
[NASA-CASE-GSC-13422-1] p 2369 N92-23462
Closed parallel-plate chiral waveguides with boundary impedance conditions
[PB92-142397] p 2366 N92-23591
Vector circuit method applied for chiral dielectric slab waveguides
[PB92-142355] p 2367 N92-23679
WEAR TESTS
Environmental effects on friction and wear of diamond and diamondlike carbon coatings
[NASA-TM-105634] p 2354 N92-23192
Deposition of adherent Ag-Ti duplex films on ceramics in a multiple-cathode sputter deposition system
[NASA-TM-105586] p 2311 N92-23225
Derated ion thruster design issues
[NASA-TM-105576] p 2337 N92-23534
WEATHER
Differences within and among surface marine datasets
[PB92-135326] p 2411 N92-23660

WEATHER FORECASTING
Computer tutorial and animation of the normal ice cycle of the Laurentian Great Lakes of North America for 1960 - 1979
[PB92-129949] p 2401 N92-23659
Tornadic supercell over Dade and Broward Counties (Florida) on January 15, 1991
[PB92-134444] p 2411 N92-23906
Diagnostic report of the National Hurricane Center: June and July 1991. Volume 4, number 1
[PB92-134501] p 2411 N92-23994
WEATHERING
Failure behaviour of high density polyethylene products with an embrittled surface layer due to UV exposure
[PB92-138494] p 2354 N92-23510
WEIGHTLESSNESS
First international Microgravity Laboratory experiment descriptions
[NASA-TM-4353] p 2356 N92-23600
Gravitropic responses of plants in the absence of a complicating G-force (6-IML-1) p 2356 N92-23601
A spaceflight experiment to investigate the effects of a range of unilateral blue light phototropic stimulations on the movements of wheat coleoptiles (6-IML-1)
p 2356 N92-23602
Microgravitational effects on chromosome behavior (7-IML-1) p 2357 N92-23604
Eggs: The role of gravity in the establishment of the dorso-ventral axis in the amphibian embryo (7-IML-1)
p 2357 N92-23607
The effect of space environment on the development and aging of Drosophila Melanogaster (7-IML-1)
p 2357 N92-23608
Effect of microgravity environment on cell wall regeneration, cell divisions, growth, and differentiation of plants from protoplasts (7-IML-1) p 2358 N92-23609
Gravity related behavior of the acellular slime mold Physarum polycephalum (7-IML-1) p 2359 N92-23618
Studies on penetration of antibiotic in bacterial cells in space conditions (7-IML-1) p 2359 N92-23619
Space adaptation syndrome experiments (8-IML-1)
p 2360 N92-23625
Modular electromagnetic levitator
[DE92-008278] p 2367 N92-23900
WELD STRENGTH
Weldline strength in injection molded glass fiber reinforced polypropylene p 2344 N92-23949
WELDED JOINTS
Nd: YAG laser welding aluminum alloys
[DE92-003131] p 2381 N92-23177
Cracking investigation of Nd:YAG laser welded gold plated glass sealing alloys
[DE92-007971] p 2387 N92-23216
Development of a crack arrest fracture toughness measurement procedure for quality assurance of plates and welds used for hydrocarbon storage tanks
[PB92-141753] p 2389 N92-23681
WELDING
JPRS report: Science and technology. Central Eurasia: Materials science
[JPRS-UMS-92-005] p 2363 N92-23708
JPRS report: Science and technology. Central Eurasia: Materials science
[JPRS-UMS-92-006] p 2363 N92-23709
WELLS
Geothermal energy program overview
[DE91-002172] p 2402 N92-23175
Geothermal direct use engineering and design guidebook
[DE92-008686] p 2404 N92-24030
WETTABILITY
Measurement of surface cleanliness by area-of-spread
[DE92-007265] p 2348 N92-23586
WHEAT
A spaceflight experiment to investigate the effects of a range of unilateral blue light phototropic stimulations on the movements of wheat coleoptiles (6-IML-1)
p 2356 N92-23602
WHEELS
Design of an omnidirectional and holonomic wheeled platform prototype
[DE92-000046] p 2382 N92-23459
Time optimal trajectories for a 2-wheeled robot
[DE92-000069] p 2430 N92-24032
WHITE NOISE
PSD computations using Welch's method
[DE92-007419] p 2370 N92-23584
WIGGLER MAGNETS
The principle and design of a high-efficiency free-electron laser p 2380 N92-23687
Report from orbit sub-group of task force for MR synchrotron radiation project
[DE92-751024] p 2441 N92-23713
WIND (METEOROLOGY)
Quasi-three-dimensional simulations of deep convection
[DE92-007204] p 2409 N92-23257
WIND MEASUREMENT
International workshop on the airborne measurement of wind, turbulence, and position
[PB92-139963] p 2410 N92-23587
WIND TUNNEL TESTS
Survey of experimental techniques for performance prediction p 2309 N92-23954
WIND VELOCITY
WAMDII: The Wide Angle Michelson Doppler Imaging Interferometer
[NASA-TM-105526] p 2441 N92-23525
Wind, current and temperature data at 0 deg, 165 deg E: January 1986 to March 1991
[PB92-143080] p 2411 N92-23682
WINDING
Analysis of a 37 kW cage-induction motor
[PB92-142116] p 2369 N92-23496
WINDPOWER UTILIZATION
PHOTO: A computer simulation program for photovoltaic and hybrid energy systems. Document and user's guide
[PB92-141928] p 2403 N92-23683
WING PROFILES
Adaptive active flutter suppression of wings in subsonic and transonic flight regimes p 2310 N92-24010
WINGS
Comparison of two-dimensional and three-dimensional droplet trajectory calculations in the vicinity of finite wings
[NASA-TM-105617] p 2373 N92-23154
Sensitivity analysis of dynamic aeroelastic responses
p 2306 N92-23229
Application of multidisciplinary optimization methods to the design of a supersonic transport
p 2307 N92-23230
Application of analytical and design tools for fighter wing aeroelastic tailoring p 2307 N92-23231
The structural optimization system OPTSYS: Current status and applications p 2307 N92-23232
Simultaneous stress and flutter optimization for the wing of a transport aircraft equipped with four engines
p 2308 N92-23238
WIRING
MBT-WIRE: Intelligent CAD in wiring design
[REPT-1.1.4] p 2419 N92-23856
On generating two dimensional CMOS cells
[REPT-1.3.2] p 2421 N92-23869
Breathing maze router for analog VLSI cell generation
[REPT-1.3.3] p 2422 N92-23870
WOOD
Influence of maleic anhydride as a coupling agent on the performance of wood fiber: Polystyrene composites
p 2343 N92-23945
Filling high density polyethylene with cellulosic fibers. 1: The effect of additives on fiber dispersion
p 2344 N92-23948
WORK
Procedure improvement enterprises
[DE92-003222] p 2453 N92-23183
WORKLOADS (PSYCHOPHYSIOLOGY)
Mental workload and performance experiment (15-IML-1) p 2361 N92-23628
WORKSTATIONS
Framework Programmable Platform for the advanced software development workstation: Framework processor design document
[NASA-CR-190173] p 2418 N92-23554
Infrastructure and training of manpower for CAD/CAM systems
[REPT-4.2.2] p 2425 N92-23888
WORMS
Genetic and molecular dosimetry of HZE radiation (7-IML-1) p 2357 N92-23603
WRINKLING
Nonlinear finite-element analysis of sandwich shells
p 2326 N92-23802

X

X RAY ANALYSIS
X ray analysis spectrometer
[DE92-615124] p 2378 N92-23219
Ion Microtomography (IMT) and Particle-Induced X ray Emission (PIXE) analysis direct drive of Inertial Confinement Fusion (ICF) targets
[DE92-008614] p 2446 N92-24067
X RAY APPARATUS
X ray based displacement measurement for hostile environments
[NASA-TM-105551] p 2378 N92-23155
X RAY BINARIES
Observations of accretion discs in interacting binaries
p 2454 N92-23673
TeV gamma ray emission from accreting binary pulsars p 2460 N92-23736
X RAY IMAGERY
Digital data registration and differencing compression system
[NASA-CASE-SSC-00010-2] p 2453 N92-23550
X RAY SOURCES
X ray based displacement measurement for hostile environments
[NASA-TM-105551] p 2378 N92-23155
Nuclear winds in active galaxies p 2457 N92-23716
X RAY SPECTRA
The origins of the cosmic x ray and gamma ray backgrounds p 2460 N92-23141
X RAY SPECTROSCOPY
An XPS study of the stability of Fomblin Z25 on the native oxide of aluminum --- x ray photoelectron spectroscopy
[NASA-TM-105594] p 2353 N92-23185
In situ XANES study of the valence state of chromium during electrochemical polarization of AlCr alloys
[DE92-007452] p 2350 N92-23197
Application of x ray absorption spectroscopy to the study of corrosion and inhibition
[DE92-007456] p 2350 N92-23198
Applications of x ray synchrotron radiation techniques to the study of dispersed electrocatalysts in high area materials
[DE92-007458] p 2346 N92-23199
X ray analysis spectrometer
[DE92-615124] p 2378 N92-23219
Quantification of surface functional groups of carbon fibers by x ray photoelectron spectroscopy
p 2343 N92-23946
X RAY STARS
Discovery of orbital decay in SMC X-1
[NASA-CR-190214] p 2317 N92-23531
X RAYS
The origins of the cosmic x ray and gamma ray backgrounds p 2460 N92-23141
X ray Fourier transform holography: Beyond the optical diffraction limit p 2377 N92-23144
Applications of x ray synchrotron radiation techniques to the study of dispersed electrocatalysts in high area materials
[DE92-007458] p 2346 N92-23199
An x ray diagnostic of electron power loss
[DE92-008599] p 2444 N92-23523
TeV gamma ray emission from accreting binary pulsars p 2460 N92-23736
Low dose neutron late effects: Cataractogenesis
[DE92-005539] p 2414 N92-24033
High-performance multilayer mirrors for soft x ray projection lithography
[DE92-008615] p 2443 N92-24049
Ion Microtomography (IMT) and Particle-Induced X ray Emission (PIXE) analysis direct drive of Inertial Confinement Fusion (ICF) targets
[DE92-008614] p 2446 N92-24067
XENON
Investigations of breakdown of rare gases by short pulses of 1.06(mu)m laser radiation
[DE92-615399] p 2379 N92-23131

Y

YAG LASERS
Nd: YAG laser welding aluminum alloys
[DE92-003131] p 2381 N92-23177
Cracking investigation of Nd:YAG laser welded gold plated glass sealing alloys
[DE92-007971] p 2387 N92-23216
YAW
Pinhole cameras as sensors for atomic oxygen in orbit: Application to attitude determination of the LDEF
p 2379 N92-23283
YTTRIUM OXIDES
NQR investigation of pressure-induced charge transfer in oxygen-deficient YBa2Cu3O(7-delta) (delta = 0.38)
[DE92-008441] p 2450 N92-24036

Z

ZIRCONIUM ALLOYS
Hydrogen absorption by zirconium alloy cladding tube with surface oxide film
[DE92-750962] p 2351 N92-23265
ZIRCONIUM OXIDES
Profiling and mapping of advanced materials using spatially resolved Raman spectroscopy
[DE92-008304] p 2347 N92-23449

Guanidine based vehicle/binders for use with oxides, metals, and ceramics
[NASA-CASE-LEW-15314-1] p 2354 N92-23461
ZONAL FLOW (METEOROLOGY)
A model of large-scale instabilities in the Jovian troposphere p 2459 N92-23704

Typical Personal Author Index Listing

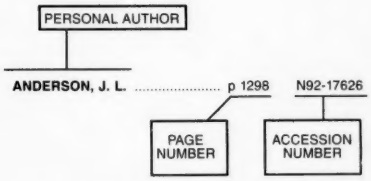

Listings in this index are arranged alphabetically by personal author. The page number helps you locate the citation in the abstract section. The accession number denotes the number by which the citation is identified.

A

ABAZOV, A. I. ..... p 2438 N92-23747
ABDELWAHAB, M. ..... p 2460 N92-23909
ABUMERI, GALIB H. ..... p 2387 N92-23196
ACKLEY, KEITH A. ..... p 2418 N92-23554
ACUNA, MARIO ..... p 2316 N92-23920
ADAMS, B. E. ..... p 2445 N92-23905
ADAMS, JAMES H., JR. ..... p 2461 N92-23307
ADIBNAZARI, SAEED ..... p 2352 N92-23725
ADLER, RICHARD M. ..... p 2427 N92-23360
AGATONOVIC, P. ..... p 2327 N92-23809
AGER, J. W., III ..... p 2347 N92-23449
AGRAWAL, GOPAL ..... p 2425 N92-23583
AHARONY, R. ..... p 2425 N92-23888
AHN, S. C. ..... p 2368 N92-23326
AHNERT, P. ..... p 2410 N92-23439
p 2410 N92-23494
p 2411 N92-23746
AHRENS, E. T. ..... p 2450 N92-24036
AIT-OUAMER, FARID ..... p 2455 N92-23695
AJAY, S. ..... p 2368 N92-23246
AKDENIZ, Z. ..... p 2350 N92-23211
AKSJONOV, STANISLAV P. ..... p 2319 N92-23757
AL-ORAINY, ABDULLAH ABDULAZIZ
p 2367 N92-24019
AL-SHUKRI, ALI MOHAMMAD S. A.
p 2457 N92-23696
ALAVA, M. J. ..... p 2444 N92-23663
ALEXANDER, HAROLD L. ..... p 2361 N92-23628
ALEXIOU, KIMON ..... p 2333 N92-23849
ALLBROOKS, M. ..... p 2336 N92-23323
ALLBROOKS, MARTHA K. ..... p 2454 N92-23313
p 2336 N92-23314
p 2336 N92-23321
p 2336 N92-23324
ALLEN, JOSEPH P. ..... p 2313 N92-23648
ALMEIDA, C. F. B. ..... p 2421 N92-23865
ALSING, PAUL MARTIN ..... p 2442 N92-23999
ALVES, BORIS KRAJNC ..... p 2387 N92-23159
AMARI, SACHIKO ..... p 2349 N92-23316
AMBROSE, BRYAN ..... p 2356 N92-23555
AMBROSE, K. R. ..... p 2412 N92-23518
AMLID, O. ..... p 2326 N92-23802
ANCIANT, M. ..... p 2435 N92-23170
ANDERSON, ALLEN JOEL ..... p 2315 N92-23915
ANDERSON, W. KYLE ..... p 2305 N92-23533
ANDERSSON, M. ..... p 2371 N92-23678
ANDERSSON, P. ..... p 2390 N92-23152
ANDREWS, HARRY ..... p 2313 N92-23646
ANGEL, S. M. ..... p 2355 N92-24068
ANGRILLI, F. ..... p 2331 N92-23834
ANGSTADT, R. ..... p 2453 N92-23212
ANGSTADT, R. D. ..... p 2368 N92-23326
ANOSOV, O. L. ..... p 2438 N92-23747
ANSELMI, ALBERTO ..... p 2316 N92-23922
ANSELMO, L. ..... p 2334 N92-23972
ANTOINE, LISA ..... p 2425 N92-23959
ANTOLAK, A. J. ..... p 2446 N92-24067
ANZ-MEADOR, P. D. ..... p 2335 N92-23978
ARAI, IKUO ..... p 2397 N92-23472
ARIKAN, E. ..... p 2417 N92-23420
p 2418 N92-23421
ARKKIO, A. ..... p 2369 N92-23496
ARMANIOS, ERIAN A. ..... p 2340 N92-23532
ARMSTRONG, T. W. ..... p 2439 N92-23292
p 2440 N92-23304
p 2440 N92-23305
ARNAUD, SARA B. ..... p 2414 N92-23424
ARNOLD, STEVEN M. ..... p 2340 N92-23195
ARUGA, TADASHI ..... p 2396 N92-23468
ASSEL, R. A. ..... p 2401 N92-23659
ASTON, D. ..... p 2436 N92-23327
ATKINSON, D. ..... p 2336 N92-23323
ATKINSON, DALE R. ..... p 2454 N92-23313
p 2336 N92-23314
p 2336 N92-23321
p 2336 N92-23324
AUGUST, R. A. ..... p 2460 N92-23293
AUGUSTEIJN, MARIJKE F. ..... p 2427 N92-23366
AWAYA, YOSHIO ..... p 2397 N92-23473
AYDORE, SAVAS ..... p 2372 N92-23146
AYIK, S. ..... p 2440 N92-23276
AYRES, J. C. ..... p 2307 N92-23233
AZUMI, MASAFUMI ..... p 2443 N92-23133

B

BABEL, HANK ..... p 2323 N92-23785
BACHMUTSKY, V. ..... p 2420 N92-23659
BACK, L. H. ..... p 2403 N92-23569
BAGAASEN, L. M. ..... p 2348 N92-23572
BAGCHI, A. ..... p 2434 N92-23505
BAGLIONI, P. ..... p 2331 N92-23834
BAKER, J. E. ..... p 2371 N92-23735
BALAKRISHNAN, A. V. ..... p 2442 N92-23567
BALBEKOV, V. I. ..... p 2436 N92-23274
BALLINGER, C. T. ..... p 2439 N92-24005
BALMINO, GEORGES ..... p 2317 N92-23925
BAMBERGER, J. A. ..... p 2459 N92-23124
BANGERT, V. ..... p 2433 N92-23599
BANSAL, NAROTTAM P. ..... p 2449 N92-23890
BANSEMIR, H. ..... p 2332 N92-23840
BARKER, A. J. ..... p 2325 N92-23800
BARKER, DANIEL K. ..... p 2307 N92-23231
BARKHOUDARIAN, S. ..... p 2320 N92-23762
BARLIER, FRANCOIS ..... p 2317 N92-23927
BARON, J. ..... p 2407 N92-24003
BARTELS, F. ..... p 2324 N92-23792
BARTHELEMY, J.-F. M. ..... p 2307 N92-23230
BARTON, J. M. ..... p 2374 N92-23542
BARTS, R. ..... p 2364 N92-23245
BASSANINO, M. ..... p 2315 N92-23914
BATTAGLIA, P. E. ..... p 2334 N92-23972
BATTLE, D. S. ..... p 2368 N92-23140
BATTRICK, B. ..... p 2333 N92-23987
BAUMGARDNER, D. ..... p 2410 N92-23587
BEAGLEY, N. R. ..... p 2329 N92-23824
BEAHM, LORRAINE P. ..... p 2461 N92-23307
BEAUJEAN, R. ..... p 2440 N92-23308
BEAUMONT, P. W. R. ..... p 2324 N92-23793
BEBEK, C. ..... p 2378 N92-23278
BEGGS, JOHN H. ..... p 2365 N92-23425
p 2366 N92-23528
BEHRMANN, H. ..... p 2392 N92-23379
p 2394 N92-23392
BELCHER, JEWELL G. ..... p 2416 N92-24044
p 2416 N92-24056
BELDI, M. ..... p 2321 N92-23811
BELLIS, HAROLD ..... p 2314 N92-23652
BEN-ARIEH, D. ..... p 2424 N92-23886
BENCH, G. S. ..... p 2446 N92-24067
BENHENNI, M. ..... p 2439 N92-24026
BENTON, E. R. ..... p 2461 N92-23302
p 2440 N92-23303
BENTON, E. V. ..... p 2439 N92-23292
p 2461 N92-23302
p 2440 N92-23303
BENZEGGAGH, M. L. ..... p 2343 N92-23943
BERG, ROBERT F. ..... p 2383 N92-23564
BERGAN, P. G. ..... p 2326 N92-23802
BERKE, L. ..... p 2388 N92-23527
BERNARD, ALAIN ..... p 2316 N92-23918
BERNELLI-ZAZZERA, F. ..... p 2330 N92-23830
BERNHARD, R. P. ..... p 2336 N92-23323
BERNHARD, RONALD P. ..... p 2458 N92-23315
BERRIOS, WILLIAM M. ..... p 2336 N92-23284
BERTHELON, T. ..... p 2324 N92-23789
BERTOGLIO, F. ..... p 2326 N92-23807
BEYSENS, D. ..... p 2362 N92-23638
BHASIN, KUL B. ..... p 2365 N92-23414
p 2365 N92-23415
BHATT, H. S. ..... p 2400 N92-23491
BIANCHINI, G. ..... p 2331 N92-23834
BIANCO, GIUSEPPE ..... p 2316 N92-23924
BIDWELL, COLIN S. ..... p 2373 N92-23154
BIEFELD, R. M. ..... p 2450 N92-24034
BIENZ, T. ..... p 2436 N92-23327
BIRD, E. L. ..... p 2353 N92-24006
BIRD, F. ..... p 2436 N92-23327
BIRMINGHAM, MARK ..... p 2402 N92-23367
BIRO, D. A. ..... p 2343 N92-23944
BISSCHOP, J. J. ..... p 2418 N92-23507
BIVAS, AVI ..... p 2424 N92-23887
BLACK, MARTIN THOMAS ..... p 2409 N92-23772
BLANC, J. P. C. ..... p 2430 N92-23508
BLANCHARD, C. ..... p 2324 N92-23790
BLEEKER, H. ..... p 2421 N92-23867
BLELLOCH, P. A. ..... p 2329 N92-23824
BLINN, THOMAS M. ..... p 2418 N92-23554
BLOCH, J. J. ..... p 2455 N92-24027
BLOCK, I. ..... p 2359 N92-23618
BLOND, EDMUND ..... p 2321 N92-23980
BOBROWSKI, S. F. ..... p 2408 N92-23741
BOEHM, M. ..... p 2410 N92-23520
BOENSCH, FRANK D. ..... p 2310 N92-23822
BOESSWETTER, C. ..... p 2392 N92-23379
p 2392 N92-23380
p 2392 N92-23383
p 2394 N92-23398
p 2395 N92-23403
p 2395 N92-23404
p 2395 N92-23405
p 2395 N92-23406
p 2395 N92-23407
p 2395 N92-23408
p 2396 N92-23410
p 2396 N92-23411
BOHLMANN, JONATHAN D. ..... p 2307 N92-23231
BONNEFOY, RENE ..... p 2315 N92-23916
BONNET, C. ..... p 2330 N92-23831
p 2331 N92-23836
BOOKER, MATTIE ..... p 2409 N92-23960
BOPPE, CHARLES W. ..... p 2309 N92-23957
BORG, JANET ..... p 2458 N92-23310
BOSCH, J. ..... p 2461 N92-23306
BOSSAERT, G. ..... p 2325 N92-23799
BOULLENGER, G. ..... p 2321 N92-23798
BOULPAEP, F. ..... p 2328 N92-23818
p 2330 N92-23832
BOUSQUET, P. W. ..... p 2324 N92-23787
BOUZAKIS, K.-D. ..... p 2422 N92-23874
BOYLE, K. M. ..... p 2374 N92-23516
BOYNTON, P. ..... p 2317 N92-23531
BOZEMAN, RICHARD J., JR. ..... p 2378 N92-23545
BRADLEY, R. A. ..... p 2405 N92-23204
p 2405 N92-23333
BRAMA, TORSTEN ..... p 2307 N92-23232
BRAMBLE, J. H. ..... p 2432 N92-23329
BRANTLEY, LARRY W. ..... p 2372 N92-24047
BRESLER, STEWART A. ..... p 2423 N92-23880
BREWE, DAVID E. ..... p 2381 N92-23226
BREWER, T. R. ..... p 2346 N92-23181
BREZINI, A. ..... p 2350 N92-23210
p 2448 N92-23581
BRIARTY, L. G. ..... p 2359 N92-23616
BRILL, YVONNE C. ..... p 2321 N92-23980
BRITT, DANIEL TURNER, III ..... p 2457 N92-23770
BROOKS, DONALD E. ..... p 2360 N92-23621
BROOKS, J. N. ..... p 2445 N92-24021
BROST, R. C. ..... p 2430 N92-23458
BROWN, ALLAN H. ..... p 2356 N92-23601
BROWN, BETH A. ..... p 2456 N92-23962

BROWN, HELEN C. p 2387 N92-23196
BROWN, LAMARR A. p 2380 N92-23961
BROWN, R. p 2448 N92-23574
BROWNING, L. p 2383 N92-23680
BROWNLEE, DON p 2336 N92-23319
BROWNLEE, DONALD E. p 2458 N92-23315
BRUSCHI, CARLO p 2357 N92-23604
BRYAN, M. A p 2368 N92-23200
BUCHER, C. G. p 2328 N92-23816
BUCK, C. p 2331 N92-23838
BUCKLEY, BRIAN p 2427 N92-23361
BUDGELL, DEREK R. p 2342 N92-23940
BUDIANSKY, BERNARD p 2321 N92-23980
BUECKER, D. H. p 2358 N92-23610
BUECKER, H. p 2361 N92-23627
BUEHLER, F. p 2459 N92-23325
BUGG, CHARLES E. p 2361 N92-23634
BUMPAS, STANLEY EUGENE p 2389 N92-23773
BUNCH, T. E. p 2336 N92-23319
BURKE, W. R. p 2322 N92-23780
BURNHAM, A. K. p 2348 N92-23904
BURNS, FORREST p 2439 N92-23296

C

CADORET, ROBERT p 2361 N92-23633
CAESAR, B. p 2333 N92-23850
CAIN, W. D. p 2425 N92-24035
CALABRO, MAX p 2320 N92-23766
CALLAGHAN, CHRISTOPHER E. p 2322 N92-23526
CALLAHAN, A. P. p 2412 N92-23518
CAMBRIDGE, VIVIEN J. p 2453 N92-23550
CAMPBELL, A. PETER p 2408 N92-23741
CAMPBELL, J. H. p 2380 N92-24065
CAMPBELL, WARREN p 2372 N92-24047
CAMURATI, P. p 2421 N92-23866
CANISTRARO, HOWARD A. p 2378 N92-23155
CAPITAINE, A. p 2324 N92-23789
CARAMARO, L. p 2342 N92-23939
CARDEN, JAMES R. p 2416 N92-24044
p 2416 N92-24056
CARDON, A. p 2328 N92-23818
p 2330 N92-23832
CARY, J. R. p 2436 N92-23217
CASELLA, G. I. p 2343 N92-23946
CASTLES, STEPHEN H. p 2378 N92-23460
CATON, RANDALL p 2369 N92-23430
CEDER, G. p 2353 N92-23984
CHABERT, B. p 2342 N92-23939
CHALLENER, S. A. p 2324 N92-23788
CHAMIS, C. C. p 2339 N92-23194
CHAMIS, CHRISTOS C. p 2388 N92-23267
CHANG, C. T. p 2304 N92-23355
CHANG, CHEN-CHUNG STEVE p 2352 N92-23718
CHANG, J. Y. p 2461 N92-23301
CHANG, YAN-TYNG p 2437 N92-23450
CHANTERANNE, JACQUES p 2319 N92-23760
CHATELAIN, J. p 2330 N92-23826
CHAU, KAM TIM p 2389 N92-23737
CHAUCHARD, J. p 2342 N92-23939
CHEATHAM, JOHN B., JR. p 2429 N92-23438
CHEMOUL, B. p 2321 N92-23797
CHEN, ANSONG p 2339 N92-23157
CHEN, BAIO p 2425 N92-23583
CHEN, CHIEN-CHUNG p 2442 N92-23551
CHEN, K. C. p 2366 N92-23575
CHEN, NANXIAN p 2351 N92-23582
CHEN, Y. C. p 2417 N92-23420
p 2418 N92-23422
CHENG, JULIAN p 2442 N92-23748
CHERN, ENGMIN J. p 2386 N92-23376
p 2388 N92-23549
CHESNUT, S. M. p 2364 N92-23173
CHESTER, MARGARET MCMATH p 2459 N92-23171
CHETTRI, SAMIR R. p 2402 N92-23367
CHIEN, STEVE p 2427 N92-23362
CHITSOMBOON, TAWIT p 2302 N92-23342
CHIU, ING-TSAU p 2425 N92-23991
CHIU, S. C. p 2444 N92-23446
CHOE, KYU YEARL p 2433 N92-23738
CHOLEWA, M. p 2446 N92-24067
CHOO, YUNG K. p 2305 N92-23563
CINGI, C. p 2350 N92-23179
CIVALE, L. p 2448 N92-23574
CLARIOU, JEAN-PIERRE p 2319 N92-23760
CLARK, G. A. p 2417 N92-23255
CLERC, CHRISTIAN p 2327 N92-23812
CLOUGH, R. L. p 2354 N92-23442
COEN, P. G. p 2307 N92-23230
COFFEY, H. E. p 2459 N92-23701
p 2460 N92-23993
COGAN, S. p 2333 N92-23848
COGOLI, AUGUSTO p 2358 N92-23613
p 2358 N92-23614
p 2359 N92-23615
COIFFIER, B. p 2308 N92-23239
COLBORN, B. L. p 2440 N92-23304
p 2440 N92-23305
COLEMAN, R. V. p 2448 N92-23721
COLOZZA, ANTHONY J. p 2404 N92-24057
COOKE, WILLIAM J. p 2458 N92-23317
COOPER, PAUL A. p 2390 N92-23992
COOPER, ROBERT S. p 2321 N92-23980
CORBET, JONATHAN M. p 2408 N92-23741
CORNUAULT, C. p 2308 N92-23239
COTANCH, S. R. p 2437 N92-23577
COTTON, JAMES DEAN p 2351 N92-23566
COTTON, W. R. p 2409 N92-23257
COUTROT, ALAIN p 2319 N92-23755
CRAWLEY, NIGEL p 2420 N92-23862
CROMP, ROBERT F. p 2402 N92-23367
p 2429 N92-23373
CRONIN, MIKE p 2314 N92-23653
CROSLEY, P. B. p 2389 N92-23681
CROSS, G. p 2320 N92-23762
CROWE, MICHAEL D. p 2322 N92-23526
CROWTHER, R. p 2318 N92-23973
CRUMP, WES p 2418 N92-23554
CRUTCHER, E. R. p 2349 N92-23286
p 2335 N92-23287
p 2349 N92-23288
p 2439 N92-23289
CSIGE, I. p 2461 N92-23302
p 2440 N92-23303
CULLEN, D. E. p 2439 N92-24005
CURRAN, T. p 2406 N92-23517
CURTIS, L. J. p 2437 N92-23448
CUTCHIN, J. H. p 2460 N92-23293
CUTTS, DANNIE E. p 2428 N92-23370

D

DADHWAL, V. K. p 2400 N92-23490
DAERDEN, I. p 2328 N92-23818
p 2330 N92-23832
DAMYANOV, B. P. p 2432 N92-23331
DANIELL, JIM p 2421 N92-23868
DANIEWICZ, STEVE p 2384 N92-23739
DAR-EL, E. M. p 2423 N92-23876
DARDEN, E. B. p 2414 N92-23139
DAVARI, SADEGH p 2425 N92-23583
DAVE, R. S. p 2344 N92-23947
DAVENPORT, A. J. p 2350 N92-23197
p 2350 N92-23198
DAVID, VALERIE p 2318 N92-23750
DAVIS, E. S. p 2316 N92-23919
DAVIS, P. L. p 2453 N92-23183
DAY, MICHAEL p 2342 N92-23940
DEAN, GARVIN p 2372 N92-24047
DEBURIJN, J. C. M. p 2354 N92-23510
DECLERQ, F. p 2325 N92-23799
DEETER, J. p 2317 N92-23531
DEFONTAINE, D. p 2353 N92-23984
DEFOURNY, P. p 2400 N92-23488
DEIS, DAN W. p 2314 N92-23654
DEJESUSLAFUENTE, CARLOS E. p 2368 N92-23963
DEJONGE, P. J. p 2432 N92-23514
DELANO, BRENDA p 2425 N92-23689
DELLACORTE, CHRISTOPHER p 2339 N92-23190
p 2381 N92-23435
DELOO, P. p 2327 N92-23814
DELVIGS, PETER p 2355 N92-24053
DEMISCH, WOLFGANG H. p 2321 N92-23980
DEMPSEY, ROBERT C. p 2458 N92-24015
DERMER, C. D. p 2438 N92-23903
DEROEY, F. p 2328 N92-23818
p 2330 N92-23832
DERRICKSON, JAMES H. p 2439 N92-23292
DESIMONI, E. p 2343 N92-23946
DESLANDES, Y. p 2343 N92-23944
DESNOYER, D. p 2329 N92-23821
p 2331 N92-23838
DEVINCENT, SANDRA M. p 2351 N92-23436
DEVISSCHER, J. p 2328 N92-23818
p 2330 N92-23832
DEZOTTI, S. p 2324 N92-23791
DHURIA, HARBANS L. p 2410 N92-23431
DIBROZOLO, F. RADICATI p 2336 N92-23319
DILTS, DAVID M. p 2424 N92-23883
DIMALANTA, ARTURO S. p 2427 N92-23366
DIMMICH, R. p 2443 N92-24029
DING, B. N. p 2368 N92-23186
DIRECTOR, STEPHEN W. p 2421 N92-23868
DOANE, GEORGE B., III p 2372 N92-24047
DOBRY, A. p 2446 N92-23270
DOGGETT, E. D. p 2411 N92-23660
DOHERTY, MICHAEL P. p 2337 N92-23252
DOMINGO, C. p 2461 N92-23306
DONG, BONIAN p 2375 N92-23997
DORFMAN, ERIK p 2429 N92-23373
DOVI, A. R. p 2307 N92-23230
DRESCHEL, T. W. p 2406 N92-23898
DREVINSKY, P. J. p 2370 N92-23562
DREW, D. A. p 2373 N92-23202
DREYSSE, H. p 2353 N92-23984
DROEGE, M. W. p 2349 N92-24064
DROEGE, T. F. p 2368 N92-23326
DROR, M. p 2424 N92-23886
DRUMMOND, CHARLES H., III p 2449 N92-23890
DRUMMOND, T. J. p 2450 N92-24034
DU, GUANG-WU p 2381 N92-23435
DUBOIS, J. p 2323 N92-23784
DUKE, JACKIE p 2357 N92-23605
DUNN, D. p 2364 N92-23245
DUNWOODIE, W. p 2436 N92-23327
DURIC, NEBOJSA p 2454 N92-23428
DURKIN, JOHN p 2427 N92-23365
DYER, C. S. p 2439 N92-23295

E

EARLY, EDWARD ALLEN p 2448 N92-23774
ECKERT, L. p 2333 N92-23850
ECKLUND, W. L. p 2401 N92-23521
ECKLUND, WAYNE p 2382 N92-23547
p 2386 N92-24059
EDULJEE, R. F. p 2343 N92-23942
EDWARDS, B. C. p 2455 N92-24027
EDWARDS, D p 2408 N92-23741
EDWARDS, D. P. p 2408 N92-23522
EDWARDS, R. p 2411 N92-23906
EFIMOCHKIN, A. F. p 2319 N92-23757
EFSTATHIOU, K. p 2422 N92-23874
EISENBERG, R. p 2347 N92-23332
EKLUND, J. E. p 2350 N92-23176
EL-KAWNI, M. I. p 2447 N92-23272
ELDER, M. L. p 2380 N92-24065
ELIASSON, PETER p 2304 N92-23168
ELROD, HAROLD G. p 2381 N92-23226
ELY, D. W. p 2460 N92-23293
ELY, R. p 2378 N92-23278
EMURIAN, H. H. p 2415 N92-23513
ENGE, W. p 2440 N92-23308
ENSMAN, LISA MARIE p 2458 N92-24017
ERBOLUKBAS, A. p 2350 N92-23211
ERCOLI-FINZI, F. p 2330 N92-23830
ERES, D. p 2447 N92-23447
ERMUTLU, M. E. p 2367 N92-23668
EROGLU, ADNAN p 2375 N92-23995
EUGSTER, O. p 2459 N92-23325
EURY, SERGE p 2319 N92-23758
p 2319 N92-23759
EVANS, DAVID J. p 2459 N92-23697
EVENSON, ERIK E. p 2385 N92-24051
EYMARD, MICHEL p 2320 N92-23767
EZELL, W. p 2320 N92-23762

F

FABRIS, G. p 2403 N92-23569
FAILOR, R. A. p 2438 N92-23903
FAIZOV, E. L. p 2438 N92-23747
FANTI, G. p 2331 N92-23834
FAORO, R. p 2406 N92-23517
FARRELL, K. p 2447 N92-23444
FAULKNER, D. N. p 2414 N92-23139
FAYER, M. D. p 2346 N92-23181
FEDDEMA, JOHANNES JAN p 2411 N92-23771
FEHL, D. L. p 2445 N92-23749
FELDMAN, JACK A. p 2421 N92-23869
FELICELLI, SERGIO DANIEL p 2353 N92-24014
FERBER, M. K. p 2354 N92-23223
FERGUSON, BRUCE W. p 2313 N92-23644
FERGUSSON, NEIL J. p 2388 N92-23427
FESSATIDIS, VASSILIOS p 2449 N92-23775
FEUER, Z. p 2423 N92-23876
FEUSTEL-BUEECHL, J. p 2318 N92-23751
FIALKO, R. W. p 2380 N92-23723
FIMPEL, H. P. p 2410 N92-23587
FINCK, BERNARD p 2320 N92-23765
FINCKENOR, MIRIA p 2335 N92-23311
FINKEL, SEYMOUR I. p 2312 N92-23240
p 2312 N92-23242
p 2312 N92-23243
p 2312 N92-23244
FINKENZELLER, H. p 2395 N92-23402
FINNEY, W. C. p 2439 N92-24031
FISA, B. p 2344 N92-23949
FISHMAN, G. J. p 2461 N92-23294
p 2440 N92-23300
FITZ-SIMONS, T. p 2406 N92-23517
FLATMAN, J. C. p 2439 N92-23295
FLEMING, RONALD H. p 2336 N92-23319
FLICKE, H.-P. p 2332 N92-23844

FLOM, YURY ... p 2388 N92-23549
FLUSS, M. J. ... p 2449 N92-23986
p 2450 N92-24007
FLYNN, M. R. ... p 2374 N92-23516
FONTIJIN, A. ... p 2347 N92-23221
FOOTE, JOHN ... p 2349 N92-23316
FOOTE, MARC C. ... p 2370 N92-23552
FOSTER, LISA M. ... p 2434 N92-23964
FOSTER, ROGER SHERMAN, III ... p 2456 N92-23126
FOURKAS, J. T. ... p 2346 N92-23181
FOX, R. J. ... p 2367 N92-23900
FRADKIN, E. S. ... p 2435 N92-23207
FRALICK, GUSTAVE C. ... p 2378 N92-23155
FRANCESCONI, DANIELE ... p 2330 N92-23827
FRANK, A. L. ... p 2461 N92-23302
p 2440 N92-23303
FRANK, N. ... p 2406 N92-23517
FRANKEL, G. S. ... p 2350 N92-23197
FRANZINI, P. ... p 2368 N92-23326
FREAS, W. ... p 2406 N92-23517
FREDERICK, MARTIN E. ... p 2403 N92-23463
FREDRICK, L. ... p 2342 N92-23938
FREITAG, H. P. ... p 2411 N92-23682
FRENKLACH, M. ... p 2348 N92-23685
FRERKING, MARGARET A. ... p 2369 N92-23464
FREY, J. D. ... p 2323 N92-23784
FRIEDBERG, W. ... p 2414 N92-23139
FRIGO, L. A. ... p 2440 N92-23303
FRITZ, H.-G. ... p 2342 N92-23941
FRULLA, G. ... p 2326 N92-23804
FUESS, D. A. ... p 2344 N92-23988
FUJIMURA, KIKUO ... p 2429 N92-23457
FUJINO, KAZUO ... p 2399 N92-23482
FUJITA, MASAHARU ... p 2396 N92-23467
FUJIYOSHI, YASUSHI ... p 2399 N92-23483
FUKUE, KIYONARI ... p 2397 N92-23469
FUKUYAMA, ATSUSHI ... p 2443 N92-23133

G

GAEDKE, MICHAEL ... p 2325 N92-23794
GAHN, RANDALL F. ... p 2404 N92-24054
GALLER, D. E. ... p 2337 N92-23982
GAMAL, Y. E. E. D. ... p 2379 N92-23131
GARAUD, X. ... p 2323 N92-23784
GARDINER, W. C. ... p 2348 N92-23685
GARG, H. K. ... p 2400 N92-23491
GARRETT, J. D. ... p 2441 N92-23445
GARSCADDEN, ALAN ... p 2354 N92-23192
GARZON, I. L. ... p 2351 N92-23573
GATES, THOMAS S. ... p 2340 N92-23434
GAUDERT, P. C. ... p 2341 N92-23937
GAUTAM, N. ... p 2400 N92-23489
GAVEL, D. T. ... p 2430 N92-24066
GAVIN, JOSEPH G., JR. ... p 2321 N92-23980
GAVRIN, V. N. ... p 2438 N92-23747
GAYLE, T. M. ... p 2337 N92-23722
GEENEN, F. ... p 2339 N92-23174
GEISS, J. ... p 2459 N92-23325
GELMAN, M. ... p 2410 N92-23439
p 2410 N92-23494
p 2411 N92-23746
GEORGES, T. M. ... p 2412 N92-23669
GEYNISMAN, M. ... p 2433 N92-23579
GHIRARDI, C. ... p 2451 N92-23206
GHOSH, M. K. ... p 2434 N92-23505
GIANGANO, D. ... p 2461 N92-23301
GIBSON, JERRY D. ... p 2417 N92-23417
p 2417 N92-23418
GIESSLER, A. ... p 2332 N92-23842
GILL, THOMAS GRANDON ... p 2454 N92-24016
GILLAND, JAMES H. ... p 2338 N92-24004
GILLEN, K. T. ... p 2354 N92-23442
GILLESPIE, J. W., JR. ... p 2343 N92-23942
GIRARD, A. ... p 2324 N92-23790
p 2330 N92-23828
GIRAUDBIT, JEAN-NOEL ... p 2327 N92-23812
GLOOS, K. ... p 2379 N92-23594
GOETTING, H. C. ... p 2328 N92-23819
GOLDSTON, R. ... p 2445 N92-24020
GOMAA, HASSAN ... p 2428 N92-23371
GOMEZ, FERNANDO ... p 2429 N92-23372
GONCALVES, F. ... p 2421 N92-23865
GONDA, STEVE R. ... p 2413 N92-24052
GONG, X. J. ... p 2343 N92-23943
GONZALEZBLASQUEZ, A. L. ... p 2321 N92-23608
GOVINDARAJAN, S. ... p 2451 N92-24040
GRANT, R. L. ... p 2323 N92-23783
GRAY, J. A. ... p 2348 N92-23715
GRECO, A. ... p 2446 N92-23270
GREENE, RICHARD J. ... p 2429 N92-23374
GREGORY, J. C. ... p 2461 N92-23294
GREGORY, JOHN C. ... p 2379 N92-23283
GRIFFIS, DIETER P. ... p 2458 N92-23318
GRINBAUM, YAKOV ... p 2419 N92-23856
GRODSINSKY, CARLOS M. ... p 2383 N92-23564
GROOM, NELSON J. ... p 2364 N92-23989
GUELPEN, JOACHIM ... p 2323 N92-23782
GUIGON, M. ... p 2341 N92-23935
GUILLAUD, V. ... p 2329 N92-23825
GUNDY-BURLET, KAREN LEANN ... p 2311 N92-23671
GUPTA, ROOP N. ... p 2374 N92-23543
GUPTA, UDAY ... p 2427 N92-23363
GUPTILL, J. D. ... p 2388 N92-23527
GUR, RON ... p 2423 N92-23878
GUREVICH, D. ... p 2431 N92-23184

H

HADLEY, ROBERT HARRISON ... p 2456 N92-23127
HAGHIGHI, H. ... p 2449 N92-23986
p 2450 N92-24007
HAGUE, J. R. ... p 2384 N92-23896
HAHS, C. A. ... p 2367 N92-23900
HAIDER, O. ... p 2332 N92-23840
HAILYE, MICHAEL ... p 2304 N92-23269
HAINES, A. B. ... p 2309 N92-23954
HAIR, L. M. ... p 2349 N92-24064
HAJJ, G. ... p 2316 N92-23919
HALEVI, GIDEON ... p 2424 N92-23885
HALL, GARDINER A. ... p 2427 N92-23363
HALL, L. E. ... p 2307 N92-23230
HALL, L. J. ... p 2456 N92-23153
HALL, TIMOTHY MATHER ... p 2408 N92-23702
HALLER, E. E. ... p 2371 N92-23985
HALLIKAINEN, M. ... p 2396 N92-23441
HALONEN, K. ... p 2370 N92-23497
HAMAMATSU, KIYOTAKA ... p 2443 N92-23133
HAMDI, M. A. ... p 2332 N92-23846
HAMILTON, DAVID A. ... p 2322 N92-23796
HAMMEL, P. C. ... p 2450 N92-24036
HAMMOND, J. K. ... p 2435 N92-23170
HAMMOUD, AHMAD N. ... p 2370 N92-23538
p 2370 N92-23561
HANOCH, COBY ... p 2422 N92-23873
HANSELKA, HOLGER ... p 2326 N92-23805
HANSEN, W. L. ... p 2371 N92-23985
HARDING, W. B. ... p 2348 N92-23586
HARIHARAN, S. I. ... p 2374 N92-23565
HARMON, B. A. ... p 2461 N92-23294
p 2440 N92-23300
HARRIS, DAVID W. ... p 2336 N92-23319
HARRIS, RONALD J. ... p 2318 N92-23752
HARSTON, CRAIG ... p 2402 N92-23368
HARVEY, D. K. ... p 2380 N92-23723
HARVEY, GALE A. ... p 2339 N92-23290
HASAN, A. ... p 2412 N92-23518
HASEGAWA, KUNIKO ... p 2397 N92-23473
HASKINS, P. S. ... p 2460 N92-23293
HASSAN, M. H. A. ... p 2444 N92-23209
HATADA, MOTOYOSHI ... p 2353 N92-23134
HAWK, CLARK W. ... p 2321 N92-23980
HEATHCOTE, DAVID G. ... p 2356 N92-23602
HEFFNER, R. H. ... p 2450 N92-24036
HEIKKINEN, D. W. ... p 2446 N92-24067
HEIKKINEN, J. A. ... p 2444 N92-23663
HEINZE, P. ... p 2308 N92-23238
HEITZER, J. ... p 2331 N92-23835
HELGESON, W. D. ... p 2371 N92-23983
HELLMAN, K. H. ... p 2383 N92-23595
HELMINCK, G. F. ... p 2431 N92-23182
HELORET, JEAN-YVES ... p 2319 N92-23758
HEMMATI, HAMID ... p 2442 N92-23551
HENCKEN, K. R. ... p 2380 N92-24070
HENDERSON, TODD L. ... p 2305 N92-23563
HENKEL, DANIEL P. ... p 2435 N92-23556
HERMAN, P. ... p 2324 N92-23791
HERNANDEZ, J. E. ... p 2417 N92-23255
HERRERA-FIERRO, PILAR ... p 2353 N92-23185
HERRMANN, A. S. ... p 2331 N92-23839
HERTENSTEIN, R. F. A. ... p 2409 N92-23257
HESAARAKI, M. ... p 2443 N92-23208
HEYWARD, ANN O. ... p 2322 N92-23187
HICKS, P. ... p 2392 N92-23379
p 2394 N92-23393
p 2394 N92-23394
p 2394 N92-23395
p 2394 N92-23397
p 2394 N92-23399
p 2395 N92-23400
p 2395 N92-23401
HIELD, CHRISTOPHER ... p 2429 N92-23374
HILL, WILLIAM C. ... p 2312 N92-23240
p 2312 N92-23243
p 2312 N92-23244
HINKLE, C. R. ... p 2406 N92-23898
HISHIDA, MASATAKA ... p 2398 N92-23476
HO, ADRIAN HSIU-TZE ... p 2380 N92-23687
HO, YUKUN ... p 2440 N92-23130
HOBBS, J. D. ... p 2438 N92-23894
HOEIJMAKERS, H. W. M. ... p 2309 N92-23955
HOERNLEIN, H. R. E. M. ... p 2308 N92-23236
HOERZ, FRIEDRICH ... p 2336 N92-23314
p 2458 N92-23315
HOFESTAEDT, H. ... p 2421 N92-23864
HOLCOMBE, C. E., JR. ... p 2353 N92-24006
HOLLIDAY, M. ... p 2379 N92-23571
HOLTZBERG, F. H. ... p 2448 N92-23574
HOMEMDEMELLO, LUIZ S. ... p 2426 N92-23357
HOMM, A. ... p 2324 N92-23792
HONDA, OSAMU ... p 2398 N92-23477
HONECY, FRANK S. ... p 2311 N92-23225
HONEY, WILLIAM BRUCE ... p 2454 N92-23673
HOPKINS, RICHARD H. ... p 2314 N92-23654
HOPPE, A. ... p 2333 N92-23850
HORII, KENZI ... p 2407 N92-23262
HORNADY, R. S. ... p 2446 N92-24067
HORTON, R. D. ... p 2444 N92-23523
HORZ, FRED ... p 2336 N92-23324
HORZ, FRIEDRICH ... p 2336 N92-23323
HOSHINO, HIDEO ... p 2312 N92-23979
HOSKEN, BRUCE ... p 2429 N92-23372
HOSOE, NOBUYUKI ... p 2312 N92-23778
HOU, P. Y. ... p 2352 N92-23893
HOUET, H. ... p 2316 N92-23923
HOWELL, R. H. ... p 2438 N92-23903
p 2449 N92-23986
p 2450 N92-24007
HSIEH, CHIH-MING ... p 2382 N92-23536
HSU, ANDREW T. ... p 2301 N92-23337
p 2302 N92-23345
p 2302 N92-23346
p 2303 N92-23347
p 2303 N92-23348
p 2303 N92-23349
HUEHNERFUSS, H. ... p 2392 N92-23379
p 2393 N92-23385
HUFFORD, G. A. ... p 2364 N92-23180
HULL, RICHARD ... p 2429 N92-23372
HUMES, DONALD H. ... p 2335 N92-23309
HUNT, BRIAN D. ... p 2370 N92-23552
HUNTER, JERRY L. ... p 2458 N92-23318
HUPP, J. T. ... p 2346 N92-23203
HURLEY, DONNA L. ... p 2440 N92-23297
HUSEK, M. ... p 2431 N92-23248
HUSTON, RONALD L. ... p 2382 N92-23536
HYYPPAE, J. ... p 2396 N92-23441

I

IDZOREK, G. C. ... p 2368 N92-23200
IIDA, HIROMASA ... p 2443 N92-23132
IKEDA, AKIO ... p 2400 N92-23486
ILAIWI, K. F. ... p 2447 N92-23272
IMAMOGLU, ATAC ... p 2379 N92-23143
IMANARI, EI-ICHI ... p 2400 N92-23486
INAGAKE, DENZO ... p 2399 N92-23480
ISAACS, H. S. ... p 2350 N92-23197
p 2350 N92-23198
ISEKI, T. ... p 2352 N92-23720
ISHII, HARUO ... p 2398 N92-23476
ISOBE, SUSUMU ... p 2351 N92-23263
ISOPI, ROBERTO ... p 2319 N92-23756
ITABE, TOSHIKAZU ... p 2396 N92-23468
IVANOV, S. V. ... p 2436 N92-23274
IWATA, KEIICHI ... p 2398 N92-23477
IZZO, MARIO ... p 2316 N92-23922

J

JACKSON, G. L. ... p 2444 N92-23446
JACQUES, P. ... p 2400 N92-23488
JAHNES, C. V. ... p 2350 N92-23197
JAIN, ABHINANDAN ... p 2385 N92-24042
p 2385 N92-24043
JAIN, K. K. ... p 2368 N92-23186
JANG, JONG HOON ... p 2373 N92-23253
JANIN, G. ... p 2318 N92-23977
JANKOWSKI, A. F. ... p 2450 N92-24069
JARED, R. ... p 2378 N92-23278
JASKOWIAK, MARTHA H. ... p 2354 N92-23461
JAW, LINK CHING ... p 2310 N92-23122
JEGLEY, DAWN C. ... p 2344 N92-23981
JEHN, R. ... p 2318 N92-23976
JELLINEK, J. ... p 2351 N92-23573
JENKINS, G. S. ... p 2410 N92-23656
JENKINS, M. G. ... p 2354 N92-23223
JENKINS, R. A. ... p 2337 N92-23722
JERMAKIAN, JOEL ... p 2403 N92-23463
JESSBERGER, ELMAR K. ... p 2349 N92-23316
JIMENEZ, E. ... p 2387 N92-23216
JIMENEZ, EDGAR, JR. ... p 2381 N92-23177
JING, SICONG ... p 2451 N92-23501
JOCHUM, A. M. ... p 2410 N92-23587

JOH, CHANGYEOL ..... p 2305 N92-23717
JOHANNSMEIER, D. ..... p 2334 N92-23974
JOHNSON, GREGORY LYNN ..... p 2402 N92-23724
JOHNSON, M. ..... p 2453 N92-23212
JOHNSON, M. E. ..... p 2368 N92-23326
JOHNSON, W. B. ..... p 2436 N92-23327
JOHNSON, W. S. ..... p 2340 N92-23433
JONATHAL, D. ..... p 2440 N92-23308
JONES, CHERIE ..... p 2323 N92-23785
JONES, G., II ..... p 2355 N92-24037
JONES, K. M. ..... p 2438 N92-23903
JONES, KEN ..... p 2313 N92-23651
JONES, R. M. ..... p 2412 N92-23669
JONES, WILLIAM R. ..... p 2353 N92-23185
JORDON, ERIC H. ..... p 2378 N92-23155
JOURDON, N. ..... p 2329 N92-23825

K

KAISER, J. H. ..... p 2449 N92-23986
p 2450 N92-24007
KAJI, KANAKO ..... p 2353 N92-23134
KALIKHOV, A. V. ..... p 2438 N92-23747
KAMESAKI, KAZUHIKO ..... p 2323 N92-23781
KANBAYASHI, AKIO ..... p 2362 N92-23635
KANDYA, A. K. ..... p 2401 N92-23492
KANKKUNEN, A. ..... p 2371 N92-23678
KANTORCIK, T. ..... p 2461 N92-23301
KANZAWA, HIROSHI ..... p 2399 N92-23481
KAO, CHENG-YAN ..... p 2426 N92-23358
KAPANIA, RAKESH K. ..... p 2306 N92-23229
KARR, CLARK ..... p 2429 N92-23372
KASHANGAKI, THOMAS A-L. ..... p 2390 N92-23990
KASSEL, PHILLIP C. ..... p 2458 N92-23317
KAUFMAN, ARIE ..... p 2419 N92-23855
KAUTZ, HAROLD E. ..... p 2386 N92-23189
KAWAGUCHI, SADAO ..... p 2399 N92-23481
KAWAMURA, TOSHIYUKI ..... p 2399 N92-23482
KEEGAN, R. ..... p 2461 N92-23306
KEINATH, WOLFGANG ..... p 2320 N92-23764
KENSEK, R. P. ..... p 2445 N92-23749
KERLEY, JAMES ..... p 2382 N92-23547
p 2386 N92-24059
KERREBROCK, JACK L. ..... p 2321 N92-23980
KERRIDGE, D. J. ..... p 2334 N92-23975
KERSCHBERG, LARRY ..... p 2428 N92-23371
KEYES, GILBERT ..... p 2313 N92-23649
KHAN, L. A. ..... p 2432 N92-23335
KHEOH, T. ..... p 2406 N92-23898
KHOROSHKIN, S. ..... p 2433 N92-23670
KIEFER, J. H. ..... p 2348 N92-24038
KILLOUGH, S. M. ..... p 2382 N92-23459
KIM, EUNSOOK ..... p 2449 N92-23776
KIM, NAM-EUNG ..... p 2345 N92-24012
KIM, SUNG-EON ..... p 2452 N92-23156
KIM, T. ..... p 2374 N92-23516
KIMURA, HARUYUKI ..... p 2444 N92-23711
KINARD, WILLIAM H. ..... p 2335 N92-23282
p 2458 N92-23317
KING, S. E. ..... p 2460 N92-23293
KINGSMILL, DAVID EDMUND ..... p 2409 N92-23121
KIPNIS, I. ..... p 2378 N92-23278
KIRBY-GALLAGHER, LUCY MARY
p 2437 N92-23674
KIRK, M. A. ..... p 2448 N92-23574
KIRNER, E. ..... p 2319 N92-23759
KIRSTEN, F. ..... p 2378 N92-23278
KISHIRO, TOSHIYA ..... p 2399 N92-23484
KISSINGER, B. ..... p 2453 N92-23188
KLEIN, M. ..... p 2324 N92-23787
p 2332 N92-23845
KLEIN, M. R. M. ..... p 2327 N92-23814
KLEIN, MICHEL ..... p 2332 N92-23843
KLEINFELDER, S. ..... p 2378 N92-23278
KLINGELE, E. ..... p 2315 N92-23915
KLINKRAD, H. ..... p 2334 N92-23970
KLUSOWSKI, ERHARD ..... p 2333 N92-23847
KNAPP, F. F., JR. ..... p 2412 N92-23518
KNODEL, T. V. ..... p 2438 N92-23747
KNYSHENKO, I. I. ..... p 2438 N92-23747
KO, FRANK ..... p 2381 N92-23435
KOBAYASHI, M. ..... p 2441 N92-23713
KOEBRUGGE, GERHARDUS WILHELMUS
p 2353 N92-23165
KOHARA, CHOJI ..... p 2353 N92-23134
KOIKE, TOSHIO ..... p 2399 N92-23483
KOIVISTO, P. K. ..... p 2366 N92-23591
p 2367 N92-23679
KOKTA, B. V. ..... p 2343 N92-23945
p 2344 N92-23948
KOMANN, WALTER ..... p 2452 N92-23929
KONDO, HIROFUMI ..... p 2312 N92-23979
KOPPENWALLNER, G. ..... p 2334 N92-23974
KOREN, ISRAEL ..... p 2421 N92-23869
KORNOUKHOV, V. N. ..... p 2438 N92-23747
KORTSCHOT, M. T. ..... p 2324 N92-23793
KOTZIAS, BERNHARD ..... p 2329 N92-23826
KOUGUCHI, TOSHIYUKI ..... p 2398 N92-23477
KOUHIA, R. ..... p 2388 N92-23664
KRAFT, U. ..... p 2392 N92-23379
p 2393 N92-23390
KRAMMER, J. ..... p 2308 N92-23236
KREIS, ANDREAS ..... p 2332 N92-23843
KRISHNAN, A. ..... p 2368 N92-23246
KUBOTA, YUSUKE ..... p 2407 N92-23262
KUENTZMANN, PAUL ..... p 2321 N92-23768
KUERTEN, J. G. M. ..... p 2373 N92-23251
KUIP, C. A. C. ..... p 2418 N92-23507
KULLA, PETER H. ..... p 2330 N92-23829
KUMAR, V. ..... p 2351 N92-23582
KUNKEL, B. ..... p 2393 N92-23387
KUNKEL, BERND A. ..... p 2392 N92-23379
KUNYAVSKII, BORIS E. ..... p 2434 N92-24061
KUNZ, KARL S. ..... p 2365 N92-23425
p 2366 N92-23528
KUNZ, P. ..... p 2436 N92-23327
KUPPERT, H. ..... p 2392 N92-23379
KUROIWA, AKIRA ..... p 2399 N92-23485
KUROSAKI, AKIO ..... p 2397 N92-23471
KURSINSKI, E. R. ..... p 2316 N92-23919
KWON, Y. ..... p 2436 N92-23327
KYLE, H. LEE ..... p 2410 N92-23431
KYRIACOU, C. ..... p 2316 N92-23919

L

LACOMBE, A. ..... p 2329 N92-23821
LAHEY, R. T., JR. ..... p 2373 N92-23202
LAIRD, C. E. ..... p 2440 N92-23300
LAKSIMI, A. ..... p 2343 N92-23943
LAL, RAVINDRA B. ..... p 2361 N92-23630
LALLEMENT, G. ..... p 2333 N92-23848
LAMAR, JOHN E. ..... p 2305 N92-23956
LAMBERT, C. R. ..... p 2412 N92-23518
LAMBERT, M. ..... p 2323 N92-23784
LAMBERT, S. J. ..... p 2412 N92-23518
LAMBETH, D. N. ..... p 2446 N92-23213
LAMPINEN, M. J. ..... p 2451 N92-23136
LANGE, GUNDOLF ..... p 2349 N92-23316
LANGEL, ROBERT ..... p 2316 N92-23920
LANGEL, ROBERT A. ..... p 2315 N92-23912
LAPEAN, J. ..... p 2364 N92-23245
LARRIEU, J. M. ..... p 2331 N92-23838
LASERSON, AVIGDOR ..... p 2419 N92-23853
LASSOURD, GERARD ..... p 2319 N92-23760
LATERZA, S. ..... p 2326 N92-23803
LAUGHLIN, D. E. ..... p 2446 N92-23213
LAURANCE, MARK R. ..... p 2458 N92-23315
LAURENT, C. ..... p 2330 N92-23833
LAURITZEN, CARL A. ..... p 2322 N92-23796
LAVALLEE, DAVID ..... p 2427 N92-23363
LAVIRON, B. ..... p 2324 N92-23791
LAWVER, B. S. ..... p 2417 N92-23255
LEDER, H. ..... p 2331 N92-23837
LEDOUX, PAUL ..... p 2323 N92-23785
LEE, CHI-CHONG ..... p 2363 N92-23719
LEE, CLINTON B. ..... p 2470 N92-23958
LEE, E. H. ..... p 2354 N92-23222
LEE, H. Q. ..... p 2347 N92-23449
LEE, HO-JUN ..... p 2387 N92-23196
LEE, KAM-PUI ..... p 2374 N92-23543
LEE, KI D. ..... p 2305 N92-23563
LEE, RICHARD Q. ..... p 2370 N92-23535
LEE, S. ..... p 2341 N92-23937
LEE, SEOK-HUA ..... p 2426 N92-23358
LEE, THOMAS S. ..... p 2382 N92-23553
LEEPER, R. J. ..... p 2445 N92-23749
LEFEVRE, Y. M. ..... p 2332 N92-23845
LEGGE, G. J ..... p 2446 N92-24067
LEGRAND, R. ..... p 2430 N92-24066
LEITH, D. W. G. S. ..... p 2436 N92-23327
LEURIDAN, J. ..... p 2325 N92-23799
LEVENSON, L. L. ..... p 2365 N92-23414
LEVI, M. ..... p 2378 N92-23278
LEVINE, A. ..... p 2317 N92-23531
LEVINE, ARLENE S. ..... p 2461 N92-23280
LEVINSON, L. ..... p 2436 N92-23327
LEWIS, M. B. ..... p 2354 N92-23222
LEWIS, N. S. ..... p 2447 N92-23275
LI, XIN KAI ..... p 2375 N92-23672
LI, Y. M. ..... p 2447 N92-23452
LICHTENBERG, BYRON K. ..... p 2321 N92-23980
LIENAU, P. J. ..... p 2404 N92-24030
LIENEWEG, UDO ..... p 2369 N92-23464
LIEWEHR, W. ..... p 2318 N92-23969
LIGHTNER, E. BURTON ..... p 2335 N92-23281
LIHTOLA, A. ..... p 2367 N92-23907
LILIUS, J. ..... p 2432 N92-23440
LILIUS, K. ..... p 2350 N92-23178
LIM, TAE W. ..... p 2390 N92-23990
LIN, C. D. ..... p 2438 N92-23895
LIN, HONG-CHIA ..... p 2375 N92-23692
LIN, X. ..... p 2342 N92-23938
LIN, ZHONGMIN ..... p 2407 N92-23142
LIND, D. L. ..... p 2459 N92-23325
LINDELL, I. V. ..... p 2364 N92-23138
p 2366 N92-23661
p 2366 N92-23666
p 2366 N92-23667
p 2367 N92-23668
p 2367 N92-23907
LINDER, W. KELLY ..... p 2335 N92-23285
LINETSKY, V. YA. ..... p 2435 N92-23207
LINTULA, P. ..... p 2380 N92-23152
LIOU, MENG-S. ..... p 2302 N92-23343
LIOU, MENG-SING ..... p 2301 N92-23336
p 2303 N92-23352
p 2304 N92-23353
LIOU, WILLIAM W. ..... p 2301 N92-23340
p 2303 N92-23351
LIPETZ, SMADAR ..... p 2423 N92-23879
LIPPMANN, S. I. ..... p 2444 N92-23446
LIU, FULING ..... p 2417 N92-23418
LIU, HUA-KUANG ..... p 2416 N92-23546
LIU, J. Z. ..... p 2450 N92-24007
LIU, M. ..... p 2446 N92-23260
LIYUAN, ZHANG ..... p 2447 N92-23273
LOGAN, B. G. ..... p 2445 N92-23987
LOHSE, U. ..... p 2331 N92-23837
LONG, MARK K. ..... p 2382 N92-23553
LOPEZ, ANTONIO M., JR. ..... p 2429 N92-23375
LORENCE, L. J., JR. ..... p 2425 N92-24041
LORENZO, L. ..... p 2344 N92-23947
LOUAAS, E. ..... p 2321 N92-23797
LOUBRIEL, G. M. ..... p 2371 N92-23983
LOVE, MICHAEL H. ..... p 2307 N92-23231
LU, SHIN-YEE ..... p 2417 N92-23255
LU, YU ..... p 2447 N92-23453
LUBKER, S. J. ..... p 2411 N92-23660
LUBZENS, D. ..... p 2422 N92-23872
LUCAS, ROLAND ..... p 2320 N92-23766
LUCERO, JOHN M. ..... p 2387 N92-23191
LUCKS, MICHAEL ..... p 2426 N92-23359
LUDWICZAK, D. R. ..... p 2329 N92-23824
LUEBBERS, RAYMOND J. ..... p 2365 N92-23425
p 2366 N92-23528
LUK, TAK-LAI DARYL ..... p 2381 N92-23158
LUKES, M. ..... p 2410 N92-23439
p 2410 N92-23494
p 2411 N92-23746
LUMLEY, JOHN L. ..... p 2376 N92-24050
LUND, P. D. ..... p 2403 N92-23592
p 2403 N92-23683
LUNEL, S. M. VERDUYN ..... p 2431 N92-23250
LUNIS, B. C. ..... p 2404 N92-24030
LUSCHER, D. ..... p 2383 N92-23680
LUST, STEVEN DAN ..... p 2389 N92-23699
LYBANON, MATTHEW ..... p 2402 N92-23369
LYON, R. E. ..... p 2355 N92-24068

M

MA, C. Y. ..... p 2337 N92-23722
MAAG, CARL R. ..... p 2335 N92-23285
MAAYAN, E. ..... p 2422 N92-23872
MACHINCHICK, MICHAEL ..... p 2381 N92-23435
MACKENZIE, K. ..... p 2310 N92-23169
MACKINNON, B. A. ..... p 2368 N92-23326
MADSEN, B. C. ..... p 2406 N92-23898
MAEDA, KOREHIRO ..... p 2396 N92-23465
p 2396 N92-23466
MAGEE, KEVIN N. ..... p 2429 N92-24038
MAGER, ARTHUR ..... p 2321 N92-23980
MAGNOTTA, F. ..... p 2438 N92-23903
MAGURA, K. ..... p 2333 N92-23968
MAHAJAN, APARAJIT J. ..... p 2387 N92-23191
MAHER, E. P. ..... p 2359 N92-23616
MAJUMDAR, T. J. ..... p 2401 N92-23492
p 2401 N92-23493
MAKARA, J. ..... p 2433 N92-23579
MALARIK, DIANE C. ..... p 2355 N92-24053
MALDAS, D. ..... p 2343 N92-23945
MANDEVILLE, J. C. ..... p 2458 N92-23310
MANGELSCHOTS, R. ..... p 2325 N92-23799
MANGIS, D. ..... p 2407 N92-24003
MANGUM, JEFFREY GARY ..... p 2457 N92-23698
MANNINEN, A. J. ..... p 2435 N92-23665
MANNINEN, L. M. ..... p 2403 N92-23683
MANNING, I. L. ..... p 2453 N92-23212
MANNINGS, VINCENT ..... p 2460 N92-23736
MANSFIELD, FRANCIS ALLEN ..... p 2376 N92-24018
MANSUR, L. K. ..... p 2354 N92-23222
p 2447 N92-23444
MARCHETTI, M. ..... p 2326 N92-23803
MARCO, ROBERTO ..... p 2357 N92-23608

MAREK, C. J. p 2304 N92-23355
MARELLI, LIVIO p 2317 N92-23926
MARLEY, GARRY M. p 2413 N92-24052
MARQUEDANT, ROY J. p 2316 N92-23920
MARR, JONATHAN MICHAEL p 2455 N92-23675
MARTEN, S. M. p 2340 N92-23585
MARTIN, GLENNA D. p 2335 N92-23282
MARTIN, J. p 2321 N92-23810
MARTNER, B. E. p 2401 N92-23521
MARUCCHI-CHIERRO, PIETRO CARLO
p 2327 N92-23813
p 2330 N92-23827
MARWICK, A. D. p 2448 N92-23574
MASERIAN, JOSEPH p 2369 N92-23464
MASSIER, P. F. p 2403 N92-23569
MASTERS, A. I. p 2337 N92-23982
MASUDA, KAZUHIKO p 2397 N92-23471
MATSUMOTO, MASAO p 2398 N92-23479
MATSUMURA, SATSUKI p 2399 N92-23484
MATSUURA, K. p 2444 N92-23261
MATTOK, C. p 2314 N92-23910
MAUL, G. A. p 2412 N92-23732
MAY, EDWARD p 2382 N92-23547
MAYBERRY, M. J. p 2444 N92-23446
MAYER, PAULA S. D. p 2418 N92-23554
MAYER, RICHARD J. p 2418 N92-23554
MCADIE, C. J. p 2411 N92-23994
MCBREEN, J. p 2346 N92-23199
MCCARTY, JOHN P. p 2319 N92-23754
MCCAY, MARY H. p 2361 N92-23631
MCCLURE, JOSEPH p 2360 N92-23624
MCCULLOUGH, R. L. p 2343 N92-23942
MCDONNELL, J. A. M. p 2336 N92-23312
p 2458 N92-23320
MCINTYRE, P. M. p 2440 N92-23334
MCKISSON, J. E. p 2460 N92-23293
MCLAUGHLIN, D. L. p 2371 N92-23983
MCLEAN, P. p 2343 N92-23944
MCLEISH, W. p 2412 N92-23732
MCNULTY, IAN LAURENCE p 2377 N92-23144
MCNULTY, S. E. p 2368 N92-23326
MCPHADEN, M. J. p 2411 N92-23682
MCPHERSON, D. W. p 2412 N92-23518
MEEHAN, T. K. p 2316 N92-23919
MEHMED, ORAL p 2387 N92-23191
MEHRHOLZ, D. p 2333 N92-23968
p 2318 N92-23969
MELBOURNE, WILLIAM G. p 2316 N92-23919
MELTON, R. B. p 2408 N92-23741
MENNIGMANN, HORST-DIETER p 2358 N92-23612
MENON, P. K. A. p 2317 N92-23529
MERCIER, F. p 2324 N92-23787
p 2328 N92-23815
MERRICK, T. p 2378 N92-23278
MESSA, KENNETH p 2402 N92-23369
MESSENGER, SCOTT p 2458 N92-23315
MEYER, DOUG p 2375 N92-23568
MEYER, P. p 2315 N92-23917
MEZENTSEVA, S. A. p 2438 N92-23747
MICHAL, GARY M. p 2351 N92-23436
MICHELS, TEUN p 2362 N92-23639
MICKNEY, MARCUS R. p 2322 N92-23526
MIEKKALA, U. p 2433 N92-23589
MIGLIACCIO, FREDERICA p 2315 N92-23914
MIGONI, R. p 2446 N92-23270
MILAM, M. BRUCE p 2382 N92-23548
MILGROME, O. p 2378 N92-23278
MILLER, A. C., JR. p 2363 N92-23899
MILLER, JEFFREY H. p 2381 N92-23435
MILLER, TERESA Y. p 2356 N92-23600
MILLS, D. L. p 2437 N92-23330
MINER, PAUL S. p 2416 N92-23559
MINNETYAN, L. p 2339 N92-23194
MIRALDI, E. p 2326 N92-23807
MIRANDA, FELIX A. p 2365 N92-23415
MIRANDA, FELIX ANTONIO p 2365 N92-23413
MIRMOV, I. N. p 2438 N92-23747
MIRZADEH, S. p 2412 N92-23518
MISHIN, VASILY B. p 2319 N92-23753
MITCHELL, T. E. p 2352 N92-23720
MITRA, PATRALEKHA p 2455 N92-24002
MIYAHARA, AKIRA p 2407 N92-23262
MIYOSHI, KAZUHISA p 2354 N92-23192
MIZIK, P. M. p 2387 N92-23216
MIZRACH, MICHAEL p 2420 N92-23858
MOELLER, P. p 2438 N92-23714
MOHAMMEDI, N. p 2451 N92-23503
MOHLER, STANLEY R., JR. p 2373 N92-23154
MOHR, W. p 2332 N92-23844
MOLL, A. J. p 2371 N92-23985
MONGEAU, LUC p 2436 N92-23726
MONROE, DARREL p 2337 N92-23151
MONTAGUE, NANCY L. p 2458 N92-23317
MONTGOMERY, B. p 2445 N92-24020
MONTGOMERY, C. KEITH p 2322 N92-23526
MOODY, R. L. p 2337 N92-23722
MOOKERJEE, A. p 2351 N92-23582
MOONEY, GEORGE DAVID p 2404 N92-23998
MOREL, J. E. p 2425 N92-24041
MOREY-HOLTON, EMILY p 2414 N92-23424
MORITA, KAZUHIKO p 2397 N92-23472
MOROHOSHI, TOSHIKAZU p 2397 N92-23474
MORRIS, C. L. p 2368 N92-23200
MORSE, D. H. p 2446 N92-24067
MOSS, C. E. p 2440 N92-23298
MOYA, ISRAEL A. p 2386 N92-24060
MOYER, C. p 2383 N92-23680
MRITUNJAY p 2400 N92-23491
MUGELLESI, R. p 2334 N92-23975
MULHOLLAND, J. DERRAL p 2458 N92-23317
MUROTA, KATSUICHI p 2312 N92-23979
MURPHY, J. L. p 2384 N92-23908
MURTHY, P. L. N. p 2339 N92-23194
MURTHY, T. V. RAMA p 2368 N92-23246
MUTHARASAN, RAJAKKANNU p 2381 N92-23435
MYERS, D. R. p 2442 N92-23748
MYERS, IRA T. p 2370 N92-23561
MYRICK, M. L. p 2355 N92-24068

N

NAGAOKA, S. p 2361 N92-23629
NAGASE, F. p 2317 N92-23531
NAKAJIMA, HAJIME p 2351 N92-23263
p 2352 N92-23712
NAKAKITA, OSAMU p 2397 N92-23473
NAKAMURA, KOUICHI p 2407 N92-23262
NAKAMURA, SEIGO p 2312 N92-23778
NAKANE, KAZURO p 2397 N92-23474
NAVIA, MANUEL A. p 2313 N92-23650
NAWIJN, W. M. p 2430 N92-23506
NAZARENKO, A. I. p 2334 N92-2397
NAZAREWICZ, W. p 2436 N92-23277
NEILAN, R. E. p 2316 N92-23919
NEILSON, H. p 2445 N92-24020
NELSON, D. J. p 2417 N92-23420
p 2418 N92-23422
NELSON, GREGORY A. p 2357 N92-23603
NELSON, P. p 2451 N92-24040
NELSON, P. A. p 2435 N92-23170
NESBITT, L. p 2412 N92-23669
NESTOR, C. W. p 2337 N92-23722
NETO, H. C. p 2420 N92-23860
NEVANLINNA, O. p 2369 N92-23495
NEVINS, B. p 2445 N92-24020
NGUYEN, B. N. p 2322 N92-23796
NIEDBAL, NORBERT p 2333 N92-23847
NIKOSKINEN, K. I. p 2364 N92-23138
p 2367 N92-23907
NISHIMURA, L. S. p 2335 N92-23287
p 2349 N92-23288
NISHIMURA, MAKOTO p 2384 N92-23779
NISHIO, FUMIHIKO p 2399 N92-23481
NISSEN-PFRANG, T. p 2384 N92-23896
NIX, J. R. p 2438 N92-23714
NOELKER, HELMUT p 2452 N92-23932
NOPONEN, E. p 2442 N92-23662
NORTON, O. A., JR. p 2369 N92-23437
NORTON, WILLIAM E. p 2416 N92-24044
p 2416 N92-24056
NOWLIN, C. H. p 2371 N92-24025
NUTTER, SCOTT LOWRY p 2460 N92-23163
NYLAND, TED W. p 2373 N92-23268

O

OBAYASHI, HARUO p 2407 N92-23262
OBRIEN, J. p 2449 N92-23986
OBRIEN, K. p 2414 N92-23139
OCHIAI, HIROAKI p 2398 N92-23478
ODAMAKI, MINORU p 2398 N92-23476
ODESS, LAWRENCE p 2419 N92-23853
ODONNELL, R. E. p 2364 N92-23901
OGAWA, S. p 2396 N92-23465
OHLY, W. p 2331 N92-23837
OHNO, KAZUKO p 2407 N92-23262
OHRI, EDITH p 2420 N92-23857
p 2422 N92-23875
OHSAKI, YUJI p 2396 N92-23467
OKADA, YOSHIHIRO p 2398 N92-23477
OKSANEN, M. I. p 2366 N92-23590
p 2366 N92-23591
p 2367 N92-23679
OLEARY, D. P. p 2432 N92-23511
OLIVEIRA, A. p 2421 N92-23865
OLIVER, JOHN P. p 2458 N92-23317
OLMEZ, ILHAN p 2439 N92-23296
OLSON, P. L. p 2368 N92-23140
OLSON, R. K. p 2410 N92-23520
OLSSON, ROBIN p 2339 N92-23167
OMALLEY, M. W. p 2371 N92-23983
OMRANI, A. p 2332 N92-23846
ONEAL, ROBERT L. p 2335 N92-23281
ORSOLINI, YVAN JOSEPH p 2459 N92-23704
ORVIS, W. J. p 2344 N92-23988
OSULLIVAN, D. p 2461 N92-23306
OSWALD, FRED B. p 2382 N92-23536
OTSUKI, FUMIO p 2323 N92-23781
OUSLEY, GILBERT W., SR. p 2316 N92-23921

P

PAHOR, J. p 2378 N92-23219
PAK, CHAN-GI p 2310 N92-24010
PALSULE, S. S. p 2400 N92-23491
PAN, JIANFU p 2409 N92-23150
PAPELL, S. STEPHEN p 2373 N92-23268
PARASKEVOPOULOU, R. p 2422 N92-23674
PARDINI, C. p 2334 N92-23972
PARET, A. p 2308 N92-23239
PARIHAR, J. S. p 2400 N92-23490
PARMA, GEORGE F. p 2382 N92-23544
PARNELL, T. A. p 2439 N92-23291
p 2439 N92-23292
p 2461 N92-23294
p 2440 N92-23300
p 2461 N92-23302
p 2440 N92-23303
PARSONS, HOWARD G. p 2359 N92-23620
PASCIAK, J. E. p 2432 N92-23329
PASWAN, G. p 2400 N92-23491
PATHAK, P. N. p 2400 N92-23489
PATKI, A. V. p 2326 N92-23801
PATNAIK, S. N. p 2388 N92-23527
PATTERSON, MICHAEL J. p 2337 N92-23534
PATTON, EDWARD MATTHEW p 2389 N92-23688
PAUL, BETH E. p 2307 N92-23231
PAULTER, N. G. p 2364 N92-23173
PAYNE, S. A. p 2380 N92-24065
PEASE, DOUGLAS M. p 2378 N92-23155
PEI, YICHUAN C. p 2456 N92-23164
PEKOLA, J. P. p 2435 N92-23665
PELIPENKO, YVES p 2320 N92-23767
PELTOLA, S. S. p 2403 N92-23592
PELTONEN, J. K. p 2368 N92-23172
PEPIN, GERARD R. p 2335 N92-24046
PEPPER, STEPHEN V. p 2353 N92-23185
PERBAL, GERALD p 2359 N92-23617
PEREIRA, F. M. B. p 2367 N92-23676
PERKINS, S. T. p 2439 N92-24005
PERL, THOMAS D. p 2370 N92-23535
PERRIER, P. p 2309 N92-23952
PERUT, CHRISTIAN p 2320 N92-23765
PETERS, H. G. p 2318 N92-23969
PETERS, PALMER N. p 2379 N92-23283
PETERSON, ROBERT B. p 2458 N92-23315
PETIAU, C. p 2308 N92-23239
PETIAU, CHRISTIAN p 2322 N92-23823
PETRIK, EDWARD J. p 2427 N92-23365
PETTY, C. C. p 2444 N92-23446
PEYROT, PATRICK p 2315 N92-23917
PHILIPP, WARREN H. p 2354 N92-23461
PHILLIPS, G. W. p 2460 N92-23293
PICHEL, WILLIAM G. p 2400 N92-23487
PIERCEY, R. B. p 2460 N92-23293
PIGGOTT, M. R. p 2341 N92-23934
PIKE, T. K. p 2394 N92-23398
PIN, F. G. p 2382 N92-23459
p 2430 N92-24032
PINSKER, R. I. p 2444 N92-23446
PIOTROWSKI, G. K. p 2383 N92-23595
PITKAERANTA, J. p 2387 N92-23137
PITT, DALE M. p 2307 N92-23235
PITZ, W. J. p 2349 N92-24064
PIURI, VICENZO p 2419 N92-23854
PLANAS, J. P. p 2330 N92-23831
PODOLAK, ESTER p 2419 N92-23856
POKHARNA, S. S. p 2401 N92-23492
POLLANO, G. p 2308 N92-23237
PONTAU, A. E. p 2446 N92-24067
POON, C. p 2341 N92-23937
PORKOLAB, M. p 2444 N92-23446
POST, G. F. p 2431 N92-23182
POTTER, A. E. p 2335 N92-23978
POURBABAI, B. p 2430 N92-23508
POURSARTIP, A. p 2342 N92-23938
POVINELLI, LOUIS A. p 2301 N92-23336
POWARS, C. p 2383 N92-23680
PRADLWARTER, H. J. p 2328 N92-23816
PRAKASH, C. V. S. p 2400 N92-23491
PRATER, R. p 2444 N92-23446
PRIMATAROWA, M. T. p 2446 N92-23271
PRINETTO, P. p 2421 N92-23866
PRINZ, RUDOLF p 2325 N92-23794
PUECH, J. F. p 2331 N92-23836

PURSIHEIMO, U. p 2451 N92-23136
PUSHPALATA p 2400 N92-23491
PYOETSIAE, J. p 2383 N92-23710

Q

QUAYLE, R. G. p 2411 N92-23660

R

RABITZ, H. p 2347 N92-23443
RACHUK, VLADIMIR S. p 2319 N92-23757
RADOK, U. p 2411 N92-23660
RADOUSKY, H. B. p 2449 N92-23986
RADUL, A. p 2431 N92-23184
p 2433 N92-23670
RAHMAN, M. S. p 2432 N92-23502
RAHMANI, M. p 2344 N92-23949
RAJ, R. G. p 2344 N92-23948
RAMAMOORTHY, V. p 2418 N92-23421
RAMAN, GANESH p 2304 N92-23269
RANSFORD, GARY A. p 2453 N92-23550
RAPP, RICHARD H. p 2315 N92-23913
RAPPAPORT, E. N. p 2411 N92-23994
RAPPAPORT, S. p 2317 N92-23531
RASH, JAMES L. p 2426 N92-23356
RASMUSSEN, OLE p 2358 N92-23609
RATCLIFF, B. N. p 2436 N92-23327
RATHJEN, P. p 2331 N92-23837
RATKOS, J. M. p 2401 N92-23659
RAVELO, ANA CHRISTINA p 2412 N92-23769
RAWLIN, VINCENT K. p 2337 N92-23534
RAYMER, DANIEL P. p 2309 N92-23953
RAYNER, S. p 2450 N92-24007
RAYNER, S. L. p 2449 N92-23986
RAZ, TAL p 2419 N92-23856
REED, J. L. p 2348 N92-23657
REEDY, R. C. p 2440 N92-23298
REILINGER, ROBERT p 2408 N92-23558
REILLY, TERRENCE W. p 2336 N92-23319
REIMERDES, HANS-G. p 2323 N92-23786
REISTER, D. B. p 2430 N92-24032
REITZ, G. p 2358 N92-23611
RESCHKE, MILLARD F. p 2360 N92-23626
RESS, D. p 2444 N92-23523
RETTER, YORAM p 2424 N92-23882
REUTER, R. p 2392 N92-23379
p 2392 N92-23381
p 2392 N92-23382
p 2393 N92-23384
p 2393 N92-23386
p 2393 N92-23388
p 2393 N92-23389
REY, SOO-JONG p 2451 N92-24040
REYES, A. P. p 2450 N92-24036
RHEE, M. J. p 2368 N92-23186
RIAHI, G. p 2342 N92-23938
RICARD, A. p 2325 N92-23795
RICE, B. W. p 2444 N92-23523
RICE, D. E. p 2412 N92-23518
RICE, EDWARD J. p 2304 N92-23269
RIGAULT, M. p 2330 N92-23831
p 2331 N92-23836
RILEY, M. F. p 2307 N92-23230
RIOS, J. F. p 2323 N92-23784
RIPLING, E. J. p 2389 N92-23681
RITCHIE, B. p 2321 N92-23811
RITTER, J. C. p 2460 N92-23293
RIVOL, G. p 2319 N92-23758
RIZZI, ARTHUR p 2304 N92-23168
ROBACK, D. M. p 2437 N92-23328
ROBERTSON, GLEN A. p 2385 N92-24055
ROBINSON, DEBORAH L. p 2442 N92-23551
ROBINSON, STEPHEN KERN p 2375 N92-23689
RODEN, JOSEPH p 2427 N92-23362
RODRIGUEZ, G. P. p 2372 N92-24063
RODRIGUEZ, GUILLERMO p 2385 N92-24042
p 2385 N92-24043
RODRIGUEZ, SUZANNE MARIE p 2453 N92-23730
ROE, N. A. p 2378 N92-23279
ROELANDT, J. M. p 2343 N92-23943
ROGERS, ROBERT DERWARD p 2460 N92-23141
ROGERS, WILLIAM A. p 2307 N92-23231
ROMEO, G. p 2326 N92-23804
p 2326 N92-23807
ROSE, M. R. p 2410 N92-23520
ROSEN, R. S. p 2443 N92-24049
ROSENBLATT, G. M. p 2347 N92-23449
ROSSI, DAVID p 2313 N92-23647
ROSSOMANDO, PHILIP J. p 2427 N92-23364
ROST, MARTIN C. p 2417 N92-23419
p 2418 N92-23423
ROTMAN, D. A. p 2404 N92-23123
ROUGES, J. M. p 2329 N92-23821
ROWLANDS, NEIL p 2460 N92-23162
ROY, N. p 2330 N92-23828
RUBINSTEIN, R. p 2374 N92-23542
RUBTSOV, V. p 2431 N92-23184
p 2433 N92-23670
RUIZ, STEVE C. p 2382 N92-23544
RUIZ, STEVE L. p 2385 N92-24051
RUMMEL, REINER p 2314 N92-23911
RUSCICA, G. p 2326 N92-23807
RUSSAK, M. A. p 2350 N92-23197
RUST, B. W. p 2432 N92-23511
RUVALDS, J. p 2446 N92-23205
RUVINETTI, G. p 2326 N92-23807
RYAN, M. A. p 2403 N92-23569
RYAN, TIMOTHY P. p 2404 N92-24054

S

SAACKS, MARGUERITE E. p 2429 N92-23375
SABADINI, R. p 2315 N92-23915
SACHER, P. W. p 2308 N92-23951
SAGALYN, PAUL p 2439 N92-23296
SAIGUSA, MIKIO p 2444 N92-23264
p 2444 N92-23711
SAITOH, YASUSHI p 2444 N92-23711
SAIYED, NASEEM H. p 2373 N92-23268
SAKAKIBARA, SEIZO p 2312 N92-23778
SAKATA, TOSHIBUMI p 2397 N92-23469
SALIMULLAH, M. p 2444 N92-23209
SALMINEN, O. p 2370 N92-23497
SALONEN, P. p 2380 N92-23152
SALVI, A. M. p 2343 N92-23946
SAMUEL, R. p 2326 N92-23801
SANDELLI, G. J. p 2403 N92-23509
SANDERS, LES p 2418 N92-23554
SANDERS, S. C. p 2449 N92-23892
SANGANI, A. S. p 2376 N92-24062
SANSO, FERNANDO p 2315 N92-23914
SANTILLI, R. M. p 2431 N92-23128
p 2431 N92-23129
p 2451 N92-23743
p 2438 N92-23744
p 2433 N92-23745
p 2434 N92-24039
SANTORO, A. p 2334 N92-23972
SAPP, CLYDE A. p 2454 N92-23313
SARGINSON, T. G. p 2379 N92-23570
SASAKI, HIDEYUKI p 2398 N92-23475
SASAKI, MASAMI p 2399 N92-23482
SATO, SATOSHI p 2398 N92-23476
SATO, T. p 2368 N92-23140
SATOH, HIDEO p 2396 N92-23466
SATTER, M. A. p 2351 N92-23582
SAWADA, HARUO p 2397 N92-23473
SAWADA, HIDEO p 2312 N92-23778
SAWADA, KOICHI p 2400 N92-23486
SAYOOD, K. p 2418 N92-23421
SAYOOD, KHALID p 2417 N92-23417
p 2417 N92-23418
p 2417 N92-23419
p 2417 N92-23420
p 2418 N92-23422
p 2418 N92-23423
SCANLON, ROBERT W. p 2307 N92-23235
SCHAEFER, R. M. p 2383 N92-23595
SCHAUS, C. F. p 2442 N92-23748
SCHIERENBECK, D. p 2308 N92-23238
SCHILLEMANS, L. p 2328 N92-23818
p 2330 N92-23832
SCHIWKOSKY, L. p 2331 N92-23837
SCHMITT, W. p 2332 N92-23842
SCHNEIDER, E. p 2323 N92-23784
SCHNEIDER, G. p 2308 N92-23236
SCHOEPE, W. p 2379 N92-23594
SCHRAWYER, L. R. p 2450 N92-24069
SCHROTT, A. G. p 2350 N92-23197
SCHUEELLER, G. I. p 2328 N92-23816
SCHUETZLE, JAMES p 2427 N92-23363
SCHUMACHER, CHRIS p 2402 N92-23368
SCHUYER, M. p 2315 N92-23916
SCHWEITZER, PAUL J. p 2423 N92-23877
SCOLAMIERO, L. p 2332 N92-23841
SCOTT, R. F. p 2341 N92-23937
SEE, T. H. p 2336 N92-23323
SEE, THOMAS p 2336 N92-23324
SEE, THOMAS H. p 2454 N92-23313
p 2336 N92-23314
p 2458 N92-23315
SEIDMANN, ABRAHAM p 2423 N92-23877
SEKI, YASUSHI p 2443 N92-23132
SELIM, RAOUF L. p 2369 N92-23430
SELTZER, JANET p 2419 N92-23853
SENICK, PAUL F. p 2311 N92-23537
SERAJI, HOMAYOUN p 2382 N92-23553
SHABBIR, AAMIR p 2301 N92-23339
SHAFIK, M. S. p 2379 N92-23131
SHAFROTH, S. M. p 2439 N92-24026
SHAH, B. S. p 2400 N92-23491
SHAH, RAHUL S. p 2345 N92-23996
SHANNON, T. p 2445 N92-24020
SHARP, J. W. p 2447 N92-23447
SHEA, M. F. p 2368 N92-23326
SHELNUTT, J. A. p 2438 N92-23894
SHELTON, R. p 2379 N92-23571
p 2450 N92-24007
SHEN, B. p 2364 N92-23245
SHENG, D. N. p 2447 N92-23452
SHENG, H. p 2448 N92-23498
SHENKMAN, A. p 2420 N92-23859
SHEPHERD, A. J. p 2411 N92-23682
SHERWOOD, R. J. p 2417 N92-23255
SHI, C. p 2420 N92-23861
SHIBATA, AKIRA p 2397 N92-23470
SHIH, T. H. p 2303 N92-23349
SHIH, T.-H. p 2303 N92-23350
p 2303 N92-23351
SHIH, TSAN-HSING p 2301 N92-23336
p 2301 N92-23338
p 2376 N92-24050
SHIMIZU, TETSUYA p 2351 N92-23263
SHIMODA, HARUHISA p 2397 N92-23469
SHINOHARA, YOSHIO p 2397 N92-23470
SHIRAKAWA, YOSHISHIGE p 2398 N92-23475
SHIRAKI, KUNIAKI p 2323 N92-23781
SHUEN, JIAN-SHUN p 2304 N92-23354
SHUI, Z. R. p 2352 N92-23893
SHUTO, KENZO p 2397 N92-23470
SHYU, KAUN-LONG p 2356 N92-23147
SIHVOLA, A. H. p 2366 N92-23661
p 2367 N92-23668
SIMOLA, J. T. p 2379 N92-23594
SIMON, CHARLES p 2349 N92-23316
SIMON, CHARLES G. p 2454 N92-23313
p 2336 N92-23314
p 2458 N92-23318
SIMONS, RAINEE N. p 2368 N92-23193
p 2370 N92-23535
SIMPSON, KAIA p 2323 N92-23785
SINGER, S. FRED p 2458 N92-23317
SINGH, D. p 2340 N92-23256
SINGH, J. P. p 2340 N92-23256
SINGHAL, SURENDRA N. p 2388 N92-23267
SIRENKO, Y. M. p 2366 N92-23580
SIROCKY, PAUL J. p 2381 N92-23435
SLATTERY, RHONDA ANN p 2430 N92-24011
SLAYTON, DEKE p 2313 N92-23645
SMIT, A. p 2461 N92-23306
SMIT, MEINT KOERT p 2441 N92-23168
SMITH, ALAN R. p 2440 N92-23297
SMITH, B. W. p 2455 N92-24027
SMITH, EDWARD J. p 2316 N92-23920
SMITH, SHELDON D. p 2322 N92-23530
SMITH, STEVEN JOSEPH p 2457 N92-23716
SMITH, SUZANNE WEAVER p 2390 N92-23990
SNEAD, L. p 2461 N92-23301
SNEE, J. M. D. p 2308 N92-23238
SNIDER, J. B. p 2401 N92-23521
SNYDER, CHRISTOPHER A. p 2311 N92-23254
SNYDER, L. p 2414 N92-23139
SNYDER, MITCHELL p 2423 N92-23879
SOBIESZCZANSKI-SOBIESKI, JAROSLAW p 2306 N92-23228
SOKAL, A. D. p 2451 N92-23578
SOLAL, F. p 2449 N92-23986
p 2450 N92-24007
SOLEL, ESTHER p 2422 N92-23870
SOLEM, J. C. p 2458 N92-24028
SOLOMON, O. M., JR. p 2370 N92-23584
SONZAREORDA, M. p 2421 N92-23866
SPAETH, WILLIBALD p 2452 N92-23930
SPEARING, S. M. p 2324 N92-23793
SRINIVASAN, SHIVAKUMAR p 2304 N92-23168
SRIVASTAVA, P. C. p 2412 N92-23518
STACHIOTTI, M. p 2446 N92-23270
STADERMANN, FRANK p 2349 N92-23316
STAFFANS, O. J. p 2433 N92-23658
STAN, MARK A. p 2365 N92-23414
STARR, LOWELL p 2314 N92-23655
STAUBER, M. p 2461 N92-23301
STEARNS, D. G. p 2443 N92-24049
STEELE, F. K. p 2364 N92-23180
STEFFEN, CHRIS J., JR. p 2304 N92-23353
STEFFEN, CHRISTOPHER J., JR. p 2302 N92-23343
p 2303 N92-23352
STEFKO, GEORGE L. p 2387 N92-23191
STEINERT, R. A. p 2384 N92-23896
STEINETZ, BRUCE p 2339 N92-23190
STEINETZ, BRUCE M. p 2381 N92-23435
STEINMAN, JEFFREY S. p 2426 N92-24045
STEN, J. C. E. p 2364 N92-23138
p 2366 N92-23667

STERNE, P. p 2449 N92-23986
STERNE, P. A. p 2450 N92-24007
STERNFELD, H. J. p 2321 N92-23768
STEVENSON, T. J. p 2336 N92-23312
STEWART, MARK E. M. p 2374 N92-23560
STOCKWELL, ALAN E. p 2390 N92-23992
STOLTE, K. p 2407 N92-24003
STOLZ, C. J. p 2379 N92-23570
STOYCHEV, K. T. p 2446 N92-23271
STRAUCH, R. G. p 2401 N92-23521
STRINGER, J. p 2352 N92-23893
STRIZ, ALFRED G. p 2307 N92-23234
STROJWAS, ANDRZEJ J. p 2422 N92-23871
STROWEIS, JEAN-PIERRE p 2423 N92-23881
STUDER, PHILIP p 2382 N92-23548
STUDER, PHILIP A. p 2386 N92-24060
STUTZMAN, W. L. p 2364 N92-23245
SU, Z. B. p 2447 N92-23452
SUEMATSU, H. p 2352 N92-23720
SUGUMARAN, VIJAYAN p 2428 N92-23371
SULLIVAN, K. p 2458 N92-23320
SUN, S. Z. p 2442 N92-23748
SUTHAR, J. L. p 2370 N92-23538
SUZUKI, KOICHI p 2312 N92-23778
SUZUKI, MASAHIRO p 2399 N92-23482
SUZUKI, TOMIO p 2352 N92-23712
SUZUKI, TSUTOMU p 2397 N92-23472
SWAN, PAT p 2349 N92-23316
SWARTZ, C. K. p 2370 N92-23562
SWIATECKI, W. J. p 2438 N92-23714
SWIS, MATTHEW J. p 2322 N92-23526
SWITENDICK, A. C. p 2447 N92-23451
SYGULLA, D. p 2327 N92-23809
SYLVESTRE, JEAN-CLAUDE p 2320 N92-23763

T

TAGHIZADEH, M. R. p 2442 N92-23662
TAKABE, MASAO p 2396 N92-23468
TAKAMIZAWA, K. p 2364 N92-23245
TAKAO, YOSHIMI p 2400 N92-23486
TAKASAKI, SHIGEYUKI p 2398 N92-23479
TAKASHIMA, TSUTOMU p 2397 N92-23471
TAKATSU, HIDEYUKI p 2443 N92-23132
TAKAYAMA, YOZO p 2397 N92-23471
TAKEUCHI, YOSHIAKI p 2398 N92-23475
TAKIGAWA, M. p 2450 N92-24036
TALLO, DONALD P. p 2427 N92-23365
TAMEISHI, HIDEO p 2398 N92-23477
TANAKA, MASATOSHI p 2443 N92-23135
TANG, BEILIN p 2353 N92-23134
TANG, LIANG p 2384 N92-23727
TAO, RUIBAO p 2448 N92-23504
TASAKI, KAZUYUKI p 2323 N92-23781
TASKINEN, P. p 2350 N92-23178
TAUB, SUSAN R. p 2368 N92-23193
TAYLOR, J. R. p 2379 N92-23570
TAYLOR, LAFAYETTE KENNETH p 2375 N92-23700
TCHVANOV, VLADIMIR K. p 2320 N92-23761
TEIXEIRA, I. M. C. p 2420 N92-23860
p 2421 N92-23865
TEIXEIRA, J. P. C. p 2420 N92-23860
p 2421 N92-23865
TELESDASILVA, A. F. p 2372 N92-23149
TEMPLETON, J. L. p 2347 N92-23499
TENGLER, NANCY E. p 2322 N92-23796
TEOPFER, ARMIN p 2452 N92-23931
THIRSK, R. B. p 2360 N92-23623
THODEN, SCOTT p 2322 N92-23526
THOMAS, D. L. p 2369 N92-23437
THOMASSEN, K. p 2445 N92-24020
THOMPSON, A. p 2461 N92-23306
THOMPSON, C. V. p 2337 N92-23722
THOMPSON, D. p 2307 N92-23233
THOMPSON, R. N. p 2368 N92-23326
THORNBURG, HUGH JOSEPH p 2372 N92-23148
THORSETT, STEPHEN ERIK p 2455 N92-24001
TIAN, ZHENGFEI p 2340 N92-23693
TINTI, S. p 2315 N92-23915
TIXADOR, R. p 2359 N92-23619
TIZZI, S. p 2326 N92-23803
TOBIN, J. p 2449 N92-23986
TOI, K. p 2444 N92-23261
TOKSOZ, M. NAFI p 2408 N92-23558
TOMAK, M. p 2447 N92-23272
TOMKINS, B. A. p 2337 N92-23722
TOMOSADA, AKIRA p 2399 N92-23480
TONG, C. H. p 2431 N92-23201
TONG, S. Y. p 2437 N92-23330
TORIZUKA, K. p 2435 N92-23665
TORRES-VERDIN, CARLOS p 2401 N92-23703
TOSI, M. P. p 2350 N92-23211
TOUBOUL, M. P. p 2316 N92-23918
TRAN, DONALD H. p 2311 N92-23254
TRAUBE, E. C. p 2368 N92-23140
TREBINO, R. p 2346 N92-23181
TRETYAKOV, S. A. p 2366 N92-23590
p 2366 N92-23591
p 2367 N92-23679
TRUCKENMULLER, F. p 2342 N92-23941
TRUMPY, S. p 2334 N92-23972
TRUSCOTT, P. R. p 2439 N92-23295
TSAI, Y.-L. PETER p 2304 N92-23354
TSUCHIYA, KIYOSHI p 2398 N92-23479
TSUJI, HIROKAZU p 2351 N92-23263
p 2352 N92-23712
TSUKADA, TAKASHI p 2352 N92-23712
TSUKAMOTO, TOORU p 2398 N92-23476
TSUZUKI, T. p 2444 N92-23261
TUCKER, GREGORY SHERIDAN p 2441 N92-23161
TUORINIEMI, J. T. p 2379 N92-23594
TURNER, B. CURTIS p 2407 N92-23965
TURNHEIM, AMIEL p 2419 N92-23856
TURUNEN, J. p 2442 N92-23662
TWARDY, H. p 2328 N92-23817
TYLKA, ALLAN J. p 2461 N92-23307
TZEMOS, S. p 2453 N92-23188

U

UBBELS, GEERTJE A. p 2357 N92-23607
UCHIDA, MASAAKI p 2351 N92-23265
UEDA, HIROSHI p 2399 N92-23483
UEHARA, SHIGETSUGU p 2397 N92-23474
ULLIO, ROBERTO p 2330 N92-23827

V

V.BOEHM, H.-D. p 2394 N92-23392
VALTONEN, M. p 2371 N92-23678
VANDEBERGHE, MARK H. p 2382 N92-23544
VANDENBERG, LODEWIJK p 2361 N92-23632
VANDERBURG, J. W. p 2373 N92-23251
VANDERDUYNSCHOUTEN, F. A. p 2430 N92-23508
VANDERGENUGTEN, B. B. p 2434 N92-23731
VANDERWAL, J. M. M. p 2436 N92-23588
VANDEVEL, M. p 2431 N92-23249
VANFOSSEN, G. JAMES p 2373 N92-23224
VANHEMELRIJCK, D. p 2328 N92-23818
p 2330 N92-23832
VANNUCCI, RAYMOND D. p 2355 N92-24053
VASARA, A. p 2442 N92-23662
VAWTER, G. A. p 2442 N92-23748
VEIRS, D. K. p 2347 N92-23449
VEITCH, LISA C. p 2354 N92-23461
VELDHUIJZEN, J. PAUL p 2357 N92-23606
VENKATESWARAN, SANKARAN p 2337 N92-23694
VENKAYYA, VIPPERLA B. p 2307 N92-23234
VERHAGEN, WILLIAM p 2429 N92-23372
VERHEUL, E. p 2431 N92-23249
VERNON, S. P. p 2443 N92-24049
VESS, T. M. p 2355 N92-24068
VEST, THOMAS W. p 2416 N92-24044
p 2416 N92-24056
VIBERT, A. J. p 2324 N92-23788
VICKERS, BRIAN p 2323 N92-23785
VIDAL, MICHEL p 2319 N92-23756
VIRKKULA, A. p 2403 N92-23683
VITNER, GAD p 2424 N92-23884
VOELLMER, GEORGE p 2381 N92-23378
p 2385 N92-24058
VOELLMER, GEORGE M. p 2381 N92-23377
VOGT, M. p 2421 N92-23864
VONBOEHM, HANS-DIETER p 2392 N92-23379
VONESTORFF, O. p 2324 N92-23792
VU-KHANH, T. p 2341 N92-23936
p 2342 N92-23939
VUORINEN, J. J. p 2350 N92-23179

W

WADA, MAKOTO p 2399 N92-23481
WAHLFRIDSSON, PETER S. H. p 2421 N92-23863
WAHLSTRAND, K. J. p 2371 N92-23902
WAINER, ILANA ELAZARI KEIN COARACY p 2404 N92-23160
WALKER, ROBERT M. p 2349 N92-23316
WALTERS, ROBERT p 2322 N92-23526
WALUKIEWICZ, W. p 2371 N92-23985
WANG, H. p 2341 N92-23936
WANG, J. C. F. p 2380 N92-24070
WANG, MENGHUA p 2392 N92-23145
WANG, XIAOGANG p 2457 N92-24000
WARNER, JOSEPH D. p 2365 N92-23415
WARNER, K. J. p 2335 N92-23287
p 2349 N92-23288
p 2439 N92-23289
WARNER, ROBERT A. p 2400 N92-23487
WARREN, JACK p 2458 N92-23315
WASCHER, W. W. p 2349 N92-23286
p 2335 N92-23287
p 2349 N92-23288
WATSON, M. M. p 2368 N92-23326
WATT, D. p 2360 N92-23625
WATTS, ALAN J. p 2336 N92-23321
WATTS, E. C. p 2405 N92-23204
p 2405 N92-23333
WATTS, G. p 2418 N92-23432
WATTS, J. W., JR. p 2461 N92-23302
p 2440 N92-23303
p 2440 N92-23304
WATTS, JOHN W. p 2439 N92-23292
WAXMAN, RONALD p 2419 N92-23852
WEBER, H. p 2331 N92-23837
p 2332 N92-23842
WEICKMANN, A. p 2412 N92-23669
WEINBERG, I. p 2370 N92-23562
WEINBERG, JERRY L. p 2458 N92-23317
WEIRUP, D. L. p 2446 N92-24067
WEISENBERGER, A. G. p 2460 N92-23293
WEISSBLUTH, M. J. p 2409 N92-23257
WEITSMAN, Y. J. p 2355 N92-23897
WENZEL, K.-P. p 2461 N92-23306
WERNTZ, P. p 2364 N92-23245
WERON, K. p 2435 N92-23220
p 2435 N92-23598
WESSELSKI, CLARENCE J. p 2385 N92-24051
WEST, LAWRENCE ALARIE, JR. p 2453 N92-23728
WEST, R. N. p 2450 N92-24007
WESTBROOK, C. K. p 2348 N92-23715
p 2349 N92-24064
WESTERHOLM, J. p 2442 N92-23662
WESTROP, JANE M. p 2306 N92-23729
WESTWATER, E. R. p 2401 N92-23521
WHEATCRAFT, LOUIS p 2427 N92-23361
WHEELER, R. p 2448 N92-23574
WHITTAKER, J. W. p 2363 N92-23899
p 2384 N92-23908
WIDGREN, BRIAN K. p 2428 N92-23370
WIENER, R. W. p 2374 N92-23516
WIERHEIM, G. p 2331 N92-23837
WIGHTMAN, J. A. p 2453 N92-23212
WILCOX, R. C. p 2356 N92-23555
WILKE, G. D. p 2380 N92-24065
WILKINS, B. R. p 2420 N92-23861
WILKINSON, R. ALLEN p 2363 N92-23640
WILLIAMS, E. R. p 2405 N92-23204
p 2405 N92-23333
WILLIAMS, M. D. p 2379 N92-23557
WILMAR, OTTO p 2326 N92-23806
WILMET, J. p 2400 N92-23488
WILT, THOMAS E. p 2340 N92-23195
WIMMER, SHMUEL p 2422 N92-23870
WING, P. C. p 2360 N92-23622
WINN, WILLARD G. p 2349 N92-23299
WISNIEWSKI, MICHAEL EDWARD p 2434 N92-23777
WOLF, DIETMAR p 2320 N92-23764
WOLFRAMM, A. P. p 2393 N92-23391
p 2394 N92-23396
WOLFRAMM, ARIBERT P. p 2392 N92-23379
WOLVERTON, C. p 2353 N92-23984
WONG, K. p 2379 N92-23571
WOODCOCK, GORDON R. p 2317 N92-24048
WOODRUFF, S. D. p 2411 N92-23660
WORGUL, B. V. p 2414 N92-24033
WORTMAN, JIM J. p 2458 N92-23317
p 2458 N92-23318
WRENN, G. A. p 2307 N92-23230
WRIGHT, JAN R. p 2333 N92-23849
WU, RICHARD L. C. p 2354 N92-23192
WUEBBLES, D. J. p 2404 N92-23123
p 2406 N92-23740

X

XING, D. Y. p 2446 N92-23260
XU, JINCHAO p 2432 N92 23329

Y

YABOROV, YU. F. p 2454 N92-23742
YAMAMOTO, MASATAKA p 2328 N92-23820
YAMANOUCHI, TAKASHI p 2399 N92-23481
YANG, Y. p 2350 N92-23178
YANG, ZHIQANG p 2301 N92-23341
YANO, T. p 2352 N92-23720
YARBROUGH, WALTHEA V. p 2364 N92-23966
YAZAKI, SHINOBU p 2397 N92-23474
YEE, J. H. p 2371 N92-23902
p 2344 N92-23988
YEE, KANE S. p 2366 N92-23528
YEN, BING KANG p 2345 N92-24013

YING, HEPING ..... p 2446 N92-23259
YORITAKA, HIROYUKI ..... p 2398 N92-23476
YOSHIZAWA, IWAO ..... p 2353 N92-23134
YOUNG, L. E. ..... p 2316 N92-23919
YU, K. M. ..... p 2371 N92-23985
YU, L. ..... p 2447 N92-23452
YU, S. T. ..... p 2304 N92-23355
YU, SHENG-TAO ..... p 2302 N92-23344
p 2304 N92-23354
YUAN, CHEN-KEE ..... p 2383 N92-23691
YUE, F. ..... p 2411 N92-23682
YUNCK, THOMAS P. ..... p 2316 N92-23919
YUNIS, I. ..... p 2329 N92-23824

Z

ZANDBERGEN, P. J. ..... p 2373 N92-23251
ZEE, R. H. ..... p 2356 N92-23555
ZEKRI, N. ..... p 2350 N92-23210
p 2448 N92-23581
ZERBINI, SUZANNA ..... p 2315 N92-23915
ZHANG, JIANBO ..... p 2446 N92-23259
ZHANG, JIPING ..... p 2387 N92-23125
ZHAO, WEI ..... p 2425 N92-23583
ZHAO, XING ..... p 2383 N92-23690
ZHOU, PING ..... p 2442 N92-23748
ZHU, H. ..... p 2355 N92-23897
ZIEBARTH, JOHN P. ..... p 2375 N92-23568
ZIMMERMAN, ROBERT K., JR. ... p 2369 N92-23462
ZIMMERMANN, H. ..... p 2308 N92-23238
ZINKLE, S. J. ..... p 2354 N92-23222
ZINNER, ERNST ..... p 2349 N92-23316
ZIOCK, K. P. ..... p 2438 N92-23903
ZOLENSKY, MICHAEL E. ..... p 2336 N92-23314
ZOLENSKY, MIKE E. ..... p 2454 N92-23313
ZOOK, HERBERT A. ..... p 2459 N92-23322
ZUTAVERN, F. J. ..... p 2371 N92-23983

Typical Corporate Source Index Listing

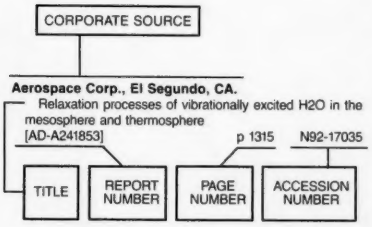

Listings in this index are arranged alphabetically by corporate source. The title of the document provides the user with a brief description of the subject matter. The report number helps to indicate the type of document cited (e.g., NASA report, translation, NASA contractor report). The accession number denotes the number by which the citation is identified. The page number helps you locate the citation in the abstract section. The titles are arranged under each corporate source in ascending accession number order.

A

AARHUS UNIV. (DENMARK).
Effect of microgravity environment on cell wall regeneration, cell divisions, growth, and differentiation of plants from protoplasts (7-IML-1) p 2358 N92-23609

ACADEMY OF SCIENCES (USSR), MOSCOW.
Family of Poisson structures on compact hermitian symmetric spaces
[PB92-149442] p 2433 N92-23670

ACUREX CORP., MOUNTAIN VIEW, CA.
White paper: Preliminary assessment of LNG vehicle technology, economics, and safety issues
[PB92-137603] p 2383 N92-23680

ADVISORY GROUP FOR AEROSPACE RESEARCH AND DEVELOPMENT, NEUILLY-SUR-SEINE (FRANCE).
Integrated Design Analysis and Optimisation of Aircraft Structures
[AGARD-R-784] p 2306 N92-23227
Special Course on Engineering Methods in Aerodynamic Analysis and Design of Aircraft
[AGARD-R-783] p 2308 N92-23950

AERONAUTICAL RESEARCH INST. OF SWEDEN, STOCKHOLM.
Experimental verification of a theory for the impact response of composite plates
[FFA-TN-1991-17] p 2339 N92-23167
Hypersonic laminar flow computations over a blunt leading edged delta wing at three different chord Reynolds numbers
[FFA-TN-1991-40] p 2304 N92-23168

AEROSPATIALE, LES MUREAUX (FRANCE).
Development status of the cryotechnical principal stage p 2319 N92-23758
Reusable launchers: New concepts and technological advances for the manufacturing of cryogenic tanks p 2319 N92-23760
Future launchers: Large size solid propellant monolithic booster p 2320 N92-23766
Multi parameter optimization on Ariane 5 p 2321 N92-23798
Mechanical behavior of composite materials and adhesive bonds at low temperatures p 2330 N92-23833

AIR FORCE SYSTEMS COMMAND, WRIGHT-PATTERSON AFB, OH.
Design challenges for the National Aero-Space Plane p 2310 N92-23822

AIRCRAFT RESEARCH ASSOCIATION LTD., BEDFORD (ENGLAND).
Survey of experimental techniques for performance prediction p 2309 N92-23954

ALABAMA A & M UNIV., HUNTSVILLE.
A study of solution crystal growth in LOW-g (2-IML-1) p 2361 N92-23630

ALABAMA UNIV., BIRMINGHAM.
Protein crystal growth (5-IML-1) p 2361 N92-23634

ALABAMA UNIV., HUNTSVILLE.
Microgravity dynamical behaviors of cryogenic liquid hydrogen reorientation and draining in space propulsion system p 2356 N92-23147
Computational fluid dynamics for propulsion technology: Geometric grid visualization in CFD-based propulsion technology research
[NASA-CR-190291] p 2375 N92-23568
Numerical simulation of fluid behaviors in microgravity environment p 2363 N92-23719
Advanced electric motor technology: Flux mapping
[NASA-CR-184317] p 2372 N92-24047

ALCATEL ESPACE, TOULOUSE (FRANCE).
Acoustic prediction on satellite structure p 2327 N92-23812

ALENIA, TORINO (ITALY).
A fin optimisation study p 2308 N92-23237

ALENIA SPAZIO S.P.A., ROME (ITALY).
Acoustic cavity and fluid/structure interaction models: A methodological deterministic approach and problems encountered p 2327 N92-23813
Modeling of honeycomb core for sandwich CTE prediction p 2332 N92-23841

ALENIA SPAZIO S.P.A., TURIN (ITALY).
Development and application of substructuring techniques for understanding and controlling residual vibrations (microgravity aspects) p 2330 N92-23827
The Aristoteles mission profile p 2316 N92-23922

ALLIED-SIGNAL AEROSPACE CO., KANSAS CITY, MO.
Nd: YAG laser welding aluminum alloys
[DE92-003131] p 2381 N92-23177
Procedure improvement enterprises
[DE92-003222] p 2453 N92-23183
Cracking investigation of Nd:YAG laser welded gold plated glass sealing alloys
[DE92-007971] p 2387 N92-23216
High strength composites evaluation
[DE92-007264] p 2340 N92-23585
Measurement of surface cleanliness by area-of-spread
[DE92-007265] p 2348 N92-23586
Improvement of laser machining processes
[DE92-007801] p 2380 N92-23723
Fabrication of a helical coil shape memory alloy actuator
[DE92-008399] p 2364 N92-23901
Replacement of hydrogen peroxide cleaning with oxygen plasma
[DE92-009020] p 2445 N92-23905

AMES LAB., IA.
Magnetic flux motion and flux pinning superconductors
[DE92-008243] p 2449 N92-23892

ARGONNE NATIONAL LAB., IL.
The effect of processing on strength of Nicalon fibers in Nicalon fiber-SiC matrix composites
[DE92-006978] p 2340 N92-23256
Search for atmospheric neutrino oscillations with the Soudan 2 detector
[DE92-007397] p 2437 N92-23328
Data exploration systems for databases p 2429 N92-23374
Melting of nickel clusters
[DE92-006986] p 2351 N92-23573
TEM study of flux pinning defects in YBa2Cu3O7-delta produced by 580 MeV Sn ion irradiation
[DE92-006991] p 2448 N92-23574
Transport calculations of chemically sputtered carbon near a plasma divertor surface
[DE92-009022] p 2445 N92-24021

ARISTOTLE UNIV. OF THESSALONIKI (GREECE).
Optimum cutting conditions determination for the NC-milling
[REPT-2.1.2] p 2422 N92-23874

ARIZONA UNIV., TUCSON.
Simulation of freckles during vertical solidification of binary alloys p 2353 N92-24014

ARKANSAS UNIV., FAYETTEVILLE.
Rapid recrystallization of semiconductor thin films for photovoltaic applications p 2404 N92-23998
Strongly coupled cavity QED p 2442 N92-23999

ASSISTANT SECRETARY OF DEFENSE (COMPTROLLER), WASHINGTON, DC.
Research, Development, Test and Evaluation (R, D, T, and E) Programs (R-1), Department of Defense budget for fiscal year 1993
[PB92-127745] p 2451 N92-23247

AUBURN UNIV., AL.
Chemical compatibility of cartridge materials
[NASA-CR-190256] p 2356 N92-23555

AVIONS MARCEL DASSAULT-BREGUET AVIATION, SAINT-CLOUD (FRANCE).
Non linear structural analysis of a thin skin carbon-carbon rigid decelerator p 2330 N92-23831
Stretched skin concept for the entry aerodynamic decelerator system of planetary probes p 2331 N92-23836

B

BATH UNIV. (ENGLAND).
The effect of fatigue-induced damage on the mechanical properties of CFRP composites p 2339 N92-23157

BEN GURION UNIV. OF THE NEGEV, BEERSHEVA (ISRAEL).
Group scheduling using group technology concepts
[REPT-3.3.2] p 2424 N92-23886

BESANCON UNIV. (FRANCE).
Matching finite element models to modal data p 2333 N92-23848

BIONETICS CORP., COCOA BEACH, FL.
Acid rain monitoring in East-Central Florida from 1977 to present
[NASA-CR-190152] p 2406 N92-23898

BOEING AEROSPACE AND ELECTRONICS CO., HUNTSVILLE, AL.
Structural assessment of the Space Station Freedom's pressurized elements p 2323 N92-23783

BOEING AEROSPACE CO., HUNTSVILLE, AL.
Space transfer concepts and analyses for exploration missions: Technical directive 10
[NASA-CR-184309] p 2317 N92-24048

BOEING CO., SEATTLE, WA.
Particle types and sources associated with LDEF p 2349 N92-23286
Migration and generation of contaminants from launch through recovery: LDEF case history p 2335 N92-23287
Quantification of contaminants associated with LDEF p 2349 N92-23288
Molecular films associated with LDEF p 2439 N92-23289

BOEING COMMERCIAL AIRPLANE CO., SEATTLE, WA.
Space Station Freedom p 2313 N92-23649

BOMBRINI PARODI-DELFINO S.P.A., COLLEFERRO (ITALY).
Manufacturing process of the Ariane 5 segmented propellant chargers p 2319 N92-23756

BOSTON UNIV., MA.
Photoinduced electron transfer in ordered polymers
[DE92-008787] p 2355 N92-24037

BRISTOL UNIV. (ENGLAND).
Applications of boundary integral methods to the study of steep free surface waves p 2372 N92-23149

BRITISH AEROSPACE PUBLIC LTD. CO., BRISTOL (ENGLAND).
Simultaneous stress and flutter optimization for the wing of a transport aircraft equipped with four engines p 2308 N92-23238
BRITISH AEROSPACE PUBLIC LTD. CO., LANCASHIRE (ENGLAND).
Application of an automated multidisciplinary analysis and optimisation system to the design of aircraft structures p 2307 N92-23233
BRITISH COLUMBIA UNIV., VANCOUVER.
Phase partitioning experiment (8-IML-1) p 2360 N92-23621
Back pain in astronauts (8-IML-1) p 2360 N92-23622
A method to determine resin flow during curing of composite laminates p 2342 N92-23938
BROOKHAVEN NATIONAL LAB., UPTON, NY.
In situ XANES study of the valence state of chromium during electrochemical polarization of AlCr alloys [DE92-007452] p 2350 N92-23197
Application of x ray absorption spectroscopy to the study of corrosion and inhibition [DE92-007456] p 2350 N92-23198
Applications of x ray synchrotron radiation techniques to the study of dispersed electrocatalysts in high area materials [DE92-007458] p 2346 N92-23199
A multilevel preconditioner for domain decomposition boundary systems [DE92-008055] p 2432 N92-23329
BROWN UNIV., PROVIDENCE, RI.
The meteorite record as clues to asteroidal regolith processes p 2457 N92-23770

C

CALGARY UNIV. (ALBERTA).
Energy expenditure in space flight (doubly labelled water method) (8-IML-1) p 2359 N92-23620
CALIFORNIA INST. OF TECH., PASADENA.
Fundamental electron transfer processes at the single crystal semiconductor/liquid interface [DE92-008132] p 2447 N92-23275
High energy physics: Report of research accomplishments and future goals, FY 1992 [DE92-008543] p 2441 N92-23576
CALIFORNIA UNIV., BERKELEY.
Constructing a pulsar timing array p 2456 N92-23126
A damage mechanics model for beams p 2387 N92-23159
High resolution studies of NGC 1275 and the galactic center p 2455 N92-23675
Continuous profiling of magnetotelluric fields p 2401 N92-23703
Transverse deformation of unidirectional fiber-reinforced metal matrix composites p 2345 N92-24013
CALIFORNIA UNIV., BERKELEY. LAWRENCE BERKELEY LAB.
Particle physics and cosmology [DE92-008301] p 2456 N92-23153
A switched capacitor array based system for high-speed calorimetry [DE92-008288] p 2378 N92-23278
Test beam results from the D0 end electromagnetic calorimeter [DE92-008299] p 2378 N92-23279
Radioactivities of Long Duration Exposure Facility (LDEF) materials: Baggage and bonanzas p 2440 N92-23297
Profiling and mapping of advanced materials using spatially resolved Raman spectroscopy [DE92-008304] p 2347 N92-23449
Potential energy surfaces and reaction dynamics of polyatomic molecules [DE92-008314] p 2437 N92-23450
The oxidation behavior of Co-15wt percent Cr alloy containing dispersed oxides formed by internal oxidation [DE92-008283] p 2352 N92-23893
Ground state searches in FCC intermetallics [DE92-008300] p 2353 N92-23984
The effect of co-implantation on the electrical activity of implanted carbon in GaAs [DE92-008307] p 2371 N92-23985
CALIFORNIA UNIV., DAVIS.
Free vibration of thick isotropic and orthotropic cylindrical shells p 2389 N92-23773
CALIFORNIA UNIV., IRVINE.
Inelastic electron scattering from surfaces [DE92-008129] p 2437 N92-23330
CALIFORNIA UNIV., LOS ANGELES.
An observational study of the internal structure of air-mass thunderstorms p 2409 N92-23121
Application of optical distributed sensing and computation to control of large space structures [NASA-CR-190293] p 2442 N92-23567
Free and forced response of nearly periodic multi-span beams and multi-bay trusses p 2389 N92-23699
Nuclear winds in active galaxies p 2457 N92-23716
Adaptive active flutter suppression of wings in subsonic and transonic flight regimes p 2310 N92-24010
CALIFORNIA UNIV., RIVERSIDE.
Gamma rays from SN1987A with the UCR double-Compton telescope p 2455 N92-23695
CALIFORNIA UNIV., SAN DIEGO.
High-temperature superconductivity: Electron-doped cuprates and composites from alloy precursors p 2448 N92-23774
CALIFORNIA UNIV., SANTA CRUZ.
Type Ib supernovae and a new radiation hydrodynamics code p 2458 N92-24017
CAMBRIDGE UNIV. (ENGLAND).
Development of fatigue damage mechanics for application to the design of damage-tolerant composite components p 2324 N92-23793
CANADIAN SPACE AGENCY, OTTAWA (ONTARIO).
Measurement of venous compliance (8-IML-1) p 2360 N92-23623
CARNEGIE-MELLON UNIV., PITTSBURGH, PA.
The role of microstructural phenomena in magnetic thin films [DE92-007960] p 2446 N92-23213
A framework for the support of VLSI (very large scale integration) design for manufacture [REPT-1.3.1] p 2421 N92-23868
Statistical process control system for VLSI fabrication [REPT-1.3.4] p 2422 N92-23871
Analytical and experimental investigation of vibratory response in adhesively bonded and composite structures p 2345 N92-24012
CASA-RI/SME, TEL AVIV (ISRAEL).
Proceedings of the International Conference on CAD/CAM and AMT. Volume 1: General sessions [ITN-92-85127] p 2418 N92-23851
CASE WESTERN RESERVE UNIV., CLEVELAND, OH.
Reaction layer formation at the graphite/copper-chromium alloy interface [NASA-CR-189147] p 2351 N92-23436
Training users of a flexible decision support system: The effects of training content and user ability p 2453 N92-23730
CENTER FOR TECHNOLOGY, HOLON (ISRAEL).
Creative search systems as specific expert systems [REPT-1.1.8] p 2420 N92-23859
CENTRE NATIONAL D'ETUDES SPATIALES, PARIS (FRANCE).
Development of solid propellant booster p 2320 N92-23767
Ariane 4 internal acoustic environment: Interpretation of flight data with a vibroacoustic model of the upper part of the launcher p 2321 N92-23811
CENTRE NATIONAL D'ETUDES SPATIALES, TOULOUSE (FRANCE).
Coupled load analysis: Scatter related to model uncertainties p 2324 N92-23787
Dynamic load cases on Ariane 5 p 2321 N92-23797
Feasibility of payload sensitivity analyses for AR4 dynamic events p 2328 N92-23815
Gravity field data products from the Aristoteles mission p 2317 N92-23925
CENTRO NAZIONALE UNIV. PER IL CALCOLO ELETTRONICO, PISA (ITALY).
Salyut-7/Kosmos-1686 reentry predictions for the Italian Civil Defence Authority p 2334 N92-23972
CHEMICAL AUTOMATICS DESIGN BUREAU, VORONEZH (USSR).
Experience of the Chemical Automatics Design Bureau in creation of RD-0120 LOX/LH2 liquid rocket engine with thrust of 2 mn for Energia launcher p 2319 N92-23757
CHIBA UNIV. (JAPAN).
Retrieval of upper precipitable water profile from MOS-1 VTIR water vapor channel p 2398 N92-23479
CHRISTOPHER NEWPORT COLL., NEWPORT NEWS, VA.
Characterizing and testing a thermally isolating superconducting link for SAFIRE-like missions [NASA-CR-190196] p 2369 N92-23430
CINCINNATI UNIV., OH.
Impinging axisymmetric jet p 2372 N92-23146
An adaptive-grid technique for simulation of complex unsteady flows p 2372 N92-23148
CIVIL AEROMEDICAL INST., OKLAHOMA CITY, OK.
Radiation exposure of air carrier crewmembers 2 [PB92-140037] p 2414 N92-23139
CLARKSON UNIV., POTSDAM, NY.
Mechanical properties of glass bead filled ductile epoxy composites p 2344 N92-23947
CLERMONT-FERRAND UNIV. (FRANCE).
Mercury iodide nucleation and crystal growth in vapor phase (4-IML-1) p 2361 N92-23633
COLORADO STATE UNIV., FORT COLLINS.
Quasi-three-dimensional simulations of deep convection [DE92-007204] p 2409 N92-23257
COLORADO UNIV., BOULDER.
Particle dynamics in a wave with variable amplitude [DE92-008340] p 2436 N92-23217
COLORADO UNIV., COLORADO SPRINGS.
Feature detection in satellite images using neural network technology p 2427 N92-23366
COLUMBIA UNIV., NEW YORK, NY.
Reconstructing the tropical Atlantic seasonal thermocline using planktonic foraminifera p 2412 N92-23769
Magnetic reconnection in magnetotail and solar plasmas p 2457 N92-24000
Low dose neutron late effects: Cataractogenesis [DE92-005539] p 2414 N92-24033
COMMISSARIAT A L'ENERGIE ATOMIQUE, GIF-SUR-YVETTE (FRANCE).
Near-critical point phenomena in fluids (19-IML-1) p 2362 N92-23638
COMMISSION OF THE EUROPEAN COMMUNITIES, BRUSSELS (BELGIUM).
Fatigue analysis under random stresses p 2325 N92-23795
COMMISSION OF THE EUROPEAN COMMUNITIES (LUXEMBOURG).
Methods for the detection of microorganisms in the environment [PB92-137454] p 2405 N92-23512
COMPUTER APPLICATION SYSTEMS, SIGNAL MOUNTAIN, TN.
Improved image classification with neural networks by fusing multispectral signatures with topological data p 2402 N92-23368
CONCEPTUAL RESEARCH CORP., SYLMAR, CA.
Configuration development p 2309 N92-23953
CONNECTICUT UNIV., STORRS.
Rotating, radiating mass imbedded in a de Sitter universe p 2456 N92-23127
CONSEJO SUPERIOR DE INVESTIGACIONES CIENTIFICAS, MADRID (SPAIN).
The effect of space environment on the development and aging of Drosophila Melanogaster (7-IML-1) p 2357 N92-23608
CONSTRUCCIONES AERONAUTICAS S.A., MADRID (SPAIN).
Brief history of the development of the EPS-structure p 2321 N92-23810
Comparison of multi-point modal test methods p 2333 N92-23849
CORNELL UNIV., ITHACA, NY.
Infrared emission lines from highly ionized regions p 2460 N92-23162
RNG in turbulence and modeling of bypass transition p 2301 N92-23341
The statics, dynamics, and control of the elasticarm: A continuous beam manipulator p 2383 N92-23691
Radar observations and dynamics of the polar summer mesosphere p 2408 N92-23702
COUNCIL ON ENVIRONMENTAL QUALITY, WASHINGTON, DC.
National acid precipitation assessment program: Mission, goals, and program plan post 1990. Public review draft [PB92-128248] p 2405 N92-23515
National acid precipitation assessment program: 1990 integrated assessment report [PB92-100346] p 2406 N92-23593
CRANFIELD INST. OF TECH., BEDFORD (ENGLAND).
Topics in numerical computation of compressible flow p 2375 N92-23692

D

DAISY/CADNETIX ISRAEL LTD., HERZLIYA.
The use of EDIF at Daisy/Cadnetix [REPT-4.2.1] p 2424 N92-23887
DASSAULT ESPACE, SAINT-CLOUD (FRANCE).
Structural optimization of aircraft practice and trends p 2308 N92-23239
The challenge of the Hermes TPS shingles p 2322 N92-23823
Computational procedures for preliminary design p 2309 N92-23952
DELAWARE UNIV., NEWARK.
Crack path prediction near an elliptical inhomogeneity p 2389 N92-23688
Evaluation of terrestrial climate variability using a moisture index p 2411 N92-23771

On the application of micromechanics to the prediction of macroscopic thermal residual stresses in short-fiber reinforced Polyetheretherketone (PEEK)
p 2343 N92-23942

DEPARTMENT OF ENERGY, WASHINGTON, DC.
Limiting net greenhouse gas emissions in the United States, volume 1
[DE92-007593] p 2405 N92-23204
Limiting net greenhouse gas emissions in the United States, volume 2
[DE92-007592] p 2405 N92-23333

DEUTSCHE AGENTUR FUER RAUMFAHRTANGELEGENHEITEN G.M.B.H., BONN (GERMANY, F.R.).
CRYOSTAT (18-IML-1) p 2362 N92-23636

DEUTSCHE FORSCHUNGSANSTALT FUER LUFT- UND RAUMFAHRT, BRUNSWICK (GERMANY, F.R.).
Characterization of interlaminar mode 1 and mode 2 fracture in CFRP laminates p 2325 N92-23794
Damping behaviour of unidirectional fibre reinforced polymers p 2326 N92-23805
Aging of polymer matrix composites at elevated temperatures p 2328 N92-23817
Experimental study of delamination growth in multidirectional CFRP-laminates under fatigue loading
p 2328 N92-23819
Notched strength of composite materials
p 2331 N92-23839

DEUTSCHE FORSCHUNGSANSTALT FUER LUFT- UND RAUMFAHRT, COLOGNE (GERMANY, F.R.).
Preconsiderations on aircraft integration
p 2395 N92-23402
Embryogenesis and organogenesis of Carausius morosus under space flight conditions (7-IML-1)
p 2358 N92-23610
Dosimetric mapping inside biorack (7-IML-1)
p 2358 N92-23611
Gravity related behavior of the acellular slime mold Physarum polycephalum (7-IML-1) p 2359 N92-23618
Biostack (14-IML-1) p 2361 N92-23627

DEUTSCHE FORSCHUNGSANSTALT FUER LUFT- UND RAUMFAHRT, GOETTINGEN (GERMANY, F.R.).
Optimal exciter placement and force vector tuning required for experimental modal analysis
p 2333 N92-23847

DISTRICT OF COLUMBIA UNIV., WASHINGTON, DC.
Clouds, surface temperature, and the tropical and subtropical radiation budget p 2410 N92-23431

DNV INGEMANSSON A.B. (SWEDEN).
Computer simulation of moisture penetration in structures p 2326 N92-23806

DORNIER SYSTEM G.M.B.H., FRIEDRICHSHAFEN (GERMANY, F.R.).
Buckling and failure of thin elliptical delaminations in composites p 2331 N92-23835
Design parameter update of dynamic mathematical models in presence of test noise and mode pairing problems p 2333 N92-23850

DU PONT DE NEMOURS (E. I.) AND CO., DEEPWATER, NJ.
Advanced Materials Center, Battelle
p 2314 N92-23652

DUBLIN INST. FOR ADVANCED STUDIES (IRELAND).
The LDEF ultra heavy cosmic ray experiment
p 2461 N92-23306

DURHAM UNIV. (ENGLAND).
TeV gamma ray emission from accreting binary pulsars p 2460 N92-23736

E

ECOLE POLYTECHNIQUE, MONTREAL (QUEBEC).
Weldline strength in injection molded glass fiber reinforced polypropylene p 2344 N92-23949

EG AND G ENERGY MEASUREMENTS, INC., GOLETA, CA.
Vapor crystal growth studies of single crystals of mercuric iodide (3-IML-1) p 2361 N92-23632

EG AND G ROCKY FLATS, INC., GOLDEN, CO.
Liquid/supercritical fluid carbon dioxide cleaning of stainless steel components
[DE92-006947] p 2348 N92-23572

EIDGENOESSISCHE TECHNISCHE HOCHSCHULE, ZURICH (SWITZERLAND).
Friend leukemia virus transformed cells exposed to microgravity in the presence of DMSO (7-IML-1)
p 2358 N92-23613
Proliferation and performance of hybridoma cells in microgravity (7-IML-1) p 2358 N92-23614
Dynamic cell culture system (7-IML-1)
p 2359 N92-23615

ELTA ELECTRONICS INDUSTRIES, ASHDOD (ISRAEL).
Deleting pads in multi-layered printed circuits
[REPT-4.2.3] p 2425 N92-23889

ENGINEERING AND ECONOMICS RESEARCH, INC., HOUSTON, TX.
Launch vehicle for orbital missions: COMET
p 2313 N92-23645

ENVIRONMENTAL PROTECTION AGENCY, ANN ARBOR, MI.
Evaluation of research prototype vehicles equipped with direct injection 2-stroke cycle engines
[PB92-143692] p 2383 N92-23595

ENVIRONMENTAL PROTECTION AGENCY, RESEARCH TRIANGLE PARK, NC.
National air quality and emissions trends report, 1990
[PB92-141555] p 2406 N92-23517

ERNO RAUMFAHRTTECHNIK G.M.B.H. BREMEN (GERMANY, F.R.).
The Columbus Free Flying Laboratory: Mechanical design aspects p 2323 N92-23782
Protection of spacecraft against meteroid/orbital debris impacts p 2323 N92-23786
On the modelling of a deployable telescope elastic beam-type element for on-orbit multibody simulations
p 2329 N92-23826

ESDU INTERNATIONAL LTD., LONDON (ENGLAND).
The statistical analysis of data from normal distributions, with particular reference to small samples
[ESDU-91041] p 2434 N92-24008
Normal force of low aspect ratio wing-body combinations up to high angles of attack at supersonic speeds
[ESDU-91042] p 2309 N92-24009

EUROPEAN SPACE AGENCY, PARIS (FRANCE).
Launcher Propulsion Towards the Year 2010
[ESA-SP-327] p 2318 N92-23750
Ariane technology: From today into the next century
p 2318 N92-23751
Spacecraft Structures and Mechanical Testing, volume 1
[ESA-SP-321-VOL-1] p 2322 N92-23780
Ariane 5 structural definition of the upper composite
p 2321 N92-23808
The Solid-Earth Mission Aristoteles
[ESA-SP-329] p 2314 N92-23910
The Reentry of Salyut-7/Kosmos-1686
[ESA-SP-345] p 2333 N92-23967

EUROPEAN SPACE AGENCY. ESRIN, FRASCATI (ITALY).
Data distribution and reduction approaches to data distribution: The Earthnet experience
p 2317 N92-23926

EUROPEAN SPACE AGENCY. EUROPEAN SPACE OPERATIONS CENTER, DARMSTADT (GERMANY, F.R.).
Aristoteles ground segment: Operational concept
p 2316 N92-23923
Salyut-7/Kosmos-1686 reentry prediction activities at ESOC p 2334 N92-23970
Prediction of solar and geomagnetic activity for ESA low-flying spacecraft p 2334 N92-23975
Salyut-7/Kosmos-1686 orbit determination from radar data p 2318 N92-23976
Lifetime of objects in geostationary transfer orbit
p 2318 N92-23977

EUROPEAN SPACE AGENCY. EUROPEAN SPACE RESEARCH AND TECHNOLOGY CENTER, ESTEC, NOORDWIJK (NETHERLANDS).
The validation of hydrocodes for orbital debris impact simulation p 2323 N92-23784
Fluid-structure interaction problems: Development of special processors p 2332 N92-23845
Introductory remarks to the mission and system aspects session p 2315 N92-23916

EUROPROPULSION, SURESNES (FRANCE).
Development status of the Ariane 5 solid propellant engine p 2319 N92-23755

F

FAR SEAS FISHERIES RESEARCH LAB., SHIMIZU (JAPAN).
The accuracy of the drift buoy positioning by MOS-1 DCS p 2399 N92-23484

FERMI NATIONAL ACCELERATOR LAB., BATAVIA, IL.
Modeling of the DZero data acquisition system
[DE92-007913] p 2453 N92-23212
A new VME based high voltage power supply for large experiments
[DE92-007199] p 2368 N92-23326
General P-T fit construction for He, N2, Ar, H2 and Ne VPT used at Fermilab
[DE92-008851] p 2433 N92-23579

FLORIDA STATE UNIV., TALLAHASSEE.
Pulsed electron beam precharger
[DE92-008693] p 2439 N92-24031

FLORIDA UNIV., GAINESVILLE.
The influence of chromium on structure and mechanical properties of B2 nickel aluminide alloys
[NASA-CR-189124] p 2351 N92-23566
Semirigid construction of topological supergravities
[DE92-008772] p 2451 N92-24040

FOOD AND AGRICULTURE ORGANIZATION OF THE UNITED NATIONS, ROME (ITALY).
Irradiation of spices, herbs, and other vegetable seasonings: A compilation of technical data for its authorization and control
[DE92-619064] p 2415 N92-24022

FORESTRY AND FOREST PRODUCTS RESEARCH INST., IBARAKI (JAPAN).
Evaluation of effective characteristic in forest field
p 2397 N92-23473

FORSCHUNGSINSTITUT FUER HOCHFREQUENZPHYSIK, WERTHHOVEN (GERMANY, F.R.).
Radar tracking and observation of noncooperative space objects by reentry of Salyut-7/Kosmos-1686
p 2333 N92-23968
Orbit analysis and lifetime prediction using radar data by reentry of Salyut-7/Kosmos-1686
p 2318 N92-23969

FRAMASOFT + CSI, PARIS (FRANCE).
Fatigue analysis under random stresses
p 2325 N92-23795

FRAUNHOFER-INST. FUER TREIB- UND EXPLOSIVSTOFFE, PFINZTAL-BERGHAUSEN (GERMANY, F.R.).
Investigations of the dynamic behaviour of compounds under preloading p 2332 N92-23842

FRAZER-NASH CONSULTANCY LTD., LEATHERHEAD (ENGLAND).
The use of modal synthesis in conjunction with nonlinear transient dynamic analysis p 2324 N92-23788

G

GENERAL ACCOUNTING OFFICE, WASHINGTON, DC.
Earth observing system: NASA's EOSDIS development approach is risky
[GAO/IMTEC-92-24] p 2401 N92-23686

GENERAL ATOMIC CO., SAN DIEGO, CA.
Fast wave current drive antenna performance on D3-D
[DE92-008052] p 2444 N92-23446

GENERAL DYNAMICS CORP., FORT WORTH, TX.
Application of analytical and design tools for fighter wing aeroelastic tailoring p 2307 N92-23231

GENERAL ELECTRIC CO., PHILADELPHIA, PA.
The achievement of spacecraft autonomy through the thematic application of multiple cooperating intelligent agents p 2427 N92-23364

GENETECH, INC., SAN FRANCISCO, CA.
Center for Cell Research, Pennsylvania State University p 2314 N92-23653

GEORGE MASON UNIV., FAIRFAX, VA.
Knowledge-based approach for generating target system specifications from a domain model
p 2428 N92-23371

GEORGE WASHINGTON UNIV., WASHINGTON, DC.
Publications of the exobiology program for 1990: A special bibliography
[NASA-TM-4364] p 2416 N92-23429

GEORGIA INST. OF TECH., ATLANTA.
Small solutions and completeness for linear functional differential equations
[PB92-149350] p 2431 N92-23250
Nonlinear feedback guidance law for aero-assisted orbit transfer maneuvers
[NASA-CR-190129] p 2317 N92-23529
Analysis of delamination related fracture processes in composites
[NASA-CR-190226] p 2340 N92-23532
The design and control of uncertain manipulator arms with decoupled inertia matrix p 2383 N92-23690

GEORGIA STATE UNIV., ATLANTA.
On the limiting astrometric accuracy of binary star speckle interferometry p 2457 N92-23896

GOSUDARSTVENNYI KOMITET PO ISPOLZOVANIYU ATOMNOI ENERGII, SERPUKHOV (USSR).
Thresholds of longitudinal instability of bunched beam in the presence of dominant inductive impedance
[DE92-617992] p 2436 N92-23274

GRUMMAN AEROSPACE CORP., BETHPAGE, NY.
Thermoluminescent dosimetry for LDEF experiment M0006 p 2461 N92-23301
Aircraft drag analysis methods p 2309 N92-23957

GTE GOVERNMENT SYSTEMS CORP., CHANTILLY, VA.
Interim Service ISDN Satellite (ISIS) hardware experiment development for advanced ISDN satellite designs and experiments
[NASA-CR-190257] p 2335 N92-24046

H

HAMBURG UNIV. (GERMANY, F.R.).
Geophysical, chemical and biological measuring parameters p 2393 N92-23385
HARVARD UNIV., CAMBRIDGE, MA.
The origins of the cosmic x ray and gamma ray backgrounds p 2460 N92-23141
Expert systems: A mapping between symbol susceptible tasks and software tools p 2454 N92-24016
HELSINKI UNIV. OF TECHNOLOGY, ESPOO (FINLAND).
Use of control theory for analyzing stability of states in continuum thermodynamics
[PB92-136571] p 2451 N92-23136
Problem of membrane locking in finite element analysis of cylindrical shells
[PB92-133941] p 2387 N92-23137
Electrostatic image solution for the interaction of two dielectric spheres
[PB92-142199] p 2364 N92-23138
Oil lubricated and water lubricated pin-on-disc wear tests with engineering ceramics
[PB92-136563] p 2380 N92-23152
Design and performance of 22 GHz coaxial low noise MESFET and HEMT amplifiers
[PB92-134071] p 2368 N92-23172
Effects of impurities on the solidification and mechanical behaviour of primary and secondary commercial purity aluminium and aluminium alloys
[PB92-133511] p 2350 N92-23176
Production of metal powders by hydrogen stripping from loaded organic extractants
[PB92-136464] p 2350 N92-23178
Casting of simple-shaped single crystals of aluminum
[PB92-136555] p 2350 N92-23179
Compositionality and analysis of algebraic high-level nets
[PB92-143551] p 2432 N92-23440
Development of a helicopter-borne 8-channel ranging scatterometer
[PB92-141977] p 2396 N92-23441
Waveform relaxation always converges for RC-circuits
[PB92-142280] p 2369 N92-23495
Analysis of a 37 kW cage-induction motor
[PB92-142116] p 2369 N92-23496
Higher order temperature compensation of bandgap voltage references (I)
[PB92-142306] p 2370 N92-23497
Semiclassical model and properties of resonant tunneling diode
[PB92-143320] p 2448 N92-23498
Theory for iterative solution of large dynamical systems using parallel computation
[PB92-143304] p 2433 N92-23589
Biisotropic polarizer shield
[PB92-141878] p 2366 N92-23590
Closed parallel-plate chiral waveguides with boundary impedance conditions
[PB92-142397] p 2366 N92-23591
Comparison of analytical and numerical modelling approaches for sizing of seasonal storage solar heating systems
[PB92-141829] p 2403 N92-23592
Microsphere viscometers for low temperature applications
[PB92-143361] p 2379 N92-23594
Sensitivity I(sup 1) minimization with boundary zeros or poles
[PB92-141803] p 2433 N92-23658
Properties of bi-isotropic Fresnel reflection coefficients
[PB92-141886] p 2366 N92-23661
Binary surface-relief gratings for array illumination in digital optics
[PB92-143585] p 2442 N92-23662
Theory study on fast wave absorption at the plasma edge
[PB92-141936] p 2444 N92-23663
Nonlinear finite element analysis of space frames
[PB92-142447] p 2388 N92-23664
Ultrasonic investigation of (3)He-A vortices in low magnetic fields
[PB92-142256] p 2435 N92-23665
Quasi-static image theory for the bi-isotropic (nonreciprocal chiral) sphere
[PB92-142371] p 2366 N92-23666
Electrostatic image theory for the dielectric sphere with an internal source
[PB92-142405] p 2366 N92-23667
Electrostatic image theory for the layered dielectric sphere
[PB92-142413] p 2367 N92-23668
MOSFET level 1 and 2 models in APLAC
[PB92-143379] p 2371 N92-23678
Vector circuit method applied for chiral dielectric slab waveguides
[PB92-142355] p 2367 N92-23679
PHOTO: A computer simulation program for photovoltaic and hybrid energy systems. Document and user's guide
[PB92-141928] p 2403 N92-23683
Mathematical model of a control valve
[PB92-141951] p 2383 N92-23710
Application of the Green function technique in the microstrip patch antenna analysis
[PB92-142173] p 2367 N92-23907
HERIOT-WATT UNIV., EDINBURGH (SCOTLAND).
Binary surface-relief gratings for array illumination in digital optics
[PB92-143585] p 2442 N92-23662
HOKKAIDO INST. OF TECH. (JAPAN).
Availability of MSR data for snow water estimation p 2399 N92-23482
HOUSTON UNIV., TX.
The subionospheric electromagnetic response to magnetopause processes p 2407 N92-23142
HOWARD UNIV., WASHINGTON, DC.
Injection seeding of a Q-switched alexandrite laser: Study of frequency stabilization p 2380 N92-23961
The use of high temperature superconductors to levitate lunar telescope p 2456 N92-23962
HUBRECHT LAB., UTRECHT (NETHERLANDS).
Eggs: The role of gravity in the establishment of the dorso-ventral axis in the amphibian embryo (7-IML-1) p 2357 N92-23607
HYPERSCHALL-TECHNOLOGIE-GOETTINGEN, LINDAU HARZ (GERMANY, F.R.).
Modelling of aerodynamic forces and heat transfer for orbital decay and reentry calculations p 2334 N92-23974

I

IBM ISRAEL SCIENTIFIC CENTER, HAIFA.
On generating two dimensional CMOS cells
[REPT-1.3.2] p 2421 N92-23869
Breathing maze router for analog VLSI cell generation
[REPT-1.3.3] p 2422 N92-23870
IKO SOFTWARE SERVICE G.M.B.H., STUTTGART (GERMANY, F.R.).
Employment of C.B. (Craig-Bampton) models for nonlinear dynamic analysis p 2327 N92-23814
ILLINOIS UNIV., CHICAGO.
Kinetics of combustion-related processes at high temperatures
[DE92-008790] p 2348 N92-24038
IMAX SPACE TECHNOLOGY, INC., HOUSTON, TX.
IMAX camera (12-IML-1) p 2363 N92-23641
IMS/VALID INTERNATIONAL, SLOUGH (ENGLAND).
An integrated test solution to address scan techniques
[REPT-1.2.3] p 2420 N92-23862
INDIAN SPACE RESEARCH ORGANIZATION, AHMEDABAD.
A note on data quality: MSR data p 2400 N92-23489
Comparative study of digital MOS-1 MESSR, LANDSAT MSS, and IRS LISS-1 data for land cover classification in Sambalpur district, India p 2400 N92-23490
Data quality evaluation results MOS-1 verification program p 2400 N92-23491
Estimation of regional evapotranspiration with MOS-1 VTIR data p 2401 N92-23492
An attempt to derive land surface temperatures from MOS-1 VTIR data using split-window channel computation technique p 2401 N92-23493
INDIAN SPACE RESEARCH ORGANIZATION, BANGALORE.
On development of automated static loading system for spacecraft structures p 2326 N92-23801
INDIANA UNIV., BLOOMINGTON.
The isotopic composition of cosmic ray helium from 500 to 1100 MeV per nucleon p 2460 N92-23163
INDUSTRIEANLAGEN-BETRIEBSGESELLSCHAFT M.B.H., OTTOBRUNN (GERMANY, F.R.).
Numerical and experimental study of noise generated by a vibrating plate p 2324 N92-23792
Numerical investigation of fluid-structure-interaction problems with the finite element method p 2332 N92-23844
INNSBRUCK UNIV. (AUSTRIA).
The response surface method: An efficient tool to determine the failure probability of large structural systems p 2328 N92-23816
INSTITUT DES HAUTES ETUDES SCIENTIFIQUES, BURES-SUR-YVETTE (FRANCE).
Non-commutative differential geometry and Yang-Baxter equation
[PB92-149459] p 2431 N92-23184
Existence of closed geodesics on 2-spheres
[PB92-149434] p 2433 N92-23599
Family of Poisson structures on compact hermitian symmetric spaces
[PB92-149442] p 2433 N92-23670
Sphere packings centered at S-units of algebraic tori
[PB92-136373] p 2434 N92-24061
INSTITUTE FOR SPACE SCIENCE AND TECHNOLOGY, INC., GAINESVILLE, FL.
Ion microprobe elemental analyses of impact features on interplanetary dust experiment sensor surfaces p 2458 N92-23318
INSTITUTO SUPERIOR TECNICO, LISBON (PORTUGAL).
Fast simulation of MOS digital networks using a physical macromodelling approach
[REPT-1.2.1] p 2420 N92-23860
Test preparation for MOS digital circuits using heuristics for reliable fault simulation
[REPT-1.2.6] p 2421 N92-23865
INTERATOM G.M.B.H., BERGISCH GLADBACH (GERMANY, F.R.).
Beryllium-thermal protection technology p 2331 N92-23837
INTERGRAPH CORP., RESTON, VA.
Center for Mapping, Ohio State University p 2314 N92-23655
INTERNATIONAL ATOMIC ENERGY AGENCY, VIENNA (AUSTRIA).
Neutron induced gamma-ray production data
[DE92-615322] p 2440 N92-23130
X ray analysis spectrometer
[DE92-615124] p 2378 N92-23219
Training guidelines in non-destructive testing techniques
[DE92-615083] p 2386 N92-23258
Method for evaluating non-consistent data using two statistical criteria
[DE92-615195] p 2454 N92-23742
Irradiation of spices, herbs, and other vegetable seasonings: A compilation of technical data for its authorization and control
[DE92-619064] p 2415 N92-24022
INTERNATIONAL CENTER FOR GENETIC ENGINEERING AND BIOTECHNOLOGY, TRIESTE (ITALY).
Microgravitational effects on chromosome behavior (7-IML-1) p 2357 N92-23604
INTERNATIONAL CENTRE FOR THEORETICAL PHYSICS, TRIESTE (ITALY).
Euclidean-isotopic symmetries
[DE92-615260] p 2431 N92-23128
Galilei-isotopic symmetries
[DE92-615261] p 2431 N92-23129
Investigations of breakdown of rare gases by short pulses of 1.06(mu)m laser radiation
[DE92-615399] p 2379 N92-23131
Beyond conventional quantum mechanics
[DE92-616892] p 2451 N92-23206
An exceptional N=8 superconformal algebra in two dimensions associated with F(4)
[DE92-616991] p 2435 N92-23207
The structure of MFD shock waves for rectilinear motion in some model of plasma
[DE92-617386] p 2443 N92-23208
Low frequency electrostatic modes in a magnetized dusty plasma
[DE92-617387] p 2444 N92-23209
Theoretical model of the density of states of random binary alloys
[DE92-617438] p 2350 N92-23210
Charged-soft-sphere potentials for trivalent metal halides
[DE92-617445] p 2350 N92-23211
A probabilistic mechanism hidden behind the universal power law for dielectric relaxation. Part 1: General relaxation equation
[DE92-615484] p 2435 N92-23220
Monte Carlo simulation of the 3-state vector Potts model on a 3-dimensional random lattice
[DE92-615489] p 2446 N92-23259
Nonequilibrium statistical operator in hot-electron transport theory
[DE92-615517] p 2446 N92-23260
Cu charge fluctuations and anomalous behaviour in the phonon spectrum of La2CuO4
[DE92-617446] p 2446 N92-23270
Solitary excitations in gyrotropic crystals
[DE92-617447] p 2446 N92-23271
Electron polarization in modulation doped heterostructures
[DE92-617490] p 2447 N92-23272
On the electronegativity of the high-T(sub c) oxide superconductor
[DE92-617537] p 2447 N92-23273
Sheaves of Schwartz distributions
[DE92-615217] p 2432 N92-23331

On the Stone-Weierstrass theorem for scalar and vector valued functions
[DE92-616916] p 2432 N92-23335
Magnetic fluctuations and normal state properties of the t-J model at finite dopings
[DE92-617538] p 2447 N92-23452
Many-body problems in high temperature superconductivity
[DE92-617539] p 2447 N92-23453
The Jordan-Schwinger realization of two-parametric quantum group Sl(sub q,s)(2)
[DE92-616891] p 2451 N92-23501
On some types of Riemannian V(sub n) with zero Ricci curvature
[DE92-616917] p 2432 N92-23502
Constant curvature and non-perturbative W(sub 3) gravity
[DE92-616919] p 2451 N92-23503
Improved spin wave theory: An application to the spin-1/2 antiferromagnetic Heisenberg model on a square lattice
[DE92-617436] p 2448 N92-23504
Mutual scattering of carriers in two quantum wires
[DE92-616890] p 2366 N92-23580
Effective mass theory for abrupt heterojunctions
[DE92-617439] p 2448 N92-23581
Ab initio pair potentials for FCC metals: An application of the method of Moebius transform
[DE92-617440] p 2351 N92-23582
A probabilistic mechanism hidden behind the universal power law for dielectric relaxation. Part 2: Discussion of the response function
[DE92-615485] p 2435 N92-23598
Inequivalence of interior and exterior dynamical problems
[DE92-615214] p 2451 N92-23743
The notion of nonrelativistic isoparticle
[DE92-615215] p 2438 N92-23744
Lie-admissible structure of Hamilton's original equations with external terms
[DE92-615216] p 2433 N92-23745
A new approach to estimate Angstrom coefficients
[DE92-619048] p 2460 N92-23909
Optical properties of metallic multi-layer films
[DE92-615486] p 2443 N92-24029
Closed systems with nonHamiltonian internal forces
[DE92-619234] p 2434 N92-24039

INTERNATIONAL FUEL CELLS CORP., SOUTH WINDSOR, CT.
Demonstration of fuel cells to recover energy from landfill gas: Conceptual study
[PB92-137520] p 2403 N92-23509

INTESPACE, TOULOUSE (FRANCE).
Acoustic absorption due to specimen in test in a reverberant chamber p 2324 N92-23790
Minimization of vibrations by broadband sensitivity approach p 2330 N92-23828

IOWA STATE UNIV. OF SCIENCE AND TECHNOLOGY, AMES.
Analysis and control of nonlinear flexible manipulator p 2384 N92-23727

ISRAEL AIRCRAFT INDUSTRIES LTD., BEN-GURION AIRPORT.
Formal methods for the evaluation of corporate CAD/CAM utilization
[REPT-1.1.1] p 2419 N92-23853
Combining a CAD/CAM system with an advanced database architecture
[REPT-3.1.5] p 2423 N92-23880
From IGES to STEP
[REPT-3.1.6] p 2423 N92-23881

ISRAEL AIRCRAFT INDUSTRIES LTD., LOD.
Shop floor scheduling through a simulation based scheduler
[REPT-2.3.3] p 2423 N92-23876

ISRAEL AIRCRAFT INDUSTRIES LTD., YEHUD.
MBT-WIRE: Intelligent CAD in wiring design
[REPT-1.1.4] p 2419 N92-23856

ISRAEL DEFENSE FORCES, TEL AVIV.
Infrastructure and training of manpower for CAD/CAM systems
[REPT-4.2.2] p 2425 N92-23888

ISRAEL MILITARY INDUSTRIES, RAMAT-HASHARON (ISRAEL).
IGES: Application generator in disguise
[REPT-3.1.7] p 2424 N92-23882

ISRAEL SOCIETY FOR CAD/CAM, TEL AVIV.
Proceedings of the International Conference on CAD/CAM and AMT. Volume 1: General sessions
[ITN-92-85127] p 2418 N92-23851

ITALIAN SPACE AGENCY, ROME.
The potential use of fiducial ground networks p 2316 N92-23924

J

JACKSON STATE COLL., MS.
Fast aurora zone analysis p 2409 N92-23960

JAPAN ATOMIC ENERGY RESEARCH INST., TOKYO.
Conceptual design of Fusion Experimental Reactor
[DE92-751036] p 2443 N92-23132
Fusion gain due to high energy ions accelerated by additional heating
[DE92-751038] p 2443 N92-23133
Radiation effects on polyethylene foam
[DE92-751046] p 2353 N92-23134
Evolution of magnetic moment due to the cyclotron resonance with field ripples in a tokamak
[DE92-751058] p 2443 N92-23135
Effect of minor elements on hot workability of Ni-Cr-W superalloys
[DE92-750951] p 2351 N92-23263
Evaluation of mode purity of ordinary and extraordinary modes by fixed elliptically polarized wave for ECH and ECCD
[DE92-750961] p 2444 N92-23264
Hydrogen absorption by zirconium alloy cladding tube with surface oxide film
[DE92-750962] p 2351 N92-23265
Conceptual design of fusion experimental reactor (FER/ITER)
[DE92-750949] p 2444 N92-23711
Effect of minor elements on corrosion behavior of Ni-Cr-W superalloys in HTGR helium
[DE92-751006] p 2352 N92-23712

JAPAN FISHERIES INFORMATION SERVICE CENTER, TOKYO.
Study of MOS-1 MESSR data for variability of the branch (Warm Streamer) from warm eddy and for fishing ground p 2398 N92-23477

JET PROPULSION LAB., CALIFORNIA INST. OF TECH., PASADENA.
Artificial intelligence approach to planning the robotic assembly of large tetrahedral truss structures p 2426 N92-23357
Evaluating model accuracy for model-based reasoning p 2427 N92-23362
Planar varactor frequency multiplier devices with blocking barrier
[NASA-CASE-NPO-18428-1-CU] p 2369 N92-23464
Optical inner product neural associative memory
[NASA-CASE-NPO-18491-1-CU] p 2416 N92-23546
Electro-optic resonant phase modulator
[NASA-CASE-NPO-18702-1-CU] p 2442 N92-23551
Method of fabricating superconducting device
[NASA-CASE-NPO-18394-1-CU] p 2370 N92-23552
Configuration control of seven-degree-of-freedom arms
[NASA-CASE-NPO-18607-1-CU] p 2382 N92-23553
Direct conversion technology
[NASA-CR-190188] p 2403 N92-23569
Genetic and molecular dosimetry of HZE radiation (7-IML-1) p 2357 N92-23603
NASA's GPS tracking system for Aristoteles p 2316 N92-23919
Controlling flexible robot arms using a high speed dynamics process
[NASA-CASE-NPO-18499-1-CU] p 2385 N92-24042
Controlling under-actuated robot arms using a high speed dynamics process
[NASA-CASE-NPO-18498-1-CU] p 2385 N92-24043
Synchronous parallel system for emulation and discrete event simulation
[NASA-CASE-NPO-18414-1-CU] p 2426 N92-24045

JOHANN-WOLFGANG-GOETHE-UNIV., FRANKFURT AM MAIN (GERMANY, F.R.).
Growth and sporulation of Bacillus subtilis under microgravity (7-IML-1) p 2358 N92-23612

JOHNS HOPKINS UNIV., BALTIMORE, MD.
Search for cosmological dust p 2456 N92-23164

JOHNSON CONTROLS, INC., BUTLER, WI.
Center for Space Power, Texas A and M University p 2313 N92-23651

JOINT FOOD AND AGRICULTURE ORGANIZATION - INTERNATIONAL ATOMIC ENERGY AGENCY, VIENNA (AUSTRIA).
Food Irradiation Newsletter, volume 15, number 2
[DE92-614951] p 2415 N92-23218

JOINT PUBLICATIONS RESEARCH SERVICE, ARLINGTON, VA.
JPRS report: Science and technology. Central Eurasia: Space
[JPRS-USP-92-002] p 2314 N92-23705
JPRS report: Science and technology. Central Eurasia: Life sciences
[JPRS-ULS-92-010] p 2412 N92-23706
JPRS report: Science and technology. USSR: Earth sciences
[JPRS-UES-91-005] p 2392 N92-23707
JPRS report: Science and technology. Central Eurasia: Materials science
[JPRS-UMS-92-005] p 2363 N92-23708
JPRS report: Science and technology. Central Eurasia: Materials science
[JPRS-UMS-92-006] p 2363 N92-23709

K

KANSAS STATE UNIV., MANHATTAN.
Atomic physics of strongly correlated systems
[DE92-008356] p 2438 N92-23895
Kansas State University electric vehicle site operator program
[DE92-008425] p 2384 N92-23896

KASSEL UNIV. (GERMANY, F.R.).
Marketing as a necessary condition for the successful development and commercialization of technological products p 2452 N92-23931
Requirements for the engineer training profile and definition of his role p 2452 N92-23932

KENT UNIV., CANTERBURY (ENGLAND).
Hypervelocity impact microfoil perforations in the LEO space environment (LDEF, MAP AO-023 experiment) p 2336 N92-23312
Dynamic (computer) modelling of the particulate environment: Transformations from the LDEF reference frame to decode geocentric and interplanetary populations p 2458 N92-23320

KIEL UNIV. (GERMANY, F.R.).
Heavy ion measurement on LDEF p 2440 N92-23308

KREIS CONSULTANCIES, PRAGG-JENAZ (SWITZERLAND).
On the analysis of liquid filled free-free tanks p 2332 N92-23843

L

LAWRENCE LIVERMORE NATIONAL LAB., CA.
Scientific development of the Advanced Parallel Chemistry (APACHE) climate model
[DE92-006657] p 2404 N92-23123
A signal and image processing object-based system using CLOS
[DE92-006826] p 2417 N92-23255
An x ray diagnostic of electron power loss
[DE92-008599] p 2444 N92-23523
Limits of survivability and damage for optical components used in a high repetition rate visible laser
[DE92-006896] p 2379 N92-23570
Vacuum mechatronic laser alignment system on the NOVA laser
[DE92-006898] p 2379 N92-23571
High-temperature ignition of propane with MTBE as an additive: Shock-tube experiments and modeling
[DE92-008557] p 2348 N92-23715
On the global warming potentials of candidate gaseous diffusion plant coolants
[DE92-006640] p 2406 N92-23740
Monte Carlo transport in semiconductor
[DE92-008404] p 2371 N92-23902
Multi-photon optical excitation of positronium
[DE92-008567] p 2438 N92-23903
VITRIMAT2: A modified model of vitrinite maturation and reflectance
[DE92-008987] p 2348 N92-23904
Electronic structure in high temperature superconducting oxides
[DE92-008566] p 2449 N92-23986
Compact Fusion Advanced Rankine (CFAR2) power cycle
[DE92-008577] p 2445 N92-23987
Metal-semiconductor, composite radiation detectors
[DE92-008980] p 2344 N92-23988
The all particle method
[DE92-008357] p 2439 N92-24005
The electron-positron momentum density and Fermi surface of YBa2Cu3O(7-x)
[DE92-008605] p 2450 N92-24007
Steady State Advanced Tokamak (SSAT): The mission and the machine
[DE92-008983] p 2445 N92-24020
High-performance multilayer mirrors for soft x ray projection lithography
[DE92-008615] p 2443 N92-24049
Modeling of the catalytic oxidative coupling of methane
[DE92-008554] p 2349 N92-24064
Optimization of the laser glass composition for the Nova upgrade fusion laser system
[DE92-008606] p 2380 N92-24065
A self-navigating mobile robot
[DE92-008612] p 2430 N92-24066

Ion Microtomography (IMT) and Particle-Induced X ray Emission (PIXE) analysis direct drive of Inertial Confinement Fusion (ICF) targets
[DE92-008614] p 2446 N92-24067
Fiber-optic Raman spectroscopy for cure monitoring of advanced polymer composites
[DE92-008619] p 2355 N92-24068
Working gas pressure and flow effects on reactively sputtered molybdenum-oxide thin films
[DE92-008624] p 2450 N92-24069

LEHIGH UNIV., BETHLEHEM, PA.
A study of aluminum-lithium alloy solidification using acoustic emission techniques
[NASA-CR-4437] p 2435 N92-23556

LMS INTERNATIONAL, LEUVEN (BELGIUM).
An advanced system for environmental sine testing: Basic principles revisited p 2325 N92-23799

LORAL AEROSYS, SEABROOK, MD.
An architecture for the development of real-time fault diagnosis systems using model-based reasoning p 2427 N92-23363

LOS ALAMOS NATIONAL LAB., NM.
Actively-stabilized photomultiplier tube base for vacuum operation
[DE92-007528] p 2368 N92-23200
Measurements of induced radioactivity in some LDEF samples p 2440 N92-23298
From ground state to fission fragments: A complex, multi-dimensional multi-path problem
[DE92-008488] p 2438 N92-23714
Hardening in AlN induced by point defects
[DE92-007717] p 2352 N92-23720
Results from the Soviet-American gallium experiment
[DE92-007414] p 2438 N92-23747
The ALEXIS data processing package: An IDL-based system
[DE92-007429] p 2455 N92-24027
Interception of comets and asteroids on collision course with Earth
[DE92-007431] p 2458 N92-24028
NQR investigation of pressure-induced charge transfer in oxygen-deficient YBa2Cu3O(7-delta) (delta = 0.38)
[DE92-008441] p 2450 N92-24036

LOUGHBOROUGH UNIV. OF TECHNOLOGY (ENGLAND).
Advanced ramjet systems for the propulsion of guided weapons
[ETN-92-91195] p 2310 N92-23169

LOUISIANA STATE UNIV., BATON ROUGE.
Modeling of physical database design and performance analysis with emphasis on VSAM files p 2452 N92-23156

LOYOLA UNIV., NEW ORLEANS, LA.
Improved interpretation of satellite altimeter data using genetic algorithms p 2402 N92-23369
Logic programming and metadata specifications p 2429 N92-23375

LYON-1 UNIV., VILLEURBANNE (FRANCE).
Morphology and mechanical performance of PPS/carbon composite p 2342 N92-23939

M

MANTECH ENVIRONMENTAL TECHNOLOGY, INC., CORVALLIS, OR.
Climate
[PB92-150457] p 2410 N92-23520

MARITIME SAFETY AGENCY, TOKYO (JAPAN).
Monitoring of ocean conditions by using MOS-1 data p 2398 N92-23476

MARYLAND UNIV., BALTIMORE.
Stress effects of human-computer interactions
[PB92-136001] p 2415 N92-23513

MARYLAND UNIV., COLLEGE PARK.
Scaling study of pseudospark produced electron beam
[DE92-003231] p 2368 N92-23186
Optimizing flow rates in a queueing network with side constraints
[PB92-149996] p 2430 N92-23508
Analysis of gravity and topography on Earth and Venus: Comparisons of lithospheric and sublithospheric processes p 2409 N92-23772

MASCHINENFABRIK AUGSBURG-NUERNBERG A.G., MUNICH (GERMANY, F.R.).
Advanced numerical analyses for the optimisation of the structural behaviour of the intersegment connection for the Ariane 5 booster case p 2327 N92-23809

MASSACHUSETTS INST. OF TECH., CAMBRIDGE.
Charged particle activation studies on the surface of LDEF spacecraft p 2439 N92-23296
Discovery of orbital decay in SMC X-1
[NASA-CR-190214] p 2317 N92-23531
The interpretation of crustal dynamics data in terms of plate interactions and active tectonics of the Anatolian plate and surrounding regions in the Middle East
[NASA-CR-188466] p 2408 N92-23558
Mental workload and performance experiment (15-IML-1) p 2361 N92-23628

MATERIALS RESEARCH LAB., INC., GLENWOOD, IL.
Development of a crack arrest fracture toughness measurement procedure for quality assurance of plates and welds used for hydrocarbon storage tanks
[PB92-141753] p 2389 N92-23681

MATRA ESPACE, TOULOUSE (FRANCE).
Improvements for interpretation of structural dynamics calculation using effective parameters for substructures p 2324 N92-23789
Maximal modal energy method: An overvaluing tool for low frequency prediction of structure acoustic response p 2324 N92-23791
Influence of microvibrations on spacecraft performances p 2329 N92-23825

MATRA MARCONI SPACE, TOULOUSE (FRANCE).
The GRADIOmeter payload p 2315 N92-23917

MCAT INST., SAN JOSE, CA.
User interface user's guide for HYPGEN
[NASA-CR-190304] p 2425 N92-23991

MCDONNELL AIRCRAFT CO., SAINT LOUIS, MO.
Design of a fighter aircraft vertical tail enhanced buffet environment survivability p 2307 N92-23235

MCDONNELL-DOUGLAS SPACE SYSTEMS CO., HUNTINGTON BEACH, CA.
Material considerations for habitable areas of manned spacecraft p 2323 N92-23785

MCGILL UNIV., MONTREAL (QUEBEC).
Space adaptation syndrome experiments (8-IML-1) p 2360 N92-23625

MESSERSCHMITT-BOELKOW-BLOHM G.M.B.H., BREMEN (GERMANY, F.R.).
Protection of spacecraft against meteroid/orbital debris impacts p 2323 N92-23786
On the modelling of a deployable telescope elastic beam-type element for on-orbit multibody simulations p 2329 N92-23826

MESSERSCHMITT-BOELKOW-BLOHM G.M.B.H., MUNICH (GERMANY, F.R.).
First approach to an integrated fin design p 2308 N92-23236
Euromar-Seastars: A definition study on modular multisensor instrumentation for airborne remote sensing of the sea
[MBB-UK-0152-91-PUB] p 2392 N92-23379
Euromar-Seastars: Summary p 2392 N92-23380
Recommended system concept p 2392 N92-23383
The imaging spectrometer p 2393 N92-23387
The imaging microwave radiometer p 2393 N92-23390
The imaging radar system p 2393 N92-23391
Passive optical and IR sensors
[MBB-UH-HE512] p 2394 N92-23392
Quick-look system p 2394 N92-23393
On board data formatting p 2394 N92-23394
On board data recording p 2394 N92-23395
Real-time radar processor p 2394 N92-23396
Ground station p 2394 N92-23397
Multisensor data fusion p 2394 N92-23398
Hardware and software modularity p 2394 N92-23399
Sensor interfaces p 2395 N92-23400
Types of operation and system control p 2395 N92-23401
Sensor compatibility/optimal sensor combinations p 2395 N92-23403
Evaluation of the sensor effectiveness p 2395 N92-23404
Current definition of some development programs p 2395 N92-23405
Realization and provisional sensor development planning p 2395 N92-23406
National user interfaces p 2395 N92-23407
Provisional cost evaluation p 2395 N92-23408
International cooperation p 2396 N92-23409
Euromar industrial partners agreement p 2396 N92-23410
An 18-point catalog description p 2396 N92-23411
Materials for liquid propellant engines p 2320 N92-23764
Strength and deformation behaviour of Kevlar and carbon composite sandwich structures for space applications p 2332 N92-23840
Symposium on Marketing for Technological Products
[MBB-UE-0014-90-PUB] p 2452 N92-23928
Market directed thinking in a technological operation p 2452 N92-23929
Marketing qualification as a requirement for operating success p 2452 N92-23930
Introduction to Special Course on Engineering Methods in Aerodynamic Analysis and Design of Aircraft p 2308 N92-23951

METEOROLOGICAL RESEARCH INST., TSUKUBA (JAPAN).
Investigations on verification of the data observed by the MESSR and VTIR, and on interannual trend in the MSR data p 2397 N92-23470
Verification of MESSR and VTIR, and time variation of MSR performance p 2397 N92-23471

METEOROLOGICAL SATELLITE CENTER, TOKYO (JAPAN).
Estimation of sea surface temperatures using MOS-1, GMS, and NOAA p 2398 N92-23475

METRAVIB, LYON (FRANCE).
Acoustic prediction on satellite structure p 2327 N92-23812

MIAMI UNIV., CORAL GABLES, FL.
Atmospheric correction of the second generation ocean color sensors p 2392 N92-23145

MICHIGAN UNIV., ANN ARBOR.
Evaluation of a mechanical beam-switching system
[PB92-139773] p 2368 N92-23140
Investigation of the Archean climate using the NCAR CCM
[NASA-CR-189878] p 2410 N92-23656

MIDWEST RESEARCH INST., GOLDEN, CO.
Geothermal energy program overview
[DE91-002172] p 2402 N92-23175

MINISTRY OF DEFENSE, MOSCOW (USSR).
Determination and prediction of satellite motion at the end of the lifetime p 2334 N92-23971

MINISTRY OF POSTS AND TELECOMMUNICATIONS, TOKYO (JAPAN).
Measurements of rain rate distribution by MOS-1 MSR p 2396 N92-23467
Application of ground-based laser beacon for Earth image calibration, 3 p 2396 N92-23468

MISSISSIPPI STATE UNIV., MISSISSIPPI STATE.
Proceedings: Nozzle Initiative Industry Advisory Committee on Standardization of Carbon-Phenolic Test Methods and Specifications
[NASA-CR-190203] p 2337 N92-23539

MISSISSIPPI STATE UNIV., STATE COLLEGE.
Unsteady three-dimensional incompressible algorithm based on artificial compressibility p 2375 N92-23700
Investigation of solution operators for the three dimensional unsteady Euler equations p 2376 N92-24018

MOSCOW INST. OF AVIATION TECHNOLOGY (USSR).
The USSR launchers programme p 2319 N92-23753

N

NAGAOKA TECHNOLOGICAL UNIV., NIIGATA (JAPAN).
Observation of lined-up cumulus rows under the winter monsoon situation using MOS-1 and radar data p 2399 N92-23483

NATIONAL ACADEMY OF SCIENCES - NATIONAL RESEARCH COUNCIL, WASHINGTON, DC.
From Earth to orbit
[NASA-CR-190216] p 2321 N92-23980

NATIONAL AERONAUTICAL LAB., BANGALORE (INDIA).
An algorithmic approach for fault-monitoring of electrical actuation system for all electric aircraft
[NAL-PD-AL-9111] p 2368 N92-23246

NATIONAL AERONAUTICS AND SPACE ADMINISTRATION, WASHINGTON, DC.
Mission safety evaluation report for STS-43, postflight edition
[NASA-TM-107801] p 2312 N92-23240
Mission safety evaluation report for STS-29, postflight edition
[NASA-TM-107773] p 2312 N92-23241
Mission safety evaluation report for STS-30, postflight edition
[NASA-TM-107774] p 2312 N92-23242
Mission safety evaluation report for STS-32, postflight edition
[NASA-TM-107775] p 2312 N92-23243
Mission safety evaluation report for STS-36, postflight edition
[NASA-TM-107780] p 2312 N92-23244
Publications of the exobiology program for 1990: A special bibliography
[NASA-TM-4364] p 2416 N92-23429
Proceedings of the Second Annual Symposium on Industrial Involvement and Successes in Commercial Space
[NASA-TM-107812] p 2312 N92-23643
Launch systems for future NASA missions p 2318 N92-23752

NATIONAL AERONAUTICS AND SPACE ADMINISTRATION. AMES RESEARCH CENTER, MOFFETT FIELD, CA.
LDEF impact craters formed by carbon-rich impactors: A preliminary report p 2336 N92-23319
Skeletal responses to spaceflight [NASA-TM-103890] p 2414 N92-23424

NATIONAL AERONAUTICS AND SPACE ADMINISTRATION. GODDARD SPACE FLIGHT CENTER, GREENBELT, MD.
The 1992 Goddard Conference on Space Applications of Artificial Intelligence [NASA-CP-3141] p 2426 N92-23356
Design of neural networks for classification of remotely sensed imagery p 2402 N92-23367
A spatial data handling system for retrieval of images by unrestricted regions of user interest p 2429 N92-23373
Method for advanced material characterization by laser induced eddy current imaging [NASA-CASE-GSC-13386-1] p 2386 N92-23376
High reliability robot friendly ORU interface [NASA-CASE-GSC-13360-1] p 2381 N92-23377
Retractable tool bit having latch type catch mechanism [NASA-CASE-GSC-13359-1] p 2381 N92-23378
Sub-Kelvin resistance thermometer [NASA-CASE-GSC-13406-1] p 2378 N92-23460
Coaxial turnstile junction [NASA-CASE-GSC-13422-1] p 2369 N92-23462
Microprocessor control of multiple peak power tracking DC/DC converters for use with solar cell arrays [NASA-CASE-GSC-13450-1] p 2403 N92-23463
WAMDII: The Wide Angle Michelson Doppler Imaging Interferometer [NASA-TM-105526] p 2441 N92-23525
Climbing robot [NASA-CASE-GSC-13442-1] p 2382 N92-23547
Helix translation device [NASA-CASE-GSC-13141-1] p 2382 N92-23548
Method and apparatus for determination of material residual stress [NASA-CASE-GSC-13451-1] p 2388 N92-23549
Mission objectives and scientific rationale for the magnetometer mission p 2315 N92-23912
The geophysical impact of the Aristoteles mission p 2315 N92-23915
Aristoteles magnetometer system p 2316 N92-23920
The Delta 2 launcher p 2316 N92-23921
Summer graduate research program for interns in science and engineering [NASA-TM-107813] p 2470 N92-23958
Retractable tool bit having slider type catch mechanism [NASA-CASE-GSC-13358-1] p 2385 N92-24058
Page turning system [NASA-CASE-GSC-13415-1] p 2386 N92-24059
Flexible robotic arm [NASA-CASE-GSC-13161-1] p 2386 N92-24060

NATIONAL AERONAUTICS AND SPACE ADMINISTRATION. JOHN C. STENNIS SPACE CENTER, BAY SAINT LOUIS, MS.
Digital data registration and differencing compression system [NASA-CASE-SSC-00010-2] p 2453 N92-23550

NATIONAL AERONAUTICS AND SPACE ADMINISTRATION. LYNDON B. JOHNSON SPACE CENTER, HOUSTON, TX.
Meteoroid and debris special investigation group data acquisition procedures p 2454 N92-23313
Meteoroid, and debris special investigation group preliminary results: Size-frequency distribution and spatial density of large impact features on LDEF p 2336 N92-23314
Preliminary analysis of LDEF instrument A0187-1: Chemistry of Micrometeoroids Experiment p 2458 N92-23315
Deriving the velocity distribution of meteoroids from the measured meteoroid impact directionality on the various LDEF surfaces p 2459 N92-23322
M and D SIG progress report: Laboratory simulations of LDEF impact features p 2336 N92-23323
Preliminary micrometeoroid and debris effects on LDEF thermal control surfaces p 2336 N92-23324
Robot-friendly connector [NASA-CASE-MSC-21864-1] p 2382 N92-23544
Smart accelerometer [NASA-CASE-MSC-21951-1] p 2378 N92-23545
Microgravity vestibular investigations (10-IML-1) p 2360 N92-23626
A review of Space Shuttle payload-bay lift-off flight data and analysis comparisons p 2322 N92-23796
Orbital decay and reentry of the Salyut-7 orbital complex p 2335 N92-23978
Quick-connect fasteners for assembling devices in space [NASA-CASE-MSC-21648-1] p 2385 N92-24051
Three-dimensional cultured glioma cell lines [NASA-CASE-MSC-21843-1-NP] p 2413 N92-24052

NATIONAL AERONAUTICS AND SPACE ADMINISTRATION. LANGLEY RESEARCH CENTER, HAMPTON, VA.
A system approach to aircraft optimization p 2306 N92-23228
Application of multidisciplinary optimization methods to the design of a supersonic transport p 2307 N92-23230
LDEF: 69 Months in Space. First Post-Retrieval Symposium, part 1 [NASA-CP-3134-PT-1] p 2461 N92-23280
Long Duration Exposure Facility: A general overview p 2335 N92-23281
Long Duration Exposure Facility (LDEF) space environments overview p 2335 N92-23282
Use of the Long Duration Exposure Facility's thermal measurement system for the verification of thermal models p 2336 N92-23284
Organic contamination of LDEF p 2339 N92-23290
Large craters on the meteoroid and space debris impact experiment p 2335 N92-23309
IDE spatio-temporal impact fluxes and high time-resolution studies of multi-impact events and long-lived debris clouds p 2458 N92-23317
Damage development in titanium metal matrix composites subjected to cyclic loading [NASA-TM-107597] p 2340 N92-23433
Matrix dominated stress/strain behavior in polymeric composites: Effects of hold time, nonlinearity and rate dependency [NASA-TM-107595] p 2340 N92-23434
Grid generation and flow solution method for Euler equations on unstructured grids [NASA-TM-4295] p 2305 N92-23533
Analysis and development of dynamic selection of laser array elements [NASA-TM-4375] p 2379 N92-23557
A verified design of a fault-tolerant clock synchronization circuit: Preliminary investigations [NASA-TM-107568] p 2416 N92-23559
High angle of attack: Aerodynamics p 2305 N92-23956
Effect of low-speed impact damage and damage location on behavior of composite panels [NASA-TP-3196] p 2344 N92-23981
Design considerations for an air core magnetic actuator [NASA-TM-104229] p 2364 N92-23989
Underlying modal data issues for detecting damage in truss structures [NASA-TM-107573] p 2390 N92-23990
Collapse of composite tubes under end moments [NASA-TM-107605] p 2390 N92-23992

NATIONAL AERONAUTICS AND SPACE ADMINISTRATION. LEWIS RESEARCH CENTER, CLEVELAND, OH.
Comparison of two-dimensional and three-dimensional droplet trajectory calculations in the vicinity of finite wings [NASA-TM-105617] p 2373 N92-23154
X ray based displacement measurement for hostile environments [NASA-TM-105551] p 2378 N92-23155
An XPS study of the stability of Fomblin Z25 on the native oxide of aluminum [NASA-TM-105594] p 2353 N92-23185
Achieving spectrum conservation for the minimum-span and minimum-order frequency assignment problems [NASA-TM-105649] p 2322 N92-23187
Detecting Lamb waves with broad-band acousto-ultrasonic signals in composite structures [NASA-TM-105557] p 2386 N92-23189
Tribological evaluation of an Al2O3-SiO2 ceramic fiber candidate for high temperature sliding seals [NASA-TM-105611] p 2339 N92-23190
Aeroelastic stability analyses of two counter rotating propfan designs for a cruise missile model [NASA-TM-105268] p 2387 N92-23191
Environmental effects on friction and wear of diamond and diamondlike carbon coatings [NASA-TM-105634] p 2354 N92-23192
A flexible CPW package for a 30 GHz MMIC amplifier [NASA-TM-105630] p 2368 N92-23193
Progressive fracture of polymer matrix composite structures: A new approach [NASA-TM-105574] p 2339 N92-23194
Influence of engineered interfaces on residual stresses and mechanical response in metal matrix composites [NASA-TM-105438] p 2340 N92-23195
Evaluation of MHOST analysis capabilities for a plate element [NASA-TM-105387] p 2387 N92-23196
Modelling and experimental verification of a water alleviation system for the NASP [NASA-TM-105661] p 2373 N92-23224
Deposition of adherent Ag-Ti duplex films on ceramics in a multiple-cathode sputter deposition system [NASA-TM-105586] p 2311 N92-23225
Numerical experiments with flows of elongated granules [NASA-TM-105567] p 2381 N92-23226
Blazing the trailway: Nuclear electric propulsion and its technology program plans [NASA-TM-105605] p 2337 N92-23252
Effects of chemical equilibrium on turbine engine performance for various fuels and combustor temperatures [NASA-TM-105399] p 2311 N92-23254
Coupled multi-disciplinary simulation of composite engine structures in propulsion environment [NASA-TM-105575] p 2388 N92-23267
Liquid hydrogen mass flow through a multiple orifice Joule-Thomson device [NASA-TM-105583] p 2373 N92-23268
The flip-flop nozzle extended to supersonic flows [NASA-TM-105570] p 2304 N92-23269
Center for Modeling of Turbulence and Transition (CMOTT). Research briefs: 1990 [NASA-TM-105243] p 2301 N92-23336
Turbulence modeling p 2301 N92-23338
Modeling of compressible turbulent shear flows p 2301 N92-23340
Development of new flux splitting schemes p 2302 N92-23343
Advancements in engineering turbulence modeling [PAPER-105] p 2303 N92-23350
On the basic equations for the second-order modeling of compressible turbulence p 2303 N92-23351
Development of a new flux splitting scheme p 2303 N92-23352
High-Order Polynomial Expansions (HOPE) for flux-vector splitting p 2304 N92-23353
Simulations of free shear layers using a compressible kappa-epsilon model p 2304 N92-23355
Intelligent fault isolation and diagnosis for communication satellite systems p 2427 N92-23365
Solid State Technology Branch of NASA Lewis Research Center [NASA-TM-105159] p 2365 N92-23412
Microwave response of high transition temperature superconducting thin films p 2365 N92-23413
Properties of large area ErBa2Cu3O(7-x) thin films deposited by ionized cluster beams p 2365 N92-23414
Dependence of the critical temperature of laser-ablated YBa2Cu3O(7-delta) thin films on LaAlO3 substrate growth technique p 2365 N92-23415
High temperature dynamic engine seal technology development [NASA-TM-105641] p 2381 N92-23435
Guanidine based vehicle/binders for use with oxides, metals, and ceramics [NASA-CASE-LEW-15314-1] p 2354 N92-23461
Singularities in optimal structural design [NASA-TM-4365] p 2388 N92-23527
Derated ion thruster design issues [NASA-TM-105576] p 2337 N92-23534
Nonplanar linearly tapered slot antenna with balanced microstrip feed [NASA-TM-105647] p 2370 N92-23535
Contact stresses in meshing spur gear teeth: Use of an incremental finite element procedure [NASA-TM-105388] p 2382 N92-23536
Effects of turbine cooling assumptions on performance and sizing of high-speed civil transport [NASA-TM-105610] p 2311 N92-23537
Renormalization group analysis of the Reynolds stress transport equation [NASA-TM-105588] p 2374 N92-23542
A two-dimensional Euler solution for an unbladed jet engine configuration [NASA-TM-105329] p 2374 N92-23560
Evaluation of high temperature capacitor dielectrics [NASA-TM-105622] p 2370 N92-23561
Defect behavior, carrier removal and predicted in-space injection annealing of InP solar cells [NASA-TM-105624] p 2370 N92-23562
Interactive solution-adaptive grid generation procedure [NASA-TM-105432] p 2305 N92-23563
NIST torsion oscillator viscometer response: Performance on the LeRC active vibration isolation platform [NASA-TM-105571] p 2383 N92-23564
Long time behavior of unsteady flow computations [NASA-TM-105584] p 2374 N92-23565

Critical fluid thermal equilibration experiment (19-IML-1) p 2363 N92-23640
Microgravity acceleration measurement and environment characterization science (17-IML-1) p 2363 N92-23642
Simulation of Space Station loads with active control systems p 2329 N92-23824
Phase transformations in SrAl2Si2O8 glass [NASA-TM-105657] p 2449 N92-23890
Kolmogorov behavior of near-wall turbulence and its application in turbulence modeling [NASA-TM-105663] p 2376 N92-24050
Vinyl capped addition polyimides [NASA-CASE-LEW-15027-2] p 2355 N92-24053
A dual anode nickel-hydrogen cell [NASA-CASE-LEW-15212-1] p 2404 N92-24054
Self-deploying photovoltaic power system [NASA-CASE-LEW-15308-1] p 2404 N92-24057

NATIONAL AERONAUTICS AND SPACE ADMINISTRATION. MARSHALL SPACE FLIGHT CENTER, HUNTSVILLE, AL.
Pinhole cameras as sensors for atomic oxygen in orbit: Application to attitude determination of the LDEF p 2379 N92-23283
Summary of ionizing radiation analysis on the Long Duration Exposure Facility p 2439 N92-23291
Prediction of LDEF ionizing radiation environment p 2439 N92-23292
The interactions of atmospheric cosmogenic radionuclides with spacecraft surfaces p 2461 N92-23294
Induced radioactivity in LDEF components p 2440 N92-23300
Radiation exposure of LDEF: Initial results p 2461 N92-23302
Charged particle LET-spectra measurements aboard LDEF p 2440 N92-23303
Ionizing radiation calculations and comparisons with LDEF data p 2440 N92-23304
Meteoroid/space debris impacts on MSFC LDEF experiments p 2335 N92-23311
Technique to eliminate computational instability in multibody simulations employing the Lagrange multiplier [NASA-TP-3220] p 2418 N92-23432
Testing and analyses of electrochemical cells using frequency response [NASA-TM-103580] p 2369 N92-23437
STS investigators' guide [NASA-TM-105523] p 2321 N92-23524
First International Microgravity Laboratory experiment descriptions [NASA-TM-4353] p 2356 N92-23600
The Critical Point Facility (CPF) p 2362 N92-23637
Rocket propulsion for NASA's Earth to orbit launchers p 2319 N92-23754
Prosthetic helping hand [NASA-CASE-MFS-28430-1] p 2416 N92-24044
Induction boiler [NASA-CASE-MFS-28634-1] p 2385 N92-24055
Bar-holding prosthetic limb [NASA-CASE-MFS-28481-1] p 2416 N92-24056

NATIONAL AERONAUTICS AND SPACE ADMINISTRATION. PASADENA OFFICE, CA.
Planar varactor frequency multiplier devices with blocking barrier [NASA-CASE-NPO-18428-1-CU] p 2369 N92-23464
Optical inner product neural associative memory [NASA-CASE-NPO-18491-1-CU] p 2416 N92-23546
Electro-optic resonant phase modulator [NASA-CASE-NPO-18702-1-CU] p 2442 N92-23551
Method of fabricating superconducting device [NASA-CASE-NPO-18394-1-CU] p 2370 N92-23552
Configuration control of seven-degree-of-freedom arms [NASA-CASE-NPO-18607-1-CU] p 2382 N92-23553
Controlling flexible robot arms using a high speed dynamics process [NASA-CASE-NPO-18499-1-CU] p 2385 N92-24042
Controlling under-actuated robot arms using a high speed dynamics process [NASA-CASE-NPO-18498-1-CU] p 2385 N92-24043
Synchronous parallel system for emulation and discrete event simulation [NASA-CASE-NPO-18414-1-CU] p 2426 N92-24045

NATIONAL AEROSPACE LAB., AMSTERDAM (NETHERLANDS).
Evaluation of the applicability of Helmholtz resonators for low frequency acoustic liners [PB92-138544] p 2436 N92-23588
Panel methods for aerodynamic analysis and design p 2309 N92-23955

NATIONAL AEROSPACE LAB., TOKYO (JAPAN).
Development of wall pressure measuring apparatus for an existing transonic wind tunnel test section [NAL-TM-565] p 2312 N92-23778
Sliding friction test of self lubricating polymer composites for rolling bearing retainer [NAL-TM-622] p 2384 N92-23779
Distributed computer system in the large scale low speed wind tunnel [NAL-TM-629] p 2312 N92-23979

NATIONAL CENTER FOR ATMOSPHERIC RESEARCH, BOULDER, CO.
GENLN2: A general line-by-line atmospheric transmittance and radiance model. Version 3.0: Description and users guide [PB92-148543] p 2408 N92-23522
International workshop on the airborne measurement of wind, turbulence, and position [PB92-139963] p 2410 N92-23587
Investigation of the Archean climate using the NCAR CCM [NASA-CR-189878] p 2410 N92-23656

NATIONAL GEOPHYSICAL DATA CENTER, BOULDER, CO.
Solar-geophysical data Number 564, August 1991. Part 2 (comprehensive reports): Data for February 1991 and miscellaneous [PB92-111699] p 2459 N92-23701
Solar-geophysical data Number 566, October 1991. Part 2 (comprehensive reports): Data for April 1991 and miscellaneous [PB92-129402] p 2460 N92-23993

NATIONAL HURRICANE CENTER, CORAL GABLES, FL.
Diagnostic report of the National Hurricane Center: June and July 1991. Volume 4, number 1 [PB92-134501] p 2411 N92-23994

NATIONAL INST. FOR FUSION SCIENCE, NAGOYA (JAPAN).
Feedback control of plasma equilibrium with control system aided by personal computer on the JIPP T-IIU tokamak [DE92-750824] p 2444 N92-23261
Development of 3-dimensional compact magnetic dosimeter for environmental magnetic field monitoring [DE92-750825] p 2407 N92-23262

NATIONAL INST. OF POLAR RESEARCH, TOKYO (JAPAN).
Preliminary report on the observation of polar atmosphere and cryosphere by MOS-1 data received at Syowa Station p 2399 N92-23481

NATIONAL INST. OF STANDARDS AND TECHNOLOGY, BOULDER, CO.
Automatic waveform analysis and measurement system user manual [PB92-132976] p 2364 N92-23173

NATIONAL INST. OF STANDARDS AND TECHNOLOGY, GAITHERSBURG, MD.
Confidence intervals for discrete approximations to ill-posed problems [PB92-143742] p 2432 N92-23511

NATIONAL LAB. FOR HIGH ENERGY PHYSICS, TSUKUBA (JAPAN).
Report from orbit sub-group of task force for MR synchrotron radiation project [DE92-751024] p 2441 N92-23713

NATIONAL MARINE FISHERIES SERVICE, SEATTLE, WA.
Our living oceans: The first annual report on the status of US living marine resources [PB92-145689] p 2412 N92-23519

NATIONAL METEOROLOGICAL CENTER, WASHINGTON, DC.
Functional precision of National Weather Service upper-air measurements using VIZ Manufacturing Co. A radiosonde (model 1492-510) [PB92-137850] p 2410 N92-23439
Functional precision of National Weather Service upper-air measurements using VIZ Manufacturing Co. B radiosonde (model 1492-520) [PB92-137868] p 2410 N92-23494
Functional precision of National Weather Service upper-air measurements using space data division radiosonde (model 909-10-01) [PB92-137843] p 2411 N92-23746

NATIONAL OCEANIC AND ATMOSPHERIC ADMINISTRATION, ANN ARBOR, MI.
Computer tutorial and animation of the normal ice cycle of the Laurentian Great Lakes of North America for 1960 - 1979 [PB92-129949] p 2401 N92-23659

NATIONAL OCEANIC AND ATMOSPHERIC ADMINISTRATION, BOULDER, CO.
Field evaluation of remote sensor measurements of wind, temperature, and moisture for ARM integrated sounding system research [PB92-140714] p 2401 N92-23521
Differences within and among surface marine datasets [PB92-135326] p 2411 N92-23660
Ocean acoustic tomography inversion in the adiabatic-invariant approximation [PB92-140466] p 2412 N92-23669

NATIONAL OCEANIC AND ATMOSPHERIC ADMINISTRATION, MIAMI, FL.
CODAR in the Straits of Florida [PB92-129964] p 2412 N92-23732

NATIONAL OCEANIC AND ATMOSPHERIC ADMINISTRATION, SEATTLE, WA.
Use of Marine Observation Satellite-1 in applied ocean science p 2400 N92-23487
Wind, current and temperature data at 0 deg, 165 deg E: January 1986 to March 1991 [PB92-143080] p 2411 N92-23682

NATIONAL PARK SERVICE, DENVER, CO.
Acid rain and air pollution in desert park areas. Proceedings of a workshop: Management recommendations [PB92-140532] p 2407 N92-24003

NATIONAL RESEARCH CENTER FOR DISASTER PREVENTION, TOKYO (JAPAN).
Verification of the effectiveness of MOS-1 MESSR in the field of disaster prevention p 2397 N92-23474

NATIONAL RESEARCH COUNCIL OF CANADA, BOUCHERVILLE (QUEBEC).
Composites, 1990 [NRC-32603] p 2341 N92-23933
Impact-induced delamination in (0(5), 90(5), 0(5)) carbon/peek composite laminates p 2341 N92-23936

NATIONAL RESEARCH COUNCIL OF CANADA, OTTAWA (ONTARIO).
WAMDII: The Wide Angle Michelson Doppler Imaging Interferometer [NASA-TM-105526] p 2441 N92-23525
Impact and compression response of composite materials containing fortifiers p 2341 N92-23937
Crystallization behavior of poly(phenylene sulphide) p 2342 N92-23940
Application of the microbond technique: Characterization of carbon-epoxy interfaces p 2343 N92-23944

NATIONAL RESEARCH INST. OF FISHERIES ENGINEERING, TOKYO (JAPAN).
Utilization of satellite images for marine resources p 2399 N92-23480
Study on drifting-data collection buoy using MOS-1: Position verification in the Bering Sea p 2400 N92-23486

NATIONAL SEMICONDUCTOR (IC) LTD., HERZLIYA (ISRAEL).
Functional design verification of ULSI components [REPT-1.3.7] p 2422 N92-23873

NATIONAL SPACE DEVELOPMENT AGENCY, IBARAKI (JAPAN).
Conceptional design to heat-resistant airframe of HOPE p 2328 N92-23820

NATIONAL SPACE DEVELOPMENT AGENCY, SAITAMA (JAPAN).
Proceedings on MOS-1 data evaluation [HE-90015] p 2396 N92-23465
Outline of utilization results of MOS-1 data p 2396 N92-23466

NATIONAL SPACE DEVELOPMENT AGENCY, TOKYO (JAPAN).
Radiation monitoring container device (16-IML-1) p 2361 N92-23629
Organic crystal growth experiment facility (13-IML-1) p 2362 N92-23635
Development of Japanese experiment module p 2323 N92-23781

NATIONAL TAIWAN UNIV., TAIPEI.
SLS-PLAN-IT: A knowledge-based blackboard scheduling system for Spacelab life sciences missions p 2426 N92-23358

NATIONAL TELECOMMUNICATIONS AND INFORMATION ADMINISTRATION, BOULDER, CO.
Tabulations of propagation data over irregular terrain in the 75- to 8400-MHz frequency range. Part 5: Virginia [PB92-137413] p 2364 N92-23180

NATIONAL TRANSPORTATION SAFETY BOARD, WASHINGTON, DC.
Aircraft accident report: Runway collision of USAir Flight 1493, Boeing 737 and Skywest Flight 5569 Fairchild Metroliner, Los Angeles International Airport, Los Angeles, CA, February 1, 1991 [PB91-910409] p 2305 N92-23596
Aircraft accident report: Ryan International Airlines DC-9-15, N565PC, loss of control on takeoff, Cleveland-Hopkins International Airport, Cleveland, Ohio, February 17, 1991 [PB91-910410] p 2305 N92-23597

NATIONAL WEATHER SERVICE, FORT WORTH, TX.
Tornadic supercell over Dade and Broward Counties (Florida) on January 15, 1991 [PB92-134444] p 2411 N92-23906

NATIONAL WEATHER SERVICE, SILVER SPRING, MD.
Functional precision of National Weather Service upper-air measurements using VIZ Manufacturing Co. A radiosonde (model 1492-510)
[PB92-137850] p 2410 N92-23439
Functional precision of National Weather Service upper-air measurements using VIZ Manufacturing Co. B radiosonde (model 1492-520)
[PB92-137868] p 2410 N92-23494
Functional precision of National Weather Service upper-air measurements using space data division radiosonde (model 909-10-01)
[PB92-137843] p 2411 N92-23746

NAVAL RESEARCH LAB., WASHINGTON, DC.
Gamma radiation survey of the LDEF spacecraft
p 2460 N92-23293
Preliminary results from the heavy ions in space experiment p 2461 N92-23307
Distributed expert systems for ground and space applications p 2427 N92-23361

NEBRASKA UNIV., LINCOLN.
Design of joint source/channel coders
[NASA-CR-189960] p 2417 N92-23416
Maximum aposteriori joint source/channel coding
p 2417 N92-23417
A joint source/channel coder design
p 2417 N92-23418
An edge preserving differential image coding scheme
p 2417 N92-23419
A robust low-rate coding scheme for packet video
p 2417 N92-23420
A hybrid LBG/lattice vector quantizer for high quality image coding p 2418 N92-23421
A robust coding scheme for packet video
p 2418 N92-23422
A progressive data compression scheme based upon adaptive transform coding: Mixture block coding of natural images p 2418 N92-23423

NEVADA UNIV., LAS VEGAS.
Climate
[PB92-150457] p 2410 N92-23520

NEW ENERGY DEVELOPMENT ORGANIZATION, TOKYO (JAPAN).
Promotion of industrial technologies on the global environment
[DE92-769377] p 2405 N92-23454
Survey on subterranean disposal and storage technology of CO2
[DE92-769378] p 2405 N92-23455
Survey on fixation and utilization of carbon dioxide by catalytic hydrogenation
[DE92-769380] p 2347 N92-23456
Investigation on effective promotion of geothermal energy development
[DE92-783370] p 2403 N92-23684
Promotion of industrial technologies on the global environment
[DE92-769374] p 2406 N92-23733
Promotion of industrial technologies on the global environment
[DE92-769375] p 2406 N92-23734
Promotion of industrial technologies on the global environment
[DE92-769376] p 2407 N92-24023
Survey on optimization of CO2 disposal system and carbon utilization technology
[DE92-769381] p 2407 N92-24024

NEW MEXICO UNIV., ALBUQUERQUE.
Annual progress report
[NASA-CR-190197] p 2454 N92-23428

NEW YORK UNIV., NEW YORK.
Improved numerical methods for quantum field theory (outstanding junior investigator award)
[DE92-008730] p 2451 N92-23578

NORTH CAROLINA AGRICULTURAL AND TECHNICAL STATE UNIV., GREENSBORO.
Using microsoft excel applications in the graduate intern program at Goddard Space Flight Center
p 2425 N92-23959

NORTH CAROLINA STATE UNIV., RALEIGH.
Theoretical nuclear reaction and structure studies using hyperons and photons
[DE92-008587] p 2437 N92-23577
Urban temperature bias as determined by polar orbiting satellite data p 2402 N92-23724
Analysis of time series with missing values
p 2434 N92-23777

NORTH CAROLINA UNIV., CHAPEL HILL.
Reductive coupling of carbon monoxide to C2 products
[DE92-007529] p 2347 N92-23499
Numerical calculation: Aspiration efficiency of aerosols into thin-walled sampling inlets
[PB92-132901] p 2374 N92-23516

NORTHWESTERN UNIV., EVANSTON, IL.
Dynamic structural effects and ultrafast biomolecular kinetics in photoinduced charge transfer reactions
[DE92-007562] p 2346 N92-23203
Research in high energy physics
[DE92-007967] p 2440 N92-23214
Research in high energy physics
[DE92-007968] p 2440 N92-23215
Research in high energy physics
[DE92-007966] p 2441 N92-23500
Localization of deformation and inelastic deformation of pressure-sensitive dilatant materials
p 2389 N92-23737

NOTTINGHAM UNIV. (ENGLAND).
Dynamic positioning by GPS p 2306 N92-23729

NPO ENERGOMASH, KHIMKI (USSR).
Oxygen-kerosene liquid rocket engines with postburning generator gas and high pressure in combustion chamber
p 2320 N92-23761

O

OAK RIDGE ASSOCIATED UNIVERSITIES, INC., TN.
Radiation exposure of air carrier crewmembers 2
[PB92-140037] p 2414 N92-23139

OAK RIDGE NATIONAL LAB., TN.
Applications of multiple-ion irradiations to metals, ceramics, and polymers
[DE92-007686] p 2354 N92-23222
Evaluation of the elevated-temperature mechanical reliability of a HIPed silicon nitride
[DE92-007838] p 2354 N92-23223
Static multipole deformations in nuclei
[DE92-008250] p 2436 N92-23277
Spectral effects in radiation embrittlement
[DE92-007837] p 2447 N92-23444
The case for exotic beams at the Holifield Heavy Ion Research Facility
[DE92-008003] p 2441 N92-23445
Temperature-dependent evolution of chemisorbed digermane in Ge thin film growth
[DE92-008098] p 2447 N92-23447
On motion planning amidst transient obstacles
[DE91-018939] p 2429 N92-23457
Design of an omnidirectional and holonomic wheeled platform prototype
[DE92-000046] p 2382 N92-23459
Nuclear medicine program
[DE92-006979] p 2412 N92-23518
Characterization of rocket propellant combustion products
[DE92-007799] p 2337 N92-23722
Empirical characterization of a high intensity LED proximity sensor
[DE91-019074] p 2371 N92-23735
Multifracture of ceramic composites
[DE92-009630] p 2355 N92-23897
Modular electromagnetic levitator
[DE92-008278] p 2367 N92-23900
An analysis of the relationship between induction motor current and shaft speed fluctuations
[DE92-007234] p 2371 N92-24025
Resonant transfer excitation: Interference effects
[DE92-007240] p 2439 N92-24026
Time optimal trajectories for a 2-wheeled robot
[DE92-000069] p 2430 N92-24032

OAK RIDGE Y-12 PLANT, TN.
Acoustic emission as a process monitor for diamond machining of metal optical components
[DE92-008037] p 2363 N92-23899
Real-time measurement of electron beam weld penetration in uranium by acoustic emission monitoring
[DE92-008040] p 2384 N92-23908
Investigation of plasma-sprayed laminates for high-temperature melting operations
[DE92-008416] p 2353 N92-24006
The use of STEP in an integrated manufacturing environment
[DE92-008417] p 2425 N92-24035

OAO CORP., GREENBELT, MD.
WAMDII: The Wide Angle Michelson Doppler Imaging Interferometer
[NASA-TM-105526] p 2441 N92-23525

OBSERVATOIRE DE LA COTE D'AZUR, NICE (FRANCE).
Possible atmospheric research with Aristoteles
p 2317 N92-23927

OFFICE NATIONAL D'ETUDES ET DE RECHERCHES AEROSPATIALES, PARIS (FRANCE).
What future for hybrid rocket propulsion?
p 2321 N92-23768
The GRADIO accelerometer: Design and development status p 2316 N92-23918

OFFICE NATIONAL D'ETUDES ET DE RECHERCHES AEROSPATIALES, TOULOUSE (FRANCE).
Study of cosmic dust particles on board LDEF: The FRECOPA experiments AO138-1 and AO138-2
p 2458 N92-23310

OHIO AEROSPACE INST., BROOK PARK.
Singularities in optimal structural design
[NASA-TM-4365] p 2388 N92-23527

OHIO STATE UNIV., COLUMBUS.
Energy cycles in the summer tropical atmosphere over the North Atlantic Ocean p 2409 N92-23150
Conception and development of improved analytical prediction models for fatigue induced tooth breakage due to cyclic bending in spur gear teeth
p 2384 N92-23739
Numerical study of the magnetic ordering and superconducting state of high-temperature superconductor p 2449 N92-23776
The Earth's gravity field from satellite geodesy: A 30 year adventure p 2315 N92-23913

OHRI (EDITH), TEL AVIV (ISRAEL).
Group technology, RCO: Rough-Cut Optimizer. The key to integration of plant operations
[REPT-1.1.6] p 2420 N92-23857
Controlling operations through procedures: APE (automated procedure editor)
[REPT-2.2.1] p 2422 N92-23875

OKLAHOMA UNIV., NORMAN.
Multidisciplinary optimization studies using ASTROS
p 2307 N92-23234

OLD DOMINION UNIV., NORFOLK, VA.
Viscous-shock-layer analysis of hypersonic flows over long slender vehicles
[NASA-CR-189614] p 2374 N92-23543

OLDENBURG UNIV. (GERMANY, F.R.).
Introduction: Ocean air observation
p 2392 N92-23381
The state of the development in Europe
p 2392 N92-23382
Sensor package for the North Sea
p 2393 N92-23384
The laser fluorosensor p 2393 N92-23386
The laser bathymeter p 2393 N92-23388
Seaborne lidar system p 2393 N92-23389

OMETRON LTD., LONDON (ENGLAND).
Non contacting measurement of vibration
p 2325 N92-23800

OPEN UNIV. (SCOTLAND).
Growth, differentiation and development of Arabidopsis thaliana under microgravity conditions (7-IML-1)
p 2359 N92-23616

ORBITAL SCIENCES CORP., FAIRFAX, VA.
Suborbital missions: The Joust p 2313 N92-23644

OREGON INST. OF TECH., KLAMATH FALLS.
Geothermal direct use engineering and design guidebook
[DE92-008686] p 2404 N92-24030

OXFORD UNIV. (ENGLAND).
Mathematical modelling and numerical approximations for two-phase flow problems p 2375 N92-23672
Observations of accretion discs in interacting binaries
p 2454 N92-23673
A study of underground muons in the Soudan 2 detector p 2437 N92-23674

P

PACIFIC NORTHWEST LAB., RICHLAND, WA.
Power beaming: Mission enabling for lunar exploration
[DE92-006727] p 2459 N92-23124
HEIS: An integrated information system for environmental restoration and monitoring at Hanford
[DE92-006467] p 2453 N92-23188
Clouds and radiation testbed data environment: Site data system and experiment center
[DE92-006732] p 2408 N92-23741

PADUA UNIV. (ITALY).
Mechanical testing on a composite flexible structure
p 2331 N92-23834

PARIS VI UNIV. (FRANCE).
Transmission of gravistimulus in the statocyte of the lentil root (7-IML-1) p 2359 N92-23617

PENNSYLVANIA STATE UNIV., UNIVERSITY PARK.
Monsoon-ENSO relationships p 2404 N92-23160
Testing the solar paradigm for chromospheric activity in RS CVN binaries: Moderate resolution spectroscopy of solar active regions p 2459 N92-23171
User's manual for three dimensional FDTD version C code for scattering from frequency-independent dielectric and magnetic materials
[NASA-CR-190109] p 2365 N92-23425
Wideband finite difference time domain implementation of surface impedance boundary conditions for good conductors
[NASA-CR-190098] p 2366 N92-23528

Basic research on natural gas combustion phenomena
[PB92-149681] p 2348 N92-23685
Analysis of solar and microwave thermal propulsion systems p 2337 N92-23694
Experimental study of the mechanism of sound generation by rotating stall in centrifugal turbomachines p 2436 N92-23726

PENNSYLVANIA UNIV., PHILADELPHIA.
Gravitropic responses of plants in the absence of a complicating G-force (6-IML-1) p 2356 N92-23601
High-temperature deformation behavior of single crystalline A15-type intermetallic compounds p 2352 N92-23718

PHILIPS TELECOMMUNICATION INDUSTRIES, HILVERSUM (NETHERLANDS).
Change in test-technology
[REPT-1.2.8] p 2421 N92-23867

POD ASSOCIATES, INC., ALBUQUERQUE, NM.
LDEF data correlation to existing NASA debris environment models p 2336 N92-23321

POLITECNICO DI MILANO (ITALY).
Harmonic wave propagation in two-dimensional periodic large space structures p 2330 N92-23830
FAPES: An expert system for designing and optimising fault-tolerant arithmetic array processors
[REPT-1.1.2] p 2419 N92-23854
Progress in the spacewise approach to Aristoteles data reduction p 2315 N92-23914

POLITECNICO DI TORINO (ITALY).
Buckling of simply supported and clamped anisotropic plates under combined loads p 2326 N92-23804
A new test facility for measuring the coefficient of moisture expansion of advanced composite materials p 2326 N92-23807
Exact probabilistic testability measures for multi-output circuits
[REPT-1.2.7] p 2421 N92-23866

PRATT AND WHITNEY AIRCRAFT, WEST PALM BEACH, FL.
Tubular copper thrust chamber design study
[NASA-CR-187206] p 2337 N92-23982

PRINCETON UNIV., NJ.
An instrument to search for small-scale anisotropy in the cosmic microwave background at 90 GHz p 2441 N92-23161
Analysis of forward and inverse problems in chemical dynamics and spectroscopy
[DE92-007732] p 2347 N92-23443
Observing millisecond and binary pulsars p 2455 N92-24001

PUERTO RICO UNIV., MAYAGUEZ.
Modifications for a communication interface board p 2368 N92-23963

Q

QUEBEC UNIV., TROIS-RIVERES.
Influence of maleic anhydride as a coupling agent on the performance of wood fiber: Polystyrene composites p 2343 N92-23945
Filling high density polyethylene with cellulosic fibers. 1: The effect of additives on fiber dispersion p 2344 N92-23948

R

RAFAEL ARMAMENT DEVELOPMENT AUTHORITY, HAIFA (ISRAEL).
Dynamic aggregate models for group technology manufacturing environment
[REPT-1.1.7] p 2420 N92-23858

RENSSELAER POLYTECHNIC INST., TROY, NY.
The continuum modelling of two-phase flow systems
[DE92-007538] p 2373 N92-23202
Kinetic measurements on elementary fossil fuel combustion reactions over wide temperatures ranges
[DE92-007535] p 2347 N92-23221
Modeling and analysis of high-temperature inelastic deformation in metal matrix composites p 2345 N92-23996

RESEARCH INST. FOR COMPUTING AND INFORMATION SYSTEMS, HOUSTON, TX.
Low thrust propulsion literature survey
[NASA-CR-190179] p 2337 N92-23151
Summary report: A preliminary investigation into the use of fuzzy logic for the control of redundant manipulators
[NASA-CR-190277] p 2429 N92-23438
Framework Programmable Platform for the advanced software development workstation: Framework processor design document
[NASA-CR-190173] p 2418 N92-23554
Architectural impact of FDDI network on scheduling hard real-time traffic
[NASA-CR-190272] p 2425 N92-23583

RICE INST., HOUSTON, TX.
An analysis of the WN shell nebula NGC 6888 using CCD imagery and spectrophotometry p 2455 N92-24002

ROCHESTER UNIV., NY.
Photochemistry and charge transfer chemistry of the platinum group elements
[DE92-007564] p 2347 N92-23332
Advances in processing rates optimization for flexible manufacturing systems
[REPT-2.3.4] p 2423 N92-23877
Annual report, 1 October 1990 - 30 September 1991
[DE92-008648] p 2380 N92-23891

ROCKWELL INTERNATIONAL CORP., CANOGA PARK, CA.
Health monitoring of reusable rocket engines p 2320 N92-23762

ROME UNIV. (ITALY).
Influence of the substrate on the solar cells interconnector: Stress distribution and fatigue life prediction p 2326 N92-23803

ROYAL AEROSPACE ESTABLISHMENT, FARNBOROUGH (ENGLAND).
Debris reentry prediction: Salyut-7/Kosmos-1686 p 2318 N92-23973

ROYAL AIR FORCE COLL., CRANWELL (ENGLAND).
Advanced ramjet systems for the propulsion of guided weapons
[ETN-92-91195] p 2310 N92-23169

ROYAL AIRCRAFT ESTABLISHMENT, FARNBOROUGH (ENGLAND).
Surface activation of Concorde by Be-7 p 2439 N92-23295

S

SAAB-SCANIA, LINKOPING (SWEDEN).
The structural optimization system OPTSYS: Current status and applications p 2307 N92-23232

SAINT ANDREW'S UNIV. (SCOTLAND).
The effects of magnetic fields on oscillations in the solar atmosphere p 2459 N92-23697

SANDIA NATIONAL LABS., ALBUQUERQUE, NM.
Oxidative degradation of polymers induced by ionizing radiation
[DE92-007657] p 2354 N92-23442
The electronic structure of icosahedral boron clusters
[DE92-008336] p 2447 N92-23451
Dynamic analysis of planar manipulation tasks
[DE91-019060] p 2430 N92-23458
Soviet articles on antenna theory
[DE92-008452] p 2366 N92-23575
PSD computations using Welch's method
[DE92-007419] p 2370 N92-23584
Versatile bistable optical switches and latching optical logic using integrated photothyristors and surface-emitting lasers
[DE92-008677] p 2442 N92-23748
A simple unfold method for Rutherford-scattering, intense ion-beam spectrographs
[DE92-008678] p 2445 N92-23749
Molecular design of substrate binding sites
[DE92-008331] p 2438 N92-23894
Electrical and optical properties of high gain GaAs switches
[DE92-008668] p 2371 N92-23983
Fermi level effects on dislocation formation in InAs(1-x)Sb(x) grown by MOCVD
[DE92-008332] p 2450 N92-24034
CEPXS/ONELD: A one-dimensional coupled electron-photon discrete ordinates code package
[DE92-003146] p 2425 N92-24041
Battery test facility hardware, software, and system operation
[DE92-008455] p 2372 N92-24063
In situ particle size measurements using a two-color laser scattering technique
[DE92-008634] p 2380 N92-24070

SANDIA NATIONAL LABS., LIVERMORE, CA.
Probing picosecond flame dynamics with transient grating experiments
[DE92-003163] p 2346 N92-23181
A comparative study of preconditioned Lanczos methods for nonsymmetric linear systems
[DE92-007530] p 2431 N92-23201

SCIENCE APPLICATIONS INTERNATIONAL CORP., GLENDORA, CA.
Measured space environmental effects to LDEF during retrieval p 2335 N92-23285

SCIENCE APPLICATIONS INTERNATIONAL CORP., ORLANDO, FL.
Aerodynamic rectifier for pulsed combustors
[PB92-142587] p 2348 N92-23657

SCIENCE APPLICATIONS INTERNATIONAL CORP., SAN DIEGO, CA.
LDEF geometry/mass model for radiation analyses p 2440 N92-23305

SECA, INC., HUNTSVILLE, AL.
Orbital Maneuvering Vehicle (OMV) plume and plume effects study
[NASA-CR-184292] p 2322 N92-23530

SIEMENS A.G., MUNICH (GERMANY, F.R.).
Using range analysis to support hierarchical test pattern generation
[REPT-1.2.5] p 2421 N92-23864

SIFU-ELEKTRONIK, STOCKHOLM (SWEDEN).
An exhaustive self-test design methodology for synchronous state machines
[REPT-1.2.4] p 2421 N92-23863

SOCIETE EUROPEENNE DE PROPULSION, SAINT-MEDARD-EN-JALLES (FRANCE).
Large thin composite thermostructural parts p 2329 N92-23821
CNSR Rosetta: Earth return capsule p 2331 N92-23838

SOCIETE EUROPEENNE DE PROPULSION, VERNON (FRANCE).
Development status of the Vulcain engine p 2319 N92-23759
Materials for high liquid propulsion in 2010 p 2320 N92-23763

SOCIETE NATIONALE DES POUDRES ET EXPLOSIFS, VERT-LE-PETIT (FRANCE).
Small or non pollutant solid propellants for space launchers p 2320 N92-23765

SOUTHAMPTON UNIV. (ENGLAND).
A frequency domain least squares method for modelling acoustic fields
[ISVR-TR-196] p 2435 N92-23170
Design for testability: Where are the goalposts?
[REPT-1.2.2] p 2420 N92-23861

SOUTHWEST RESEARCH INST., SAN ANTONIO, TX.
Probabilistic Structural Analysis Methods (PSAM) for select space propulsion system components, part 2
[NASA-CR-187200] p 2388 N92-23426

SPACE INDUSTRIES, INC., WEBSTER, TX.
The Wake Shield Facility: A space experiment platform p 2313 N92-23648

SPACE TELESCOPE SCIENCE INST., BALTIMORE, MD.
Detecting opportunities for parallel observations on the Hubble Space Telescope p 2426 N92-23359

SPACEHAB, INC., WASHINGTON, DC.
Spacehab p 2313 N92-23647

STANFORD LINEAR ACCELERATOR CENTER, CA.
Recent results on K(omega) and (pi)(pi) systems from LASS
[DE92-007389] p 2436 N92-23327

STANFORD UNIV., CA.
Control of a helicopter engine in low altitude flight p 2310 N92-23122
Lasers without inversion: Theory and experiment p 2379 N92-23143
Turbulence modeling p 2301 N92-23338
Computations of unsteady multistage turbomachinery flows p 2311 N92-23671
The principle and design of a high-efficiency free-electron laser p 2380 N92-23687
The kinematics of turbulent boundary layer structure p 2375 N92-23689
Optimal control of closed chain robotic systems p 2430 N92-24011

STATE UNIV. OF NEW YORK, BUFFALO.
Experiments and modeling p 2301 N92-23339

STATE UNIV. OF NEW YORK, STONY BROOK.
X ray Fourier transform holography: Beyond the optical diffraction limit p 2377 N92-23144
Voxel-based solid modeling
[REPT-1.1.3] p 2419 N92-23855

STEVENS INST. OF TECH., HOBOKEN, NJ.
Magnetotransport and responses of semiconductor microstructures p 2449 N92-23775

STUTTGART UNIV. (GERMANY, F.R.).
Injection molding of long fiber reinforced thermoplastics: A comparison of extruded and pultruded materials with direct addition of roving strands p 2342 N92-23941

SVERDRUP TECHNOLOGY, INC., BROOK PARK, OH.
A study of start-up characteristics of a potassium heat pipe from the frozen state
[NASA-CR-189173] p 2373 N92-23253
Characterization of polybenzimidazole (PBI) film at high temperatures
[NASA-CR-189174] p 2370 N92-23538
Synergistic use of high and low thrust propulsion systems for piloted missions to Mars
[NASA-CR-189138] p 2338 N92-24004

SVERDRUP TECHNOLOGY, INC., CLEVELAND, OH.
The study of PDF turbulence models in combustion p 2301 N92-23337

Progress of simulations for reacting shear layers
p 2302 N92-23344
The study of PDF turbulence models in combustion
[PAPER-107] p 2302 N92-23345
On recontamination and directional-bias problems in Monte Carlo simulation of PDF turbulence models
p 2302 N92-23346
Progress in the development of PDF turbulence models for combustion
[PAPER-213] p 2303 N92-23347
A study of hydrogen diffusion flames using PDF turbulence model p 2303 N92-23348
An improved k-epsilon model for near wall turbulence
p 2303 N92-23349
Three-dimensional calculations of supersonic reacting flows using an LU scheme p 2304 N92-23354

SYMBIOTICS, INC., CAMBRIDGE, MA.
Coordinating complex problem-solving among distributed intelligent agents p 2427 N92-23360

SYRACUSE UNIV., NY.
Numerical and physical modelling of bubbly flow phenomena
[DE92-008642] p 2376 N92-24062

T

TADIRAN ISRAEL ELECTRONICS INDUSTRIES LTD., GIVAT-SHMUEL.
Writing a simulation of a communications network using SIMSCRIPT/DISS
[REPT-2.3.6] p 2423 N92-23879

TADIRAN ISRAEL ELECTRONICS INDUSTRIES LTD., TEL AVIV.
CIM implementation at CVALIM, D.T.C. Division, Bet-Shean, Israel
[REPT-3.2.4] p 2424 N92-23884

TAMPERE UNIV. OF TECHNOLOGY (FINLAND).
Oil lubricated and water lubricated pin-on-disc wear tests with engineering ceramics
[PB92-136563] p 2380 N92-23152

TECHNICAL RESEARCH CENTRE OF FINLAND, ESPOO.
Oil lubricated and water lubricated pin-on-disc wear tests with engineering ceramics
[PB92-136563] p 2380 N92-23152
MOSFET level 1 and 2 models in APLAC
[PB92-143379] p 2371 N92-23678

TECHNICAL UNIV. OF LISBON (PORTUGAL).
Variable bit rate video coding
[PB92-134279] p 2367 N92-23676

TECHNION - ISRAEL INST. OF TECH., HAIFA.
Statistical optimization of integrated circuits in order to reduce the sensitivity to variations in process parameters and environmental conditions
[REPT-1.3.6] p 2422 N92-23872
CIM: The future technology
[REPT-3.3.1] p 2424 N92-23885

TECHNISCHE UNIV., DELFT (NETHERLANDS).
On the kinetics of structural relaxation in some metallic glasses
[PB92-1287272] p 2353 N92-23165
Integrated optics in silicon-based aluminum oxide
[ISBN-90-9004261-X] p 2441 N92-23166
Characterization of organic coatings with impedance measurements: A study of coating structure, adhesion and underfilm corrosion
[PB92-133479] p 2339 N92-23174
Failure behaviour of high density polyethylene products with an embrittled surface layer due to UV exposure
[PB92-138494] p 2354 N92-23510
Analysis of ordering scheme for the unknowns during the solving of geodetic least squares systems
[PB92-137355] p 2432 N92-23514
On the principle of Aristoteles p 2314 N92-23911

TECHNISCHE UNIV., TWENTE (NETHERLANDS).
Geometry of differential difference equations
[PB92-148774] p 2431 N92-23182
Improved shock-capturing of Jameson's scheme for the Euler equations
[PB92-148758] p 2373 N92-23251
Stochastic games with average payoff criterion
[PB92-148634] p 2434 N92-23505
Control problem for a multi server loss system
[PB92-148675] p 2430 N92-23506
Hierarchical sets in mathematical programming modeling languages
[PB92-148683] p 2418 N92-23507

TEL-AVIV UNIV. (ISRAEL).
Flexible Design Environment (FDE) for operation systems design
[REPT-2.3.5] p 2423 N92-23878

TELEDYNE BROWN ENGINEERING, HUNTSVILLE, AL.
The use of artificial intelligence techniques to improve the multiple payload integration process
p 2428 N92-23370

TEMPLE UNIV., PHILADELPHIA, PA.
Mathematical analysis techniques for modeling the space network activities p 2434 N92-23964
Use of the maximum entropy method to retrieve the vertical atmospheric ozone profile and predict atmospheric ozone content p 2407 N92-23965

TENNESSEE TECHNOLOGICAL UNIV., COOKEVILLE.
Studies of fluctuation processes in nuclear collisions
[DE92-008144] p 2440 N92-23276

TENNESSEE UNIV. SPACE INST., TULLAHOMA.
An optical study of grain formation: Casting and solidification technology (2-IML-1) p 2361 N92-23631

TEWISOFT G.M.B.H., SOECHTENAU (GERMANY, F.R.).
The continuous elements method
p 2330 N92-23829

TEXAS A&M UNIV., COLLEGE STATION.
New technology for linear colliders
[DE92-007912] p 2440 N92-23334
A joint source/channel coder design
p 2417 N92-23418
The market for computer readable information
p 2453 N92-23728

TEXAS UNIV., AUSTIN.
Determination of crustal motions using satellite laser ranging
[NASA-CR-190246] p 2408 N92-23540
Precision GPS ephemerides and baselines
[NASA-CR-190247] p 2306 N92-23541
Basic research on natural gas combustion phenomena
[PB92-149681] p 2348 N92-23685

TEXAS UNIV. HEALTH SCIENCE CENTER, HOUSTON.
Chrondrogenesis in micromass cultures of embryonic mouse limb mesenchymal cells exposed to microgravity (7-IML-1) p 2357 N92-23605

TILBURG UNIV. (NETHERLANDS).
Optimizing flow rates in a queueing network with side constraints
[PB92-149996] p 2430 N92-23508
Density of the F-statistic in the linear model with arbitrarily normal distributed errors
[PB92-128792] p 2434 N92-23731

TOBA MERCHANT MARINE COLL. (JAPAN).
Applicability of MESSR and VTIR data for marine observation p 2398 N92-23478

TOKAI REGIONAL FISHERIES RESEARCH LAB., TOKYO (JAPAN).
Research project for practical usage of MOS-1 data collection system p 2399 N92-23485

TOKAI UNIV., TOKYO (JAPAN).
Estimation of MTF of MOS-1 MESSR images
p 2397 N92-23469

TOKYO UNIV., TANASHI (JAPAN).
The 7th INS Scientific Computational Programs
[DE92-750967] p 2417 N92-23266

TOLEDO UNIV., OH.
Semiempirical studies of atomic structure
[DE92-008143] p 2437 N92-23448
Line profile asymmetries in chromospherically active stars p 2458 N92-24015

TORONTO UNIV. (ONTARIO).
Failure processes in the fibre-polymer interphase
p 2341 N92-23934

TOULOUSE UNIV. (FRANCE).
Studies on penetration of antibiotic in bacterial cells in space conditions (7-IML-1) p 2359 N92-23619

TURKU UNIV. (FINLAND).
Use of control theory for analyzing stability of states in continuum thermodynamics
[PB92-136571] p 2451 N92-23136

U

UNIVERSITA DEGLI STUDI DELLA BASILICATA, POTENZA (ITALY).
Quantification of surface functional groups of carbon fibers by x ray photoelectron spectroscopy
p 2343 N92-23946

UNIVERSITE CATHOLIQUE DE LOUVAIN (BELGIUM).
Multitemporal and multisensor approach with MOS data to natural resources evaluation in dry tropical Africa (Burkina Faso) p 2400 N92-23488

UNIVERSITE DE TECHNOLOGIE DE COMPIEGNE (FRANCE).
A symmetric coupling between BEM and FEM for dynamical analysis of spacecraft p 2332 N92-23846
Microstructure and mechanical properties of carbon fibres: Relationship with the fibre-matrix adhesion in a carbon-epoxy composite p 2341 N92-23935
On the test of mode 1 delamination and the importance of laminate lay-ups p 2343 N92-23943

UNIVERSITY CITY SCIENCE CENTER, PHILADELPHIA, PA.
Gravitropic responses of plants in the absence of a complicating G-force (6-IML-1) p 2356 N92-23601
A spaceflight experiment to investigate the effects of a range of unilateral blue light phototropic stimulations on the movements of wheat coleoptiles (6-IML-1)
p 2356 N92-23602

UNIVERSITY COLL. OF NORTH WALES, BANGOR.
Mutual interference in multichannel fibre communication systems p 2367 N92-24019

UNIVERSITY OF CENTRAL FLORIDA, ORLANDO.
Combining factual and heuristic knowledge in knowledge acquisition p 2429 N92-23372

UNIVERSITY OF ELECTRO-COMMUNICATIONS, TOKYO (JAPAN).
Signal processing of the data obtained by MOS-1 MSR p 2397 N92-23472

UNIVERSITY OF NORTHERN ARIZONA, FLAGSTAFF.
Radiation exposure of air carrier crewmembers 2
[PB92-140037] p 2414 N92-23139

UNIVERSITY OF WESTERN ONTARIO, LONDON.
Positional and spontaneous nystagmus (8-IML-1)
p 2360 N92-23624

UTAH STATE UNIV., LOGAN.
The interstellar gas experiment p 2459 N92-23325

UTAH UNIV., SALT LAKE CITY.
The fracture behavior of carbon/epoxy laminates containing part through-the-thickness fiber breakage
p 2340 N92-23693
Investigation of fretting fatigue mechanisms on 7075-T6 aluminum alloy and Ti-6Al-4V titanium alloy
p 2352 N92-23725

V

VAN DER WAALS LAB., AMSTERDAM (NETHERLANDS).
Study of density distribution in a near-critical simple fluid (19-IML-1) p 2362 N92-23639

VERITAS RESEARCH A.S., HOVIK (NORWAY).
Nonlinear finite-element analysis of sandwich shells
p 2326 N92-23802

VERTEX PHARMACEUTICALS, CAMBRIDGE, MA.
Center for Macromolecular Crystallography, University of Alabama in Birmingham p 2313 N92-23650

VIGYAN RESEARCH ASSOCIATES, INC., HAMPTON, VA.
Turbulence modeling in supersonic combusting flows
p 2302 N92-23342

VIRGINIA POLYTECHNIC INST. AND STATE UNIV., BLACKSBURG.
Sensitivity analysis of dynamic aeroelastic responses
p 2306 N92-23229
Feasibility study of a synthesis procedure for array feeds to improve radiation performance of large distorted reflector antennas
[NASA-CR-190191] p 2364 N92-23245
Solar-electric-propulsion cargo vehicles for split/sprint Mars mission
[NASA-CR-189983] p 2322 N92-23526
Sensitivity l(sup 1) minimization with boundary zeros or poles
[PB92-141803] p 2433 N92-23658
Efficient and robust design optimization of transonic airfoils p 2305 N92-23717
Applications of industrial engineering
p 2364 N92-23966
Numerical simulations of wakes, blade-vortex interaction, flutter, and flutter suppression by feedback control p 2375 N92-23997

VIRGINIA UNIV., CHARLOTTESVILLE.
Superconducting materials
[DE92-007748] p 2446 N92-23205
The free and forced vibrations of structures using the finite dynamic element method
[NASA-CR-190184] p 2388 N92-23427
The throes of star formation: A study of the Orion-KL and DR21(OH) molecular clouds p 2457 N92-23698
Surface structure and analysis with scanning tunneling microscopy and electron tunneling spectroscopy
[DE92-007747] p 2448 N92-23721
The need for standards in design automation
[P-1-1] p 2419 N92-23852

VRIJE UNIV., AMSTERDAM (NETHERLANDS).
Some topological problems I met
[PB92-149327] p 2431 N92-23248
Isometric embedding of median algebras into L1 (mu) spaces
[PB92-149343] p 2431 N92-23249
Small solutions and completeness for linear functional differential equations
[PB92-149350] p 2431 N92-23250
Effect of microgravity and mechanical stimulation on the in vitro mineralization and resorption of fetal mouse long bones (7-IML-1) p 2357 N92-23606

VRIJE UNIV., BRUSSELS (BELGIUM).
The torsional fatigue behaviour of the in-plane and out-of-plane shear moduli of composite materials
p 2328 N92-23818
Dynamic characterization of composite materials
p 2330 N92-23832

W

WASHINGTON UNIV., SAINT LOUIS, MO.
SIMS chemical analysis of extended impact features from the trailing edge portion of experiment AO187-2
p 2349 N92-23316
WASHINGTON UNIV., SEATTLE.
A model of large-scale instabilities in the Jovian troposphere p 2459 N92-23704
The discontinuous finite element method with the Taylor-Galerkin approach for nonlinear hyperbolic conservation laws p 2433 N92-23738
An experimental investigation of entrainment and mixing in pulsed and exponential transverse jets
p 2375 N92-23995
WATERLOO UNIV. (ONTARIO).
Computer integrated enterprise: The next step in CIM evolution
[REPT-3.2.2] p 2424 N92-23883
WEST VIRGINIA UNIV., MORGANTOWN.
Automated synthesis of robot arm motion for robot arm collision avoidance p 2381 N92-23158
WESTINGHOUSE DEFENSE AND ELECTRONIC SYSTEMS CENTER, BALTIMORE, MD.
Systems for COMET p 2313 N92-23646
WESTINGHOUSE ELECTRIC CORP., PITTSBURGH, PA.
Center for Space Power and Advanced Electronics, Auburn University p 2314 N92-23654
WESTINGHOUSE SAVANNAH RIVER CO., AIKEN, SC.
Gamma ray spectrometry of LDEF samples at SRL
p 2349 N92-23299
WISCONSIN UNIV., MILWAUKEE.
Boundary element analysis of fracture mechanics problems p 2387 N92-23125
WORLD HEALTH ORGANIZATION, GENEVA (SWITZERLAND).
Irradiation of spices, herbs, and other vegetable seasonings: A compilation of technical data for its authorization and control
[DE92-619064] p 2415 N92-24022
WORLD METEOROLOGICAL ORGANIZATION, GENEVA (SWITZERLAND).
Climate System Monitoring (CSM). El Nino/Southern Oscillation (ENSO) diagnostic advisory, special issue
p 2411 N92-23677

Typical Contract Number Index Listing

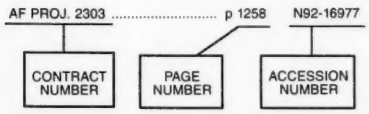

Listings in this index are arranged alphanumerically by contract number. Under each contract number the accession numbers denoting documents that have been produced as a result of research done under that contract are arranged in ascending order. The page number helps to locate the citation in the abstract section. The accession number denotes the number by which the citation is identified.

BMFT-MFU-06021 ..... p 2392 N92-23379
BRITE PROJ. P2381-5 ..... p 2325 N92-23795
DA PROJ. 1L1-61102-AH-45 ..... p 2381 N92-23226
DA PROJ. 1L1-62211-A-47A ..... p 2382 N92-23536
DE-AC02-76CH-00016 ..... p 2350 N92-23197
p 2350 N92-23198
p 2346 N92-23199
p 2432 N92-23329
DE-AC02-76CH-03000 ..... p 2453 N92-23212
p 2368 N92-23326
p 2433 N92-23579
DE-AC02-76ER-02289 ..... p 2440 N92-23214
p 2440 N92-23215
p 2441 N92-23500
DE-AC02-76ER-03071 ..... p 2451 N92-24040
DE-AC02-83CH-10093 ..... p 2402 N92-23175
DE-AC02-85ER-40236 ..... p 2440 N92-23334
DE-AC03-76SF-00098 ..... p 2456 N92-23153
p 2378 N92-23278
p 2378 N92-23279
p 2440 N92-23297
p 2347 N92-23449
p 2437 N92-23450
p 2352 N92-23893
p 2353 N92-23984
p 2371 N92-23985
DE-AC03-76SF-00515 ..... p 2436 N92-23327
DE-AC03-81ER-40050 ..... p 2441 N92-23576
DE-AC03-89ER-51114 ..... p 2444 N92-23446
DE-AC04-76DP-00613 ..... p 2381 N92-23177
p 2453 N92-23183
p 2387 N92-23216
p 2340 N92-23585
p 2348 N92-23586
p 2380 N92-23723
p 2364 N92-23901
p 2445 N92-23905
DE-AC04-76DP-00789 ..... p 2354 N92-23442
p 2447 N92-23451
p 2430 N92-23458
p 2366 N92-23575
p 2370 N92-23584
p 2348 N92-23715
p 2442 N92-23748
p 2445 N92-23749
p 2438 N92-23894
p 2371 N92-23983
p 2450 N92-24034
p 2425 N92-24041
p 2372 N92-24063
DE-AC04-76DR-00789 ..... p 2346 N92-23181
p 2431 N92-23201
p 2380 N92-24070
DE-AC05-84OR-21400 ..... p 2354 N92-23222
p 2354 N92-23223
p 2436 N92-23277
p 2447 N92-23444
p 2441 N92-23445
p 2444 N92-23446
p 2447 N92-23447
p 2429 N92-23457
p 2382 N92-23459
p 2412 N92-23518
p 2337 N92-23722
p 2371 N92-23735
p 2355 N92-23897
p 2367 N92-23900
p 2371 N92-24025
p 2439 N92-24026
p 2430 N92-24032
DE-AC05-84OS-21400 ..... p 2363 N92-23899
p 2384 N92-23908
p 2353 N92-24006
p 2425 N92-24035
DE-AC06-76RL-01830 ..... p 2459 N92-23124
p 2453 N92-23188
p 2408 N92-23741
DE-AC07-76ID-01570 ..... p 2404 N92-24030
DE-AC09-89SR-18035 ..... p 2349 N92-23299
DE-AC34-90DP-62349 ..... p 2348 N92-23572
DE-AC35-89ER-40486 ..... p 2378 N92-23278
DE-AI01-86CE-90237 ..... p 2403 N92-23569
DE-FC03-85DP-40200 ..... p 2380 N92-23891
DE-FC07-91ID-13074 ..... p 2384 N92-23896
DE-FG02-84ER-13224 ..... p 2347 N92-23221
DE-FG02-85ER-13384 ..... p 2348 N92-24038
DE-FG02-86ER-13480 ..... p 2347 N92-23443
DE-FG02-86ER-13489 ..... p 2373 N92-23202
DE-FG02-86ER-13596 ..... p 2438 N92-23895
DE-FG02-86ER-40302 ..... p 2436 N92-23217
DE-FG02-87ER-13808 ..... p 2346 N92-23203
DE-FG02-88ER-13905 ..... p 2355 N92-24037
DE-FG02-90ER-14125 ..... p 2347 N92-23332
DE-FG02-90ER-14136 ..... p 2376 N92-24062
DE-FG02-90ER-40581 ..... p 2451 N92-23578
DE-FG02-90ER-45423 ..... p 2446 N92-23213
DE-FG02-90ER-61009 ..... p 2414 N92-24033
DE-FG02-90ER-61066 ..... p 2409 N92-23257
DE-FG03-84ER-45083 ..... p 2437 N92-23330
DE-FG03-88ER-13932 ..... p 2447 N92-23275
DE-FG05-84ER-45072 ..... p 2448 N92-23721
DE-FG05-84ER-45113 ..... p 2446 N92-23205
DE-FG05-85ER-13430 ..... p 2347 N92-23499
DE-FG05-86ER-40272 ..... p 2451 N92-24040
DE-FG05-88ER-13958 ..... p 2437 N92-23448
DE-FG05-88ER-40461 ..... p 2437 N92-23577
DE-FG05-89ER-40530 ..... p 2440 N92-23276
DE-FG05-91ER-40642 ..... p 2368 N92-23186
DE-FG07-90ID-13040 ..... p 2404 N92-24030
DE-FG22-89PC-89768 ..... p 2439 N92-24031
EPA-R-815152 ..... p 2374 N92-23516
EPA-68-D1-0008 ..... p 2403 N92-23509
ESA-6468/86/NL/PH ..... p 2332 N92-23845
ESA-7821/88 ..... p 2324 N92-23790
ESTEC-AOP/WK/303284 ..... p 2349 N92-23316
ESTEC-8219/89 ..... p 2333 N92-23848
EUREKA PROJ. EU-494 ..... p 2392 N92-23379
FFF-6/546 ..... p 2328 N92-23816
GIT PROJ. E16-654 ..... p 2340 N92-23532
GRI-5086-254-1363 ..... p 2389 N92-23681
GRI-5086-260-1307 ..... p 2348 N92-23685
GRI-5086-260-1320 ..... p 2348 N92-23685
GRI-5090-260-1970 ..... p 2348 N92-23657
GRI-5091-292-2153 ..... p 2383 N92-23680
NAGW-1545 ..... p 2317 N92-23531
NAGW-2066 ..... p 2459 N92-23325
NAGW-2717 ..... p 2306 N92-23541
NAGW-812 ..... p 2379 N92-23283
NAG1-1074 ..... p 2442 N92-23567
NAG1-1174 ..... p 2349 N92-23316
NAG1-1214 ..... p 2458 N92-23318
NAG1-1218 ..... p 2458 N92-23317
p 2458 N92-23318
NAG1-1221 ..... p 2365 N92-23425
p 2366 N92-23528
NAG1-1242 ..... p 2369 N92-23430
NAG1-1243 ..... p 2317 N92-23529
NAG1-346 ..... p 2374 N92-23543
NAG1-637 ..... p 2340 N92-23532
NAG1-859 ..... p 2364 N92-23245
NAG1-956 ..... p 2470 N92-23958
NAG10-0058 ..... p 2429 N92-23372
NAG3-1004 ..... p 2378 N92-23155
NAG3-1079 ..... p 2351 N92-23566
NAG3-806 ..... p 2417 N92-23417
p 2417 N92-23418
NAG5-1012 ..... p 2410 N92-23431
NAG5-1118 ..... p 2408 N92-23540
NAG5-1239 ..... p 2454 N92-23428
NAG5-753 ..... p 2408 N92-23558
NAG5-916 ..... p 2417 N92-23416
p 2417 N92-23417
p 2417 N92-23418
p 2417 N92-23419
p 2418 N92-23422
p 2418 N92-23423
NAG8-168 ..... p 2461 N92-23302
p 2440 N92-23303
NAG8-545 ..... p 2337 N92-23539
NAG8-762 ..... p 2317 N92-23531
NAG8-846 ..... p 2356 N92-23555
NASA ORDER C-99066-G ..... p 2374 N92-23560
NASA ORDER C-99066-6 ..... p 2301 N92-23336
NASA ORDER H-06815-D ..... p 2440 N92-23297
NASW-4003 ..... p 2321 N92-23980
NASW-4324 ..... p 2416 N92-23429
NASW-4435 ..... p 2322 N92-23526
NASW-4520 ..... p 2335 N92-24046
NAS1-16550 ..... p 2458 N92-23317
NAS1-18224 ..... p 2349 N92-23286
p 2335 N92-23287
p 2349 N92-23288
p 2439 N92-23289
NAS1-18471 ..... p 2306 N92-23229
NAS10-10285 ..... p 2406 N92-23898
NAS10-11606 ..... p 2427 N92-23360
NAS10-11763 ..... p 2427 N92-23360
NAS10-8986 ..... p 2406 N92-23898
NAS10-9841 ..... p 2406 N92-23898
NAS13-435 ..... p 2402 N92-23368
NAS2-5266 ..... p 2303 N92-23348
NAS3-23858 ..... p 2337 N92-23982
NAS3-24389 ..... p 2388 N92-23426
NAS3-25266 ..... p 2368 N92-23193
p 2373 N92-23253
p 2388 N92-23267
p 2304 N92-23269
p 2303 N92-23347
p 2370 N92-23535
p 2370 N92-23538
p 2338 N92-24004
NAS7-918 ..... p 2369 N92-23464
p 2416 N92-23546
p 2442 N92-23551
p 2370 N92-23552
p 2382 N92-23553
p 2385 N92-24042
p 2426 N92-24045
NAS8-35866 ..... p 2440 N92-23305
NAS8-36645 ..... p 2379 N92-23283
NAS8-36955 ..... p 2369 N92-23437
p 2375 N92-23568
p 2372 N92-24047
NAS8-37857 ..... p 2317 N92-24048
NAS8-38243 ..... p 2322 N92-23530
NAS8-38566 ..... p 2440 N92-23304
NAS8-918 ..... p 2385 N92-24043
NAS9-17884 ..... p 2426 N92-23358
NCC2-692 ..... p 2425 N92-23991
NCC3-233 ..... p 2374 N92-23542
p 2374 N92-23565
p 2376 N92-24050
NCC3-94 ..... p 2351 N92-23436
NCC9-16 ..... p 2337 N92-23151
p 2429 N92-23438
p 2418 N92-23554
p 2425 N92-23583
NGT-50343 ..... p 2388 N92-23427
NGT-50417 ..... p 2435 N92-23556
NGT-70120 ..... p 2410 N92-23656
NSF ATM-87-09659 ..... p 2410 N92-23656
NSF DCR-86-03603 ..... p 2419 N92-23855
NSF DMS-89-21189 ..... p 2374 N92-23565
NSF MIP-88-05130 ..... p 2419 N92-23855
NSG3-188 ..... p 2382 N92-23536
PHS-OH-02614-01A1 ..... p 2415 N92-23513
PROJ. 90-18 ..... p 2369 N92-23437

RICIS PROJ. AI-02	p 2429	N92-23438
RICIS PROJ. SE-21	p 2337	N92-23151
RICIS PROJ. SE-37	p 2418	N92-23554
VUB-8356/89/NL/FG(SG)	p 2304	N92-23168
W-31-109-ENG-36	p 2340	N92-23256
W-31-109-ENG-38	p 2437	N92-23328
	p 2351	N92-23573
	p 2448	N92-23574
	p 2445	N92-24021
W-7405-ENG-36	p 2368	N92-23200
	p 2438	N92-23714
	p 2352	N92-23720
	p 2438	N92-23747
	p 2455	N92-24027
	p 2458	N92-24028
	p 2450	N92-24036
W-7405-ENG-48	p 2404	N92-23123
	p 2417	N92-23255
	p 2444	N92-23523
	p 2379	N92-23570
	p 2379	N92-23571
	p 2348	N92-23715
	p 2406	N92-23740
	p 2371	N92-23902
	p 2438	N92-23903
	p 2348	N92-23904
	p 2449	N92-23986
	p 2445	N92-23987
	p 2344	N92-23988
	p 2439	N92-24005
	p 2450	N92-24007
	p 2445	N92-24020
	p 2443	N92-24049
	p 2349	N92-24064
	p 2380	N92-24065
	p 2430	N92-24066
	p 2446	N92-24067
	p 2355	N92-24068
	p 2450	N92-24069
W-7405-ENG-82	p 2449	N92-23892
030-09-01-25	p 2426	N92-23356
196-88-00-03	p 2461	N92-23280
199-40-42-01	p 2414	N92-23424
307-50-00	p 2388	N92-23527
323-51-66-01	p 2435	N92-23556
505-33-13	p 2353	N92-23185
505-59-53-01	p 2305	N92-23533
505-62-OK	p 2381	N92-23226
505-62-21	p 2301	N92-23336
	p 2374	N92-23542
	p 2374	N92-23560
	p 2374	N92-23565
	p 2376	N92-24050
505-62-52	p 2304	N92-23269
	p 2305	N92-23563
505-63-40	p 2351	N92-23436
505-63-5A	p 2339	N92-23190
	p 2351	N92-23566
505-63-50-04	p 2340	N92-23434
505-63-50-08	p 2344	N92-23981
505-63-53	p 2339	N92-23194
	p 2388	N92-23267
505-64-10-05	p 2416	N92-23559
505-68-10	p 2373	N92-23154
505-69-40	p 2311	N92-23254
505-90-01	p 2378	N92-23155
506-40-91-02	p 2374	N92-23543
506-41-11	p 2370	N92-23562
506-41-41-01	p 2379	N92-23557
506-41-41	p 2370	N92-23538
	p 2370	N92-23561
506-42-31	p 2337	N92-23534
506-42-73	p 2373	N92-23268
506-43-11	p 2354	N92-23192
	p 2311	N92-23225
506-43-71-01	p 2340	N92-23433
506-44-2C	p 2368	N92-23193
	p 2370	N92-23535
506-59-4C	p 2365	N92-23412
510-01-50	p 2386	N92-23189
	p 2340	N92-23195
	p 2449	N92-23890
510-10-50	p 2387	N92-23196
535-03-0B	p 2387	N92-23191
537-01-22	p 2311	N92-23537
553-13-00	p 2388	N92-23426
590-13-21	p 2373	N92-23253
590-14-11-02	p 2364	N92-23989
590-14-31-01	p 2390	N92-23990
	p 2390	N92-23992
593-12-21	p 2337	N92-23982
593-72-00	p 2337	N92-23252
	p 2338	N92-24004
643-10-01	p 2322	N92-23187
694-03-0K	p 2383	N92-23564
763-22-00	p 2373	N92-23224
763-22-41	p 2381	N92-23435

Typical Report Number Index Listing

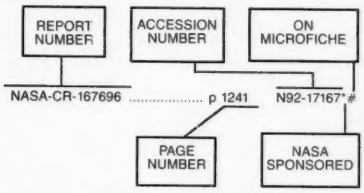

Listings in this index are arranged alphanumerically by report number. The accession number denotes the number by which the citation is identified. The page number helps to locate the citation in the abstract section. An asterisk (*) indicates that the item is a NASA report. A pound sign (#) indicates that the item is available on microfiche.

A-91232 p 2414 N92-23424 * #

AGARD-R-783 p 2308 N92-23950 #
AGARD-R-784 p 2306 N92-23227 #

AIAA-91-2346 p 2338 N92-24004 * #
AIAA-91-3441 p 2337 N92-23252 * #
AIAA-92-0645 p 2373 N92-23154 * #
AIAA-92-1960 p 2322 N92-23187 * #
AIAA-92-2881 p 2373 N92-23268 * #

ANL-HEP-CP-92-03 p 2437 N92-23328 #

ANL/CP-73627 p 2448 N92-23574 #
ANL/CP-73727 p 2351 N92-23573 #
ANL/CP-73895 p 2340 N92-23256 #

ANL/FPP/TM-259 p 2445 N92-24021 #

AVSCOM-TR-90-C-029 p 2382 N92-23536 * #
AVSCOM-TR-91-C-006 p 2381 N92-23226 * #

B-247178 p 2401 N92-23686 #

BNL-45024 p 2346 N92-23199 #
BNL-45259 p 2350 N92-23198 #
BNL-46984 p 2432 N92-23329 #
BNL-47016 p 2350 N92-23197 #

C-228 p 2380 N92-23152 #

CCFD-92-01 p 2375 N92-23568 * #

CESAR-91/41 p 2371 N92-23735 #

CMOTT-91-07 p 2301 N92-23336 * #
CMOTT-92-03 p 2374 N92-23542 * #
CMOTT-92-06 p 2376 N92-24050 * #

CONF-850406-15 p 2380 N92-24070 #
CONF-900557-34 p 2444 N92-23523 #
CONF-9103145-3 p 2348 N92-23715 #
CONF-910328-7 p 2350 N92-23198 #
CONF-9104333-1-EXTD-ABST p 2447 N92-23444 #
CONF-910505-439 p 2368 N92-23186 #
CONF-910626-15 p 2445 N92-23987 #
CONF-9107115-71 p 2443 N92-24049 #
CONF-9108150-7 p 2438 N92-23903 #
CONF-9108150-8 p 2449 N92-23986 #
CONF-9108150-9 p 2450 N92-24007 #
CONF-910864-10 p 2436 N92-23327 #
CONF-910869-27 p 2444 N92-23446 #
CONF-910872-9 p 2347 N92-23449 #
CONF-9109332-3 p 2436 N92-23277 #
CONF-9109348-1 p 2384 N92-23908 #
CONF-9109348-2 p 2363 N92-23899 #
CONF-910983-3 p 2439 N92-24005 #
CONF-9110242-2 p 2346 N92-23199 #
CONF-9110281-5 p 2378 N92-23279 #
CONF-9110281-6 p 2378 N92-23278 #
CONF-9110289-4 p 2441 N92-23445 #
CONF-9110313-5 p 2439 N92-24026 #
CONF-9110323-1 p 2417 N92-23255 #
CONF-911033-5 p 2351 N92-23573 #
CONF-911033-6 p 2447 N92-23451 #
CONF-9110332-1 p 2438 N92-23747 #
CONF-9110335-1-EXTD-ABST p 2438 N92-23895 #
CONF-911047-17 p 2350 N92-23197 #
CONF-911050-4 p 2354 N92-23223 #
CONF-911064-2 p 2379 N92-23570 #
CONF-911106-65 p 2379 N92-23571 #
CONF-911106-73 p 2368 N92-23326 #
CONF-911106-80 p 2453 N92-23212 #
CONF-911107-54 p 2453 N92-23188 #
CONF-9111141-3 p 2437 N92-23328 #
CONF-9111182-3 p 2456 N92-23153 #
CONF-9111183-1 p 2453 N92-23183 #
CONF-9111185-1 p 2455 N92-24027 #
CONF-911132-21 p 2446 N92-24067 #
CONF-911154-2 p 2354 N92-23222 #
CONF-911202-49 p 2448 N92-23574 #
CONF-911202-55 p 2352 N92-23720 #
CONF-911202-59 p 2447 N92-23447 #
CONF-911202-61 p 2353 N92-23984 #
CONF-911202-63 p 2371 N92-23985 #
CONF-911202-64 p 2450 N92-24034 #
CONF-911221-1 p 2442 N92-23748 #
CONF-911296-1 p 2346 N92-23181 #
CONF-911296-3 p 2381 N92-23177 #
CONF-911296-4 p 2387 N92-23216 #
CONF-920104-27 p 2459 N92-23124 #
CONF-920124-12 p 2371 N92-23983 #
CONF-920141-2 p 2450 N92-24036 #
CONF-920144-1 p 2340 N92-23256 #
CONF-920163-1 p 2408 N92-23741 #
CONF-920174-1 p 2409 N92-23257 #
CONF-920180-1 p 2458 N92-24028 #
CONF-920192-1 p 2438 N92-23714 #
CONF-920213-1 p 2432 N92-23329 #
CONF-920235-2 p 2380 N92-24065 #
CONF-920277-1 p 2425 N92-24041 #
CONF-920305-6 p 2367 N92-23900 #
CONF-920362-3 p 2445 N92-23749 #
CONF-920388-1 p 2354 N92-23442 #
CONF-920392-1 p 2425 N92-24035 #
CONF-920439-1 p 2450 N92-24069 #
CONF-920444-14 p 2438 N92-23894 #
CONF-920444-15 p 2349 N92-24064 #
CONF-920458-1 p 2352 N92-23893 #
CONF-920474-1 p 2371 N92-24025 #
CONF-9205100-1 p 2353 N92-24006 #
CONF-920540-15 p 2430 N92-24066 #
CONF-920540-1 p 2429 N92-23457 #
CONF-920540-4 p 2430 N92-23458 #
CONF-920540-7 p 2382 N92-23459 #
CONF-920540-8 p 2430 N92-24032 #
CONF-920572-2 p 2355 N92-24068 #

CSR-HEA-92-02 p 2317 N92-23531 * #

CT-8 p 2371 N92-23678 #

CTN-92-60405 p 2341 N92-23933 #

DE91-002172 p 2402 N92-23175 #
DE91-018939 p 2429 N92-23457 #
DE91-019060 p 2430 N92-23458 #
DE91-019074 p 2371 N92-23735 #
DE92-000046 p 2382 N92-23459 #
DE92-000069 p 2430 N92-24032 #
DE92-003131 p 2381 N92-23177 #
DE92-003146 p 2425 N92-24041 #
DE92-003163 p 2346 N92-23181 #
DE92-003222 p 2453 N92-23183 #
DE92-003231 p 2368 N92-23186 #
DE92-005539 p 2414 N92-24033 #
DE92-006467 p 2453 N92-23188 #
DE92-006640 p 2406 N92-23740 #
DE92-006657 p 2404 N92-23123 #
DE92-006727 p 2459 N92-23124 #
DE92-006732 p 2408 N92-23741 #
DE92-006826 p 2417 N92-23255 #
DE92-006868 p 2403 N92-23569 * #
DE92-006896 p 2379 N92-23570 #
DE92-006898 p 2379 N92-23571 #
DE92-006947 p 2348 N92-23572 #
DE92-006978 p 2340 N92-23256 #
DE92-006979 p 2412 N92-23518 #
DE92-006986 p 2351 N92-23573 #
DE92-006991 p 2448 N92-23574 #
DE92-007199 p 2368 N92-23326 #
DE92-007204 p 2409 N92-23257 #
DE92-007234 p 2371 N92-24025 #
DE92-007240 p 2439 N92-24026 #
DE92-007264 p 2340 N92-23585 #
DE92-007265 p 2348 N92-23586 #
DE92-007389 p 2436 N92-23327 #
DE92-007397 p 2437 N92-23328 #
DE92-007414 p 2438 N92-23747 #
DE92-007419 p 2370 N92-23584 #
DE92-007429 p 2455 N92-24027 #
DE92-007431 p 2458 N92-24028 #
DE92-007452 p 2350 N92-23197 #
DE92-007456 p 2350 N92-23198 #
DE92-007458 p 2346 N92-23199 #
DE92-007528 p 2368 N92-23200 #
DE92-007529 p 2347 N92-23499 #
DE92-007530 p 2431 N92-23201 #
DE92-007535 p 2347 N92-23221 #
DE92-007538 p 2373 N92-23202 #
DE92-007562 p 2346 N92-23203 #
DE92-007564 p 2347 N92-23332 #
DE92-007592 p 2405 N92-23333 #
DE92-007593 p 2405 N92-23204 #
DE92-007657 p 2354 N92-23442 #
DE92-007686 p 2354 N92-23222 #
DE92-007717 p 2352 N92-23720 #
DE92-007732 p 2347 N92-23443 #
DE92-007747 p 2448 N92-23721 #
DE92-007748 p 2446 N92-23205 #
DE92-007799 p 2337 N92-23722 #
DE92-007801 p 2380 N92-23723 #
DE92-007837 p 2447 N92-23444 #
DE92-007838 p 2354 N92-23223 #
DE92-007912 p 2440 N92-23334 #
DE92-007913 p 2453 N92-23212 #
DE92-007960 p 2446 N92-23213 #
DE92-007966 p 2441 N92-23500 #
DE92-007967 p 2440 N92-23214 #
DE92-007968 p 2440 N92-23215 #
DE92-007971 p 2387 N92-23216 #
DE92-008003 p 2441 N92-23445 #
DE92-008037 p 2363 N92-23899 #
DE92-008040 p 2384 N92-23908 #
DE92-008052 p 2444 N92-23446 #
DE92-008055 p 2432 N92-23329 #
DE92-008098 p 2447 N92-23447 #
DE92-008129 p 2437 N92-23330 #
DE92-008132 p 2447 N92-23275 #
DE92-008143 p 2437 N92-23448 #
DE92-008144 p 2440 N92-23276 #
DE92-008243 p 2449 N92-23892 #
DE92-008250 p 2436 N92-23277 #
DE92-008278 p 2367 N92-23900 #
DE92-008283 p 2352 N92-23893 #
DE92-008288 p 2378 N92-23278 #
DE92-008299 p 2378 N92-23279 #
DE92-008300 p 2353 N92-23984 #
DE92-008301 p 2456 N92-23153 #
DE92-008304 p 2347 N92-23449 #
DE92-008307 p 2371 N92-23985 #
DE92-008314 p 2437 N92-23450 #
DE92-008331 p 2438 N92-23894 #
DE92-008332 p 2450 N92-24034 #
DE92-008336 p 2447 N92-23451 #
DE92-008340 p 2436 N92-23217 #
DE92-008356 p 2438 N92-23895 #
DE92-008357 p 2439 N92-24005 #
DE92-008399 p 2364 N92-23901 #
DE92-008404 p 2371 N92-23902 #
DE92-008416 p 2353 N92-24006 #

DE92-008417 ..... p 2425 N92-24035 #
DE92-008425 ..... p 2384 N92-23896 #
DE92-008441 ..... p 2450 N92-24036 #
DE92-008452 ..... p 2366 N92-23575 #
DE92-008455 ..... p 2372 N92-24063 #
DE92-008488 ..... p 2438 N92-23714 #
DE92-008543 ..... p 2441 N92-23576 #
DE92-008554 ..... p 2349 N92-24064 #
DE92-008557 ..... p 2348 N92-23715 #
DE92-008566 ..... p 2449 N92-23986 #
DE92-008567 ..... p 2438 N92-23903 #
DE92-008577 ..... p 2445 N92-23987 #
DE92-008587 ..... p 2437 N92-23577 #
DE92-008599 ..... p 2444 N92-23523 #
DE92-008605 ..... p 2450 N92-24007 #
DE92-008606 ..... p 2380 N92-24065 #
DE92-008612 ..... p 2430 N92-24066 #
DE92-008614 ..... p 2446 N92-24067 #
DE92-008615 ..... p 2443 N92-24049 #
DE92-008619 ..... p 2355 N92-24068 #
DE92-008624 ..... p 2450 N92-24069 #
DE92-008634 ..... p 2380 N92-24070 #
DE92-008642 ..... p 2376 N92-24062 #
DE92-008648 ..... p 2380 N92-23891 #
DE92-008668 ..... p 2371 N92-23983 #
DE92-008677 ..... p 2442 N92-23748 #
DE92-008678 ..... p 2445 N92-23749 #
DE92-008686 ..... p 2404 N92-24030 #
DE92-008693 ..... p 2439 N92-24031 #
DE92-008730 ..... p 2451 N92-23578 #
DE92-008772 ..... p 2451 N92-24040 #
DE92-008787 ..... p 2355 N92-24037 #
DE92-008790 ..... p 2348 N92-24038 #
DE92-008851 ..... p 2433 N92-23579 #
DE92-008980 ..... p 2344 N92-23988 #
DE92-008983 ..... p 2445 N92-24020 #
DE92-008987 ..... p 2348 N92-23904 #
DE92-009020 ..... p 2445 N92-23905 #
DE92-009022 ..... p 2445 N92-24021 #
DE92-009630 ..... p 2355 N92-23897 #
DE92-614951 ..... p 2415 N92-23218 #
DE92-615083 ..... p 2386 N92-23258 #
DE92-615124 ..... p 2378 N92-23219 #
DE92-615195 ..... p 2454 N92-23742 #
DE92-615214 ..... p 2451 N92-23743 #
DE92-615215 ..... p 2438 N92-23744 #
DE92-615216 ..... p 2433 N92-23745 #
DE92-615217 ..... p 2432 N92-23331 #
DE92-615260 ..... p 2431 N92-23128 #
DE92-615261 ..... p 2431 N92-23129 #
DE92-615322 ..... p 2440 N92-23130 #
DE92-615399 ..... p 2379 N92-23131 #
DE92-615484 ..... p 2435 N92-23220 #
DE92-615485 ..... p 2435 N92-23598 #
DE92-615486 ..... p 2443 N92-24029 #
DE92-615489 ..... p 2446 N92-23259 #
DE92-615517 ..... p 2446 N92-23260 #
DE92-616890 ..... p 2366 N92-23580 #
DE92-616891 ..... p 2451 N92-23501 #
DE92-616892 ..... p 2451 N92-23206 #
DE92-616916 ..... p 2432 N92-23335 #
DE92-616917 ..... p 2432 N92-23502 #
DE92-616919 ..... p 2451 N92-23503 #
DE92-616991 ..... p 2435 N92-23207 #
DE92-617386 ..... p 2443 N92-23208 #
DE92-617387 ..... p 2444 N92-23209 #
DE92-617436 ..... p 2448 N92-23504 #
DE92-617438 ..... p 2350 N92-23210 #
DE92-617439 ..... p 2448 N92-23581 #
DE92-617440 ..... p 2351 N92-23582 #
DE92-617445 ..... p 2350 N92-23211 #
DE92-617446 ..... p 2446 N92-23270 #
DE92-617447 ..... p 2446 N92-23271 #
DE92-617490 ..... p 2447 N92-23272 #
DE92-617537 ..... p 2447 N92-23273 #
DE92-617538 ..... p 2447 N92-23452 #
DE92-617539 ..... p 2447 N92-23453 #
DE92-617992 ..... p 2436 N92-23274 #
DE92-619048 ..... p 2460 N92-23909 #
DE92-619064 ..... p 2415 N92-24022 #
DE92-619234 ..... p 2434 N92-24039 #
DE92-750824 ..... p 2444 N92-23261 #
DE92-750825 ..... p 2407 N92-23262 #
DE92-750949 ..... p 2444 N92-23711 #
DE92-750951 ..... p 2351 N92-23263 #
DE92-750961 ..... p 2444 N92-23264 #
DE92-750962 ..... p 2351 N92-23265 #
DE92-750967 ..... p 2417 N92-23266 #
DE92-751006 ..... p 2352 N92-23712 #
DE92-751024 ..... p 2441 N92-23713 #
DE92-751036 ..... p 2443 N92-23132 #
DE92-751038 ..... p 2443 N92-23133 #
DE92-751046 ..... p 2353 N92-23134 #
DE92-751058 ..... p 2443 N92-23135 #
DE92-769374 ..... p 2406 N92-23733 #
DE92-769375 ..... p 2406 N92-23734 #
DE92-769376 ..... p 2407 N92-24023 #
DE92-769377 ..... p 2405 N92-23454 #
DE92-769378 ..... p 2405 N92-23455 #
DE92-769380 ..... p 2347 N92-23456 #
DE92-769381 ..... p 2407 N92-24024 #
DE92-783370 ..... p 2403 N92-23684 #

DOE/CH-10093/95 ..... p 2402 N92-23175 #

DOE/DP-40200/184 ..... p 2380 N92-23891 #

DOE/ER-02289/2 ..... p 2441 N92-23500 #
DOE/ER-02289/3 ..... p 2440 N92-23214 #
DOE/ER-02289/4 ..... p 2440 N92-23215 #
DOE/ER-13224/16 ..... p 2347 N92-23221 #
DOE/ER-13384/5 ..... p 2348 N92-24038 #
DOE/ER-13430/T1 ..... p 2347 N92-23499 #
DOE/ER-13480/2 ..... p 2347 N92-23443 #
DOE/ER-13489/6 ..... p 2373 N92-23202 #
DOE/ER-13596/25 ..... p 2438 N92-23895 #
DOE/ER-13808/4 ..... p 2346 N92-23203 #
DOE/ER-13905/4 ..... p 2355 N92-24037 #
DOE/ER-13932/T1 ..... p 2447 N92-23275 #
DOE/ER-13958/28 ..... p 2437 N92-23448 #
DOE/ER-14125/2 ..... p 2347 N92-23332 #
DOE/ER-14136/T1 ..... p 2376 N92-24062 #
DOE/ER-40050/T7 ..... p 2441 N92-23576 #
DOE/ER-40236/T2 ..... p 2440 N92-23334 #
DOE/ER-40272/129 ..... p 2451 N92-24040 #
DOE/ER-40302/6 ..... p 2436 N92-23217 #
DOE/ER-40461/4 ..... p 2437 N92-23577 #
DOE/ER-40530/3 ..... p 2440 N92-23276 #
DOE/ER-40581/2 ..... p 2451 N92-23578 #
DOE/ER-45072/50 ..... p 2448 N92-23721 #
DOE/ER-45083/T1 ..... p 2437 N92-23330 #
DOE/ER-45113/T3 ..... p 2446 N92-23205 #
DOE/ER-45423/2 ..... p 2446 N92-23213 #
DOE/ER-61009/2 ..... p 2414 N92-24033 #
DOE/ER-61066/3 ..... p 2409 N92-23257 #

DOE/ID-13040/T3 ..... p 2404 N92-24030 #
DOE/ID-13074/T2 ..... p 2384 N92-23896 #

DOE/PC-89768/T3 ..... p 2439 N92-24031 #

DOE/PE-0101-VOL-1 ..... p 2405 N92-23204 #
DOE/PE-0101-VOL-2 ..... p 2405 N92-23333 #

DOT/FAA-AM-92/2 ..... p 2414 N92-23139 #

D615-10051 ..... p 2317 N92-24048 * #

E-6447 ..... p 2365 N92-23412 * #
E-6570 ..... p 2301 N92-23336 * #
E-6686 ..... p 2388 N92-23527 * #
E-6691 ..... p 2374 N92-23560 * #
E-6754 ..... p 2370 N92-23535 * #
E-6773 ..... p 2387 N92-23196 * #
E-6776 ..... p 2382 N92-23536 * #
E-6795 ..... p 2311 N92-23254 * #
E-6806 ..... p 2373 N92-23154 * #
E-6853 ..... p 2305 N92-23563 * #
E-6866 ..... p 2340 N92-23195 * #
E-6872 ..... p 2378 N92-23155 * #
E-6881 ..... p 2386 N92-23189 * #
E-6891 ..... p 2381 N92-23226 * #
E-6895 ..... p 2304 N92-23269 * #
E-6896 ..... p 2383 N92-23564 * #
E-6900 ..... p 2339 N92-23194 * #
E-6901 ..... p 2388 N92-23267 * #
E-6902 ..... p 2337 N92-23534 * #
E-6910 ..... p 2373 N92-23268 * #
E-6912 ..... p 2374 N92-23565 * #
E-6914 ..... p 2311 N92-23225 * #
E-6917 ..... p 2374 N92-23542 * #
E-6926 ..... p 2353 N92-23185 * #
E-6940 ..... p 2338 N92-24004 * #
E-6941 ..... p 2337 N92-23252 * #
E-6945 ..... p 2381 N92-23435 * #
E-6948 ..... p 2311 N92-23537 * #
E-6949 ..... p 2339 N92-23190 * #
E-6957 ..... p 2370 N92-23538 * #
E-6960 ..... p 2370 N92-23561 * #
E-6961 ..... p 2351 N92-23436 * #
E-6963 ..... p 2370 N92-23562 * #
E-6973 ..... p 2368 N92-23193 * #
E-6977 ..... p 2354 N92-23192 * #
E-7001 ..... p 2387 N92-23191 * #
E-7010 ..... p 2322 N92-23187 * #
E-7021 ..... p 2449 N92-23890 * #
E-7026 ..... p 2373 N92-23224 * #
E-7031 ..... p 2373 N92-23253 * #

EPA/AA/CTAB-92/01 ..... p 2383 N92-23595 #

EPA/450/4-91/023 ..... p 2406 N92-23517 #
EPA/600/A-92/023 ..... p 2410 N92-23520 #
EPA/600/R-92/007 ..... p 2403 N92-23509 #
EPA/600/3-91/075 ..... p 2374 N92-23516 #

ESA-SP-321-VOL-1 ..... p 2322 N92-23780 #
ESA-SP-327 ..... p 2318 N92-23750 #
ESA-SP-329 ..... p 2314 N92-23910 #
ESA-SP-345 ..... p 2333 N92-23967 #

ESDU-68014 ..... p 2434 N92-24008
ESDU-68016 ..... p 2434 N92-24008
ESDU-68017 ..... p 2434 N92-24008
ESDU-68022 ..... p 2309 N92-24009
ESDU-91041 ..... p 2434 N92-24008
ESDU-91042 ..... p 2309 N92-24009

ETN-92-91073 ..... p 2392 N92-23379 #
ETN-92-91074 ..... p 2452 N92-23928 #
ETN-92-91142 ..... p 2353 N92-23165 #
ETN-92-91143 ..... p 2441 N92-23166 #
ETN-92-91187 ..... p 2333 N92-23967 #
ETN-92-91193 ..... p 2339 N92-23167 #
ETN-92-91194 ..... p 2304 N92-23168 #
ETN-92-91195 ..... p 2310 N92-23169 #
ETN-92-91196 ..... p 2435 N92-23170 #
ETN-92-91208 ..... p 2322 N92-23780 #
ETN-92-91381 ..... p 2318 N92-23750 #
ETN-92-91383 ..... p 2314 N92-23910 #

FCR-11900A ..... p 2403 N92-23509 #

FEW-500 ..... p 2434 N92-23731 #
FEW-511 ..... p 2430 N92-23508 #

FFA-TN-1991-17 ..... p 2339 N92-23167 #
FFA-TN-1991-40 ..... p 2304 N92-23168 #

FNAL-TM-1767 ..... p 2433 N92-23579 #

FNAL/C-91/310 ..... p 2368 N92-23326 #
FNAL/C-91/351 ..... p 2453 N92-23212 #

FR-21385 ..... p 2337 N92-23982 * #

GA-A-20694 ..... p 2444 N92-23446 #

GAO/IMTEC-92-24 ..... p 2401 N92-23686 #

GRI-91/0227 ..... p 2389 N92-23681 #
GRI-91/0333 ..... p 2348 N92-23685 #
GRI-91/0347 ..... p 2383 N92-23680 #
GRI-91/0401 ..... p 2348 N92-23657 #

HE-90015 ..... p 2396 N92-23465 #

IAEA-R-5017-F ..... p 2378 N92-23219 #
IAEA-R-5234-F ..... p 2440 N92-23130 #

IAEA-TECDOC-628/S ..... p 2386 N92-23258 #
IAEA-TECDOC-639 ..... p 2415 N92-24022 #

IC-91/226 ..... p 2443 N92-23208 #
IC-91/246 ..... p 2435 N92-23220 #
IC-91/247 ..... p 2435 N92-23598 #
IC-91/257 ..... p 2432 N92-23335 #
IC-91/258 ..... p 2451 N92-23743 #
IC-91/259 ..... p 2434 N92-24039 #
IC-91/262 ..... p 2431 N92-23128 #
IC-91/263 ..... p 2431 N92-23129 #
IC-91/265 ..... p 2438 N92-23744 #
IC-91/266 ..... p 2433 N92-23745 #
IC-91/272 ..... p 2432 N92-23331 #
IC-91/276 ..... p 2443 N92-24029 #
IC-91/277 ..... p 2446 N92-23260 #
IC-91/279 ..... p 2350 N92-23211 #
IC-91/281 ..... p 2446 N92-23270 #
IC-91/288 ..... p 2446 N92-23259 #
IC-91/289 ..... p 2447 N92-23273 #
IC-91/293 ..... p 2446 N92-23271 #
IC-91/294 ..... p 2366 N92-23580 #
IC-91/297 ..... p 2447 N92-23272 #
IC-91/298 ..... p 2460 N92-23909 #
IC-91/310 ..... p 2451 N92-23503 #
IC-91/312 ..... p 2432 N92-23502 #
IC-91/315 ..... p 2448 N92-23504 #
IC-91/317 ..... p 2447 N92-23452 #
IC-91/318 ..... p 2444 N92-23209 #
IC-91/322 ..... p 2350 N92-23210 #
IC-91/323 ..... p 2448 N92-23581 #
IC-91/335 ..... p 2451 N92-23501 #
IC-91/336 ..... p 2451 N92-23206 #
IC-91/339 ..... p 2447 N92-23453 #
IC-91/348 ..... p 2435 N92-23207 #
IC-91/351 ..... p 2351 N92-23582 #

ICOMP-91-17 ..... p 2301 N92-23336 * #

ICOMP-91-22 ..... p 2374 N92-23560 * #
ICOMP-92-04 ..... p 2374 N92-23565 * #
ICOMP-92-06 ..... p 2374 N92-23542 * #
ICOMP-92-10 ..... p 2376 N92-24050 * #

IFVE-OUNK-91-14 ..... p 2436 N92-23274 #

IHEP-OUNK-91-14 ..... p 2436 N92-23274 #

IHES/M/91/70 ..... p 2434 N92-24061 #
IHES/M/91/88 ..... p 2431 N92-23184 #
IHES/M/91/91 ..... p 2433 N92-23670 #
IHES/M/91/92 ..... p 2433 N92-23599 #

IMI-90D-000-1063-G ..... p 2341 N92-23933 #

INDC(CCP)-343/L ..... p 2454 N92-23742 #

INIS-MF-13047-VOL-15-NO-2 ..... p 2415 N92-23218 #

INS-T-503 ..... p 2417 N92-23266 #

IS-T-1604 ..... p 2449 N92-23892 #

ISBN-0-85679-803-7 ..... p 2434 N92-24008
ISBN-0-85679-804-5 ..... p 2309 N92-24009
ISBN-90-9004261-X ..... p 2441 N92-23166 #
ISBN-92-835-0652-9 ..... p 2308 N92-23950 #
ISBN-92-835-0653-7 ..... p 2306 N92-23227 #
ISBN-92-9092-126-9 ..... p 2322 N92-23780 #
ISBN-92-9092-150-1 ..... p 2318 N92-23750 #
ISBN-92-9092-158-7 ..... p 2314 N92-23910 #
ISBN-92-9092-222-2 ..... p 2333 N92-23967 #
ISBN-951-22-0334-0 ..... p 2368 N92-23172 #
ISBN-951-22-0358-8 ..... p 2350 N92-23179 #
ISBN-951-22-0391-X ..... p 2380 N92-23152 #
ISBN-951-22-0395-2 ..... p 2350 N92-23178 #
ISBN-951-22-0458-4 ..... p 2370 N92-23497 #
ISBN-951-22-0465-7 ..... p 2403 N92-23683 #
ISBN-951-22-0476-2 ..... p 2367 N92-23679 #
ISBN-951-22-0485-1 ..... p 2387 N92-23137 #
ISBN-951-22-0486-X ..... p 2366 N92-23666 #
ISBN-951-22-0522-X ..... p 2369 N92-23495 #
ISBN-951-22-0526-2 ..... p 2444 N92-23663 #
ISBN-951-22-0550-5 ..... p 2366 N92-23591 #
ISBN-951-22-0573-4 ..... p 2366 N92-23667 #
ISBN-951-22-0583-1 ..... p 2403 N92-23592 #
ISBN-951-22-0600-5 ..... p 2367 N92-23907 #
ISBN-951-22-0610-2 ..... p 2367 N92-23668 #
ISBN-951-22-0733-8 ..... p 2396 N92-23441 #
ISBN-951-22-0741-9 ..... p 2442 N92-23662 #
ISBN-951-22-0756-7 ..... p 2364 N92-23138 #
ISBN-951-22-0757-5 ..... p 2369 N92-23496 #
ISBN-951-22-0762-1 ..... p 2383 N92-23710 #
ISBN-951-22-0787-7 ..... p 2371 N92-23678 #
ISBN-951-22-0792-3 ..... p 2366 N92-23590 #
ISBN-951-22-0802-4 ..... p 2366 N92-23661 #
ISBN-951-22-0803-2 ..... p 2433 N92-23658 #
ISBN-951-22-0828-8 ..... p 2432 N92-23440 #
ISBN-951-22-0846-6 ..... p 2433 N92-23589 #
ISBN-951-22-0854-7 ..... p 2448 N92-23498 #

ISSN-0141-397X ..... p 2309 N92-24009
ISSN-0141-4089 ..... p 2434 N92-24008
ISSN-0141-4097 ..... p 2434 N92-24008
ISSN-0379-6566 ..... p 2322 N92-23780 #
ISSN-0379-6566 ..... p 2314 N92-23910 #
ISSN-0379-6566 ..... p 2333 N92-23967 #
ISSN-0452-2982 ..... p 2312 N92-23778 #
ISSN-0452-2982 ..... p 2384 N92-23779 #
ISSN-0452-2982 ..... p 2312 N92-23979 #
ISSN-9058-0379 ..... p 2434 N92-24008

ISVR-TR-196 ..... p 2435 N92-23170 #

ITN-92-85127 ..... p 2418 N92-23851 #

JAERI-M-91-094 ..... p 2444 N92-23711 #
JAERI-M-91-116 ..... p 2351 N92-23263 #
JAERI-M-91-126 ..... p 2443 N92-23132 #
JAERI-M-91-131 ..... p 2444 N92-23264 #
JAERI-M-91-132 ..... p 2351 N92-23265 #
JAERI-M-91-134 ..... p 2353 N92-23134 #
JAERI-M-91-136 ..... p 2352 N92-23712 #
JAERI-M-91-156 ..... p 2443 N92-23133 #
JAERI-M-91-168 ..... p 2443 N92-23135 #

JPL-D-9263 ..... p 2403 N92-23569 * #

JPRS-UES-91-005 ..... p 2392 N92-23707 #

JPRS-ULS-92-010 ..... p 2412 N92-23706 #

JPRS-UMS-92-005 ..... p 2363 N92-23708 #
JPRS-UMS-92-006 ..... p 2363 N92-23709 #

JPRS-USP-92-002 ..... p 2314 N92-23705 #

JTN-92-80274 ..... p 2396 N92-23465 #
JTN-92-80309 ..... p 2312 N92-23778 #
JTN-92-80310 ..... p 2384 N92-23779 #
JTN-92-80327 ..... p 2312 N92-23979 #

KCP-613-4477 ..... p 2380 N92-23723 #
KCP-613-4556 ..... p 2340 N92-23585 #
KCP-613-4616 ..... p 2364 N92-23901 #
KCP-613-4626 ..... p 2348 N92-23586 #
KCP-613-4653 ..... p 2445 N92-23905 #
KCP-613-4675 ..... p 2381 N92-23177 #
KCP-613-4687 ..... p 2387 N92-23216 #
KCP-613-4758 ..... p 2453 N92-23183 #

KEK-91-5 ..... p 2441 N92-23713 #

K243 ..... p 2354 N92-23510 #

L-17031 ..... p 2344 N92-23981 * #
L-17042-PT-1 ..... p 2461 N92-23280 * #
L-17043 ..... p 2379 N92-23557 * #

LA-UR-91-4163 ..... p 2455 N92-24027 #
LA-UR-92-231 ..... p 2458 N92-24028 #
LA-UR-92-338 ..... p 2438 N92-23747 #
LA-UR-92-429 ..... p 2450 N92-24036 #
LA-UR-92-578 ..... p 2438 N92-23714 #
LA-UR-92-73 ..... p 2352 N92-23720 #

LA-11623-MS ..... p 2368 N92-23200 #

LAMP-91/6 ..... p 2379 N92-23131 #

LBL-30462 ..... p 2347 N92-23449 #
LBL-31207 ..... p 2371 N92-23985 #
LBL-31497 ..... p 2378 N92-23279 #
LBL-31622 ..... p 2437 N92-23450 #
LBL-31671 ..... p 2352 N92-23893 #
LBL-31677 ..... p 2378 N92-23278 #
LBL-31678 ..... p 2456 N92-23153 #
LBL-31831 ..... p 2353 N92-23984 #

L16986 ..... p 2305 N92-23533 * #

M-681 ..... p 2356 N92-23600 * #
M-687 ..... p 2418 N92-23432 * #

MBB-UE-0014-90-PUB ..... p 2452 N92-23928 #

MBB-UH-HE512 ..... p 2394 N92-23392 #

MBB-UK-0152-91-PUB ..... p 2392 N92-23379 #

MEMO-985 ..... p 2434 N92-23505 #
MEMO-989 ..... p 2430 N92-23506 #
MEMO-990 ..... p 2418 N92-23507 #
MEMO-997 ..... p 2373 N92-23251 #
MEMO-999 ..... p 2431 N92-23182 #

MRL-7043 ..... p 2389 N92-23681 #

NAL-PD-AL-9111 ..... p 2368 N92-23246 #

NAL-TM-565 ..... p 2312 N92-23778 #
NAL-TM-622 ..... p 2384 N92-23779 #
NAL-TM-629 ..... p 2312 N92-23979 #

NAS 1.15:103580 ..... p 2369 N92-23437 * #
NAS 1.15:103890 ..... p 2414 N92-23424 * #
NAS 1.15:104229 ..... p 2364 N92-23989 * #
NAS 1.15:105159 ..... p 2365 N92-23412 * #
NAS 1.15:105243 ..... p 2301 N92-23336 * #
NAS 1.15:105268 ..... p 2387 N92-23191 * #
NAS 1.15:105329 ..... p 2374 N92-23560 * #
NAS 1.15:105387 ..... p 2387 N92-23196 * #
NAS 1.15:105388 ..... p 2382 N92-23536 * #
NAS 1.15:105399 ..... p 2311 N92-23254 * #
NAS 1.15:105432 ..... p 2305 N92-23563 * #
NAS 1.15:105438 ..... p 2340 N92-23195 * #
NAS 1.15:105523 ..... p 2321 N92-23524 * #
NAS 1.15:105526 ..... p 2441 N92-23525 * #
NAS 1.15:105551 ..... p 2378 N92-23155 * #
NAS 1.15:105557 ..... p 2386 N92-23189 * #
NAS 1.15:105567 ..... p 2381 N92-23226 * #
NAS 1.15:105570 ..... p 2304 N92-23269 * #
NAS 1.15:105571 ..... p 2383 N92-23564 * #
NAS 1.15:105574 ..... p 2339 N92-23194 * #
NAS 1.15:105575 ..... p 2388 N92-23267 * #
NAS 1.15:105576 ..... p 2337 N92-23534 * #
NAS 1.15:105583 ..... p 2373 N92-23268 * #
NAS 1.15:105584 ..... p 2374 N92-23565 * #
NAS 1.15:105586 ..... p 2311 N92-23225 * #
NAS 1.15:105588 ..... p 2374 N92-23542 * #
NAS 1.15:105594 ..... p 2353 N92-23185 * #
NAS 1.15:105605 ..... p 2337 N92-23252 * #
NAS 1.15:105610 ..... p 2311 N92-23537 * #
NAS 1.15:105611 ..... p 2339 N92-23190 * #
NAS 1.15:105617 ..... p 2373 N92-23154 * #
NAS 1.15:105622 ..... p 2370 N92-23561 * #
NAS 1.15:105624 ..... p 2370 N92-23562 * #
NAS 1.15:105630 ..... p 2368 N92-23193 * #
NAS 1.15:105634 ..... p 2354 N92-23192 * #
NAS 1.15:105641 ..... p 2381 N92-23435 * #
NAS 1.15:105647 ..... p 2370 N92-23535 * #
NAS 1.15:105649 ..... p 2322 N92-23187 * #
NAS 1.15:105657 ..... p 2449 N92-23890 * #
NAS 1.15:105661 ..... p 2373 N92-23224 * #
NAS 1.15:105663 ..... p 2376 N92-24050 * #
NAS 1.15:107568 ..... p 2416 N92-23559 * #
NAS 1.15:107573 ..... p 2390 N92-23990 * #
NAS 1.15:107595 ..... p 2340 N92-23434 * #
NAS 1.15:107597 ..... p 2340 N92-23433 * #
NAS 1.15:107605 ..... p 2390 N92-23992 * #
NAS 1.15:107773 ..... p 2312 N92-23241 * #
NAS 1.15:107774 ..... p 2312 N92-23242 * #
NAS 1.15:107775 ..... p 2312 N92-23243 * #
NAS 1.15:107780 ..... p 2312 N92-23244 * #
NAS 1.15:107801 ..... p 2312 N92-23240 * #
NAS 1.15:107812 ..... p 2312 N92-23643 * #
NAS 1.15:107813 ..... p 2470 N92-23958 * #
NAS 1.15:4295 ..... p 2305 N92-23533 * #
NAS 1.15:4353 ..... p 2356 N92-23600 * #
NAS 1.15:4364 ..... p 2416 N92-23429 * #
NAS 1.15:4365 ..... p 2388 N92-23527 * #
NAS 1.15:4375 ..... p 2379 N92-23557 * #
NAS 1.26:184292 ..... p 2322 N92-23530 * #
NAS 1.26:184309 ..... p 2317 N92-24048 * #
NAS 1.26:184317 ..... p 2372 N92-24047 * #
NAS 1.26:187200 ..... p 2388 N92-23426 * #
NAS 1.26:187206 ..... p 2337 N92-23982 * #
NAS 1.26:188466 ..... p 2408 N92-23558 * #
NAS 1.26:189124 ..... p 2351 N92-23566 * #
NAS 1.26:189138 ..... p 2338 N92-24004 * #
NAS 1.26:189147 ..... p 2351 N92-23436 * #
NAS 1.26:189173 ..... p 2373 N92-23253 * #
NAS 1.26:189174 ..... p 2370 N92-23538 * #
NAS 1.26:189614 ..... p 2374 N92-23543 * #
NAS 1.26:189878 ..... p 2410 N92-23656 * #
NAS 1.26:189960 ..... p 2417 N92-23416 * #
NAS 1.26:189983 ..... p 2322 N92-23526 * #
NAS 1.26:190098 ..... p 2366 N92-23528 * #
NAS 1.26:190109 ..... p 2365 N92-23425 * #
NAS 1.26:190129 ..... p 2317 N92-23529 * #
NAS 1.26:190152 ..... p 2406 N92-23698 * #
NAS 1.26:190173 ..... p 2418 N92-23554 * #
NAS 1.26:190179 ..... p 2337 N92-23151 * #
NAS 1.26:190184 ..... p 2388 N92-23427 * #
NAS 1.26:190188 ..... p 2403 N92-23569 * #
NAS 1.26:190191 ..... p 2364 N92-23245 * #
NAS 1.26:190196 ..... p 2369 N92-23430 * #
NAS 1.26:190197 ..... p 2454 N92-23428 * #
NAS 1.26:190203 ..... p 2337 N92-23539 * #
NAS 1.26:190214 ..... p 2317 N92-23531 * #
NAS 1.26:190216 ..... p 2321 N92-23980 * #
NAS 1.26:190226 ..... p 2340 N92-23532 * #
NAS 1.26:190246 ..... p 2408 N92-23540 * #
NAS 1.26:190247 ..... p 2306 N92-23541 * #
NAS 1.26:190256 ..... p 2356 N92-23555 * #
NAS 1.26:190257 ..... p 2335 N92-24046 * #
NAS 1.26:190272 ..... p 2425 N92-23583 * #
NAS 1.26:190277 ..... p 2429 N92-23438 * #
NAS 1.26:190291 ..... p 2375 N92-23568 * #
NAS 1.26:190293 ..... p 2442 N92-23567 * #
NAS 1.26:190304 ..... p 2425 N92-23991 * #
NAS 1.26:4437 ..... p 2435 N92-23556 * #
NAS 1.55:3134-PT-1 ..... p 2461 N92-23280 * #
NAS 1.55:3141 ..... p 2426 N92-23356 * #
NAS 1.60:3196 ..... p 2344 N92-23981 * #
NAS 1.60:3220 ..... p 2418 N92-23432 * #
NAS 1.71:GSC-13141-1 ..... p 2382 N92-23548 * #
NAS 1.71:GSC-13161-1 ..... p 2386 N92-24060 * #
NAS 1.71:GSC-13358-1 ..... p 2385 N92-24058 * #
NAS 1.71:GSC-13359-1 ..... p 2381 N92-23378 * #
NAS 1.71:GSC-13360-1 ..... p 2381 N92-23377 * #
NAS 1.71:GSC-13386-1 ..... p 2386 N92-23376 * #
NAS 1.71:GSC-13406-1 ..... p 2378 N92-23460 * #
NAS 1.71:GSC-13415-1 ..... p 2386 N92-24059 * #
NAS 1.71:GSC-13422-1 ..... p 2369 N92-23462 * #
NAS 1.71:GSC-13442-1 ..... p 2382 N92-23547 * #
NAS 1.71:GSC-13450-1 ..... p 2403 N92-23463 * #
NAS 1.71:GSC-13451-1 ..... p 2388 N92-23549 * #
NAS 1.71:LEW-15027-2 ..... p 2355 N92-24053 * #
NAS 1.71:LEW-15212-1 ..... p 2404 N92-24054 * #
NAS 1.71:LEW-15308-1 ..... p 2404 N92-24057 * #
NAS 1.71:LEW-15314-1 ..... p 2354 N92-23461 * #
NAS 1.71:MFS-28430-1 ..... p 2416 N92-24044 * #
NAS 1.71:MFS-28481-1 ..... p 2416 N92-24056 * #
NAS 1.71:MFS-28634-1 ..... p 2385 N92-24055 * #
NAS 1.71:MSC-21648-1 ..... p 2385 N92-24051 * #
NAS 1.71:MSC-21843-1-NP ..... p 2413 N92-24052 * #

NAS 1.71:MSC-21864-1 ..... p 2382 N92-23544 * #
NAS 1.71:MSC-21951-1 ..... p 2378 N92-23545 * #
NAS 1.71:NPO-18394-1-CU ..... p 2370 N92-23552 * #
NAS 1.71:NPO-18414-1-CU ..... p 2426 N92-24045 * #
NAS 1.71:NPO-18428-1-CU ..... p 2369 N92-23464 * #
NAS 1.71:NPO-18491-1-CU ..... p 2416 N92-23546 * #
NAS 1.71:NPO-18498-1-CU ..... p 2385 N92-24043 * #
NAS 1.71:NPO-18499-1-CU ..... p 2385 N92-24042 * #
NAS 1.71:NPO-18607-1-CU ..... p 2382 N92-23553 * #
NAS 1.71:NPO-18702-1-CU ..... p 2442 N92-23551 * #
NAS 1.71:SSC-00010-2 ..... p 2453 N92-23550 * #

NASA-CASE-GSC-13141-1 ..... p 2382 N92-23548 * #
NASA-CASE-GSC-13161-1 ..... p 2386 N92-24060 * #
NASA-CASE-GSC-13358-1 ..... p 2385 N92-24058 * #
NASA-CASE-GSC-13359-1 ..... p 2381 N92-23378 * #
NASA-CASE-GSC-13360-1 ..... p 2381 N92-23377 * #
NASA-CASE-GSC-13386-1 ..... p 2386 N92-23376 * #
NASA-CASE-GSC-13406-1 ..... p 2378 N92-23460 * #
NASA-CASE-GSC-13415-1 ..... p 2386 N92-24059 * #
NASA-CASE-GSC-13422-1 ..... p 2369 N92-23462 * #
NASA-CASE-GSC-13442-1 ..... p 2382 N92-23547 * #
NASA-CASE-GSC-13450-1 ..... p 2403 N92-23463 * #
NASA-CASE-GSC-13451-1 ..... p 2388 N92-23549 * #

NASA-CASE-LEW-15027-2 ..... p 2355 N92-24053 * #
NASA-CASE-LEW-15212-1 ..... p 2404 N92-24054 * #
NASA-CASE-LEW-15308-1 ..... p 2404 N92-24057 * #
NASA-CASE-LEW-15314-1 ..... p 2354 N92-23461 * #

NASA-CASE-MFS-28430-1 ..... p 2416 N92-24044 * #
NASA-CASE-MFS-28481-1 ..... p 2416 N92-24056 * #
NASA-CASE-MFS-28634-1 ..... p 2385 N92-24055 * #

NASA-CASE-MSC-21648-1 ..... p 2385 N92-24051 * #
NASA-CASE-MSC-21843-1-NP .... p 2413 N92-24052 * #
NASA-CASE-MSC-21864-1 ..... p 2382 N92-23544 * #
NASA-CASE-MSC-21951-1 ..... p 2378 N92-23545 * #

NASA-CASE-NPO-18394-1-CU .... p 2370 N92-23552 * #
NASA-CASE-NPO-18414-1-CU .... p 2426 N92-24045 * #
NASA-CASE-NPO-18428-1-CU .... p 2369 N92-23464 * #
NASA-CASE-NPO-18491-1-CU .... p 2416 N92-23546 * #
NASA-CASE-NPO-18498-1-CU .... p 2385 N92-24043 * #
NASA-CASE-NPO-18499-1-CU .... p 2385 N92-24042 * #
NASA-CASE-NPO-18607-1-CU .... p 2382 N92-23553 * #
NASA-CASE-NPO-18702-1-CU .... p 2442 N92-23551 * #

NASA-CASE-SSC-00010-2 ..... p 2453 N92-23550 * #

NASA-CP-3134-PT-1 ..... p 2461 N92-23280 * #
NASA-CP-3141 ..... p 2426 N92-23356 * #

NASA-CR-184292 ..... p 2322 N92-23530 * #
NASA-CR-184309 ..... p 2317 N92-24048 * #
NASA-CR-184317 ..... p 2372 N92-24047 * #
NASA-CR-187200 ..... p 2388 N92-23426 * #
NASA-CR-187206 ..... p 2337 N92-23982 * #
NASA-CR-188466 ..... p 2408 N92-23558 * #
NASA-CR-189124 ..... p 2351 N92-23566 * #
NASA-CR-189138 ..... p 2338 N92-24004 * #
NASA-CR-189147 ..... p 2351 N92-23436 * #
NASA-CR-189173 ..... p 2373 N92-23253 * #
NASA-CR-189174 ..... p 2370 N92-23538 * #
NASA-CR-189614 ..... p 2374 N92-23543 * #
NASA-CR-189878 ..... p 2410 N92-23656 * #
NASA-CR-189960 ..... p 2417 N92-23416 * #
NASA-CR-189983 ..... p 2322 N92-23526 * #
NASA-CR-190098 ..... p 2366 N92-23528 * #
NASA-CR-190109 ..... p 2365 N92-23425 * #
NASA-CR-190129 ..... p 2317 N92-23529 * #
NASA-CR-190152 ..... p 2406 N92-23898 * #
NASA-CR-190173 ..... p 2418 N92-23554 * #
NASA-CR-190179 ..... p 2337 N92-23151 * #
NASA-CR-190184 ..... p 2388 N92-23427 * #
NASA-CR-190188 ..... p 2403 N92-23569 * #
NASA-CR-190191 ..... p 2364 N92-23245 * #
NASA-CR-190196 ..... p 2369 N92-23430 * #
NASA-CR-190197 ..... p 2454 N92-23428 * #
NASA-CR-190203 ..... p 2337 N92-23539 * #
NASA-CR-190214 ..... p 2317 N92-23531 * #
NASA-CR-190216 ..... p 2321 N92-23980 * #
NASA-CR-190226 ..... p 2340 N92-23532 * #
NASA-CR-190246 ..... p 2408 N92-23540 * #
NASA-CR-190247 ..... p 2306 N92-23541 * #
NASA-CR-190256 ..... p 2356 N92-23555 * #
NASA-CR-190257 ..... p 2335 N92-24046 * #
NASA-CR-190272 ..... p 2425 N92-23583 * #
NASA-CR-190277 ..... p 2429 N92-23438 * #
NASA-CR-190291 ..... p 2375 N92-23568 * #
NASA-CR-190293 ..... p 2442 N92-23567 * #
NASA-CR-190304 ..... p 2425 N92-23991 * #
NASA-CR-4437 ..... p 2435 N92-23556 * #

NASA-TM-103580 ..... p 2369 N92-23437 * #
NASA-TM-103890 ..... p 2414 N92-23424 * #

NASA-TM-104229 ..... p 2364 N92-23989 * #
NASA-TM-105159 ..... p 2365 N92-23412 * #
NASA-TM-105243 ..... p 2301 N92-23336 * #
NASA-TM-105268 ..... p 2387 N92-23191 * #
NASA-TM-105329 ..... p 2374 N92-23560 * #
NASA-TM-105387 ..... p 2387 N92-23196 * #
NASA-TM-105388 ..... p 2382 N92-23536 * #
NASA-TM-105399 ..... p 2311 N92-23254 * #
NASA-TM-105432 ..... p 2305 N92-23563 * #
NASA-TM-105438 ..... p 2340 N92-23195 * #
NASA-TM-105523 ..... p 2321 N92-23524 * #
NASA-TM-105526 ..... p 2441 N92-23525 * #
NASA-TM-105551 ..... p 2378 N92-23155 * #
NASA-TM-105557 ..... p 2386 N92-23189 * #
NASA-TM-105567 ..... p 2381 N92-23226 * #
NASA-TM-105570 ..... p 2304 N92-23269 * #
NASA-TM-105571 ..... p 2383 N92-23564 * #
NASA-TM-105574 ..... p 2339 N92-23194 * #
NASA-TM-105575 ..... p 2388 N92-23267 * #
NASA-TM-105576 ..... p 2337 N92-23534 * #
NASA-TM-105583 ..... p 2373 N92-23268 * #
NASA-TM-105584 ..... p 2374 N92-23565 * #
NASA-TM-105586 ..... p 2311 N92-23225 * #
NASA-TM-105588 ..... p 2374 N92-23542 * #
NASA-TM-105594 ..... p 2353 N92-23185 * #
NASA-TM-105605 ..... p 2337 N92-23252 * #
NASA-TM-105610 ..... p 2311 N92-23537 * #
NASA-TM-105611 ..... p 2339 N92-23190 * #
NASA-TM-105617 ..... p 2373 N92-23154 * #
NASA-TM-105622 ..... p 2370 N92-23561 * #
NASA-TM-105624 ..... p 2370 N92-23562 * #
NASA-TM-105630 ..... p 2368 N92-23193 * #
NASA-TM-105634 ..... p 2354 N92-23192 * #
NASA-TM-105641 ..... p 2381 N92-23435 * #
NASA-TM-105647 ..... p 2370 N92-23535 * #
NASA-TM-105649 ..... p 2322 N92-23187 * #
NASA-TM-105657 ..... p 2449 N92-23890 * #
NASA-TM-105661 ..... p 2373 N92-23224 * #
NASA-TM-105663 ..... p 2376 N92-24050 * #
NASA-TM-107568 ..... p 2416 N92-23559 * #
NASA-TM-107573 ..... p 2390 N92-23990 * #
NASA-TM-107595 ..... p 2340 N92-23434 * #
NASA-TM-107597 ..... p 2340 N92-23433 * #
NASA-TM-107605 ..... p 2390 N92-23992 * #
NASA-TM-107773 ..... p 2312 N92-23241 * #
NASA-TM-107774 ..... p 2312 N92-23242 * #
NASA-TM-107775 ..... p 2312 N92-23243 * #
NASA-TM-107780 ..... p 2312 N92-23244 * #
NASA-TM-107801 ..... p 2312 N92-23240 * #
NASA-TM-107812 ..... p 2312 N92-23643 * #
NASA-TM-107813 ..... p 2470 N92-23958 * #
NASA-TM-4295 ..... p 2305 N92-23533 * #
NASA-TM-4353 ..... p 2356 N92-23600 * #
NASA-TM-4364 ..... p 2416 N92-23429 * #
NASA-TM-4365 ..... p 2388 N92-23527 * #
NASA-TM-4375 ..... p 2379 N92-23557 * #

NASA-TP-3196 ..... p 2344 N92-23981 * #
NASA-TP-3220 ..... p 2418 N92-23432 * #

NCAR/CT-132 ..... p 2410 N92-23656 * #

NCAR/TN-365+PROC ..... p 2410 N92-23587 #
NCAR/TN-376+STR ..... p 2408 N92-23522 #

NEDO-ITE-9002-1 ..... p 2406 N92-23733 #
NEDO-ITE-9002-2 ..... p 2406 N92-23734 #
NEDO-ITE-9002-4 ..... p 2407 N92-24023 #
NEDO-ITE-9002-5 ..... p 2405 N92-23454 #
NEDO-ITE-9003 ..... p 2407 N92-24024 #
NEDO-ITE-9006 ..... p 2405 N92-23455 #
NEDO-ITE-9008 ..... p 2347 N92-23456 #

NEDO-P-9009 ..... p 2403 N92-23684 #

NIFS-MEMO-1 ..... p 2444 N92-23261 #
NIFS-MEMO-2 ..... p 2407 N92-23262 #

NISTIR-3978 ..... p 2364 N92-23173 #
NISTIR-4720 ..... p 2432 N92-23511 #

NLR-TR-88148-U ..... p 2436 N92-23588 #

NOAA-DR-ERL-PMEL-36 ..... p 2411 N92-23682 #

NOAA-TM-ERL-GLERL-76 ..... p 2401 N92-23659 #

NOAA-TM-ERL-WPL-217 ..... p 2412 N92-23669 #

NOAA-TM-ERL-211 ..... p 2401 N92-23521 #

NOAA-TM-NMFS-F/SPO-1 ..... p 2412 N92-23519 #

NOAA-TM-NWS-SR-140 ..... p 2411 N92-23906 #

NOAA-TR-ERL-447-AOML-35 ..... p 2412 N92-23732 #

NOAA-TR-NWS-44 ..... p 2410 N92-23439 #
NOAA-TR-NWS-45 ..... p 2410 N92-23494 #
NOAA-TR-NWS-46 ..... p 2411 N92-23746 #

NPS/NRAQD/NRTR-91/02 ..... p 2407 N92-24003 #

NRC-32603 ..... p 2341 N92-23933 #

NTIA-91-282 ..... p 2364 N92-23180 #

NTSB/AAR-91/08 ..... p 2305 N92-23596 #
NTSB/AAR-91/09 ..... p 2305 N92-23597 #

ORNL-6703 ..... p 2355 N92-23897 #

ORNL/TM-11759 ..... p 2337 N92-23722 #
ORNL/TM-11972 ..... p 2371 N92-23735 #
ORNL/TM-11992 ..... p 2412 N92-23518 #

P-1-1 ..... p 2419 N92-23852 #

PAPER-105 ..... p 2303 N92-23350 * #
PAPER-107 ..... p 2302 N92-23345 * #
PAPER-213 ..... p 2303 N92-23347 * #

PB91-910409 ..... p 2305 N92-23596 #
PB91-910410 ..... p 2305 N92-23597 #
PB92-100346 ..... p 2406 N92-23593 #
PB92-111699 ..... p 2459 N92-23701 #
PB92-127745 ..... p 2451 N92-23247 #
PB92-128248 ..... p 2405 N92-23515 #
PB92-1287272 ..... p 2353 N92-23165 #
PB92-128792 ..... p 2434 N92-23731 #
PB92-129402 ..... p 2460 N92-23993 #
PB92-129949 ..... p 2401 N92-23659 #
PB92-129964 ..... p 2412 N92-23732 #
PB92-132901 ..... p 2374 N92-23516 #
PB92-132976 ..... p 2364 N92-23173 #
PB92-133479 ..... p 2339 N92-23174 #
PB92-133511 ..... p 2350 N92-23176 #
PB92-133941 ..... p 2387 N92-23137 #
PB92-134071 ..... p 2368 N92-23172 #
PB92-134279 ..... p 2367 N92-23676 #
PB92-134444 ..... p 2411 N92-23906 #
PB92-134501 ..... p 2411 N92-23994 #
PB92-135326 ..... p 2411 N92-23660 #
PB92-136001 ..... p 2415 N92-23513 #
PB92-136373 ..... p 2434 N92-24061 #
PB92-136464 ..... p 2350 N92-23178 #
PB92-136555 ..... p 2350 N92-23179 #
PB92-136563 ..... p 2380 N92-23152 #
PB92-136571 ..... p 2451 N92-23136 #
PB92-137355 ..... p 2432 N92-23514 #
PB92-137413 ..... p 2364 N92-23180 #
PB92-137454 ..... p 2405 N92-23512 #
PB92-137520 ..... p 2403 N92-23509 #
PB92-137603 ..... p 2383 N92-23680 #
PB92-137843 ..... p 2411 N92-23746 #
PB92-137850 ..... p 2410 N92-23439 #
PB92-137868 ..... p 2410 N92-23494 #
PB92-138494 ..... p 2354 N92-23510 #
PB92-138544 ..... p 2436 N92-23588 #
PB92-139773 ..... p 2368 N92-23140 #
PB92-139963 ..... p 2410 N92-23587 #
PB92-140037 ..... p 2414 N92-23139 #
PB92-140466 ..... p 2412 N92-23669 #
PB92-140532 ..... p 2407 N92-24003 #
PB92-140714 ..... p 2401 N92-23521 #
PB92-141555 ..... p 2406 N92-23517 #
PB92-141753 ..... p 2389 N92-23681 #
PB92-141803 ..... p 2433 N92-23658 #
PB92-141829 ..... p 2403 N92-23592 #
PB92-141878 ..... p 2366 N92-23590 #
PB92-141886 ..... p 2366 N92-23661 #
PB92-141928 ..... p 2403 N92-23683 #
PB92-141936 ..... p 2444 N92-23663 #
PB92-141951 ..... p 2383 N92-23710 #
PB92-141977 ..... p 2396 N92-23441 #
PB92-142116 ..... p 2369 N92-23496 #
PB92-142173 ..... p 2367 N92-23907 #
PB92-142199 ..... p 2364 N92-23138 #
PB92-142256 ..... p 2435 N92-23665 #
PB92-142280 ..... p 2369 N92-23495 #
PB92-142306 ..... p 2370 N92-23497 #
PB92-142355 ..... p 2367 N92-23679 #
PB92-142371 ..... p 2366 N92-23666 #
PB92-142397 ..... p 2366 N92-23591 #
PB92-142405 ..... p 2366 N92-23667 #
PB92-142413 ..... p 2367 N92-23668 #
PB92-142447 ..... p 2388 N92-23664 #
PB92-142587 ..... p 2348 N92-23657 #
PB92-143080 ..... p 2411 N92-23682 #
PB92-143304 ..... p 2433 N92-23589 #
PB92-143320 ..... p 2448 N92-23498 #
PB92-143361 ..... p 2379 N92-23594 #
PB92-143379 ..... p 2371 N92-23678 #

PB92-143551 ..... p 2432 N92-23440 #
PB92-143585 ..... p 2442 N92-23662 #
PB92-143692 ..... p 2383 N92-23595 #
PB92-143742 ..... p 2432 N92-23511 #
PB92-145389 ..... p 2412 N92-23519 #
PB92-148543 ..... p 2408 N92-23522 #
PB92-148634 ..... p 2434 N92-23505 #
PB92-148675 ..... p 2430 N92-23506 #
PB92-148683 ..... p 2418 N92-23507 #
PB92-148758 ..... p 2373 N92-23251 #
PB92-148774 ..... p 2431 N92-23182 #
PB92-149327 ..... p 2431 N92-23248 #
PB92-149343 ..... p 2431 N92-23249 #
PB92-149350 ..... p 2431 N92-23250 #
PB92-149434 ..... p 2433 N92-23599 #
PB92-149442 ..... p 2433 N92-23670 #
PB92-149459 ..... p 2431 N92-23184 #
PB92-149681 ..... p 2348 N92-23685 #
PB92-149996 ..... p 2430 N92-23508 #
PB92-150457 ..... p 2410 N92-23520 #

PNL-SA-19713 ..... p 2459 N92-23124 #
PNL-SA-19800 ..... p 2453 N92-23188 #
PNL-SA-19880 ..... p 2408 N92-23741 #

REPT-1.1.1 ..... p 2419 N92-23853 #
REPT-1.1.2 ..... p 2419 N92-23854 #
REPT-1.1.3 ..... p 2419 N92-23855 #
REPT-1.1.4 ..... p 2419 N92-23856 #
REPT-1.1.6 ..... p 2420 N92-23857 #
REPT-1.1.7 ..... p 2420 N92-23858 #
REPT-1.1.8 ..... p 2420 N92-23859 #
REPT-1.2.1 ..... p 2420 N92-23860 #
REPT-1.2.2 ..... p 2420 N92-23861 #
REPT-1.2.3 ..... p 2420 N92-23862 #
REPT-1.2.4 ..... p 2421 N92-23863 #
REPT-1.2.5 ..... p 2421 N92-23864 #
REPT-1.2.6 ..... p 2421 N92-23865 #
REPT-1.2.7 ..... p 2421 N92-23866 #
REPT-1.2.8 ..... p 2421 N92-23867 #
REPT-1.3.1 ..... p 2421 N92-23868 #
REPT-1.3.2 ..... p 2421 N92-23869 #
REPT-1.3.3 ..... p 2422 N92-23870 #
REPT-1.3.4 ..... p 2422 N92-23871 #
REPT-1.3.6 ..... p 2422 N92-23872 #
REPT-1.3.7 ..... p 2422 N92-23873 #
REPT-1/91 ..... p 2350 N92-23176 #
REPT-102 ..... p 2366 N92-23590 #
REPT-103 ..... p 2366 N92-23661 #
REPT-109 ..... p 2388 N92-23664 #
REPT-18 ..... p 2370 N92-23497 #
REPT-2.1.2 ..... p 2422 N92-23874 #
REPT-2.2.1 ..... p 2422 N92-23875 #
REPT-2.3.3 ..... p 2423 N92-23876 #
REPT-2.3.4 ..... p 2423 N92-23877 #
REPT-2.3.5 ..... p 2423 N92-23878 #
REPT-2.3.6 ..... p 2423 N92-23879 #
REPT-3.1.5 ..... p 2423 N92-23880 #
REPT-3.1.6 ..... p 2423 N92-23881 #
REPT-3.1.7 ..... p 2424 N92-23882 #
REPT-3.2.2 ..... p 2424 N92-23883 #
REPT-3.2.4 ..... p 2424 N92-23884 #
REPT-3.3.1 ..... p 2424 N92-23885 #
REPT-3.3.2 ..... p 2424 N92-23886 #
REPT-4.2.1 ..... p 2424 N92-23887 #
REPT-4.2.2 ..... p 2425 N92-23888 #
REPT-4.2.3 ..... p 2425 N92-23889 #
REPT-46 ..... p 2451 N92-23136 #
REPT-4 ..... p 2396 N92-23441 #
REPT-79 ..... p 2367 N92-23679 #
REPT-81 ..... p 2366 N92-23666 #
REPT-85 ..... p 2366 N92-23591 #
REPT-88 ..... p 2366 N92-23667 #
REPT-90 ..... p 2367 N92-23907 #
REPT-91-4 ..... p 2432 N92-23514 #
REPT-91 ..... p 2367 N92-23668 #
REPT-92-008 ..... p 2425 N92-23991 * #
REPT-92B00045 ..... p 2426 N92-23356 * #
REPT-99 ..... p 2364 N92-23138 #

RFP-4476 ..... p 2348 N92-23572 #

RR-A290 ..... p 2387 N92-23137 #
RR-A291 ..... p 2369 N92-23495 #
RR-A301 ..... p 2433 N92-23658 #
RR-A304 ..... p 2433 N92-23589 #

S-186 ..... p 2368 N92-23172 #

SAND-85-8869 ..... p 2380 N92-24070 #
SAND-91-0720 ..... p 2366 N92-23575 #
SAND-91-1059 ..... p 2372 N92-24063 #
SAND-91-1196C ..... p 2447 N92-23451 #
SAND-91-1533 ..... p 2370 N92-23584 #
SAND-91-1561C ..... p 2450 N92-24034 #
SAND-91-1562C ..... p 2371 N92-23983 #
SAND-91-1584C ..... p 2442 N92-23748 #
SAND-91-2041C ..... p 2430 N92-23458 #
SAND-91-2921C ..... p 2438 N92-23894 #
SAND-91-8240 ..... p 2431 N92-23201 #
SAND-92-0064C ..... p 2445 N92-23749 #
SAND-92-0236C ..... p 2354 N92-23442 #
SAND-92-0261C ..... p 2425 N92-24041 #
SAND-92-8408J ..... p 2346 N92-23181 #

SATCOM-92-2 ..... p 2364 N92-23245 * #

SECA-TR-92-02 ..... p 2322 N92-23530 * #

SER-A-16 ..... p 2432 N92-23440 #

SGD-564-PT-2 ..... p 2459 N92-23701 #
SGD-566-PT-2 ..... p 2460 N92-23993 #

SU-SLAC-PUB-5722 ..... p 2436 N92-23327 #

TKK-F-A670 ..... p 2403 N92-23683 #
TKK-F-A675 ..... p 2403 N92-23592 #
TKK-F-A678 ..... p 2444 N92-23663 #
TKK-F-A690 ..... p 2442 N92-23662 #
TKK-F-A691 ..... p 2435 N92-23665 #
TKK-F-A692 ..... p 2379 N92-23594 #

TKK-V-B59 ..... p 2350 N92-23178 #

UAH-5-32640 ..... p 2372 N92-24047 * #

UCB-PTH-92/01 ..... p 2456 N92-23153 #

UCRL-ID-108256 ..... p 2371 N92-23902 #
UCRL-ID-109159 ..... p 2344 N92-23988 #
UCRL-ID-109227 ..... p 2406 N92-23740 #
UCRL-ID-109264 ..... p 2404 N92-23123 #
UCRL-ID-109807 ..... p 2445 N92-24020 #
UCRL-ID-109903 ..... p 2348 N92-23904 #

UCRL-JC-103284 ..... p 2444 N92-23523 #
UCRL-JC-106407 ..... p 2445 N92-23987 #
UCRL-JC-106910 ..... p 2348 N92-23715 #
UCRL-JC-107010 ..... p 2438 N92-23903 #
UCRL-JC-108061 ..... p 2439 N92-24005 #
UCRL-JC-108069 ..... p 2379 N92-23570 #
UCRL-JC-108266 ..... p 2449 N92-23986 #
UCRL-JC-108299 ..... p 2443 N92-24049 #
UCRL-JC-108409 ..... p 2417 N92-23255 #
UCRL-JC-108475 ..... p 2380 N92-24065 #
UCRL-JC-108592 ..... p 2430 N92-24066 #
UCRL-JC-108620 ..... p 2450 N92-24069 #
UCRL-JC-108674 ..... p 2450 N92-24007 #
UCRL-JC-108752 ..... p 2379 N92-23571 #
UCRL-JC-109030 ..... p 2446 N92-24067 #
UCRL-JC-109148 ..... p 2349 N92-24064 #
UCRL-JC-109213 ..... p 2355 N92-24068 #

UFIFT-HEP-91-10 ..... p 2451 N92-24040 #

UMTRI-91-45 ..... p 2368 N92-23140 #

UPR-0472T ..... p 2451 N92-24040 #

US-PATENT-APPL-SN-754828 ..... p 2386 N92-24060 * #
US-PATENT-APPL-SN-754875 ..... p 2382 N92-23548 * #
US-PATENT-APPL-SN-758977 ..... p 2386 N92-23376 * #
US-PATENT-APPL-SN-765069 ..... p 2385 N92-24058 * #
US-PATENT-APPL-SN-765070 ..... p 2378 N92-23460 * #
US-PATENT-APPL-SN-772200 ..... p 2381 N92-23377 * #
US-PATENT-APPL-SN-772741 ..... p 2369 N92-23462 * #
US-PATENT-APPL-SN-787993 ..... p 2403 N92-23463 * #
US-PATENT-APPL-SN-796496 ..... p 2381 N92-23378 * #
US-PATENT-APPL-SN-799460 ..... p 2382 N92-23544 * #
US-PATENT-APPL-SN-801141 ..... p 2388 N92-23549 * #
US-PATENT-APPL-SN-803828 ..... p 2413 N92-24052 * #
US-PATENT-APPL-SN-812932 ..... p 2386 N92-24059 * #
US-PATENT-APPL-SN-824806 ..... p 2385 N92-24051 * #
US-PATENT-APPL-SN-824858 ..... p 2355 N92-24053 * #
US-PATENT-APPL-SN-825895 ..... p 2385 N92-24055 * #
US-PATENT-APPL-SN-832569 ..... p 2416 N92-24044 * #
US-PATENT-APPL-SN-834451 ..... p 2378 N92-23545 * #
US-PATENT-APPL-SN-836490 ..... p 2404 N92-24054 * #
US-PATENT-APPL-SN-842297 ..... p 2369 N92-23464 * #
US-PATENT-APPL-SN-842300 ..... p 2442 N92-23551 * #
US-PATENT-APPL-SN-842313 ..... p 2354 N92-23461 * #
US-PATENT-APPL-SN-842956 ..... p 2453 N92-23550 * #
US-PATENT-APPL-SN-843861 ..... p 2382 N92-23547 * #
US-PATENT-APPL-SN-849613 ..... p 2370 N92-23552 * #
US-PATENT-APPL-SN-849629 ..... p 2382 N92-23553 * #
US-PATENT-APPL-SN-862113 ..... p 2404 N92-24057 * #
US-PATENT-APPL-SN-862861 ..... p 2385 N92-24042 * #
US-PATENT-APPL-SN-866779 ..... p 2385 N92-24043 * #
US-PATENT-APPL-SN-873931 ..... p 2416 N92-24056 * #
US-PATENT-APPL-SN-880210 ..... p 2416 N92-23546 * #
US-PATENT-APPL-SN-880211 ..... p 2426 N92-24045 * #

VAL-1/90 ..... p 2350 N92-23179 #

WS-378 ..... p 2431 N92-23248 #
WS-383 ..... p 2431 N92-23250 #
WS-384 ..... p 2431 N92-23249 #

WSS/CI-91-17 ..... p 2348 N92-23715 #

Y/DV-1096 ..... p 2353 N92-24006 #

Y/DW-1050 ..... p 2363 N92-23899 #
Y/DW-1053 ..... p 2384 N92-23908 #

Y/EN-4562 ..... p 2425 N92-24035 #

Typical Accession Number Index Listing

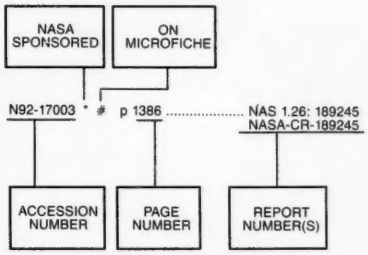

Listings in this index are arranged alphanumerically by accession number. The page number helps to locate the citation in the abstract section. An asterisk (*) indicates that the item is a NASA report. A pound sign (#) indicates that the item is available on microfiche.

N92-23121 p 2409 ..... NO REPORT NUMBER
N92-23122 p 2310 ..... NO REPORT NUMBER
N92-23123 # p 2404 ..... DE92-006657
UCRL-ID-109264
N92-23124 # p 2459 ..... CONF-920104-27
DE92-006727
PNL-SA-19713
N92-23125 p 2387 ..... NO REPORT NUMBER
N92-23126 p 2456 ..... NO REPORT NUMBER
N92-23127 p 2456 ..... NO REPORT NUMBER
N92-23128 # p 2431 ..... DE92-615260
IC-91/262
N92-23129 # p 2431 ..... DE92-615261
IC-91/263
N92-23130 # p 2440 ..... DE92-615322
IAEA-R-5234-F
N92-23131 # p 2379 ..... DE92-615399
LAMP-91/6
N92-23132 # p 2443 ..... DE92-751036
JAERI-M-91-126
N92-23133 # p 2443 ..... DE92-751038
JAERI-M-91-156
N92-23134 # p 2353 ..... DE92-751046
JAERI-M-91-134
N92-23135 # p 2443 ..... DE92-751058
JAERI-M-91-168
N92-23136 # p 2451 ..... PB92-136571
REPT-46
N92-23137 # p 2387 ..... ISBN-951-22-0485-1
PB92-133941
RR-A290
N92-23138 # p 2364 ..... ISBN-951-22-0756-7
PB92-142199
REPT-99
N92-23139 # p 2414 ..... DOT/FAA-AM-92/2
PB92-140037
N92-23140 # p 2368 ..... PB92-139773
UMTRI-91-45
N92-23141 p 2460 ..... NO REPORT NUMBER
N92-23142 p 2407 ..... NO REPORT NUMBER
N92-23143 p 2379 ..... NO REPORT NUMBER
N92-23144 p 2377 ..... NO REPORT NUMBER
N92-23145 p 2392 ..... NO REPORT NUMBER
N92-23146 p 2372 ..... NO REPORT NUMBER
N92-23147 p 2356 ..... NO REPORT NUMBER
N92-23148 p 2372 ..... NO REPORT NUMBER
N92-23149 p 2372 ..... NO REPORT NUMBER
N92-23150 p 2409 ..... NO REPORT NUMBER
N92-23151 * # p 2337 ..... NAS 1.26:190179
NASA-CR-190179
N92-23152 # p 2380 ..... C-228
ISBN-951-22-0391-X
PB92-136563
N92-23153 # p 2456 ..... CONF-9111182-3
DE92-008301
LBL-31678
UCB-PTH-92/01
N92-23154 * # p 2373 ..... AIAA-92-0645
E-6806
NAS 1.15:105617
NASA-TM-105617
N92-23155 * # p 2378 ..... E-6872
NAS 1.15:105551
NASA-TM-105551
N92-23156 p 2452 ..... NO REPORT NUMBER
N92-23157 p 2339 ..... NO REPORT NUMBER
N92-23158 p 2381 ..... NO REPORT NUMBER
N92-23159 p 2387 ..... NO REPORT NUMBER
N92-23160 p 2404 ..... NO REPORT NUMBER
N92-23161 p 2441 ..... NO REPORT NUMBER
N92-23162 p 2460 ..... NO REPORT NUMBER
N92-23163 p 2460 ..... NO REPORT NUMBER
N92-23164 p 2456 ..... NO REPORT NUMBER
N92-23165 # p 2353 ..... ETN-92-91142
PB92-1287272
N92-23166 # p 2441 ..... ETN-92-91143
ISBN-90-9004261-X
N92-23167 # p 2339 ..... ETN-92-91193
FFA-TN-1991-17
N92-23168 # p 2304 ..... ETN-92-91194
FFA-TN-1991-40
N92-23169 # p 2310 ..... ETN-92-91195
N92-23170 # p 2435 ..... ETN-92-91196
ISVR-TR-196
N92-23171 p 2459 ..... NO REPORT NUMBER
N92-23172 # p 2368 ..... ISBN-951-22-0334-0
PB92-134071
S-186
N92-23173 # p 2364 ..... NISTIR-3978
PB92-132976
N92-23174 # p 2339 ..... PB92-133479
N92-23175 # p 2402 ..... DE91-002172
DOE/CH-10093/95
N92-23176 # p 2350 ..... PB92-133511
REPT-1/91
N92-23177 # p 2381 ..... CONF-911296-3
DE92-003131
KCP-613-4675
N92-23178 # p 2350 ..... ISBN-951-22-0395-2
PB92-136464
TKK-V-B59
N92-23179 # p 2350 ..... ISBN-951-22-0358-8
PB92-136555
VAL-1/90
N92-23180 # p 2364 ..... NTIA-91-282
PB92-137413
N92-23181 # p 2346 ..... CONF-911296-1
DE92-003163
SAND-92-8408J
N92-23182 # p 2431 ..... MEMO-999
PB92-148774
N92-23183 # p 2453 ..... CONF-9111183-1
DE92-003222
KCP-613-4758
N92-23184 # p 2431 ..... IHES/M/91/88
PB92-149459
N92-23185 * # p 2353 ..... E-6926
NAS 1.15:105594
NASA-TM-105594
N92-23186 # p 2368 ..... CONF-910505-439
DE92-003231
N92-23187 * # p 2322 ..... AIAA-92-1960
E-7010
NAS 1.15:105649
NASA-TM-105649
N92-23188 # p 2453 ..... CONF-911107-54
DE92-006467
PNL-SA-19800
N92-23189 * # p 2386 ..... E-6881
NAS 1.15:105557
NASA-TM-105557
N92-23190 * # p 2339 ..... E-6949
NAS 1.15:105611
NASA-TM-105611
N92-23191 * # p 2387 ..... E-7001
NAS 1.15:105268
NASA-TM-105268
N92-23192 * # p 2354 ..... E-6977
NAS 1.15:105634
NASA-TM-105634
N92-23193 * # p 2368 ..... E-6973
NAS 1.15:105630
NASA-TM-105630
N92-23194 * # p 2339 ..... E-6900
NAS 1.15:105574
NASA-TM-105574
N92-23195 * # p 2340 ..... E-6866
NAS 1.15:105438
NASA-TM-105438
N92-23196 * # p 2387 ..... E-6773
NAS 1.15:105387
NASA-TM-105387
N92-23197 # p 2350 ..... BNL-47016
CONF-911047-17
DE92-007452
N92-23198 # p 2350 ..... BNL-45259
CONF-910328-7
DE92-007456
N92-23199 # p 2346 ..... BNL-45024
CONF-9110242-2
DE92-007458
N92-23200 # p 2368 ..... DE92-007528
LA-11623-MS
N92-23201 # p 2431 ..... DE92-007530
SAND-91-8240
N92-23202 # p 2373 ..... DE92-007538
DOE/ER-13489/6
N92-23203 # p 2346 ..... DE92-007562
DOE/ER-13808/4
N92-23204 # p 2405 ..... DE92-007593
DOE/PE-0101-VOL-1
N92-23205 # p 2446 ..... DE92-007748
DOE/ER-45113/T3
N92-23206 # p 2451 ..... DE92-616892
IC-91/336
N92-23207 # p 2435 ..... DE92-616991
IC-91/348
N92-23208 # p 2443 ..... DE92-617386
IC-91/226
N92-23209 # p 2444 ..... DE92-617387
IC-91/318
N92-23210 # p 2350 ..... DE92-617438
IC-91/322
N92-23211 # p 2350 ..... DE92-617445
IC-91/279
N92-23212 # p 2453 ..... CONF-911106-80
DE92-007913
FNAL/C-91/351
N92-23213 # p 2446 ..... DE92-007960
DOE/ER-45423/2
N92-23214 # p 2440 ..... DE92-007967
DOE/ER-02289/3
N92-23215 # p 2440 ..... DE92-007968
DOE/ER-02289/4
N92-23216 # p 2387 ..... CONF-911296-4
DE92-007971
KCP-613-4687
N92-23217 # p 2436 ..... DE92-008340
DOE/ER-40302/6
N92-23218 # p 2415 ..... DE92-614951
INIS-MF-13047-VOL-15-NO-2
N92-23219 # p 2378 ..... DE92-615124
IAEA-R-5017-F
N92-23220 # p 2435 ..... DE92-615484
IC-91/246
N92-23221 # p 2347 ..... DE92-007535
DOE/ER-13224/16
N92-23222 # p 2354 ..... CONF-911154-2
DE92-007686
N92-23223 # p 2354 ..... CONF-911050-4
DE92-007838
N92-23224 * # p 2373 ..... E-7026
NAS 1.15:105661
NASA-TM-105661
N92-23225 * # p 2311 ..... E-6914
NAS 1.15:105586
NASA-TM-105586
N92-23226 * # p 2381 ..... AVSCOM-TR-91-C-006
E-6891
NAS 1.15:105567
NASA-TM-105567

N92-23227 # p 2306 ..... AGARD-R-784
ISBN-92-835-0653-7
N92-23228* # p 2306 ..... NO REPORT NUMBER
N92-23229* # p 2306 ..... NO REPORT NUMBER
N92-23230* # p 2307 ..... NO REPORT NUMBER
N92-23231 # p 2307 ..... NO REPORT NUMBER
N92-23232 # p 2307 ..... NO REPORT NUMBER
N92-23233 # p 2307 ..... NO REPORT NUMBER
N92-23234 # p 2307 ..... NO REPORT NUMBER
N92-23235 # p 2307 ..... NO REPORT NUMBER
N92-23236 # p 2308 ..... NO REPORT NUMBER
N92-23237 # p 2308 ..... NO REPORT NUMBER
N92-23238 # p 2308 ..... NO REPORT NUMBER
N92-23239 # p 2308 ..... NO REPORT NUMBER
N92-23240* # p 2312 ..... NAS 1.15:107801
NASA-TM-107801
N92-23241* # p 2312 ..... NAS 1.15:107773
NASA-TM-107773
N92-23242* # p 2312 ..... NAS 1.15:107774
NASA-TM-107774
N92-23243* # p 2312 ..... NAS 1.15:107775
NASA-TM-107775
N92-23244* # p 2312 ..... NAS 1.15:107780
NASA-TM-107780
N92-23245* # p 2364 ..... NAS 1.26:190191
NASA-CR-190191
SATCOM-92-2
N92-23246 # p 2368 ..... NAL-PD-AL-9111
N92-23247 # p 2451 ..... PB92-127745
N92-23248 # p 2431 ..... PB92-149327
WS-378
N92-23249 # p 2431 ..... PB92-149343
WS-384
N92-23250 # p 2431 ..... PB92-149350
WS-383
N92-23251 # p 2373 ..... MEMO-997
PB92-148758
N92-23252* # p 2337 ..... AIAA-91-3441
E-6941
NAS 1.15:105605
NASA-TM-105605
N92-23253* # p 2373 ..... E-7031
NAS 1.26:189173
NASA-CR-189173
N92-23254* # p 2311 ..... E-6795
NAS 1.15:105399
NASA-TM-105399
N92-23255 # p 2417 ..... CONF-9110323-1
DE92-006826
UCRL-JC-108409
N92-23256 # p 2340 ..... ANL/CP-73895
CONF-920144-1
DE92-006978
N92-23257 # p 2409 ..... CONF-920174-1
DE92-007204
DOE/ER-61066/3
N92-23258 # p 2386 ..... DE92-615083
IAEA-TECDOC-628/S
N92-23259 # p 2446 ..... DE92-615489
IC-91/288
N92-23260 # p 2446 ..... DE92-615517
IC-91/277
N92-23261 # p 2444 ..... DE92-750824
NIFS-MEMO-1
N92-23262 # p 2407 ..... DE92-750825
NIFS-MEMO-2
N92-23263 # p 2351 ..... DE92-750951
JAERI-M-91-116
N92-23264 # p 2444 ..... DE92-750961
JAERI-M-91-131
N92-23265 # p 2351 ..... DE92-750962
JAERI-M-91-132
N92-23266 # p 2417 ..... DE92-750967
INS-T-503
N92-23267* # p 2388 ..... E-6901
NAS 1.15:105575
NASA-TM-105575
N92-23268* # p 2373 ..... AIAA-92-2881
E-6910
NAS 1.15:105583
NASA-TM-105583
N92-23269* # p 2304 ..... E-6895
NAS 1.15:105570
NASA-TM-105570
N92-23270 # p 2446 ..... DE92-617446
IC-91/281
N92-23271 # p 2446 ..... DE92-617447
IC-91/293
N92-23272 # p 2447 ..... DE92-617490
IC-91/297
N92-23273 # p 2447 ..... DE92-617537
IC-91/289
N92-23274 # p 2436 ..... DE92-617992
IFVE-OUNK-91-14
IHEP-OUNK-91-14
N92-23275 # p 2447 ..... DE92-008132
DOE/ER-13932/T1
N92-23276 # p 2440 ..... DE92-008144
DOE/ER-40530/3
N92-23277 # p 2436 ..... CONF-9109332-3
DE92-008250
N92-23278 # p 2378 ..... CONF-9110281-6
DE92-008288
LBL-31677
N92-23279 # p 2378 ..... CONF-9110281-5
DE92-008299
LBL-31497
N92-23280* # p 2461 ..... L-17042-PT-1
NAS 1.55:3134-PT-1
NASA-CP-3134-PT-1
N92-23281* # p 2335 ..... NO REPORT NUMBER
N92-23282* # p 2335 ..... NO REPORT NUMBER
N92-23283* # p 2379 ..... NO REPORT NUMBER
N92-23284* # p 2336 ..... NO REPORT NUMBER
N92-23285* # p 2335 ..... NO REPORT NUMBER
N92-23286* # p 2349 ..... NO REPORT NUMBER
N92-23287* # p 2335 ..... NO REPORT NUMBER
N92-23288* # p 2349 ..... NO REPORT NUMBER
N92-23289* # p 2439 ..... NO REPORT NUMBER
N92-23290* # p 2339 ..... NO REPORT NUMBER
N92-23291* # p 2439 ..... NO REPORT NUMBER
N92-23292* # p 2439 ..... NO REPORT NUMBER
N92-23293* # p 2460 ..... NO REPORT NUMBER
N92-23294* # p 2461 ..... NO REPORT NUMBER
N92-23295* # p 2439 ..... NO REPORT NUMBER
N92-23296* # p 2439 ..... NO REPORT NUMBER
N92-23297* # p 2440 ..... NO REPORT NUMBER
N92-23298* # p 2440 ..... NO REPORT NUMBER
N92-23299* # p 2349 ..... NO REPORT NUMBER
N92-23300* # p 2440 ..... NO REPORT NUMBER
N92-23301* # p 2461 ..... NO REPORT NUMBER
N92-23302* # p 2461 ..... NO REPORT NUMBER
N92-23303* # p 2440 ..... NO REPORT NUMBER
N92-23304* # p 2440 ..... NO REPORT NUMBER
N92-23305* # p 2440 ..... NO REPORT NUMBER
N92-23306* # p 2461 ..... NO REPORT NUMBER
N92-23307* # p 2461 ..... NO REPORT NUMBER
N92-23308* # p 2440 ..... NO REPORT NUMBER
N92-23309* # p 2335 ..... NO REPORT NUMBER
N92-23310* # p 2458 ..... NO REPORT NUMBER
N92-23311* # p 2335 ..... NO REPORT NUMBER
N92-23312* # p 2336 ..... NO REPORT NUMBER
N92-23313* # p 2454 ..... NO REPORT NUMBER
N92-23314* # p 2336 ..... NO REPORT NUMBER
N92-23315* # p 2458 ..... NO REPORT NUMBER
N92-23316* # p 2349 ..... NO REPORT NUMBER
N92-23317* # p 2458 ..... NO REPORT NUMBER
N92-23318* # p 2458 ..... NO REPORT NUMBER
N92-23319* # p 2336 ..... NO REPORT NUMBER
N92-23320* # p 2458 ..... NO REPORT NUMBER
N92-23321* # p 2336 ..... NO REPORT NUMBER
N92-23322* # p 2459 ..... NO REPORT NUMBER
N92-23323* # p 2336 ..... NO REPORT NUMBER
N92-23324* # p 2336 ..... NO REPORT NUMBER
N92-23325* # p 2459 ..... NO REPORT NUMBER
N92-23326 # p 2368 ..... CONF-911106-73
DE92-007199
FNAL/C-91/310
N92-23327 # p 2436 ..... CONF-910864-10
DE92-007389
SU-SLAC-PUB-5722
N92-23328 # p 2437 ..... ANL-HEP-CP-92-03
CONF-9111141-3
DE92-007397
N92-23329 # p 2432 ..... BNL-46984
CONF-920213-1
DE92-008055
N92-23330 # p 2437 ..... DE92-008129
DOE/ER-45083/T1
N92-23331 # p 2432 ..... DE92-615217
IC-91/272
N92-23332 # p 2347 ..... DE92-007564
DOE/ER-14125/2
N92-23333 # p 2405 ..... DE92-007592
DOE/PE-0101-VOL-2
N92-23334 # p 2440 ..... DE92-007912
DOE/ER-40236/T2
N92-23335 # p 2432 ..... DE92-616916
IC-91/257
N92-23336* # p 2301 ..... CMOTT-91-07
E-6570
ICOMP-91-17
NAS 1.15:105243
NASA-TM-105243
N92-23337* # p 2301 ..... NO REPORT NUMBER
N92-23338* # p 2301 ..... NO REPORT NUMBER
N92-23339* # p 2301 ..... NO REPORT NUMBER
N92-23340* # p 2301 ..... NO REPORT NUMBER
N92-23341* # p 2301 ..... NO REPORT NUMBER
N92-23342* # p 2302 ..... NO REPORT NUMBER
N92-23343* # p 2302 ..... NO REPORT NUMBER
N92-23344* # p 2302 ..... NO REPORT NUMBER
N92-23345* # p 2302 ..... PAPER-107
N92-23346* # p 2302 ..... NO REPORT NUMBER
N92-23347* # p 2303 ..... PAPER-213
N92-23348* # p 2303 ..... NO REPORT NUMBER
N92-23349* # p 2303 ..... NO REPORT NUMBER
N92-23350* # p 2303 ..... PAPER-105
N92-23351* # p 2303 ..... NO REPORT NUMBER
N92-23352* # p 2303 ..... NO REPORT NUMBER
N92-23353* # p 2304 ..... NO REPORT NUMBER
N92-23354* # p 2304 ..... NO REPORT NUMBER
N92-23355* # p 2304 ..... NO REPORT NUMBER
N92-23356* # p 2426 ..... NAS 1.55:3141
NASA-CP-3141
REPT-92B00045
N92-23357* # p 2426 ..... NO REPORT NUMBER
N92-23358* # p 2426 ..... NO REPORT NUMBER
N92-23359* # p 2426 ..... NO REPORT NUMBER
N92-23360* # p 2427 ..... NO REPORT NUMBER
N92-23361* # p 2427 ..... NO REPORT NUMBER
N92-23362* # p 2427 ..... NO REPORT NUMBER
N92-23363* # p 2427 ..... NO REPORT NUMBER
N92-23364* # p 2427 ..... NO REPORT NUMBER
N92-23365* # p 2427 ..... NO REPORT NUMBER
N92-23366* # p 2427 ..... NO REPORT NUMBER
N92-23367* # p 2402 ..... NO REPORT NUMBER
N92-23368* # p 2402 ..... NO REPORT NUMBER
N92-23369* # p 2402 ..... NO REPORT NUMBER
N92-23370* # p 2428 ..... NO REPORT NUMBER
N92-23371* # p 2428 ..... NO REPORT NUMBER
N92-23372* # p 2429 ..... NO REPORT NUMBER
N92-23373* # p 2429 ..... NO REPORT NUMBER
N92-23374* # p 2429 ..... NO REPORT NUMBER
N92-23375* # p 2429 ..... NO REPORT NUMBER
N92-23376* # p 2386 ..... NAS 1.71:GSC-13386-1
NASA-CASE-GSC-13386-1
US-PATENT-APPL-SN-758977
N92-23377* # p 2381 ..... NAS 1.71:GSC-13360-1
NASA-CASE-GSC-13360-1
US-PATENT-APPL-SN-772200
N92-23378* # p 2381 ..... NAS 1.71:GSC-13359-1
NASA-CASE-GSC-13359-1
US-PATENT-APPL-SN-796496
N92-23379 # p 2392 ..... ETN-92-91073
MBB-UK-0152-91-PUB
N92-23380 # p 2392 ..... NO REPORT NUMBER
N92-23381 # p 2392 ..... NO REPORT NUMBER
N92-23382 # p 2392 ..... NO REPORT NUMBER
N92-23383 # p 2392 ..... NO REPORT NUMBER
N92-23384 # p 2393 ..... NO REPORT NUMBER
N92-23385 # p 2393 ..... NO REPORT NUMBER
N92-23386 # p 2393 ..... NO REPORT NUMBER
N92-23387 # p 2393 ..... NO REPORT NUMBER
N92-23388 # p 2393 ..... NO REPORT NUMBER
N92-23389 # p 2393 ..... NO REPORT NUMBER
N92-23390 # p 2393 ..... NO REPORT NUMBER
N92-23391 # p 2393 ..... NO REPORT NUMBER
N92-23392 # p 2394 ..... MBB-UH-HE512
N92-23393 # p 2394 ..... NO REPORT NUMBER
N92-23394 # p 2394 ..... NO REPORT NUMBER
N92-23395 # p 2394 ..... NO REPORT NUMBER
N92-23396 # p 2394 ..... NO REPORT NUMBER
N92-23397 # p 2394 ..... NO REPORT NUMBER
N92-23398 # p 2394 ..... NO REPORT NUMBER
N92-23399 # p 2394 ..... NO REPORT NUMBER
N92-23400 # p 2395 ..... NO REPORT NUMBER
N92-23401 # p 2395 ..... NO REPORT NUMBER
N92-23402 # p 2395 ..... NO REPORT NUMBER
N92-23403 # p 2395 ..... NO REPORT NUMBER
N92-23404 # p 2395 ..... NO REPORT NUMBER
N92-23405 # p 2395 ..... NO REPORT NUMBER
N92-23406 # p 2395 ..... NO REPORT NUMBER
N92-23407 # p 2395 ..... NO REPORT NUMBER
N92-23408 # p 2395 ..... NO REPORT NUMBER
N92-23409 # p 2396 ..... NO REPORT NUMBER
N92-23410 # p 2396 ..... NO REPORT NUMBER
N92-23411 # p 2396 ..... NO REPORT NUMBER
N92-23412* # p 2365 ..... E-6447
NAS 1.15:105159
NASA-TM-105159
N92-23413* # p 2365 ..... NO REPORT NUMBER
N92-23414* # p 2365 ..... NO REPORT NUMBER
N92-23415* # p 2365 ..... NO REPORT NUMBER
N92-23416* # p 2417 ..... NAS 1.26:189960
NASA-CR-189960
N92-23417* # p 2417 ..... NO REPORT NUMBER
N92-23418* # p 2417 ..... NO REPORT NUMBER
N92-23419* # p 2417 ..... NO REPORT NUMBER
N92-23420* # p 2417 ..... NO REPORT NUMBER
N92-23421* # p 2418 ..... NO REPORT NUMBER
N92-23422* # p 2418 ..... NO REPORT NUMBER
N92-23423* # p 2418 ..... NO REPORT NUMBER
N92-23424* # p 2414 ..... A-91232
NAS 1.15:103890
NASA-TM-103890
N92-23425* # p 2365 ..... NAS 1.26:190109
NASA-CR-190109

N92-23426* # p 2388 ..... NAS 1.26:187200
NASA-CR-187200
N92-23427* # p 2388 ..... NAS 1.26:190184
NASA-CR-190184
N92-23428* # p 2454 ..... NAS 1.26:190197
NASA-CR-190197
N92-23429* # p 2416 ..... NAS 1.15:4364
NASA-TM-4364
N92-23430* # p 2369 ..... NAS 1.26:190196
NASA-CR-190196
N92-23431* # p 2410 ..... NO REPORT NUMBER
N92-23432* # p 2418 ..... M-687
NAS 1.60:3220
NASA-TP-3220
N92-23433* # p 2340 ..... NAS 1.15:107597
NASA-TM-107597
N92-23434* # p 2340 ..... NAS 1.15:107595
NASA-TM-107595
N92-23435* # p 2381 ..... E-6945
NAS 1.15:105641
NASA-TM-105641
N92-23436* # p 2351 ..... E-6961
NAS 1.26:189147
NASA-CR-189147
N92-23437* # p 2369 ..... NAS 1.15:103580
NASA-TM-103580
N92-23438* # p 2429 ..... NAS 1.26:190277
NASA-CR-190277
N92-23439 # p 2410 ..... NOAA-TR-NWS-44
PB92-137850
N92-23440 # p 2432 ..... ISBN-951-22-0828-8
PB92-143551
SER-A-16
N92-23441 # p 2396 ..... ISBN-951-22-0733-8
PB92-141977
REPT-4
N92-23442 # p 2354 ..... CONF-920388-1
DE92-007657
SAND-92-0236C
N92-23443 # p 2347 ..... DE92-007732
DOE/ER-13480/2
N92-23444 # p 2447 ... CONF-9104333-1-EXTD-ABST
DE92-007837
N92-23445 # p 2441 ..... CONF-9110289-4
DE92-008003
N92-23446 # p 2444 ..... CONF-910869-27
DE92-008052
GA-A-20694
N92-23447 # p 2447 ..... CONF-911202-59
DE92-008098
N92-23448 # p 2437 ..... DE92-008143
DOE/ER-13958/28
N92-23449 # p 2347 ..... CONF-910872-9
DE92-008304
LBL-30462
N92-23450 # p 2437 ..... DE92-008314
LBL-31622
N92-23451 # p 2447 ..... CONF-911033-6
DE92-008336
SAND-91-1196C
N92-23452 # p 2447 ..... DE92-617538
IC-91/317
N92-23453 # p 2447 ..... DE92-617539
IC-91/339
N92-23454 # p 2405 ..... DE92-769377
NEDO-ITE-9002-5
N92-23455 # p 2405 ..... DE92-769378
NEDO-ITE-9006
N92-23456 # p 2347 ..... DE92-769380
NEDO-ITE-9008
N92-23457 # p 2429 ..... CONF-920540-1
DE91-018939
N92-23458 # p 2430 ..... CONF-920540-4
DE91-019060
SAND-91-2041C
N92-23459 # p 2382 ..... CONF-920540-7
DE92-000046
N92-23460* # p 2378 ..... NAS 1.71:GSC-13406-1
NASA-CASE-GSC-13406-1
US-PATENT-APPL-SN-765070
N92-23461* # p 2354 ..... NAS 1.71:LEW-15314-1
NASA-CASE-LEW-15314-1
US-PATENT-APPL-SN-842313
N92-23462* # p 2369 ..... NAS 1.71:GSC-13422-1
NASA-CASE-GSC-13422-1
US-PATENT-APPL-SN-772741
N92-23463* # p 2403 ..... NAS 1.71:GSC-13450-1
NASA-CASE-GSC-13450-1
US-PATENT-APPL-SN-787993
N92-23464* # p 2369 ..... NAS 1.71:NPO-18428-1-CU
NASA-CASE-NPO-18428-1-CU
US-PATENT-APPL-SN-842297
N92-23465 # p 2396 ..... HE-90015
JTN-92-80274
N92-23466 # p 2396 ..... NO REPORT NUMBER
N92-23467 # p 2396 ..... NO REPORT NUMBER
N92-23468 # p 2396 ..... NO REPORT NUMBER
N92-23469 # p 2397 ..... NO REPORT NUMBER
N92-23470 # p 2397 ..... NO REPORT NUMBER
N92-23471 # p 2397 ..... NO REPORT NUMBER
N92-23472 # p 2397 ..... NO REPORT NUMBER
N92-23473 # p 2397 ..... NO REPORT NUMBER
N92-23474 # p 2397 ..... NO REPORT NUMBER
N92-23475 # p 2398 ..... NO REPORT NUMBER
N92-23476 # p 2398 ..... NO REPORT NUMBER
N92-23477 # p 2398 ..... NO REPORT NUMBER
N92-23478 # p 2398 ..... NO REPORT NUMBER
N92-23479 # p 2398 ..... NO REPORT NUMBER
N92-23480 # p 2399 ..... NO REPORT NUMBER
N92-23481 # p 2399 ..... NO REPORT NUMBER
N92-23482 # p 2399 ..... NO REPORT NUMBER
N92-23483 # p 2399 ..... NO REPORT NUMBER
N92-23484 # p 2399 ..... NO REPORT NUMBER
N92-23485 # p 2399 ..... NO REPORT NUMBER
N92-23486 # p 2400 ..... NO REPORT NUMBER
N92-23487 # p 2400 ..... NO REPORT NUMBER
N92-23488 # p 2400 ..... NO REPORT NUMBER
N92-23489 # p 2400 ..... NO REPORT NUMBER
N92-23490 # p 2400 ..... NO REPORT NUMBER
N92-23491 # p 2400 ..... NO REPORT NUMBER
N92-23492 # p 2401 ..... NO REPORT NUMBER
N92-23493 # p 2401 ..... NO REPORT NUMBER
N92-23494 # p 2410 ..... NOAA-TR-NWS-45
PB92-137868
N92-23495 # p 2369 ..... ISBN-951-22-0522-X
PB92-142280
RR-A291
N92-23496 # p 2369 ..... ISBN-951-22-0757-5
PB92-142116
N92-23497 # p 2370 ..... ISBN-951-22-0458-4
PB92-142306
REPT-18
N92-23498 # p 2448 ..... ISBN-951-22-0854-7
PB92-143320
N92-23499 # p 2347 ..... DE92-007529
DOE/ER-13430/T1
N92-23500 # p 2441 ..... DE92-007966
DOE/ER-02289/2
N92-23501 # p 2451 ..... DE92-616891
IC-91/335
N92-23502 # p 2432 ..... DE92-616917
IC-91/312
N92-23503 # p 2451 ..... DE92-616919
IC-91/310
N92-23504 # p 2448 ..... DE92-617436
IC-91/315
N92-23505 # p 2434 ..... MEMO-985
PB92-148634
N92-23506 # p 2430 ..... MEMO-989
PB92-148675
N92-23507 # p 2418 ..... MEMO-990
PB92-148683
N92-23508 # p 2430 ..... FEW-511
PB92-149996
N92-23509 # p 2403 ..... EPA/600/R-92/007
FCR-11900A
PB92-137520
N92-23510 # p 2354 ..... K243
PB92-138494
N92-23511 # p 2432 ..... NISTIR-4720
PB92-143742
N92-23512 # p 2405 ..... PB92-137454
N92-23513 # p 2415 ..... PB92-136001
N92-23514 # p 2432 ..... PB92-137355
REPT-91-4
N92-23515 # p 2405 ..... PB92-128248
N92-23516 # p 2374 ..... EPA/600/3-91/075
PB92-132901
N92-23517 # p 2406 ..... EPA/450/4-91/023
PB92-141555
N92-23518 # p 2412 ..... DE92-006979
ORNL/TM-11992
N92-23519 # p 2412 ..... NOAA-TM-NMFS-F/SPO-1
PB92-145689
N92-23520 # p 2410 ..... EPA/600/A-92/023
PB92-150457
N92-23521 # p 2401 ..... NOAA-TM-ERL-211
PB92-140714
N92-23522 # p 2408 ..... NCAR/TN-376+STR
PB92-148543
N92-23523 # p 2444 ..... CONF-900557-34
DE92-008599
UCRL-JC-103284
N92-23524* # p 2321 ..... NAS 1.15:105523
NASA-TM-105523
N92-23525* # p 2441 ..... NAS 1.15:105526
NASA-TM-105526
N92-23526* # p 2322 ..... NAS 1.26:189983
NASA-CR-189983
N92-23527* # p 2388 ..... E-6686
NAS 1.15:4365
NASA-TM-4365
N92-23528* # p 2366 ..... NAS 1.26:190098
NASA-CR-190098
N92-23529* # p 2317 ..... NAS 1.26:190129
NASA-CR-190129
N92-23530* # p 2322 ..... NAS 1.26:184292
NASA-CR-184292
SECA-TR-92-02
N92-23531* # p 2317 ..... CSR-HEA-92-08
NAS 1.26:190214
NASA-CR-190214
N92-23532* # p 2340 ..... NAS 1.26:190226
NASA-CR-190226
N92-23533* # p 2305 ..... L16986
NAS 1.15:4295
NASA-TM-4295
N92-23534* # p 2337 ..... E-6902
NAS 1.15:105576
NASA-TM-105576
N92-23535* # p 2370 ..... E-6754
NAS 1.15:105647
NASA-TM-105647
N92-23536* # p 2382 ..... AVSCOM-TR-90-C-029
E-6776
NAS 1.15:105388
NASA-TM-105388
N92-23537* # p 2311 ..... E-6948
NAS 1.15:105610
NASA-TM-105610
N92-23538* # p 2370 ..... E-6957
NAS 1.26:189174
NASA-CR-189174
N92-23539* # p 2337 ..... NAS 1.26:190203
NASA-CR-190203
N92-23540* # p 2408 ..... NAS 1.26:190246
NASA-CR-190246
N92-23541* # p 2306 ..... NAS 1.26:190247
NASA-CR-190247
N92-23542* # p 2374 ..... CMOTT-92-03
E-6917
ICOMP-92-06
NAS 1.15:105588
NASA-TM-105588
N92-23543* # p 2374 ..... NAS 1.26:189614
NASA-CR-189614
N92-23544* # p 2382 ..... NAS 1.71:MSC-21864-1
NASA-CASE-MSC-21864-1
US-PATENT-APPL-SN-799460
N92-23545* # p 2378 ..... NAS 1.71:MSC-21951-1
NASA-CASE-MSC-21951-1
US-PATENT-APPL-SN-834451
N92-23546* # p 2416 ..... NAS 1.71:NPO-18491-1-CU
NASA-CASE-NPO-18491-1-CU
US-PATENT-APPL-SN-880210
N92-23547* # p 2382 ..... NAS 1.71:GSC-13442-1
NASA-CASE-GSC-13442-1
US-PATENT-APPL-SN-843861
N92-23548* # p 2382 ..... NAS 1.71:GSC-13141-1
NASA-CASE-GSC-13141-1
US-PATENT-APPL-SN-754875
N92-23549* # p 2388 ..... NAS 1.71:GSC-13451-1
NASA-CASE-GSC-13451-1
US-PATENT-APPL-SN-801141
N92-23550* # p 2453 ..... NAS 1.71:SSC-00010-2
NASA-CASE-SSC-00010-2
US-PATENT-APPL-SN-842956
N92-23551* # p 2442 ..... NAS 1.71:NPO-18702-1-CU
NASA-CASE-NPO-18702-1-CU
US-PATENT-APPL-SN-842300
N92-23552* # p 2370 ..... NAS 1.71:NPO-18394-1-CU
NASA-CASE-NPO-18394-1-CU
US-PATENT-APPL-SN-849613
N92-23553* # p 2382 ..... NAS 1.71:NPO-18607-1-CU
NASA-CASE-NPO-18607-1-CU
US-PATENT-APPL-SN-849629
N92-23554* # p 2418 ..... NAS 1.26:190173
NASA-CR-190173
N92-23555* # p 2356 ..... NAS 1.26:190256
NASA-CR-190256
N92-23556* # p 2435 ..... NAS 1.26:4437
NASA-CR-4437
N92-23557* # p 2379 ..... L-17043
NAS 1.15:4375
NASA-TM-4375
N92-23558* # p 2408 ..... NAS 1.26:188466
NASA-CR-188466
N92-23559* # p 2416 ..... NAS 1.15:107568
NASA-TM-107568
N92-23560* # p 2374 ..... E-6691
ICOMP-91-22
NAS 1.15:105329
NASA-TM-105329
N92-23561* # p 2370 ..... E-6960
NAS 1.15:105622
NASA-TM-105622
N92-23562* # p 2370 ..... E-6963
NAS 1.15:105624

NASA-TM-105624
N92-23563* # p 2305 ..... E-6853
NAS 1.15:105432
NASA-TM-105432
N92-23564* # p 2383 ..... E-6896
NAS 1.15:105571
NASA-TM-105571
N92-23565* # p 2374 ..... E-6912
ICOMP-92-04
NAS 1.15:105584
NASA-TM-105584
N92-23566* # p 2351 ..... NAS 1.26:189124
NASA-CR-189124
N92-23567* # p 2442 ..... NAS 1.26:190293
NASA-CR-190293
N92-23568* # p 2375 ..... CCFD-92-01
NAS 1.26:190291
NASA-CR-190291
N92-23569* # p 2403 ..... DE92-006868
JPL-D-9263
NAS 1.26:190188
NASA-CR-190188
N92-23570 # p 2379 ..... CONF-911064-2
DE92-006896
UCRL-JC-108069
N92-23571 # p 2379 ..... CONF-911106-65
DE92-006898
UCRL-JC-108752
N92-23572 # p 2348 ..... DE92-006947
RFP-4476
N92-23573 # p 2351 ..... ANL/CP-73727
CONF-911033-5
DE92-006986
N92-23574 # p 2448 ..... ANL/CP-73627
CONF-911202-49
DE92-006991
N92-23575 # p 2366 ..... DE92-008452
SAND-91-0720
N92-23576 # p 2441 ..... DE92-008543
DOE/ER-40050/T7
N92-23577 # p 2437 ..... DE92-008587
DOE/ER-40461/4
N92-23578 # p 2451 ..... DE92-008730
DOE/ER-40581/2
N92-23579 # p 2433 ..... DE92-008851
FNAL-TM-1767
N92-23580 # p 2366 ..... DE92-616890
IC-91/294
N92-23581 # p 2448 ..... DE92-617439
IC-91/323
N92-23582 # p 2351 ..... DE92-617440
IC-91/351
N92-23583* # p 2425 ..... NAS 1.26:190272
NASA-CR-190272
N92-23584 # p 2370 ..... DE92-007419
SAND-91-1533
N92-23585 # p 2340 ..... DE92-007264
KCP-613-4556
N92-23586 # p 2348 ..... DE92-007265
KCP-613-4626
N92-23587 # p 2410 ..... NCAR/TN-365+PROC
PB92-139963
N92-23588 # p 2436 ..... NLR-TR-88148-U
PB92-138544
N92-23589 # p 2433 ..... ISBN-951-22-0846-6
PB92-143304
RR-A304
N92-23590 # p 2366 ..... ISBN-951-22-0792-3
PB92-141878
REPT-102
N92-23591 # p 2366 ..... ISBN-951-22-0550-5
PB92-142397
REPT-85
N92-23592 # p 2403 ..... ISBN-951-22-0583-1
PB92-141829
TKK-F-A675
N92-23593 # p 2406 ..... PB92-100346
N92-23594 # p 2379 ..... PB92-143361
TKK-F-A692
N92-23595 # p 2383 ..... EPA/AA/CTAB-92/01
PB92-143692
N92-23596 # p 2305 ..... NTSB/AAR-91/08
PB91-910409
N92-23597 # p 2305 ..... NTSB/AAR-91/09
PB91-910410
N92-23598 # p 2435 ..... DE92-615485
IC-91/247
N92-23599 # p 2433 ..... IHES/M/91/92
PB92-149434
N92-23600* # p 2356 ..... M-681
NAS 1.15:4353
NASA-TM-4353
N92-23601* # p 2356 ..... NO REPORT NUMBER
N92-23602* # p 2356 ..... NO REPORT NUMBER
N92-23603* # p 2357 ..... NO REPORT NUMBER
N92-23604* # p 2357 ..... NO REPORT NUMBER
N92-23605* # p 2357 ..... NO REPORT NUMBER
N92-23606* # p 2357 ..... NO REPORT NUMBER
N92-23607* # p 2357 ..... NO REPORT NUMBER
N92-23608* # p 2357 ..... NO REPORT NUMBER
N92-23609* # p 2358 ..... NO REPORT NUMBER
N92-23610* # p 2358 ..... NO REPORT NUMBER
N92-23611* # p 2358 ..... NO REPORT NUMBER
N92-23612* # p 2358 ..... NO REPORT NUMBER
N92-23613* # p 2358 ..... NO REPORT NUMBER
N92-23614* # p 2358 ..... NO REPORT NUMBER
N92-23615* # p 2359 ..... NO REPORT NUMBER
N92-23616* # p 2359 ..... NO REPORT NUMBER
N92-23617* # p 2359 ..... NO REPORT NUMBER
N92-23618* # p 2359 ..... NO REPORT NUMBER
N92-23619* # p 2359 ..... NO REPORT NUMBER
N92-23620* # p 2359 ..... NO REPORT NUMBER
N92-23621* # p 2360 ..... NO REPORT NUMBER
N92-23622* # p 2360 ..... NO REPORT NUMBER
N92-23623* # p 2360 ..... NO REPORT NUMBER
N92-23624* # p 2360 ..... NO REPORT NUMBER
N92-23625* # p 2360 ..... NO REPORT NUMBER
N92-23626* # p 2360 ..... NO REPORT NUMBER
N92-23627* # p 2361 ..... NO REPORT NUMBER
N92-23628* # p 2361 ..... NO REPORT NUMBER
N92-23629* # p 2361 ..... NO REPORT NUMBER
N92-23630* # p 2361 ..... NO REPORT NUMBER
N92-23631* # p 2361 ..... NO REPORT NUMBER
N92-23632* # p 2361 ..... NO REPORT NUMBER
N92-23633* # p 2361 ..... NO REPORT NUMBER
N92-23634* # p 2361 ..... NO REPORT NUMBER
N92-23635* # p 2362 ..... NO REPORT NUMBER
N92-23636* # p 2362 ..... NO REPORT NUMBER
N92-23637* # p 2362 ..... NO REPORT NUMBER
N92-23638* # p 2362 ..... NO REPORT NUMBER
N92-23639* # p 2362 ..... NO REPORT NUMBER
N92-23640* # p 2363 ..... NO REPORT NUMBER
N92-23641* # p 2363 ..... NO REPORT NUMBER
N92-23642* # p 2363 ..... NO REPORT NUMBER
N92-23643* # p 2312 ..... NAS 1.15:107812
NASA-TM-107812
N92-23644* # p 2313 ..... NO REPORT NUMBER
N92-23645* # p 2313 ..... NO REPORT NUMBER
N92-23646* # p 2313 ..... NO REPORT NUMBER
N92-23647* # p 2313 ..... NO REPORT NUMBER
N92-23648* # p 2313 ..... NO REPORT NUMBER
N92-23649* # p 2313 ..... NO REPORT NUMBER
N92-23650* # p 2313 ..... NO REPORT NUMBER
N92-23651* # p 2313 ..... NO REPORT NUMBER
N92-23652* # p 2314 ..... NO REPORT NUMBER
N92-23653* # p 2314 ..... NO REPORT NUMBER
N92-23654* # p 2314 ..... NO REPORT NUMBER
N92-23655* # p 2314 ..... NO REPORT NUMBER
N92-23656* # p 2410 ..... NAS 1.26:189878
NASA-CR-189878
NCAR/CT-132
N92-23657 # p 2348 ..... GRI-91/0401
PB92-142587
N92-23658 # p 2433 ..... ISBN-951-22-0803-2
PB92-141803
RR-A301
N92-23659 # p 2401 ..... NOAA-TM-ERL-GLERL-76
PB92-129949
N92-23660 # p 2411 ..... PB92-135326
N92-23661 # p 2366 ..... ISBN-951-22-0802-4
PB92-141886
REPT-103
N92-23662 # p 2442 ..... ISBN-951-22-0741-9
PB92-143585
TKK-F-A690
N92-23663 # p 2444 ..... ISBN-951-22-0526-2
PB92-141936
TKK-F-A678
N92-23664 # p 2388 ..... PB92-142447
REPT-109
N92-23665 # p 2435 ..... PB92-142256
TKK-F-A691
N92-23666 # p 2366 ..... ISBN-951-22-0486-X
PB92-142371
REPT-81
N92-23667 # p 2366 ..... ISBN-951-22-0573-4
PB92-142405
REPT-88
N92-23668 # p 2367 ..... ISBN-951-22-0610-2
PB92-142413
REPT-91
N92-23669 # p 2412 ..... NOAA-TM-ERL-WPL-217
PB92-140466
N92-23670 # p 2433 ..... IHES/M/91/91
PB92-149442
N92-23671 p 2311 ..... NO REPORT NUMBER
N92-23672 p 2375 ..... NO REPORT NUMBER
N92-23673 p 2454 ..... NO REPORT NUMBER
N92-23674 p 2437 ..... NO REPORT NUMBER
N92-23675 p 2455 ..... NO REPORT NUMBER
N92-23676 # p 2367 ..... PB92-134279
N92-23677 # p 2411 ..... NO REPORT NUMBER
N92-23678 # p 2371 ..... CT-8
ISBN-951-22-0787-7
PB92-143379
N92-23679 # p 2367 ..... ISBN-951-22-0476-2
PB92-142355
REPT-79
N92-23680 # p 2383 ..... GRI-91/0347
PB92-137603
N92-23681 # p 2389 ..... GRI-91/0227
MRL-7043
PB92-141753
N92-23682 # p 2411 ..... NOAA-DR-ERL-PMEL-36
PB92-143080
N92-23683 # p 2403 ..... ISBN-951-22-0465-7
PB92-141928
TKK-F-A670
N92-23684 # p 2403 ..... DE92-783370
NEDO-P-9009
N92-23685 # p 2348 ..... GRI-91/0333
PB92-149681
N92-23686 # p 2401 ..... B-247176
GAO/IMTEC-92-24
N92-23687 p 2380 ..... NO REPORT NUMBER
N92-23688 p 2389 ..... NO REPORT NUMBER
N92-23689 p 2375 ..... NO REPORT NUMBER
N92-23690 p 2383 ..... NO REPORT NUMBER
N92-23691 p 2383 ..... NO REPORT NUMBER
N92-23692 p 2375 ..... NO REPORT NUMBER
N92-23693 p 2340 ..... NO REPORT NUMBER
N92-23694 p 2337 ..... NO REPORT NUMBER
N92-23695 p 2455 ..... NO REPORT NUMBER
N92-23696 p 2457 ..... NO REPORT NUMBER
N92-23697 p 2459 ..... NO REPORT NUMBER
N92-23698 p 2457 ..... NO REPORT NUMBER
N92-23699 p 2389 ..... NO REPORT NUMBER
N92-23700 p 2375 ..... NO REPORT NUMBER
N92-23701 # p 2459 ..... PB92-111699
SGD-564-PT-2
N92-23702 p 2408 ..... NO REPORT NUMBER
N92-23703 p 2401 ..... NO REPORT NUMBER
N92-23704 p 2459 ..... NO REPORT NUMBER
N92-23705 # p 2314 ..... JPRS-USP-92-002
N92-23706 # p 2412 ..... JPRS-ULS-92-010
N92-23707 # p 2392 ..... JPRS-UES-91-005
N92-23708 # p 2363 ..... JPRS-UMS-92-005
N92-23709 # p 2363 ..... JPRS-UMS-92-006
N92-23710 # p 2383 ..... ISBN-951-22-0762-1
PB92-141951
N92-23711 # p 2444 ..... DE92-750949
JAERI-M-91-094
N92-23712 # p 2352 ..... DE92-751006
JAERI-M-91-136
N92-23713 # p 2441 ..... DE92-751024
KEK-91-5
N92-23714 # p 2438 ..... CONF-920192-1
DE92-008488
LA-UR-92-578
N92-23715 # p 2348 ..... CONF-9103145-3
DE92-008557
UCRL-JC-106910
WSS/CI-91-17
N92-23716 p 2457 ..... NO REPORT NUMBER
N92-23717 p 2305 ..... NO REPORT NUMBER
N92-23718 p 2352 ..... NO REPORT NUMBER
N92-23719 p 2363 ..... NO REPORT NUMBER
N92-23720 # p 2352 ..... CONF-911202-55
DE92-007717
LA-UR-92-73
N92-23721 # p 2448 ..... DE92-007747
DOE/ER-45072/50
N92-23722 # p 2337 ..... DE92-007799
ORNL/TM-11759
N92-23723 # p 2380 ..... DE92-007801
KCP-613-4477
N92-23724 p 2402 ..... NO REPORT NUMBER
N92-23725 p 2352 ..... NO REPORT NUMBER
N92-23726 p 2436 ..... NO REPORT NUMBER
N92-23727 p 2384 ..... NO REPORT NUMBER
N92-23728 p 2453 ..... NO REPORT NUMBER
N92-23729 p 2306 ..... NO REPORT NUMBER
N92-23730 p 2453 ..... NO REPORT NUMBER
N92-23731 # p 2434 ..... FEW-500
PB92-128792
N92-23732 # p 2412 ..... NOAA-TR-ERL-447-AOML-35
PB92-129964
N92-23733 # p 2406 ..... DE92-769374
NEDO-ITE-9002-1
N92-23734 # p 2406 ..... DE92-769375
NEDO-ITE-9002-2
N92-23735 # p 2371 ..... CESAR-91/41
DE91-019074
ORNL/TM-11972
N92-23736 p 2460 ..... NO REPORT NUMBER
N92-23737 p 2389 ..... NO REPORT NUMBER
N92-23738 p 2433 ..... NO REPORT NUMBER
N92-23739 p 2384 ..... NO REPORT NUMBER

N92-23740 # p 2406 ..... DE92-006640
UCRL-ID-109227
N92-23741 # p 2408 ..... CONF-920163-1
DE92-006732
PNL-SA-19880
N92-23742 # p 2454 ..... DE92-615195
INDC(CCP)-343/L
N92-23743 # p 2451 ..... DE92-615214
IC-91/258
N92-23744 # p 2438 ..... DE92-615215
IC-91/265
N92-23745 # p 2433 ..... DE92-615216
IC-91/266
N92-23746 # p 2411 ..... NOAA-TR-NWS-46
PB92-137843
N92-23747 # p 2438 ..... CONF-9110332-1
DE92-007414
LA-UR-92-338
N92-23748 # p 2442 ..... CONF-911221-1
DE92-008677
SAND-91-1584C
N92-23749 # p 2445 ..... CONF-920362-3
DE92-008678
SAND-92-0064C
N92-23750 # p 2318 ..... ESA-SP-327
ETN-92-91381
ISBN-92-9092-150-1
N92-23751 # p 2318 ..... NO REPORT NUMBER
N92-23752*# p 2318 ..... NO REPORT NUMBER
N92-23753 # p 2319 ..... NO REPORT NUMBER
N92-23754*# p 2319 ..... NO REPORT NUMBER
N92-23755 # p 2319 ..... NO REPORT NUMBER
N92-23756 # p 2319 ..... NO REPORT NUMBER
N92-23757 # p 2319 ..... NO REPORT NUMBER
N92-23758 # p 2319 ..... NO REPORT NUMBER
N92-23759 # p 2319 ..... NO REPORT NUMBER
N92-23760 # p 2319 ..... NO REPORT NUMBER
N92-23761 # p 2320 ..... NO REPORT NUMBER
N92-23762 # p 2320 ..... NO REPORT NUMBER
N92-23763 # p 2320 ..... NO REPORT NUMBER
N92-23764 # p 2320 ..... NO REPORT NUMBER
N92-23765 # p 2320 ..... NO REPORT NUMBER
N92-23766 # p 2320 ..... NO REPORT NUMBER
N92-23767 # p 2320 ..... NO REPORT NUMBER
N92-23768 # p 2321 ..... NO REPORT NUMBER
N92-23769 p 2412 ..... NO REPORT NUMBER
N92-23770 p 2457 ..... NO REPORT NUMBER
N92-23771 p 2411 ..... NO REPORT NUMBER
N92-23772 p 2409 ..... NO REPORT NUMBER
N92-23773 p 2389 ..... NO REPORT NUMBER
N92-23774 p 2448 ..... NO REPORT NUMBER
N92-23775 p 2449 ..... NO REPORT NUMBER
N92-23776 # p 2449 ..... NO REPORT NUMBER
N92-23777 p 2434 ..... NO REPORT NUMBER
N92-23778 # p 2312 ..... ISSN-0452-2982
JTN-92-80309
NAL-TM-565
N92-23779 # p 2384 ..... ISSN-0452-2982
JTN-92-80310
NAL-TM-622
N92-23780 # p 2322 ..... ESA-SP-321-VOL-1
ETN-92-91208
ISBN-92-9092-126-9
ISSN-0379-6566
N92-23781 # p 2323 ..... NO REPORT NUMBER
N92-23782 # p 2323 ..... NO REPORT NUMBER
N92-23783 # p 2323 ..... NO REPORT NUMBER
N92-23784 # p 2323 ..... NO REPORT NUMBER
N92-23785 # p 2323 ..... NO REPORT NUMBER
N92-23786 # p 2323 ..... NO REPORT NUMBER
N92-23787 # p 2324 ..... NO REPORT NUMBER
N92-23788 # p 2324 ..... NO REPORT NUMBER
N92-23789 # p 2324 ..... NO REPORT NUMBER
N92-23790 # p 2324 ..... NO REPORT NUMBER
N92-23791 # p 2324 ..... NO REPORT NUMBER
N92-23792 # p 2324 ..... NO REPORT NUMBER
N92-23793 # p 2324 ..... NO REPORT NUMBER
N92-23794 # p 2325 ..... NO REPORT NUMBER
N92-23795 # p 2325 ..... NO REPORT NUMBER
N92-23796*# p 2322 ..... NO REPORT NUMBER
N92-23797 # p 2321 ..... NO REPORT NUMBER
N92-23798 # p 2321 ..... NO REPORT NUMBER
N92-23799 # p 2325 ..... NO REPORT NUMBER
N92-23800 # p 2325 ..... NO REPORT NUMBER
N92-23801 # p 2326 ..... NO REPORT NUMBER
N92-23802 # p 2326 ..... NO REPORT NUMBER
N92-23803 # p 2326 ..... NO REPORT NUMBER
N92-23804 # p 2326 ..... NO REPORT NUMBER
N92-23805 # p 2326 ..... NO REPORT NUMBER
N92-23806 # p 2326 ..... NO REPORT NUMBER
N92-23807 # p 2326 ..... NO REPORT NUMBER
N92-23808 # p 2321 ..... NO REPORT NUMBER
N92-23809 # p 2327 ..... NO REPORT NUMBER
N92-23810 # p 2321 ..... NO REPORT NUMBER
N92-23811 # p 2321 ..... NO REPORT NUMBER
N92-23812 # p 2327 ..... NO REPORT NUMBER
N92-23813 # p 2327 ..... NO REPORT NUMBER
N92-23814 # p 2327 ..... NO REPORT NUMBER
N92-23815 # p 2328 ..... NO REPORT NUMBER
N92-23816 # p 2328 ..... NO REPORT NUMBER
N92-23817 # p 2328 ..... NO REPORT NUMBER
N92-23818 # p 2328 ..... NO REPORT NUMBER
N92-23819 # p 2328 ..... NO REPORT NUMBER
N92-23820 # p 2328 ..... NO REPORT NUMBER
N92-23821 # p 2329 ..... NO REPORT NUMBER
N92-23822 # p 2310 ..... NO REPORT NUMBER
N92-23823 # p 2322 ..... NO REPORT NUMBER
N92-23824*# p 2329 ..... NO REPORT NUMBER
N92-23825 # p 2329 ..... NO REPORT NUMBER
N92-23826 # p 2329 ..... NO REPORT NUMBER
N92-23827 # p 2330 ..... NO REPORT NUMBER
N92-23828 # p 2330 ..... NO REPORT NUMBER
N92-23829 # p 2330 ..... NO REPORT NUMBER
N92-23830 # p 2330 ..... NO REPORT NUMBER
N92-23831 # p 2330 ..... NO REPORT NUMBER
N92-23832 # p 2330 ..... NO REPORT NUMBER
N92-23833 # p 2330 ..... NO REPORT NUMBER
N92-23834 # p 2331 ..... NO REPORT NUMBER
N92-23835 # p 2331 ..... NO REPORT NUMBER
N92-23836 # p 2331 ..... NO REPORT NUMBER
N92-23837 # p 2331 ..... NO REPORT NUMBER
N92-23838 # p 2331 ..... NO REPORT NUMBER
N92-23839 # p 2331 ..... NO REPORT NUMBER
N92-23840 # p 2332 ..... NO REPORT NUMBER
N92-23841 # p 2332 ..... NO REPORT NUMBER
N92-23842 # p 2332 ..... NO REPORT NUMBER
N92-23843 # p 2332 ..... NO REPORT NUMBER
N92-23844 # p 2332 ..... NO REPORT NUMBER
N92-23845 # p 2332 ..... NO REPORT NUMBER
N92-23846 # p 2332 ..... NO REPORT NUMBER
N92-23847 # p 2333 ..... NO REPORT NUMBER
N92-23848 # p 2333 ..... NO REPORT NUMBER
N92-23849 # p 2333 ..... NO REPORT NUMBER
N92-23850 # p 2333 ..... NO REPORT NUMBER
N92-23851 # p 2418 ..... ITN-92-85127
N92-23852 # p 2419 ..... P-1-1
N92-23853 # p 2419 ..... REPT-1.1.1
N92-23854 # p 2419 ..... REPT-1.1.2
N92-23855 # p 2419 ..... REPT-1.1.3
N92-23856 # p 2419 ..... REPT-1.1.4
N92-23857 # p 2420 ..... REPT-1.1.6
N92-23858 # p 2420 ..... REPT-1.1.7
N92-23859 # p 2420 ..... REPT-1.1.8
N92-23860 # p 2420 ..... REPT-1.2.1
N92-23861 # p 2420 ..... REPT-1.2.2
N92-23862 # p 2420 ..... REPT-1.2.3
N92-23863 # p 2421 ..... REPT-1.2.4
N92-23864 # p 2421 ..... REPT-1.2.5
N92-23865 # p 2421 ..... REPT-1.2.6
N92-23866 # p 2421 ..... REPT-1.2.7
N92-23867 # p 2421 ..... REPT-1.2.8
N92-23868 # p 2421 ..... REPT-1.3.1
N92-23869 # p 2421 ..... REPT-1.3.2
N92-23870 # p 2422 ..... REPT-1.3.3
N92-23871 # p 2422 ..... REPT-1.3.4
N92-23872 # p 2422 ..... REPT-1.3.6
N92-23873 # p 2422 ..... REPT-1.3.7
N92-23874 # p 2422 ..... REPT-2.1.2
N92-23875 # p 2422 ..... REPT-2.2.1
N92-23876 # p 2423 ..... REPT-2.3.3
N92-23877 # p 2423 ..... REPT-2.3.4
N92-23878 # p 2423 ..... REPT-2.3.5
N92-23879 # p 2423 ..... REPT-2.3.6
N92-23880 # p 2423 ..... REPT-3.1.5
N92-23881 # p 2423 ..... REPT-3.1.6
N92-23882 # p 2424 ..... REPT-3.1.7
N92-23883 # p 2424 ..... REPT-3.2.2
N92-23884 # p 2424 ..... REPT-3.2.4
N92-23885 # p 2424 ..... REPT-3.3.1
N92-23886 # p 2424 ..... REPT-3.3.2
N92-23887 # p 2424 ..... REPT-4.2.1
N92-23888 # p 2425 ..... REPT-4.2.2
N92-23889 # p 2425 ..... REPT-4.2.3
N92-23890*# p 2449 ..... E-7021
NAS 1.15:105657
NASA-TM-105657
N92-23891 # p 2380 ..... DE92-008648
DOE/DP-40200/184
N92-23892 # p 2449 ..... DE92-008243
IS-T-1604
N92-23893 # p 2352 ..... CONF-920458-1
DE92-008283
LBL-31671
N92-23894 # p 2438 ..... CONF-920444-14
DE92-008331
SAND-91-2921C
N92-23895 # p 2438 ... CONF-9110335-1-EXTD-ABST
DE92-008356
DOE/ER-13596/25
N92-23896 # p 2384 ..... DE92-008425
DOE/ID-13074/T2
N92-23897 # p 2355 ..... DE92-009630
ORNL-6703
N92-23898*# p 2406 ..... NAS 1.26:190152
NASA-CR-190152
N92-23899 # p 2363 ..... CONF-9109348-2
DE92-008037
Y/DW-1050
N92-23900 # p 2367 ..... CONF-920305-6
DE92-008278
N92-23901 # p 2364 ..... DE92-008399
KCP-613-4616
N92-23902 # p 2371 ..... DE92-008404
UCRL-ID-108256
N92-23903 # p 2438 ..... CONF-9108150-7
DE92-008567
UCRL-JC-107010
N92-23904 # p 2348 ..... DE92-008987
UCRL-ID-109903
N92-23905 # p 2445 ..... DE92-009020
KCP-613-4653
N92-23906 # p 2411 ..... NOAA-TM-NWS-SR-140
PB92-134444
N92-23907 # p 2367 ..... ISBN-951-22-0600-5
PB92-142173
REPT-90
N92-23908 # p 2384 ..... CONF-9109348-1
DE92-008040
Y/DW-1053
N92-23909 # p 2460 ..... DE92-619048
IC-91/298
N92-23910 # p 2314 ..... ESA-SP-329
ETN-92-91383
ISBN-92-9092-158-7
ISSN-0379-6566
N92-23911 # p 2314 ..... NO REPORT NUMBER
N92-23912*# p 2315 ..... NO REPORT NUMBER
N92-23913 # p 2315 ..... NO REPORT NUMBER
N92-23914 # p 2315 ..... NO REPORT NUMBER
N92-23915*# p 2315 ..... NO REPORT NUMBER
N92-23916 # p 2315 ..... NO REPORT NUMBER
N92-23917 # p 2315 ..... NO REPORT NUMBER
N92-23918 # p 2316 ..... NO REPORT NUMBER
N92-23919*# p 2316 ..... NO REPORT NUMBER
N92-23920*# p 2316 ..... NO REPORT NUMBER
N92-23921*# p 2316 ..... NO REPORT NUMBER
N92-23922 # p 2316 ..... NO REPORT NUMBER
N92-23923 # p 2316 ..... NO REPORT NUMBER
N92-23924 # p 2316 ..... NO REPORT NUMBER
N92-23925 # p 2317 ..... NO REPORT NUMBER
N92-23926 # p 2317 ..... NO REPORT NUMBER
N92-23927 # p 2317 ..... NO REPORT NUMBER
N92-23928 # p 2452 ..... ETN-92-91074
MBB-UE-0014-90-PUB
N92-23929 # p 2452 ..... NO REPORT NUMBER
N92-23930 # p 2452 ..... NO REPORT NUMBER
N92-23931 # p 2452 ..... NO REPORT NUMBER
N92-23932 # p 2452 ..... NO REPORT NUMBER
N92-23933 # p 2341 ..... CTN-92-60405
IMI-90D-000-1063-G
NRC-32603
N92-23934 # p 2341 ..... NO REPORT NUMBER
N92-23935 # p 2341 ..... NO REPORT NUMBER
N92-23936 # p 2341 ..... NO REPORT NUMBER
N92-23937 # p 2341 ..... NO REPORT NUMBER
N92-23938 # p 2342 ..... NO REPORT NUMBER
N92-23939 # p 2342 ..... NO REPORT NUMBER
N92-23940 # p 2342 ..... NO REPORT NUMBER
N92-23941 # p 2342 ..... NO REPORT NUMBER
N92-23942 # p 2343 ..... NO REPORT NUMBER
N92-23943 # p 2343 ..... NO REPORT NUMBER
N92-23944 # p 2343 ..... NO REPORT NUMBER
N92-23945 # p 2343 ..... NO REPORT NUMBER
N92-23946 # p 2343 ..... NO REPORT NUMBER
N92-23947 # p 2344 ..... NO REPORT NUMBER
N92-23948 # p 2344 ..... NO REPORT NUMBER
N92-23949 # p 2344 ..... NO REPORT NUMBER
N92-23950 # p 2308 ..... AGARD-R-783
ISBN-92-835-0652-9
N92-23951 # p 2308 ..... NO REPORT NUMBER
N92-23952 # p 2309 ..... NO REPORT NUMBER
N92-23953 # p 2309 ..... NO REPORT NUMBER
N92-23954 # p 2309 ..... NO REPORT NUMBER
N92-23955 # p 2309 ..... NO REPORT NUMBER
N92-23956*# p 2305 ..... NO REPORT NUMBER
N92-23957 # p 2309 ..... NO REPORT NUMBER
N92-23958*# p 2470 ..... NAS 1.15:107813
NASA-TM-107813
N92-23959*# p 2425 ..... NO REPORT NUMBER
N92-23960*# p 2409 ..... NO REPORT NUMBER
N92-23961*# p 2380 ..... NO REPORT NUMBER
N92-23962*# p 2456 ..... NO REPORT NUMBER
N92-23963*# p 2368 ..... NO REPORT NUMBER
N92-23964*# p 2434 ..... NO REPORT NUMBER
N92-23965*# p 2407 ..... NO REPORT NUMBER
N92-23966*# p 2364 ..... NO REPORT NUMBER
N92-23967 # p 2333 ..... ESA-SP-345
ETN-92-91187

ISBN-92-9092-222-2
ISSN-0379-6566
N92-23968 # p 2333 ..... NO REPORT NUMBER
N92-23969 # p 2318 ..... NO REPORT NUMBER
N92-23970 # p 2334 ..... NO REPORT NUMBER
N92-23971 # p 2334 ..... NO REPORT NUMBER
N92-23972 # p 2334 ..... NO REPORT NUMBER
N92-23973 # p 2318 ..... NO REPORT NUMBER
N92-23974 # p 2334 ..... NO REPORT NUMBER
N92-23975 # p 2334 ..... NO REPORT NUMBER
N92-23976 # p 2318 ..... NO REPORT NUMBER
N92-23977 # p 2318 ..... NO REPORT NUMBER
N92-23978* # p 2335 ..... NO REPORT NUMBER
N92-23979 # p 2312 ..... ISSN-0452-2982
JTN-92-80327
NAL-TM-629
N92-23980* # p 2321 ..... NAS 1.26:190216
NASA-CR-190216
N92-23981* # p 2344 ..... L-17031
NAS 1.60:3196
NASA-TP-3196
N92-23982* # p 2337 ..... FR-21385
NAS 1.26:187206
NASA-CR-187206
N92-23983 # p 2371 ..... CONF-920124-12
DE92-008668
SAND-91-1562C
N92-23984 # p 2353 ..... CONF-911202-61
DE92-008300
LBL-31831
N92-23985 # p 2371 ..... CONF-911202-63
DE92-008307
LBL-31207
N92-23986 # p 2449 ..... CONF-9108150-8
DE92-008566
UCRL-JC-108266
N92-23987 # p 2445 ..... CONF-910626-15
DE92-008577
UCRL-JC-106407
N92-23988 # p 2344 ..... DE92-008980
UCRL-ID-109159
N92-23989* # p 2364 ..... NAS 1.15:104229
NASA-TM-104229
N92-23990* # p 2390 ..... NAS 1.15:107573
NASA-TM-107573
N92-23991* # p 2425 ..... NAS 1.26:190304
NASA-CR-190304
REPT-92-008
N92-23992* # p 2390 ..... NAS 1.15:107605
NASA-TM-107605
N92-23993 # p 2460 ..... PB92-129402
SGD-566-PT-2
N92-23994 # p 2411 ..... PB92-134501
N92-23995 p 2375 ..... NO REPORT NUMBER
N92-23996 p 2345 ..... NO REPORT NUMBER
N92-23997 p 2375 ..... NO REPORT NUMBER
N92-23998 p 2404 ..... NO REPORT NUMBER
N92-23999 p 2442 ..... NO REPORT NUMBER
N92-24000 p 2457 ..... NO REPORT NUMBER
N92-24001 p 2455 ..... NO REPORT NUMBER
N92-24002 p 2455 ..... NO REPORT NUMBER
N92-24003 # p 2407 ..... NPS/NRAQD/NRTR-91/02
PB92-140532
N92-24004* # p 2338 ..... AIAA-91-2346
E-6940
NAS 1.26:189138
NASA-CR-189138
N92-24005 # p 2439 ..... CONF-910983-3
DE92-008357
UCRL-JC-108061
N92-24006 # p 2353 ..... CONF-9205100-1
DE92-008416
Y/DV-1096
N92-24007 # p 2450 ..... CONF-9108150-9
DE92-008605
UCRL-JC-108674
N92-24008 p 2434 ..... ESDU-68014
ESDU-68016
ESDU-68017
ESDU-91041
ISBN-0-85679-803-7
ISSN-0141-4089
ISSN-0141-4097
ISSN-9058-0379
N92-24009 p 2309 ..... ESDU-68022
ESDU-91042
ISBN-0-85679-804-5
ISSN-0141-397X
N92-24010 p 2310 ..... NO REPORT NUMBER
N92-24011 p 2430 ..... NO REPORT NUMBER
N92-24012 p 2345 ..... NO REPORT NUMBER
N92-24013 p 2345 ..... NO REPORT NUMBER
N92-24014 p 2353 ..... NO REPORT NUMBER
N92-24015 p 2458 ..... NO REPORT NUMBER
N92-24016 p 2454 ..... NO REPORT NUMBER
N92-24017 p 2458 ..... NO REPORT NUMBER
N92-24018 p 2376 ..... NO REPORT NUMBER
N92-24019 p 2367 ..... NO REPORT NUMBER
N92-24020 # p 2445 ..... DE92-008983
UCRL-ID-109807
N92-24021 # p 2445 ..... ANL/FPP/TM-259
DE92-009022
N92-24022 # p 2415 ..... DE92-619064
IAEA-TECDOC-639
N92-24023 # p 2407 ..... DE92-769376
NEDO-ITE-9002-4
N92-24024 # p 2407 ..... DE92-769381
NEDO-ITE-9003
N92-24025 # p 2371 ..... CONF-920474-1
DE92-007234
N92-24026 # p 2439 ..... CONF-9110313-5
DE92-007240
N92-24027 # p 2455 ..... CONF-9111185-1
DE92-007429
LA-UR-91-4163
N92-24028 # p 2458 ..... CONF-920180-1
DE92-007431
LA-UR-92-231
N92-24029 # p 2443 ..... DE92-615486
IC-91/276
N92-24030 # p 2404 ..... DE92-008686
DOE/ID-13040/T3
N92-24031 # p 2439 ..... DE92-008693
DOE/PC-89768/T3
N92-24032 # p 2430 ..... CONF-920540-8
DE92-000069
N92-24033 # p 2414 ..... DE92-005539
DOE/ER-61009/2
N92-24034 # p 2450 ..... CONF-911202-64
DE92-008332
SAND-91-1561C
N92-24035 # p 2425 ..... CONF-920392-1
DE92-008417
Y/EN-4562
N92-24036 # p 2450 ..... CONF-920141-2
DE92-008441
LA-UR-92-429
N92-24037 # p 2355 ..... DE92-008787
DOE/ER-13905/4
N92-24038 # p 2348 ..... DE92-008790
DOE/ER-13384/5
N92-24039 # p 2434 ..... DE92-619234
IC-91/259
N92-24040 # p 2451 ..... DE92-008772
DOE/ER-40272/129
UFIFT-HEP-91-10
UPR-0472T
N92-24041 # p 2425 ..... CONF-920277-1
DE92-003146
SAND-92-0261C
N92-24042* # p 2385 ..... NAS 1.71:NPO-18499-1-CU
NASA-CASE-NPO-18499-1-CU
US-PATENT-APPL-SN-862861
N92-24043* # p 2385 ..... NAS 1.71:NPO-18498-1-CU
NASA-CASE-NPO-18498-1-CU
US-PATENT-APPL-SN-866779
N92-24044* # p 2416 ..... NAS 1.71:MFS-28430-1
NASA-CASE-MFS-28430-1
US-PATENT-APPL-SN-832569
N92-24045* # p 2426 ..... NAS 1.71:NPO-18414-1-CU
NASA-CASE-NPO-18414-1-CU
US-PATENT-APPL-SN-880211
N92-24046* # p 2335 ..... NAS 1.26:190257
NASA-CR-190257
N92-24047* # p 2372 ..... NAS 1.26:184317
NASA-CR-184317
UAH-5-32640
N92-24048* # p 2317 ..... D615-10051
NAS 1.26:184309
NASA-CR-184309
N92-24049 # p 2443 ..... CONF-9107115-71
DE92-008615
UCRL-JC-108299
N92-24050* # p 2376 ..... CMOTT-92-06
ICOMP-92-10
NAS 1.15:105663
NASA-TM-105663
N92-24051* # p 2385 ..... NAS 1.71:MSC-21648-1
NASA-CASE-MSC-21648-1
US-PATENT-APPL-SN-824806
N92-24052* # p 2413 ..... NAS 1.71:MSC-21843-1-NP
NASA-CASE-MSC-21843-1-NP
US-PATENT-APPL-SN-803828
N92-24053* # p 2355 ..... NAS 1.71:LEW-15027-2
NASA-CASE-LEW-15027-2
US-PATENT-APPL-SN-824858
N92-24054* # p 2404 ..... NAS 1.71:LEW-15212-1
NASA-CASE-LEW-15212-1
US-PATENT-APPL-SN-836490
N92-24055* # p 2385 ..... NAS 1.71:MFS-28634-1
NASA-CASE-MFS-28634-1
US-PATENT-APPL-SN-825895
N92-24056* # p 2416 ..... NAS 1.71:MFS-28481-1
NASA-CASE-MFS-28481-1
US-PATENT-APPL-SN-873931
N92-24057* # p 2404 ..... NAS 1.71:LEW-15308-1
NASA-CASE-LEW-15308-1
US-PATENT-APPL-SN-862113
N92-24058* # p 2385 ..... NAS 1.71:GSC-13358-1
NASA-CASE-GSC-13358-1
US-PATENT-APPL-SN-765069
N92-24059* # p 2386 ..... NAS 1.71:GSC-13415-1
NASA-CASE-GSC-13415-1
US-PATENT-APPL-SN-812932
N92-24060* # p 2386 ..... NAS 1.71:GSC-13161-1
NASA-CASE-GSC-13161-1
US-PATENT-APPL-SN-754828
N92-24061 # p 2434 ..... IHES/M/91/70
PB92-135373
N92-24062 # p 2376 ..... DE92-008642
DOE/ER-14136/T1
N92-24063 # p 2372 ..... DE92-008455
SAND-91-1059
N92-24064 # p 2349 ..... CONF-920444-15
DE92-008554
UCRL-JC-109148
N92-24065 # p 2380 ..... CONF-920235-2
DE92-008606
UCRL-JC-108475
N92-24066 # p 2430 ..... CONF-920540-15
DE92-008612
UCRL-JC-108592
N92-24067 # p 2446 ..... CONF-911132-21
DE92-008614
UCRL-JC-109030
N92-24068 # p 2355 ..... CONF-920572-2
DE92-008619
UCRL-JC-109213
N92-24069 # p 2450 ..... CONF-920439-1
DE92-008624
UCRL-JC-108620
N92-24070 # p 2380 ..... CONF-850406-15
DE92-008634
SAND-85-8869

Appendix

NASA SCIENTIFIC AND TECHNICAL INFORMATION PROGRAM PRODUCTS AND SERVICES

The NASA Scientific and Technical Information (STI) Program provides for the collection and announcement of aerospace-related reports and literature obtained worldwide through agreements and exchanges. The result of the collection is the comprehensive NASA STI Database that covers aeronautics, space, and supporting disciplines.

The STI Database, documents generated or obtained by NASA, and products and services derived from or supporting the database are made available to the NASA research community and to the public. Descriptions and sources of these items are presented in the following pages.

Scientific and Technical Aerospace Reports (*STAR*) is an abstract journal, listing citations with abstracts for aerospace-related reports obtained from worldwide sources. *STAR* is issued on the 8th and 23rd of each month and announces current documents that have been entered into the NASA STI Database during the previous two weeks. The reports are of the following types:

- NASA, NASA contractor, and NASA grantee reports;
- Reports issued by other U.S. Government agencies, domestic and foreign institutions, universities, and private firms;
- Translations in report form;
- NASA-owned patents and patent applications;
- Other U.S. Government agency and foreign patents and patent applications;
- Domestic and foreign dissertations and theses.

Journal, book, and conference literature, journal translations, and certain foreign dissertations having the same subject scope as *STAR* are announced in a companion journal, *International Aerospace Abstracts* (*IAA*). *IAA* is issued on the 1st and 15th of each month and is available from the American Institute of Aeronautics and Astronautics, Technical Information Service, 555 West 57th Street, 12th Floor, New York, NY 10019.

ELIGIBILITY AND REGISTRATION FOR NASA STI PRODUCTS AND SERVICES

Organizations of the type listed below that have registered with NASA can receive products and services.

- NASA offices and installations, contractors, subcontractors, grantees, and consultants;
- Other U.S. Government agencies and their contractors;
- Libraries in the United States that have arrangements with NASA to maintain collections of NASA documents for public reference;
- Other organizations in the United States having a need for NASA documents in work related to aeronautics and space research;
- Organizations abroad that have established reciprocal documents exchange arrangements with NASA.

Only the central service points or central points of document acquisition and control within qualified organizations are eligible to register for NASA STI products and services. Domestic organizations that may be eligible to receive various classes of NASA publications and services should address their requests for registration or further information to:

NASA Center for AeroSpace Information
ATTN: Registration Services
P.O. Box 8757
Baltimore, MD 21240-0757
301-621-0153

Organizations abroad should direct requests to:

National Aeronautics and Space Administration
Director, Scientific and Technical Information Program
Code JTT
Washington, DC 20546
USA
703-271-5640

SUBJECT SCOPE

The subject scope of *STAR* and *IAA* includes all aspects of aeronautics and space research and development, supporting basic and applied research, and applications. Aerospace aspects of Earth resources, energy development, conservation, oceanography, environmental protection, urban transportation, and other topics of high national priority are also covered.

HOW TO USE *STAR* SUBJECT CATEGORIES

Abstracts in *STAR* are categorized by 10 major subject divisions that are divided further into 76 specific subject categories. The subject divisions and categories are listed in the Table of Contents together with a note for each that defines its scope and provides any cross-references. For example:

16 SPACE TRANSPORTATION
Includes passenger and cargo space transportation, e.g., shuttle operations; and space rescue techniques. For related information see also *03 Air Transportation and Safety* and *18 Spacecraft Design, Testing and Performance.* For space suits see *54 Man/System Technology and Life Support.*

CROSS-REFERENCES

Individual *STAR* abstracts are not ordinarily cross-referenced, except for certain conference reports or book translations that have had separate abstracts written for their component papers or chapters. Citations and abstracts of the components follow immediately after those of the parent document. When the subject content of a component differs sufficiently from the general content of the parent, a cross-reference citation also is printed at the end of the category to which it normally would have been assigned if it were independent.

DOCUMENTS ON MICROFICHE

Documents available on microfiche are designated by a pound sign (#) following the accession number.

LIMITED REPRODUCIBILITY

A note of limited reproducibility appears in the citation, if there are factors affecting the reproducibility of more than 20% of the document. These factors include faint or broken type, color photographs, black and white photographs, foldouts, dot matrix print, or some other factor that limits the reproducibility of the document. This notation also appears on the microfiche header with the specific factor checked off on a list visible in the second frame.

COLOR COPIES

An increasing number of NASA scientific and technical reports are being produced with color graphs, charts, illustrations, and photographs. An indication that a document has color pages follows the source and pricing (SAP) information in the *STAR* citation.

Registered users of the NASA Scientific and Technical Information Program will receive ordered documents with color at no additional cost, as long as stock copies of the document are available. Otherwise, an additional fee of $2.00 per color page will be charged. The NASA Center for AeroSpace Information staff will contact registered users to determine individual user's needs.

NASA PATENTS AND PATENT APPLICATIONS

Patents and patent applications owned by NASA are announced in *STAR* under appropriate subject categories and are referenced in the *STAR* indexes. In the Report/Accession Number Index, patents are indexed by the NASA Case Number, and the U.S. Patent Class. Patent applications are indexed by the NASA Case Number and the U.S. Patent Application Serial Number.

Printed copies of patents (which are not microfiched) are available for purchase from the U.S. Patent and Trademark Office.

NASA patent application specifications are sold in both paper copy and microfiche by the National Technical Information Service (NTIS). The US-Patent-Appl-SN-number should be used in ordering either paper copy or microfiche from NTIS.

When ordering patents, the U.S. Patent Number should be used, and payment must be remitted in advance, by money order or check payable to the Commissioner of Patents and Trademarks. Prepaid purchase coupons for ordering are also available from the U.S. Patent and Trademark Office.

The patents and patent applications announced in *STAR* are owned by NASA and are available for royalty-free licensing. Requests for licensing terms and further information should be addressed to:

National Aeronautics and Space Administration
Associate General Counsel for Intellectual Property
Code GP
Washington, DC 20546

SOURCES FOR DOCUMENTS

One or more sources from which a document announced in *STAR* is available to the public is given in each citation. The most commonly indicated sources and their acronyms or abbreviations are listed on page A-6. If the publication is available from a source other than those listed, the publisher and address will be displayed on the availability line or in combination with the corporate source line.

Avail: NTIS. Sold by the National Technical Information Service. Prices for hard copy (HC) and microfiche (MF) are indicated by a price code following the letters HC or MF in the *STAR* citation. Current values for the price codes are given in the tables on page A-7.

Initially distributed microfiche under the NTIS SRIM (Selected Research in Microfiche) is available at greatly reduced unit prices. For this service and for information concerning subscription to NASA printed reports, consult the NTIS Subscription Section, Springfield, VA 22161.

NOTE ON ORDERING DOCUMENTS: When ordering NASA publications (those followed by the * symbol), use the N accession number. NASA patent applications (only the specifications are offered) should be ordered by the US-Patent-Appl-SN number. Non-NASA publications (no asterisk) should be ordered by the AD, PB, or other *report number* shown on the last line of the citation, not by the N accession number. It is also advisable to cite the title and other bibliographic identification.

Avail: SOD (or GPO). Sold by the Superintendent of Documents, U.S. Government Printing Office, in hard copy. The current price and order number are given following the availability line. (NTIS will fill microfiche requests, as indicated above, for those documents identified by a # symbol.)

Avail: BLL (formerly NLL): British Library Lending Division, Boston Spa, Wetherby, Yorkshire, England. Photocopies available from this organization at the price shown. (If none is given, address inquiry to the BLL.)

Avail: DOE Depository Libraries. Organizations in U.S. cities and abroad that maintain collections of Department of Energy reports, usually in microfiche form, are listed in *Energy Research Abstracts.* Services available from the DOE and its depositories are described in a booklet, *DOE Technical Information Center - Its Functions and Services* (TID-4660), which may be obtained without charge from the DOE Technical Information Center.

Avail: ESDU. Pricing information on specific data, computer programs, and details on Engineering Sciences Data Unit (ESDU) topic categories can be obtained from ESDU International Ltd. Requesters in North America should use the Virginia address while all other requesters should use the London address, both of which are on page A-6.

Avail: Fachinformationszentrum, Karlsruhe. Sold by the Fachinformationszentrum Energie, Physik, Mathematik GMBH, Eggenstein Leopoldshafen, Federal Republic of Germany, at the price shown in deutschmarks (DM).

Avail: HMSO. Publications of Her Majesty's Stationery Office are sold in the U.S. by Pendragon House, Inc. (PHI), Redwood City, CA. The U.S. price (including a service and mailing charge) is given, or a conversion table may be obtained from PHI.

Avail: NASA Public Document Rooms. Documents so indicated may be examined at or purchased from the National Aeronautics and Space Administration, Public Documents Room (Room 126), 600 Independence Ave., S.W., Washington, DC 20546, or public document rooms located at NASA installations, and the NASA Pasadena Office at the Jet Propulsion Laboratory.

Avail: Univ. Microfilms. Documents so indicated are dissertations selected from *Dissertation Abstracts* and are sold by University Microfilms as xerographic copy (HC) and microfilm. All requests should cite the author and the Order Number as they appear in the citation.

Avail: US Patent and Trademark Office. Sold by Commissioner of Patents and Trademarks, U.S. Patent and Trademark Office, at the standard price of $1.50 each, postage free. (See discussion of NASA patents and patent applications below.)

Avail: (US Sales Only). These foreign documents are available to users within the United States from the National Technical Information Service (NTIS). They are available to users outside the United States through the International Nuclear Information Service (INIS) representative in their country, or by applying directly to the issuing organization.

Avail: USGS. Originals of many reports from the U.S. Geological Survey, which may contain color illustrations, or otherwise may not have the quality of illustrations preserved in the microfiche or facsimile reproduction, may be examined by the public at the libraries of the USGS field offices whose addresses are listed on page A-6. The libraries may be queried concerning the availability of specific documents and the possible utilization of local copying services, such as color reproduction.

Avail: Issuing Activity, or Corporate Author, or no indication of availability. Inquiries as to the availability of these documents should be addressed to the organization shown in the citation as the corporate author of the document.

FEDERAL DEPOSITORY LIBRARIES: To provide the general public with greater access to U.S. Government publications, Congress established the Federal Depository Library Program under the Government Printing Office (GPO), with 53 regional depositories responsible for permanent retention of material, inter-library loan, and reference services. (These libraries are not sales outlets.) At least one copy of nearly every NASA and NASA-sponsored publication, either in printed or microfiche format, is received and retained by the 53 regional depositories. A list of the regional GPO libraries, appears on page A-8. A local library can contact a regional depository library to help locate specific reports, or direct contact may be made by an individual.

PUBLIC COLLECTION OF NASA DOCUMENTS

An extensive collection of NASA and NASA-sponsored publications is maintianed by the British Library Lending Divison, Boston Spa, Wetherby, Yorkshire, England, for public access. The British Library Lending Division also has available many of the non-NASA publications cited in *STAR*.

European requesters may purchase facsimile copy or microfiche of NASA and NASA-sponsored documents, those identified by both the symbols # and * from ESA—Information Retrieval Service, European Space Agency, 8-10 rue Mario-Nikis, 75738 Paris CEDEX 15, France.

SUBMITTING DOCUMENTS

All users of this abstract service are urged to forward reports to be considered for announcement in *STAR*. This will aid NASA in its efforts to provide the fullest possible coverage of all scientific and technical publications that might support aeronautics and space research and development. If you have prepared relevant reports (other than those you will transmit to NASA, DOD, or DOE through the usual contract- or grant-reporting channels), please send them for consideration to the NASA Center for AeroSpace Information, P.O. Box 8757, Baltimore, MD 21240-0757.

Reprints of journal articles, book chapters, and conference papers are also welcome. These will be considered for announcement in *STAR*'s companion journal, *IAA*.

You may specify a particular source to be included in a report announcement if you wish; otherwise the report will be placed on a public sale at the National Technical Information Service. Copyrighted publications will be announced but not distributed or sold.

PURCHASE OF *STAR*

STAR is publicly available on annual subscription from the Superintendent of Documents, U.S. Government Printing Office, Washington, DC 20402.

STAR is available to registered users on annual subscription from the NASA Center for AeroSpace Information, ATTN: Registration Services, P.O. Box 8757, Baltimore, MD 21240-0757.

Microfiche of the abstract sections of *STAR* are available, on annual subscription only, from NTIS as PB92-911300, Attn: Subscriptions, 5285 Port Royal Road, Springfield, VA 22161. Annual subscription rates are $100.00 North America; $200.00 foreign. Abstract sections for previous years retroactive to 1964 are available at the current rates.

ADDRESSES OF ORGANIZATIONS

American Institute of Aeronautics and Astronautics
Technical Information Service
555 West 57th Street, 12th Floor
New York, New York 10019

British Library Lending Division,
Boston Spa, Wetherby, Yorkshire,
England

Commissioner of Patents and Trademarks
U.S. Patent and Trademark Office
Washington, DC 20231

Department of Energy
Technical Information Center
P.O. Box 62
Oak Ridge, Tennessee 37830

European Space Agency-Information Retrieval Service
ESRIN
Via Galileo Galilei
00044 Frascati (Rome) Italy

Engineering Sciences Data Unit International
P.O. Box 1633
Manassas, Virginia 22110

Engineering Sciences Data Unit International, Ltd.
251-259 Regent Street
London, W1R 7AD, England

Fachinformationszentrum Energie, Physik, Mathematik
GMBH
7514 Eggenstein Leopoldshafen
Federal Republic of Germany

Her Majesty's Stationery Office
P.O. Box 569, S.E. 1
London, England

NASA Center for AeroSpace Information
P.O. Box 8757
Baltimore, Maryland 21240-0757

National Aeronautics and Space Administration
Scientific and Technical Information Program (JTT)
Washington, DC 20546-0001

National Technical Information Service
5285 Port Royal Road
Springfield, Virginia 22161

Pendragon House, Inc.
899 Broadway Avenue
Redwood City, California 94063

Superintendent of Documents
U.S. Government Printing Office
Washington, DC 20402

University Microfilms
A Xerox Company
300 North Zeeb Road
Ann Arbor, Michigan 48106

University Microfilms, Ltd.
Tylers Green
London, England

U.S. Geological Survey Library National Center
MS 950
12201 Sunrise Valley Drive
Reston, Virginia 22092

U.S. Geological Survey Library
2255 North Gemini Drive
Flagstaff, Arizona 86001

U.S. Geological Survey
345 Middlefield Road
Menlo Park, California 94025

U.S. Geological Survey Library
Box 25046
Denver Federal Center, MS914
Denver, Colorado 80225

NTIS PRICE SCHEDULES

(Effective October 1, 1991)

Schedule A
STANDARD PRICE DOCUMENTS AND MICROFICHE**

PRICE CODE	NORTH AMERICAN PRICE	FOREIGN PRICE
A01	$ 9.00	$ 18.00
A02	12.50	25.00
A03	17.00	34.00
A04-A05	19.00	38.00
A06-A09	26.00	52.00
A10-A13	35.00	70.00
A14-A17	43.00	86.00
A18-A21	50.00	100.00
A22-A25	59.00	118.00
A99	*	*
N01	60.00	120.00
N02	59.00	118.00
N03	20.00	40.00

Schedule E
EXCEPTION PRICE DOCUMENTS AND MICROFICHE**

PRICE CODE	NORTH AMERICAN PRICE	FOREIGN PRICE
E01	$11.00	$ 22.00
E02	14.00	28.00
E03	16.00	32.00
E04	19.00	38.00
E05	21.00	42.00
E06	24.00	48.00
E07	27.00	54.00
E08	30.00	60.00
E09	33.00	66.00
E10	36.00	72.00
E11	39.00	78.00
E12	43.00	86.00
E13	46.00	92.00
E14	50.00	100.00
E15	54.00	108.00
E16	59.00	118.00
E17	64.00	128.00
E18	69.00	138.00
E19	76.00	152.00
E20	88.00	176.00
E99	*	*

* Contact NTIS for price quote.

** Effective January 1, 1991, the microfiche copy of any new document entering the NTIS collection will be priced the same as the paper copy of the document.

IMPORTANT NOTICE

NTIS Shipping and Handling Charges

U.S., Canada, Mexico — ADD $3.00 per TOTAL ORDER

All Other Countries — ADD $4.00 per TOTAL ORDER

Exceptions — Does NOT apply to:

ORDERS REQUESTING NTIS RUSH HANDLING
ORDERS FOR SUBSCRIPTION OR STANDING ORDER PRODUCTS *ONLY*

NOTE: Each additional delivery address on an order requires a separate shipping and handling charge.

FEDERAL REGIONAL DEPOSITORY LIBRARIES

ALABAMA

AUBURN UNIV. AT MONTGOMERY LIBRARY
Documents Dept.
7300 University Drive
Montgomery, AL 36117-3596
(205) 244-3650 FAX: (205) 244-0678

UNIV. OF ALABAMA
Amelia Gayle Gorgas Library
Govt. Documents
Box 870266
Tuscaloosa, AL 35487-0266
(205) 348-6046 FAX: (205) 348-8833

ARIZONA

DEPT. OF LIBRARY, ARCHIVES, AND PUBLIC RECORDS
Federal Documents
Third Floor State Capitol
1700 West Washington
Phoenix, AZ 85007
(602) 542-4121 FAX: (602) 542-4400; 542-4500

ARKANSAS

ARKANSAS STATE LIBRARY
State Library Services
One Capitol Mall
Little Rock, AR 72201
(501) 682-2869

CALIFORNIA

CALIFORNIA STATE LIBRARY
Govt. Publications Section
914 Capitol Mall - P.O. Box 942837
Sacramento, CA 94237-0001
(916) 322-4572 FAX: (916) 324-8120

COLORADO

UNIV. OF COLORADO - BOULDER
Norlin Library
Govt. Publications
Campus Box 184
Boulder, CO 80309-0184
(303) 492-8834 FAX: (303) 492-2185

DENVER PUBLIC LIBRARY
Govt. Publications Dept. BS/GPD
1357 Broadway
Denver, CO 80203
(303) 571-2135

CONNECTICUT

CONNECTICUT STATE LIBRARY
231 Capitol Avenue
Hartford, CT 06106
(203) 566-4971 FAX: (203) 566-3322

FLORIDA

UNIV. OF FLORIDA LIBRARIES
Documents Dept.
Library West
Gainesville, FL 32611-2048
(904) 392-0366 FAX: (904) 392-7251

GEORGIA

UNIV. OF GEORGIA LIBRARIES
Govt. Documents Dept.
Jackson Street
Athens, GA 30602
(404) 542-8949 FAX: (404) 542-6522

HAWAII

UNIV. OF HAWAII
Hamilton Library
Govt. Documents Collection
2550 The Mall
Honolulu, HI 96822
(808) 948-8230 FAX: (808) 956-5968

IDAHO

UNIV. OF IDAHO LIBRARY
Documents Section
Moscow, ID 83843
(208) 885-6344 FAX: (208) 885-6817

ILLINOIS

ILLINOIS STATE LIBRARY
Reference Dept.
300 South Second
Springfield, IL 62701-1796
(217) 782-7596 FAX: (217) 524-0041

INDIANA

INDIANA STATE LIBRARY
Serials/Documents Section
140 North Senate Avenue
Indianapolis, IN 46204
(317) 232-3678 FAX: (317) 232-3728

IOWA

UNIV. OF IOWA LIBRARIES
Govt. Publications Dept.
Washington & Madison Streets
Iowa City, IA 52242
(319) 335-5926 FAX: (319) 335-5830

KANSAS

UNIV. OF KANSAS
Govt. Documents & Map Library
6001 Malatt Hall
Lawrence, KS 66045-2800
(913) 864-4660 FAX: (913) 864-5380

KENTUCKY

UNIV. OF KENTUCKY LIBRARIES
Govt. Publications/Maps Dept.
Lexington, KY 40506-0039
(606) 257-3139 FAX: (606) 257-1563; 257-8379

LOUISIANA

LOUISIANA STATE UNIV.
Middleton Library
Govt. Documents Dept.
Baton Rouge, LA 70803
(504) 388-2570 FAX: (504) 388-6992

LOUISIANA TECHNICAL UNIV.
Prescott Memorial Library
Govt. Documents Dept.
305 Wisteria Street
Ruston, LA 71270-9985
(318) 257-4962 FAX: (318) 257-2447

MAINE

TRI-STATE DOCUMENTS DEPOSITORY
Raymond H. Fogler Library
Govt. Documents & Microforms Dept.
Univ. of Maine
Orono, ME 04469
(207) 581-1680

MARYLAND

UNIV. OF MARYLAND
Hornbake Library
Govt. Documents/Maps Unit
College Park, MD 20742
(301) 454-3034 FAX: (301) 454-4985

MASSACHUSETTS

BOSTON PUBLIC LIBRARY
Govt. Documents Dept.
666 Boylston Street
Boston, MA 02117
(617) 536-5400 ext. 226
FAX: (617) 267-8273; 267-8248

MICHIGAN

DETROIT PUBLIC LIBRARY
5201 Woodward Avenue
Detroit, MI 48202-4093
(313) 833-1440; 833-1409
FAX: (313) 833-5039

LIBRARY OF MICHIGAN
Govt. Documents Unit
P.O. Box 30007
Lansing, MI 48909
(517) 373-0640 FAX: (517) 373-3381

MINNESOTA

UNIV. OF MINNESOTA
Wilson Library
Govt. Publications Library
309 19th Avenue South
Minneapolis, MN 55455
(612) 624-5073 FAX: (612) 626-9353

MISSISSIPPI

UNIV. OF MISSISSIPPI
J.D. Williams Library
Federal Documents Dept.
106 Old Gym Bldg.
University, MS 38677
(601) 232-5857 FAX: (601) 232-5453

MISSOURI

UNIV. OF MISSOURI - COLUMBIA
Ellis Library
Govt. Documents
Columbia, MO 65201
(314) 882-6733 FAX: (314) 882-8044

MONTANA

UNIV. OF MONTANA
Maureen & Mike Mansfield Library
Documents Div.
Missoula, MT 59812-1195
(406) 243-6700 FAX: (406) 243-2060

NEBRASKA

UNIV. OF NEBRASKA - LINCOLN
D.L. Love Memorial Library
Documents Dept.
Lincoln, NE 68588
(402) 472-2562

NEVADA

UNIV. OF NEVADA
Reno Library
Govt. Publications Dept.
Reno, NV 89557
(702) 784-6579 FAX: (702) 784-1751

NEW JERSEY

NEWARK PUBLIC LIBRARY
U.S. Documents Div.
5 Washington Street -
P.O. Box 630
Newark, NJ 07101-0630
(201) 733-7812 FAX: (201) 733-5648

NEW MEXICO

UNIV. OF NEW MEXICO
General Library
Govt. Publications Dept.
Albuquerque, NM 87131-1466
(505) 277-5441 FAX: (505) 277-6019

NEW MEXICO STATE LIBRARY
325 Don Gaspar Avenue
Santa Fe, NM 87503
(505) 827-3826 FAX: (505) 827-3820

NEW YORK

NEW YORK STATE LIBRARY
Documents/Gift & Exchange Section
Federal Depository Program
Cultural Education Center
Albany, NY 12230
(518) 474-5563 FAX: (518) 474-5786

NORTH CAROLINA

UNIV. OF NORTH CAROLINA - CHAPEL HILL
CB#3912, Davis Library
BA/SS Dept.—Documents
Chapel Hill, NC 27599
(919) 962-1151 FAX: (919) 962-0484

NORTH DAKOTA

NORTH DAKOTA STATE UNIV. LIBRARY
Documents Office
Fargo, ND 58105
(701) 237-8886 FAX: (701) 237-7138
In cooperation with Univ. of North Dakota, Chester Fritz Library
Grand Forks

OHIO

STATE LIBRARY OF OHIO
Documents Dept.
65 South Front Street
Columbus, OH 43266
(614) 644-7051 FAX: (614) 752-9178

OKLAHOMA

OKLAHOMA DEPT. OF LIBRARIES
U.S. Govt. Information Div.
200 NE 18th Street
Oklahoma City, OK 73105-3298
(405) 521-2502, ext. 252, 253
FAX: (405) 525-7804

OKLAHOMA STATE UNIV.
Edmon Low Library
Documents Dept.
Stillwater, OK 74078
(405) 744-6546 FAX: (405) 744-5183

OREGON

PORTLAND STATE UNIV.
Millar Library
934 SW Harrison - P.O. Box 1151
Portland, OR 97207
(503) 725-3673 FAX: (503) 725-4527

PENNSYLVANIA

STATE LIBRARY OF PENN.
Govt. Publications Section
Walnut St. & Commonwealth Ave. -
P.O. Box 1601
Harrisburg, PA 17105
(717) 787-3752

SOUTH CAROLINA

CLEMSON UNIV.
Cooper Library
Public Documents Unit
Clemson, SC 29634-3001
(803) 656-5174 FAX: (803) 656-3025
In cooperation with Univ. of South Carolina, Thomas Cooper Library, Columbia

TENNESSEE

MEMPHIS STATE UNIV. LIBRARIES
Govt. Documents
Memphis, TN 38152
(901) 678-2586 FAX: (901) 678-2511

TEXAS

TEXAS STATE LIBRARY
United States Documents
P.O. Box 12927 - 1201 Brazos
Austin, TX 78711
(512) 463-5455 FAX: (512) 463-5436

TEXAS TECH. UNIV. LIBRARY
Documents Dept.
Lubbock, TX 79409
(806) 742-2268 FAX: (806) 742-1920

UTAH

UTAH STATE UNIV.
Merrill Library & Learning Resources Center, UMC-3000
Documents Dept.
Logan, UT 84322-3000
(801) 750-2684 FAX: (801) 750-2677

VIRGINIA

UNIV. OF VIRGINIA
Alderman Library
Govt. Documents
Charlottesville, VA 22903-2498
(804) 924-3133 FAX: (804) 924-4337

WASHINGTON

WASHINGTON STATE LIBRARY
Document Section
MS AJ-11
Olympia, WA 98504-0111
(206) 753-4027 FAX: (206) 753-3546

WEST VIRGINIA

WEST VIRGINIA UNIV. LIBRARY
Govt. Documents Section
P.O. Box 6069
Morgantown, WV 26506
(304) 293-3640

WISCONSIN

ST. HIST. SOC. OF WISCONSIN LIBRARY
Govt. Publications Section
816 State Street
Madison, WI 53706
(608) 262-2781 FAX: (608) 262-4711
In cooperation with Univ. of Wisconsin-Madison, Memorial Library

MILWAUKEE PUBLIC LIBRARY
Documents Div.
814 West Wisconsin Avenue
Milwaukee, WI 53233
(414) 278-2167 FAX: (414) 278-2137

* U.S. G.P.O.:1992-313-125:60014

National Aeronautics and
Space Administration
Code JTT
Washington, D.C.
20546-0001

Official Business
Penalty for Private Use, $300

SPECIAL FOURTH-CLASS RATE
POSTAGE & FEES PAID
NASA
PERMIT No. G27

NASA

POSTMASTER: If Undeliverable (Section 158
Postal Manual) Do Not Return